

DRAG REDUCTION BY POLYMER SOLUTIONS IN RIBLET PIPES

by

EDDIE KOURY

B.A.
University of Cambridge
(1989)

M.Eng.
University of Cambridge
(1990)

Submitted to the Department of Chemical Engineering in Partial Fulfillment of the
Requirements for the Degree of

DOCTOR OF PHILOSOPHY
in Chemical Engineering

at the

MASSACHUSETTS INSTITUTE OF TECHNOLOGY

June, 1995

© Massachusetts Institute of Technology, 1995
All rights reserved

Signature of Author
Department of Chemical Engineering
May 24, 1995

Certified by
Preetinder Singh Virk
Associate Professor
Thesis Advisor

Accepted by
Robert E. Cohen
Chairman, Committee on Graduate Students

MASSACHUSETTS INSTITUTE
OF TECHNOLOGY

JUL 12 1995

V. I.
LIBRARIES

ARCHIVES

DRAG REDUCTION BY POLYMER SOLUTIONS IN RIBLET PIPES

by

EDDIE KOURY

Submitted to the Department of Chemical Engineering on May 24, 1995 in partial fulfillment of the requirements for the Degree of Doctor of Philosophy in Chemical Engineering

ABSTRACT

Flows of dilute polymer solutions were investigated in four longitudinally grooved pipes, fabricated from combinations of 10.21 and 7.82 mm ID smooth pipes and geometrically similar V-groove vinyl riblets of nominal heights 0.15 and 0.11 mm (3M Co.). Five homologous polyethyleneoxides, of molecular weights, M_w from 0.16 to 7.9×10^6 and two homologous polyacrylamides, $M_w = 2.9$ and 7.4×10^6 were used, at concentrations c from 1 to 5000 wppm, to investigate drag reduction in the riblet pipes. Diametral Reynolds numbers were varied from 300 to 150000. Measurements in each riblet pipe were accompanied by simultaneous measurements in a smooth pipe of the same nominal diameter placed in tandem. The chosen conditions provided turbulent drag reductions from zero to the asymptotic maximum possible.

In the smooth pipes, the polymer solutions followed established patterns of Type A drag reduction, namely:

- (i) An onset of drag reduction at a wall shear stress that was approximately inversely proportional to the square of the polymer radius of gyration but independent of polymer concentration and pipe diameter.
- (ii) A polymeric regime "fan", in which the extent of drag reduction increased linearly on Prandtl-Karman (P-K) coordinates, the slope for a polymer solution exceeding that of the solvent by an amount δ (slope increment) that was approximately proportional to the square root of polymer concentration and independent of pipe diameter; further, within a homologous series of polymers, the specific slope increment, δ/c , increased linearly with M_w .
- (iii) An asymptotic maximum drag reduction that was independent of polymer concentration, polymer molecular weight, polymer skeletal structure and pipe diameter.

In the riblet pipes, the onset of polymer-induced drag reduction occurred at the same wall shear stress as observed in the tandem smooth pipes. In the polymeric regime, following onset, the polymer solutions initially exhibited linear segments on P-K coordinates, akin to those seen in the smooth pipes. The maximum drag reduction observed in the riblet pipes was independent of polymeric properties but depended on the ratio of pipe radius to riblet height, $d/2h$. Under conditions of maximum drag reduction, $1/\sqrt{f}$ in the riblet pipes typically followed the smooth pipe friction factors up to $Re\sqrt{f} \approx 1000$, then diverged upwards, in most cases, for a short range of $Re\sqrt{f}$, before decreasing, and becoming appreciably lower than smooth at the highest $Re\sqrt{f}$.

Flow in the riblet pipes relative to the tandem smooth pipes was characterized by a riblet-induced flow enhancement, $R' = [1/\sqrt{f_{\text{riblet}}} - 1/\sqrt{f_{\text{smooth}}}]_{\text{Re}, f, \text{fluid}}$. Solvent flows exhibited three regimes, namely:

- (i) Hydraulically smooth. The riblets induced no drag reduction for nondimensional riblet heights $h^+ = u_\tau h/\nu < 5$.
- (ii) Riblet drag reduction. It was observed that $R' > 0$ for $5 < h^+ < 22$, the maximum $R' \approx 0.5$ occurring at $h^+ \approx 15$.
- (iii) Riblet drag enhancement. It was found that $R' < 0$ for $22 < h^+ < 110$, with $R' \rightarrow -2.2$ for $h^+ > 70$.

Polymer solution flows in the riblet pipes also exhibited all three of the regimes noted above, with the following differences:

- (i) The hydraulically smooth regime extended to $h^+ \approx 10$ at maximum drag reduction.
- (ii) In the riblet drag reduction regime, R' was a function of both h^+ and the polymer-induced flow enhancement, $S' = [1/\sqrt{f_{\text{polymer}}} - 1/\sqrt{f_{\text{solvent}}}]_{\text{Re}, f, \text{pipe}}$. At low S' , the upper limit of the regime lay at higher h^+ than in solvent, which at high h^+ the opposite was true; also, the maximum R' in polymer solutions was generally higher than in solvent.
- (iii) Riblet drag enhancement was observed in all polymer solutions at high h^+ , the more so as S' increased; the greatest drag enhancement in polymer solutions, $R' \approx -8 \pm 1$ at $h^+ \approx 50$ and $S' \approx 20$, considerably exceeded that in solvent.

A serrated sublayer model was proposed to decouple the drag reduction inherently induced by the riblets from the drag enhancement caused by their increased wetted surface area. In this model, the hydraulic diameter of the riblet pipes was derived from the shape of the viscous sub-layer as a function of h^+ . Application of the model to solvent flow suggested that the inherent riblet-induced drag reduction extended from $5 < h^+ < 65$, over a considerably wider range than the physically observed regime of riblet drag reduction, $5 < h^+ < 22$; also, the maximum inherent $R' = 1.5$ was thrice the observed maximum, $R' = 0.5$. Application of the model at conditions of maximum polymer-induced drag reduction suggested a thickening of the viscous sublayer to about twice its Newtonian value. Such thickening has previously been observed in rough pipes operating at maximum drag reduction.

Three-dimensional representations of riblet- and polymer-induced drag reductions versus turbulent flow parameters revealed a hitherto unknown "dome" region, $8 < h^+ < 31$, $0 < S' < 13$, $0 < R' < 1.5$, containing a broad maximum. The existence of a dome was physically interpreted to suggest that riblets and polymers reduce drag by separate mechanisms. In terms of the turbulent burst cycle comprising (1) lift-up of sublayer streaks, (2) vortex growth, and (3) vortex breakdown, with axial to transverse energy transfer, it was suggested that the riblets primarily interfere with stage (2) while the polymer solutions retard axial to transverse energy transfer in stage (3).

Thesis Supervisor: Dr. Preetinder Singh Virk
Title: Professor of Chemical Engineering

**Dedicated to my Parents:
Moufidy and Issam Koury**

and to the memory of Paul Jenkins

ACKNOWLEDGEMENTS

I would like to thank my thesis advisor, Professor Preetinder Singh Virk, for his invaluable insight and education on both my work and on the nature of things; the members of my thesis committee: E.W. Merrill, Professors K.A. Smith, and M. T. Landahl for their support and encouragement. I would also like to acknowledge Stone and Webster for its partial financial support during the course of this study and Mr. Frank Marentic, formerly of 3M Co., for graciously supplying the riblets used for this study.

Heartfelt appreciation and thanks go out to the numerous members of the department for their camaraderie and understanding (too numerous to name all, after all I'm trying to keep the number of pages of this thesis to a minimum). Specifically, I would like to thank the Tester group with whom I shared an office; Elaine Aufiero-Peters, whose friendship and support I cherished; Mike Thompson, who still cannot beat me at racquetball; David Waggoner for his guidance during the initial stages of my work, and Dr. Vikki Vlastnik for her inestimable understanding and support.

I would like to acknowledge Sonia Edghill, Audrey Tolman, Gervase and Leslie Warner, Scott and Ianthe Hilton-Clarke for their friendship outside of M.I.T. Finally, I would just like to add that apart from my parents, I would not have been here if it were not for Mr. E.N. Lambert, my high school teacher, and the single incident that changed my academic life on December 15, 1980.

CONTENTS

1	INTRODUCTION	28
	1.1 Motivation and Objectives	28
	1.2 Turbulent Flow Drag Reduction: Literature Review	29
	1.2.1 Gross Flow	29
	<i>1.2.1.1 Definitions</i>	29
	<i>1.2.1.2 Dilute Polymer Solutions</i>	30
	<i>1.2.1.3 Riblets</i>	35
	1.2.2 Mean Velocity Profiles	38
	<i>1.2.2.1 Newtonian Flow over Smooth Surfaces</i>	38
	<i>1.2.2.2 Dilute Polymer Solutions</i>	42
	<i>1.2.2.3 Riblets</i>	46
	1.2.3 Turbulence Structures	48
	<i>1.2.3.1 Newtonian Flow over Smooth Surfaces</i>	48
	<i>1.2.3.2 Dilute Polymer Solutions</i>	51
	<i>1.2.3.3 Riblets</i>	58
	1.2.4 Polymer Drag Reduction over Wall Modified Surfaces	65
	<i>1.2.4.1 Rough Walls</i>	65
	<i>1.2.4.2 Riblet Walls</i>	66
	1.3 Properties of Polyethylene oxide and Polyacrylamide Solutions	69
	1.3.1 Dilute Solutions	69
	1.3.2 Intrinsic Viscosity	69
	<i>1.3.2.1 Evaluation</i>	68
	<i>1.3.2.2 Interpretation</i>	70
	1.3.3 Molecular Weight and Radius of Gyration	71
	1.3.4 Polydispersity	74
2	EXPERIMENTAL APPARATUS	159
	2.1 General Flow System Description	159
	2.2 Detailed Description	161

2.2.1 Test System	161
2.2.1.1 <i>Riblets.</i>	161
2.2.1.2 <i>Smooth Test Section Fabrication</i>	162
2.2.1.3 <i>Riblet Test Section Fabrication.</i>	164
2.2.1.4 <i>Trailing Smooth Test Section.</i>	166
2.2.1.5 <i>Pressure Transducer Interface Unit.</i>	167
2.2.2 Upstream System	168
2.2.2.1 <i>Tanks.</i>	168
2.2.2.2 <i>Pump Unit.</i>	169
2.2.2.3 <i>Calming Chamber.</i>	169
2.2.3 Downstream System	170
2.2.3.1 <i>Flow Controller.</i>	170
2.2.3.2 <i>Temperature Probe.</i>	170
2.2.3.3 <i>Flow Diverter.</i>	171
2.3 Measuring Devices	172
2.3.1 Pressure Transducer and Carrier Demodulator.	172
2.3.2 Data Acquisition System.	172
2.4 Other Related Equipment	173
2.4.1 Manometers	173
2.4.2 Small Scale Mixing System	174
2.5 Chemicals	174
3 EXPERIMENTAL PROCEDURES	185
3.1 Calibrations	185
3.1.1 Tank Calibrations	185
3.1.2 Pump Calibrations	186
3.1.3 Transducer Calibrations	188
3.1.4 Thermistor Calibration	191
3.1.5 Measured and Calculated Pipe Diameters	192
3.1.5.1 <i>Smooth Pipe</i>	192
3.1.5.2 <i>Riblet Pipes</i>	193

3.2	Polymer Solution Master Batch Preparation and Classification	194
3.2.1	Preparation	194
3.2.2	Classification	196
3.3	Experimental Runs	197
3.3.1	Preparation	197
3.3.2	Procedure	200
3.4	Data Reduction	203
4	RESULTS	226
4.1	Experimental Grid	226
4.2	Solvent Flow	227
4.2.1	Flow Development	227
4.2.2	Laminar Flow	228
4.2.3	Pressure Gradient Ratio	229
4.2.4	Prandtl-Karman Representation	233
4.2.5	Flow Enhancement Parameters	237
4.3	Polymer Solution Flow	238
4.3.1	A Representative Example	238
<i>4.3.1.1</i>	<i>Prandtl-Karman Representation</i>	238
<i>4.3.1.2</i>	<i>Flow Enhancement Parameters</i>	240
4.3.2	Effect of Polymer Concentration	241
4.3.3	Effect of Degradation	245
<i>4.3.3.1</i>	<i>Degradation Experiments</i>	245
<i>4.3.3.2</i>	<i>Examples</i>	246
<i>4.3.3.3</i>	<i>Quantitative Results</i>	251
4.3.4	Effect of Polymer Molecular Weight	257
<i>4.3.4.1</i>	<i>N-10 Solutions</i>	257
<i>4.3.4.2</i>	<i>N-750 Solutions</i>	259
<i>4.3.4.3</i>	<i>N-6CK Solutions</i>	261
<i>4.3.4.4</i>	<i>P-309 Solutions</i>	264
<i>4.3.4.5</i>	<i>PEO Comparisons</i>	266

4.3.5	Effect of Polymer Skeletal Structure	269
4.3.5.1	<i>N-300L Solutions</i>	269
4.3.5.2	<i>N-300 Solutions</i>	272
4.3.6	Riblet Pipe Reproductions	275
4.3.6.1	<i>Solvent Flow in the Riblet Pipe</i>	275
4.3.6.2	<i>Polymer-induced Flow Enhancement in the Smooth Pipe</i>	276
4.3.6.3	<i>Riblet-induced Flow Enhancement</i>	277
4.3.7	Effect of Riblet Pipe Geometry	279
4.3.7.1	<i>7.82 mm pipe/0.11 mm riblets (S1 and R1A)</i>	279
4.3.7.2	<i>7.82 mm pipe/0.15 mm riblets (S1 and R1B)</i>	292
4.3.7.3	<i>10.21 mm pipe/0.11 mm riblets (S2 and R2A)</i>	299
4.3.7.4	<i>Pipe Comparisons</i>	311
4.4	Maximum Drag Reduction	314
4.4.1	Pressure Gradient Ratio	315
4.4.2	Prandtl-Karman Representation	317
4.4.2.1	<i>Smooth Pipes</i>	317
4.4.2.1	<i>Riblet Pipes</i>	318
4.4.3	Flow Enhancement Parameters	319
4.5	Laminar Flow Parameters	320
4.5.1	Relative Viscosity	320
4.6	Turbulent Flow Parameters	321
4.6.1	Onset Wall Shear Stress, τ_w^*	321
4.6.1.1	<i>Smooth Pipes</i>	321
4.6.1.2	<i>Riblet Pipes</i>	322
4.6.2	Slope Increment, δ	323
4.6.2.1	<i>Smooth Pipes</i>	323
4.6.2.2	<i>Riblet Pipes</i>	323
4.7	Summary	324
4.7.1	Solvent Flow	324
4.7.2	Polymer Solution Flow	324

	<i>4.7.2.1 Polymer-induced Flow Enhancement in the Smooth Pipes</i>	325
	<i>4.7.2.2 Polymer-induced Flow Enhancement in the Riblet Pipes</i>	326
	<i>4.7.2.3 Riblet-induced Flow Enhancement</i>	327
5	DISCUSSION	457
	5.1 Smooth Pipes	457
	5.1.1 Onset	457
	5.1.2 Polymeric Regime	458
	5.1.3 Maximum Drag Reduction	459
	5.1.3 Polymer Degradation	460
	5.2 Riblet Pipes: Solvent Flow	461
	5.2.1 Laminar Flow	461
	5.2.2 Comparison to Previous Work	462
	5.2.3 Serrated Sublayer Model	463
	<i>5.2.3.1 Model Development</i>	463
	<i>5.2.3.2 Riblet Drag Reduction</i>	467
	<i>5.2.3.3 Comparison to Rough Pipes</i>	468
	<i>5.2.3.4 Comparison with other Models of Riblet Drag Reduction</i>	469
	5.2 Riblet Pipes: Polymer Solution Flow	470
	5.3.1 Riblet-Polymer Matrix	470
	5.3.2 Onset	471
	5.3.3 Polymeric Regime	472
	<i>5.3.3.1 Effectively Smooth</i>	472
	5.3.4 Maximum Drag Reduction	474
	<i>5.3.4.1 Riblet-induced Flow Enhancement</i>	474
	<i>5.3.4.2 Serrated Sublayer Model at MDR</i>	475
	<i>5.3.4.3 Comparison to Rough Pipes</i>	476
	5.3.5 Effect of Degradation	477
	5.4. Relation between Riblet- and Polymer-induced Flow Enhancements	481
	5.4.1 Additive Equivalence	481
	5.4.2 3-D Representation	482

5.4.3	Scaling	481
5.4.2	Other 3-D Representations: Prandtl-Karman and f -Re	485
5.5	Mechanism	486
6	SUMMARY	534
6.1	Background	534
6.2	Experimental	537
6.2.1	Riblets	537
6.2.2	Flow System	537
6.3	Results	539
6.3.1	Solvent Flow	539
6.3.2	Polymer Solution Flow	540
6.3.2.1	<i>Example</i>	540
6.3.2.2	<i>Drag Reduction Parameters</i>	542
6.3.2.3	<i>Polymer-induced Flow Enhancement in the Smooth Pipes</i>	542
6.3.2.4	<i>Polymer-induced Flow Enhancement in the Riblet Pipes</i>	544
6.3.2.5	<i>Riblet-induced Flow Enhancement</i>	545
6.4	Discussion	547
6.4.1	Smooth Pipes	547
6.4.2	Riblet Pipes	548
6.4.2.1	<i>Solvent Flow</i>	548
6.4.2.2	<i>Polymer Solution Flow</i>	549
6.4.3	Mechanism	552
7	RECOMMENDATIONS	553
8	APPENDICES	
A	Laminar Flow Re-Development after a Sudden Contraction in Pipe Flow	555
B	Contour Plot Generation	558
C	Nomenclature	562

D References

566

E Data

576

LIST OF TABLES

Table 1.2.1.	Some characteristics of fast swimming sharks. Physical sizes are those of Reif (1982)	75
Table 1.2.2.	External flow over riblets: Experimental riblet configurations.	76
Table 1.2.3.	Internal flow over riblets: Experimental riblet configurations.	78
Table 1.2.4.	Additive mean velocity profiles: Representative literature experimental conditions.	79
Table 1.2.5.	Additive turbulence intensity: Representative literature experimental conditions.	80
Table 1.2.6.	Riblet turbulence intensity: Representative literature experimental and computational configurations.	81
Table 1.2.7.	Polymer solution flow over wall modified surfaces: (a) rough pipes, (b) external flow over V-groove riblet surfaces and (c) V-groove riblet pipes.	82
Table 1.3.1.	Characterization of aqueous PEO solutions.	83
Table 1.3.2.	Characterization of aqueous PAM solutions.	84
Table 1.3.3.	Characteristics of high molecular weight aqueous PEO solutions ($M_w > 10^5$ g/mol).	85
Table 1.3.4.	Characteristics of high molecular weight aqueous PAM solutions ($M_w > 10^5$ g/mol).	86
Table 2.2.1	Pipe designation and fabrication specifications	175
Table 2.5.1	Series designation and approximate molecular weights for water soluble polymers.	176
Table 3.1.1.	Summary of pump calibrations.	205
Table 3.1.2.	Two factor Analysis of Variance (ANOVA) for the linear regression coefficients	205
Table 3.1.3.	Calculated and measured pipe diameters	206
Table 3.4.1.	Data reduction spreadsheet summary	207
Table 4.1.1.	Experimental grid	330
Table 4.2.1.	Flow regimes of pressure gradient ratio for solvent flow.	331
Table 4.2.2.	Summary of solvent flow regimes in smooth and riblet pipes	332
Table 4.3.1.	Summary of Drag Reduction by PEO W-301 in S2 and R2B.	333

Table 4.3.2a.	Polymer degradation experiments.	334
Table 4.3.2b.	Drag Reduction Results at Station 1 for Polymer batches used in Degradation Experiments.	335
Table 4.3.3.	Summary of Drag Reduction by PEO N-10 in S2 and R2B.	336
Table 4.3.4.	Summary of Drag Reduction by PEO N-750 in S2 and R2B.	337
Table 4.3.5.	Summary of Drag Reduction by PEO N-60K in S2 and R2B.	338
Table 4.3.6.	Summary of Drag Reduction by PEO P-309 in S2 and R2B.	339
Table 4.3.7.	Summary of Drag Reduction by PAM N-300L in S2 and R2B.	340
Table 4.3.8.	Summary of Drag Reduction by PAM N-300 in S2 and R2B.	341
Table 4.3.9.	Summary of Drag Reduction by PEO W-301 and PEO P-309 in S2 and R2BR.	342
Table 4.3.10.	Summary of Drag Reduction by PEO N-750 in S1 and R1A.	343
Table 4.3.11.	Summary of Drag Reduction by PEO N-60K in S1 and R1A.	344
Table 4.3.12.	Summary of Drag Reduction by PEO W-301, PEO P-309 and PAM N-300 in S1 and R1A.	345
Table 4.3.13.	Summary of Drag Reduction by PEO N-60K and 100 wppm W-301 in S1 and R1AR.	346
Table 4.3.14.	Summary of Drag Reduction by PEO W-301 in S1 and R1AR.	347
Table 4.3.15.	Summary of Drag Reduction by PEO N-750 in S1 and R1B.	348
Table 4.3.16.	Summary of Drag Reduction by PEO N-60K in S1 and R1B.	349
Table 4.3.17.	Summary of Drag Reduction by PEO W-301, PEO P-309 and PAM N-300 in S1 and R1B.	350
Table 4.3.18.	Summary of Drag Reduction by PEO N-750 in S2 and R2A.	351
Table 4.3.19.	Summary of Drag Reduction by PEO N-60K in S2 and R2A.	352
Table 4.3.20.	Summary of Drag Reduction by PEO W-301 in S2 and R2A.	353
Table 4.3.21.	Summary of Drag Reduction by PEO P-309 in S2 and R2A.	354
Table 4.3.22.	Summary of Drag Reduction by PEO P-309 in S2 and R2AR.	355
Table 4.4.1.	Experiments at maximum drag reduction.	356
Table 4.4.2.	Flow regimes of pressure gradient ratio at maximum drag reduction.	357

Table 4.4.3.	Summary of maximum drag reduction in smooth and riblet pipes.	358
Table 4.5.1.	Experimental relative and intrinsic viscosities calculated from laminar flow data.	359
Table 4.5.2.	Polymeric parameters inferred from intrinsic viscosities.	361
Table 4.6.1.	Average regressed onset wall shear stress for additives in 10.21 mm and 7.82 mm hydraulically smooth pipes.	362
Table 4.6.2.	Type A model intrinsic slope increment, $\delta/c^{1/2}$, for additives in 10.21 mm and 7.82 mm hydraulically smooth pipes.	363
Table 5.1.1.	Degradation parameters in the polymeric regime.	488
Table 5.2.1.	Smooth and riblet pipe data.	489
Table 5.3.1.	The Riblet-Polymer Matrix for all polymers in the 7.82 mm pipe, 0.11 mm riblets.	490
Table 5.3.2.	The Riblet-Polymer Matrix for all polymers in the 7.82 mm pipe, 0.15 mm riblets.	491
Table 5.3.3.	The Riblet-Polymer Matrix for all polymers in the 10.21 mm pipe, 0.11 mm riblets.	492
Table 5.3.4.	The Riblet-Polymer Matrix for all polymers in the 10.21 mm pipe, 0.15 mm riblets.	493
Table 5.3.5.	Onset wall shear stress and non-dimensional riblet height in riblet pipes.	494
Table 5.4.1.	Summary of the regions that define the relation between the riblet-induced flow enhancement, R' , the polymer-induced flow enhancement, S_s' , and the non-dimensional riblet height, h^+ .	495

LIST OF FIGURES

Figure 1.2.1.	Aspects of type-A drag reduction (Virk, 1975a)	87
Figure 1.2.2.	Aspects of type-B drag reduction (Virk and Wagger, 1989)	88
Figure 1.2.3a.	External, subsonic flow over V-groove riblet surfaces ($h/s = 1$)	89
Figure 1.2.3b.	External, subsonic flow over V-groove riblet surfaces ($h/s = 1$)	90
Figure 1.2.4a.	External, transonic flow over V-groove riblet surfaces ($h/s = 1$)	91
Figure 1.2.4b.	External, transonic flow over V-groove riblet surfaces ($h/s = 1$)	92
Figure 1.2.5a.	External flow over V-groove riblet surfaces ($h/s > 1$)	93
Figure 1.2.5b.	External flow over V-groove riblet surfaces ($h/s > 1$)	94
Figure 1.2.6a.	External flow over V-groove riblet surfaces ($h/s < 1$)	95
Figure 1.2.6b.	External flow over V-groove riblet surfaces ($h/s < 1$)	96
Figure 1.2.7a.	External flow over U-groove riblet surfaces	97
Figure 1.2.7b.	External flow over U-groove riblet surfaces	98
Figure 1.2.8a.	External flow over rectangular riblet surfaces	99
Figure 1.2.8b.	External flow over rectangular riblet surfaces	100
Figure 1.2.9a	Internal flow over riblet surfaces ($h/s = 1$)	101
Figure 1.2.9b.	Internal flow over riblet surfaces ($h/s = 1$)	102
Figure 1.2.10a.	Internal flow over riblet surfaces ($h/s < 1$)	103
Figure 1.2.10b.	Internal flow over riblet surfaces ($h/s < 1$)	104
Figure 1.2.11.	Variation of maximum riblet-induced flow enhancement, R'_{max} , with aspect ratio, h/s .	105
Figure 1.2.12.	Variation of h^+ at R'_{max} , with aspect ratio, h/s .	106
Figure 1.2.13.	Variation of h_c^+ with aspect ratio, h/s .	107
Figure 1.2.14.	Turbulent, Newtonian, mean velocity profiles	108
Figure 1.2.15.	Three-zone mean velocity profile model for the flow of dilute polymer solutions (Virk, 1971)	109
Figure 1.2.16.	Mean velocity profiles for the flow of dilute polymer solutions (Mizushima and Usui, 1977)	110

Figure 1.2.17.	Mean velocity profiles for the flow of dilute polymer solutions (Schummer and Thielen, 1980)	111
Figure 1.2.18.	Mean velocity profiles for the flow of dilute polymer solutions (Bartels et al., 1985)	112
Figure 1.2.19.	Mean velocity profiles for the flow of dilute polymer solutions (Willmarth et al., 1987 and Gampert and Yong, 1990)	113
Figure 1.2.20.	Mean velocity profile for the flow of centerline injected 0.2% polymer solution (Bewersdorff, 1984)	114
Figure 1.2.21.	Mean velocity profiles for Newtonian flow over riblets (Sawyer and Winter, 1987)	115
Figure 1.2.22.	Mean velocity profiles for Newtonian flow over riblets (Wallace, 1987)	116
Figure 1.2.23.	Calculated spanwise variation of shear stress on V-groove riblet surface (Choi et al., 1993)	117
Figure 1.2.24.	Spanwise variation of the mean velocity over a V-groove riblet surface (Hooshmand et al., 1983)	118
Figure 1.2.25.	Newtonian, turbulent intensity profiles in pipe flow at $Re = 50,000$ (Laufer, 1954)	119
Figure 1.2.26.	Newtonian, turbulent intensity profiles in pipe flow at $Re = 500,000$ (Laufer, 1954)	120
Figure 1.2.27.	Newtonian, turbulent Reynolds stress profiles in pipe flow at $Re = 50,000$ and $500,000$ (Laufer, 1954)	121
Figure 1.2.28.	u-v correlation coefficient in pipe flow at $Re = 50,000$ and $500,000$ (Laufer, 1954)	122
Figure 1.2.29a-b	Aspects of the structure of turbulence	123
Figure 1.2.29c-d	Aspects of the structure of turbulence	124
Figure 1.2.30.	Axial and radial intensity profiles for the flow of dilute polymer solutions in a 14.0 mm ID pipe (Schummer and Thielen, 1980)	125
Figure 1.2.31.	Axial intensity profiles for the flow of dilute polymer solutions in a 25.3 mm ID pipe at maximum drag reduction (Mizushima and Usui, 1977)	126
Figure 1.2.32.	Axial intensity profiles for the flow of dilute polymer solutions in a 16.4 mm ID pipe (Bartels et al., 1985)	127
Figure 1.2.33.	Radial intensity profiles for the flow of dilute polymer solutions in a 16.4 mm ID pipe (Bartels et al., 1985)	128

Figure 1.2.34.	Tangential intensity profiles for the flow of dilute polymer solutions in a 16.4 mm ID pipe (Bartels et al., 1985)	129
Figure 1.2.35.	Axial intensity profiles for the flow of dilute polymer solutions in a 44 mm ID pipe (Bartels et al., 1985)	130
Figure 1.2.36.	Radial intensity profiles for the flow of dilute polymer solutions in a 44 mm ID pipe (Bartels et al., 1985)	131
Figure 1.2.37.	Variation of the magnitude and position of the maximum axial turbulent intensity with the extent of polymeric drag reduction relative to that at maximum drag reduction	132
Figure 1.2.38.	Reynolds stress profiles for the flow of dilute polymer solutions	133
Figure 1.2.39.	Ratio of the polymer solution to solvent u-v correlation coefficient	134
Figure 1.2.40.	Variation of the non-dimensional streak spacing with the extent of polymeric drag reduction, measured as S^+	135
Figure 1.2.41.	Variation of the normalized turbulent burst times with the extent of polymeric drag reduction, measured as S^+	136
Figure 1.2.42.	Streamwise and normal turbulent intensity profiles over V-groove riblets (Walsh, 1979)	137
Figure 1.2.43.	Streamwise turbulent intensity profiles over V-groove riblets (Hooshmand et al., 1983)	138
Figure 1.2.44.	Streamwise turbulent intensity profiles over V-groove riblets (Bacher and Smith, 1985)	139
Figure 1.2.45.	Streamwise and normal turbulent intensity profiles over V-groove riblets under drag reducing conditions (Pulles, 1988)	140
Figure 1.2.46.	Streamwise and normal turbulent intensity profiles over V-groove riblets under drag enhancing conditions (Pulles, 1988)	141
Figure 1.2.47.	Streamwise, normal and tangential turbulent intensity profiles over tapered rectangular riblets (Choi, 1989)	142
Figure 1.2.48.	Spanwise variation of the streamwise turbulent intensity over an isolated rectangular riblet (Wilkinson and Lazos, 1987)	143
Figure 1.2.49.	Reynolds stress profile over V-groove riblets (Walsh, 1979)	144
Figure 1.2.50.	Reynolds stress profile over V-groove riblets under drag reducing conditions (Pulles, 1988)	145
Figure 1.2.51.	Reynolds stress profile over V-groove riblets under drag enhancing conditions (Pulles, 1988)	146

Figure 1.2.52.	Reynolds stress profile over tapered rectangular riblets (Choi, 1989)	147
Figure 1.2.53.	Ratio of the riblet to smooth u-v correlation coefficient	148
Figure 1.2.54.	The onset of drag reduction in rough pipes (Virk, 1971)	149
Figure 1.2.55.	Fractional slip in rough and smooth pipes (Virk, 1971)	150
Figure 1.2.56.	Maximum, asymptotic, drag reduction in smooth and rough pipes (Virk, 1971)	151
Figure 1.2.57.	Fractional slip in rough and smooth pipes (Bewersdorff and Petersmann, 1987)	152
Figure 1.2.58.	Polymer-induced flow enhancement over a smooth and riblet-lined axysymmetric body: (a) incremental flow enhancement (R') and differential flow enhancement or slip (S') (Beauchamps and Philips, 1986, 1987)	153
Figure 1.2.59.	Polymer-induced flow enhancement in smooth and riblet pipes (a) incremental flow enhancement (R'); (b) riblet pipe differential flow enhancement (S'_r); (c) smooth pipe differential flow enhancement (S'_s) (Anderson et al., 1993)	154
Figure 1.2.60.	Riblet drag reduction in smooth and riblet pipes for 0-50 wppm of (a) PAM and (b) PEO solutions (Christodoulou et al, 1991)	155
Figure 1.3.1.	Relation between K and a in the Mark-Houwink intrinsic viscosity-molecular weight relations for aqueous PEO and PAM solutions	156
Figure 1.3.2.	Characterization of aqueous PEO solutions	157
Figure 1.3.3.	Characterization of aqueous PAM solutions	158
Figure 2.1.1.	Experimental flow system	177
Figure 2.2.1.	3M V-groove riblets	178
Figure 2.2.2.	Pipe interface and pressure tap housing	179
Figure 2.2.3.	Pressure Transducer Interface (PTI) boards	180
Figure 2.2.4.	Flow controller	181
Figure 2.2.5.	Flow diverter	182
Figure 2.3.1.	Pressure transducer and carrier demodulator	183
Figure 2.4.1.	Water and Mercury manometers	184
Figure 3.1.1a.	Left tank calibration	209

Figure 3.1.1b.	Right tank calibration	210
Figure 3.1.2.	Pump calibration #1: 10.21 mm pipe, 0.15 mm riblets, distilled water	211
Figure 3.1.3.	Pump calibration #2: 10.21 mm pipe, 0.15 mm riblets, 50 wppm P-309	212
Figure 3.1.4.	Pump calibration #3: 10.21 mm pipe, 0.11 mm riblets, distilled water	213
Figure 3.1.5.	Pump calibration #4: 10.21 mm pipe, 0.11 mm riblets, 50 wppm P-309	214
Figure 3.1.6.	Pump calibration #5: 7.82 mm pipe, 0.15 mm riblets, distilled water	215
Figure 3.1.7.	Pump calibration #6: 7.82 mm pipe, 0.15 mm riblets, 50 wppm P-309	216
Figure 3.1.8.	Pump calibration summary accounting for the effect of pump back pressure	217
Figure 3.1.9.	Representative 0.1-psid pressure transducer calibration (CAL #775)	218
Figure 3.1.10.	Representative 1.0-psid pressure transducer calibration (CAL #523)	219
Figure 3.1.11.	Representative 10-psid pressure transducer calibration (CAL #740)	220
Figure 3.1.12.	5 k Ω thermistor calibration	221
Figure 3.3.1.	Pump-driven fluid flow path	222
Figure 3.3.2.	Gravity-driven fluid flow path	223
Figure 3.3.3.	Pump bypass-driven fluid flow path	224
Figure 3.4.1.	Representative data reduction spreadsheet (RUN237.R1A.P-309.100 wppm)	225
Figure 4.1.1.	Experimental grid depicting the expected flow regimes for five PEO solutions in the 10.21 mm and 7.82 mm smooth pipes.	364
Figure 4.1.2.	Experimental grid depicting the expected flow regimes for two PAM solutions in the 10.21 mm and 7.82 mm smooth pipes.	365
Figure 4.2.1.	Laminar and turbulent flow development in the 7.82 mm and 10.21 mm smooth pipes.	366
Figure 4.2.2.	Laminar flow pressure gradient-flowrate relation in the 7.82 mm pipes S1, R1A, R1B.	367
Figure 4.2.3.	Laminar flow pressure gradient-flowrate relation in the 10.21 mm pipes S2, R2A, R2B.	368
Figure 4.2.4.	Variations of the smooth to riblet pipe pressure gradient ratios versus flowrate.	369

Figure 4.2.5.	Prandtl-Karman friction factors for solvent flow in the 10.21 mm id smooth pipe.	370
Figure 4.2.6.	Prandtl-Karman friction factors for solvent flow in the 7.82 mm id smooth pipe.	371
Figure 4.2.7.	Prandtl-Karman friction factors for solvent flow in the 10.21 mm id smooth pipe and in the 10.21 mm pipe lined with 0.15 mm riblets.	372
Figure 4.2.8.	Effect of riblet-pipe diameter on Prandtl-Karman friction factors for $h^+ < 5$ in the 10.21 mm id smooth and 10.21 mm pipe lined with 0.15 mm riblets.	373
Figure 4.2.9.	Prandtl-Karman friction factors for solvent flow in the 7.82 mm id smooth and 7.82 mm pipe lined with 0.11 mm riblets.	374
Figure 4.2.10.	Prandtl-Karman friction factors for solvent flow in the 7.82 mm id smooth and 7.82 mm pipe lined with 0.15 mm riblets.	375
Figure 4.2.11.	Prandtl-Karman friction factors for solvent flow in the 10.21 mm id smooth and 10.21 mm pipe lined with 0.11 mm riblets.	376
Figure 4.2.12.	The riblet-induced flow enhancement for the flow of solvent in all riblet pipes.	377
Figure 4.2.13.	Error analysis of riblet-induced flow enhancement for the flow of solvent in all riblet pipes.	378
Figure 4.2.14.	The riblet-induced fractional flow enhancement for the flow of solvent in all riblet pipes.	379
Figure 4.3.1.	Flow of solvent and a 3 wppm solution of PEO W-301 in S2 and R2B.	380
Figure 4.3.2.	Flow of solvent and a 3 wppm solution of PEO W-301 in S2 and R2B. The vertical line <u>abcd</u> at $Re\sqrt{f} = 1510$ illustrates the definitions of polymer- and riblet-induced flow enhancements.	381
Figure 4.3.3.	Effect of polymer concentration on drag reduction by W-301 in S2 and R2B.	382
Figure 4.3.4.	Analysis of riblet- and polymer-induced flow enhancements by solvent and PEO W-301 solutions in S2 and R2B.	383
Figure 4.3.5.	Comparison between the effects of riblets and polymer degradation in the flow of 3 wppm W-301 in pipes S2 and R2B; upstream station 1, downstream station 2.	384
Figure 4.3.6.	Comparison between the effects of riblets and polymer degradation in the flow of 3 wppm W-301 in pipes S1 and R1B; upstream station 1, downstream station 2.	385

Figure 4.3.7.	Comparison between the effects of riblets and polymer degradation in the flow of 100 wppm W-301 in pipes S1 and R1A; upstream station 1, downstream station 2.	386
Figure 4.3.8.	Effect of downstream distance on degradation in the 10.21 mm pipe for PEO W-301 solutions.	387
Figure 4.3.9.	Effect of polymer molecular weight and pipe diameter on degradation between upstream and downstream hydraulically smooth sections.	388
Figure 4.3.10.	Friction factors for solutions of PEO N-10 in S2 and R2B.	389
Figure 4.3.11.	Analysis of riblet- and polymer-induced flow enhancements by solvent and PEO N-10 solutions in S2 and R2B.	390
Figure 4.3.12.	Friction factors for solutions of PEO N-750 in S2 and R2B.	391
Figure 4.3.13.	Analysis of riblet- and polymer-induced flow enhancements by solvent and PEO N-750 solutions in S2 and R2B.	392
Figure 4.3.14.	Friction factors for solutions of PEO N-60K in S2 and R2B.	393
Figure 4.3.15.	Analysis of riblet- and polymer-induced flow enhancements by solvent and PEO N-60K solutions in S2 and R2B.	394
Figure 4.3.16.	Friction factors for solutions of PEO P-309 in S2 and R2B.	395
Figure 4.3.17.	Analysis of riblet- and polymer-induced flow enhancements by solvent and PEO P-309 solutions in S2 and R2B.	396
Figure 4.3.18.	Friction factors for solutions of PAM N-300L in S2 and R2B.	397
Figure 4.3.19.	Analysis of riblet- and polymer-induced flow enhancements by solvent and PAM N-300L solutions in S2 and R2B.	398
Figure 4.3.20.	Friction factors for solutions of PAM N-300 in S2 and R2B.	399
Figure 4.3.21.	Analysis of riblet- and polymer-induced flow enhancements by solvent and PAM N-300 solutions in S2 and R2B.	400
Figure 4.3.22.	Analysis of riblet- and polymer-induced flow enhancements by solvent and PEO W-301 solutions in S2 and R2B, repeated pipe.	401
Figure 4.3.23.	Analysis of riblet- and polymer-induced flow enhancements by solvent and PEO P-309 solutions in S2 and R2B, repeated pipe.	402
Figure 4.3.24.	Friction factors for solutions of PEO N-750 in S1 and R1A.	403
Figure 4.3.25.	Analysis of riblet- and polymer-induced flow enhancements by solvent and PEO N-750 solutions in S1 and R1A.	404
Figure 4.3.26.	Friction factors for solutions of PEO N-60K in S1 and R1A..	405

Figure 4.3.27.	Analysis of riblet- and polymer-induced flow enhancements by solvent and PEO N-60K solutions in S1 and R1A.	406
Figure 4.3.28.	Friction factors for solutions of PEO W-301 in S1 and R1A.	407
Figure 4.3.29.	Friction factors for solutions of PEO P-309 in S1 and R1A.	408
Figure 4.3.30.	Friction factors for solutions of PEO N-300 in S1 and R1A.	409
Figure 4.3.31.	Analysis of riblet- and polymer-induced flow enhancements by solvent and PEO W-301 solutions in S1 and R1A.	410
Figure 4.3.32.	Analysis of riblet- and polymer-induced flow enhancements by solvent and PEO P-309 solutions in S1 and R1A.	411
Figure 4.3.33.	Analysis of riblet- and polymer-induced flow enhancements by solvent and PEO N-300 solutions in S1 and R1A.	412
Figure 4.3.34.	Analysis of riblet- and polymer-induced flow enhancements by solvent and PEO N-60K solutions in S1 and R1A, repeated pipe.	413
Figure 4.3.35.	Analysis of riblet- and polymer-induced flow enhancements by solvent and 100 wppm PEO W-301 solutions in S1 and R1AR.	414
Figure 4.3.36.	Friction factors for solutions of PEO W-301 in S1 and R1BR.	415
Figure 4.3.37.	Analysis of riblet- and polymer-induced flow enhancements by solvent and PEO W-301 solutions in S1 and R1AR.	416
Figure 4.3.38.	Friction factors for solutions of PEO N-750 in S1 and R1B.	417
Figure 4.3.39.	Analysis of riblet- and polymer-induced flow enhancements by solvent and PEO N-750 solutions in S1 and R1B.	418
Figure 4.3.40.	Friction factors for solutions of PEO N-60K in S1 and R1B.	419
Figure 4.3.41.	Analysis of riblet- and polymer-induced flow enhancements by solvent and PEO N-60K solutions in S1 and R1B.	420
Figure 4.3.42.	Friction factors for solutions of PEO W-301 in S1 and R1B.	421
Figure 4.3.43.	Friction factors for solutions of PEO P-309 in S1 and R1B.	422
Figure 4.3.44.	Friction factors for solutions of PEO N-300 in S1 and R1B.	423
Figure 4.3.45.	Analysis of riblet- and polymer-induced flow enhancements by solvent and PEO W-301 solutions in S1 and R1B.	424
Figure 4.3.46.	Analysis of riblet- and polymer-induced flow enhancements by solvent and PEO P-309 solutions in S1 and R1B.	425
Figure 4.3.47.	Analysis of riblet- and polymer-induced flow enhancements by solvent and PEO N-300 solutions in S1 and R1B.	426

Figure 4.3.48.	Friction factors for solutions of PEO N-750 in S2 and R2A.	427
Figure 4.3.49.	Analysis of riblet- and polymer-induced flow enhancements by solvent and PEO N-750 solutions in S2 and R2A.	428
Figure 4.3.50.	Friction factors for solutions of PEO N-60K in S2 and R2A.	429
Figure 4.3.51.	Analysis of riblet- and polymer-induced flow enhancements by solvent and PEO N-60K solutions in S2 and R2A.	430
Figure 4.3.52.	Friction factors for solutions of PEO W-301 in S2 and R2A.	431
Figure 4.3.53.	Analysis of riblet- and polymer-induced flow enhancements by solvent and PEO W-301 solutions in S2 and R2A.	432
Figure 4.3.54.	Friction factors for solutions of PEO P-309 in S2 and R2A.	433
Figure 4.3.55.	Analysis of riblet- and polymer-induced flow enhancements by solvent and PEO P-309 solutions in S2 and R2A.	434
Figure 4.3.56.	Analysis of riblet- and polymer-induced flow enhancements by solvent and PEO P-309 solutions in S2 and R2AR.	435
Figure 4.3.57.	Variation of h^+ , at the cross-over from riblet drag reduction to drag enhancement, with polymer-induced flow enhancement, S_s' .	436
Figure 4.3.58.	Variation of maximum riblet drag reduction, R'_{max} , with polymer-induced flow enhancement, S_s' .	437
Figure 4.3.59.	Variation of h^+ at the maximum riblet drag reduction with polymer-induced flow enhancement, S_s' .	438
Figure 4.4.1.	Variations of the smooth to riblet pipe pressure gradient ratios versus flowrate at maximum drag reduction.	439
Figure 4.4.2.	Prandtl-Karman friction factors at maximum drag reduction in the 10.21 mm id smooth pipe.	440
Figure 4.4.3.	Friction factors at maximum drag reduction in the 7.82 mm id smooth pipe.	441
Figure 4.4.4.	Friction factors at maximum drag reduction in the 7.82 mm pipe lined with 0.11 mm riblets.	442
Figure 4.4.5.	Friction factors at maximum drag reduction in the 7.82 mm pipe lined with 0.15 mm riblets.	443
Figure 4.4.6.	Friction factors at maximum drag reduction in the 10.21 mm pipe lined with 0.11 mm riblets.	444
Figure 4.4.7.	Friction factors at maximum drag reduction in 10.21 mm pipe lined with 0.15 mm riblets.	445

Figure 4.4.8.	Analysis of riblet- and polymer-induced flow enhancements by solvent and at maximum drag reduction in S1 and R1A.	446
Figure 4.4.9.	Analysis of riblet- and polymer-induced flow enhancements by solvent and at maximum drag reduction in S1 and R1B.	447
Figure 4.4.10.	Analysis of riblet- and polymer-induced flow enhancements by solvent and at maximum drag reduction in S2 and R2A.	448
Figure 4.4.11.	Analysis of riblet- and polymer-induced flow enhancements by solvent and at maximum drag reduction in S2 and R2B.	449
Figure 4.6.1.	Definitions of visual and regressed onset wall shear stress in smooth pipes.	450
Figure 4.6.2.	Regressed onset wall shear stresses in the 10.21 mm id smooth pipe.	451
Figure 4.6.3.	Regressed onset wall shear stresses in the 7.82 mm id smooth pipe.	452
Figure 4.6.4.	Variation of the onset $Re\sqrt{f}^*$ in the riblet pipes with $Re\sqrt{f}^*$ in the corresponding smooth pipes.	453
Figure 4.6.5.	Slope increments in the 7.82 mm id smooth pipe.	454
Figure 4.6.6.	Slope increments in the 10.21 mm id smooth pipe.	455
Figure 4.6.7.	Variation of the slope of the first polymeric segment in a riblet pipe with the slope of the linear polymeric segment in the corresponding smooth pipe.	456
Figure 5.1.1.	Onset correlations for PEO and PAM solutions in the smooth 7.82 mm and 10.21 mm pipes	496
Figure 5.1.2.	Specific slope increment correlations for PEO and PAM solutions in the smooth 7.82 mm and 10.21 mm pipes	497
Figure 5.1.3.	Variation of the apparent degradation rate with wall shear stress	498
Figure 5.2.1.	Experimental and computational laminar flow in riblet channels	499
Figure 5.2.2.	Comparison of riblet-induced flow enhancement between current work and previous work for riblets with $h \approx s$	500
Figure 5.2.3.	Serrated-sublayer model.	501
Figure 5.2.4.	Variation of normalized equivalent hydraulic diameter, $\xi = d_{h\alpha}/d_{h0}$, with h^+ .	502
Figure 5.2.5.	The inherent riblet induced flow enhancement in Newtonian pipe flows.	503

Figure 5.2.6.	Comparison between physical and inherent riblet-induced flow enhancements.	504
Figure 5.2.7.	The inherent riblet induced fractional flow enhancement for Newtonian pipe flows.	505
Figure 5.2.8.	Comparison between riblet and rough pipes for Newtonian flows	506
Figure 5.2.9.	Comparison between predictive models for inherent riblet-induced flow enhancement	507
Figure 5.3.1.	Comparison of polymer-induced fractional flow enhancements for PEO N-60K in all pipes	508
Figure 5.3.2.	Comparison of polymer-induced fractional flow enhancements for PEO N-750 in all pipes	509
Figure 5.3.3.	Comparison of polymer-induced fractional flow enhancements for PEO W-301 in all pipes	510
Figure 5.3.4.	Analysis of polymer-induced fractional flow enhancements (Anderson et al., 1993 and Christodoulou et al., 1991)	511
Figure 5.3.5.	The riblet induced flow enhancement for flows in riblet pipes at maximum drag reduction	512
Figure 5.3.6.	The inherent riblet induced flow enhancement flows in riblet pipes at maximum drag reduction	513
Figure 5.3.7.	Comparison between riblet and rough pipes for Newtonian and maximum drag reducing flows	514
Figure 5.3.8.	The riblet-induced flow enhancement for the flows of PEO W-301 in R2B based on upstream and downstream smooth pipe results	515
Figure 5.3.9.	The riblet-induced flow enhancement for the flows of PEO W-301 in R1A based on upstream and downstream smooth pipe results	516
Figure 5.3.10.	The degradation model riblet-induced flow enhancement for the flows of PEO W-301 in R2B; bounded by upstream and downstream smooth pipe results	517
Figure 5.3.11.	The degradation model riblet-induced flow enhancement for the flows of PEO W-301 in R1A; bounded by upstream and downstream smooth pipe results	518
Figure 5.3.12.	Analysis of riblet- and polymer-induced flow enhancements by solvent and PEO N-60K solutions in S1 and R1AR. (—— uncorrected data, ----- corrected data)	519

Figure 5.3.13.	Analysis of riblet- and polymer-induced flow enhancements by solvent and PEO N-60K solutions in S2 and R2B. (—— uncorrected data, --- corrected data)	520
Figure 5.3.14.	Analysis of riblet- and polymer-induced flow enhancements by solvent and PEO W-301 solutions in S1 and R1AR. (—— uncorrected data, ----- corrected data)	521
Figure 5.3.15.	Analysis of riblet- and polymer-induced flow enhancements by solvent and PEO W-301 solutions in S2 and R2B. (—— uncorrected data, --- corrected data)	522
Figure 5.4.1.	Example of additive equivalence at an isoslip point in the 7.82 mm pipe system	523
Figure 5.4.2.	Example of additive equivalence at an isoslip point in the 10.21 mm pipe system	524
Figure 5.4.3.	3-D contour representation of the relation between riblet- and polymer-induced drag reduction in turbulent flow of all polymer solutions in R1A	525
Figure 5.4.4.	3-D contour representation of the relation between riblet- and polymer-induced drag reduction in turbulent flow of all polymer solutions in R1B	526
Figure 5.4.5.	3-D contour representation of the relation between riblet- and polymer-induced drag reduction in turbulent flow of all polymer solutions in R2A	527
Figure 5.4.6.	3-D contour representation of the relation between riblet- and polymer-induced drag reduction in turbulent flow of all polymer solutions in R2B	528
Figure 5.4.7.	Analysis of literature in relation to 3-D contour representation of the polymer- and riblet-induced flow enhancement in pipe R2B	529
Figure 5.4.8.	3-D contour representation of the riblet-induced flow enhancement, R' , using normalized polymer-induced flow enhancement.	530
Figure 5.4.9.	3-D contour representation of the average riblet-induced flow enhancement, R' , on normalized coordinates for ALL riblet pipes	531
Figure 5.4.10.	3-D contour representation of the average riblet-induced flow enhancement, R' , on Prandtl-Karman coordinates	532
Figure 5.4.11.	3-D contour representation of the riblet-induced percentage drag reduction, %DR, on f - Re coordinates	533

Chapter 1

Introduction

This chapter sets forth the motivation behind and the objectives of this thesis. In particular, the literature for drag reduction by polymer solutions and by riblets is detailed, followed by a review of the pertinent studies of polymer drag reduction over wall modified surfaces, and ending with a recapitulation of relevant macromolecular characterization.

1.1 Motivation and Objectives

Turbulent drag reduction remains a topic of turbulence research, on account of the economic benefits to be derived from the reduction of frictional resistance, and also for the insights it provides into the nature of turbulence. Drag reduction can be achieved either by additives, which alter fluid composition and thence its flow, or by passive devices which directly affect the flow, without altering the fluid. Details and applications of these devices may be sought out in Bushnell and Hefner (1990).

The primary aim of this thesis is to investigate the interaction between two established drag reducing devices, namely, dilute polymer solutions and small streamwise-aligned grooves called riblets. It is hoped that this study would yield insight into the behavior of each device separately and, even more ambitious, into the features of turbulence that are affected to produce drag reduction.

Chapter 2 reviews the pertinent drag reduction literature; Chapters 3 and 4 respectively detail the experimental equipment and procedures necessary to carry out the thesis objectives. Chapter 5 presents the experimental results and in Chapter 6, these results

are analyzed, correlated, compared with the literature, and, wherever possible, physically interpreted.

1.2 Turbulent Flow Drag Reduction: Literature Review

1.2.1 Gross Flow

1.2.1.1 Definitions

Skin friction in internal and external flows is characterized by surface stresses (τ_w) at a corresponding average flow velocity (U_{av}). In dimensionless form, these parameters are represented by a skin-friction coefficient (f) and a Reynolds number (Re) defined, in the most general terms, by:

$$f = \frac{2\bar{\tau}_w}{\rho U_{av}^2} \quad \text{and} \quad Re_l = \frac{U_{av} l}{\nu} \quad (1.2-1)$$

where l is a characteristic geometric length. For example, in external flows over a flat plate, l is typically the length of the plate, L , and for internal pipe flows it corresponds to the diameter, d , of the pipe. In turbulent channel and pipe flows, it is often convenient to represent these quantities in terms of turbulent scales, such as the friction velocity, $u_\tau = (\tau_w/\rho)^{1/2}$, which is the basis for the Prandtl-Karman (PK) coordinate system:

$$\frac{1}{\sqrt{f}} = \frac{U_{av}}{\sqrt{2} u_\tau} \quad \text{and} \quad Re\sqrt{f} = \frac{\sqrt{2} du_\tau}{\nu} \quad (1.2-2)$$

Physically, the abscissa, $Re\sqrt{f}$, a turbulence Reynolds number, is a ratio of the largest to smallest turbulent eddy sizes; while the ordinate, $1/\sqrt{f}$, is a ratio of the bulk to turbulent velocities.

Based on the preceding, drag reduction may be quantified either as a fractional (or percentage) change in the skin-friction coefficient at a given Reynolds number:

$$DR = \left(1 - \frac{f}{f_0}\right)_{Re} \quad (1.2-3a)$$

$$\%DR = 100 \left(1 - \frac{f}{f_0}\right)_{Re} \quad (1.2-3b)$$

or as a flow enhancement parameter or 'slip', S' , at a given $Re\sqrt{f}$:

$$S' = \left(\frac{1}{\sqrt{f}} - \frac{1}{\sqrt{f_0}}\right)_{Re\sqrt{f}} \quad (1.2-4)$$

Eq. (1.2-3) is often used in the literature, particularly for passive drag reducing devices such as riblets, but Eq. (1.2-4) has the advantage that it is directly proportional to shifts in the velocity profile. Because $\%DR$ and S' are measured with different variables held constant, they may be coupled only if the reference friction factor, f_0 , is known for all Re or $Re\sqrt{f}$.

1.2.1.2 Dilute Polymer Solutions

Early work by Toms (1948) and Mysels (1949) revealed the profound effect additives have on turbulent Newtonian flow. Toms, while investigating the mechanical degradation of polymethylmethacrylate in monochlorobenzene, noted that the polymer offered reduced resistance to flow at a given pressure drop relative to the solvent alone. Mysels evaluated the enhanced flow of gasoline thickened with an aluminum di-soap (Napalm) during World War II and noted a reduction in turbulent drag in this solution. The gross flow of dilute polymer solutions has been subsequently well documented in several reviews (Lumley, 1969; Virk, 1975a; White and Hemmings, 1976; Berman, 1978; Sellin et al., 1982; Virk, 1985; Giesekus & Hibberd, 1989).

Virk (1975a) defined the flow of dilute solutions of random coiling molecules and collapsed electrolytes (Type A) as being asymptotically bounded by theoretical laws and empirical relationships:

- (i) **Laminar Flow (abbr. L):** For $Re < 2000$, the flow of dilute polymer solutions obey Poiseuille's Law:

$$1/\sqrt{f} = Re\sqrt{f} / 16 \quad (1.2-5)$$

- (ii) **Newtonian Regime (N):** A regime of no drag reduction, the friction factors for polymer solutions are identical to those for solvent flow, which, for hydraulically smooth pipes, is:

$$1/\sqrt{f} = 4.0 \log_{10}(Re\sqrt{f}) - 0.4 \quad (1.2-6)$$

- (iii) **Polymeric Regime (P):** The onset of drag reduction occurs at a characteristic wall shear stress, τ_w^* , that depends on the molecular weight of the polymer but is essentially independent of concentration. After onset, the extent of drag reduction increases as the flow rate, polymer molecular weight and solution concentration increases:

$$1/\sqrt{f} = 4.0 \log_{10}(Re\sqrt{f}) - 0.4 + \delta \log_{10}(Re\sqrt{f}/P.e\sqrt{f}^*) \quad (1.2-7)$$

where $\delta \log_{10}(Re\sqrt{f}/Re\sqrt{f}^*)$ is equal to the slip, $S' = \left(\frac{1}{\sqrt{f}_p} - \frac{1}{\sqrt{f}_n} \right)_{Re\sqrt{f}}$. The term, δ , is a slope increment and * refers to the condition at the onset of drag reduction. The subscripts p and n refer to polymer solution and Newtonian solvent, respectively.

- (iv) **Maximum Drag Reduction (M):** There is an apparent upper limit to drag reduction. This polymer independent asymptote is correlated by:

$$1/\sqrt{f} = 19 \log_{10}(Re\sqrt{f}) - 32.4 \quad (1.2-8)$$

Figure 1.2.1 shows the experimental results used by Virk (1975a) in formulating the above description. Figure 1.2.1a depicts some aspects of the polymeric regime, namely: (i) that $Re\sqrt{f}$ at onset increases as the polymer molecular weight decreases, and (ii) as the molecular weight decreases, higher concentrations are required to achieve the same slope increments. Figure 1.2.1b depicts typical gross flow trajectories that exhibit maximum drag reduction. For example, the flow of 450 wppm PEO solution, $M_w = 6.1 \times 10^6$, in a 32.1 mm i.d. pipe exhibits three segments in turbulent flow, namely: (i) Newtonian, $250 < Re\sqrt{f} < 380$, wherein the data obey the Prandtl-Karman law (Eq. 1.2-6); (ii) Polymeric, $380 < Re\sqrt{f} < 900$; a well defined onset of drag reduction occurs at $Re\sqrt{f}^* \approx 380$, beyond which the polymer solution data diverge upwards from solvent. The segment is approximately linear from onset to $Re\sqrt{f} = 900$, with slope exceeding that of the solvent line (Eq. 1.2-6) by an amount $\delta \approx 37$; (iii) Maximum Drag Reduction, $Re\sqrt{f} > 900$, wherein the data obey Eq. (1.2-8). Figure 1.2.1c depicts the data of several investigators that approximately follow the maximum drag reduction asymptote. The asymptote is independent of polymer type, molecular weight, concentration and pipe diameter.

Onset. Virk (1975a) inferred that the onset of drag reduction results from a change in the conformational state of the polymer molecules in solution, namely from a collapsed to an extended state. It is not known if, during drag reduction, the polymer molecules are partially or fully extended. The extension of a polymer molecule in a turbulent flow field must result from the interaction between some characteristic scale of the flow and the polymer molecule, so as to overcome the resistance inherent in altering the equilibrium collapsed state of the polymer molecule. Walsh (1967) examined onset quantitatively by an energy balance between turbulent fluctuations and the stored internal energy of a polymer molecule. The stored energy of a polymer molecule is proportional to $M\eta\eta_s/RT$, assuming polymer molecules behave as Hookean springs. The total stored energy per unit volume is thus the product of the stored energy per molecule and the number of molecules per unit

volume, $c|\eta|$. The turbulent kinetic energy per unit volume is scaled by τ_w . Equating the energies:

$$\frac{\tau_w^* |\eta|^2 M c}{RT} = C_E \quad (1.2-9)$$

This model, however, predicts a strong concentration dependence for onset not noted experimentally in the literature. Virk and Merrill (1969) proposed a scale of interaction based upon length. The characteristic macromolecular length scale was chosen to be the radius of gyration, R_g , while the turbulence length scales as $\sqrt{\tau_w}$. The ratio of the macromolecular to turbulence length scales are assumed to be constant such that:

$$R_G^2 \tau_w^* = C_L \quad (1.2-10a)$$

or
$$R_G W^* = \Omega_L \quad (1.2-10b)$$

where W^* is an onset wavenumber, u_τ^*/v_s . Fabula et al. (1966) and Lumley (1969) noted that the microscale of turbulence at onset is several orders of magnitude larger than R_g . They suggested a relation between the shear rate of the flow, τ_w/η , and the relaxation time of a polymer molecule, $0.42M|\eta|\eta_s/RT$, described by the theory of Rouse (1953) and Zimm (1956). Moreover, the ratio of the time scales should be ~ 1 , hence:

$$\frac{\tau_w^* |\eta|\eta_s M}{\eta RT} = \hat{C}_T \quad (1.2-11)$$

where $\hat{C}_T \approx 2.4$ based on theory. The relaxation time is linked to the product of the polymer molecular weight, M , and the solution intrinsic viscosity, $|\eta|$, which is the classical volume per unit macromolecule, and thus directly proportional to R_g^3 . Consequently, this hypothesis predicts:

$$\tau_w^* R_g^3 = \Omega_T \quad (1.2-12)$$

Experimental evidence on the variation of τ_w with R_g (Virk, 1975a) for solutions of polyethylene oxide in water, polyacrylamide in water, partially hydrolyzed polyacrylamide in 0.1m NaCl and polyisobutylene in various solvents do not provide conclusive proof of either a length or time scale hypothesis.

Slope Increment (δ): After the onset of drag reduction, the variation of $1/\sqrt{f}$ with $Re\sqrt{f}$ is approximately linear in Prandtl-Karman coordinates up to the MDR asymptote. The difference between the slope of this line and the slope of the Newtonian regime is defined as the slope increment, δ . The value of δ is approximately proportional to the square root of the solution concentration, c , and the molecular weight, M . This led to the definition of an intrinsic slope increment, Π , that is uniquely linked to the number of backbone chain links, $N = M/m_0$:

$$\Pi = \frac{\delta}{(cM)^{1/2}} \quad (1.2-13)$$

and:

$$\Pi = \kappa N^{3/2} \quad (1.2-14)$$

The quantity κ is defined as a slope modulus and has values from 70×10^{-6} for carbon-carbon backbones to 1500×10^{-6} for cellulosic backbones.

Virk (1975b) defined a second type of drag reduction (type B) related to the behavior of extended polyelectrolytes, for which $1/\sqrt{f}$ follow a trajectory that is nearly parallel to the Prandtl-Karman law (Virk and Wagger, 1989 - Figure 1.2.2). The flow of extended macromolecules does not exhibit an onset as in type A drag reduction but, instead, a typical gross flow trajectory commences on MDR then deviates into the polymeric regime after a "retro-onset". Type B drag reduction is also exhibited by fibers of asbestos (Sharma et al., 1978) and nylon (Vaseleski and Metzner, 1974) though much larger concentrations are required than polymer solutions to effect the same drag reduction.

Kane (1990) summarized that flexibility and low aspect ratios are necessary to produce significant drag reduction in dilute fiber suspensions.

1.2.1.3 Riblets

Riblets are small, longitudinally, grooved surfaces that alter the turbulence structure near the wall resulting in a small but significant drag reduction (4-9%) over a range of non-dimensional riblet height, typically $h^+ < 22$. The historical development of riblets stems from several independent fluid dynamic observations. In a German patent, Kramer (1937) described the use of suspended streamwise wires to shield the near wall region from the outer layer. The patent was conceptual and no data were presented to support Kramer's claim. Kennedy et al. (1973) noted that the shear stress is significantly reduced for turbulent flows in the corners of rectangular ducts. Working at the Iowa Institute of Hydraulic Research, they found that small longitudinal fins produced a reduction in the average shear stress, of order 22%, for $h^+ < 20$. Drag reduction by streamwise grooves is also thought to occur in fast swimming sharks. Shark scales or dermal denticles have three dimensional ridges that are aligned with the flow. Reif (1978) estimated that the ridges reduced the drag on fast-swimming sharks by stabilizing the boundary layer. The characteristics of some typical fast swimming sharks are summarized in Table 1.2.1. At top speeds, the nondimensional primary groove height is typically less than 20 wall units, where it is believed the scales offer reduced drag. Laboratory attempts to produce drag reduction by a shark skin have not met with much success (Bechert et al., 1985).

The development of the commercial riblets stemmed from the work on external boundary layers conducted at NASA, Langley by M.J. Walsh and his co-workers (Walsh, 1979, 1982, 1983, 1990a, 1990b; Walsh and Weinstein, 1979; Walsh and Lindemann, 1984). The parameters which determine the extent of drag reduction are the riblet height; width; spacing and geometry. The optimization of these parameters has led to the commercial manufacture of symmetric V-groove riblets by 3M Co. of nominal heights

0.0013, 0.003, 0.0045 and 0.006 in. Gross flow results have been presented in the literature either in terms of DR or 1-DR ($= f_r/f_s$) and a non-dimensional riblet height (or spacing), $h^+ = \frac{h}{d} \frac{Re\sqrt{f}}{\sqrt{2}}$. In order to bring riblet drag reduction data in line with polymer solutions, an incremental flow enhancement parameter, R' , is defined that is analogous to S' in polymer solution flow:

$$R' = \left(\frac{1}{\sqrt{f_r}} - \frac{1}{\sqrt{f_s}} \right)_{Re\sqrt{f}} \quad (1.2-15)$$

Unfortunately, some literature results do not include the values of f_s for the reference smooth surface. Where necessary, smooth surface friction factors are determined from the correlations for a turbulent boundary layer over a flat plate (Schlichting, 1979):

$$f = \frac{0.455}{(\log Re)^{2.58}} \quad (1.2-16)$$

or in equivalent Prandtl-Karman coordinates:

$$\frac{1}{\sqrt{f}} = 3.7 \log (Re\sqrt{f}) - 2.1 \quad (1.2-17)$$

Table 1.2.2 summarizes the external flow studies conducted on various riblet geometries, the results of which are presented in Figures 1.2.3-1.2.8 in both (1-DR) - h^+ and R' - h^+ coordinates.

Figures 1.2.3 and 1.2.4 depict the drag characteristics for symmetric V-groove riblets with equal height and spacing in subsonic and transonic (Mach nos. = 0.3-0.83) flows respectively. For $h^+ < 25$, the friction factors on the riblet surface are lower than those on the smooth surface, with a maximum drag reduction ~4-10% ($R' = 0.2-0.7$) at $h^+ \approx 12-15$. For $h^+ > 25$, the riblets are drag enhancing with respect to the smooth surface, with a maximum enhancement ~15% at $h^+ \approx 45$. Figures 1.2.5 and 1.2.6 are, respectively, the drag characteristics for symmetric V-groove riblets with $h/s > 1$ and $h/s < 1$. When plotted against h^+ , the results for $h/s > 1$ exhibit an analogous behavior to the $h/s = 1$ data,

with a maximum drag reduction $\sim 3\%$ at $h^+ \approx 16$. For $h/s < 1$, as h/s decreases, the region of drag reduction decreases in bandwidth from $h^+ < 20$ for $h/s = 0.78$ to $h^+ < 9$ for $h/s = 0.22$. A similar trend is observed in the results of U-groove riblets, depicted in Figure 1.2.7 where the drag reduction region decreases from $h^+ < 22$ for $h/s = 0.79$ to $h^+ < 12$ for $h/s = 0.33$. It also appears that the maximum drag reduction also decreases as h/s decreases, though it is not possible to make any definitive statement because of the scatter in the data. It appears that maximum benefit is obtained by riblets for which $h/s \approx 1$.

Drag characteristics over rectangular riblets have been investigated by Wilkinson and Lazos (1987) and Enyutin et al. (1987), depicted in Figure 1.2.8. The maximum drag reduction decreases from $\sim 10\%$ at $h^+ \approx 10$ for $h/s \approx 1$ riblets to $\sim 3\%$ at $h^+ \approx 10$ for $h/s \approx 0.1$ riblets. The crossover from drag reduction to drag enhancement occurs between $h^+ \approx 10$ for $h/s = 0.07$ and $h^+ \approx 22$ for $h/s = 0.83$, which is qualitatively similar to the observations for V- and U-groove riblets.

Other riblet geometries have been tested, including convex semicircular; embedded V-groove; axysymmetric V-groove (Walsh, 1982) and three dimensional scalloped riblets (Bechert, 1987), depicted schematically in Table 1.2.2.

Flows of air and water in pipes lined with riblets (henceforth referred to as riblet pipes) have been investigated by Nitschke (1983); Liu et al. (1989); Nakao (1990) and by the research group at the Naval Oceans Systems Center in San Diego (Reidy and Anderson, 1988; Rohr et al., 1990; Anderson et al., 1993). The geometries used in internal flow investigations are summarized in Table 1.2.3. Because riblets alter the cross section of the pipe, the definition of a pipe diameter is of fundamental importance to any internal flow study. In the literature, the diameter of a riblet pipe was unanimously taken as the value for an equivalently smooth pipe, d_c , with the same cross-sectional area, A_c :

$$d_c = \sqrt{\frac{4A_c}{\pi}} \quad (1.2-18)$$

For symmetric, V-groove riblets, Eq. (1.2-18) gives an apparent origin which is midway between the riblet peak and valley. With the exception of Reidy and Anderson (1988), flows inside riblet pipes show the same qualitative behavior as flows over external riblets, as depicted in Figures 1.2.9 and 1.2.10.

In summary, the friction characteristics observed in internal and external flows over riblets may be decomposed, at this stage, into two regimes:

(i) **Riblet Drag Reduction:** $h^+ < h_c^+$, where h_c^+ is the zero cross-over into regime (ii).

Figure 1.2.11 depicts the variation of maximum drag reduction, R'_{\max} , with h/s for V-groove, U-groove and rectangular riblets. Amid the scatter, it may be inferred that R'_{\max} increases from ≈ 0.1 for $h/s \approx 0.2$ to ≈ 0.5 at $h/s \approx 1$ then decreases to ≈ 0.2 at $h/s \approx 2$. This supports the general consensus that riblets with $h = s$ are most effective drag reducers; however, it is not clear whether one riblet geometry is superior to another. Figure 1.2.12 depicts the variation of h^+ at R'_{\max} with h/s . Clearly, h^+ at R'_{\max} increases as h/s increases, which may be correlated by $h^+ R'_{\max} \approx (14 \pm 1) (h/s)$ implying that $s^+ R'_{\max} \approx 14 \pm 1$. This seems to suggest that the mechanism of drag reduction appears to be related to the spanwise scale of the riblets.

(ii) **Riblet Drag Enhancement:** $h^+ > h_c^+$. Figure 1.2.13 depicts the variation of h_c^+ with h/s . h_c^+ increases monotonically from ≈ 6 at $h/s \approx 0.2$ to ≈ 22 at $h/s \approx 1$. R' decreases as h^+ increases, with a maximum enhancement $R' \sim -2.2$ at $h^+ \approx 80$.

1.2.2 Mean Velocity Profiles

1.2.2.1 Newtonian Flow over Smooth Surfaces

At the cornerstone of fluid mechanics are the continuity and momentum equations, expressed in the most general form by:

$$\frac{D\rho}{Dt} = -\rho \nabla \cdot \mathbf{v} \quad (1.2-19)$$

$$\rho \frac{D\mathbf{v}}{Dt} = -\nabla p + \nabla \cdot \boldsymbol{\tau} + \rho \mathbf{g} \quad (1.2-20)$$

where D/Dt is the material derivative; ρ is the density, \mathbf{v} is the velocity vector, $\boldsymbol{\tau}$ is the stress tensor; p is the pressure and $\rho \mathbf{g}$ is the gravity force. The former is a statement of conservation of mass and the latter is a momentum balance on the elements of fluid. The velocity field is thus obtained from the solution of Eqs. (1.2-19) and (1.2-20) and by invoking a constitutive equation which relates the stress tensor to the velocity field. For incompressible, Newtonian fluids, Eqs. (1.2-19) and (1.2-20) may be expressed in terms of the velocity field only:

$$\nabla \cdot \mathbf{v} = 0 \quad (1.2-21)$$

$$\frac{D\mathbf{v}}{Dt} = -\frac{\nabla p}{\rho} + \nu \nabla^2 \mathbf{v} + \mathbf{g} \quad (1.2-22)$$

Furthermore, in turbulent flow, the velocity field is mathematically treated as the superposition of stationary time-averaged and fluctuating velocity components:

$$\mathbf{v} = \bar{\mathbf{v}} + \mathbf{v}' \quad (1.2-23)$$

Substituting Eq. (1.2-23) into Eqs. (1.2-21) and (1.2-22) yield, after some manipulating, the turbulent form of the continuity and Navier-Stokes equations:

$$\nabla \cdot \bar{\mathbf{v}} = 0 \quad (1.2-24)$$

$$\frac{D\bar{\mathbf{v}}}{Dt} = -\frac{\nabla \bar{p}}{\rho} + \nu \nabla^2 \bar{\mathbf{v}} + \nabla \cdot (\overline{\mathbf{v}'\mathbf{v}'}) + \mathbf{g} \quad (1.2-25)$$

The term, $\nabla \cdot (\overline{\mathbf{v}'\mathbf{v}'})$, in Eq. (1.2-25) is an additional stress term called the Reynolds stress that is responsible for the increased friction in turbulent flow relative to laminar flow. Two noteworthy points warrant mention; first, if the fluctuating components are independent,

the Reynolds stress averages to zero. Second, the turbulent equations cannot be solved analytically because the three unknowns, v , p and $\overline{v'v'}$ cannot be obtained from two equations, continuity and Navier-Stokes. In 1877, Boussinesq suggested that the Reynolds stress may be written analogous to the viscous stress term:

$$-\overline{v'v'} = \epsilon \nabla v \quad (1.2-26)$$

where ϵ is called an eddy diffusivity which must vary with distance from the wall in order for the fluid to display turbulence characteristics. In turbulent, one-dimensional, Newtonian flows such as in pipes and channels, the mean velocity profiles in the near wall region are normally represented in terms of velocities and distances from the wall scaled by the friction velocity:

$$u^+ = \frac{u}{u_\tau} \quad y^+ = \frac{yu_\tau}{\nu} \quad (1.2-27)$$

In the region very close to the wall, $y^+ < 5$, viscous stresses dominate because the fluctuating components, v' , near the wall must vanish, consequently $\nu \gg \epsilon$ and the solution to Eq. (1.2-25) becomes, for steady, horizontal, one-dimensional flow:

$$u^+ = y^+ \quad (1.2-28)$$

This region is called the viscous sub-layer; earlier works often referred to this regime as a laminar sublayer because of its laminar-like velocity profile.

For $y^+ > 30$, turbulent stresses are much greater than viscous stresses, $\epsilon \gg \nu$. However, Eq. (1.2-25) cannot be integrated unless the functionality of ϵ with y is known. Prandtl (1925) proposed a mixing length, $\ell = \chi y$ (i.e. $\epsilon/\nu = \ell^{+2} |du^+/dy^+|$), which represents the distance over which momentum may be transferred. For one-dimensional flow, the velocity profile thus becomes:

$$u^+ = \frac{1}{\chi} \ln(y^+) + B \quad (1.2-29)$$

where the values of χ typically range from 0.38-0.42 and B from 5-5.5 in the literature.

The most widely used values are those of Nikuradse (1933):

$$u^+ = 2.5 \ln(y^+) + 5.5 \quad (1.2-30)$$

The region between the viscous sublayer and the logarithmic layer is termed the buffer layer where the viscous and turbulent stresses are of the same order, $\epsilon/\nu \approx 1$. There are numerous single and two equation models that attempt to completely define the law of the wall region, including the buffer layer. For example, van Driest (1956) proposed an eddy viscosity model of the form:

$$\frac{\epsilon}{\nu} = (0.4y^+)^2 (1 - e^{-(y^+/26)}) \left| \frac{du^+}{dy^+} \right| \quad (1.2-31)$$

that completely spans the wall region. Thus, the velocity profile for the entire law of the wall region, $y \geq 0$, is thus:

$$u^+ = \int_0^{y^+} \frac{2dy^+}{1 + \{1 + 0.64y^{+2} [1 - \exp(-y^+/26)]^2\}^{1/2}} \quad (1.2-32)$$

which may not be integrated analytically, a shortcoming of increasing the complexity of the mixing length model. Other contributors to the velocity profile pool include Reichardt (1951); Deissler (1954); Rannie (1956) and Spalding (1961); all of which are essentially variations of the central mixing length theme.

The simple assumption on the mixing length, $\ell = \chi y$, does not hold true for the whole pipe diameter or channel width since the gradient at the center-line, $du/dy = u_\tau/\chi y$, is

clearly incorrect. Coles (1956) proposed an empirical correction function based on the similarity between the outer region and wake flow:

$$u^+ = 2.5 \ln(y^+) + 5.5 + 2.5\Phi w\left(\frac{y}{R}\right) \quad (1.2-33)$$

where Φ is a profile parameter that is independent of y . Values of Φ may be inferred from the conditions at $y = R$:

$$u_{\max}^+ = 2.5 \ln(R^+) + 5.5 + 2.5\Phi w(1) \quad (1.2-34)$$

which is in turn related to gross flow correlations. Hinze (1959) proposed an antisymmetrical function:

$$w\left(\frac{y}{R}\right) = 1 + \sin\left(\frac{y}{R} - 0.5\right)\pi \quad (1.2-35)$$

to approximate the wake function, w , for many practical applications. For turbulent pipe flow, $\Phi \approx 0.2$.

Figure 1.2.14 summarizes the mathematical description of the velocity profiles in Newtonian pipe flow. The experimental data are those of Laufer (1954) taken at $Re = 50,000$ and $500,000$ ($R^+ = 1,030$ and $8,950$) for air flow through a 0.247 m pipe. The velocity profile model representations correspond to Eqs. (1.2-28) and (1.2-30) (Prandtl, 1945; Nikuradse, 1933); Eq. (1.2-32) (van Driest, 1956); and Eq. (1.2-33) (Coles, 1956).

1.2.2.2 Dilute Polymer Solutions

Average flow quantities are obtained by integrating over the boundary layer of the flow. Thus, the gross flow behavior associated with drag reduction is a manifestation of upward shifts in the velocity profile. Virk (1971b) proposed a three-zone mean velocity profile during drag reduction which corresponds to: (i) a viscous sub-layer; (ii) an elastic

sublayer where the mixing-length constant is derived from the maximum drag reduction asymptote ($\chi_m = 0.085$); and (iii) an outer Newtonian core with $\chi_n = 0.4$. The resulting zones may be represented quantitatively by:

$$\text{Viscous sublayer (VSL)} \quad u^+ = y^+ \quad y^+ < y_v^+ \quad (1.2-36)$$

$$\text{Elastic sublayer (ESL)} \quad u^+ = 11.7 \ln(y^+) - 17 \quad y_v^+ < y^+ < y_e^+ \quad (1.2-37)$$

$$\text{Newtonian core (N)} \quad u^+ = 1.5 \ln(y^+) + 5 + S^+ \quad y_e^+ < y^+ < R^+ \quad (1.2-38)$$

S^+ is the shift in the log layer and is related to the elastic sublayer thickness, y_e^+ , by:

$$S^+ = 9.2 \ln\left(\frac{y_e^+}{y_v^+}\right) \quad (1.2-39)$$

Virk's three layer profile is shown in Figure 1.2.15. Since PK coordinates result from an integration of the mean velocity profile (i.e. $\int u^+ dy^+ = U_{av}^+ = \sqrt{\frac{2}{f}}$), then changes in the mean velocity profile may be inferred from the apparent slip in PK coordinates:

$$S^+ = \sqrt{2} S' = \sqrt{2} \left(\frac{1}{\sqrt{f_p}} - \frac{1}{\sqrt{f_n}} \right)_{Re\sqrt{f}} \quad (1.2-40)$$

The thickness of the elastic sublayer is also related to the gross flow regimes, N, P and M:

$$\text{Newtonian Regime:} \quad y_e^+ = y_v^+ \quad (1.2-41)$$

$$\text{Polymeric Regime:} \quad y_e^+ = y_v^+ (R^+ / R^{+\bullet})^\psi \quad (1.2-42)$$

$$\text{Maximum Drag Reduction:} \quad y_e^+ = R^+ \quad (1.2-43)$$

This qualitatively infers that as drag reduction increases, the elastic sublayer expands at the expense of the Newtonian core toward the center of the pipe until, at the condition of maximum drag reduction, it pervades the entire cross section.

In his 1975 review, Virk examined the mean velocity profile data of several groups, the results of which supported the three zone model. There has subsequently been a number of studies on the mean velocity profile that roughly support the elastic sublayer proposal. Of these, the results of Mizushima and Usui (1977); Schummer and Thielen (1980); Bartels et al. (1985); Willmarth et al. (1987); and Gampert and Yong (1990) are presented here to serve as a representative cross-section of the literature for homogeneous polymer solution flow since Virk's original review. Table 1.2.4 summarizes the experimental conditions under which the profiles were obtained.

Mizushima and Usui (1977) measured mean velocity profiles of dilute solutions of a single PEO polymer ($M_w = 4.6 \times 10^6$) in a 25.3 mm tube by an LDA. Figure 1.2.16 depicts the mean velocity profiles obtained at $Re \approx 13000$ and 35000 and polymer drag reductions from 0 to ~80% (MDR). The results are qualitatively similar to Virk's three-zone model with increasing upward displacements of the velocity profile as the extent of polymer drag reduction increases. The data follow a more sigmoidal shape even at MDR, which the authors attribute to the existence of the turbulent core at high drag reductions. At MDR, $R^+ \approx 300-500$, for which the inner layer may not be well defined.

In a well conceived experiment, Schummer and Thielen (1980) measured mean velocity profiles in each of the flow regimes, N, P and M at $Re\sqrt{f} \approx 600$ and 950. Results were obtained by an LDA for the flow of 100-1000 wppm PAM ($M_w \approx 5 \times 10^6$) in a 14 mm tube. Figure 1.2.17 depicts the mean velocity profiles, which exhibit similar sigmoidal shapes to those of Mizushima and Usui (1977). They proposed a model for the velocity profile over the entire pipe radius, thereby accounting for the R^+ dependence of the data:

$$u^+ = - \int_0^{y^+} \frac{1}{2\chi^2 y^{+2}} \left[1 - \left(1 + 4\chi^2 y^{+2} \left(1 - \frac{y^+}{R^+} \right) \right)^{1/2} \right] dy^+ \quad (1.2-44)$$

where χ was chosen to be 0.055 in order to match their data at maximum drag reduction.

Bartels et al. (1985) measured the mean velocity profiles for flows of 25-500 wppm PAM solutions (Separan AP30) in a 16.4 mm tube at $Re = 20000$, results of which are depicted in Figure 1.2.18. Flows of 25, 100 and 200 wppm solutions were in the polymeric regime whereas 300 and 500 wppm solutions exhibited maximum drag reduction. The profiles are consistent with the observations discussed earlier.

Figure 1.2.19 depicts the mean velocity profiles of Willmarth et al. (1987) and Gampert and Yong (1990); both used laser Doppler anemometry to investigate the influence of polymer additives on the mean turbulent velocity profiles in rectangular channel flow. Willmarth et al. (1987) used 10 wppm of a single polyethyleneoxide polymer of molecular weight 2.6×10^6 in a rectangular channel (254 x 2.54 x 30.48 cm). The polymer solution was delivered by injecting 100 wppm polymer at four points in a settling chamber; the homogenous concentration of 10 wppm was determined assuming complete mixing. In this configuration the observed drag reduction was 38.5% ($S' \approx 3.5$). Their results show a viscous sublayer for $y^+ < 5$ and a Newtonian core for $y^+ > 50$. In the buffer region, the data are shifted to the right of the expected ultimate profile. It is not clear whether this is a feature of low drag reducing flows or non-uniform mixing of the polymer in the settling chamber. Gampert and Yong (1990) carried out experiments in a recirculating channel (320 x 1.0 x 19.0 cm). Data were presented for high drag reducing flows of 50 and 100 wppm of PAM for which the flow was approximately at MDR. For $y^+ > 10$, the data depart from Eq. (1.2-36) but follow Virk's ultimate profile at maximum drag reduction for $y^+ > 30$.

The term heterogeneous drag reduction has been coined to describe the turbulent flow drag reduction by polymer injections. Though it is now believed that drag reduction by polymer injection occurs due to polymer diffusion into wall region (Gyr, 1993), it nevertheless produces a unique phenomenon in the velocity profile. Figure 1.2.20 depicts the velocity profile obtained for the flow of 0.2% polyacrylamide injected at the centerline of a 50 mm pipe (Bewersdorff, 1984). The Reynolds number was 20000, at which the

observed polymer drag reduction was 36%. The mean velocity profile closely follows the Newtonian up to $y^+ \approx 35$, then diverges in the direction of increasing u^+ to a value of $u^+ \approx 25$ ($S^+ \approx 4.5$) at $y^+ \approx 500$. For $y^+ > 100$, the data follow a path that is approximately parallel to the Newtonian logarithmic law line. One plausible explanation arises if one assumes that the polymer diffuses from the centerline toward the wall. As the polymer diffuses, the flow is still of Newtonian character akin to the Newtonian core region of homogeneous drag reduction. As the wall is approached, the strain field is sufficiently large so as to produce an analogous elastic sublayer effect. This effect diminishes to the Newtonian baseline closer to the wall because the polymer has not diffused into the buffer region.

1.2.2.3 Riblets

Because the azimuthal variation of shear stress transverse to a riblet surface is not constant, determining the friction velocity and a virtual origin is essential in the analysis of experimental data. The virtual origin is defined as the location of an imaginary flat surface, say y_0 from the riblet base, which (i) has the same drag as the riblet surface and (ii) matches the velocity defect profile for smooth (and rough) surfaces between the viscous sublayer and the wake region. Hooshmand et al. (1983) employed a variation to the method of Clauser (1954) for a rough surface. They found that the apparent origin is at the riblet base, $y_0/h = 0$, and the friction velocity at that location is larger than the corresponding smooth plate under drag reducing conditions, which contradicts the measured drag reduction of $\approx 7\%$. They subsequently used a method which extrapolated the linear velocity profile within the viscous sublayer to $u = 0$, yielding $y_0/h = 0.5$. Squire and Savill (1987) and Choi (1989) defined the virtual origin in such a way that the velocity defect profile over a riblet surface should be the same as that for a smooth plate when plotted against the non-dimensional distance, $yu_\tau/\delta U_\infty$, except for the inner region of the turbulent boundary layer. Squire and Savill (1987) found $y_0/h = 0.75$ for symmetric V-groove riblets in transonic

flow and Choi (1989) produced $y_0/h = 0.85$ for rectangular riblets at $h^+ \approx 20$. Bechert et al. (1985, 1986), Djenidi et al. (1989) and Luchini et al. (1991) determined the apparent origin by solving the viscous flow equations in laminar flow over a riblet surface. Bechert et al. (1985, 1986) employed a conformal mapping to transform the solution to zero pressure gradient viscous flow over a flat plate to a riblet surface. The apparent origin approaches an asymptotic value of $y_0/s = 1 - \ln 2/\pi = 0.78$ as $h/s \rightarrow \infty$. Bechert et al. (1985) defined a protrusion height, $h_p (= h - y_0)$, which measures how far the riblet tips *protrude* into the boundary layer. Choi et al. (1993) carried out direct numerical simulations over a V-groove riblet surface at $h^+ = 20$ and 40 in turbulent channel flow with a non-dimensional channel half width, $\delta^+ = 180$. They recognized that any method based on changes in the logarithmic profile would not give accurate representations of the virtual origin because this region is not well defined in their computations. Instead, they matched the location of the maximum intensity of the streamwise velocity fluctuations for smooth and riblet surfaces. This yielded results which are similar to those of Bechert et al. (1985).

The effect of riblets on the mean velocity profile was first investigated by Hooshmand et al. (1983) using a single-sensor hot-wire probe to study the characteristics of the velocity distribution over a flat plate with V-groove riblets ($h = 1.27$ mm, $s = 2.54$ mm). The mean velocity profile was measured at a free stream velocity of 3.74 m/s, which corresponded to $h^+ \approx 9$ and $\%DR \approx 7\%$. They showed that the logarithmic profile is shifted upward relative to the smooth plate profile during riblet drag reduction. Shifts in the logarithmic region are best illustrated by the results of Sawyer and Winter (1987) who measured the mean velocity profile for four configurations of V- and U-groove riblets in the region $5 < h^+ < 50$, within which the riblets exhibited both drag reducing and drag enhancing behavior. Velocity profiles were measured with the apparent origin at the riblet peak. Figure 1.2.21 illustrates three representative mean velocity profiles taken at $h^+ = [12, 22, 40]$ corresponding to, respectively, drag reduction ($R' = 0.42$), no effect ($R' = -0.01$) and drag enhancement ($R' = -1.1$) by V-groove riblets. For $h^+ = [12, 22, 40]$, the shifts in

the velocity profile are respectively $S^+ = [0.9, 0, -1.5]$ units, which differ from the measured R' by a factor $\approx \sqrt{2}$.

Vukoslavcevic et al. (1987, 1992) used a hot-wire sensor, 0.5 mm long and 2.5 μm in diameter, to probe the variation of the mean velocity profile close to a V-groove riblet surface at three locations, namely at the peak, midpoint and valley. Figure 1.2.22 depicts the variation of the mean velocity with distance from the riblet surface for a free stream velocity of 1.23 m/s, at which $h^+ \approx 17.5$. The difference between the mean velocity profiles is negligible beyond $y = 2h$. The shear stress at the peak is of order 10 times greater than the value for the smooth plate but is practically zero in the valley. The variation of wall shear stress along a V-groove riblet surface is illustrated by the direct numerical simulation results of Choi et al. (1993) in Figure 1.2.23. The shear stress is a maximum at the peak but falls steeply to the flat plate value within 0.1h of the riblet peak, then decreases gradually to a value ~ 0 in the riblet valley.

Figure 1.2.24 depicts the spanwise variation of the mean velocity above a riblet surface (Hooshmand et al., 1983). The average velocity varies periodically with the riblet spacing; the amplitude of the variations decrease rapidly with the distance above the riblet surface and are approximately zero for $y^+ > 1.5 h^+$. This conclusion was also derived at by Bechert et al. (1986) and is clearly seen in the results of Vukoslavcevic et al. (1987, 1992) in Figure 1.2.22.

1.2.3 Turbulence Structures

1.2.3.1 Newtonian Flow over Smooth Surfaces

Turbulence intensities and Reynolds stresses. Quantitative measurements of turbulence are treated in terms of averaged quantities with respect to time, space or

ensemble. The average values of the r.m.s. fluctuating velocity components, $v' = [u' \ v' \ w']$, are a measure of the intensity of turbulence. In Newtonian pipe flow, detailed hot wire measurements of fluctuating velocity components were made by Laufer (1954) on air flow in a 0.247 m pipe at $Re = 50,000$ and $500,000$. Figures 1.2.25 and 1.2.26 show, respectively, the variation of the wall normalized turbulent intensities, u'^+ , v'^+ and w'^+ with normalized distance from the wall at $Re = 50,000$ and $500,000$. The axial intensity increases from zero at the wall to a maximum $u'^+ \approx 2.5$ at $y^+ \approx 15$, then decreases to $u'^+ \approx 0.7$ at the centerline of the pipe. The radial and tangential intensity profiles, though qualitatively similar, are lower in magnitude and broader than the axial intensity profile. For example, at $y^+ \approx 50$, $u'^+ \approx 2$, $v'^+ \approx 1.4$ and $w'^+ \approx 0.9$. At the centerline, $u'^+ = v'^+ = w'^+ \approx 0.7$. Figure 1.2.27 depicts the variation of the wall normalized turbulence shear stress, $-\langle uv \rangle^+$, with normalized distance from the wall. The abscissa is dually scaled with u_τ/ν in the wall region ($y^+ < 90$) and with R in the outer region ($y/R > 0.1$). In the near wall region, the data for both $Re = 50,000$ and $500,000$ collapse onto a single line when scaled with y^+ , despite almost 10-fold difference in R^+ . The turbulence shear stress grows rapidly from zero at the wall to a maximum $-\langle uv \rangle^+ \approx 0.9$ at $y^+ \sim 100$. In the outer region ($y/R > 0.1$), The turbulence shear stress decreases linearly with y/R , from $-\langle uv \rangle^+ \approx 0.9$ to zero at the centerline. For $y/R > 0.1$, the viscous contribution to the total shear stress is negligible, so the normalized turbulence shear stress must equal to the total shear stress, where $\tau/\tau_w = 1-y/R$, hence the scaling with R .

Figure 1.2.28 depicts the variation of the u-v correlation coefficient, $C_{uv} = \langle uv \rangle / u'v'$ with normalized distance from the wall, with values computed from the Reynolds stress, axial and radial turbulent intensity data of Laufer (1954). The abscissa is dually scaled similar to that of Figure 1.2.27. The correlation coefficient is approximately constant over much of the pipe cross-section with $C_{uv} = 0.46 \pm 0.04$ for $y/R < 0.6$. For $y/R > 0.6$, C_{uv} , scaled by y/R , decreases to zero at $y = R$.

Coherent Structures. From a mechanistic view point, the origin of turbulence stresses stems from an apparent cyclic series of events which ultimately leads to an ejection process that results in the transfer of momentum. Conceptualization of this process is inferred from hydrogen bubble flow visualization studies of turbulent boundary layers (Kline et. al., 1967; Kim et al., 1971; Clark and Markland 1970; Grass, 1971); particle seeding flow visualization (Corino and Brodsky, 1969), hot-wire anemometry (Willmarth and Lu, 1972) and direct numerical simulations (Brachet, 1991, 1994).

The conceptual model of turbulence begins with the formation of a U-shaped vortex which is oriented in the mean flow direction as depicted in Figure 1.2.29a. The length, l_1 , and the cross-section, l_2 , of the vortex is of the order of the boundary layer and viscous sub-layer thicknesses respectively; Kline et al. (1967) and Clark and Markland (1970) reported that the average spanwise spacing between U-shaped vortices was $z^+ \approx 100$. The top of the vortex, labeled T, lifts away from the wall due to self-induction, that is to say, a slight deformation in the x-z plane induces a velocity component, v , normal to the wall. As the top of the vortex moves into a region of higher velocity, it is stretched into a horseshoe-shaped (Ω -shaped) vortex. The increased curvature in the neighborhood of the peak increases the vorticity, and results in strong increases in the u and v velocity components. The effect on the instantaneous velocity is illustrated by the hot wire anemometer measurements of Muiswinkel (Hinze, 1975, pp.608-609) in Figure 1.2.29b. The deformation of the instantaneous profile produces a thin region of high velocity gradients in the region $5 < y^+ < 30$, called a horizontal shear-layer, a region of inflexional instability that breaks down, appearing as a “burst” in a velocity oscillogram. High turbulence intensity, low momentum fluid is ejected and convected away from the wall while, simultaneously, high momentum fluid is swept in almost parallel to the wall (at 5° to 15°). The ejection of low speed fluid produces a defect in the instantaneous velocity profile, $U - \langle U \rangle < 0$, while the inrush produces $U - \langle U \rangle > 0$, illustrated in the left panel of Figure 1.2.29c (Grass, 1972). Perusal of Figure 1.2.29c reveals that in the region $y = 10$ -15 mm,

$-uv < 0$ for both $u, v > 0$, implying a “negative” contribution to the turbulence stress. Willmarth and Lu (1972) determined that ~ 80% of the total Reynolds stress is due to bursts ($u < 0, v > 0$); ~40% to sweeps ($u > 0, v < 0$), and ~10% to each of the negative productions ($u,v > 0$ and $u,v < 0$).

Figure 1.2.29d illustrates the model and attempts to ascribe a cyclic nature to turbulence. The average time between bursts in turbulent Newtonian flows, T_b , have been inferred from numerous flow visualization studies (Kim et al., 1971; Laufer and Badri Narayanan, 1971; Donohue et al., 1972; Achia and Thompson, 1977, Mizushima and Usui, 1977; Rao et al., 1971; Tiederman et al., 1985). When scaled with the friction velocity, the non-dimensional burst times, in general, vary with the Reynolds number based on the boundary layer thickness or channel half width:

$$T_b^+ = \frac{T_b u_\tau^2}{\nu} = a Re^n \quad (1.2-45)$$

Values of n reported in the literature range from 0, implying T_b^+ is independent of Re , to ≈ 1 , implying a strong Re dependence. Kim et al. (1971) noted that their data, for which $n = 0.63$, scaled with the outer region variables, U and δ , with $T_b U_0 / \delta \approx 5 \pm 2$. They pointed out that the lifting of low speed streaks seems to be triggered by large scale disturbances in the flow, hence T_b should scale with outer-region variables.

1.2.3.2 Dilute Polymer Solutions

Turbulence intensities and Reynolds stresses. Recent laser anemometry measurements for turbulent velocity fluctuations have been made by Mizushima and Usui (1977); Schummer and Thielen (1980); Bartels (1985); Willmarth et al. (1987); and Luchik and Tiederman (1988).

Schummer and Thielen (1980) measured axial and radial fluctuating velocity profiles using an LDA in a recirculating flow system with a 14 mm ID plexiglas test pipe. Polyacrylamide solutions were used to effect drag reduction. Velocity measurements were made in each of the gross flow regimes, N, P and M at $Re\sqrt{f} \approx 600$ and 950, the results of which are depicted in Figure 1.2.30. In the polymeric regime, the axial turbulent intensity grows as the extent of drag reduction increases, with a maximum intensity that ranges from $u^{+} \approx 2.70$ at $y^{+} \approx 15$ in the Newtonian case to $u^{+} \approx 3.70$ at $y^{+} \approx 48$ for the flow of 100 wppm polymer solutions. This observation is consistent with the prevailing literature (Virk, 1975a). Curiously, at MDR, the axial turbulent intensity profile is damped to about the Newtonian level and broadened with a maximum $u^{+} \approx 2.8$ at $y^{+} \approx 60$. Table 1.2.5 summarizes the values and positions of the maximum axial intensities in the regimes investigated. For Newtonian flow, the radial intensity varies gradually for $10 < y^{+} < 400$, with $v' \sim 1$. For polymer solution flows, v' is significantly damped with $v' \sim [0.5, 0.2]$ for $S' = [12.7, 13.7]$.

Prior to Schummer and Thielen's work, Mizushina and Usui (1977) similarly observed the damping of axial turbulent intensities at MDR. Data were obtained by an LDA in a flow system that consisted of a 25.3 mm ID polyester tube. Figure 1.2.31 depicts the results for the flow of 50-500 wppm polyethyleneoxide ($M_w \approx 4.6 \times 10^6$) for which the flow was at MDR. The profile is approximately independent of the polymer concentration and Reynolds numbers and has a peak value of $u^{+} \approx 2.1$ at $y^{+} \approx 60$; a result that is qualitatively similar to that of Schummer and Thielen (1980).

Bartels et al. (1985) investigated the turbulent intensity profiles for the flow of 25-500 wppm of polyacrylamide solutions in 16.4 mm and 44 mm tubes. In the smaller tube, the axial, radial and tangential intensity profiles are depicted in Figures 1.2.32-1.2.34. The axial intensity profile results for solvent flow were presented only for $y^{+} > 60$, with $u^{+} = 1.8$ at $y^{+} = 60$ decreasing as y^{+} increases to $u^{+} = 0.7$ at $y^{+} = R^{+} = 570$. These results are

consistent with the data of Laufer (1954). In the polymeric regime, the axial turbulent intensity increases for 100 to 200 wppm solutions, then decreases for 300 and 500 wppm solutions corresponding to MDR. For example, at $y^+ = 60$, $u'^+ = [1.8, 2.8, 3.1, 2.6, 2.3]$ corresponding to $S' = [0, 6.6, 8.0, 12.6, 13.1]$, respectively. As $y^+ \rightarrow R^+$, the axial intensity profiles all converge to the Newtonian level of $u'^+ = 0.7$. The data for the $c = [300, 500]$ wppm solutions exhibit shallow maxima at $y^+ \approx [60, 75]$ for which $u'^+ \approx [2.7, 2.3]$. Radial intensity profiles were presented for 25, 200 and 300 wppm solutions. The radial intensity profile for solvent flow span $60 < y^+ < 570$, with $v'^+ = 0.85$ at $y^+ = 60$, increasing slightly to a shallow maximum, $v'^+ = 0.92$ at $y^+ \approx 120$ then decreases to $v'^+ = 0.6$ at $y^+ = R^+ = 570$. As drag reduction increases, the radial intensity profile is increasingly damped. For example, at $y^+ = 100$, $v'^+ = [0.90, 0.74, 0.6, 0.53]$ corresponding to $S' = [0, 1.2, 8.0, 12.6]$. Figure 1.2.34 depicts the variation of the tangential intensity for 200 and 300 wppm solutions. The solid line corresponds to the results of Laufer (1954) for $Re = 50000$ since no data were presented for solvent flow. Relative to Laufer (1954), the intensity profiles are increasingly damped as drag reduction increases for all y^+ . At $y^+ = 100$, for example, $w'^+ = [1.3, 0.92, 0.66]$ for $s' = [0, 7.5, 13.6]$. Figures 1.2.35 and 1.2.36 show, respectively, axial and radial intensity profiles in the 44 mm tube. The axial turbulent intensity monotonically increases as drag reduction increases; the maximum intensity increases and its position moves coreward from $u'^+ \approx 3.0$ at $y^+ \approx 22$ for the 40 wppm solution ($S' \approx 2.1$) to $u'^+ \approx 3.6$ at $y^+ \approx 36$ for 160 and 320 wppm solutions ($S' \approx 6.6$). As column 7 of Table 1.2.5 shows, their results for the 44 mm pipe were all obtained for flows in the polymeric regime. As with the smaller tube, the radial intensity profile decreases monotonically with increasing S' .

Figure 1.2.37 is a plot of the maximum axial turbulence intensity, u'^+_{\max} , and its position from the wall, $y^+_{u'^+_{\max}}$, versus the ratio of the turbulent flow enhancement to that at MDR, S'/S'_{MDR} . The plot also includes the single polymer, low drag reduction results of Willmarth et al. (1987); and Luchik and Tiederman (1988) summarized in Table 1.2.5.

Values of u^+_{\max} and $y^+_{u^+_{\max}}$ increase with S' for $S'/S'_{\text{MDR}} < 0.6$. For $0.6 < S'/S'_{\text{MDR}} < 1$, values of $y^+_{u^+_{\max}}$ continue to increase monotonically up to $y^+_{u^+_{\max}} \approx 80 \pm 20$ at $S'/S'_{\text{MDR}} = 1$. The profile of u^+_{\max} apparently exhibits a turning point which eventually leads to values of $u^+_{\max} \approx 2.1$ at MDR. Gampert and Rensch (1993, 1995) proposed that this behavior is associated with molecular overlapping at the high concentrations used to effect maximum drag reduction.

Schummer and Thielen (1980); Bewersdorff (1984) and Luchik and Tiederman (1988) measured Reynolds stress components, $-\langle uv \rangle^+$, in dilute polymer solution flow. Figure 1.2.38 depicts the variation of $-\langle uv \rangle^+$ with distance from the wall normalized with the centerline distance, y/R . As the extent of drag reduction increases, the Reynolds stress profile varies in the following manner: (i) the profile is shallower; (ii) the peak value of $-\langle uv \rangle^+$ decreases; and (iii) the peak $-\langle uv \rangle^+$ is located further from the wall. These observations have prompted an approach to modeling polymer flow by defining a stress deficit, G , which appears in the modified form of the Navier-Stokes equation (Willmarth et al., 1987):

$$\frac{-\langle uv \rangle}{u_t^2} = 1 - \frac{y}{R} - \frac{du^+}{dy^+} - G \quad (1.2-46)$$

Alhousseini (1989) and Berman (1990) have attempted to relate G to the properties of polymer solutions with little success except at very low drag reduction.

Figure 1.2.39 depicts the results of Schummer and Thielen (1980) and Luchik and Tiederman (1988) for the ratio of the u - v correlation coefficient of polymer solutions to that of solvent, $(C_{uv})_p/(C_{uv})_n$. These two representative investigations were chosen because turbulent intensity and Reynolds stress profiles were obtained at the same wall shear stress for both polymer solution and solvent flows. For the low drag reduction results of Luchik and Tiederman (1988), $(C_{uv})_p \approx 0.5 (C_{uv})_n$ at $y^+ \approx 20$, then increases approximately to the

Newtonian level for $y^+ > 60$. At maximum drag reduction, the u - v correlation coefficient is significantly lower than the Newtonian value, with $(C_{uv})_p \sim 0.4 (C_{uv})_n$. Because both v'^+ and $-\langle uv \rangle^+$ profiles are significantly lowered at MDR, the error in the $(C_{uv})_p / (C_{uv})_n$ profiles is large, ~ 0.2 , which precludes a more detailed inference of the results in this regime. The reduction in C_{uv} in the wall region for low drag reducing polymer solutions, and over the entire pipe cross section at maximum drag reduction implies that the elastic sublayer is associated with a decoupling of the axial and radial velocity components. It is not known what effect polymer molecules have on the $-\langle uw \rangle$ and $-\langle vw \rangle$ components of the Reynolds stress tensor.

Streak spacing and burst statistics. Donohue et al. (1972); Achia and Thompson (1977); Oldaker and Tiederman (1977); and Tiederman et al. (1985) have employed different methods of flow visualization to ascertain the spacing of low-speed streaks in dilute polymer solution flows. The spanwise streak spacing in the literature show $Z_n^+ \approx 100$ in Newtonian flows (Hinze, 1975). In drag reducing polymer flows, Z_p^+ then becomes a function of the extent of drag reduction, depicted in Figure 1.2.40. Virk (1975a) correlated streak spacing with S^+ for the earlier experimental work and arrived at:

$$\ln \left(\frac{Z_p^+}{Z_n^+} \right) = 0.11 S^+ \quad (1.2-47)$$

The ratio of the polymer to Newtonian streak spacing is roughly equal to the ratio of the elastic to viscous sublayer thickness. The ratio of spanwise to radial scales are consequently preserved in the inner region during drag reduction.

For drag reducing polymer flows, burst times have been reported by Donohue et al. (1972), Achia and Thompson (1977), Mizushima and Usui (1977) and McComb and Rabie (1982). Figure 1.2.41 depicts the variation of the ratio of polymer to Newtonian burst times, at the same friction velocity, with the extent of polymer drag reduction, measured as

S^+ . Amid the scatter, the burst times roughly increase as S^+ . To facilitate comparison between burst times and flow scales, the data are correlated in a manner similar to Eq. (1.2-47), yielding:

$$\ln \left(\frac{T_{b,p}}{T_{b,n}} \right)_{u_*} = (0.045 \pm 0.05) S^+ \quad (1.2-48)$$


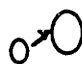



On immediate inspection, it appears as though the streak spacing roughly scales as the square of the burst times. Whether this is true or not requires further testing.

On the mechanism of polymer drag reduction. One of the most widely accepted explanations of drag reduction by additives assumes that polymer molecules produce a non-Newtonian effect in regions of high deformation. Lumley (1969) proposed that the extension of the polymer molecule produces an enhancement of the viscosity which alters the viscous limit of turbulent eddies to lower wavenumbers producing an apparent increase of the viscous sublayer. Landahl (1973) proposed that the anisotropic stress caused by an extended polymer molecule has a stabilizing effect on the inflexional instabilities of the boundary layer. The direct numerical simulations of den Toonder et al. (1995a,b) suggest that the viscous, not elastic, anisotropic stress is responsible for polymer drag reduction.

Based on evidence on polymer drag reduction in rough pipes (Virk, 1971a - § 1.2.4.1), drag reduction appears to originate in the buffer layer in the vicinity of the plane of peak turbulent energy production, $y^+ \approx 15$. At the onset of drag reduction, the macromolecular relaxation time is of the order of the turbulent burst times whereas the polymer radius of gyration is $\sim 10^{-3}$ times the smallest turbulent length scale. The formation of an elastic sublayer results from an attenuation of the eddy viscosity in the vicinity of $\epsilon/\nu \sim 1$ ($y^+ \sim 15$); the region of reduced eddy viscosity then increases both in an outward and inward direction as the drag reduction increases. Attenuation of the eddy viscosity very near the wall, where $\epsilon/\nu = \alpha y^{+3}$, is supported by the mass transfer results of Virk and

Suraiya (1977), in which they found that the concentration required to achieve maximum mass transfer reduction was larger than that required to attain maximum drag reduction. Inward attenuation does not significantly affect momentum transport, but does affect mass transport which occurs closer to the wall as the Schmidt number, Sc , increases. The decrease in the eddy viscosity is equivalent to a decoupling of the axial and radial turbulent flow fields.

The polymer-turbulence interaction responsible for drag reduction was examined by Virk (1975a) in terms of the interaction between additive states and burst events described by an “additive-burst” matrix:

Additive States \ Burst Events	Lift-Up 	Growth 	Breakdown $U \rightarrow u'$ $u' \rightarrow v', w'$
Random-Coil 			
Coiling-Uncoiling 			
Extended 			

The rows of the matrix correspond to the macromolecular states, namely, (i) random-coiled, (ii) coiling-uncoiling, (iii) extended. The columns denote the burst events which are (i) lift up, (ii) growth and (iii) breakdown. Experimental evidence suggests that the interaction between the extended polymer molecule and vortex breakdown, [3,3], is responsible for drag reduction by polymer solutions.

In a recent study, van Dam (1993) suggested that polymers truncate the turbulent cascade in the core, so that the turbulent kinetic energy cannot be transferred to smaller, dissipative scales. In recent computational (She et al., 1990) and experimental (Douady et

al., 1991) studies, it was found that the formation of large scale eddies is related to the breakdown of high-vorticity, filamentary structures which have widths and lengths on the order of the dissipation and largest scales respectively. van Dam (1993) observed that drag reducing polymer solutions inhibit the formation of these high-vorticity filaments, which is accompanied by the reduction in the rate of formation of large eddies. The polymer solution, therefore, affects the equilibrium distribution of all eddies present in the turbulent system, resulting in a strong decrease in the turbulent energy dissipation. Gyr et al. (1995) proposed that polymer additives are concentrated in the regions of high turbulent activity; they found that the concentration of polymer in the core of a vortex in a tube was 10% higher than in the original solution. However it is not known how a small inhomogeneity in distribution of polymer additives may produce significant drag reductions.

1.2.3.3 Riblets

Turbulence intensities and Reynolds stresses. Turbulent intensity profiles over riblet surfaces have been obtained experimentally by Walsh (1979); Hooshmand et al. (1983); Bacher and Smith (1985); Vukoslavcevic et al. (1987, 1992); Pulles (1988); Choi (1989a, 1989b); Suzuki and Kasagi (1994) and computationally by Chu and Karniadakis (1993) and Choi et al. (1993). The experimental conditions are summarized in Table 1.2.6.

Walsh (1979) measured the streamwise and normal turbulent intensities over V-groove riblets ($h = 0.25$ mm, $s = 0.51$ mm) machined on a flat plate in a low speed wind tunnel. Hot-wire probe measurements were made at a free stream velocity of 13 m/s, for which the boundary layer thickness was 9.9 mm and $h^+ \approx 8.5$ at $x = 0.222$ m downstream of the test section. Figure 1.2.42 is a plot of the streamwise and normal intensities, normalized with respect to the free stream velocity, versus the distance from the wall, y/δ .

Both $u'_{\text{rms}}/U_{\infty}$ and $v'_{\text{rms}}/U_{\infty}$ over the riblet surface are decreased by $\approx 3\text{-}5\%$ over much of the boundary layer relative to the smooth plate ($0.2 < y/\delta < 1.2$).

Hooshmand et al. (1983) measured the variation of the streamwise turbulent intensity over V-groove riblets ($h = s/2 = 1.27$ mm) in a wind tunnel at a free stream velocity of 3.74 m/s, for which $h^+ \approx 8.7$. They observed a significant decrease in the maximum intensity of order 10% over the riblet surface, as depicted in Figure 1.2.43. The location of the peak intensity appears unchanged at $y^+ \approx 15$.

Bacher and Smith (1985) investigated the variation of the streamwise intensity against the distance from the wall for V-groove riblets ($h = s = 1.6$ mm) machined on a flat surface. Measurements were taken at a streamwise position 1.15 m downstream of the leading edge of the riblet plate, at a free stream velocity of 0.2 m/s, which corresponded to $h^+ \approx 15$ and a 10% reduction in the momentum thickness compared to the smooth surface. The streamwise turbulent intensity over the riblet surface was found to be greater than that over the smooth one for $8 < y^+ < 100$, as depicted in Figure 1.2.44. This was the only report of an increase in the turbulent intensity over a riblet surface under drag reducing conditions; no explanation was offered by the authors as to the contradiction with previous results.

Pulles (1988) investigated the variation of the streamwise and normal turbulent intensities over triangular riblets on a flat plate in a water tunnel using an LDA. The riblets were roughly triangular in shape with equal height and base width (2.5 mm) spaced 5.0 mm apart (Table 1.2.6). Pulles reported results for the turbulent intensities at two free stream velocities, $U_{\infty} = 95$ and 140 mm/s which, respectively, corresponded to 2% drag reduction at $h^+ \approx 11.7$ and 12% drag enhancement at $h^+ \approx 20.7$. Figures 1.2.45 and 1.2.46 depict the results in the coordinates chosen by Pulles, namely u^+ vs y^+ scaled in both surfaces by the friction velocity of the smooth plate. The data show a lower streamwise turbulent intensity over the riblet surface in both the drag reducing and drag enhancing

cases by $\sim 10\%$. The inferences are not significantly altered if the intensities are normalized with the friction velocity of each surface. There is no significant change in the normal intensity between the smooth and riblet surfaces.

Choi (1989a, 1989b) measured the turbulent intensity profiles over a chamfered rectangular riblet array of height, $h = 1.6\text{mm}$, base thickness, $t = 0.5\text{ mm}$ and spaced, $s = 2.5\text{ mm}$ apart in a wind tunnel. The height of the riblets was 13 wall units at a mean stream velocity of 3 m/s. The axial (u'/U_∞), normal (v'/U_∞), and spanwise (w'/U_∞) turbulence intensities, were all reduced by up to 10% over the riblet surface compared with the smooth surface (Figure 1.2.47). This reduction was only observed in the near wall region, say $y^+ < 70$, with the maximum axial turbulence intensity occurring at $y^+ \approx 18$ over both surfaces.

The direct numerical studies of Chu and Karniadakis (1993) and Choi et al. (1993) showed reductions in all three components of the turbulent intensity over riblet surfaces during drag reduction. For $h^+ = 17$, the maximum turbulent intensities are reduced by $\sim 5\%$ in the streamwise direction and up to 10% in the normal and spanwise components. Choi et al. (1993) reported that in the drag enhancement regime, at $h^+ = 37$, the streamwise component is decreased by as much as 15% in the riblet valley and increased by $\approx 5\%$ above the riblet peak.

Wilkinson and Lazos (1987) investigated the spanwise variation of u' above a single thin element riblet at a free stream velocity of 10.5 m/s corresponding to $h^+ \approx 13$. Noteworthy is the 40% decrease in u' just above the riblet element (Figure 1.2.48). For $y^+ > 2h^+$, the spanwise variation approaches that of a flat plate. Wilkinson and Lazos (1987) attributed this observation to the formation of vortex pairs on either side of the element which tends to accelerate (stabilize) vortex downwash regions and retard (destabilize) up-wash regions in the vicinity of the riblet peak.

Experimental measurements of the Reynolds stress were reported by Walsh (1979), Hooshmand (1985); Pulles (1988); Choi (1989), and Suzuki and Kasagi (1994). Walsh (1979) measured a significant decrease in the Reynolds stresses that extended throughout the boundary layer, with a maximum reduction $\approx 16\%$ (Figure 1.2.49). Hooshmand (1985) measured a reduction in the Reynolds stress away from the wall but an increase for $y/\delta < 0.2$. Wallace and Balint (1987) pointed out that the results for smooth surfaces do not compare well with Hooshmand's results. Pulles (1988) measured a decrease in the Reynolds stress for drag reduction (Figure 1.2.50) and a slight increase for drag enhancement (Figure 1.1.51) in the region $y^+ < 80$, despite the observation that the streamwise fluctuating component is reduced in both cases. Choi (1989) reported a reduction in the Reynolds stress of order 18% over riblet surfaces, nearly twice as much as the reduction he found for the turbulence intensities (Figure 1.2.52). Computational studies of Chu and Karniadakis (1993) and Choi et al. (1993) show that the Reynolds stress is reduced by up to 12% over a riblet surface relative to that above a flat plate. Choi et al. (1993) noted that, for $s^+ = 20$ ($h^+ = 17$), the Reynolds stress above the riblets is significantly increased at the riblet peak but relatively unchanged in the riblet valley compared to the flat plate.

Figure 1.2.53 depicts the ratio of the u-v correlation over the riblet surface to that of the smooth surface, calculated from the u' , v' and $\langle uv \rangle$ data of Walsh (1979), Pulles (1988) and Choi (1989). The data of Pulles indicate u-v correlation coefficient over the riblet surface relative to the smooth surface is reduced by up to 15% in the vicinity of $y^+ \approx 6$, increases to the smooth surface value for $y^+ \sim 25$, then decreases to $(C_{uv})_r \sim 0.85$ $(C_{uv})_s$. The results of Choi for $14 < y^+ < 80$ imply that $(C_{uv})_r$ is essentially constant in this range, which evidently differs from the results of Pulles (1988). The results of Walsh (1979) suggest that $(C_{uv})_r/(C_{uv})_s$ decreases as y^+ increases; which is not consistent with the near wall ($y = 3h$) domain of riblet influence. However, the fractional error in C_{uv} increases as y increases in the outer region because $\langle uv \rangle \rightarrow 0$ as $y \rightarrow \delta$. Many authors

turbulent shear stress, reduced relative to their respective magnitudes over smooth surfaces at the same free stream velocities. Interestingly, despite the general reduction in turbulent intensities, axial to transverse velocity correlations near the riblet surface remain much the same as those near a smooth surface. Suzuki and Kasagi (1994) proposed that in the vicinity of the valley, the redistribution of kinetic energy from streamwise to spanwise components is impeded, suggesting a reduction in streamwise vorticity. Drag enhancement by riblets at high h^+ was attributed by Walsh (1979, 1990) to the adverse effects of the increased riblet wetted surface area overwhelming the riblet-induced drag reduction. Tani (1988) compared the results of Sawyer and Winter (1987) to those of Nikuradse (1933) for sand-roughened pipes. He re-analyzed the data of Nikuradse (1933) using a smaller diameter that accounted for an apparent origin over rough surfaces and found that rough pipes exhibited a regime of uniform drag reduction for $1 < h^+ < 5$. Believing this to be a genuine phenomenon, he concluded that the mechanism of riblet drag reduction and enhancement is similar to that for sand-roughened pipes, though he did not declare what that mechanism might be. Baron et al. (1993) attempted to decouple riblet drag reduction by defining two functions, $F(s^+)$ and $G(h_p^+)$, that, respectively, modeled the drag reduction interaction between riblets and near-wall structures, and drag enhancement due to the increase in the wetted surface area. The drag enhancement function, $G(h_p^+)$, is equal to 1 for the riblets within the viscous sublayer, $h^+ < y_v^+$, and equal to the ratio of the wetted areas of the riblet to smooth surfaces for $h^+ \gg y_v^+$, for which the riblets are completely out of the viscous sub-layer. Interpreting their numerical calculations in terms of coherent structures, Choi et al. (1993) suggested that riblets reduce drag when the streamwise vortices above them are aligned such that only a small portion of the riblet, near the tip, is exposed to their “downwash”; at higher h^+ , the streamwise vortices become smaller relative to the riblets, and their downwash affects a greater fraction of the riblet surface, enhancing drag.

1.2.4 Polymer Drag Reduction over Wall Modified Surfaces

1.2.4.1 Rough Walls

Virk (1971a) investigated the drag reduction caused by dilute solutions of four PEO ($M_w = 0.1-8 \times 10^6$) and one PAM ($M_w = 0.1-8 \times 10^6$) solutions in one smooth and three sand roughened pipes ($R/k \approx 15, 23, 35$); the experimental parameters are summarized in Table 1.2.7. The onset of drag reduction in the rough pipes occurred at the same wall shear stress as in the smooth pipe, independent of the flow regime within which onset occurred, namely, the hydraulically smooth, transitional and fully rough, as depicted in Figure 1.2.54. The onset wall shear stress was inversely proportional to the square of the polymer radius of gyration, which was consistent with earlier observations (Virk and Merrill, 1969). Since onset is independent of the existence of a viscous sublayer, Virk (1971a) inferred that drag reduction must be associated with the buffer layer. Following the onset, the flow in the polymeric regime was characterized by a fractional slip, $S_F = (\sqrt{T_s/T_p} - 1)_{Re_s \sqrt{f}} = S'(1/\sqrt{f_s})$, which measured the fractional increase in the mean velocity relative to the solvent. Figure 1.2.55 depicts the variation of S_F with $Re_s \sqrt{f}$. Despite striking differences between gross flow in smooth and rough pipes, the fractional slip was essentially the same in both pipes below some critical non-dimensional roughness height, $k_{es}^+ \sim 50$. Virk (1971a) defined the regime from the onset k^{+*} to k_{es}^+ as the "effectively smooth regime". For $k^+ > k_{es}^+$, the fractional slip in the rough pipe was less than that in the smooth pipe which depended on the relative roughness as well and the flow and polymeric properties. At MDR, depicted in Prandtl-Karman coordinates by Figure 1.2.56 for the flows of high molecular weight PEO and PAM, the onset of roughness occurred at $k^+ \approx 12$ indicating that the viscous sublayer is thickened to approximately 2.5 times the Newtonian value.

Evidence of the effectively smooth regime is also supported by the observations of Bewersdorff and Petersmann (1987) for the flow of 20 and 50 wppm of a polyacrylamide

polymer (Separan AP-30) through a hydraulically smooth 30.7 mm i.d. pipe and a rough pipe ($R/k = 6.8$). The fractional slip, depicted in Figure 1.2.57, is essentially the same in both pipes for $k^+ < 45$ which is in qualitative agreement with the results of Virk (1971a).

1.2.4.2 Riblet Walls

The combined effects of riblets and polymers have been investigated in external flow by Philips et al. (1987); Beauchamps and Philips (1988) and Choi et al. (1990) and in pipe flow by two research groups: one at the Naval Ocean System Center in San Diego, California (Reidy and Anderson, 1988; Rohr et al., 1990; Anderson et al., 1993) and the other at the University of Minnesota (Christodoulou et al., 1991), summarized in Table 1.2.7.

The first experiments on the combined use of riblets and polymers in external flow were conducted during May, 1986 - September, 1987 by C.H. Beauchamps and R.B. Philips at the Naval Underwater Systems Center at Newport, Rhode Island (Philips et al., 1987 and Beauchamps and Philips, 1988). They carried out two series of experiments on an axysymmetric body, 1.21 m long and 102 mm in diameter lined with 0.033 and 0.076 mm 3M V-groove riblets, projected into a tank containing 125 wppm of polyethylene oxide ($M_w \approx 3 \times 10^6$). The terminal velocity of the model was determined by lasers which tripped a timer when the beams were interrupted. Given the model's terminal velocity and weight, the drag coefficient was directly calculated. The authors then assumed that the contribution of skin friction to the total drag force was 45% which facilitated the determination of the skin friction coefficient. Experiments were carried out for $7 < h^+ < 25$ and polymer drag reductions from 0% to 20%. The effect of the polymer solution compared to the solvent for the smooth projectile is depicted in Figure 1.2.58a. The drag reduction in the polymer solution ocean differed between the 1986 and 1987 experiments even though the concentration and type of polymer used remained the same. An onset is observed in the

1986 data which suggests that the molecular weight of the polymer was lower in the earlier experiments. The effects of the riblet-lined compared to the smooth projectile for both solvent and 125 wppm PEO are depicted, in $R^+ - h^+$ coordinates, by Figure 1.2.58b. The results for the solvent ocean follow the established riblet regimes, namely: (i) for $h^+ < 21$, the riblets are drag reducing with a maximum of $\approx 5\%$ at $h^+ \approx 13$; (ii) for $h^+ > 21$, the riblets are drag enhancing. For the polymer solution, the 1986 data reveal that the riblets are further able to reduce the drag by polymer solutions by as much as 6% at $h^+ \approx 5$. The 1987 data show no significant effect of the riblets on the drag reduction experienced in the polymer solution ocean up to $h^+ \approx 21$.

Reidy and Anderson (1988) published the first experimental results on the combined effects of riblets and polymer solutions in pipe flow. They investigated the effect of 2 wppm of an unspecified polyacrylamide in a 156.2 mm pipe lined with 0.076 mm 3M V-groove riblets. The experiments were conducted for $4 < h^+ < 25$, corresponding to $3 \times 10^5 < Re < 13 \times 10^5$. For solvent flow alone, the maximum drag reduction in the riblet pipe was of the order of 20% at $h^+ \approx 10$ (see Figure 1.2.9). They reported that the flow of 2 wppm polymer through hydraulically smooth 25.4 mm and 156.2 mm pipes produced the same polymeric drag reduction at the same wall shear stress, a result that is characteristic of type B drag reduction. For the flow of 2 wppm polymer solution through the riblet pipe, they found that riblets contributed an additional drag reduction to that of 2 wppm polymer flow in smooth pipes. At low Reynolds numbers, the additional drag reduction was less than the sum of the two techniques alone, but greater than the sum at high Reynolds numbers. Within the same research group, Rohr et al. (1990) studied the flow of 2.5, 10 and 40 wppm polyethylene oxide (Union Carbide Polyox WSR-301) solutions in a 12.7 mm pipe lined with 0.076 mm V-groove riblets (3M co.). These experiments spanned non-dimensional riblet heights from 1 to 4 and polymer induced drag reductions from 0-50%. The riblets produced no observable effect on the polymer solution flows. Recently, Anderson et al. (1993) have reported additional results for the flow of 2, 4 and 8 wppm

WSR-301 and 100 wppm Guar gum solutions in a 25.4 mm pipe lined with 0.15 mm V-groove riblets (3M co.). This work spanned non-dimensional riblet heights $4 < h^+ < 90$, and polymer drag reductions from 0 - 40%. Figure 1.2.59 depicts, in registry, the variation of S'_s , S'_r and R' with h^+ . The middle and lowermost panels represent the effect of the polymer solution relative to solvent in each of the smooth and riblet pipes respectively, while the uppermost panel depicts the effect of the riblets relative to the smooth pipe for a given solution concentration. For solvent flows, the riblet pipe exhibited drag reduction for $4 < h^+ < 22$, the maximum $R' \approx 0.5$ at $h^+ \approx 15$, and drag enhancement for $h^+ > 22$, up to $R' \approx -2.2$ at $h^+ \approx 90$. For polymer solution flows, the onset of drag reduction for PEO solutions occurred at the same wall shear stress, $\tau_w^* \approx 2.8 \text{ N/m}^2$ in both smooth and riblet pipes, corresponding to $h^{*+} \approx 8$ in the riblet pipe. The behavior of the riblet pipe relative to the smooth was substantially the same in the region $h^+ < 22$ as observed in the solvent alone, regardless of the extent of drag reduction induced by the polymer solution. For $h^+ > 22$, the maximum drag enhancement increases from $R' \approx -2.2$ at $h^+ \approx 90$ for solvent to $R' \approx -4.0$ at $h^+ \approx 100$ for 8 wppm PEO.

Christodoulou et al. (1991) investigated the effects of 2-50 wppm of polyethylene oxide (WSR-301) and polyacrylamide solutions in a 25.4 mm pipe lined with 0.11 mm V-groove riblets (3M co.) over the range $4 < h^+ < 22$ and polymeric drag reductions, quoted for 10 wppm PEO, from 0-20%. Figure 1.2.60 depicts the drag reduction in the riblet pipe relative to the smooth one, measured as %DR. With the exception of 20 and 50 wppm PEO solutions, their results show that the drag reduction induced by the riblets relative to the smooth pipe decreased from a maximum $\approx 6\%$ in solvent alone to $\approx 2\%$ in 10 wppm PEO and 10 wppm PAM to 0-1% in 20 and 50 wppm PAM. This apparent decrease in the riblet-related drag reduction with increasing polymer concentration (and presumably drag reduction) evidently differs from the findings of Anderson et al. (1993).

1.3 Properties of Polyethylene oxide and Polyacrylamide Solutions

1.3.1 Dilute Solutions

Up to now, the term "dilute polymer solution" has been used rather loosely in association with turbulent flow drag reduction. "Dilute" refers to concentrations below some critical concentration, $c^{\#}$, at which the polymer chains begin to overlap. $c^{\#}$ is approximately given by $c^{\#} \approx M/N_A R_G^3$, where M is the molecular weight of the molecule, R_G is the root-mean-square radius of gyration of the molecule and N_A is Avogadro's constant.

1.3.2 Intrinsic Viscosity

1.3.2.1 Evaluation

Dilute polymer solutions have viscosities that are greater than the solvent due to the differences in size between the polymer and solvent molecules. In dilute solution viscometry, it is often not necessary to determine the absolute viscosity values, only the values of the solution viscosity relative to the solvent. There are several measures of comparative viscosity terms that are used including relative viscosity ($\eta_{rel} = \eta_p/\eta_n$); specific viscosity ($\eta_{sp} = \eta_{rel} - 1$); reduced viscosity ($\eta_{red} = \eta_{sp}/c$); inherent viscosity ($\eta_{inh} = \ln(\eta_{rel}/c)$) and intrinsic viscosity ($[\eta_{inh}] = (\eta_{red})_{c \rightarrow 0} = (\eta_{inh})_{c \rightarrow 0}$). Use of the intrinsic viscosity simplifies the interpretation of experimental data by eliminating polymer-polymer interactions, allowing theories for single polymer molecules to be related to polymer properties.

Intrinsic viscosities are determined from relative viscosity measurements at finite concentrations. In the most general form, the relation between intrinsic and solution viscosities takes the form of a power series expansion in concentration:

$$\eta_{sp} = [\eta]c + k_1[\eta]^2c^2 + k_2[\eta]^3c^3 + \dots \quad (1.3-1)$$

Huggins (1942) proposed a relation based on the truncation of the series to the second order term:

$$\frac{\eta_{sp}}{c} = [\eta] + k_1[\eta]^2c \quad (1.3-2)$$

where k_1 ranges from 0.3 for "good" solvent-polymer pairs to 0.5 for "poor" pairs. The intrinsic viscosity is obtained experimentally by extrapolating η_{sp}/c vs c curves to $c = 0$. For convenience, methods for the determination of intrinsic viscosity from a single $\eta_{sp} - c$ point are also available, the simplest of which was proposed by Solomon and Citua (1962):

$$[\eta] = \frac{[2(\eta_{sp} - \ln(\eta_{sp}))]^{1/2}}{c} \quad (1.3-3)$$

which is based on $k_1 = 0.33$.

1.3.2.2 Interpretation

The hydrodynamic behavior of polymer molecules in solution is a function of the polymer chemical and skeletal structure. The hydrodynamic effects may be defined by two extremes, namely (i) a free-draining model, wherein the solvent molecules may pass undisturbed through the coil and (ii) non-draining for which the solvent within the coil is trapped and must follow coil deformation and rotation; the external solvent is disturbed and must flow around the coil.

In the free-draining model, each segment of the polymer chain has an equal contribution to the friction coefficient, f , of the polymer molecules hence $f \propto N$, the

number of segments. The intrinsic viscosity may be shown to depend on the ratio R_{G0}^3/M (Kirkwood and Riseman, 1948), where R_{G0} is the root-mean-square radius of gyration of the unperturbed polymer molecule.

A deficiency of the free-draining model is the use of unperturbed dimensions for the polymer molecule. In good solvents, polymer molecules expand beyond their unperturbed dimensions due to volume exclusion effects; the radius of gyration of a polymer molecule in solution is given by:

$$R_G = \alpha R_{G0} \quad (1.3-4)$$

where α is an expansion coefficient. Only when polymer-solvent effects counteract volume exclusion effects does $\alpha = 1$, at which the solution is said to be under θ -conditions. Flory and Fox (1951) modified the ideas of Kirkwood and Riseman (1948) to include Eq. (1.3-4) in an expression for $[\eta]$:

$$[\eta] = K_{\theta} \alpha^3 M^{1/2} \quad (1.3-5)$$

where

$$K_{\theta} = 6^{3/2} \Phi \left[\frac{R_{G0}^2}{M} \right]^{3/2} \quad (1.3-6)$$

and $\Phi = 2.5 \pm 0.5 \times 10^{23}$, a "universal" constant. To account for the use of good solvents instead of θ -solvents, a factor of 0.8 is introduced such that $\Phi' = 0.8 \Phi = 2.0 \times 10^{23}$.

1.3.3. Molecular Weight and Radius of Gyration

At θ conditions, the Flory-Fox equation predicts $[\eta] \propto M^{1/2}$. For departures from θ conditions, experiments suggest that $\log(\alpha^3) \propto \log(M)$, such that:

$$[\eta] = KM^a \quad (1.3-7)$$

Equation (1.3-7) is commonly known as the Mark-Houwink equation. If the polymer in solution is polydisperse, equation (1.3-7) is expressed in terms of a viscosity average molecular weight:

$$[\eta] = K\bar{M}_v^a \quad (1.3-8)$$

where

$$\bar{M}_v^a = \left[\frac{\sum w_i M_i^a}{\sum w_i} \right]^{1/a} \quad (1.3-9)$$

and w_i is the weight of molecules of molecular weight M_i . Generally $0.5 < a < 0.8$ for flexible chains, $0.8 < a < 1.0$ for stiff molecules (e.g. cellulosic backbones) and $1.0 < a < 1.7$ for highly extended molecules. K tends to decrease as a increases. If the molecular weight distribution is assumed to be of the same functional form for different samples, then the relation between $[\eta]$ and the weight average molecular weight, M_w , is of the same form as Eq. (1.3-8):

$$[\eta] = K'M_w^a \quad (1.3-10)$$

Generally, a plot of $\log [\eta]$ against $\log M_w$ is fitted to a straight line from which K and a are determined. This plot is not linear over all molecular weights; curvature for low molecular weights are observed, a consequence of the non-Gaussian character of short flexible chains.

Empirical values of (K, a) have been widely reported in the literature for PEO and PAM solutions. For PEO solutions, the relation between intrinsic viscosity, determined from η - c data extrapolated to $c = 0$, and molecular weight have been investigated by Rempp (1957); Bailey et al. (1958); Bailey and Callard (1959); Rossi and Cuniberti (1964); Shin (1965); Ring et al. (1966); Hammes and Robertis (1968); Nabi (1968) and Crouzet and Marchal (1973). The experimental techniques used, solvent, temperature, molecular weight range and Mark-Houwink parameters are summarized in Table 1.3.1. For aqueous PAM

solutions, the relation between intrinsic viscosity and molecular weight have been investigated by Scholotan (1954); American Cyanamid Co. (1955); Collinson et al. (1957); Kline and Conrad (1978); Munk et al. (1980); Kulicke et al. (1982) and McCormick et al. (1990); details of which are summarized in Table 1.3.2. What is striking about the experimental (K , a) values in both PEO and PAM solutions is the increase in a and corresponding decrease in K as the molecular weights investigated increase. For example, ($K \times 10^5$, a) \approx (8, 0.8) for $M_w > 10^5$ g/mol as compared to ($K \times 10^5$, a) \approx (150, 0.5) for $M_w < 10^3$ for PEO solutions. Figure 1.3.1 depicts the variation of K with a . The data may be correlated by:

$$K = \varphi_1 \exp(\varphi_2 a) \quad (1.3-11)$$

where (φ_1 , φ_2) has values (0.41, -9.9) for PEO and (0.22, -10.4) for PAM solutions.

Dilute polymer solutions are effective drag reducers for molecular weights typically greater than 10^5 g/mol. In the range of present interest, Figures 1.3.2 and 1.3.3 depict the variation of intrinsic viscosity with the weight average molecular weight summarized in Table 1.3.3 and 1.2.4 for aqueous PEO and PAM solutions respectively. Regression of the literature data give, for PEO solutions:

$$[\eta] = (7.87 \pm 1.54) \times 10^{-5} M_w^{(0.804 \pm 0.014)} \quad (1.3-12)$$

and for PAM:

$$[\eta] = (7.27 \pm 2.40) \times 10^{-5} M_w^{(0.780 \pm 0.036)} \quad (1.3-13)$$

where $[\eta]$ is in dl/g. These correlations will subsequently be used to interpret the laminar flow data.

Independent measurements of the radius of gyration from light scattering experiments have been determined by Shin (1965) and Kezirian (1993) for aqueous PEO

solutions and by Kline and Conrad (1979), Muller et al. (1979) and Kulicke et al. (1982) for aqueous PAM solutions. The variation of R_G with M_w is similarly depicted in Figures 1.3.2 and 1.3.3 for PEO and PAM solutions respectively. For PEO solutions:

$$R_G = (1.58 \pm 0.08) \times 10^{-1} M_w^{(0.469 \pm 0.033)} \quad (1.3-14)$$

and for PAM:

$$R_G = (3.11 \pm 2.20) \times 10^{-3} M_w^{(0.707 \pm 0.045)} \quad (1.3-15)$$

where R_G is in nm.

1.3.1 Polydispersity

For a monodisperse polymer solution, independent determination of the molecular weight and the radius of gyration should satisfy Eqs. (1.3-5) and (1.3-6). However, commercial polymer samples are not monodisperse. The classical measure of polydispersity is the "polydispersity index", s , which is the ratio of the weight average to number average molecular weights (M_w/M_n). However, determination of the number and weight average molecular weights requires separate experiments which are seldom available for the range of interest. Virk (1975a) proposed that since R_G , which may be determined simultaneously with M_w in light scattering experiments, is related to the "z-average" molecular weight, then deviations from Eqs. (1.3-5) and (1.3-6) may be used as a measure of polydispersity:

$$H = \frac{29.5 \times 10^{23} R_G^3}{M_w[\eta]} \quad (1.3-16)$$

Values of H are summarized in Column 5 of Tables 1.3.3 and 1.3.4 for PEO and PAM solutions respectively. Commercial PEO solutions exhibit a very wide range of heterogeneity indices ranging from $(H, M_w \times 10^{-6}) = (28.7, 0.3)$ to $(3.2, 8.5)$. Commercial PAM solutions have a much narrower molecular weight distribution with $H = 2.4 \pm 0.8$ being essentially independent of the molecular weight of the polymer.

Table 1.2.1. Some characteristics of fast swimming sharks. Physical sizes are those of Reif (1982)

Shark	L (m)	h [†] (mm)	s [†] (mm)	CRUISING			SPRINTING		
				¹ U (m/s)	Re _L x 10 ⁶	h ⁺	² U (m/s)	Re _L x 10 ⁶	h ⁺
Carcharhinus falciformis (Silky)	2.2	0.020	0.060	0.71	1.55	2	18	39.9	21
Lamna nasus (Porbeagle)	1.3	0.020	0.070	0.56	0.73	1	6.3	8.24	10
Carcharodon carcharias (Great white)	1.9	0.015	0.065	0.66	1.26	1	14	25.7	13
Isurus oxyrinchus (shortfin mako)	1.1	0.015	0.040	0.52	0.58	1	4.5	4.99	6
Carcharhinus galapagensis (Galapagos)	2.5	0.018	0.080	0.75	1.86	1	23	58.6	23
Carcharhinus obscurus (Dusky)	1.2	0.025	0.060	0.54	0.65	2	5.4	6.48	11
Prionace glauca (Blue)	1.5	0.026	0.090	0.60	0.90	2	8.4	12.7	16

¹ $U = 0.503 L^{0.43}$: Weihs (1977)

² $U = 0.6L^2/2T$ where T is the muscle contraction time ≈ 0.08 s for $L \approx 2$ m : Wardle (1975)

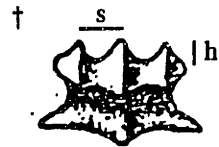
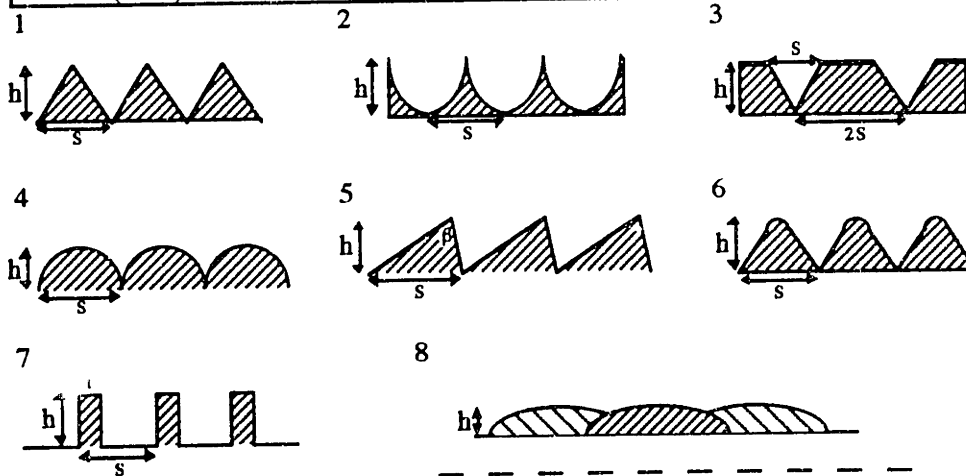


Table 1.2.2. External flow over riblets: Experimental riblet configurations.

SOURCE	RIBLET SHAPE	h (mm)	h/s	h ⁺ RANGE
Walsh et al. (Walsh, 1979,1982, 1983, 1990a, 1990b; Walsh & Weinstein, 1979; Walsh & Lindemann, 1984)	v ¹	0.51	1.00	11-47
	V	0.30	1.00	6-22
	V	0.20	2.00	12-47
	V	0.10	2.00	5-24
	V	0.25	1.92	4-43
	V	0.25	0.49	5-25
	V	0.25	0.22	6-22
	U ²	0.15	0.33	4-17
	U	0.46	0.79	11-46
	embed. V ³	0.25	0.49	5-25
	semicir. ⁴	0.25	0.50	5-25
	assym. V ^{5†}	0.25	0.28	6-35
	assym. V	0.25	0.17	6-35
	assym. V	0.25	0.49	6-35
assym. V	0.25	0.49	6-35	
Sawyer & Winter (1987)	V	0.39	0.78	5-44
	V	0.48	0.48	7-53
	U	0.20	0.40	3-21
	U	0.44	0.45	6-51
Reidy (1987)	V	0.08	1.00	7-18
Coustols et al. (1987)	V	0.25	1.00	9-23
	V	0.25	0.50	10-23
	V	0.20	0.33	8-18
	round V ⁶	0.13	0.29	5-11
Philips & Beauchamps (1987); Beauchamps & Philips (1988)	V	0.03	1.00	7-14
	V	0.08	1.00	12-26

Table 1.2.2. cont'd

SOURCE	RIBLET SHAPE	h (mm)	h/s	h ⁺ RANGE
Wilkinson & Lazos (1987)	rectang. ^{7†}	0.25	0.07	5-14
	rectang	0.25	0.16	5-24
	rectang	0.33	0.16	6-26
	rectang	0.51	0.31	2-44
	rectang	0.51	0.80	11-45
	rectang	0.64	1.00	4-35
Enyutin et al. (1987)	V	0.08	0.80	3-16
	V	0.17	0.68	8-27
	rectang. [†]	0.22	0.83	5-27
McClellan et al. (1987)	V	0.03	1.00	6-15
	V	0.08	1.00	13-38
Squire & Savill (1987)	V	0.03	1.00	15-19
	V	0.05	1.00	24-26
	V	0.08	1.00	28-41
	V	0.11	1.00	35-50
Bechert (1987)	3-D ⁸	0.25	0.5	8-45



† Walsh et al. $h/s = 0.28$ $b = 40^\circ$
 Walsh et al. $h/s = 0.43$ $b = 90^\circ$
 Walsh et al. $h/s = 0.17$ $b = 45^\circ$
 Walsh et al. $h/s = 0.49$ $b = 64^\circ$
 Wilkinson & Lazos ALL $h/s t = 0.051$ mm
 Enyutin et al. ALL $h/s t = 0.0096$ mm

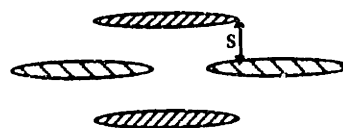
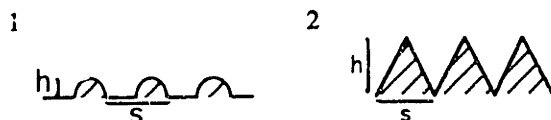


Table 1.2.3. Internal flow over riblets: Experimental riblet configurations.

SOURCE	RIBLET SHAPE	h (mm)	h/s	d_r^\dagger (mm)	d_s (mm)	h^+ RANGE
Nitschke (1983)	humped ¹	0.13	0.26	38.20	39.89	2-15
	humped	0.50	0.91	42.13	42.31	5-60
Nakao (1990)	V ²	0.86	0.48	51.3	50.8	2-37
	V	0.68	0.96	50.7	50.8	5-30
	V	0.40	0.24	48.6	50.8	2-18
	V	0.55	0.48	51.2	50.8	3-23
	V	0.64	0.40	50.6	50.8	3-28
	V	0.55	0.27	51.3	50.8	1-23
Liu et al. (1989)	V	0.11	1.00	24.98	25.4	7-23
	V	0.11	1.00	50.38	50.8	4-28
Reidy and Anderson (1988)	V	0.076	1.00	155.8	156.2	5-25
Rohr et al. (1989)	V	0.15	1.00	12.24	12.7	5-28
	V	0.076	1.00	12.32	12.7	3-22
Anderson et al. (1993)	V	0.15	1.00	24.70	25.2	4-87



$$\dagger d_R = \sqrt{\frac{4A_c}{\pi}}$$

Table 1.2.4. Additive mean velocity profiles: Representative literature experimental conditions.

Source	Poly.	M $\times 10^{-6}$	c (wppm)	Pipe ID (mm)	Re/f	1/f	S'	R ⁺
Mizushina	-	-	0	25.3	1066	11.7	0	377
	PEO	4.6	20	25.3	777	14.8	3.6	275
	PEO	4.6	50	25.3	622	19.9	9.2	220
	PEO	4.6	100	25.3	591	22.3	11.6	209
	PEO	4.6	300	25.3	634	22.7	12.0	204
	PEO	4.6	10	25.3	1999	19.0	6.2	707
	PEO	4.6	20	25.3	1877	19.9	7.2	664
	PEO	4.6	50	25.3	1616	21.3	8.9	571
	PEO	4.6	100	25.3	1311	25.8	13.7	463
Schummer	-	-	0	14	1374	12.2	0	486
	PAM	5	100	14	625	14.4	3.6	221
	PAM	5	100	14	966	18.6	7.3	341
	PAM	5	250	14	579	20.3	9.6	205
	PAM	5	250	14	959	24.0	12.7	339
	PAM	5	1000	14	926	24.9	13.7	328
Bartels	-	-	0	16.4	1374	12.4	0	569
	PAM	*	25	16.4	738	13.5	1.2	525
	PAM	*	100	16.4	1005	18.3	6.6	386
	PAM	*	200	16.4	637	19.7	8.0	360
	PAM	*	300	16.4	955	23.9	12.6	296
	PAM	*	500	16.4	907	24.4	13.1	290
Willmarth	-	-	0	46.8 [†]	3232	13.1	0	571
	PEO	2.6	10	46.8	2739	16.6	3.5	482
Gampert	-	-	0	19 [†]	879	11.4	0	311
	-	-	0	19	1251	12.0	0	442
	-	-	0	19	1965	12.8	0	695
	PAM	3.4	50	19	402	16.2	6.2	142
	PAM	3.4	50	19	523	18.9	8.5	185
	PAM	3.4	50	19	794	21.1	10.0	281
	PAM	3.4	100	19	334	14.4	4.7	118
	PAM	3.4	100	19	438	17.3	7.2	155
	PAM	3.4	100	19	715	20.9	9.8	253

Mizushina: Mizushina & Usui (1977); pipe flow

Schummer: Schummer and Thielen, 1980; pipe flow

Bartels: Bartels et al., 1985; pipe flow

Willmarth: Willmarth et al. 1987; rectangular channel flow

Gampert: Gampert and Yong, 1990; rectangular channel flow

* no data given

† hydraulic diameter

Table 1.2.5. Additive turbulence intensity: Representative literature experimental conditions.

Source	Poly.	M $\times 10^{-6}$	c (wppm)	R ⁺	S'	S'/S'MDR	u' ⁺ _{max}	y' ⁺ _{max}
Laufer	-	-	0	1020	0	0	2.62	16
	-	-	0	8940	0	0	2.60	15
Mizushina	PEO	4.6	50	456	14.7	1.0	2.16	90
	PEO	4.6	100	419	14.1	1.0	1.96	96
	PEO	4.6	300	312	12.2	1.0	2.11	75
	PEO	4.6	200	206	9.5	1.0	2.14	88
	PEO	4.6	500	178	8.5	1.0	2.00	80
Schummer	-	-	0	486	0	0	2.70	15
	PAM	5	100	221	3.6	0.36	3.20	30
	PAM	5	100	341	7.3	0.57	3.70	48
	PAM	5	250	205	9.6	1.0	2.85	25
	PAM	5	250	339	12.7	1.0	2.80	62
	PAM	5	1000	328	13.7	1.0	2.25	65
Bartels	-	-	0	569	0	0	-	-
16.4 mm pipe	PAM	*	100	386	6.6	0.48	-	-
	PAM	*	200	360	8.0	0.61	-	-
	PAM	*	300	296	12.6	1.0	2.66	60
	PAM	*	500	290	13.1	1.0	2.30	75
Bartels	-	-	0	562	0	0	-	-
44 mm pipe	PAM	*	40	470	2.1	0.14	3.06	22
	PAM	*	80	375	3.7	0.28	3.24	27
	PAM	*	80	441	4.4	0.30	3.38	33
	PAM	*	160	406	6.2	0.44	3.52	36
	PAM	*	320	393	6.6	0.48	3.53	35
Willmarth	-	-	0	571	0	0	2.70	18
	PEO	2.6	10	482	3.5	0.23	3.35	29
Luchik	-	-	0	519	0	0	2.63	18
	PAM	*	2.1	519	2.7	0.17	2.90	28

Mizushina: Mizushina & Usui, 1977; pipe flow

Schummer: Schummer and Thielen, 1980; pipe flow

Bartels: Bartels et al., 1985; pipe flow

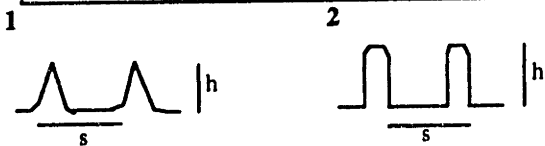
Willmarth: Willmarth et al. 1987; rectangular channel flow

Luchik: Luchik and Tiederman, 1988; rectangular channel flow

* no data given

Table 1.2.6. Riblet turbulence intensity: Representative literature experimental and computational configurations.

Source	Riblet			Experimental		
	Shape	h (mm)	s (mm)	U_∞/u_τ (smooth)	S^+	h^+
Walsh (1979)	V-groove	0.25	0.25	21.54	0.79	8.5
Hooshmand et al. (1983)	V-groove	1.27	2.54	26.14	1.85	8.7
Bacher and Smith (1985)	V-groove	1.60	1.60	22.62	0.91	15
Vukoslavcevic et al. (1987)	V-groove	5.00	10.0	22.22	-	17.5
Pulles (1988)	triang. ¹	2.5	2.5	19.98	0.33	11.7
		2.5	2.5	20.73	-1.36	20.7
Suzuki and Kasagi (1994)	triang. ¹	2.2	3.5	18.02	(?)	9.1
		2.2	3.5	19.68	(?)	19
Choi (1989)	tapered rectang. ²	1.6	2.5	26.09	1.44	13
Chu and Karniadakis (1993)†	V-groove	$h/s = 1$		17.17	0.41	17.1
Choi et al. (1993)†	V-groove	$h/s = 0.865$		22.93	-1.00	34.6
	V-groove	$h/s = 0.865$		23.15	1.00	17.3



Note: †computational
 $R' = \sqrt{2} S^+$
 Values in parentheses are estimated

Table 1.2.7. Polymer solution flow over wall modified surfaces: (a) rough pipes, (b) external flow over V-groove riblet surfaces and (c) V-groove riblet pipes.

(a) Polymer solution flow in rough pipes

Source	ID (mm)	R/k	k+ Range	Type	Mw x 10 ⁶	c (wppm)	Range of Polymeric Drag Reduction
Virk (1971)				PEO	0.12	2240 - 5830	0 - 15%
	8.69	35	4 - 70	PEO	0.57	43.6 - 939	0 - 45%
	8.76	22.8	5 - 150	PEO	5.5	18.7 - 82.5	0 - 80%
	8.64	14.6	7 - 220	PEO	8.0	110	~ 80%
				PAM	12.5	110	~ 80%
Bewersdorff & Petersmann (1987)	30.7	6.8	30 - 270	PAM	-	20-50	0 - 80%

(b) External flow of polymer solutions over riblet surfaces

Source	L (mm)	h (mm)	h/s	h ⁺ Range	Type	Mw x 10 ⁶	c (wppm)	Range of Polymeric Drag Reduction
Beauchamps & Philips ¹ (1986, 1987)	1212	0.033	1.00	6 - 12	PEO [†]	~ 3	120	0 - 15%
	1212	0.076	1.00	7 - 25	PEO [†]	~ 3	120	10 - 35%

(c) Polymer solution flow in V-groove riblet pipes

Source	ID (mm)	h (mm)	h/s	h ⁺ Range	Type	Mw x 10 ⁶	c (wppm)	Range of Polymeric Drag Reduction
Reidy & Anderson (1988)	156.0	0.006	1.00	5 - 25	PAM	-	2	0 - 50%
Rohr et al. (1990)	12.47	0.006	1.00	1 - 4	PEO [†]	-	2.5-40	~ 20%
Christodoulou et al. (1991)	25.14	0.11	1.00	6 - 20	PEO [†]	-	5-50	-
	25.14	0.11	1.00	6 - 22	PAM	-	2-50	-
Anderson et al. (1993)	25.01	0.15	1.00	5 - 88	PEO [†]	-	2-8	0 - 40%

1. axisymmetric model, 102 mm diameter

† POLYOX WSR-301

Table 1.3.1. Characterization of aqueous PEO solutions.

Source	Experimental			M_w range (g/mol)	$[\eta] = K'M_w^a$	
	Technique	solvent	T (°C)		$K' \times 10^{-5}$ (dl/g)	a
Rempp (1957)	V	H ₂ O	20	6E2 - 3E4	33	0.72
Bailey et al. (1958) [†]	V/L/S	H ₂ O	30	3E4 - 1E7	12.5	0.78
Bailey and Callard (1959) [†]	V	H ₂ O	35	3E4 - 4E6	6.40	0.82
	V	H ₂ O	45	3E4 - 4E6	6.90	0.81
Rossi and Cuniberti (1964)	V/E	H ₂ O	25	2E2 - 8E3	156	0.5
Shin (1965) [†]	V/L	H ₂ O	25	3E5 - 8.5E6	8.79	0.79
Ring et al. (1966)	V	H ₂ O	25	5E3 - 3E5	24	0.73
Hammes and Roberts (1968)	V	H ₂ O	10	1E3 - 2E4	75	0.63
Nabi (1968)	V/L	H ₂ O	25	5E5 - 4E6	11.9	0.76
Crouzet and Marchal (1973)	V/L/S	H ₂ O	25	6E2 - 3E4	29	0.72

V = Viscosity; L = Light Scattering; S = Sedimentation; E = Endgroup analysis

[†] POLYOX™ Water-Soluble-Resins (Union Carbide)

Table 1.3.2. Characterization of aqueous PAM solutions.

Source	Experimental			M_w range (g/mol)	$[\eta] = K'M_w^a$	
	Technique	solvent	T (°C)		$K' \times 10^{-5}$ (dl/g)	a
Scholotan (1954)	V/S	H ₂ O	25	2E4 - 5E5	6.31	0.80
American Cyanamid Co. (1955)	?	1N NaNO ₃	30	?	37.3	0.66
Collinson et al. (1957)	V/FeT	H ₂ O	25	1E4 - 3E5	68.0*	0.66
Kline and Conrad (1978)	V/L	H ₂ O	25?	5E5 - 5E6	4.90	0.80
Munk et al. (1980)	V/S	H ₂ O	20	2.5E5 - 1E7	30.9	0.67
	V/S	0.2N NaCl	20	2.5E5 - 1E7	30.2	0.68
	V/S	1N NaCl	20	2.5E5 - 1E7	28.8	0.69
Kulicke et al. (1982)	V/L	H ₂ O	20	3.8E4 - 9E6	10.0	0.76
	V/L	θ solvent	25	0.5E5 - 6.0E6	79.0	0.50
McCormick et al. (1990)	V/L	0.5N NaCl	25	3.9E6 - 2.8E7	9.06	0.77

V = Viscosity; L = Light Scattering; S = Sedimentation; FeT = ferric ion termination of polymerisation reaction

* based on number average molecular weight, M_n

Table 1.3.3. Characteristics of high molecular weight aqueous PEO solutions ($M_w > 10^5$ g/mol).

Source	M_w (g/mole)	$[\eta]$ (dl/g)	R_G^\dagger (nm)	H (Eq. 2.3-16)
Shin (1965) (T = 25°C)	302000	1.8	81	28.7
	492000	3.0	75.5	8.6
	622000	3.5	82	7.4
	1226000	5.4	128	9.4
	2580000	8.2	144	4.1
	2820000	11.4	151	3.1
	4270000	16.5	194	3.0
	5180000	17.6	222	3.5
	8450000	27.0	292	3.2
Kezirian (1993) (T = 25°C)	5660000	16.8 (20.1)*	266	5.8 (4.9)
Bailey et al. (1958) (T = 30°C)	306900	2.3	-	-
	580300	3.91	-	-
	756800	4.65	-	-
	698800	5.41	-	-
	1817000	7.66	-	-
	1769000	10.6	-	-
	1968000	11.4	-	-
	2021000	10.3	-	-
	2635000	9.8	-	-
	4480000	21.8	-	-
	7035000	24.7	-	-
Bailey and Callard (1959) (T = 35°C)	171800	1.16	-	-
	447000	2.65	-	-
	703100	4.05	-	-
	3991000	16.7	-	-
Bailey and Callard (1959) (T = 45°C)	165900	1.14	-	-
	701700	3.95	-	-
	3921000	17.7	-	-
	6183000	23.4	-	-

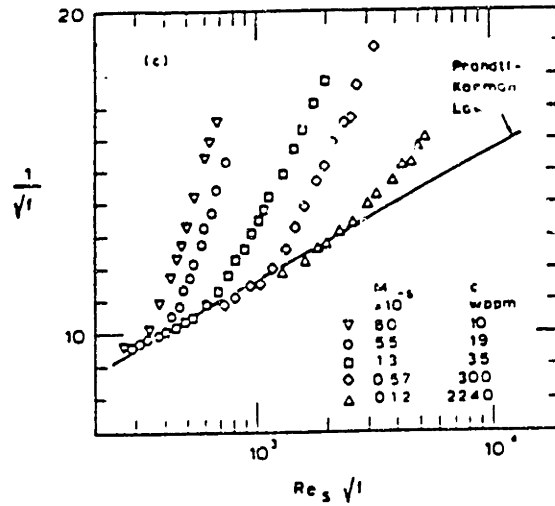
$\dagger R_G = \langle R_G^2 \rangle_z^{1/2}$ - z-average radius of gyration

* Values in parentheses correspond to intrinsic viscosity measurements in current work. The viscometer used by Kezirian may have caused mechanical degradation of the samples.

Table 1.3.4. Characteristics of high molecular weight aqueous PAM solutions ($M_w > 10^5$ g/mol).

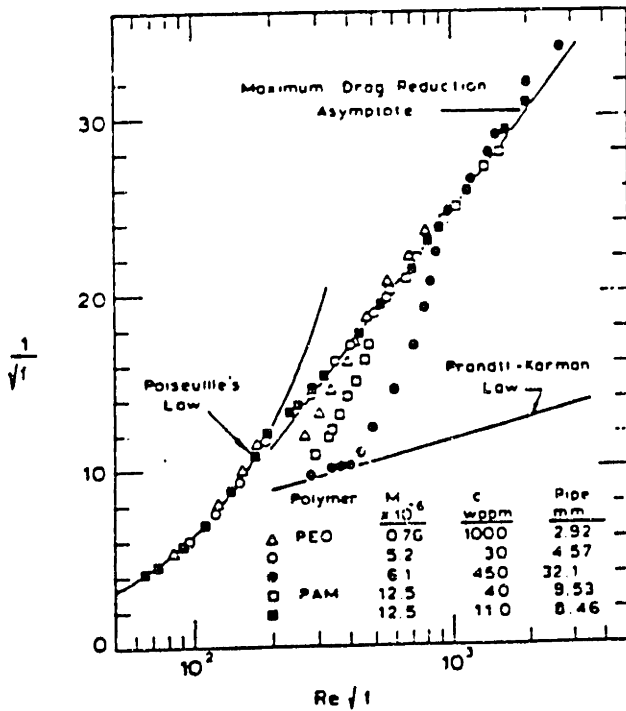
Source	M_w (g/mole)	$[\eta]$ (dl/g)	R_G^\dagger (nm)	H (Eq. 1.3-16)
Kline and Conrad (1978) (T = 25°C?)	490000	1.83	37.4	1.7
	540000	2.09	49.3	3.1
	560000	2.13	49.9	3.1
	770000	2.63	40.5	1.0
	1050000	2.46	62.3	2.8
	1100000	3.45	63.4	2.0
	1250000	4.12	69.9	1.9
	2020000	6.06	90.7	1.8
	2660000	7.40	111.7	2.1
	2860000	7.38	106.5	1.7
	3090000	7.38	106.9	1.6
	5610000	13.6	167.3	1.8
Muller et al. (1979) (T = 25°C)	3700000	7.90	169	4.9
	3800000	8.10	144	2.9
	4000000	7.00	150	3.5
Kulicke et al. (1982) (T = 20°C)	813000	3.31	61	2.5
	4240000	9.5	140	2.0
	4314000	11.1	170	3.0
	4950000	10.7	164	2.5
	5044000	14.0	184	2.6
	5050000	15.0	182	2.3
	7060000	16.2	197	2.0
	7560000	14.6	207	2.4
McCormick et al. (1990) (T = 25°C)	3960000	8.4	-	-
	6900000	16	-	-
	7500000	18	-	-
	24000000	34	-	-
	25000000	52	-	-
	28000000	47	-	-

$\dagger R_G = \langle R_G^2 \rangle_z^{1/2}$ - z-average radius of gyration



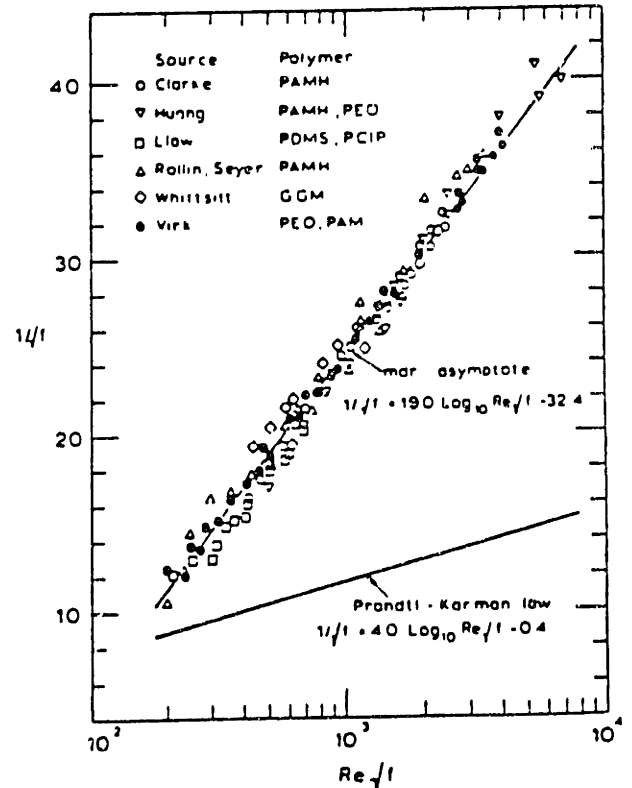
Aspects of the polymeric regime: Effect of molecular weight. Pipe I.D. 8.46 and 9.45 mm, temperature 25 C, solvent distilled water, polymer PEO. ($M \times 10^{-6}$, c wppm) as follows: (8.0, 10), (5.5, 10), (1.3, 35), (0.57, 300), (0.12, 2240).

a



Gross flow trajectories exhibiting maximum drag reduction. In all cases solvent was distilled water, temperature 25 C. (Polymer, $M \times 10^{-6}$, c wppm, d mm) as follows: (PEO, 0.76, 1000, 2.92), (PEO, 5.2, 30, 4.57), (PEO, 6.1, 450, 32.1), (PAM, 12.5, 40, 9.53), (PAM, 12.5, 110, 8.46).

b



The maximum drag reduction asymptote in pipe flow of polymer solutions. See Table 4 for experimental details.

c

Figure 1.2.1. Aspects of type-A drag reduction (Virk, 1975a)

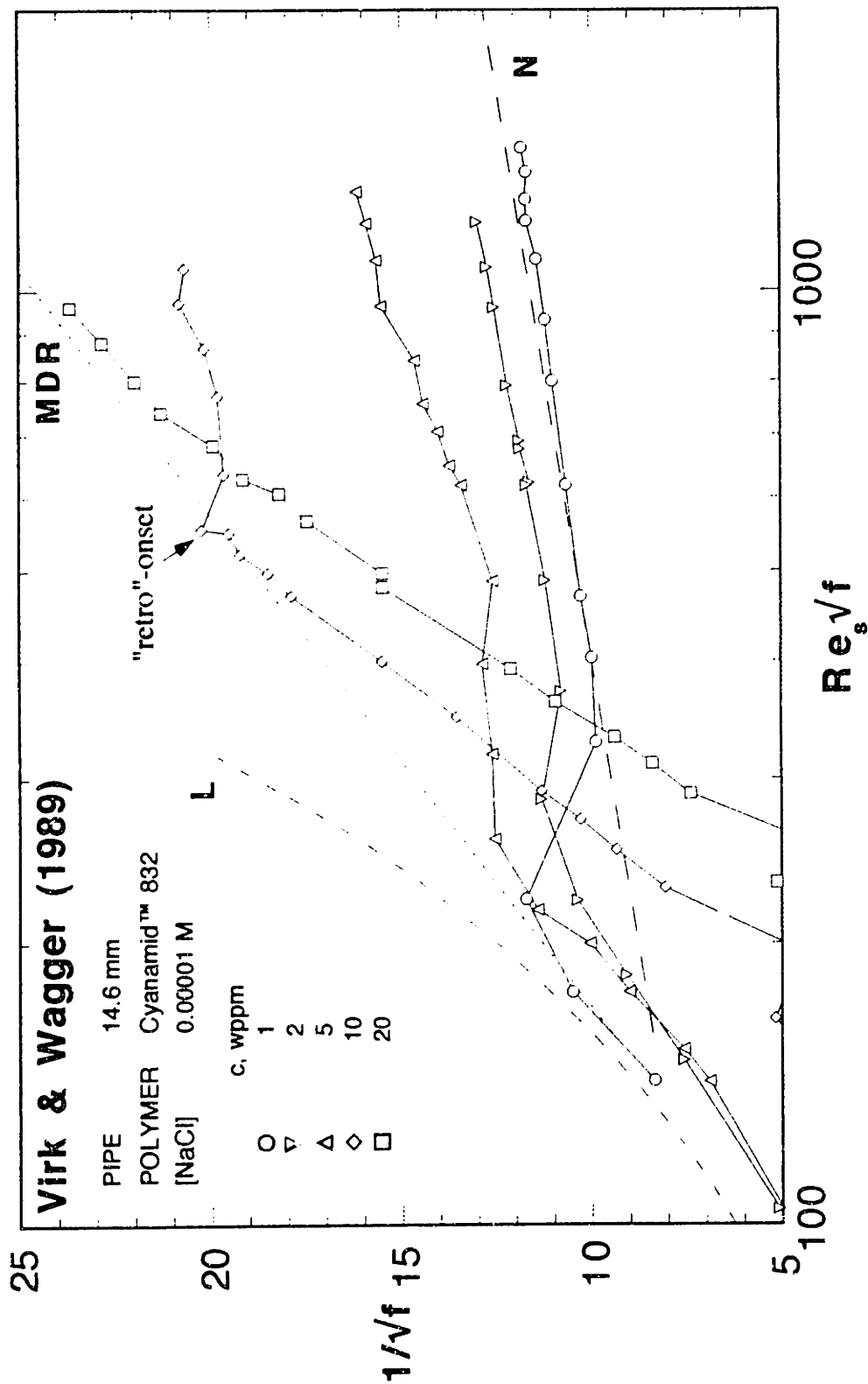


Figure 1.2.2 Aspects of type-B drag reduction (Virk and Wagger, 1989)

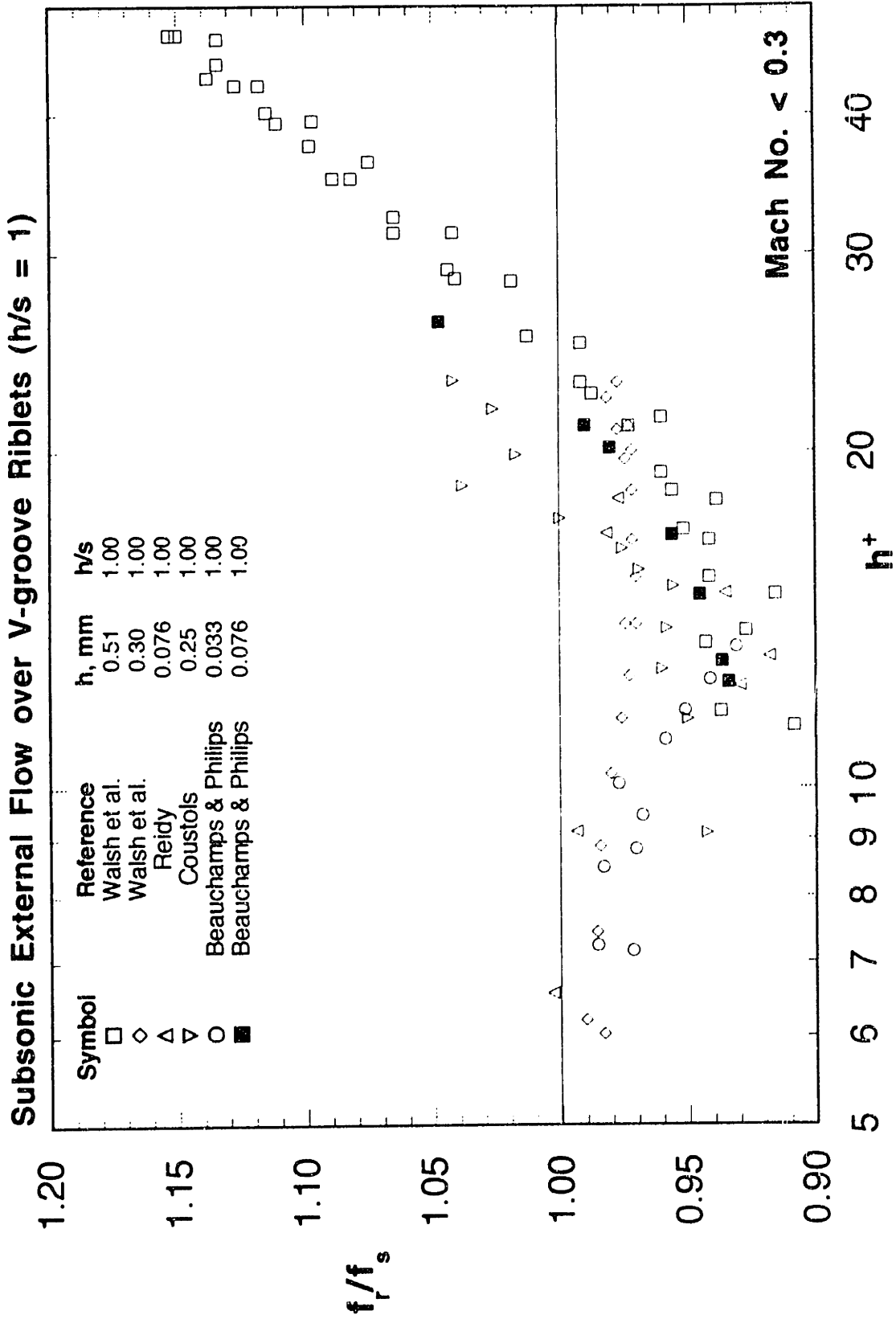


Figure 1.2.3a External, subsonic flow over V-groove riblet surfaces ($h/s = 1$)

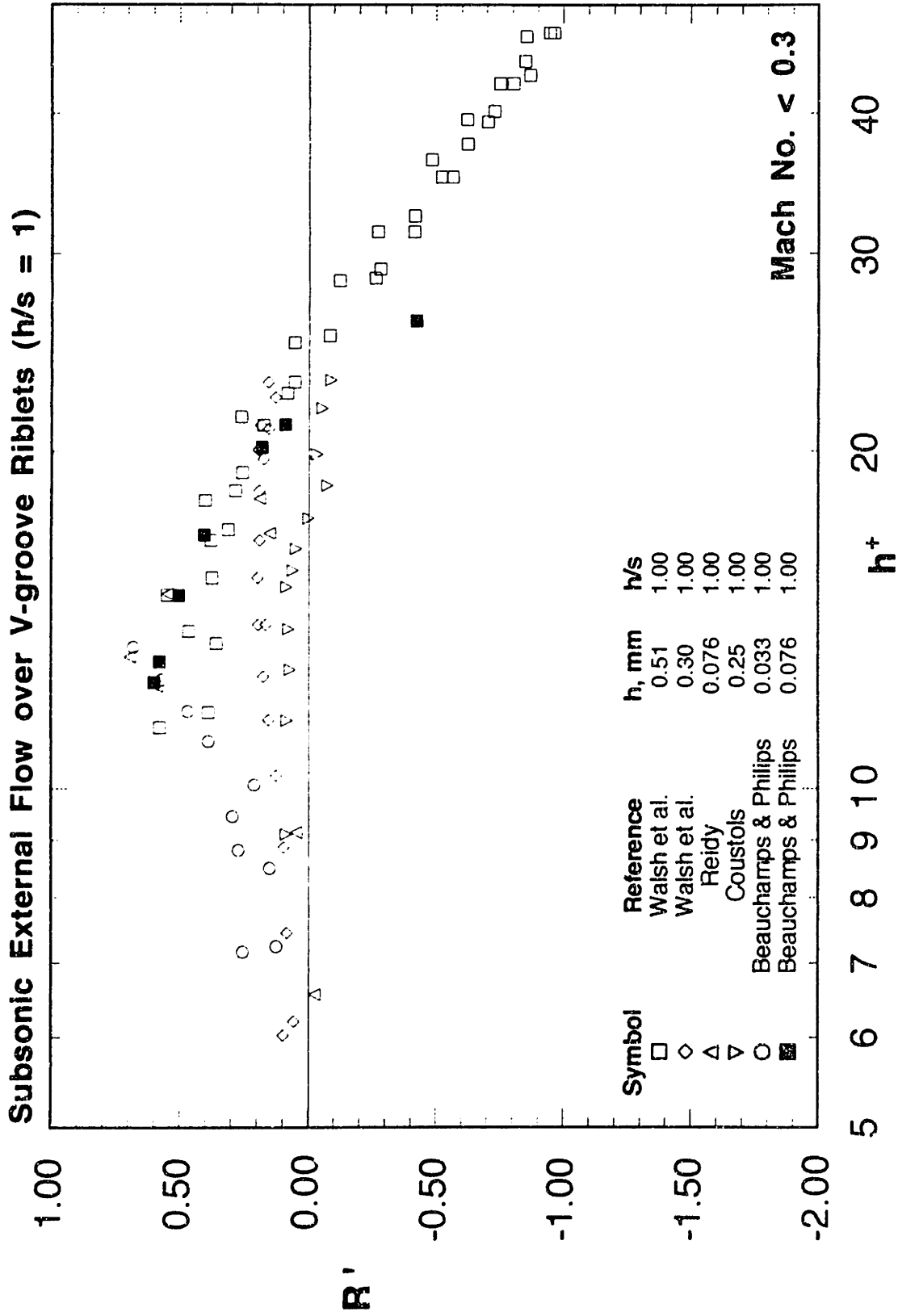


Figure 1.2.3b External, subsonic flow over V-groove riblet surfaces ($h/s = 1$)

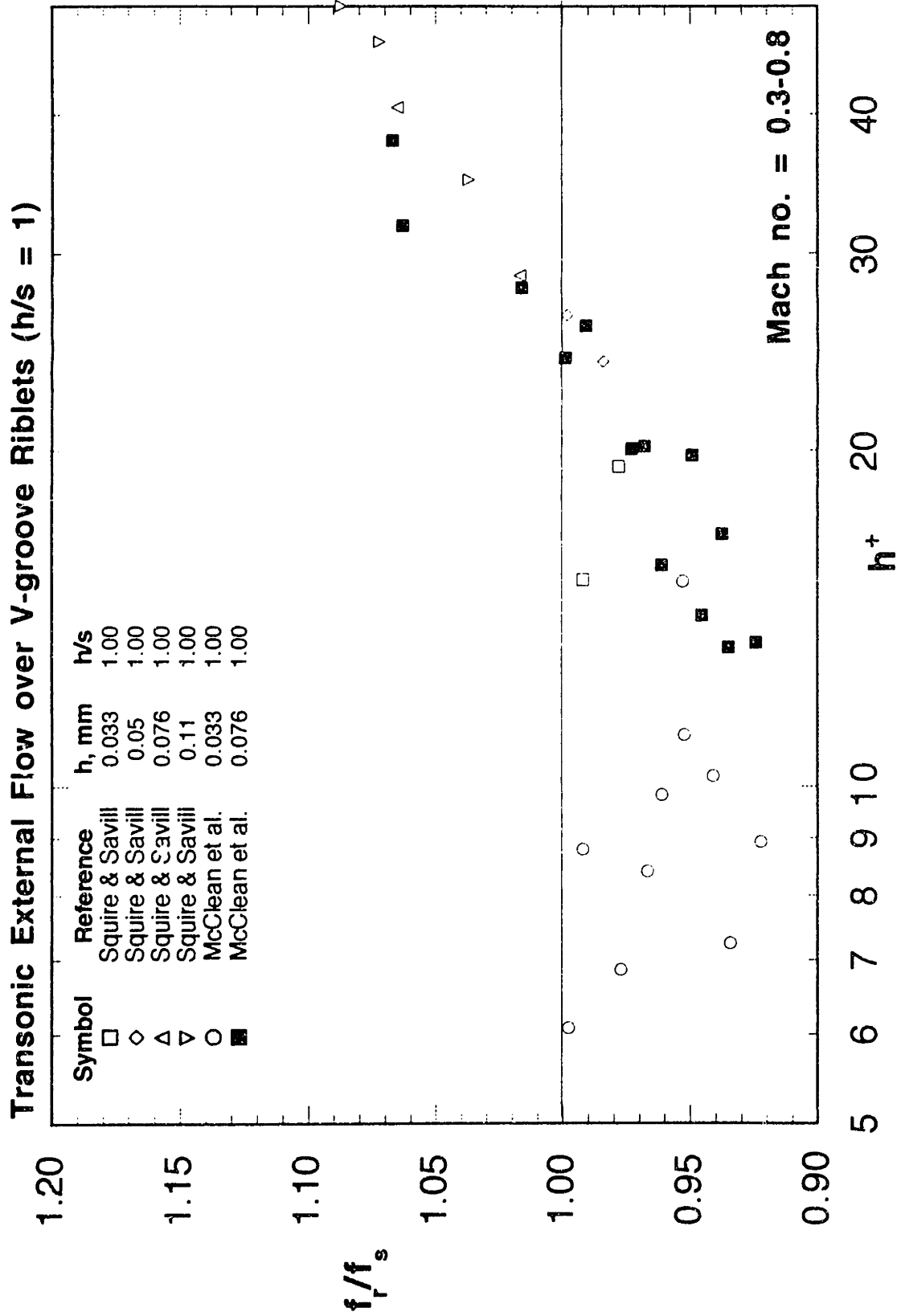


Figure 1.2.4a External, transonic flow over V-groove riblet surfaces ($h/s = 1$)

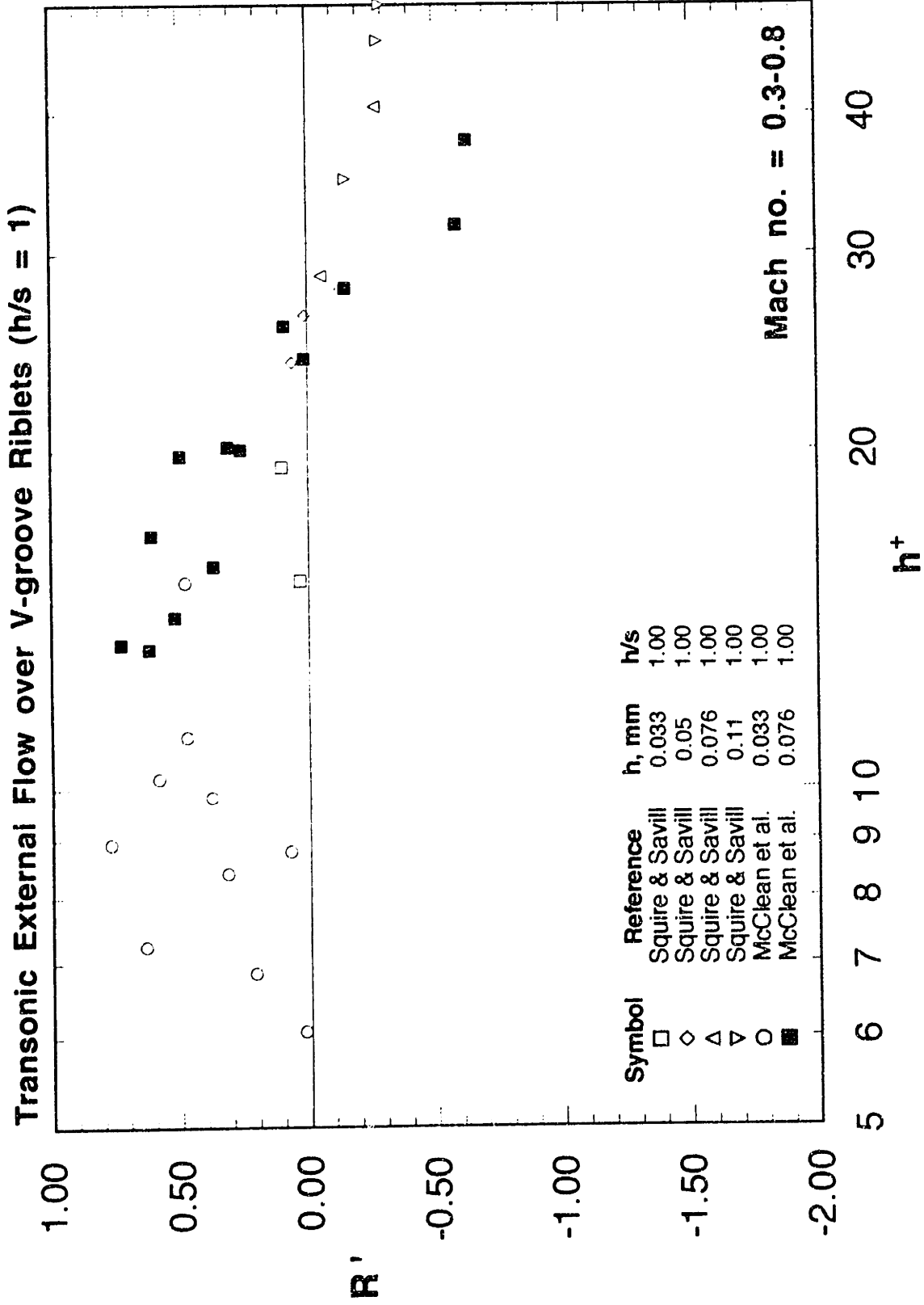


Figure 1.2.4b External, transonic flow over V-groove riblet surfaces ($h/s = 1$)

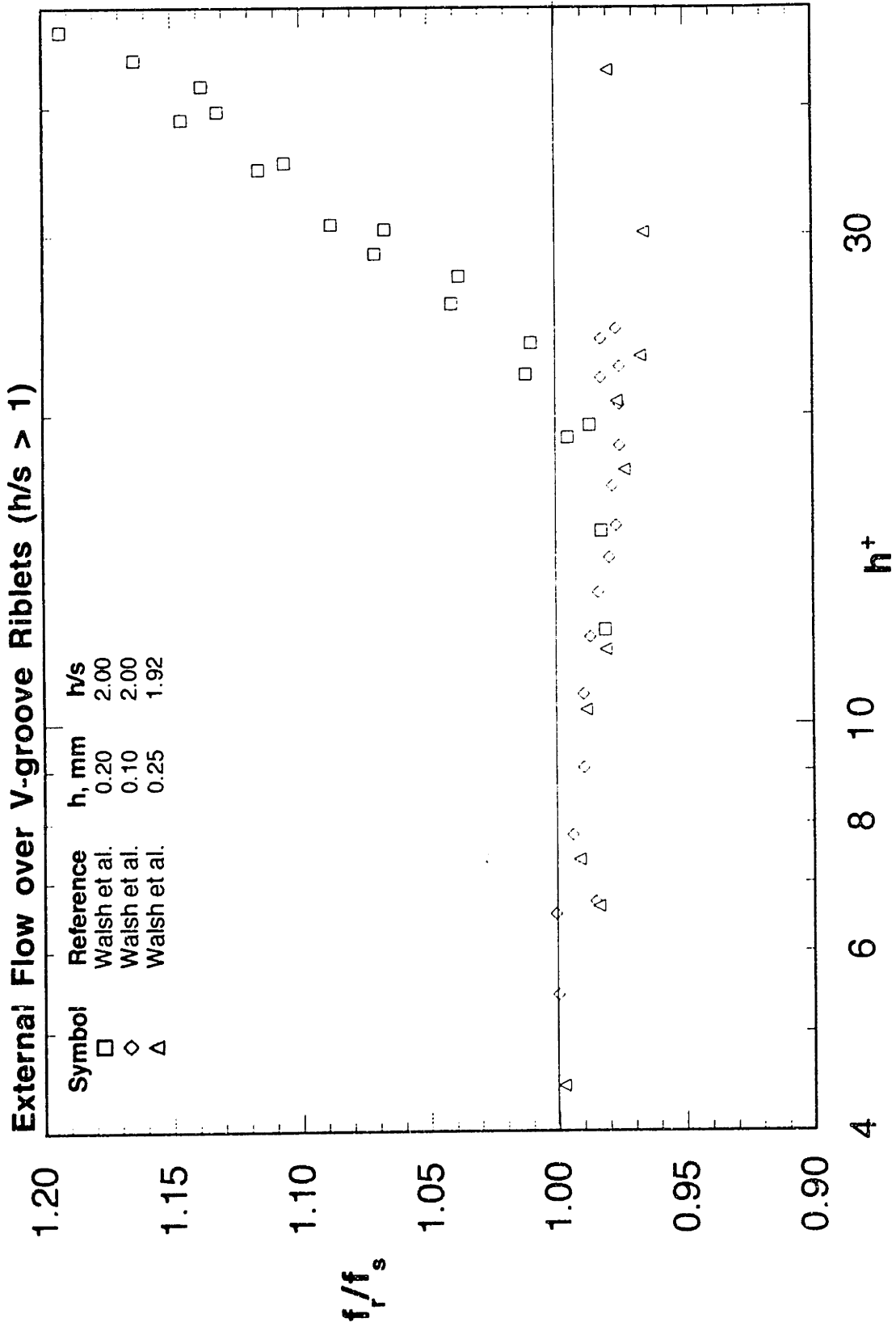


Figure 1.2.5a External flow over V-groove riblet surfaces ($h/s > 1$)

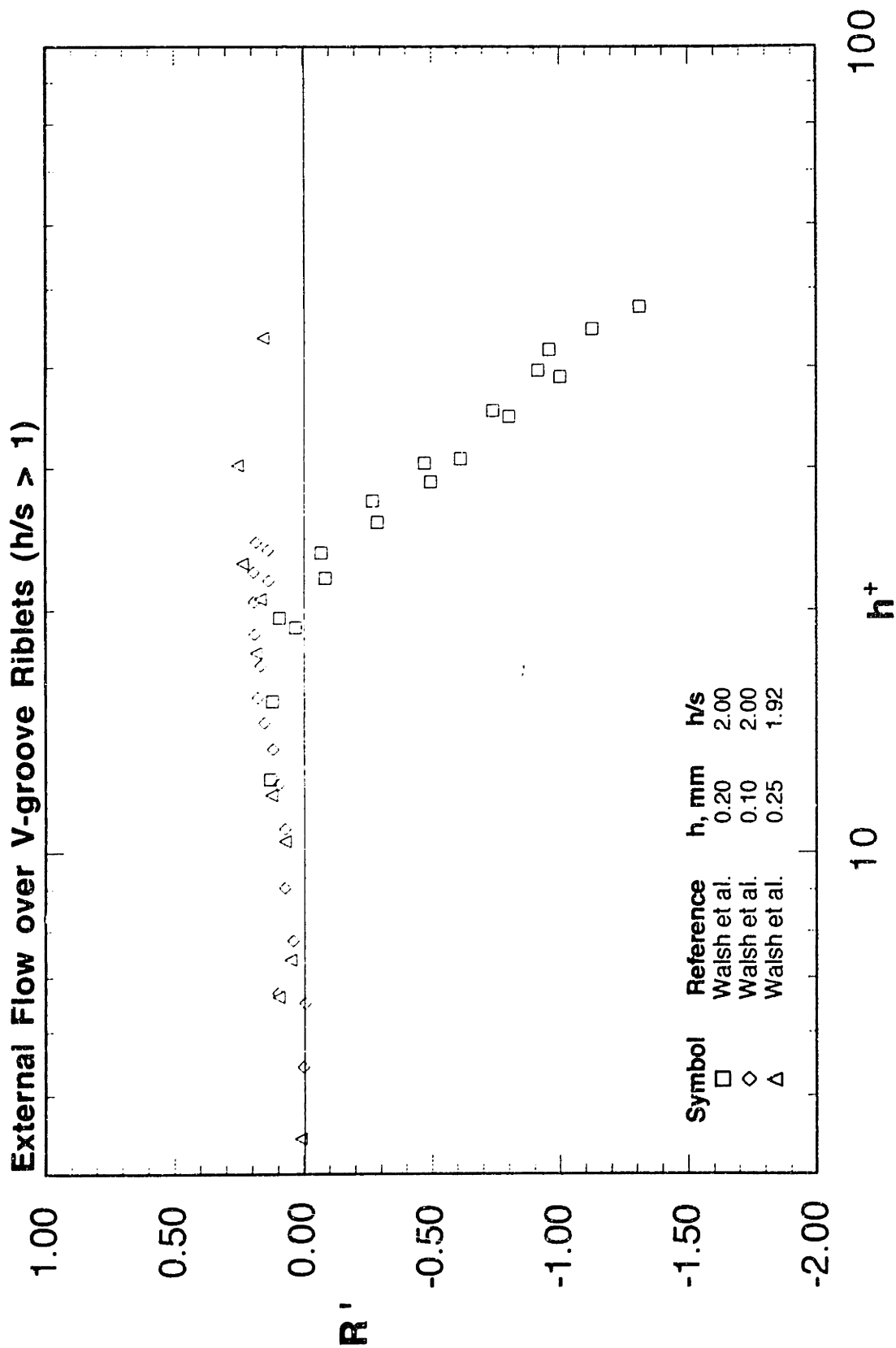


Figure 1.2.5b External flow over V-groove riblet surfaces ($h/s > 1$)

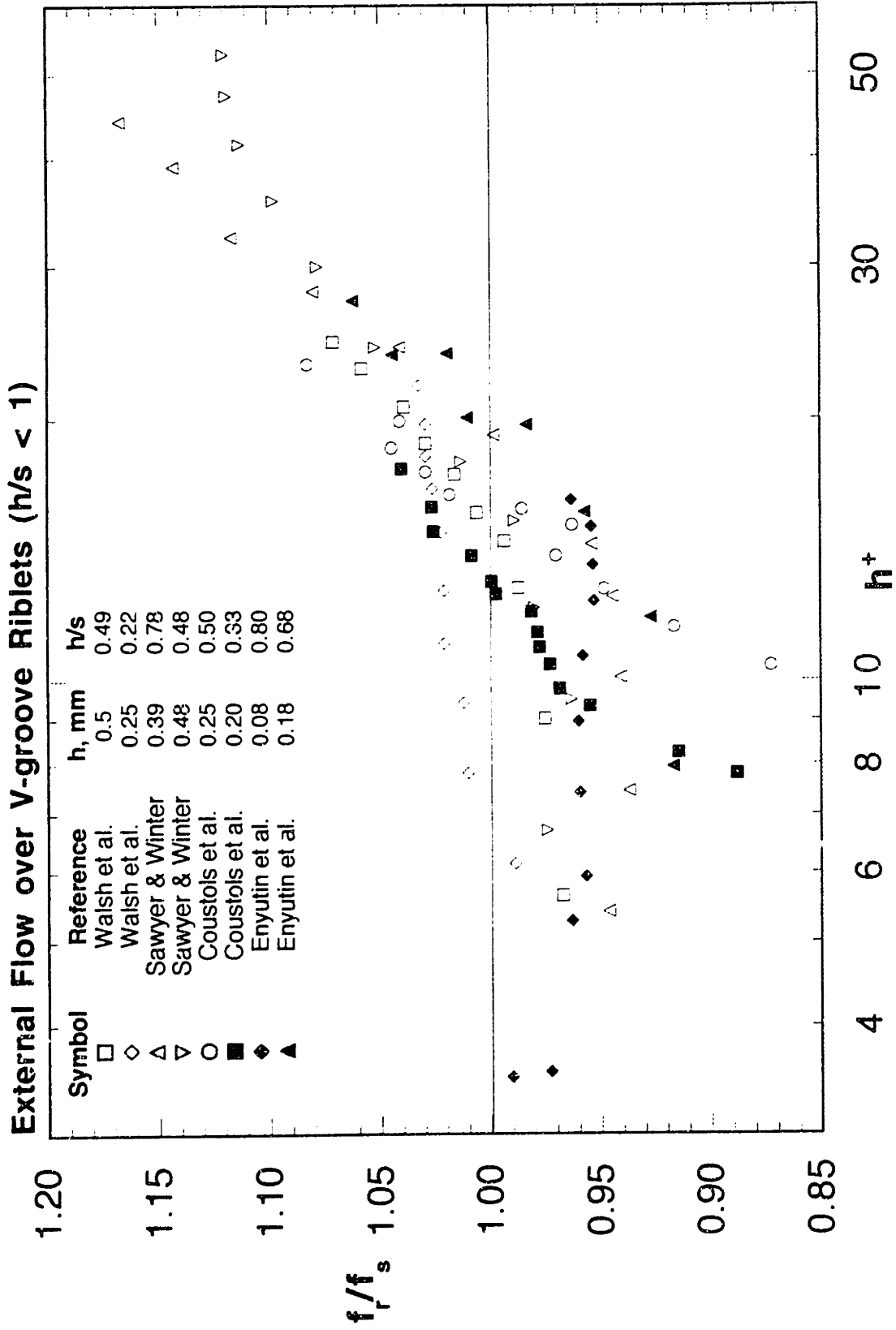


Figure 1.2.6a External flow over V-groove riblet surfaces ($h/s < 1$)

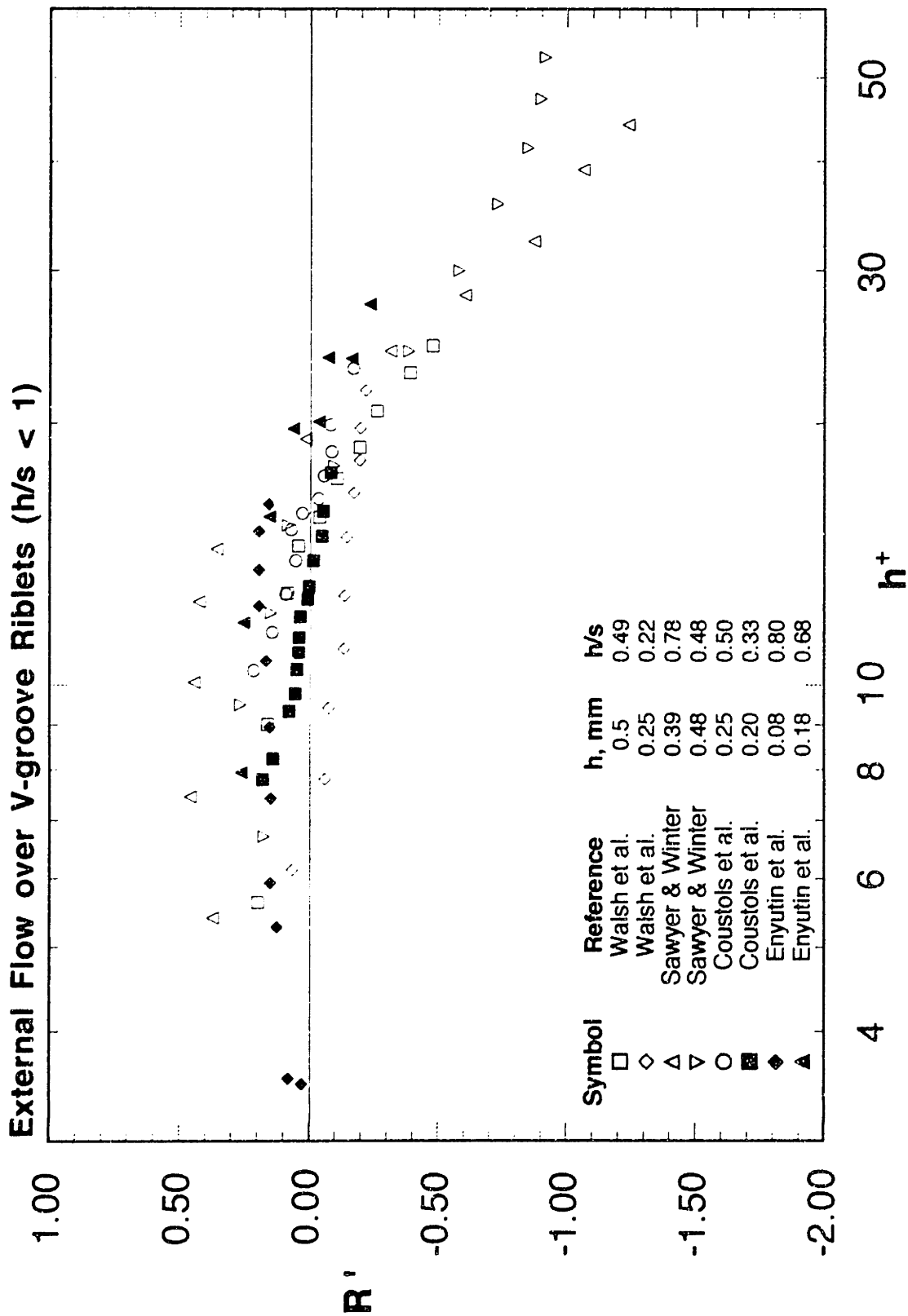


Figure 1.2.6b External flow over V-groove riblet surfaces ($h/s < 1$)

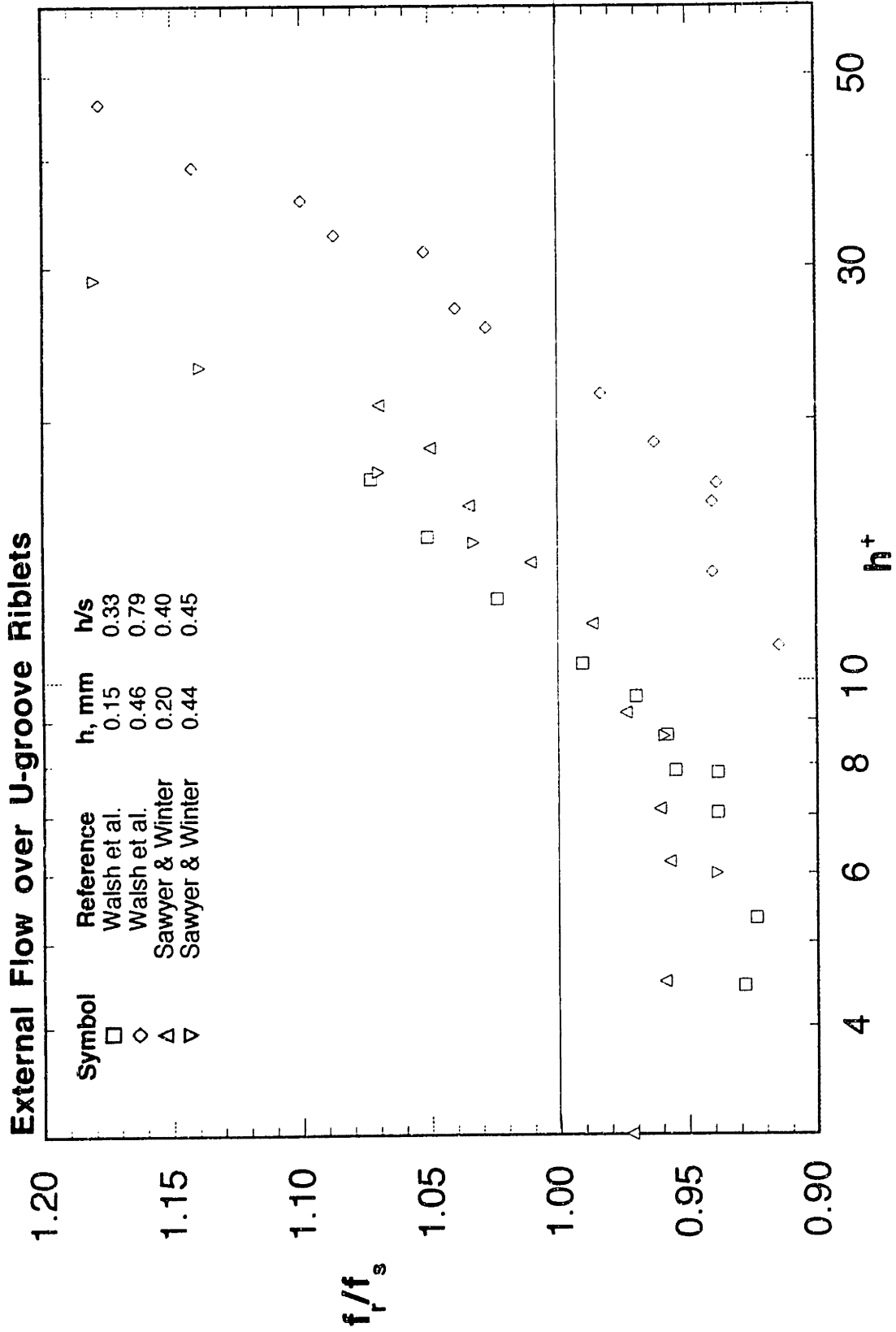


Figure 1.2.7a External flow over U-groove riblet surfaces

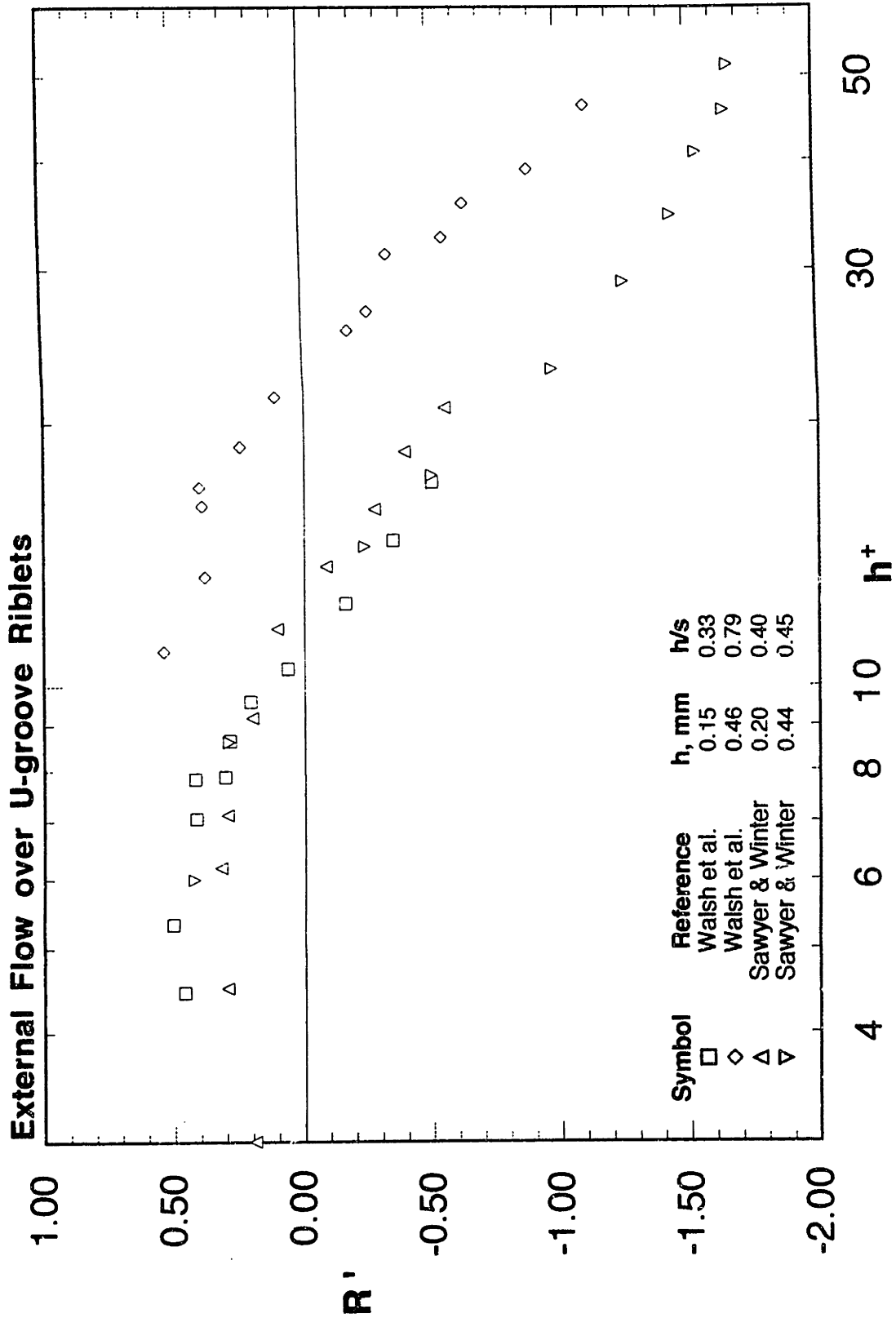


Figure 1.2.7b External flow over U-groove riblet surfaces

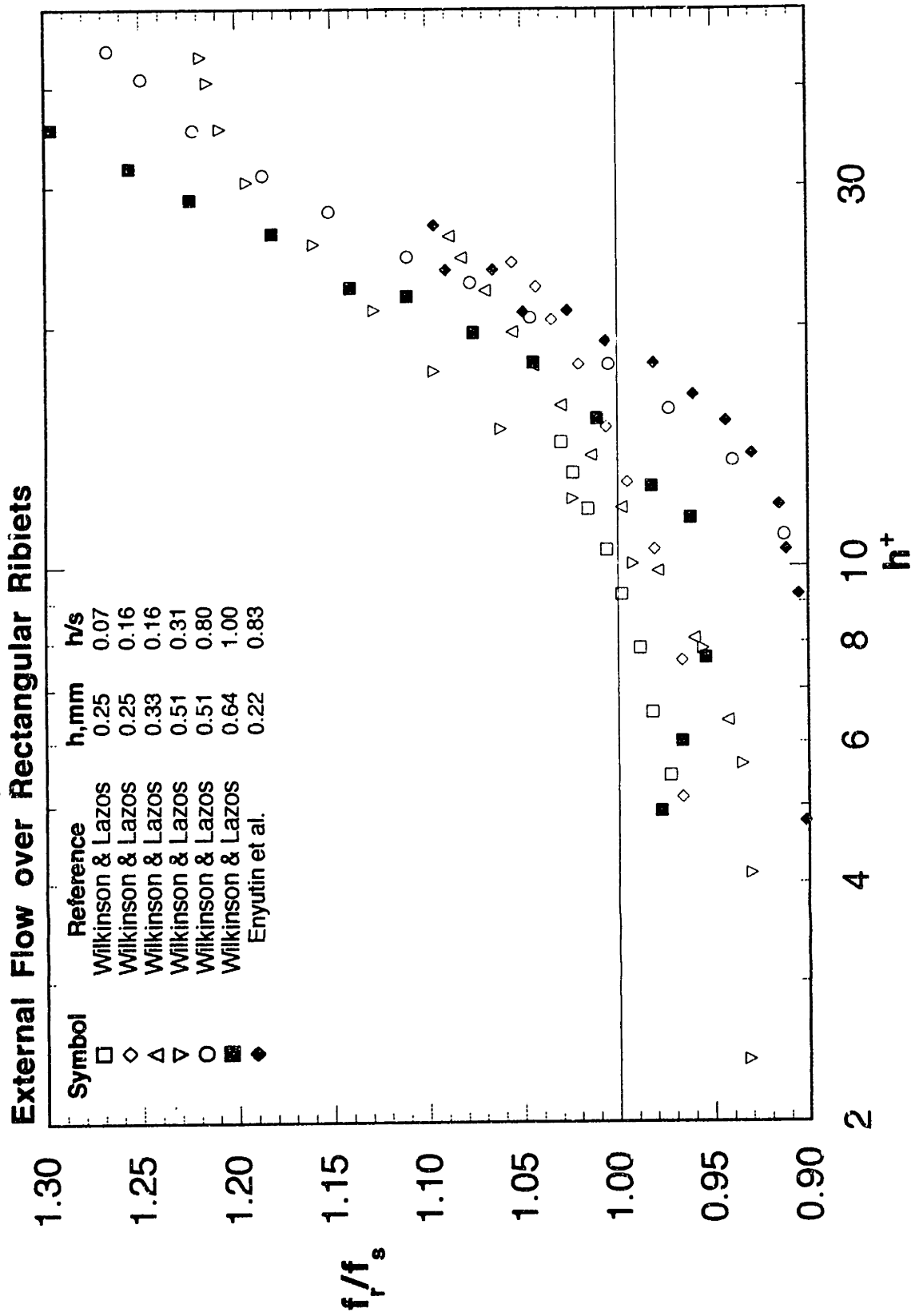


Figure 1.2.8a External flow over rectangular riblet surfaces

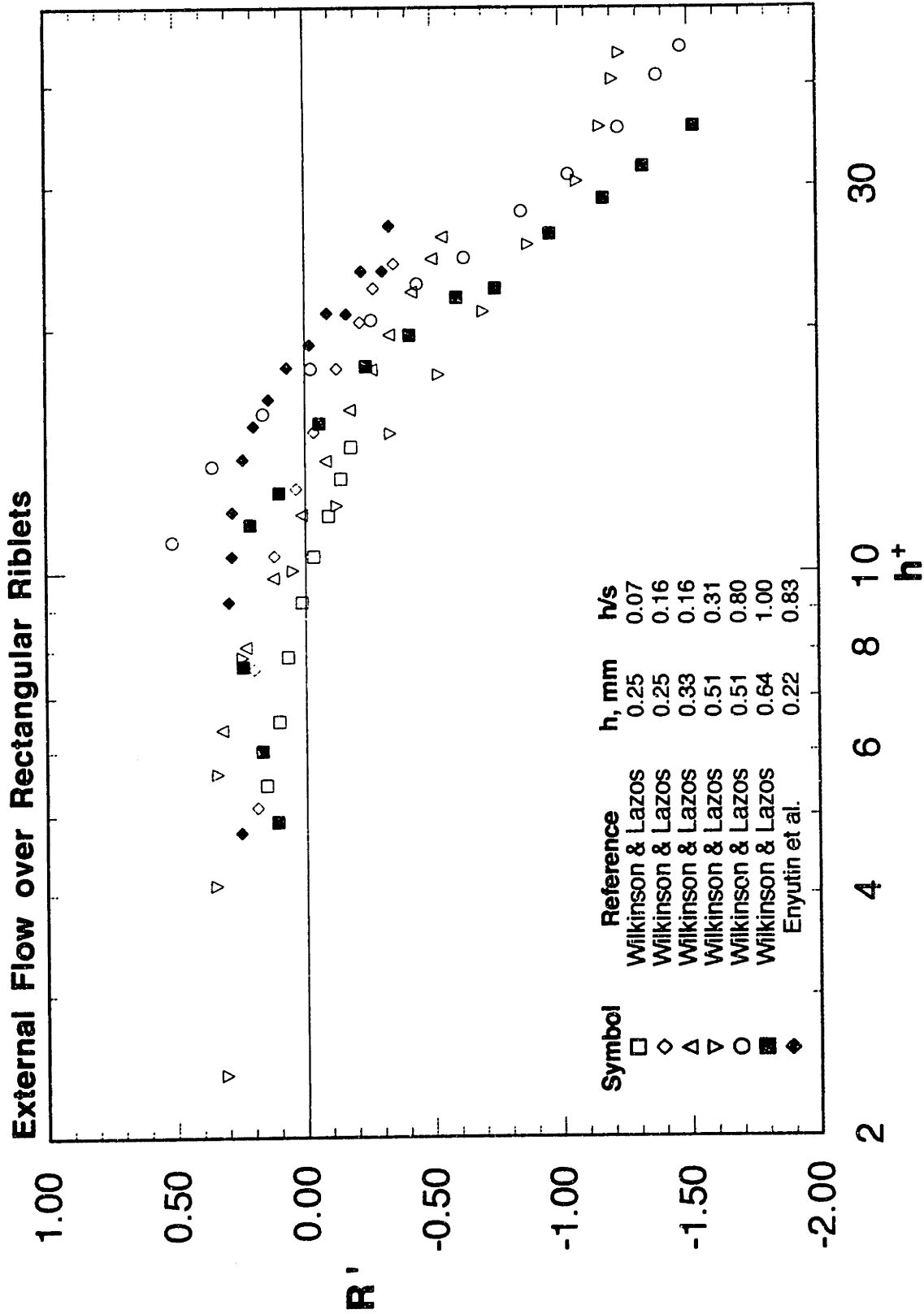


Figure 1.2.8b External flow over rectangular riblet surfaces

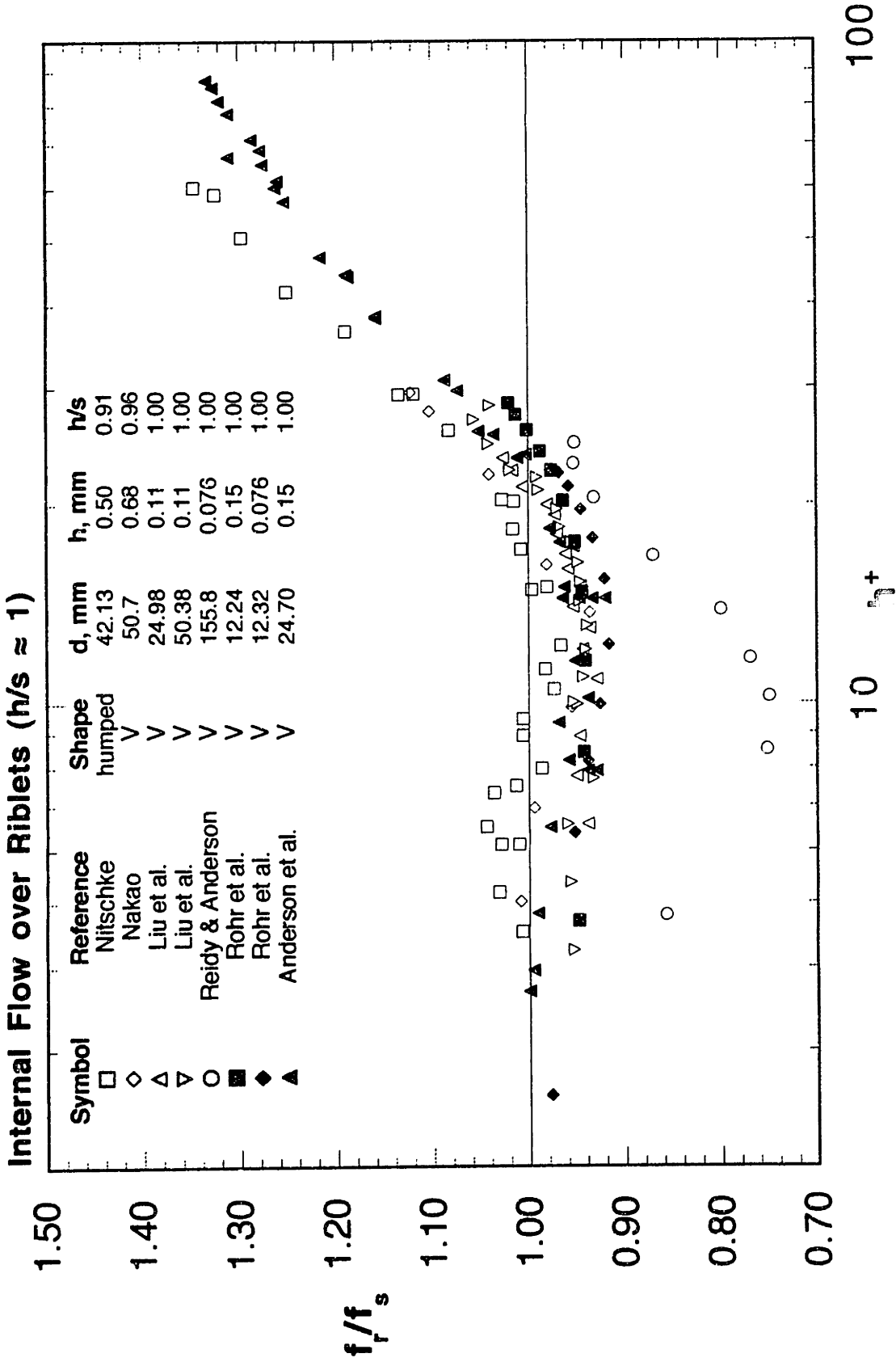


Figure 1.2.9a Internal flow over riblet surfaces ($h/s = 1$)

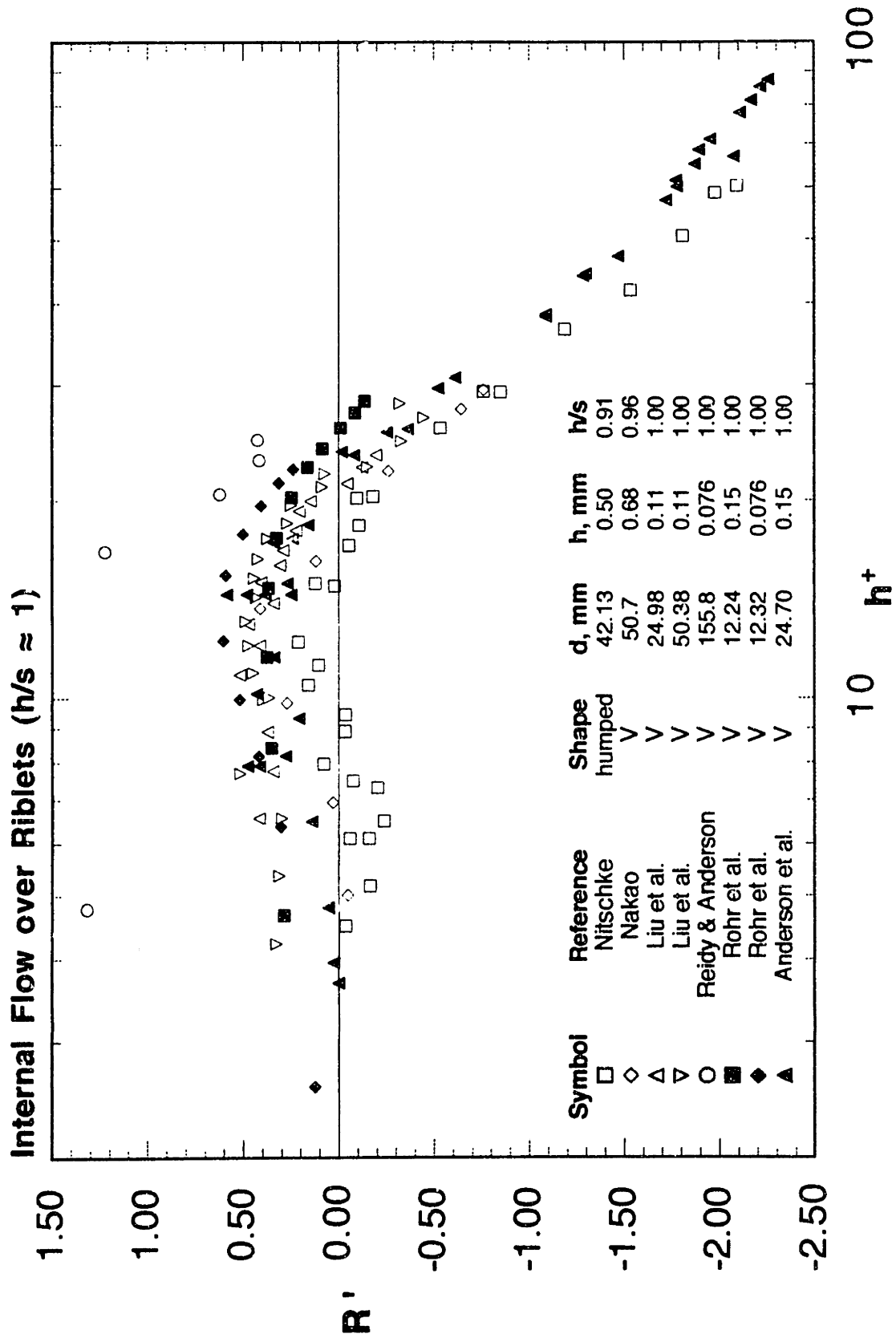


Figure 1.2.9b Internal flow over riblet surfaces ($h/s = 1$)

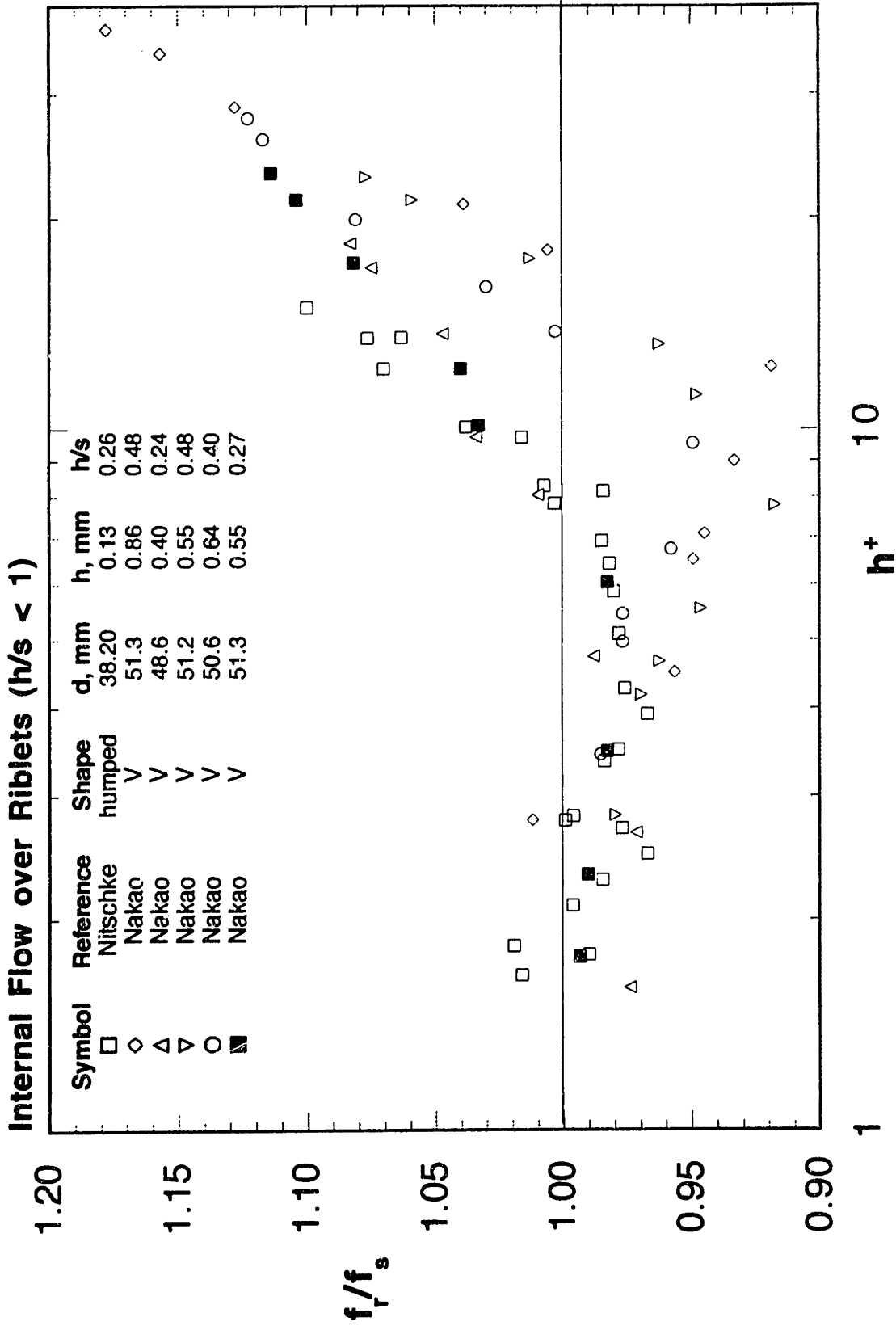


Figure 1.2.10a Internal flow over riblet surfaces ($h/s < 1$)

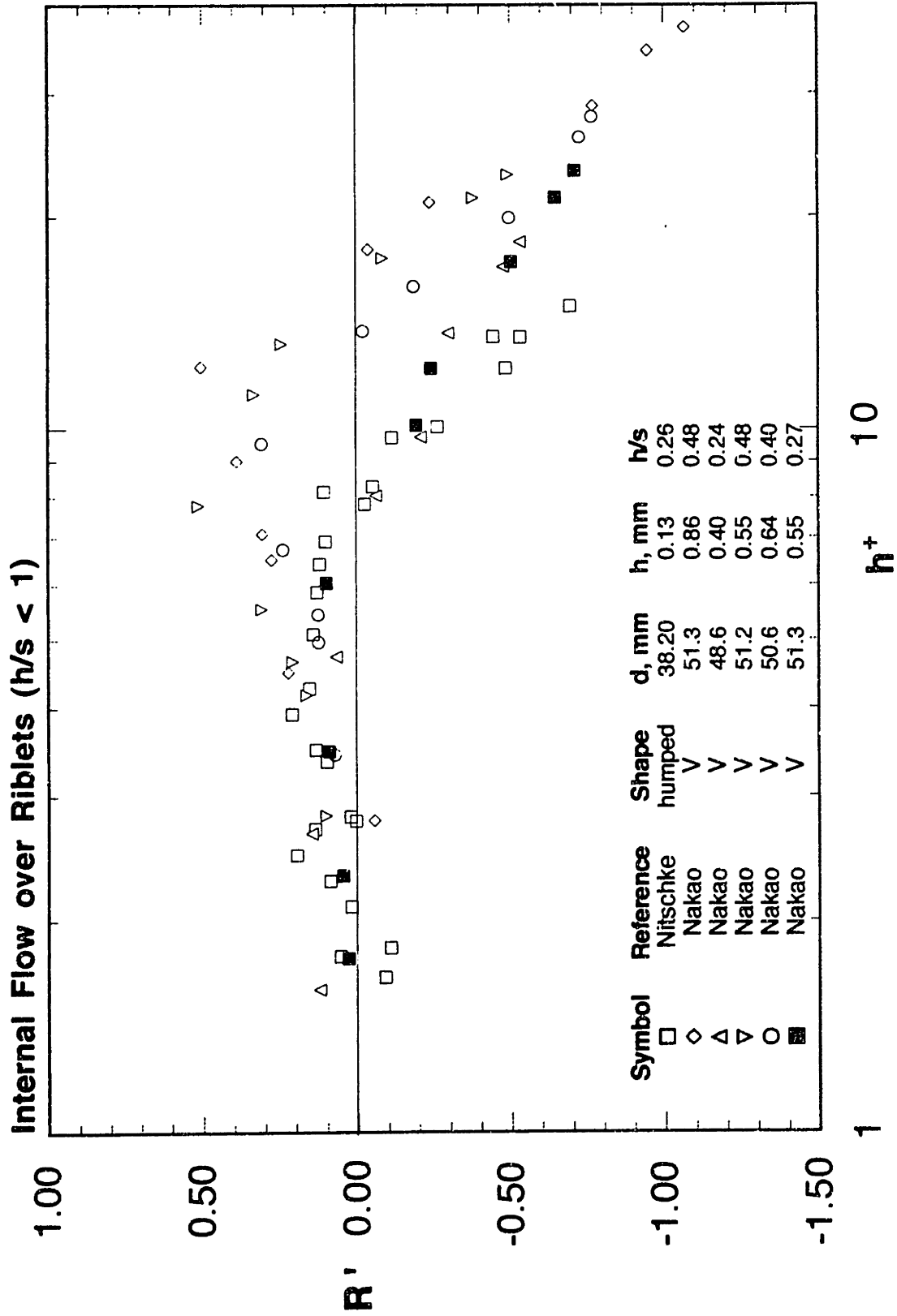


Figure 1.2.10b Internal flow over riblet surfaces ($h/s < 1$)

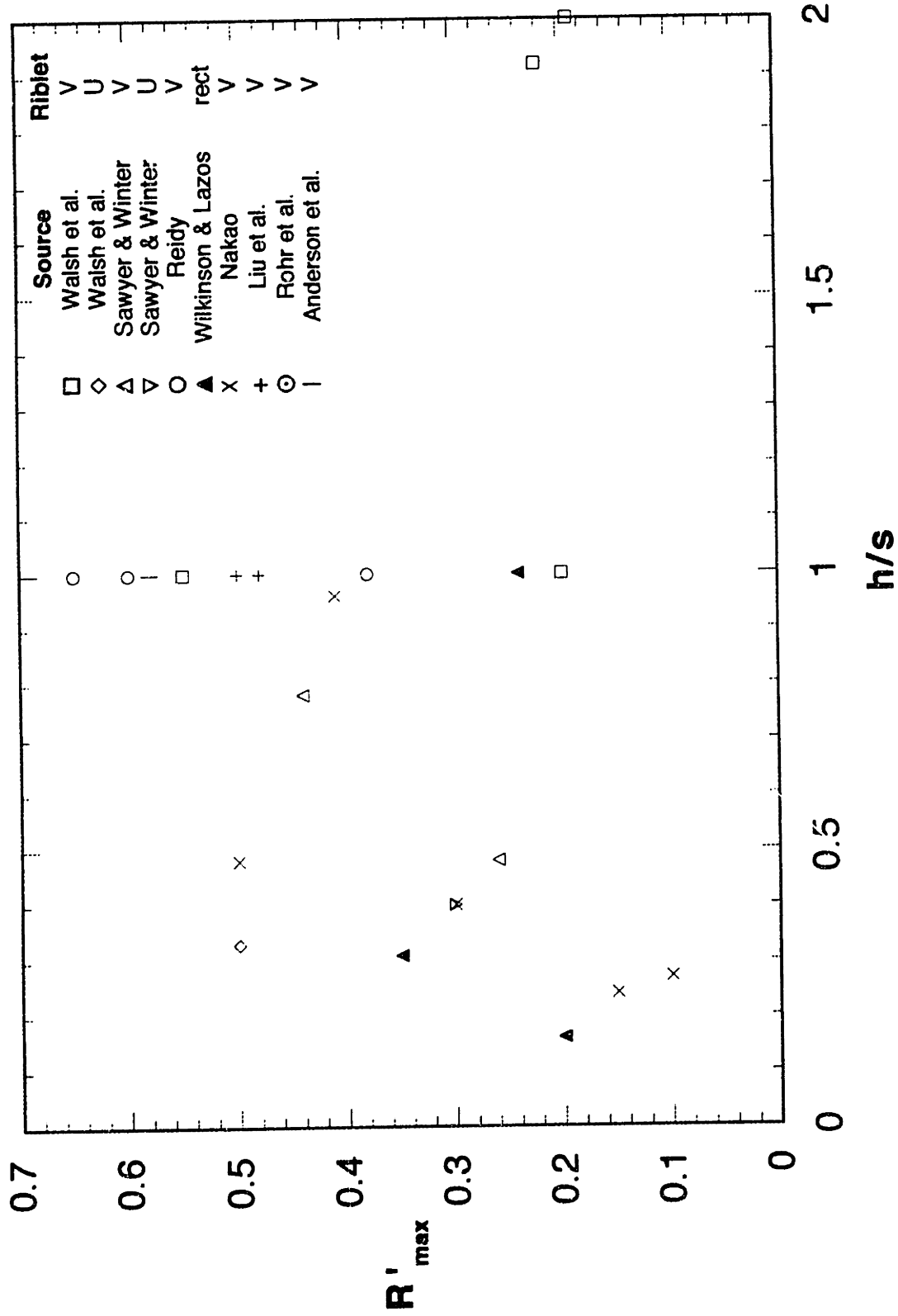


Figure 1.2.11 Variation of maximum riblet-induced flow enhancement, R'_{max} with aspect ratio, h/s .

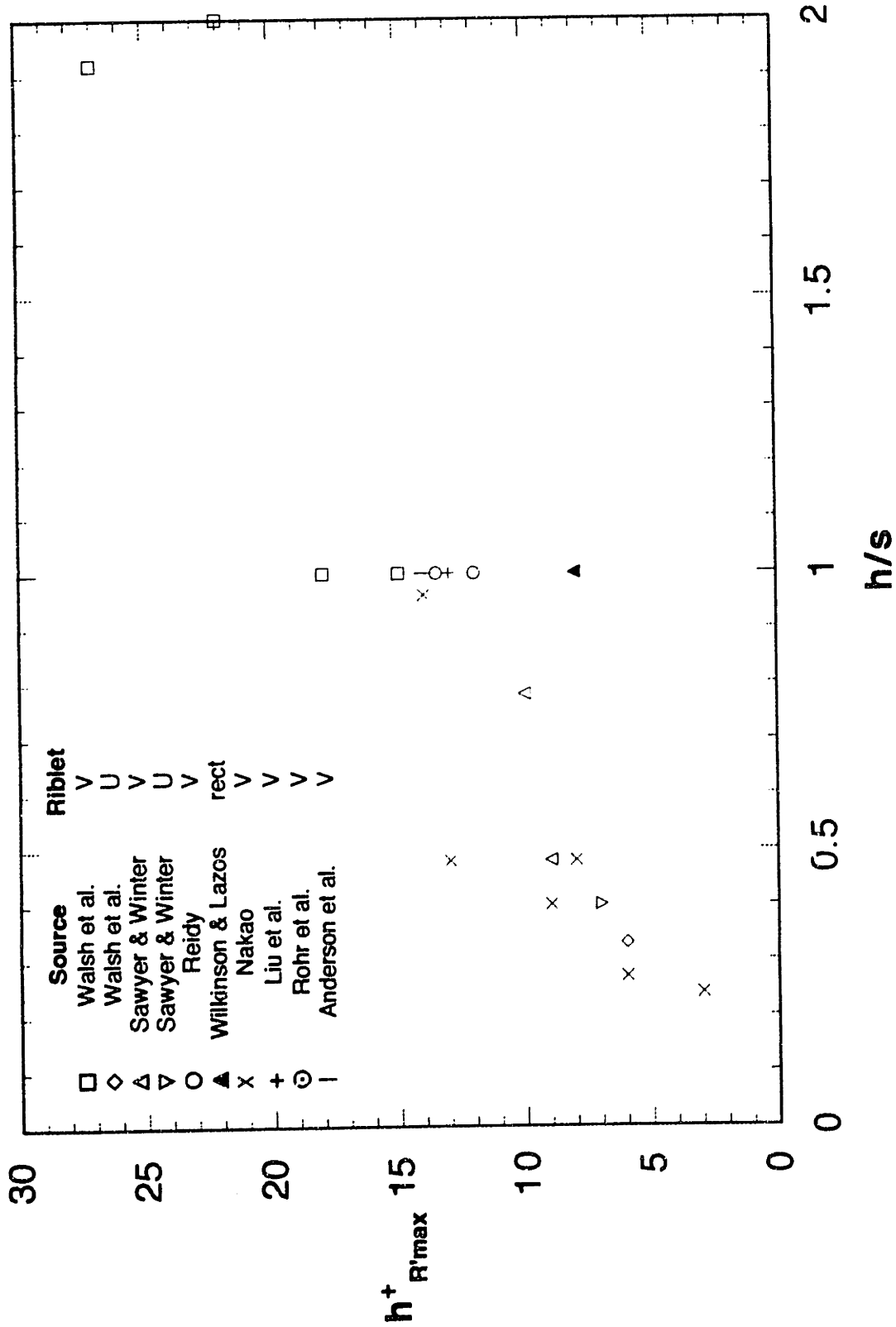


Figure 1.2.12 Variation of h^+ at R'_{max} , with aspect ratio, h/s .

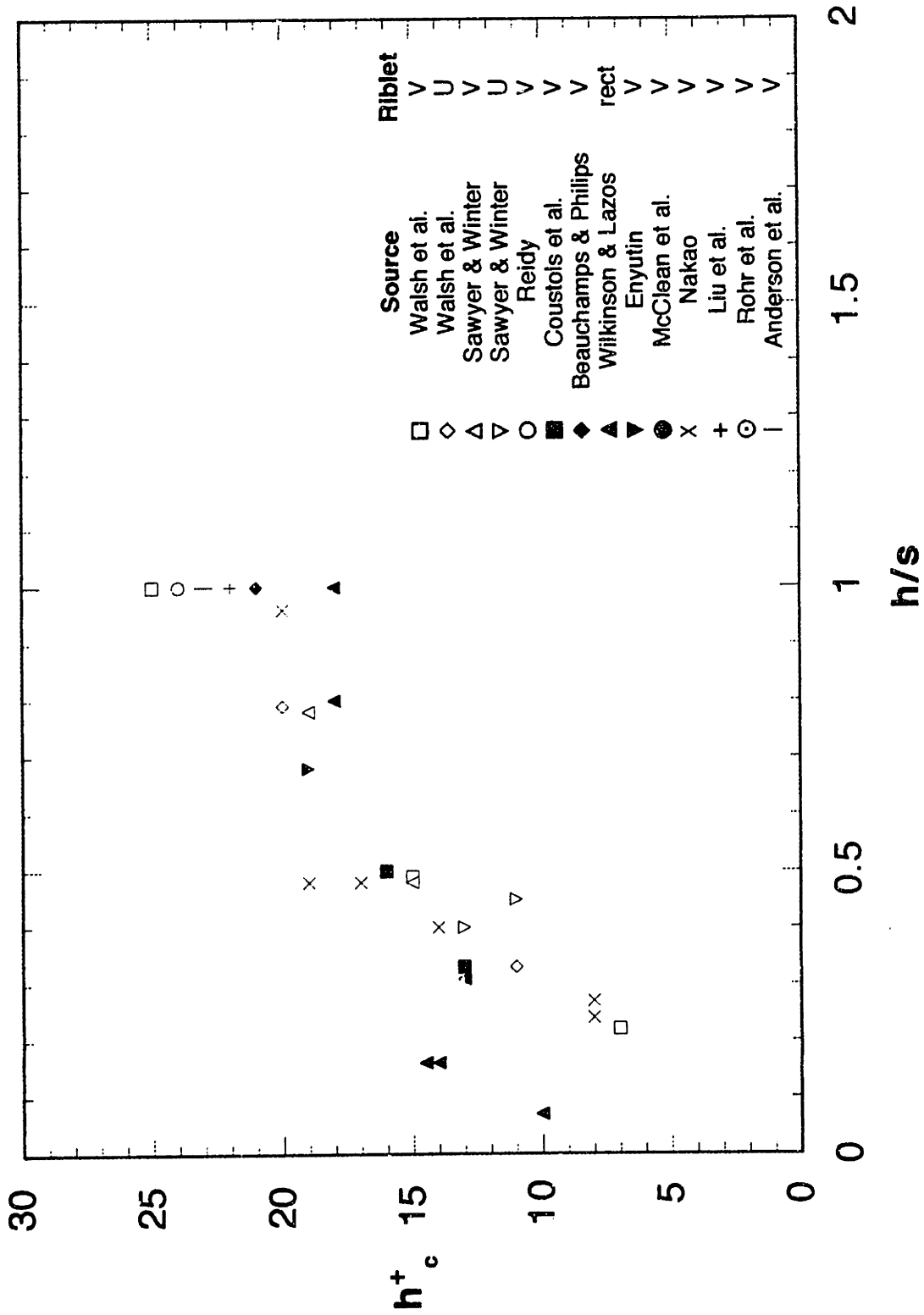


Figure 1.2.13 Variation of h_c^+ with aspect ratio, h/s .

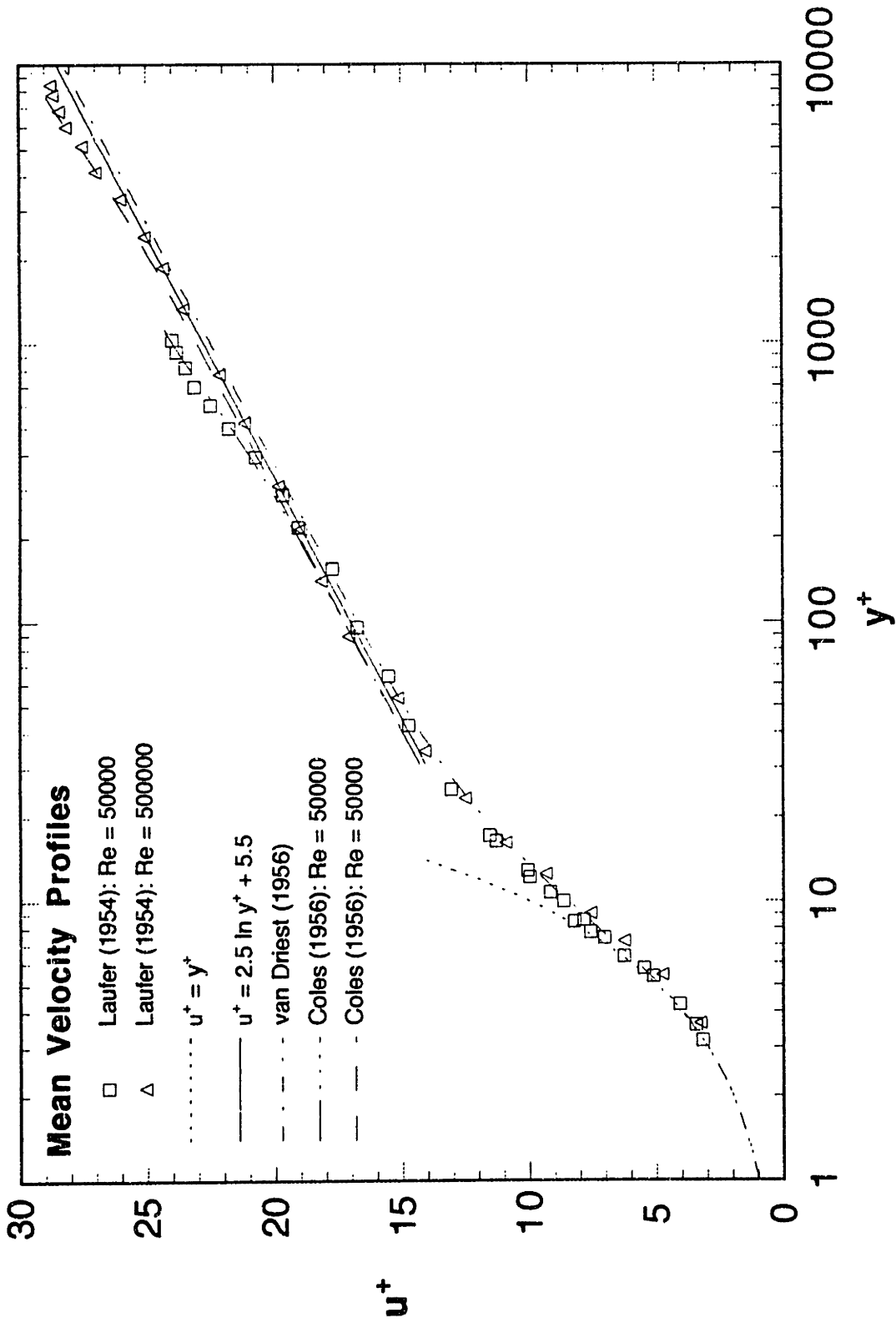


Figure 1.2.14 Turbulent, Newtonian, mean velocity profiles

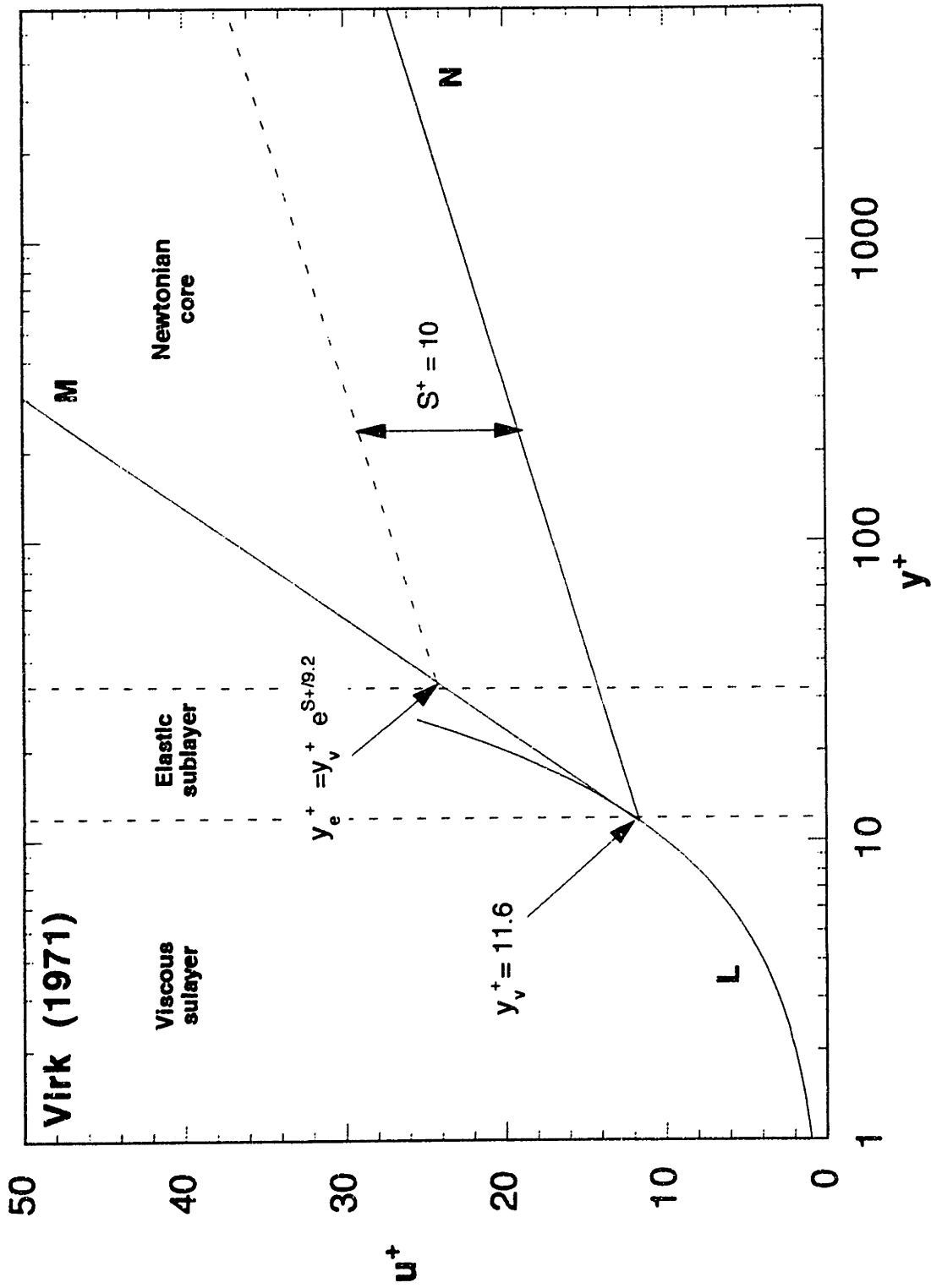


Figure 1.2.15 Three-zone mean velocity profile model for the flow of dilute polymer solutions (Virk, 1971)

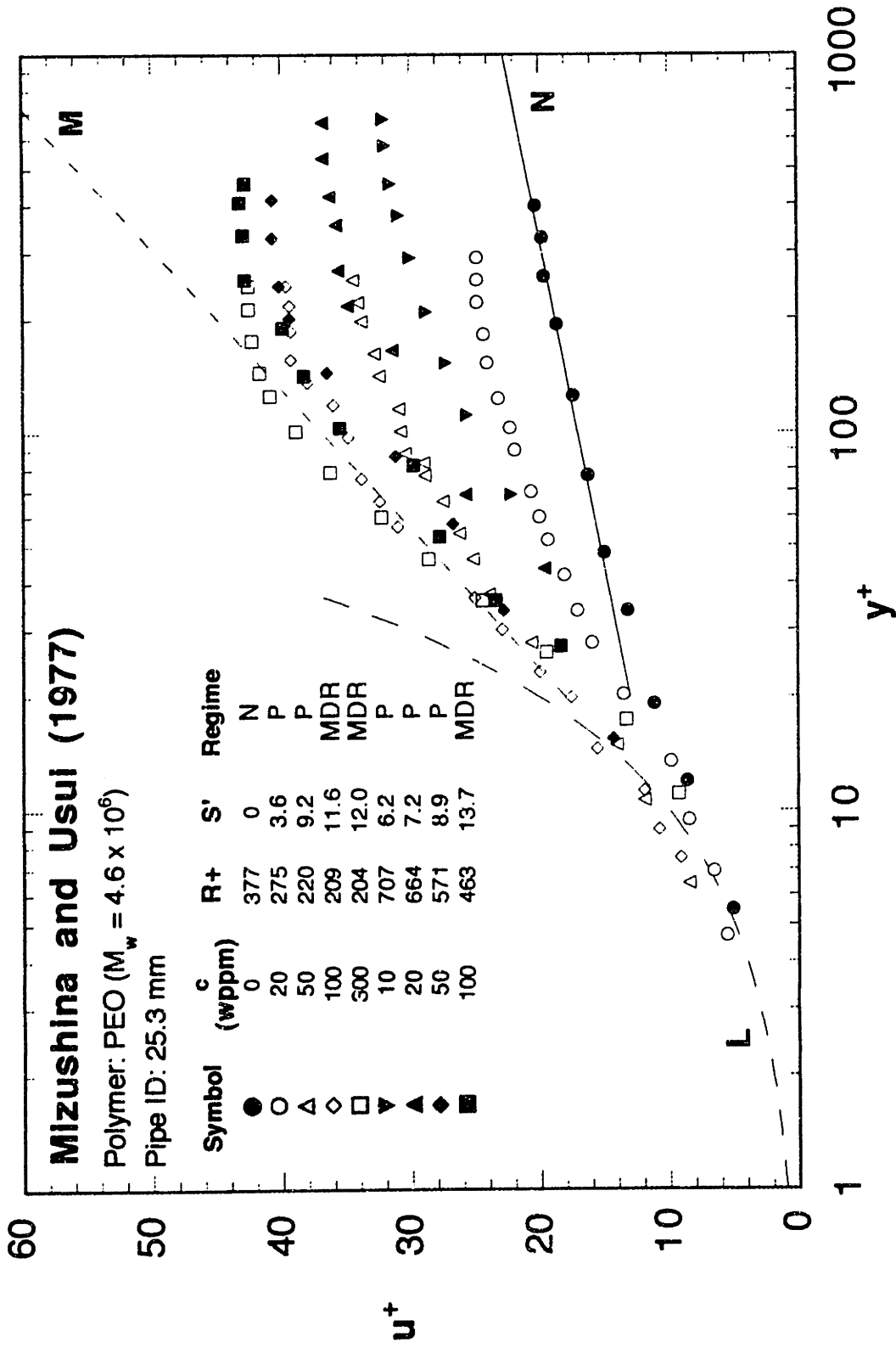


Figure 1.2.16 Mean velocity profiles for the flow of dilute polymer solutions (Mizushina and Usui, 1977)

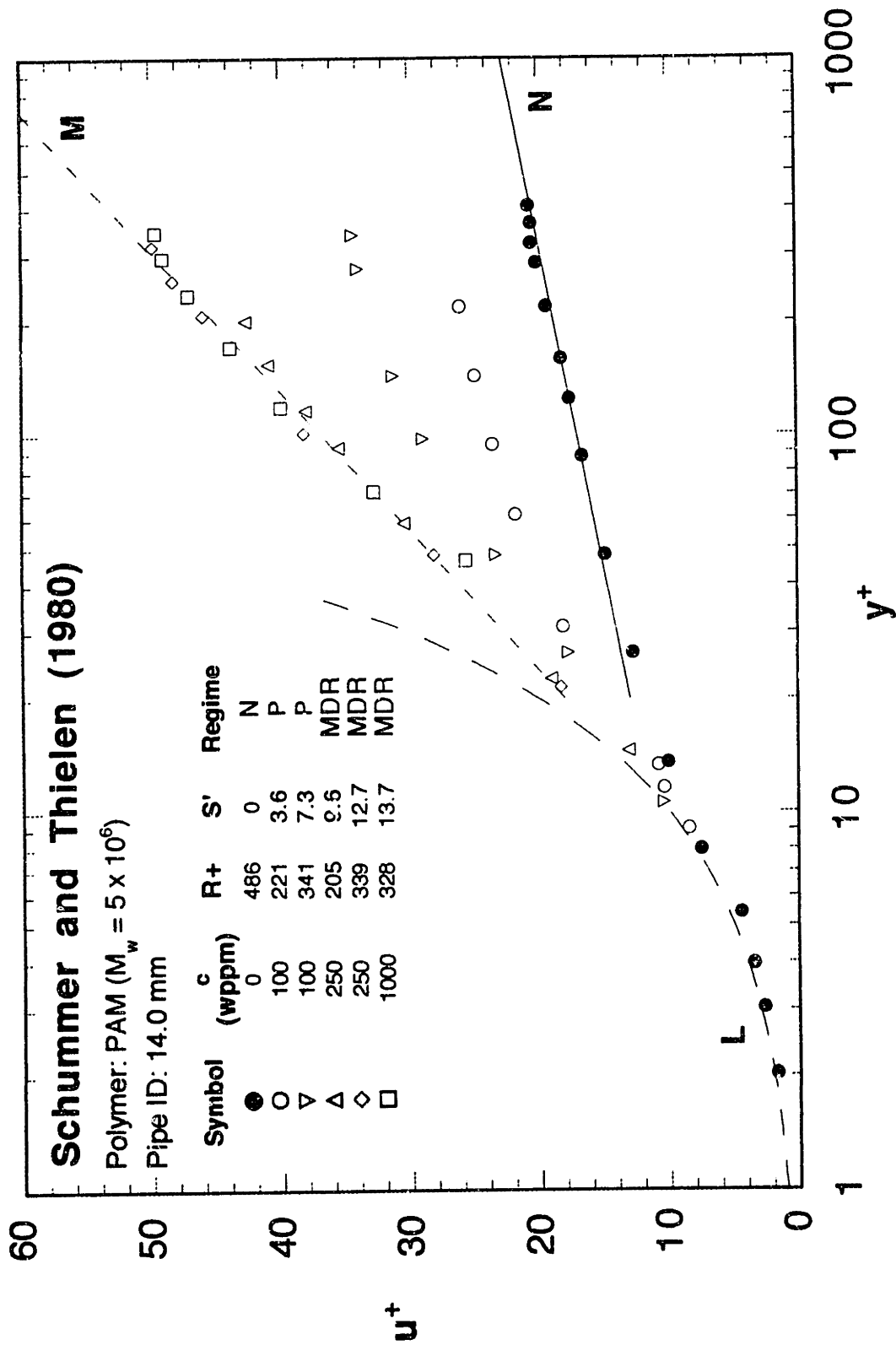


Figure 1.2.17 Mean velocity profiles for the flow of dilute polymer solutions (Schummer and Thielen, 1980)

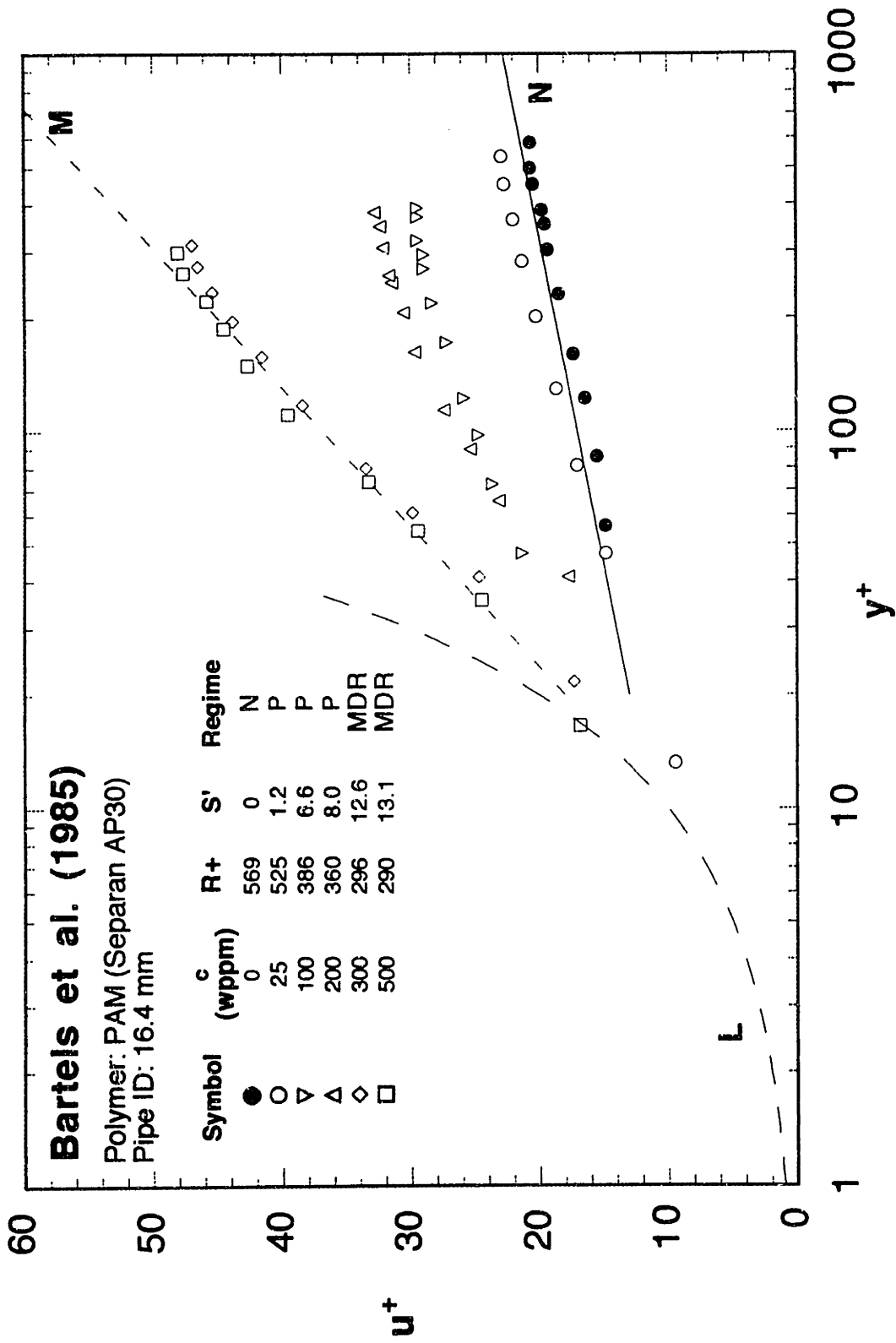


Figure 1.2.18 Mean velocity profiles for the flow of dilute polymer solutions (Bartels et al., 1985)

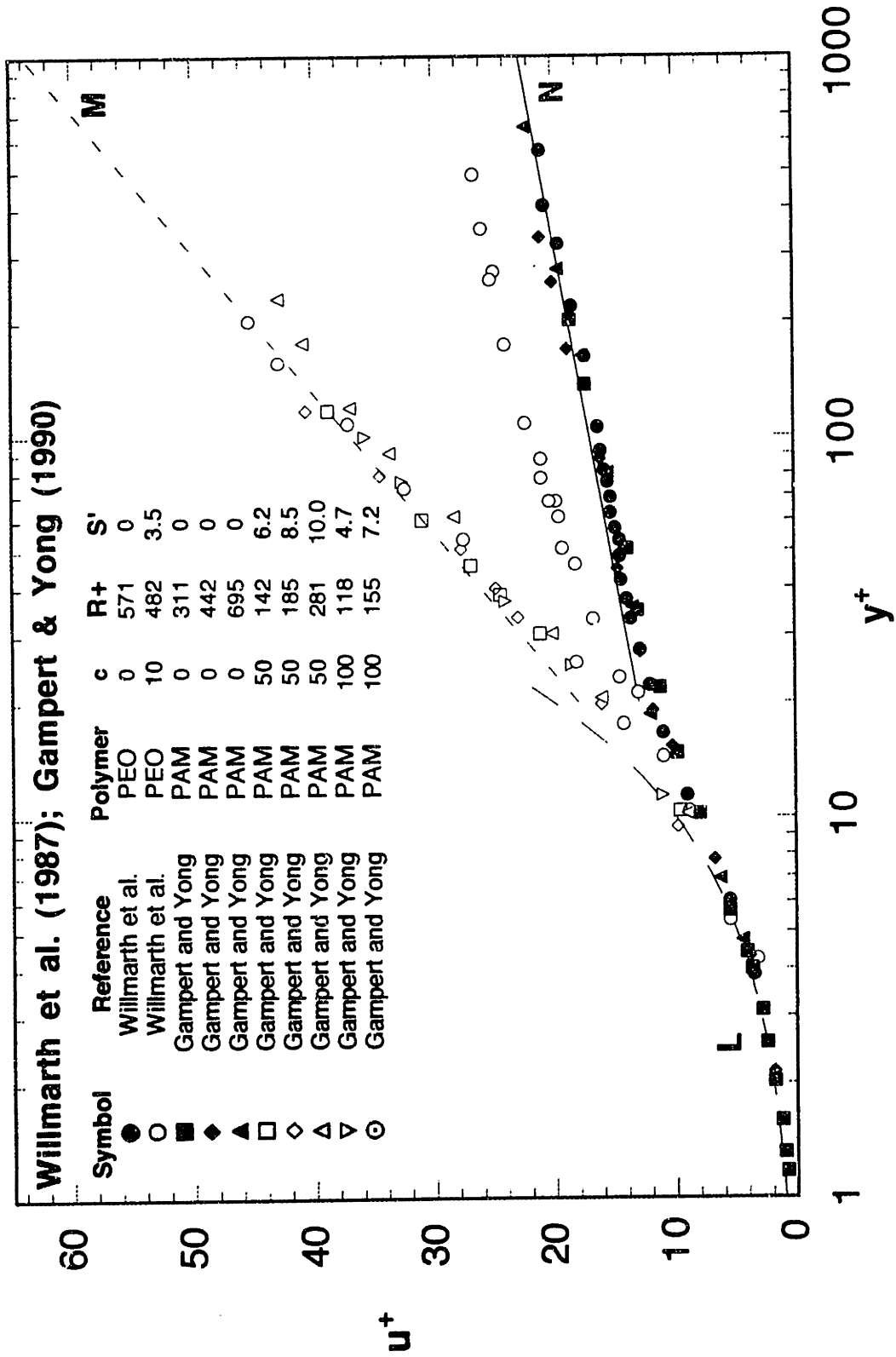


Figure 1.2.19 Mean velocity profiles for the flow of dilute polymer solutions (Willmarth et al., 1987 and Gampert and Yong, 1990)

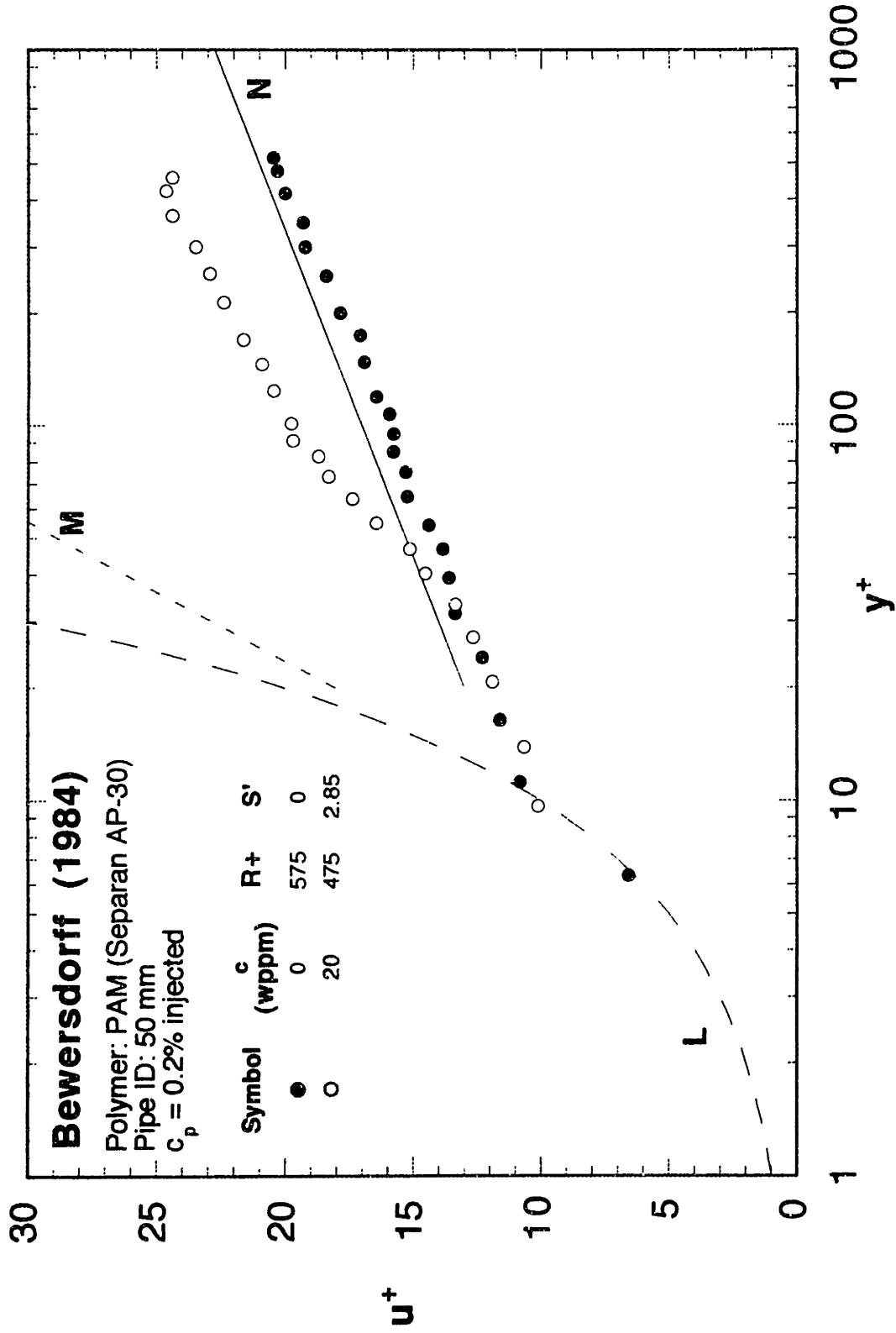


Figure 1.2.20 Mean velocity profile for the flow of centerline injected 0.2% polymer solution (Bewersdorff, 1984)

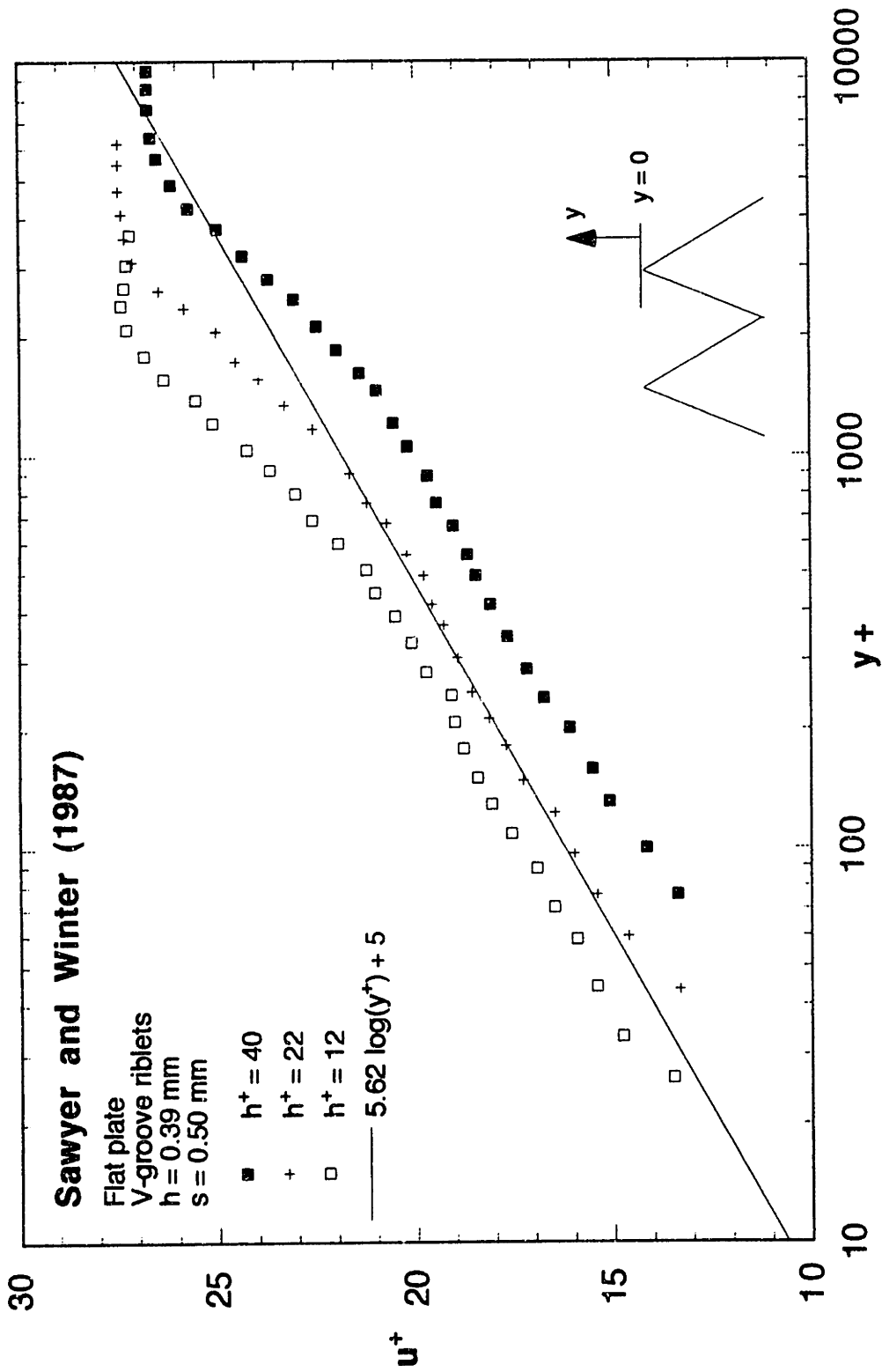


Figure 1.2.21 Mean velocity profiles for Newtonian flow over riblets (Sawyer and Winter, 1987)

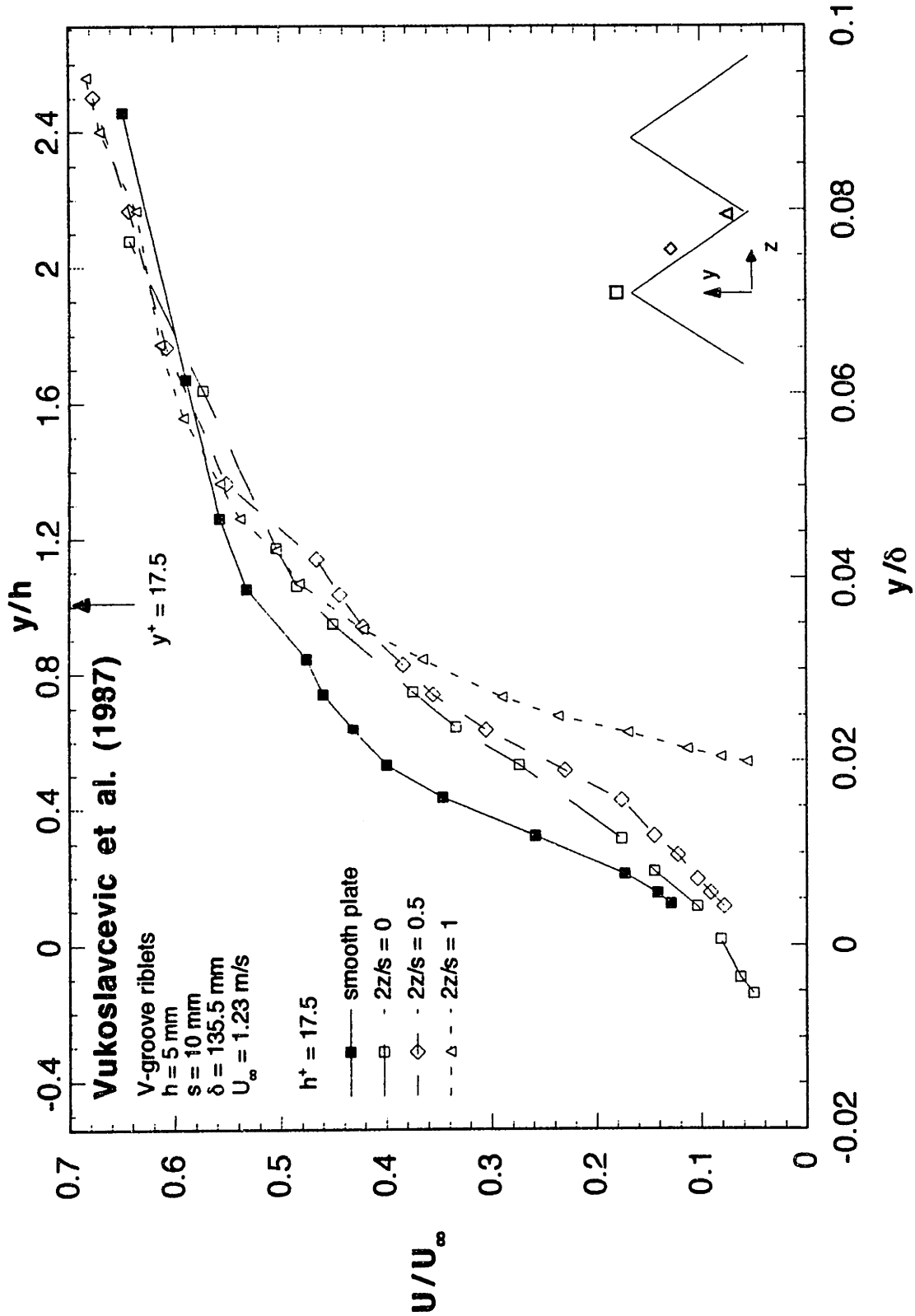


Figure 1.2.22 Mean velocity profiles for Newtonian flow over riblets (Wallace, 1987)

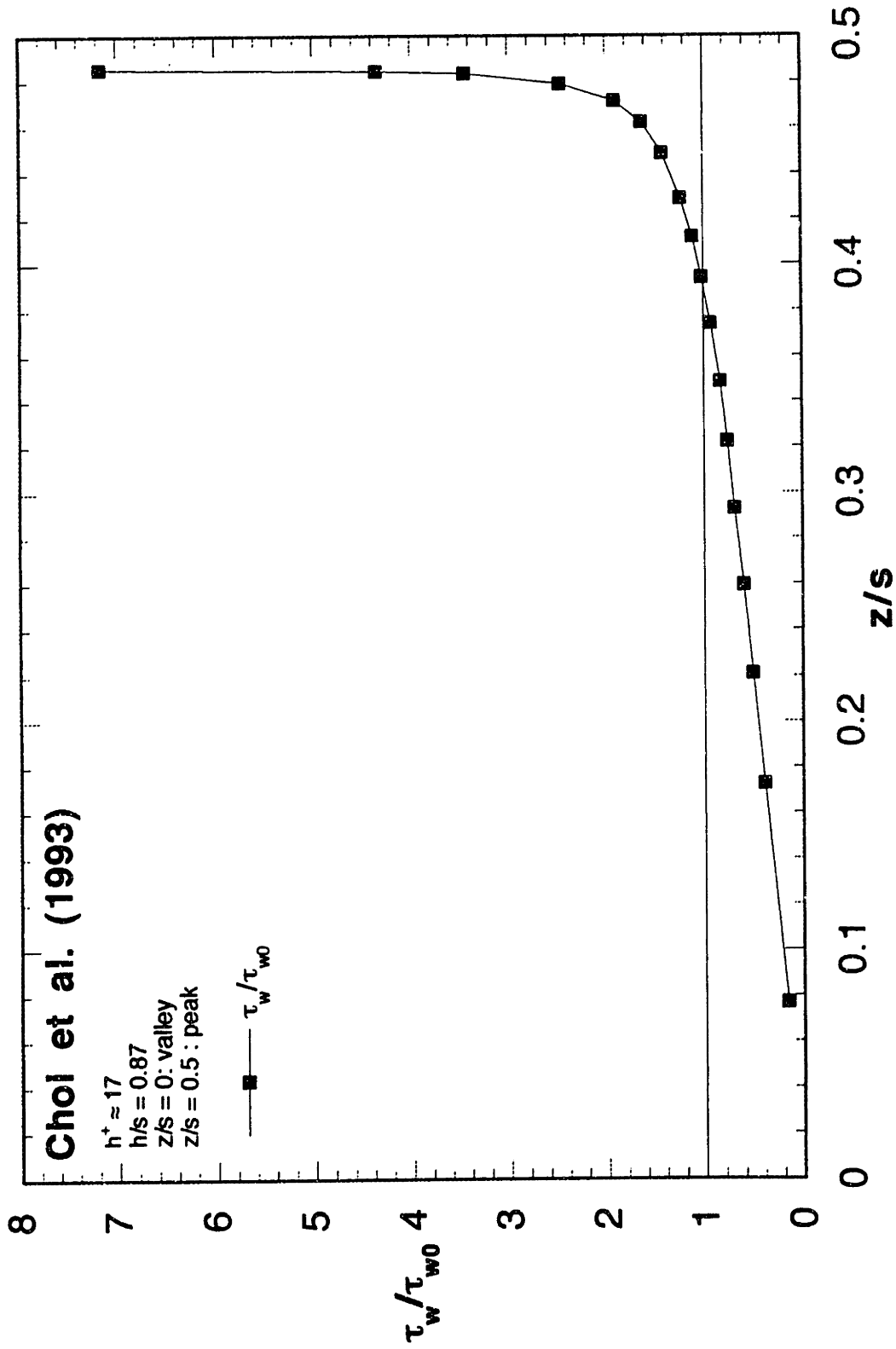


Figure 1.2.23 Calculated spanwise variation of shear stress on V-groove riblet surface (Choi et al., 1993)

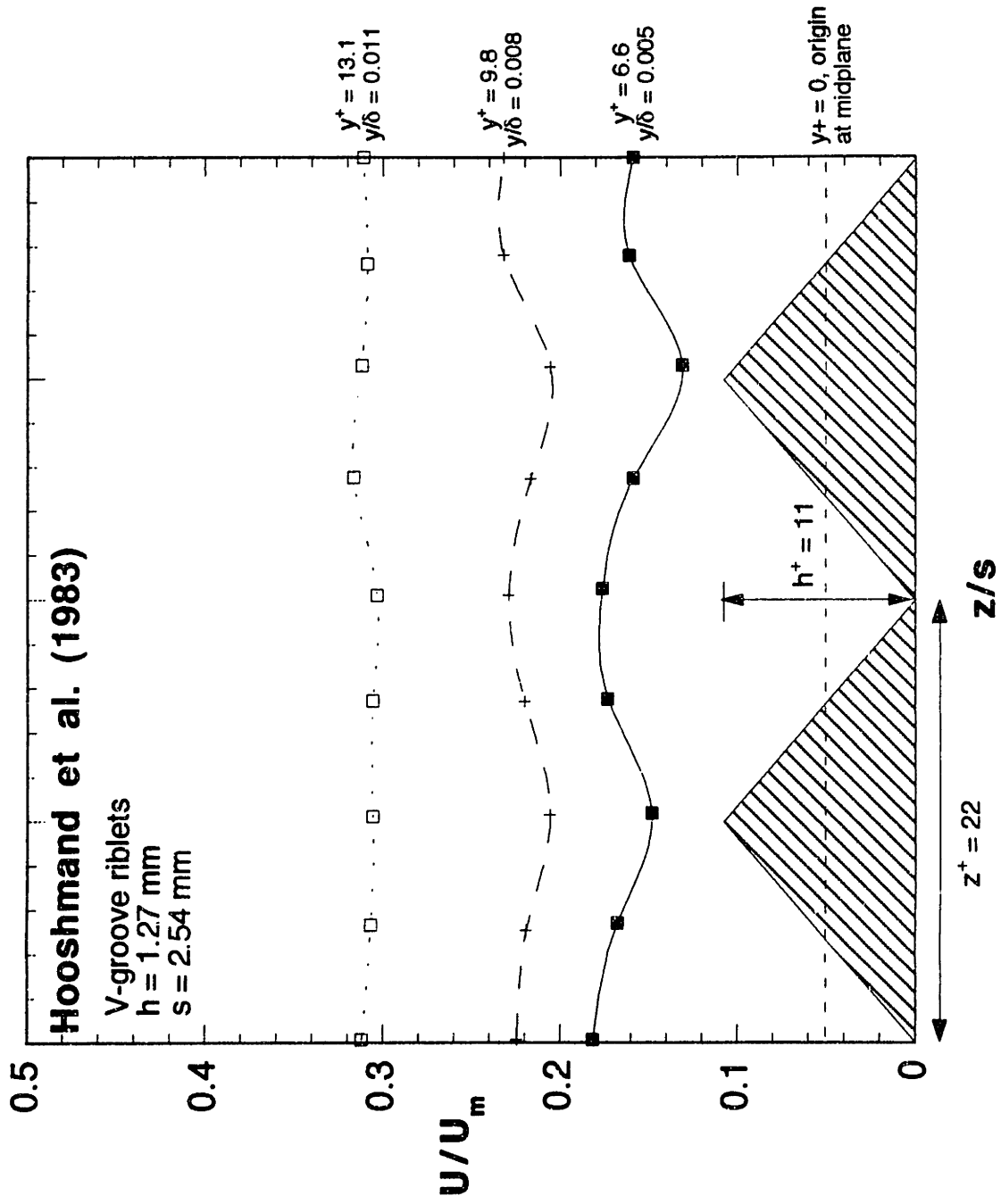


Figure 1.2.24 Spanwise variation of the mean velocity over a V-groove riblet surface (Hooshmand et al., 1983)

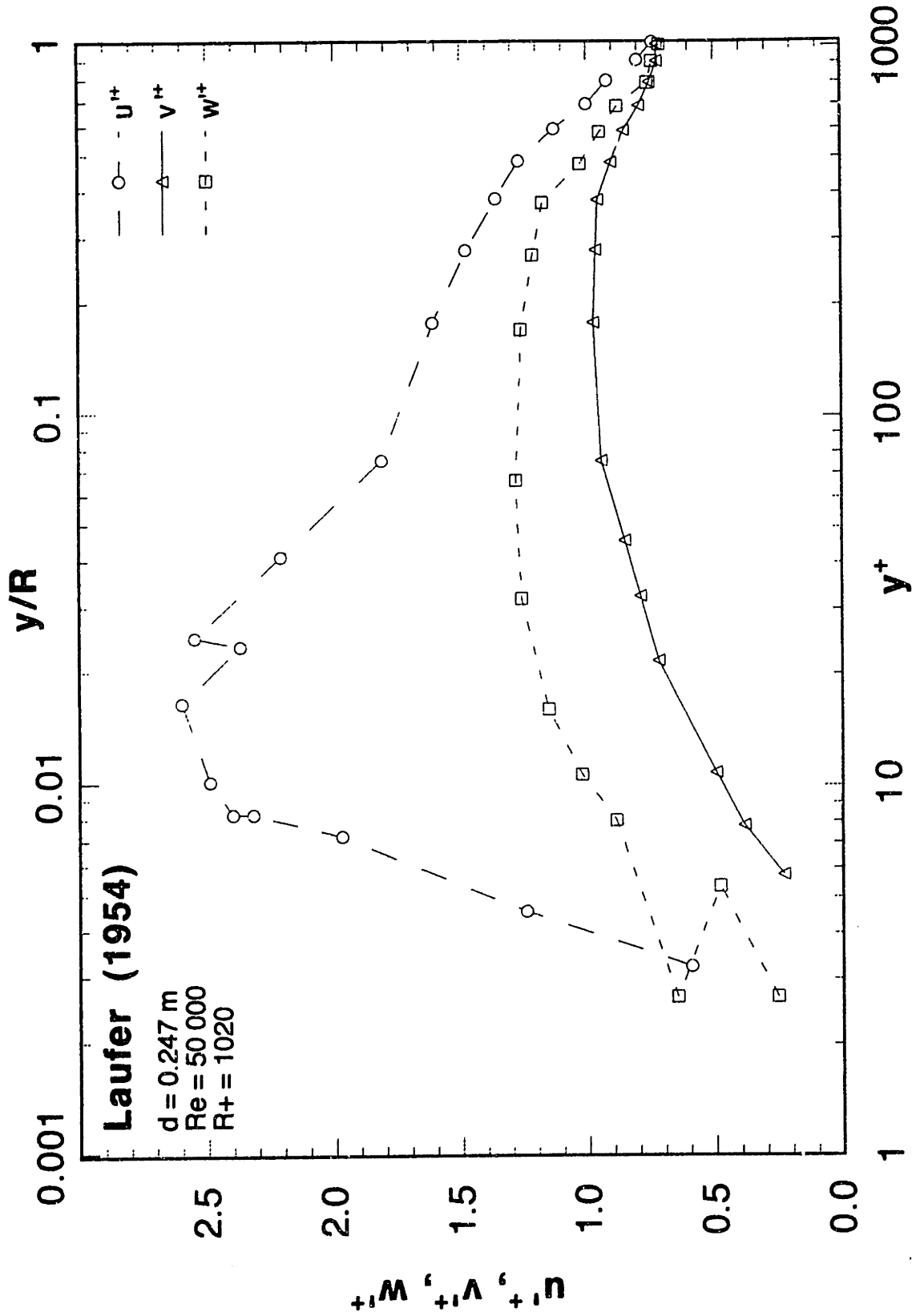


Figure 1.2.25 Newtonian, turbulent intensity profiles in pipe flow at $Re = 50,000$ (Laufer, 1954)

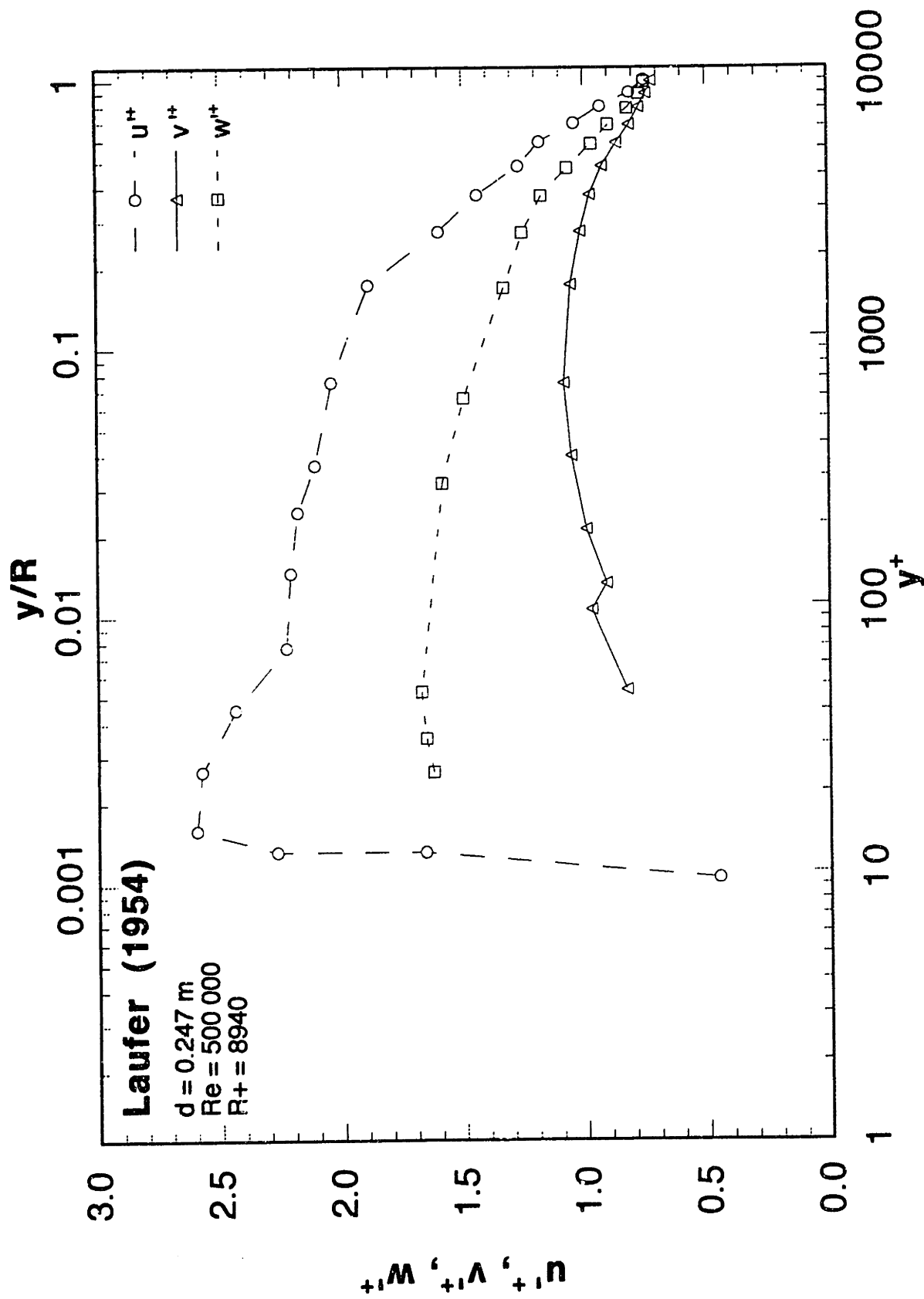


Figure 1.2.26 Newtonian, turbulent intensity profiles in pipe flow at $Re = 500,000$ (Laufer, 1954)

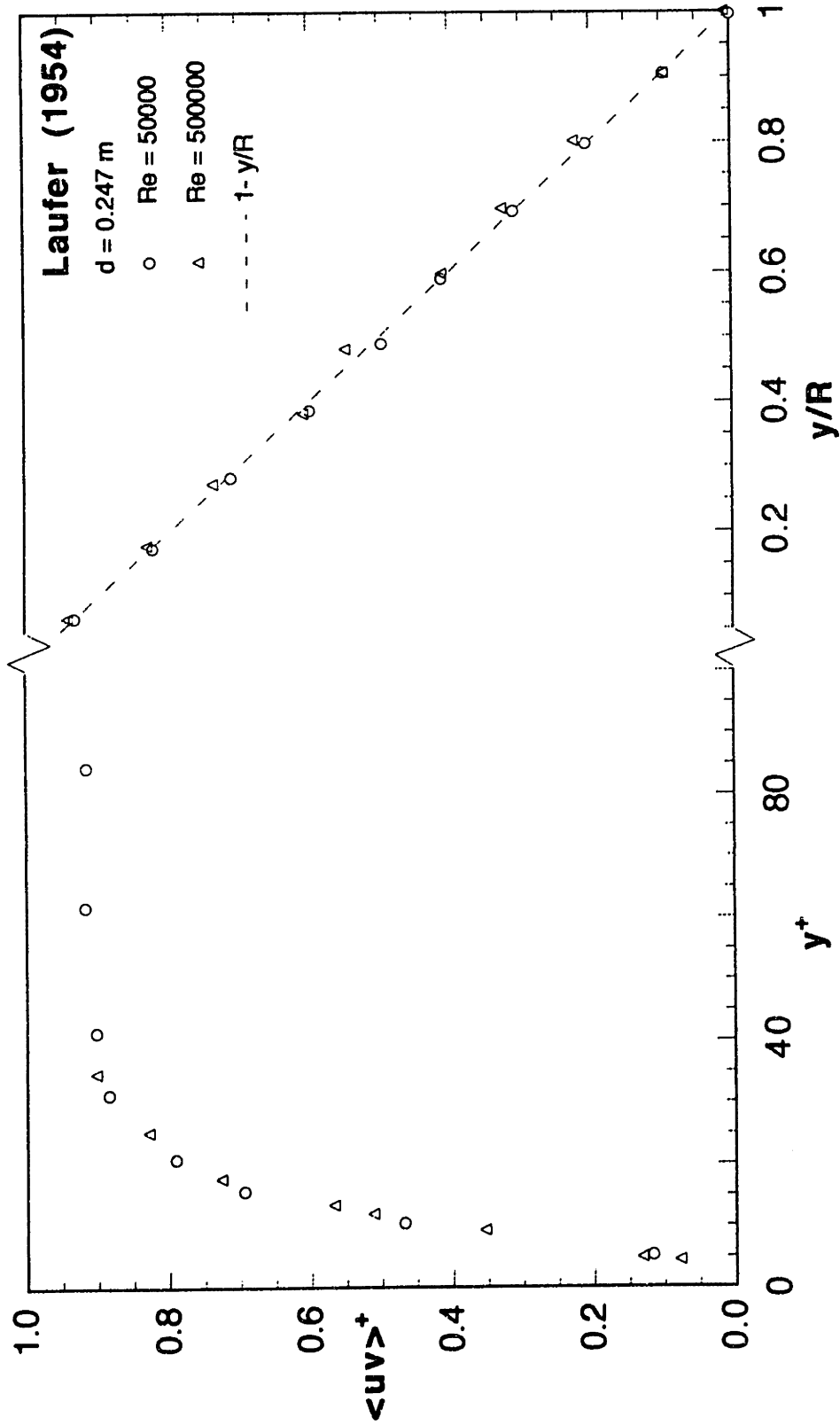


Figure 1.2.27 Newtonian, turbulent Reynolds stress profiles in pipe flow at $Re = 50,000$ and $500,000$ (Laufer, 1954)

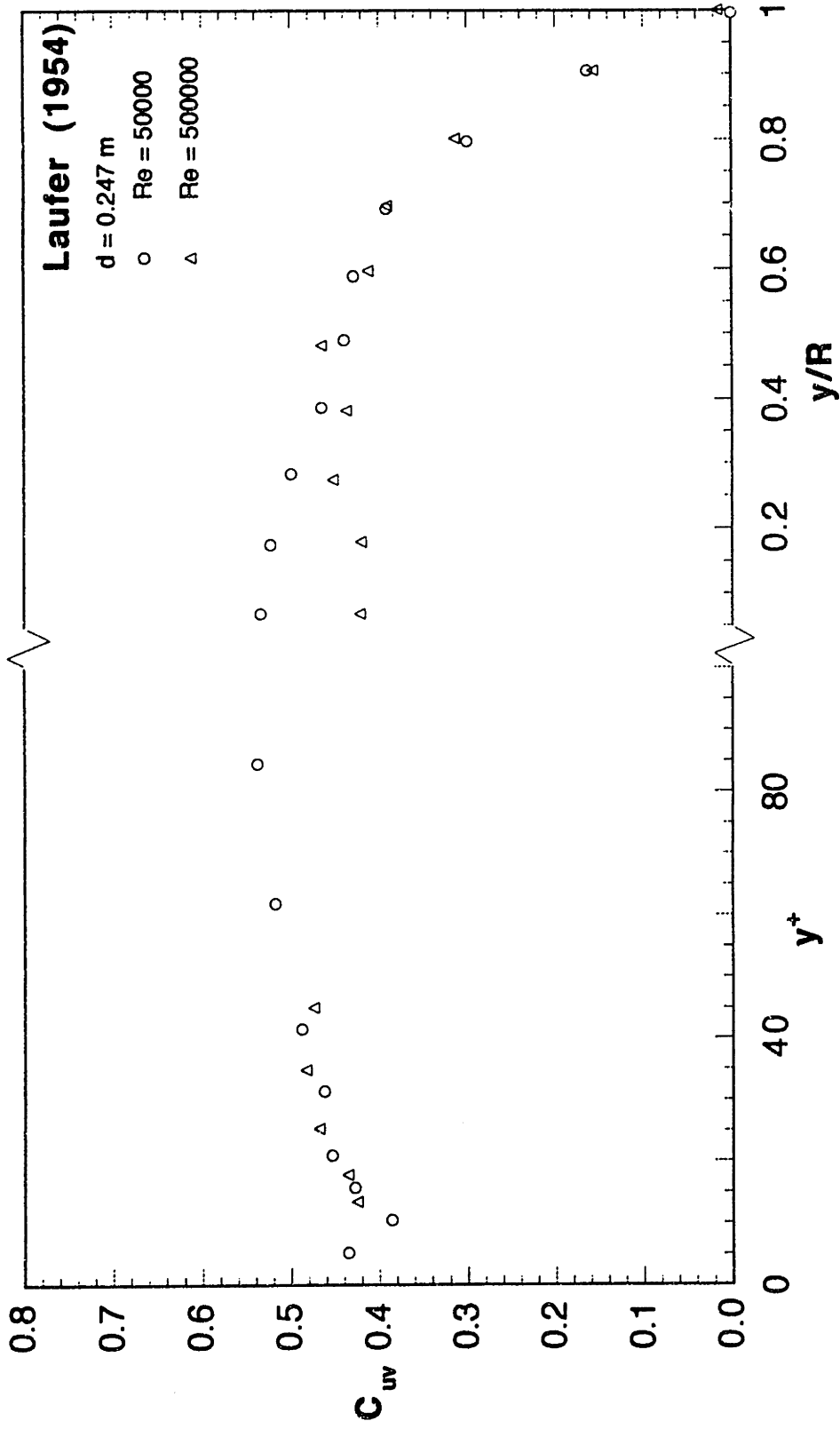
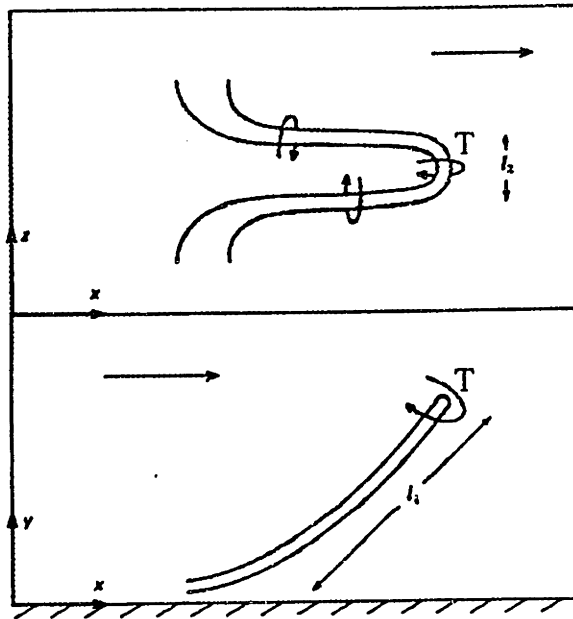
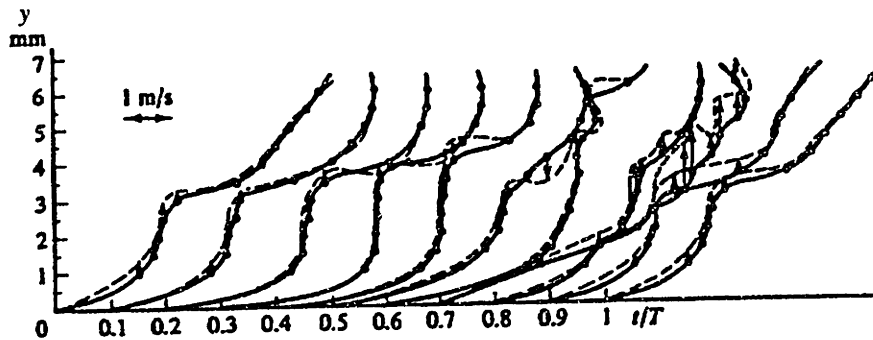


Figure 1.2.28 u-v correlation coefficient in pipe flow at $Re = 50,000$ and $500,000$ (Laufer, 1954)

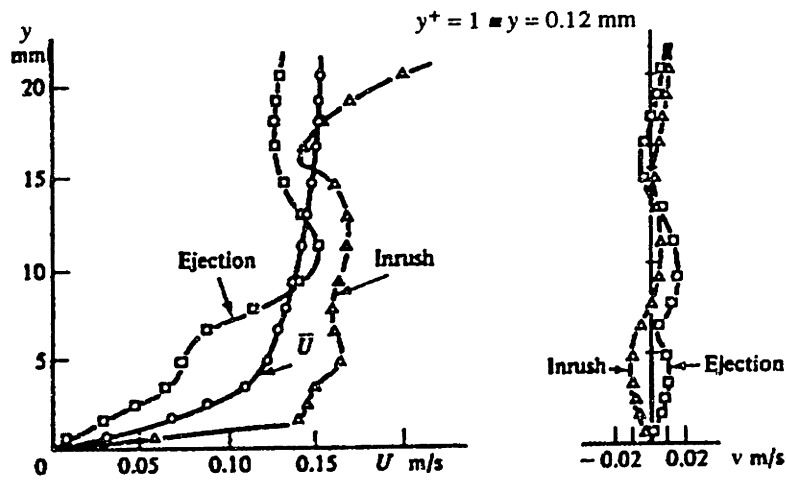


(a) A horseshoe vortex: model of coherent structure in turbulent boundary layers (Tritton, 1988)

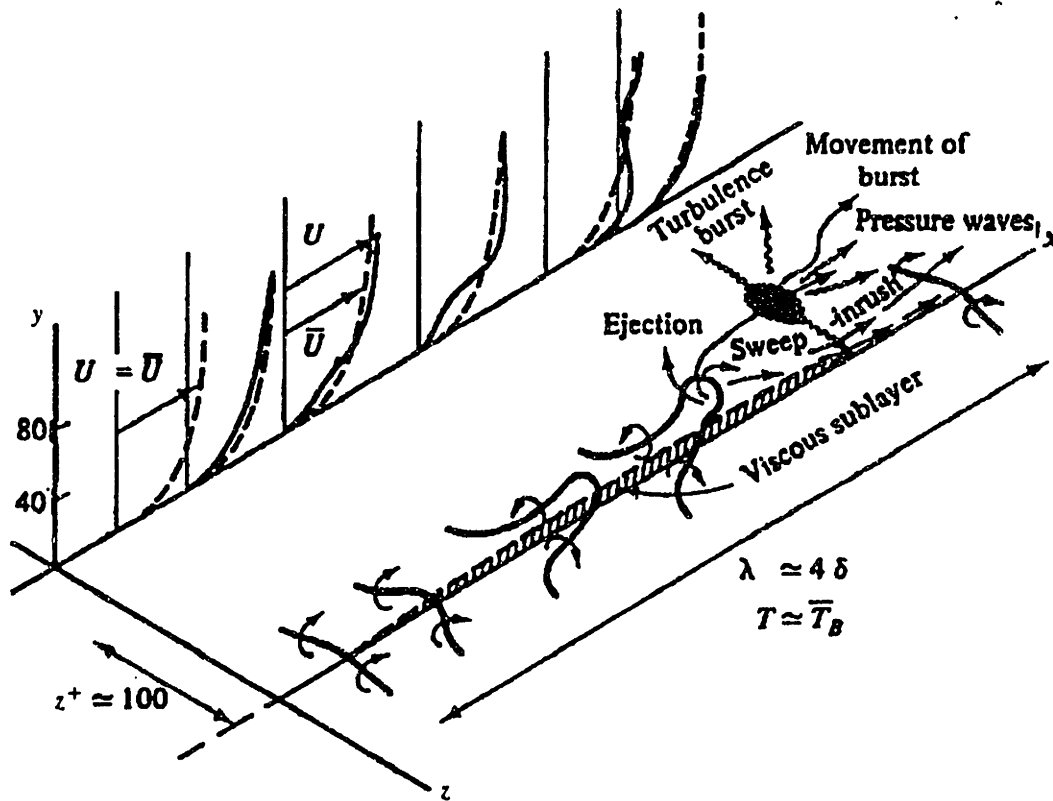


(b) Measured instantaneous velocity profiles during one cycle, T . $U_0 = 7.7$ m/s; $\delta \approx 6$ mm; $T = 0.015$ s (Muiswinkel - unpublished, Hinze, 1975)

Figure 1.2.29 Aspects of the structure of turbulence



(c) Instantaneous lateral distributions of U and v during an ejection and inrush phase (Grass, 1972)



(d) Conceptual model of the turbulence near the wall during a "cyclic" process (Hinze, 1975)

Figure 1.2.29 Aspects of the structure of turbulence

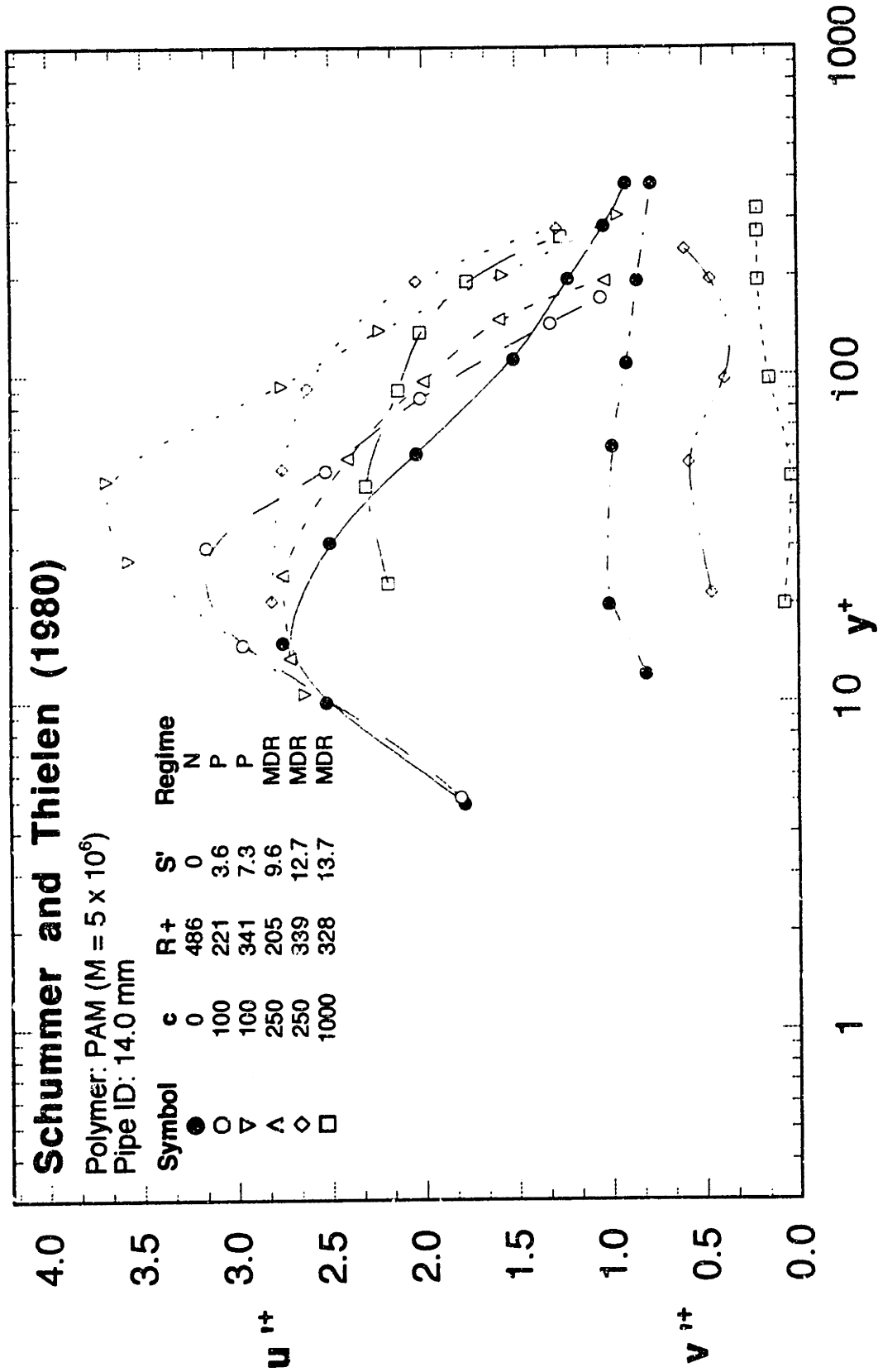


Figure 1.2.30 Axial and radial intensity profiles for the flow of dilute polymer solutions in a 14.0 mm ID pipe (Schummer and Thielen, 1980)

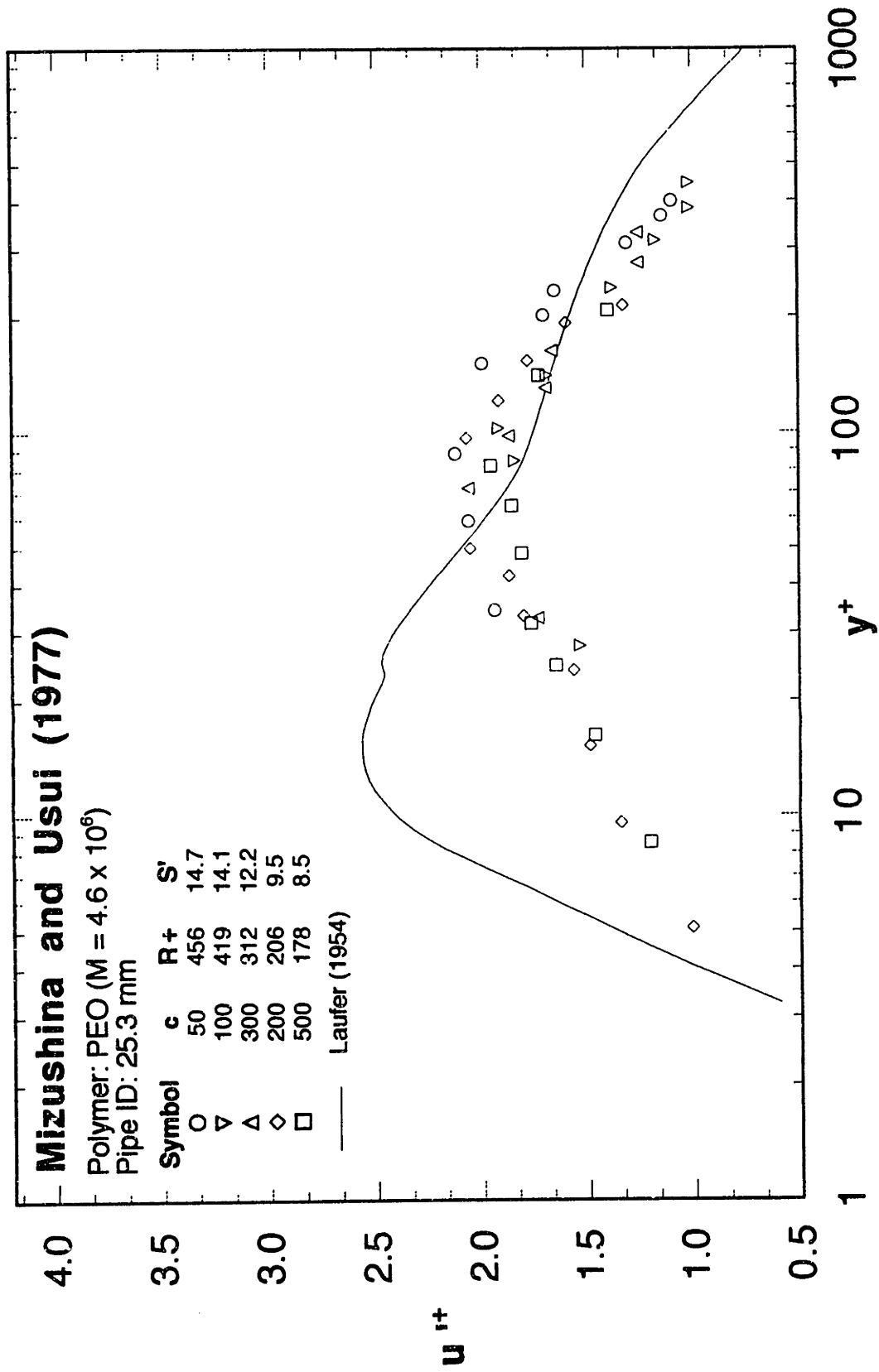


Figure 1.2.31 Axial intensity profiles for the flow of dilute polymer solutions in a 25.3 mm ID pipe at maximum drag reduction (Mizushima and Usui, 1977)

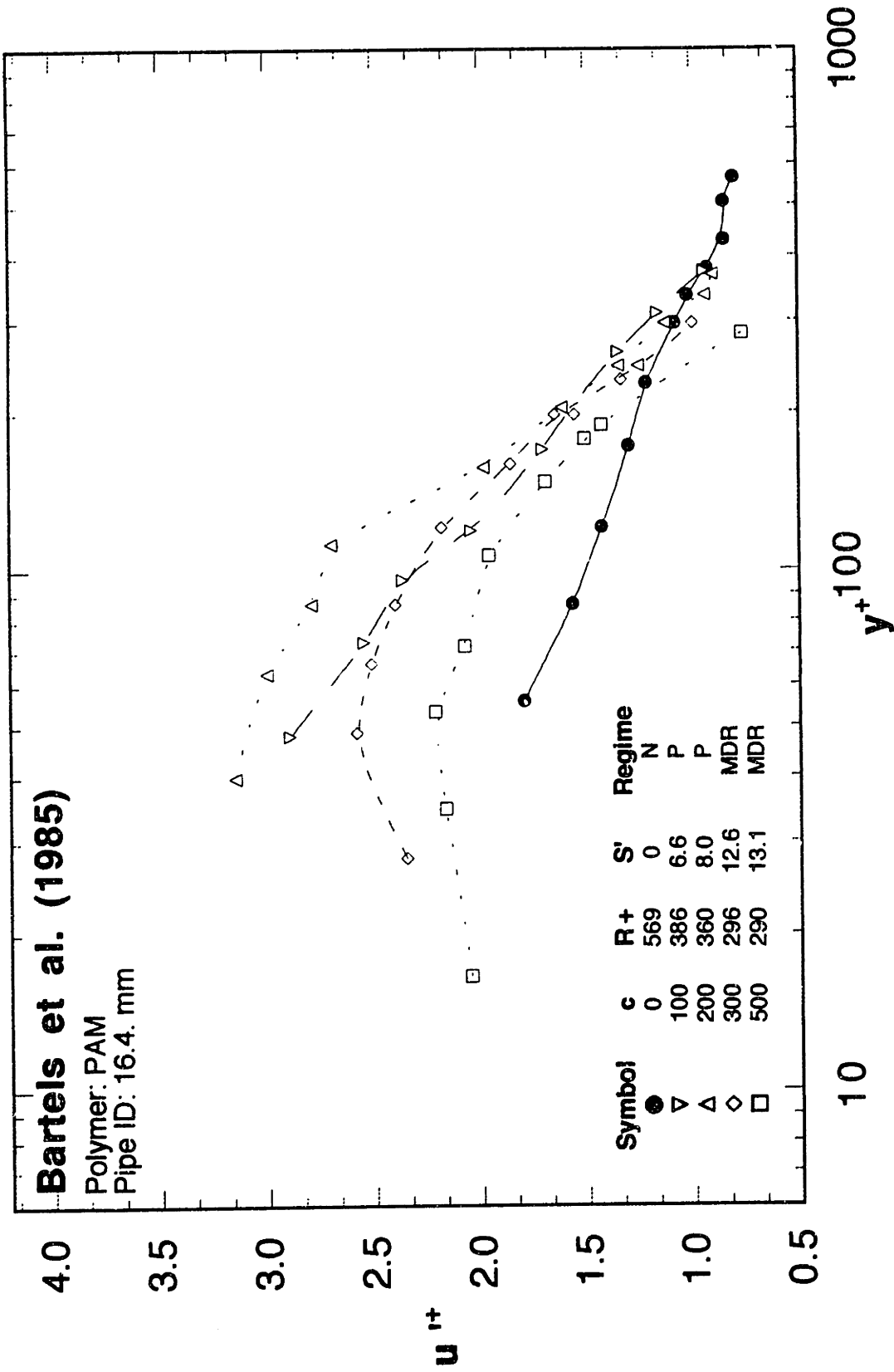


Figure 1.2.32 Axial intensity profiles for the flow of dilute polymer solutions in a 16.4 mm ID pipe (Bartels et al., 1985)

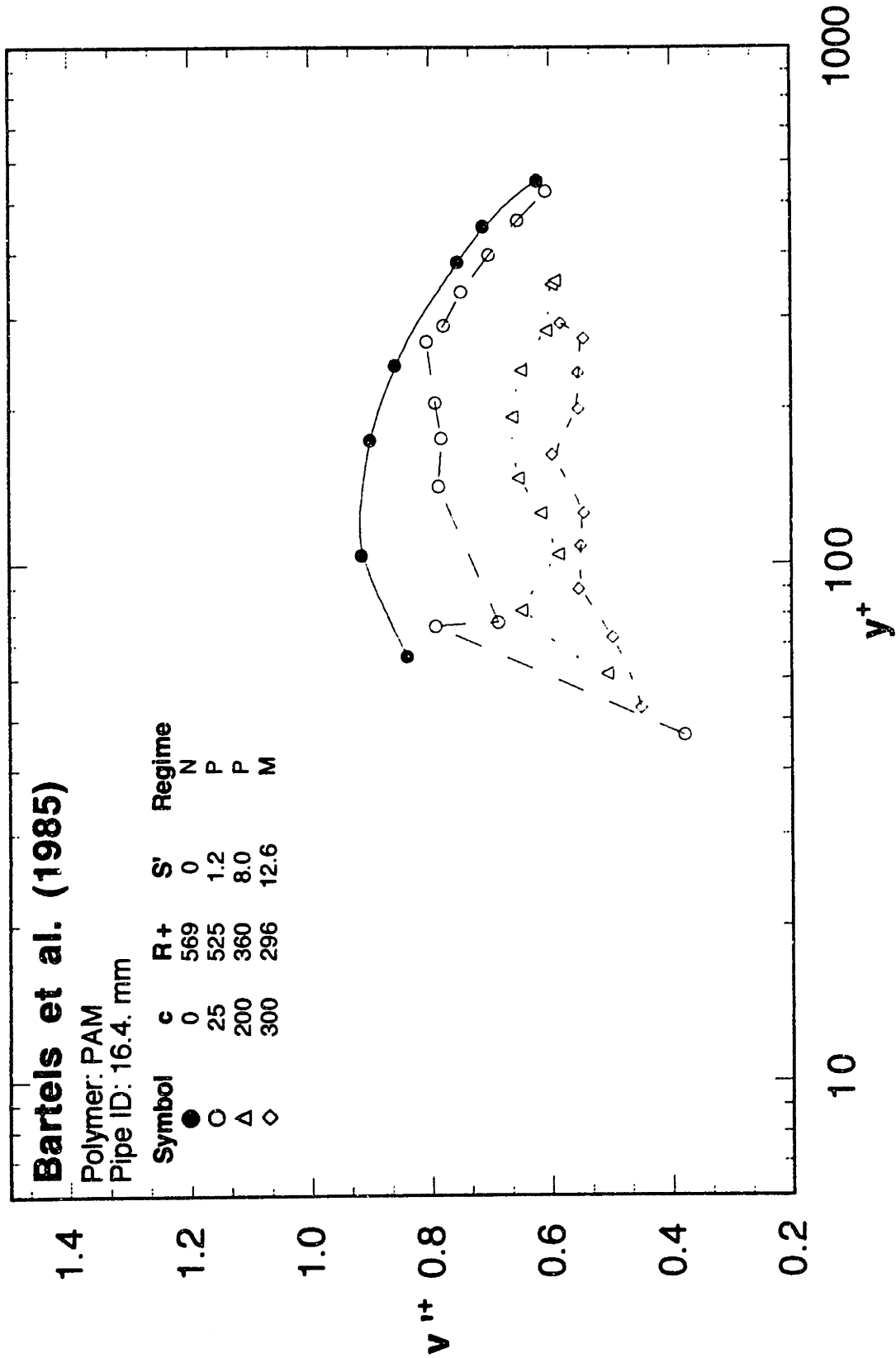


Figure 1.2.33 Radial intensity profiles for the flow of dilute polymer solutions in a 16.4 mm ID pipe (Bartels et al., 1985)

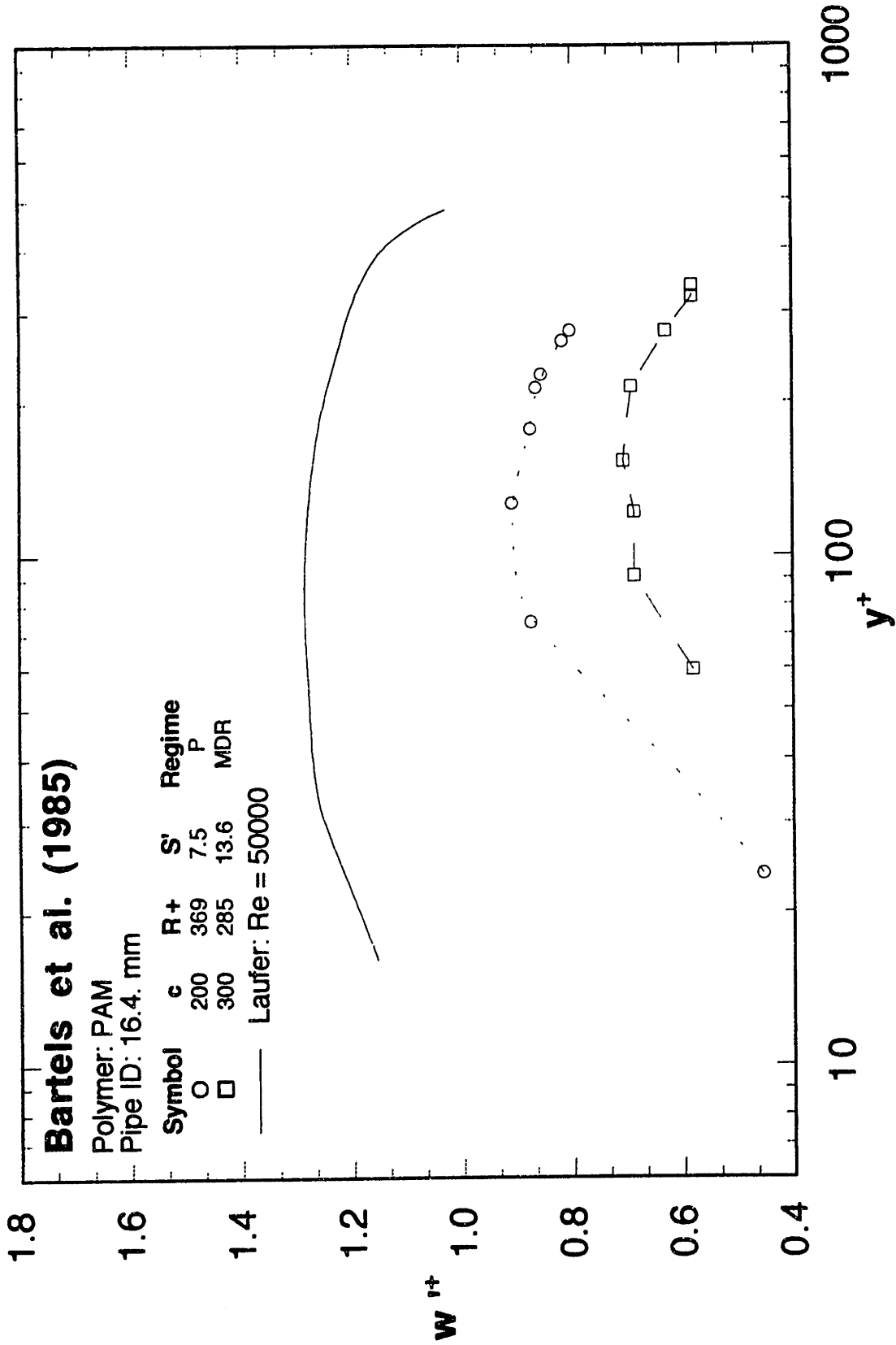


Figure 1.2.34 Tangential intensity profiles for the flow of dilute polymer solutions in a 16.4 mm ID pipe (Bartels et al., 1985)

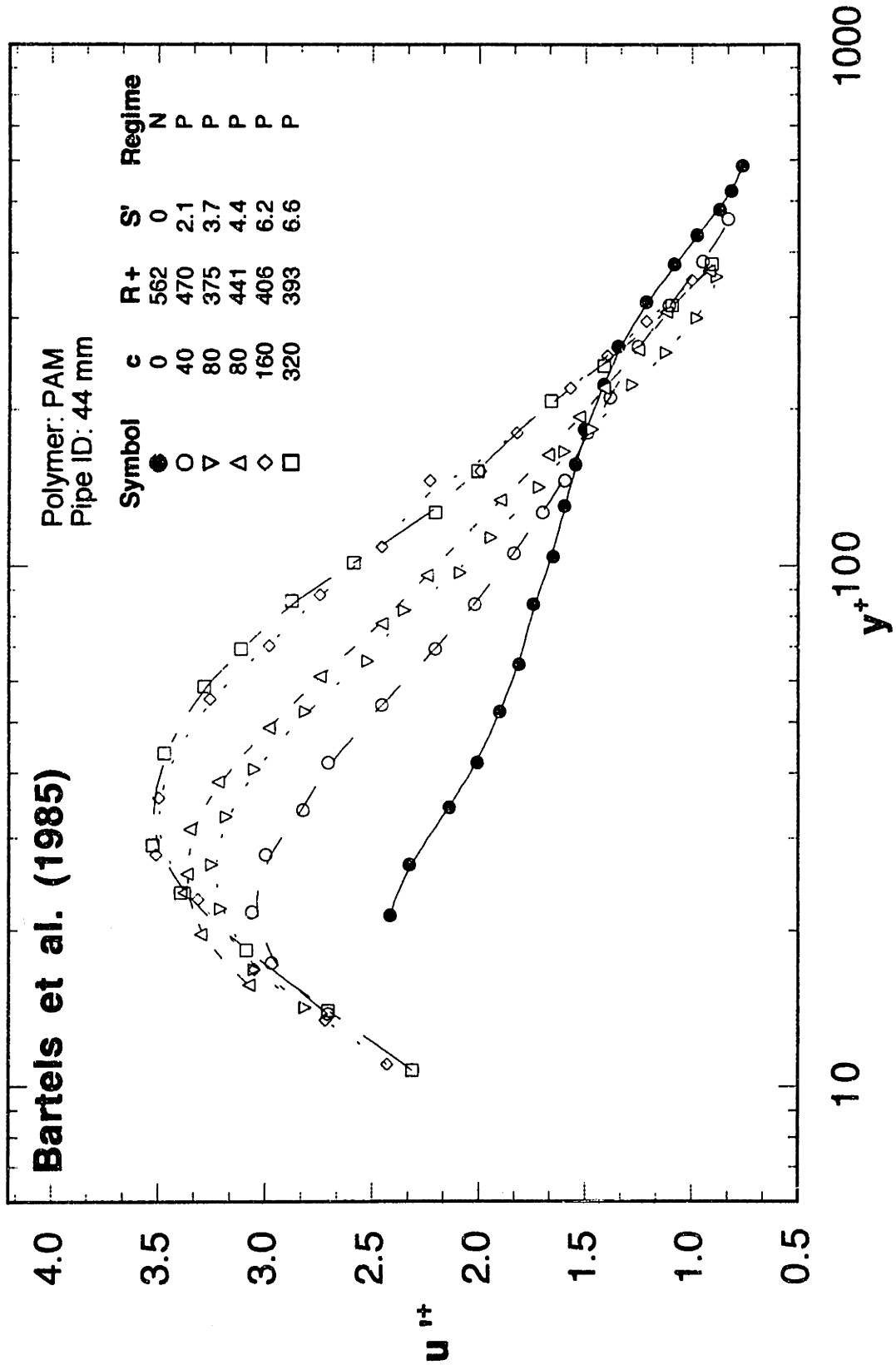


Figure 1.2.35 Axial intensity profiles for the flow of dilute polymer solutions in a 44 mm ID pipe (Bartels et al., 1985)

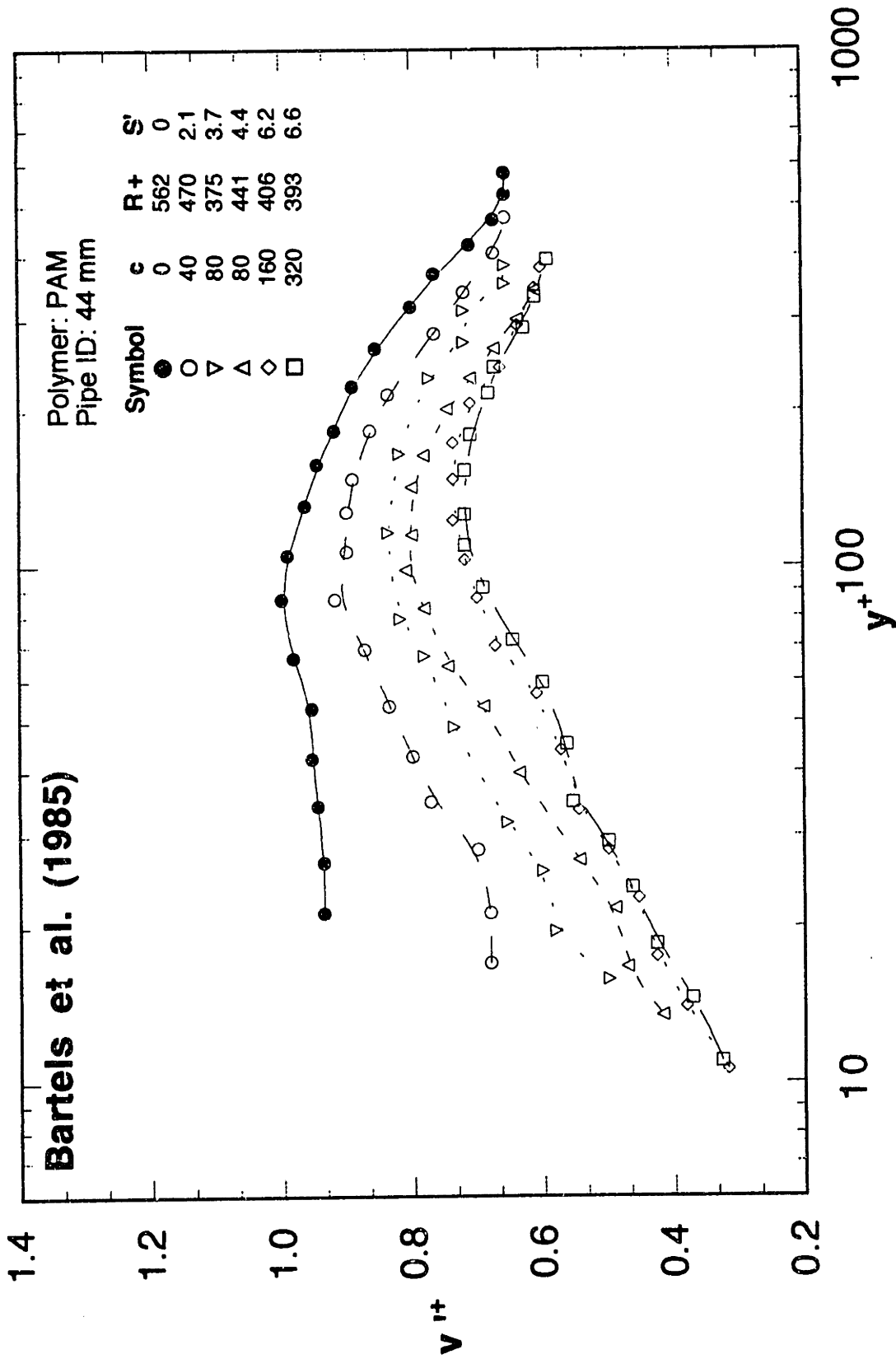


Figure 1.2.36 Radial intensity profiles for the flow of dilute polymer solutions in a 44 mm ID pipe (Bartels et al., 1985)

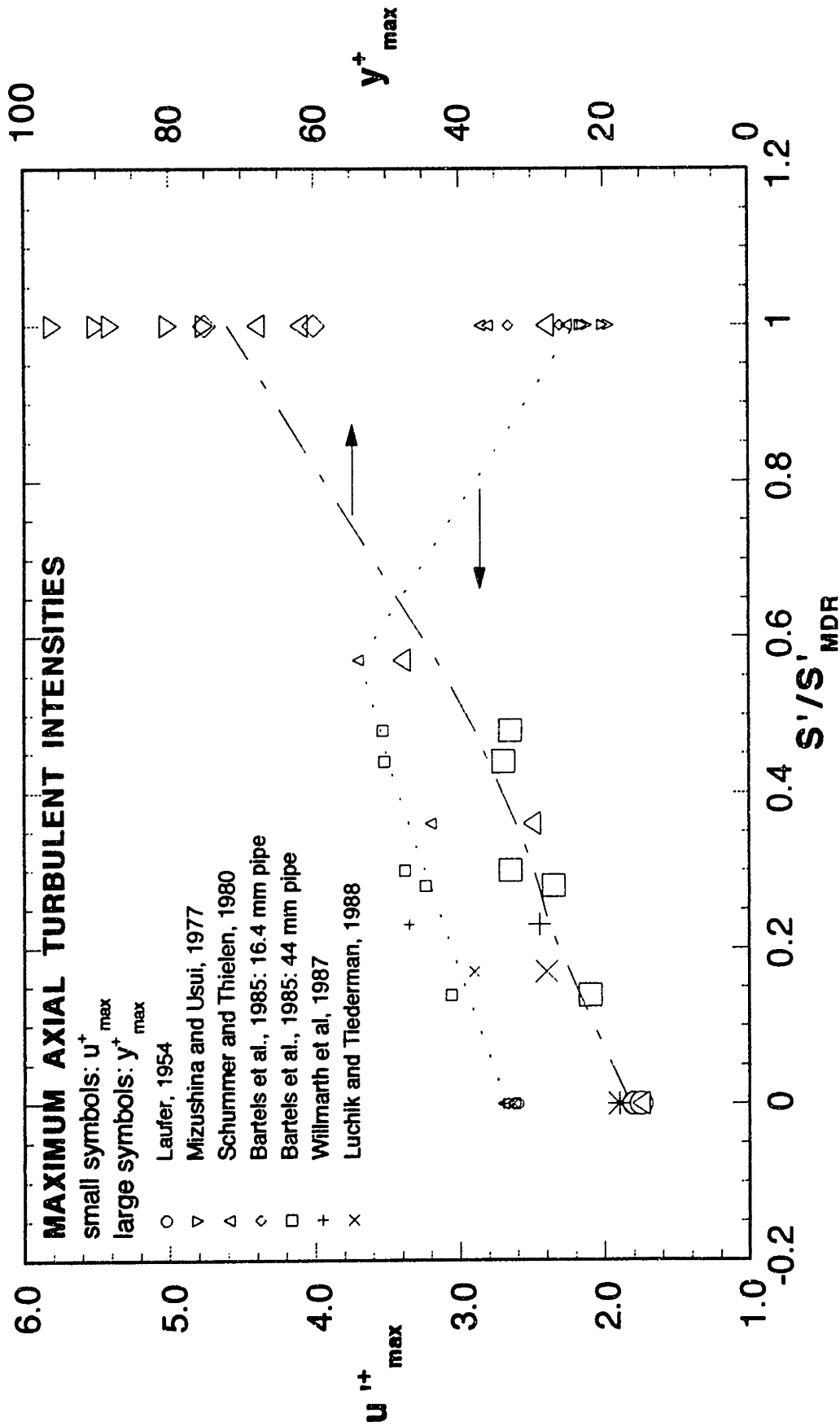


Figure 1.2.37 Variation of the magnitude and position of the maximum axial turbulent intensity with the extent of polymeric drag reduction relative to that at maximum drag reduction

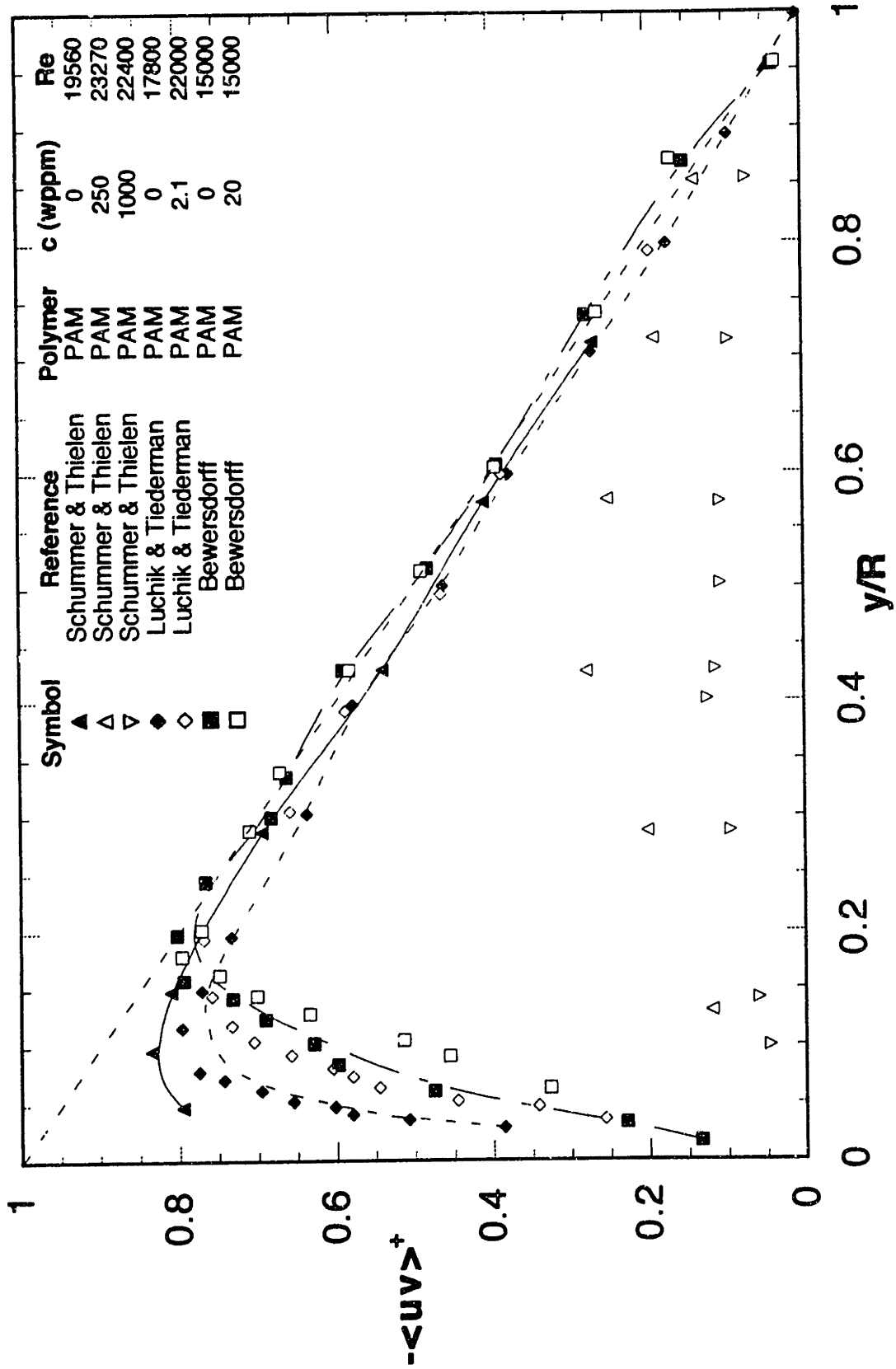


Figure 1.2.38 Reynolds stress profiles for the flow of dilute polymer solutions

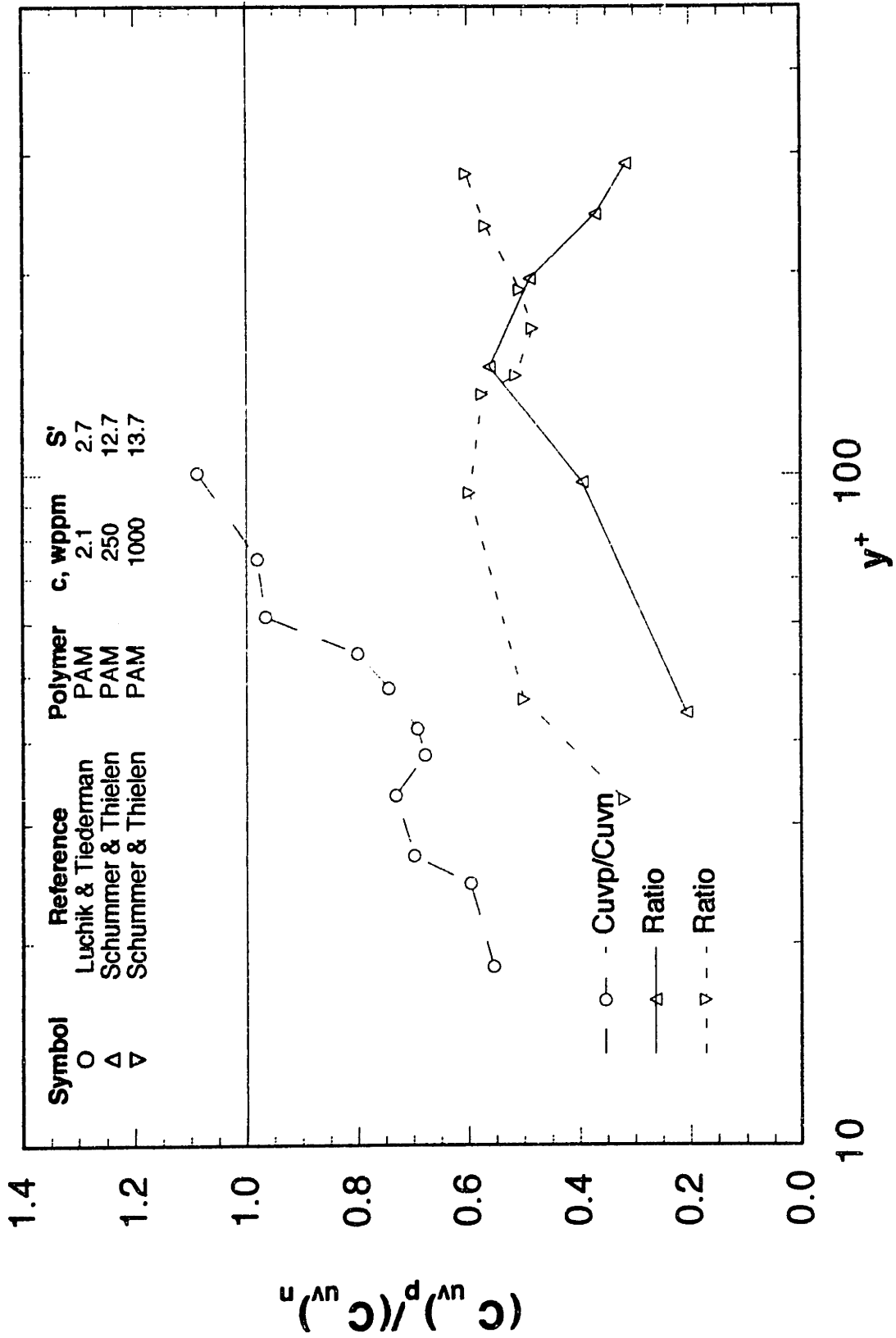


Figure 1.2.39 Ratio of the polymer solution to solvent u-v correlation coefficient

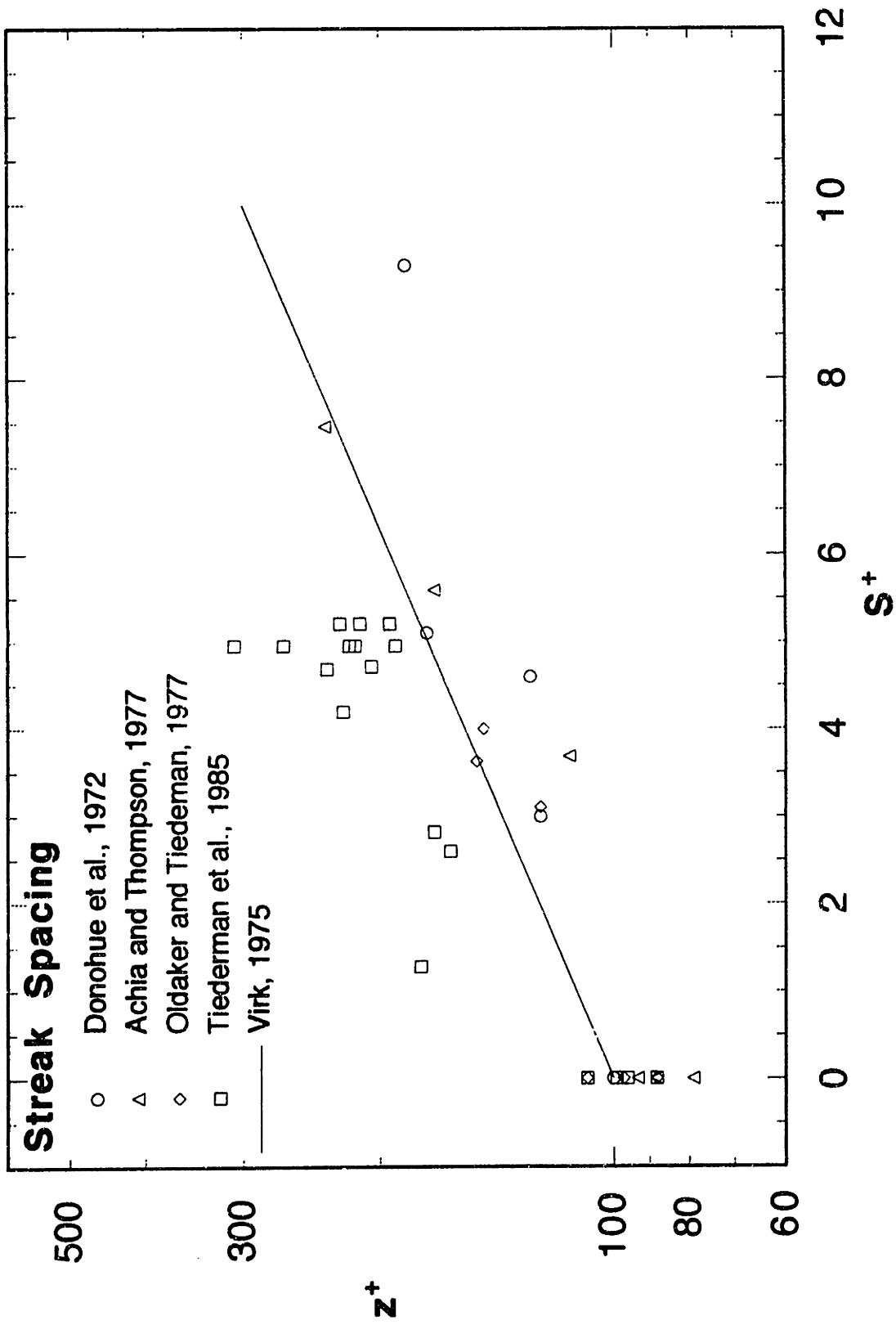


Figure 1.2.40 Variation of the non-dimensional streak spacing with the extent of polymeric drag reduction, measured as S^+

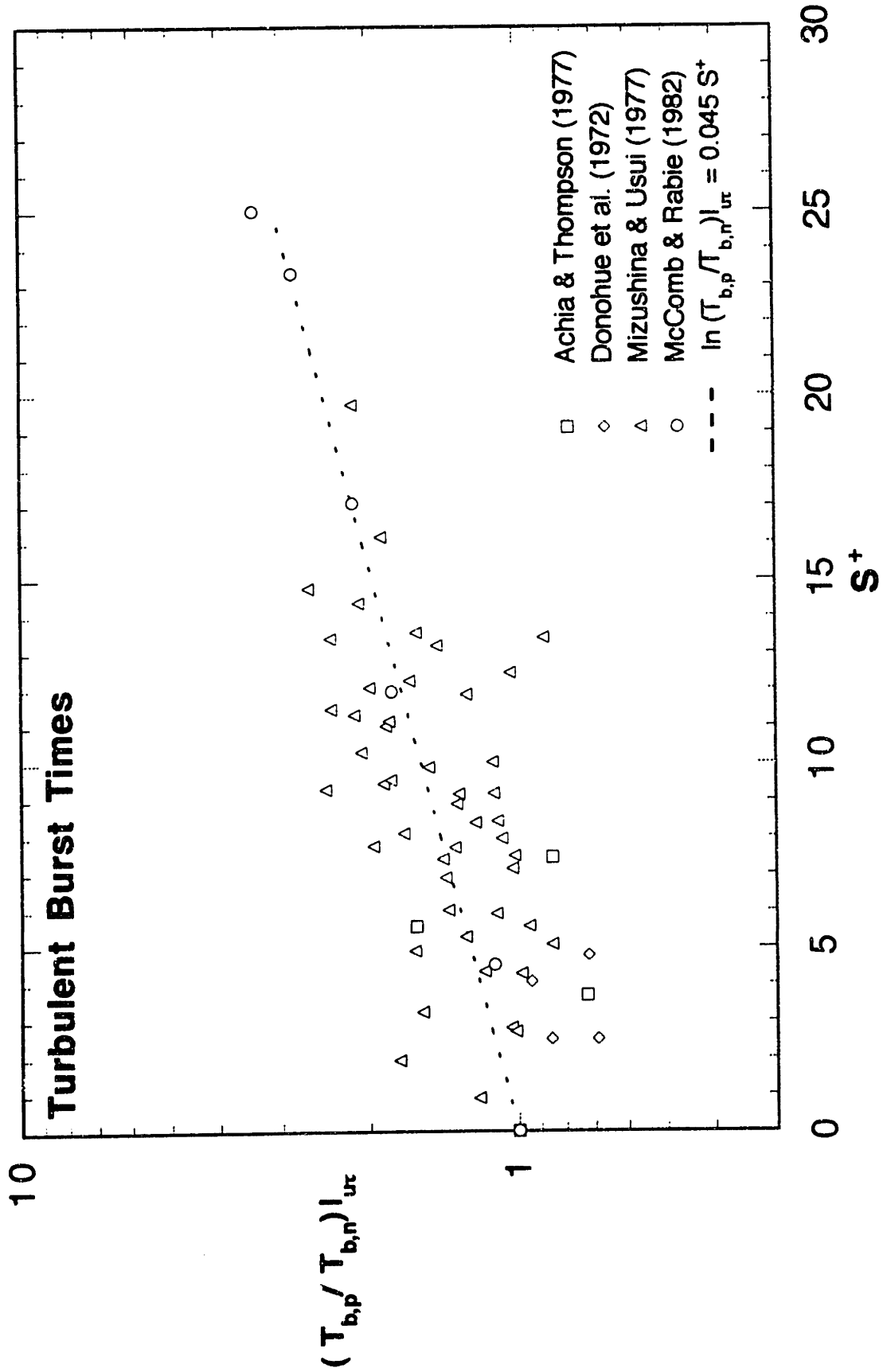


Figure 1.2.41 Variation of the normalized turbulent burst times with the extent of polymeric drag reduction, measured as S^+

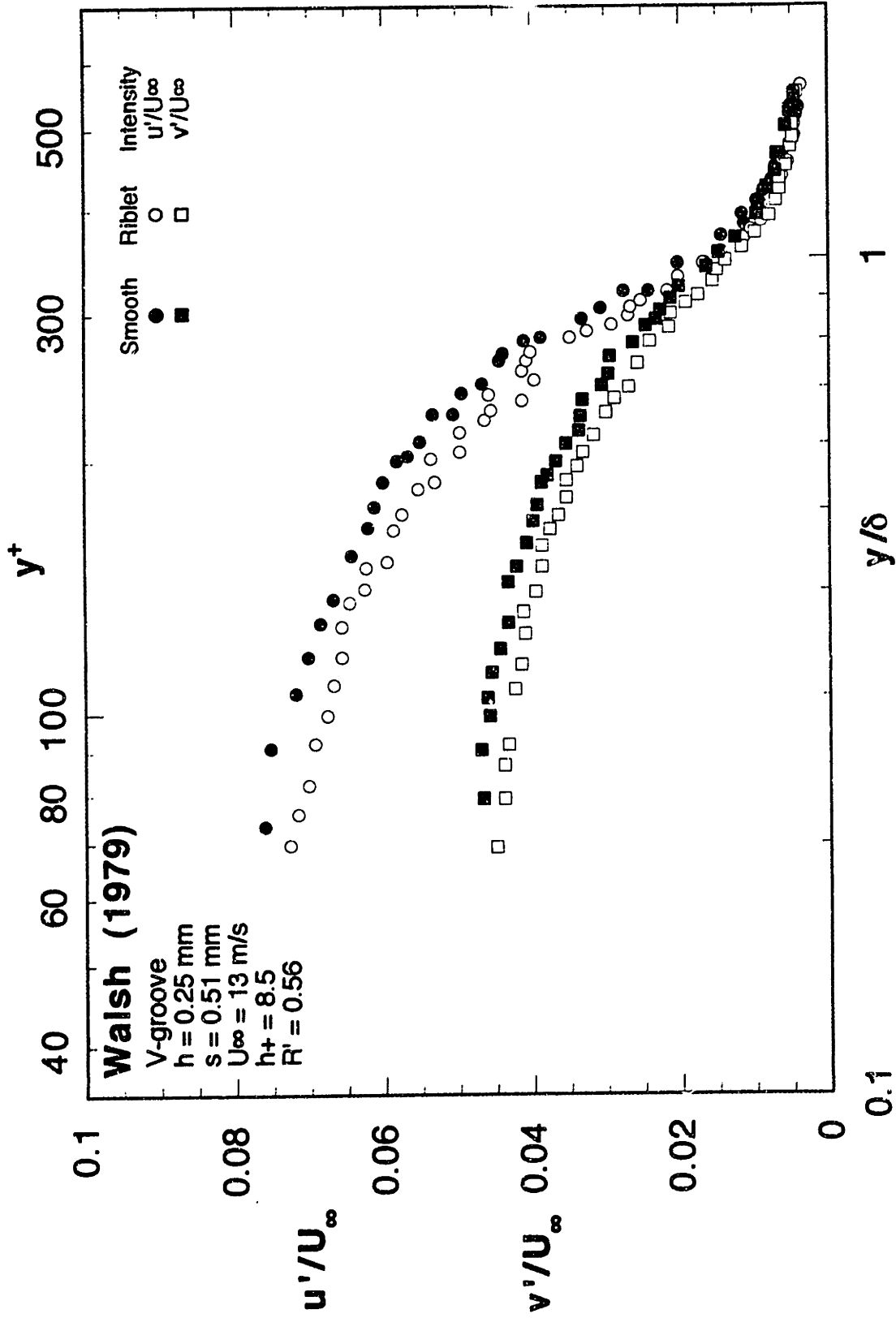


Figure 1.2.42 Streamwise and normal turbulent intensity profiles over V-groove riblets (Walsh, 1979)

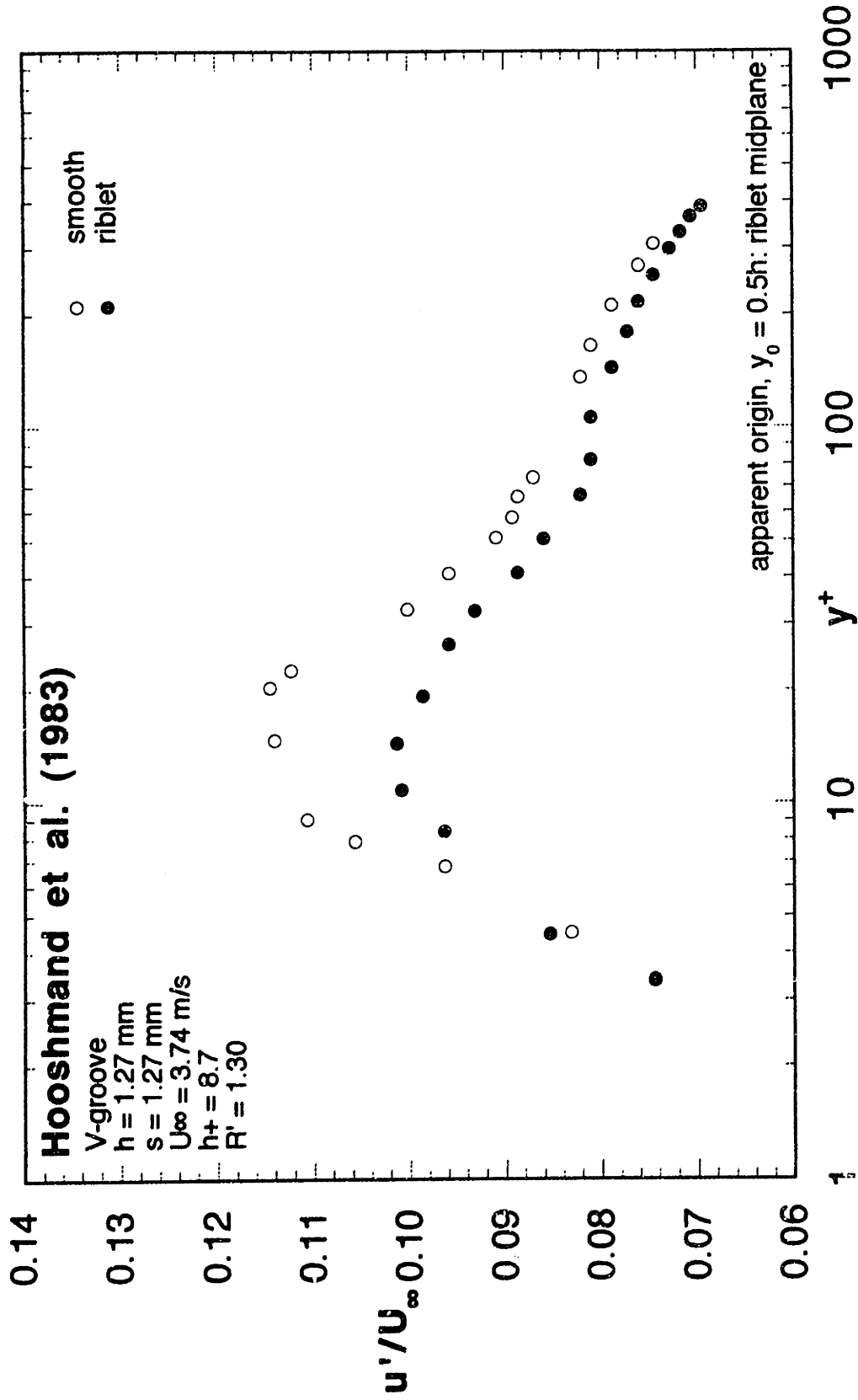


Figure 1.2.43 Streamwise turbulent intensity profiles over V-groove riblets (Hooshmand et al., 1983)

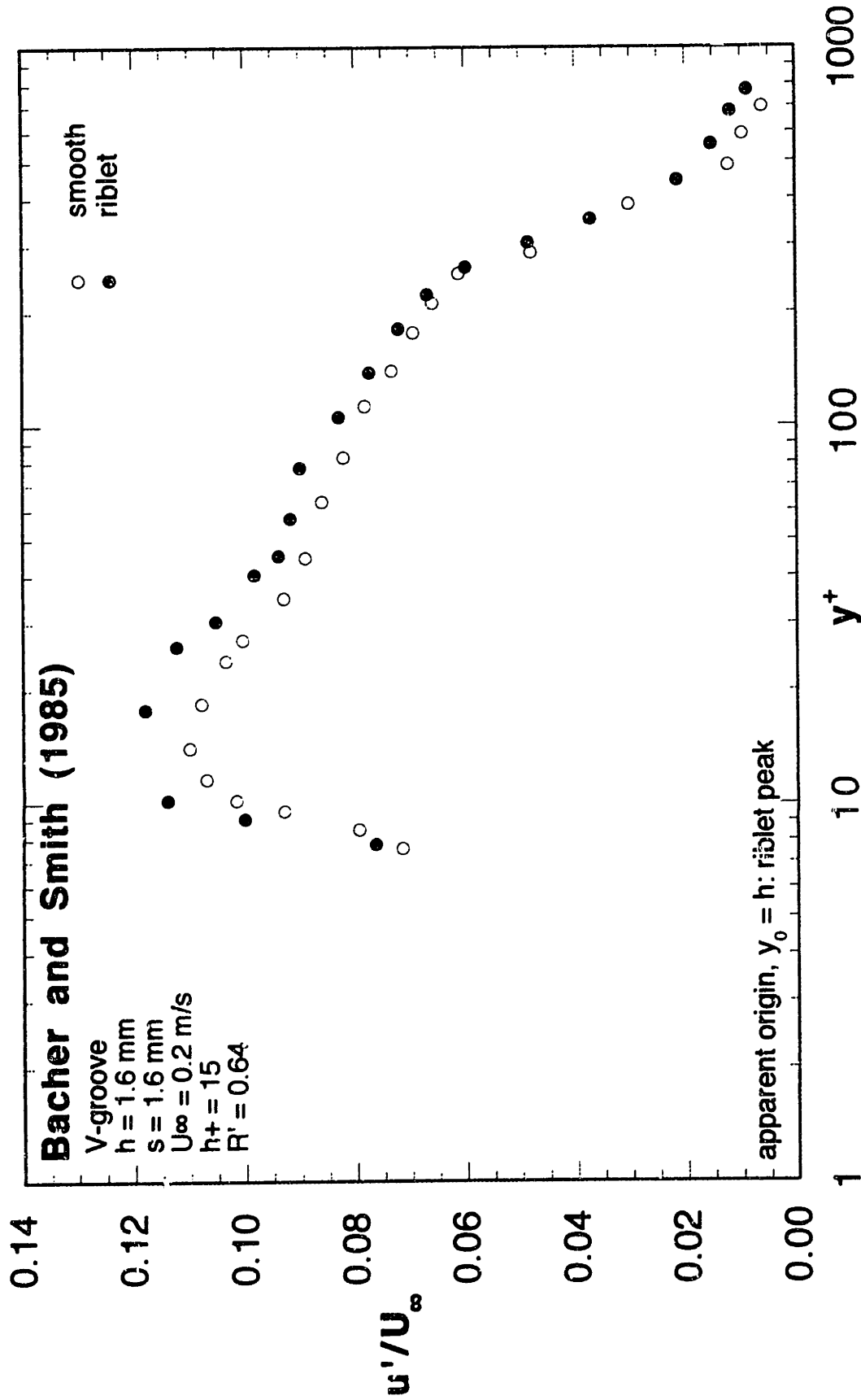


Figure 1.2.44 Streamwise turbulent intensity profiles over V-groove riblets (Bacher and Smith, 1985)

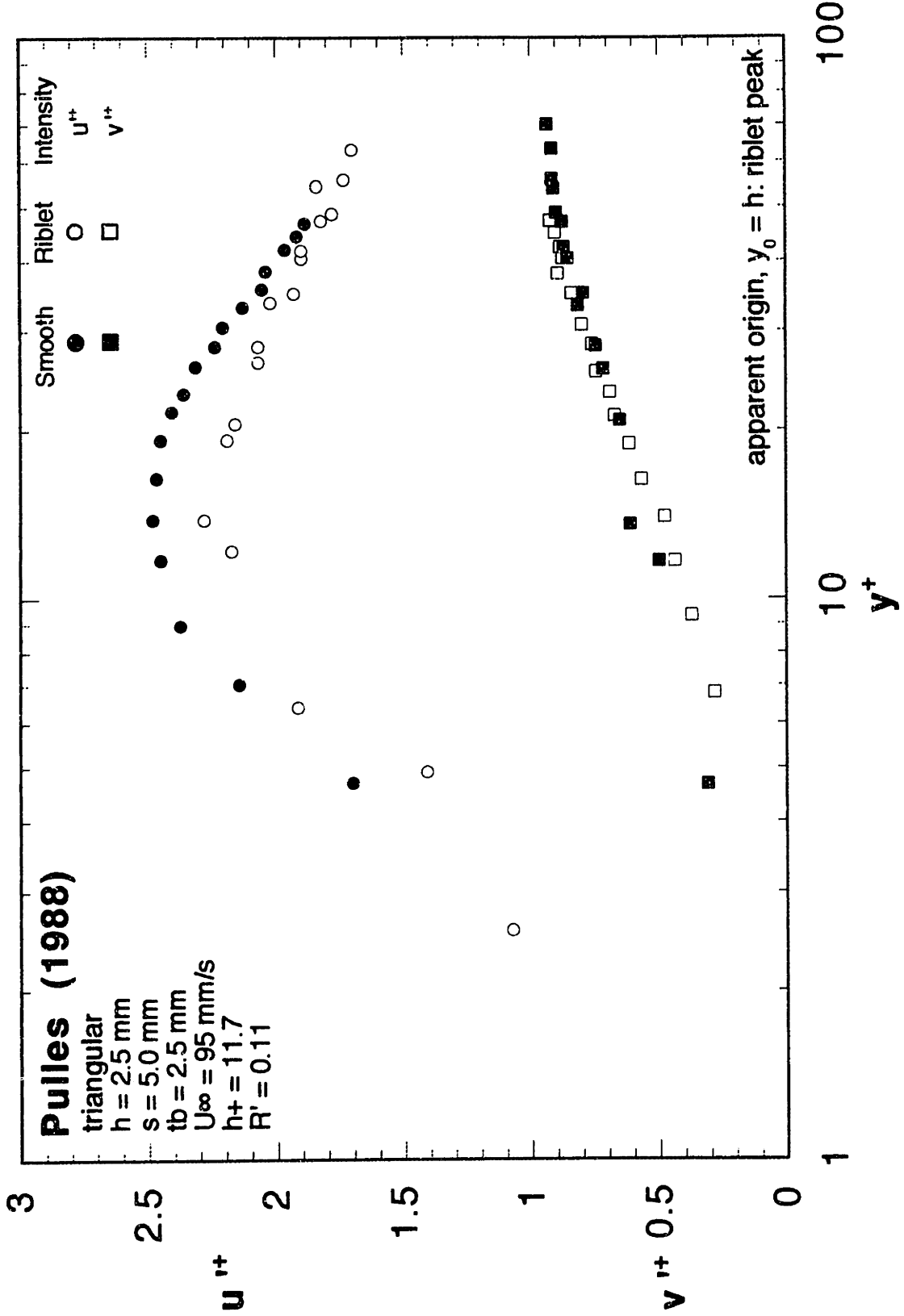


Figure 1.2.45 Streamwise and normal turbulent intensity profiles over V-groove riblets under drag reducing conditions (Pulles, 1988)

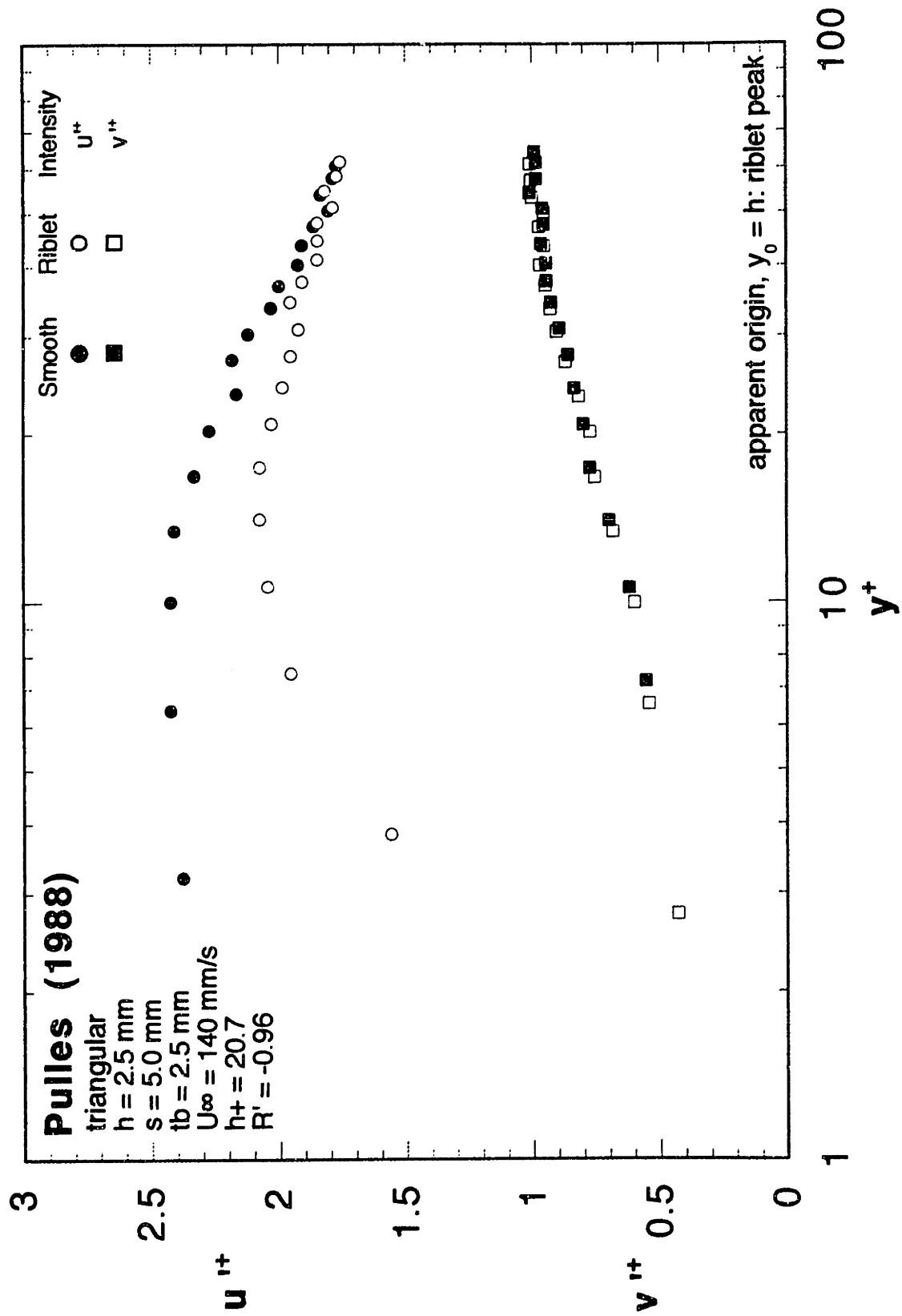


Figure 1.2.46 Streamwise and normal turbulent intensity profiles over V-groove riblets under drag enhancing conditions (Pulles, 1988)

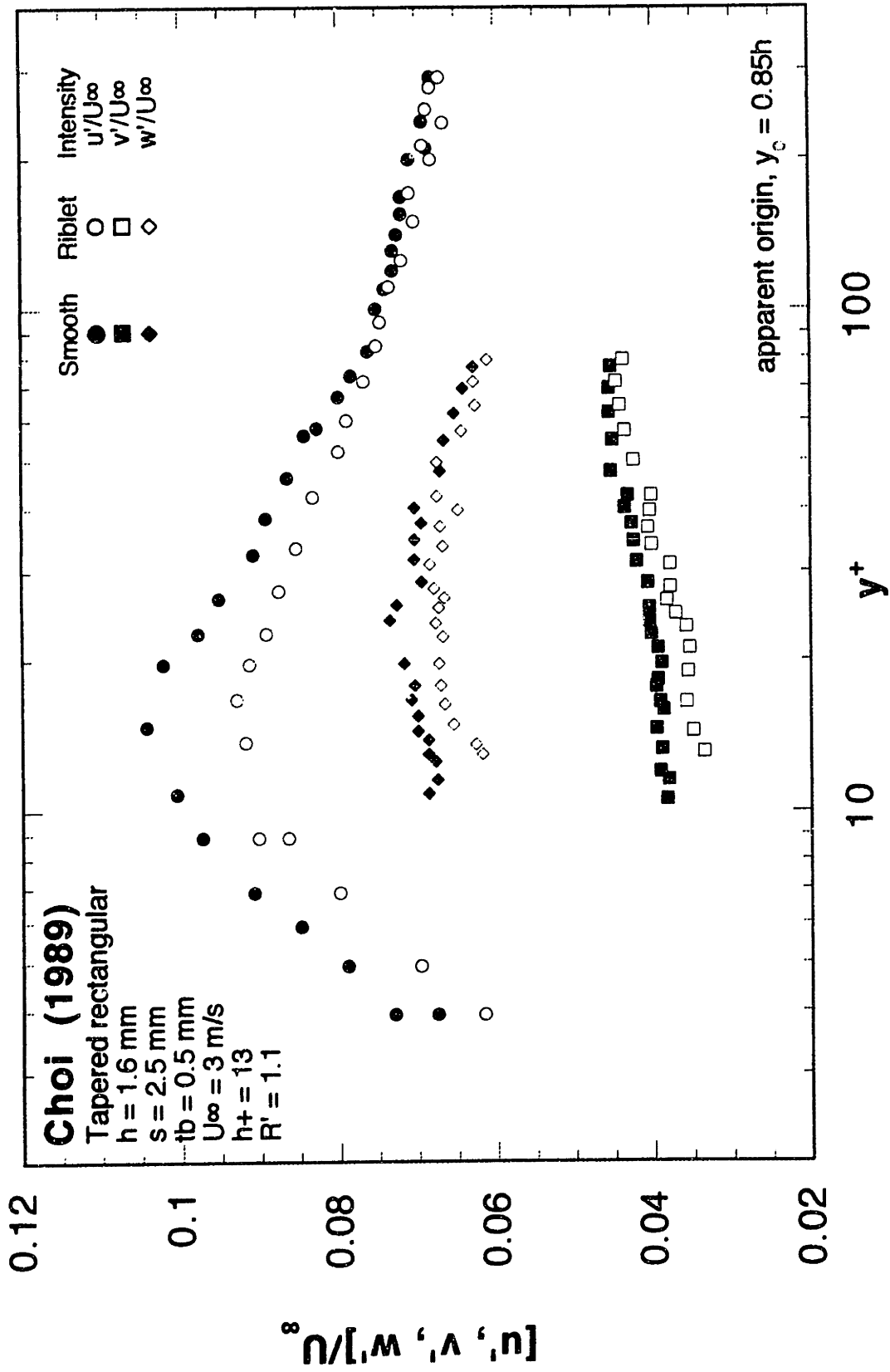


Figure 1.2.47 Streamwise, normal and tangential turbulent intensity profiles over tapered rectangular riblets (Choi, 1989)

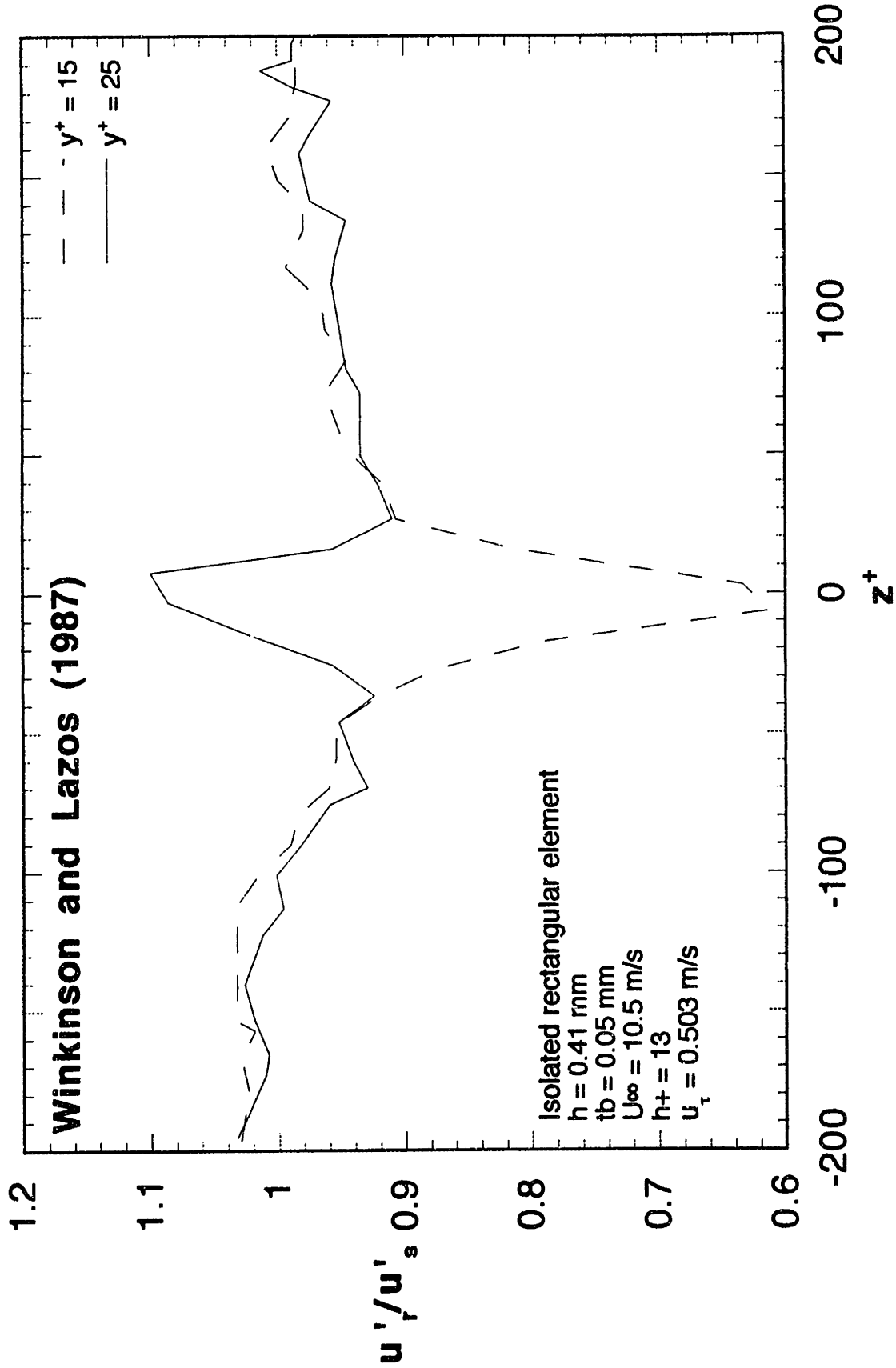


Figure 1.2.48 Spanwise variation of the streamwise turbulent intensity over an isolated rectangular riblet (Winkinson and Lazos, 1987)

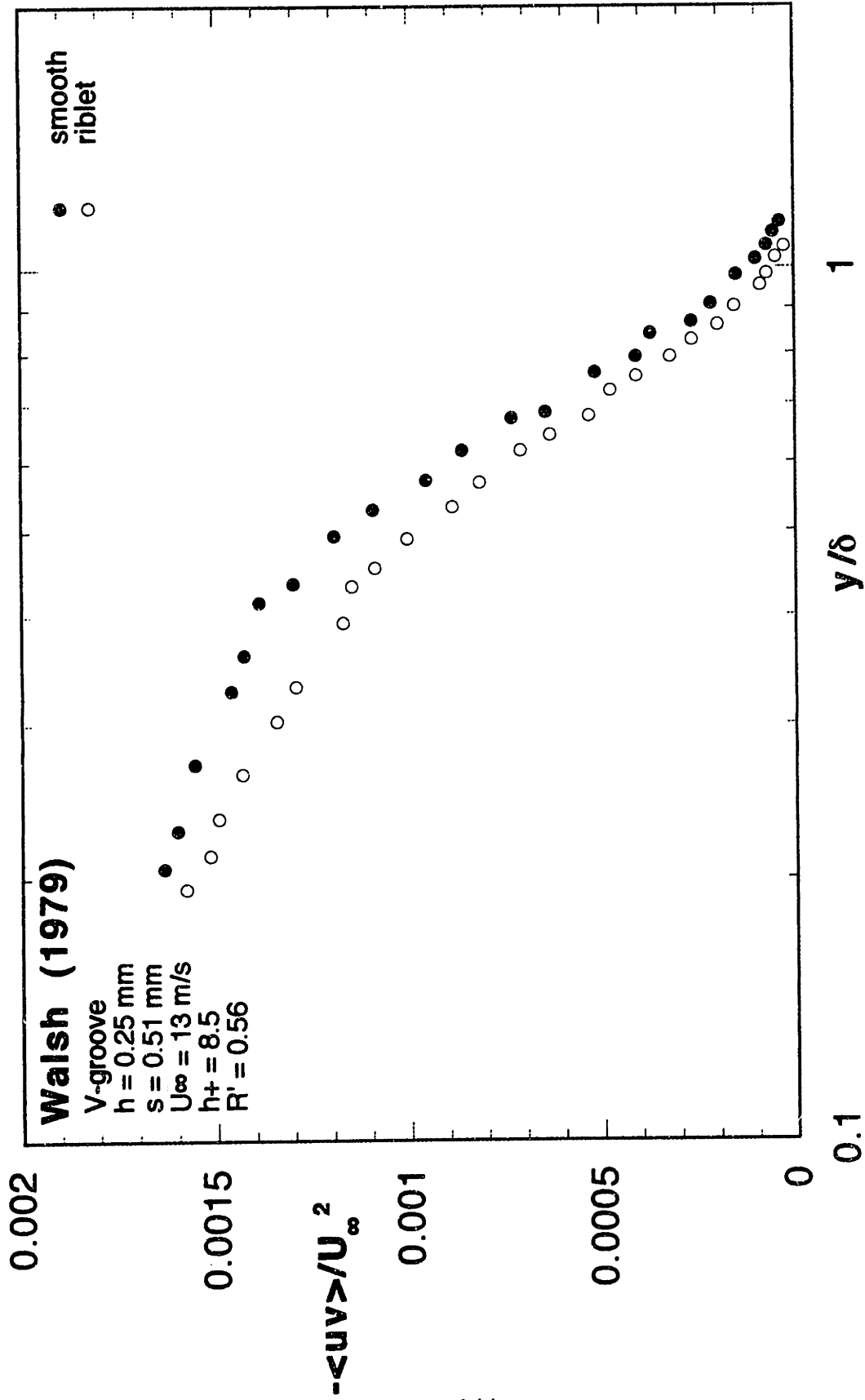


Figure 1.2.49 Reynolds stress profile over V-groove riblets (Walsh, 1979)

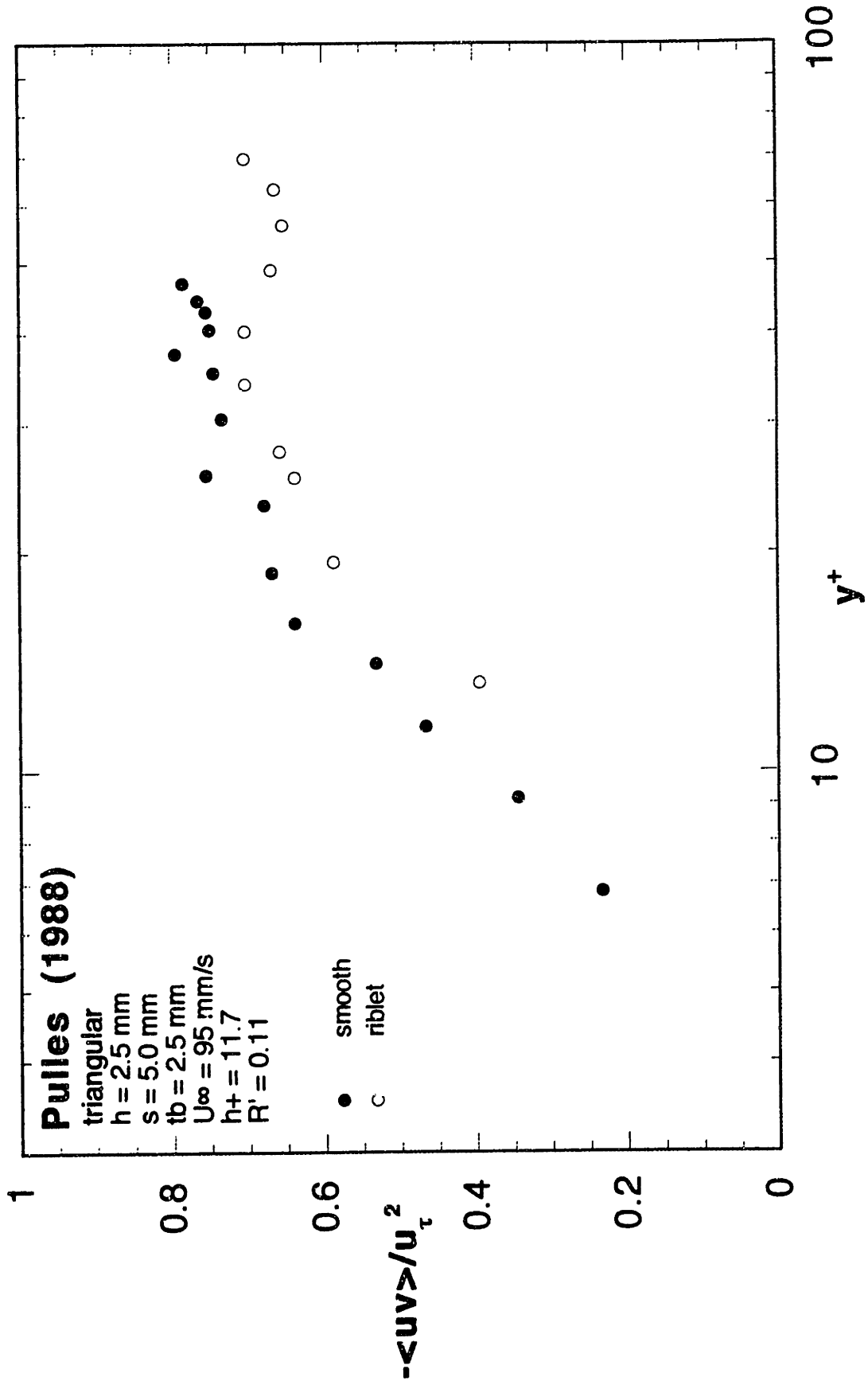


Figure 1.2.50 Reynolds stress profile over V-groove riblets under drag reducing conditions (Pulles, 1988)

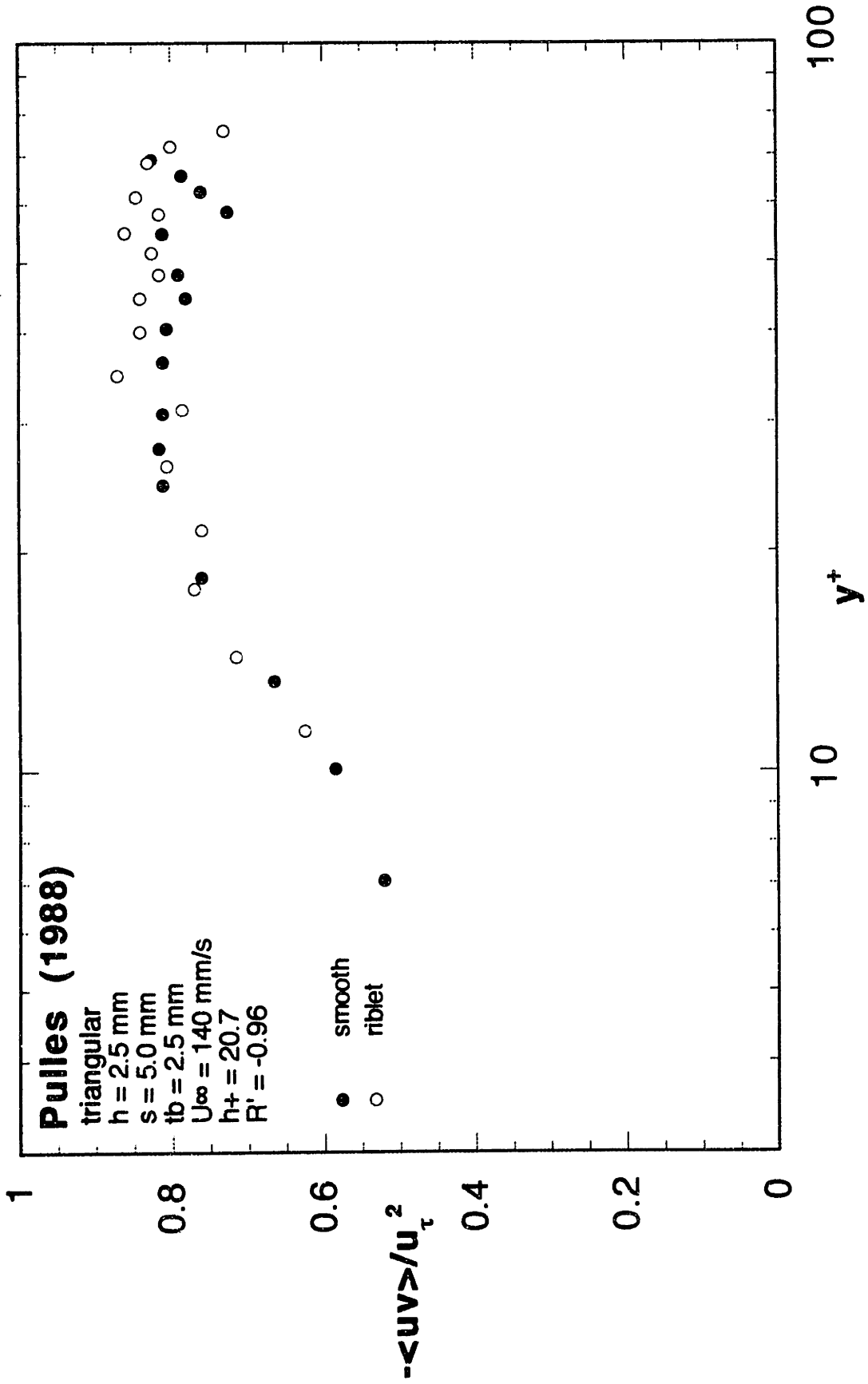


Figure 1.2.51 Reynolds stress profile over V-groove riblets under drag enhancing conditions (Pulles, 1988)

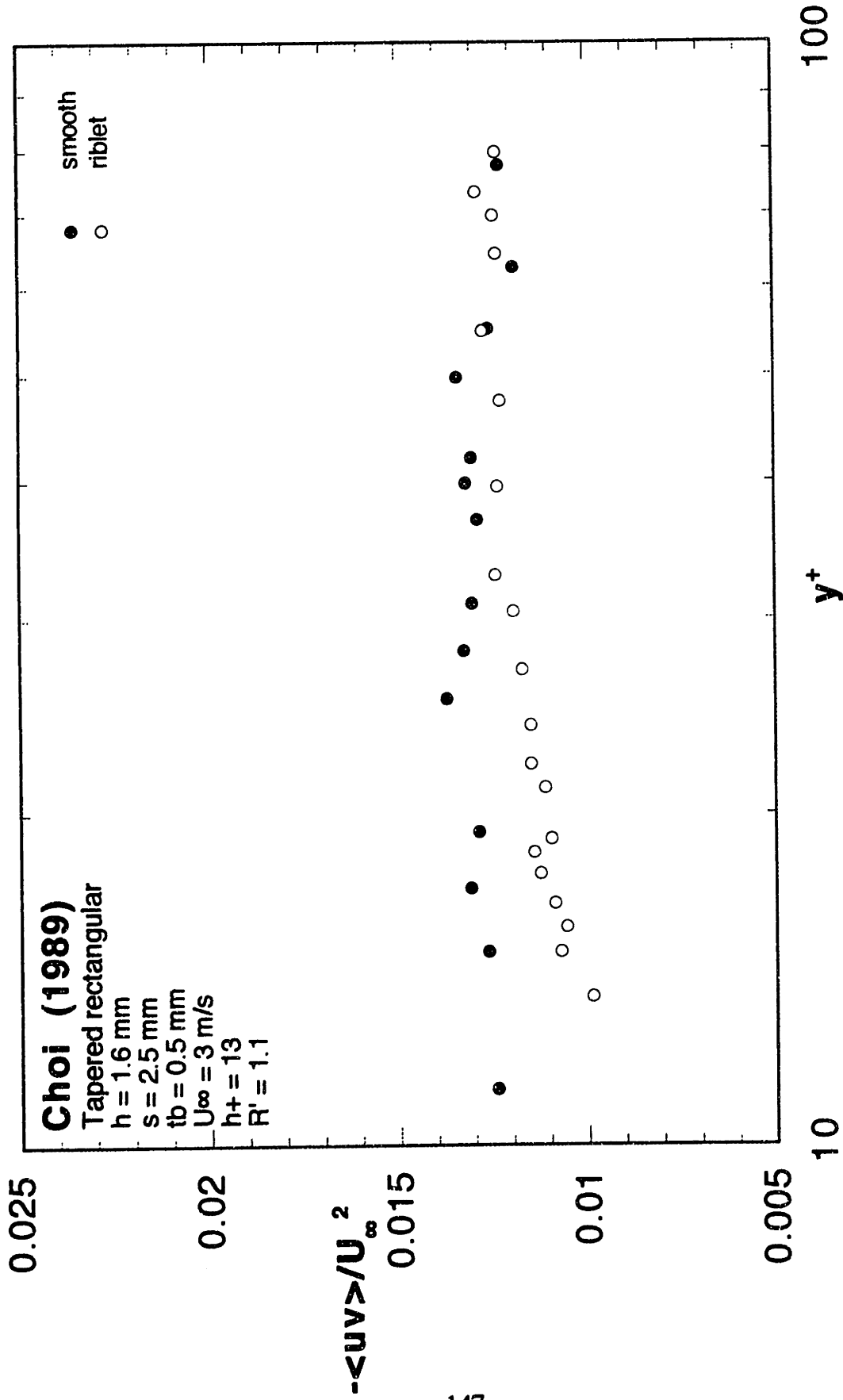


Figure 1.2.52 Reynolds stress profile over tapered rectangular riblets (Choi, 1989)

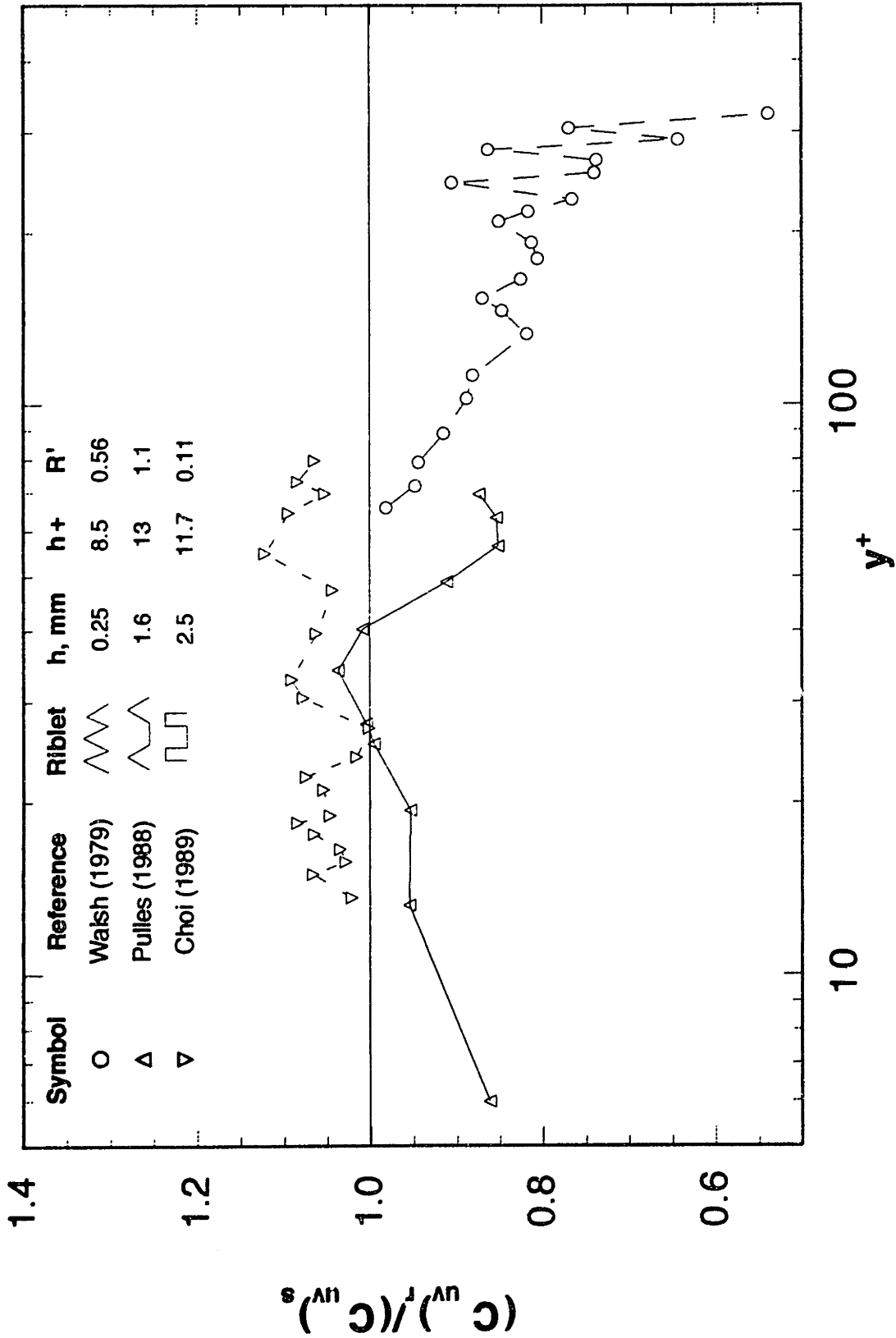
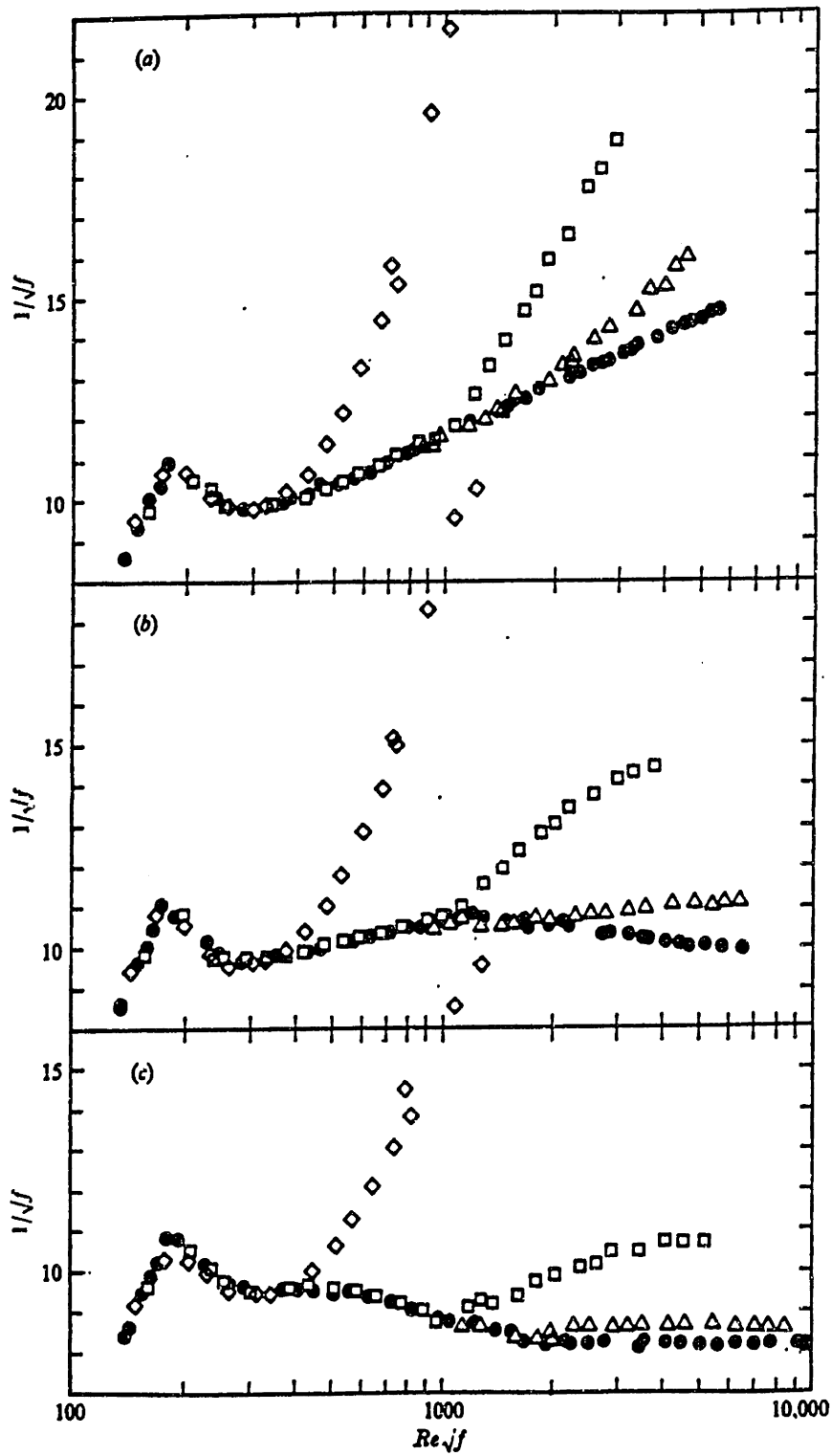


Figure 1.2.53 Ratio of the riblet to smooth u-v correlation coefficient



The onset of drag reduction in rough pipes. (a) Smooth, (b) $R/k = 35$, (c) $R/k = 14.6$.

Symbol	Polymer	c , w.p.p.m.
◇	W301	18.7
□	N750	296
△	N10	2240
●	Solvent	—

Figure 1.2.54. The onset of drag reduction in rough pipes (Virk, 1971)

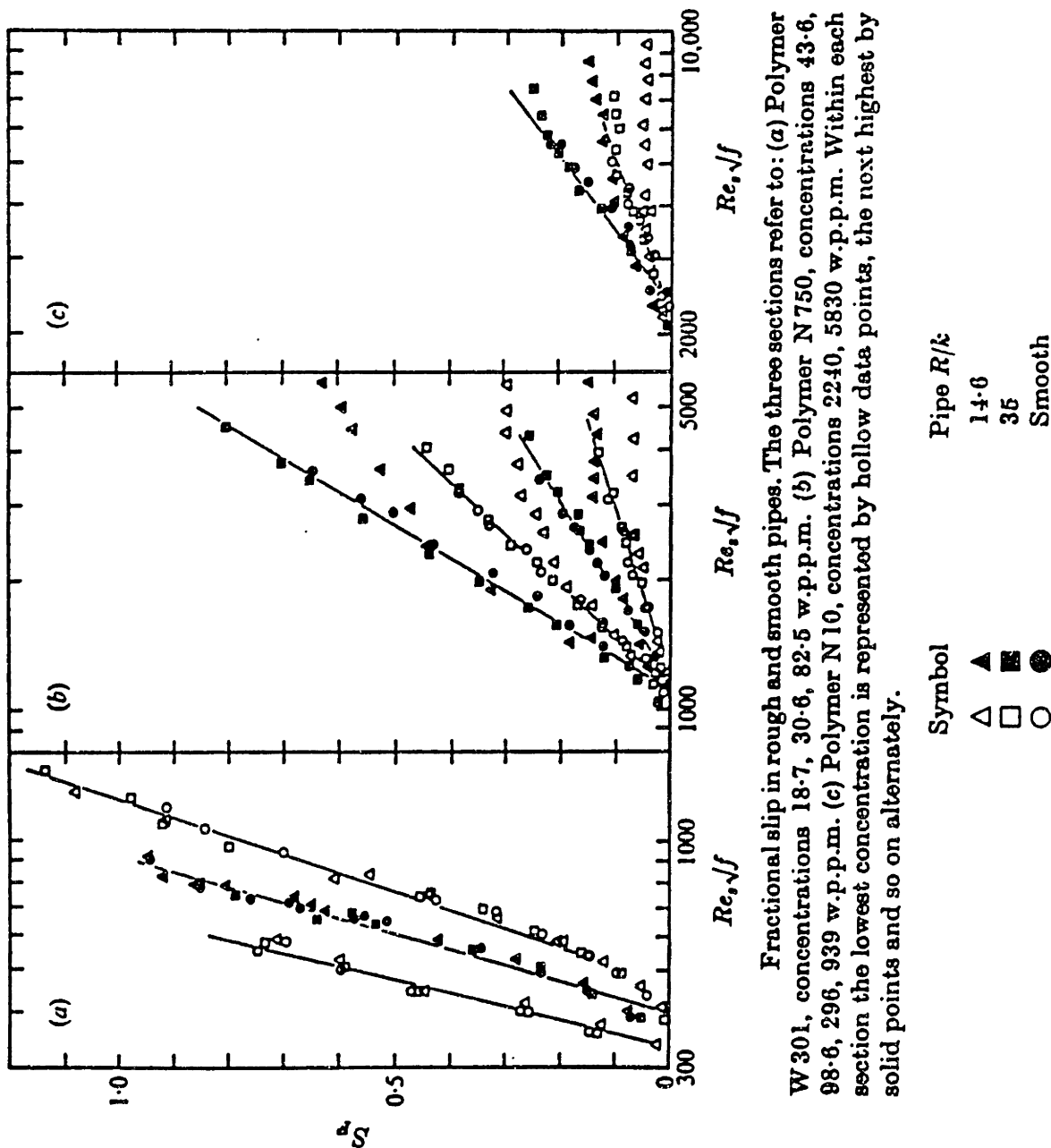
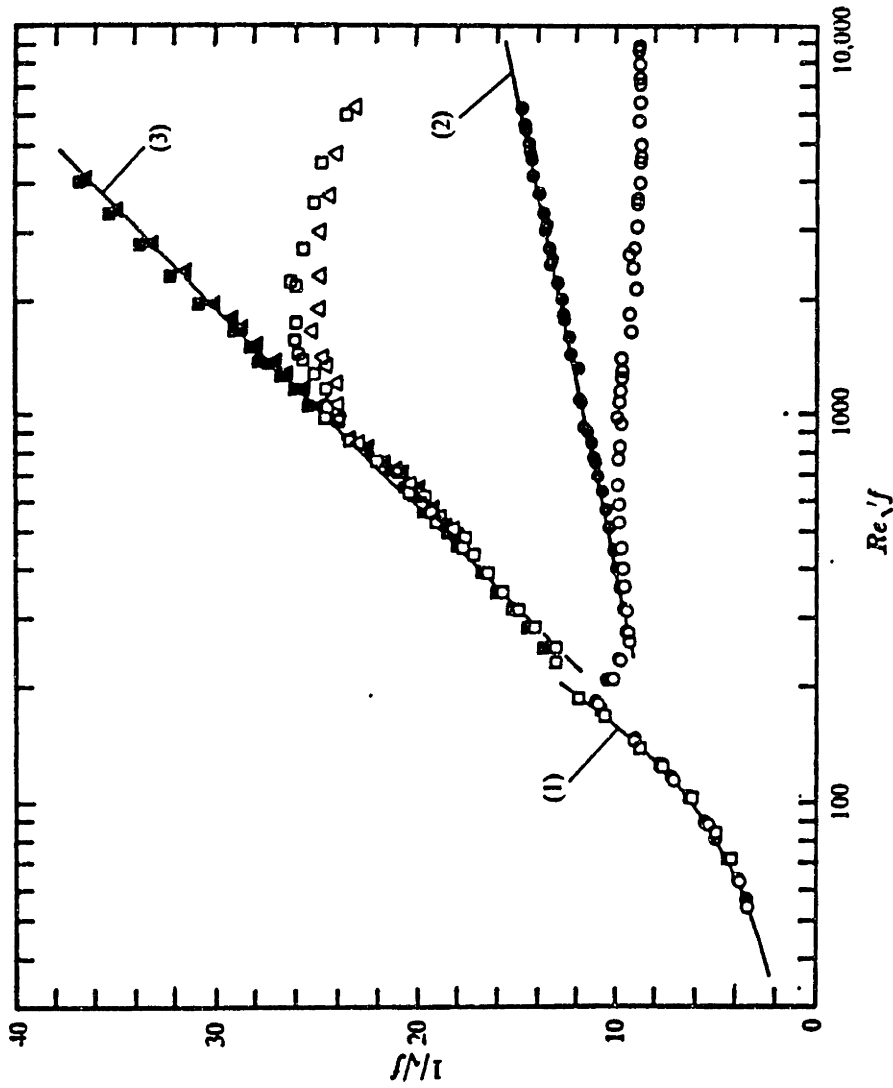


Figure 1.2.55. Fractional slip in rough and smooth pipes (Virk, 1971)



Maximum, asymptotic, drag reduction. Solid lines correspond to indicated equations in text.

Smooth	Symbol	Polymer	$c, w.p.p.m.$
▲	△	FR-A	110
■	□	E117	110
●	○	Solvent	—

Figure 1.2.56. Maximum, asymptotic, drag reduction in smooth and rough pipes (Virk, 1971)

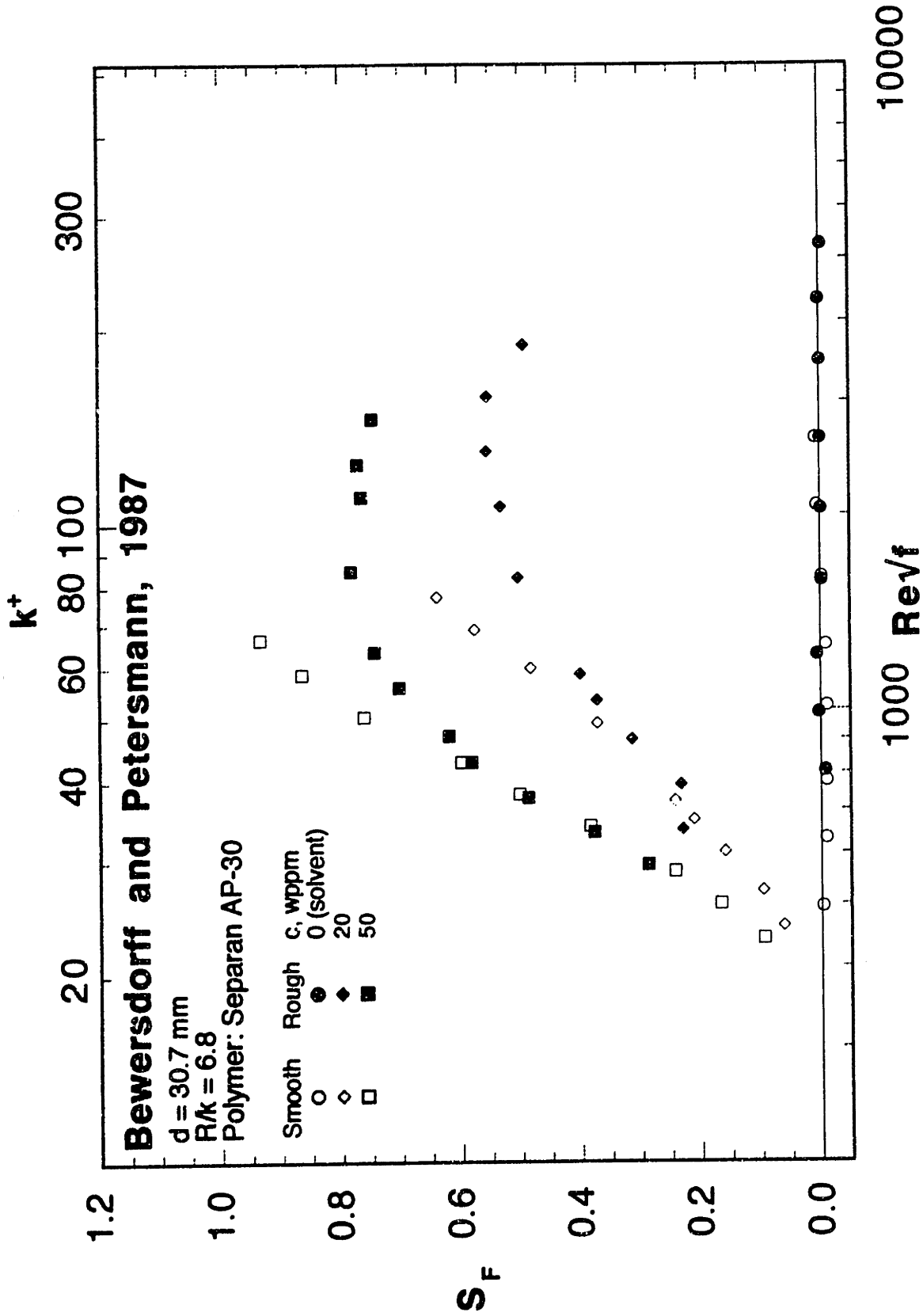


Figure 1.2.57 Fractional slip in rough and smooth pipes (Bewersdorff and Petersmann, 1987)

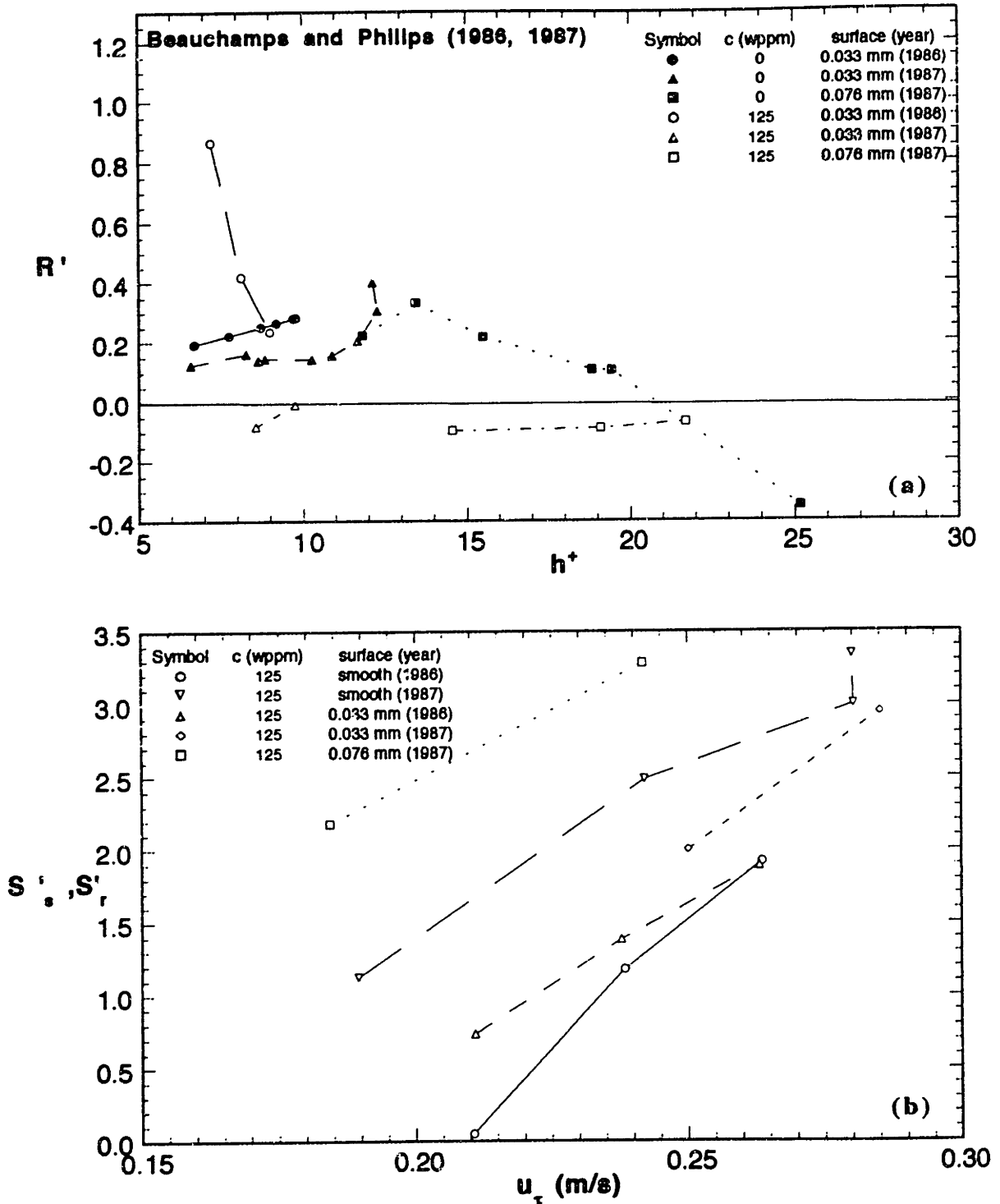


Figure 1.2.58 Polymer-induced flow enhancement over a smooth and riblet-lined axisymmetric body: (a) incremental flow enhancement (R') and (b) differential flow enhancement or slip (S') (Beauchamps and Phillips, 1986, 1987)

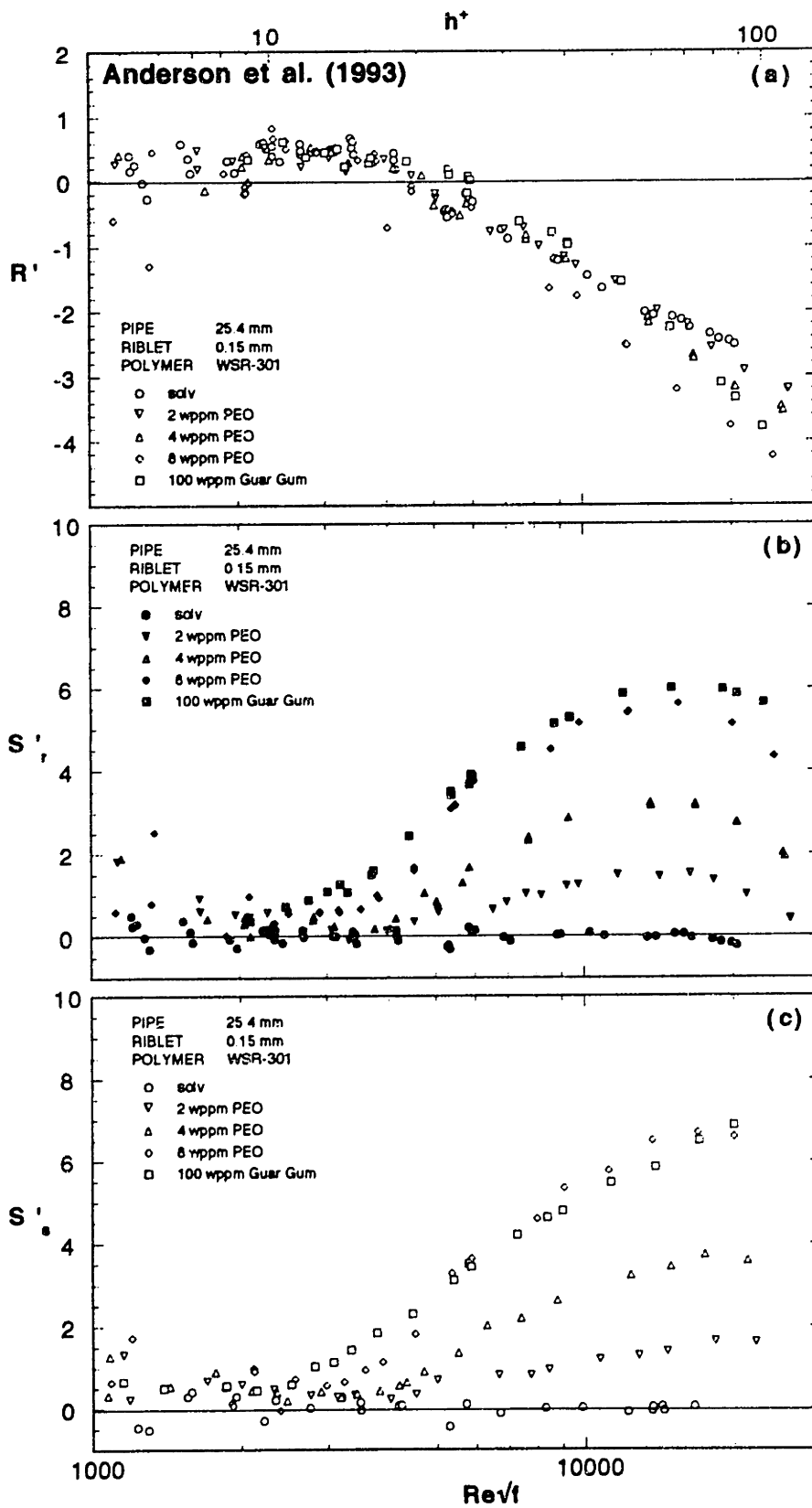


Figure 1.2.59 Polymer-induced flow enhancement in smooth and riblet pipes
 (a) incremental flow enhancement (R');
 (b) riblet pipe differential flow enhancement (S_r');
 (c) smooth pipe differential flow enhancement (S_s') (Anderson 1993)

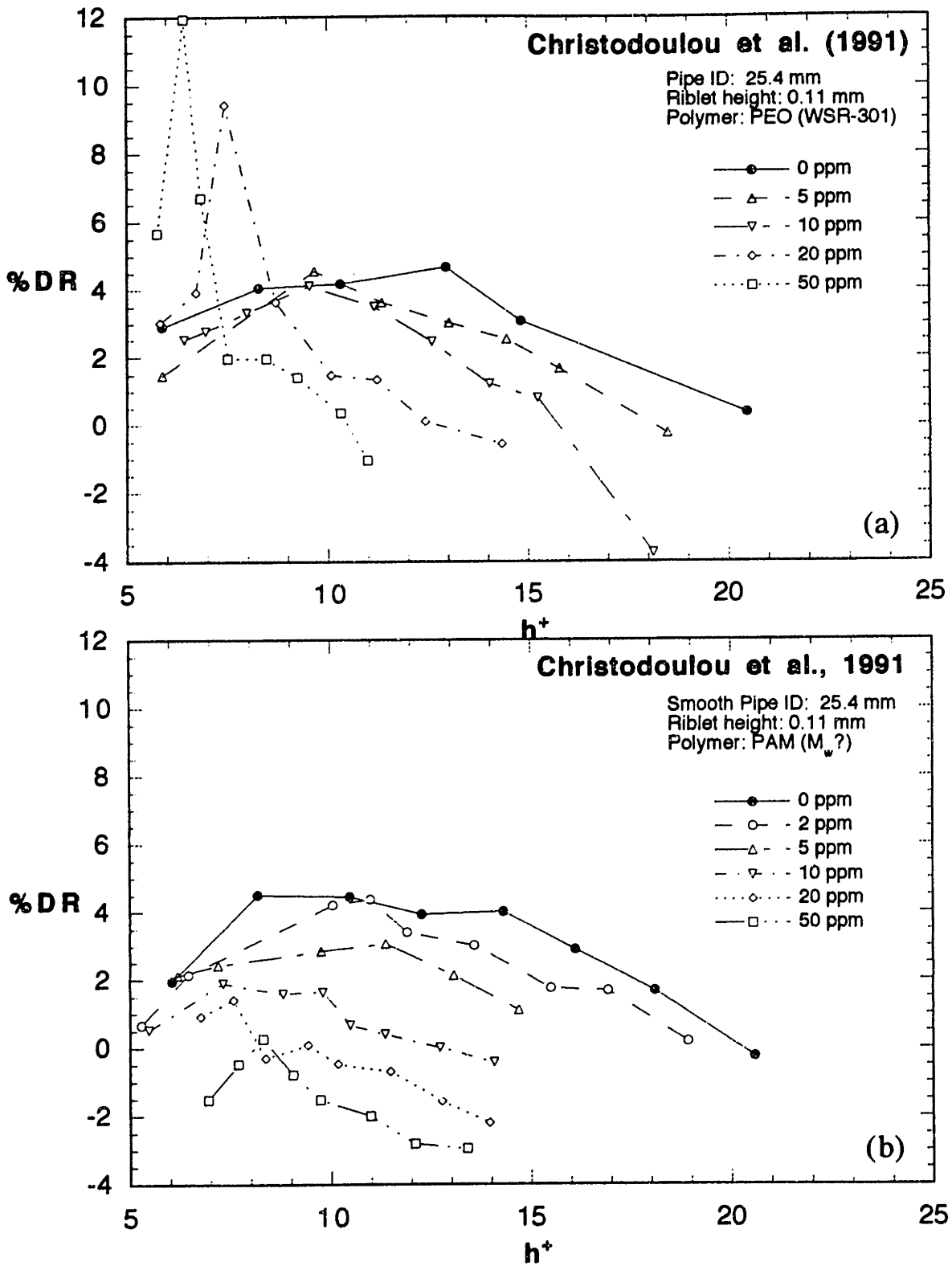


Figure 1.2.60 Riblet drag reduction in smooth and riblet pipes for 0-50 wppm of (a) PAM and (b) PEO solutions (Christodoulou et al, 1991)

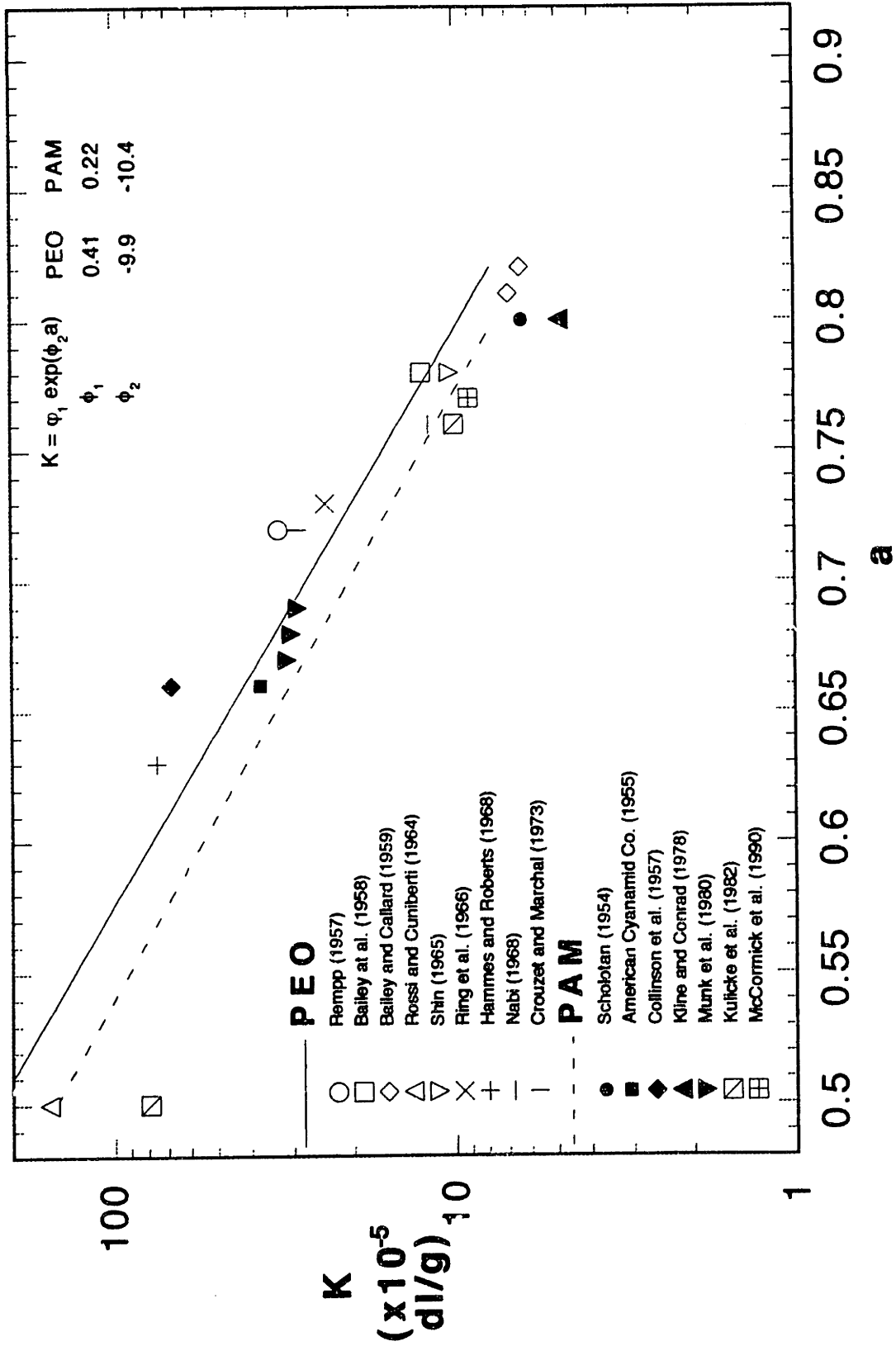


Figure 1.3.1 Relation between K and a in the Mark-Houwink intrinsic viscosity-molecular weight relations for aqueous PEO and PAM solutions

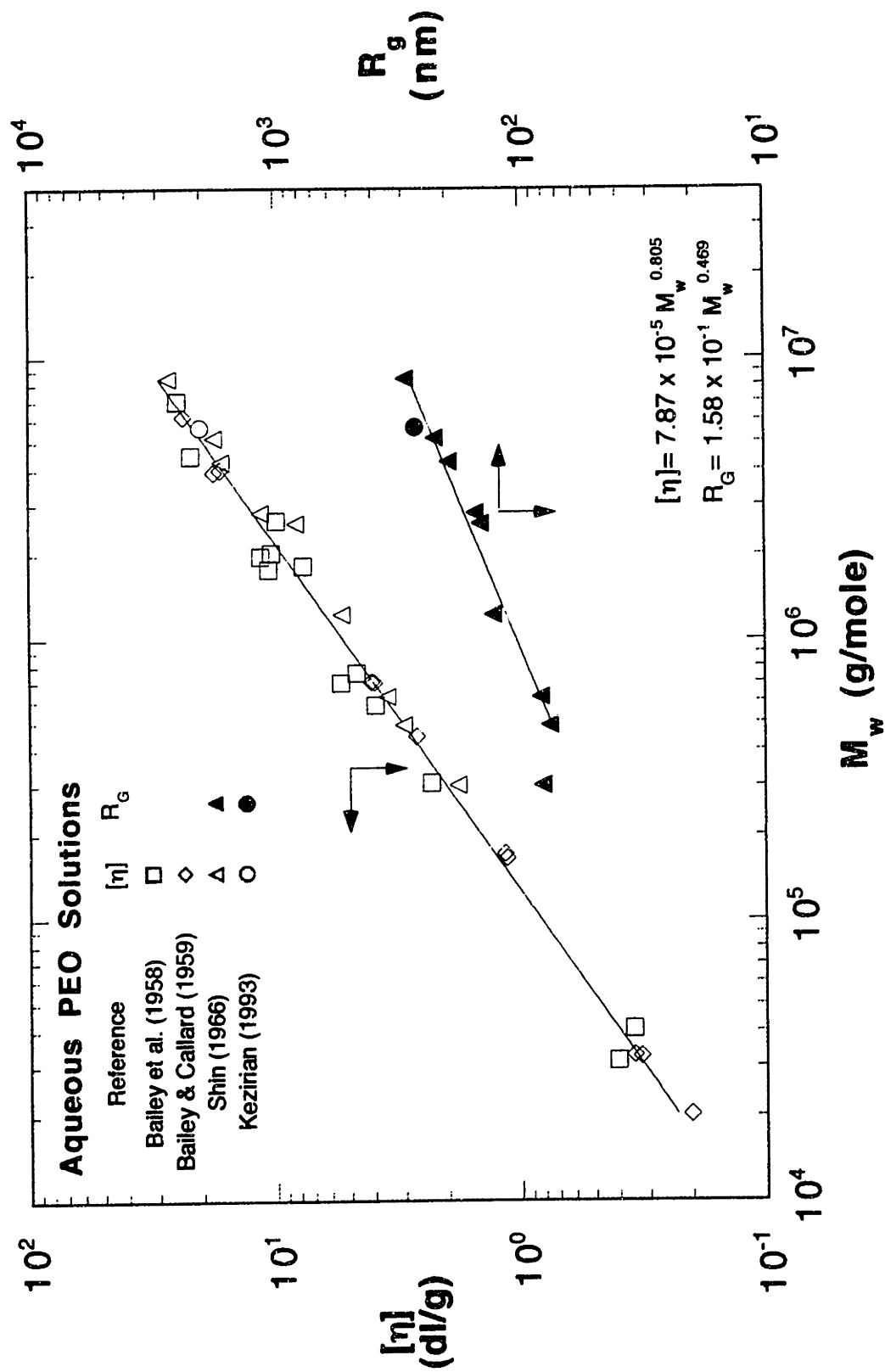


Figure 1.3.2 Characterization of aqueous PEO solutions

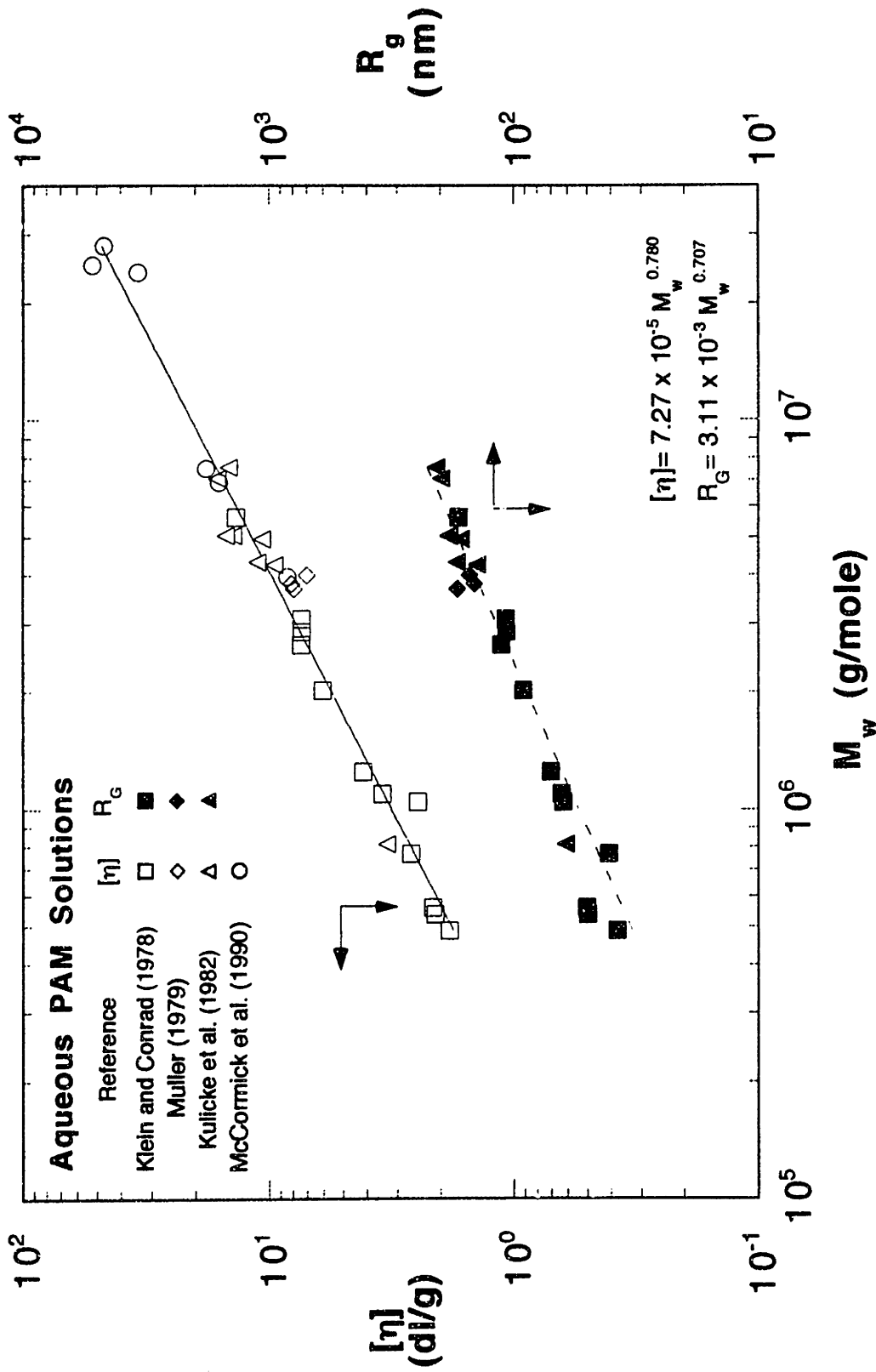


Figure 1.3.3 Characterization of aqueous PAM solutions

Chapter 2

Experimental Apparatus

This chapter describes the present experimental apparatus, which was based on a flow system originally built by Wagger (1992). The modifications made to Wagger's original experimental setup include the fabrication and implementation of new smooth and riblet test sections as well as improvements in the original control and measuring equipment in order to facilitate and improve the accuracy of results obtained.

2.1 General Flow System Description

Figure 2.1.1, parts (a-d), illustrate the experimental apparatus in order of increasing detail.

Figure 2.1.1(a) depicts a plan view of the flow system. At the most upstream end, two 55-gallon tanks, mounted 1.7 m above the floor on a unistrut support, were used to mix, heat and store the solutions under investigation. The flows in to and out of the right and left tanks were controlled by ball valves, VR and VL respectively. Valve, V1, controlled the flow to the test system and valve VB controlled tank drainage. Low flowrates from 0.001-0.13 l/s were achieved by gravity-driven flow through a bypass line with valves V3 and V4 open. Under conditions of gravity-driven flow, the flow was triggered at the entrance to the test sections by a partially closed 3/8" ball valve, VTr. Flowrates were controlled by a flow controller unit comprising a 3/4" ball valve, VFC1, in parallel with a 3/4" stainless steel, 10-turn needle valve, VFC2. The mass flowrate of the effluent was determined by weighing a collected volume of effluent, diverted using a pivoting arm connected to a snap switch, in a measured elapsed time. A 5 k Ω thermistor, housed in a stainless steel union tee, measured the effluent temperature. Between the thermistor and the

flow diverter, a 3/4" ball valve, VFC3, was used to start and stop the flow. In the smaller pipe system, the maximum flow rate, under conditions of gravity-driven solvent flow, was 0.085 l/s. Under pump flow operation, a Moyno positive displacement pump provided flowrates of 0.13-1.2 l/s. The pump operated with valves, V2, V3 and V4, in the bypass line closed. Between the pump discharge and the entrance to the test section, 2" OD, 3" long, 1/8" cell honeycomb sections were inserted into a flange ended 2" flexible hose to calm the flow leaving the pump rotor stages. Intermediate flowrates were subsequently achieved by operating the pump at 0.4 l/s and bypassing most of the flow back through the bypass arm, with V2, V3 and V4 open, to the drain. Flow control was achieved by using both the flow controller unit and V4 and the mass flow rate measured as it was under gravity-driven flow conditions.

Output signals from the pressure transducers and thermistors were monitored, logged and outputted using a HP-3467A Logging Multimeter (which eventually failed) then subsequently a Fluke Hydra 2625A Data Logger interfaced to an IBM PC.

Figure 2.1.1(b) is an expanded view of the test pipe section assembly which consisted of a developing smooth section, a riblet-lined test section and a trailing smooth section. Four riblet pipe configurations were tested using a combination of two pipe sizes (10.21 mm and 7.82 mm ID) and two nominal riblet sizes (0.15 and 0.11 mm V-groove riblets with equal height and spacing). In the 10.21 mm flow system, three test sections were arranged sequentially with smooth test sections at the upstream and downstream ends of a riblet pipe test section. In the 7.82 mm flow system, the downstream or trailing smooth section was removed initially because including it would cause the pressure drop across the system to exceed the safety limits on the pump (100 psid) at high flowrates.

The upstream smooth test section consisted of [3, 2] lengths of tubing cut from a single length of [(1/2" OD, 10.21 mm ID), (3/8" OD, 7.82 mm ID)] low carbon, stainless

steel, micro smooth tubing. An entry length of [77.3 ID, 56.7 ID] was provided to ensure fully developed flow in the test section.

The riblet test sections each consisted of two lengths of pipe cut from a single length of smooth tubing lined with riblets. The riblets were inserted by first wrapping a riblet rectangular strip (length = length of pipe, width = inner circumference of pipe) around a felt-covered dowel with the adhesive side, sprayed with a detergent solution, facing outward. As the dowel was inserted into the pipe, the riblets unwrapped onto the inner wall of the pipe producing an almost seamless fit. Excess detergent was removed by carefully expanding a length of pure gum rubber tubing, under pressure, inside the pipe.

The trailing smooth 10.21 mm test section consisted of two sections cut from a single length of tubing and contained two pressure taps and a flow re-development length of 32.0 ID. The pressure taps may be connected to either set of transducers.

The sections were held firmly in place and realigned with bored through [1/2", 3/8"] unions. Each length contained 0.025" OD pressure tap holes, over which were inserted bored through [1/2", 3/8"] union tees (Figure 1.3.1(c)). An independent set of calibrated 0.1, 1.0 and 10-psid transducers allowed simultaneous measurement of the pressure drop across the pressure taps in both the smooth and riblet test sections.

2.2 Detailed Description

2.2.1 Test System

2.2.1.1 Riblets.

The riblets used in this investigation were 3M Scotchcal™ Brand Drag Reduction Tape: a thin, flexible, clear, PVC tape with a precoated pressure sensitive adhesive,

protected by a plastic liner. Two types of riblets were tested of heights 0.11 mm and 0.15 mm. Figure 2.2.1a and b are photographs of the riblets cross-section taken at 220x magnification using an environmental scanning electron microscope (ESEM). The sections were prepared by cutting transverse to the riblets with an Xacto knife in a guillotine manner, then mounted vertically into the vacuum chamber of the ESEM. The triangular riblet serrations had sharp peaks, but blunt valleys, with a flat gap, g , at the bottom of adjacent serrations. For the nominal 0.11 and 0.15 mm riblets, $[h, s, g, t] = [0.145 \pm 0.001, 0.165 \pm 0.001, 0.011 \pm 0.001, 0.081 \pm 0.001]$ mm and $[h, s, g, t] = [0.105 \pm 0.001, 0.108 \pm 0.001, 0.015 \pm 0.001, 0.081 \pm 0.001]$, respectively where s is now defined as the peak-to-peak distance. The values were averaged over several snapshots. A schematic of the riblets indicating the dimensions $[h, s, g, t]$ is shown in Figure 2.2.1c.

2.2.1.2 Smooth Test Section Fabrication.

Two pipe sizes, 1/2" OD, 10.21 mm, $< 5 \mu\text{m}$ roughness and 3/8" OD, 7.82 mm ID, $< 10 \mu\text{m}$ roughness, made from 316 stainless steel seamless tubing with electropolished inner walls, were used in this investigation. The upstream smooth test sections featured a flow development length and a measurement length along which pressure measurements were taken. The 10.21 mm ID and 7.82 mm ID pipe fabrications are separately detailed.

(1) 10.21 mm Pipe

Cut from a single length of tubing, the test pipes consisted of three sections, designated $S2_{a-c}$. The original length of tubing was labeled and marked prior to cutting to permit exact realignment of its sections when they were inserted into the flow system. All sections were faced off and deburred to provide an unobstructed, almost seamless fit between the sections. $S2_a$, of length 859 mm (84.1 ID) provided a flow development

length and contained the first pressure tap, T1, located 69.67 mm from the downstream end. The flow development length was therefore 841 (77.3 ID). S2_b and S2_c were 397 mm (38.9 ID) and 396 (38.8 ID) long, respectively, and contained pressure taps, T2 and T3, located 69.8 and 69.6 mm from the downstream ends. The inter-tap distances were thus [T2-T3, T1-T3] = [397 mm (38.8 ID), 793 mm (77.7 ID)].

The pressure taps were 0.025" holes drilled into the pipe, normal to the pipe wall, using a No.72 H.S. Cobalt drill bit. A manually rotated drill bit was moved in and out of the hole to ensure the hole was unobstructed. Excess material and burrs were removed by carefully filing the inner wall of the tube at the hole. This process was repeated until a circular, burr-free hole was obtained. This was confirmed with a 20x magnifying glass looking perpendicular to the hole with the hole illuminated on the inside using a small flashlight held against one end of the tube.

The length of the pipes and the distance between adjacent tap pairs were measured with a dial caliper. Each hole was then fitted with a bored through Swagelok 1/2" stainless steel union tee fitting with the tap hole aligned with the axis of the vertical branch of the tee as shown in Figure 2.2.2. The tee was bored through using a 1/2" drill bit and then honed to provide a snug fit over the pipe. The tee provided a seal above the pressure tap hole, and its port accommodated a pressure line to the transducers. Separate sections were realigned, and the held firmly in place, by bored through stainless steel unions with nylon ferrules that ensured a fluid tight, almost seamless junction. The foregoing information regarding the smooth 10.21 mm pipe sections is summarized in Table 2.2.1.

(2) 7.82 mm Pipe

Cut from a single length of tubing, the smaller diameter test pipes consisted of two sections, designated S1_{a-b}. The original length of tubing was labeled, cut and deburred in the manner described above. S1_a, of length 638 mm (81.6 ID) provided a flow

development length and contained the first pressure tap, T1, located 59.69 mm from the downstream end. The flow development length was therefore 579 (56.7 ID). S1_b, of length 286 (36.5 ID) housed both pressure taps T2 and T3 located 59.7 mm from both ends. The inter-tap distances were therefore [T2-T3, T1-T3] = [164 (21.0 ID), 286 mm (36.3 ID)].

The pressure tap holes (0.025"), enclosed tees and connecting unions were fabricated in a manner analogous to that for the 10.21 pipe. The dimensions of the 10.21 mm smooth pipe sections are summarized in Table 2.2.1.

2.2.1.3 Riblet Test Section Fabrication.

In each pipe size-riblet geometry studied, two sections of approximately equal length were cut from a single section of tube. Four riblet test configurations were fabricated, designated R1A and R1B for the 0.11 mm and 0.15 mm riblets in the 7.82 pipe respectively; and R2A and R2B for the 0.11 mm and 0.15 mm riblets in the 10.21 mm pipe respectively. The lengths of all riblet pipe sections, together with their inter-tap distances, are summarized in Table 2.2.1.

The fabrication of the riblet sections, prior to the insertion of the riblets, mirrored the smooth pipe sections. The riblets were then inserted into the each pipe section as follows:

- (i) The riblet sheet was laid flat onto a table with the plastic backing facing outward and secured with tape.
- (ii) A strip of riblet was marked with length equal to the length and width equal to the inner circumference of the test section. A 6" rule with 1/100" divisions was used to measure these dimensions accurately.

- (iii) The strip was cut using a sharp, thin blade in a single fluid motion guided by a metal rule secured so that its edge exactly matched the marks made.
- (iv) The plastic backing was then carefully removed and the adhesive thus exposed sprayed with copious amounts of a liquid detergent solution comprising 8% of household washing detergent (Joy™) in distilled water.
- (v) The riblet strip was wrapped, with the adhesive side out, around a felt-covered dowel with a diameter approximately 2.5 mm smaller than that of the pipe. Care was taken to ensure a straight riblet seam along the axis of the dowel.
- (vi) The dowel was carefully inserted into the pipe, intermittently spraying with the detergent solution to facilitate smooth straight-line motion of the dowel.
- (vii) When the dowel emerged from the other end, it was removed, minus the riblets, by carefully moving it from side to side while pulling it out. This served not only to dislodge the riblets from the felt, but also to remove some of the excess detergent between the riblets and the pipe wall allowing the riblets to adhere to the pipe while the dowel was removed.
- (viii) A length of pure gum rubber tubing, with an OD marginally smaller than the ID of the pipe lined with riblets, was inserted into the pipe and one end connected to a compressed air line.
- (ix) With air flowing through the gum rubber tube, the free end was slowly pinched, causing the tubing to expand against the pipe inner wall, which forced excess detergent between the riblets and the pipe wall out through the ends of the tube. To minimize deformation of the riblets, the flexible tubing was only expanded for about 2 s at a time.

- (x) The tube was clamped vertically for about 10 min. and then carefully flushed with distilled water to remove detergent from the riblet surface.
- (xi) The tube was again clamped vertically and allowed to dry for 24 hr..
- (xii) Once dry, the dowel was reinserted and pressed against the section of the wall containing the pressure tap holes. The 0.025" drill bit was used to puncture a hole through the riblet film. A sharp jab was preferred to re-drilling because it was feared that a rotating drill would tend to tear the riblets beyond the region of the hole.
- (xiii) Excess material around the pressure tap hole was removed by the sequential process of filing and re-boring, as described above. Care was taken not to excessively file the material from the inner wall in order to minimize axial disturbances of the fluid flow.
- (xiv) A small amount of epoxy was placed at the entrance to the riblet section to prevent the riblets from peeling when the fluid underwent a contraction from the smooth to the riblet pipe.

Bored through Swagelok tees and unions completed the assembly of the riblet test section in the manner detailed earlier for the smooth test sections.

2.2.1.4 Trailing Smooth Test Section.

In each pipe system, a trailing smooth test section was placed downstream of the upstream smooth and riblet test sections to assess polymer degradation effects in the pipes.

In the 10.21 mm test system, two sections, designated S2D_{a-b}, were cut from a single tube. S2D_a, of length 422 mm (41.4 ID) had a flow re-development length and

contained pressure tap T8 located 95.25 mm from the downstream end. The recovery length for the flow exiting the riblet pipe was thus 327 mm (32.0 ID). S2D_b, of length 374 mm (36.7 ID) housed tap T9 located 71.12 mm from the downstream end resulting in an inter-tap distance [T8-T9] = [398 mm (39.0 ID)].

In the 7.82 mm test system, two sections, designated S1D_{a-b}, were cut from a single tube. S1D_a, of length 220 mm (28.0 ID) provided the flow re-development length. S1D_b, of length 253 mm (32.4 ID) housed taps T8 and T9 located 71.1 mm from the upstream and downstream ends respectively resulting in an inter-tap distance [T8-T9] = [134 mm (17.1 ID)]

The fabrication of the pressure tap holes, as well as the assembly of the test section with bored through fittings mirrored the procedure described earlier for the upstream smooth test sections.

2.2.1.5 Pressure Transducer Interface Unit.

Each test section pressure tap was connected to the pressure transducers via an interface, constructed from 1/4" 2-way valves, 3-way valves, crosses, and 1/4"-1/8" reducers mounted on an aluminum frame, which allowed variation of the tap pairs across which pressure drop was required.

The upstream smooth pressure transducer interface (PTI), shown in Figure 2.2.3a, interfaced pressure taps T1, T2 and T3 to the pressure transducers. Taps T1 and T2 were connected, via 1/4" 2-way ball valves, to the high pressure arm of the PTI and subsequently to the high pressure side of the pressure transducer by 1/8" flexible tubing. Tap T3 was connected to the low pressure arm of the PTI through a 1/4" 2-way ball valve. A 2-way valve physically connected the high and low pressure lines of the PTI allowing

pressure equalization in both arms. This PTI therefore allowed tap pairs T1-T3 or T2-T3 to be on-line during experimental runs.

The riblet PTI, shown in Figure 2.2.3b, connected taps T4-T7 to a second independent set of pressure transducers mounted on an aluminum frame. Tap T4 was connected, via a 1/4" 2-way valve, to the high pressure arm of the interface while tap T7 was connected to the low pressure arm of the PTI. Taps T5 and T6 may be toggled between the high and low pressure lines via 1/4" 3-way valves. This configuration allowed tap pairs T4-T5; T4-T7; T5-T6; T5-T7 or T6-T7 to be on-line during an experimental run. The high and low pressure lines were physically connected by a 2-way valve for pressure equalization.

The trailing smooth section PTI connected taps T8 and T9 to the pressure transducers mounted on the upstream smooth interface (Figure 2.2.3c). Tap T8 was connected via a 2-way valve, to the high pressure arm of the PTI and tap T9 was similarly connected to the low pressure line. A 2-way valve allowed pressure equalization between the two arms.

2.2.2 Upstream System

2.2.2.1 Tanks.

Two 55-gallon tanks, positioned with their bases approximately 1.7 m above the floor, were used to mix and store the solutions under investigation. The tanks were filled, via flexible tubing, from the main distilled water line. Prior to experimental runs, the volume in each tank was approximately 180 l; the exact volume was determined by measuring the fluid height, via clamped, vertical, metal rulers with 1/16" divisions, and employing a pre-established volume-height calibration. The fluid in the tanks was heated by

band heaters located approximately 20 cm from the base of the tanks and the temperature monitored independently in each tank by calibrated 5 k Ω thermistors connected to the data acquisition system. A Lightning[®] Model-10 mixer, clamped onto either tank rim, with an A-310 impeller, ensured efficient mixing with minimal mechanical degradation of the polymer solution.

A 2" PVC wye provided multiple flow paths for the fluid entering and leaving the tanks. Valves VL and VR controlled the flow to and from the left and right tanks respectively such that each tank could be isolated at any time; valve V1 controlled the flow entering the pump through a length of 2" flexible tubing and VB controlled the flow to the drain through a length of 1 1/4" flexible tubing.

2.2.2.2 Pump Unit.

The pump unit comprised a Moyno positive displacement pump, model 3L4-SSQ-AAA which was driven, through a series of timing belts and pulleys, by a Reliance 2 Hp TEFC-XE motor. The motor was controlled by a T.B. Woods 2 Hp variable-frequency E-trAC AC inverter. The pump was designed to operate between 100 rpm and 940 rpm with a discharge rate of 0.13-1.07 l/s. However, the 2 Hp motor was under powered and subsequently one of the three rotor stages was removed resulting in an operating range of 0.15-1.2 l/s. The discharge rate was remotely adjusted by the inverter which provided variable frequencies, at constant torque, to the motor.

2.2.2.3 Calming Chamber.

Three pieces of Spiral Wrap Tricomb Honeycomb were placed into the flexible corrugated hose connecting the pump discharge to the test section. Each piece was 3" long,

2" OD with 1/4" cell honeycomb encased in a stainless steel sleeve. Wagger (1992) estimated that the presence of the honeycomb reduced the wall shear stress in the hose by a factor ~ 5000 with the Reynolds number in each cell of approximately 2100, thus creating low disturbance fluid prior to entry into the test section.

2.2.3 Downstream System

2.2.3.1 Flow Controller.

Under conditions of gravity flow, the flowrate was controlled sensitively by two valves placed in parallel (Figure 2.2.4). The lower valve, FCV1, a 3/4" stainless steel ball valve with 3/4" female NPT fittings, allowed diversion of fluid to the bypass line of the controller which contained a 10-turn, 3/4" needle valve, FCV2, allowing sensitive control of the fluid through the system. The entire assembly was mounted on a 10" x 12" x 1/8" aluminum plate and affixed to the unistrut support.

2.2.3.2 Temperature Probe.

The temperature of the fluid exiting the flow controller was measured by a 5 k Ω thermistor connected to the data logger. The original data logger (section 2.2.3) was internally configured to calculate and display temperature directly. In the newer data logger, the thermistor resistance was measured directly and the temperature determined from a temperature-resistance calibration curve (section 3.1.4). The thermistor was housed in a 1/8" stainless steel casing and immersed in the flow through the vertical branch of a 3/4" stainless steel union tee.

2.2.3.3 *Flow Diverter*

Under conditions of gravity flow, the mass flow rate was determined by measuring the mass of effluent per unit elapsed time. The unit consists of an electronic timer, a snap switch mounted on a pivoting diverter arm and a digital balance which was used to weigh the effluent collected in a 6 l container, schematically shown in Figure 2.2.5.

The original electronic timer used was a DX100 Solid State Time/Count Totalizer that was configured through appropriate connections to display elapsed time with 0.1 s resolution. The timer was reset by a remote switch housed in a 2 1/4" x 2 1/4" x 5" aluminum box that signaled open and closed circuits by red and green lights respectively. This timer eventually failed on 30 May 1993 and was replaced by a Duran Model 45610-100 Single Preset, Six Digit Count/Time Controller. The controller was configured to display elapsed time, with 0.1 s resolution, through a series of DIP switches located on both sides of the unit. A panel mounted reset switch eliminated the need for the remote reset switch box. A snap switch, connected next to the pivot arm, controlled the start/stop operations of the timer. The position of the switch was adjusted by the pivoting arm via a screw that would either press or release the snap switch.

The pivoting arm consisted of a 1/2" copper tubing, 380 mm long with a 90° bend at the discharge end. The tube was supported by a bored through rod end connector, which had a second, perpendicular hole into which the rod comprising the pivot axis was inserted. The tube was connected to the discharge valve, VFC3, by flexible tubing. The mass of diverted effluent was measured by an digital top pan balance with a maximum reading of 5 kg and 1 g resolution. The effluent was collected in a 6 l graduated container. Undirected effluent discharged to the drain through a supported funnel and flexible tubing, The funnel was positioned so that it overlapped with the container in order to prevent spillage when the flow was diverted.

2.3 Measuring Devices

2.3.1 Pressure Transducer and Carrier Demodulator.

Three differential pressure transducers, with full-scale ranges 0.1, 1.0 and 10 psid, were used to measure the pressure drops across the test section pressure taps. The transducers were Model CJ3D Variable Reluctance transducers supplied by C.J. Enterprises. Constructed of stainless steel, the transducers consisted of a flat pressure sensing diaphragm clamped between two matched case halves each with electrical pickups that form part of bridge circuit (Figure 2.3.1a) with the bridge output being proportional to the pressure drop. Bleed screws were provided to enable complete liquid filling of the cavity surrounding the diaphragm. The output voltage was linear with pressure with rated accuracy $\pm 0.5\%$ of full scale. Hysteresis was 0.5% of full scale and over pressure was 2 times the range with 0.5% full scale maximum zero shift. The transducers were connected by a 1/8"-27NPT connector to the PT interface board.

The output reluctance from the pressure transducers was converted to a DC signal via a Model CJCD-411 Carrier Demodulator designed for ± 10 VDC full scale output (Figure 2.3.1b). The response time of the unit was rated less than 50 ms and zero and span controls are facilitated by external, graduated, knobs. The accuracy of the unit was $\pm 0.5\%$ full scale, including linearity and drift. The connection between the pressure transducers and carrier demodulator was made via shielded, 3-wire cables with WK-3-32S connectors.

2.3.2 Data Acquisition System.

Initially, a 4-channel Hewlet Packard Logging Multimeter, model HP3467, simultaneously displayed and printed the output from the carrier demodulator and

temperature probe. Each channel may be configured to measure DC voltage, AC voltage, resistance and temperature. However the system failed on 15 August 1992 and was replaced by a Fluke Hydra Data Logger, model 2625A. The data logger featured 21 analog and digital channels able to measure DC voltage, AC voltage, temperature via thermocouples and RTDs, resistance and frequency. Each channel was configured via Hydra Data Logger software allowing full instrument control from an IBM PC through the RS-232 port. During experimental runs, the maximum sampling rate was approximately 2 samples per channel per second. Logged measurements may be stored in an ASCII file format or outputted directly onto an IBM PC Printer. The former was most often employed as it allowed direct access by all modern spreadsheet software packages.

2.4 Other Related Equipment

2.4.1 Manometers

The 0.1 and 1.0 psid transducers were calibrated with a water filled manometer comprising of two glass tubes clamped vertically. Each tube may be connected, via 1/8" flexible tubing, to either the high or low pressure side of the transducers. The tubes were also connected by a stopcock which allowed pressure equalization in both tubes. With the stopcock closed and each arm isolated, the differential pressure may be altered by adjusting the height of a water reservoir connected to the high pressure arm of the manometer (Figure 2.4.1a).

The 10 psid transducer was calibrated with a mercury manometer consisting of a U-tube with one end connected to a compressed nitrogen cylinder, via a 1/4" union cross through a regulating valve and the other end open to the air through a mercury trap (Figure 2.4.1b). One branch of the cross was connected, via 1/8" flexible tubing, to the high pressure port of the transducer and the other, through a 2-way valve, to the atmosphere.

2.4.2 Small Scale Mixing System

Master batch polymer solutions were prepared using a Lightin® LabMaster™ Model TSR1516 mixer with an A310 impeller rated at speeds from 0-600 rpm. Solutions were mixed in a 6 l baffled stainless steel vessel which ensured efficient mixing.

2.5 Chemicals

Five grades of Union Carbide POLYOX™ Water Soluble Resins (polyethyleneoxide) and two grades of American Cyanamid CYANAMER™ (polyacrylamide) were used to effect turbulent flow drag reduction. The polyethyleneoxide polymers were >95% polymer with < 3% fumed silica; < 0.02% ammonium salts; < 0.02% ethyl amine; < 0.0005% monomer and < 0.72% calcium salts. The polyacrylamide polymers were > 98% polymer with < 1% acrylic acid; < 0.5% monomer and < 0.5% "water insolubles". Table 2.5.1 summarizes the designation of the polymer series, both the manufacturer's and the abbreviated form used throughout this work, and an approximate molecular weight supplied by the manufacturer.

Table 2.2.1 Pipe designation and fabrication specifications

PIPE SECTION DESIGNATION	NOMINAL ID* (mm)	NOMINAL RIBLET HEIGHT (mm)	LENGTH		TAP-PAIR DISTANCES (mm)
			(mm)	(smooth pipe ID)	
S1 _a	7.82	-	638	81.6	[T1-T3, T2-T3] [286, 166]
S1 _b	7.82	-	286	36.5	
S2 _a [†]	10.21	-	810	84.1	[T1-T3, T2-T3] [793, 397]
S2 _b [†]	10.21	-	397	38.9	
S2 _c [†]	10.21	-	396	38.8	
R1A _a	7.82	0.11	236	30.2	[T4-T7, T5-T7, T6-T7] [400, 283, 164]
R1A _b	7.82	0.11	283	36.2	
R1B _a	7.82	0.15	232	29.8	[T4-T7, T5-T7, T6-T7] [345, 233, 113]
R1B _b	7.82	0.15	232	29.7	
R2A _a	10.21	0.11	283	27.7	[T4-T7, T5-T7, T6-T7] [440, 297, 157]
R2A _b	10.21	0.11	297	29.1	
R2B _a	10.21	0.15	360	35.3	[T4-T7, T5-T7, T6-T7] [577, 359, 216]
R2B _b	10.21	0.15	359	35.1	
S1D _a	7.82	-	220	28.0	[T8-T9] [134]
S1D _b	7.82	-	253	32.4	
S2D _a	10.21	-	422	41.4	[T8-T9] [398]
S2D _b	10.21	-	374	36.7	

[†] fabricated by Wagger (1992)

* measured riblet dimensions: 0.11 mm: $h = 0.105 \pm 0.001$ mm; $s = 0.145 \pm 0.001$ mm; $t = 0.081 \pm 0.002$ mm
0.15 mm: $h = 0.108 \pm 0.001$ mm; $s = 0.165 \pm 0.001$ mm; $t = 0.081 \pm 0.002$ mm

Table 2.5.1 Series designation and approximate molecular weights for water soluble polymers.

POLYMER	SERIES DESIGNATION		APPROXIMATE MOLECULAR WEIGHT $M_w \times 10^6$
	Manufacturer	This Work	
PEO	WSR N-10	N-10	0.1
PEO	WSR N-750	N-750	0.3
PEO	WSR N-60K	N-60K	2.0
PEO	WSR-301	W-301	5.0
PEO	UCARFLOC™ Polymer 309	P-309	8.0
PAM	CYANAMER™ N-300 LMW	N-300L	5.0
PAM	CYANAMER™ N-300	N-300	15

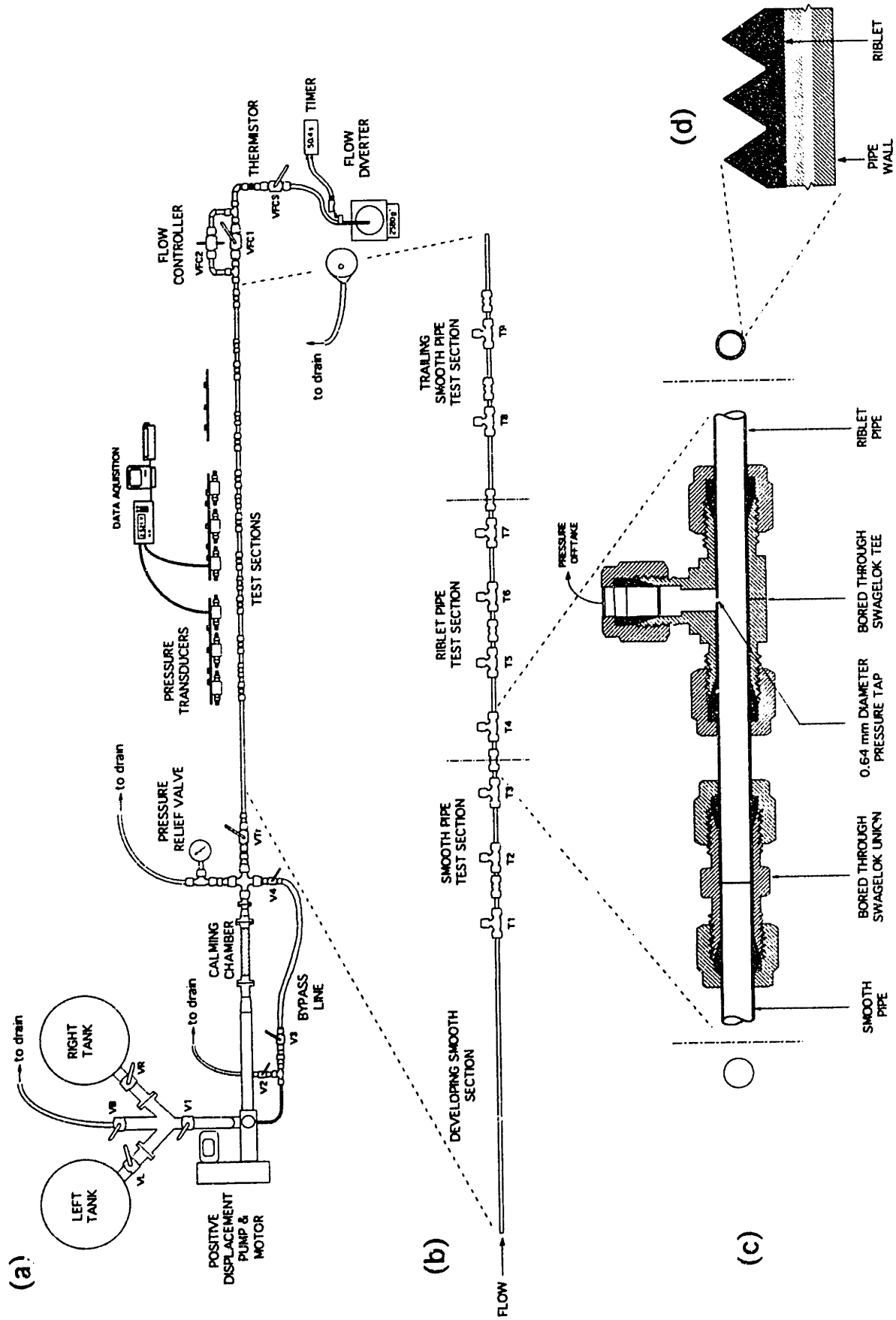
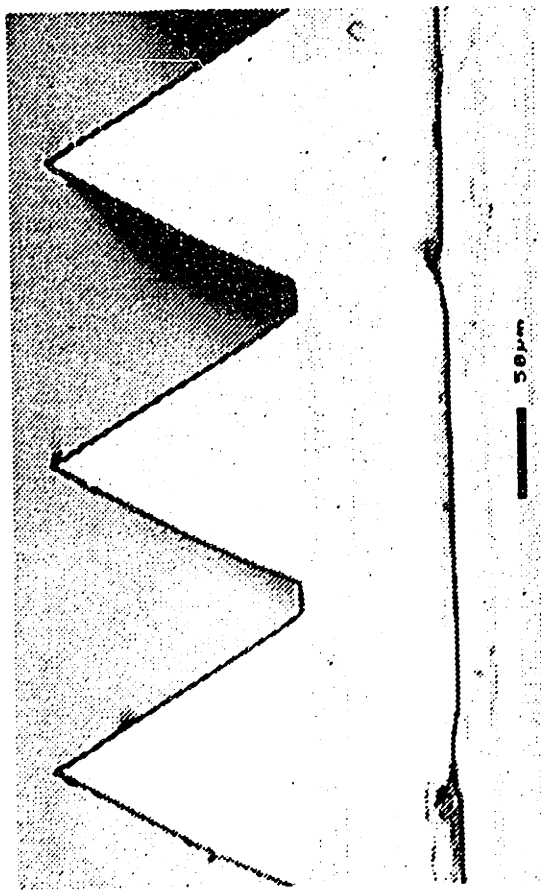
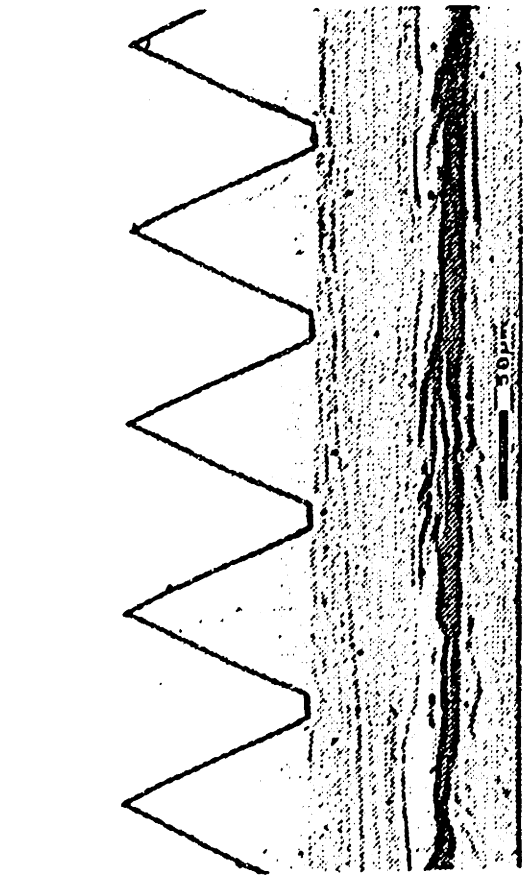


Figure 2.1.1 Experimental apparatus

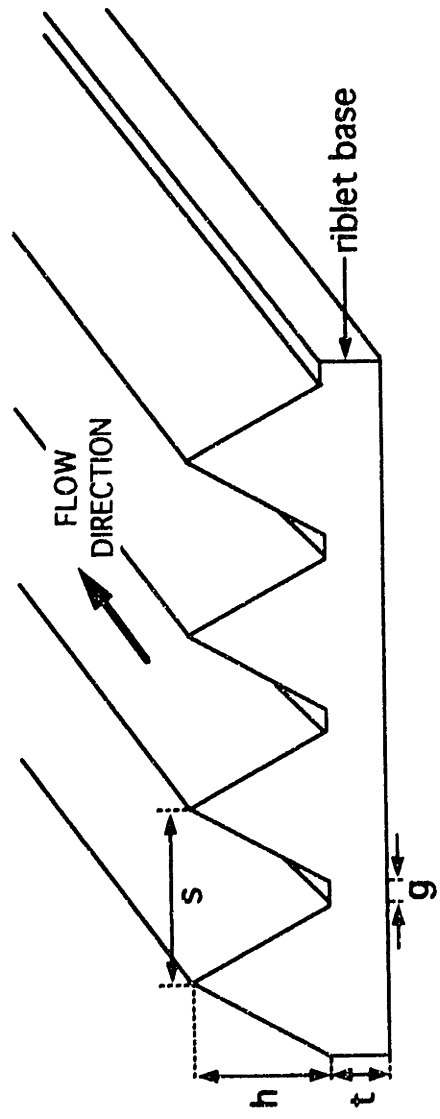


(ii) Nominal 0.0060" Riblets



(i) Nominal 0.0045" Riblets

(b) ENVIRONMENTAL SCANNING ELECTRON MICROSCOPE PHOTOGRAPHS OF 3M V-GROOVE RIBLET SURFACES



(b) V-GROOVE RIBLET SCHEMATIC

Figure 2.1.2 3M V-groove riblets

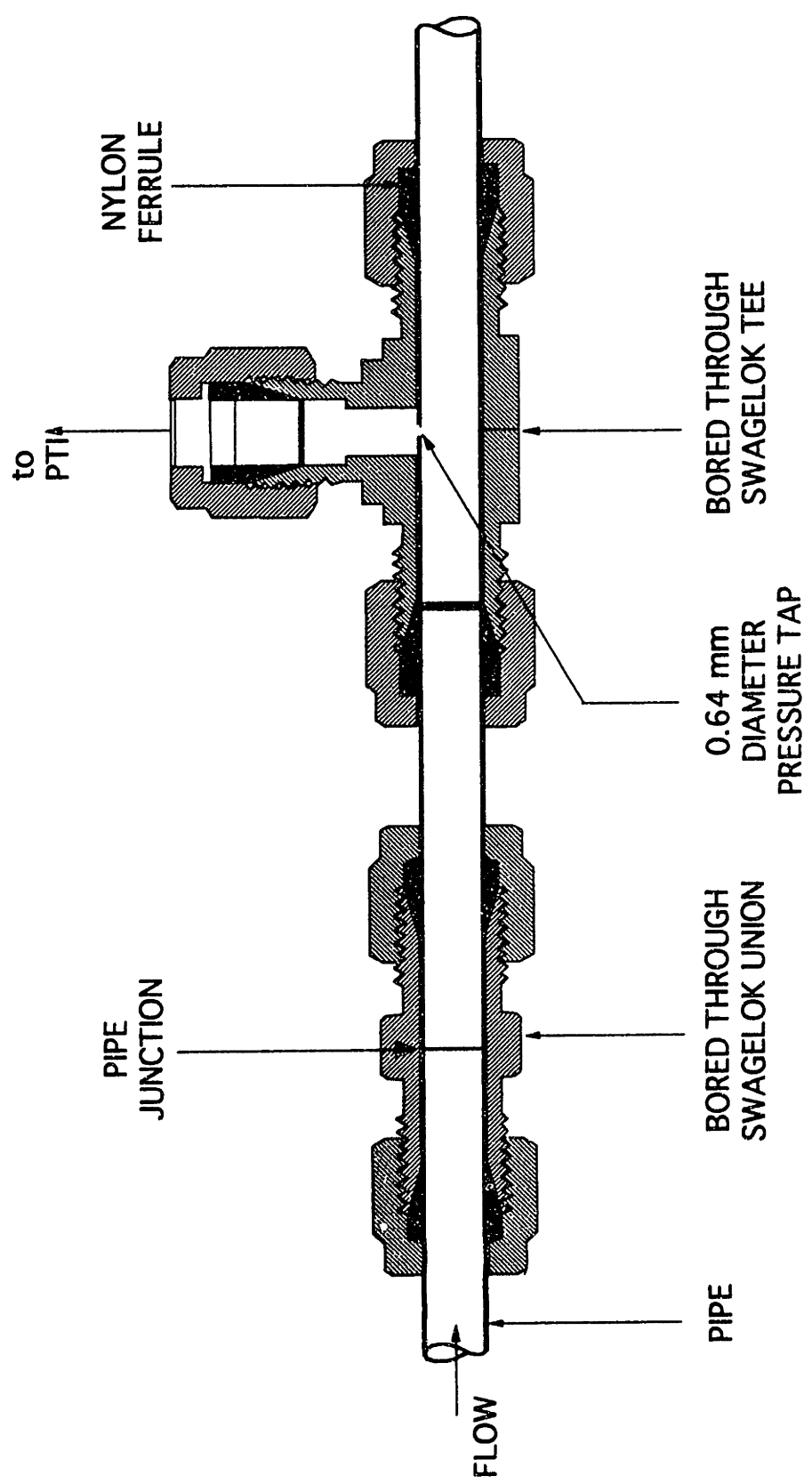
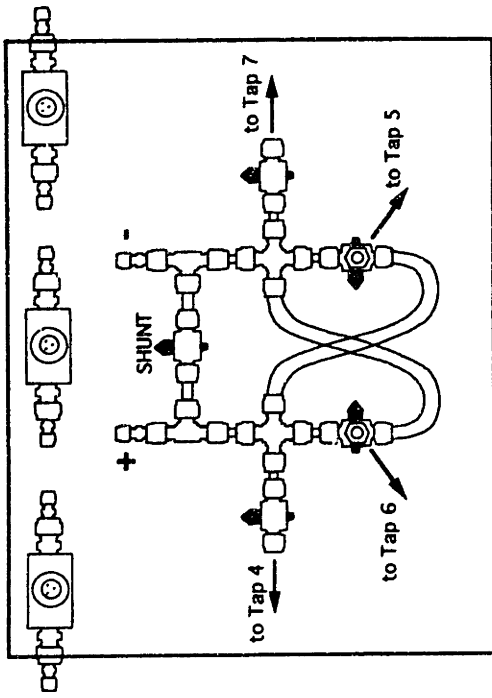
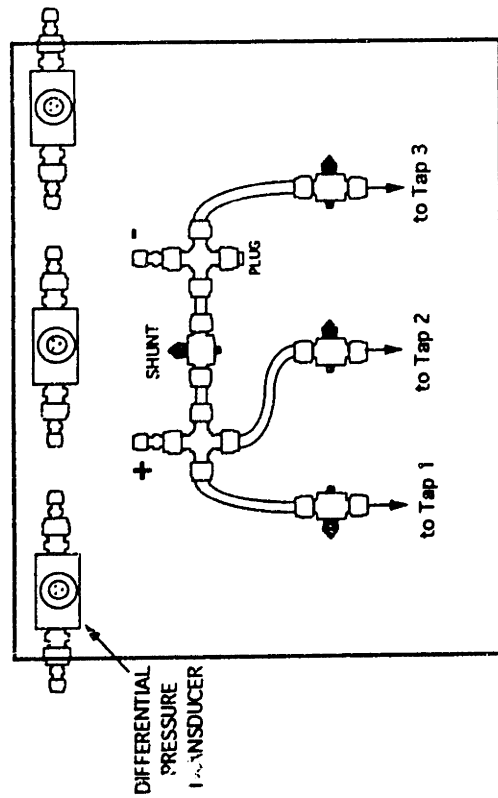


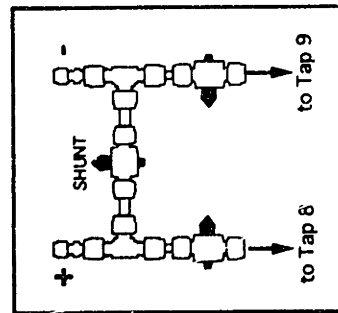
Figure 2.2.2. Pipe interface and pressure tap housing



(b) Riblet PTI



(a) Upstream Smooth PTI



(c) Trailing Smooth PTI

Figure 2.2.3. Pressure Transducer Interface (PTI) boards

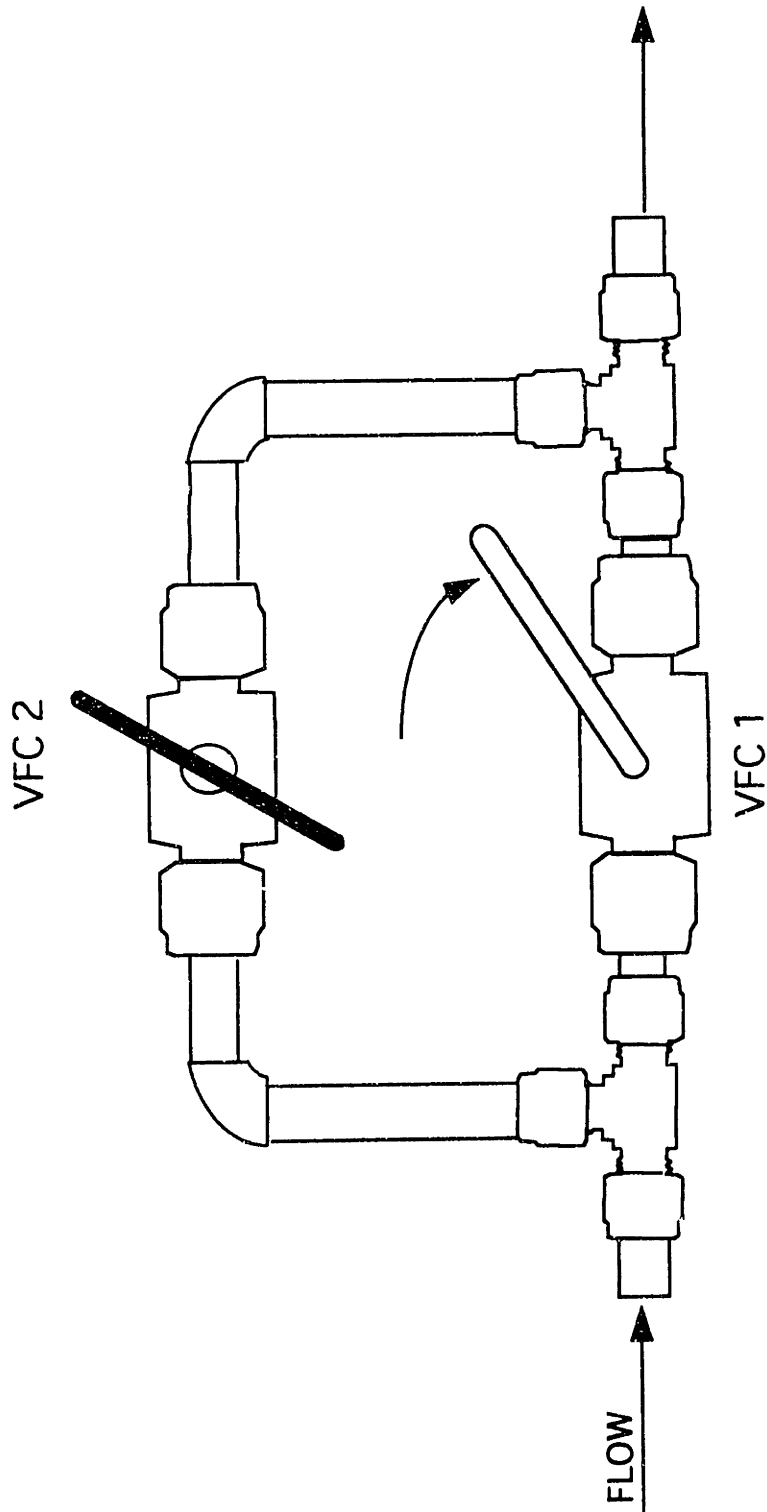


Figure 2.2.4. Flow controller unit

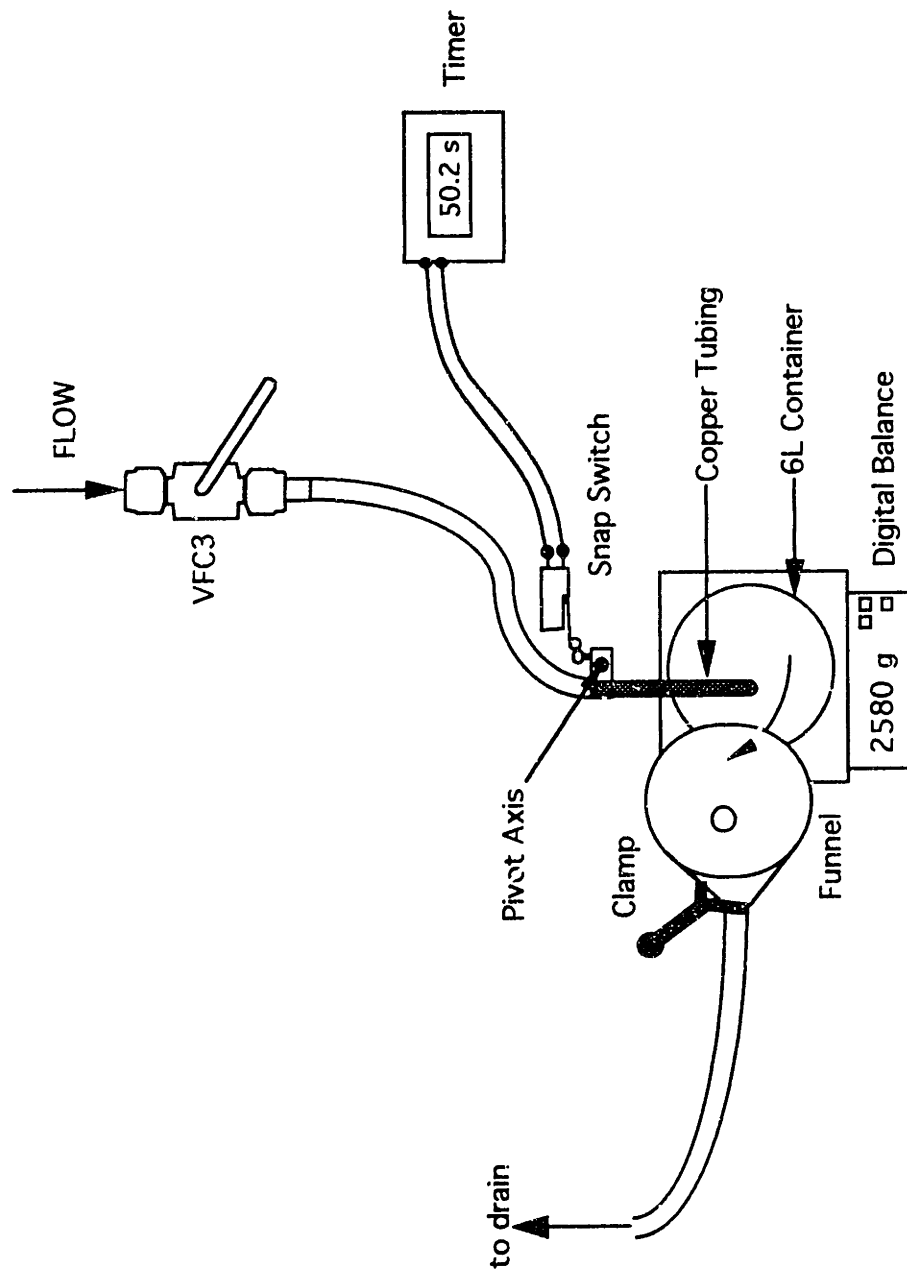


Figure 2.2.5. Flow diverter unit

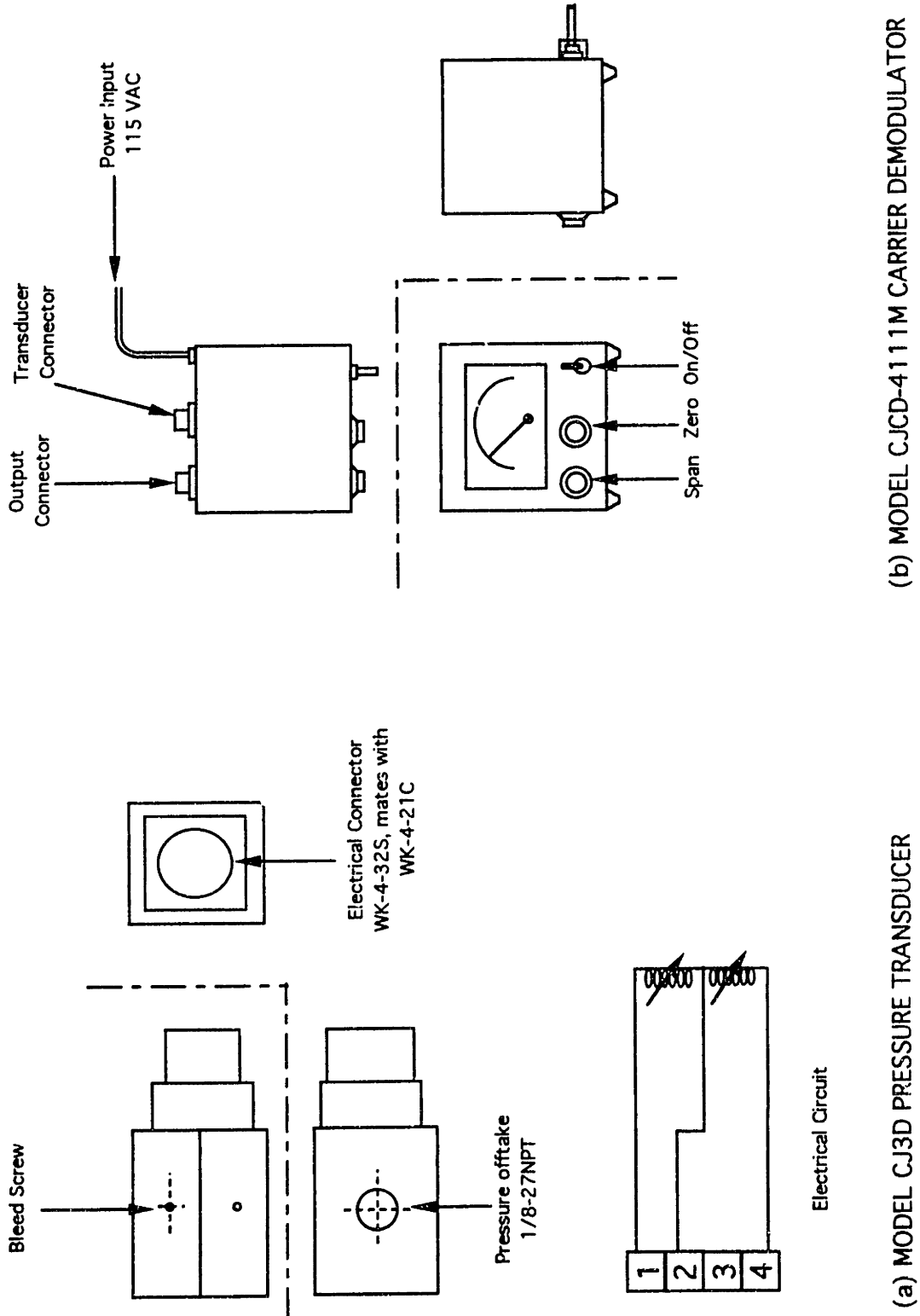
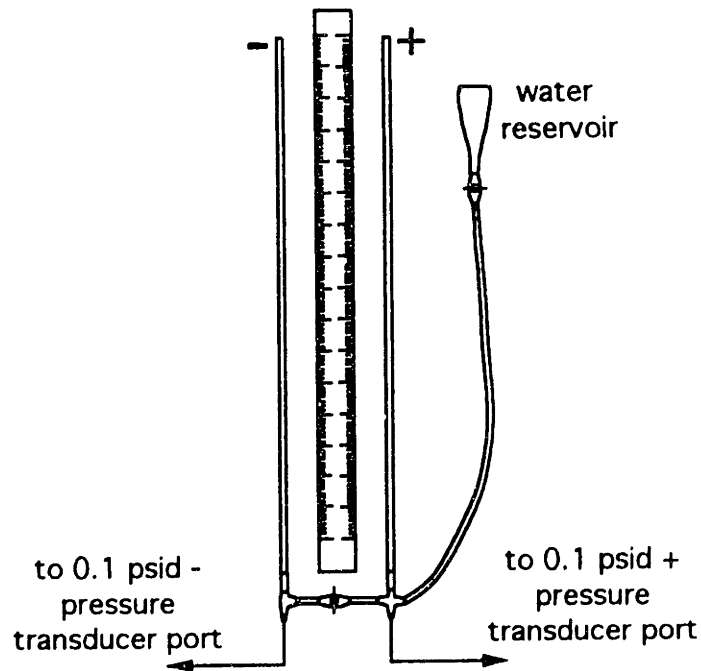
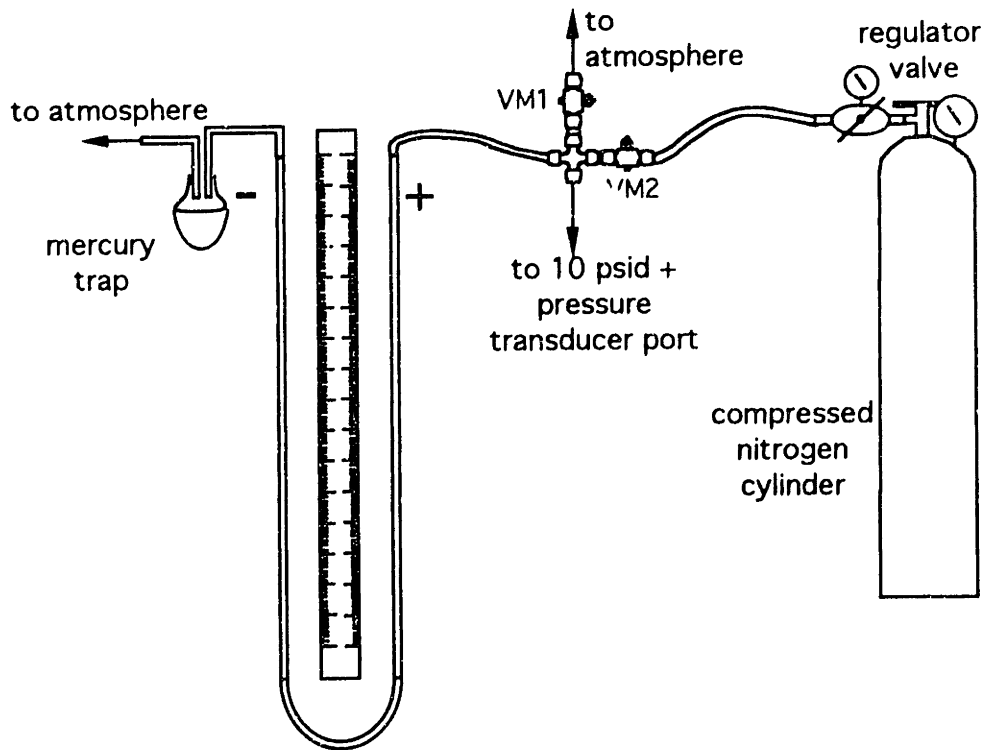


Figure 2.3.1. Pressure transducer and carrier demodulator



(a) Water Manometer



(b) Mercury Manometer

Figure 2.4.1. Water and Mercury manometers

Chapter 3

Experimental Procedures

This chapter describes the experimental procedures employed in order to achieve the aims of this work. The procedures are presented in the following order: equipment calibrations; polymer solution master batch preparation and classification, experimental run procedures and data reduction.

3.1 Calibrations

3.1.1 Tank Calibrations

The two 55-gallon tanks used, though cylindrical in shape, had slightly convex bottoms. This meant that the calculated cylindrical volume ($\pi d^2 h$) overestimated the volume in the tank and thus introduced systematic errors when the concentration of polymer solutions were calculated (section 3.3.1). Wagger (1992) calibrated the tanks by recording cumulative fluid volume in the tanks, added in 2 l increments, and measuring the liquid height relative to the tank base.

Figures 3.1.1a and 3.1.1b are, respectively, plots of the volume of the left and right tanks, in liters, against the liquid level height, in inches. A linear relation, based on least squares parameter estimation, was fit to the data yielding the following volume-height relations:

$$\text{Left Tank:} \quad \text{Volume (l)} = -1.75820 + 6.62538 \text{ Height (in)} \quad (3.1-1a)$$

$$\text{Right Tank:} \quad \text{Volume (l)} = -1.35260 + 6.64321 \text{ Height (in)} \quad (3.1-1b)$$

3.1.2 Pump Calibrations

The procedure for determining the flow rate through the system as a function of the controller frequency and back pressure was as follows, with reference to the flow system diagram, Figure 2.1.1:

- (i) With the tanks initially empty, valves VL and VR were closed and the tanks then filled with approximately 175 l of distilled water each via the distilled water line.
- (ii) With VR closed, VL was opened allowing liquid from the left tank to pass through the system.
- (iii) The bypass line was isolated by closing valve V4.
- (iv) Valves VTr and VFC1-VFC3 were fully open producing a flow path through the test system.
- (v) The E-trAC inverter was supplied with power and preset to 35 Hz, a value that ensured the pressure safety limit on the pump would not be exceeded at initial startup: the frequency at which the back pressure was 100 psig was determined by incrementing the frequency by 5 Hz at a time while the pump was operational.
- (vi) The motor was engaged.
- (vii) The fluid in the tank was allowed to settle, after which a stopwatch was started at a recorded initial height and stopped at a noted final height. The back pressure was measured during the run.
- (viii) The controller frequency was changed to a new value and steps (vi) - (vii) were repeated.

- (ix) When the fluid in the tank had reached a low level, making heights difficult to read, valve VL was closed and VR opened and step (viii) was repeated.
- (x) After obtaining a number of readings (including repetitions), the fluid heights, elapsed time, controller frequency and back pressure were entered into a spreadsheet which calculated volumetric flow rate.

Six pump calibrations were conducted; four in the 10.21 mm pipe system and two in the 7.82 mm system. The fluid in the tanks alternated between distilled water and 50 wppm solutions of P-309, allowing a wide range of back pressures to be investigated. Details of the calibrations are summarized in Table 3.1.1.

Figures 3.1.2 - 3.1.7 are plots of the flow rate, in l/s, versus the controller frequency, in Hz, for each of the calibrations. The data were fit with both linear and quadratic relations with zero intercept based on least squares regression. The values of the calibration parameters are summarized in Table 3.1.1.

Table 3.1.2 summarizes the results of a two-factor analysis of variance (ANOVA) that examines the dependence of the calibration constants on the pipe configuration and on the solution composition. A comparison of columns 4 and 5 of Table 3.1.2 show that the calibration constants based on a linear regression are dependent on both the pipe configuration and solution at the 95% significance level. The dependence on the solution viscosity is not clear but the analysis points to a strong dependence on the back pressure experienced by the pump. At a given controller frequency, the flowrate decreased as the back pressure increased. This may be accounted for in the calibration by a correction term such that:

$$Q \text{ (l/s)} = A_1 F \text{ (Hz)} + A_P P \text{ (psig)} \quad (3.1-2)$$

or:

$$\frac{Q}{F} = A_1 + A_P \frac{P}{F} \quad (3.1-3)$$

A plot of Q/F versus P/F is shown on Figure 3.1.8 and includes the data for the calibration runs of Wagger (1992). Amidst the scatter, a linear trend may be inferred providing some validity to the functionality of Eq. (3.1-2). A linear least squares regression gives values of $A_1 = (2.023 \pm 0.050) \times 10^{-3} \text{ l}$ and $A_p = (-5.660 \pm 0.354) \times 10^{-4} \text{ l/s.psig}$.

During an experimental run, controller frequencies were converted into flowrates using, as a default, the coefficients of the quadratic expression corresponding to the pipe configuration. As an example, for solvent flow in the 10.21 mm test system with 0.15 mm riblets, a controller frequency set at 40 Hz produced a flowrate of 0.787 l/s. For the linear calibration, the corresponding flowrate would be 0.775 l/s; a small but significant difference of 1.5% from the value obtained by the quadratic regression.

3.1.3 Transducer Calibrations

Prior to each experimental run, the 0.1-, 1.0- and 10-psid transducers were calibrated. The 0.1-psid transducers were also calibrated at the end of each run since they were very sensitive and prone to drift in the calibration constants. Since there were six pressure transducers, over 1100 calibrations were performed during the course of this work. For the most part, the calibration constants did not change significantly with time but step changes occurred after the transducers were taken off-line for maintenance, because the calibrations were sensitive to the tightness of the screws that held the case halves together.

The 0.1- and 1.0- psid differential transducers were calibrated with the water manometer and the 10-psid transducer calibrated with the mercury manometer. The procedure for calibrating with the water manometer was as follows:

- (i) The temperature of the water in the reservoir was recorded. This temperature was used to calculate the density of the water.
- (ii) The pressure transducer was connected to the water manometer via long 1/8" flexible tubings with stainless steel nuts and nylon ferrules.
- (iii) The bleed screws were opened to release trapped air in the transducer cavity. The bleed screws were then closed.
- (iv) The transducer was connected, via a shielded cable with appropriate connectors, to the carrier demodulator.
- (v) The zero and span were adjusted to the values required for an experimental run. Under normal experimental conditions, the transducers were set at maximum sensitivity (span = 10).
- (vi) The arms of the manometers were isolated by closing the connecting stopcock. The level in each arm was recorded together with the initial zero reading, V_0 , in volts, displayed on the data logger.
- (vii) The water reservoir was raised incrementally in approximately 20 mm and 20 cm steps in the 0.1- and 1.0-psid transducers respectively. At each reservoir level, the height of water in each arm and the voltage reading, V , were recorded. When the maximum range was reached, the reservoir was lowered incrementally, recording level heights and voltages at each position. Taking measurements with both positive and negative height changes served as a check on the voltage drifts in the transducer readings.
- (viii) The data were entered into a spreadsheet where the heights were converted into a pressure drop, ΔP , in psid. The calibration constants, $K_{PT} = dV/d\Delta P$, in volts/psid, were obtained by a linear regression of the data with K_{PT} representing the slope of

the regressed line. Figures 3.1.9 and 3.1.10 illustrate the regression of ΔP versus V for the 0.1- and 1.0-psid transducers respectively. The hollow circles (○) represent an increasing increment, abbreviated "+ increments" in the legend and closed circles (●) represent a decreasing increment, abbreviated "- increments". Calibrations were immediately repeated whenever the correlation coefficient, R^2 , was less than 0.999500, thereby ensuring strict control on the accuracy of the calibration coefficients.

The calibration constants in the 0.1-psid transducers were respectively 42-46 and 84-90 V/psid in the smooth and riblet transducers with the span set at maximum (=10). Prior to this, values of K_{PT} was as high as 115 V/psid in the riblet pipe transducer but the sensitivity could not be reproduced once the old diaphragm failed and replaced with a new one.

The calibration procedure for the 10-psid differential transducers was as follows:

- (i) The ambient temperature was recorded. This was the temperature used in calculating the density of the mercury in the manometer.
- (ii) The positive pressure side of the 10-psid differential transducer was connected to the union cross of the mercury manometer by a 1/8" length of flexible tubing. The negative pressure side of the transducer was left unconnected at atmospheric pressure. The mercury levels in each arm and the voltage reading were recorded.
- (iii) The transducer was electrically connected to the carrier demodulator and the span and zero values adjusted as required by the experiment.
- (iv) With valves VM1 and VM2 closed (see Figure 2.3.2) and the pressure regulator valve closed, the valve on the nitrogen cylinder was opened.

- (v) Valve VM2 was opened and the regulator valve opened slightly resulting in a drop in the mercury level in the high pressure arm and a rise in the level on the atmospheric side of the manometer. The manometer was then isolated from the tanks by closing VM2. It was found that the mercury levels, and hence the voltages, slowly increased if the manometer was left connected to the nitrogen cylinder.
- (vi) The mercury levels and voltage reading were recorded.
- (vii) Steps (iv) and (v) were repeated in incremental steps.
- (viii) At the maximum range or voltage, the mercury level was then decreased incrementally by closing valve VM2 and using VM1 to carefully release nitrogen, thereby lowering the pressure above the mercury in the positive pressure arm of the manometer. At each level, the mercury levels and voltage reading were recorded.
- (ix) The data were entered into a spreadsheet and the calibration constant, K_{PT} , obtained by linear regression detailed earlier. Figure 3.1.11 illustrates the regression of a typical calibration with symbols and legends identical to those described for the regression of the 0.1- and 1.0-psid transducer calibrations.

The 10-psid transducers were typically operated with maximum span (=10) which produced values of $K_{PT} \approx 3.7$ and 4.2 V/psid in the smooth and riblet transducers respectively.

3.1.4 Thermistor Calibration

The original data logger was configured to output temperature, in °C, directly. However, the newer data logger did not have the internal circuitry required for $5 \text{ k}\Omega$

thermistors, hence a temperature-resistance relation was required to convert resistance output of the thermistor to temperature.

- (i) A 500 ml flask was filled with water at a temperature $\approx 30^\circ\text{C}$.
- (ii) The temperature of the water was measured with a mercury thermometer with 0.1°C resolution and the resistance of the thermistor immersed in the flask was measured by the data logger.
- (iii) Approximately 50 ml was removed from the flask and replaced with 50 ml colder water ($\approx 10^\circ\text{C}$).
- (iv) Step (ii) was repeated.
- (v) Steps (ii)-(iv) were repeated until the water temperature was $\approx 10^\circ\text{C}$.

Figure 3.1.12 is a semi-logarithmic plot of the temperature, in $^\circ\text{C}$, versus thermistor resistance, in $\text{k}\Omega$. The data were regressed to give the following relation:

$$T (^\circ\text{C}) = 60.7662 - 51.0843 \log (R(\text{k}\Omega)) \quad (3.1-4)$$

3.1.5 Measured and Calculated Pipe Diameters

3.1.5.1 Smooth Pipe

The internal diameter of the smooth pipes was determined by two methods. In the first, five measurements were made of the diameter at each end of the test sections with a vernier calipers with $0.001''$ divisions, then averaged. The smooth pipe diameters obtained by this method were $d_s = [7.82 \pm 0.02, 10.21 \pm 0.02]$ mm for [S1, S2]. In the second method, the diameter of the pipes was calculated from the pipe volume; this procedure was as follows:

- (i) One end of the pipe was sealed with a thin plastic strip mounted flush with the pipe end and secured with paraffin wax and tape. The pressure tap holes were sealed with paraffin wax.
- (ii) The pipe was positioned vertically, with the sealed end freely resting on a top pan balance.
- (iii) A burette containing distilled water was clamped vertically above the open pipe end.
- (iv) The balance was tared and the burette stopcock was opened allowing the pipe to be filled with water.
- (v) The stopcock was closed when the water level reached about 5 mm below the upper end. A pipette was used to slowly add water until the water level was equal to the upper end. The weight and temperature of the water was measured.
- (vi) The volume of the water in the pipe was calculated, and the volume of the pipe, V , calculated by subtracting the volume of the tap holes, which was calculated based on the hole diameter and pipe thickness. The cross sectional diameter of the pipe was calculated:

$$d_c = \sqrt{\frac{4A_c}{\pi}} = \sqrt{\frac{4V/L}{\pi}} \quad (3.1-5)$$

This method yielded $d_s = [7.82 \pm 0.02, 10.21 \pm 0.02]$ mm for [S1, S2].

3.1.5.2 Riblet Pipes

Riblet pipes are not circular, so there is no single measure of the diameter. If d_s is the ID of the smooth pipe in which the riblets were installed, then the distances that can be used to describe a riblet pipe include:

$$(i) \text{ valley-to-valley diameter: } d_v = d_s - 2t \quad (3.1-6)$$

$$(ii) \text{ cross sectional diameter: } d_c = \sqrt{\frac{4A_c}{\pi}} = d_s - 2t - h \quad (3.1-7)$$

$$(iii) \text{ tip-to-tip diameter: } d_t = d_s - 2t - 2h \quad (3.1-8)$$

$$(iv) \text{ hydraulic diameter: } d_H = 4A_c / P_w = d_v / \sqrt{1 + \frac{4h^2}{s^2}} \quad (3.1-9)$$

The four "diameters" may be calculated based on the riblet geometry, assuming no deformation of the riblets during their installation in the pipe. Of these, only the cross-sectional diameter can be measured experimentally by determining the pipe volume per unit length. Values of the d_v , d_c (both calculated and measured), d_t , and d_H are summarized in Table 3.1.3.

3.2 Polymer Solution Master Batch Preparation and Classification

3.2.1 Preparation

Two methods, one for PEO and one for PAM, were used to prepare polymer solution master batches. Polyox PEO, a fine powder, may be dispersed in organic solvents such as 1,2-propanediol or 2-propanol whereas Cyanamid PAM, a grainy material, does not readily form suspensions and takes longer to dissolve in water.

A. PEO

- (i) The 6 l baffled, stainless steel vessel was filled with approximately 5 l of distilled water.

- (ii) Approximately 50 ml of formaldehyde solution was added.
- (iii) Depending on the polymer molecular weight and required solution concentration, a quantity of PEO was weighed in a 500 ml glass beaker.
- (iv) 1,2-propanediol was added to the PEO powder in the beaker until the resulting suspension may be well dispersed by stirring with a glass rod. For example, about 36 g of polymer typically required about 250 ml of 1,2-propanediol for efficient dispersion.
- (v) The mixer shaft and impeller were immersed into the water and the mixer speed was set at 500 rpm.
- (vi) The polymer suspension was added slow enough to ensure dispersion in the agitated water but fast enough to prevent addition into a viscous solution (≈ 5 s). This was particularly essential for the high molecular weight polymers.
- (vii) When the polymer had dispersed, the mixer speed was reduced to 300 rpm for about 5 minutes and then reduced to 150 rpm for about 2 hours.
- (viii) The mixer was stopped, the impeller and shaft were removed and cleaned, the vessel was then covered with four layers of clear plastic film (Saran Wrap™) and secured by a rubber band over the lip of the vessel.
- (ix) The master batch was left undisturbed for about 10 hours.

B. PAM

- (i) The 5 l baffled stainless steel vessel was filled with approximately 5 l of distilled water.
- (ii) Approximately 50 ml of formaldehyde solution was added to the distilled water.
- (iii) Approximately 24 g of PAM was weighed in a plastic boat.
- (iv) The mixer speed was set initially to 500 rpm.
- (v) The polymer was added **slowly** into the churning water.
- (vi) After all the polymer was added, the mixer speed was reduced to 300 rpm and maintained for about 15 minutes.
- (vii) The mixer speed was reduced to 200 rpm for about three hours and then to 120 rpm for another three.
- (viii) The mixer was stopped, the impeller and shaft were removed and cleaned and the vessel covered with four layers of Saran Wrap™ as above.
- (ix) The master batch was left undisturbed for 24 hours.

3.2.2 Classification

- (i) Approximately 60 ml of master batch was withdrawn using a plastic syringe.
- (ii) The exterior of the syringe was wiped clean and the vessel re-covered.
- (iii) Four aluminum weighing boats were weighed empty on a top pan balance with 0.0001g resolution. The boats were handled with forceps to reduce contamination.

- (iv) Approximately 15 ml of solution was put into each boat and immediately weighed.
- (v) The receptacles were placed into a vacuum oven.
- (vi) The samples were desiccated in the oven at 60 °C and 40 mm Hg absolute for approximately 16 hours.
- (vii) After desiccation, the oven was switched off and allowed to cool to ambient temperature.
- (viii) The polymer-residue boats were weighed. The average weight concentration, c , and the standard deviation, σ_c for the master batch were calculated. The fractional error, σ_c/c , was typically less than 0.008 in PEO and 0.015 in PAM master batches. New master batches were prepared if σ_c/c exceeded 0.02.

3.3 Experimental Runs

3.3.1 Preparation

- (i) Given a target solution concentration in each tank, c_{tank} wppm, and a tank volume, V_{tank} , of approximately 180 l, an amount of master batch of mass, m_{MB} , of concentration c_{MB} wppm, was weighed in a 10 l bucket where:

$$m_{\text{MB}}(\text{kg}) = 180 \frac{c_{\text{tank}}}{c_{\text{MB}}} \quad (3.3-1)$$

- (ii) The solution in the bucket was diluted by distilled water to a volume of about 8 l. This helped to reduce the time required for mixing in the tank and thus reduced degradation.
- (iii) With VL closed, the left tank was filled with approximately 150 l of distilled water.

- (iv) The mixer was clamped onto the lip of the tank with the impeller immersed into the water and engaged on the highest speed setting.
- (v) The diluted solution was slowly added into the tank away from the impeller. When very viscous solutions were used, polymer threads tended to migrate to the impeller shaft where they were quickly broken up. This may have degraded the solution but it was unavoidable in order to ensure a homogeneous solution in the tank.
- (vi) The bucket was thoroughly rinsed with distilled water and its contents poured into the tank ensuring all the master batch weighed went into the tank.
- (vii) The mixer was switched off.
- (vii) The level of the solution in the tank was increased with distilled water until the tank volume was:

$$V_{\text{tank}} = \frac{m_{\text{MB}} C_{\text{MB}}}{\rho_{\text{tank}} C_{\text{tank}}} \quad (3.3-2)$$

where ρ_t is the density of the fluid in the tank, calculated from density-temperature tables.

- (viii) The mixer was switched on with the lowest speed setting. The mixer speed was sensitively controlled by altering the voltage input, via a Variac, to the motor.
- (ix) A 1" dowel was used to manually agitate the fluid near the bottom of the tank where it was felt that the mixer may be inefficient.
- (x) The mixer was operated for 30 s at intervals of about 5 minutes.
- (xi) Steps (i)-(x) were repeated for the right tank.

- (xii) If the water temperature was initially below 25 °C, the tank heaters were switched on and the temperatures monitored until the liquid temperature was about 25.8 °C.
- (xiii) Valves VL and VR were opened.
- (xiv) The 0.1, 1.0 and 10-psid transducers were calibrated.
- (xv) The bypass line was isolated by closing V4.
- (xvi) VFC3 was closed followed by opening V1.
- (xvii) The 10-psid transducers were connected to the data logger. All the valves on the PT boards were initially closed. Each valve was opened individually to release trapped air in the lines. All the valves were then opened and the PTIs shunted to remove trapped air within the fittings. All valves were then closed and the PTI lines were connected to the transducers. The valves corresponding to the desired tap pairs were opened and the system shunted. The bleed screws on the transducers were opened to release trapped air in the transducer cavity and then were closed. The span and zero values of the carrier demodulator were set to the desired values and the high and low pressure lines isolated by closing the shunt valve. If the zero values differed significantly from that during calibration, the process was repeated. Much of the problems that arose had to do with trapped air in the lines which caused readings to fluctuate wildly.
- (xviii) The controller frequency was set to its highest safe operating value.
- (xix) The data logger was configured via the software package to measure the thermistor resistance and the output voltages from each carrier demodulator. The software wrote the data to an ASCII file called RUN***.DAT where *** is the run number.

3.3.2 Procedure

A. Pump-Driven Flow

Figure 3.3.1 illustrates the flow path of fluid through the system during conditions of pump-driven flow. In this configuration, the flow diverter was replaced by 1" flexible tubing to drain.

- (i) The data logger was enabled to record the zero values of the 10-psid transducer.
- (ii) Data acquisition was paused and valve VFC3 opened.
- (iii) The pump was started and residual water was flushed from the system before data acquisition resumed.
- (iv) About 5-10 voltage readings were obtained per flowrate. The higher flowrates had fewer samples because of limited solution volume.
- (v) The frequency was reduced by increments which decreased as the flowrate decreased. For example, a typical run might have recorded frequencies: 50, 40, 33, 27, 24, 20, 17, 15, 13, 11, 10, 9, 8, 7 Hz. Decreasing increments ensured that the data points on a logarithmic scale are approximately equally spaced.
- (vi) At the end of the run, the pump was switched off, data acquisition paused, valve V4 opened and VFC3 closed. This ensured that the conditions at the end of the run mirrored those at the beginning. The zero value of the transducer at the end of the run was recorded.

B. Gravity Driven Flow

Figure 3.3.2 illustrates the flow path of fluid through the system during conditions of gravity-driven flow.

- (i) If the pressure drop across the 10 psid transducers fell below 0.1 psid, the lines were transferred to the 0.1 psid transducers in the manner described in section 3.3.1(xvii). If not the 10-psid transducer remained in use. Prior to RUN 140, the 1.0 psid transducers were used but zero drift and linearity problems subsequently made their results error prone. The 10-psid transducers were robust in their readings even at low pressure drops.
- (ii) The diverter was connected to the end of the system. The position of the funnel was adjusted so that the timer started when the diverter arm was directly above the edge of the funnel. The tension in the flexible tubing allowed the diverter to snap back into the undiverted position rapidly.
- (iii) Valves VFC1 and VFC2 were initially fully open. Valve V4 was opened creating a fluid path through the bypass line. Valve VFC3 was initially closed and VTr was slightly closed at an angle of about 15° to trigger the flow at the entrance to the test system.
- (iv) Data acquisition was resumed, recording the zero values of the transducers.
- (v) Valve VFC3 was opened and the flow diverted. The maximum mass of effluent collected was constrained by the range of the balance (≈ 4300 g) and data were collected during an elapsed time of about 50 s allowing ≈ 25 readings to be collected per channel per flowrate .
- (vi) Data acquisition was paused, the diverter snapped back to its original position, and valve VFC3 closed.
- (vii) VFC1 was closed and steps (iv) - (vi) repeated.
- (viii) The flowrate was then controlled by incrementally closing the needle valve. At each needle valve position steps (iv) - (vi) were repeated. The increments of adjustment,

measured in turns of the handle, followed a similar logarithmic pattern as those for the pump for the same reasons. Transition to turbulence occurred typically after $8^{1/2}$ - $9^{1/4}$ turns of the handle depending on the level of liquid in the tanks.

C. Pump-Driven Bypassed Flow

In the big pipe system, the lowest flowrate under conditions of pump-driven flow overlapped with the highest flowrate of gravity-driven flow. In the 7.82 mm pipe, there was insufficient gravity head to overlap pump- and gravity-driven flows. The following procedure was used to bridge the flow rates between the pump- and gravity-driven ranges:

- (i) Valve VL was closed, isolating the left tank from the rest of the system. The drain line emanating from valve V2 was clamped onto the rim of the left tank so that fluid flowing through this line fed directly into the tank.
- (ii) Valves V2-V4 were all opened creating a flow path, when the pump was switched on, through the bypass (in the reverse direction) and into the left tank.
- (iii) The controller frequency was set to 20 Hz.
- (iv) Data acquisition was resumed then paused after recording the zero values of the appropriate transducers.
- (v) Valve VFC3 was opened and the pump switched on. The flow rate through the test system was then controlled by V4, VFC1 and VFC2. Closing V4 allowed higher flowrates through the system, i.e. a smaller bypassed fraction.
- (vi) The flow was diverted and data acquisition resumed. The diverter arm was returned to its original position after an elapsed time and the data acquisition paused.

- (vii) Only about 3-5 flow rates were sufficient to bridge the gap between pump- and gravity-driven flows.

Figure 3.3.3 illustrates the bifurcation of fluid at the entrance to the test section during operating conditions when some of the fluid was diverted through the bypass line and into the left tank.

On completion of an experimental run, the 0.1-psid transducers were re-calibrated to account for any drift in the calibration coefficient. The drift was typically of order 1% in the calibration constant. The tanks were emptied and rinsed thoroughly with distilled water. The system was then flushed of residual solution by flowing distilled water at high flowrates. The pressure lines were also flushed with distilled water to remove any polymer solution that may have entered them when the transducers were bled.

3.4 Data Reduction

For each experimental run, the following unprocessed data were obtained: pressure transducer type; calibration coefficients for each of the transducers used; tap pairs; thermistor resistance; pump controller frequency; mass of diverted effluent; elapsed time of effluent collection; and voltage outputs from smooth and riblet pipe pressure transducers.

The data file RUN***.DAT was first imported into the spreadsheet software, Microsoft Excel™. The columns contained the elapsed time after the data acquisition was started (not to be confused with the elapsed time of collecting the effluent); thermistor resistance (Ω) and two non-zero columns of voltage outputs (V). A column was inserted to calculate the temperature of the effluent from Eq. 3.1-4. The data were parsed to separate each flowrate and three more columns were created into which the averages of the temperatures, the zero-flow voltages, V_0 , and the flow-voltages, V , were calculated.

A template spreadsheet file named RUN<run number>. <pipe>. <polymer>. <concentration> (e.g. RUN160.R1.N-60K.100ppm) contained the formulae necessary to calculate all the dimensional and dimensionless variables necessary to define the behavior of the fluid consistent with the literature. Details of the test sections including inter-tap distances and the pump coefficients were previously entered when setting up the template. The run information, test pipe section (smooth or riblet), pressure transducer calibration constants; pump frequency, mass of effluent and collection times were entered manually and the temperature and voltages were imported from RUN***.DAT. The following variables were calculated in the spreadsheet: volumetric flow rate, Q (l/s); fluid density, ρ (kg/m³); solvent viscosity, μ (cP); average velocity, U_{av} (m/s); solvent based Reynolds number, Re_n ; pressure gradient, $\Delta p/\Delta x$ (Pa/m³); wall shear stress, τ_w (N/m²); turbulent friction velocity, u_τ (m/s); friction factor, f ; $1/\sqrt{f}$; $Re_n\sqrt{f}$; relative viscosity, η_r ; non-dimensional riblet height, h^+ ; $Re\sqrt{f}$.

Figure 3.4.1 is a representative example of the output from a typical run. Table 3.4.1 summarizes the information, including the formulae used, that is contained within each spreadsheet. A typical printed output may have some of the columns hidden to fit the data onto a single page but no information was withheld since the columns hidden may be calculated from the quantities displayed.

Table 3.1.1. Summary of pump calibrations.

Cal. No.	Solution	Pipe (mm)	Riblet (mm)	Freq. Range (Hz)	DP Range (psid)	Linear Fit	Quadratic Fit	
							a1 x 10 ²	a2 x 10 ⁶
1	DW	10.21	0.15	15-50	12.5-80	1.9378	1.9690	-8.1455
2	50 ppm P-309	10.21	0.15	15-50	5-35	1.9939	2.0006	-3.0600
3	DW	10.21	0.11	15-50	12-75	1.9501	1.9940	-11.072
4	50 ppm P-309	10.21	0.11	15-55	7-38	1.9973	1.9878	2.2311
5	DW	7.82	0.15	15-35	23-90	1.8834	1.9405	-19.888
6	50 ppm P-309	7.82	0.15	15-50	12-83	1.9078	1.9290	-5.8164

Table 3.1.2. Two factor Analysis of Variance (ANOVA) for the linear regression coefficients

Source of Variation	SS	df	MS	F	F _{crit} (95%)
Solution	2.718E-07	1	2.718E-07	20.334	18.513
Pipe configuration	7.398E-07	2	3.699E-07	27.673	19.000
Error	2.673E-08	2	1.337E-08		
Total	1.038E-06	5			

Table 3.1.3. Calculated and measured pipe diameters

PIPE → DIAMETER, mm ↓	S 1	S 2	R1A	R1B	R2A	R2B
h	-	-	0.105	0.145	0.105	0.145
s	-	-	0.108	0.165	0.108	0.165
d_s	7.82	10.21	7.82	7.82	10.21	10.21
d_v	-	-	7.66	7.66	10.05	10.05
d_c , calculated	7.82	10.21	7.55	7.51	9.94	9.90
d_c , measured	7.82	10.22	7.56	7.50	9.95	9.90
d_t	-	-	7.45	7.37	9.84	9.76
d_H	-	-	3.50	3.79	4.60	4.97

Notes:

$$d_v = d_s - 2t$$

$$d_c = d_s - 2t - h$$

$$d_t = d_s - 2t - 2h$$

$$d_H = d_v / \sqrt{1 + \frac{4h^2}{s^2}}$$

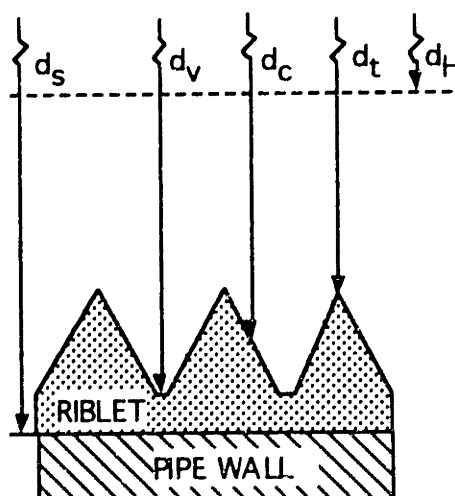


Table 3.4.1. Data reduction spreadsheet summary

Column	Variable	Symbol	Units	Formula
A-F	run information	-	-	-
G	data number	-	-	-
H	temperature	T	°C	-
I	frequency	F	Hz	-
J	effluent mass	W	g	-
K	elapsed time	t	s	-
L	flowrate	Q	l/s	$K_{\text{pump}} F$ for pump-driven or $W/\rho t$ for gravity-driven
M	PT type	-	-	-
N	zero-flow voltage	V_0	V	-
O	flow voltage	V	V	-
P	tap pair	-	-	-
R	fluid density	ρ	kg/m ³	$(999.83952 + 16.945176 T - 0.0079870401 T^2 - 0.000046170461 T^3 + 0.00000010556302 T^4 - 0.00000000028054253 T^5) / (1 + 0.01687985 T)^1$
S	solvent viscosity	μ	cP	$1.002 * 10^4 ((1.3272 (20 - T) - 0.001053 (T - 20)^2) / (T + 105))^1$
T	average velocity	U_{av}	m/s	$(4Q/(\pi d^2))/1000$

Table 3.4.1. cont'd

Column	Variable	Symbol	Units	Formula
U	solvent Reynolds number	Re_s	-	$U_{av}d/(\mu 0.001/\rho)$
V	PT coefficient	K	V/psid	-
W	tap pair distance	Δx	m	-
X	pressure gradient	$\Delta p/\Delta x$	N/m^3	$6894.7544 (V-V_0)/K/\Delta x$
Y	wall shear stress	τ_w	N/m^2	$(\Delta p/\Delta x) d/4$
Z	friction velocity	u_t	m/s	$\sqrt{(\tau_w/\rho)}$
AA	friction factor	f	-	$2\tau_w/(\rho U_{av}^2)$
AB	$Re_s\sqrt{f}$	$Re_s\sqrt{f}$	-	$Re_s\sqrt{f}$
AC	$1/\sqrt{f}$	$1/\sqrt{f}$	-	$1/\sqrt{f}$
AD	$1/\sqrt{f}$ (PK)	-	-	$4.0 \log (Re\sqrt{f}) - 0.4$
AE	non-dimensional riblet height	h^+	-	$Re\sqrt{f}/\sqrt{2} (h/d)$
AF	relative viscosity	μ_r	-	$Re_s f/16$ for $Re < 1200$
AG	$Re\sqrt{f}$	-	-	$Re_s\sqrt{f}/\mu_r$

¹ Perry and Green (1984)

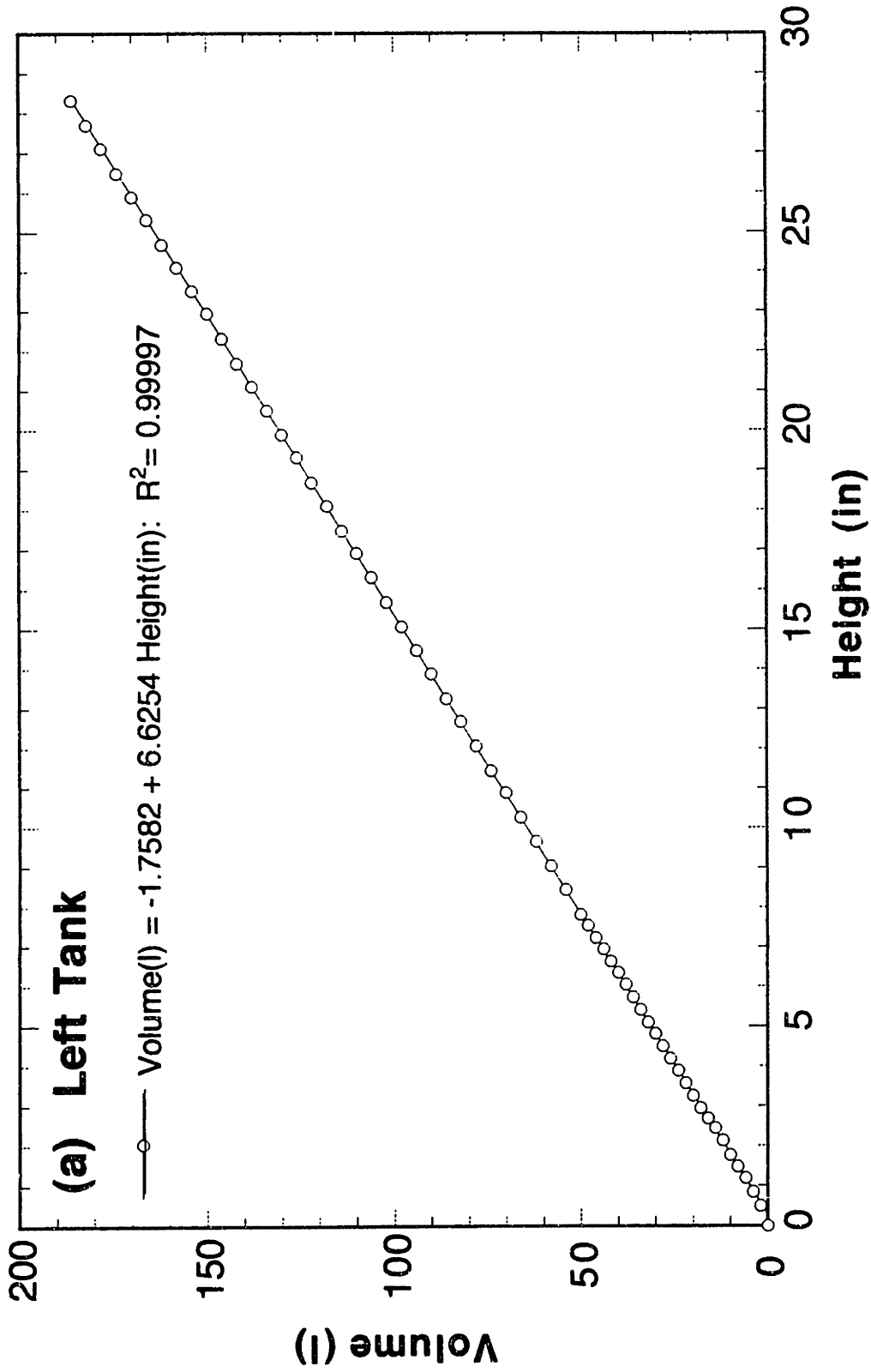


Figure 3.1.1a Left tank calibration

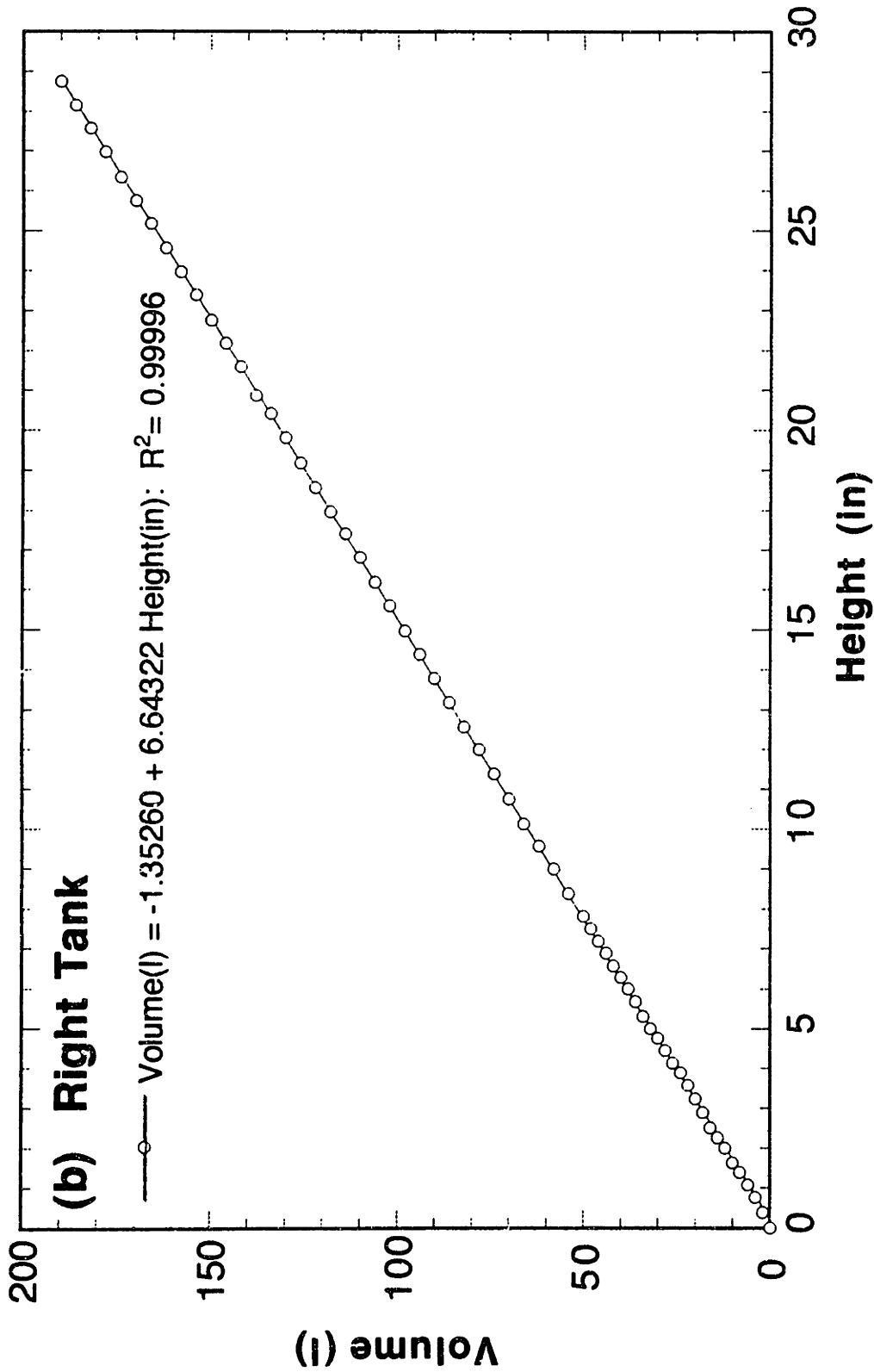


Figure 3.1.1b Right tank calibration

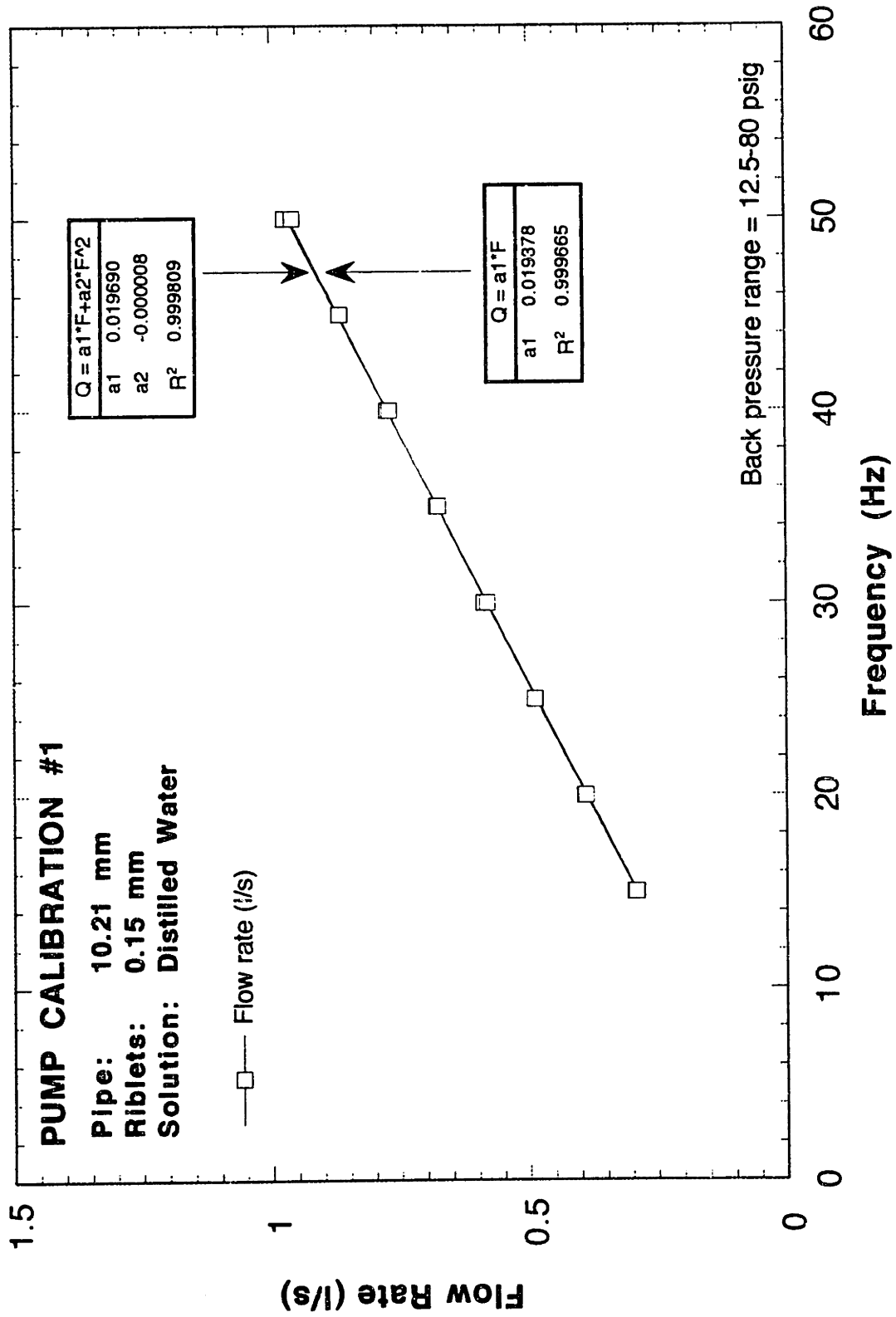


Figure 3.1.2 Pump calibration #1: 10.21 mm pipe, 0.15 mm riblets, distilled water

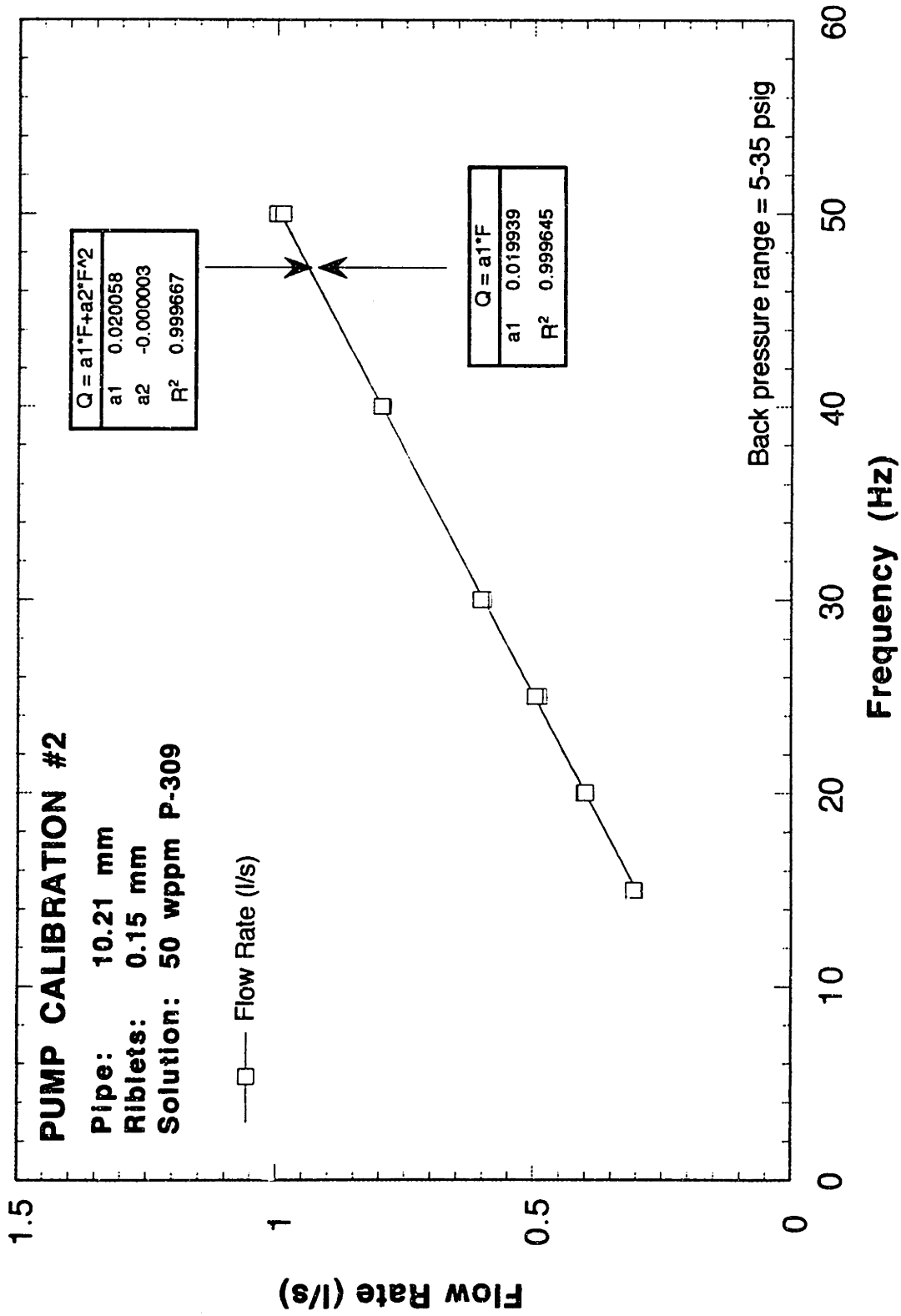


Figure 3.1.3 Pump calibration #2: 10.21 mm pipe, 0.15 mm riblets, 50 wppm P-309

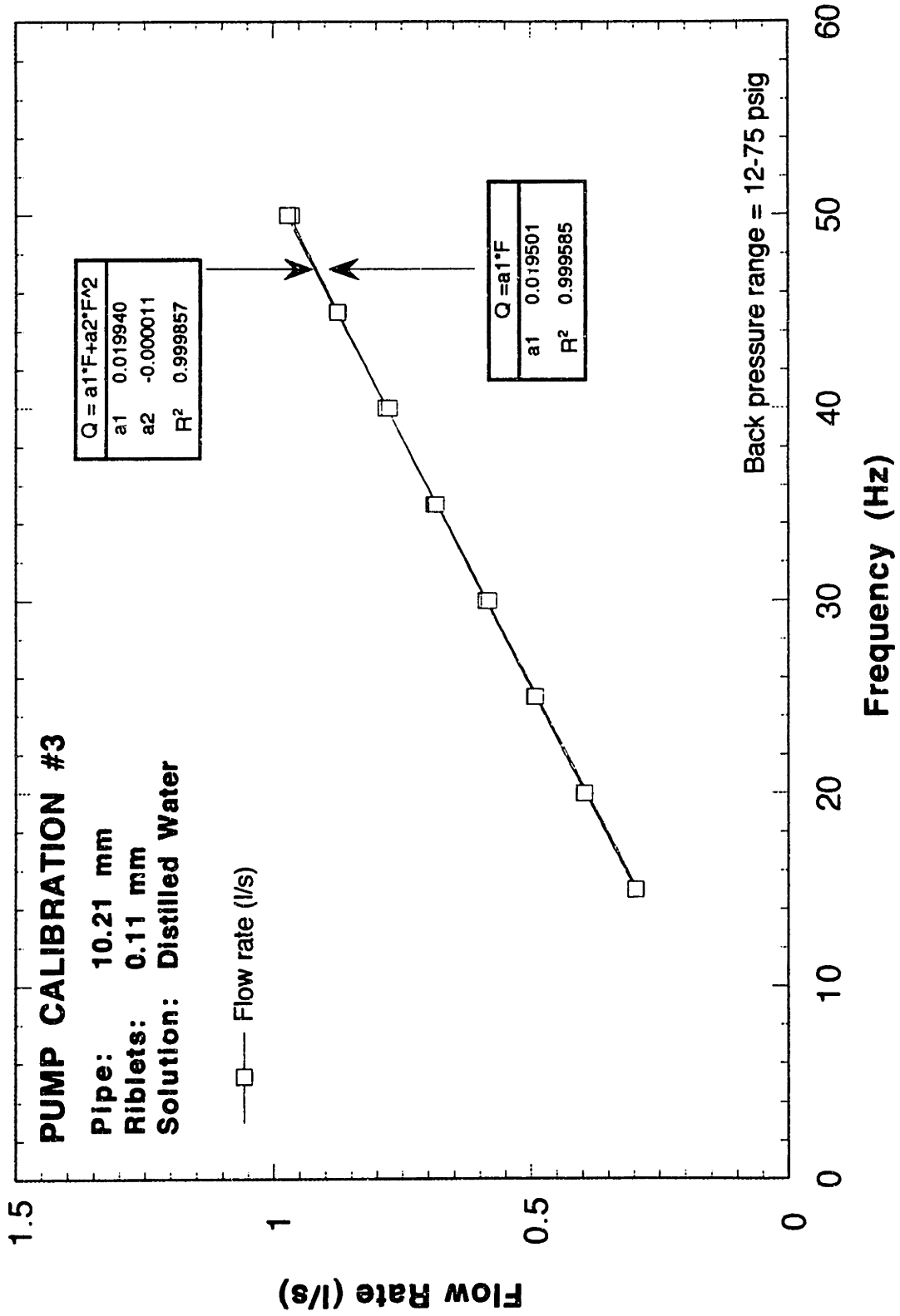


Figure 3.1.4 Pump calibration #3: 10.21 mm pipe, 0.11 mm riblets, distilled water

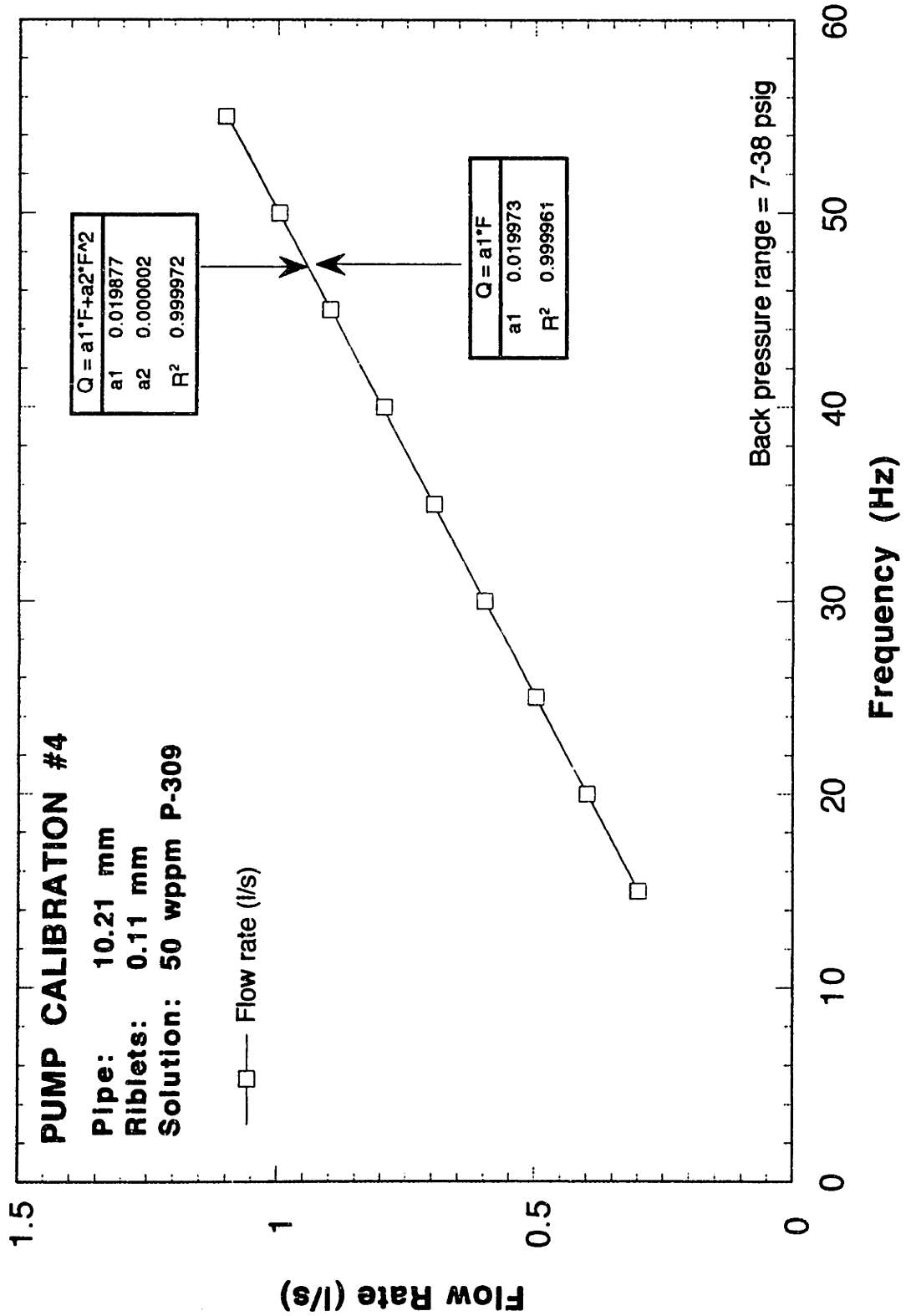


Figure 3.1.5 Pump calibration #4: 10.21 mm pipe, 0.11 mm riblets, 50 wppm P-309

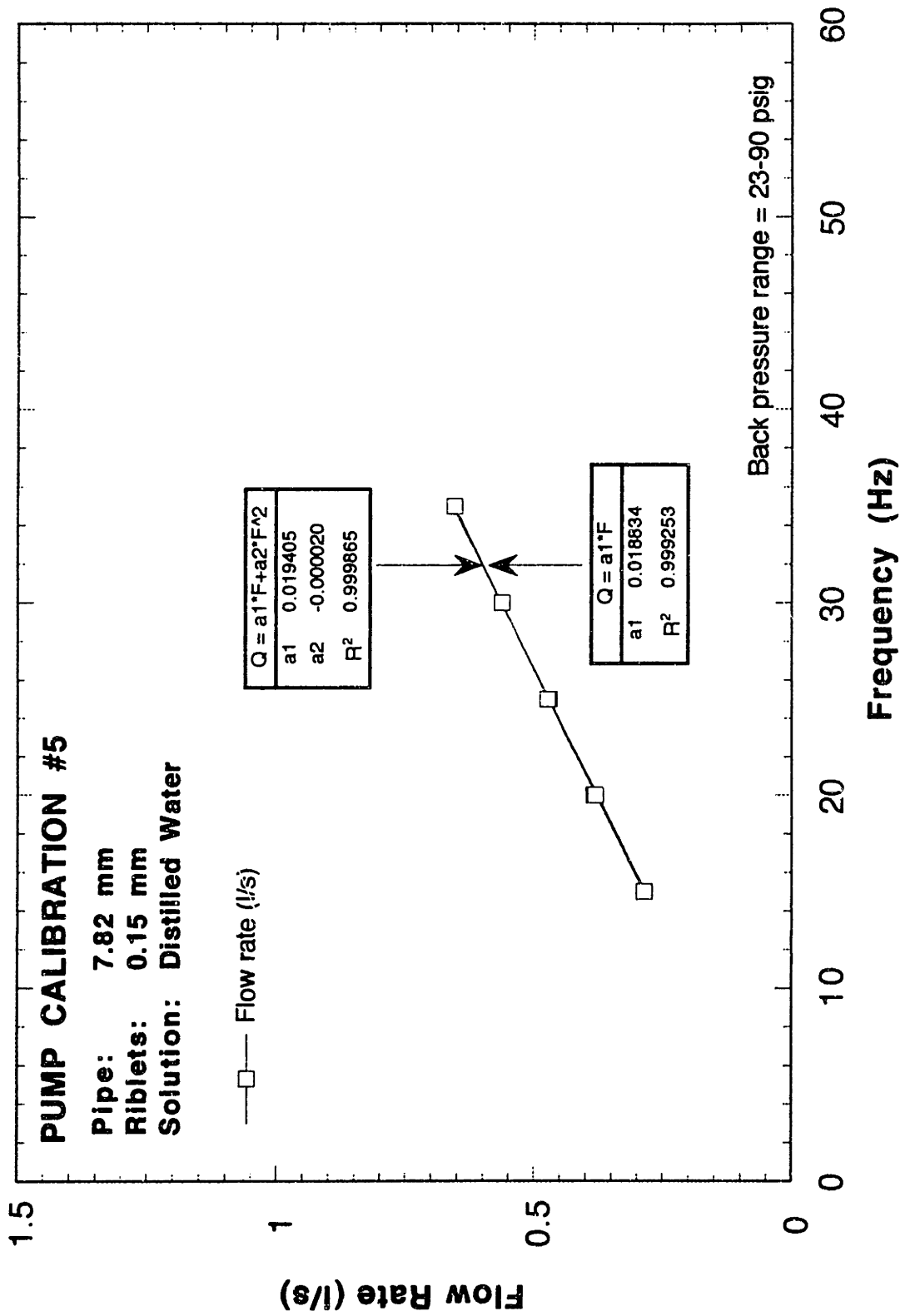


Figure 3.1.6 Pump calibration #5: 7.82 mm pipe, 0.15 mm riblets, distilled water

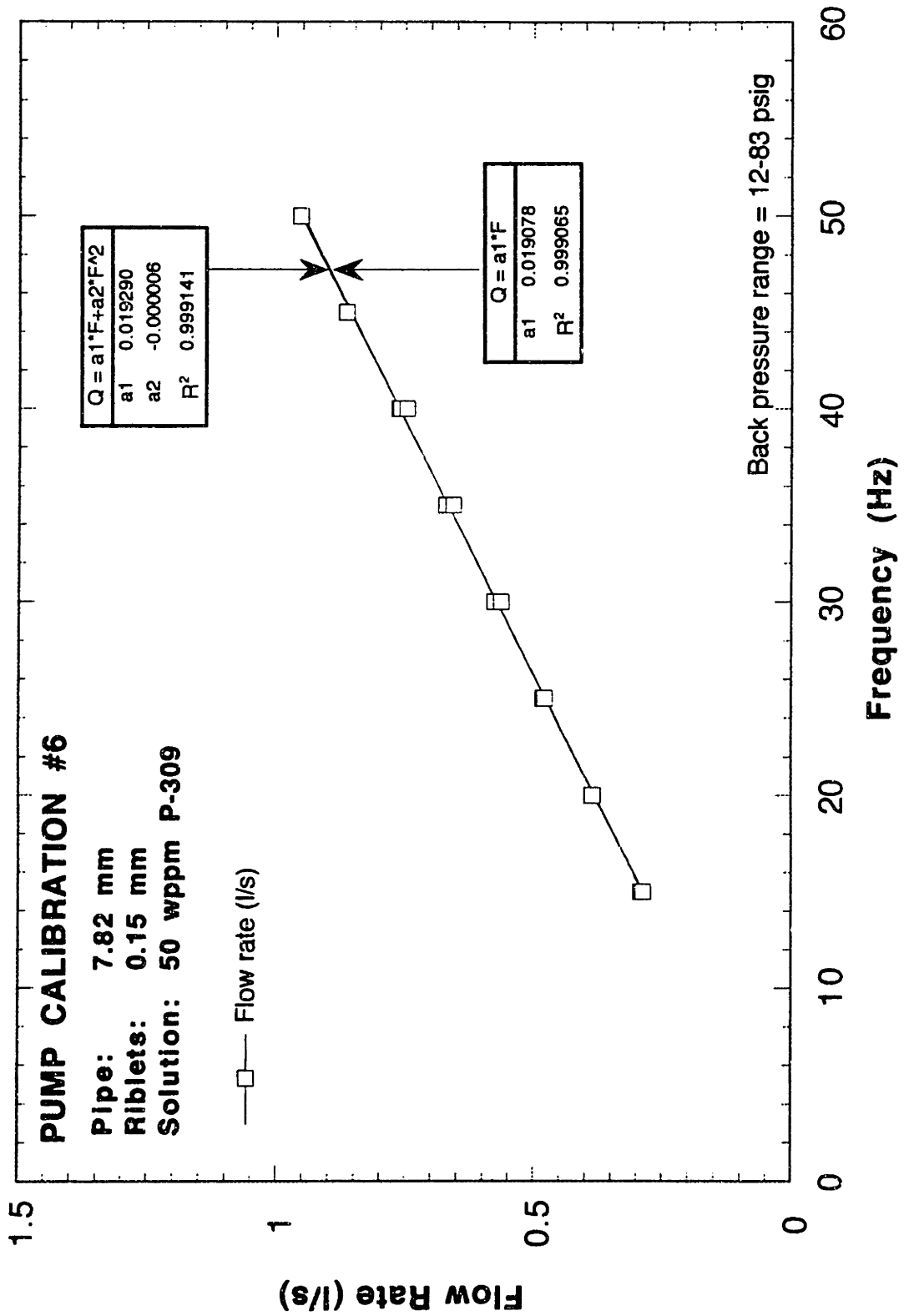


Figure 3.1.7 Pump calibration #6: 7.82 mm pipe, 0.15 mm riblets, 50 wppm P-309

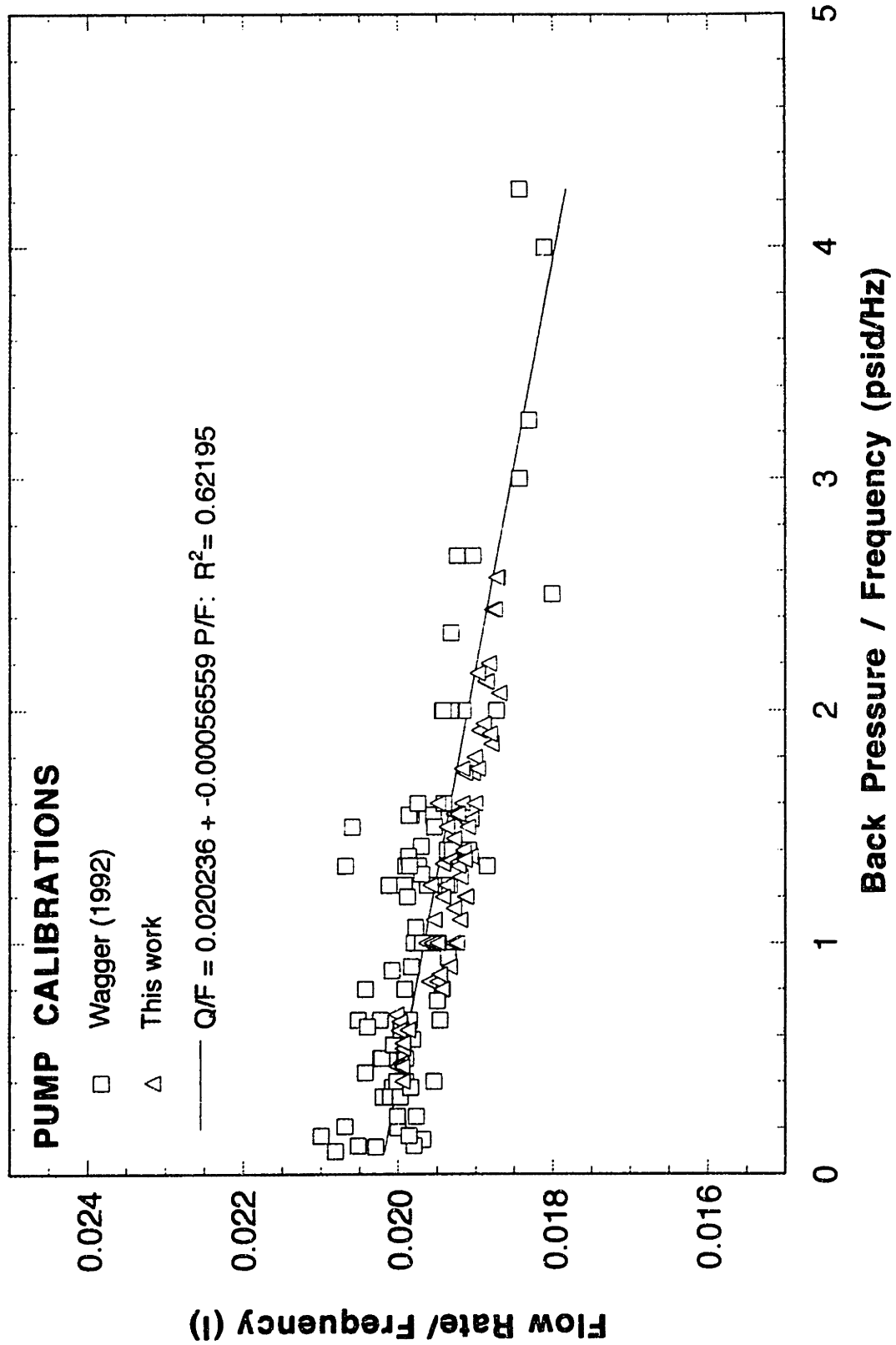


Figure 3.1.8 Pump calibration summary accounting for the effect of pump back pressure

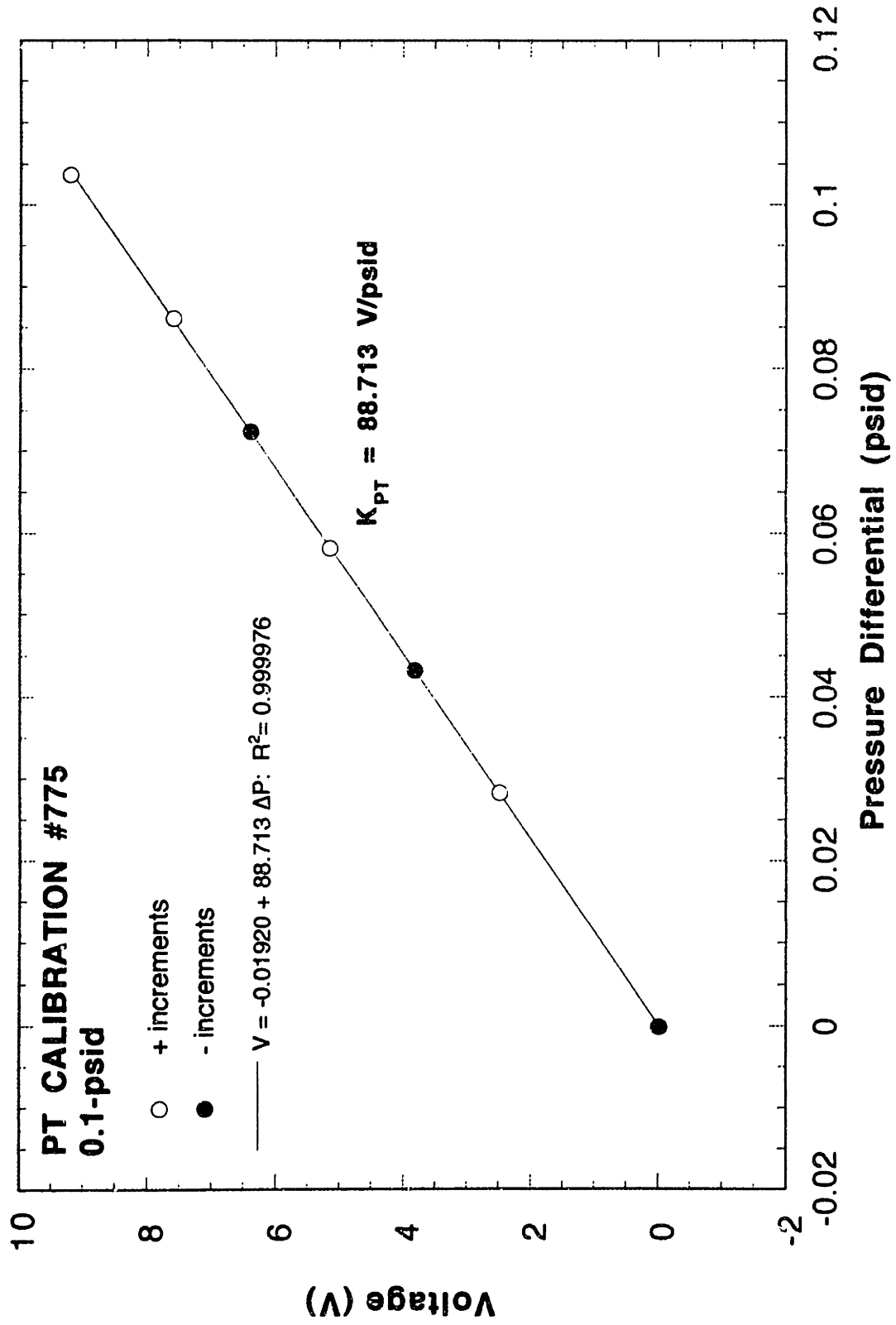


Figure 3.1.9 Representative 0.1-psid pressure transducer calibration (CAL #775)

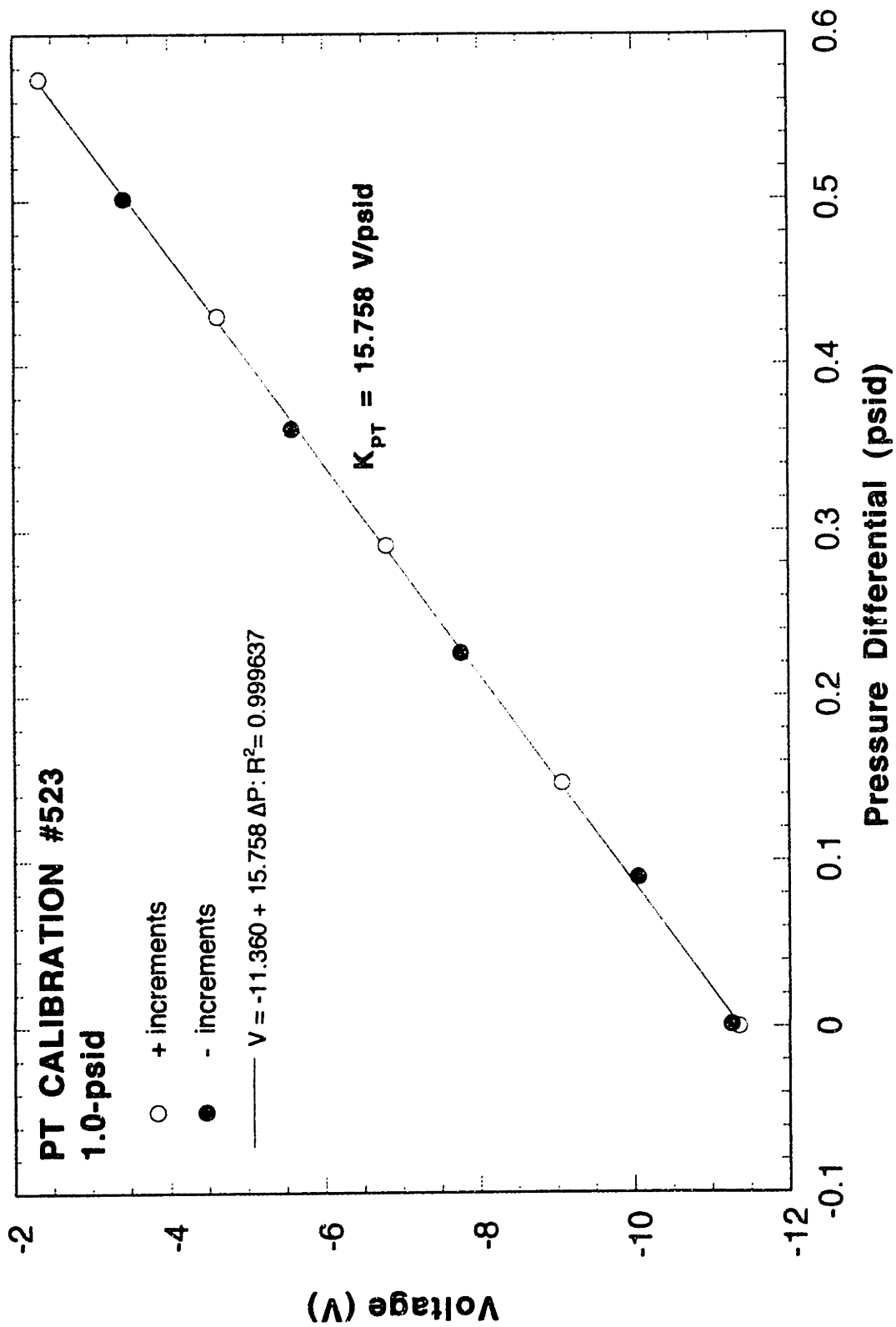


Figure 3.1.10 Representative 1.0-psid pressure transducer calibration (CAL #523)

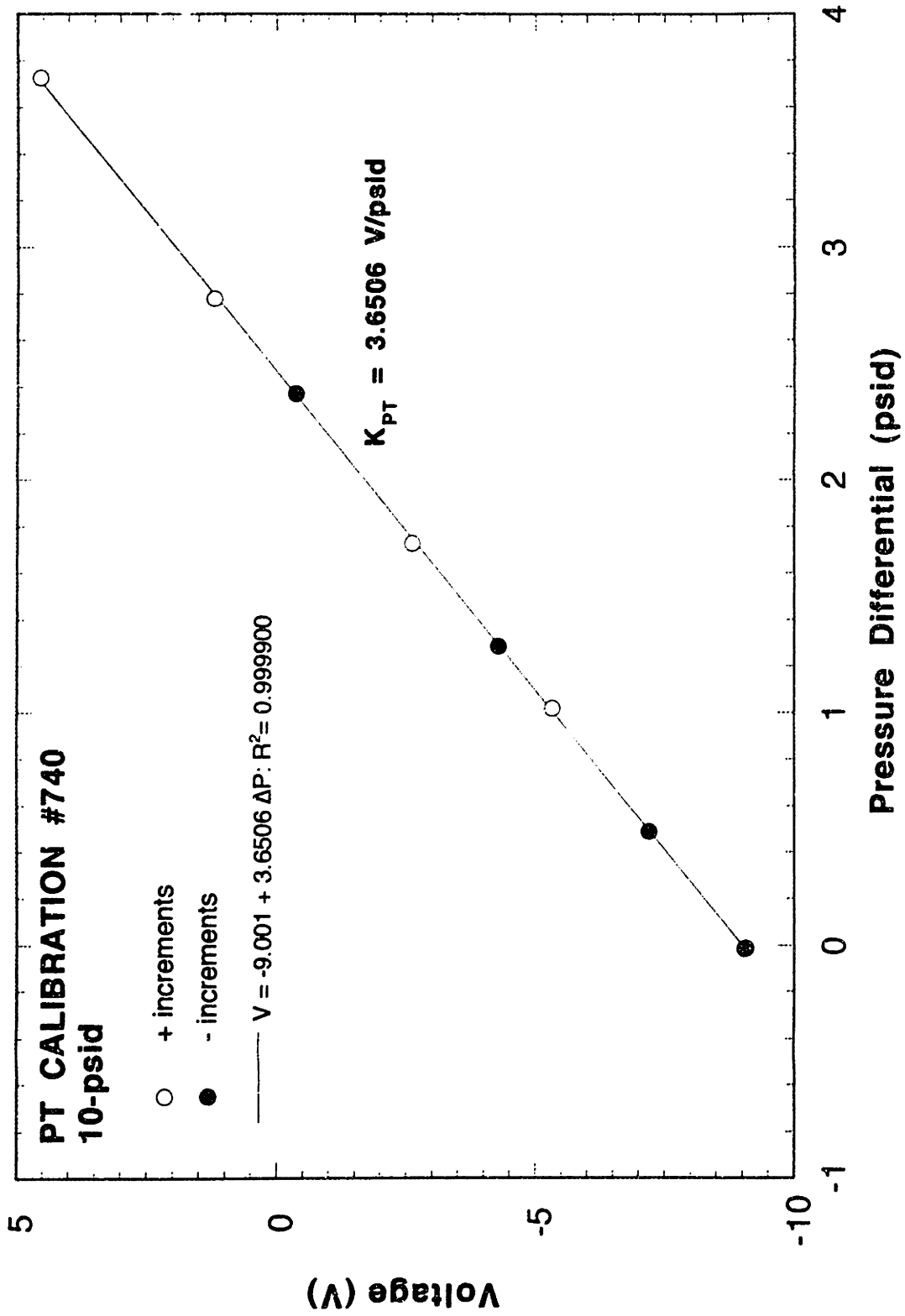


Figure 3.1.11 Representative 10-psid pressure transducer calibration (CAL #740)

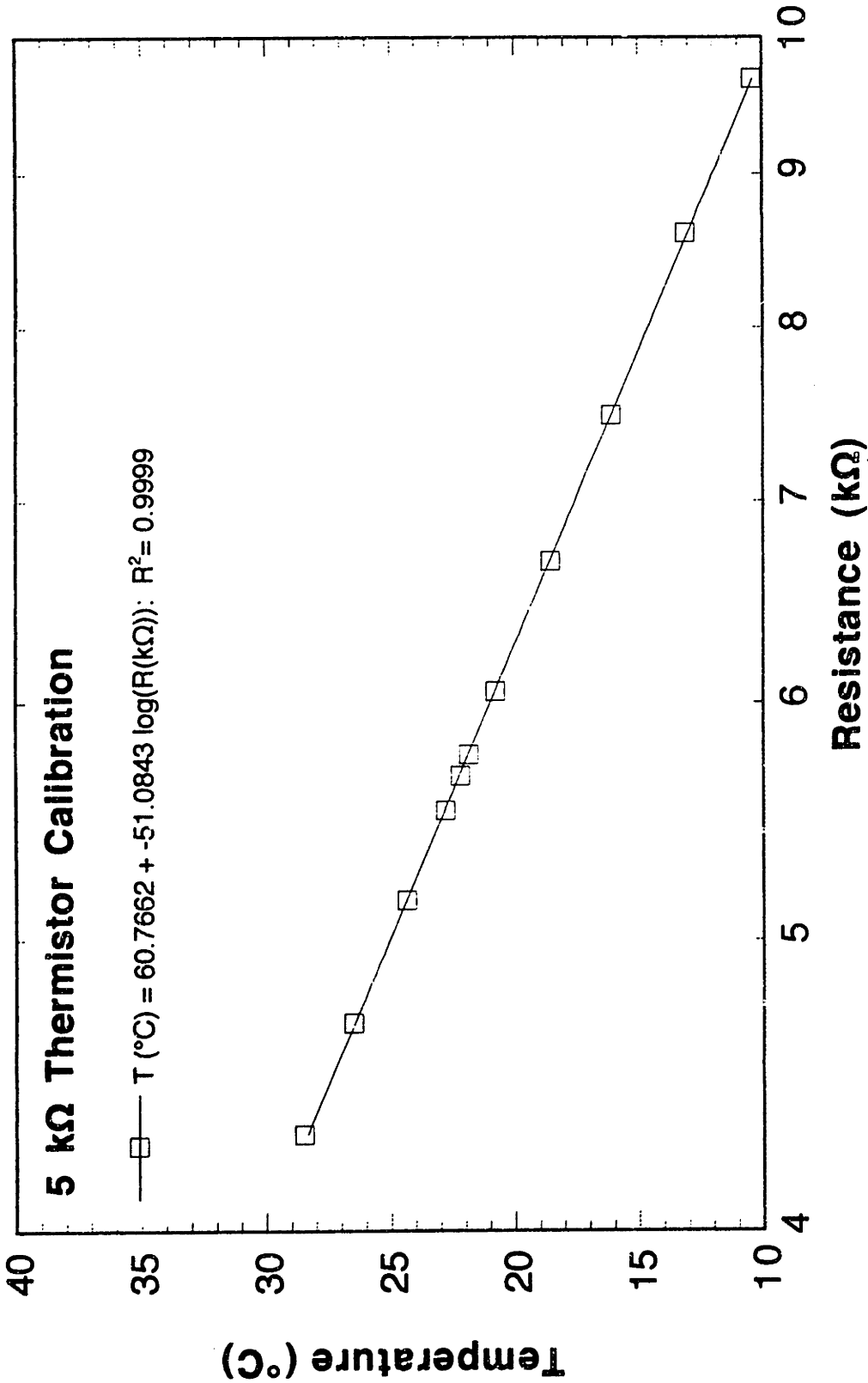


Figure 3.1.12 5 kΩ thermistor calibration

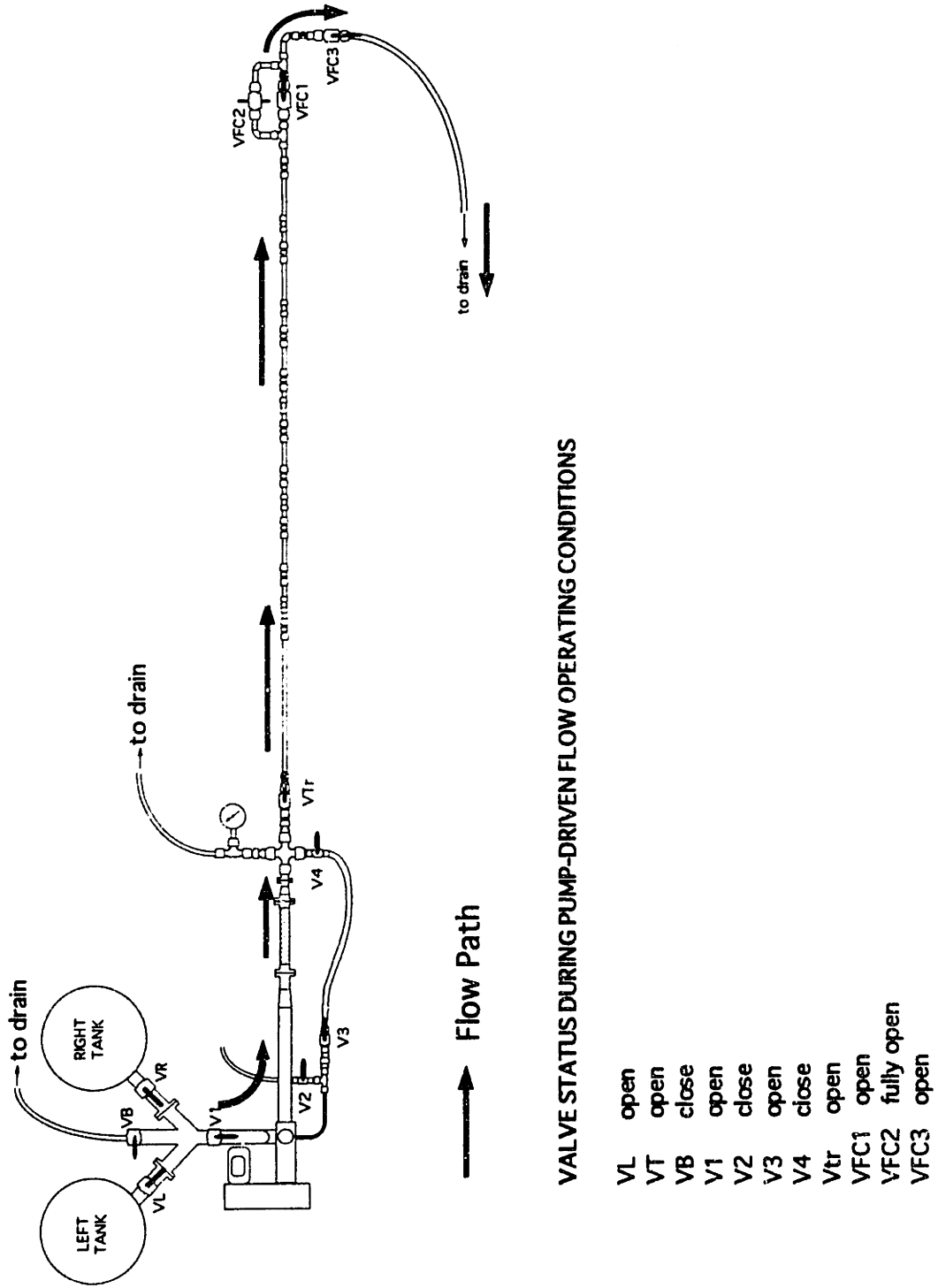
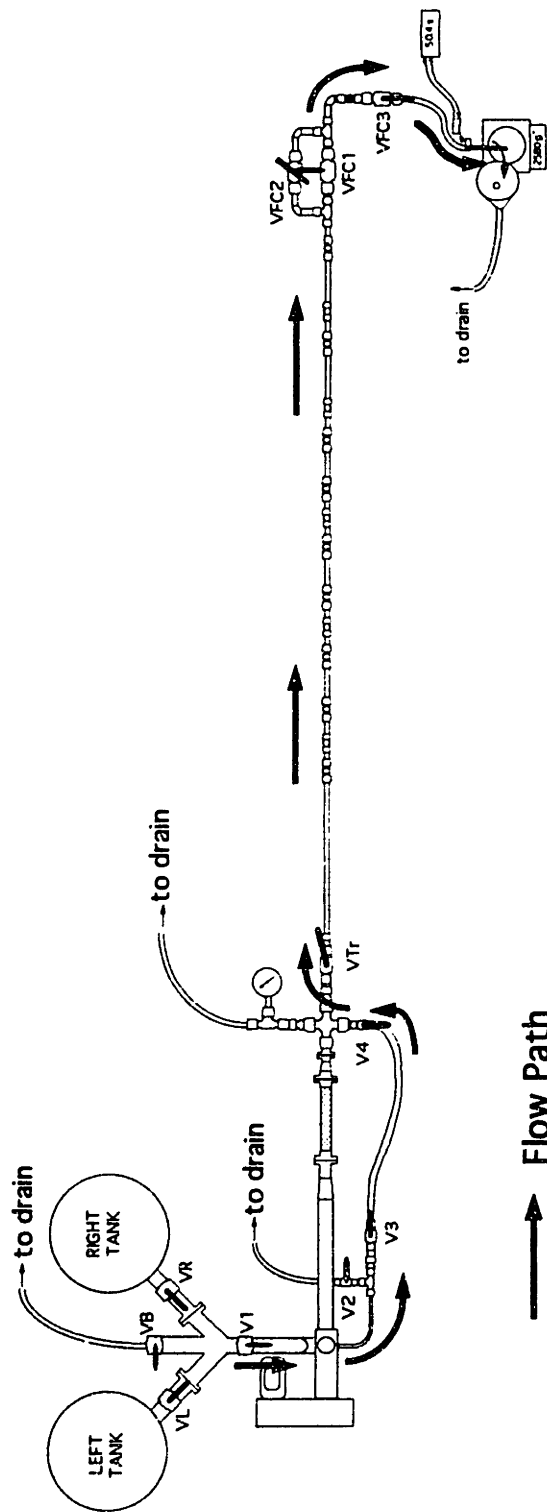


Figure 3.3.1. Pump-driven fluid flow path

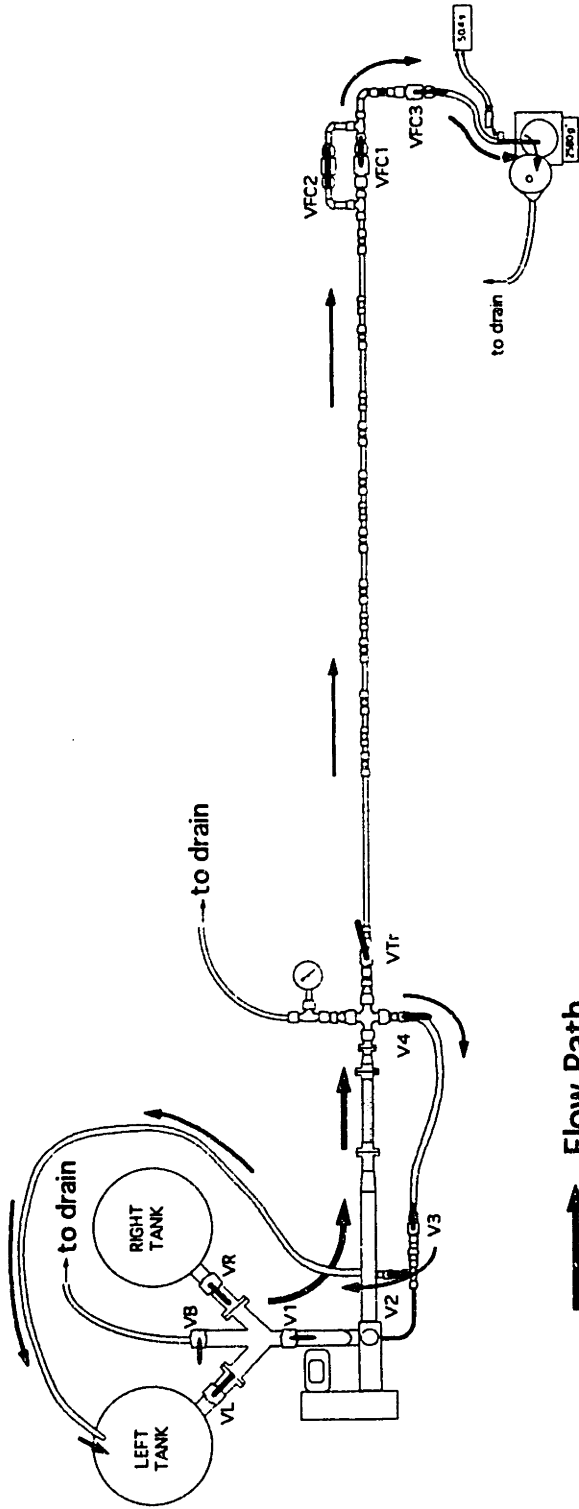


→ Flow Path

VALVE STATUS DURING GRAVITY_DRIVEN FLOW OPERATING CONDITIONS

- VL open
- VT open
- VB close
- V1 open
- V2 close
- V3 open
- V4 open
- Vtr 15° close
- VFC1 open/close
- VFC2 incrementally open
- VFC3 open

Figure 3.3.2. Gravity-driven fluid flow path



→ Flow Path

VALVE STATUS DURING PUMP-BYPASSED FLOW OPERATING CONDITIONS

- VL open
- VT open
- VB close
- V1 open
- V2 open
- V3 open
- V4 open
- Vtr open
- VFC1 open
- VFC2 open
- VFC3 open

Figure 3.3.3. Pump bypass-driven fluid flow path

A	B	C	D	E	F	G	H	I	J	K	L	M	N	O	P	Q	R	S	T	U	V	W	X	Y	Z	AA	AB	AC	AD	AE	AF	AG	AH				
1	RUN NO.	237	RIA																																		
2	DATE	1-Sep-93																																			
3	START	12:00 AM																																			
4	STOP	11:30 AM																																			
5	PT Coeff.	X																																			
10	PT(0.1)	81.4539	(V/puls)																																		
11	PT(1)		(V/puls)																																		
12	PT(10)	4.1896	(V/puls)																																		
14	PLM Coeff	0.018435	(V/s/Hz)																																		
15		-6.51E-06																																			
16	POLYMER:	PEO																																			
17	Series	P-309																																			
19	MW(x10^6)	-																																			
20	S	5																																			
21	c (wppm)	100																																			
24	Temp	4.7	119.38	0.11938	Δx (m)																																
25	12	11.249	295.72	0.2857246																																	
26	13	13.761	400.33	0.4003294																																	
27	47	11.163	283.54	0.2835402																																	
28	57	6.463	164.16	0.1641602																																	
29	67																																				
30	PPEDATA	D (m)	D (mm)	D (m)																																	
32	RM	0.297	7.5438	0.0075438																																	
33	Diameter	0.297	7.5438	0.0075438																																	
34	X sec diameter(R)	0.297	7.5438	0.0075438																																	
35																																					
36																																					
37																																					
38																																					
39																																					

Figure 3.4.1. Representative data reduction spreadsheet (RUN237.R1A.P-309.100 wppm)

Chapter 4

Results

4.1 Experimental Grid

The flows of dilute polymer solutions were investigated in four riblet pipes, fabricated from combinations of 10.21 and 7.82 mm ID smooth pipes, and V-groove vinyl riblets (3M Co.) of nominal heights 0.15 and 0.11 mm. Five homologous polyethylenoxides (PEO), namely N-10; N-750; N-60K; W-301, and P-309, and two homologous polyacrylamides (PAM), N-300L and N-300, were used to investigate drag reduction in the riblet pipes. The polymer concentrations used are summarized in Table 4.1.1, and the physical basis behind the choice of the polymer solution is elaborated in Figures 4.1.1 and 4.1.2.

Figure 4.1.1a attempts to anticipate the drag reduction for PEO solutions used in the 10.21 mm ID pipe system. The plot is logarithmic with dual abscissae, the lower of which is the polymer molecular weight as supplied by the manufacturer (Table 2.5.1), while the upper is $Re\sqrt{f}^*$, at the onset of drag reduction in the smooth pipe, as determined from the onset correlations in Chapter 2. For $Re\sqrt{f}^* > 400$, gross flow data in the smooth pipe are expected to follow an L→N transition, leading to a clearly defined onset, whereas for $Re\sqrt{f}^* < 400$, they should follow either L→P or L→M transitions, some of which should lead to flow at the MDR asymptote. The lower dashed and upper solid lines in the figure define the loci of $c-M_w$ for which slope increments $\delta = 4$ and 40 respectively. Most of the polymer solutions used provided slope increments, $4 < \delta < 40$. Solutions of 100 wppm W-301, 50 and 100 wppm P-309, which were estimated to exhibit high $\delta > 40$, were used to study the MDR regime. Figure 4.1.1b depicts the experimental grid for the smaller 7.82 mm ID smooth and riblet pipes. The figure provides information similar to that in Figure 4.1.1a; its upper axis is shifted relative to that in Figure 4.1.1a by a factor

(7.82/10.21) to reflect the dependence of $Re\sqrt{f}^*$ on d , with τ_w^* unchanged. Figures 4.1.2 a and b are analogous to Figures 4.1.1 a and b, depicting the concentrations of solutions of PAM used in this investigation. Note that both the loci of c - M_w corresponding to $\delta = 4$ and 40, and the $Re\sqrt{f}^*$ axes in Figure 4.1.2 are different from those in Figure 4.1.1 because the molecular weight per backbone chain link and slope modulus $[m_0, \kappa] = [35.5, 95 \times 10^{-6}]$ of PAM differ from those, $[14.4, 75 \times 10^{-6}]$, of PEO.

4.2 Solvent Flow

4.2.1 Flow Development

The results that are presented in this chapter and the subsequent interpretation of these results are based on the assumption that the flow is fully developed. Typical development lengths in pipes are $L_e/d \approx 0.06Re$ for laminar flow (Atkinson, 1969) and $L_e/d \approx 40$ for turbulent flow (Nikuradse, 1933). The right panel of Figure 4.2.1 depicts the variation of the pressure drop, $|\Delta P|$, with the distance downstream of tap 1 for solvent flow in the smooth 10.21 mm ID pipe. The readings spanned both laminar (hollow symbols) and turbulent (solid symbols) regimes for $295 < Re < 83000$. Each pressure drop is scaled by a constant, C , which depends on the Reynolds number. The scaling constants chosen enabled all the results, which spanned about four orders of magnitude in pressure drop from $Re = 295$ to $Re = 83000$, to be presented on the same arithmetic plot. The pressure drop varied linearly with downstream distance from tap 1 with a maximum difference of 1% between the pressure gradients calculated using tap pairs 12 and 13. The solid lines in Figure 4.2.1 are the linear best-fit relations passing through the origin. The left panel of Figure 4.2.1 depicts the variation of the scaled pressure drop with distance downstream of Tap 1 in the 7.82 mm ID smooth pipe for $485 < Re < 67100$. The pressure drop varies linearly with downstream distance from tap 1, with a maximum difference between the pressure gradients calculated using tap pairs 12 and 13 of 1% for $Re < 5490$ and 2% for Re

> 5490. From these figures it is evident that the development lengths of $L_e/d = [77, 57]$ for the pipes of $d_s = [10.21, 7.82]$ provided fully developed flow between taps 1, 2 and 3 in the upstream smooth test sections.

The fully developed velocity profile in the smooth pipe will be disturbed upon entrance into the riblet section, where it develops into a new profile. The reduction in cross-sectional area from smooth to riblet pipes varied from 2.6% to 4.0%. Treating the change in cross-section between the smooth and riblet pipes as a simple contraction (Appendix A.1), the flow development length for laminar flow is estimated to be $L_e/d \approx Re/50$; for example, $[Re, L_e/d] = [1000, 20]$. The development length for turbulent flow is typically much smaller than that for laminar flow. For example, at $Re = 2000$, the development length for fully developed laminar flow from an initially plug flow is ≈ 60 , which is approximately the same as for turbulent flow, $L_e/d \approx 30-80$. The upstream smooth to riblet flow redevelopment lengths of $[35d, 41d]$ in the $[10.21, 7.82]$ mm ID pipes are therefore assumed to be adequate for this work.. The flow redevelopment length between riblet and trailing smooth sections was also adequate, as will be shown in subsequent data taken with the downstream smooth sections.

4.2.2 Laminar Flow

In any fully developed, internal, laminar flow, the pressure gradient is directly proportional to the flowrate. The pressure gradient-flowrate relation in Newtonian pipe flow is given by Poiseuille's Law:

$$\nabla P = \frac{|\Delta P|}{\Delta z} = \frac{128\eta Q}{\pi d^4} \quad (4.2-1)$$

or in nondimensional form:

$$f.Re = 16 \quad (4.2-2)$$

Figure 4.2.2 depicts the variation of the pressure gradient, ∇P , versus the flowrate-viscosity product, ηQ , in each of the 7.82 mm pipes, S1, R1A and R1B. The data for all three pipes are correlated by separate straight lines passing through the origin with correlation coefficients, $R^2 > 0.998$, and slopes $[10.871, 12.782, 13.816] \times 10^9 \text{ m}^{-4}$ for [S1, R1A, R1B], respectively. The abscissa chosen has the virtue that the slopes of the regressed lines are a function of pipe geometry only. The slope observed for the smooth pipe yields $d = 7.82 \text{ mm}$ from Eq. (4.2.1), which agrees identically with caliper measurements of the pipe ID as reported in section 3.1.5. Formal application of Eq. (4.2.1) provided apparent laminar diameters $d = [7.51, 7.37] \text{ mm}$ for [R1A, R1B].

Figure 4.2.3 depicts the variation of ∇P versus ηQ , in each of the 10.21 mm pipes, S2, R2A and R2B. The data for all three pipes are correlated by separate straight lines passing through the origin with correlation coefficients, $R^2 > 0.999$, and slopes $[3.750, 4.281, 4.480] \times 10^9 \text{ m}^{-4}$ for [S2, R2A, R2B], respectively. The slope observed for the smooth pipe yields $d = 10.21 \text{ mm}$ from Eq. (4.2.1), which agrees identically with caliper measurements of the pipe ID as reported in section 3.1.5. Formal application of Eq. (4.2.1) provided apparent laminar diameters $d = [9.88, 9.76] \text{ mm}$ for [R2A, R2B].

4.2.3 Pressure Gradient Ratio

Figure 4.2.4 depicts the variation of the ratio of the pressure gradients in the smooth to riblet pipes at the same volumetric flow rate:

$$P = \frac{[(\nabla P)_s]}{[(\nabla P)_r]_Q} \quad (4.2-3)$$

versus the volumetric flowrate, Q . The advantage of using P is that it facilitates comparison between smooth and riblet pipes without introducing the diameter of the riblet pipes, which has not as yet been defined. The four, semi-logarithmic graphs, each corresponding to a single riblet pipe, are arranged with parts [a,b] and [c,d] respectively depicting, in registry, the variation of P in the smaller and larger pipes. For each pipe size, the upper axis corresponds to the Reynolds number in the smooth pipe.

Consider, first, the variation of P in R2B depicted by Figure 4.2.4d . The results span three flow regimes, namely:

- (i) Laminar flow in both pipes: $0.0021 < Q < 0.015$ l/s, $290 < Re_s < 2070$. In this regime, the pressure gradient ratio is roughly independent of flowrate with $P = P_L = 0.839 \pm 0.006$. The observation that P is independent of Q implies that the pressure gradients in both the smooth and riblet pipes vary with Q in a similar functional form. This was earlier seen in section 4.2.2, where ∇P varied linearly with Q . We may interpret the results in two ways. First, if we assume that the riblet pipe behaves as a smooth one such that $f.Re = 16$, then $d_r/d_s = 0.948$ or $d_r = 9.76$ mm. Second, in anticipation of later results, if $d_r = 9.80$ mm, then $f.Re = 16.22$
- (ii) Transition in either pipe: $0.015 < Q < 0.026$ l/s, $2070 < Re_s < 3600$. In this regime, values of P fluctuate from 0.78 to 0.98, evidently reflecting the unstable, intermittent flows in each pipe, sampled at random.
- (iii) Turbulent flow in both pipes: $0.026 < Q < 1.070$ l/s, $3600 < Re_s < 148000$. Perusal of the results reveal P to be a complex function of Q , that may be sub-divided into three further regimes:
 - (1) $P = P_{T0} = 0.824 \pm 0.003$: $0.026 < Q < 0.040$ l/s, $3600 < Re_s < 5530$. In this regime, P is roughly independent of flowrate; that is, the pressure gradients in the

smooth and riblet pipes vary with Q in similar functional ways. The riblet pipe may be considered as an "equivalently" smooth pipe of a different diameter, say d_r . For hydraulically smooth pipes, ∇P may be directly related to Q via the Blasius expression for the friction in turbulent flow:

$$\nabla P \propto Q^{1.75} d^{4.75} \quad \text{for } Re < 10^5 \quad (4.2-4)$$

If the riblet pipe were to obey the same smooth friction factor relationship, then $P_{T0} \approx (d_r/d_s)^{4.75}$, from which $d_r \approx 9.80$ mm.

- (2) $P > P_{T0}$: $0.040 < Q < 0.210$ l/s, $5530 < Re_s < 29000$. P increases with increasing Q up to $P_{\max} = 0.912$ at $[Q, Re_s] = [0.122$ l/s, $16800]$ then decreases, crossing the $P = P_{T0}$ line at $[Q, Re_s] = [0.210$ l/s, $29000]$. It is noteworthy that the drag in the riblet pipe relative to smooth in this regime is smaller than it was in the preceding regime (1). However, the maximum value of P never exceeds unity, implying that the pressure gradient in the riblet pipe was always greater than that in the smooth pipe.
- (3) $P < P_{T0}$: $0.210 < Q < 1.070$ l/s, $29000 < Re_s < 148000$. P decreases monotonically with increasing Q to $P = 0.643$ at $[Q, Re_s] = [0.580$ l/s, $80200]$, beyond which it becomes essentially constant with $P \rightarrow P_{T\infty} = 0.643 \pm 0.008$ for $0.580 < Q < 1.070$ l/s ($80200 < Re_s < 148000$). There exists a two-fold range of Q for which P is constant. This suggests that at high flowrates the riblet pipe asymptotically behaves as an "equivalently" smooth pipe of diameter, $d_r = 9.30$ mm, rather smaller than $d_r = 9.80$ mm established in regime (1).

It can be seen in Figures 4.2.4a-c that the other three riblet pipes also exhibit the features described in the preceding example. The ranges of $[Q, Re_s]$ that define all regimes are summarized in Table 4.2.1. In laminar flow, we observe $P = P_L = [0.851, 0.783,$

0.875, 0.839] for pipes [R1A, R1B, R2A, R2B], respectively. In turbulent flow, the variation of P with Q may be further divided into three regimes:

- (1) $P = P_{T0}$. P is roughly independent of Q , with $P_{T0} = [0.843, 0.875, 0.824]$ for [R1A, R2A, R2B]. In R1B, there is no region of constant P , which increases immediately past $P = 0.790$ at $[Q, Re_s] = [0.016 \text{ l/s}, 2980]$. If the riblet pipes follow the same friction factor relation as the smooth pipe, then the observed value of P_{T0} provide the equivalent riblet pipe diameters of $d_r = [7.54, 7.44, 9.93, 9.80]$ mm for pipes [R1A, R1B, R2A, R2B], respectively; the value in *italics* is inferred from $P = 0.790$ for R1B.
- (2) $P > P_{T0}$. P increases with increasing Q to a maximum $P = [0.910, 0.843, 0.922, 0.912]$ at $Q = [0.085, 0.057, 0.172, 0.135]$ l/s for [R1A, R1B, R2A, R2B], respectively then decreases, back to $P = P_{T0}$ at $Q = [0.140, 0.096, 0.250, 0.210]$ l/s, respectively.
- (3) $P < P_{T0}$. P decreases monotonically with increasing Q , then becomes essentially constant with $P \rightarrow P_{T\infty} = [0.627, 0.577, 0.643]$ at $Q > [0.58, 0.34, 0.58]$ l/s for [R1A, R1B, R2B]. The latter segment is not observed for R2A, which exhibits $P_{\min} = 0.680$ at $[Q, Re_s] = [0.975 \text{ l/s}, 133000]$.

We now address the riblet pipe diameter, which must be defined to form the dimensionless groups used henceforth. Following the literature, the flow regimes in riblet pipes will be scaled by the non-dimensional riblet height, h^+ :

$$h^+ = \frac{u_\tau h}{\nu} = \sqrt{\frac{\tau_w}{\rho}} \frac{h}{\nu} = \sqrt{\frac{VP_r \cdot d_r}{4\rho}} \frac{h}{\nu} \quad (4.2-5)$$

Table 4.2.1 summarizes the approximate ranges of h^+ associated with the turbulent flow regimes, based on the calculated cross sectional diameters of the riblet pipes, d_c . Since the differences between the various possible riblet pipe diameters are small, the estimated h^+

will not vary significantly when refinements are made. The turbulent regimes (1) - (3) are found to be spanned by roughly the same h^+ range in all the riblet pipes, namely: (1) $P_T = P_{T0}$ for $h^+ < 5.3$; (2) $P_T > P_{T0}$ for $5.3 < h^+ < 22$, with a maximum P_T at $h^+ = 15$; (3) $P_T < P_{T0}$ for $h^+ > 22$ with $P_T \rightarrow P_{T\infty}$ for $h^+ > 75$. Since rough pipes are considered hydraulically smooth when the non-dimensional roughness height $k^+ < 5$ (Nikuradse, 1933), we can, by analogy, consider riblet to be hydraulically smooth for $h^+ < 5$, which would produce $P = \text{constant}$, as observed in regime (1) of our data. The diameter of a riblet pipe will henceforth be defined as that value which produces the same f - Re relation as the smooth pipe for $h^+ < 5$, corresponding to $P_T = P_{T0}$.

4.2.4 Prandtl-Karman Representation

Smooth Pipes

Figure 4.2.5 is a plot, in P-K coordinates, for solvent flow in the 10.21 mm smooth pipe (O), with data taken from seven experimental runs. The dashed and solid lines correspond to Poiseuille's and the Prandtl-Karman laws respectively. The data span three flow regimes, namely:

- (i) $Re\sqrt{f} < 175$, laminar flow, adhering to Poiseuille's law, $f.Re = 16$ to within 0.3%;
- (ii) $175 < Re\sqrt{f} < 300$, laminar to turbulent transition, and
- (iii) $300 < Re\sqrt{f} < 9100$, turbulent flow, adhering to the Prandtl-Karman law, Eq. (2.2-6); the r.m.s. deviation in $1/\sqrt{f}$ between the data and the P-K law being 0.7%.

Figure 4.2.6 depicts solvent flow in the 7.82 mm smooth pipe, showing regimes of laminar ($Re\sqrt{f} < 180$), transitional ($180 < Re\sqrt{f} < 300$) and turbulent flow ($300 < Re\sqrt{f} < 9200$). In the turbulent flow regime, the data obey the P-K law with a r.m.s. deviation of 0.5% in $1/\sqrt{f}$.

Riblet Pipes

As a representative example, depicted in Figure 4.2.7, consider the P-K representation of the data in R2B (●), using riblet pipe diameter $d_r = 9.80$ mm, derived from the analysis in section 4.2.3. An upper abscissa of the nondimensional riblet, h^+ , is included in Figure 4.2.7. The data span three flow regimes, namely:

- (i) Laminar flow: $Re\sqrt{f} < 180$. Poiseuille's law is not followed exactly, the data being displaced $\approx 1.5\%$ below it, corresponding to $f.Re = 16.2$.
- (ii) Transition: $180 < Re\sqrt{f} < 310$. The data depart downwards from the laminar line towards the Prandtl-Karman law.
- (iii) Turbulent flow: $310 < Re\sqrt{f} < 9880$. The turbulent flow data in the riblet pipe may be divided into three regimes, namely:
 - (1) Hydraulically smooth: $310 < Re\sqrt{f} < 480$ ($3.4 < h^+ < 5.6$). $1/\sqrt{f}$ in the riblet pipe is identical to that in the smooth pipe at the same $Re\sqrt{f}$. This was, of course, the basis for defining the riblet pipe diameter.
 - (2) Riblet drag reduction: $480 < Re\sqrt{f} < 2000$ ($5.6 < h^+ < 22$). The data in the riblet pipe lie above those in the smooth pipe, exhibiting riblet-induced drag reduction. The maximum difference of about 0.6 units in $1/\sqrt{f}$ occurs at $Re\sqrt{f} = 1300$ ($h^+ = 14$) which corresponds to a flow enhancement of 5% relative to smooth (%DR = 8.0).
 - (3) Riblet drag enhancement: $2000 < Re\sqrt{f} < 9880$ ($22 < h^+ < 110$). The riblet pipe data lie below those in the smooth pipe, indicating drag enhancement. This regime consists of two segments, namely: (i) for $2000 < Re\sqrt{f} < 6300$ ($22 < h^+ < 67$), $1/\sqrt{f}$ is, at most, a weak function of $Re\sqrt{f}$, with:

$$1/\sqrt{f} = 12.7 \pm 0.1 \quad (4.2-6)$$

and (ii) for $6300 < Re\sqrt{f} < 9880$ ($67 < h^+ < 110$), the riblet pipe data follow a trajectory that is roughly parallel to, but displaced downward from, the P-K line, correlated by:

$$1/\sqrt{f} = 4.0 \log Re\sqrt{f} - 2.28; \quad R^2 = 0.990 \quad (4.2-7)$$

In this regime, the data therefore lie 1.88 units of $1/\sqrt{f}$ below smooth, corresponding to a flow reduction of 13% ($\%DR = -27$).

The boundary between the smooth and riblet drag reduction regimes at $h^+ \approx 5$ is diffuse because the riblet data only gradually lift off the smooth pipe in this vicinity, whereas the demarcation between the riblet drag reduction and riblet drag enhancement regimes at $h^+ = 22$ is sharp, the riblet data intersecting the smooth at a considerable angle.

Figure 4.2.8 illustrates the effect of using different riblet diameters to convert pressure drop-flow rate measurements to P-K coordinates. The diameters chosen are $d_r = [d_v, d_c, d, d_t] = [10.06, 9.91, 9.80, 9.75]$ mm respectively representing the riblet valley-to-valley, the riblet pipe cross-sectional, the diameter arrived at in section 4.2.3 and used hereafter and riblet tip-to-tip, denoted by $[\square, \diamond, \blacksquare, \circ]$; the experimental error in $1/\sqrt{f}$ is $\pm 0.5\%$. To compare to the P-K law, the transformed data, regressed to the form $1/\sqrt{f} = 4.0 \log(Re\sqrt{f}) + B$, exhibit $B = [-1.10, -0.77, -0.42, -0.28]$. Thus, for example, choosing $d_r = d_c$ causes the data to lie ≈ 0.35 units of $1/\sqrt{f}$ below the P-K law, and decreases the maximum flow enhancement (not shown) from $R'_{\max} = 0.55$ ($\%DR_{\max} = 7.5$) to $R'_{\max} = 0.20$ ($\%DR_{\max} = 3.0$), and the maximum drag enhancement from $R' = -1.88$ to $R' = -1.65$. This illustrates the sensitivity of riblet drag reduction and enhancement to the choice of riblet pipe diameter.

Figures 4.2.9 - 4.2.11 depict the results, in P-K coordinates with an upper h^+ abscissa, for solvent flow in the riblet pipes R1A, R1B, and R2A. Table 4.2.2 summarizes

the solvent flow regimes observed in all pipes. Three flow regimes are observed in the riblet pipes, namely: (i) laminar flow, in which the data are displaced downward from Poiseuille's law by 1.5% to 4%, with $f.Re = [16.26, 16.66, 16.34, 16.22]$ for [R1A, R1B, R2A, R2B] ; (ii) transition, and (iii) turbulent flow, which may be further subdivided into three regimes, namely:

- (1) **Hydraulically smooth:** The riblet pipe data (solid symbols) essentially follow those in the smooth pipe (hollow symbols) for $Re\sqrt{f} < [490, -, 700, 480]$ in [R1A, R1B, R2A, R2B], respectively, corresponding to non-dimensional riblet heights $h^+ < [5.2, -, 5.6, 5.3]$. This region does not exist in R1B, for which we previously estimated $d_r = 7.44$ mm.
- (2) **Riblet drag reduction:** The riblet pipe data lie above those in the smooth pipe, by as much as $[0.55, 0.44, 0.48, 0.60]$ units of $1/\sqrt{f}$ for [R1A, R1B, R2A, R2B], respectively, occurring at $Re\sqrt{f} = [1400, 1000, 1800, 1350]$, which interestingly corresponds to $h^+ \approx 14.5 \pm 0.2$ in all riblet pipes.
- (3) **Riblet drag enhancement:** The riblet pipes lie below those in the corresponding smooth for $Re\sqrt{f} > [2200, 1600, 2680, 2000]$ all of which correspond to $h^+ > 23 \pm 1$. This regime may be divided into two segments, namely (i) a segment of approximately constant $1/\sqrt{f} \approx [13.0, 12.3, 13.3, 12.7]$ for [R1A, R1B, R2A, R2B], respectively, and (ii) a segment wherein the data follow a trajectory that is approximately parallel to the P-K line but displaced downwards from it. This displacement by $[-2.17, -2.43, -1.85, -1.88]$ units of $1/\sqrt{f}$ occurs in [R1A, R1B, R2A, R2B], respectively, for $h^+ > [79, 81, 80, 67]$.

4.2.5 Flow Enhancement Parameters

For solvent flow, the effect of the riblet pipes (r) relative to the corresponding smooth pipes (s) at a fixed $Re\sqrt{f}$ can be defined in terms of the riblet induced flow enhancement:

$$R' = \left[\left(\frac{1}{\sqrt{f}} \right)_r - \left(\frac{1}{\sqrt{f}} \right)_s \right]_{Re\sqrt{f}} \quad (4.2-8)$$

or as the riblet-induced fractional flow enhancement:

$$R_F = R' / \left(\frac{1}{\sqrt{f}} \right)_s = \left[\frac{\left(\frac{1}{\sqrt{f}} \right)_r}{\left(\frac{1}{\sqrt{f}} \right)_s} - 1 \right]_{Re\sqrt{f}} \quad (4.2-9)$$

Figure 4.2.12 depicts the variation of R' with h^+ , showing similarities between the results for all pipes, as summarized in Table 4.2.2. Figure 4.2.13 shows error bars for R' corresponding to an experimental error of $\pm 0.5\%$ in $1/\sqrt{f}$ (individual symbols omitted for clarity). The error in R' is the sum of the absolute errors of the riblet and smooth pipes and is of the order of ± 0.13 units in R' . It is evident that, within experimental error, solvent data in all riblet pipes follow the same universal R' - h^+ relation. . The three turbulent flow segments defined earlier can now be described in terms of flow enhancement parameters:

- (1) Hydraulically smooth: $R' = 0$; $h^+ < 5$.
- (2) Riblet drag reduction: $R' > 0$; $5 < h^+ < 23$, with a maximum $R' = 0.5 \pm 0.05$ at $h^+ = 14 \pm 1$.
- (3) Riblet drag enhancement: $R' < 0$; $h^+ > 23$. R' decreases approximately linearly with increasing h^+ to $h^+ \approx 80$, the slope of this segment, $dR'/d\log h^+ \approx -3.9 \pm 0.1$. For $h^+ > 80$, R' essentially tend to constants with $R' \rightarrow R'_\infty \approx [-2.17, -2.43, -1.88]$.

It should be noted here that the diameter of R1B, which exhibited a very small hydraulically smooth regime, was defined such that the cross over from regimes (2) and (3) occurred at $h^+ = 23$; this diameter agreed with the diameter determined from the single point P_{T0} in Table 4.2.1.

The foregoing comments regarding R' are also apparent in the variation of R_F with h^+ , depicted in Figure 4.2.14.

4.3 Polymer Solution Flow

4.3.1 A Representative Example

4.3.1.1 Prandtl-Karman Representation

Figure 4.3.1 depicts the flow of solvent and a 3 wppm solution of W-301 through S2 and R2B using P-K coordinates, with an upper abscissa added to indicate non-dimensional riblet height, h^+ . In the smooth pipe, the polymer solution exhibits regimes of laminar, $Re\sqrt{f} < 180$, transitional, $180 < Re\sqrt{f} < 300$, and turbulent flow, $300 < Re\sqrt{f} < 9000$, the latter having two segments:

- (i) Newtonian: $300 < Re\sqrt{f} < 550$. The polymer solution (Δ) follows the solvent (\circ).
- (ii) Polymeric: $550 < Re\sqrt{f} < 9000$. A well defined onset of drag reduction occurs at $Re\sqrt{f}^* = 550$, beyond which the polymer solution data diverge upwards from solvent. The segment is approximately linear from onset to $Re\sqrt{f} = 4000$, with slope exceeding that of the solvent line (Eq. 2) by an amount $\delta = 11$. The data exhibit a shallow maximum at $Re\sqrt{f} = 5000$ and then decline slightly to $1/\sqrt{f} = 21$ at $Re\sqrt{f} = 9000$, their decline at the highest $Re\sqrt{f}$ likely caused by polymer degradation.

In the riblet pipe, the polymer solution exhibits laminar, transitional and turbulent flow regimes similar to those seen in the smooth pipe. The turbulent flow data are viewed in two ways. First, the effect of the polymeric additive is revealed by viewing the polymer solution relative to solvent flow in the riblet pipe. The polymer solution data exhibit two segments, akin to those seen in the smooth pipe, namely:

- (i) Newtonian: $300 < Re\sqrt{f} < 550$. The polymer solution (\blacktriangle) follows the solvent (\bullet).
- (ii) Polymeric: $550 < Re\sqrt{f} < 9000$. The onset of polymeric drag reduction in the riblet pipe occurs at $Re\sqrt{f}^* = 550$, the same as that in the smooth pipe. After onset, the polymeric segment in the riblet pipe is initially akin to that seen in the smooth pipe, increasing roughly linearly, with slope 17, from onset to $Re\sqrt{f} = 2500$, at which point it reaches a maximum and abruptly switches to a second roughly linear segment, slope -5, that persists to the highest $Re\sqrt{f} = 9000$. Detailed scrutiny of the riblet polymeric segment shows it to possess a complex sigmoidal shape that differs from that of the corresponding smooth polymeric segment in much the same manner as the riblet solvent curve differs from the smooth solvent line.

Second, the influence of the riblet wall is seen by viewing the flow of the same polymer solution in the riblet and smooth pipes. The data exhibit three turbulent regimes that mirror those earlier seen for solvent flow, namely:

- (i) Hydraulically smooth: $Re\sqrt{f} < 900$ ($h^+ < 10$). The riblet pipe data (\blacktriangle) essentially follow those in the smooth pipe (Δ).
- (ii) Riblet drag reduction: $900 < Re\sqrt{f} < 2700$ ($10 < h^+ < 30$). The riblet pipe data lie above those in the smooth pipe, by as much as 1.6 units of $1/\sqrt{f}$ at $Re\sqrt{f} = 1900$ ($h^+ = 21$).

(iii) Riblet drag enhancement: $2700 < Re\sqrt{f} < 9000$ ($30 < h^+ < 100$). The riblet pipe data lie below those in the smooth pipe, by 2.3 units of $1/\sqrt{f}$ at the highest $Re\sqrt{f} = 9000$ ($h^+ = 100$).

4.3.1.2 Flow Enhancement Parameters

The two facets of drag reduction by polymer solutions in riblet pipes, as described above, can be quantified as follows. First, the effect of the polymer solution (p) relative to the solvent (n) at a fixed $Re\sqrt{f}$ for a given pipe, either smooth (s) or riblet (r) is defined by S' , the polymer-induced flow enhancement, or by S_F , the polymer-induced fractional flow enhancement:

$$S' = \left[\left(\frac{1}{\sqrt{f}} \right)_p - \left(\frac{1}{\sqrt{f}} \right)_n \right]_{Re\sqrt{f}, \text{ pipe}} \quad (4.3-1)$$

$$S_F = S' / \left(\frac{1}{\sqrt{f}} \right)_n = \left[\left(\frac{1}{\sqrt{f}} \right)_p / \left(\frac{1}{\sqrt{f}} \right)_n - 1 \right]_{Re\sqrt{f}, \text{ pipe}} \quad (4.3-2)$$

The evaluation of S' , and hence S_F , from experimental data is illustrated in Figure 4.3.2; the dashed vertical line abcd at $Re\sqrt{f} = 1510$ provides the smooth pipe $S'_s = \underline{ac} = 4.5$; $S_{Fs} = 0.37$ and the riblet pipe $S'_r = \underline{bd} = 5.6$; $S_{Fr} = 0.43$.

Second, the effect of the riblet pipe (r) relative to the smooth pipe (s) at a fixed $Re\sqrt{f}$ for a given fluid, either solvent (n) or polymer solution (p), is defined by R' , the riblet-induced flow enhancement, or by R_F , the riblet-induced fractional flow enhancement:

$$R' = \left[\left(\frac{1}{\sqrt{f}} \right)_r - \left(\frac{1}{\sqrt{f}} \right)_s \right]_{\text{Re}\sqrt{f}, \text{ solution}} \quad (4.3-3)$$

$$R_F = R' / \left(\frac{1}{\sqrt{f}} \right)_s = \left[\left(\frac{1}{\sqrt{f}} \right)_r / \left(\frac{1}{\sqrt{f}} \right)_s - 1 \right]_{\text{Re}\sqrt{f}, \text{ solution}} \quad (4.3-4)$$

Eqs. (4.3-3) and (4.3-4) are the more general form of Eqs. (4.2-8) and (4.2-9). Figure 4.3.2 also shows the evaluation of R' , and hence R_F ; at $\text{Re}\sqrt{f} = 1510$, line abcd provides for the solvent $R_n' = \underline{ab} = 0.4$, $R_{Fn} = 0.035$ and the polymer solution $R_p' = \underline{cd} = 1.5$, $R_{Fp} = 0.089$.

4.3.2 Effect of Polymer Concentration

Figure 4.3.3 shows the effect of polymer concentration, respectively 0 (solvent), 3, 10, 30 and 100 wppm W-301, on drag reduction in S2 and R2B, using the P-K coordinates, an upper h^+ abscissa and notation of Figure 4.3.1. In the smooth pipe (hollow points) the polymer solutions exhibit laminar, $\text{Re}\sqrt{f} < 180$, transitional, $180 < \text{Re}\sqrt{f} < 300$, and turbulent flow, $\text{Re}\sqrt{f} > 300$. All three known regimes of turbulent drag reduction by polymers (Virk, 1975a) are visible, namely:

- (i) Newtonian, wherein the polymer solutions follow the solvent. Both 3 and 10 wppm solutions exhibit Newtonian segments from $300 < \text{Re}\sqrt{f} < 500$.
- (ii) Polymeric, wherein, after onset, the polymer solution data diverge upwards from solvent, exhibiting drag reduction that is dependent upon both flow and polymeric parameters. All four polymer solutions exhibit polymeric segments. The 3 and 10 wppm solutions show well-defined onsets, at $\text{Re}\sqrt{f}^* = 550$ and 450 respectively, followed by roughly linear polymeric segments with slope increments $\delta = 11$ ($550 <$

$Re\sqrt{f} < 4000$) and 19 ($450 < Re\sqrt{f} < 3000$) respectively. The 30 and 100 wppm solutions transit from laminar flow directly into the polymeric regime. Of these, the 30 wppm polymeric segment has a slope increment $\delta = 25$ ($400 < Re\sqrt{f} < 1000$) and an apparent onset at $Re\sqrt{f}^* = 350$, inferred by extrapolation back to the solvent line, but the 100 wppm polymeric segment is too short ($300 < Re\sqrt{f} < 500$) for the derivation of reliable onset and slope parameters.

- (iii) Maximum Drag Reduction, wherein the polymer solutions follow an asymptote that is independent of polymeric parameters and universal in P-K coordinates. Data from both the 30 and 100 wppm solutions lie close to the MDR asymptote, over the respective ranges $1500 < Re\sqrt{f} < 4000$ and $500 < Re\sqrt{f} < 4000$.

Polymer-induced drag reduction regimes seen in the smooth pipe are summarized in Table 4.3.1a.

In the riblet pipe (solid points) the polymer solutions again exhibit laminar, $Re\sqrt{f} < 180$, transitional, $180 < Re\sqrt{f} < 300$, and turbulent flow, $Re\sqrt{f} > 300$. Viewing the turbulent data first relative to solvent (solid circles), to discern the effect of the polymeric additive, we find regimes of polymer solution flow in the riblet pipe similar to those seen in the smooth pipe, namely:

- (i) Newtonian, wherein the polymer solutions follow the solvent. Both 3 and 10 wppm solutions exhibit Newtonian segments from, approximately, $300 < Re\sqrt{f} < 500$.
- (ii) Polymeric, wherein, after onset, the polymer solution data diverge upwards from solvent, exhibiting drag reduction that is dependent upon both flow and polymeric parameters. All four polymer solutions exhibit polymeric segments. The 3 and 10 wppm solutions show well-defined onsets, at $Re\sqrt{f}^* = 550$ and 400 respectively,

while the 30 and 100 wppm solutions transit from laminar flow directly into the polymeric regime. An apparent onset at $Re\sqrt{f}^* = 300$ can be inferred for the 30 wppm solution. For each of the 3, 10 and 30 wppm solutions, the onset of drag reduction in the riblet pipe occurred at essentially the same $Re\sqrt{f}^*$ as in the smooth pipe. Following onset, the polymer solutions initially exhibit roughly linear segments, akin to those seen in the smooth pipe, the slopes of which increase with increasing polymer concentration. However, beyond a certain characteristic $Re\sqrt{f} = [2500, 2000, 1100, 800]$ for $c = [3, 10, 30, 100]$ wppm, respectively, each polymer solution trajectory switches, almost discontinuously, to a second roughly linear segment of lower slope that persists to the highest $Re\sqrt{f}$; it is interesting that the slope of the second segment is ≈ 20 (P-K units) less than that of the initial segment for all four solutions.

- (iii) Maximum Drag Reduction, wherein the polymer solutions follow an asymptote that is independent of polymer concentration. It can be verified on Figure 4.3.3 that the maximum drag reduction (highest $1/\sqrt{f}$) in the riblet pipe is limited by an asymptote:

$$1/\sqrt{f} = 8 \log Re\sqrt{f} - 1.5 ; 800 < Re\sqrt{f} < 5500. \quad (4.3-5)$$

This asymptote is attained by both the 30 and 100 wppm solutions in their second polymeric regime segments, which essentially coincide over the respective ranges $1100 < Re\sqrt{f} < 5500$ and $800 < Re\sqrt{f} < 5000$.

Polymer-induced drag reduction regimes observed in the riblet pipe are summarized in Table 4.3.1b.

Analysis of riblet-induced regimes, and their relation to polymer-induced drag reduction, is attempted in Figure 4.3.4 using, respectively, the flow enhancement

parameters R' and S' , extracted from the data in Figure 4.3.3. Figure 4.3.4 comprise two semi-log plots of (a) the riblet-induced flow enhancement R' and (b) the polymer-induced flow enhancement S' , respectively, versus $Re\sqrt{f}$, and an arithmetic plot of (c) R' versus the smooth pipe polymer-induced flow enhancement S'_s . Part (a) has an upper abscissa showing h^+ , and its ordinate is expanded roughly twofold relative to that of part (b). Perusal of the three panels of Figure 4.3.4 reveal the riblet regimes:

- (i) Hydraulically smooth, $R_p' \approx 0$. For $3 < h^+ < 10$, riblet-induced drag reduction was negligible in all the polymer solutions, amid varying, and considerable, polymer-induced drag reduction, $0 < S'_s < 10$. The hydraulically smooth regime in polymer solutions appeared to extend somewhat beyond that in solvent ($3 < h^+ < 5$), but this is uncertain, on account of both the greater scatter in the polymer solution data relative to solvent and the inherently diffuse upper boundary of this regime.
- (ii) Riblet drag reduction, $R_p' > 0$. The riblets induced drag reduction in the 3 and 10 wppm solutions, over the ranges $10 < h^+ < 30$ and $9 < h^+ < 15$, with respective maxima $(R_p', h^+) = (1.6, 20)$ and $(0.8, 11)$ both occurring at moderate $S'_s \approx 5$; further, there was no instance of $R_p' > 0$ for $S'_s > 8$. Thus the greatest riblet-induced drag reduction in polymer solutions occurred at only moderate polymer-induced drag reductions. Also, in solvent ($S'_s = 0$), riblet drag reduction for $5 < h^+ < 22$ had maximum $(R_p', h^+) = (0.6, 14)$, so that the maximum riblet-induced flow enhancement in the polymer solutions can considerably exceed that in solvent while the h^+ corresponding to this maximum can lie either above or below that in solvent.
- (iii) Riblet drag enhancement, $R_p' < 0$. Riblet-induced drag enhancement occurred in all polymer solutions, those of $c = [3, 10, 30, 100]$ wppm exhibiting $R_p' < 0$ for $h^+ > [30, 15, 11, 9]$, respectively. At the quoted h^+ , the corresponding polymer-induced flow enhancements were $S'_s = [8, 9, 10, 10]$, and it was further found that $R_p' < 0$ for all $S'_s > 10$, that is, beyond a certain extent of polymer-induced drag reduction, the

riblets always induced drag enhancement. At fixed high $h^+ > 30$, R_p' generally decreased with increasing S_s' , while at a fixed high $S_s' > 10$, R_p' was relatively independent of h^+ but decreased with increasing S_s' . The solvent ($S_s' = 0$) showed riblet drag enhancement for $h^+ > 22$, with minimum $R_n' = -2$ for $50 < h^+ < 100$. The 3 and 10 wppm solutions, both confined to the polymeric drag reduction regime, straddled the solvent, each exhibiting the tendency $R_p' \rightarrow R_n'$ as $h^+ \rightarrow 50$. The 30 and 100 wppm solutions, both close to the asymptotic maximum drag reduction, crossed the minimum solvent $R_n' = -2$ at $h^+ = 15$ where $S_s' = 13$, and their drag enhancements then increased monotonically with increasing h^+ (and S_s'), to $R_p' = -7 \pm 1$ at $h^+ = 40$ where $S_s' = 20$.

Riblet-related flow regimes observed in solvent and in W-301 solutions are summarized in Table 4.3.1c.

4.3.3 Effect of Polymer Degradation.

The downward curvature of the 3 wppm W301 data for $Re\sqrt{f} > 3000$ in the smooth pipe S2, as seen in the preceding Figure 4.3.1, was, we will show, symptomatic of polymer degradation; that is, the scission of the original polymer macromolecules into smaller fragments, of lower molecular weight. Turbulent drag reduction by polymer solutions is invariably accompanied by polymer degradation. In seeking the effect of riblets on the flow of polymer solutions, it is particularly important to account for polymer degradation because the latter can cause differences between polymer-induced drag reductions in successive pipe sections that are of the same magnitude as the sought-after riblet-induced drag reductions and enhancements relative to a smooth pipe.

4.3.3.1 Degradation Experiments

Table 4.3.2a lists the experiments conducted to detect and define polymer degradation. The flow system, earlier sketched in Figure 2.1.1, had smooth pipe test sections both upstream and downstream of the riblet pipe sections. In what follows, "Station 1" refers to measurements obtained from a pair of pressure taps in the upstream smooth test section, at $L = 0.78$ and 1.38 m, respectively, for the 7.82 mm and 10.21 mm pipes, where L is the distance from the pipe entrance to midway between the two pressure taps. Station 2 refers to measurements obtained from a pair of pressure taps in a downstream smooth test section, at $L = 1.51$ and 2.25 m, respectively, for the 7.82 and 10.21 mm pipes. Station 2 was separated from Station 1 by the developing section of 0.11 mm riblet pipe, respectively 0.22 and 0.42 m long in the 7.82 mm and 10.21 mm systems; in this configuration the downstream smooth Station 2 lay approximately at the axial location occupied by the riblet test section. Finally, Station 3, used only with the 7.82 mm pipe system to explore the effect of downstream distance, refers to measurements obtained from a pair of pressure taps in a downstream smooth test section at $L = 1.79$ m; Station 3 was separated from Station 1 by both the developing and test sections of 0.11 mm riblet pipe, respectively 0.22 and 0.25 m long; in this configuration, Stations 1 and 3 were at approximately equal distances up- and down-stream of the riblet test section. Experiments were conducted with solvent (control) and with several concentrations of each of two of the highest molecular weight PEO polymers, N-60K and W301, to systematically examine polymer degradation effects as a function of (i) downstream position, (ii) polymer concentration and molecular weight, and (iii) pipe diameter.

4.3.3.2 Examples

Figures 4.3.5-4.3.7 are friction factor plots, P-K coordinates, that illustrate the differences between riblet and smooth pipes on the one hand and between upstream and downstream smooth sections on the other, the latter caused by polymer degradation.

Figure 4.3.5 shows two sets of data for each of solvent and 3 wppm W301 in the 10.21 mm pipe system. The first data set comprises measurements in the smooth and riblet pipes, S2 and R2B, and is a repetition, for comparative purposes, of the information previously presented in Figure 4.3.1; the measurements ascribed to smooth pipe S2 all refer to the upstream Station 1. The second data set comprises measurements from Stations 1 and 2, respectively upstream and downstream of the riblet pipe. For the flow of solvent, friction factors from both Stations, 1(∇) and 2(\blacktriangledown), were virtually identical, and followed the Newtonian Prandtl-Karman relation (N). For the flow of 3 wppm W301, friction factors from Station 2 (\blacksquare) were essentially identical to those from Station 1 (\square) at the lowest $Re\sqrt{f} \approx 2000$, but then diverged progressively downwards with increasing $Re\sqrt{f}$, lying ≈ 0.5 units of $1/\sqrt{f}$ lower at $Re\sqrt{f} = 3500$ and ≈ 1.3 units lower at the highest $Re\sqrt{f} = 7100$. Evidently, the polymer solution degraded while flowing, exhibiting less drag reduction at Station 2 than it did at Station 1. This can be viewed in two equivalent ways; either the polymer solution, of fixed total concentration, had a lower average molecular weight at Station 2 than it had at Station 1, or, the polymer solution contained a lower concentration of the original polymer macromolecules at Station 2 than it had at Station 1. It is also noteworthy that the $Re\sqrt{f} \approx 3500$ at which the friction factors from Stations 1 and 2 begin to diverge appreciably also marks the point beyond which the data from both stations begin to exhibit the downward curvature characteristic of degradation in smooth pipes.

In comparing the two sets of data presented in Figure 4.3.5, we note that friction factors for solvent flow in the smooth pipe from Station 1 (∇) of the second set were identical to those in S2 (\circ) of the first set. However, for the flow of 3 wppm W301, the smooth pipe data (\diamond) of the first set lie above those from Station 1 (\square) of the second set, by ≈ 1 unit of $1/\sqrt{f}$ for $2000 < Re\sqrt{f} < 3500$; this stems from differences between the W301 polymer batches used, that of the first set being of slightly higher molecular weight than that of the second. Nevertheless, the downward curvature symptomatic of polymer degradation becomes apparent at roughly the same $Re\sqrt{f} = 3500 \pm 500$ in both sets (\diamond and

□) of smooth pipe data, and the two sets virtually coalesce at the highest $Re\sqrt{f} \approx 7000$. Turning to the riblet pipe R2B of the first set, the data for 3 wppm W301 (◆) were previously shown to exhibit three regimes, namely: (i) $R' = 0$, hydraulically smooth, $350 < Re\sqrt{f} < 900$, (ii) $R' > 0$, riblet drag reduction, $900 < Re\sqrt{f} < 3000$, and (iii) $R' < 0$, riblet drag enhancement, $3000 < Re\sqrt{f} < 9000$. Recall now that riblet-induced drag reduction, $R' = (1/\sqrt{f_r} - 1/\sqrt{f_s})Re\sqrt{f}$, was defined, Eq. (4.2-8), with respect to the friction factor for the same solution in a smooth pipe at the same $Re\sqrt{f}$. As long as polymer degradation is imperceptible, and friction factors in the smooth sections upstream and downstream of the riblet pipe are identical, we can employ $1/\sqrt{f_{s,Station 1}} = 1/\sqrt{f_s} = 1/\sqrt{f_{s,Station 2}}$, and evaluate R' without ambiguity; in the present case, the second set of 3 wppm W301 data (□ and ■) shows this condition to prevail for $Re\sqrt{f} < 3500$, over which range, therefore, our assessment of riblet-induced drag reduction is unaffected by polymer degradation. However, as polymer degradation becomes appreciable, and friction factors in the downstream smooth section diverge downwards from those in the upstream smooth section, we can only bracket the reference smooth pipe friction factor within the limits $1/\sqrt{f_{s,Station 1}} \geq 1/\sqrt{f_s} \geq 1/\sqrt{f_{s,Station 2}}$, and it becomes difficult to evaluate R' precisely. In the present case, at $Re\sqrt{f} = 7000$, for example, we have $R' = -2.3$ from the first data set (◇ and ◆), based on $1/\sqrt{f_s} = 1/\sqrt{f_{s,Station 1}}$; however, from the second data set (□ and ■) $1/\sqrt{f_{s,Station 2}} - 1/\sqrt{f_{s,Station 1}} = -1.3$, so we estimate $R' = -1.0$ based on $1/\sqrt{f_s} = 1/\sqrt{f_{s,Station 2}}$; the riblet-induced drag reduction is thus bracketed between the wide limits $-2.3 < R' < -1.0$, which illustrates the uncertainty that polymer degradation can introduce into evaluations of R' at the highest $Re\sqrt{f}$.

Figure 4.3.6 shows two sets of data for each of solvent and 3 wppm W301 in the 7.82 mm pipe system. The first data set comprises measurements in the smooth and riblet pipes, S1 and R1A, while the second data set comprises measurements from smooth pipe Stations 1 and 2. For the flow of solvent, friction factors from both Stations, 1(▼) and 2(▼), were virtually identical, and followed the Newtonian Prandtl-Karman relation (N) in

the turbulent regime. For the flow of 3 wppm W301, friction factors from Station 2 (■) were essentially identical to those from Station 1 (□) over the turbulent range $300 < Re\sqrt{f} < 2200$, but then diverged downwards with increasing $Re\sqrt{f}$, lying ≈ 1.5 units of $1/\sqrt{f}$ lower for $3000 < Re\sqrt{f} < 7000$. This is evidence of polymer degradation. The $Re\sqrt{f} \approx 2200$ at which the friction factors from Stations 1 and 2 begin to diverge is also where the data from both stations begin to exhibit the downward curvature symptomatic of degradation.

Comparing the two sets of data in Figure 4.3.6, friction factors for solvent flow in the smooth pipe (○) of the first set were identical to those from Station 1 (▽) of the second set. For the flow of 3 wppm W301, the smooth pipe data (◇) of the first set lie slightly below those from Station 1 (□) of the second set, by ≈ 0.5 unit of $1/\sqrt{f}$ for $800 < Re\sqrt{f} < 7000$, on account of the W301 polymer batch of the first set being of slightly lower molecular weight than that of the second. In both sets (◇ and □), the downward curvature symptomatic of polymer degradation becomes apparent at roughly the same $Re\sqrt{f} = 2200 \pm 200$. Turning to the riblet pipe R1A of the first set, the data for 3 wppm W301 (◆) exhibit three regimes, namely: (i) $R' = 0$, hydraulically smooth, $350 < Re\sqrt{f} < 450$, (ii) $R' > 0$, riblet drag reduction, $450 < Re\sqrt{f} < 1200$, and (iii) $R' < 0$, riblet drag enhancement, $1200 < Re\sqrt{f} < 8000$. Polymer degradation was imperceptible, and therefore does not affect the assessment of riblet-induced drag reduction R' , for $Re\sqrt{f} < 2200$. At the highest $Re\sqrt{f} = 7000$, we have $R' = -2.6$ from the first data set (◇ and ◆), based on $1/\sqrt{f_s} = 1/\sqrt{f_{s,Station 1}}$; however, from the second data set (□ and ■), $1/\sqrt{f_{s,Station 2}} - 1/\sqrt{f_{s,Station 1}} = -1.4$, so we estimate $R' = -1.2$ based on $1/\sqrt{f_s} = 1/\sqrt{f_{s,Station 2}}$; the riblet-induced drag reduction is thus bracketed between the limits $-2.6 < R' < -1.2$.

As a final example, Figure 4.3.7 shows two sets of data for each of solvent and 100 wppm W301 in the 7.82 mm pipe system, respectively comprising measurements in pipes S1 and R1A and from Stations 1 and 2. For the flow of 100 wppm W301, friction factors from Station 2 (■) were essentially identical to those from Station 1 (□), with both

closely adhering to the maximum drag reduction asymptote (MDR) for smooth pipes over the range $300 < Re\sqrt{f} < 3000$. Evidence of polymer degradation is barely visible at the very highest $Re\sqrt{f} \approx 3300$, where the data from Station 2 lie ≈ 1 unit of $1/\sqrt{f}$ below those of Station 1.

Comparing the two sets of data in Figure 4.3.7, friction factors for the flow of 100 wppm W301 in the smooth pipe (\diamond) of the first set are virtually identical to those from Station 1 (\square) of the second set, both following the smooth pipe MDR relation for $300 < Re\sqrt{f} < 3000$. In the riblet pipe R1A of the first set, the data for 100 wppm W301 (\blacklozenge) exhibit three regimes, namely: (i) $R' = 0$, hydraulically smooth, $350 < Re\sqrt{f} < 750$, (ii) $R' > 0$, riblet drag reduction, $750 < Re\sqrt{f} < 1000$, and (iii) $R' < 0$, riblet drag enhancement, $1000 < Re\sqrt{f} < 5500$. Polymer degradation was imperceptible, and therefore does not affect the assessment of riblet-induced drag reduction R' , for $Re\sqrt{f} < 3000$. At $Re\sqrt{f} = 3300$, we have $R' = -6.3$ from the first data set (\diamond and \blacklozenge), based on $1/\sqrt{f_s} = 1/\sqrt{f_{s,Station 1}}$; from the second data set (\square and \blacksquare), $1/\sqrt{f_{s,Station 2}} - 1/\sqrt{f_{s,Station 1}} = -1.1$, so we estimate $R' = -5.2$ based on $1/\sqrt{f_s} = 1/\sqrt{f_{s,Station 2}}$; the riblet-induced drag reduction is thus bracketed between the limits $-6.3 < R' < -5.2$.

The foregoing observations regarding polymer degradation can be summarized thus:

1. In the polymeric regime of drag reduction, exemplified by flows of 3 wppm W301, polymer degradation was imperceptible for $Re\sqrt{f} < 2200$ in the 7.82 mm pipe and for $Re\sqrt{f} < 3500$ in the 10.21 mm pipe. Thus, for the present set of smooth and riblet pipes, the evaluation of riblet-induced flow enhancement R' was essentially unaffected by polymer degradation over the whole of the hydraulically smooth and riblet drag reduction regimes. In the riblet drag enhancement regime, polymer degradation generally affected the evaluation of R' , introducing very little uncertainty in the early, low $Re\sqrt{f}$, portions of the regime, but causing uncertainties on the order of ± 1 unit of

$1/\sqrt{f}$ at the highest $Re\sqrt{f} \approx 7000$. It should also be noted that PEO W301 was one of the highest molecular weight polymers used in the present investigation, and thus the most susceptible to degradation; we can therefore anticipate riblet pipe data from other polymers to be even less affected by degradation.

2. In the regime of asymptotic maximum drag reduction, exemplified by flows of 100 wppm W301, polymer degradation was imperceptible for $Re\sqrt{f} < 3000$ in the 7.82 mm pipe. Thus the evaluation of riblet-induced flow enhancement R' was essentially unaffected by polymer degradation over the whole of the hydraulically smooth and riblet drag reduction regimes and for most of the riblet drag enhancement regime. Polymer degradation caused uncertainties on the order of ± 0.5 unit of $1/\sqrt{f}$ in the evaluation of R' at the highest $Re\sqrt{f} \approx 3500$ in the riblet drag enhancement regime. It should also be noted that, since the 7.82 mm pipe generally engendered more degradation than the 10.21 mm pipe, riblet pipe data at maximum drag reduction in the larger pipe will be even less affected by polymer degradation.

4.3.3.3 *Quantitative Results.*

Before attempting to quantify degradation effects, it is appropriate to assess the variations between the nominally identical polymer batches used in these experiments. The detailed friction factor measurements made to define degradation are collected and analyzed in Appendix E, with the onset wall shear stresses and specific slope increments obtained at Station 1 for each of the five polymer batches used summarized in Table 4.3.2b. This table shows that the two batches of N-60K polymer exhibited essentially the same τ_w^* and δ/\sqrt{c} , within experimental uncertainties. Of the three batches of W-301 polymer, the tow used in the 7.82 mm pipe experiments exhibited the same τ_w^* and δ/\sqrt{c} , within experimental uncertainties, while the third, used in the 10.21 mm pipe, showed τ_w^* somewhat higher

and δ/\sqrt{c} somewhat lower than the other two, which suggests its molecular weight was slightly lower than theirs. Thus we can conclude that there was little variation between different batches of a given polymer.

Quantitative results for polymer degradation as a function of downstream distance, polymer concentration and molecular weight, and pipe diameter are presented in Figures 4.3.8a,b and 4.3.9a-d, using data from all the experiments listed in Table 4.3.2a. Both figures employ semi-logarithmic coordinates of a degradation parameter Δ' versus the wall shear stress τ_w N/m². The difference between the P-K friction factors at the downstream (j) and upstream (k) smooth pipe stations:

$$\Delta_{jk} = \left[\left(\frac{1}{\sqrt{f}} \right)_{s,j} - \left(\frac{1}{\sqrt{f}} \right)_{s,k} \right]_{Re\sqrt{f}} \quad (4.3-6)$$

was chosen as an appropriate degradation parameter; it can be viewed as a degradation-induced flow enhancement that is inherently ≤ 0 . Also, since degradation was observed to increase strongly with increasing $Re\sqrt{f}$, the latter was a natural abscissa for depicting the former; an abscissa closely related to $Re\sqrt{f}$, namely, wall shear stress τ_w , was finally used because it better correlated the point at which degradation became perceptible.

For solutions of polymer W301 in the 7.82 mm pipe, Figure 4.3.8 depicts, in registry, (a) the variation of Δ'_{21} , between Stations 2 and 1, versus wall shear stress τ_w N/m² for $c = [1, 3, 10, 30, 100]$ wppm and (b) the variation of Δ'_{31} versus τ_w for $c = [1, 10, 100]$ wppm. The influence of downstream location, and some of the physics of degradation, are derived by following the data for a particular polymer solution. For $c = 10$ wppm we see in part (a), upper panel, that degradation is imperceptible at the lower wall shear stresses, $\Delta'_{21} = 0.0 \pm 0.4$ for $1 < \tau_w$ N/m² < 13 , but then increases rapidly with increasing wall shear stress, to $\Delta'_{21} = -1.9$ at $\tau_w = 30$ N/m², before reaching a nearly constant level at the highest wall shear stresses, $\Delta'_{\min,21} = -2.4 \pm 0.1$, for $40 < \tau_w$ N/m² $<$

200. A similar pattern is visible for the 10 wppm solution in part (b), lower panel, with degradation imperceptible, $\Delta'_{31} = 0.0 \pm 0.2$, for $1 < \tau_w \text{ N/m}^2 < 12$, then increasing rapidly, to $\Delta'_{31} = -4.7$ at $\tau_w = 30 \text{ N/m}^2$, before reaching a nearly constant level, $\Delta'_{\min,31} = -5.0 \pm 0.2$, for $40 < \tau_w \text{ N/m}^2 < 120$ [it is possible that, after reaching a minimum, Δ'_{31} slowly increases with increasing τ_w in this range]. In both of the preceding cases, there is a characteristic wall shear stress, hereafter called τ_w^\wedge , above which degradation becomes perceptible. The values of $\tau_w^\wedge_{21} \approx 13 \text{ N/m}^2$ and $\tau_w^\wedge_{31} \approx 12 \text{ N/m}^2$, respectively, in parts (a) and (b), show τ_w^\wedge to be essentially independent of downstream location over the present variation of L/d_s , respectively 100, 193 and 230 at Stations 1, 2 and 3. Beyond τ_w^\wedge , however, the rapid increase in degradation with increasing τ_w , is clearly dependent upon downstream location, with $\Delta'_{21} = -1.9$ in (a) while $\Delta'_{31} = -4.7$ in (b) at the same $\tau_w = 30 \text{ N/m}^2$. The nearly constant levels of degradation seen at the highest wall shear stresses, $\tau_w > 40 \text{ N/m}^2$, also depend upon downstream location, being (a) $\Delta'_{\min,21} = -2.4$ and (b) $\Delta'_{\min,31} = -5.0$.

The foregoing observations for $c = 10$ wppm qualitatively apply to $c = 1$ wppm also, which exhibits (a) degradation imperceptible, $\Delta'_{21} = 0.0 \pm 0.4$, for $1 < \tau_w \text{ N/m}^2 < 15$, then increasing to $\Delta'_{21} = -0.4$ at $\tau_w = 30 \text{ N/m}^2$, before reaching a nearly constant level, $\Delta'_{\min,21} = -0.8 \pm 0.1$, for $60 < \tau_w \text{ N/m}^2 < 300$, and (b) degradation imperceptible, $\Delta'_{31} = 0.0 \pm 0.2$, for $1 < \tau_w \text{ N/m}^2 < 13$, then increasing rapidly, to $\Delta'_{31} = -0.9$ at $\tau_w = 30 \text{ N/m}^2$, before reaching a nearly constant level, $\Delta'_{\min,31} = -1.2 \pm 0.2$, for $60 < \tau_w \text{ N/m}^2 < 300$. In this case too, the shear stresses above which degradation becomes perceptible, $\tau_w^\wedge_{21} \approx 15 \text{ N/m}^2$ and $\tau_w^\wedge_{31} \approx 13 \text{ N/m}^2$, are relatively independent of downstream location, while for $\tau_w > \tau_w^\wedge$, the extents of degradation, $\Delta'_{21} = -0.4$ and $\Delta'_{31} = -0.9$ at the same $\tau_w = 30 \text{ N/m}^2$, are dependent upon downstream location.

Solutions of $c = 100$ wppm exhibit (a) degradation imperceptible, $\Delta'_{21} = 0.0 \pm 0.4$, for $1 < \tau_w \text{ N/m}^2 < 70$, then increasing rapidly, to $\Delta'_{21} = -0.8$ at $\tau_w = 100 \text{ N/m}^2$, before

reaching a nearly constant level, $\Delta'_{\min,21} = -0.8 \pm 0.1$, for $100 < \tau_w \text{ N/m}^2 < 120$, and (b) degradation imperceptible, $\Delta'_{31} = 0.0 \pm 0.2$, for $1 < \tau_w \text{ N/m}^2 < 60$, then increasing rapidly, to $\Delta'_{31} = -1.4$ at $\tau_w = 100 \text{ N/m}^2$. Here too, the shear stresses above which degradation becomes perceptible, $\tau_w^{\wedge 21} \approx 70 \text{ N/m}^2$ and $\tau_w^{\wedge 31} \approx 60 \text{ N/m}^2$, are relatively independent of downstream location, while for $\tau_w > \tau_w^{\wedge}$, the extents of degradation, $\Delta'_{21} = -0.8$ and $\Delta'_{31} = -1.4$ at the same $\tau_w = 100 \text{ N/m}^2$, depend upon downstream location.

It may be verified by reference to Figure 4.3.8 that the features described above also apply to all of the other polymer solutions therein, which generally exhibit regions of (i) imperceptible degradation, $\Delta' \approx 0$ for $\tau_w < \tau_w^{\wedge}$, and (ii) perceptible degradation, $\Delta' < 0$ for $\tau_w > \tau_w^{\wedge}$, the degradation increasing rapidly with increasing τ_w beyond τ_w^{\wedge} but then reaching an almost constant level Δ'_{\min} at the highest τ_w .

The influence of polymer concentration upon degradation can also be discerned from the data in Figure 4.3.8.

Solutions associated with the polymeric regime of drag reduction, namely $c = [1, 3, 10, 30]$ wppm in part (a) and $c = [1, 10]$ wppm in part (b), all show perceptible degradation above approximately the same wall shear stresses, (a) $\tau_w^{\wedge 21} = 14 \pm 3 \text{ N/m}^2$ and (b) $\tau_w^{\wedge 31} = 12 \pm 1 \text{ N/m}^2$, which are essentially independent of polymer concentration and only weakly dependent, if at all, on downstream distance. The average $\tau_w^{\wedge} \approx 13 \text{ N/m}^2$ is about 7 times higher than the onset wall shear stress $\tau_w^* = 1.8 \pm 0.5 \text{ N/m}^2$ above which these polymer solutions exhibit drag reduction; this provides an interesting indication of the range, $\tau_w^* \leq \tau_w \leq \tau_w^{\wedge}$, over which drag reduction data are unswayed by polymer degradation effects. At fixed $\tau_w = 30 \text{ N/m}^2 > \tau_w^{\wedge}$, the above solutions show (a) $\Delta'_{21} = [-0.4, -1.0, -1.9, -1.4]$ and (b) $\Delta'_{31} = [-0.9, -4.7]$, while at the highest wall shear stresses, roughly $50 < \tau_w \text{ N/m}^2 < 200$, the essentially constant degradation levels are (a) $\Delta'_{\min,21} = [-0.8, -1.4, -2.4, -3.8]$ and (b) $\Delta'_{\min,31} = [-1.2, -5.0]$. It is evident that for any fixed τ_w

$> \tau_w^\wedge$, Δ' generally increased with increasing polymer concentration and with increasing downstream distance. At the highest τ_w , we find $\Delta'_{\min,21} = (0.75 \pm 0.06)\sqrt{c}$ and $\Delta'_{\min,31} = (1.4 \pm 0.2)\sqrt{c}$, both increasing approximately as the square root of polymer concentration; at any $\tau_w > \tau_w^\wedge$, it is also found that $\Delta'_{31} \approx 2 \Delta'_{21}$. The observed variation of $\Delta'_{\min} \propto \sqrt{c}$ at fixed $\tau_w > \tau_w^\wedge$ is interesting because it parallels the known variation of the polymer-induced flow enhancement, $S' \propto \sqrt{c}$, in the present polymeric regime; this implies that a normalized “severity” of degradation, of the form (Δ'_{\min}/S') , might actually be independent of polymer concentration, that is, polymer degradation is kinetically a first order process.

Finally, the solution associated with the asymptotic maximum drag reduction, $c = 100$ wppm, showed perceptible degradation above (a) $\tau_w^\wedge_{21} \approx 70 \text{ N/m}^2$ and (b) $\tau_w^\wedge_{31} \approx 60 \text{ N/m}^2$. The average $\tau_w^\wedge \approx 65 \text{ N/m}^2$ for $c = 100$ wppm at MDR considerably exceeds $\tau_w^\wedge \approx 13 \text{ N/m}^2$ observed for all the other solutions in the polymeric regime. At fixed $\tau_w = 100 \text{ N/m}^2 > \tau_w^\wedge$, the 100 wppm solution showed (a) $\Delta'_{21} = -0.8$ and (b) $\Delta'_{31} = -1.4$. Thus degradation increases with increasing downstream distance at MDR also, with $\Delta'_{31} \approx 2 \Delta'_{21}$; however, the magnitudes of Δ' observed with $c = 100$ wppm at MDR are considerably smaller than those observed at comparable τ_w with $c = 10$ and 30 wppm solutions, of lower concentration, operating in the polymeric regime.

Figure 4.3.9 shows the effects of polymer molecular weight and pipe diameter on degradation using two PEO polymers, N-60K and W-301, of nominal $M_w = 2.0 \times 10^6$ and 5.0×10^6 , and making measurements between Stations 1,3 in the 7.82 mm pipe and Stations 1,2 in the 10.21 mm pipe, respectively. The figure has four parts, a-d, the pairs a,b and c,d, each in vertical registry, referring to the 7.82 and 10.21 pipes, while the pairs a,c and b,d, each in horizontal registry, refer to N-60K and W-301 polymers, respectively; note that Figure 4.3.9b here is the same as the earlier Figure 4.3.8b.

Consider first the effect of molecular weight on degradation, for solutions in the polymeric regime of drag reduction. Within the a,b pair, in the 7.82 mm pipe, we see that in part (a), $c = [3, 10]$ wppm of N-60K exhibit degradation beyond $\tau_w^{\wedge}{}_{31} = 17 \pm 5 \text{ N/m}^2$, with $\Delta'_{31} = [-1.2, -2.2]$ at $\tau_w = 100 \text{ N/m}^2$, while in part (b), $c = [1, 10]$ wppm of W-301 exhibit degradation beyond $\tau_w^{\wedge}{}_{31} = 12 \pm 1 \text{ N/m}^2$, with $\Delta'_{31} = [-1.3, -4.8]$ at $\tau_w = 100 \text{ N/m}^2$. Next, within the c,d pair, 10.21 mm pipe, in part (c), $c = [3, 10, 30]$ wppm of N-60K exhibit degradation beyond $\tau_w^{\wedge}{}_{21} = 40 \pm 5 \text{ N/m}^2$, with $\Delta'_{21} = [-0.5, -0.7, -0.9]$ at $\tau_w = 100 \text{ N/m}^2$, while in part (d), $c = [3, 10]$ wppm of W-301 exhibit degradation beyond $\tau_w^{\wedge}{}_{21} = 14 \pm 1 \text{ N/m}^2$, with $\Delta'_{21} = [-1.0, -1.6]$ at $\tau_w = 100 \text{ N/m}^2$. In both pairs of comparisons between N-60K and W-301, the latter exhibited the lower τ_w^{\wedge} , and the higher Δ' at fixed c and $\tau_w > \tau_w^{\wedge}$, showing that increasing polymer molecular weight causes degradation to become perceptible at lower wall shear stresses, and to be of greater severity thereafter. Quantitatively, the ratio of degradation-inducing wall shear stresses $\tau_w^{\wedge}(\text{W-301})/\tau_w^{\wedge}(\text{N-60K}) = 0.71$ and 0.33 in the 7.82 and 10.21 mm pipes, while for equal concentrations $c = [3, 10]$ wppm at constant $\tau_w = 100 \text{ N/m}^2$, the ratio of degradation extents $\Delta'(\text{W-301})/\Delta'(\text{N-60K}) = [2.0, 2.2]$ and $[2.0, 2.3]$ in the 7.82 and 10.21 mm pipes. Since the ratio of the polymer molecular weights, $M_w(\text{W-301})/M_w(\text{N-60K}) \approx 2.5$, the observed degradation extent ratios of similar magnitudes imply that degradation extent is approximately proportional to polymer molecular weight, $\Delta' \propto M_w$.

The effect of pipe diameter on degradation can be inferred directly from information in the preceding paragraph, by making pair-wise comparisons between parts a,c and b,d of Figure 4.3.9. Broadly, increasing pipe diameter did not greatly affect the wall shear stress at which degradation became perceptible but appreciably reduced the severity of degradation thereafter. More quantitatively, we should note that proper inference of pipe diameter effects requires constant transit times between measuring stations, as well as identical polymer molecular weights between tests, in each pipe. The nondimensional separations used between Stations 1,3 in the 7.82 mm pipe and Stations 1,2 in the 10.21

mm pipe, respectively $L/d_s = 129$ and 85 , provided approximately equal transit times at a fixed wall shear stress in turbulent flow, and it has been shown in Table 4.3.2b that there were only small variations between polymer batches. The ratio of degradation-inducing to onset wall shear stresses $(\tau_w^\wedge/\tau_w^*) = [6.7, 5.6, 3.4, 7.3]$ in parts [b, d, a, c] is essentially the same, $\approx 6.2 \pm 0.6$, for W301 in both pipes, but varies considerably, 5.4 ± 2.0 , for N60K. At constant $\tau_w = 100 \text{ N/m}^2 > \tau_w^\wedge$, using the same polymer solution, the ratio of degradation extents in the two pipes is $\Delta'_{21} (10.21 \text{ mm}) / \Delta'_{31} (7.82 \text{ mm}) = [0.42, 0.33, 0.42, 0.32]$ for $c = [1, 10]$ wppm W301 and $[3, 10]$ wppm N60K. The foregoing correspond to a power-law of the form: $\Delta' \propto d_s^{-3.7}$, illustrating the powerful dependence of degradation extent upon pipe diameter.

The foregoing quantitative results will be more comprehensively correlated in the next chapter, with a view to applying appropriate “degradation corrections” to our riblet pipe results at the highest flow rates.

4.3.4 Effect of Polymer Molecular Weight

4.3.4.1 N-10 Solutions

Figure 4.3.10 shows drag reduction by 2435 and 5138 wppm N-10 in S2 and R2B, using P-K coordinates, an upper h^+ abscissa and the notation of Figure 4.3.1, which will be adopted as the standard hereafter. In the smooth pipe (hollow points) the polymer solutions exhibit laminar, $Re\sqrt{f} < 180$, transitional, $180 < Re\sqrt{f} < 300$, and turbulent flow, $Re\sqrt{f} > 300$. Only two of the three known regimes of turbulent drag reduction by polymers are visible, namely:

- (i) Newtonian, wherein the polymer solutions follow the solvent. The [2435, 5138] wppm solutions exhibit Newtonian segments for $Re\sqrt{f} < [2000, 1200]$, respectively.

- (ii) Polymeric, wherein the polymer solutions exhibit drag reduction. The [2435, 5138] wppm solutions onset at $Re\sqrt{f}^* = [2000, 1200]$ respectively, followed by roughly linear polymeric segments with slope increments $\delta = [4.6, 6.8]$, respectively.

Polymer-induced drag reduction regimes for N-10 solutions observed in the smooth pipe, S2, are summarized in Table 4.3.3a.

In the riblet pipe the polymer solutions again exhibit laminar, $Re\sqrt{f} < 180$, transitional, $180 < Re\sqrt{f} < 300$, and turbulent flow, $Re\sqrt{f} > 300$. Viewing the turbulent data first relative to solvent (solid circles), to discern the effect of the polymeric additive, we find regimes of polymer solution flow in the riblet pipe similar to those seen in the smooth pipe, namely:

- (i) Newtonian, wherein the polymer solutions follow the solvent. Both [2435, 5138] wppm solutions exhibit Newtonian segments for $Re\sqrt{f} < [1800, 1200]$, respectively.
- (ii) Polymeric, wherein the polymer solutions exhibits drag reduction. The [2435, 5138] wppm solutions onset at $Re\sqrt{f}^* = [1800, 1200]$, corresponding to $h^{+*} = [25, 19]$, respectively. The onset of drag reduction in the riblet pipe occurred at approximately the same $Re\sqrt{f}^*$ as in the smooth pipe for the same concentration. Following onset, the polymer solutions exhibit roughly linear segments, akin to those seen in the smooth pipe, the slopes of which increase with increasing polymer concentration.

Polymer-induced drag reduction regimes for N-10 solutions observed in the riblet pipe, R2B, are summarized in Table 4.3.3b.

Analysis of riblet-induced regimes, and their relation to polymer-induced drag reduction, is attempted in Figure 4.3.11. Perusal of the three panels reveal the riblet regimes:

- (i) Hydraulically smooth, $R_p' \approx 0$. For $3 < h^+ < 5$, riblet-induced drag reduction was negligible in the polymer solutions, both of which lay in their Newtonian regime, with no polymer-induced drag reduction, $S_s' = 0$.
- (ii) Riblet drag reduction, $R_p' > 0$. The riblet induced drag reduction in the [2435, 5136] wppm solutions occurred over the ranges [$5 < h^+ < 30$, $5 < h^+ < 27$]. The respective maxima $R_p' = [0.55, 0.50]$, at $h^+ = [15, 15]$, occurred while $S_s' = 0$, the onsets of polymer-induced drag reduction being at $h^{+*} = [25, 19]$. For $h^+ < h^{+*}$, the polymer solution data closely follow the solvent, while for $h^+ > h^{+*}$ these data lie above the solvent.
- (iii) Riblet drag enhancement, $R_p' < 0$. Riblet-induced drag enhancement occurred in both [2435, 5136] wppm solutions for $h^+ > [30, 27]$, respectively. At the quoted h^+ , the corresponding polymer-induced flow enhancements were $S_s' = [0.5, 3]$. As h^+ increases, both solution trajectories lay above the solvent for $h^+ < 50$, by as much as 1 unit of $1/\sqrt{f}$; the 2435 wppm solution exhibited $R_p' \approx R_n'$ for $50 < h^+ < 80$.

Riblet-related flow regimes observed in solvent and in N-10 solutions are summarized in Table 4.3.3c.

4.3.4.2 N-750 Solutions

Figure 4.3.12 shows drag reduction by [100, 250, 900, 2073] wppm N-750 in S2 and R2B. In the smooth pipe (hollow points) the polymer solutions exhibit laminar, $Re\sqrt{f} < 180$, transitional, $180 < Re\sqrt{f} < 300$, and turbulent flow, $Re\sqrt{f} > 300$. Only two of the three known regimes of turbulent drag reduction by polymers are visible, namely:

- (i) Newtonian, wherein the polymer solutions follow the solvent. The [100, 250, 900, 2073] wppm solutions exhibit Newtonian segments for $Re\sqrt{f} < [1200, 1100, 950, 600]$, respectively.
- (ii) Polymeric, wherein the polymer solutions exhibit drag reduction. The [100, 250, 900, 2073] wppm solutions onset at $Re\sqrt{f}^* = [1200, 1100, 950, 600]$, respectively, followed by roughly linear polymeric segments with slope increments $\delta = [7.8, 10.2, 17.3, 30.3]$, respectively.

Polymer-induced drag reduction regimes for N-750 solutions observed in the smooth pipe, S2, are summarized in Table 4.3.4a.

In the riblet pipe the polymer solutions again exhibit laminar, $Re\sqrt{f} < 180$, transitional, $180 < Re\sqrt{f} < 300$, and turbulent flow, $Re\sqrt{f} > 300$. Viewing the turbulent data first relative to solvent (solid circles), to discern the effect of the polymeric additive, we find regimes of polymer solution flow in the riblet pipe similar to those seen in the smooth pipe, namely:

- (i) Newtonian, wherein the polymer solutions follow the solvent. The [100, 250, 900, 2073] wppm solutions exhibit Newtonian segments for $Re\sqrt{f} < [1100, 1100, 950, 600]$, respectively.
- (ii) Polymeric, wherein, after onset, the polymer solution data diverge upwards from solvent, exhibiting drag reduction that is dependent upon both flow and polymeric parameters. The [100, 250, 900, 2073] wppm solutions onset at $Re\sqrt{f}^* = [1100, 1100, 950, 600]$, corresponding to $h^{+*} = [12, 12, 10, 6]$, respectively. The onset of drag reduction in the riblet pipe occurred at approximately the same $Re\sqrt{f}^*$ as in the smooth pipe for the same concentration. Following onset, the polymer solutions exhibit roughly linear segments, the slopes of which increase with increasing polymer concentration.

Polymer-induced drag reduction regimes for N-750 solutions observed in the riblet pipe, R2B, are summarized in Table 4.3.4b.

Analysis of riblet-induced regimes, and their relation to polymer-induced drag reduction, is attempted in Figure 4.3.13, revealing the riblet regimes:

- (i) Hydraulically smooth, $R_p' \approx 0$. For $3 < h^+ < 6$, riblet-induced drag reduction was negligible in all the polymer solutions, occurring in the Newtonian regime, where in $S_s' = 0$.
- (ii) Riblet drag reduction, $R_p' > 0$. The riblets induced drag reduction in the 100, 250, 900 and 2073 wppm solutions over the ranges $6 < h^+ < 40$, $6 < h^+ < 43$, $5 < h^+ < 34$, and $5 < h^+ < 23$ with respective maxima $(R_p', h^+) = (1.1, 30)$, $(1.8, 25)$, $(2.0, 22)$ and $(1.9, 13)$. The greatest riblet-induced drag reduction in polymer solutions occurred at only low to moderate polymer-induced drag reductions, $1 < S_s' < 5$. It is noteworthy that the range of riblet-induced flow enhancement in the polymer solutions initially increased, exceeding solvent, as concentration increased from 100 to 250 wppm solutions then decreased from 900 to 2073 wppm solutions, approaching the solvent range.
- (iii) Riblet drag enhancement, $R_p' < 0$. Riblet-induced drag enhancement occurred in all polymer solutions, those of $c = [100, 250, 900, 2073]$ wppm exhibiting $R_p' < 0$ for $h^+ > [40, 43, 34, 23]$, respectively. At the quoted h^+ , the corresponding polymer-induced flow enhancements were $S_s' = [2, 3, 6, 10]$, and it was further found that $R_p' < 0$ for all $S_s' > 10$. At fixed high $h^+ > 60$, the trajectories for the [100, 250, 900] wppm solutions approached the solvent trajectory.

Riblet-related flow regimes observed in solvent and in N-750 solutions are summarized in Table 4.3.4c.

4.3.4.3 N-60K Solutions

Figure 4.3.14 shows drag reduction by [3, 10, 30, 100] wppm N-60K in S2 and R2B. In the smooth pipe (hollow points) the polymer solutions exhibit laminar, $Re\sqrt{f} < 180$, transitional, $180 < Re\sqrt{f} < 300$, and turbulent flow, $Re\sqrt{f} > 300$. Only two of the three known regimes of turbulent drag reduction by polymers are visible, namely:

- (i) Newtonian, wherein the polymer solutions follow the solvent. The [3, 10, 30, 100] wppm solutions exhibit Newtonian segments for $Re\sqrt{f} < [1150, 1050, 950, 650]$, respectively.
- (ii) Polymeric, wherein the polymer solutions exhibit drag reduction. The [3, 10, 30, 100] wppm solutions onset at $Re\sqrt{f}^* = [1150, 1050, 950, 650]$, respectively, followed by roughly linear polymeric segments with slope increments $\delta = [5.2, 10.4, 16.4, 27.0]$, respectively.

Polymer-induced drag reduction regimes for N-60K solutions observed in the smooth pipe, S2, are summarized in Table 4.3.5a.

In the riblet pipe the polymer solutions again exhibit laminar, $Re\sqrt{f} < 180$, transitional, $180 < Re\sqrt{f} < 300$, and turbulent flow, $Re\sqrt{f} > 300$. Viewing the turbulent data first relative to solvent (solid circles), to discern the effect of the polymeric additive, we find regimes of polymer solution flow in the riblet pipe similar to those seen in the smooth pipe, namely:

- (i) Newtonian, wherein the polymer solutions follow the solvent. The [3, 10, 30, 100] wppm solutions exhibit Newtonian segments for $Re\sqrt{f} < [1200, 1050, 850, 650]$, respectively.

- (ii) Polymeric, wherein, after onset, the polymer solution exhibit drag reduction. The [3, 10, 30, 100] wppm solutions onset at $Re\sqrt{f}^* = [1200, 1050, 850, 650]$, corresponding to $h^+ = [13, 11, 9, 7]$, respectively. The onset of drag reduction in the riblet pipe occurred at approximately the same $Re\sqrt{f}^*$ as in the smooth pipe for the same concentration. Following onset, the polymer solutions exhibit roughly linear segments, akin to those seen in the smooth pipe, the slopes of which increase with increasing polymer concentration. The switch to a second segment is uncertain for 3 and 10 wppm solutions, but more pronounced for 30 and 100 wppm solutions. For 10, 30, and 100 wppm solutions, the slope of the second segment is ≈ 18 (P-K units) less than that of the initial segment.

Polymer-induced drag reduction regimes for N-60K solutions observed in the riblet pipe, R2B, are summarized in Table 4.3.5b.

Analysis of riblet-induced regimes, and their relation to polymer-induced drag reduction, is attempted in Figure 4.3.15, revealing the riblet regimes:

- (i) Hydraulically smooth, $R_p' \approx 0$. For $3 < h^+ < 5$, riblet-induced drag reduction was negligible in all the polymer solutions, occurring in the Newtonian regime, wherein $S_s' = 0$.
- (ii) Riblet drag reduction, $R_p' > 0$. The riblets induced drag reduction in the 3, 10, 30 and 100 wppm solutions over the ranges $5 < h^+ < 32$, $5 < h^+ < 40$, $5 < h^+ < 42$, and $5 < h^+ < 24$ with respective maxima $(R_p', h^+) = (0.7, 15)$, $(1.5, \approx 20)$, $(2.2, 22)$ and $(0.9, \approx 16)$. The greatest riblet-induced drag reduction in polymer solutions occurred at $2 < S_s' < 10$. It is noteworthy that the ranges of riblet-induced flow enhancement in the polymer solutions increasingly exceeded solvent for 3, 10, and 30 wppm solutions but then decreased to approximately the solvent range for the 100 wppm solution.

- (iii) Riblet drag enhancement, $R_p' < 0$. Riblet-induced drag enhancement occurred in all polymer solutions, those of $c = [3, 10, 30, 100]$ wppm exhibiting $R_p' < 0$ for $h^+ > [32, 40, 42, 24]$, respectively. At the quoted h^+ , the corresponding polymer-induced flow enhancements were $S_s' = [3, 6, 8, 10]$, and it was further found that $R_p' < 0$ for all $S_s' > 10$. At fixed high $h^+ > 60$, the trajectories for the $[3, 10, 30]$ wppm solutions approached the solvent trajectory even at moderate to high slips, $3 < S_s' < 12$, whereas for 100 wppm solution, $R_p' < R_n'$ for $h^+ > 25$.

Riblet-related flow regimes observed in solvent and in N-60K solutions are summarized in Table 4.3.5c.

4.3.4.4 P-309 Solutions

Figure 4.3.16 shows drag reduction by $[50, 100]$ wppm P-309 in S2 and R2B. In the smooth pipe (hollow points) the polymer solutions exhibit laminar, $Re\sqrt{f} < 180$, and turbulent flow, $Re\sqrt{f} > 300$. The transition between laminar and turbulent flow is not well defined: the 50 wppm solution transits into the polymeric regime and the 100 wppm solution into the regime of maximum drag reduction. The Newtonian flow regime is not observed; the other two regimes of turbulent drag reduction by polymers are visible:

- (ii) Polymeric, wherein the polymer solutions exhibit drag reduction. Only the 50 wppm solution exhibits a polymeric segment, for $300 < Re\sqrt{f} < 750$; the segment is too short for the derivation of reliable onset and slope parameters.
- (iii) Maximum Drag Reduction, wherein the polymer solutions follow an asymptote that is independent of polymeric parameters and universal in P-K coordinates. Data from both the 50 and 100 wppm solutions lie close to the MDR asymptote, over the respective ranges $750 < Re\sqrt{f} < 3700$ and $300 < Re\sqrt{f} < 3200$.

Polymer-induced drag reduction regimes for P-309 solutions observed in the smooth pipe, S2, are summarized in Table 4.3.6a.

In the riblet pipe the polymer solutions again exhibit laminar, $Re\sqrt{f} < 180$ and turbulent flow, $Re\sqrt{f} > 300$; the transition between laminar and turbulent flows is not well defined. Viewing the turbulent data first relative to solvent (solid circles), to discern the effect of the polymeric additive, we find regimes of polymer solution flow in the riblet pipe similar to those seen in the smooth pipe, namely:

- (ii) Polymeric, wherein, after onset, the polymer solution data exhibit drag reduction. Only the 50 wppm solution exhibits a polymeric trajectory for $300 < Re\sqrt{f} < 750$, the segment is too short for the derivation of reliable onset and slope parameters.
- (iii) Maximum Drag Reduction, wherein the polymer solutions follow an asymptote that is independent of polymeric parameters and universal in P-K coordinates. The data initially follow the smooth pipe MDR relation, then switch to a second segment for $Re\sqrt{f} > 800$. The maximum drag reduction (highest $1/\sqrt{f}$) in the riblet pipe is approximately given by:

$$1/\sqrt{f} = 11 \log Re\sqrt{f} - 9.5 ; 600 < Re\sqrt{f} < 4000. \quad (4.3-7)$$

These results will be combined with other maximum drag reduction data in the subsequent section 4.4.

Polymer-induced drag reduction regimes for P-309 solutions observed in the riblet pipe, R2B, are summarized in Table 4.3.6b.

Analysis of riblet-induced regimes, and their relation to polymer-induced drag reduction, is attempted in Figure 4.3.17, revealing the riblet regimes:

- (i) Hydraulically smooth, $R_p' \approx 0$. For $3 < h^+ < 9$, at which $5 < S_s' < 10$; the riblet-induced drag reduction was negligible in all the polymer solutions.
- (ii) There is no discernible regime of riblet drag reduction.
- (iii) Riblet drag enhancement, $R_p' < 0$. Riblet-induced drag enhancement occurred in both 50 and 100 wppm which exhibited $R_p' < 0$ for $h^+ > 9$. At $h^+ \approx 9$, the corresponding polymer-induced flow enhancement was $S_s' = 10$, and it was further found that $R_p' < 0$ for all $S_s' > 10$. At fixed h^+ , trajectories for the 50 and 100 wppm solutions were identical, both falling more steeply than solvent flow to reach $R'_{\min} \approx -6$ at $h^+ \approx 45$.

Riblet-related flow regimes observed in solvent and in P-309 solutions are summarized in Table 4.3.6c.

4.3.4.5 PEO Comparisons

Polymer-induced Flow Enhancement in the Smooth Pipe

In the smooth pipe, both concentrations of N-10; all concentrations of each of N-750 and N-60K, as well as 3 and 10 wppm of W-301 exhibited well defined onsets of drag reduction. For a given molecular weight, $Re\sqrt{f}^*$ decreased somewhat as concentration increased; for example, for $c = [100, 250, 900, 2073]$ N-750 solutions, $Re\sqrt{f}^* = [1200, 1100, 950, 650]$, respectively. It is noteworthy, however, that the values of the onset wall shear stress, $\tau_w^* = [5.1, 5.8, 5.4, 5.8]$ N/m², were essentially independent of polymer concentration. For polymer solutions that exhibited the same slope increment, $Re\sqrt{f}^*$ increased as the molecular weight decreased; for example, $Re\sqrt{f}^* = 2000$ for 2435 wppm N-10 $>$ $Re\sqrt{f}^* = 1100$ for 250 wppm N-750 $>$ $Re\sqrt{f}^* = 1050$ for 10 wppm N-60K $>$ $Re\sqrt{f}^* = 550$ for 3 wppm W-301, for all of which $\delta \approx 10$. After onset, the data exhibited a linear P-K segment, with slope increments that increased with increasing molecular weight for a given solution concentration. For example, for 3 wppm solutions, $\delta = 11$ for W-301

$\delta = 5.2$ for N-60K; and for 100 wppm solutions, $\delta = 27.0$ for N-60K $\delta = 7.8$ for N-750. Detailed analyses of onset and slope parameters are presented in section 4.6. For [3, 10, 30] wppm N-60K and [3, 10, 30] wppm W-301 solutions, the data exhibited a downward curvature, caused by polymer degradation. Maximum drag reduction was observed for [30, 100] wppm W-301 for $Re\sqrt{f} > [1500, 500]$ and [50, 100] wppm P-309 for $Re\sqrt{f} > [750, 300]$.

Polymer-induced Flow Enhancement in the Riblet Pipe

All the polymer solutions that exhibited well defined onsets in the smooth pipe, also did so in the riblet pipe, with values of $Re\sqrt{f}^*$ in the riblet pipe essentially the same as in the smooth pipe. Following onset, the polymer solutions initially exhibited linear segments akin to those seen in the smooth pipe, the slopes of which increased with increasing molecular weight for a given solution concentration. For example, for 3 wppm solutions, the slope of the first polymeric segment was 17.1 for W-301 > 9.0 for N-60K; and for 100 wppm solutions the slope was 27.5 for N-60K > 6.1 for N-750. For the higher molecular weight polymers namely, N-60K, W-301 and P-309, the polymer solution trajectory switched, almost discontinuously in W-301 and P-309, to a second roughly linear segment of a lower slope that persisted to the highest $Re\sqrt{f}$. The slope of the second polymeric segment increased with increasing concentration to a maximum value ≈ 10 for the highest concentrations. With the exception of 3 wppm N-60K, the slope of the second polymeric segment was $\approx 18 \pm 4$ (P-K units) less than that of the initial segment. Maximum drag reduction was exhibited by solutions of [30, 100] wppm W-301 for $Re\sqrt{f} > [1400, 700]$ and [50, 100] wppm P-309 for $Re\sqrt{f} > [750, 300]$. The polymer solution data in the riblet pipe followed the smooth pipe MDR asymptote up to $Re\sqrt{f} \approx 1000 \pm 100$, then abruptly diverged downwards to a second, roughly linear segment, correlated by:

$$1/\sqrt{f} = (9.5 \pm 0.5) \log Re\sqrt{f} - (6.0 \pm 1.5); \quad Re\sqrt{f} > 1000. \quad (4.3-8)$$

Riblet-induced Flow Enhancement

In the hydraulically smooth regime, the riblet-induced drag reduction was negligible in all the polymer solutions investigated. For the lower molecular weight polymers, namely N-10, N-750, and N-60K, the hydraulically smooth regime occurred at $3 < h^+ < 5$, within the Newtonian regime ($S' = 0$) of polymer drag reduction. For the two highest molecular weight PEO polymer solutions, W-301 and P-309, the hydraulically smooth regime, which was observed over a considerable range of polymer-induced drag reduction, $0 < S' < 10$, appeared to extend over a range, $3 < h^+ < 10$. The upper boundary of this regime was better defined for P-309 solutions than for W-301 because P-309 solutions did not exhibit a riblet drag reduction regime, the transition from hydraulically smooth to riblet drag enhancement occurring almost discontinuously.

With the exception of [30, 100] wppm W-301 and [50, 100] wppm P-309 solutions, riblet-induced drag reduction was observed in all the solutions investigated. For N-10, this regime coincided with the corresponding solvent regime for $5 < h^+ < 20$, wherein $S' = 0$. For N-750, N-60K and W-301 solutions, amid scatter, the riblet drag reduction regime extended to greater h^+ than that in solvent for $S'_s < 5$. The maximum riblet-induced flow enhancement in polymer solutions exceeded that in solvent for $3 < S'_s < 5$, while the h^+ corresponding to this maximum typically exceeded the solvent $h^+ = 14$. For $5 < S'_s < 10$, the range of h^+ over which the riblets were drag reducing decreased, and eventually vanished for $S'_s > 10$. For [50, 100] wppm P-309 solutions, there was no observed riblet drag reduction regime, the transition from hydraulically smooth to riblet drag enhancement occurring at $h^+ \approx 9$, $S'_s = 10$. There was no instance of $R_p' > 0$ for $S'_s > 10$.

Riblet-induced drag enhancement occurred in all polymer solutions. At low to moderate $S'_s < 10$, $R_p' < 0$ occurred typically for $h^+ > 22$, a value greater than that for

solvent. At high $h^+ > 50$, $R_p' \rightarrow R_n'$ for low $S_s' < 4$, as seen in the data for [2435, 5138] wppm N-10; 100 wppm N-750; 3 wppm N-60K, and 3 wppm W-301. In the polymeric regime, for $S_s' > 4$ and a fixed high $h^+ > 30$, R_p' generally decreased with increasing S_s' . Close to the asymptotic maximum drag reduction, R_p' decreased monotonically with increasing h^+ . The segment is approximately linear with slope, $dR_p'/d\log h^+ = -8 \pm 1$, decreasing to $R_p' = -7 \pm 1$ at $h^+ \approx 50$, where $S_s' = 20$.

4.3.5 Effect of Polymer Skeletal Structure

The effect of polymer skeletal structure was examined by solutions of two PAM polymers, N-300L and N-300, of nominal molecular weight, $M_w \approx 5 \times 10^6$, and 15×10^6 , respectively. It is noteworthy that the ratio of manufacturers' quoted molecular weights between PAM N-300L to PEO N-60K, = 2.5, is similar to the ratio between PAM N-300 to PEO W-301, = 3.0. Both ratios are further approximately equal to the ratio of PAM to PEO repeat unit molecular weights, $m_0(\text{PAM})/m_0(\text{PEO}) = 35/14 = 2.5$, so PAM N-300L possesses roughly the same number of backbone chain links as PEO N-60K, while PAM N-300 has roughly the same number of backbone links as PEO W-301.

4.3.5.1 N-300L Solutions

Figure 4.3.18 depicts drag reduction by solutions of PAM N-300L in pipes S2 and R2B. In the smooth pipe (hollow points) the PAM solutions exhibit laminar, $Re\sqrt{f} < 180$, transitional, $180 < Re\sqrt{f} < 300$, and turbulent flow, $Re\sqrt{f} > 300$. All three known regimes of turbulent drag reduction by polymers are visible, namely:

- (i) Newtonian, wherein the polymer solutions follow the solvent. The [10, 30, 100, 300] wppm solutions exhibit Newtonian segments for $Re\sqrt{f} < [850, 700, 500, 400]$, respectively.

- (ii) Polymeric, wherein, after onset, the polymer solutions exhibit drag reduction. The [10, 30, 100, 300] wppm solutions onset at $Re\sqrt{f}^* = [850, 700, 500, 400]$, respectively, followed by roughly linear polymeric segments with slope increments $\delta = [6.9, 12.3, 18.7, 30.8]$, respectively. At the highest $Re\sqrt{f} > 4200$, the 10 and 30 wppm solution data exhibit some downward curvature, symptomatic of polymer degradation.
- (iii) Maximum drag reduction, wherein the 300 wppm N-300L polymer solution follows the smooth pipe MDR asymptote for $Re\sqrt{f} > 1400$.

Polymer-induced drag reduction regimes seen for N-300L solutions in S2 are summarized in Table 4.3.7a.

In the riblet pipe (solid points) the polymer solutions exhibit laminar, $Re\sqrt{f} < 180$, transitional, $180 < Re\sqrt{f} < 300$, and turbulent flow, $Re\sqrt{f} > 300$. Relative to solvent (solid circles), the turbulent data in the riblet pipe exhibit regimes of polymer solution flow similar to those seen in the smooth pipe, namely:

- (i) Newtonian, wherein the polymer solutions follow the solvent. The [10, 30, 100, 300] wppm solutions exhibit Newtonian segments for $Re\sqrt{f} < [850, 700, 500, 400]$, respectively.
- (ii) Polymeric, wherein, after onset, the polymer solution exhibit drag reduction. The [10, 30, 100, 300] wppm solutions onset at $Re\sqrt{f}^* = [850, 650, 450, 400]$, corresponding to $h^{+*} = [9, 7, 5, 4]$, respectively. The onset of drag reduction in the riblet pipe occurred at approximately the same $Re\sqrt{f}^*$ as in the smooth pipe for the same concentration. Following onset, the polymer solutions exhibit roughly linear segments, the initial slopes of which increase with increasing polymer concentration. At high $Re\sqrt{f}$, the 30 and 100 wppm solutions switch to second, roughly linear

segments, the slopes of which are ≈ 18 (P-K units) less than those of the initial segments.

- (iii) Maximum drag reduction: For $Re\sqrt{f} > 1440$, the 300 wppm N-300L solution follows a trajectory close to Eq. 4.3-8, the maximum drag reduction asymptote earlier observed for PEO solutions in this riblet pipe.

Polymer-induced drag reduction regimes seen for N-300L solutions in R2B are summarized in Table 4.3.7b.

Figure 4.3.19 is an analysis of the riblet-induced regimes and their relation to polymer-induced drag reduction for solutions of N-300L. Three riblet-induced regimes drag are observed, namely:

- (i) Hydraulically smooth, $R_p' \approx 0$. For $3 < h^+ < 5$, riblet-induced drag reduction was negligible in all the polymer solutions.
- (ii) Riblet drag reduction. $R_p' > 0$. The riblets induced drag reduction in the [10, 30, 100, 300] wppm solutions over the ranges $5 < h^+ < 30$, $5 < h^+ < 38$, $5 < h^+ < 30$, and $5 < h^+ < 12$ with respective maxima $(R_p', h^+) = (1.0, 23)$, $(1.2, 16)$, $(2.6, 15)$ and $(0.8, 8)$. Riblet-induced drag reduction in polymer solutions occurred at $2 < S_s' < 12$. It is noteworthy that the h^+ ranges of riblet-induced flow enhancement in the 10, 30, and 100 wppm solutions were wider than the range of riblet drag reduction in solvent, but the range of riblet drag reduction for the 300 wppm solution was narrower than that in solvent.
- (iii) Riblet drag enhancement, $R_p' < 0$. Riblet-induced drag enhancement occurred in all polymer solutions, those of $c = [10, 30, 100, 300]$ wppm exhibiting $R_p' < 0$ for $h^+ > [30, 38, 30, 12]$, respectively. At the quoted h^+ , the corresponding polymer-induced flow enhancements were $S_s' = [4, 7, 12, 10]$, and it was further found that $R_p' < 0$

for all $S_s' > 12$. At fixed high $h^+ > 60$, the trajectories for the [10, 30, 100] wppm solutions approached the solvent trajectory even at moderate to high slips, $3 < S_s' < 12$, whereas for 300 wppm solution, $R_p' < R_n'$ for $h^+ > 12$. It should be noted that for $Re\sqrt{f} > 2500$, $h^+ > 27$, R_p' data for the 10 and 30 wppm solutions require (small) corrections for polymer degradation.

Riblet-related flow regimes observed in solvent and in PAM N-300L solutions in R2B are summarized in Table 4.3.7c.

It is noteworthy that solutions of N-300L behave much like those of PEO N-60K. The onset of polymer induced drag reduction occurs at slightly higher $Re\sqrt{f}^*$ with N-300L than with N-60K solutions of the same concentration; and the slope increments in the smooth pipe as well as the slopes of the first and second polymeric segments in the riblet pipe, and the ranges and magnitude of the riblet-induced flow enhancement regimes in N-300L are all similar to those in N-60K.

4.3.5.1 N-300 Solutions

Figure 4.3.20 depicts drag reduction by solutions of PAM N-300 in S2 and R2B. In the smooth pipe (hollow points) the PAM solutions exhibit laminar, $Re\sqrt{f} < 180$, transitional, $180 < Re\sqrt{f} < 300$, and turbulent flow, $Re\sqrt{f} > 300$. All three known regimes of turbulent drag reduction by polymers are visible, namely:

- (i) Newtonian, wherein the polymer solutions follow the solvent. Only the 3 wppm solution exhibits a Newtonian segment from $300 < Re\sqrt{f} < 550$.
- (ii) Polymeric. All four polymer solutions exhibit polymeric segments. The 3 wppm solution shows a well-defined onset, at $Re\sqrt{f}^* = 550$; the [10, 30, 100] wppm solutions transit from laminar flow directly into the polymeric regime, with onsets at

$Re\sqrt{f}^* = [350, 320]$ for [10, 30] wppm solutions, respectively, estimated by extrapolation back to the solvent line. The slope increment increases with increasing concentration with $\delta = [9.1, 17.7, 22.7]$ for $c = [3, 10, 30]$ wppm solutions, respectively; the 100 wppm polymeric segment is too short for the derivation of reliable onset and slope parameters. For $Re\sqrt{f} > 2500$ in the 3 and 10 wppm solutions and for $Re\sqrt{f} > 3500$ in the 30 wppm solution, the data exhibit some downward curvature, associated with polymer degradation.

- (iii) Maximum Drag Reduction, wherein the polymer solutions follow an asymptote that is independent of polymeric parameters and universal in P-K coordinates. Data from both the 30 and 100 wppm solutions lie close to the MDR asymptote, over the respective ranges $2000 < Re\sqrt{f} < 4000$ and $600 < Re\sqrt{f} < 3800$.

Polymer-induced drag reduction regimes seen in S2 are summarized in Table 4.3.8a.

In the riblet pipe (solid points) N-300 solutions exhibit laminar, $Re\sqrt{f} < 180$, transitional, $180 < Re\sqrt{f} < 300$, and turbulent flow, $Re\sqrt{f} > 300$. Relative to solvent (solid circles), the turbulent data in riblet pipes exhibit regimes of polymer solution flow similar to those seen in smooth pipes, namely:

- (i) Newtonian, wherein the polymer solutions follow the solvent. Only the 3 wppm solution exhibits a Newtonian segment from $300 < Re\sqrt{f} < 550$.
- (ii) Polymeric, wherein, after onset, the polymer solutions exhibit drag reduction that is dependent on polymer concentration. The 3 wppm solution shows a well-defined onset, at $Re\sqrt{f}^* = 550$, the same value as in the smooth pipe. The 10 and 30 wppm solutions transit into the polymeric regime directly; however, short extrapolation back to the solvent suggests onsets at $Re\sqrt{f}^* \approx 300-350$, similar to those estimated in the smooth pipe. Following onset, the polymer solutions exhibit linear segments, the slopes of which increase with increasing concentration. Beyond a certain

characteristic $Re\sqrt{f}$, each polymer solution trajectory switches to a second roughly linear segment of lower slope, that persists to the highest $Re\sqrt{f}$.

- (iii) Maximum Drag Reduction is observed for [30, 100] wppm solutions for $Re\sqrt{f} > [2000, 500]$. It can be verified on Figure 4.3.20 that the maximum drag reduction (highest $1/\sqrt{f}$) in the riblet pipe is limited by an asymptote:

$$1/\sqrt{f} = 9.5 \log Re\sqrt{f} - 6.1 ; 800 < Re\sqrt{f} < 5500; \quad (4.3-9)$$

which is followed by the 30 wppm solution for $2000 < Re\sqrt{f} < 4200$ and by the 100 wppm solution for $500 < Re\sqrt{f} < 4500$. Eq. (4.3-9) for PAM N-300 solutions agrees with Eq. (4.3-6), the asymptote for PEO solutions.

Polymer-induced drag reduction regimes seen for N-300 solutions in R2B are summarized in Table 4.3.8b.

Figure 4.3.21 is an analysis of riblet-induced regimes and their relation to polymer-induced drag reduction for solutions of N-300. Three riblet-induced regimes are observed, namely:

- (i) Hydraulically smooth. This regime is observed over the range $h^+ < 5$ for [3, 10] wppm N-300, within which the polymeric drag reduction was small, $S_g' < 2$. For [30, 100] wppm N-300 solutions, the hydraulically smooth regime extended over the range $3 < h^+ < 10$, amid considerable polymer induced drag reduction, $S_g' < 10$.
- (ii) Riblet drag reduction. The riblets induced drag reduction in the 3 and 10 wppm solutions, over the ranges $6 < h^+ < 34$ and $6 < h^+ < 21$, with respective maxima $(R_p', h^+) = (1.5, 20)$ and $(0.8, \approx 10)$ both occurring at moderate $S_g' \approx 5$; further, there was no instance of $R_p' > 0$ for $S_g' > 8$.

- (iii) Riblet drag enhancement. This regime is observed in all the N-300 solutions, with $R_p' \rightarrow R_n'$ for $h^+ > 50$ and $S' < 10$, as seen in the data for [3, 10] wppm solutions. However, these solutions are most affected by degradation. For [30, 100] wppm solutions, close to the asymptotic maximum drag reduction, R_p' decreases monotonically with increasing h^+ . The segment is approximately linear with slope, $dR_p'/d\log h^+ = -8$, decreasing to $R_p' = -6$ at $h^+ \approx 50$, where $S_s' \approx 18$.

Riblet-related flow regimes observed in solvent and in N-300 solutions in R2B are summarized in Table 4.3.8c.

Solutions of PAM N-300 behave quantitatively as those of PEO W-301 in pipes S2 and R2B. The onset of polymer induced-drag reduction; the slope increments in the smooth pipe; the slopes of the first and second polymeric segments in the riblet pipe, and the ranges and magnitude of the riblet-induced flow enhancement regimes are all almost identical for the two polymers.

4.3.6 Riblet Pipe Reproductions

A second riblet test section, designated R2BR, was fabricated from the 10.21 mm pipe and 0.15 mm riblets. The fabrication method was identical to that used for the original pipe. Flows of solvent, [3, 10] wppm W-301 and [50, 100] wppm P-309 in R2BR were investigated, the results of which are summarized in Table 4.3.9 and Figures 4.3.22 and 4.3.23 using the flow enhancement parameters. The table and plots convey all the information about polymer-induced flow enhancement in the smooth and replicated riblet pipes (table sections a, b and plot b), and riblet-induced flow enhancement for solvent and polymer solution flows (table section c and plot a).

4.3.6.1 Solvent Flow in the Riblet Pipe

For solvent flow, depicted by the solid circles in Figures 4.3.21 and 4.3.22, the three riblet-induced regimes are observed, namely:

- (i) Hydraulically smooth, $R_n' = 0$, for $h^+ < 5$.
- (ii) Riblet drag reduction, $R_n' > 0$, for $5 < h^+ < 22$, with a maximum $R_n' = 0.45$ at $h^+ = 15$.
- (iii) Riblet drag enhancement, $R_n' < 0$, for $22 < h^+ < 110$, wherein R_n' decreases with increasing h^+ , reaching an asymptotic value $R_{n\infty}' = -2.33$ for $h^+ > 80$.

The extent of the riblet drag reduction regime observed in pipe R2BR was the same as that in the original pipe R2B; the maximum $R_n' = 0.45$ in R2BR was slightly lower than $R_n' = 0.60$ observed in R2B and occurred in both pipes at $h^+ = 15$. In the riblet drag enhancement regime, the asymptotic minimum value of $R_{n\infty}' \rightarrow -2.3$ reached for $h^+ > 80$ in R2BR is to be compared with $R_{n\infty}' \rightarrow -1.9$ for $h^+ > 67$ in R2B. These solvent results provide an estimate of the differences that can be expected between observations in two riblet pipes fabricated by the present techniques. Specifically, the maximum riblet-induced flow enhancement varied by ± 0.1 unit of $1/\sqrt{f}$; h^+ at the maximum by ± 0 units, the upper limit of the riblet drag reduction regime by ± 0 units of h^+ , and the asymptotic riblet drag enhancement by ± 0.2 units of $1/\sqrt{f}$.

4.3.6.2 Polymer-induced Flow Enhancement in the Smooth Pipe

A comparison between parts (a) of Table 4.3.9, columns 2 and 3, and those in Table 4.3.1, as well as between Figures 4.3.21b and 4.3.4b reveals qualitatively similar trends in the trajectories of [3, 10] wppm W-301 solutions in the smooth pipe, namely an onset of drag reduction followed by an initially linear polymeric segment whose slope

increases with increasing concentration, followed by a downward curvature, associated with degradation. There are however quantitative differences between the two results. In the repeated run, $Re\sqrt{f}^* = [800, 600]$, and $\delta = [12, 19]$ for $c = [3, 10]$ wppm, respectively, differs from $Re\sqrt{f}^* = [550, 450]$, and $\delta = [11, 19]$ in the original pipe. The $[3, 10]$ wppm solution trajectories in the repeated runs in the smooth pipe are approximately parallel to, but downwardly displaced by about 2 units of $1/\sqrt{f}$ from, the earlier runs. These differences most probably reflect variations between the polymer batches used in the two series of runs.

Trajectories observed for $[50, 100]$ P-309 solutions in the original and reproduced experiments were almost identical, as seen by comparing Table 4.3.9 columns 4 and 5 with Table 4.3.6 columns 2 and 3, and also by comparing Figure 4.3.23b with 4.3.17b. Both solutions exhibit maximum drag reduction for $Re\sqrt{f} > 500$ in both the present and original experiments.

4.3.6.3 Riblet-induced Flow Enhancement

Results for W-301 solutions in the replicated pipe R2BR can be compared with those in the original riblet pipe R2B by perusal of the corresponding columns in parts (b) and (c) of Tables 4.3.9 and 4.3.1 and the three respective panels in each of Figures 4.3.21 and 4.3.4. Essentially, the 3 wppm W-301 solution in R2BR exhibited all three riblet regimes, namely: (i) hydraulically smooth, (ii) riblet drag reduction, and (iii) riblet drag enhancement, as in the original pipe R2B, with qualitative similarities and quantitative differences. For example, the respective $R'_{p,max}$ were 0.9 versus 1.6, occurring at $h^+ = 21$ versus 20, with the riblet drag reduction regime visible for $6 < h^+ < 28$ versus $10 < h^+ < 33$; also in the riblet drag enhancement regime, $R'_p \rightarrow R'_n$ for $h^+ > 40$ versus $h^+ > 45$. The 10 wppm W-301 solution in R2BR exhibited all three riblet regimes, with qualitative similarities and quantitative differences relative to R2B. For example, the respective

$R'_{p,max}$ were 1.6 versus 0.8, occurring at $h^+ = 18$ versus 11, with the riblet drag reduction regime visible for $5 < h^+ < 25$ versus $9 < h^+ < 15$; also in the riblet drag enhancement regime, $R'_p \approx R'_n$ for $h^+ > 30$ versus $h^+ \approx 50$.

Though the W-301 polymer solution results in the two riblet pipes R2BR and R2B differ somewhat, it is interesting to note that the results for the 3 wppm solution in R2BR are intermediate between solvent and 3 wppm results in R2B; while the results for the 10 wppm solution in R2BR are intermediate between 3 and 10 wppm results in R2B. These observations accord with the differences observed between gross flow trajectories of the solutions in the smooth pipe during the repeated runs when compared to the original, and therefore mostly reflect small differences between the polymer batches used rather than differences between the riblet pipes.

Results for P-309 solutions in R2BR can be compared with those in R2B by perusal of the corresponding columns in parts (b) and (c) of Tables 4.3.10 and 4.3.6 as well as the three respective panels of Figures 4.3.22 and 4.3.16. Both 50 and 100 wppm solutions followed almost identical trajectories in R2BR, as they had in R2B, indicative of their attaining the asymptotic maximum drag reduction. The (i) hydraulically smooth and (iii) riblet drag enhancement flow regimes exhibited in R2BR are similar to those seen in R2B, with some differences. The extents of the hydraulically smooth regions, $3 < h^+ < 11$ versus $3 < h^+ < 9$, and the riblet drag enhancement regions, $11 < h^+ < 50$ versus $9 < h^+ < 45$, differ slightly between R2BR and R2B, the riblet drag enhancement region commences at somewhat higher h^+ (9 versus 11) and polymer-induced flow enhancements S' (12 versus 10), and showing about 1.5 units of $1/\sqrt{f}$ less drag enhancement. There is a possibility that regime (ii), riblet drag reduction, occurred in pipe R2BR in the region $7 < h^+ < 11$ with both 50 and 100 wppm P-309, though these data are within the experimental scatter, typically 0.5 $1/\sqrt{f}$ units, at high polymer drag reductions. It will be recalled that data for P-309 solutions in the original pipe R2B did not exhibit riblet drag reduction.

The foregoing show that the replicated riblet pipe R2BR exhibited all of the flow regimes and physics seen in the original pipe R2B with solvent, polymer solutions in the polymeric regime of drag reduction, and at maximum drag reduction. It also provides quantitative measures of the (small) variations in performance that might be expected between identical riblet pipes fabricated by the present procedures.

4.3.7 Effect of Riblet Pipe Geometry

4.3.7.1 7.82 mm pipe/0.11 mm riblets (S1 and R1A)

Flows of dilute polymer solutions were investigated in one 7.82 mm smooth pipe, designated S1, and two 7.82 mm pipes lined with 0.11 mm riblets. In the first riblet pipe, designated R1A, the following solutions were investigated: [100, 300, 1000] wppm N-750; [3, 10, 30, 100] wppm N-60K; 100 wppm W-301; [50, 100] wppm P-309; and 100 wppm N-300. In the second, repeated pipe, R1AR, flows of [3, 10, 30, 100] N-60K and [1, 3, 10, 30, 100] wppm W-301 were investigated.

N-750 Solutions

Figure 4.3.24 shows drag reduction by [100, 300, 1000] wppm N-750 in S1 and R1A, on P-K coordinates. In the smooth pipe, two of the three known regimes of turbulent drag reduction by polymers are visible, namely:

- (i) Newtonian, wherein the polymer solutions follow the solvent. The [100, 300, 1000] wppm solutions exhibit Newtonian segments for $300 < Re\sqrt{f} < [1250, 950, 700]$, respectively.
- (ii) Polymeric, wherein the polymer solutions exhibit drag reduction. The [100, 300, 1000] wppm solutions onset at $Re\sqrt{f}^* = [1250, 950, 700]$, respectively, followed by

roughly linear polymeric segments with slope increments $\delta = [7.6, 11.7, 19.8]$, respectively.

Polymer-induced drag reduction regimes for N-750 solutions observed in the smooth pipe, S1, are summarized in Table 4.3.10a.

In the riblet pipe, we find regimes of polymer solution flow similar to those seen in the smooth pipe, namely:

- (i) Newtonian, wherein the polymer solutions follow the solvent. The [100, 300, 1000] wppm solutions exhibit Newtonian segments for $300 < Re\sqrt{f} < [1250, 950, 700]$, respectively.
- (ii) Polymeric, wherein, after onset, the polymer solution data diverge upwards from solvent, exhibiting drag reduction that is dependent upon both flow and polymeric parameters. The [100, 300, 100] wppm solutions onset at $Re\sqrt{f}^* = [1250, 950, 700]$, corresponding to $h^{+*} = [14, 10, 8]$, respectively. For a given concentration, the onset of drag reduction in the riblet pipe occurred at approximately the same $Re\sqrt{f}^*$ as in the smooth pipe. Following onset, the polymer solutions exhibit roughly linear segments, akin to those seen in the smooth pipe, the slopes of which increase with increasing polymer concentration.

Polymer-induced drag reduction regimes for N-750 solutions observed in the riblet pipe, R1A, are summarized in Table 4.3.10b.

Analysis of riblet-induced regimes, and their relation to polymer-induced drag reduction, is attempted in Figure 4.3.25, revealing the riblet regimes:

- (i) Hydraulically smooth, $R_p' \approx 0$. For $3 < h^+ < 5$, riblet-induced drag reduction was negligible in all the polymer solutions. Further, the polymer solutions were all in their Newtonian regime prior to onset, wherein $S_s' = 0$.
- (ii) Riblet drag reduction, $R_p' > 0$. The riblets induced drag reduction in the 100, 300 and 1000 wppm solutions over the ranges $5 < h^+ < 23$, $5 < h^+ < 23$, and $5 < h^+ < 20$ with respective maxima $(R_p', h^+) = (0.5, 14)$, $(0.5, 14)$, and $(0.5, 14)$. The greatest riblet-induced drag reduction in polymer solutions occurred at only low polymer-induced drag reductions, $0 < S_s' < 4$. Both the range and magnitude of riblet-induced flow enhancement in the polymer solutions closely followed the solvent.
- (iii) Riblet drag enhancement, $R_p' < 0$. Riblet-induced drag enhancement occurred in all polymer solutions, those of $c = [100, 300, 1000]$ wppm exhibiting $R_p' < 0$ for $h^+ > [23, 23, 20]$, respectively, at which the corresponding polymer-induced flow enhancements were $S_s' = [2, 3, 6]$. For $h^+ > 30$, the trajectories for the 100 and 300 wppm solutions approached that of the solvent, whereas the 1000 wppm solution data lay considerably below the solvent, with $R_p' = -6$ at $h^+ = 60$ and $S_s' = 14$.

Riblet-related flow regimes observed in solvent and in N-750 solutions are summarized in Table 4.3.10c.

N-60K Solutions

Figure 4.3.26 shows drag reduction by [3, 10, 30, 100] wppm N-60K in S1 and R1A. All three regimes of turbulent drag reduction by polymers are visible in the smooth pipe, namely:

- (i) Newtonian, wherein the polymer solutions follow the solvent. The [3, 10, 30, 100] wppm solutions exhibit Newtonian segments for $300 < Re\sqrt{f} < [750, 650, 600, 500]$, respectively.

- (ii) Polymeric, wherein the polymer solutions exhibit drag reduction. The [3, 10, 30, 100] wppm solutions onset at $Re\sqrt{f}^* = [750, 650, 600, 500]$, respectively, followed by roughly linear polymeric segments with slope increments $\delta = [7.8, 13.7, 20.7, 32]$, respectively. At the highest $Re\sqrt{f} > 4000$, the 3, 10 and 30 wppm data exhibit downward curvatures, indicative of polymer degradation.
- (iii) Maximum Drag Reduction. The 100 wppm solution data, of initial slope 32 in the polymeric regime, abruptly decrease slope at $Re\sqrt{f} \approx 1700$, becoming essentially parallel to the MDR asymptote, but lying below it by about 2 units of $1/\sqrt{f}$.

Polymer-induced drag reduction regimes for N-60K solutions in the smooth pipe, S1, are summarized in Table 4.3.11a.

In the riblet pipe, all three regimes of turbulent drag reduction by polymers are visible, namely:

- (i) Newtonian, wherein the polymer solutions follow the solvent. The [3, 10, 30, 100] wppm solutions exhibit Newtonian segments for $Re\sqrt{f} < [750, 650, 550, 450]$, respectively.
- (ii) Polymeric, wherein the polymer solutions exhibit drag reduction. The [3, 10, 30, 100] wppm solutions onset at $Re\sqrt{f}^* = [750, 650, 550, 450]$, respectively, which are essentially the same as the onsets observed in the smooth pipe, and correspond to $h^{+*} = [8, 7, 6, 5]$. After onset, the polymer solution data describe roughly linear initial segments, the slopes of which increase with increasing polymer concentration. With increasing $Re\sqrt{f}$, the initial linear segment is commonly followed by a second segment, of lower slope. For 10, 30, and 100 wppm solutions, the slope of the second segment is $\approx 18 \pm 3$ (P-K units) less than that of the initial segment, in agreement with earlier observations for N-60K solutions in riblet pipe R2B.

- (iii) Maximum Drag Reduction. The 100 wppm solution data, of initial segment slope 27 in the polymeric regime, changes to a second segment given by $1/\sqrt{f} = 5.3 \log(\text{Re}\sqrt{f}) - 7.5$ for $1700 < \text{Re}\sqrt{f} < 5100$, that appears to represent the asymptotic maximum drag reduction in this riblet pipe (see following sections).

Polymer-induced drag reduction regimes for N-60K solutions observed in the riblet pipe, R1A, are summarized in Table 4.3.11b.

Analysis of riblet-induced regimes, and their relation to polymer-induced drag reduction, is attempted in Figure 4.3.27, revealing the riblet regimes:

- (i) Hydraulically smooth, $R_p' \approx 0$. For $3 < h^+ < 5$, riblet-induced drag reduction was negligible in all the polymer solutions, which exhibited little or no polymer-induced drag reduction, $S_s' < 1$.
- (ii) Riblet drag reduction, $R_p' > 0$. The riblets induced drag reduction in the 3, 10, 30 and 100 wppm solutions over the ranges $5 < h^+ < 22$, $5 < h^+ < 20$, $5 < h^+ < 16$, and $5 < h^+ < 11$ with respective maxima $(R_p', h^+) = (0.5, 12)$, $(0.6, 10)$, $(1.0, 10)$ and $(1.2, 8)$. Riblet-induced drag reduction in these polymer solutions was observed at $0 < S_s' < 8$. With increasing polymer-induced drag reduction, the data for 3 and 10 wppm solutions tended to follow the solvent whereas in the 30 and 100 wppm solutions, the magnitude of riblet-induced drag reduction exceeded that observed in solvent, but the range of h^+ over which riblet drag reduction was observed was narrower than that in solvent.
- (iii) Riblet drag enhancement, $R_p' < 0$. Riblet-induced drag enhancement occurred in all polymer solutions, those of $c = [3, 10, 30, 100]$ wppm exhibiting $R_p' < 0$ for $h^+ > [22, 20, 16, 11]$, respectively, at which $S_s' = [3, 5, 7, 10]$. With increasing h^+ , the 3 and 10 wppm solutions approached the solvent riblet drag enhancement relationship, while the 30 and 100 wppm solutions exhibited R' decreasing well below solvent. It

should be kept in mind that observation at the highest $h^+ > 30$ suffer from polymer degradation and will require (small) corrections to account for it.

Riblet-induced flow regimes observed in N-60K solutions are summarized in Table 4.3.11c.

W-301, P-309, and N-300 Solutions

Results for 100 wppm W-301, [50, 100] wppm P-309 and 100 wppm N-300 are presented collectively since all these polymer solutions essentially exhibited maximum drag reduction.

Figures 4.3.28-4.3.30 show drag reduction by 100 wppm W-301, [50, 100] wppm P-309 and 100 wppm N-300, respectively, in S2 and R2B. In the smooth pipe, the Newtonian regime was absent, with only the regimes of turbulent drag reduction by polymers visible, namely:

- (ii) Polymeric. The data for 50 wppm P-309 and 100 wppm N-300 solutions exhibit L→P type transitions, directly from laminar to the polymeric regime of drag reduction. These solutions then exhibit short polymeric segments for $300 < Re\sqrt{f} < 600$ and $300 < Re\sqrt{f} < 400$, respectively; the segments are too short for the derivation of reliable onset and slope parameters.
- (iii) Maximum Drag Reduction, wherein the polymer solutions follow an asymptote that is independent of polymeric parameters and universal in P-K coordinates. The 100 wppm W-301 and 100 wppm P-309 solutions both exhibit L→M type transitions, directly from laminar to turbulent flow at maximum drag reduction. The 50 wppm P-309 and 100 wppm N-300 solutions attain MDR for $Re\sqrt{f} > 600$ and 400, respectively, and remain close to it up to their highest $Re\sqrt{f} \approx 4000$.

Polymer-induced drag reduction regimes for W-301, P-309, and N-300 solutions observed in the smooth pipe, S1, are summarized in Table 4.3.12a.

In the riblet pipe, we find polymer solution flow regimes similar to those seen in smooth pipes, namely:

- (ii) Polymeric. The 50 wppm P-309 and 100 wppm N-300 solutions both exhibit L→P transitions, and form short polymeric segments for $300 < Re\sqrt{f} < 600$ and $300 < Re\sqrt{f} < 400$, respectively, which are essentially identical to those seen in the smooth pipe; these segments are too short for the derivation of reliable onset and slope parameters.
- (iii) Maximum Drag Reduction, wherein the polymer solutions follow an asymptote that is independent of polymeric parameters and universal in P-K coordinates. The data for 100 wppm W-301 and 100 wppm P-309 exhibit L→M transitions and then can be seen to follow the corresponding smooth pipe MDR data for $250 < Re\sqrt{f} < 1100$. The 50 wppm P-309 and 100 wppm N-300 solutions, also following their corresponding smooth pipe data, attain and then follow the smooth MDR for $600 < Re\sqrt{f} < 1200$ and $400 < Re\sqrt{f} < 1200$, respectively. At $Re\sqrt{f} = 1100 \pm 100$, the riblet pipe data for all four solutions abruptly switch to a second segment, of lower slope and still independent of polymeric parameters, that persists to the highest $Re\sqrt{f} \approx 4000$. The maximum drag reduction (highest $1/\sqrt{f}$) in the riblet pipe is thus limited by an asymptote:

$$1/\sqrt{f} = 4.3 \log Re\sqrt{f} - 11.6 ; 1100 < Re\sqrt{f} < 4000 \quad (4.3-10)$$

At the very highest $Re\sqrt{f} \approx 5000$, a data point or two from each of 100 wppm W-301, 50 wppm P-309 and 100 wppm N-300 fall below Eq. (4.3-10), likely due to polymer degradation.

Polymer-induced drag reduction regimes for W-301, P-309, and N-300 solutions observed in the riblet pipe, R1A, are summarized in Table 4.3.12b.

Analysis of riblet-induced regimes, and their relation to polymer-induced drag reduction, is attempted in Figures 4.3.31-4.3.33, revealing the riblet regimes:

- (i) Hydraulically smooth, $R_p' \approx 0$. For $3 < h^+ < 10$, riblet-induced drag reduction was negligible in all the polymer solutions, all of which exhibited maximum possible polymer-induced drag reduction, $5 < S_s' < 12$.
- (ii) Riblet Drag Reduction. There appears to be a narrow range, $10 < h^+ < 14$, wherein the riblets reduce drag with a maximum $R_p' = 0.8$ at $h^+ = 11$. Unfortunately, the magnitude of R_p' is of the same order as the uncertainty in $1/\sqrt{f}$, typically 0.5 units, at the present high polymeric drag reductions.
- (iii) Riblet drag enhancement, $R_p' < 0$. Riblet-induced drag enhancement occurred in all polymer solutions, for $h^+ > 14$, at which the corresponding polymer-induced flow enhancement was $S_s' = 13$. With increasing h^+ (and S_s'), riblet-induced drag enhancement increased greatly, and more steeply than for solvent flow, reaching $R'_{\min} \approx -9$ at $h^+ \approx 50$.

Riblet-related flow regimes observed in solvent and in W-301, P-309, and N-300 solutions are summarized in Table 4.3.12c.

Replicated Pipe, R1AR

A second riblet test section, designated R1AR, was fabricated from the 7.82 mm pipe and 0.11 mm riblets. The fabrication method was identical to that used for the original pipe. For comparison with the original riblet pipe, R1A, flows of solvent, [3, 10, 30, 100] wppm N-60K and 100 wppm W-301 were investigated, the results of which are summarized in Table 4.3.13 and Figures 4.3.34 and 4.3.35 using the flow enhancement

parameters. In addition, flows of [1, 3, 10, 30] wppm were also investigated in R1AR and will be subsequently described under a separate W-301 heading.

Solvent Flow in the Riblet Pipe. For solvent flow, depicted by the solid circles in Figures 4.3.34 and 4.3.35, the three riblet-induced regimes are observed, namely:

- (i) Hydraulically smooth, $R_n' = 0$, for $h^+ < 5$.
- (ii) Riblet drag reduction, $R_n' > 0$, for $5 < h^+ < 21$, with a maximum $R_n' = 0.48$ at $h^+ = 14$.
- (iii) Riblet drag enhancement, $R_n' < 0$, for $h^+ > 21$, wherein R_n' decreases with increasing h^+ , reaching an asymptotic value $R_{n\infty}' = -2.19$ for $80 < h^+ < 110$.

The extent of the riblet drag reduction regime observed in pipe R1AR was the same as that in the original pipe R1A; the maximum $R_n' = 0.48$ in R1AR was slightly lower than $R_n' = 0.55$ observed in R1A and occurred in both pipes at $h^+ = 14$. In the riblet drag enhancement regime, the asymptotic minimum value of $R_{n\infty}' \rightarrow -2.2$ reached for $h^+ > 80$ in R2BR is similar to $R_{n\infty}' \rightarrow -2.2$ for $h^+ > 79$ in R1A. These solvent results provide an estimate of the differences that can be expected between observations in two riblet pipes fabricated by the present techniques. Specifically, the maximum drag reduction varied by ± 0.05 units of $1/\sqrt{f}$; h^+ at the maximum by ± 0 units, the upper limit of the riblet drag reduction regime by ± 1 units of h^+ , and the asymptotic riblet drag enhancement by ± 0 units of $1/\sqrt{f}$.

Polymer-induced Flow Enhancement in the Smooth Pipe. A comparison between parts (a) of Table 4.3.13, columns 2-5, and those in Table 4.3.11, as well as between Figures 4.3.34b with 4.3.27b reveals qualitatively similar trends in the trajectories of [3, 10, 30, 100] wppm N-60K solutions in the smooth pipe, namely an onset of drag reduction followed by an initially linear polymeric segment whose slope increases with

increasing concentration, followed by a downward curvature, associated with degradation. There are small quantitative differences between the two results. In the repeated pipe, $Re\sqrt{f}^* = [900, 700, 550, 500]$ and $\delta = [8.8, 15.5, 21.1, 30.3]$ for $c = [3, 10, 30, 100]$ wppm, respectively, differs from $Re\sqrt{f}^* = [750, 650, 600, 500]$ and $\delta = [7.8, 13.7, 20.7, 32.0]$ in the original pipe. These variations are probably due to differences in polymer batches between the two series of runs.

The trajectory observed for the 100 wppm W-301 solution in the replicated pipe was almost identical to that in the original pipe, as seen by comparing Table 4.3.13 column 6 with Table 4.3.12 column 2, and also by comparing Figure 4.3.35b with 4.3.31b. Both solutions exhibit maximum drag reduction for $Re\sqrt{f} > 300$ in both the present and original experiments.

Riblet-induced Flow Enhancement. Results for N-60K solutions in the replicated pipe R1AR can be compared with those in the original riblet pipe R1A by perusal of the corresponding columns in parts (b) and (c) of Tables 4.3.13 and 4.3.11 and the three respective panels in each of Figures 4.3.34 and 4.3.27. Essentially, the [3, 10, 30, 100] wppm N-60K solutions in R1AR exhibited all three riblet regimes, namely: (i) hydraulically smooth, (ii) riblet drag reduction, and (iii) riblet drag enhancement, as in the original pipe R1A, with qualitative similarities and quantitative differences. For example, the respective $R'_{p,max}$ were [0.8, 0.9, 0.8, 1.5] versus [0.5, 0.6, 1.0, 1.2], occurring at $h^+ = [11, 11, 10, 7]$ versus [12, 10, 10, 8], with the riblet drag reduction regime visible for $[5 < h^+ < 21, 5 < h^+ < 17, 5 < h^+ < 14, 5 < h^+ < 11]$, versus $[5 < h^+ < 22, 5 < h^+ < 20, 5 < h^+ < 16, 5 < h^+ < 11]$. In the riblet drag enhancement regime, at a fixed h^+ , R'_p decreased with increasing S_s' ; for example, at $h^+ = 30$, $R'_p = [-0.6, -2, -5, -5]$ in R1AR versus $[-0.6, -1.6, -3.8, -4.5]$ in R1A for [3, 10, 30, 100] wppm N-60K solutions, respectively.

Results for the 100 wppm W-301 solution in R1AR can be compared with that in R1A by perusal of the corresponding columns in parts (b) and (c) of Tables 4.3.13 and 4.3.12 as well as the three respective panels of Figures 4.3.35 and 4.3.31. The data for the 100 wppm solution in R1AR, which exhibited maximum polymer-induced drag reduction, was similar to those in R1A up to $Re\sqrt{f} \approx 1500$, then diverged to lower slips, with a maximum difference of ≈ 2 $1/\sqrt{f}$ units at $Re\sqrt{f} \approx 3200$. The flow regimes exhibited in R1AR, namely: (i) hydraulically smooth, (ii) riblet drag reduction, and (iii) riblet drag enhancement were similar to those seen in R1A, with some differences. The extents of the hydraulically smooth regions, $4 < h^+ < 8$ versus $3 < h^+ < 8$, the riblet drag reduction regions $8 < h^+ < 10$ versus $8 < h^+ < 12$, and the riblet drag enhancement regions, $10 < h^+ < 49$ versus $12 < h^+ < 45$, all differed slightly between R1AR and R1A. Within the narrow riblet drag reduction regime, the maximum $R_p' = 0.45$ occurred at $h^+ = 9$ in R1AR, differing slightly, but within the experimental uncertainty, from $R_p' = 0.75$ at $h^+ = 11$ in R1A.

The foregoing show that the replicated riblet pipe R1AR exhibited all of the flow regimes and physics seen in the original pipe R1A with solvent, polymer solutions in the polymeric regime of drag reduction, and at maximum drag reduction.

W-301 Solutions. Figure 4.3.36 shows drag reduction by [1, 3, 10, 30, 100] wppm W-301 solutions in S1 and R1AR. In the smooth pipe S1, all three known regimes of turbulent drag reduction by polymers are visible, namely:

- (i) Newtonian, wherein the polymer solutions follow the solvent. The [1, 3, 10] wppm solutions exhibit Newtonian segments for $300 < Re\sqrt{f} < [750, 600, 400]$, respectively.
- (ii) Polymeric, wherein, after onset, the polymer solutions exhibit drag reduction. The [1, 3, 10] wppm solutions onset at $Re\sqrt{f}^* = [750, 600, 400]$ respectively, followed

by roughly linear polymeric segments with slope increments $\delta = [6.5, 12.1, 21.7]$, respectively. At high $Re\sqrt{f} > 2500$, data for 1, 3 and 10 wppm solutions show downward curvature, indicative of polymer degradation. The 30 wppm solution exhibits L→P type transition, the polymeric segment being too short for the derivation of reliable onset and slope increments.

- (iii) Maximum Drag Reduction, wherein the polymer solutions follow an asymptote that is independent of polymeric parameters and universal in P-K coordinates. The 30 wppm attains MDR for $500 < Re\sqrt{f} < 3000$, beyond which the data fall below the smooth pipe MDR relation, indicative of degradation. The 100 wppm W-301 solution exhibits L→M type transitions and exhibits maximum drag reduction over the entire range $300 < Re\sqrt{f} < 4000$.

Polymer-induced drag reduction regimes for W-301 solutions observed in the smooth pipe, S1, are summarized in Table 4.3.14a.

In the riblet pipe, we find regimes of polymer solution flow similar to those in the smooth pipe, namely:

- (i) Newtonian, wherein the polymer solutions follow the solvent. The [1, 3, 10] wppm solutions exhibit Newtonian segments for $300 < Re\sqrt{f} < [700, 550, 400]$, respectively.
- (ii) Polymeric, wherein, after onset, the polymer solutions exhibit drag reduction. The [1, 3, 10] wppm solutions onset at $Re\sqrt{f}^* = [700, 550, 400]$, corresponding to $h^{+*} = [8, 6, 4]$, respectively. For a given concentration, the onset of drag reduction in the riblet pipe occurred at approximately the same $Re\sqrt{f}^*$ as in the smooth pipe. Following onset, the polymer solutions initially exhibit roughly linear segments, akin to those seen in the smooth pipe, the slopes of which increase with increasing

polymer concentration. At a certain high $Re\sqrt{f}$, all solutions switch to a second segment of lower slope. It should be noted that the 1, 3 and 10 wppm solutions likely suffer from polymer degradation, as was apparent from their smooth pipe trajectories.

- (iii) Maximum Drag Reduction, wherein the polymer solutions follow an asymptote that is independent of polymeric parameters and universal in P-K coordinates. The 100 wppm solution exhibits L→M transition and then follows the corresponding smooth pipe MDR data for $300 < Re\sqrt{f} < 1100$; at $Re\sqrt{f} = 1100 \pm 100$, it abruptly switches to a second segment of lower slope that persists to the highest $Re\sqrt{f} \approx 5000$. The 30 wppm solution, also following its corresponding smooth pipe data, attains and then follows the smooth MDR for $600 < Re\sqrt{f} < 1100$; at $Re\sqrt{f} = 1100 \pm 100$ it switches to a second segment, of lower slope, which coincides with the corresponding 100 wppm data for a short span $1100 < Re\sqrt{f} < 1600$, before falling below the latter, likely on account of polymer degradation as shown in Figure 4.3.9(b).

Polymer-induced drag reduction regimes for W-301 solutions in the riblet pipe, R1AR, are summarized in Table 4.3.14b.

Analysis of riblet-induced regimes, and their relation to polymer-induced drag reduction, is attempted in Figure 4.3.37, revealing the riblet regimes for W-301:

- (i) Hydraulically smooth, $R_p' \approx 0$. For $3 < h^+ < 5$, riblet-induced drag reduction was negligible in all the polymer solutions, for which $0 < S_s' < 8$.
- (ii) Riblet drag reduction, $R_p' > 0$. The riblets induced drag reduction in the 1, 3, 10, 30 and 100 wppm solutions over the ranges $5 < h^+ < 21$, $5 < h^+ < 14$, $5 < h^+ < 10$, $5 < h^+ < 11$, and $5 < h^+ < 10$ with respective maxima $(R_p', h^+) = (0.57, 14)$, $(0.71, 9)$, $(0.95, 7)$, $(0.38, 9)$, and $(0.35, 9)$. Riblet-induced drag reduction in polymer solutions occurred for $0 < S_s' < 6$ for $1 < c < 10$, and at $S' = 11 \pm 1$ for $c = 30$ and 100.

(iii) Riblet drag enhancement, $R_p' < 0$. Riblet-induced drag enhancement occurred in all polymer solutions, those of $c = [1, 3, 10, 30, 100]$ wppm exhibiting $R_p' < 0$ for $h^+ > [21, 14, 10, 11, 11]$, respectively. The data for 1 wppm solution follow solvent; those for 3 wppm lie below solvent up to $h^+ = 60$, then follow the solvent $R' - h^+$ relation; the data for 10 wppm exhibit a minimum at $(R_p', h^+) = (-6, 30)$ then curve upwards towards the solvent. It is interesting to note that the minimum approximately coincides with the departure from a linear polymeric segment at high $Re\sqrt{f} = 2300$ ($h^+ = 25$), suggesting that as degradation decreases the drag reduction to moderate slips, R_p' approaches the trajectory exhibited by lower concentration solutions, namely towards the solvent. For 30, 100 wppm solutions, which are either at or close to the maximum polymer-induced drag reduction, R_p' decreases monotonically with increasing h^+ to a minimum $R_p' = -9$ at $h^+ = 55$, where $S' \approx 18$.

Riblet-induced drag reduction regimes for W-301 solutions observed in R1AR are summarized in Table 4.3.14c.

4.3.7.2 7.82 mm pipe/0.15 mm riblets (S1 and R1B)

Flows of [100, 300] wppm N-750; [3, 10, 30, 100] wppm N-60K; 100 wppm W-301; [50, 100] wppm P-309; and 100 wppm N-300 solutions were investigated in the 7.82 mm smooth pipe and in a 7.82 mm pipe lined with 0.15 mm riblets, designated R1B.

N-750 Solutions

Figure 4.3.38 shows drag reduction by [100, 300] wppm N-750 in S1 and R1B. In the smooth pipe two turbulent regimes are visible, namely:

- (i) Newtonian, wherein the polymer solutions follow the solvent. The [100, 300] wppm solutions exhibit Newtonian segments for $300 < Re\sqrt{f} < [1200, 900]$, respectively.

(ii) Polymeric, wherein the polymer solutions exhibit drag reduction. The [100, 300] wppm solutions onset at $Re\sqrt{f}^* = [1200, 900]$, respectively, followed by roughly linear polymeric segments with slope increments $\delta = [9.1, 12.9]$, respectively.

Polymer-induced drag reduction regimes for N-750 solutions observed in the smooth pipe, S1, are summarized in Table 4.3.15a.

In the riblet pipe, we find turbulent flow regimes similar to those seen in the smooth pipe, namely:

- (i) Newtonian, wherein the polymer solutions follow the solvent. The [100, 300] wppm solutions exhibit Newtonian segments for $300 < Re\sqrt{f} < [1110, 850]$, respectively.
- (ii) Polymeric, wherein, after onset, the polymer solution data diverge upwards from solvent, exhibiting drag reduction that is dependent upon both flow and polymeric parameters. The [100, 300] wppm solutions onset at $Re\sqrt{f}^* = [1110, 850]$, corresponding to $h^{+*} = [18, 13]$, respectively. For a given concentration, the onset of drag reduction in the riblet pipe occurred at approximately the same $Re\sqrt{f}^*$ as in the smooth pipe. Following onset, the polymer solutions exhibit roughly linear segments, akin to those seen in the smooth pipe, the slopes of which increase with increasing polymer concentration.

Polymer-induced drag reduction regimes for N-750 solutions observed in the riblet pipe, R1B, are summarized in Table 4.3.15b.

Analysis of riblet-induced regimes, and their relation to polymer-induced drag reduction, is attempted in Figure 4.3.39, revealing the riblet regimes:

- (i) There is no hydraulically smooth regime. The riblets reduce drag for $h^+ > 5$, directly after fully turbulent flow is established.

- (ii) Riblet drag reduction, $R_p' > 0$. The riblets induced drag reduction in the 100 and 300 wppm solutions over the ranges $5 < h^+ < 28$, and $5 < h^+ < 28$, with respective maxima $(R_p', h^+) = (0.55, 15)$, and $(0.6, 14)$. Riblet-induced drag reduction in the polymer solutions was observed at $S_s' \approx 0$. It is noteworthy that both the range and magnitude of riblet-induced flow enhancement in the polymer solutions closely follows the solvent.
- (iii) Riblet drag enhancement, $R_p' < 0$. Riblet-induced drag enhancement occurred in both 100 and 300 wppm polymer solutions, which exhibited $R_p' < 0$ for $h^+ > [28, 28]$, respectively, where the corresponding polymer-induced flow enhancements were $S_s' = [1, 2]$. For $30 < h^+ < 80$, R_p' in the [100, 300] wppm solutions was within 0.5 units of that in solvent, falling to ≈ 1 unit below solvent at the highest $h^+ \approx 100$.

Riblet-related flow regimes observed in solvent and in N-750 solutions are summarized in Table 4.3.15c.

N-60K Solutions

Figure 4.3.40 shows drag reduction by [3, 10, 30, 100] wppm N-60K in S1 and R1B. In the smooth pipe, all three regimes of turbulent drag reduction by polymers are visible, namely:

- (i) Newtonian, wherein the polymer solutions follow the solvent. The [3, 10, 30, 100] wppm solutions exhibit Newtonian segments for $300 < Re\sqrt{f} < [750, 700, 600, 450]$, respectively.
- (ii) Polymeric, wherein the polymer solutions exhibit drag reduction. The [3, 10, 30, 100] wppm solutions onset at $Re\sqrt{f}^* = [750, 700, 600, 450]$, respectively, followed by roughly linear polymeric segments with slope increments $\delta = [7.5, 13.1, 21.4, 33]$, respectively. At the highest $Re\sqrt{f} > 4000$, data for 3, 10 and 30 wppm exhibit downward curvature, indicative of polymer degradation.

- (iii) **Maximum Drag Reduction.** The 100 wppm solution data, of initial slope 37 in the polymeric regime, abruptly decrease slope at $Re\sqrt{f} \approx 1400$, becoming essentially parallel to the MDR asymptote, but lying below it by about 2 units of $1/\sqrt{f}$.

Polymer-induced drag reduction regimes for N-60K solutions observed in the smooth pipe, S1, are summarized in Table 4.3.16a.

In the riblet pipe, all three regimes of turbulent drag reduction by polymers are visible, namely:

- (i) **Newtonian**, wherein the polymer solutions follow the solvent. The [3, 10, 30, 100] wppm solutions exhibit Newtonian segments for $300 < Re\sqrt{f} < [750, 650, 550, 450]$, respectively.
- (ii) **Polymeric**, wherein the polymer solutions exhibit drag reduction. The [3, 10, 30, 100] wppm solutions onset at $Re\sqrt{f}^* = [750, 650, 550, 450]$, respectively, which are essentially the same as the onsets observed in the smooth pipe, and correspond to $h^{+*} = [11, 10, 8, 7]$. After onset, the polymer solution data describe roughly linear initial segments, the slopes of which increase with increasing polymer concentration. With increasing $Re\sqrt{f}$, the initial linear segment is commonly followed by a second segment, of lower slope. For 10, 30, and 100 wppm solutions, the slope of the second segment is $\approx 18 \pm 5$ (P-K units) less than that of the initial segment.
- (iii) **Maximum Drag Reduction.** The 100 wppm solution data, of initial segment slope 27 in the polymeric regime, changes to a second segment correlated by $1/\sqrt{f} = 10 \log(Re\sqrt{f}) - 9.1$ for $1600 < Re\sqrt{f} < 5000$.

Polymer-induced drag reduction regimes for N-60K solutions in the riblet pipe, R1B, are summarized in Table 4.3.16b.

Analysis of riblet-induced regimes, and their relation to polymer-induced drag reduction, is attempted in Figure 4.3.41, revealing the riblet regimes:

- (i) No hydraulically smooth regime is observed. The riblets reduce drag for $h^+ > 5$ directly after fully turbulent flow is established.
- (ii) Riblet drag reduction, $R_p' > 0$. The riblets induced drag reduction in the 3, 10, 30 and 100 wppm solutions over the ranges $5 < h^+ < 23$, $5 < h^+ < 23$, $5 < h^+ < 20$, and $5 < h^+ < 14$ with respective maxima $(R_p', h^+) = (0.6, 14)$, $(0.8, 13)$, $(0.6, 14)$ and $(1.0, 10)$. Riblet-induced flow enhancement in the polymer solutions was observed at $0 < S_s' < 7$. The 3 and 10 wppm solutions tended to follow the solvent R' versus h^+ , relation whereas in the 30 and 100 wppm solutions, the maximum riblet-induced flow enhancement exceeded that observed in solvent, but the range of h^+ over which riblet drag reduction occurred was narrower than that in solvent.
- (iii) Riblet drag enhancement, $R_p' < 0$. Riblet-induced drag enhancement occurred in all polymer solutions, those of $c = [3, 10, 30, 100]$ wppm exhibiting $R_p' < 0$ for $h^+ > [23, 22, 20, 14]$, respectively, at which $S_s' = [2, 4, 6, 8]$. With increasing h^+ , the 3 and 10 wppm solutions essentially followed the solvent R' versus h^+ relationship up to $h^+ = 60$, then fell below solvent, to $R_p' = -4.1$ at $h^+ = 130$; the polymer-induced flow enhancement in these solutions was $0 < S_s' < 8$. In the 30 and 100 wppm solutions, R_p' decreased to well below solvent, being $R_p' \approx -6$ at $h^+ \approx 50$, where $S_s' \approx 18$. It should be kept in mind that observations at the highest $h^+ > 50$ suffer from polymer degradation and will require (small) corrections to account for it

Riblet-related flow regimes observed in solvent and in N-60K solutions are summarized in Table 4.3.16c.

W-301, P-309 and N-300 Solutions

Figures 4.3.42-4.3.44 show drag reduction by 100 wppm W-301, [50, 100] wppm P-309 and 100 wppm N-300, respectively, in S1 and R1B. These results are again presented collectively because all results are close to the asymptotic maximum polymer-induced drag reduction. In the smooth pipe, the Newtonian regime was absent, with only the regimes of turbulent drag reduction by polymers visible, namely:

- (ii) Polymeric. The 100 wppm N-300 solution exhibits an L→P type transition, the polymeric segment, $300 < Re\sqrt{f} < 400$, is too short for the derivation of reliable onset and slope parameters.
- (iii) Maximum Drag Reduction, wherein the polymer solutions follow an asymptote that is independent of polymeric parameters and universal in P-K coordinates. The 100 wppm W-301 and [50, 100] wppm P-309 solutions exhibit L→M type transitions and then follow the MDR asymptote over the entire range, $300 < Re\sqrt{f} < 4000$. The 100 wppm N-300 solution attains MDR for $Re\sqrt{f} > 400$ and remains close to it up to its highest $Re\sqrt{f} \approx 4200$.

Polymer-induced drag reduction regimes for W-301, P-309, and N-300 solutions observed in the smooth pipe, S1, are summarized in Table 4.3.17a.

In the riblet pipe, we find polymer solution flow regimes similar to those seen in smooth pipes, namely:

- (ii) Polymeric. The 100 wppm N-300 solution exhibits L→P transition, and forms a short polymeric segment for $300 < Re\sqrt{f} < 400$, which is essentially identical to that seen in the smooth pipe; this segment is too short for the derivation of reliable onset and slope parameters.

- (iii) Maximum Drag Reduction, wherein the polymer solutions follow an asymptote that is independent of polymeric parameters and universal in P-K coordinates. The data for 100 wppm W-301 and [50, 100] wppm P-309 exhibit L→M transitions and then can be seen to follow the corresponding smooth pipe MDR data for $300 < Re\sqrt{f} < 1000$. The 100 wppm N-300 solutions, also following their corresponding smooth pipe data, attain and then follow the smooth MDR for $400 < Re\sqrt{f} < 1000$, respectively. At $Re\sqrt{f} = 1000 \pm 100$, the riblet pipe data for all four solutions abruptly switch to a common second segment, of lower slope and still independent of polymeric parameters, that persists to the highest $Re\sqrt{f} \approx 5000$. The maximum drag reduction (highest $1/\sqrt{f}$) in the riblet pipe is thus limited by an asymptote:

$$1/\sqrt{f} = 10.1 \log Re\sqrt{f} - 7.3 ; 1100 < Re\sqrt{f} < 4000 \quad (4.3-11)$$

At the very highest $Re\sqrt{f} \approx 5000$, a data point or two from each of 100 wppm W-301, 50 wppm P-309 and 100 wppm N-300 fall below Eq. (4.3-11), likely due to polymer degradation, as seen in Figure 4.3.9(b).

Polymer-induced drag reduction regimes for W-301, P-309, and N-300 solutions observed in the riblet pipe, R1A, are summarized in Table 4.3.17b.

Analysis of riblet-induced regimes, and their relation to polymer-induced drag reduction, is attempted in Figures 4.3.45-4.3.47, revealing the riblet regimes:

- (i) Hydraulically smooth, $R_p' \approx 0$. For $3 < h^+ < 9$, riblet-induced drag reduction was negligible in all the polymer solutions, all of which exhibited the maximum possible polymer-induced drag reduction, $5 < S_s' < 10$.
- (ii) Riblet Drag Reduction. There appears to be a narrow range, $9 < h^+ < 14$, wherein the riblets reduce drag with a maximum $R_p' = 0.8$ at $h^+ = 11$. Unfortunately, the

magnitude of R_p' is of the same order as the uncertainty in $1/\sqrt{f}$, typically 0.5 units, at the present high polymeric drag reductions.

- (iii) Riblet drag enhancement, $R_p' < 0$. Riblet-induced drag enhancement occurred in all polymer solutions, for $h^+ > 14$, at which the corresponding polymer-induced flow enhancement was $S_s' = 13$. With increasing h^+ (and S_s'), riblet-induced drag enhancement increased greatly, and more steeply than for solvent flow, reaching $R'_{\min} \approx -7$ at $h^+ \approx 70$, where $S_s' \approx 20$.

Riblet-related flow regimes observed in solvent and in W-301, P-309, and N-300 solutions are summarized in Table 4.3.17c.

4.3.7.3 10.21 mm pipe/0.11 mm riblets (S2 and R2A)

Flows of dilute polymer solutions were investigated in one 10.21 mm smooth pipe, designated S1, and two 10.21 mm pipes lined with 0.11 mm riblets. In the first riblet pipe, designated R2A, the following solutions were investigated: [100, 250, 1000] wppm N-750; [3, 10, 30, 100] wppm N-60K; [3, 10, 30, 100] wppm W-301, and [50, 100, 200] wppm P-309. In the second, repeated pipe, R2AR, flows of 50 and 100 wppm P-309 were investigated.

N-750 Solutions

Figure 4.3.48 shows drag reduction by [100, 250, 1000] wppm N-750 in S2 and R2A. Two turbulent flow regimes are visible, namely:

- (i) Newtonian, wherein the polymer solutions follow the solvent. The [100, 250, 1000] wppm solutions exhibit Newtonian segments for $300 < Re\sqrt{f} < [2100, 1200, 1000]$, respectively.

- (ii) Polymeric, wherein the polymer solutions exhibit drag reduction. The [100, 250, 1000] wppm solutions onset at $Re\sqrt{f}^* = [2100, 1200, 1000]$, respectively, followed by linear polymeric segments with slope increments $\delta = [9.3, 12.6, 18.9]$, respectively.

Polymer-induced drag reduction regimes for N-750 solutions in the smooth pipe, S1, are summarized in Table 4.3.18a.

In the riblet pipe, we find turbulent flow regimes similar to those seen in the smooth pipe, namely:

- (i) Newtonian, wherein the polymer solutions follow the solvent. The [100, 250, 1000] wppm solutions exhibit Newtonian segments for $300 < Re\sqrt{f} < [2000, 1300, 1000]$, respectively.
- (ii) Polymeric, wherein, after onset, the polymer solution data diverge upwards from solvent, exhibiting drag reduction that is dependent upon both flow and polymeric parameters. The [100, 250, 1000] wppm solutions onset at $Re\sqrt{f}^* = [2000, 1300, 1000]$, corresponding to $h^{+*} = [16, 11, 8]$, respectively. For a given polymer concentration, the onset of drag reduction in the riblet pipe occurred at approximately the same $Re\sqrt{f}^*$ as in the smooth pipe. Following onset, the polymer solutions exhibit roughly linear segments, akin to those seen in the smooth pipe, the slopes of which increase with increasing polymer concentration.

Polymer-induced drag reduction regimes for N-750 solutions in the riblet pipe, R2A, are summarized in Table 4.3.18b.

Analysis of riblet-induced regimes, and their relation to polymer-induced drag reduction, is attempted in Figure 4.3.49, revealing the riblet regimes:

- (i) Hydraulically smooth, $R_p' \approx 0$. For $3 < h^+ < 5$, riblet-induced drag reduction was negligible in all the polymer solutions, and occurred in the Newtonian regime, prior to the onset of polymeric drag reduction, wherein $S_s' = 0$.
- (ii) Riblet drag reduction, $R_p' > 0$. The riblets induced drag reduction in the 100, 250, and 1000 wppm solutions over the ranges $5 < h^+ < 21$, $6 < h^+ < 20$, and $5 < h^+ < 20$ with respective maxima $(R_p', h^+) = (0.5, 14)$, $(0.5, 14)$, and $(0.7, 13)$. The greatest riblet-induced drag reduction in polymer solutions occurred only at low polymer-induced drag reductions, $0 < S_s' < 2$. The R_p' versus h^+ trajectories for all three polymer solutions approximately follow the solvent data.
- (iii) Riblet drag enhancement, $R_p' < 0$. Riblet-induced drag enhancement occurred in all three polymer solutions, with [100, 250, 1000] wppm exhibiting $R_p' < 0$ for $h^+ > [21, 20, 20]$, respectively, at which the corresponding polymer-induced flow enhancements were $S_s' = [1, 2, 4]$. As h^+ increased, the trajectories for the [100, 250] wppm solutions approached the solvent trajectory even at moderate slips, $S_s' < 6$. The trajectory for the 1000 wppm solution followed the solvent up to $h^+ = 30$, then diverged lower, to a minimum $R_p' = -2.3$ at $h^+ = 40$, where $S_s' \approx 10$.

Riblet-related flow regimes observed in solvent and in N-750 solutions are summarized in Table 4.3.18c.

N-60K Solutions

Figure 4.3.50 shows drag reduction by [3, 10, 30, 100] wppm N-60K in S2 and R2B. Two turbulent flow regimes are visible, namely:

- (i) Newtonian, wherein the polymer solutions follow the solvent. The [3, 10, 30, 100] wppm solutions exhibit Newtonian segments for $300 < Re\sqrt{f} < [1100, 900, 700, 550]$, respectively.

- (ii) Polymeric, wherein the polymer solutions exhibit drag reduction. The [3, 10, 30, 100] wppm solutions onset at $Re\sqrt{f}^* = [1100, 900, 700, 550]$, respectively, followed by roughly linear polymeric segments with slope increments $\delta = [7.8, 13.0, 19.5, 28.9]$, respectively. The data for 3 and 10 wppm solutions exhibit slight downward curvature at the highest $Re\sqrt{f} > 4000$, indicative of (slight) polymer degradation.

Polymer-induced drag reduction regimes for N-60K solutions in the smooth pipe, S2, are summarized in Table 4.3.19a.

In the riblet pipe, we find regimes of polymer solution flow similar to those seen in the smooth pipe, namely:

- (i) Newtonian, wherein the polymer solutions follow the solvent. The [3, 10, 30, 100] wppm solutions exhibit Newtonian segments for $300 < Re\sqrt{f} < [1100, 850, 700, 550]$, respectively.
- (ii) Polymeric, wherein, after onset, the polymer solution exhibit drag reduction. The [3, 10, 30, 100] wppm solutions onset at $Re\sqrt{f}^* = [1100, 850, 700, 550]$, respectively, which are essentially the same as the onsets observed in the smooth pipe, and correspond to $h^{+*} = [9, 7, 6, 4]$. After onset, the polymer solution data describe roughly linear initial segments, akin to those seen in the smooth pipe, the slopes of which increase with increasing polymer concentration. At higher $Re\sqrt{f} \approx 2000$, all the polymer solutions switch to a second linear segment of lower slope.

Polymer-induced drag reduction regimes for N-60K solutions in the riblet pipe, R2A, are summarized in Table 4.3.19b.

Analysis of riblet-induced regimes, and their relation to polymer-induced drag reduction, is attempted in Figure 4.3.51, revealing the riblet regimes:

- (i) Hydraulically smooth, $R_p' \approx 0$. For $3 < h^+ < 5$, riblet-induced drag reduction was negligible in all the polymer solutions, of which [3, 10, 30] wppm solutions were in their Newtonian regimes, wherein $S_s' = 0$, while the 100 wppm solution was barely past onset, with $S_s' < 2$.
- (ii) Riblet drag reduction, $R_p' > 0$. The riblets induced drag reduction in the 3, 10, 30 and 100 wppm solutions over the ranges $5 < h^+ < 23$, $5 < h^+ < 22$, $5 < h^+ < 21$, and $5 < h^+ < 14$ with respective maxima $(R_p', h^+) = (0.6, 15)$, $(1.0, 15)$, $(1.6, 14)$ and $(1.4, 11)$. Riblet-induced drag reduction in polymer solutions occurred for $2 < S_s' < 10$. It is noteworthy that the h^+ range of riblet-induced flow enhancement in the polymer solutions is approximately the same as solvent for 3, 10, and 30 wppm solutions but then decreases for 100 wppm solutions, the magnitude of $R_p'_{\max}$ increasing monotonically from 0.48 in solvent to 1.5 ± 0.1 in the 30 and 100 wppm solutions.
- (iii) Riblet drag enhancement, $R_p' < 0$. Riblet-induced drag enhancement occurred in all polymer solutions, those of $c = [3, 10, 30, 100]$ wppm exhibiting $R_p' < 0$ for $h^+ > [23, 22, 21, 14]$, respectively, at which the corresponding polymer-induced flow enhancements were $S_s' = [3, 6, 10, 10]$. It was further found that $R_p' < 0$ for all $S_s' > 10$. With increasing $h^+ > 60$, the [3, 10] wppm solutions approached the solvent R' - h^+ relation, despite exhibiting moderate polymer drag reduction, $3 < S_s' < 8$, while the [30, 100] wppm solutions lay well below solvent, with $R_p' < R_n'$ for $h^+ > 25$, reaching a minimum $R_p' \approx -4$ at $h^+ \approx 60$, where $S_s' \approx 15$.

Riblet-related flow regimes observed in solvent and in N-60K solutions are summarized in Table 4.3.19c.

W-301 Solutions

Figure 4.3.52 shows drag reduction [3, 10, 30, 100] wppm W-301 in S2 and R2A. All three known regimes of turbulent drag reduction by polymers are visible, namely:

- (i) Newtonian, wherein the polymer solutions follow the solvent. Only the [3, 10] wppm solutions exhibit Newtonian segments for $300 < Re\sqrt{f} < [700, 500]$, respectively.
- (ii) Polymeric, wherein, after onset, the polymer solutions exhibit drag reduction. All four polymer solutions exhibit polymeric segments. The [3, 10] wppm solutions onset at $Re\sqrt{f}^* = [700, 500]$ respectively, followed by roughly linear polymeric segments with slope increments $\delta = [11.8, 20.4]$ respectively. At high $Re\sqrt{f} > 3500$, data for both 3 and 10 wppm solutions show downward curvature, indicative of polymer degradation. The 30 and 100 wppm solutions transit from laminar flow directly into the polymeric regime. Of these, the 30 wppm polymeric segment has a slope increment $\delta = 28.1$ and an apparent onset at $Re\sqrt{f}^* = 400$, inferred by extrapolation back to the solvent line, but the 100 wppm polymeric segment is too short for the derivation of reliable onset and slope parameters.
- (iii) Maximum Drag Reduction, wherein the polymer solutions follow an asymptote that is independent of polymeric parameters and universal in P-K coordinates. Data from both the 30 and 100 wppm solutions lie close to the MDR asymptote, over the respective ranges $1400 < Re\sqrt{f} < 4400$ and $700 < Re\sqrt{f} < 3800$.

Polymer-induced drag reduction regimes for W-301 solutions observed in the smooth pipe, S2, are summarized in Table 4.3.20a.

In the riblet pipe, we find regimes of polymer solution flow similar to those in the smooth pipe, namely:

- (i) Newtonian, wherein the polymer solutions follow the solvent. The [3, 10] wppm solutions exhibit Newtonian segments for $300 < Re\sqrt{f} < [700, 500]$, respectively.
- (ii) Polymeric, wherein, after onset, the polymer solution exhibit drag reduction. The [3, 10, 30] wppm solutions onset at $Re\sqrt{f}^* = [700, 500, (400)]$, corresponding to $h^{+*} = [6, 4, (3)]$, respectively. The onset of drag reduction in the riblet pipe occurred at approximately the same $Re\sqrt{f}^*$ as in the smooth pipe for the same concentration. Following onset, the polymer solutions initially exhibit roughly linear segments, akin to those seen in the smooth pipe, the slopes of which increase with increasing polymer concentration. At a certain high $Re\sqrt{f}$, all solutions switch to a second segment of lower slope; this is most pronounced for 10, 30 and 100 wppm solutions, for all of which the second segment slopes are $\approx 24 \pm 3$ units smaller than the first. It should be noted that the 3 and 10 wppm solutions likely suffer from polymer degradation, apparent in their smooth pipe data.
- (iii) Maximum Drag Reduction, wherein the polymer solutions follow an asymptote that is independent of polymer concentration. The maximum drag reduction (highest $1/\sqrt{f}$) in the riblet pipe is limited by an asymptote:

$$1/\sqrt{f} = 8.2 \log Re\sqrt{f} + 1.1 ; 1600 < Re\sqrt{f} < 5500. \quad (4.3-12)$$

This asymptote is attained by both the 30 and 100 wppm solutions in their second polymeric regime segments, which essentially coincide over the respective ranges $1600 < Re\sqrt{f} < 4900$ and $700 < Re\sqrt{f} < 4200$.

Polymer-induced drag reduction regimes for W-301 solutions in the riblet pipe, R2A, are summarized in Table 4.3.20b.

Analysis of riblet-induced regimes, and their relation to polymer-induced drag reduction, is attempted in Figure 4.3.53, reveal the riblet regimes:

- (i) Hydraulically smooth, $R_p' \approx 0$. For $3 < h^+ < 5$, riblet-induced drag reduction was negligible in all the polymer solutions, amid varying, and considerable, polymer-induced drag reduction, $0 < S_s' < 10$. The hydraulically smooth regime in polymer solutions extended over much the same range as that in solvent, with some uncertainty, on account of both the greater scatter in the polymer solution data relative to solvent and the inherently diffuse upper boundary of this regime.
- (ii) Riblet drag reduction, $R_p' > 0$. The riblets induced drag reduction in the 3, 10, 30 and 100 wppm solutions over the ranges $5 < h^+ < 23$, $5 < h^+ < 19$, $5 < h^+ < 15$, and $5 < h^+ < 14$ with respective maxima $(R_p', h^+) = (0.7, 18)$, $(1.3, 12)$, $(1.2, 10)$ and $(1.6, 9)$. Riblet-induced drag reduction occurred at $5 < S_s' < 14$. With increasing polymer concentration, and the associated higher S_s' , the maximum R' increasingly exceeded that observed in solvent, while the h^+ ranges over which riblet drag reduction occurred narrowed relative to solvent.
- (iii) Riblet drag enhancement, $R_p' < 0$. Riblet-induced drag enhancement occurred in all polymer solutions, those of $c = [3, 10, 30, 100]$ wppm exhibiting $R_p' < 0$ for $h^+ > [23, 19, 15, 14]$, respectively, at which $S_s' = [7, 12, 15, 15]$. The 3 wppm solution followed the solvent for $25 < h^+ < 60$, whereas R_p' decreased with increasing $S_s' > 5$ for $[10, 30, 100]$ wppm solutions, to a minimum $R_p' \approx -4$ at $h^+ \approx 40$, where $S_s' \approx 20$. It should be noted that for $h^+ > 25$, R_p' data for the 3 and 10 wppm solutions require (small) corrections for polymer degradation.

Riblet-related flow regimes observed in solvent and in W-301 solutions are summarized in Table 4.3.20c.

P-309 Solutions

Figure 4.3.54 shows drag reduction by [50, 100, 200] wppm P-309 in S2 and R2B. In the smooth pipe the Newtonian turbulent regime was absent, with two drag reduction regimes visible, namely:

- (ii) **Polymeric.** The 50 wppm solution transits from laminar flow into the polymeric regime, where it remains for $300 < Re\sqrt{f} < 500$, the segment too short for the derivation of reliable onset and slope parameters.
- (iii) **Maximum Drag Reduction,** wherein the polymer solutions follow an asymptote that is independent of polymeric parameters and universal in P-K coordinates. The 50 wppm solution attains MDR at $Re\sqrt{f} \approx 500$, while the 100 and 200 wppm solutions transit directly from laminar flow to MDR at $Re\sqrt{f} \approx 300$. Data from both the 50 and 100 wppm solutions then lie close to the MDR asymptote over the respective ranges $500 < Re\sqrt{f} < 4000$ and $300 < Re\sqrt{f} < 3500$. The data for the 200 wppm solution lie somewhat above the MDR asymptote for $500 < Re\sqrt{f} < 2800$, probably due to slight shear thinning of this polymer solution.

Polymer-induced drag reduction regimes for P-309 solutions in the smooth pipe, S2, are summarized in Table 4.3.21b.

In the riblet pipe, we find polymer solution flow regimes similar to those in smooth pipes, namely:

- (i) **No Newtonian regime** was observed .
- (ii) **Polymeric.** wherein, after onset, the polymer solution data exhibit drag reduction. Following an L→P type transition, the 50 wppm solution exhibits a polymeric segment for $300 < Re\sqrt{f} < 500$, too short for the derivation of reliable onset and slope parameters.

- (iii) Maximum Drag Reduction, wherein the polymer solutions follow an asymptote that is independent of polymeric parameters and universal in P-K coordinates. The data for 100 and 200 wppm P-309 exhibit L→M transitions and then follow the smooth pipe data for $300 < Re\sqrt{f} < 900$, being joined by the 50 wppm data, which climb upward from the polymeric regime, for $500 < Re\sqrt{f} < 900$. Then, for $900 < Re\sqrt{f} < 1800$, both solutions lie somewhat above the smooth pipe data, exhibiting riblet-induced drag reduction. Finally, at the highest flowrates, $1800 < Re\sqrt{f} < 4000$, all the solutions switch to an approximately linear segment that diverges downward from the smooth pipe data and is given, for 50 and 100 wppm solutions, by the relation:

$$1/\sqrt{f} = 8.4 \log Re\sqrt{f} + 2.2 ; 1800 < Re\sqrt{f} < 5500. \quad (4.3-13)$$

Polymer-induced drag reduction regimes for P-309 solutions observed in the riblet pipe, R2A, are summarized in Table 4.3.21b.

Analysis of riblet-induced regimes, and their relation to polymer-induced drag reduction, is attempted in Figure 4.3.55, revealing the riblet regimes:

- (i) Hydraulically smooth, $R_p' \approx 0$. For $3 < h^+ < 6$, riblet-induced drag reduction was negligible in all the polymer solutions, which exhibited the maximum possible polymer-induced drag reductions, $5 < S_s' < 12$.
- (ii) Riblet drag reduction, $R_p' > 0$. The riblets induced drag reduction in the [50, 100, 200] wppm solutions over the range $6 < h^+ < 17$ with maximum $R_p' = 2.5 \pm 0.5$ at $h^+ \approx 10$. Riblet-induced drag reduction occurred while the polymer-induced drag reductions varied from $11 < S_s' < 18$, the maximum possible. Unlike any of the preceding pipes, this regime of riblet drag reduction at MDR was pronounced in pipe R2A; it extended over a somewhat narrower range of h^+ than in solvent, but the maximum riblet-induced flow enhancement was ≈ 3 times that in solvent .

- (iii) Riblet drag enhancement, $R_p' < 0$. Riblet-induced drag enhancement occurred in all polymer solutions, which exhibited $R_p' < 0$ for $17 < h^+ < 30$, at which $16 < S_s' < 20$. The [50, 100, 200] wppm solutions followed similar R_p' - h^+ relations, lying below solvent and decreasing more steeply than solvent, to $R'_{\min} \approx -2$ at $h^+ \approx 32$.

Riblet-related flow regimes observed in solvent and in P-309 solutions are summarized in Table 4.3.21c.

Replicated Pipe, R2AR

A second riblet test section, designated R2AR, was fabricated from the 10.21 mm pipe and 0.11 mm riblets. The fabrication method was identical to that in the original pipe. Flows of solvent and [50, 100] wppm P-309 were investigated, the results of which are summarized in Table 4.3.22 and Figure 4.3.56.

Solvent Flow in the Riblet Pipe. For solvent flow, depicted by the solid circles in Figure 4.3.56a, the three riblet-induced regimes are observed, namely:

- (i) Hydraulically smooth, $R_n' = 0$, for $h^+ < 5$.
- (ii) Riblet drag reduction, $R_n' > 0$, for $5 < h^+ < 24$, with a maximum $R_n' = 0.54$ at $h^+ = 14$.
- (iii) Riblet drag enhancement, $R_n' < 0$, for $h^+ > 24$, wherein R_n' decreases with increasing h^+ , to a minimum $R_n' = -2.2$ at $h^+ \approx 80$.

The riblet drag reduction regime observed in pipe R2AR from $5 < h^+ < 24$ was about the same as that in the original pipe R2A, $5 < h^+ < 22$; the maximum $R_n' = 0.54$ in R2AR was slightly higher than $R_n' = 0.48$ observed in R2A and occurred in both pipes at $h^+ = 14$. The minimum value of $R_n' = -2.20$ at $h^+ = 80$ in R2BR is to be compared with the corresponding minimum $R_n' = -1.84$ at $h^+ = 80$ in R2A. The extents of the riblet drag

reduction regime thus varied by ± 1 unit of h^+ ; $R_n'_{\max}$ varied by ± 0.03 units of $1/\sqrt{f}$ and h^+ at this maximum by ± 0 units; in the riblet drag enhancement regime the minimum R_n' observed at $h^+ \approx 80$, varied by ± 0.2 units of $1/\sqrt{f}$.

Polymer-induced Flow Enhancement in the Smooth Pipe Trajectories observed for [50, 100] P-309 solutions in the original and reproduced experiments were almost identical, as seen by comparing Table 4.3.22 with Table 4.3.21, and also by comparing Figure 4.3.56b with 4.3.55b. Both solutions exhibited maximum drag reduction for $500 < Re\sqrt{f} < 3500$ in both the present and original experiments.

Riblet-induced Flow Enhancement. Results for P-309 solutions in R2AR can be compared with those in R2A by perusal of the corresponding columns in parts (b) and (c) of Tables 4.3.22 and 4.3.21 as well as the three respective panels of Figures 4.3.56 and 4.3.55. Both 50 and 100 wppm solutions exhibited: (i) hydraulically smooth, (ii) riblet-drag reduction, and (iii) riblet drag enhancement regimes in R2AR, similar to those seen in R2A. In R2AR, the riblet drag reduction regime occurs for $7 < h^+ < 14$ in the 50 wppm solution and for $5 < h^+ < 14$ in the 100 wppm solution, while the maximum $R_p' \approx 1.5$ at $h^+ \approx 8$ is the same in both solutions. The extents of the hydraulically smooth regions, $6 \pm 1 < h^+ < 14$ versus $6 < h^+ < 17$, and the riblet drag enhancement regions, $14 < h^+ < 30$ versus $17 < h^+ < 28$, differ slightly between the replicated R2AR and the original R2A pipes. The maximum $R_p' \approx 1.5$ at $h^+ \approx 8$ in R1AR was lower than that, $R_p' \approx 1.9$ at $h^+ \approx 10$, observed in R1A.

The foregoing show that the replicated riblet pipe R2BR exhibited all of the flow regimes and physics seen in the original pipe R2B with solvent and at maximum drag reduction. It also provides quantitative measures of the (small) variations in performance that might be expected between identical riblet pipes fabricated by the present procedures.

4.3.7.4 Pipe Comparisons

Polymer-induced Flow Enhancement in the Smooth Pipes

Onset. The onset of polymer drag reduction was characterized by $Re\sqrt{f^*}$ which :

- (i) decreased slowly with increasing concentration for a given polymer molecular weight and pipe diameter [M_w , d_s]. The effect of concentration on the onset wall shear stress, $\tau_w^* = \frac{\rho}{2} \left[\frac{v Re\sqrt{f^*}}{d_s} \right]^2$, which has been used in the literature to describe Type

A drag reduction, is examined in section 4.6.1,

- (ii) decreased with increasing molecular weight for a given [c , d_s], and
 (iii) was smaller in the 7.82 mm pipe than in the 10.21 mm pipe for a given solution [c , M_w]. It is noteworthy that for a given [c , M_w] solution that exhibits a well defined onset, the ratio of $Re\sqrt{f^*}$ (7.82 mm pipe)/ $Re\sqrt{f^*}$ (10.21 mm pipe) = 0.75 ± 0.10 , is approximately equal to the ratio of the pipe diameters, $7.82/10.21 = 0.76$.

Slope Increment. The extent of drag reduction in the polymeric regime following onset was characterized by the slope increment of the initial linear polymeric segment, δ , which :

- (i) increased with increasing concentration for a given [M_w , d_s],
 (ii) increased with increasing molecular weight for a given [c , d_s], and
 (iii) was approximately independent of pipe diameter. For a given, [c , M_w], the ratio δ (7.82 mm pipe)/ δ (10.21 mm pipe) = 1.08 ± 0.08 .

Maximum Drag Reduction. An asymptote of maximum drag reduction was observed in both pipes; it was independent of pipe diameter, polymer concentration, polymer molecular weight, and polymer skeletal structure. Detailed analysis of MDR is presented in section 4.4.

Polymer-induced Flow Enhancement in the Riblet Pipes

Onset. In the riblet pipes, the onset of drag reduction occurred at approximately the same $Re\sqrt{f}^*$ as in the corresponding smooth pipe, regardless of the riblet pipe geometry $d_r/2h$, and the riblet-induced flow regime within which onset occurred. For a polymer solution of a given $[c, M_w]$, the ratio $Re\sqrt{f}^*(\text{riblet pipe})/Re\sqrt{f}^*(\text{tandem smooth pipe}) = 0.97 \pm 0.05$.

Slope. Following onset, the riblet pipe data follow an initially linear polymeric segment, the slope of which:

- (i) increased with increasing concentration for a given $[M_w, d_r/2h]$,
- (ii) increased with increasing molecular weight for a given $[c, d_r/2h]$, and
- (iii) was approximately independent of the riblet pipe geometry, $d_r/2h$, for a given $[c, M_w]$.

However, beyond a certain characteristic $Re\sqrt{f}$, the polymer solution trajectory switched to a second, roughly linear segment of lower slope that persisted to the highest $Re\sqrt{f}$. This switch was not observed for solutions of N-10 and N-750, was weak for low concentrations of N-60K and became more pronounced for the higher concentrations of N-60K and the higher molecular weight polymers. It is interesting that the slope of the second segment was typically $\approx 18 \pm 5$ (P-K units) less than that of the initial segment for all riblet pipes.

Maximum Drag Reduction. At maximum drag reduction, the data for all riblet pipes initially, that is at low $Re\sqrt{f}$, followed the smooth pipe MDR relation. Then, depending upon the riblet pipe geometry $d_r/2h$, the data lay above the smooth MDR relation for a small range of $Re\sqrt{f}$, and finally, at the highest $Re\sqrt{f}$, switched to a second, polymer independent, relation that exhibited lower drag reduction than smooth.

Riblet-induced Flow Enhancement

The flow of each polymer solution in the riblet pipe was also viewed relative to its flow in the smooth pipe, to discern the influence of the riblet wall. Three regimes of riblet-induced flow enhancement were observed, namely:

- (i) **Hydraulically smooth.** This regime, of negligible riblet-induced drag reduction, was observed in all of the riblet pipes, amid varying, and considerable, polymer-induced drag reduction, $0 < S_s' < 10$. At low slips, $S_s' < 4$, the hydraulically smooth regime was typically observed for $3 < h^+ < 5$, over the same range as solvent. Close to the maximum polymer-induced drag reduction, the hydraulically smooth regime appeared to extend somewhat beyond that in solvent, for $3 < h^+ < 10$, but this is uncertain, on account of both the greater scatter in the polymer solution data relative to solvent and the inherently diffuse upper boundary of the regime.
- (ii) **Riblet drag reduction.** The regime of riblet-induced drag reduction was defined in terms of an h^+ range (the upper bound is denoted by $h^+ = h^+_z$), and a magnitude and position of the maximum flow enhancement, R'_{\max} . It was found that the riblet drag reduction regime depended on both the polymer-induced flow enhancement and the riblet pipe geometry. Figure 4.3.57 depicts the variation of h^+_z with S_s' for each of the riblet pipes investigated. Amid wide scatter, some trends are visible. For pipes R1A, R1B and R2A, $h^+_z \approx 22$, approximately equal to the solvent value, for $0 < S_s' < 7$, then decreased below the solvent value, to $h^+_z \approx 12 \pm 3$ at higher slips of $7 < S_s' < 16$. For pipe R2B, h^+_z increased with increasing S_s' from the solvent value $h^+_z = 22$ at $S_s' = 0$ to $h^+_z \approx 32 \pm 10$ for $1 < S_s' < 8$, then decreased to below the solvent level, with $h^+_z = 11 \pm 4$ for $S_s' = 11 \pm 2$. Figure 4.3.58 depicts the variation of R'_{\max} with S_s' for each of the riblet pipes. For all pipes, at low slips, $0 < S_s' < 7$, R'_{\max} increased with increasing S_s' from the solvent value $R'_{n,\max} \approx 0.55$ at $S_s' \approx 0$ to $R'_{p,\max} \approx 1.5 \pm 0.5$ for $2 < S_s' < 7$. At the highest slips, $S_s' \approx 12 \pm 2$, associated with maximum polymer-

induced drag reduction, $R'_{p,max}$ decreased back to the solvent level in riblet pipes R1A and R1B, but in pipe R2A, $R'_{p,max} \approx 1.5 \pm 0.5$ remained larger than the solvent value, while in pipe R2B, there was no discernible riblet-induced drag reduction. Figure 4.3.59 depicts the variation of h^+ at R'_{max} (abbr. $h^+@max$) with S_s' for each of the riblet pipes. For R1A, R2A and R2B, $h^+@max \approx 10 \pm 2$ for $2 < S_s' < 12$, typically lower than the solvent value, while for R2B, $h^+@max$ increased from $h^+@max \approx 14$ at $S_s' \approx 0$ to $h^+@max \approx 25 \pm 5$ for $2 < S_s' < 4$, then decreased to $h^+@max \approx 15 \pm 5$ for $4 < S_s' < 6$.

(iii) Riblet drag enhancement. The riblets enhanced drag in all polymer solutions, and in all riblet pipes investigated. For low $S_s' < 5$, riblet drag enhancement was essentially the same as in solvent, that is R_p' decreased with increasing h^+ , with $R_p' \rightarrow -2$ for $h^+ > 70$. At higher $S_s' > 5$, and at high $h^+ > 30$, R_p' generally decreased with increasing S_s' for flows in the polymeric regime. At the highest S_s' , close to the asymptotic maximum drag reduction, R_p' decreased monotonically, and approximately linearly, with increasing h^+ the slopes of these segments, $dR_p'/d\log h^+ \approx -9.0 \pm 0.2$ being more than twice as steep as the greatest slope seen in solvent.

4.4 Maximum Drag Reduction

The presentation of riblet pipe results at maximum drag reduction (MDR) mirrors that for solvent flow in section 4.2. The polymer species, types and concentrations that exhibited MDR in the smooth and riblet pipes are listed in Table 4.4.1, along with the $Re\sqrt{f}$ ranges over which they did so. Of these solutions, 100 wppm PEO W-301, [50, 100] wppm PEO P-309, and 100 wppm PAM N-300 in both the original and replicated riblet pipes were analyzed in detail, being common to most of the riblet pipes.

4.4.1 Pressure Gradient Ratio

Figure 4.4.1 depicts the variation of the pressure gradient ratio, P , versus the volumetric flowrate, Q . The four, semi-logarithmic graphs, each corresponding to a single riblet pipe, are arranged with parts [a,b] and [c,d] respectively depicting, in registry, the variation of P in the smaller and larger pipes. For each pipe size, the upper axis corresponds to the Reynolds number in the smooth pipe with solvent viscosity. Data for all the polymer solutions that induced MDR are presented without distinguishing individual cases but with the original and replicated pipes represented by separate symbols, \circ and \square , respectively.

Consider, first, the variation of P in R1B depicted by Figure 4.4.1b. The results span three flow regimes, namely:

- (i) Laminar flow in both pipes: $0.0040 < Q < 0.0086$ l/s, $730 < Re_s < 1580$. In this regime, the pressure gradient ratio is roughly independent of flowrate with $P = P_L = 0.786 \pm 0.026$, which is roughly equal to the value for solvent, $P_L = 0.783 \pm 0.005$.
- (ii) Transition in either pipe: $0.0086 < Q < 0.030$ l/s, $1580 < Re_s < 5500$. In this regime, values of P fluctuate from 0.56 to 0.80, evidently reflecting the unstable, intermittent flows in each pipe, sampled at random.
- (iii) Turbulent flow in both pipes: $0.030 < Q < 1.020$ l/s, $5500 < Re_s < 187000$. Perusal of the results reveal that P is a complex function of Q , but may be divided into three regimes similar to those witnessed in solvent flows, namely:
 - (1) $P = P_{T0} = 0.793 \pm 0.028$: $0.030 < Q < 0.062$ l/s, $5500 < Re_s < 11300$. In this segment, P is roughly independent of flowrate; that is, the pressure gradients in the smooth and riblet pipes vary with Q in similar functional ways. It is noteworthy that this regime did not exist for solvent flows in this particular pipe, R1B. To facilitate

comparison to solvent flow, the f - Re relation at MDR may be represented by a Blasius-type power-law expression (Virk, 1975a):

$$f \approx 0.58 Re^{-0.58}; \quad 4000 < Re < 40000 \quad (4.4-1)$$

It should be noted that, on f - Re coordinates, experimental data at MDR exhibit greater curvature than solvent data, and are thus modeled only approximately by Eq. (4.4-1), whence:

$$\Delta P/\Delta z \propto Q^{1.42} d^{4.42} \quad \text{for } Re < 4 \times 10^4 \quad (4.4-2)$$

Assuming the riblet pipe obeys the same friction relationship as the smooth one, with $d_r \approx 7.44$ mm as in solvent flow, then $P_{T0} \approx (d_r/d_s)^{4.42} = 0.802$, in approximate agreement with the experimentally observed value.

- (2) $P > P_{T0}$: $0.062 < Q < 0.157$ l/s, $11300 < Re_s < 28700$. P increases with increasing Q up to $P_{\max} = 0.860$ at $[Q, Re_s] = [0.100 \text{ l/s}, 15500]$ then decreases, crossing the $P = P_{T0}$ line at $[Q, Re_s] = [0.157 \text{ l/s}, 28700]$. It is noteworthy that the relative drag in this regime is smaller than in regime (1), implying that maximum drag reduction in the smooth pipe is exceeded by the riblet pipe in this regime.
- (3) $P < P_{T0}$: $0.157 < Q < 1.020$ l/s, $28700 < Re_s < 187000$. P decreases monotonically with increasing Q to $P = 0.54 \pm 0.01$ at $[Q, Re_s] = [1.020 \text{ l/s}, 187000]$. P decreases somewhat less steeply with increasing Q , but does not attain a regime of constant P_T up to the highest flowrates. Though the maximum flowrate achieved at MDR exceeds that for solvent, the maximum observed $h^+ = 72 < 80$, the lower bound for which $P_T \rightarrow P_{T\infty}$ was observed in solvent flow.

It can be seen in Figures 4.4.1a,b,d, that the other three riblet pipes exhibit either all or most of the features described in the preceding example. The ranges of $[Q, Re_s]$ that define the regimes are summarized in Table 4.4.2. The variation of P with Q exhibit (i)

laminar flow, for which $P = P_L = [0.838, 0.786, 0.873, 0.840]$ for [R1A, R1B, R2A, R2B] pipes; (ii) transition, (iii) turbulent flow. In the turbulent regime, the variation of P with Q may be further divided into three regimes:

- (1) $P = P_{T0}$. P is roughly independent of Q , with $P_{T0} = [0.839, 0.793, 0.881, 0.837]$ for [R1A, R1B, R2A, R2B]. Assuming that the riblet pipes follow the same relation as the smooth pipe, Eq. (4.4-1), with $d_r = [7.54, 7.44, 9.93, 9.80]$ mm; then the expected $P_{T0} = [0.851, 0.802, 0.884, 0.834]$, in close agreement with the experimentally observed values.
- (2) $P > P_{T0}$. P increases with increasing Q to a maximum $P = [0.880, 0.860, 0.992, -]$ at $Q = [0.085, 0.057, 0.172, -]$ l/s for [R1A, R1B, R2A, R2B] then decreases, back to $P = P_{T0}$ at $Q = [0.200, 0.157, 0.516, 0.132]$ l/s.
- (c) $P < P_{T0}$. P decreases monotonically with increasing Q from $P = P_{T0}$ as given above, to $P_{\min} = [0.49, 0.54, 0.75, 0.58]$ at $Q = [0.920, 1.02, 1.10, 1.10]$ l/s for [R1A, R1B, R2A, R2B]. Unlike solvent flows, there is no tendency towards constant $P_T \rightarrow P_{T\infty}$ at the highest Q .

4.4.2 Prandtl-Karman Representation

4.4.2.1 Smooth Pipes

Figure 4.4.2 is a plot, in P-K coordinates, for flows of [50, 100] wppm P-309; 100 wppm W-301 and 100 wppm N-300 in the 10.21 mm smooth pipe; the data were taken from several reproduced, experimental runs, and truncated such that only laminar flow and MDR are depicted. In the turbulent regime, the maximum drag reduction is limited by a polymer-independent asymptote:

$$1/\sqrt{f} = (18.9 \pm 0.2) \log \text{Re}\sqrt{f} - (33.4 \pm 0.8) \quad R^2 = 0.973 \quad (4.4-3)$$

which is in agreement with Virk's MDR correlation (Eq. 2.2-8). Figure 4.4.3 depicts regimes of laminar and turbulent maximum drag reduction in the 7.82 mm smooth pipe. The maximum drag reduction in the turbulent regime is limited by a polymer-independent asymptote:

$$1/\sqrt{f} = (19.1 \pm 0.2) \log \text{Re}\sqrt{f} - (33.4 \pm 0.5) \quad R^2 = 0.981 \quad (4.4-4)$$

which also agrees with Eq. 2.2-8.

Aspects of maximum drag reduction observed in the smooth pipes are summarized in Table 4.4.3a

4.4.2.2 Riblet Pipes

Figures 4.4.4-4.4.7 depict the results, in P-K coordinates with an upper h^+ abscissa, of the riblet pipes [R1A, R1AR], R1B, [R2A, R2AR], and [R2B, R2BR]. For clarity, the 10.21 mm and 7.82 mm smooth pipe data are represented by Eqs. (4.4-3) and (4.4-4), respectively, and the original and replicated pipes are not distinguished, having been previously shown to be similar. There is considerably worse scatter at MDR than was observed in solvent runs. Direct recognition of the regimes of riblet flow enhancement relative to smooth is therefore difficult in P-K coordinates and requires a more sensitive analysis in terms of the flow enhancement parameter R' . Perusal of the P-K plots reveals polymer independent asymptotes that are unique to each pipe. In general, at maximum drag reduction, the riblet pipes exhibit two, roughly linear segments. The first segment, at low $\text{Re}\sqrt{f}$, has roughly the same slope as the smooth pipe asymptote with slopes, $\Delta_1 = [20.4, 20.6, 23.2, 16.7]$ for $\text{Re}\sqrt{f} < [1200, 1000, 1150, 850]$ in [R1A, R1B, R2A, R2B]. At higher $\text{Re}\sqrt{f}$, the riblet pipe data follow a second, roughly linear segment which is drag

enhancing relative to the smooth pipe, with slopes, $\Delta_2 = [4.5, 10.1, 8.0, 9.7]$ for $Re\sqrt{f} > [1300, 1400, 1150, 1100]$ in [R1A, R1B, R2A, R2B], respectively.

Aspects of maximum drag reduction observed in the riblet pipes are summarized in Table 4.4.3b.

4.4.3 Flow Enhancement Parameters

Figures 4.4.8 through 4.4.11 depict the analysis of riblet-induced flow regimes at MDR and their relation to the polymer-induced maximum drag reduction in the smooth pipes, with axes and notation of Figure 4.3.4, original and replicated pipes are not distinguished. Detailed examination of the figures reveal the riblet regimes defined previously, namely:

- (i) Hydraulically smooth, $R_p' \approx 0$. The hydraulically smooth regime at maximum drag reduction appeared to extend from $3 < h^+ < 9$, somewhat beyond that in solvent, $3 < h^+ < 5$, but this is uncertain, on account of both the greater scatter in the polymer solution data relative to solvent and the inherently diffuse upper boundary of this regime. The uncertainty in the polymer solution data is ≈ 0.5 units of R' at MDR, resulting from the larger absolute values of $1/\sqrt{f}$ and larger errors due to increased voltage fluctuations at MDR relative to solvent. Unfortunately, this is the same order as the drag reduction by riblets for solvent flow. The upper bound of the hydraulically smooth regime occurred at $h^+ \approx [9, 9, 7, 9]$ in [R1A, R1B, R2A, R2B].
- (ii) Riblet drag reduction, $R_p' > 0$. The riblets induced drag reduction in pipes [R1A, R1B, R2A] over the ranges $[9 < h^+ < 14, 9 < h^+ < 14, 7 < h^+ < 16]$ with maxima $R_p' = [0.8, 1.0, 1.8]$ at $h^+ = [11, 11, 10]$. There was no observed regime of riblet drag reduction in the original pipe R2B, the transition from hydraulically smooth to riblet drag

enhancement occurs at $h^+ \approx 9$; however the replicated pipe R2BR provided a hint of riblet drag reduction over the range $7 < h^+ < 10$ with $R'_{p,max} \approx 0.7$ at $h^+ \approx 8$. It is noteworthy that the extent of the riblet drag reduction regime at MDR, typically $9 < h^+ < 14$, is narrower than that in solvent, $5 < h^+ < 23$; also $R'_{max} = 1.2 \pm 0.6$ at MDR observed at $h^+ \approx 10$, was higher than $R'_{max} = 0.55$ in solvent, observed at $h^+ = 14$.

(iii) Riblet drag enhancement, $R_p' > 0$. Riblet-induced drag enhancement occurred in all pipes. R_p' decreased approximately linearly with increasing h^+ to $R_{min}' = [-9 \pm 1, -7 \pm 1, -2.4 \pm, -6 \pm 2]$ at $h^+ = [50, 80, 35, 50]$ for [R1A, R1B, R2A, R2B], respectively; the slopes of these segments, $dR_p'/d\log h^+ \approx -9.0 \pm 0.2$, being more than twice as steep as the greatest slope seen in solvent. In all but R2A, the riblet-induced drag enhancement at MDR far exceeded that observed that in solvent at the same h^+ . Finally, at MDR, the data for R' versus h^+ decreased monotonically to the highest $h^+ \approx 50$, showing no evidence of the asymptotic minimum attained in solvent at $h^+ > 80$.

Aspects of the riblet-induced flow regimes observed in the riblet pipes at maximum polymer-induced drag reduction are summarized in Table 4.4.3c.

4.5 Laminar Flow Parameters

4.5.1 Relative Viscosity

Polymeric properties such as molecular weight and radius of gyration were inferred from intrinsic viscosities obtained from laminar flow data in the smooth pipe. For each experimental run, laminar flow provides information on the solution relative viscosity via Poiseuille's law:

$$Re_p f_p = Re_n f_n = 16 \quad (4.5-1)$$

$$\eta_{rel} = \frac{\eta_p}{\eta_n} = \frac{Re_n}{Re_p} = \frac{f_p}{f_n} = \frac{Re_n f_p}{16} \quad (4.5-2)$$

Both the solvent based Reynolds number, Re_n , and the polymer solution friction factor, f_p , are calculated for each data point, the relative viscosity determined from the average over all laminar flow data. Table 4.5.1 summarizes the relative and intrinsic viscosities for each experimental run, in which $\eta_{rel} > 1.05$. The intrinsic viscosities were calculated both from a 1-point estimate, Eq. 2.2-3 (Solomon and Ciuta, 1962) and from Flory-Huggins equation, Eq. 2.2-2, with $k_1 = [0.36, 0.37]$ for [PEO, PAM]; the differences between the two estimates are small, $\approx 0.5\%$. Table 4.5.2 summarizes the molecular weight, number of backbone chain links, radius of gyration and contour length of all the polymer species used in this investigation, the associated error limits (\pm) being inferred from the standard deviations of the intrinsic viscosity.

4.6 Turbulent Flow Parameters

4.6.1 Onset Wall Shear Stress, τ_w^*

4.6.1.1 Smooth Pipes

The model of Type A drag reduction in smooth pipes presumes a discontinuous change from Newtonian to a linear polymeric segment. In many of the solutions investigated, the data depart from the Newtonian baseline rather weakly, then ascend into the polymeric regime along a shallow knee, before finally forming a well-defined linear polymeric segment. As shown in the $S' - \tau_w$ plot of Figure 4.6.1 for 3 wppm W-301 in S2, the visually determined onset point, $\tau_w^* = 1.5 \text{ N/m}^2$, need not coincide with the value inferred from regression of the linear segment back the Newtonian regime ($S' = 0$), $\tau_w^* =$

2.0 N/m². The use of S' - τ_w plots enables τ_w^* to be determined directly by extrapolation to a horizontal Newtonian baseline, $S' = 0$.

Figures 4.6.2 and 4.6.3 show the concentration dependence of the regressed onset wall shear stress for all additives in the smooth 10.21 and 7.82 mm pipes, respectively. The error bars in the data are inferred from the errors in the regression of the linear polymeric segment. In both pipes, $\tau_{w,s}^*$ is, at most, a weak, decreasing function of c . The data are best represented by a power law fit:

$$\tau_{w,s}^* = \text{constant} \times c^n \quad (4.6-1)$$

where $n = -0.15 \pm 0.08$ for all polymer solutions. Because the ideal Type A fan radiates from a single point on the Newtonian baseline, the onset wall shear stress has one concentration-independent value. Experimentally, this is taken as the average of the values over all concentrations, summarized in Table 4.6.1, from which it is seen that $\tau_{w,s}^*$ is approximately independent of pipe diameter.

4.6.1.1 Riblet Pipes

The onset of polymer-induced drag reduction in the riblet pipes is examined in Figure 4.6.4 which depicts the variation of $Re\sqrt{f}^*$ in the riblet pipe versus $Re\sqrt{f}^*$ in the corresponding smooth pipe for a given solution. The data show that onset $Re\sqrt{f}^*$ in the riblet and smooth pipes were the same; regression yields:

$$Re\sqrt{f}_r^* = (0.97 \pm 0.03) Re\sqrt{f}_s^* \quad (4.6-2)$$

If we use the diameter of the riblet pipe as the basis for calculating the onset "wall" shear stress, then Eq. (4.6-2) corresponds to the relation $\tau_{w,r}^* = 1.04 \tau_{w,s}^*$.

4.6.2 Slope Increment, δ

4.6.2.1 Smooth Pipes

Figures 4.6.5 and 4.6.6 are dual logarithmic plots of the slope increment, δ , versus concentration for all additives in the 10.21 mm and 7.82 mm smooth pipes, respectively. The data are best represented by a power law expression:

$$\delta = \text{constant} \times c^n \quad (4.6-3)$$

where n is represented by a single value, 0.4 ± 0.01 , that differs somewhat from the Type A model for which $d \propto c^{0.5}$.

Table 4.6.2 summarizes values of the Type A model specific slope increment, $\delta/c^{0.5}$ for the larger and smaller pipes, indicating that pipe diameter has a weak effect on the Type A fan.

4.6.2.1 Riblet Pipes

Figure 4.6.7 depicts the variation of the slope of the initial polymeric segment in the riblet pipes versus the slope of the linear segment of the polymeric regime in the corresponding smooth pipe; the ratio of the two slopes is 0.84 ± 0.10 . Whereas the smooth pipe data are referenced to a line of constant slope = 4.0, yielding a slope increment δ , the riblet pipes gets referred to the solvent line whose slope changes from 4 for $h^+ < 5$, to ≈ 6 for $5 < h^+ < 14$, ≈ 0 for $14 < h^+ < 80$, and ≈ 4 for $h^+ > 80$. It is uncertain how best to determine an analogous slope increment in the riblet pipes.

4.7 Summary

The following is a summary of the results presented in detail in the preceding sections. This summary examines the features observed for flows of distilled water and dilute polymer solutions in smooth and riblet pipes.

4.7.1 Solvent Flow

In the smooth pipes, flows of distilled water exhibited regimes of (i) laminar flow, $Re\sqrt{f} < 180$, wherein the data adhere to Poiseuille's law, $f.Re = 16$; (ii) laminar to turbulence transition, $180 < Re\sqrt{f} < 300$, and (iii) turbulent flow, $Re\sqrt{f} > 300$, wherein the data were correlated by the Prandtl-Karman law, $1/\sqrt{f} = 4.0 \log(Re\sqrt{f}) - 0.4$.

In the riblet pipes, flows of distilled water exhibited regimes of (i) laminar flow, $Re\sqrt{f} < 180$, in which the data were downwardly displaced 1.5 to 4% from Poiseuille's law; (ii) transition, $180 < Re\sqrt{f} < 300$, and (iii) turbulent flows, $Re\sqrt{f} > 300$. Within the turbulent regime, the data may be further divided into three regimes:

- (i) Hydraulically smooth, $h^+ < 5$, wherein the P-K law for smooth pipes was obeyed. This was the basis for defining the riblet pipe diameter
- (ii) Riblet drag reduction, $5 < h^+ < 22$, wherein $1/\sqrt{f}$ exceeded the P-K law, with the greatest riblet-induced flow enhancement $R_n' = 0.5 \pm 0.05$ ($1/\sqrt{f}$ units) at $h^+ = 14 \pm 1$.
- (iii) Riblet drag enhancement, $22 < h^+ < 160$, wherein $1/\sqrt{f}$ lay below the P-K law, the more so at the higher h^+ , until $R_n' \rightarrow -2.2 \pm 0.4$ for $h^+ > 70$.

4.7.2 Polymer Solution Flow

Flows of dilute solutions of five polyethyleneoxide and two polyacrylamide polymer solutions in two smooth and four riblet-lined pipes were studied at diametral Reynolds numbers from 300 to 150000. Friction factor measurements in the riblet pipe were accompanied by simultaneous measurements in a smooth pipe of the same diameter placed in tandem. The chosen conditions provided turbulent drag reductions from zero to the asymptotic maximum possible.

4.7.2.1 Polymer-induced Flow Enhancement in the Smooth Pipes

Polymer solution flows in the smooth pipe followed previously established patterns of Type A drag reduction, exhibiting:

- (1) A well defined onset of drag reduction, which was characterized by an onset wall shear stress, τ_w^* , was examined in terms of:
 - (i) molecular weight. For a fixed solution concentration, τ_w^* decreased with increasing molecular weight.
 - (ii) concentration. The onset wall shear stress, τ_w^* was, at most, a weak function of concentration, $\propto c^{-0.15 \pm 0.08}$.
 - (iii) pipe diameter. For a solution of fixed concentration and molecular weight, τ_w^* was approximately independent of pipe diameter.

- (2) A polymeric regime "fan", in which the extent of drag reduction increased with increasing Re/f . The trajectory exhibited an initially linear segment, with slope that exceeded that of the solvent line by an amount δ (slope increment) that was examined in terms of:
 - (i) concentration. δ increased with increasing concentration, $\propto c^{0.40 \pm 0.01}$

- (ii) molecular weight. For a fixed solution concentration, δ increased with increasing molecular weight.
 - (iii) pipe diameter. For a fixed polymer solution, δ was approximately independent of pipe diameter.
- (3) Polymer degradation. In certain cases, associated with the highest molecular weight polymers at high $Re\sqrt{f}$, polymer solution data deviated downwards from a linear trajectory in P-K coordinates. The extent of deviation depended on:
- (i) downstream location. Degradation was detected as a bifurcation between the friction factors measured at an upstream and a downstream smooth pipe measuring station. This occurred at a characteristic wall shear stress, τ_w^\wedge , that was roughly independent of concentration for flows in the polymeric regime. At a fixed τ_w , the severity of degradation increased with increasing downstream distance.
 - (ii) molecular weight. For a given concentration, the wall shear stress for incipient degradation in the polymeric regime was roughly proportional to polymer molecular weight. Furthermore, at a fixed τ_w , the severity of degradation increased with increasing molecular weight .
 - (iii) pipe diameter. The wall shear stress at incipient degradation was approximately independent of pipe diameter. For a given concentration and τ_w , degradation was more severe in the smaller pipe.
- (4) Maximum drag reduction was attained by solutions of the highest molecular weight polymers, which closely followed the universal MDR asymptote, $1/\sqrt{f} = 19 \log Re\sqrt{f}$ - 32.4.

4.7.2.2 Polymer-induced Flow Enhancement in the Riblet Pipes

In the riblet pipe the flow of polymer solutions was first viewed relative to solvent, to discern the effect of the polymeric additive:

- (1) The onset of drag reduction in the riblet pipe occurred at the same $Re\sqrt{f}^*$ as in the smooth pipe, and the corresponding onset wall shear stress was also approximately the same as in the smooth pipe.
- (2) In the polymeric regime, following onset, the polymer solutions initially exhibited linear segments on P-K coordinates, akin to those seen in the smooth pipe, with slopes that depended on:
 - (i) concentration. The slope increased with increasing polymer concentration.
 - (ii) molecular weight. For a fixed solution concentration, the slope increased with increasing molecular weight.
 - (iii) pipe diameter. For a fixed polymer solution, the slope was approximately independent of pipe diameter.

However, beyond a characteristic $Re\sqrt{f}$, which decreased with increasing concentration, each polymer solution trajectory switched to a second roughly linear segment of lower slope, which persisted to the highest $Re\sqrt{f}$. The slope of this segment was typically 18 units less than the initial segment.

- (3) The maximum drag reduction in the riblet pipe was limited by an asymptote attained by solutions of the highest molecular weight polymers. The maximum asymptotic drag reduction approximately followed the smooth pipe asymptote up to $Re\sqrt{f} \approx 1000 - 1400$, then switched to a second, polymer independent segment, the equation of which depended on $d_r/2h$.

4.7.2.3 Riblet-induced Flow Enhancement

The flow of each polymer solution in the riblet pipe was also viewed relative to its flow in the smooth pipe, to discern the influence of the riblet wall. Three regimes of riblet-induced flow enhancement were observed, namely:

- (i) **Hydraulically smooth.** This regime, with negligible riblet-induced drag reduction, was observed in all of the riblet pipes, amid varying, and considerable, polymer-induced drag reduction, $0 < S_s' < 10$. At low slips, $S_s' < 4$, the hydraulically smooth regime was observed for $3 < h^+ < 5$, as in solvent. Close to the maximum polymer-induced drag reduction, this regime appeared to extend for $3 < h^+ < 10$, somewhat beyond that in solvent, but this is uncertain, on account of both the greater scatter in the polymer solution data relative to solvent and the inherently diffuse upper boundary of this regime.
- (ii) **Riblet drag reduction.** The regime of riblet-induced drag reduction was defined in terms of an h^+ range (the upper bound being better defined than the more diffuse lower bound), and the magnitude and position of the maximum flow enhancement, R'_{\max} . It was found that the riblet drag reduction regime depended on:
 - (1) the polymer-induced flow enhancement, S_s' . For solvent flow, $S_s' = 0$, riblet drag reduction occurred over the range $5 < h^+ < 22$, with the greatest riblet-induced flow enhancement $R_n' = 0.5$ at $h^+ = 14$. For low to moderate slips, $0 < S_s' < 5$, the upper h^+ bound was typically close to or greater than the solvent upper bound, $h^+ = 22$, depending on the riblet pipe. Within this range of polymer-induced flow enhancement, the maximum R' increased with S_s' from $R_n' = 0.50$ to $R_p' \approx 1-2$ depending on the riblet pipe, occurring at $h^+ \leq 14$ for R1A, R1B, R2A and $h^+ \geq 14$ for R2B. For moderate to high slips, $S_s' > 7$, the

upper bound $h^+ < 22$, typically, with a maximum $R_p' \approx 0.5-1.0$ at $h^+ < 14$ for pipes R1A and R2A; pipe R2A exhibited a maximum $R_p' \approx 1.5$ even at high $S_s' \approx 12$, and pipe R2B exhibited no discernible drag reduction regime at high slips.

(2) riblet pipe. All riblet pipes exhibited a riblet drag reduction regime, the upper bound of which followed the same trends in pipes R1A, R1B, and R2A, but not in R2B which exhibited larger upper bounds than the solvent for $S_s' < 7$. The maximum enhancement exhibited similar trends in R1A, R1B, R2A and R2B at low to moderate slips, $S_s' < 5$, but at the highest slips, $S_s' \approx 10$, the maximum enhancement in pipe R2A exceeded those of the smaller diameter riblet pipes, and R2B exhibited no perceptible riblet drag reduction. However, the uncertainty in the results at high polymer-induced drag reductions, $\approx 0.5 1/\sqrt{f}$ units, precludes firmer conclusions concerning the effect of the riblet pipe.

(iii) Riblet drag enhancement, $R_p' < 0$. At high h^+ , the riblets enhanced drag in all polymer solutions, and in all riblet pipes investigated. For low $S_s' < 5$, the riblet drag enhancement was essentially the same as in solvent, that is R_p' decreased with increasing h^+ , with $R_p' \rightarrow -2$ for $h^+ > 70$. At higher $S_s' > 5$, and at higher $h^+ > 30$, R_p' generally decreased with increasing S_s' for flows in the polymeric regime. Close to the asymptotic maximum drag reduction, R_p' decreased monotonically, and approximately linearly, with increasing h^+ , the slopes of these segments, $dR_p'/d\log h^+ \approx -9.0 \pm 0.2$, being considerably steeper than observed in solvent.

Table 4.1.1. Experimental grid

Pipe designation		S1/R1A	S1/R1B	S2/R2A	S2/R2B
d_s , mm		7.82	7.82	10.21	10.21
h, mm		0.11	0.15	0.11	0.15
$*d_s/2h$		36	26	46	34
Species	Type				
PEO	N-10	-	-	-	2435, 5138
	N-750	100, 300, 1000	100, 300	100, 250, 1000	100, 250, 900, 2073
	N-60K	<i>3, 10, 30,</i> <i>100</i>	3, 10, 30, 100	3, 10, 30, 100, 300	3, 10, 30, 100
	W-301	<i>1, 3, 10, 30,</i> <i>100</i>	100	3, 10, 30, 100	<i>3, 10, 30,</i> <i>100</i>
	P-309	50, 100	50, 100	50, 100, 200	50, 100
PAM	N-300L	-	-	-	10, 30, 100, 300
	N-300	100	100	-	3, 10, 30, 100

Note: PEO = polyethyleneoxide
PAM = polyacrylamide

Numbers in **bold** indicate replicated experimental runs in original pipe.
Numbers in *italics* indicate experimental runs in replicated pipe.

***Note:** Relative riblet height $d_s/2h$ is here with respect to nominal smooth pipe diameters because precise riblet pipe diameters are yet to be defined.

Table 4.2.1. Flow regimes of pressure gradient ratio for solvent flow.

Pipes→		S1 & R1A	S1 & R1B	S2 & R2A	S2 & R2B
Flow Regime ↓					
Laminar					
P_L		0.851 ± 0.003	0.783 ± 0.005	0.875 ± 0.007	0.839 ± 0.006
Q range (l/s)		0.0033-0.0089	0.0037-0.0080	0.0025-0.012	0.0021-0.015
Re _s range		610-1650	690-1490	350-1660	290-2070
Transition					
Q range (l/s)		0.0089-0.017	0.0080-0.016	0.012-0.025	0.015-0.026
Re _s range		1650-3160	1490-2980	1660-3460	2070-3600
Turbulent					
$P_T = P_{T0}$	P_{T0}	0.843 ± 0.002	(0.790)	0.875 ± 0.004	0.824 ± 0.003
	Q range (l/s)	0.017-0.027	-	0.025-0.051	0.026-0.040
	Re _s range	3160-5020	-	3460-7050	3600-5530
	≈ h ⁺ range	3.0-5.4	-	2.7-5.2	3.9-5.3
$P_T > P_{T0}$	Q range (l/s)	0.027-0.140	0.016-0.096	0.051-0.250	0.040-0.210
	Re _s range	5020-26000	2980-17900	7050-34600	5530-29000
	≈ h ⁺ range	5.4-23	5.7-24	5.2-22	5.3-21
	P_{Tmax}	0.910	0.843	0.922	0.912
	h ⁺ at P_{Tmax}	14.3	15.3	14.6	14.5
$P_T < P_{T0}$	Q range (l/s)	0.140-0.690	0.096-0.740	0.250-0.975	0.210-1.070
	Segment 1 Q range (l/s)	0.140-0.480	0.096-0.340	0.250-0.975	0.210-0.580
	Re _s range	26000-89300	17900-63200	34600-135000	29000-80200
	≈ h ⁺ range	23-77	24-80	22-80	21-70
Segment 2	$P_{T∞}$	0.627 ± 0.002	0.577 ± 0.004	-	0.643 ± 0.008
	Q range (l/s)	0.480-0.690	0.340-0.740	-	0.580-1.070
	Re _s range	89300-128000	63200-138000	-	80200-148000
	≈ h ⁺ range	77-110	80-160	-	70-115

Table 4.2.2. Summary of solvent flow regimes in smooth and riblet pipes

Pipe →		S 1	S 2	R 1 A	R 1 B	R 2 A	R 2 B
d_p		7.82	10.21	7.54	7.44	9.93	9.80
h		-	-	0.11	0.15	0.11	0.15
$d_p/2h$		-	-	35.9	25.7	47.3	33.8
Flow Regime ↓							
Laminar	Re \sqrt{f} range	< 180	< 175	< 180	< 185	< 190	< 180
	fRe based on d	16.0	16.0	16.26	16.66	16.34	16.22
Transition	Re \sqrt{f} range	180 - 300	175 - 300	180 - 300	185 - 300	190 - 300	180 - 300
Turbulent Hydraulically smooth	d, mm	7.82	10.21	7.54	7.44	9.93	9.80
	Re \sqrt{f} range	300 - 9200	300 - 9100	300 - 490	-	300 - 700	300 - 480
	h^+ range	-	-	3.6 - 5.2	-	2.8 - 5.6	3.4 - 5.3
Riblet drag reduction	Re \sqrt{f} range	-	-	490 - 2200	370 - 1600	700 - 2680	480 - 2000
	h^+ range	-	-	5.2 - 24	5.4 - 23	5.6 - 22	5.3 - 22
	R' max	-	-	0.55	0.44	0.48	0.59
	RF _{max} (%)	-	-	4.5	3.8	3.8	4.8
	h^+ at max	-	-	14.3	14.5	14.3	14.6
Riblet drag enhancement	Re \sqrt{f} range	-	-	2200 - 10000	1600 - 9900	2680 - 9700	2000 - 9880
	Segment 1 Re \sqrt{f} range	-	-	2200 - 7450	1600 - 5600	2680 - 9700	2000 - 6200
	h^+ range	-	-	24 - 79	23 - 81	22 - 80	22 - 67
	$\approx 1/\sqrt{f}$	-	-	13.0±0.1	12.3±0.1	13.3±0.1	12.7±0.1
	Segment 2 Re \sqrt{f} range	-	-	7450 - 10000	5600 - 9900	2680 - 9700	6200 - 9880
	h^+ range	-	-	79 - 110	81 - 150	-	67 - 110
	R' _∞	-	-	-2.17	-2.43	(-1.84)	-1.88
	RF _∞ (%)	-	-	-14.0	-16.0	(-11.9)	-12.5

Values in parentheses correspond to minimum values in regime

Table 4.3.1. Summary of Drag Reduction by PEO W-301 in S2 and R2B. $d_s = 10.21 \text{ mm}; d_r = 9.80 \text{ mm}$ $h = 0.15 \text{ mm}; d/h = 65$

POLYMER: W-301

c, wppm		0 (solvent)	3	10	30	100
(a) Smooth Pipe: Polymer Solutions wrt Solvent.						
Turbulent Regime						
(i) Newtonian	Re \sqrt{f} range	300-9000	300-550	300-450	-	-
(ii) Polymeric	Re \sqrt{f} range	-	550-9000	450-4000	300-1500	300-500
(iii) MDR	Re \sqrt{f} range	-	-	-	1500-4500	500-4000
Parameters						
Onset	Re \sqrt{f} *	-	550	450	(350)	-
Slope Increment	δ	-	11	19	25	-
Linear Segment	Re \sqrt{f} range	-	550-4000	450-3000	400-1000	-
Poly. Drag Reduction	S' $_{\max}$	-	8.0	14	20	20
	Re \sqrt{f} @ max	-	4000	3000	4200	3800
(b) Riblet Pipe: Polymer Solutions wrt Solvent.						
Turbulent Regime						
(i) N	Re \sqrt{f} range	300-10000	300-550	300-400	-	-
(ii) P	Re \sqrt{f} range	-	550-9000	400-5000	300-1100	300-800
(iii) MDR	Re \sqrt{f} range	-	-	-	1100-5500	800-5000
Parameters						
Onset	Re \sqrt{f} *	-	550	400	(300)	-
Polymeric Segment 1	Slope	-	17	22	26	26
	Re \sqrt{f} range	-	550-2500	400-2000	300-1100	300-800
Polymeric Segment 2	Slope	-	-5	3	8	8
	Re \sqrt{f} range	-	2500-9000	2000-5000	1100-5500	800-5000
Poly. Drag Reduction	S' $_{\max}$	-	8.0	13	16	15
	Re \sqrt{f} @ max	-	3000	4000	5200	4700
(c) Polymer Solutions: Riblet wrt Smooth Wall.						
Turbulent Regime						
(i) HS	h $^+$ range	3.4-5.3	3.9-10	4.0-8.7	3.9-11	3.9-7.5
(ii) RDR	h $^+$ range	5.3-22	10-33	8.7-15	-	-
(iii) RDE	h $^+$ range	22-110	33-97	15-58	11-58	7.5-52
Parameters						
RDR	R' $_{\max}$	0.6	1.6	0.8	-	-
	h $^+$ @ max	15	20	11	-	-
RDE	R' $_{\min}$	-1.88	-2.3	-2.5	-6.1	-8.0
	h $^+$ @ min	110	97	58	58	52

Table 4.3.2a. Polymer degradation experiments.

Pipe designation		S1	S1D		S2	S2D	
d _s , mm		7.82	7.82		10.21	10.21	
*Station		1	2	3	1	2	3
L, m		0.780	1.510	1.790	1.450	2.540	-
L/d		100	193	230	142	249	-
Polymer	c, wppm						
none	0	✓	✓	✓	✓	✓	
N-60K	3	✓		✓	✓	✓	
	10	✓		✓	✓	✓	
	30				✓	✓	
W-301	1	✓✓	✓	✓			
	3	✓	✓		✓	✓	
	10	✓✓	✓	✓	✓	✓	
	30	✓	✓		✓	✓	
	100	✓✓	✓	✓	✓	✓	

* Station positions:

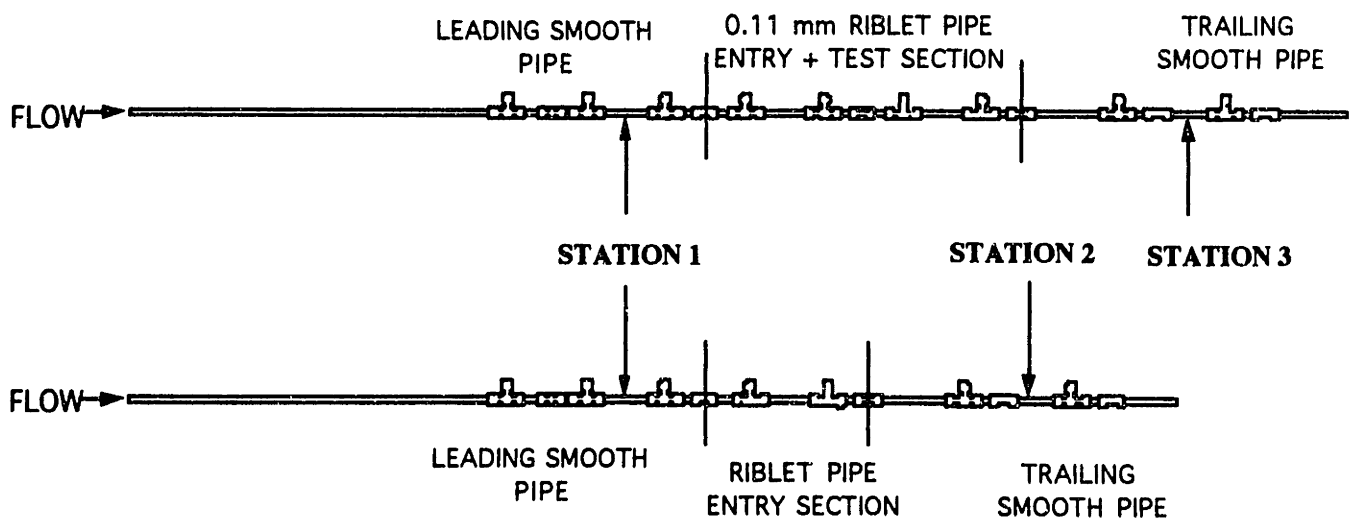


Table 4.3.2b. Drag Reduction Results at Station 1 for Polymer batches used in Degradation Experiments.

Batch	d_s , mm	Stations	Polymer	M_w	c wppm	τ_w^* N/m ²	$\delta/\nu c$
1	7.82	13	N-60K	2×10^6	3, 10	5.0 ± 0.8	3.5 ± 0.1
2	10.21	12	N-60K	2×10^6	3, 10, 30	5.5 ± 1.0	3.5 ± 0.2
3	7.82	12	W-301	5.5×10^6	1, 3, 10	1.9 ± 0.8	7.0 ± 0.2
4	7.82	13	W-301	5.5×10^6	1, 10	1.8 ± 0.7	7.3 ± 0.2
5	10.21	12	W-301	5.5×10^6	3, 10	2.5 ± 0.7	6.6 ± 0.1

Table 4.3.3. Summary of Drag Reduction by PEO N-10 in S2 and R2B. $d_s = 10.21$ mm; $d_r = 9.80$ mm $h = 0.145$ mm; $d/h = 65$

POLYMER: N-10

c, wppm		0 (solvent)	2435	5138
(a) Smooth Pipe: Polymer Solutions wrt Solvent.				
Turbulent Regime				
(i) Newtonian	Re \sqrt{f} range	300-9000	300-2000	300-1200
(ii) Polymeric	Re \sqrt{f} range	-	2000-5800	1200-4400
(iii) MDR	Re \sqrt{f} range	-	-	-
Parameters				
Onset	Re \sqrt{f} *	-	2000	1200
Slope Increment	δ	-	4.6	6.8
Linear Segment	Re \sqrt{f} range	-	2000-5800	1200-4400
Poly. Drag Reduction	S' _{max}	-	1.6	3.7
	Re \sqrt{f} @ max	-	5800	4400
(b) Riblet Pipe: Polymer Solutions wrt Solvent.				
Turbulent Regime				
(i) N	Re \sqrt{f} range	300-10000	300-1800	300-1200
(ii) P	Re \sqrt{f} range	-	1800-6800	1200-4800
(iii) MDR	Re \sqrt{f} range	-	-	-
Parameters				
Onset	Re \sqrt{f} *	-	1800	1200
Polymeric Segment 1	Slope	-	2.8	8.3
	Re \sqrt{f} range	-	1800-7000	1400-4800
Polymeric Segment 2	Slope	-	-	-
	Re \sqrt{f} range	-	-	-
Poly. Drag Reduction	S' _{max}	-	1.64	4.8
	Re \sqrt{f} @ max	-	6800	4800
(c) Polymer Solutions: Riblet wrt Smooth Wall.				
Turbulent Regime				
(i) HS	h ⁺ range	3.4-5.3	3-5	3-5
(ii) RDR	h ⁺ range	5.3-22	5-30	5-27
(iii) RDE	h ⁺ range	22-110	30-71	27-51
Parameters				
RDR	R' _{max}	0.6	0.55	0.50
	h ⁺ @ max	15	15	15
RDE	R' _{min}	-1.88	-2.3	-0.78
	h ⁺ @ min	110	71	51

Table 4.3.4. Summary of Drag Reduction by PEO N-750 in S2 and R2B. $d_s = 10.21 \text{ mm}; d_r = 9.80 \text{ mm}$ $h = 0.145 \text{ mm}; d/h = 65$

POLYMER: N-750

c, wppm		0 (solvent)	100	250	900	2073
(a) Smooth Pipe: Polymer Solutions wrt Solvent.						
Turbulent Regime						
(i) Newtonian	Rev/f range	300-9000	300-1200	300-1100	300-950	300-600
(ii) Polymeric	Rev/f range	-	1200-7600	1100-5500	950-5000	600-2450
(iii) MDR	Rev/f range	-	-	-	-	-
Parameters						
Onset	Rev/f *	-	1200	1100	950	600
Slope Increment	δ	-	7.8	10.2	17.3	30.3
Linear Segment	Rev/f range	-	2900-7600	2000-5500	1800-5000	1000-2450
Poly. Drag Reduction	S'_{max}	-	4.7	5.8	9.2	13.3
	Rev/f @ max	-	7600	5500	5000	2450
(b) Riblet Pipe: Polymer Solutions wrt Solvent.						
Turbulent Regime						
(i) N	Rev/f range	300-10000	300-1100	300-1100	300-950	300-600
(ii) P	Rev/f range	-	1100-8500	1100-7200	950-5200	600-2600
(iii) MDR	Rev/f range	-	-	-	-	-
Parameters						
Onset	Rev/f *	-	1100	1100	950	600
Polymeric Segment 1	Slope	-	6.1	10.8	15.0	28.1
	Rev/f range	-	1100-8500	1600-7200	1300-5200	800-2600
Polymeric Segment 2	Slope	-	-	-	-	-
	Rev/f range	-	-	-	-	-
Poly. Drag Reduction	S'_{max}	-	5.0	6.7	10.4	13.8
	Rev/f @ max	-	8500	7200	5200	2600
(c) Polymer Solutions: Riblet wrt Smooth Wall.						
Turbulent Regime						
(i) HS	h^+ range	3.4-5.3	3-6	3-6	3-5	3-5
(ii) RDR	h^+ range	5.3-22	6-40	6-43	5-34	5-23
(iii) RDE	h^+ range	22-110	40-94	43-74	34-55	23-27
Parameters						
RDR	$[R', R_F\%]_{max}$	0.6, 4.8	1.1, 7.5	1.8, 11.4	2.0, 12.8	1.9, 12.3
	h^+ @ max	15	30	25	22	13
RDE	R'_{min}	-1.88	-2.0	-3.0	-0.7	-0.5
	h^+ @ min	110	94	74	55	27

Table 4.3.5. Summary of Drag Reduction by PEO N-60K in S2 and R2B. $d_s = 10.21$ mm; $d_r = 9.80$ mm $h = 0.15$ mm; $d/h = 65$

POLYMER: PEO N-60K

c, wppm		0 (solvent)	3	10	30	100
(a) Smooth Pipe: Polymer Solutions wrt Solvent.						
Turbulent Regime						
(i) Newtonian	Re ν f range	300-9000	300-1150	300-1050	300-950	300-650
(ii) Polymeric	Re ν f range	-	1150-8000	1050-6350	950-5350	650-4350
(iii) MDR	Re ν f range	-	-	-	-	-
Parameters						
Onset	Re ν f *	-	1150	1050	950	650
Slope Increment	δ	-	5.2	10.4	16.4	27.0
Linear Segment	Re ν f range	-	1200-6000	1050-5400	1000-5350	800-4350
Poly. Drag Reduction	S' ν max	-	3.8	7.5	12.3	7.5
	Re ν f @ max	-	7000	6000	5400	4400
(b) Riblet Pipe: Polymer Solutions wrt Solvent.						
Turbulent Regime						
(i) N	Re ν f range	300-10000	300-1200	300-1050	300-850	300-650
(ii) P	Re ν f range	-	1200-9500	1050-7050	850-5800	650-5200
(iii) MDR	Re ν f range	-	-	-	-	-
Parameters						
Onset	Re ν f *	-	1200	1050	850	650
Polymeric Segment 1	Slope	-	9.0	18.6	25.2	27.5
	Re ν f range	-	1200-4200	1200-2700	1000-2400	700-1900
Polymeric Segment 2	Slope	-	-2.0	0.4	6.8	10.6
	Re ν f range	-	4600-9000	3000-7100	2800-5600	2000-5200
Poly. Drag Reduction	S' ν max	-	4.2	7.8	12.6	15.6
	Re ν f @ max	-	4800	6000	5800	5200
(c) Polymer Solutions: Riblet wrt Smooth Wall.						
Turbulent Regime						
(i) HS	h $^+$ range	3.4-5.3	3.4-5	3.4-5	3.4-5	3.4-5
(ii) RDR	h $^+$ range	5.3-22	5-32	5-40	5-42	5-24
(iii) RDE	h $^+$ range	22-110	40-98	32-77	42-64	24-57
Parameters						
RDR	R' ν max	0.6	0.7	1.5	2.2	0.9
	h $^+$ @ max	15	15	\approx 20	22	\approx 16
RDE	R' ν min	-1.88	-2.0	-2.0	-2.4	-5.7
	h $^+$ @ min	110	98	77	64	57

Table 4.3.6. Summary of Drag Reduction by PEO P-309 in S2 and R2B. $d_s = 10.21 \text{ mm}$; $d_r = 9.80 \text{ mm}$ $h = 0.145 \text{ mm}$; $d/h = 65$

POLYMER: P-309

c, wppm		0 (solvent)	50	100
(a) Smooth Pipe: Polymer Solutions wrt Solvent.				
Turbulent Regime				
(i) Newtonian	Re \sqrt{f} range	300-9000	-	-
(ii) Polymeric	Re \sqrt{f} range	-	300-750	-
(iii) MDR	Re \sqrt{f} range	-	750-3700	300-3200
Parameters				
Onset	Re \sqrt{f} *	-	-	-
Slope Increment	δ	-	-	-
Linear Segment	Re \sqrt{f} range	-	-	-
Poly. Drag Reduction	S' $_{\text{max}}$	-	20.3	19.9
	Re \sqrt{f} @ max	-	3700	3200
(b) Riblet Pipe: Polymer Solutions wrt Solvent.				
Turbulent Regime				
(i) N	Re \sqrt{f} range	300-10000	-	-
(ii) P	Re \sqrt{f} range	-	300-750	-
(iii) MDR	Re \sqrt{f} range	-	750-4400	300-3900
Parameters				
Onset	Re \sqrt{f} *	-	-	-
Polymeric Segment 1	Slope	-	21.3	17.8
	Re \sqrt{f} range	-	300-800	300-800
Polymeric Segment 2	Slope	-	11.6	10.8
	Re \sqrt{f} range	-	800-4400	900-3900
Poly. Drag Reduction	S' $_{\text{max}}$	-	16.6	15.7
	Re \sqrt{f} @ max	-	4400	3900
(c) Polymer Solutions: Riblet wrt Smooth Wall.				
Turbulent Regime				
(i) HS	h $^+$ range	3.4-5.3	3-9	3-9
(ii) RDR	h $^+$ range	5.3-22	-	-
(iii) RDE	h $^+$ range	22-110	9-48	9-42
Parameters				
RDR	R' $_{\text{max}}$	0.6	-	-
	h $^+$ @ max	15	-	-
RDE	R' $_{\text{min}}$	-1.88	-5.8	-6.8
	h $^+$ @ min	110	48	42

Table 4.3.7. Summary of Drag Reduction by PAM N-300L in S2 and R2B. $d_s = 10.21 \text{ mm}; d_r = 9.80 \text{ mm}$ $h = 0.145 \text{ mm}; d/h = 65$

POLYMER: N-300L

c, wppm		0 (solvent)	10	30	100	300
(a) Smooth Pipe: Polymer Solutions wrt Solvent.						
Turbulent Regime						
(i) Newtonian	Re ν f range	300-9000	300-850	300-700	300-500	300-400
(ii) Polymeric	Re ν f range	-	850-7800	700-6200	500-480	400-1400
(iii) MDR	Re ν f range	-	-	-	-	1400-3400
Parameters						
Onset	Re ν f *	-	850	700	500	400
Slope Increment	δ	-	6.9	12.3	18.7	30.8
Linear Segment	Re ν f range	-	900-4200	900-3500	700-3400	700-1100
Poly. Drag Reduction	S' $_{\text{max}}$	-	5.0	9.5	15.7	20.0
	Re ν f @ max	-	5500	6200	4800	3400
(b) Riblet Pipe: Polymer Solutions wrt Solvent.						
Turbulent Regime						
(i) N	Re ν f range	300-10000	300-850	300-650	300-450	300-400
(ii) P	Re ν f range	-	850-9100	650-7000	450-5300	400-1500
(iii) MDR	Re ν f range	-	-	-	-	1500-4100
Parameters						
Onset	Re ν f *	-	850	650	450	400
Polymeric Segment 1	Slope	-	10.0	16.6	25.8	25.5
	Re ν f range	-	900-3600	700-3600	600-2400	400-1600
Polymeric Segment 2	Slope	-	-2.0	11.0	9.0	10.3
	Re ν f range	-	3600-9100	3600-7000	240-5300	1600-4100
Poly. Drag Reduction	S' $_{\text{max}}$	-	5.5	9.7	15.3	15.9
	Re ν f @ max	-	4200	3600	5300	4100
(c) Polymer Solutions: Riblet wrt Smooth Wall.						
Turbulent Regime						
(i) HS	h $^+$ range	3.4-5.3	3-5	3-5	3-5	3-5
(ii) RDR	h $^+$ range	5.3-22	5-30	5-38	5-30	5-12
(iii) RDE	h $^+$ range	22-110	30-100	38-77	30-58	12-45
Parameters						
RDR	R' $_{\text{max}}$	0.6	1.0	1.2	2.6	0.8
	h $^+$ @ max	15	23	16	14	8
RDE	R' $_{\text{min}}$	-1.88	-2.5	-2.0	-2.6	-7.0
	h $^+$ @ min	110	100	77	50	45

Table 4.3.8. Summary of Drag Reduction by PAM N-300 in S2 and R2B. $d_s = 10.21 \text{ mm}; d_r = 9.80 \text{ mm}$ $h = 0.145 \text{ mm}; d/h = 65$

POLYMER: N-300

c, wppm		0 (solvent)	3	10	30	100
(a) Smooth Pipe: Polymer Solutions wrt Solvent.						
Turbulent Regime						
(i) Newtonian	Re ν f range	300-9000	300-550	-	-	-
(ii) Polymeric	Re ν f range	-	550-7500	300-6400	300-1100	300-600
(iii) MDR	Re ν f range	-	-	-	2000-4000	600-3800
Parameters						
Onset	Re ν f *	-	550	(350)	(320)	-
Slope Increment	δ	-	9.1	17.7	22.7	-
Linear Segment	Re ν f range	-	650-2300	450-1700	350-900	-
Poly. Drag Reduction	S' $_{\text{max}}$	-	5.9	13.1	19.2	20.9
	Re ν f @ max	-	3200	2700	3500	3800
(b) Riblet Pipe: Polymer Solutions wrt Solvent.						
Turbulent Regime						
(i) N	Re ν f range	300-10000	300-550	-	-	-
(ii) P	Re ν f range	-	550-9200	300-7700	300-1400	300-500
(iii) MDR	Re ν f range	-	-	-	2000-4200	500-4500
Parameters						
Onset	Re ν f *	-	550	(350)	(320)	-
Polymeric Segment 1	Slope	-	10.1	21.0	22.1	26.2
	Re ν f range	-	550-2300	400-1900	300-1400	320-900
Polymeric Segment 2	Slope	-	-5.0	-11.5	6.9	13.1
	Re ν f range	-	2600-9200	3000-7700	2000-4000	1000-4000
Poly. Drag Reduction	S' $_{\text{max}}$	-	7.5	12.4	15.7	17.6
	Re ν f @ max	-	2400	2700	5400	4500
(c) Polymer Solutions: Riblet wrt Smooth Wall.						
Turbulent Regime						
(i) HS	h $^+$ range	3.4-5.3	3-6	3-6	3-10	3-10
(ii) RDR	h $^+$ range	5.3-22	6-34	6-21	-	-
(iii) RDE	h $^+$ range	22-110	34-100	21-85	10-59	10-49
Parameters						
RDR	R' $_{\text{max}}$	0.6	1.5	0.8	-	-
	h $^+$ @ max	15	21	\approx 10	-	-
RDE	R' $_{\text{min}}$	-1.88	-2.2	-3.3	-5.1	-6.0
	h $^+$ @ min	110	100	85	59	49

Table 4.3.9. Summary of Drag Reduction by PEO W-301 and P-309 in S2 and R2BR.

$d_s = 10.21$ mm; $d_f = 9.80$ mm
 $h = 0.145$ mm; $d/h = 65$
 POLYMERS: W-301 and P-309

c, wppm		0 (solvent)	3 W301	10 W301	50 P309	100 P309
(a) Smooth Pipe: Polymer Solutions wrt Solvent.						
Turbulent Regime						
(i) Newtonian	Re ν f range	300-10000	300-800	300-600	-	-
(ii) Polymeric	Re ν f range	-	800-6700	600-5700	300-400	300-400
(iii) MDR	Re ν f range	-	-	-	400-4000	400-3700
Parameters						
Onset	Re ν f *	-	800	600	-	-
Slope Increment	δ	-	12.4	18.8	-	-
Linear Segment	Re ν f range	-	900-2900	700-2900	-	-
Poly. Drag Reduction	S' $_{max}$	-	5.9	11.8	20.2	20.7
	Re ν f @ max	-	6300	4700	4000	3700
(b) Riblet Pipe: Polymer Solutions wrt Solvent.						
Turbulent Regime						
(i) N	Re ν f range	300-10000	300-800	300-600	-	-
(ii) P	Re ν f range	-	800-7900	600-6700	300-400	300-400
(iii) MDR	Re ν f range	-	-	-	400-4000	400-3700
Parameters						
Onset	Re ν f *	-	800	600	-	-
Polymeric Segment 1	Slope	-	16.3	23.5	20	22
	Re ν f range	-	900-2400	700-1800	400-1000	400-1000
Polymeric Segment 2	Slope	-	-4.4	-2.5	9.9	9.6
	Re ν f range	-	4000-7900	3700-6700	1100-4400	1100-4400
Poly. Drag Reduction	S' $_{max}$	-	6.8	12.1	17.9	17.5
	Re ν f @ max	-	4200	4300	4500	4400
(c) Polymer Solutions: Riblet wrt Smooth Wall.						
Turbulent Regime						
(i) HS	h $^+$ range	4-5	4-6	4-5	3-11	3-11
(ii) RDR	h $^+$ range	5-22	6-28	5-25	(8-11)	(7-10)
(iii) RDE	h $^+$ range	22-110	28-87	25-73	11-49	11-48
Parameters						
RDR	R' $_{max}$	0.45	0.87	1.6	(0.5)	(0.6)
	h $^+$ @ max	15	21	18	(11)	(8)
RDE	R' $_{min}$	-2.33	-2.3	-2.8	-4.7	-6.4
	h $^+$ @ min	110	87	73	43	48

Note: Numbers in parentheses are uncertain

Table 4.3.10. Summary of Drag Reduction by PEO N-750 in S1 and R1A.

$d_s = 7.82 \text{ mm}; d_r = 7.54 \text{ mm}$

$h = 0.105 \text{ mm}; d/h = 71$

POLYMER: N-750

c, wppm		0 (solvent)	100	300	1000
(a) Smooth Pipe: Polymer Solutions wrt Solvent.					
Turbulent Regime					
(i) Newtonian	Revf range	300-9000	300-1250	300-950	300-700
(ii) Polymeric	Revf range	-	1250-6400	950-5900	700-4700
(iii) MDR	Revf range	-	-	-	-
Parameters					
Onset	Revf *	-	1250	950	700
Slope Increment	δ	-	7.6	11.7	19.8
Linear Segment	Revf range	-	130-6400	940-5900	1000-4700
Poly. Drag Reduction	S' max	-	5.1	8.2	13.3
	Revf @ max	-	6400	5900	4700
(b) Riblet Pipe: Polymer Solutions wrt Solvent.					
Turbulent Regime					
(i) N	Revf range	300-10000	300-1250	300-950	300-700
(ii) P	Revf range	-	1250-7000	950-6600	700-5600
(iii) MDR	Revf range	-	-	-	-
Parameters					
Onset	Revf *	-	1250	950	700
Polymeric Segment 1	Slope	-	8.3	11.0	14.9
	Revf range	-	1100-7000	1100-6600	1000-5600
Polymeric Segment 2	Slope	-	-	-	-
	Revf range	-	-	-	-
Poly. Drag Reduction	S' max	-	5.5	8.1	10.7
	Revf @ max	-	7000	6600	5600
(c) Polymer Solutions: Riblet wrt Smooth Wall.					
Turbulent Regime					
(i) HS	h^+ range	3.6-5.2	3-5	3-5	3-5
(ii) RDR	h^+ range	5.2-24	5-23	5-23	5-20
(iii) RDE	h^+ range	24-110	20-72	23-69	20-58
Parameters					
RDR	R' max	0.55	0.5	0.5	0.5
	h^+ @ max	14	14	14	14
RDE	R' min	-2.17	-1.8	-2.5	-6.2
	h^+ @ min	110	72	69	58

Table 4.3.11. Summary of Drag Reduction by PEO N-60K in S1 and R1A.

$d_s = 7.82 \text{ mm}; d_r = 7.54 \text{ mm}$

$h = 0.105 \text{ mm}; d/h = 71$

POLYMER: N-60K

c, wppm		0 (solvent)	3	10	30	100
(a) Smooth Pipe: Polymer Solutions wrt Solvent.						
Turbulent Regime						
(i) Newtonian	Re ν f range	300-9000	300-750	300-650	300-600	300-500
(ii) Polymeric	Re ν f range	-	750-600	650-6000	600-5600	500-1700
(iii) MDR	Re ν f range	-	-	-	-	1700-4400
Parameters						
Onset	Re ν f *	-	750	650	600	500
Slope Increment	δ	-	7.8	13.7	20.7	32.0
Linear Segment	Re ν f range	-	900-2400	900-2600	800-2800	700-1500
Poly. Drag Reduction	S' $_{\max}$	-	4.4	8.3	14.3	19.4
	Re ν f @ max	-	3800	4300	4600	4400
(b) Riblet Pipe: Polymer Solutions wrt Solvent.						
Turbulent Regime						
(i) N	Re ν f range	300-10000	300-750	300-650	300-550	300-450
(ii) P	Re ν f range	-	750-7200	650-7100	550-7000	450-1700
(iii) MDR	Re ν f range	-	-	-	-	1700-5900
Parameters						
Onset	Re ν f *	-	750	650	550	450
Polymeric Segment 1	Slope	-	11.8	17.9	21.7	26.7
	Re ν f range	-	900-2400	800-1900	700-1700	500-1400
Polymeric Segment 2	Slope	-	-3.0	1.8	2.5	5.3
	Re ν f range	-	3000-7200	2900-580	2200-6700	1800-5100
Poly. Drag Reduction	S' $_{\max}$	-	4.1	7.2	10.6	14.2
	Re ν f @ max	-	3800	5800	5600	5100
(c) Polymer Solutions: Riblet wrt Smooth Wall.						
Turbulent Regime						
(i) HS	h $^+$ range	3.6-5.2	3-5	3-5	3-5	3-5
(ii) RDR	h $^+$ range	5.2-24	5-22	5-20	5-16	5-11
(iii) RDE	h $^+$ range	24-110	22-73	20-73	16-72	11-61
Parameters						
RDR	R' $_{\max}$	0.55	0.5	0.6	1.0	1.2
	h $^+$ @ max	14	12	10	10	8
RDE	R' $_{\min}$	-2.17	-2.3	-2.8	-5.2	-9.6
	h $^+$ @ min	110	73	73	53	61

Table 4.3.12. Summary of Drag Reduction by PEO W-301, PEO P-309 and PAM N-300 in S1 and R1A. $d_s = 7.82 \text{ mm}; d_r = 7.54 \text{ mm}$ $h = 0.105 \text{ mm}; d/h = 71$

POLYMERS: W-301, P-309 and N-300

c, wppm		0 (solvent)	100 W301	50 P309	100 P309	100 N300
(a) Smooth Pipe: Polymer Solutions wrt Solvent.						
Turbulent Regime						
(i) Newtonian	Re ν f range	300-9000	-	-	-	-
(ii) Polymeric	Re ν f range	-	-	300-600	-	300-400
(iii) MDR	Re ν f range	-	300-3700	600-4100	300-3700	400-4000
Parameters						
Onset	Re ν f *	-	-	-	-	-
Slope Increment	δ	-	-	-	-	-
Linear Segment	Re ν f range	-	-	-	-	-
Poly. Drag Reduction	S' $_{\text{max}}$	-	21.1	20.7	21.3	21.8
	Re ν f @ max	-	3700	4100	3700	4000
(b) Riblet Pipe: Polymer Solutions wrt Solvent.						
Turbulent Regime						
(i) N	Re ν f range	300-10000	-	-	-	-
(ii) P	Re ν f range	-	-	300-600	-	300-400
(iii) MDR	Re ν f range	-	300-4900	600-5500	300-4700	400-5900
Parameters						
Onset	Re ν f *	-	-	-	-	-
Polymeric Segment 1	Slope	-	20.0	21.7	20.2	21.9
	Re ν f range	-	300-1200	300-1500	300-1300	300-1100
Polymeric Segment 2	Slope	-	2.9	1.3	2.4	1.6
	Re ν f range	-	1200-4500	1500-4800	1300-4700	1400-4400
Poly. Drag Reduction	S' $_{\text{max}}$	-	14.5	14.4	15.0	14
	Re ν f @ max	-	4500	4900	4700	5000
(c) Polymer Solutions: Riblet wrt Smooth Wall.						
Turbulent Regime						
(i) HS	h $^+$ range	3.6-5.2	3-8	3-10	3-10	3-10
(ii) RDR	h $^+$ range	5.2-24	8-12	10-14	10-14	10-13
(iii) RDE	h $^+$ range	24-110	12-45	14-58	14-44	13-46
Parameters						
RDR	R' $_{\text{max}}$	0.55	0.75	0.7	0.7	0.9
	h $^+$ @ max	14	11	11	11	11
RDE	R' $_{\text{min}}$	-2.17	-9.5	-9.5	-9.6	-9.8
	h $^+$ @ min	110	45	58	44	46

Table 4.3.13. Summary of Drag Reduction by PEO N-60K and 100 wppm W-301 in S1 and R1AR. $d_s = 7.82 \text{ mm}; d_r = 7.54 \text{ mm}$ $h = 0.105 \text{ mm}; d/h = 71$

POLYMER: N-60K and 100 wppm W-301

c, wppm		0 (solvent)	3 N60K	10 N60K	30 N60K	100 N60K	100 W301
(a) Smooth Pipe: Polymer Solutions wrt Solvent.							
Turbulent Regime							
(i) Newtonian	Re/f range	300-10000	300-900	300-700	300-550	300-500	-
(ii) Polymeric	Re/f range	-	900-7000	700-5600	550-4700	500-1400	-
(iii) MDR	Re/f range	-	-	-	-	1400-4000	300-3700
Parameters							
Onset	Re/f *	-	900	700	550	500	-
Slope Increment	δ	-	8.8	15.5	21.1	30.3	-
Linear Segment	Re/f range	-	1200-3100	900-2700	800-2400	550-1300	-
Poly. Drag Reduction	S'_{max}	-	4.8	9.3	15	19	20
	Re/f @ max	-	7000	5100	4700	4000	3700
(b) Riblet Pipe: Polymer Solutions wrt Solvent.							
Turbulent Regime							
(i) N	Re/f range	300-10000	300-800	300-650	300-550	300-450	-
(ii) P	Re/f range	-	800-8400	650-6700	550-6100	450-1400	-
(iii) MDR	Re/f range	-	-	-	-	1400-5400	300-4700
Parameters							
Onset	Re/f *	-	800	650	550	450	-
Polymeric Segment 1	Slope	-	10.2	13.6	18.7	24.5	19.0
	Re/f range	-	850-3000	700-2900	600-1700	450-1400	300-1100
Polymeric Segment 2	Slope	-	-2.9	1.7	3.4	-0.8	7.9
	Re/f range	-	4000-8400	3500-8400	2300-6100	2200-5400	1100-3800
Poly. Drag Reduction	S'_{max}	-	4.8	8.0	11	13	16
	Re/f @ max	-	4300	5100	6100	2800	3400
(c) Polymer Solutions: Riblet wrt Smooth Wall.							
Turbulent Regime							
(i) HS	h^+ range	3.1-5.1	3.8-5.1	4.0-5.2	4.0-5.0	3.7-4.6	3.8-8.0
(ii) RDR	h^+ range	5.1-21	5.1-21	5.2-17	5.0-14	4.6-11	8.0-10
(iii) RDE	h^+ range	21-110	21-85	17-69	14-63	11-50	10-49
Parameters							
RDR	R'_{max}	0.48	0.76	0.85	0.81	1.5	0.35
	$h^+ @ max$	14	11	10.8	10.1	7.3	8.9
RDE	R'_{min}	-2.19	-2.4	-2.8	-2.8	-8.9	-8.3
	$h^+ @ min$	110	85	63	69	50	49

Table 4.3.14. Summary of Drag Reduction by PEO W-301 in S1 and R1AR. $d_s = 7.82 \text{ mm}; d_r = 7.54 \text{ mm}$ $h = 0.105 \text{ mm}; d/h = 71$

POLYMER: W-301

c, wppm		0 (solvent)	1	3	10	30	100
(a) Smooth Pipe: Polymer Solutions wrt Solvent.							
Turbulent Regime							
(i) Newtonian	Re ν f range	300-10000	300-750	300-600	300-400	-	-
(ii) Polymeric	Re ν f range	-	750-7200	600-6700	400-5400	300-500	-
(iii) MDR	Re ν f range	-	-	-	-	500-4200	300-3700
Parameters							
Onset	Re ν f *	-	750	600	400	(300)	-
Slope Increment	δ	-	6.5	12.1	21.7	-	-
Linear Segment	Re ν f range	-	900-2700	800-2200	600-1500	-	-
Poly. Drag Reduction	S' $_{\max}$	-	3.3	7.0	14.6	18.6	20.4
	Re ν f @ max	-	3400	3100	2800	420	3700
(b) Riblet Pipe: Polymer Solutions wrt Solvent.							
Turbulent Regime							
(i) N	Re ν f range	300-10000	300-700	300-550	300-400	-	-
(ii) P	Re ν f range	-	700-8600	550-8100	400-6800	300-500	-
(iii) MDR	Re ν f range	-	-	-	-	500-5800	300-4700
Parameters							
Onset	Re ν f *	-	700	550	400	-	-
Polymeric Segment 1	Slope	-	9.2	12.8	24.4	24.3	19.0
	Re ν f range	-	700-2200	600-1900	500-1100	500-1100	300-1100
Polymeric Segment 2	Slope	-	-3.0	-4.0	-2.1	-5.3	7.9
	Re ν f range	-	2400-8600	2900-8100	2100-5700	2100-5800	1100-3800
Poly. Drag Reduction	S' $_{\max}$	-	3.3	5.9	9.3	13.5	16.0
	Re ν f @ max	-	3400	3600	3300	1900	3400
(c) Polymer Solutions: Riblet wrt Smooth Wall.							
Turbulent Regime							
(i) HS	h $^+$ range	3.1-5.1	3.6-5.1	3.6-5.1	3.5-5.2	3.8-8.1	3.8-8.0
(ii) RDR	h $^+$ range	5.1-21	5.1-21	5.1-14	5.2-10	8.1-11	8.0-10
(iii) RDE	h $^+$ range	21-110	21-89	14-84	10-70	11-60	10-49
Parameters							
RDR	R' $_{\max}$	0.48	0.57	0.71	0.95	0.38	0.35
	h $^+$ @ max	14	9.1	8.7	7.1	9.1	8.9
RDE	R' $_{\min}$	-2.19	-2.1	-2.4	5.8	-9.6	-8.3
	h $^+$ @ min	110	89	84	31	60	49

Table 4.3.15. Summary of Drag Reduction by PEO N-750 in S1 and R1B.

$d_s = 7.82 \text{ mm}$; $d_r = 7.44 \text{ mm}$
 $h = 0.145 \text{ mm}$; $d/h = 51$
 POLYMER: N-750

c, wppm		0 (solvent)	100	300
(a) Smooth Pipe: Polymer Solutions wrt Solvent.				
Turbulent Regime				
(i) Newtonian	Re \sqrt{f} range	300-9000	300-1200	300-900
(ii) Polymeric	Re \sqrt{f} range	-	1200-6800	900-6000
(iii) MDR	Re \sqrt{f} range	-	-	-
Parameters				
Onset	Re \sqrt{f} *	-	1200	900
Slope Increment	δ	-	9.1	12.9
Linear Segment	Re \sqrt{f} range	-	1800-6800	1800-6000
Poly. Drag Reduction	S' $_{\max}$	-	5.9	8.5
	Re \sqrt{f} @ max	-	6800	6000
(b) Riblet Pipe: Polymer Solutions wrt Solvent.				
Turbulent Regime				
(i) N	Re \sqrt{f} range	300-10000	300-1100	300-850
(ii) P	Re \sqrt{f} range	-	1100-8000	850-7100
(iii) MDR	Re \sqrt{f} range	-	-	-
Parameters				
Onset	Re \sqrt{f} *	-	1100	850
Polymeric Segment 1	Slope	-	7.8	10.6
	Re \sqrt{f} range	-	1400-8000	1400-7100
Polymeric Segment 2	Slope	-	-	-
	Re \sqrt{f} range	-	-	-
Poly. Drag Reduction	S' $_{\max}$	-	5.7	8.3
	Re \sqrt{f} @ max	-	8000	7100
(c) Polymer Solutions: Riblet wrt Smooth Wall.				
Turbulent Regime				
(i) HS	h $^+$ range	-	-	-
(ii) RDR	h $^+$ range	5.4-23	5-28	5-28
(iii) RDE	h $^+$ range	23-150	28-113	28-100
Parameters				
RDR	R' $_{\max}$	0.44	0.55	0.60
	h $^+$ @ max	14	15	14
RDE	R' $_{\min}$	-2.43	-3.4	-3.6
	h $^+$ @ min	150	113	100

Table 4.3.16. Summary of Drag Reduction by PEO N-60K in S1 and R1B. $d_s = 7.82 \text{ mm}; d_r = 7.44 \text{ mm}$ $h = 0.145 \text{ mm}; d/h = 51$

POLYMER: N-60K

c, wppm		0 (solvent)	3	10	30	100
(a) Smooth Pipe: Polymer Solutions wrt Solvent.						
Turbulent Regime						
(i) Newtonian	Re \sqrt{f} range	300-9000	300-750	300-700	300-600	300-450
(ii) Polymeric	Re \sqrt{f} range	-	750-7300	700-7000	600-5900	450-1400
(iii) MDR	Re \sqrt{f} range	-	-	-	-	1400-4400
Parameters						
Onset	Re \sqrt{f} *	-	750	700	600	450
Slope Increment	δ	-	7.5	13.1	21.4	33.0
Linear Segment	Re \sqrt{f} range	-	850-3300	800-2900	850-2000	800-1400
Poly. Drag Reduction	S' $_{max}$	-	4.1	8.3	13.4	18.7
	Re \sqrt{f} @ max	-	7300	4400	4100	4400
(b) Riblet Pipe: Polymer Solutions wrt Solvent.						
Turbulent Regime						
(i) N	Re \sqrt{f} range	300-10000	300-750	300-650	300-550	300-450
(ii) P	Re \sqrt{f} range	-	750-9500	650-9000	550-7600	450-1400
(iii) MDR	Re \sqrt{f} range	-	-	-	-	1400-5500
Parameters						
Onset	Re \sqrt{f} *	-	750	650	550	450
Polymeric Segment 1	Slope	-	8.2	13.1	18.0	22.9
	Re \sqrt{f} range	-	800-2700	800-2500	700-2000	500-1000
Polymeric Segment 2	Slope	-	-3.2	-2.2	5.0	9.5
	Re \sqrt{f} range	-	3400-9300	4000-9000	2500-6100	1500-5000
Poly. Drag Reduction	S' $_{max}$	-	4.1	7.6	11.1	15.4
	Re \sqrt{f} @ max	-	4100	4200	4700	5500
(c) Polymer Solutions: Riblet wrt Smooth Wall.						
Turbulent Regime						
(i) HS	h $^+$ range	-	-	-	-	-
(ii) RDR	h $^+$ range	5.4-23	5-23	5-22	5-20	5-14
(iii) RDE	h $^+$ range	23-150	23-133	22-128	20-107	14-79
Parameters						
RDR	R' $_{max}$	0.44	0.6	0.8	0.6	1.0
	h $^+$ @ max	14	14	13	14	10
RDE	R' $_{min}$	-2.43	-4.1	-4.1	-4.8	-6.6
	h $^+$ @ min	150	133	128	107	79

Table 4.3.17. Summary of Drag Reduction by PEO W-301, PEO P-309 and PAM N-300 in S1 and R1B. $d_s = 7.82 \text{ mm}; d_r = 7.44 \text{ mm}$ $h = 0.145 \text{ mm}; d/h = 51$

POLYMERS: W-301, P-309, N-300

c, wppm		0 (solvent)	100 W301	50 P309	100 P309	100 N300
(a) Smooth Pipe: Polymer Solutions wrt Solvent.						
Turbulent Regime						
(i) Newtonian	Re \sqrt{f} range	300-9000	-	-	-	-
(ii) Polymeric	Re \sqrt{f} range	-	-	-	-	300-400
(iii) MDR	Re \sqrt{f} range	-	300-3900	300-4500	300-3800	400-4200
Parameters						
Onset	Re \sqrt{f} *	-	-	-	-	-
Slope Increment	δ	-	-	-	-	-
Linear Segment	Re \sqrt{f} range	-	-	-	-	-
Poly. Drag Reduction	S' $_{\max}$	-	21.1	21.4	21.3	21.9
	Re \sqrt{f} @ max	-	390	4500	3800	4200
(b) Riblet Pipe: Polymer Solutions wrt Solvent.						
Turbulent Regime						
(i) N	Re \sqrt{f} range	300-10000	-	-	-	-
(ii) P	Re \sqrt{f} range	-	-	-	-	300-400
(iii) MDR	Re \sqrt{f} range	-	300-4900	300-5800	300-4700	400-5600
Parameters						
Onset	Re \sqrt{f} *	-	-	-	-	-
Polymeric Segment 1	Slope	-	20.3	20.3	20.7	21.2
	Re \sqrt{f} range	-	300-1000	300-1000	300?-1000	300-1000
Polymeric Segment 2	Slope	-	11.8	12.5	13.5	8.6
	Re \sqrt{f} range	-	2000-4200	2200-4100	2200-4500	1900-4500
Poly. Drag Reduction	S' $_{\max}$	-	17.3	16.8	17.6	16.2
	Re \sqrt{f} @ max	-	4900	5800	4700	5600
(c) Polymer Solutions: Riblet wrt Smooth Wall.						
Turbulent Regime						
(i) HS	h $^+$ range	-	5-8	5-9	5-8	5-9
(ii) RDR	h $^+$ range	5.4-23	8-14	9-14	8-14	9-14
(iii) RDE	h $^+$ range	23-150	14-70	14-83	14-66	14-80
Parameters						
RDR	R' $_{\max}$	0.44	0.9	0.80	0.80	0.4
	h $^+$ @ max	14	10	11	11	11
RDE	R' $_{\min}$	-2.43	-7.2	-7.4	-7.3	-9.2
	h $^+$ @ min	150	70	83	66	80

Table 4.3.18. Summary of Drag Reduction by PEO N-750 in S2 and R2A. $d_s = 10.21 \text{ mm}$; $d_r = 9.93 \text{ mm}$ $h = 0.105 \text{ mm}$; $d/h = 95$

POLYMER: N-750

c, wppm		0 (solvent)	100	250	1000
(a) Smooth Pipe: Polymer Solutions wrt Solvent.					
Turbulent Regime					
(i) Newtonian	Revf range	300-9000	300-2100	300-1200	300-1000
(ii) Polymeric	Revf range	-	2100-7400	1200-6700	1000-4800
(iii) MDR	Revf range	-	-	-	-
Parameters					
Onset	Revf *	-	2100	1200	1000
Slope Increment	δ	-	9.3	12.6	18.9
Linear Segment	Revf range	-	2300-7400	2400-6700	1700-4800
Poly. Drag Reduction	S'_{\max}	-	4.9	6.9	9.9
	Revf @ max	-	7400	6700	4800
(b) Riblet Pipe: Polymer Solutions wrt Solvent.					
Turbulent Regime					
(i) N	Revf range	300-10000	300-2000	300-1300	300-1000
(ii) P	Revf range	-	2000-8100	1300-7100	1000-5200
(iii) MDR	Revf range	-	-	-	-
Parameters					
Onset	Revf *	-	2000	1300	1000
Polymeric Segment 1	Slope	-	10.1	13.1	17.3
	Revf range	-	2600-8100	2100-7100	1900-5200
Polymeric Segment 2	Slope	-	-	-	-
	Revf range	-	-	-	-
Poly. Drag Reduction	S'_{\max}	-	5.5	17.3	9.7
	Revf @ max	-	8100	7100	5200
(c) Polymer Solutions: Riblet wrt Smooth Wall.					
Turbulent Regime					
(i) HS	h^+ range	2.8-5.6	3-5	3-5	3-5
(ii) RDR	h^+ range	5.6-22	5-21	5-20	5-20
(iii) RDE	h^+ range	23-80	21-62	20-55	20-41
Parameters					
RDR	R'_{\max}	0.48	0.5	0.5	0.7
	h^+ @ max	14	14	14	13
RDE	R'_{\min}	-1.84	-1.3,	-1.6	-2.3
	h^+ @ min	80	62	55	41

Table 4.3.19. Summary of Drag Reduction by PEO N-60K in S2 and R2A. $d_s = 10.21$ mm; $d_r = 9.93$ mm $h = 0.105$ mm; $d/h = 95$

POLYMER: N-60K

c, wppm		0 (solvent)	3	10	30	100
(a) Smooth Pipe: Polymer Solutions wrt Solvent.						
Turbulent Regime						
(i) Newtonian	Revf range	300-9000	300-1100	300-900	300-700	300-550
(ii) Polymeric	Revf range	-	1100-8000	900-6700	700-5500	550-3300
(iii) MDR	Revf range	-	-	-	-	-
Parameters						
Onset	Revf *	-	1100	900	700	550
Slope Increment	δ	-	7.8	13.0	19.5	28.9
Linear Segment	Revf range	-	1400-3900	1200-3700	1100-360	1200-3300
Poly. Drag Reduction	S'_{max}	-	4.6	8.3	12.8	17
	Revf @ max	-	6100	6700	5500	3300
(b) Riblet Pipe: Polymer Solutions wrt Solvent.						
Turbulent Regime						
(i) N	Revf range	300-10000	300-1100	300-850	300-700	300-550
(ii) P	Revf range	-	1100-9300	850-7500	700-6200	550-5000
(iii) MDR	Revf range	-	-	-	-	-
Parameters						
Onset	Revf *	-	1100	850	700	550
Polymeric Segment 1	Slope	-	11.0	17.7	22.9	27.4
	Revf range	-	1300-3500	1200-2600	1000-2600	900-4800
Polymeric Segment 2	Slope	-	-1.3	4.5	7.2	19.0
	Revf range	-	3800-9200	2600-7000	2600-6200	1500-4900
Poly. Drag Reduction	S'_{max}	-	4.3	7.7	11	16.8
	Revf @ max	-	5100	7500	6200	5000
(c) Polymer Solutions: Riblet wrt Smooth Wall.						
Turbulent Regime						
(i) HS	h^+ range	2.8-5.6	3-5	3-5	3-5	3-5
(ii) RDR	h^+ range	5.6-22	5-23	5-22	5-21	5-14
(iii) RDE	h^+ range	23-80	23-73	22-59	21-49	14-38
Parameters						
RDR	R'_{max}	0.48	0.6	1.0	1.6	1.4
	h^+ @ max	14	15	15	14	11
RDE	R'_{min}	-1.84	-2.1	-2.3	-3.4	-3.8
	h^+ @ min	80	73	59	49	30

Table 4.3.20. Summary of Drag Reduction by PEO W-301 in S2 and R2A.

$d_s = 10.21 \text{ mm}; d_r = 9.93 \text{ mm}$

$h = 0.105 \text{ mm}; d/h = 95$

POLYMER: W-301

c, wppm		0 (solvent)	3	10	30	100
(a) Smooth Pipe: Polymer Solutions wrt Solvent.						
Turbulent Regime						
(i) Newtonian	Revf range	300-9000	300-700	300-500	-	-
(ii) Polymeric	Revf range	-	700-6700	500-5700	300-1400	300-700
(iii) MDR	Revf range	-	-	-	1400-4400	700-3800
Parameters						
Onset	Revf *	-	700	500	(400)	-
Slope Increment	δ	-	11.8	20.4	28.1	-
Linear Segment	Revf range	-	800-3200	800-2800	600-1200	-
Poly. Drag Reduction	S'_{\max}	-	7.4	13.2	19.8	19.9
	Revf @ max	-	4000	3600	4400	3800
(b) Riblet Pipe: Polymer Solutions wrt Solvent.						
Turbulent Regime						
(i) N	Revf range	300-10000	300-700	300-500	-	-
(ii) P	Revf range	-	700-7600	500-6500	300-1600	300-700
(iii) MDR	Revf range	-	-	-	1600-4900	700-4200
Parameters						
Onset	Revf *	-	700	500	(400)	-
Polymeric Segment 1	Slope	-	18.2	25.3	29.0	28.2
	Revf range	-	1000-2300	900-2200	500-1600	300-1100
Polymeric Segment 2	Slope	-	-3.7	-2.7	6.5	7.9
	Revf range	-	3300-7500	2300-5200	1800-4100	1500-3600
Poly. Drag Reduction	S'_{\max}	-	7.2	11.9	17.4	18.2
	Revf @ max	-	4100	3500	4900	4200
(c) Polymer Solutions: Riblet wrt Smooth Wall.						
Turbulent Regime						
(i) HS	h^+ range	2.8-5.6	3-5	3-5	3-5	3-5
(ii) RDR	h^+ range	5.6-22	5-23	5-19	5-15	5-14
(iii) RDE	h^+ range	23-80	23-60	19-51	15-39	14-33
Parameters						
RDR	R'_{\max}	0.48	0.70	1.3	1.2	1.6
	h^+ @ max	14	18	12	10	9
RDE	R'_{\min}	-1.84	-1.8	-2.6	-4.5	-3.3
	h^+ @ min	80	60	51	39	33

Table 4.3.21. Summary of Drag Reduction by PEO P-309 in S2 and R2A. $d_s = 10.21$ mm; $d_r = 9.93$ mm $h = 0.105$ mm; $d/h = 95$

POLYMER: P-309

c, wppm		0 (solvent)	50	100	200
(a) Smooth Pipe: Polymer Solutions wrt Solvent.					
Turbulent Regime					
(i) Newtonian	Re \sqrt{f} range	300-9000	-	-	-
(ii) Polymeric	Re \sqrt{f} range	-	300-500	-	-
(iii) MDR	Re \sqrt{f} range	-	500-4000	300-3500	300-2800
Parameters					
Onset	Re \sqrt{f} *	-	-	-	-
Slope Increment	δ	-	-	-	-
Linear Segment	Re \sqrt{f} range	-	-	-	-
Poly. Drag Reduction	S' $_{max}$	-	19.9	20.4	20.7
	Re \sqrt{f} @ max	-	4000	3500	2800
(b) Riblet Pipe: Polymer Solutions wrt Solvent.					
Turbulent Regime					
(i) N	Re \sqrt{f} range	300-10000	-	-	-
(ii) P	Re \sqrt{f} range	-	300-500	-	-
(iii) MDR	Re \sqrt{f} range	-	500-4200	300-3800	300-3000
Parameters					
Onset	Re \sqrt{f} *	-	-	-	-
Polymeric Segment 1	Slope	-	21.3	22.1	27
	Re \sqrt{f} range	-	300-1200	400-1200	300-1500
Polymeric Segment 2	Slope	-	8.3	8.8	6.0
	Re \sqrt{f} range	-	1600-4200	1600-3800	1600-3000
Poly. Drag Reduction	S' $_{max}$	-	19.4	19.3	19.2
	Re \sqrt{f} @ max	-	4200	3800	3800
(c) Polymer Solutions: Riblet wrt Smooth Wall.					
Turbulent Regime					
(i) HS	h $^+$ range	2.8-5.6	3-6	3-6	3-6
(ii) RDR	h $^+$ range	5.6-22	7-17	7-17	6-17
(iii) RDE	h $^+$ range	23-80	17-34	17-30	17-25
Parameters					
RDR	R' $_{max}$	0.48	1.9	1.9	2.8
	h $^+$ @ max	14	10	10	10
RDE	R' $_{min}$	-1.84	-1.8	-2.1	-2.4
	h $^+$ @ min	80	34	30	25

Table 4.3.22. Summary of Drag Reduction by PEO P-309 in S2 and R2AR.

$$d_s = 10.21 \text{ mm}; d_r = 9.93 \text{ mm}$$

$$h = 0.105 \text{ mm}; d/h = 95$$

POLYMER: P-309

c, wppm		0 (solvent)	50	100
(a) Smooth Pipe: Polymer Solutions wrt Solvent.				
Turbulent Regime				
(i) Newtonian	Re/f range	300-9000	-	-
(ii) Polymeric	Re/f range	-	300-500	-
(iii) MDR	Re/f range	-	500-3800	300-3300
Parameters				
Onset	Re/f *	-	-	-
Slope Increment	δ	-	-	-
Linear Segment	Re/f range	-	-	-
Poly. Drag Reduction	S' max	-	20.7	20.4
	Re/f @ max	-	3800	3300
(b) Riblet Pipe: Polymer Solutions wrt Solvent.				
Turbulent Regime				
(i) N	Re/f range	300-10000	-	-
(ii) P	Re/f range	-	300-500	-
(iii) MDR	Re/f range	-	500-4300	300-3700
Parameters				
Onset	Re/f *	-	-	-
Polymeric Segment 1	Slope	-	23.8	21.5
	Re/f range	-	500-1500	300-1500
Polymeric Segment 2	Slope	-	6.2	6.8
	Re/f range	-	1500-4200	1500-3700
Poly. Drag Reduction	S' max	-	18.3	17.7
	Re/f @ max	-	4300	3700
(c) Polymer Solutions: Riblet wrt Smooth Wall.				
Turbulent Regime				
(i) HS	h^+ range	3.3-5.0	3-7	3-5
(ii) RDR	h^+ range	5.0-24	7-14	5-14
(iii) RDE	h^+ range	24-80	14-33	14-29
Parameters				
RDR	R' max	0.54	1.5	1.5
	h^+ @ max	14	8	7
RDE	R' min	-2.20	-3.8	-3.7
	h^+ @ min	80	33	29

Table 4.4.1. Experiments at maximum drag reduction.

Pipe designation			S1/R1A	S1/R1B	S2/R2A	S2/R2B
	d_s , mm		7.82	7.82	10.21	10.21
	h , mm		0.11	0.15	0.11	0.15
	$d_r/2h$		36	26	47	34
Species	Type	c , wppm	Rev/f range	Rev/f range	Rev/f range	Rev/f range
PEO	P-309	50	600-5500	300-5800	500-4200	750-4400
		100	300-4700	300-4700	300-3800	300-3900
		200	-	-	300-3000	-
	W-301	30	<i>500-5800</i>	-	1600-4900	1100-5500
		100	300-4900	300-4900	700-4200	500-5000
	N-60K	100	<i>1700-5900</i>	1400-5500	-	-
PAM	N-300	30	-	-	-	2000-4200
		100	400-5900	400-5600	-	500-4500
	N-300L	100	-	-	-	1500-4100

Note: PEO = polyethyleneoxide
PAM = polyacrylamide

Numbers in **bold** indicate results used in the analysis of maximum drag reduction.
Numbers in *italic* indicate experimental runs in the replicated pipe.

Table 4.4.2. Flow regimes of pressure gradient ratio at maximum drag reduction.

Pipes→	S1 & R1A	S1 & R1B	S2 & R2A	S2 & R2B
Flow Regime ↓				
Laminar				
P_L	0.838±0.024	0.786±0.026	0.873±0.038	0.840±0.019
Q range (ml/s)	3.4-9.7	4.0-8.6	10-21	3.0-12
Re_s range	530-1510	730-1580	1200-2500	360-1400
Transition				
Q range (ml/s)	9.7-30	8.6-30	21-42	12-42
Re_s range	1510-4700	1580-5500	2500-5000	1400-5000
Turbulent				
$P_T = P_{T0}$				
P_{T0}	0.839±0.010	0.793±0.028	0.881±0.007	0.837±0.021
Q range (ml/s)	30-122	30-62	42-122	42-132
Re_s range	4700-19000	5500-11300	5000-14500	5000-15800
$\approx h^+$ range	3-10	4.7-8.5	2.3-5.5	4.1-9.3
$P_T > P_{T0}$				
Q range (ml/s)	122-200	62-157	122-516	-
Re_s range	19000-31200	11300-28700	14500-61500	-
$\approx h^+$ range	10-15	8.5-17	5.5-17	-
P_{Tmax}	0.880	0.860	0.992	-
h^+ at P_{Tmax}	11.7	12.6	11.2	-
$P_T < P_{T0}$				
Q range (ml/s)	200-920	157-1020	516-1100	132-1100
Segment 1				
Q range (ml/s)	200-920	157-1020	516-1100	132-1100
Re_s range	31200-144000	28700-187000	61500-131000	15800-131000
$\approx h^+$ range	15-54	17-72	17-30	9.3-41
P_{Tmin}	0.49±0.02	0.54±0.01	0.75±0.04	0.58±0.03
Segment 2				
$P_{T\infty}$	-	-	-	-
Q range (ml/s)	-	-	-	-
Re_s range	-	-	-	-
$\approx h^+$ range	-	-	-	-

Table 4.4.3. Summary of maximum drag reduction in smooth and riblet pipes.

Pipe		S1/R1A	S1/R1B	S2/R2A	S2/R2B
d_s , mm		7.82	7.82	10.21	10.21
h , mm		0.11	0.15	0.11	0.15
$d_r/2h$		35.9	25.7	47.3	33.8
(a) Smooth Pipe: Polymer Solutions wrt Solvent.					
Turbulent Regime					
MDR	Re \sqrt{f} range	350-4100	350-4300	400-4200	350-3800
Parameters					
$1/\sqrt{f} = A \log(\text{Re}\sqrt{f}) + B$	A	19.2±0.2	19.1±0.1	18.7±0.4	19.1±0.2
	B	-33.7±0.5	-33.1±0.3	-33.3±1.3	-33.5±0.7
	Re \sqrt{f} range	350-4100	350-4300	400-4200	350-3800
Poly. Drag Reduction	S' $_{\max}$	21.6	21.8	20.2	20.3
	Re \sqrt{f} @ max	4100	4300	4200	3800
(b) Riblet Pipe: Polymer Solutions wrt Solvent.					
Turbulent Regime					
MDR	Re \sqrt{f} range	350-4300	350-4800	350-4300	350-4400
Parameters					
Polymeric Segment 1					
$1/\sqrt{f} = A \log(\text{Re}\sqrt{f}) + B$	A	20.4±0.5	20.6±0.3	23.2±0.8	19.6±2.0
	B	-36.9±1.5	-37.2±1.0	-35.0±1.6	-33.8±5.0
	Re \sqrt{f} range	350-1200	350-1000	350-1150	350-850
Polymeric Segment 2					
$1/\sqrt{f} = A \log(\text{Re}\sqrt{f}) + B$	A	4.3±0.3	10.1±0.4	8.0±1.5	9.7±0.6
	B	-11.6±0.5	-7.7±1.3	3.1±3.0	-7.4±2.1
	Re \sqrt{f} range	1300-4300	1400-4800	1150-4300	1100-4000
Poly. Drag Reduction	S' $_{\max}$	14.5	17.3	19.0	16.1
	Re \sqrt{f} @ max	4300	4800	4300	4000
(c) Polymer Solutions: Riblet wrt Smooth Wall.					
Turbulent Regime					
(i) HS	h^+ range	4-9	5-9	3-7	4-9
(ii) RDR	h^+ range	9-14	9-14	7-16	(7-10)
(iii) RDE	h^+ range	14-50	14-80	16-35	9-50
Parameters					
RDR	R' $_{\max}$	0.8	0.7	1.8	(0.6)
	h^+ @ max	11	11	10	(8)
RDE	R' $_{\min}$	-9.5	-7.3	-2.4	-6.9
	h^+ @ min	50	80	35	50

Values in parentheses are uncertain

Table 4.5.1. Experimental relative and intrinsic viscosities calculated from laminar flow data.

RUN	POLY.	SERIES	c wppm	η_r	η/c^* 1 point estimation	η_l dl/g	η/c^{**} Flory- Huggins	η_l dl/g
149	PEO	P-309	200	1.608	0.516	25.80	0.513	25.65
64	PEO	P-309	100	1.330	0.299	29.93	0.298	29.78
65	PEO	P-309	100	1.302	0.276	27.59	0.275	27.45
142	PEO	P-309	100	1.300	0.274	27.42	0.273	27.29
144	PEO	P-309	100	1.306	0.279	27.91	0.278	27.78
219	PEO	P-309	100	1.251	0.233	23.25	0.231	23.15
237	PEO	P-309	100	1.260	0.241	24.05	0.239	23.94
249	PEO	P-309	100	1.260	0.241	24.07	0.240	23.96
66	PEO	P-309	50	1.139	0.133	26.63	0.133	26.54
146	PEO	P-309	50	1.150	0.143	28.66	0.143	28.57
148	PEO	P-309	50	1.151	0.144	28.71	0.143	28.62
220	PEO	P-309	50	1.135	0.129	25.86	0.129	25.78
238	PEO	P-309	50	1.141	0.135	27.03	0.135	26.94
250	PEO	P-309	50	1.138	0.132	26.36	0.131	26.28
72	PEO	W-301	100	1.229	0.214	21.38	0.213	21.29
99	PEO	W-301	100	1.219	0.205	20.47	0.204	20.38
156	PEO	W-301	100	1.208	0.195	19.53	0.195	19.45
222	PEO	W-301	100	1.209	0.196	19.62	0.195	19.54
252	PEO	W-301	100	1.205	0.192	19.23	0.192	19.16
270	PEO	W-301	100	1.191	0.180	18.00	0.179	17.94
280	PEO	W-301	100	1.196	0.184	18.45	0.184	18.38
166	PEO	N-60K	300	1.317	0.289	9.62	0.287	9.57
74	PEO	N-60K	100	1.086	0.084	8.40	0.084	8.38
85	PEO	N-60K	100	1.087	0.084	8.43	0.084	8.41
164	PEO	N-60K	100	1.097	0.094	9.36	0.093	9.33
224	PEO	N-60K	100	1.092	0.090	8.97	0.090	8.95
240	PEO	N-60K	100	1.104	0.100	10.05	0.100	10.02
287	PEO	N-60K	100	1.100	0.097	9.67	0.096	9.64
97	PEO	N-750	2072.7	1.892	0.714	3.44	0.710	3.43
170	PEO	N-750	1000	1.330	0.300	3.00	0.298	2.98
248	PEO	N-750	1000	1.336	0.304	3.04	0.302	3.02
93	PEO	N-750	900	1.278	0.255	2.84	0.254	2.82
230	PEO	N-750	300	1.102	0.099	3.30	0.099	3.29
91	PEO	N-750	250	1.074	0.072	2.90	0.072	2.89
169	PEO	N-750	250	1.084	0.082	3.27	0.082	3.26
95	PEO	N-10	2435	1.303	0.277	1.14	0.276	1.13
115	PEO	N-10	5138	1.777	0.636	1.24	0.632	1.23
104	PAM	N-300	100	1.177	0.168	16.75	0.167	16.69
231	PAM	N-300	100	1.177	0.168	16.75	0.167	16.69
253	PAM	N-300	100	1.176	0.166	16.62	0.166	16.56
105	PAM	N-300	30	1.050	0.049	16.27	0.049	16.25
113	PAM	N300LMW	300	1.254	0.236	7.85	0.234	7.81
110	PAM	N300LMW	100	1.084	0.082	8.20	0.082	8.18

* intrinsic viscosity determined from a single point estimation: $[\eta] = \frac{1}{c} \left[2(\eta_{sp}) - \ln(\eta_r) \right]^{1/2}$ (Solomon & Ciuta, 1962)

** intrinsic viscosity determined from Flory Huggins equation: $\frac{\eta_{sp}}{c} = [\eta] + k_1[\eta]^2 c$

Table 4.5.2. Polymeric parameters inferred from intrinsic viscosities.

Polymer Type	Species	η_l (dl/g)	Polymer Parameters inferred via Eqs. 2.3-12 2.3-15			
			$M_w \times 10^{-6}$ (g/mole)	$N \times 10^{-5}$	R_G (nm)	L_c (μm)
PEO	P-309	27.5 \pm 4.2	7.9 \pm 1.5	5.25 \pm 1.00	267 \pm 24	168 \pm 31
	W-301	20.0 \pm 0.9	5.3 \pm 0.3	3.53 \pm 0.20	223 \pm 6	113 \pm 6
	N-60K	9.11 \pm 0.65	2.0 \pm 0.2	1.33 \pm 0.12	141 \pm 6	42 \pm 4
	N-750	3.10 \pm 0.23	0.52 \pm 0.05	0.35 \pm 0.03	75.1 \pm 3.3	11 \pm 1
	N-10	1.18 \pm 0.07	0.16 \pm 0.01	0.10 \pm 0.01	42.8 \pm 1.5	3.4 \pm .3
PAM	N-300	16.6 \pm 0.2	7.4 \pm 0.1	2.09 \pm 0.03	224 \pm 3	104 \pm 2
	N-300L	8.00 \pm 0.26	2.9 \pm 0.1	0.82 \pm 0.03	115 \pm 3	41 \pm 2

Polymer Backbone Chain

	m_0 , g/mole	b_0 , nm
PEO	14.7	0.32
PAM	35.5	0.50

Table 4.6.1. Average regressed onset wall shear stress for additives in 10.21 mm and 7.82 mm smooth pipes.

		Ensemble Average τ_w^* (N/m ²)	
Polymer↓	Pipe→	10.21 mm	7.82 mm
W-301		1.3 ± 0.4	1.8 ± 0.5
N-60K		3.6 ± 0.7	3.6 ± 1.0
N-750		13.7 ± 2.0	12.4 ± 0.9
N-10		38 ± 6	-
N-300		0.87 ± 0.25	-
N-300L		2.3 ± 0.4	-

Table 4.6.2. Type A model intrinsic slope increment, $\delta/c^{1/2}$, for additives in 10.21 mm and 7.82 mm smooth pipes.

Polymer↓	Pipe→	Model Specific Slope Increment, $\delta/c^{1/2}$	
		10.21 mm	7.82 mm
W-301		5.6 ± 0.2	6.8 ± 0.2
N-60K		3.0 ± 0.1	3.4 ± 0.1
N-750		0.64 ± 0.02	0.70 ± 0.03
N-10		0.090 ± 0.005	-
N-300		4.4 ± 0.3	-
N-300L		1.8 ± 0.1	-

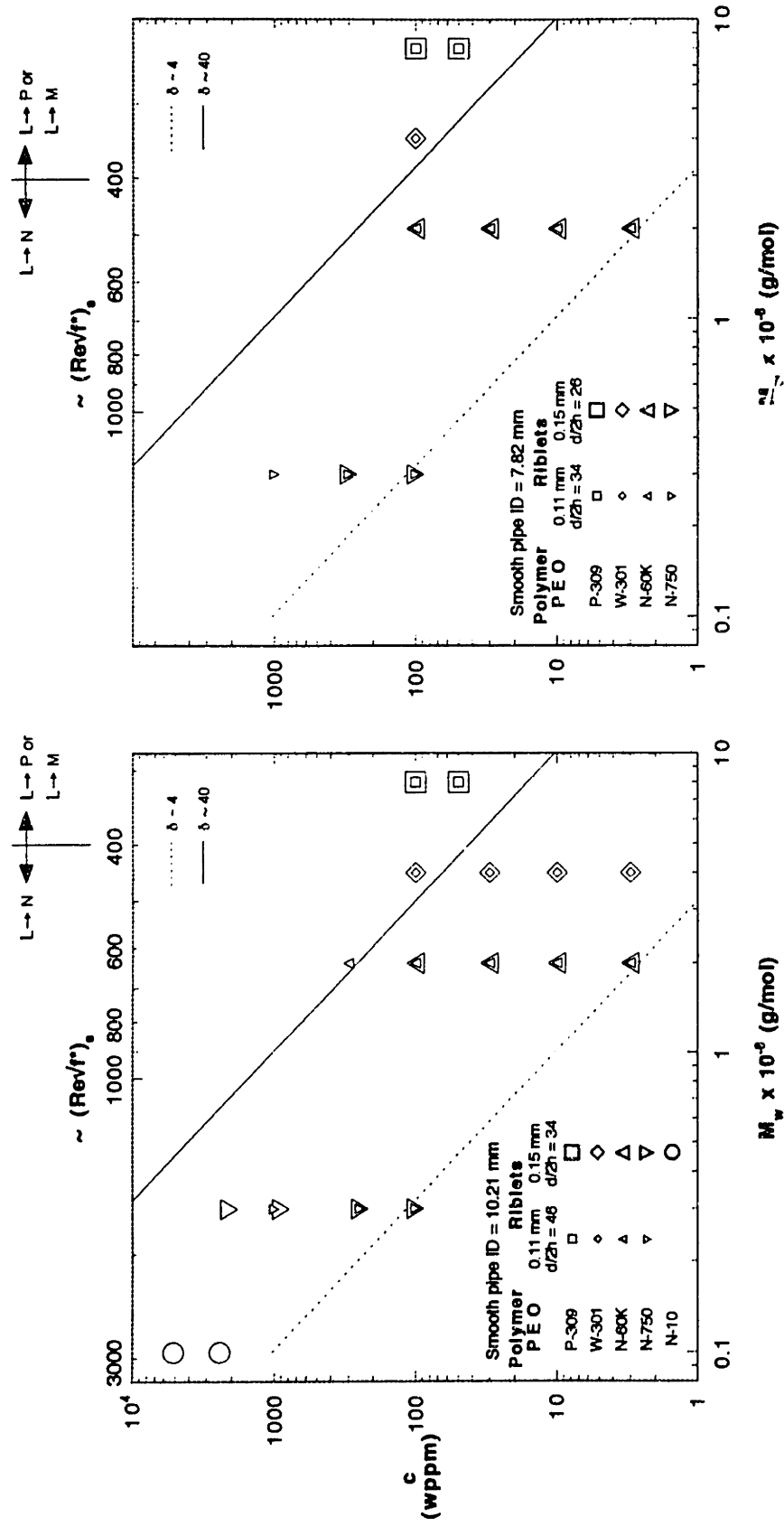


Figure 4.1.1. Experimental grid depicting the expected flow regimes for five PEO solutions in the 10.21 mm and 7.82 mm smooth pipes.

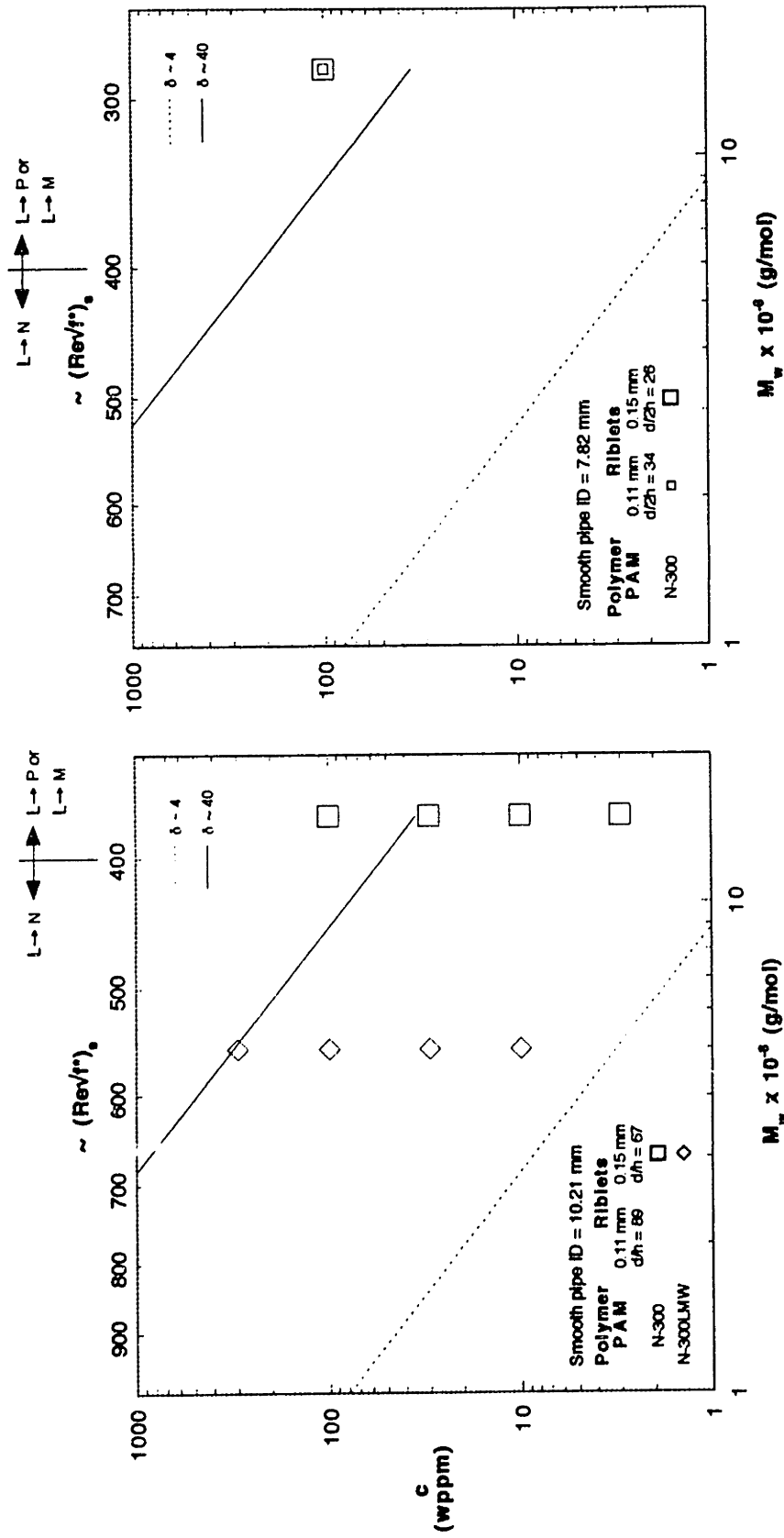


Figure 4.1.2 Experimental grid depicting the expected flow regimes for two PAM solutions in the 10.21 mm and 7.82 mm smooth pipes

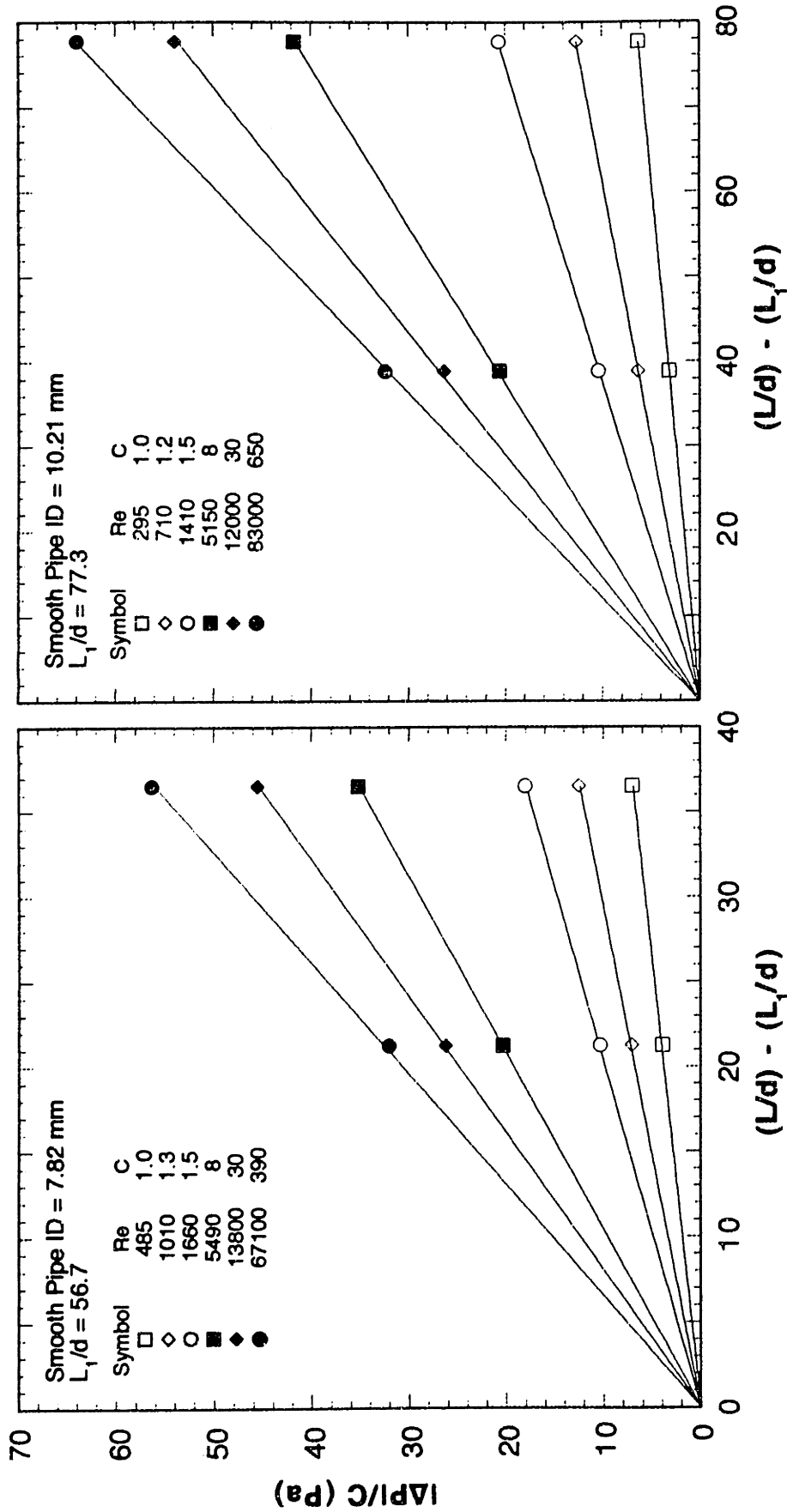


Figure 4.2.1 Laminar and turbulent flow development in the 7.82 mm and 10.21 mm smooth pipes

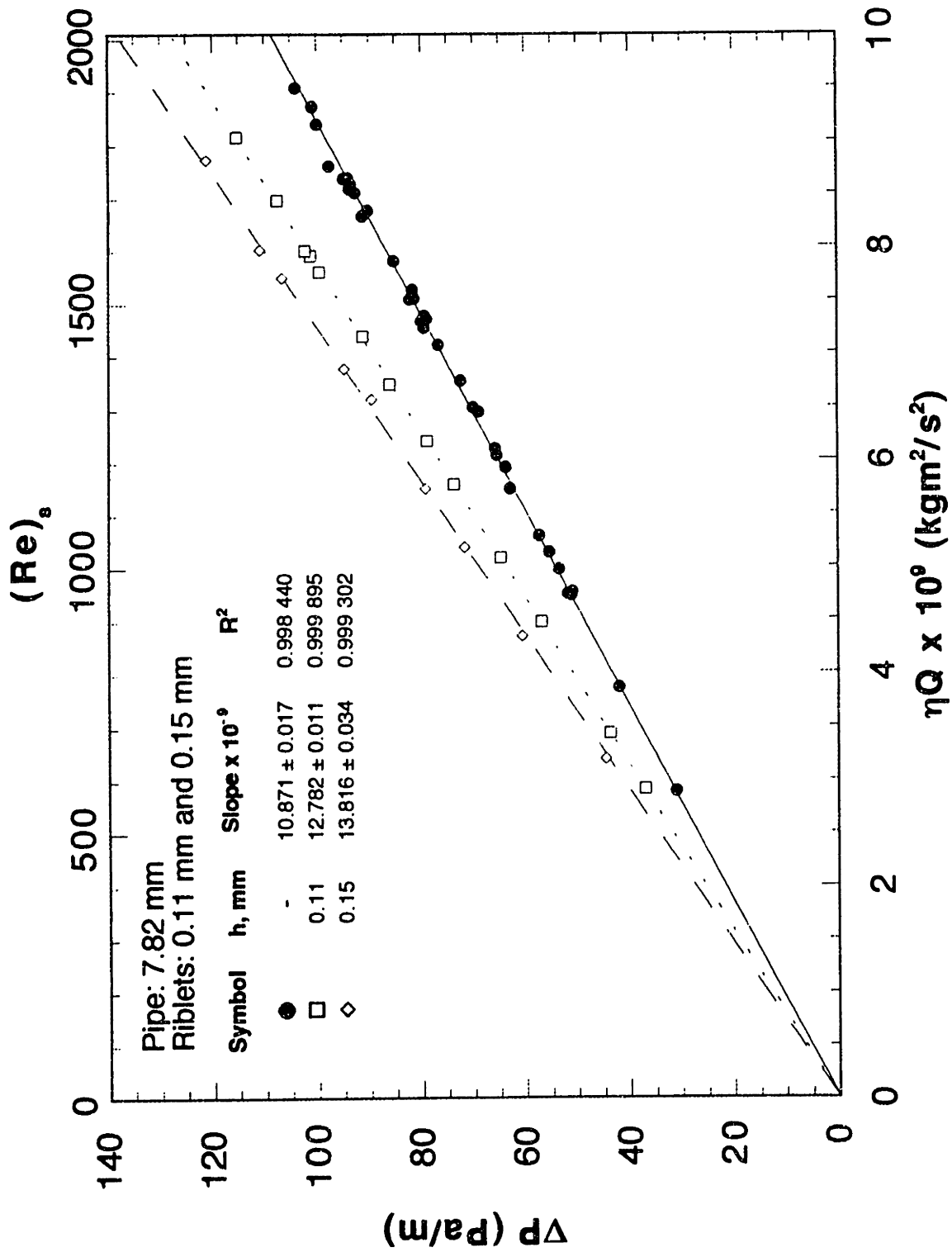


Figure 4.2.2 Laminar flow pressure gradient-flowrate relation in the 7.82 mm pipes S1, R1A, R1B

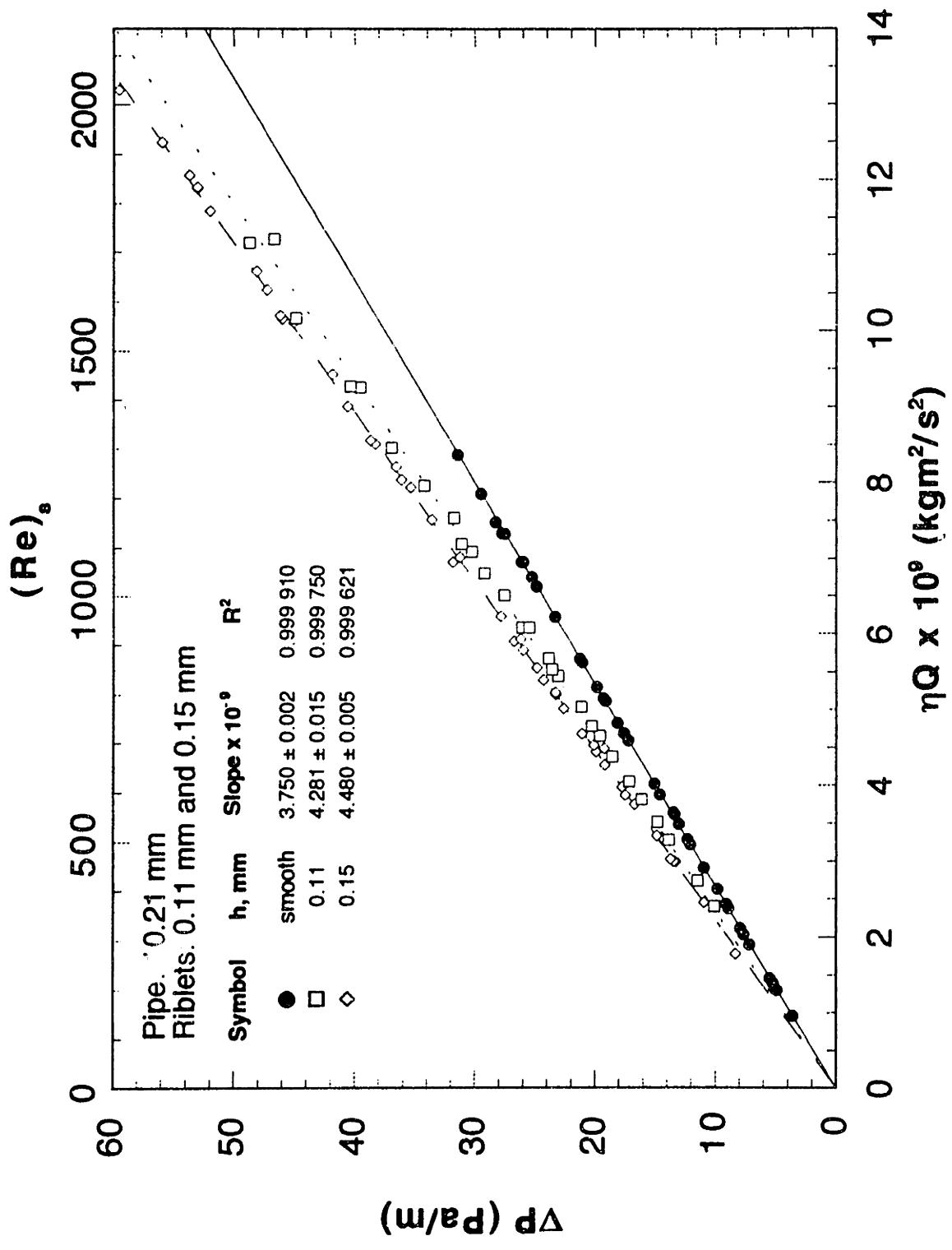


Figure 4.2.3 Laminar flow pressure gradient-flowrate relation in the 10.21 mm pipes S2, R2A, R2B

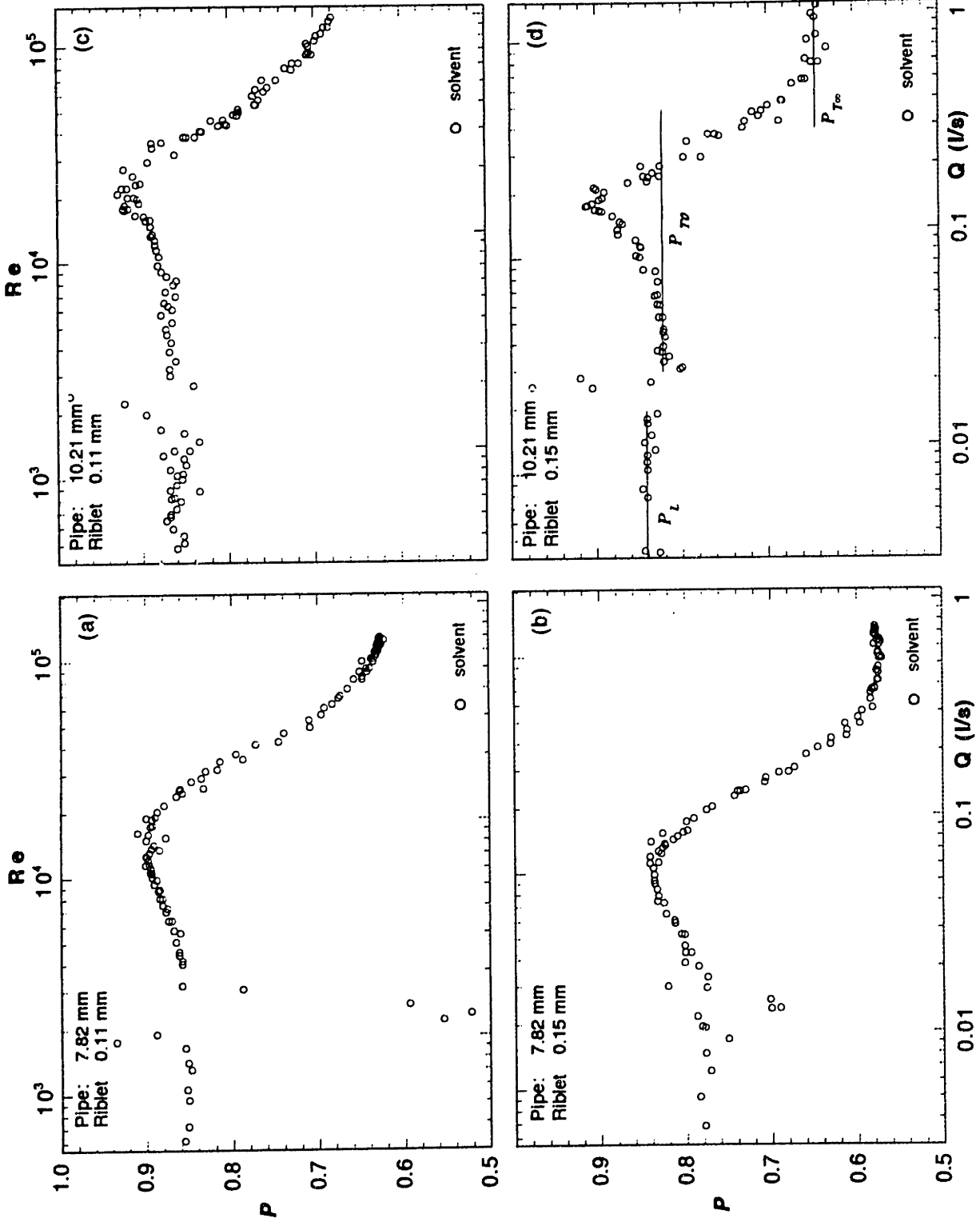


Figure 4.2.4 Variations of the smooth to riblet pipe pressure gradient ratios versus flowrate

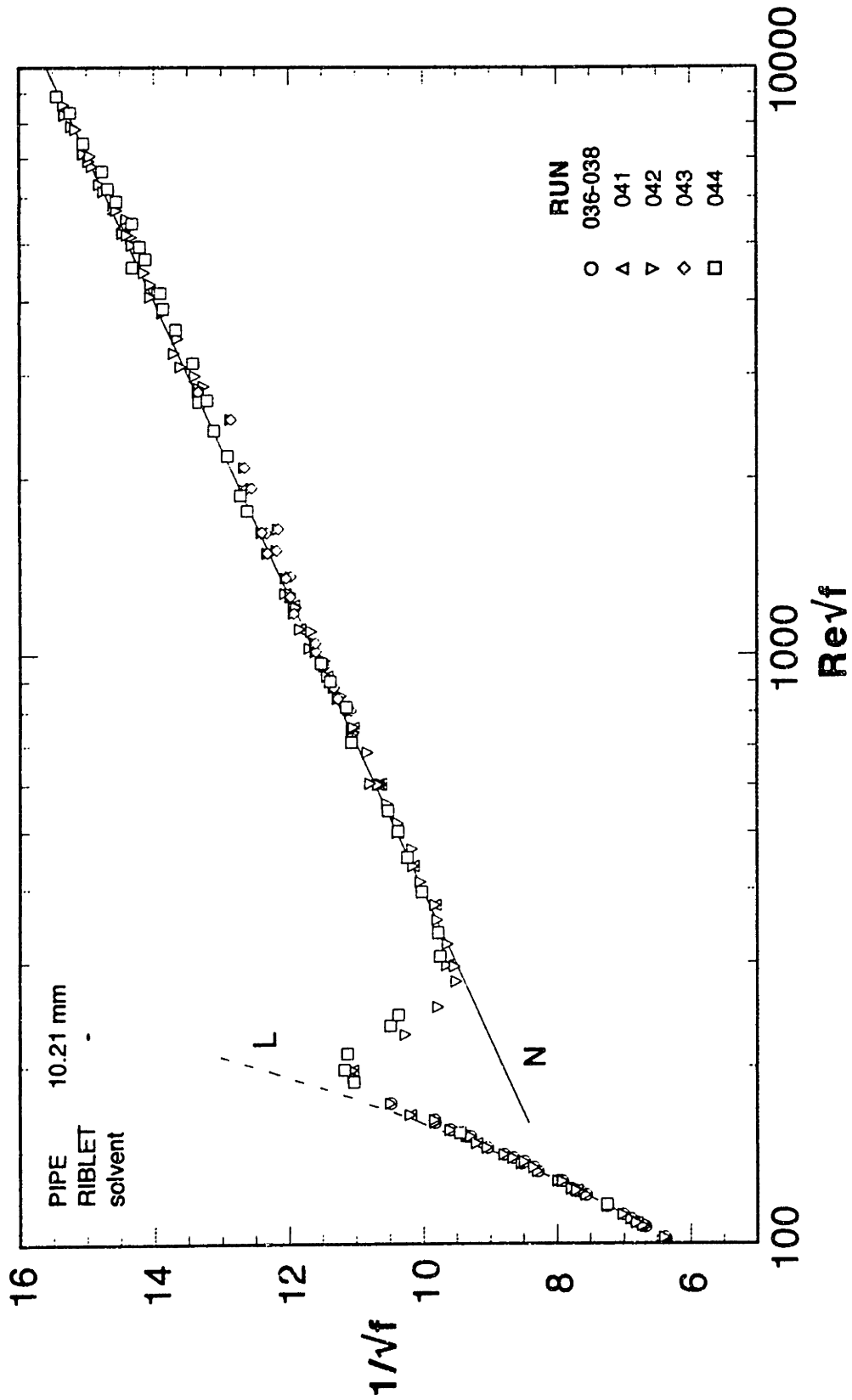


Figure 4.2.5 Prandtl-Karman friction factors for solvent flow in the 10.21 mm id smooth pipe.

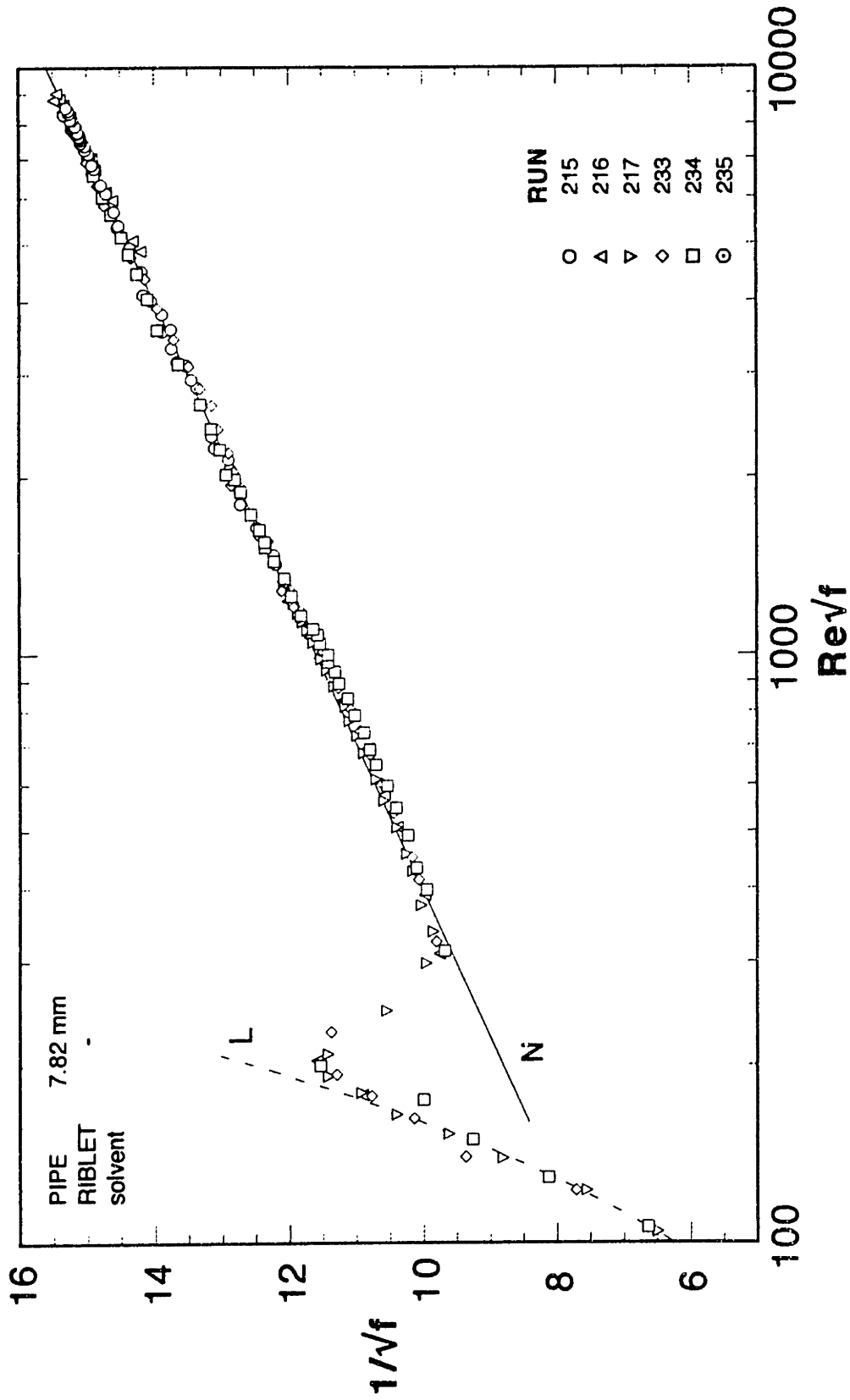


Figure 4.2.6 Prandtl-Karman friction factors for solvent flow in the 7.82 mm id smooth pipe

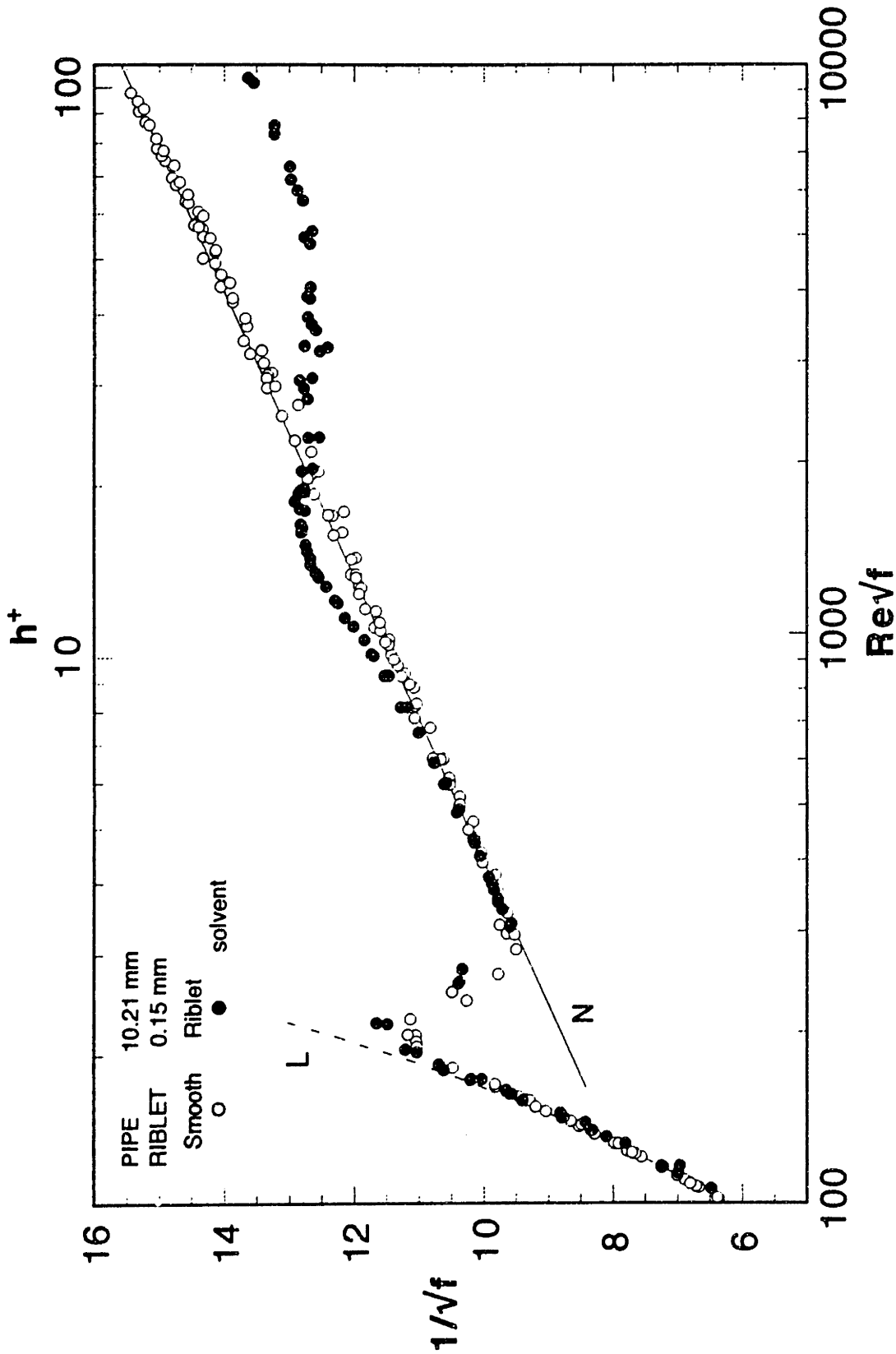


Figure 4.2.7 Prandtl-Karman friction factors for solvent flow in the 10.21 mm id smooth pipe and in the 10.21 mm pipe lined with 0.15 mm riblets.

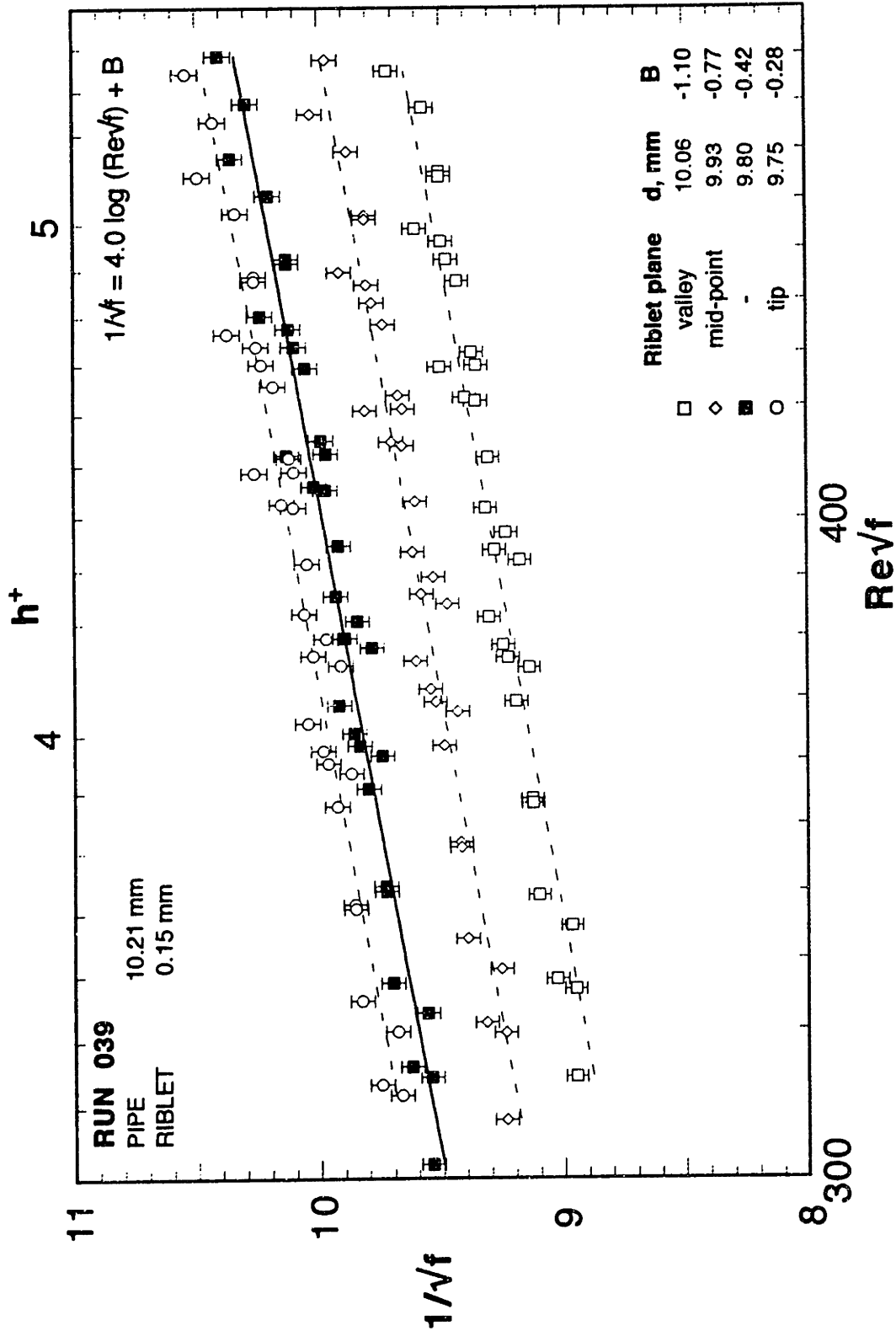


Figure 4.2.8 Effect of riblet-pipe diameter on Prandtl-Karman friction factors for $h^+ < 5$ in the 10.21 mm id smooth and 10.21 mm pipe lined with 0.15 mm riblets.

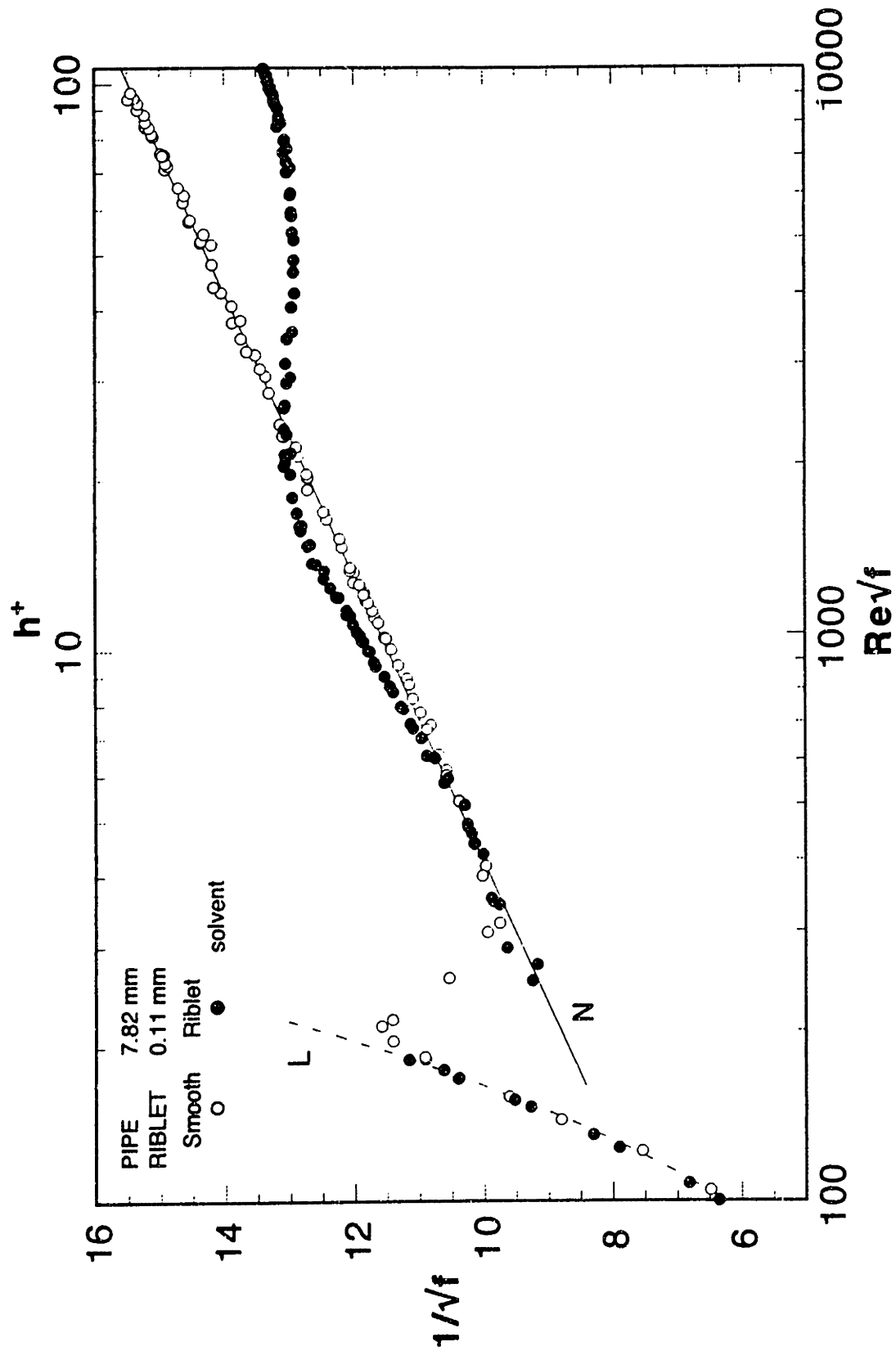


Figure 4.2.9 Prandtl-Karman friction factors for solvent flow in the 7.82 mm id smooth and 7.82 mm pipe lined with 0.11 mm riblets.

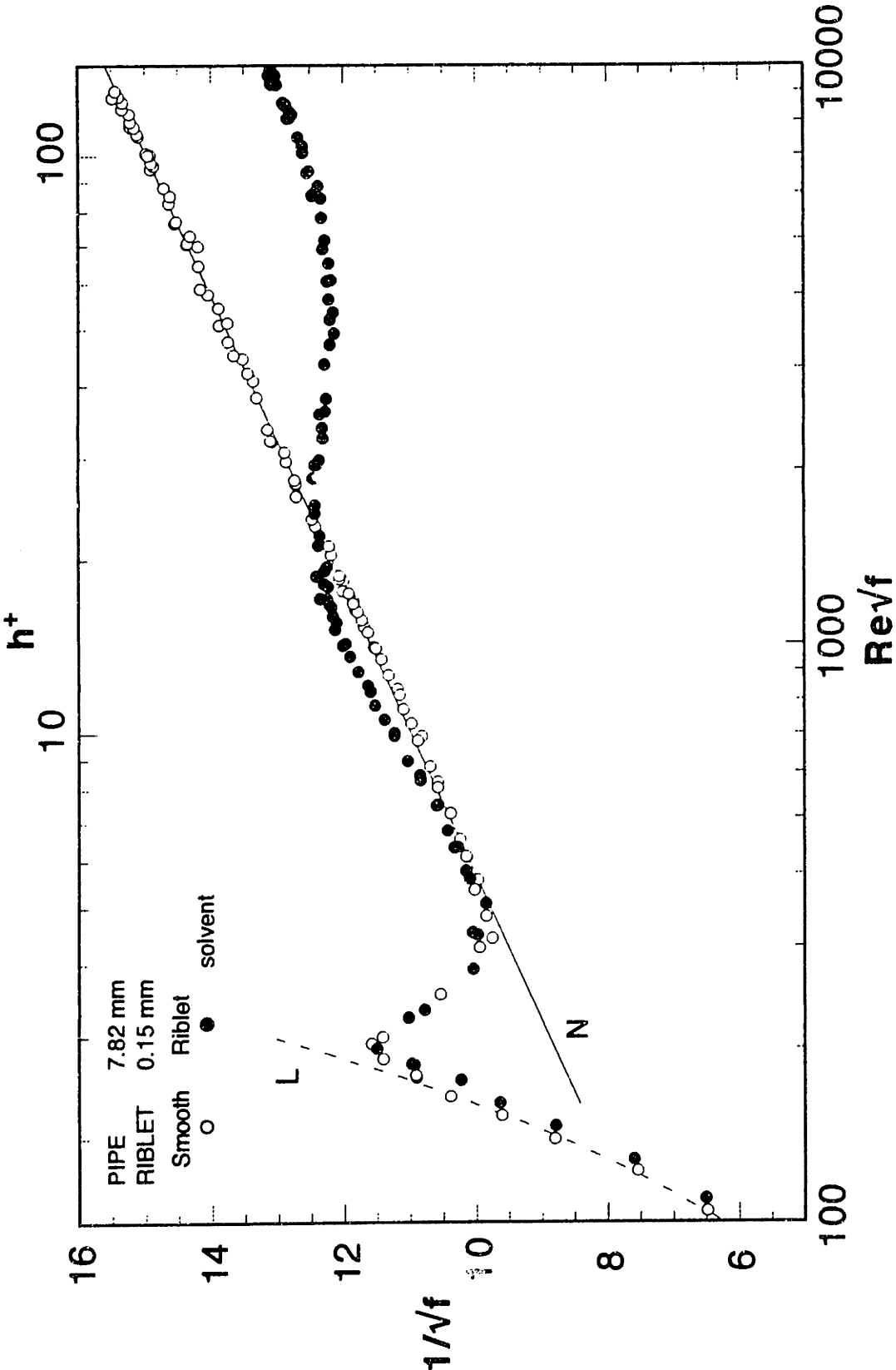


Figure 4.2.10 Prandtl-Karman friction factors for solvent flow in the 7.82 mm id smooth and 7.82 mm pipe lined with 0.15 mm riblets.

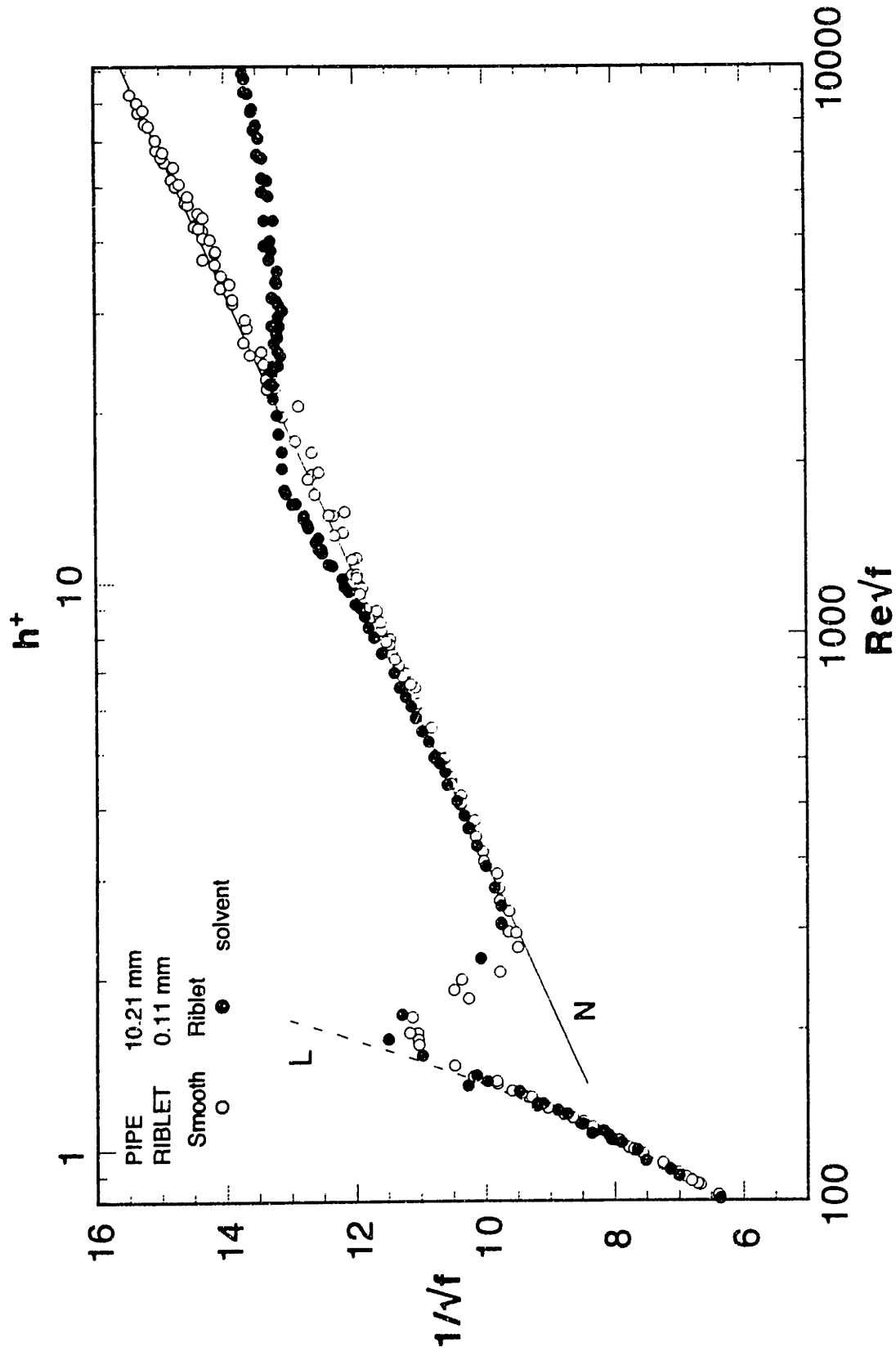


Figure 4.2.11 Prandtl-Karman friction factors for solvent flow in the 10.21 mm id smooth and 10.21 mm pipe lined with 0.11 mm riblets.

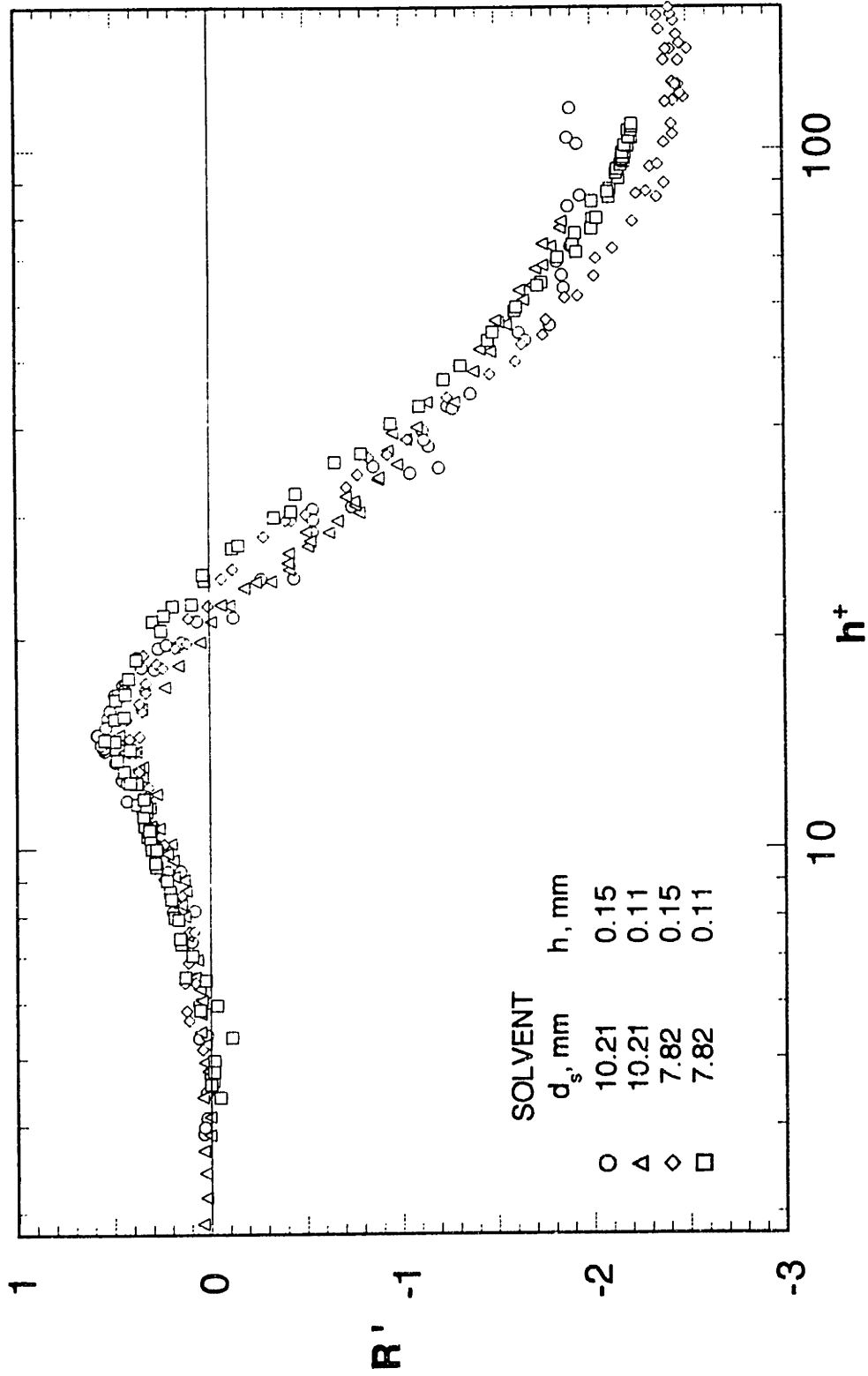


Figure 4.2.12 The riblet-induced flow enhancement for the flow of solvent in all riblet pipes

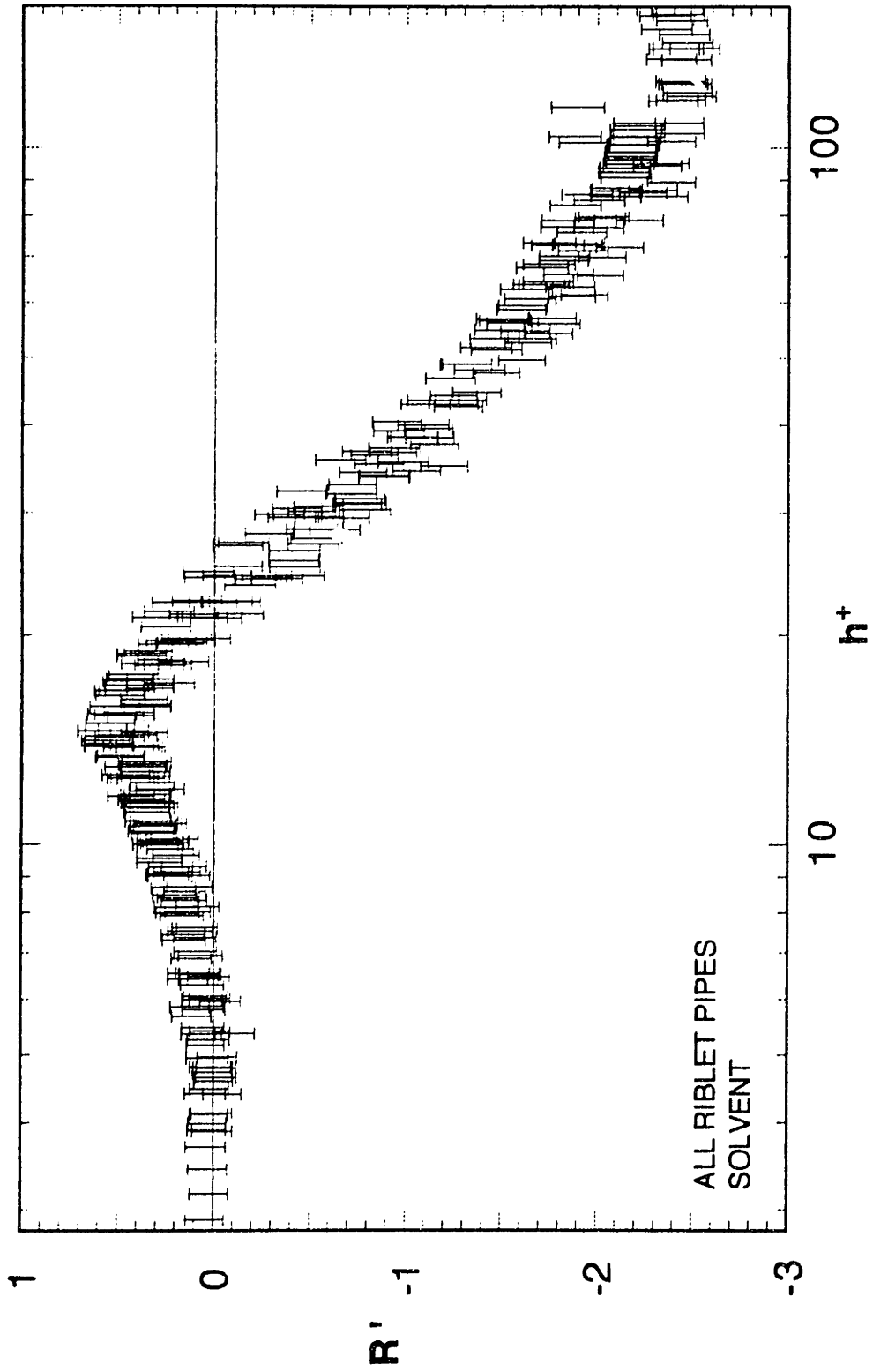


Figure 4.2.13 Error analysis of riblet-induced flow enhancement for the flow of solvent in all riblet pipes

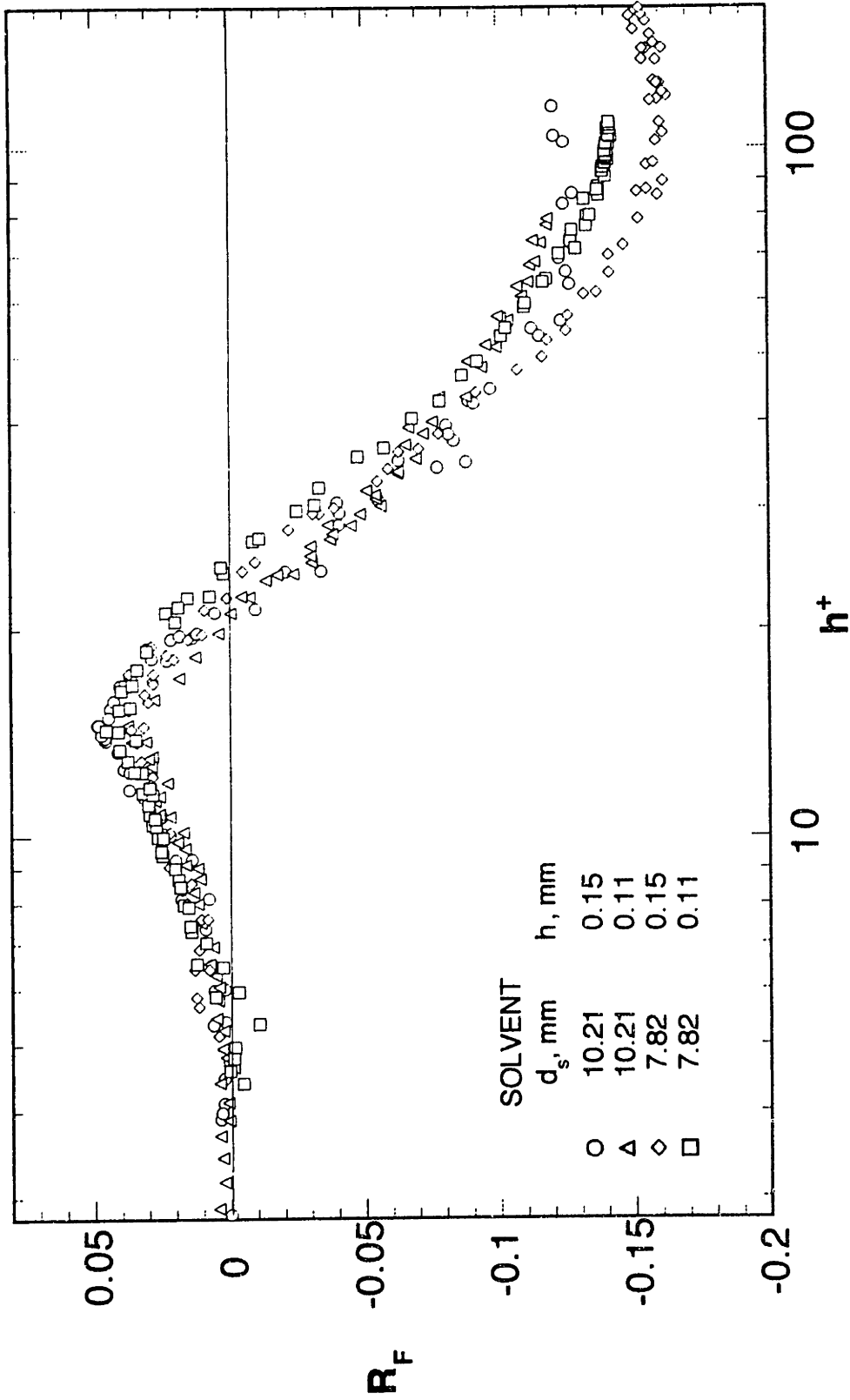


Figure 4.2.14 The riblet-induced fractional flow enhancement for the flow of solvent in all riblet pipes

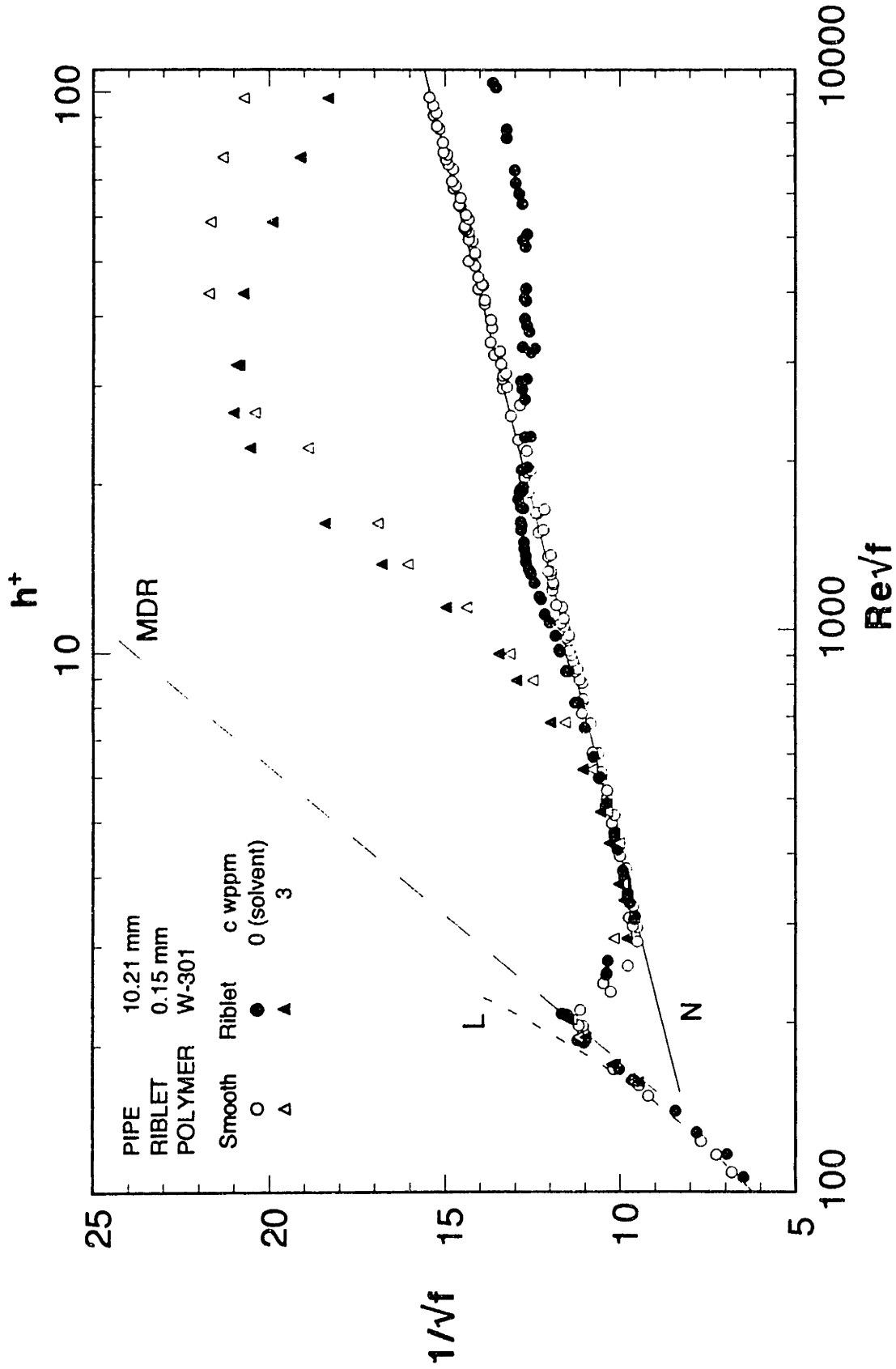


Figure 4.3.1 Flow of solvent and a 3 wppm solution of PEO W-301 in S2 and R2B

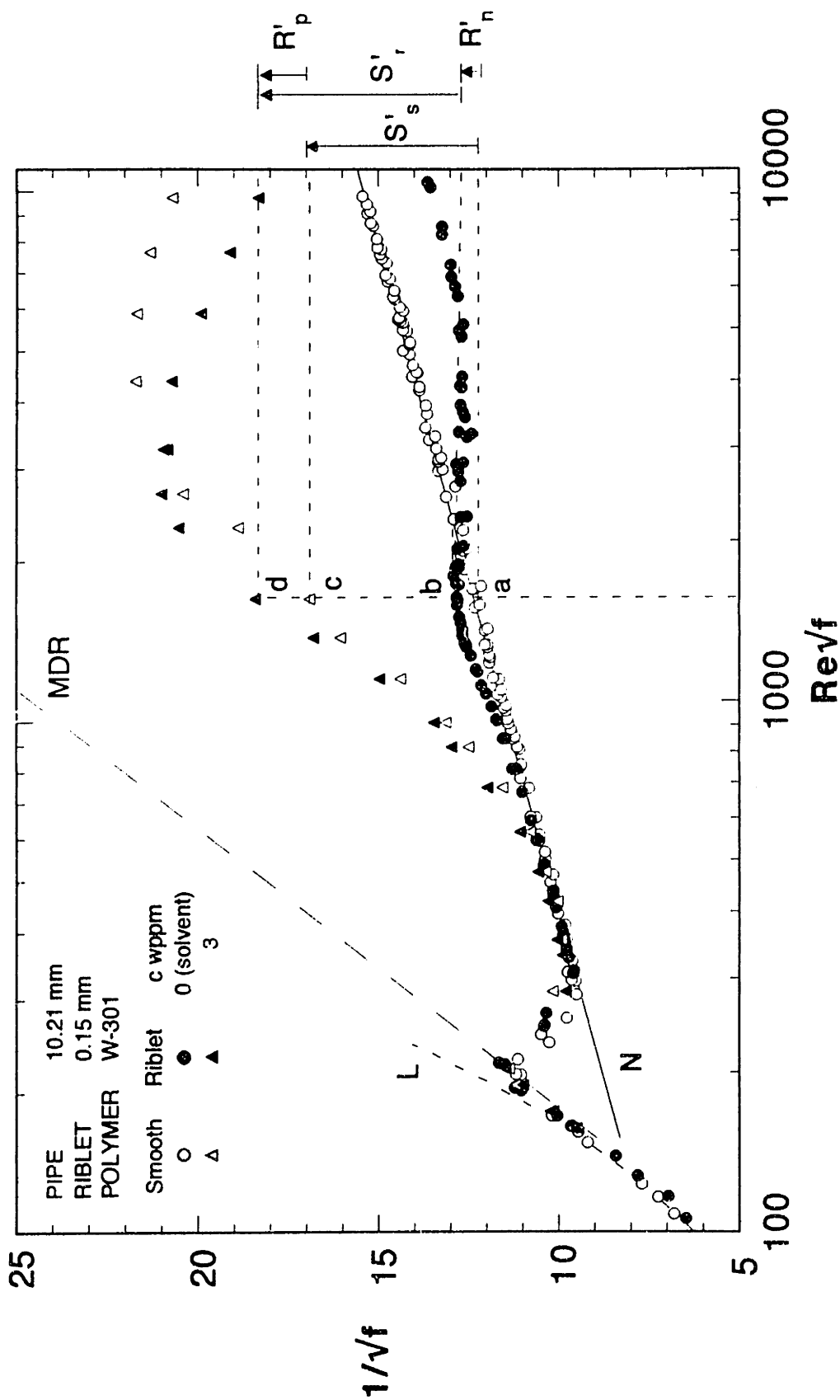


Figure 4.3.2 Flow of solvent and a 3 wppm solution of PEO W-301 in S2 and R2B. The vertical line abcd at $Rev/f = 1510$ illustrates the definitions of polymer- and riblet-induced flow enhancements

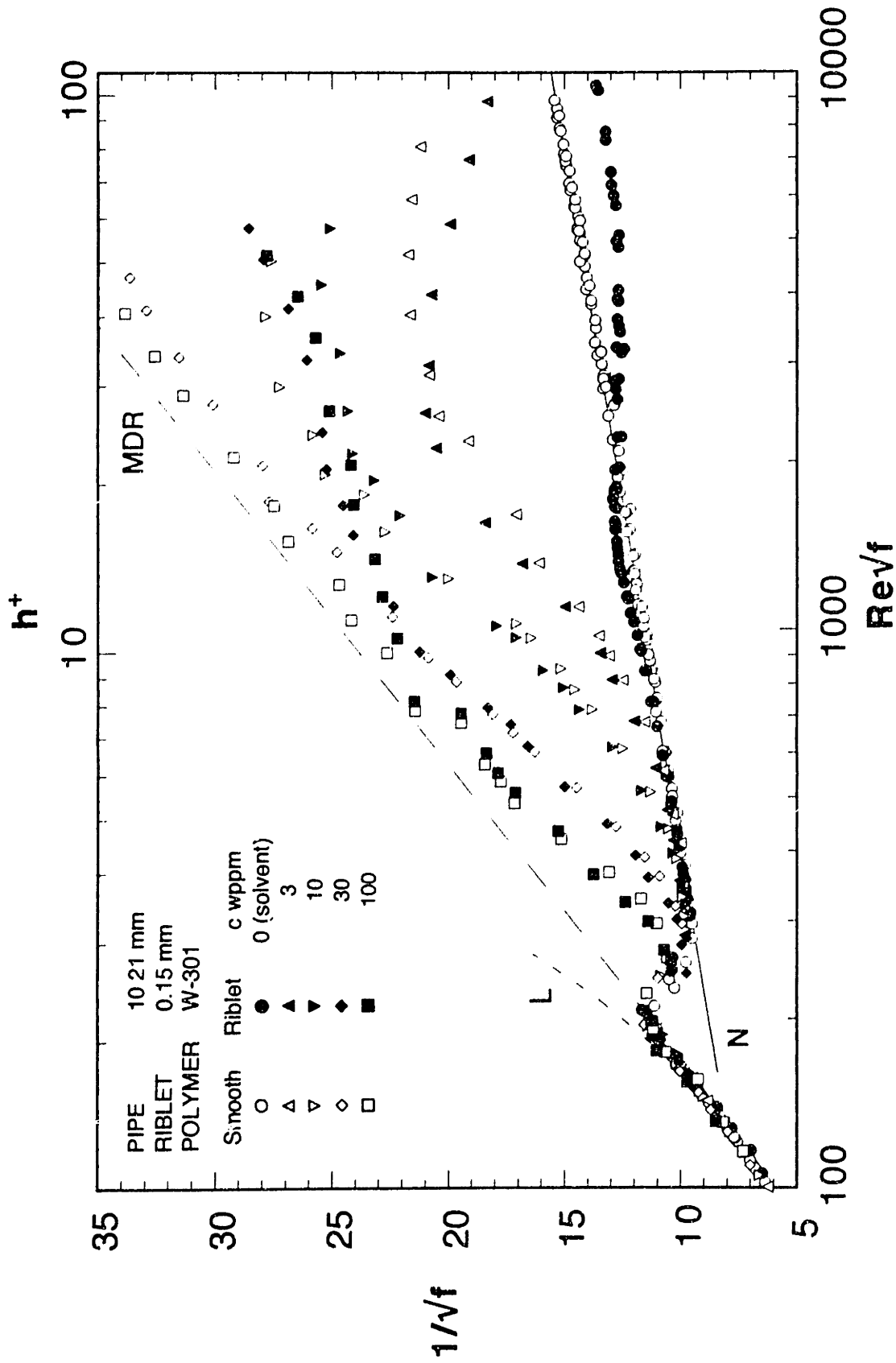


Figure 4.3.3 Effect of polymer concentration on drag reduction by W-301 in S2 and R2B.

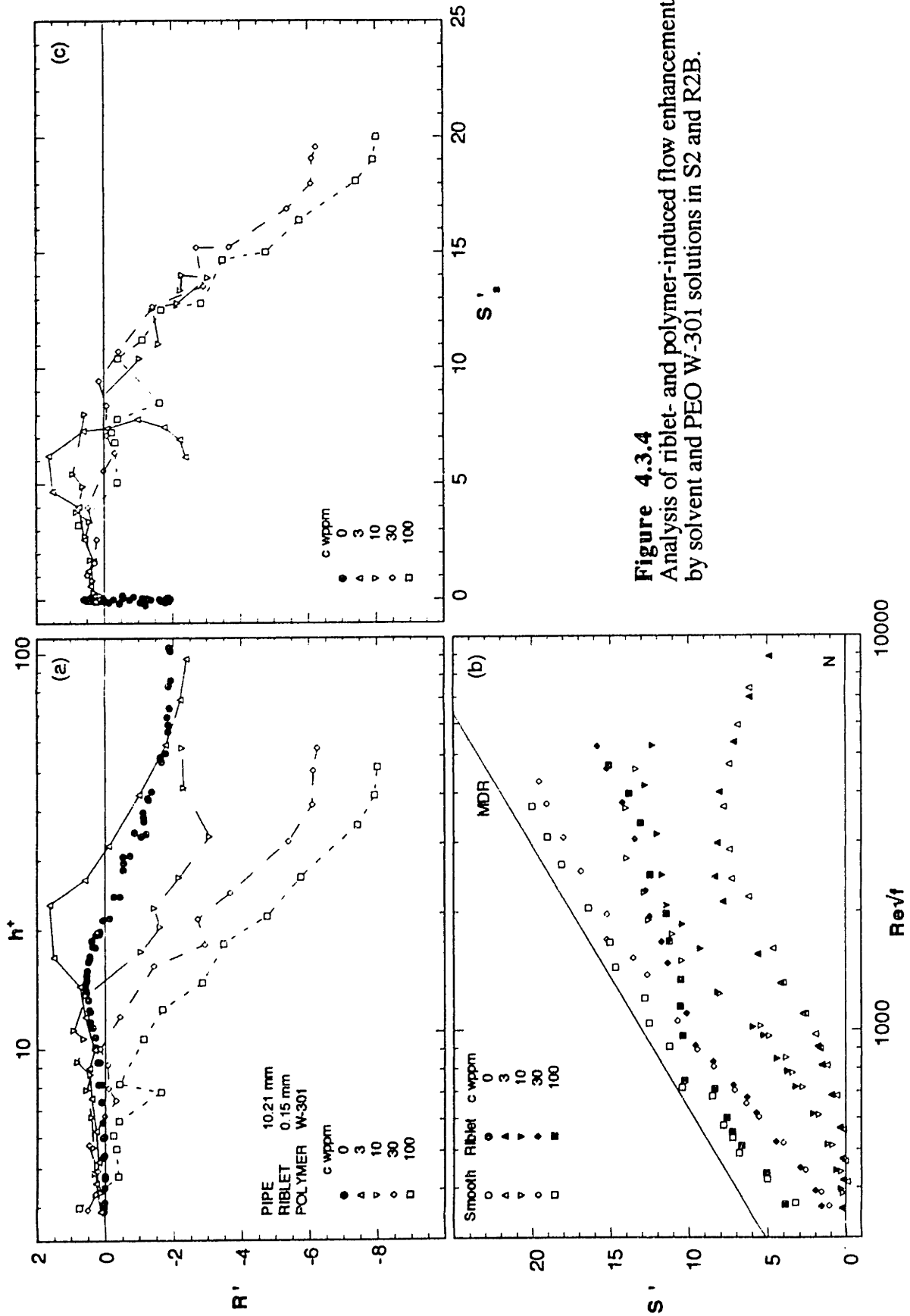


Figure 4.3.4
Analysis of riblet- and polymer-induced flow enhancements
by solvent and PEO W-301 solutions in S2 and R2B.

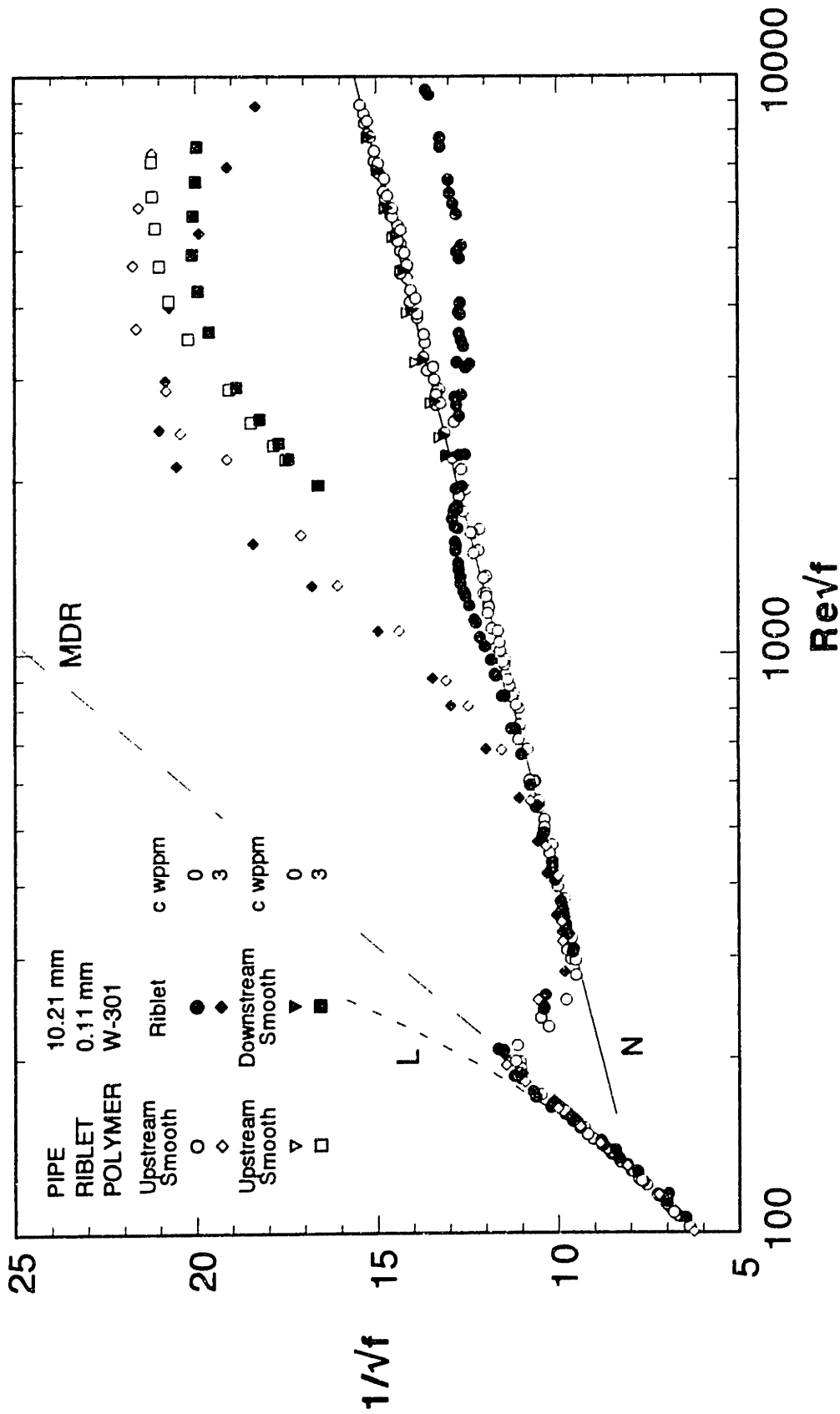


Figure 4.3.5 Comparison between the effects of riblets and polymer degradation in the flow of 3 wppm W-301 in pipes S2 and R2B; upstream station 1, downstream station 2

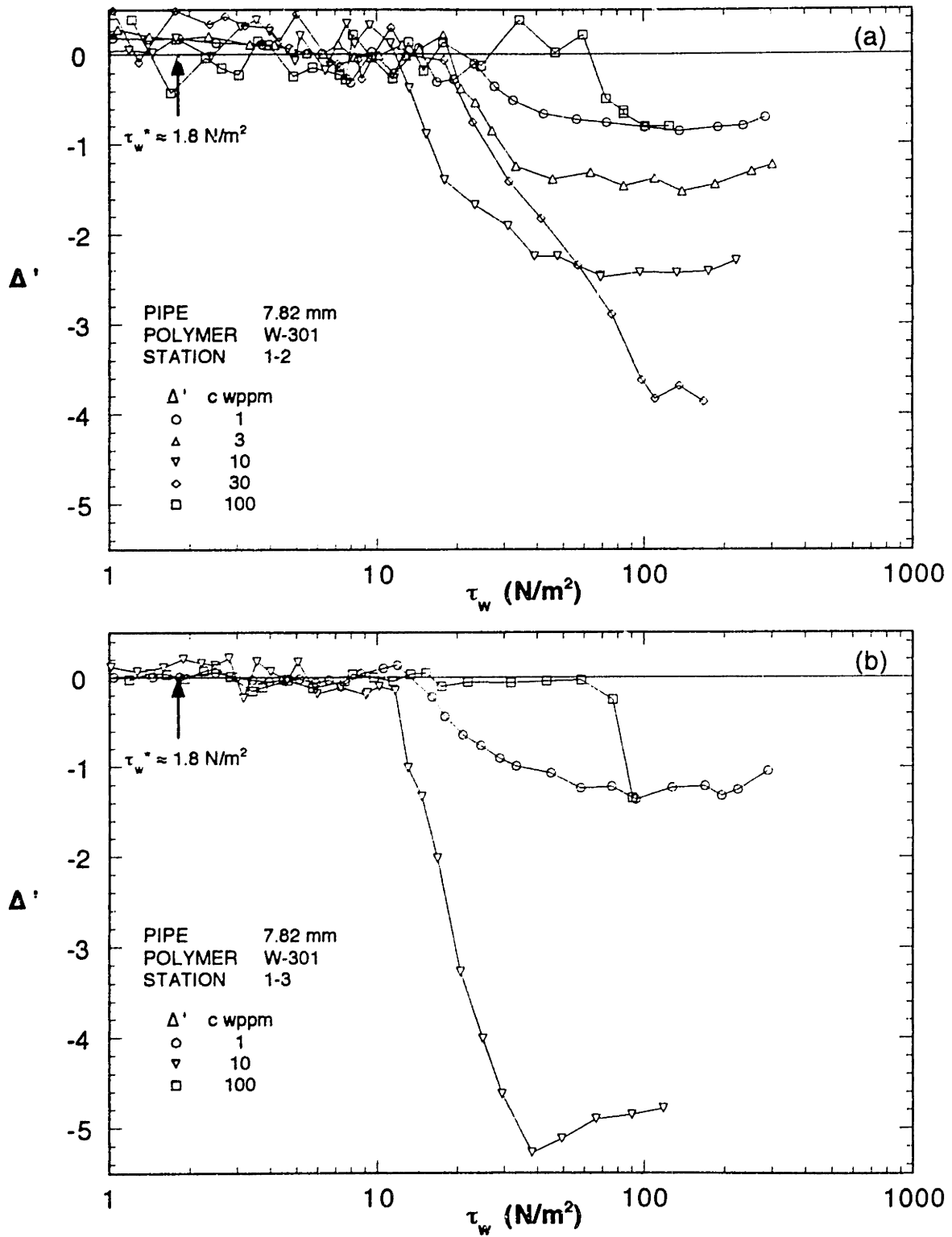


Figure 4.3.8 Effect of downstream distance on degradation in the 10.21 mm pipe for PEO W-301 solutions

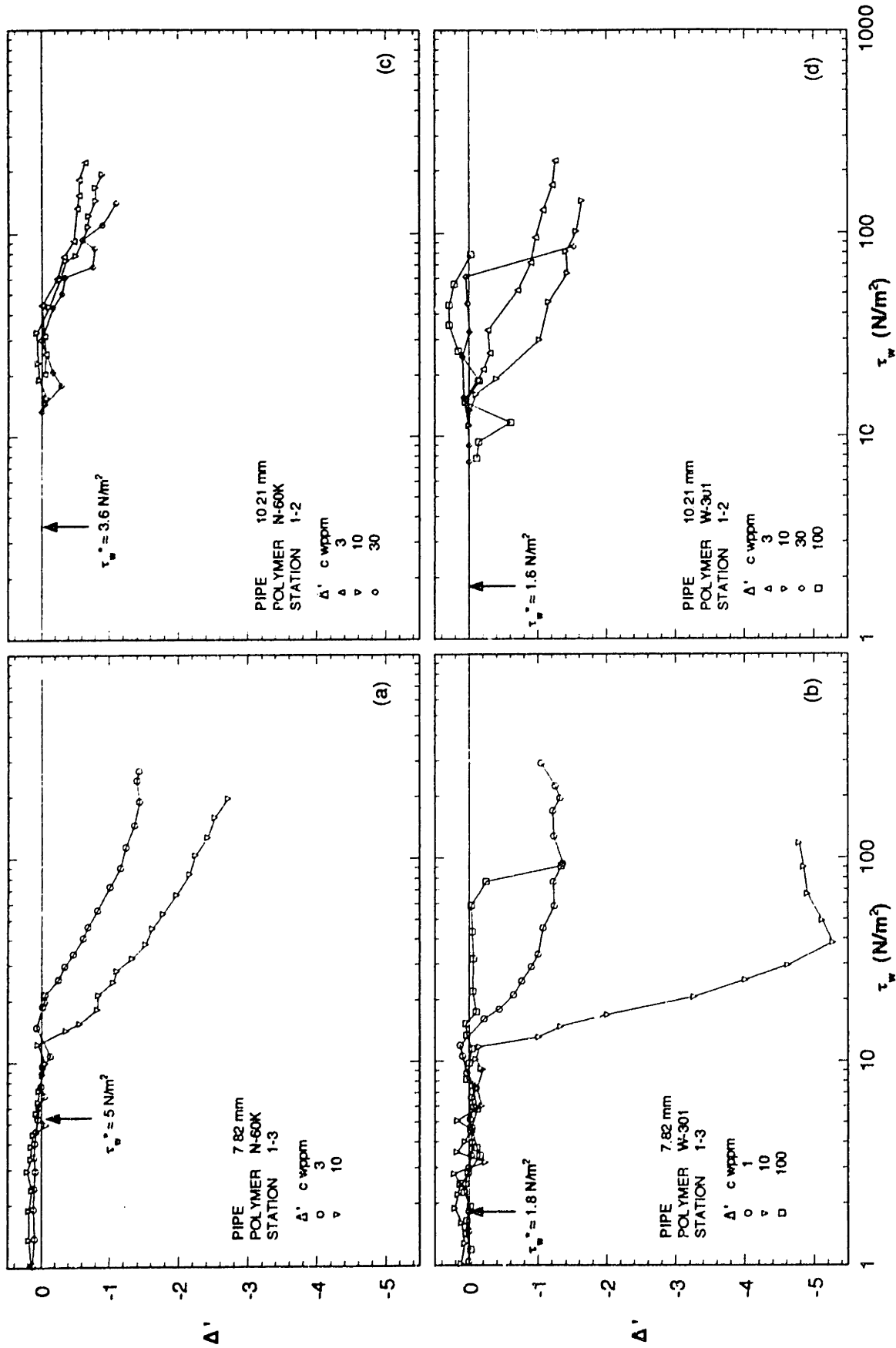


Figure 4.3.9 Effect of polymer molecular weight and pipe diameter on degradation between upstream and downstream hydraulically smooth sections.

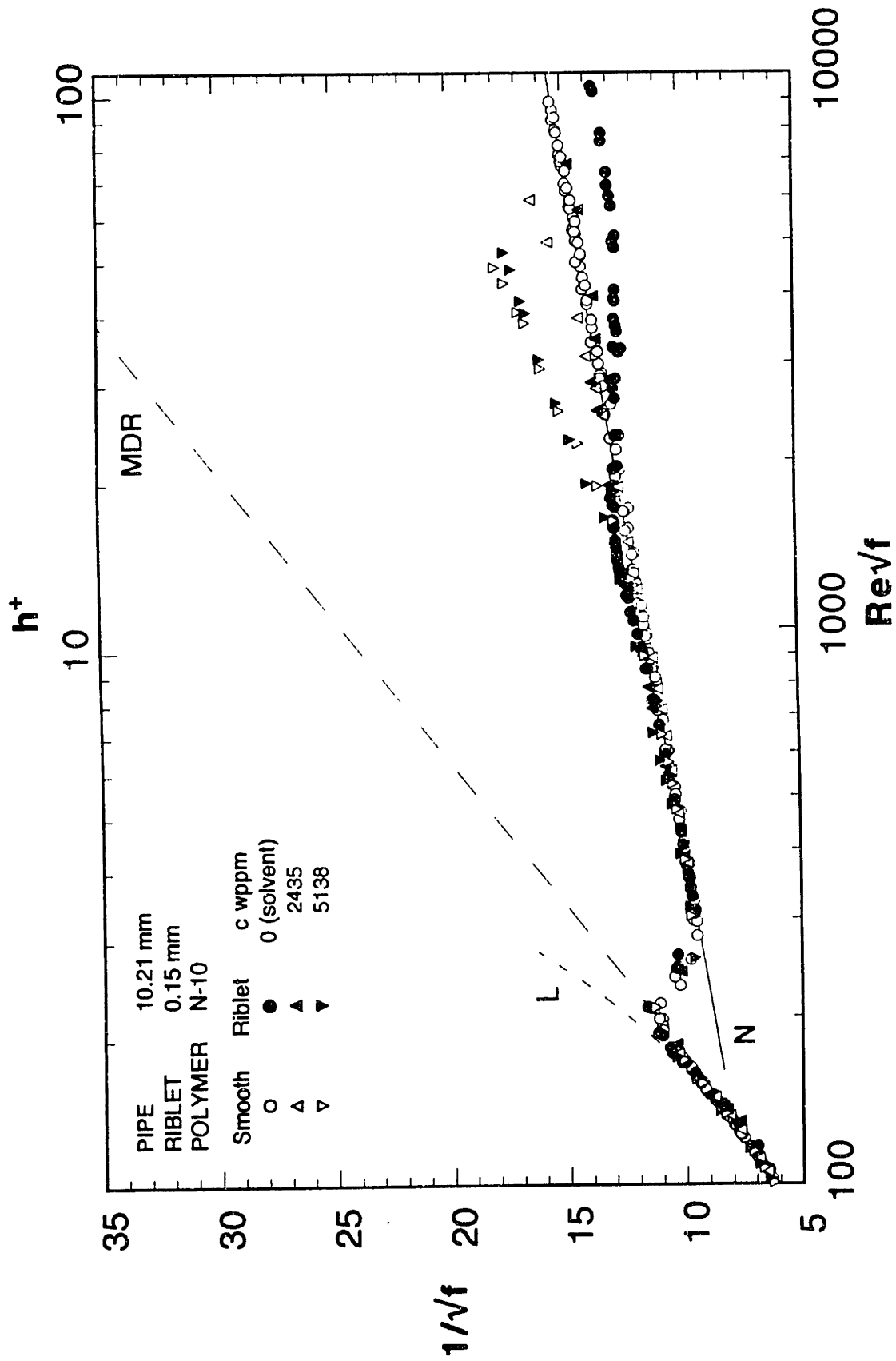


Figure 4.3.10 Friction factors for solutions of PEO N-10 in S2 and R2B.

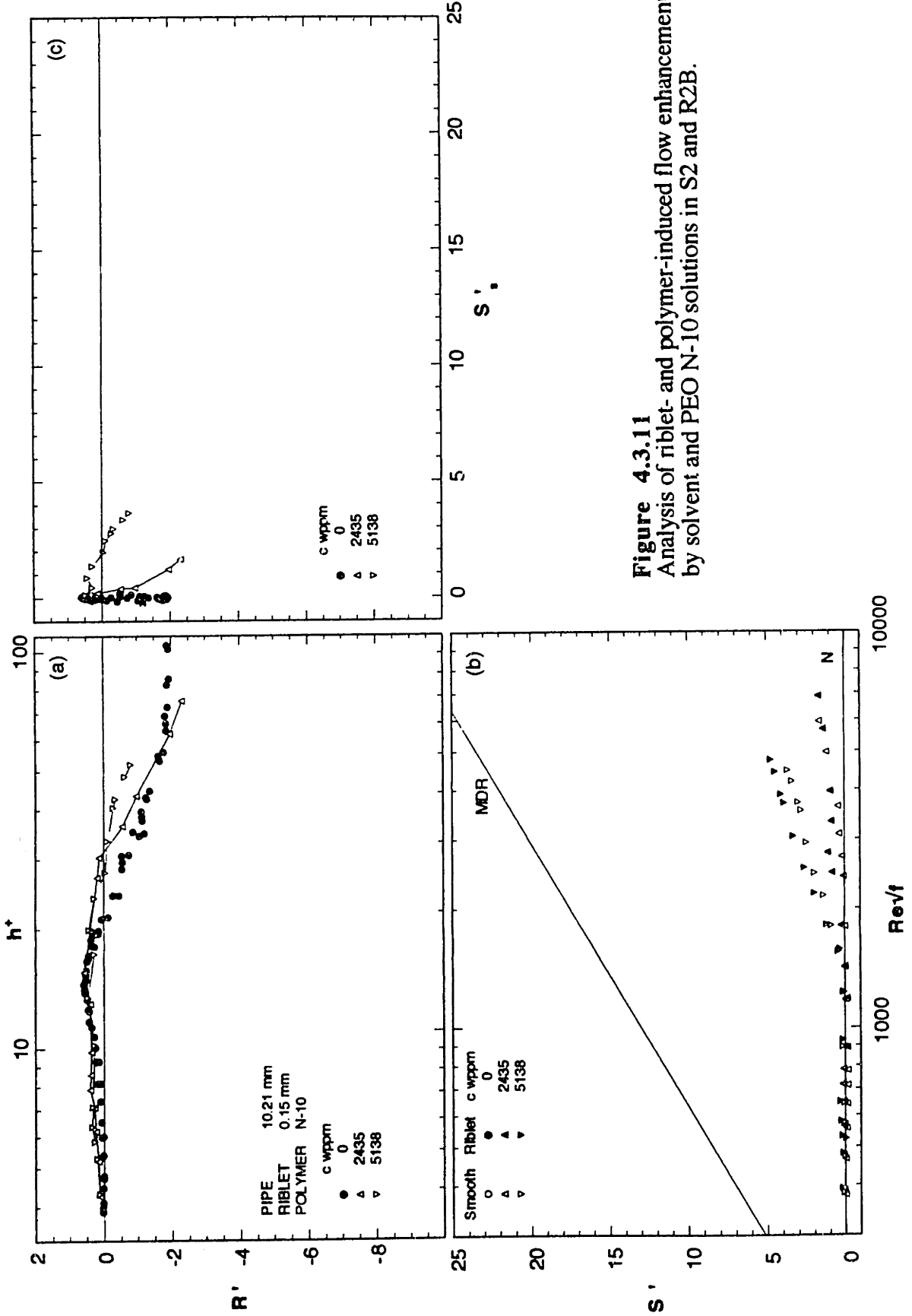


Figure 4.3.11
Analysis of riblet- and polymer-induced flow enhancements
by solvent and PEO N-10 solutions in S2 and R2B.

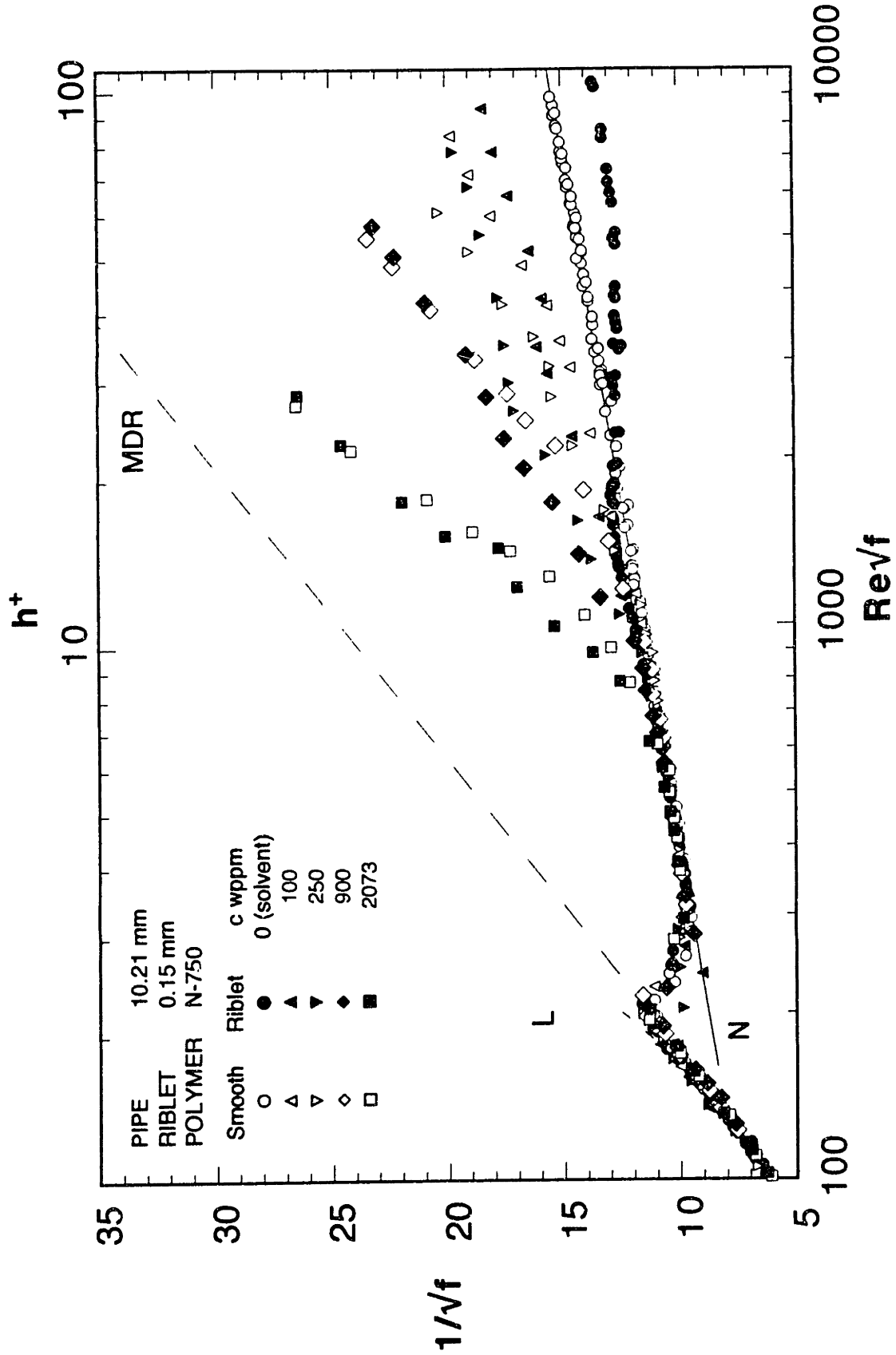


Figure 4.3.12 Friction factors for solutions of PEO N-750 in S2 and R2B.

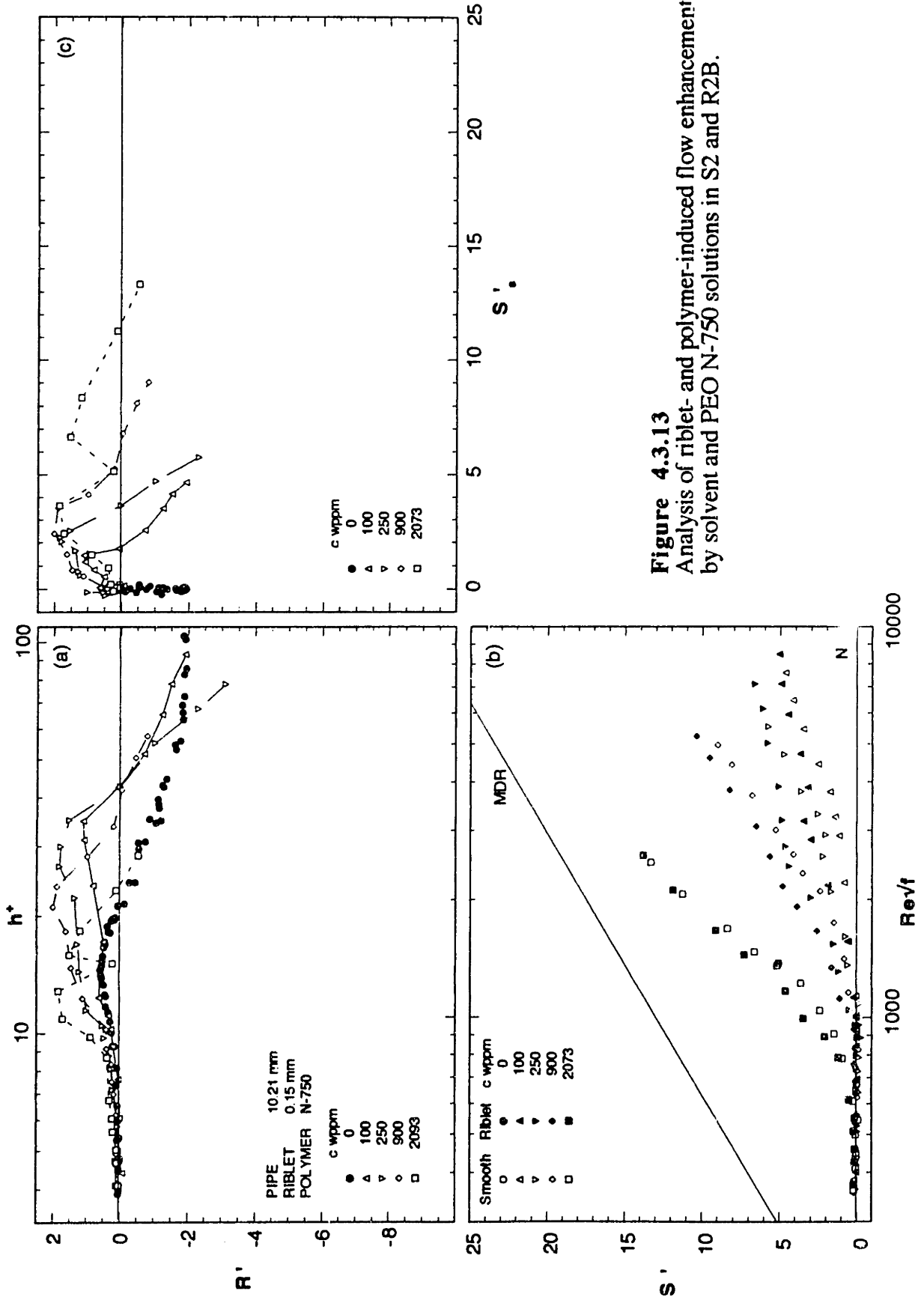


Figure 4.3.13
 Analysis of riblet- and polymer-induced flow enhancements by solvent and PEO N-750 solutions in S2 and R2B.

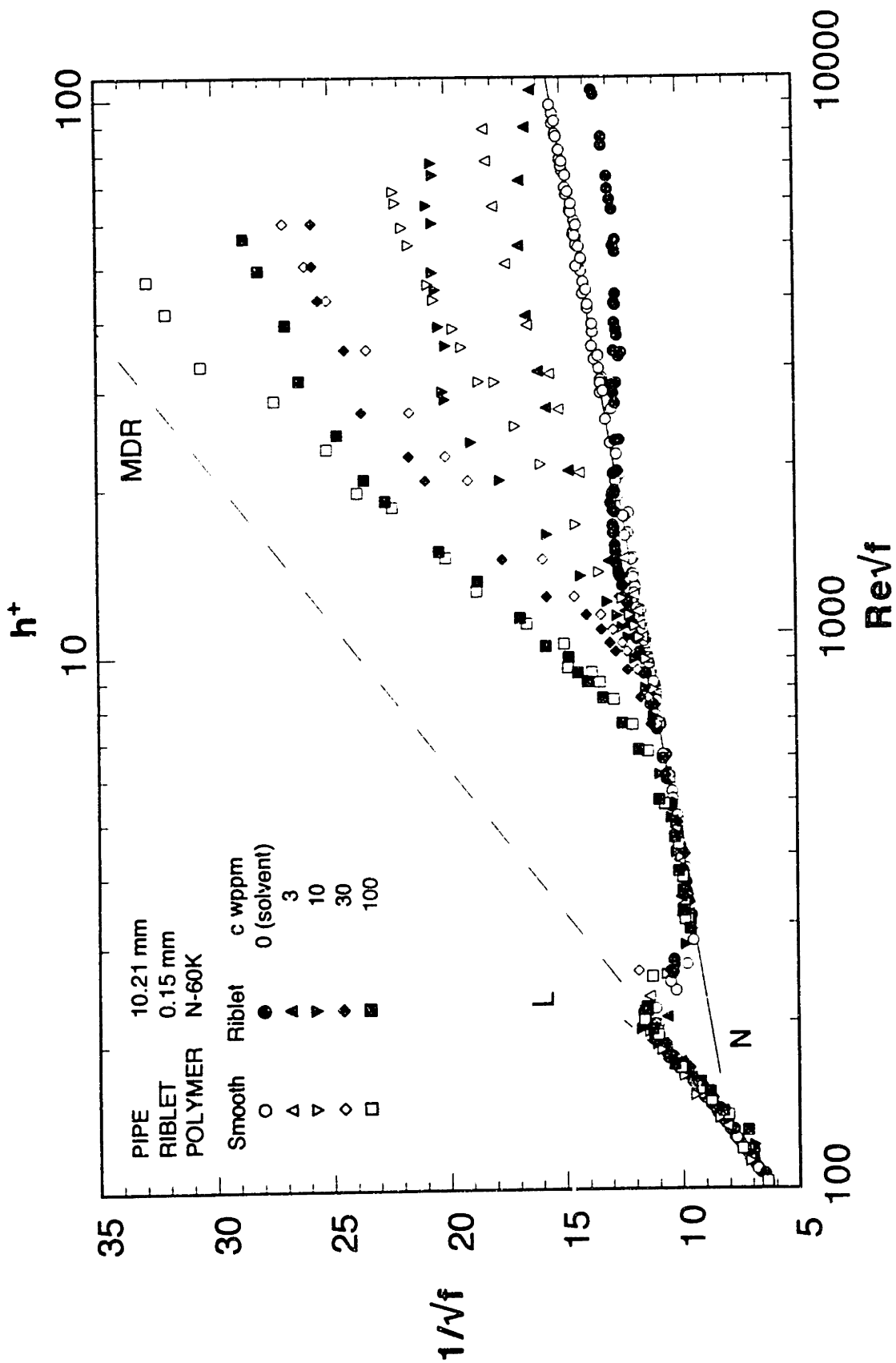


Figure 4.3.14 Friction factors for solutions of PEO N-60K in S2 and R2B.

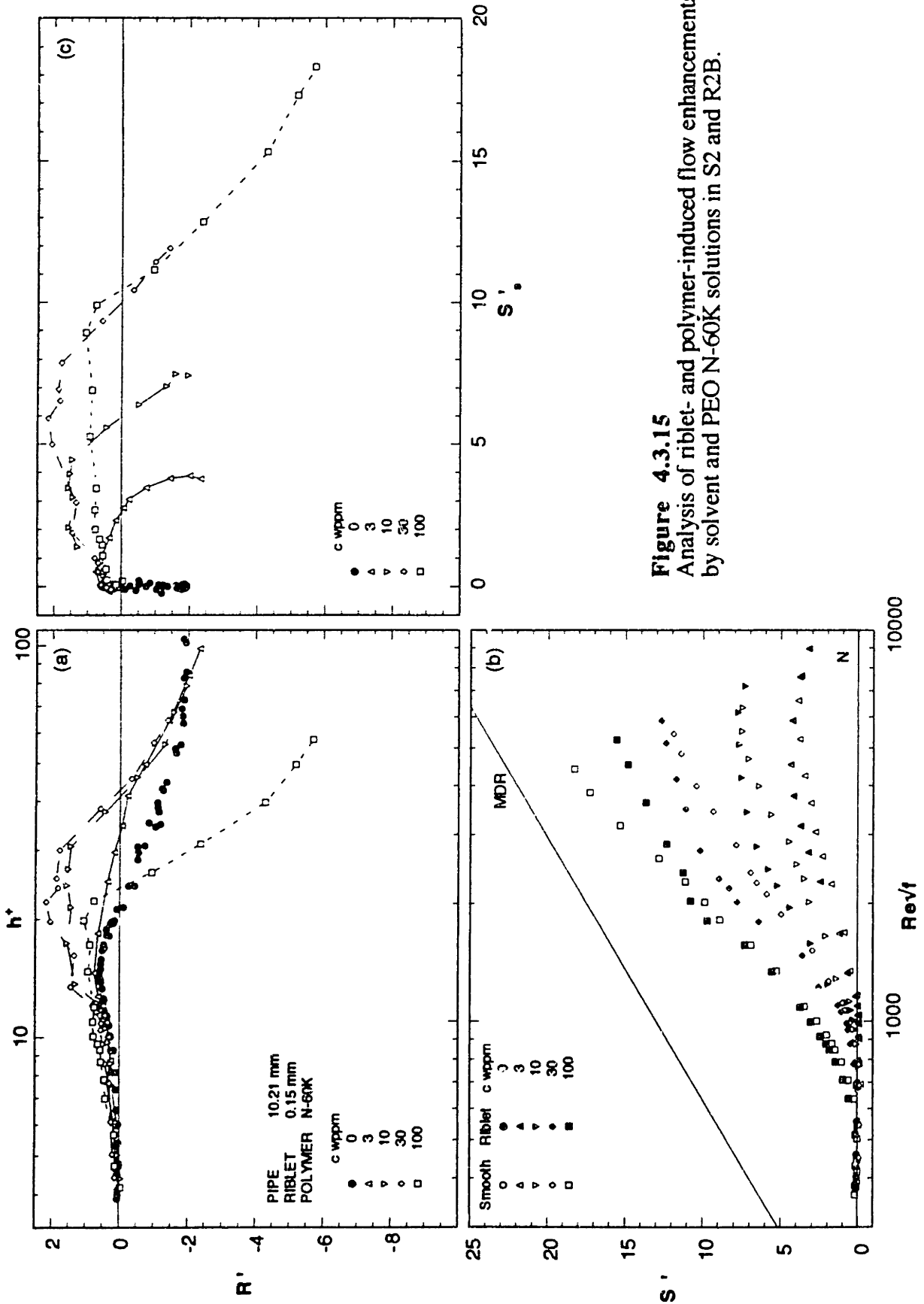


Figure 4.3.15
Analysis of riblet- and polymer-induced flow enhancements by solvent and PEO N-60K solutions in S2 and R2B.

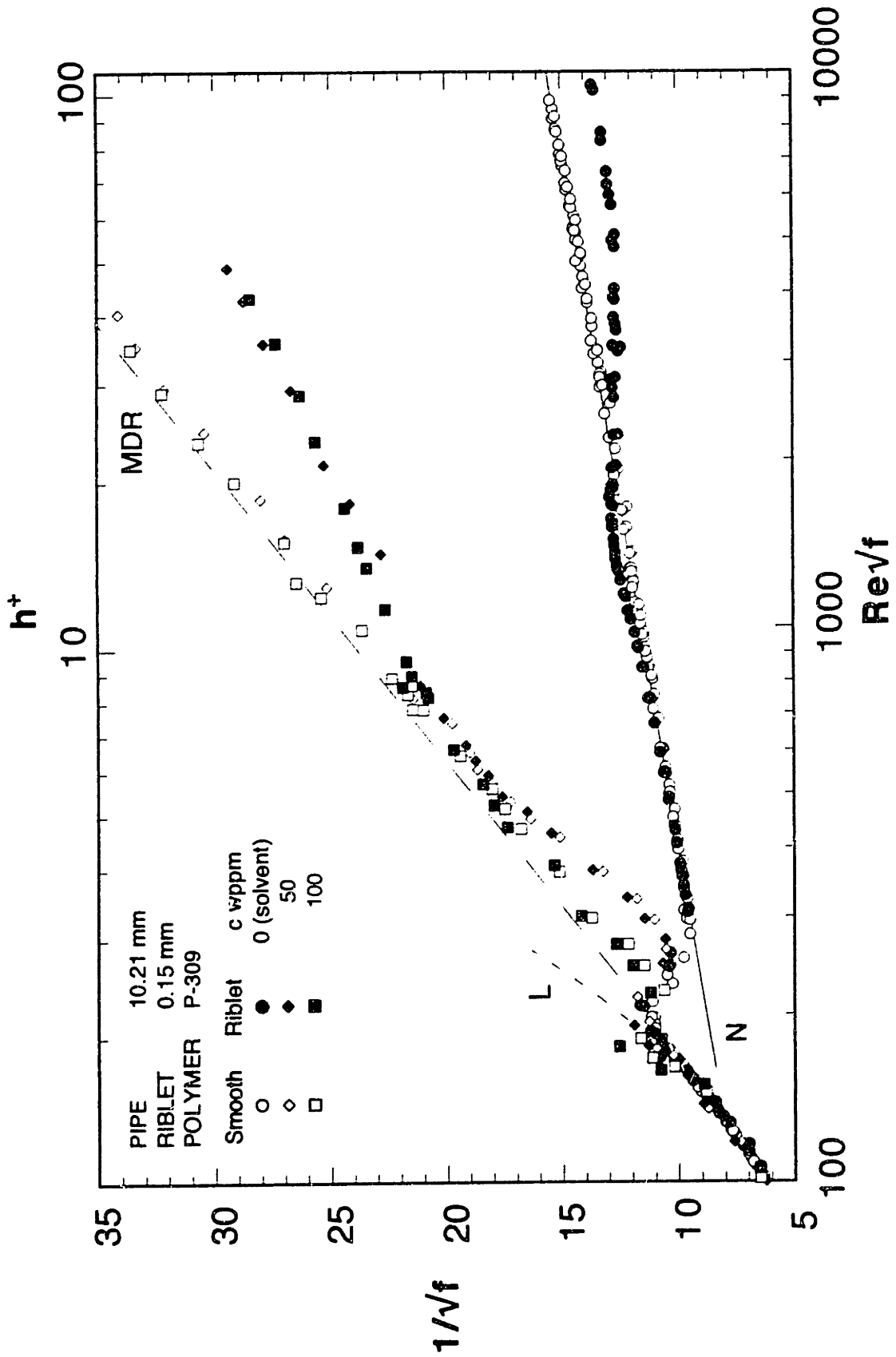


Figure 4.3.16 Friction factors for solutions of PEO P-309 in S2 and R2B.

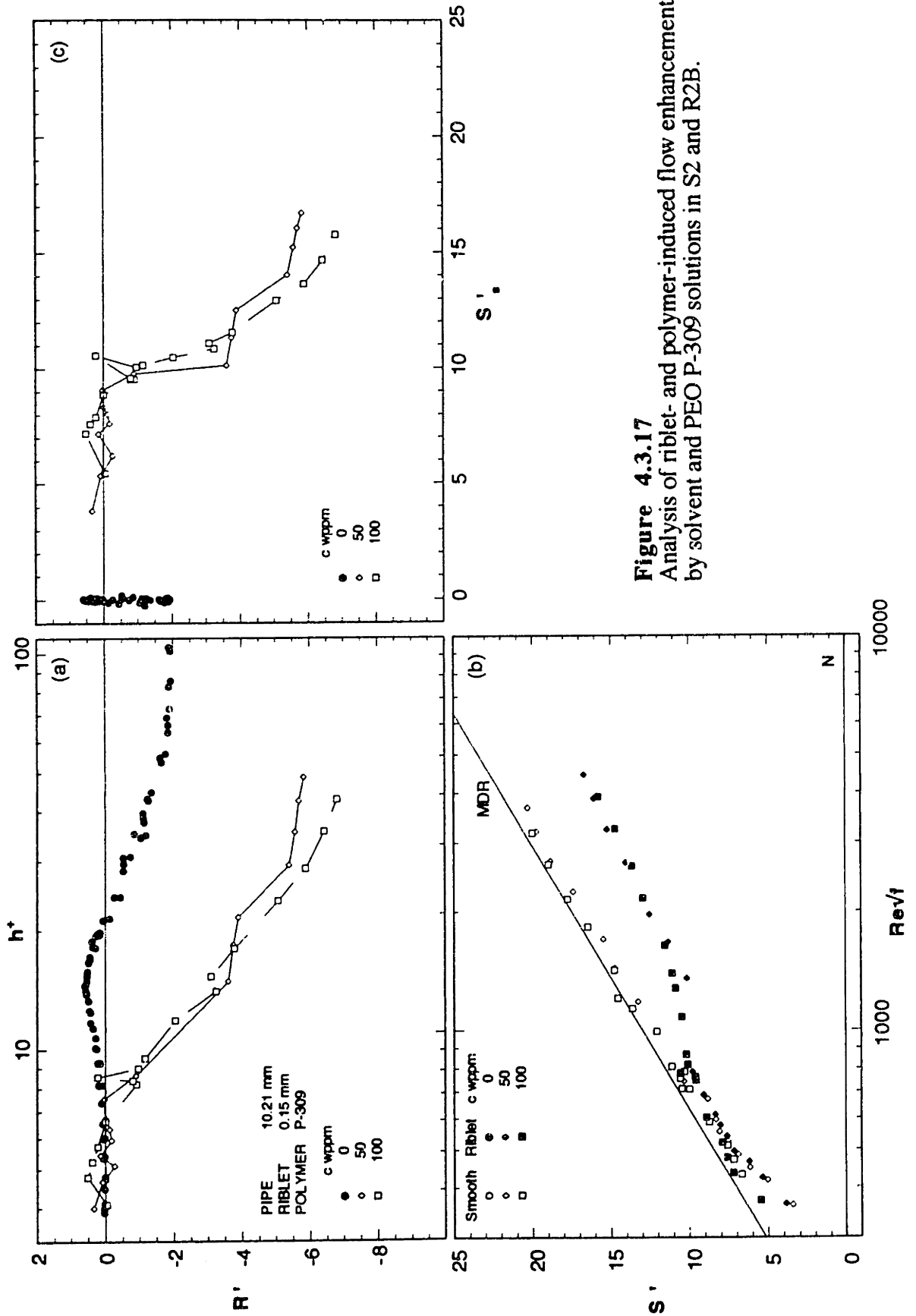


Figure 4.3.17
 Analysis of riblet- and polymer-induced flow enhancements by solvent and PEO P-309 solutions in S2 and R2B.

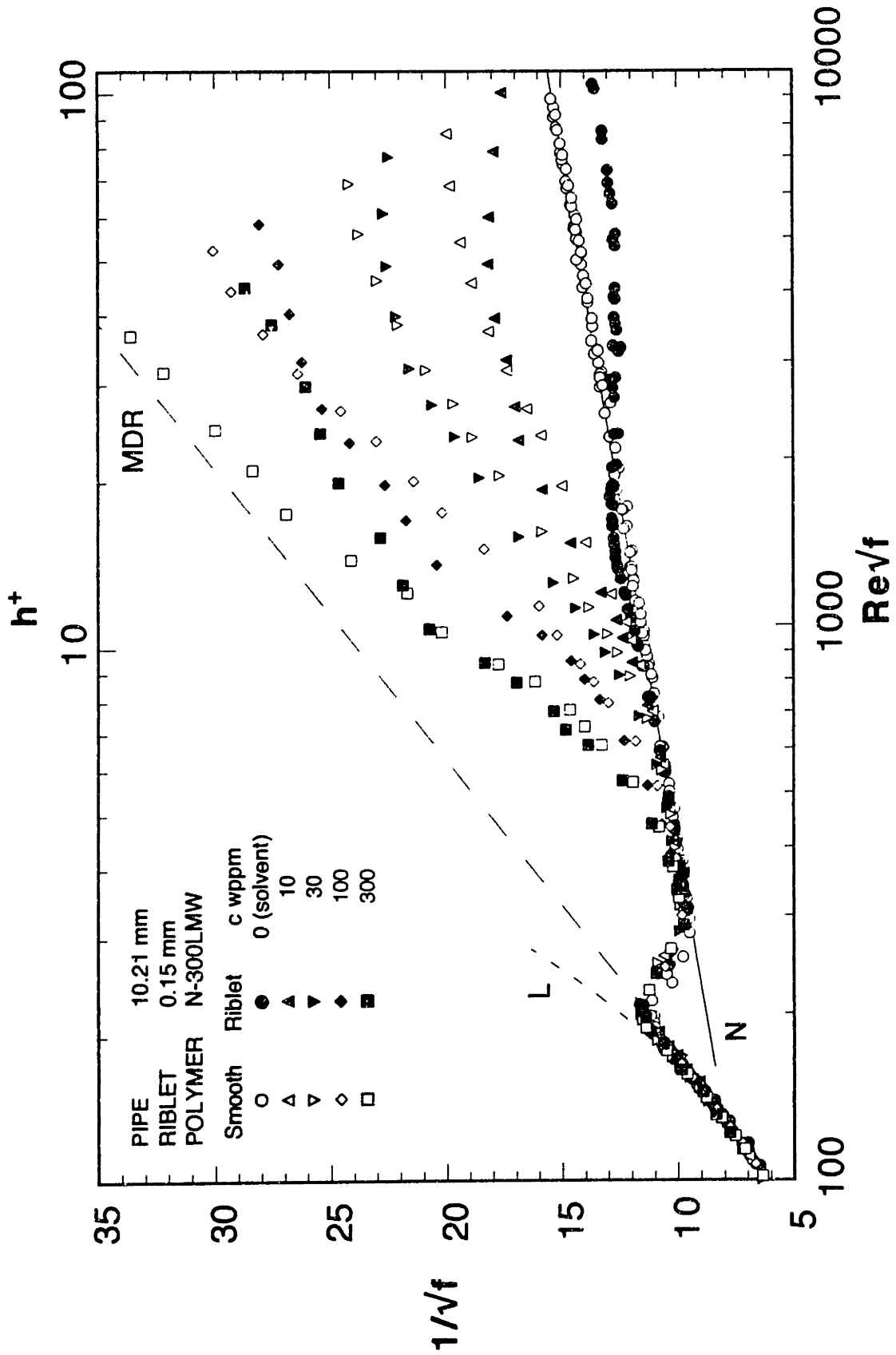


Figure 4.3.18 Friction factors for solutions of PAM N-300L in S2 and R2B.

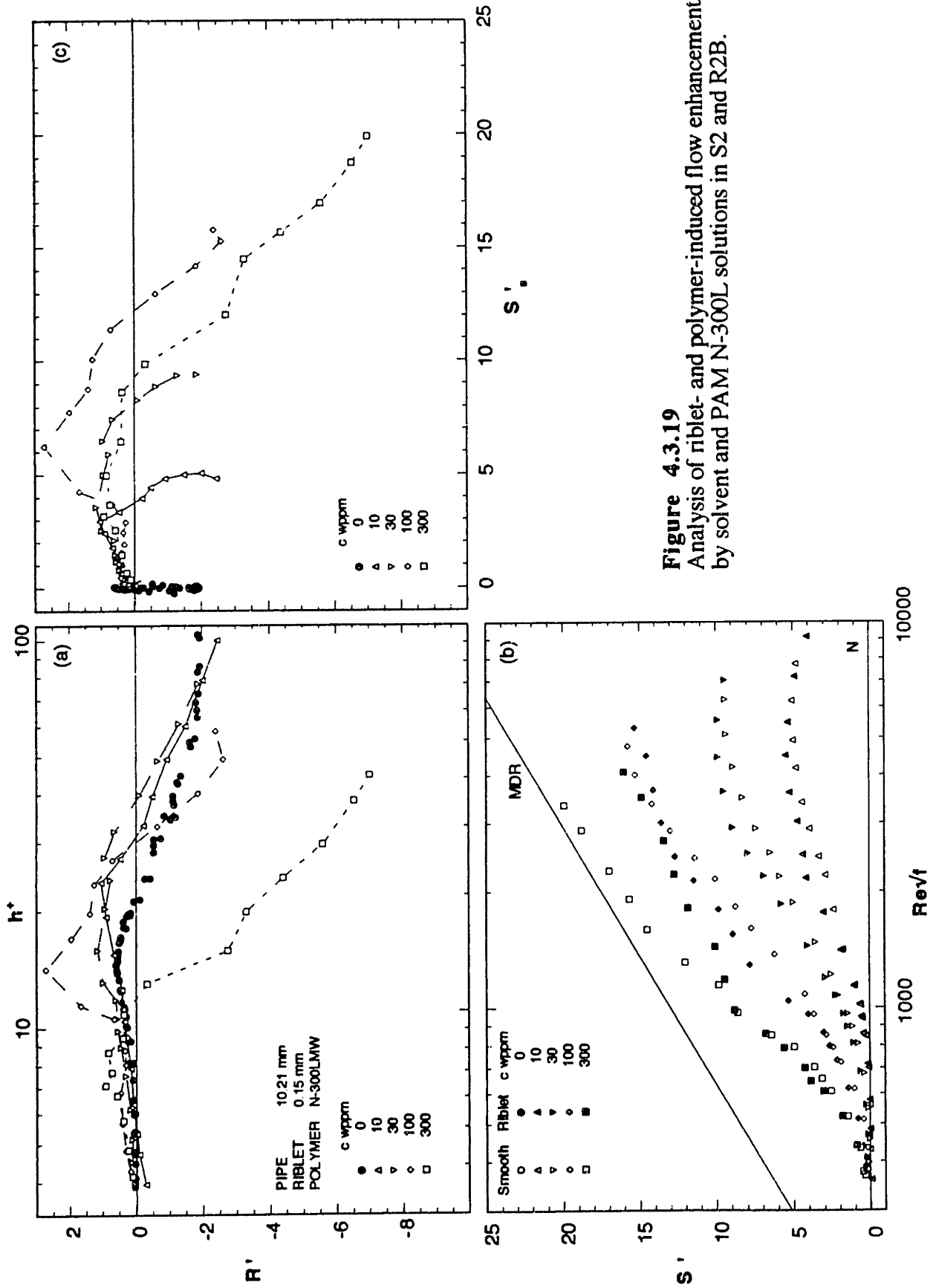


Figure 4.3.19
 Analysis of riblet- and polymer-induced flow enhancements by solvent and PAM N-300L solutions in S2 and R2B.

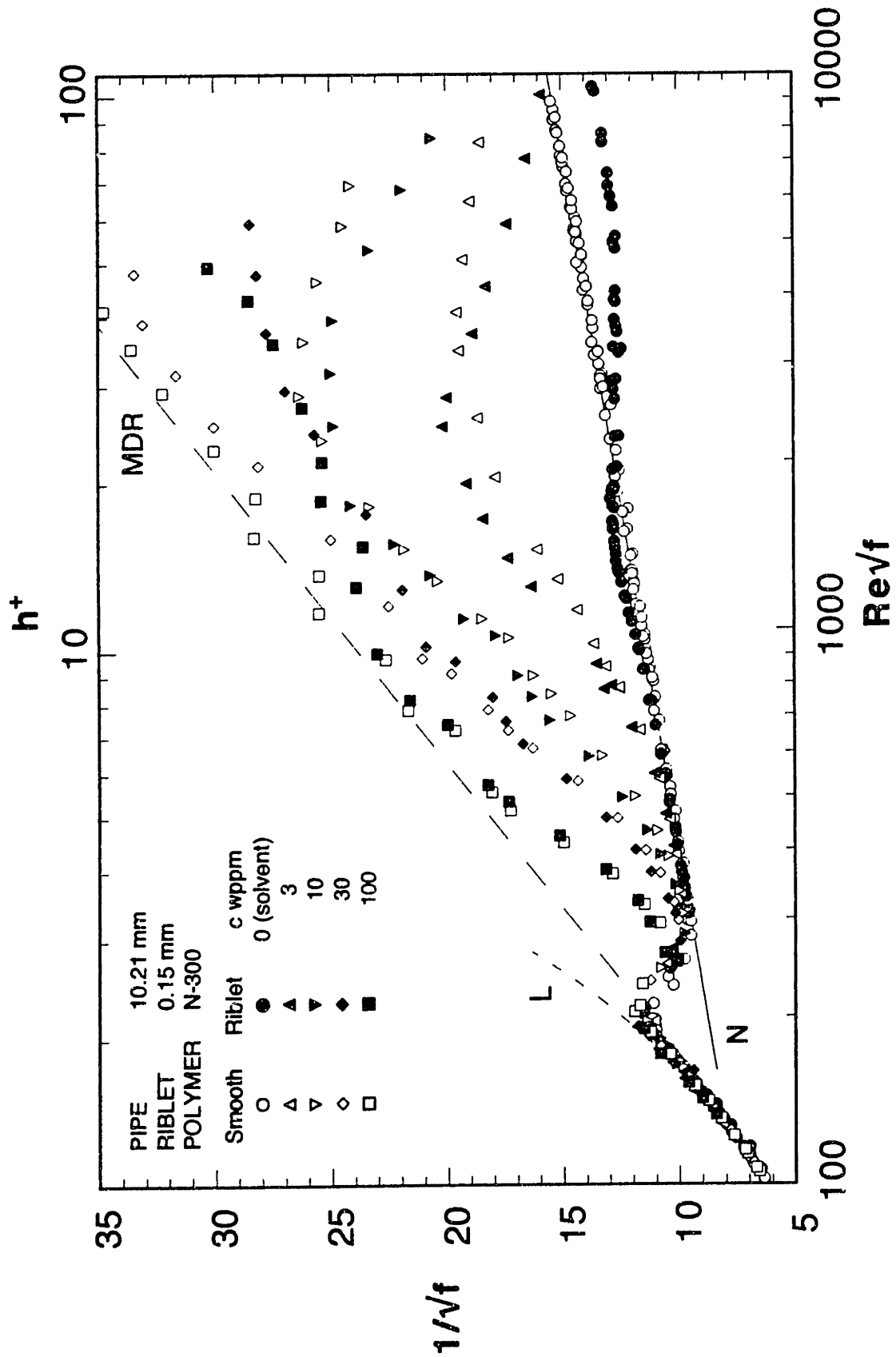


Figure 4.3.20 Friction factors for solutions of PAM N-300 in S2 and R2B.

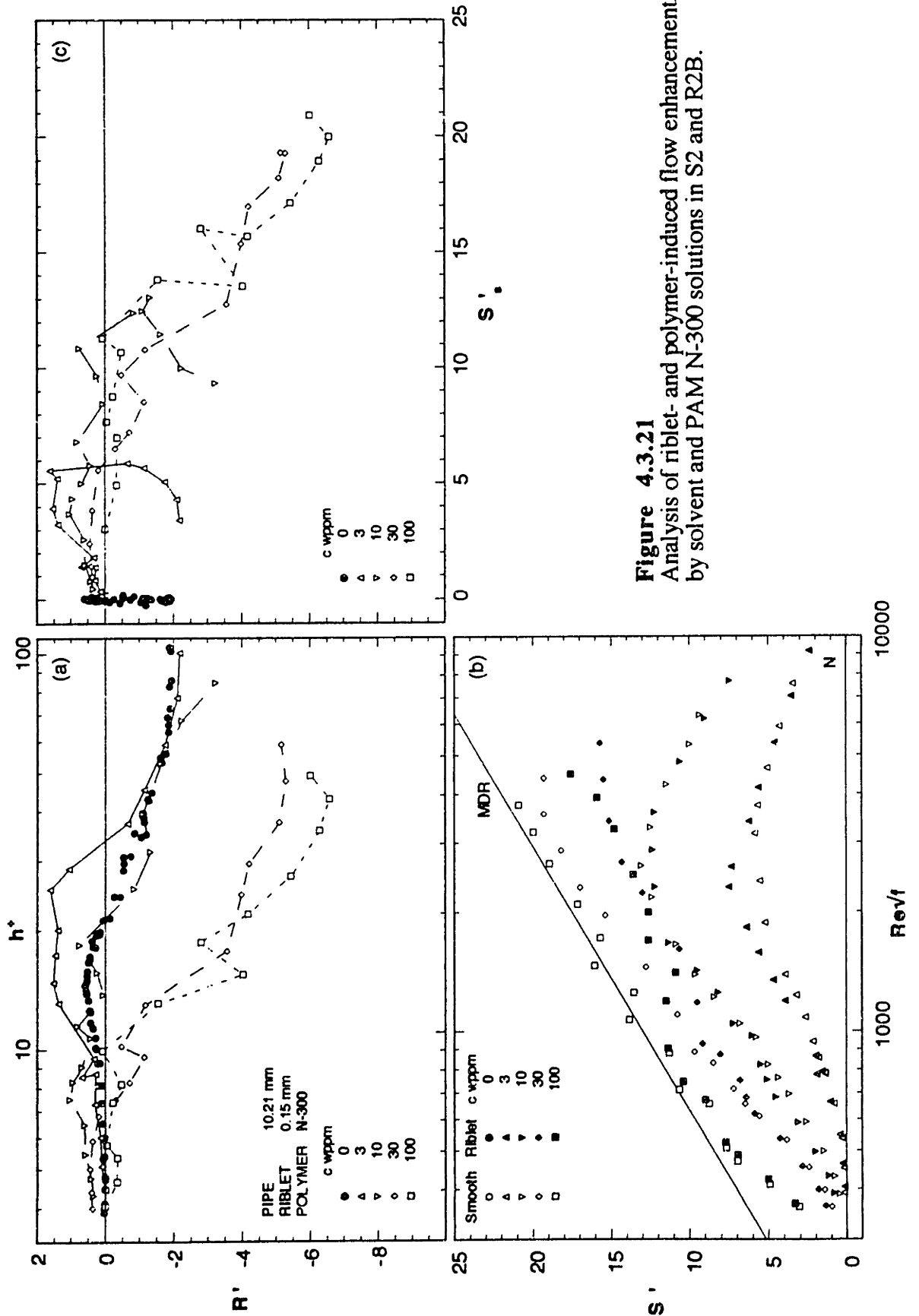
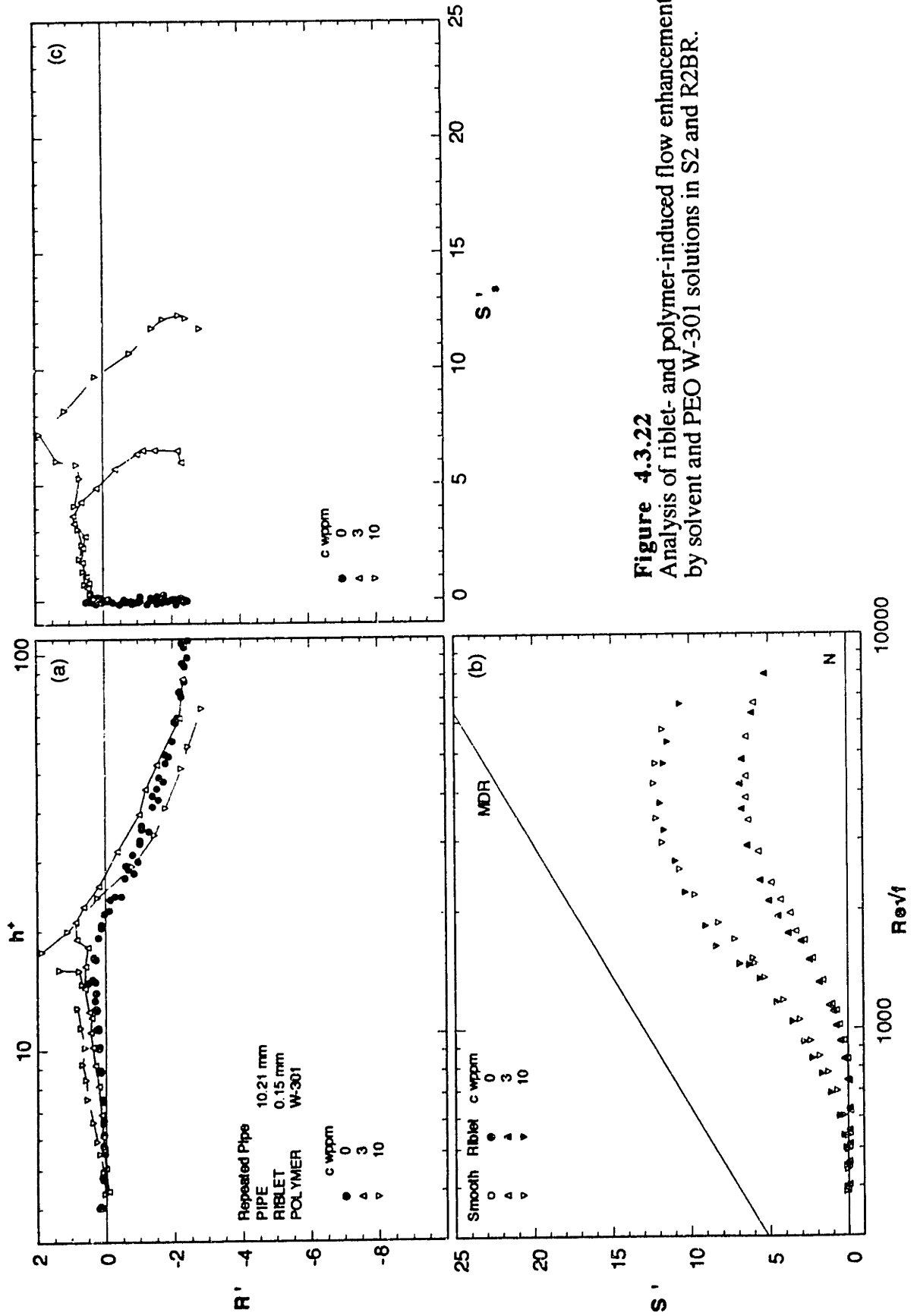


Figure 4.3.21
Analysis of riblet- and polymer-induced flow enhancements by solvent and PAM N-300 solutions in S2 and R2B.



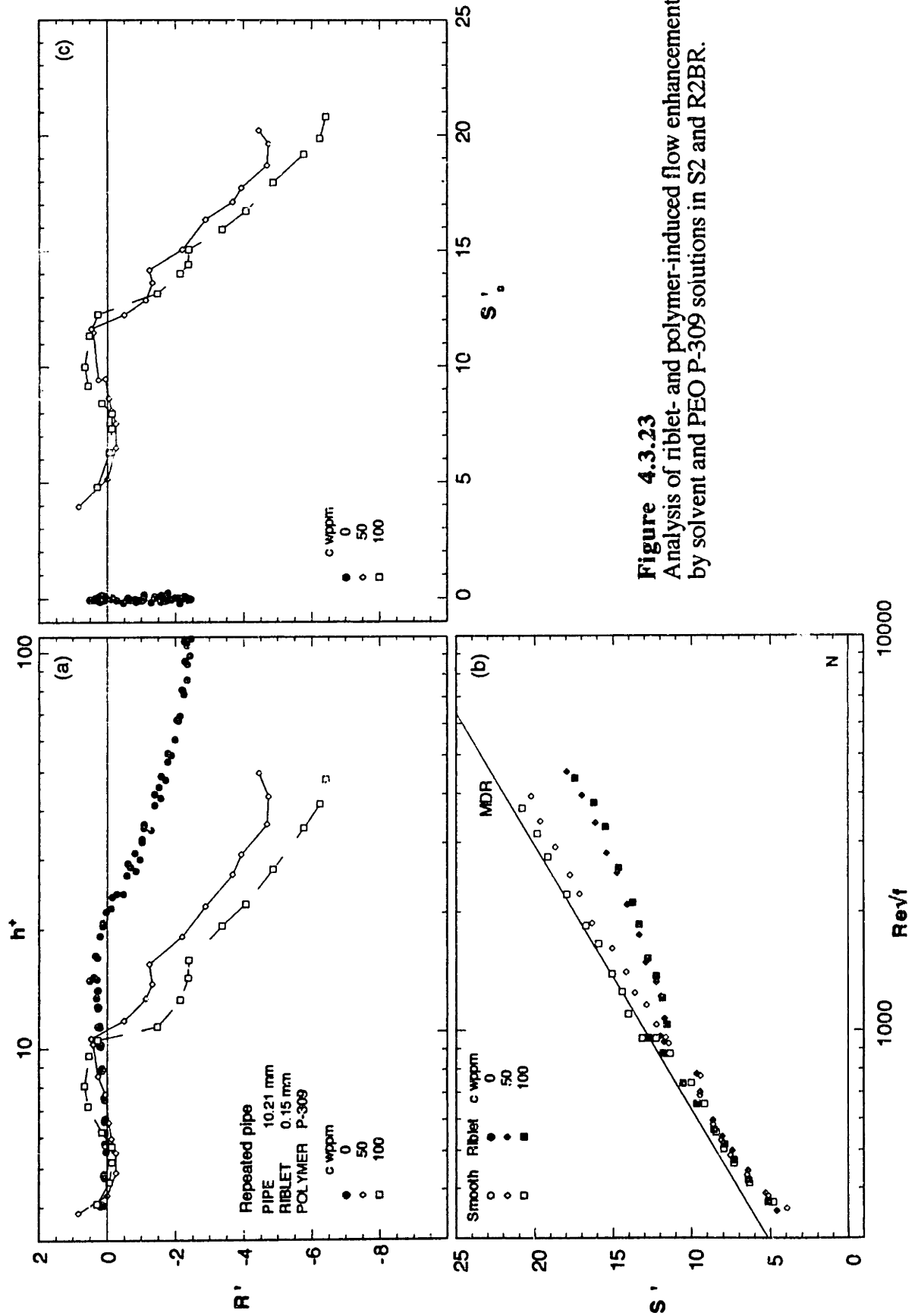


Figure 4.3.23
Analysis of riblet- and polymer-induced flow enhancements by solvent and PEO P-309 solutions in S2 and R2BR.

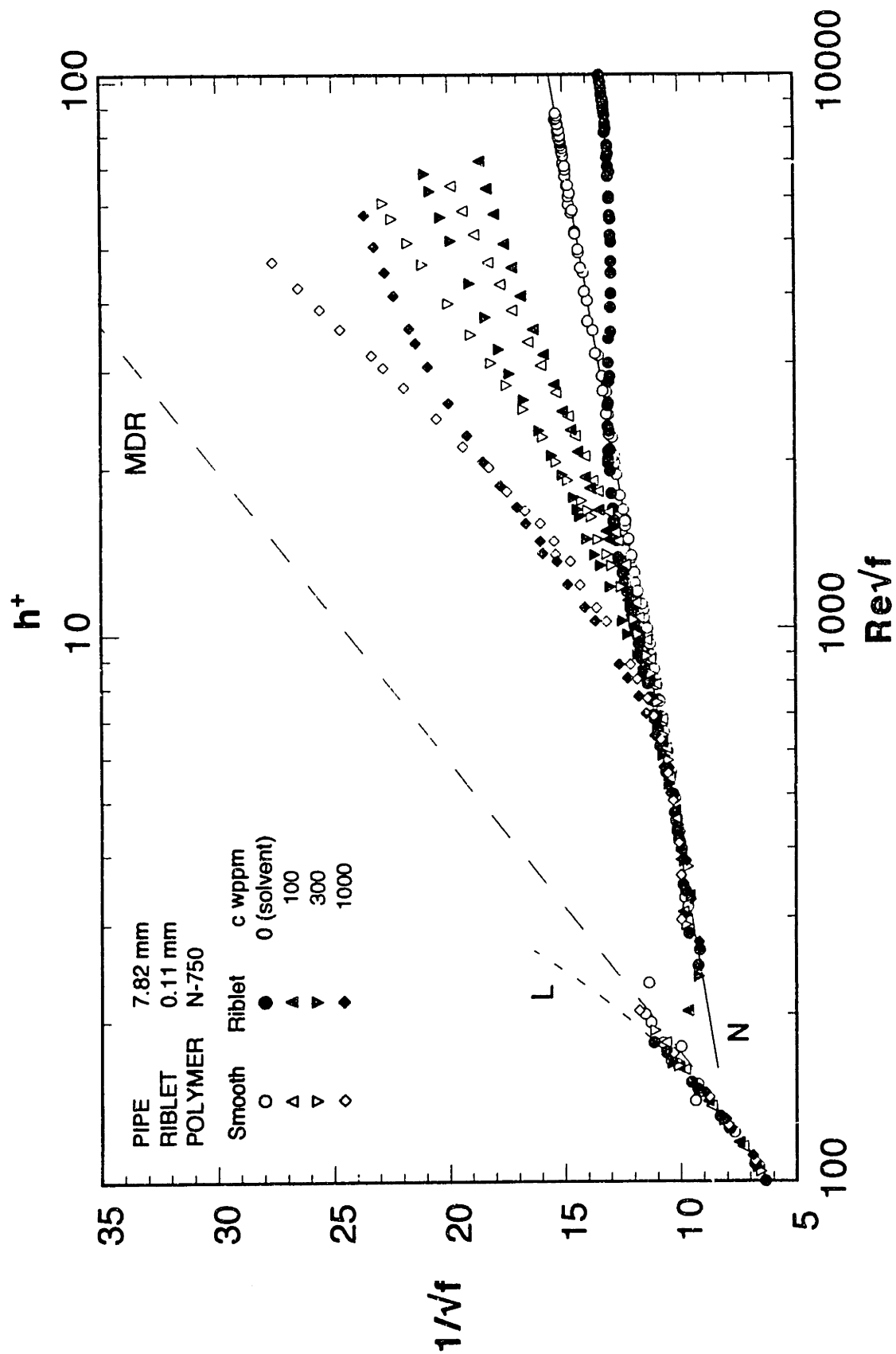


Figure 4.3.24 Friction factors for solutions of PEO N-750 in S1 and R1A.

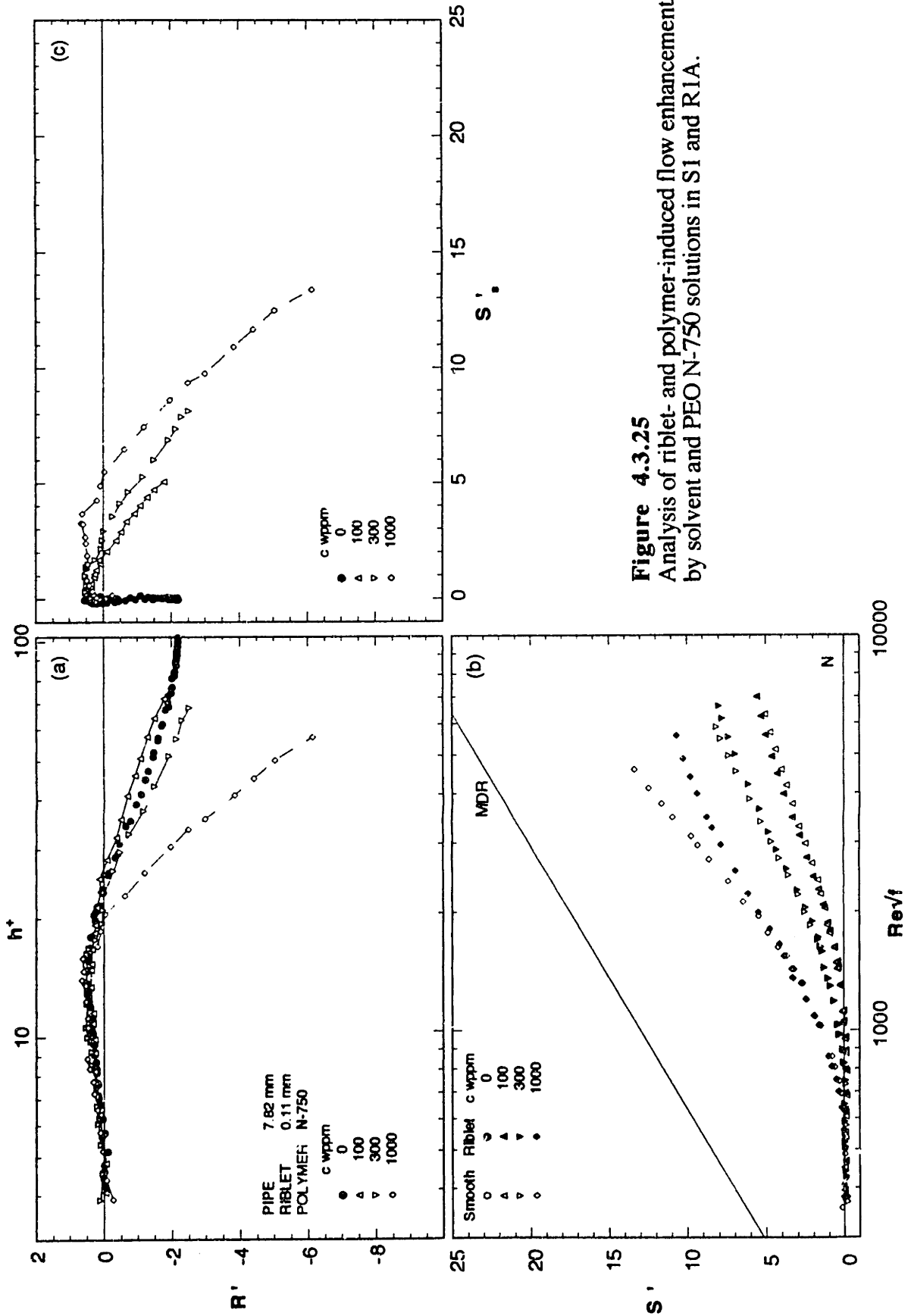


Figure 4.3.25
 Analysis of riblet- and polymer-induced flow enhancements by solvent and PEO N-750 solutions in S1 and R1A.

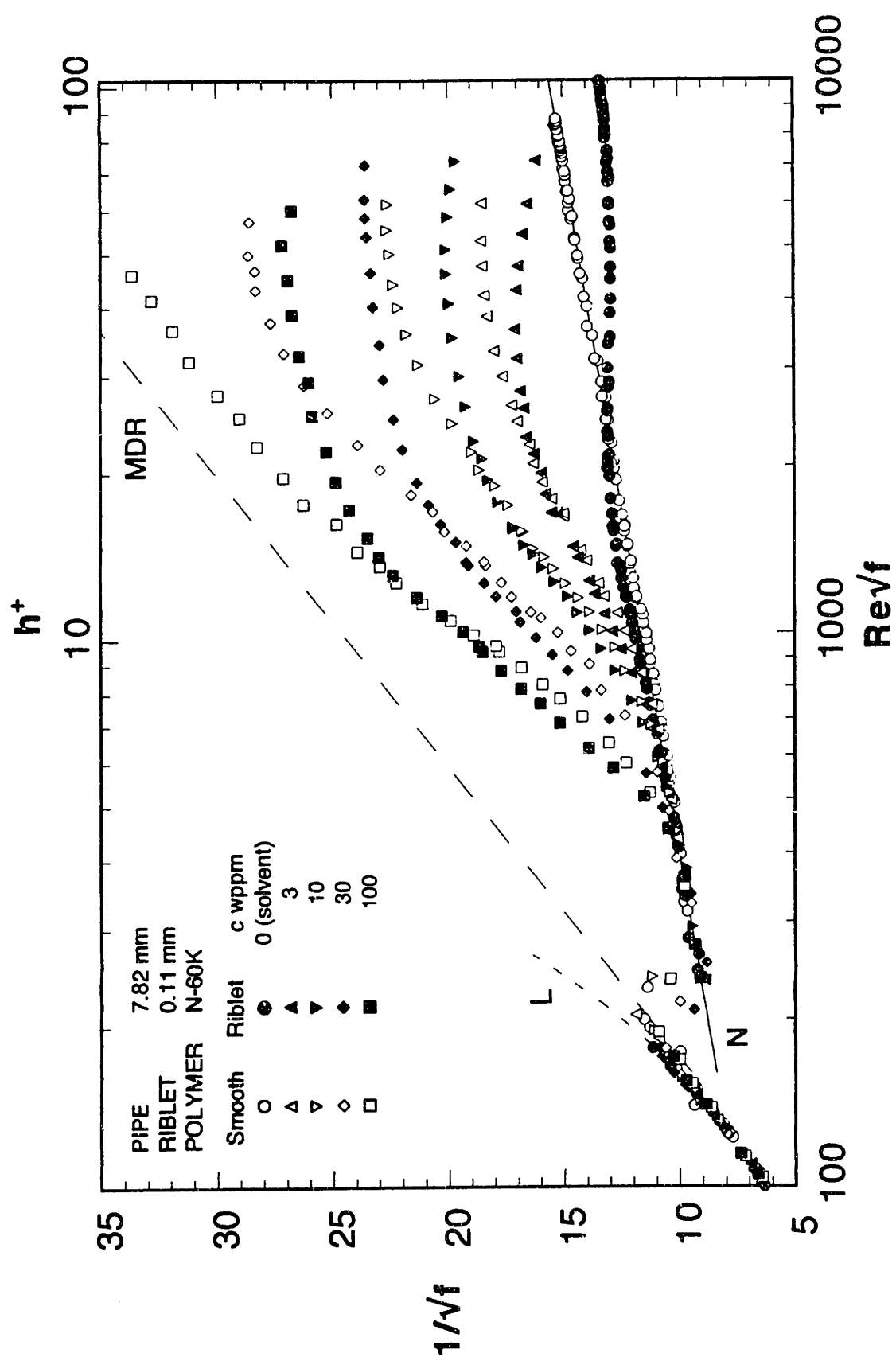


Figure 4.3.26 Friction factors for solutions of PEO N-60K in S1 and R1A.

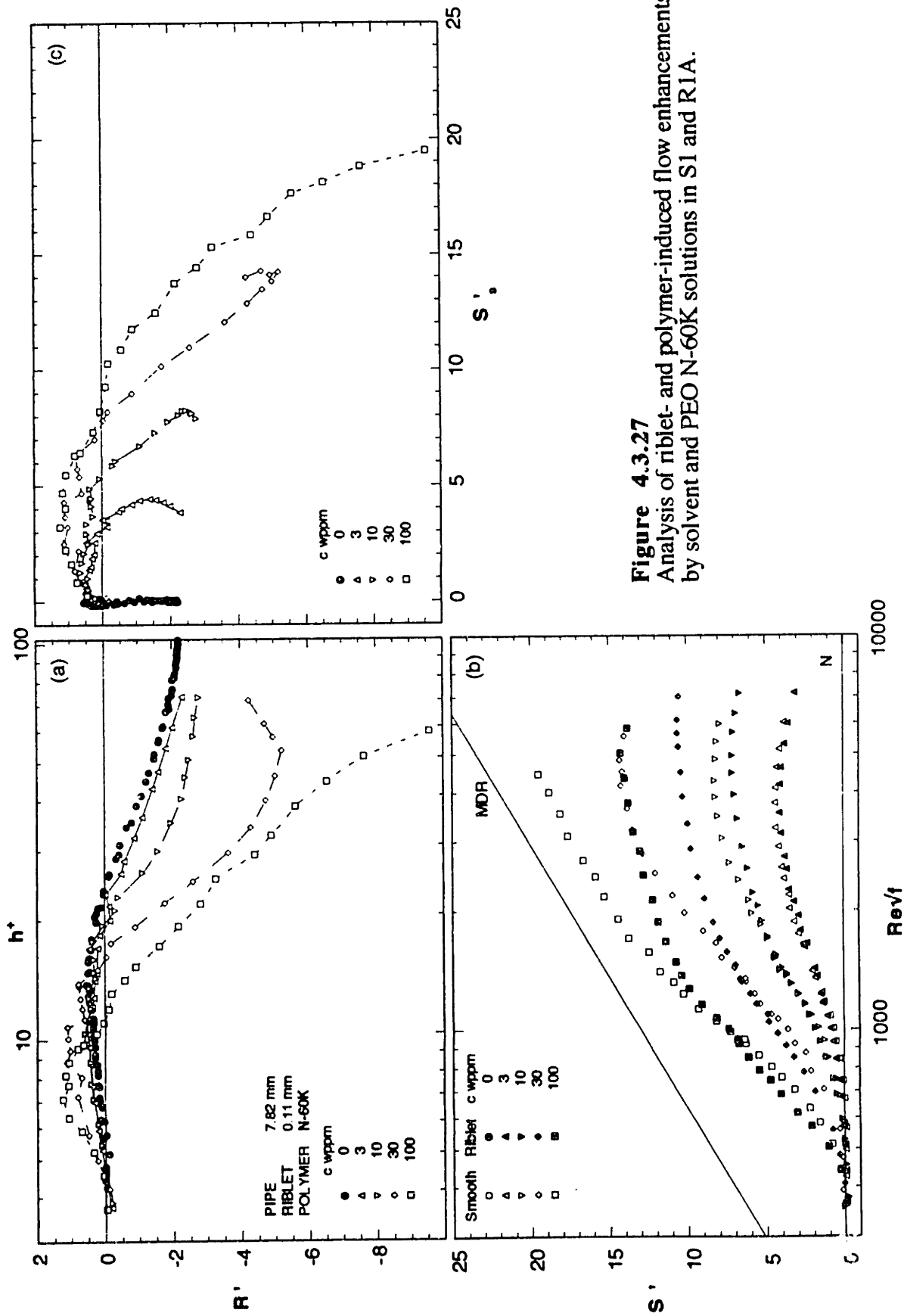


Figure 4.3.27
 Analysis of riblet- and polymer-induced flow enhancements by solvent and PEO N-60K solutions in S1 and R1A.

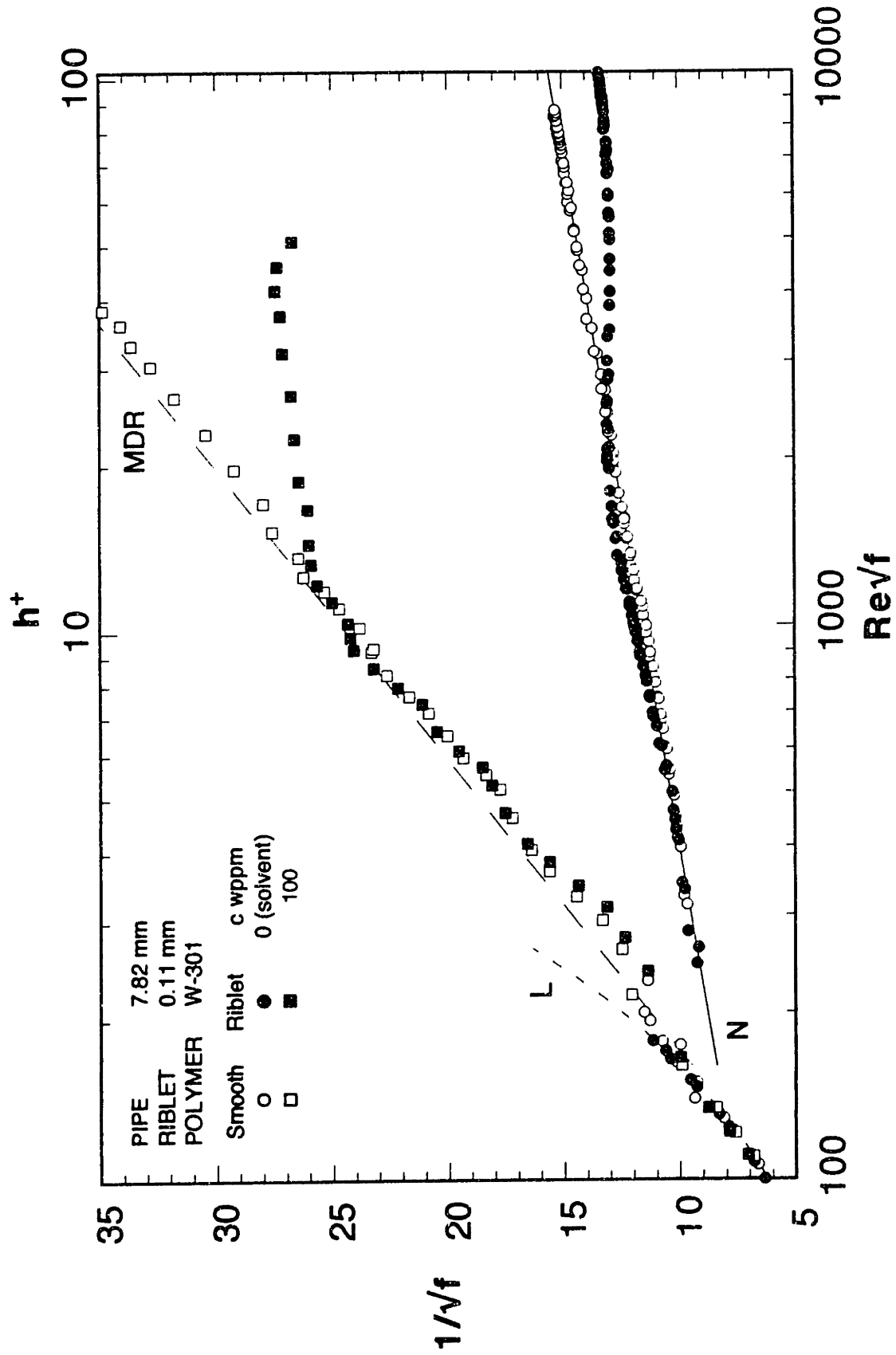


Figure 4.3.28 Friction factors for solutions of PEO W-301 in S1 and R1A.

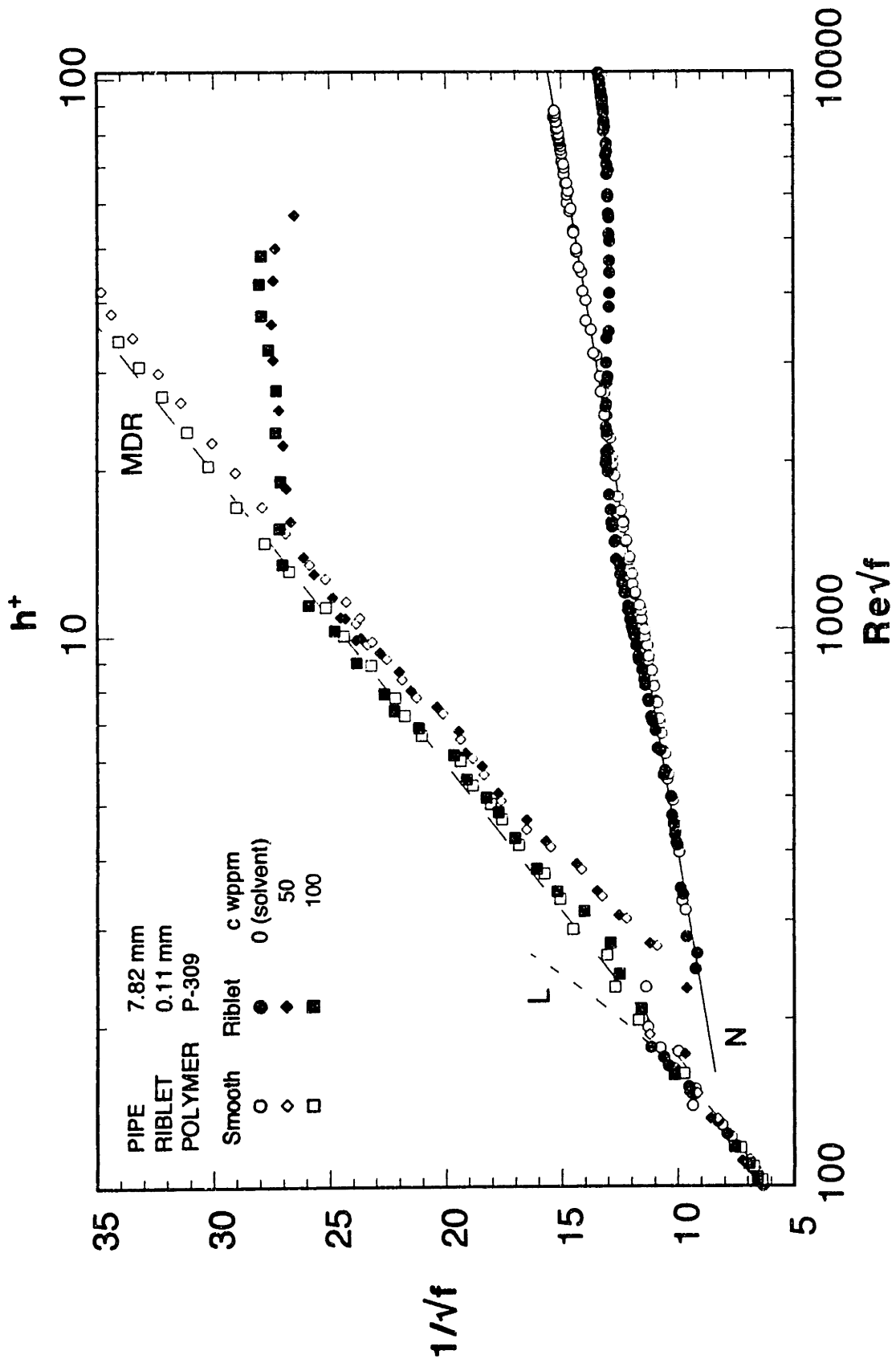


Figure 4.3.2.9 Friction factors for solutions of PEO P-309 in S1 and R1A.

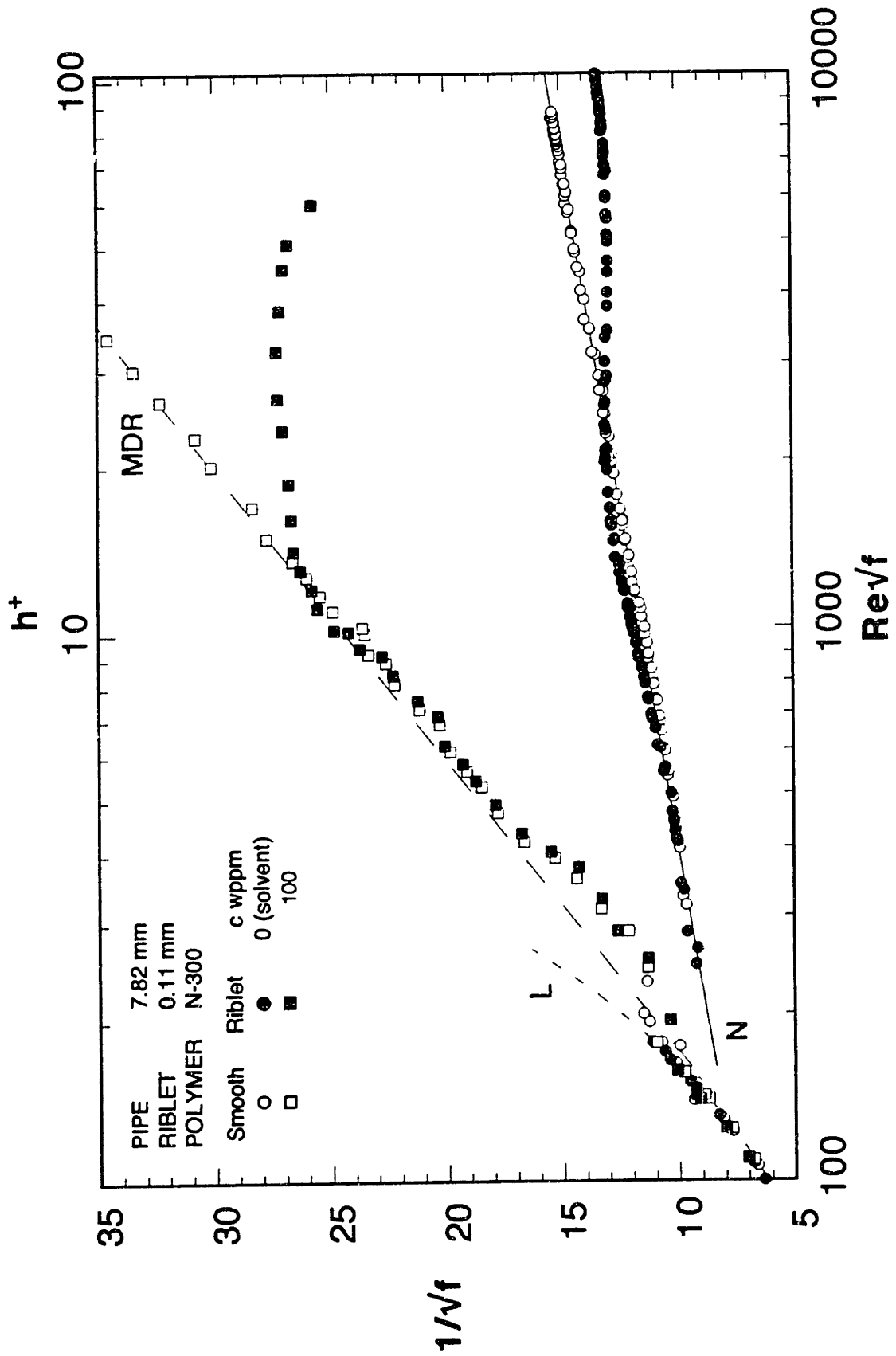


Figure 4.3.30 Friction factors for solutions of PAM N-300 in S1 and R1A.

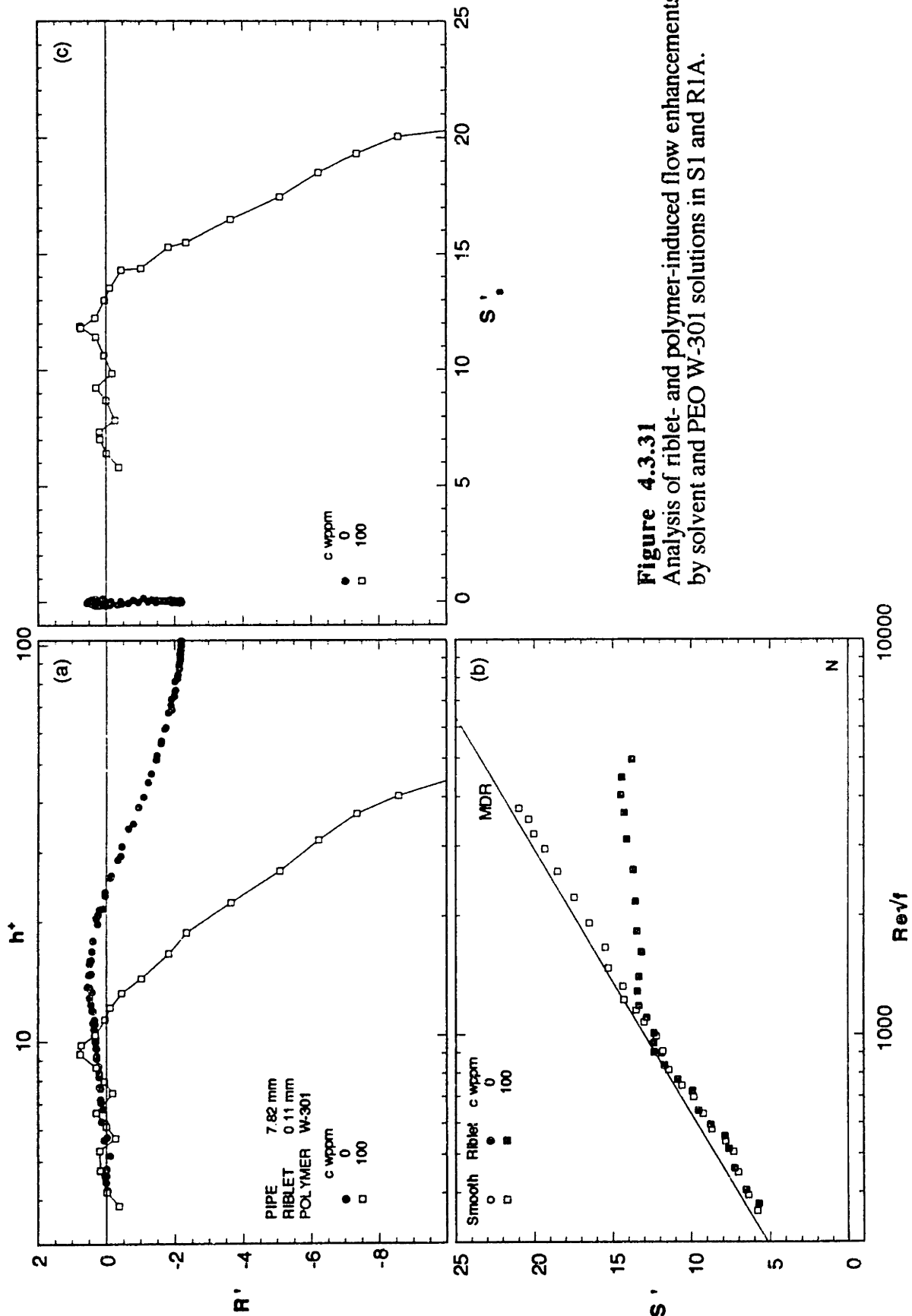


Figure 4.3.31
 Analysis of riblet- and polymer-induced flow enhancements by solvent and PEO W-301 solutions in S1 and R1A.

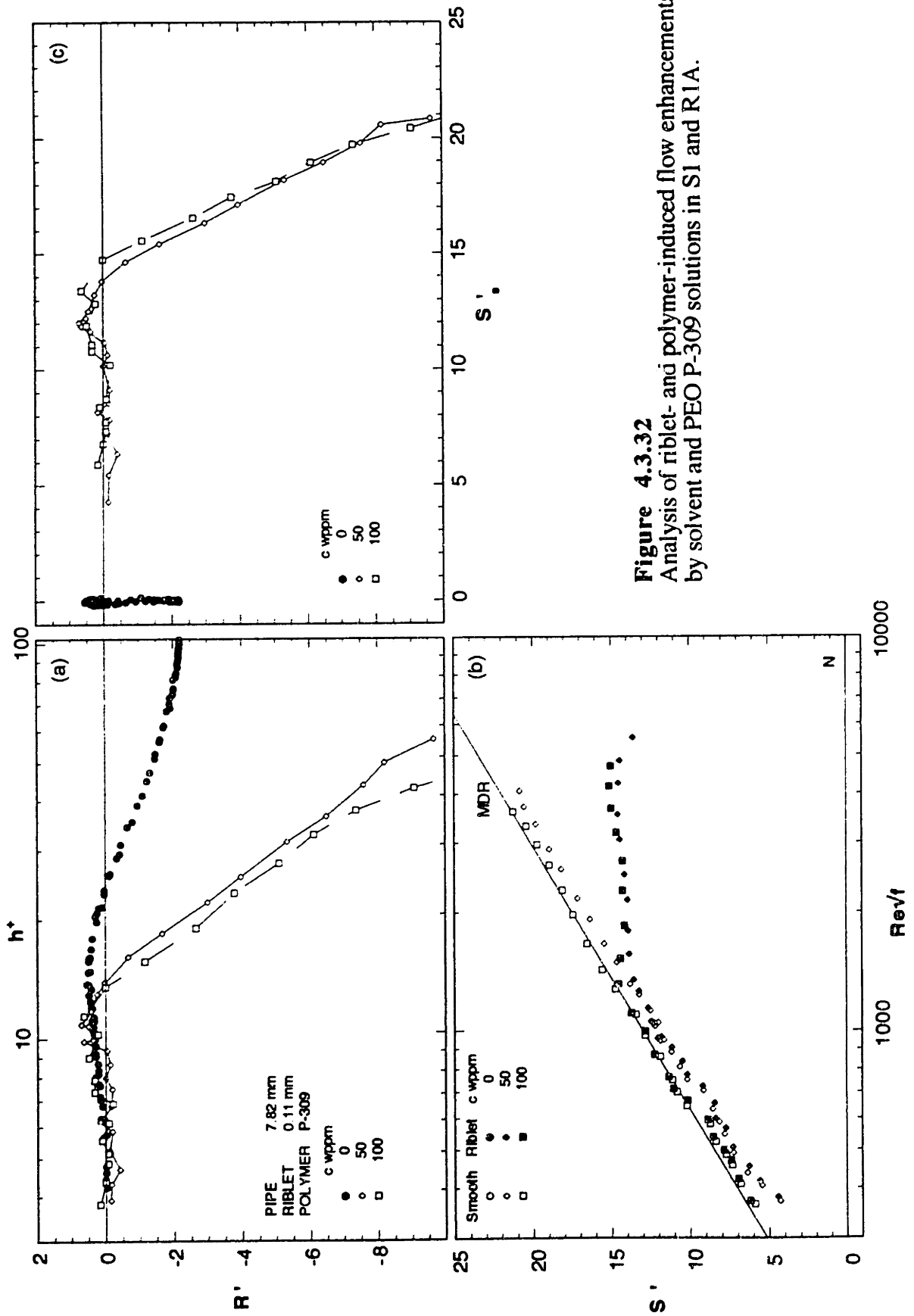


Figure 4.3.32
 Analysis of riblet- and polymer-induced flow enhancements
 by solvent and PEO P-309 solutions in S1 and R1A.

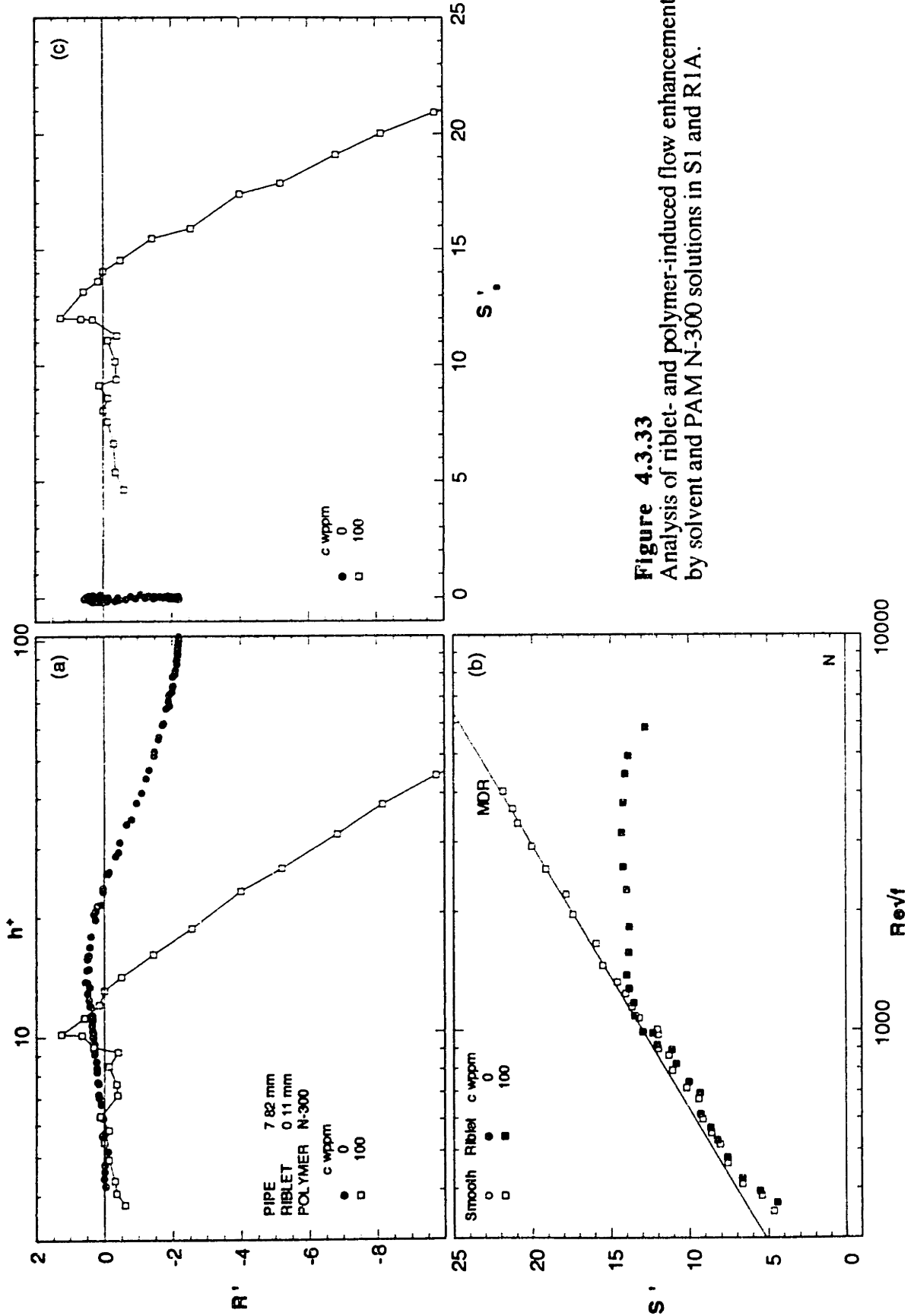


Figure 4.3.33
 Analysis of riblet- and polymer-induced flow enhancements by solvent and PAM N-300 solutions in S1 and R1A.

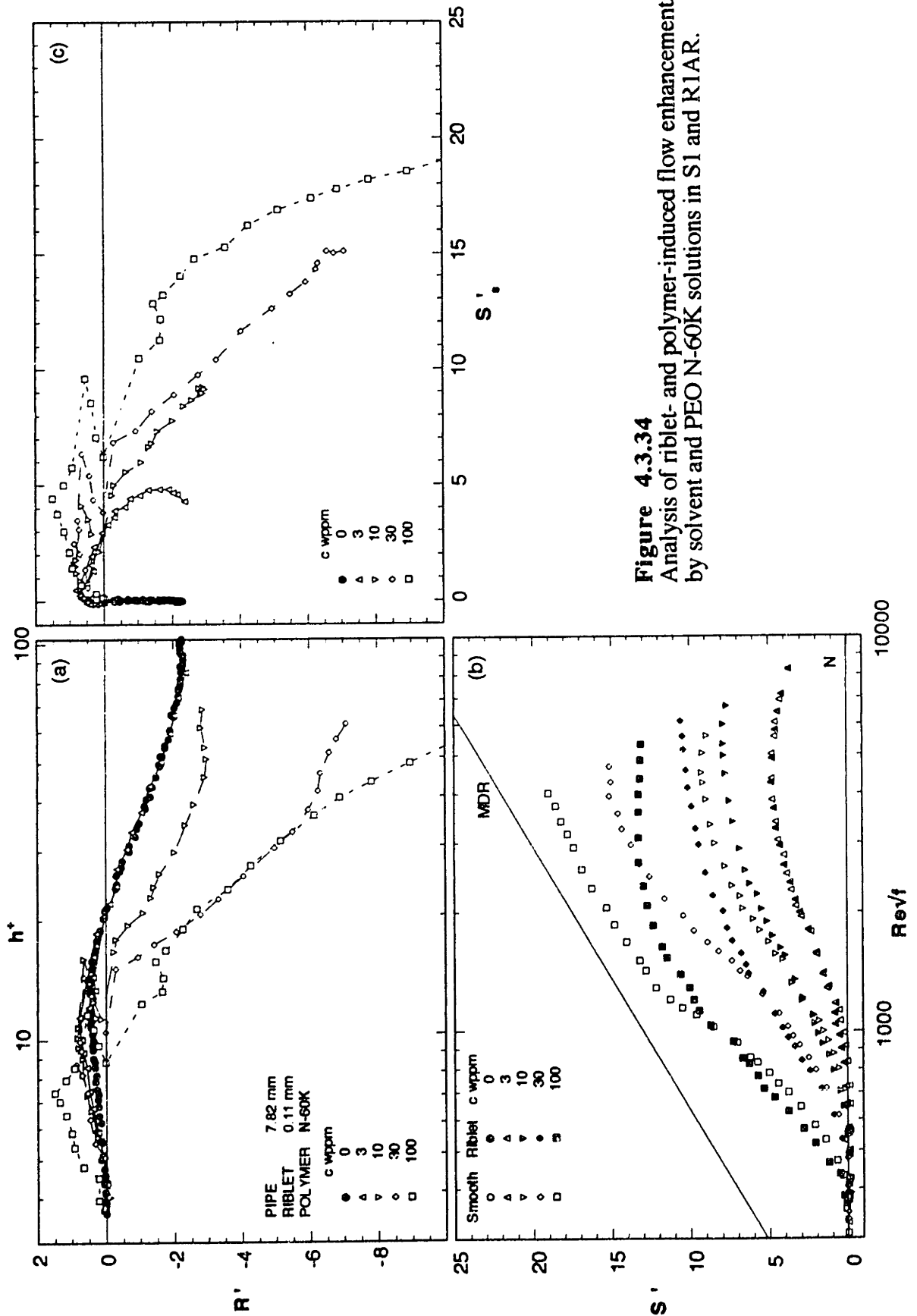


Figure 4.3.34
 Analysis of riblet- and polymer-induced flow enhancements
 by solvent and PEO N-60K solutions in S1 and RIAR.

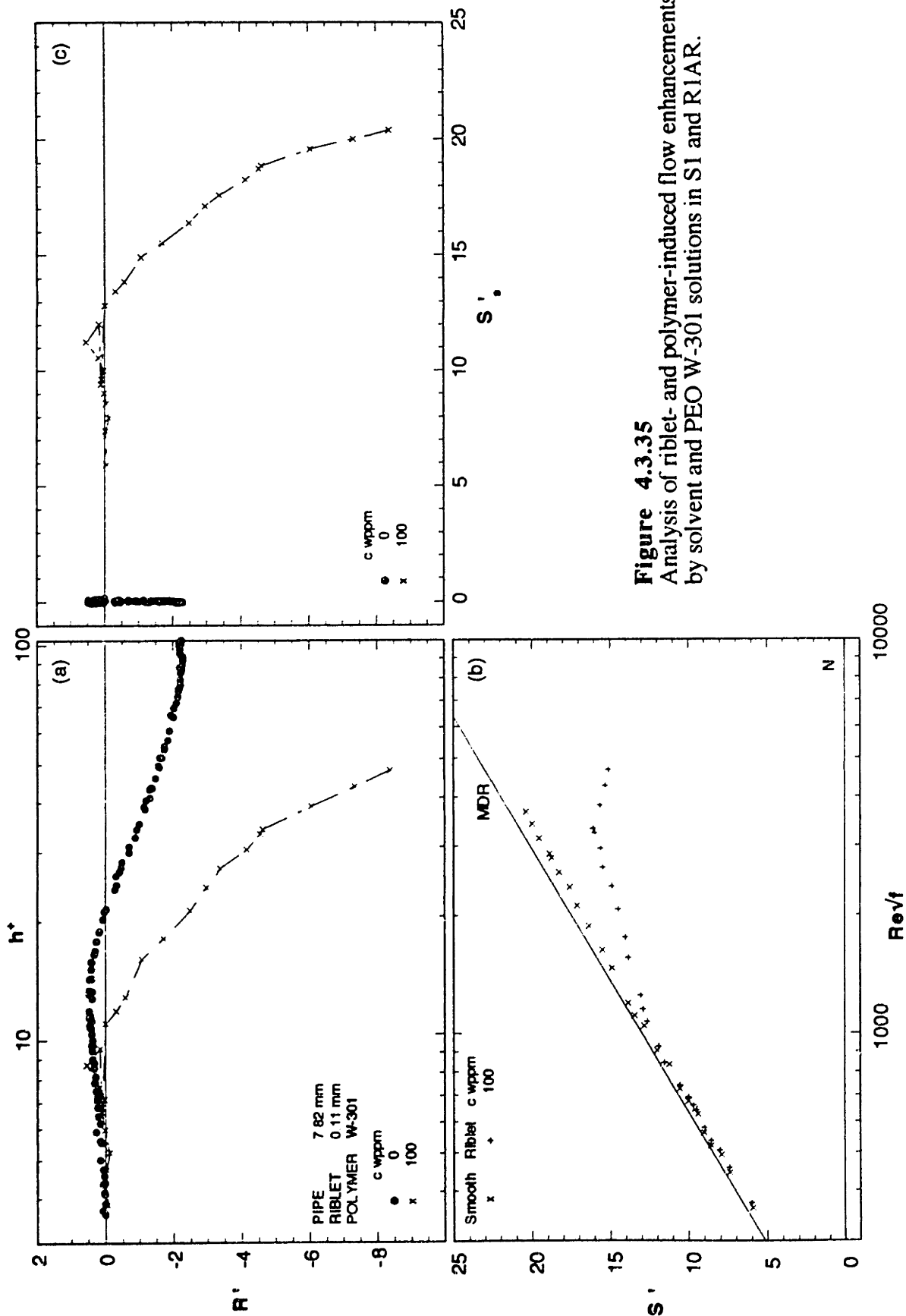


Figure 4.3.35
Analysis of riblet- and polymer-induced flow enhancements by solvent and PEO W-301 solutions in S1 and RIAR.

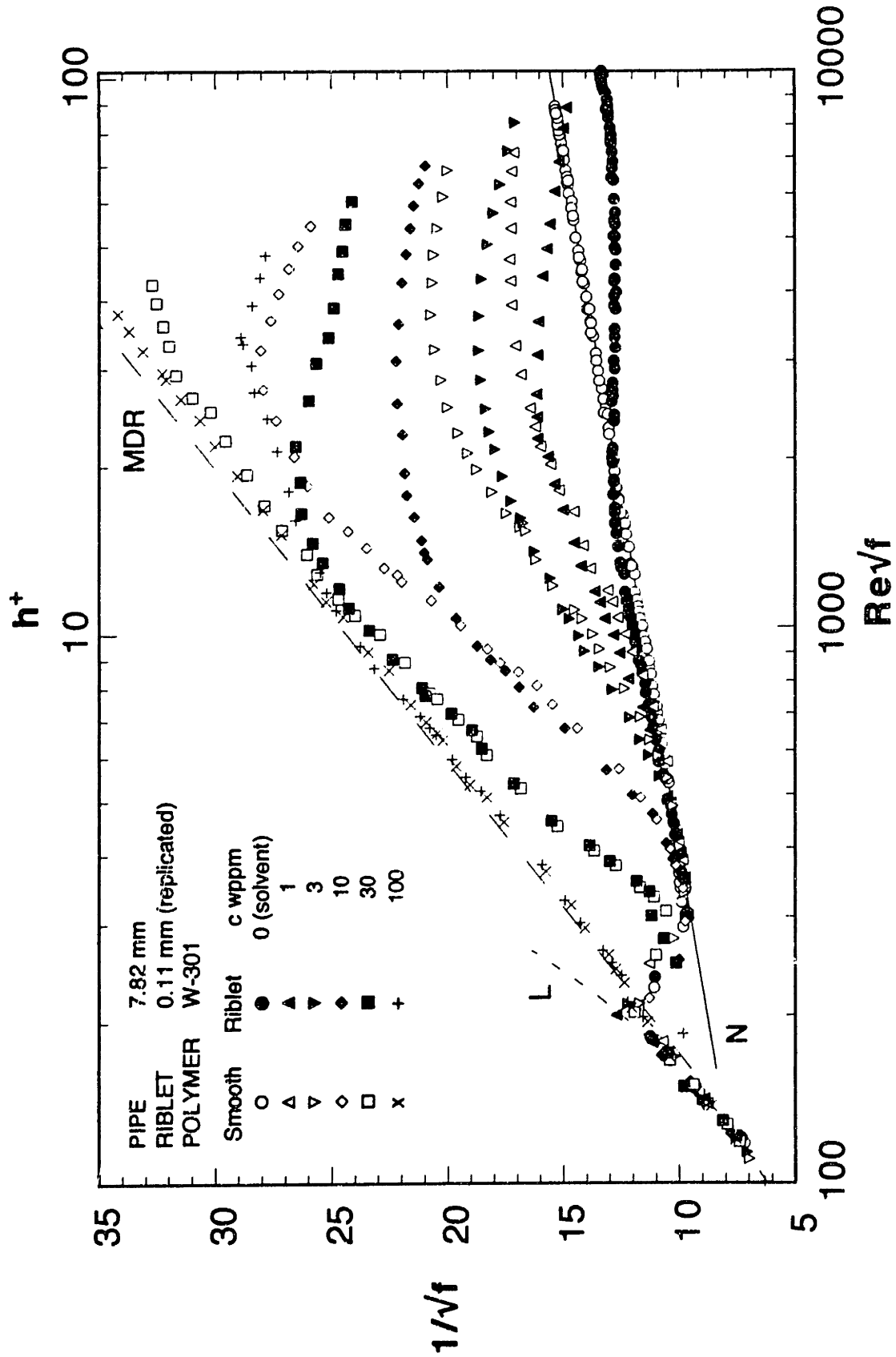


Figure 4.3.36 Friction factors for solutions of PEO W-301 in SI and RIAR.

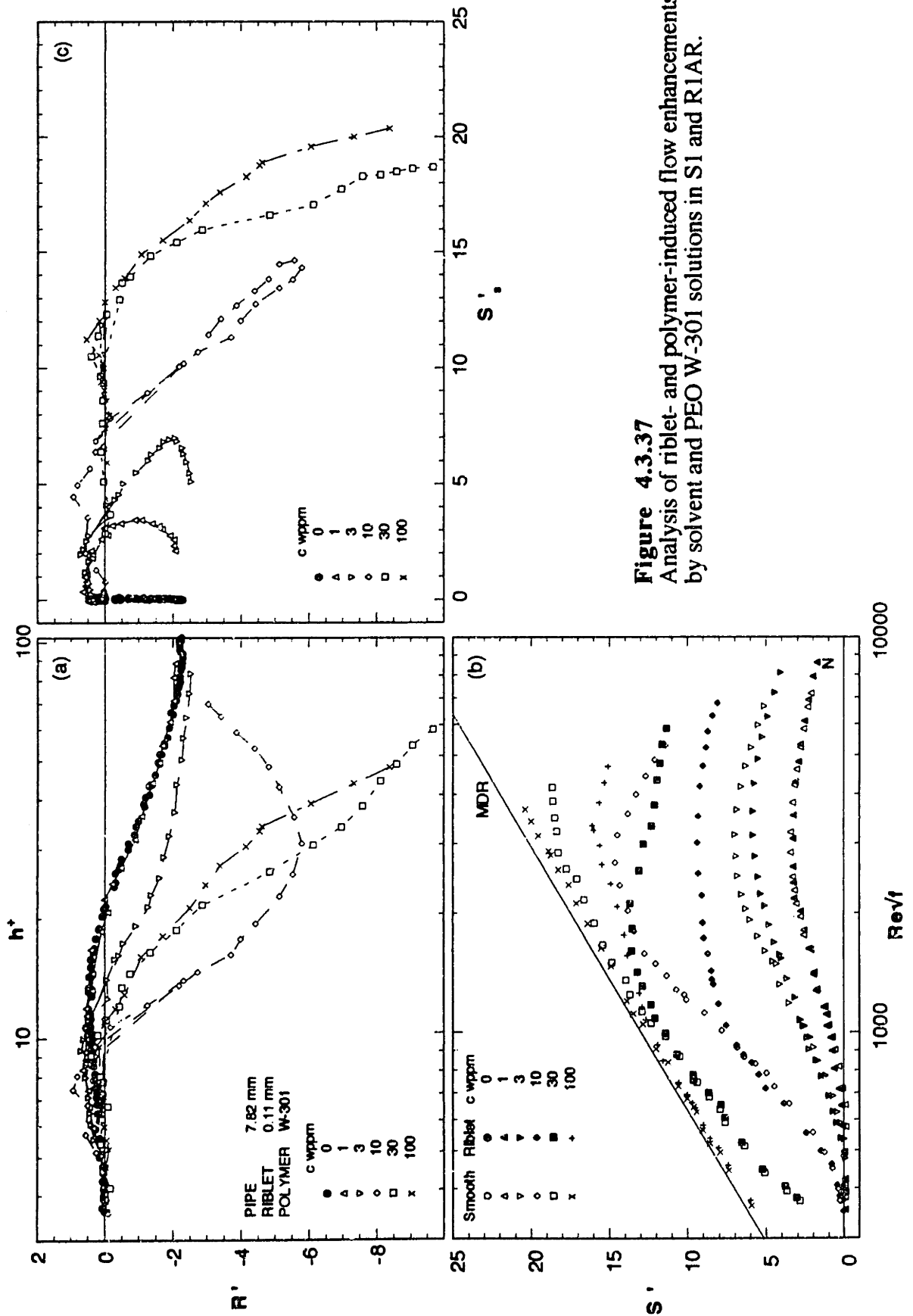


Figure 4.3.37
 Analysis of riblet- and polymer-induced flow enhancements
 by solvent and PEO W-301 solutions in S1 and R1AR.

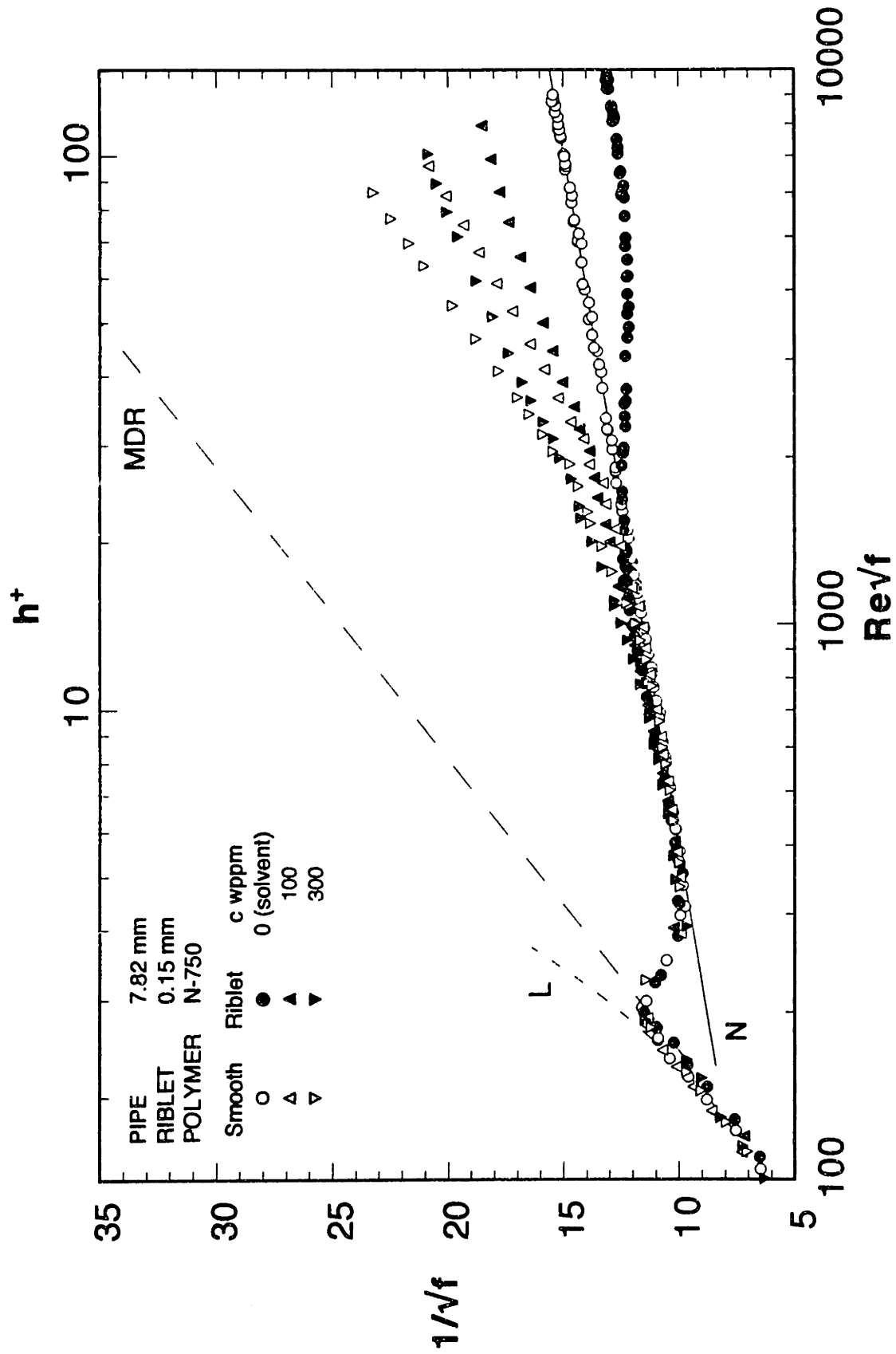


Figure 4.3.38 Friction factors for solutions of PEO N-750 in S1 and R1B.

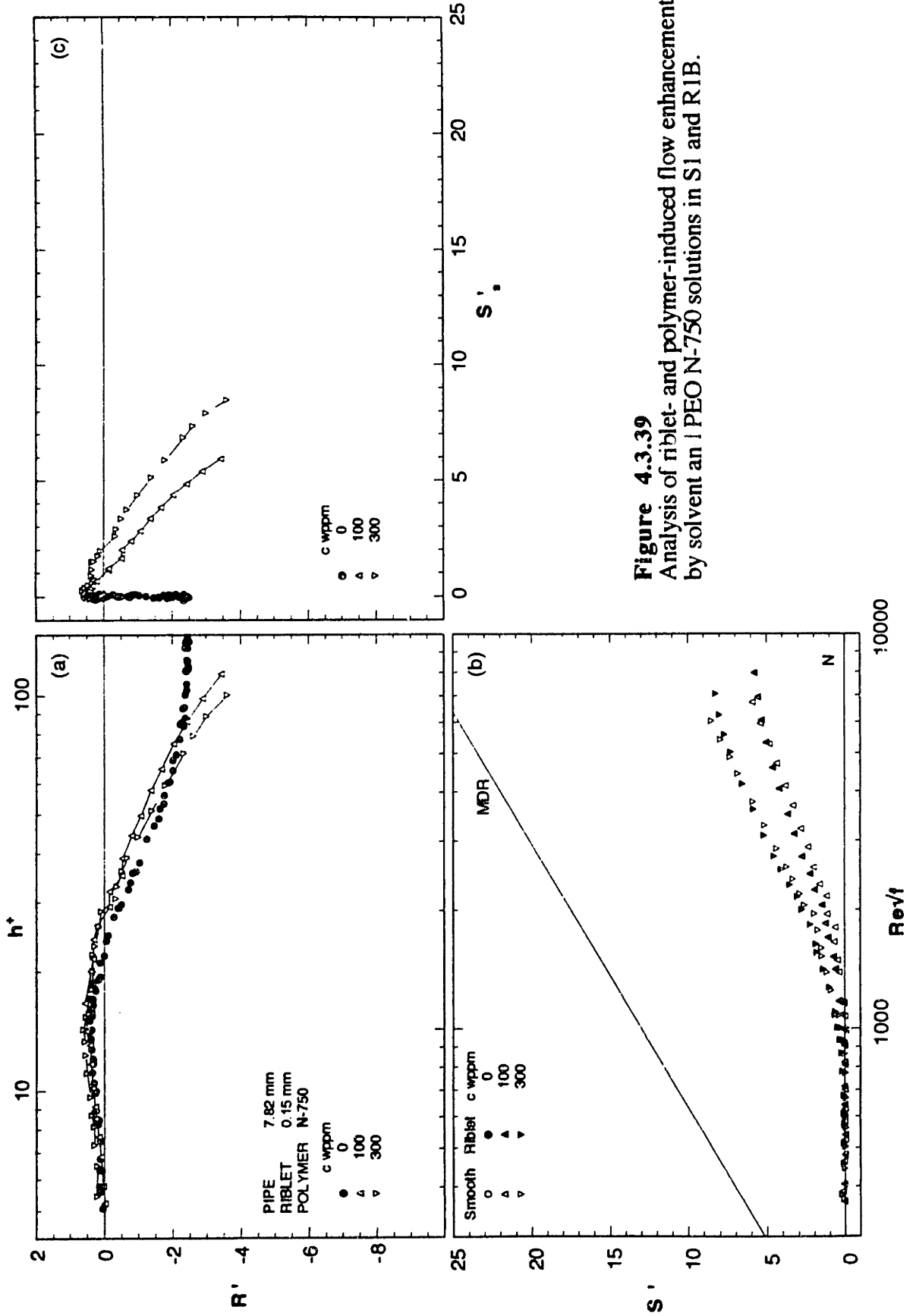


Figure 4.3.39
 Analysis of riblet- and polymer-induced flow enhancements by solvent an I PEO N-750 solutions in S1 and R1B.

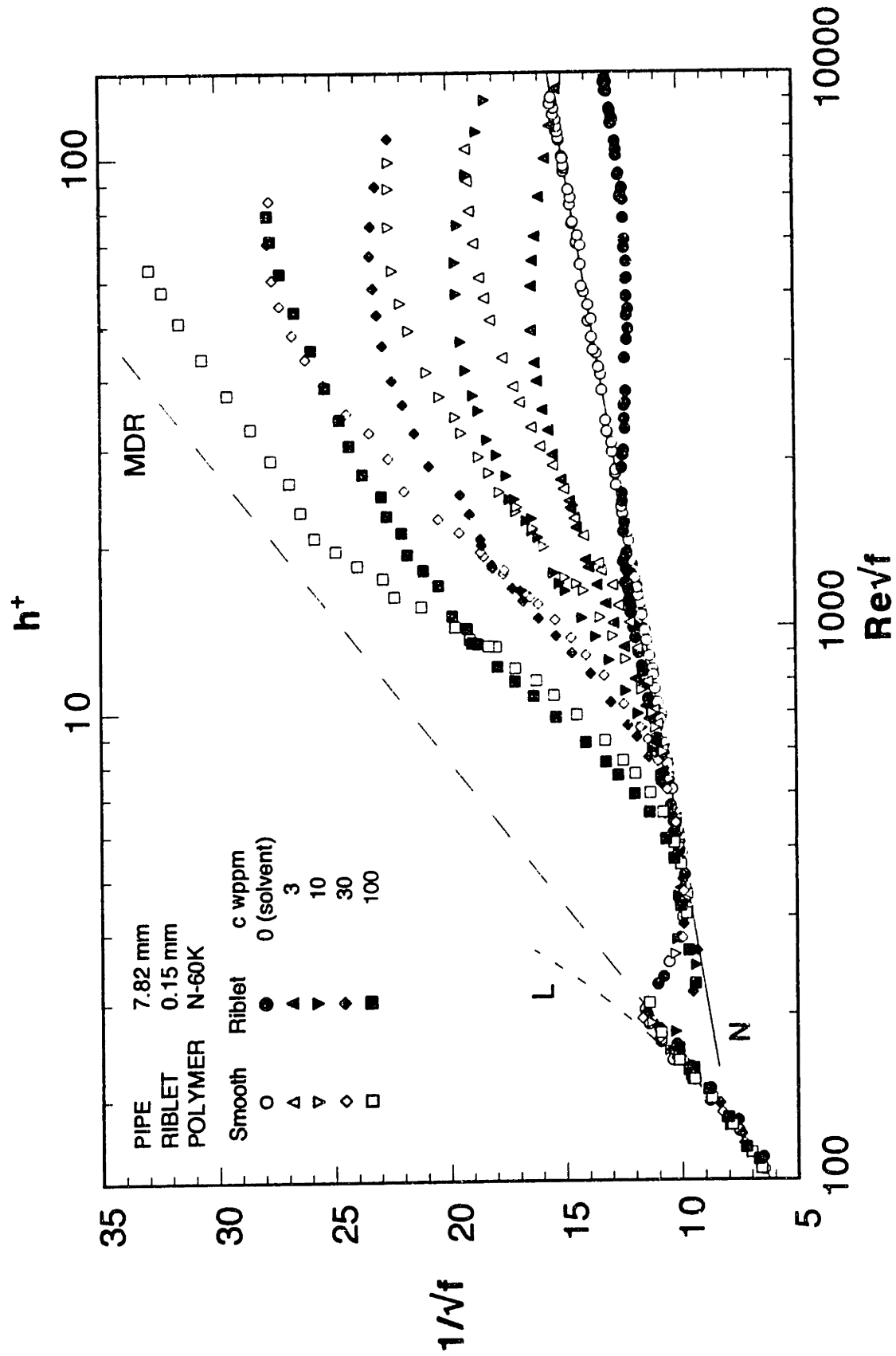


Figure 4.3.40 Friction factors for solutions of PEO N-60K in S1 and R1B.

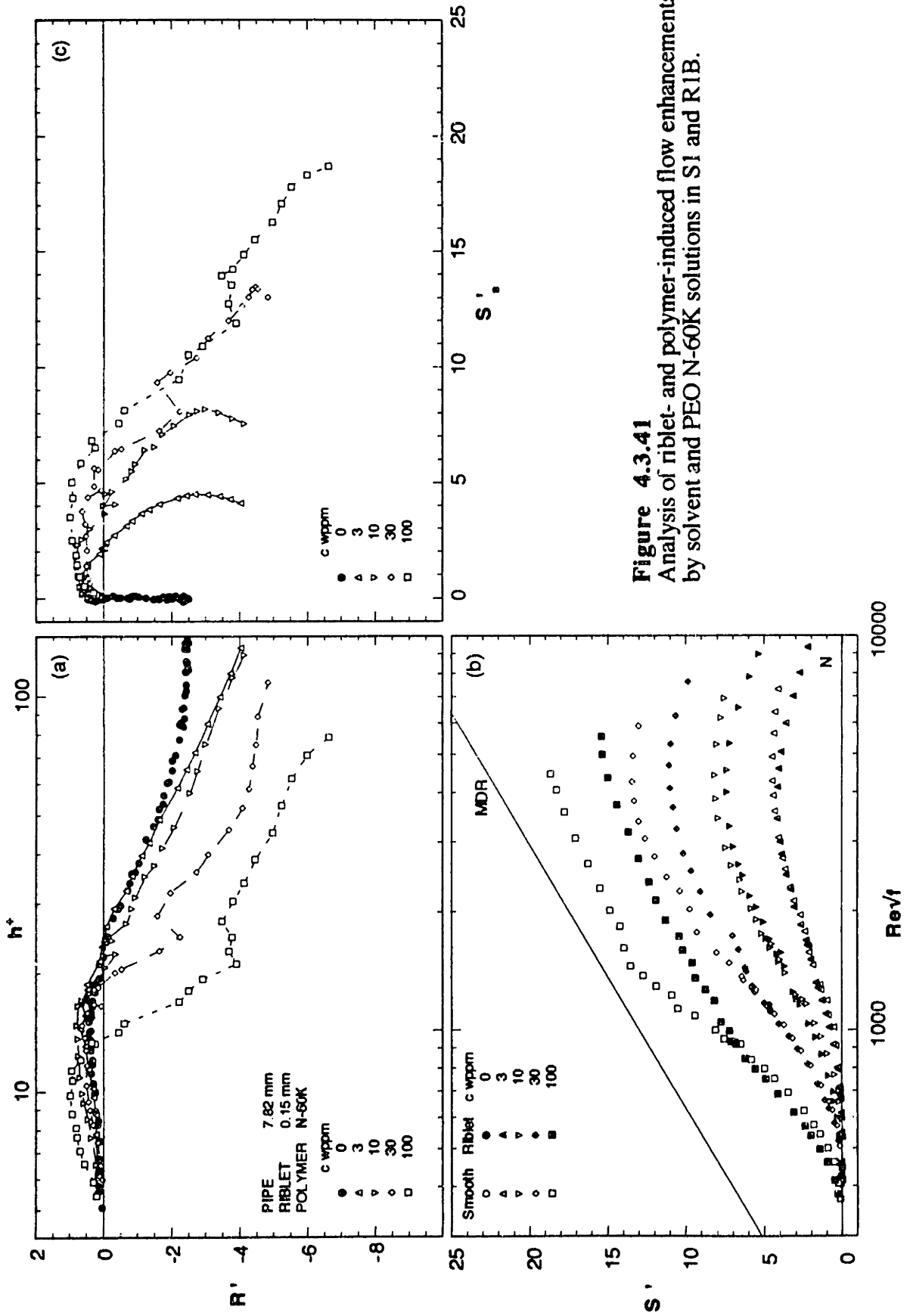


Figure 4.3.41
Analysis of riblet- and polymer-induced flow enhancements by solvent and PEO N-60K solutions in S1 and R1B.

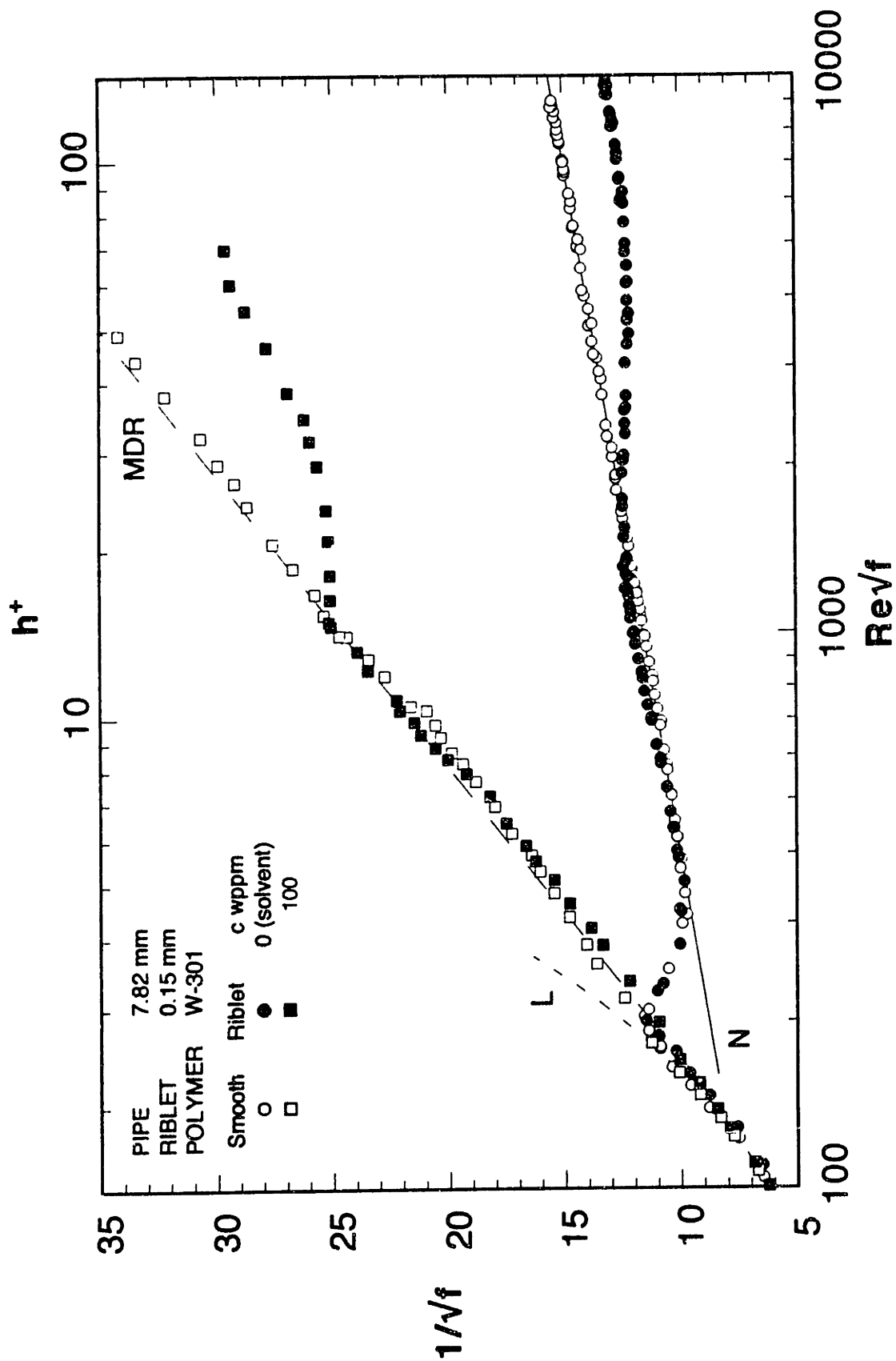


Figure 4.3.42 Friction factors for solutions of PEO W-301 in S1 and R1B.

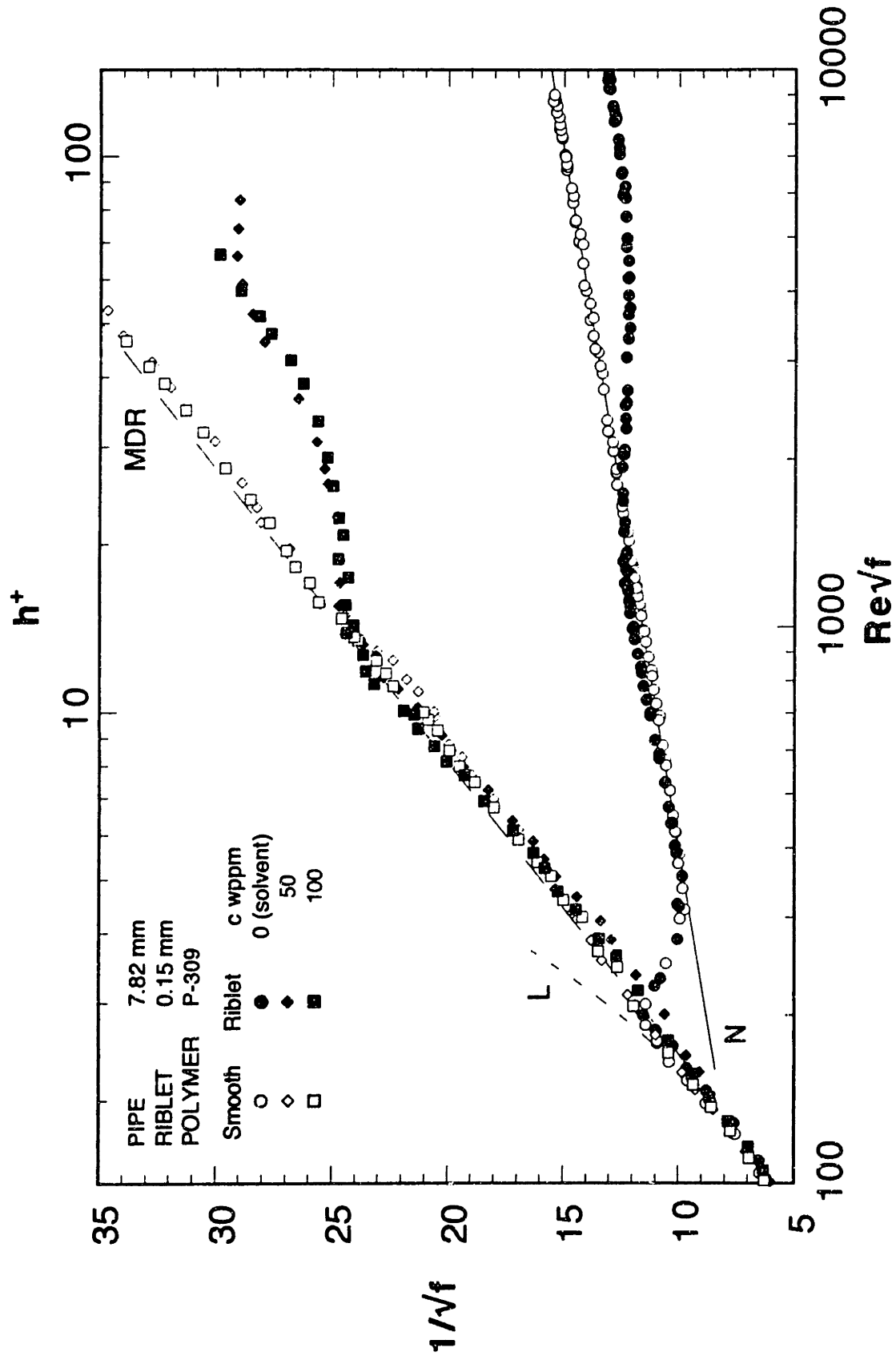


Figure 4.3.43 Friction factors for solutions of PEO P-309 in SI and RIB.

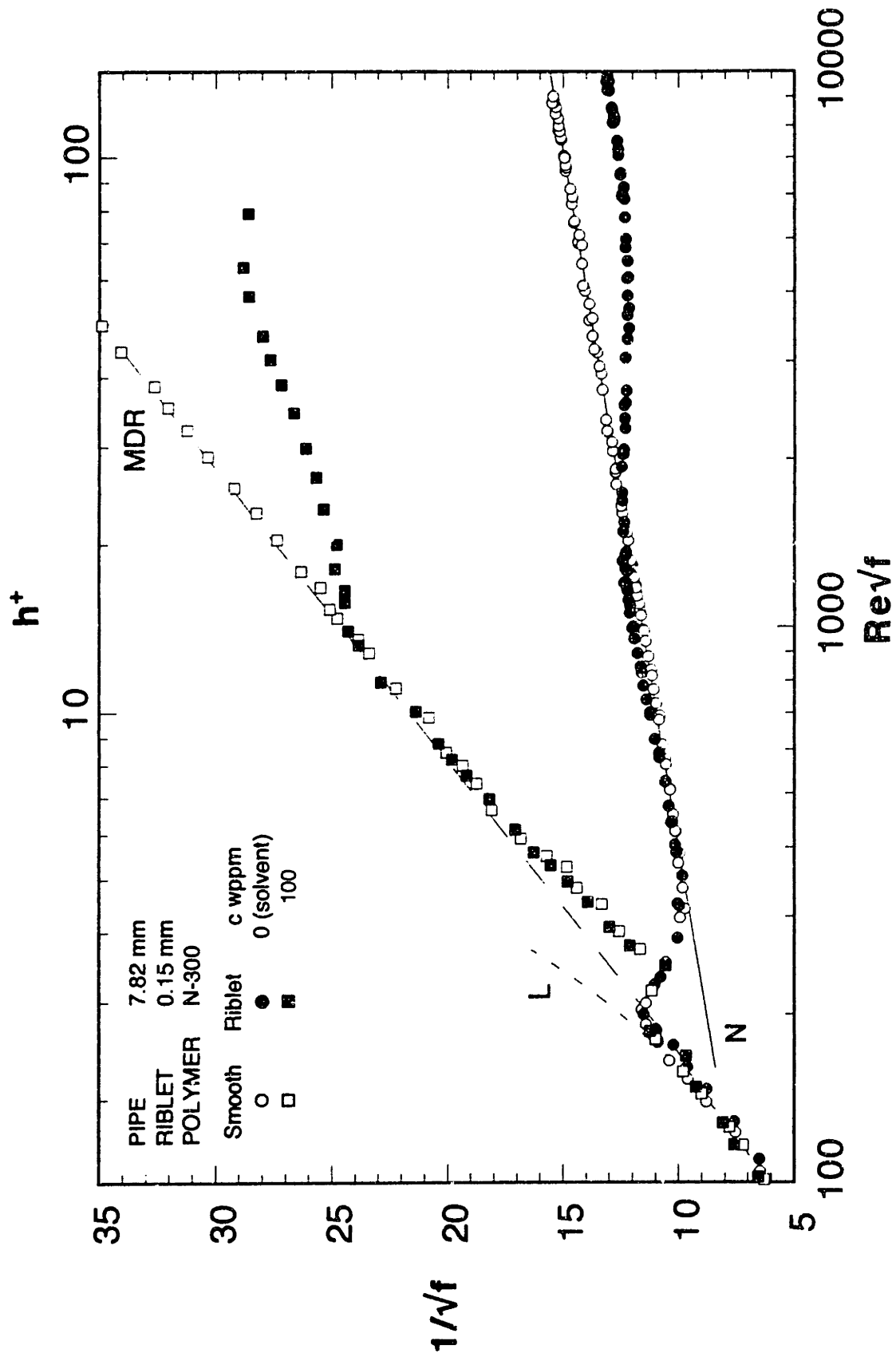


Figure 4.3.44 Friction factors for solutions of PAM N-300 in S1 and R1B.

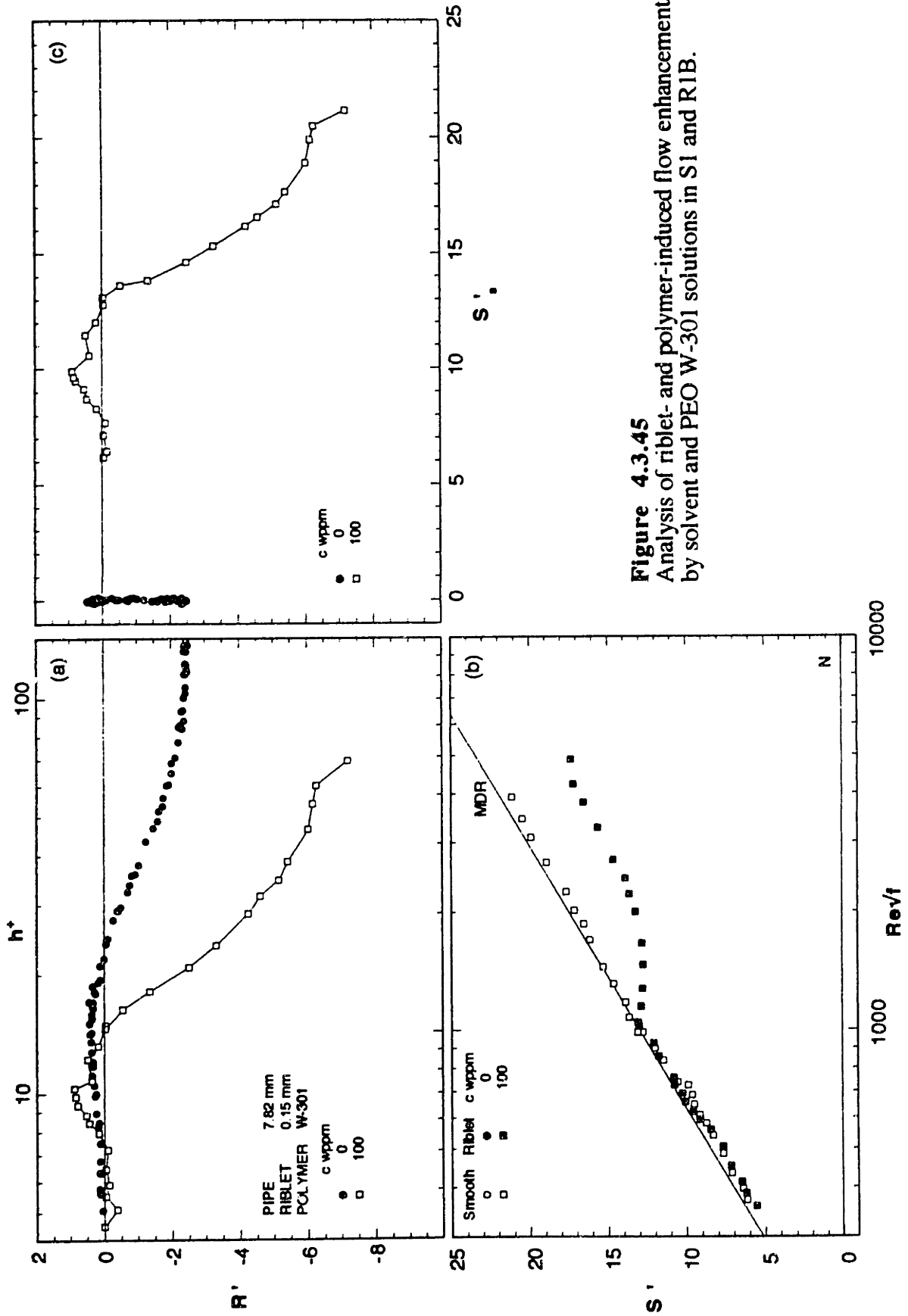


Figure 4.3.45
Analysis of riblet- and polymer-induced flow enhancements by solvent and PEO W-301 solutions in S1 and R1B.

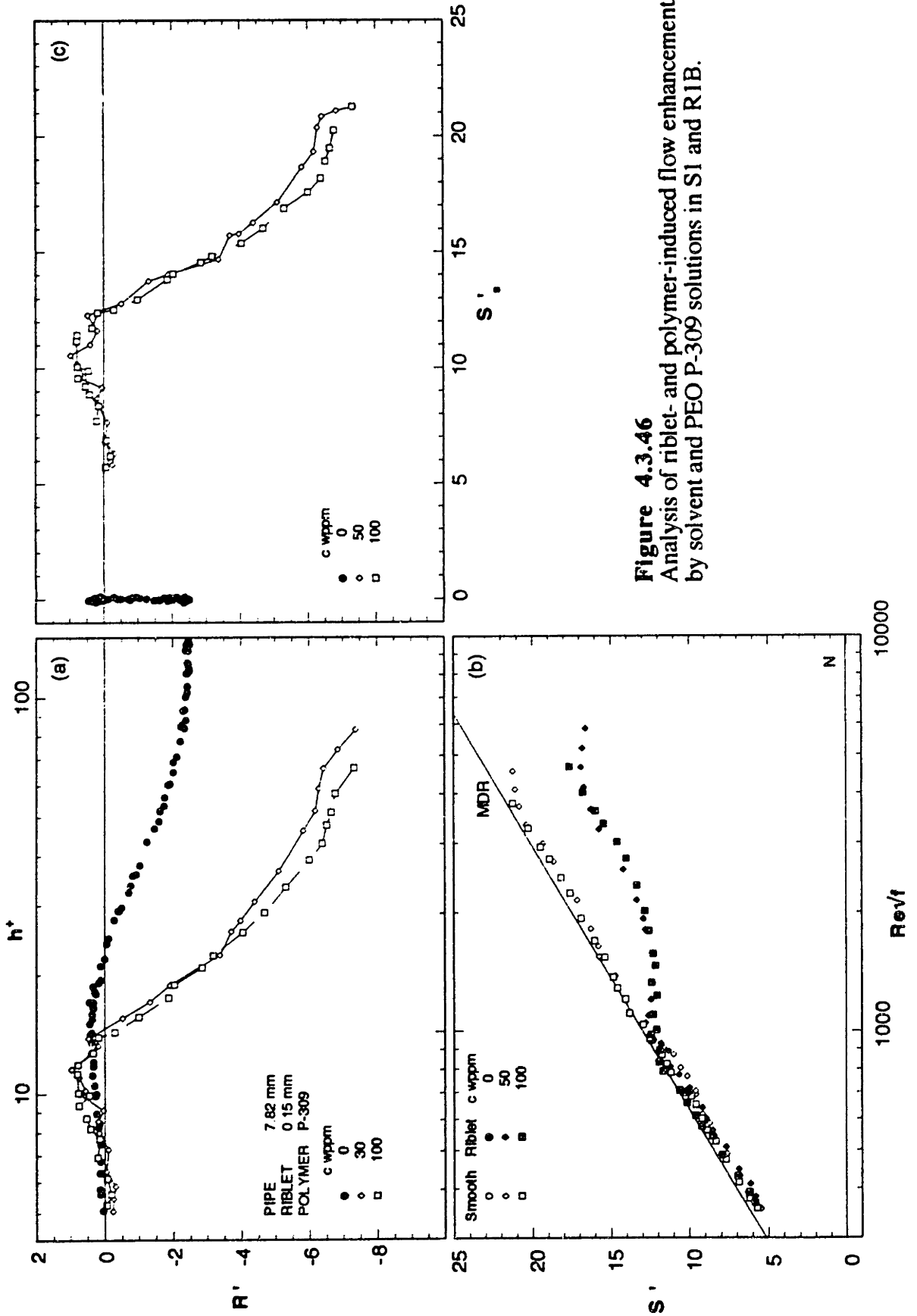


Figure 4.3.46
 Analysis of riblet- and polymer-induced flow enhancements by solvent and PEO P-309 solutions in S1 and RIB.

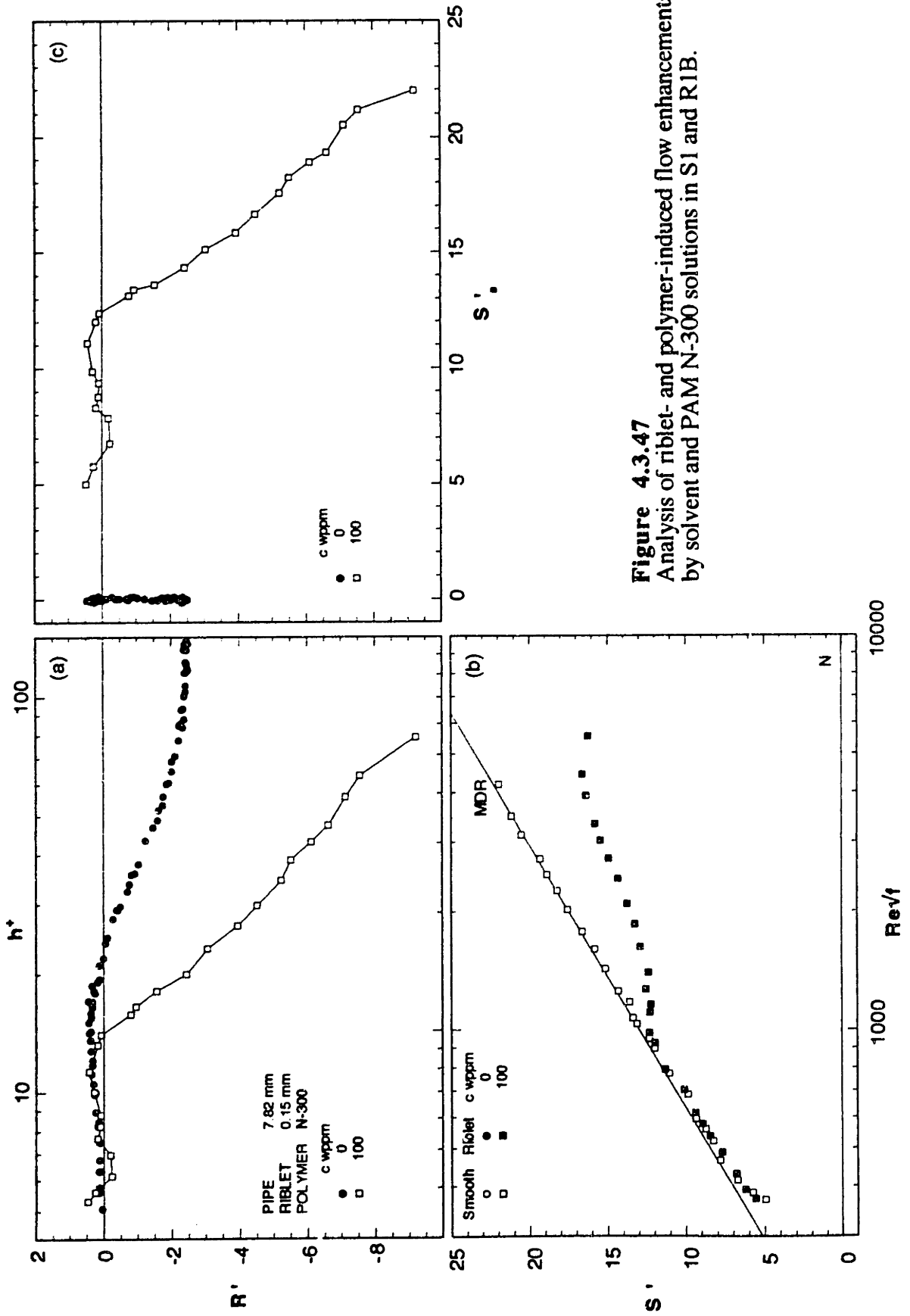


Figure 4.3.47
Analysis of riblet- and polymer-induced flow enhancements by solvent and PAM N-300 solutions in S1 and R1B.

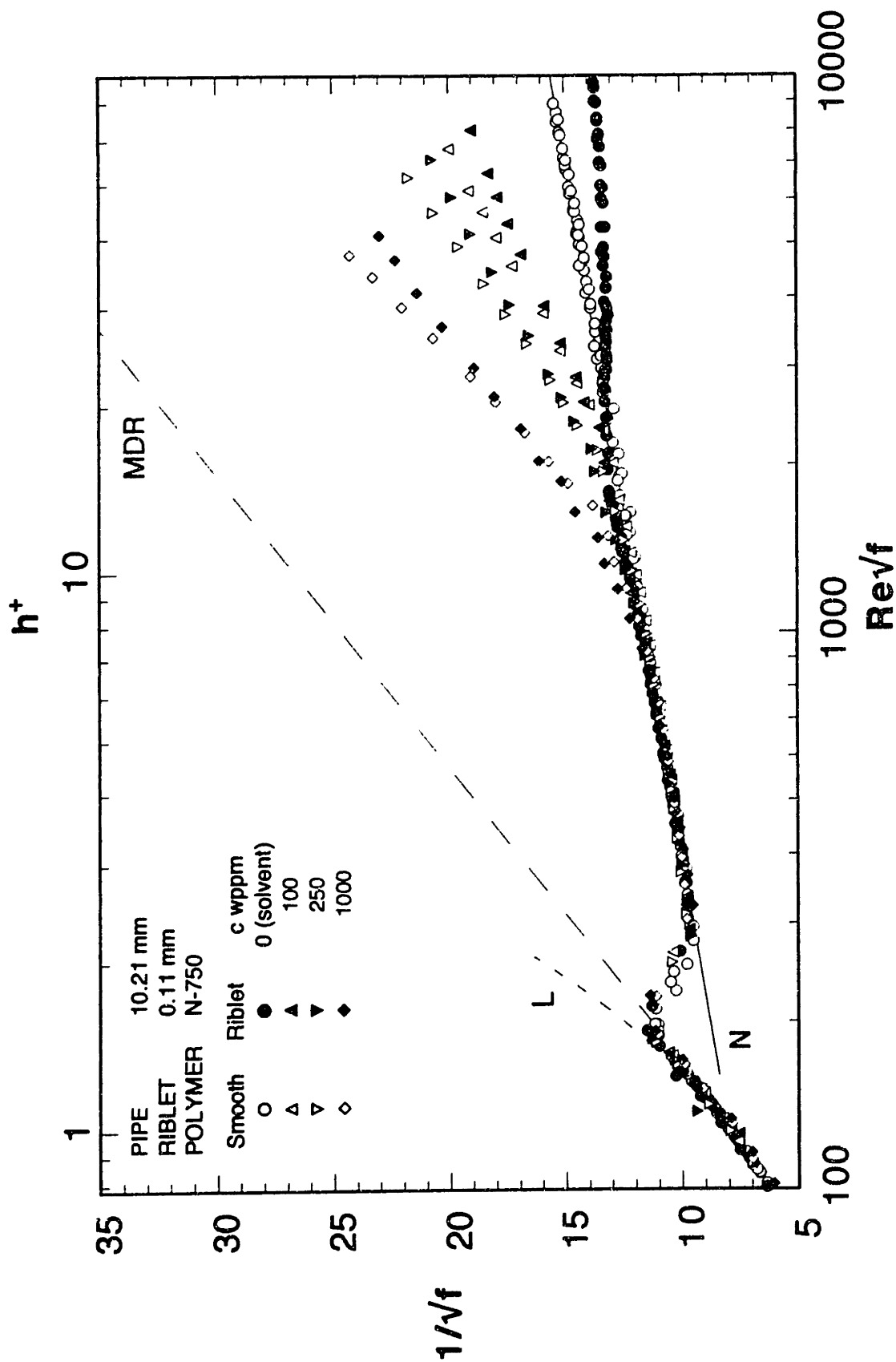


Figure 4.3.48 Friction factors for solutions of PEO N-750 in S2 and R2A.

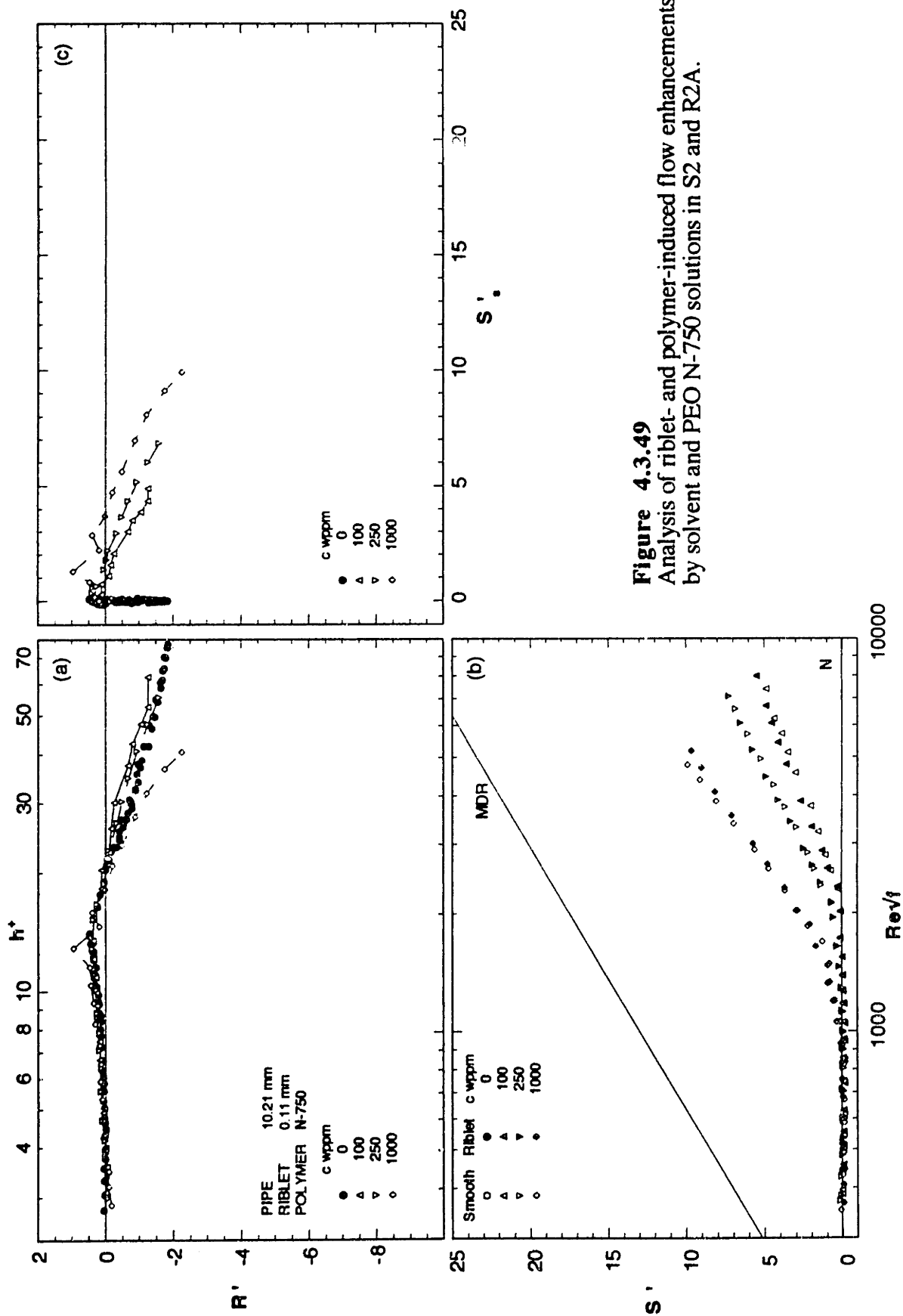


Figure 4.3.49
 Analysis of riblet- and polymer-induced flow enhancements
 by solvent and PEO N-750 solutions in S2 and R2A.

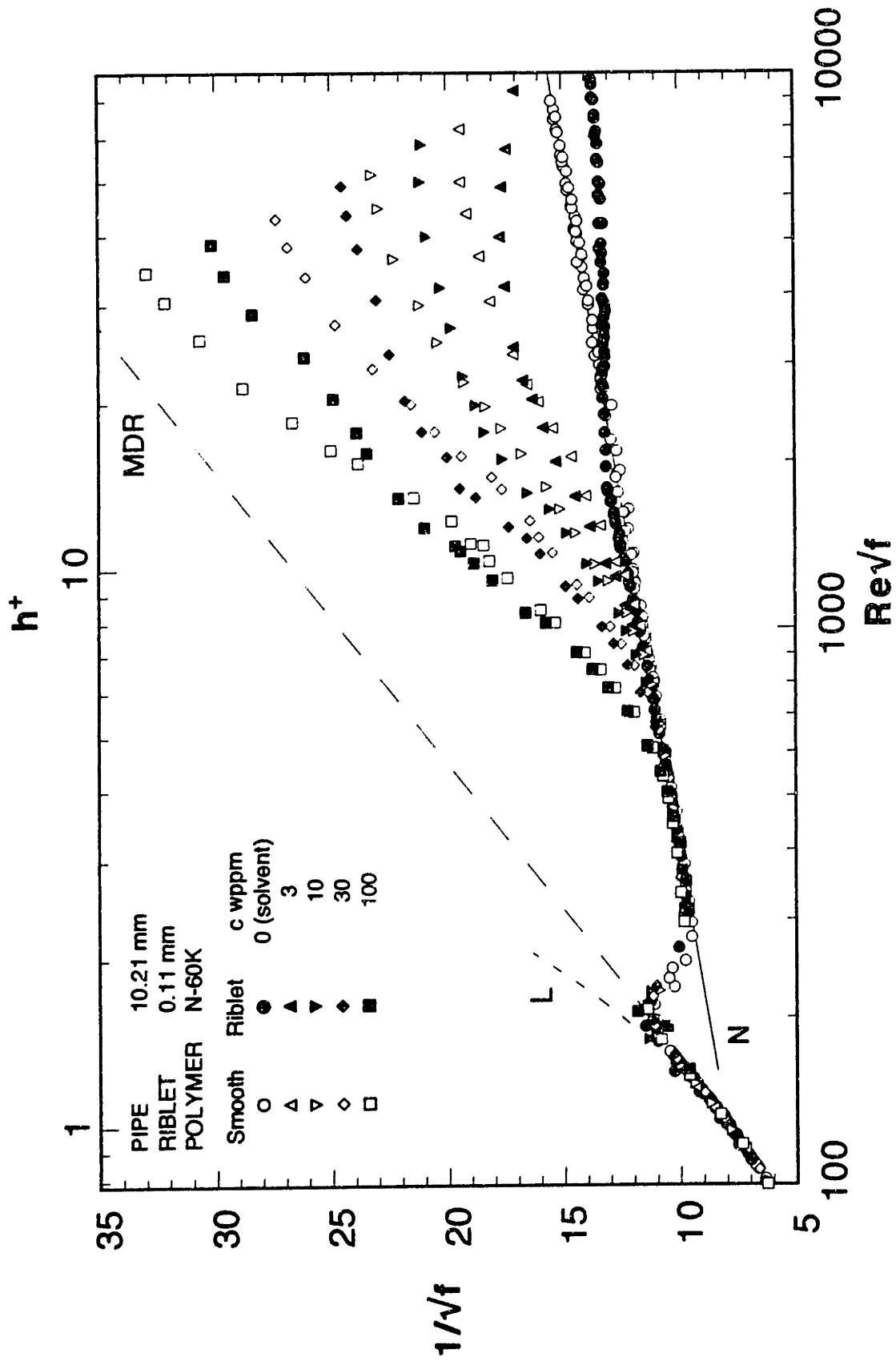


Figure 4.3.50 Friction factors for solutions of PEO N-60K in S2 and R2A.

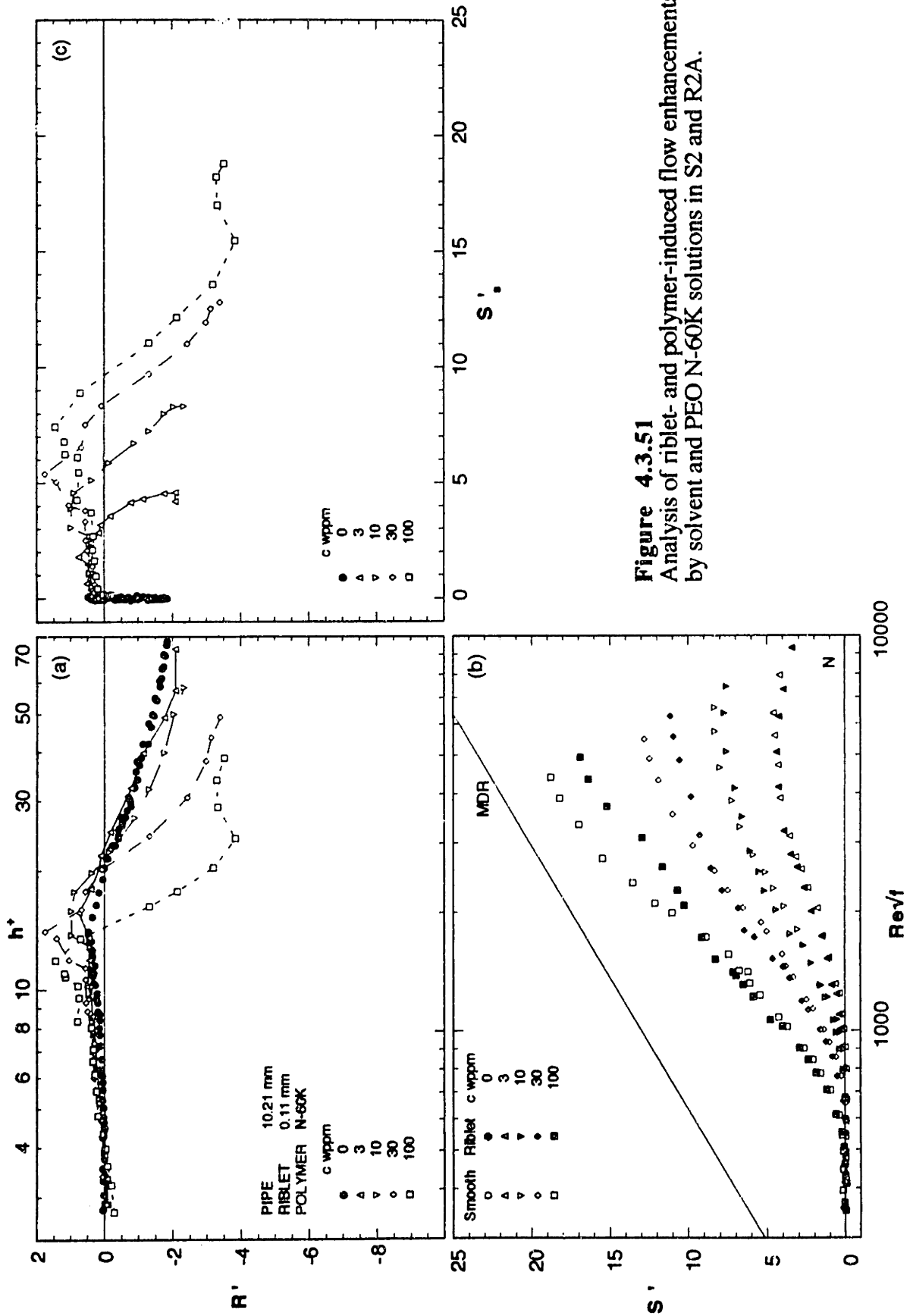


Figure 4.3.51
Analysis of riblet- and polymer-induced flow enhancements by solvent and PEO N-60K solutions in S2 and R2A.

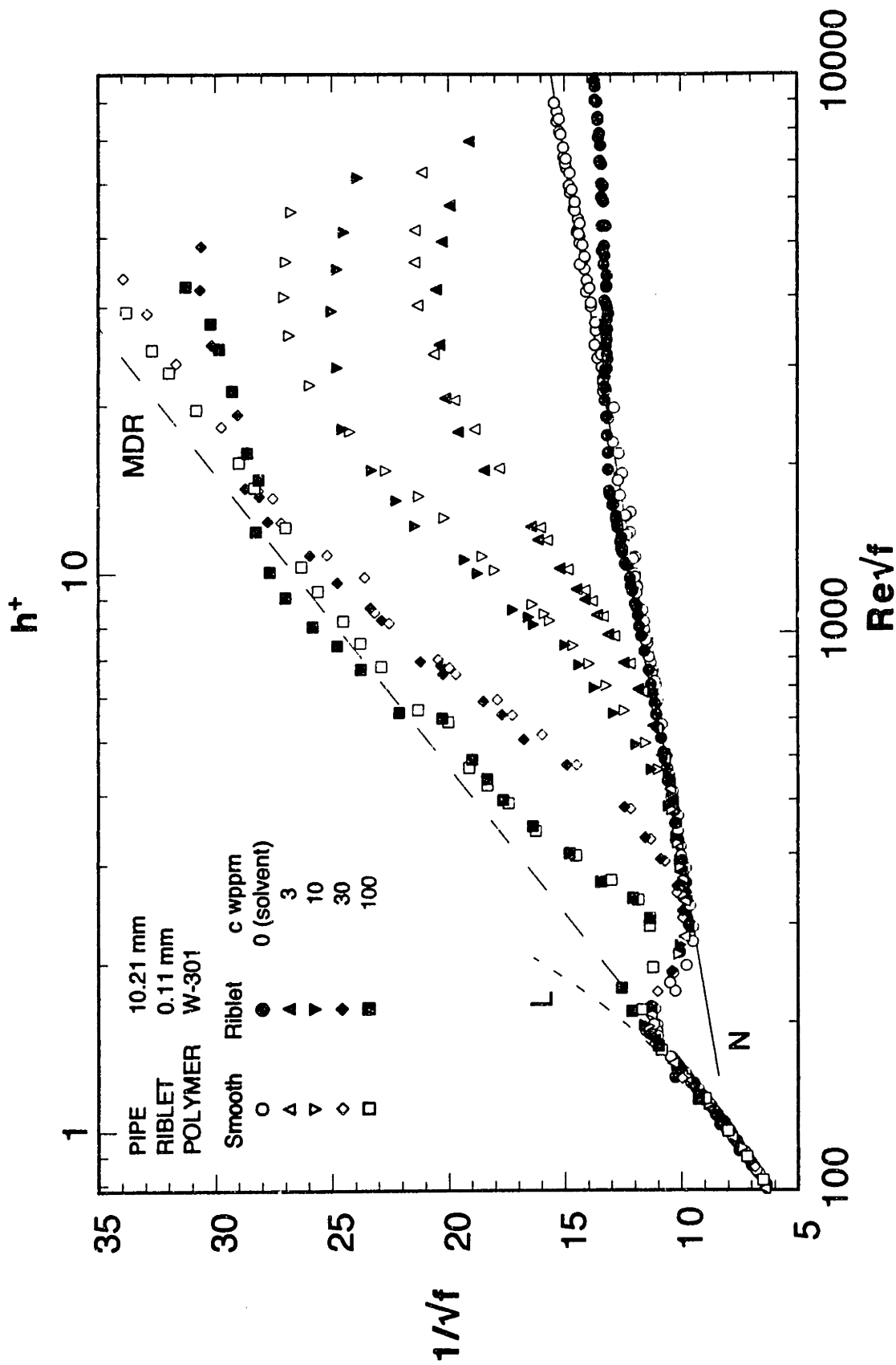


Figure 4.3.52 Friction factors for solutions of PEO W-301 in S2 and R2A.

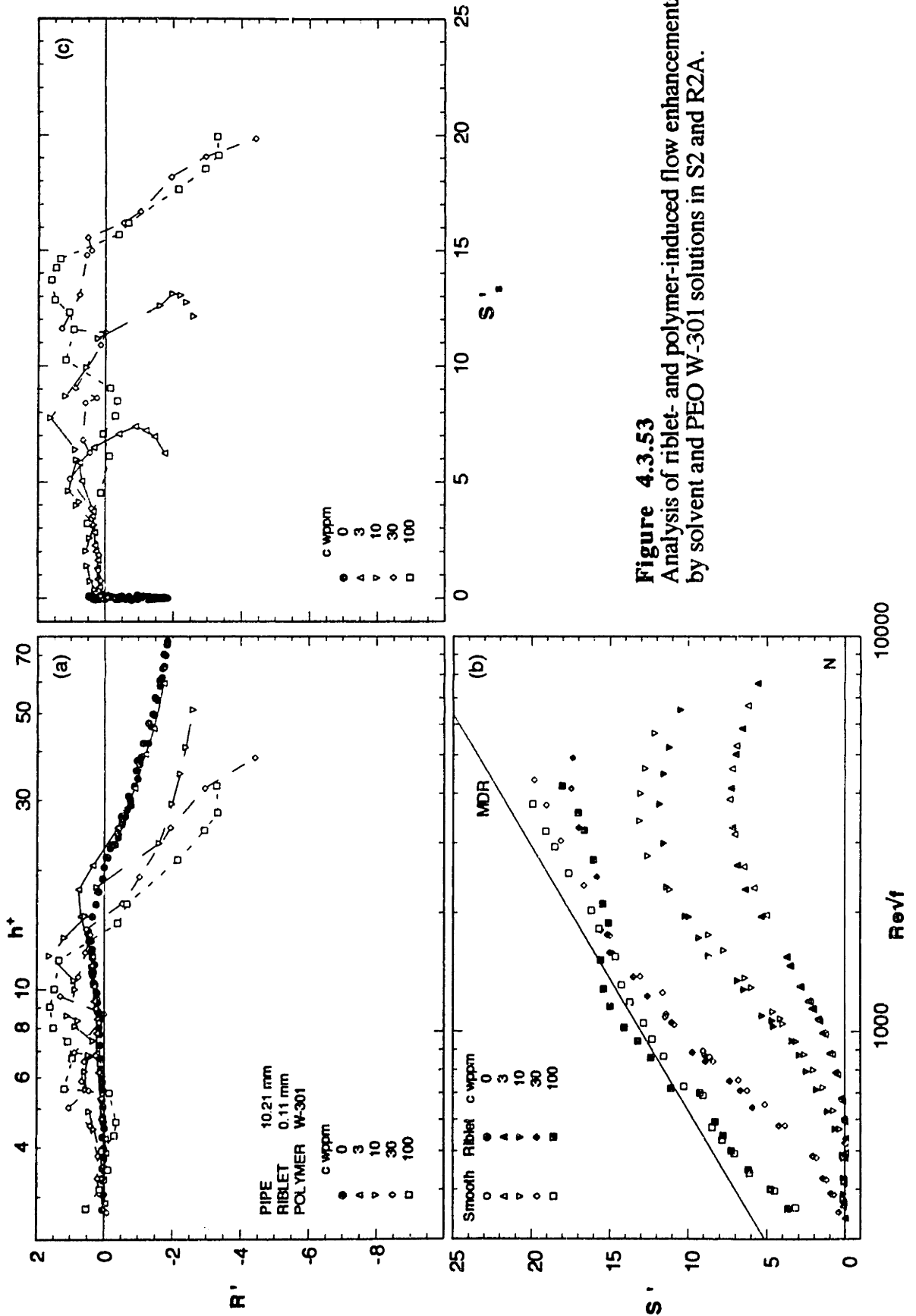


Figure 4.3.53
Analysis of riblet- and polymer-induced flow enhancements by solvent and PEO W-301 solutions in S2 and R2A.

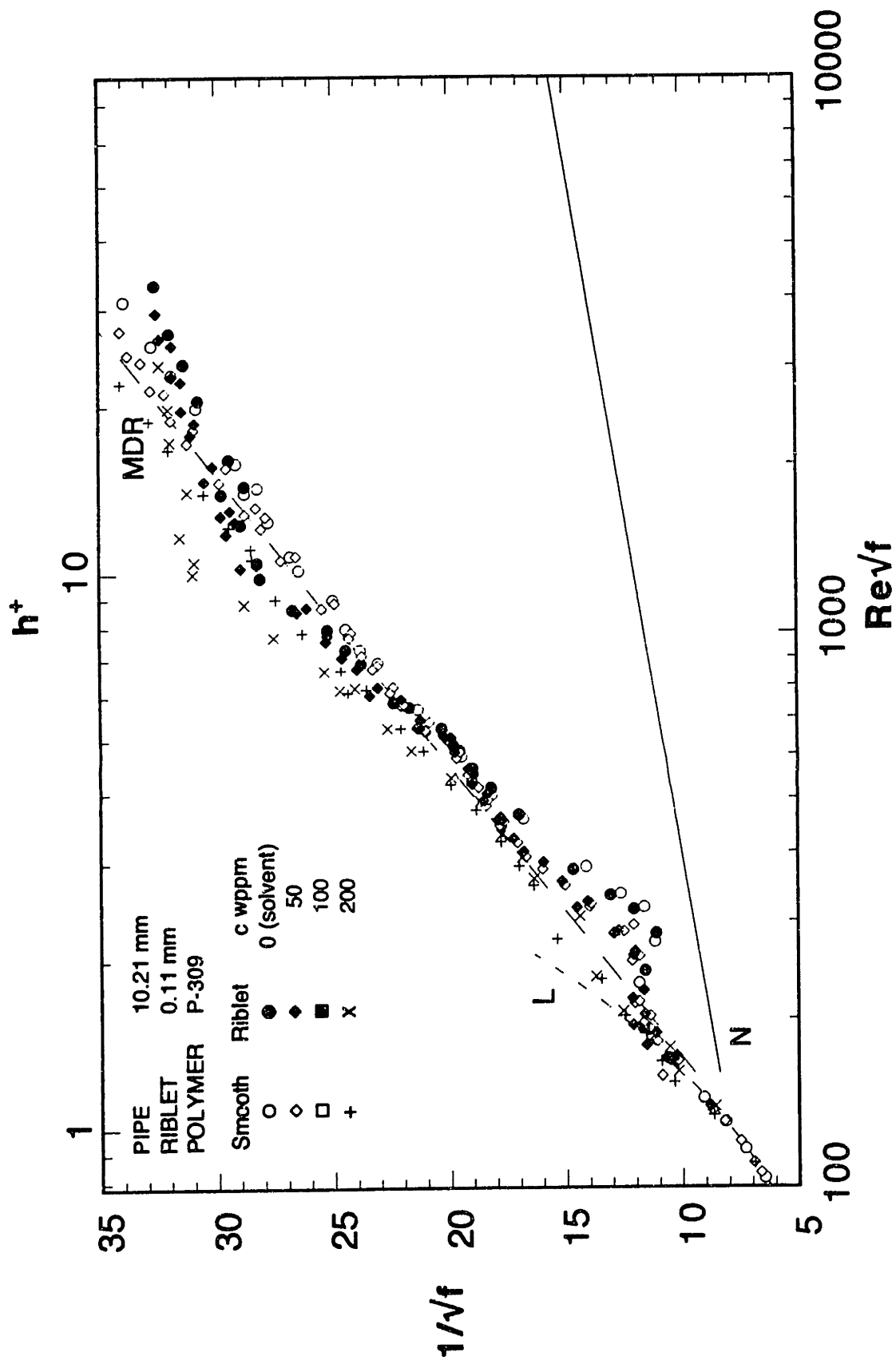


Figure 4.3.54 Friction factors for solutions of PEO P-309 in S2 and R2A.

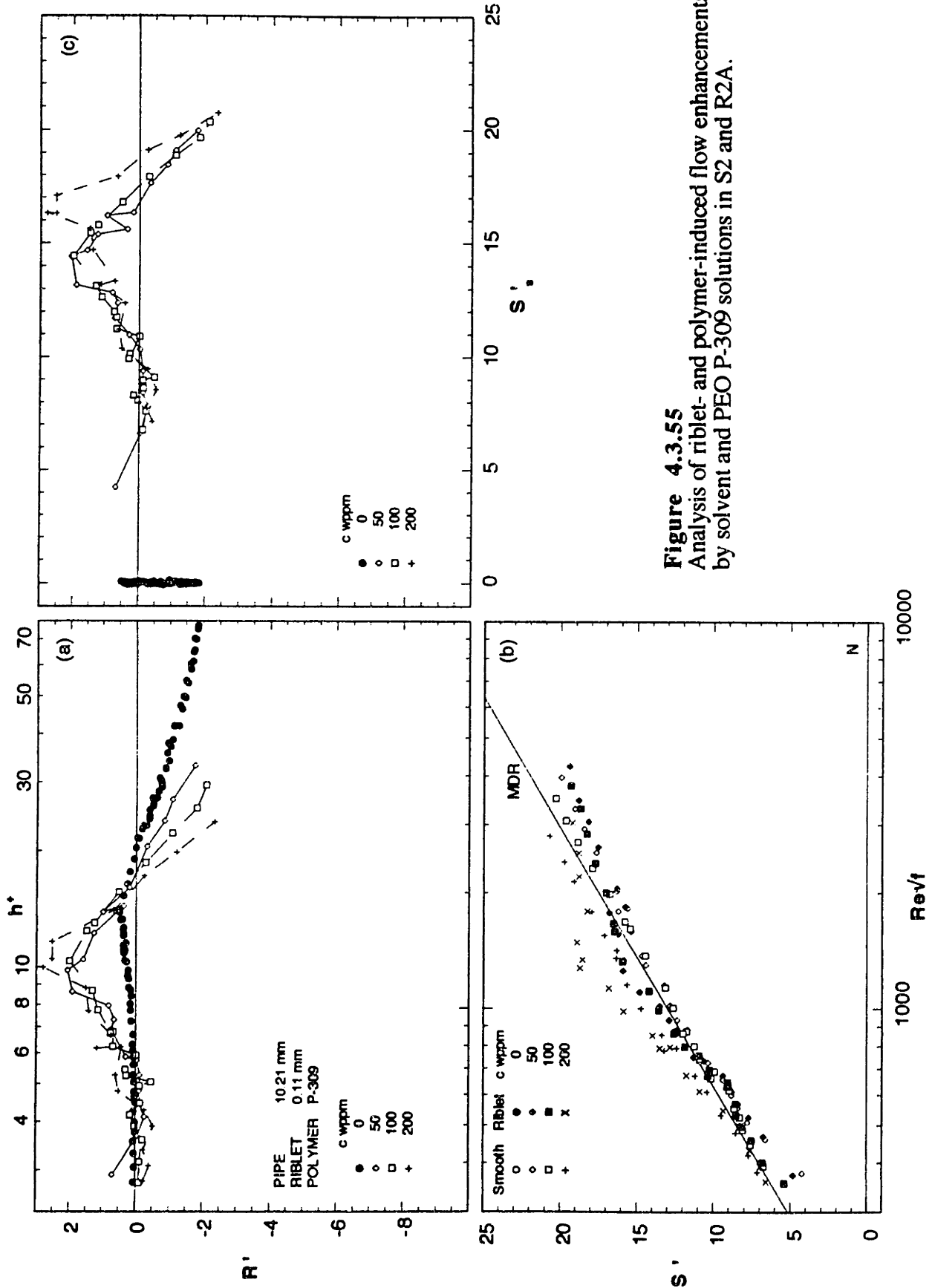


Figure 4.3.55
Analysis of riblet- and polymer-induced flow enhancements
by solvent and PEO P-309 solutions in S2 and R2A.

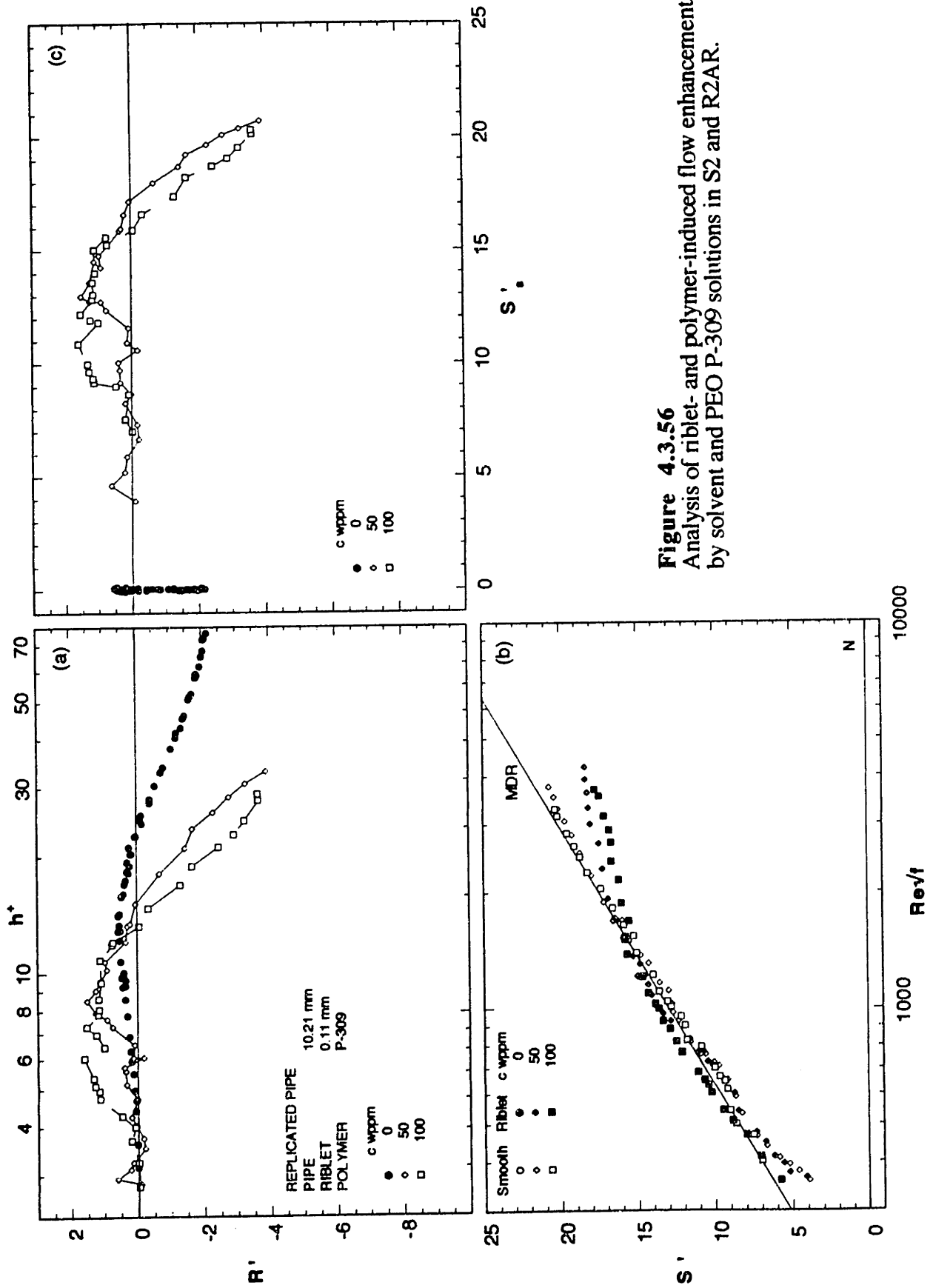


Figure 4.3.56
Analysis of riblet- and polymer-induced flow enhancements
by solvent and PEO P-309 solutions in S2 and R2AR.

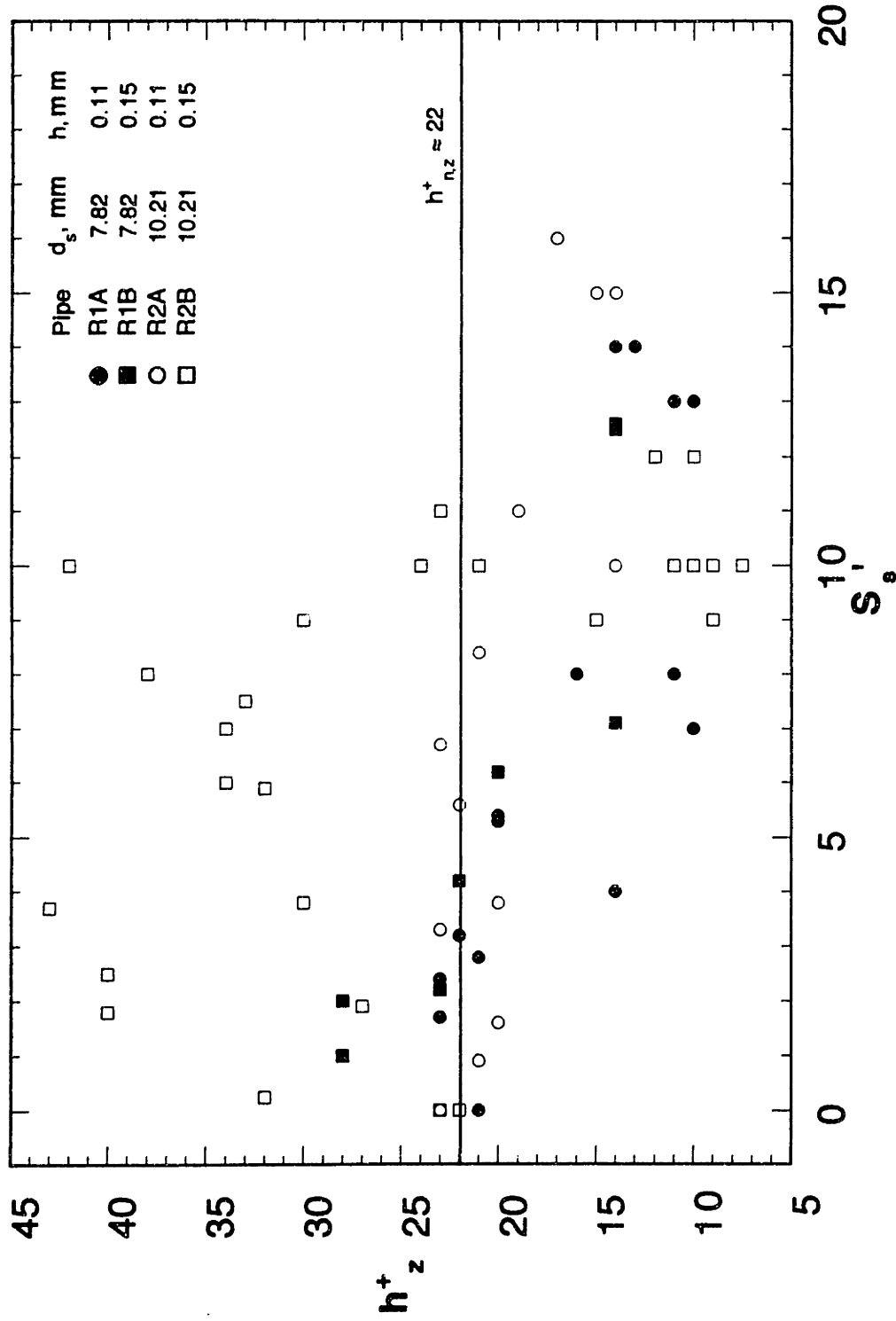


Figure 4.3.57 Variation of h_z^+ , at the cross-over from riblet drag reduction to drag enhancement, with polymer-induced flow enhancement, S_s' .

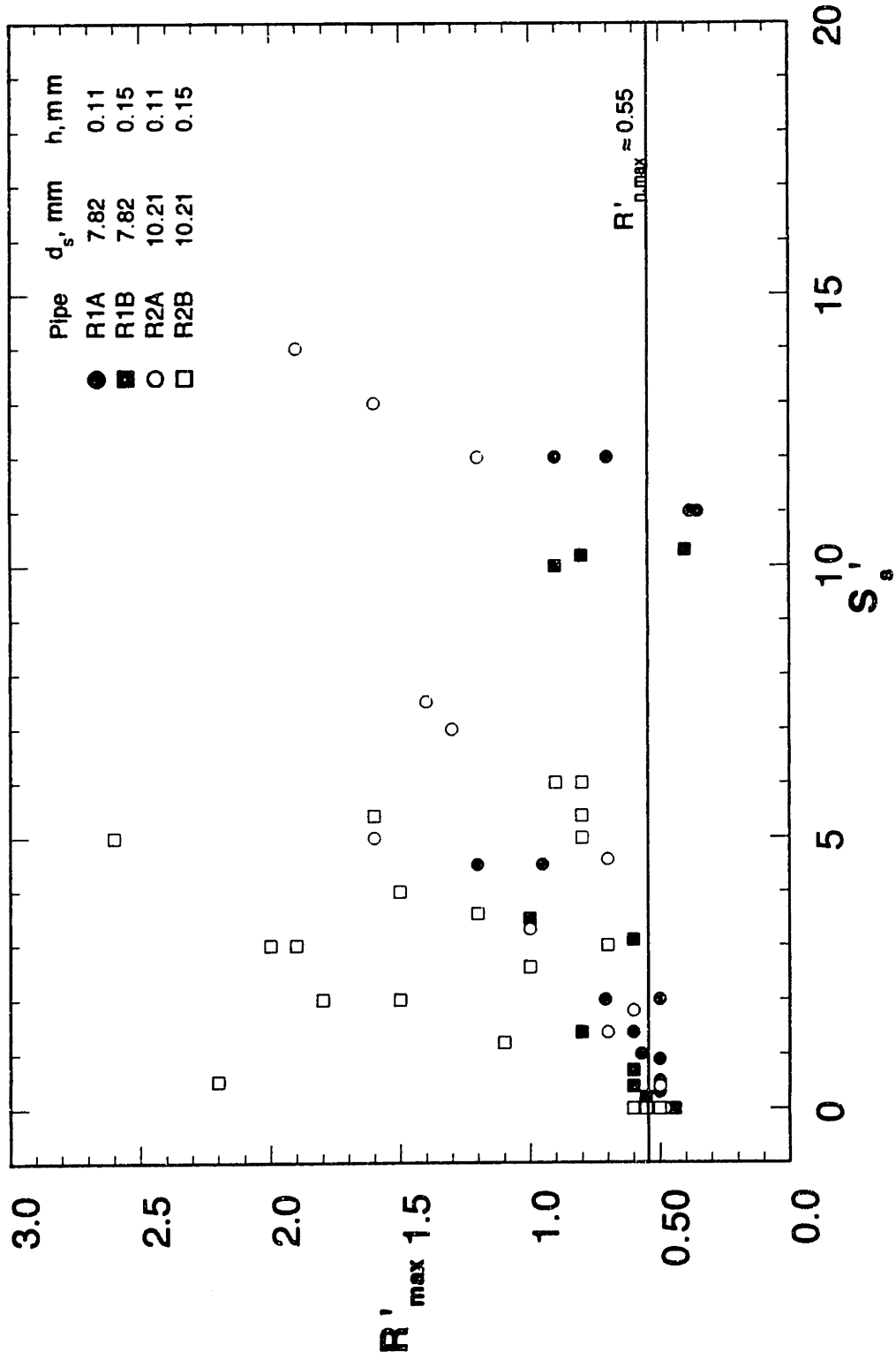


Figure 4.3.58 Variation of maximum riblet drag reduction, R'_{max} , with polymer-induced flow enhancement, S'_s

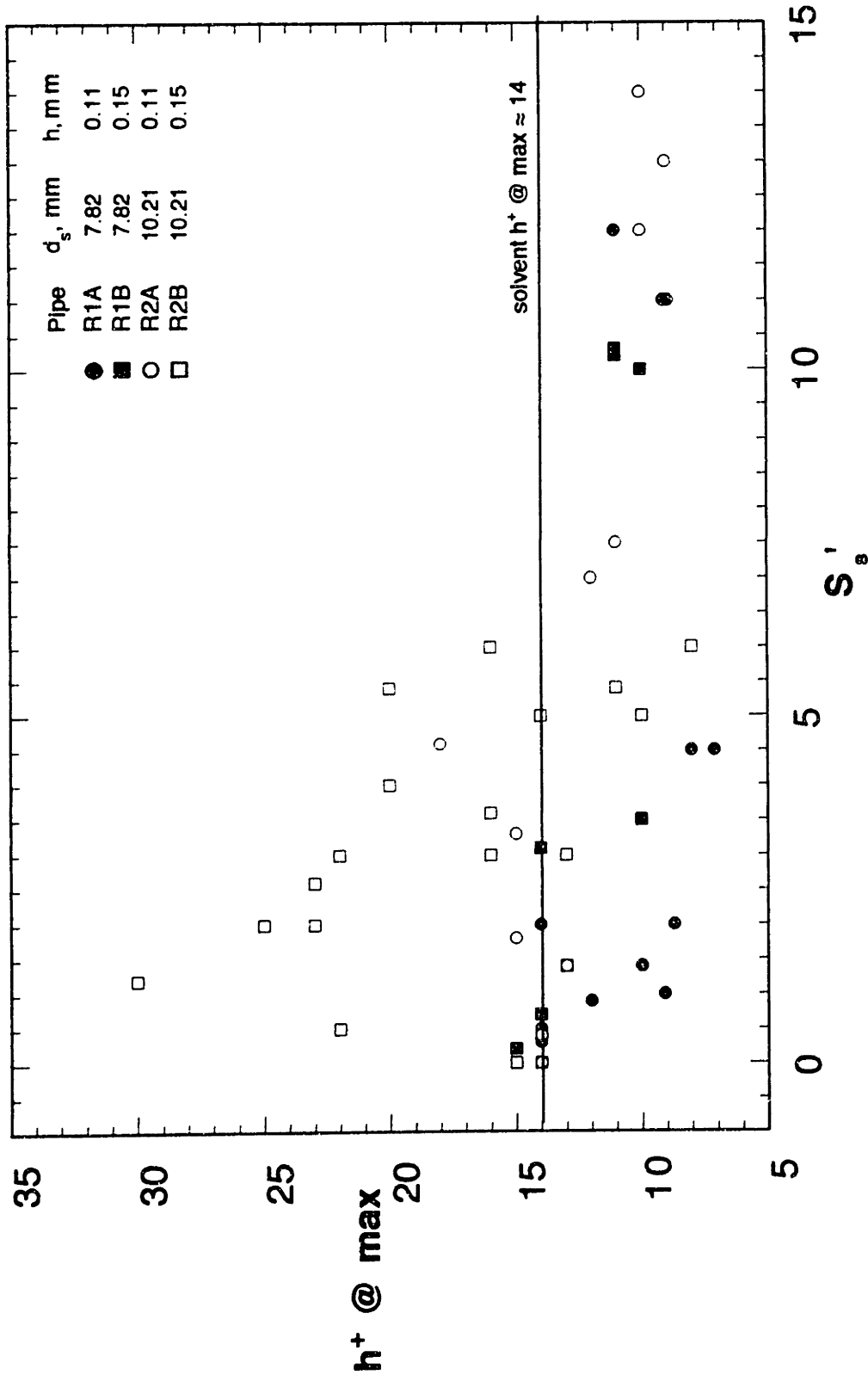


Figure 4.3.59 Variation of h^+ at the maximum riblet drag reduction with polymer-induced flow enhancement, S'_s

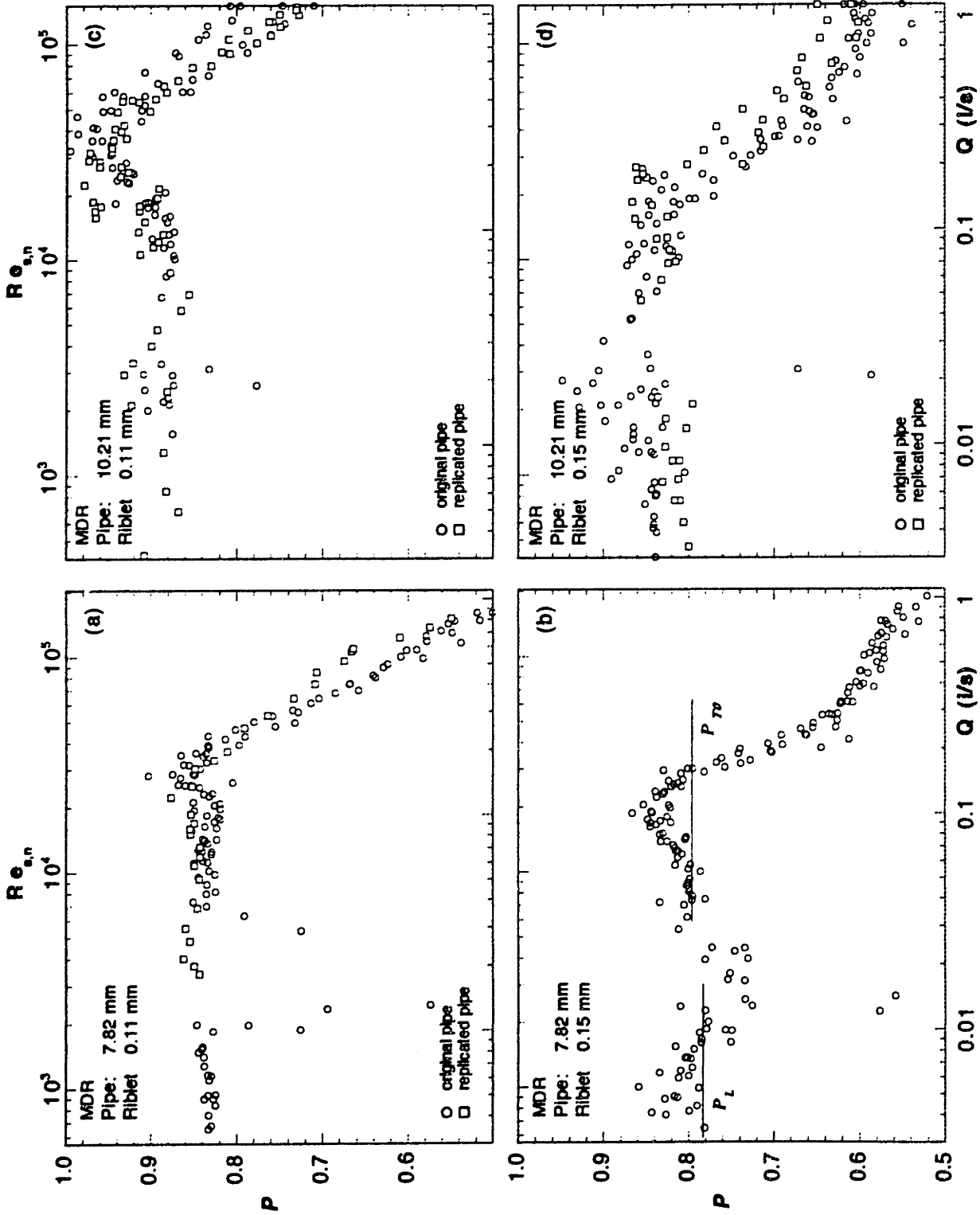


Figure 4.4.1 Variations of the smooth to riblet pipe pressure gradient ratios versus flowrate at maximum drag reduction.

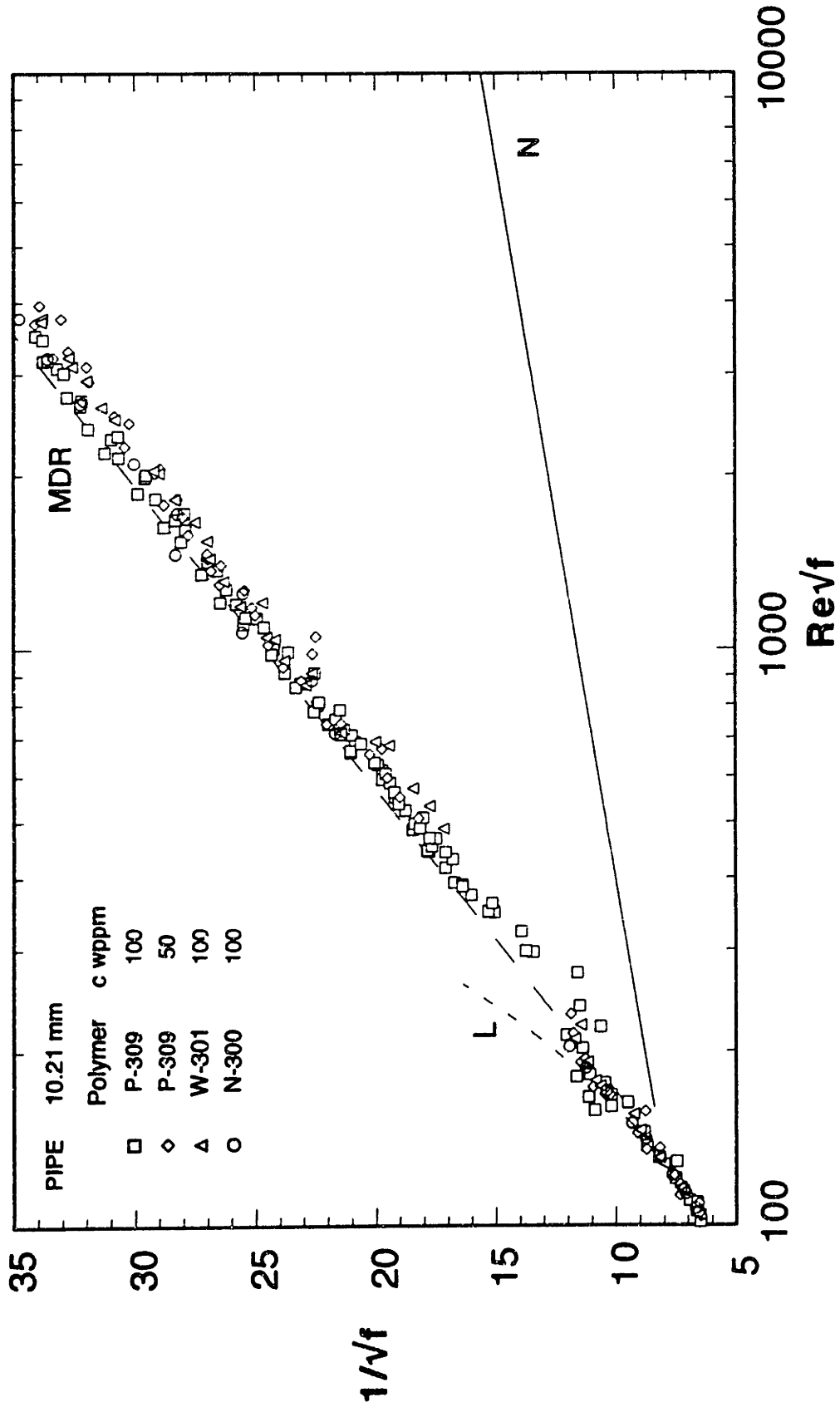


Figure 4.4.2 Prandtl-Karman friction factors at maximum drag reduction in the 10.21 mm id smooth pipe.

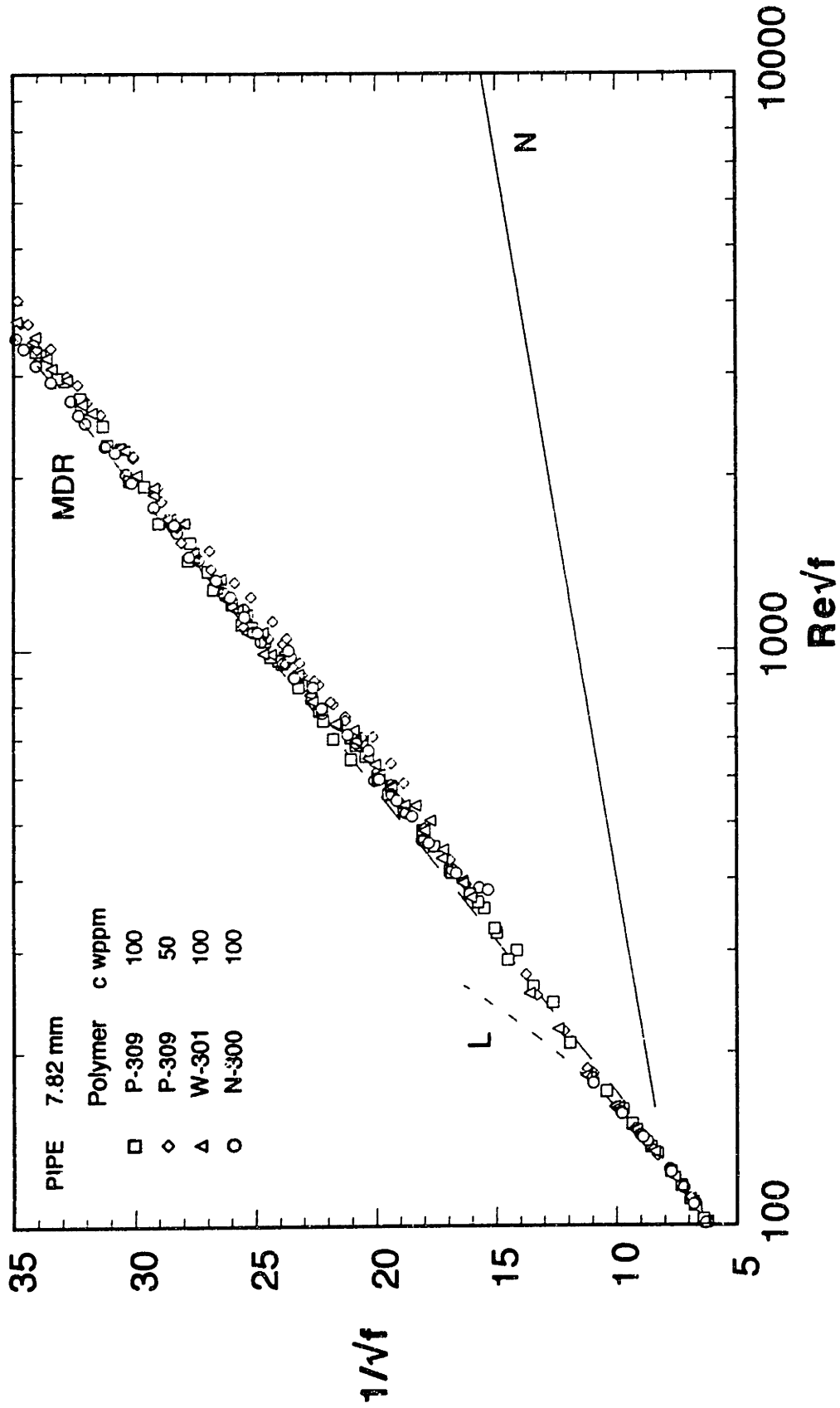


Figure 4.4.3 Friction factors at maximum drag reduction in the 7.82 mm id smooth pipe.

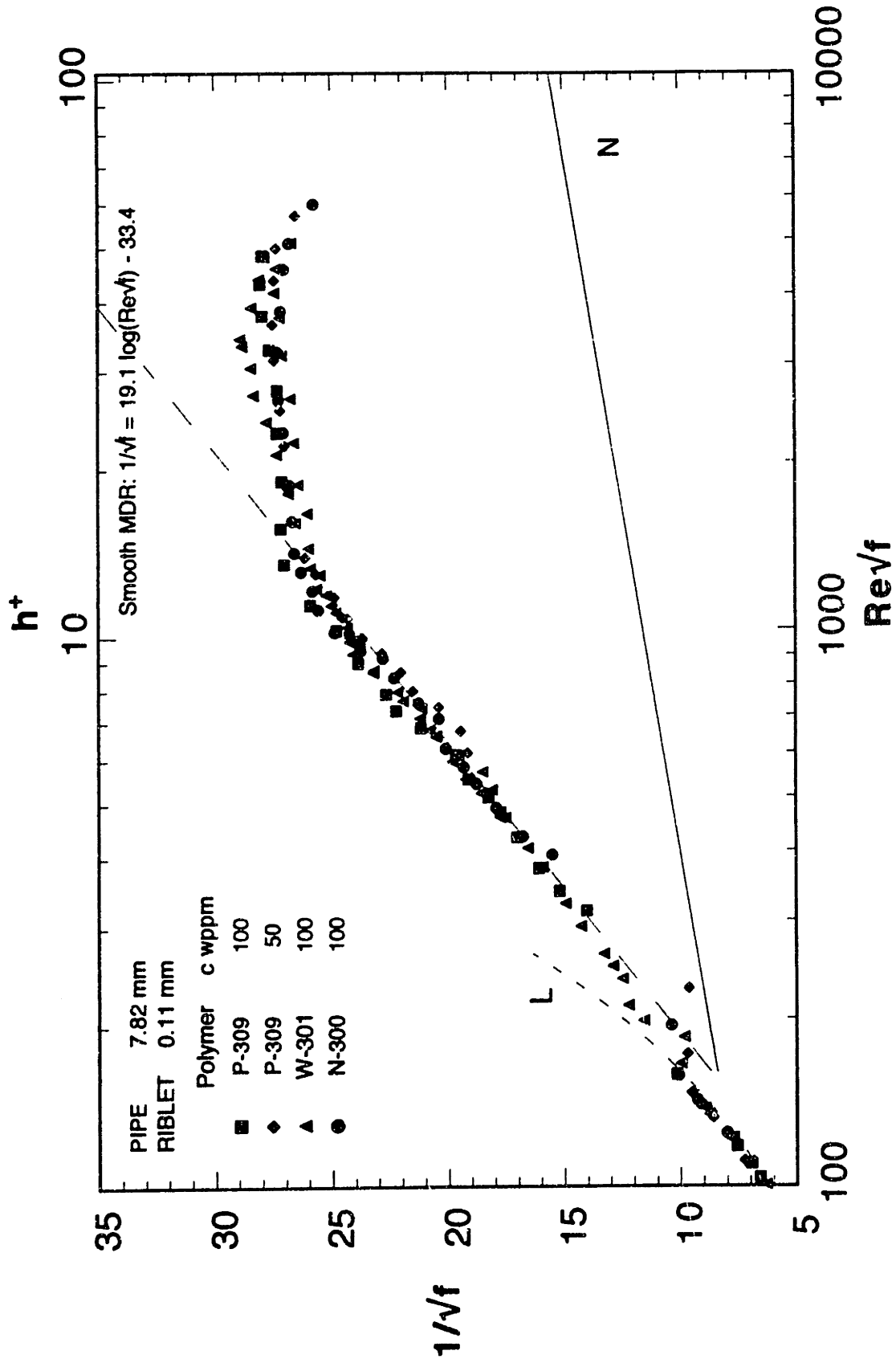


Figure 4.4.4 Friction factors at maximum drag reduction in the 7.82 mm pipe lined with 0.11 mm riblets.

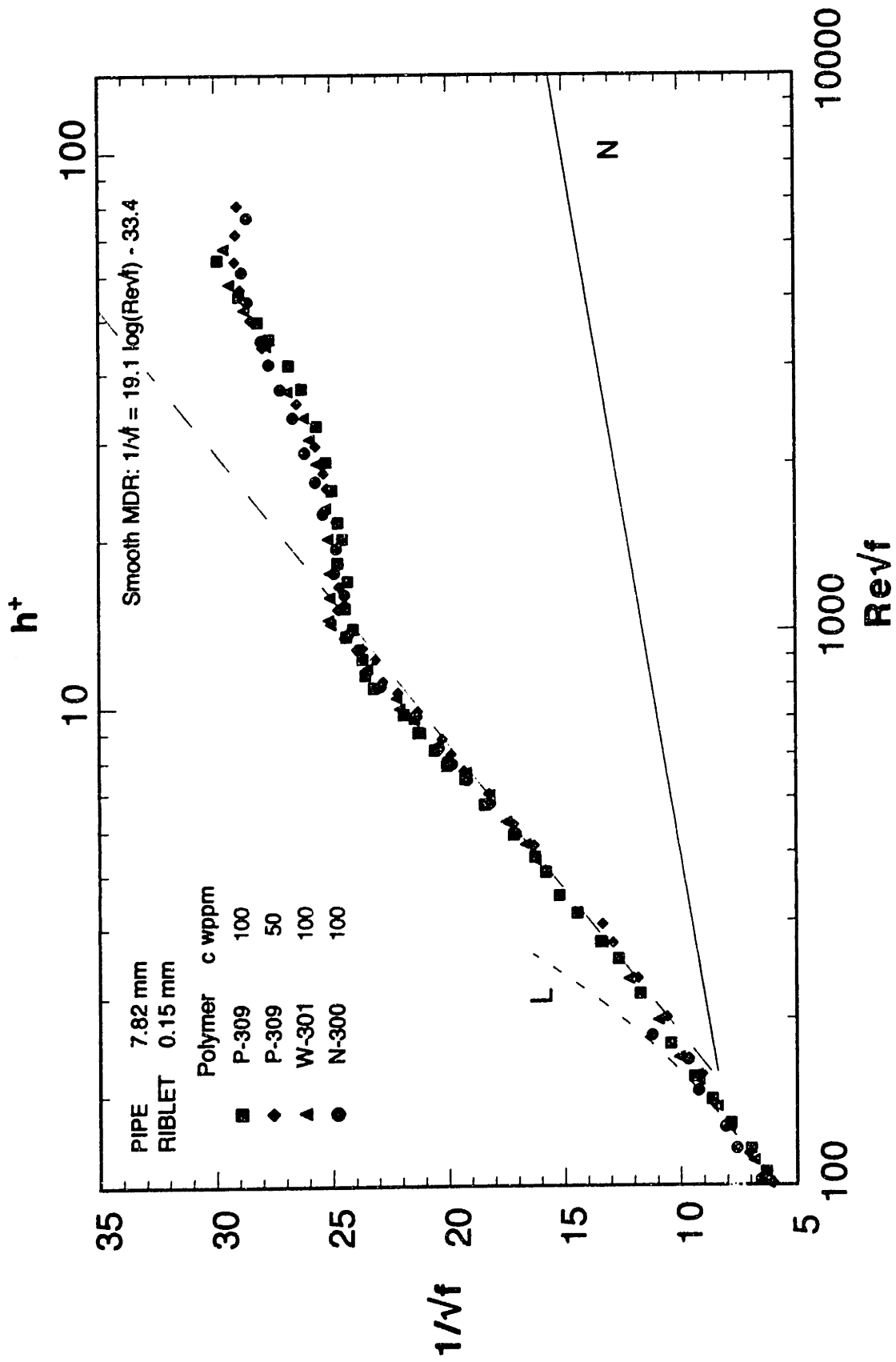


Figure 4.4.5 Friction factors at maximum drag reduction in the 7.82 mm pipe lined with 0.15 mm riblets.

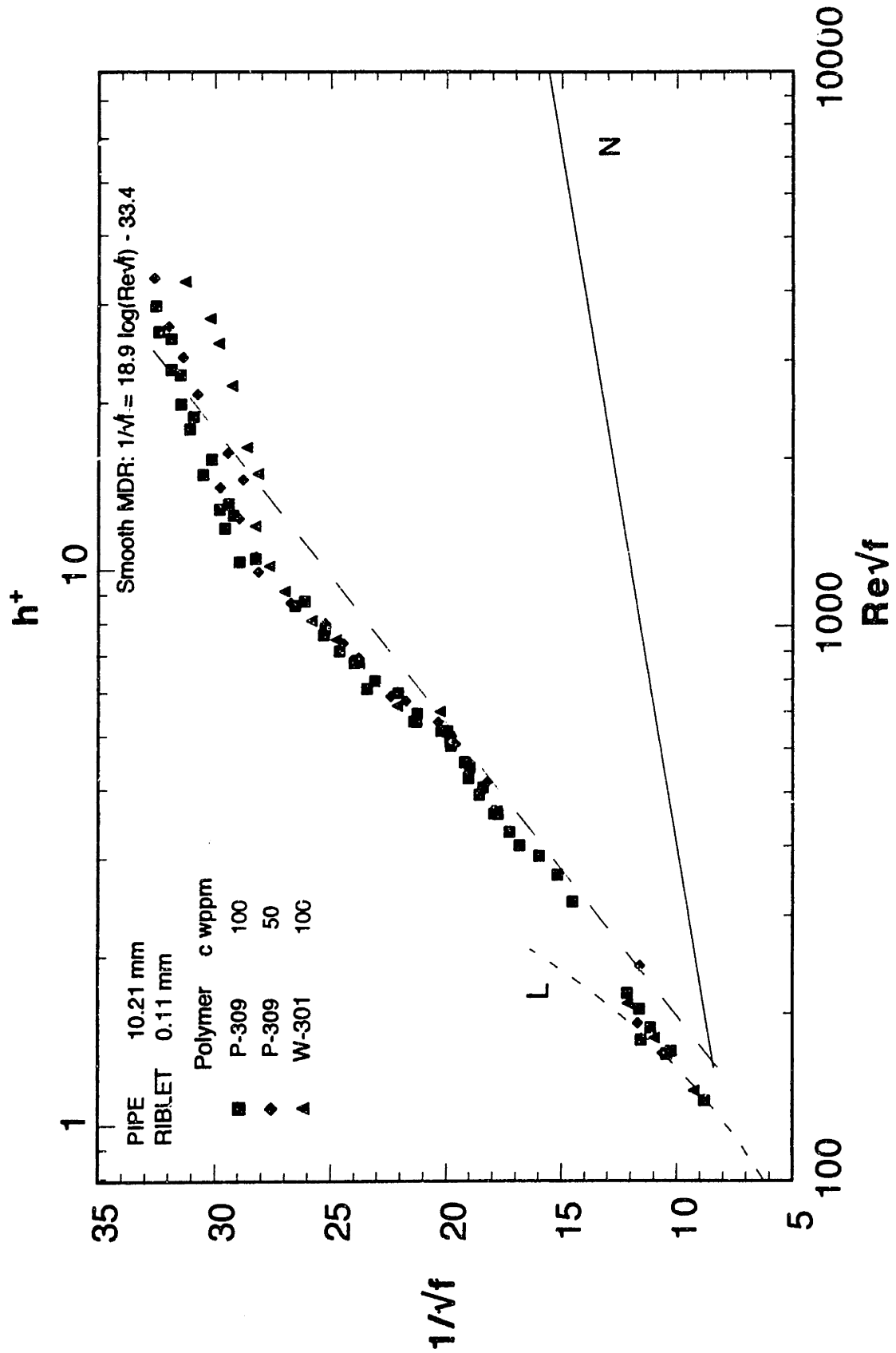


Figure 4.4.6 Friction factors at maximum drag reduction in the 10.21 mm pipe lined with 0.11 mm riblets.

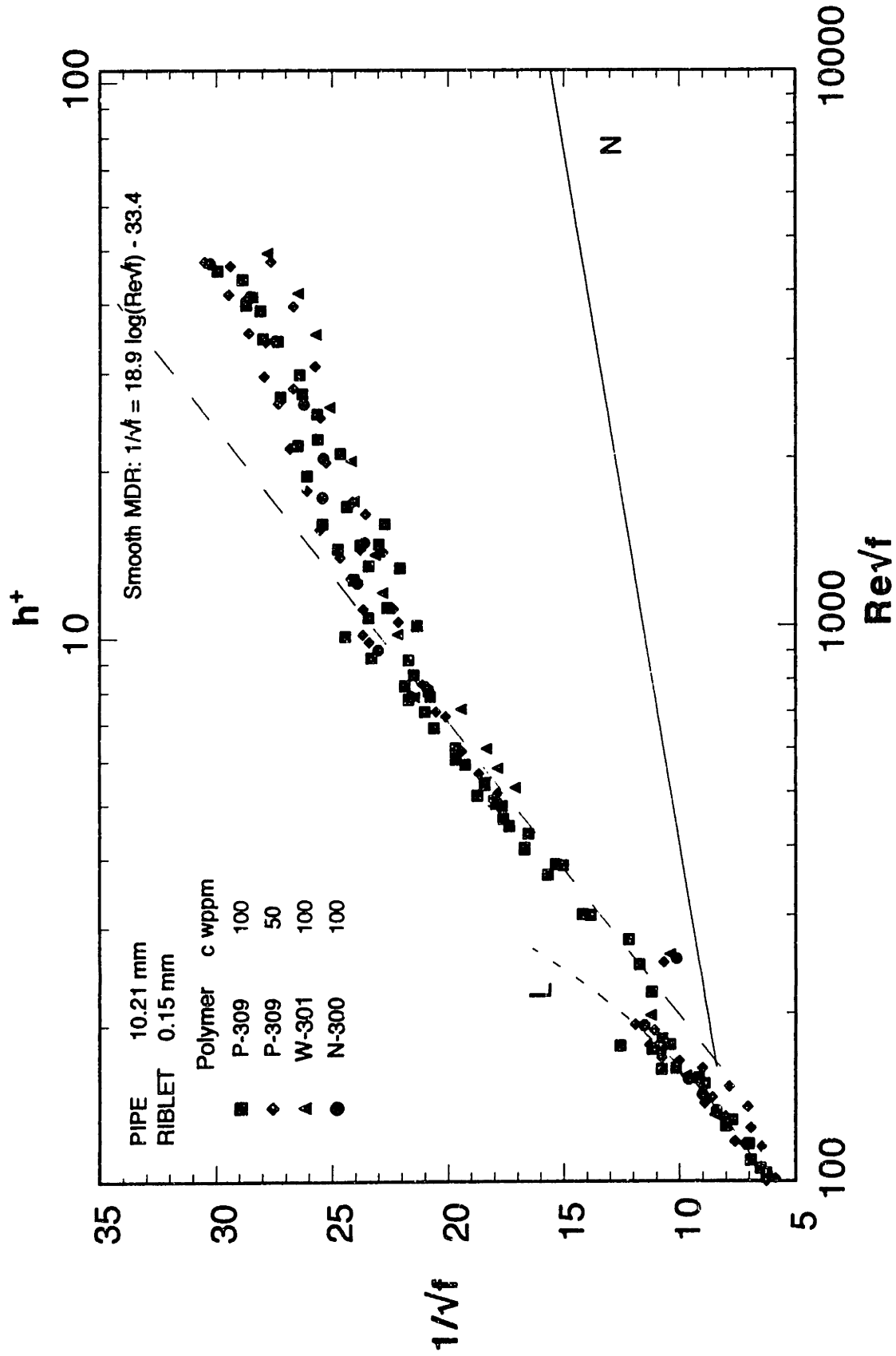


Figure 4.4.7 Friction factors at maximum drag reduction in the 10.21 mm pipe lined with 0.15 mm riblets.

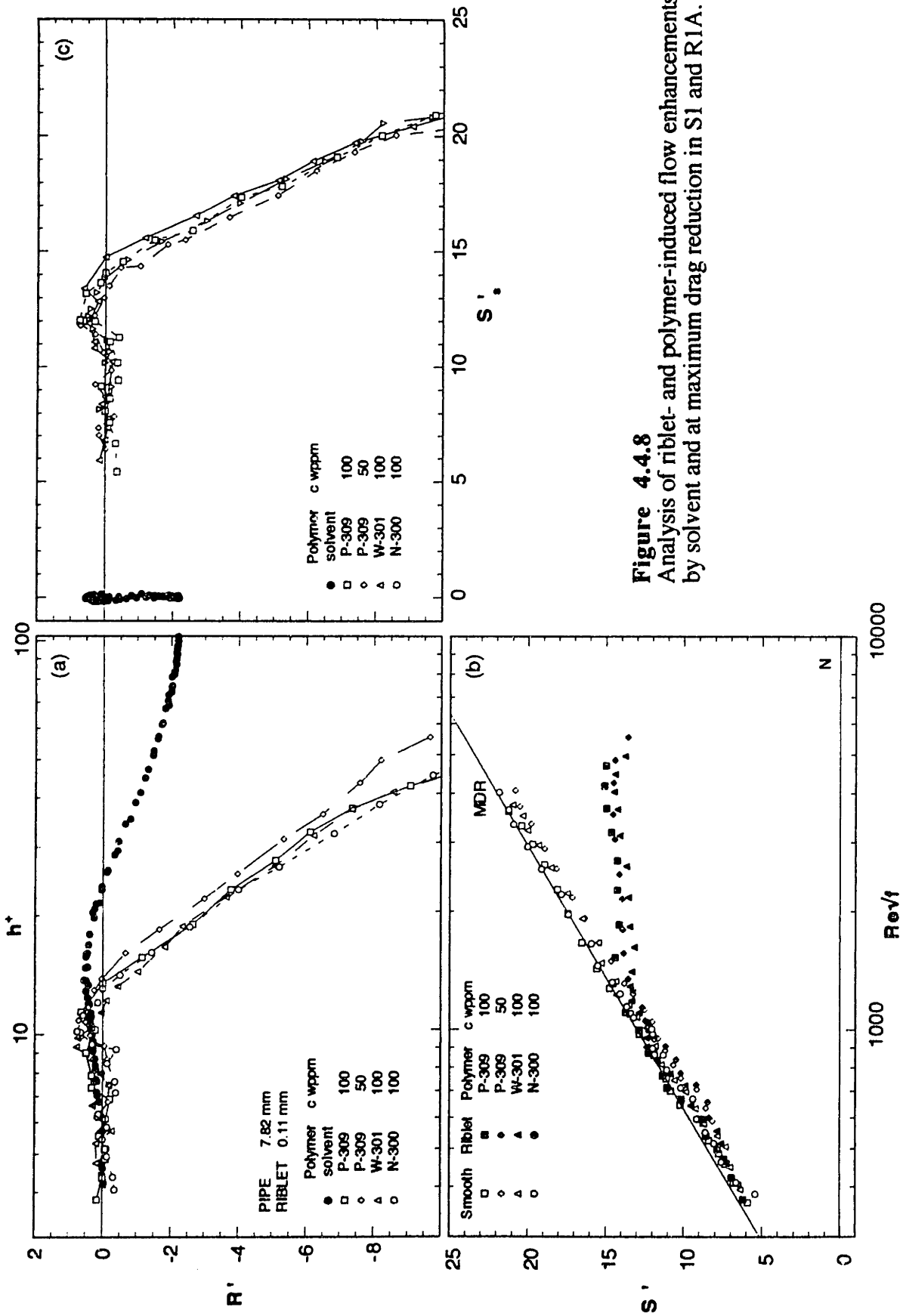


Figure 4.4.8
Analysis of riblet- and polymer-induced flow enhancements by solvent and at maximum drag reduction in S1 and R1A.

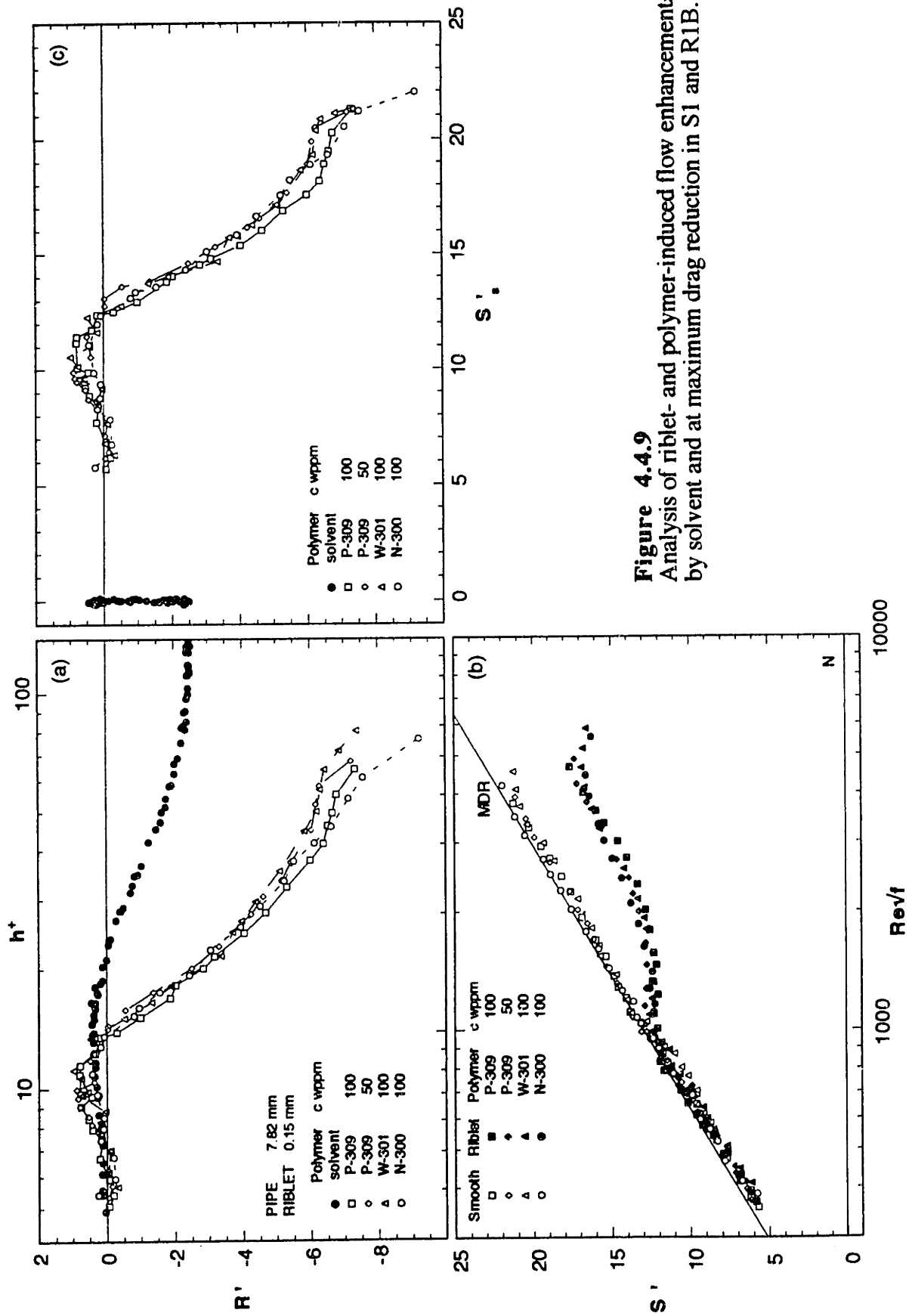


Figure 4.4.9
Analysis of riblet- and polymer-induced flow enhancements by solvent and at maximum drag reduction in S1 and R1B.

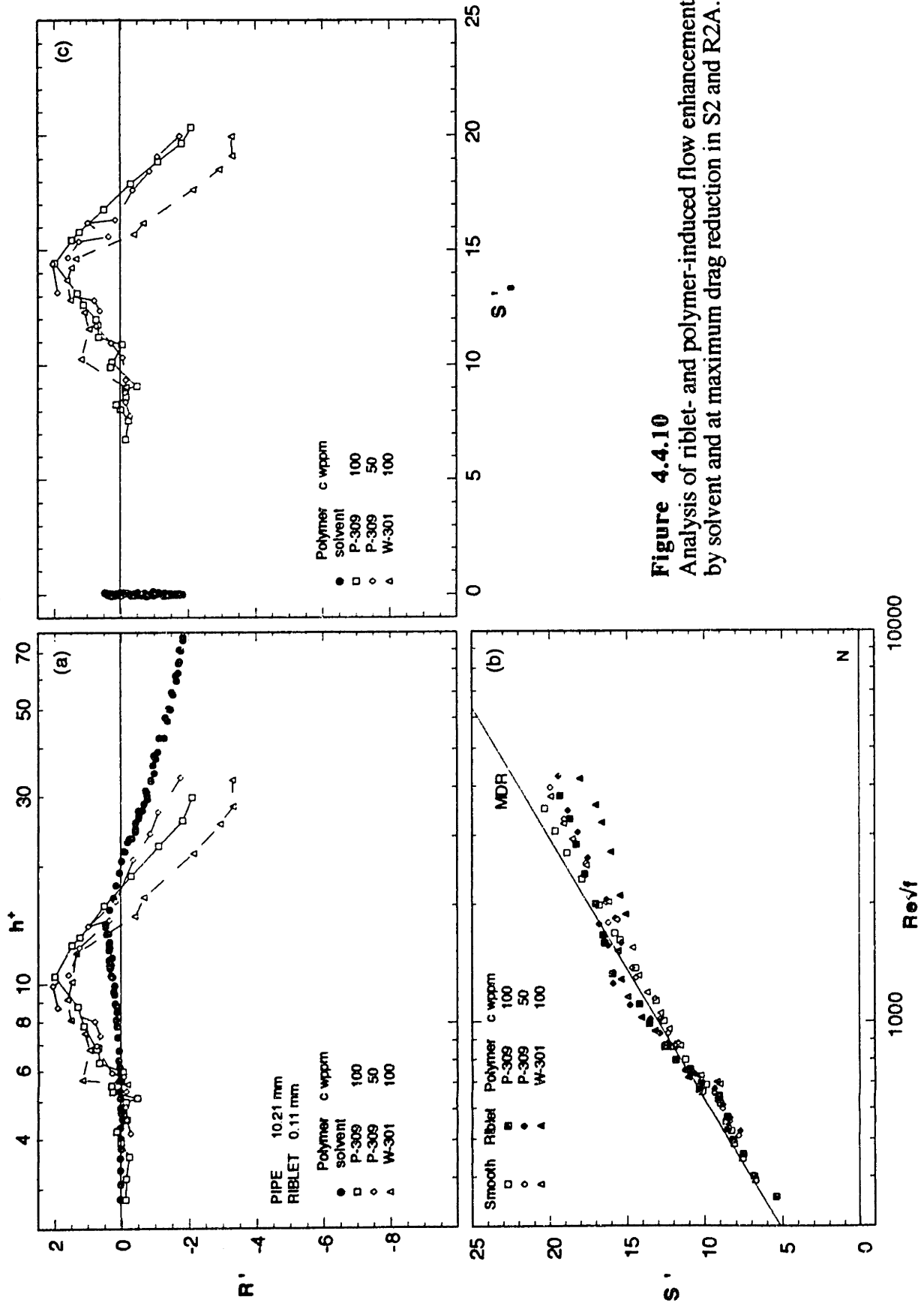


Figure 4.4.10
 Analysis of riblet- and polymer-induced flow enhancements by solvent and at maximum drag reduction in S2 and R2A.

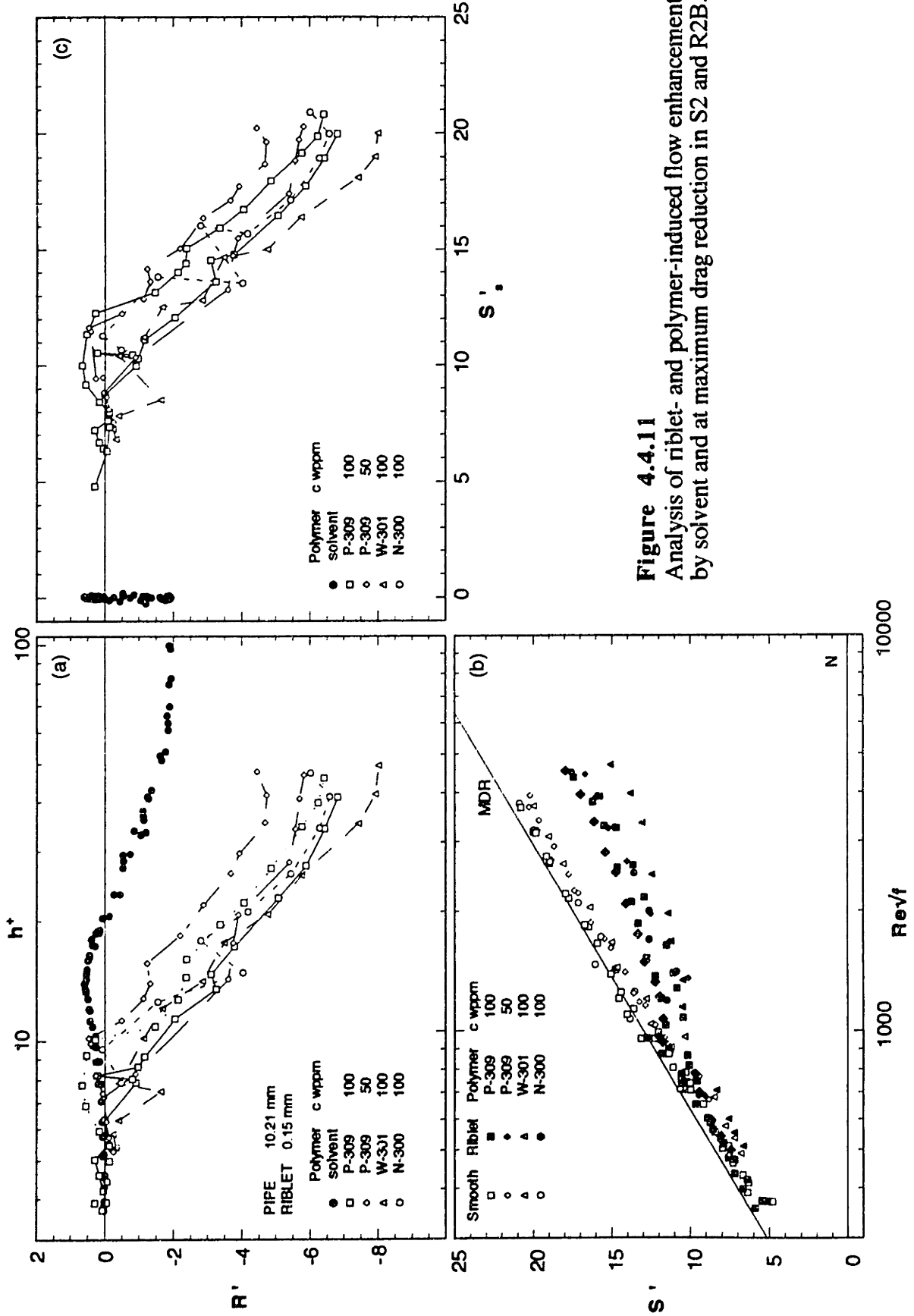


Figure 4.4.11
Analysis of riblet- and polymer-induced flow enhancements by solvent and at maximum drag reduction in S2 and R2B.

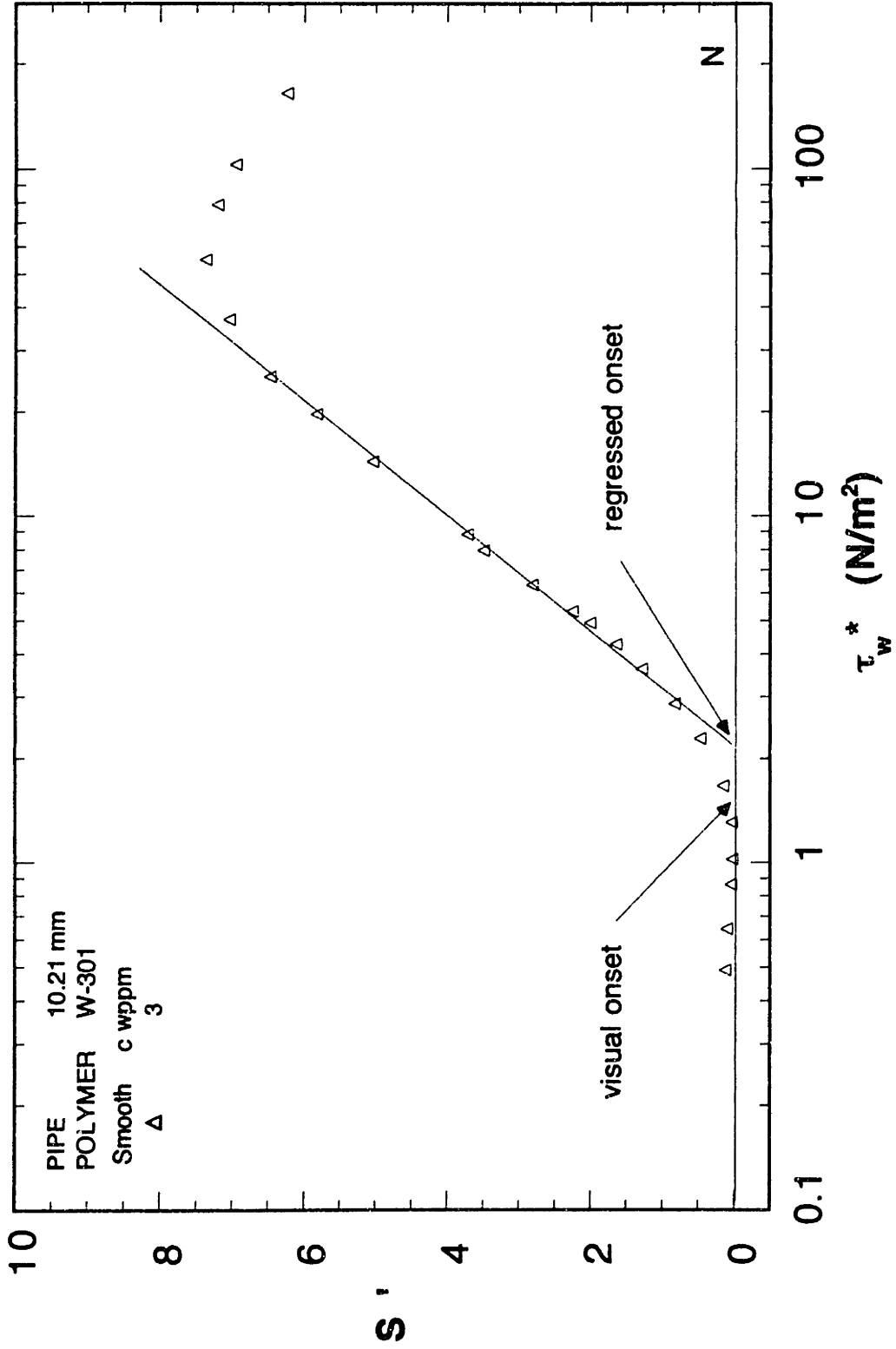


Figure 4.6.1 Definition of visual and regressed onsets of polymer-induced drag reduction

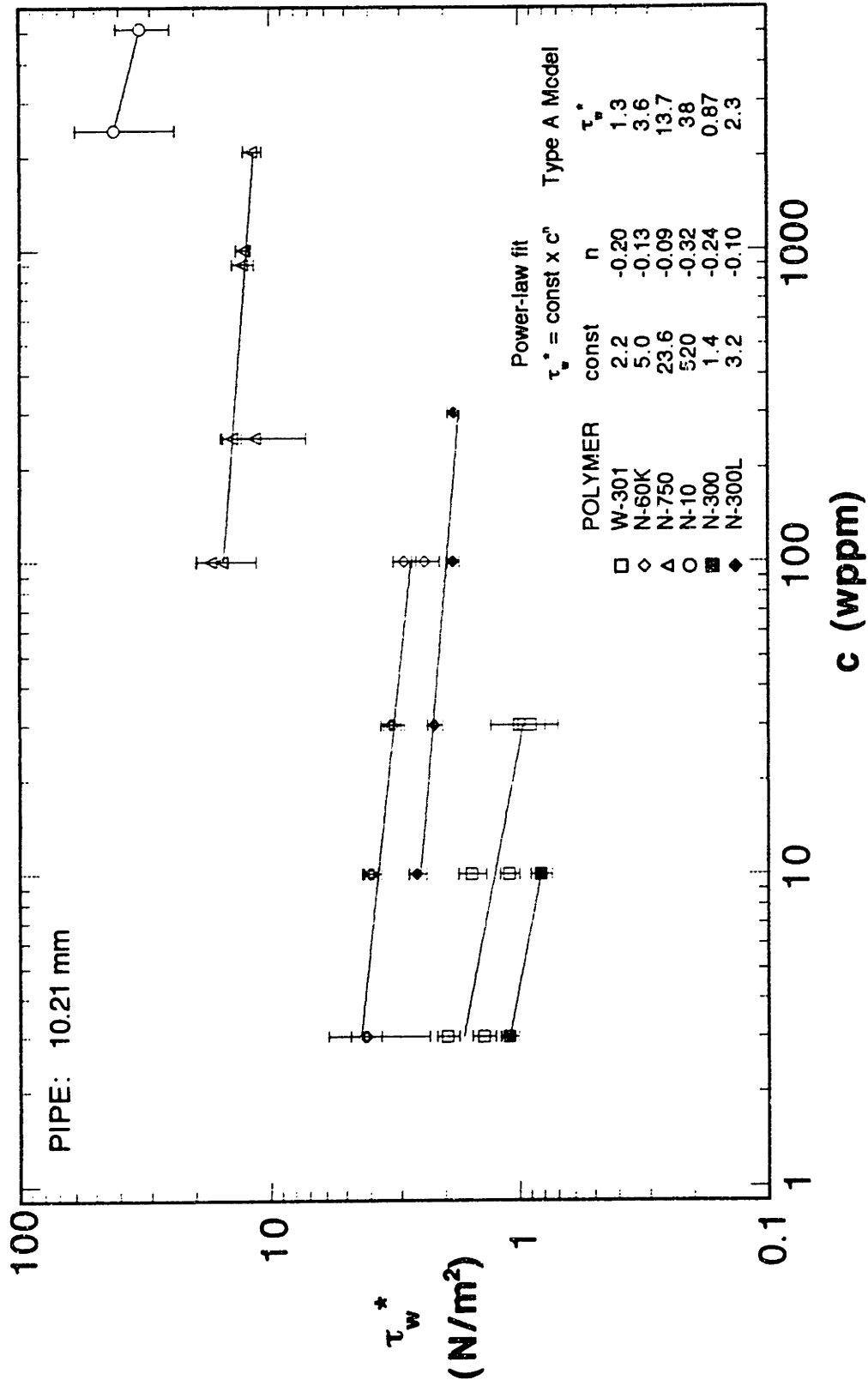


Figure 4.6.2 Regressed onset wall shear stresses in the 10.21 mm smooth pipe

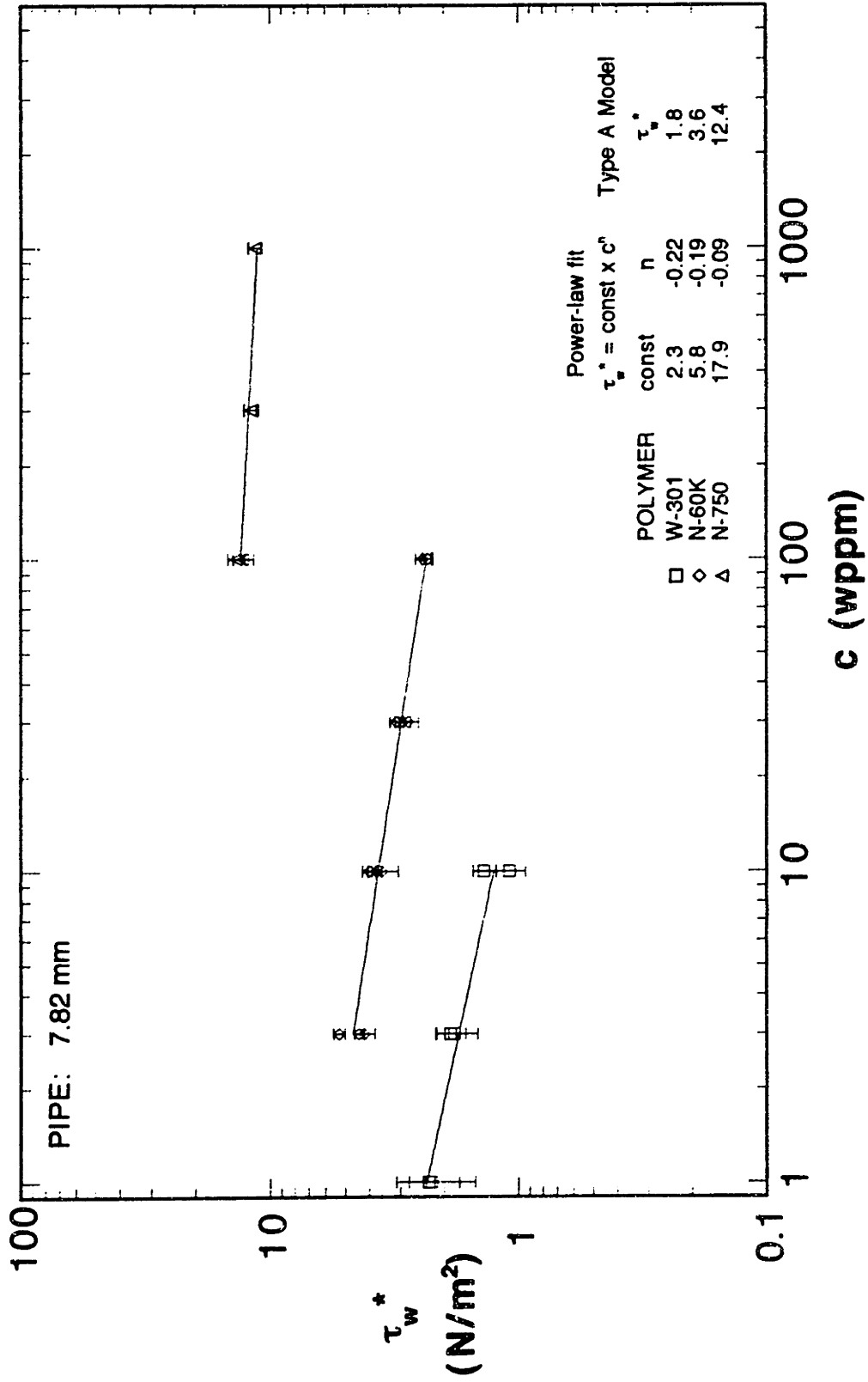


Figure 4.6.3 Regressed onset wall shear stresses in the 7.82 mm smooth pipe

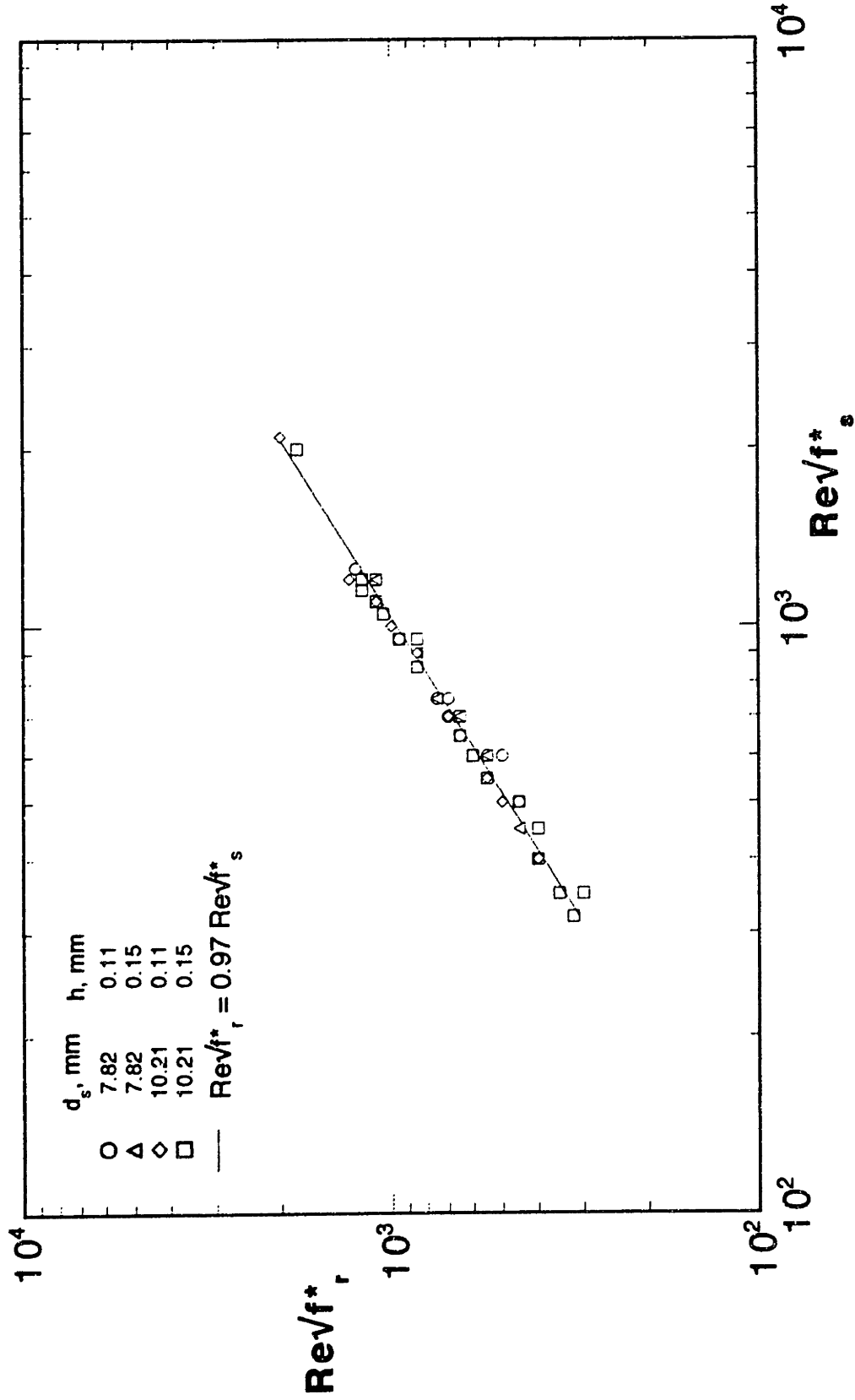


Figure 4.6.4 Variation of the onset Rev^*_r in the riblet pipes with Rev^*_s in the corresponding smooth pipes

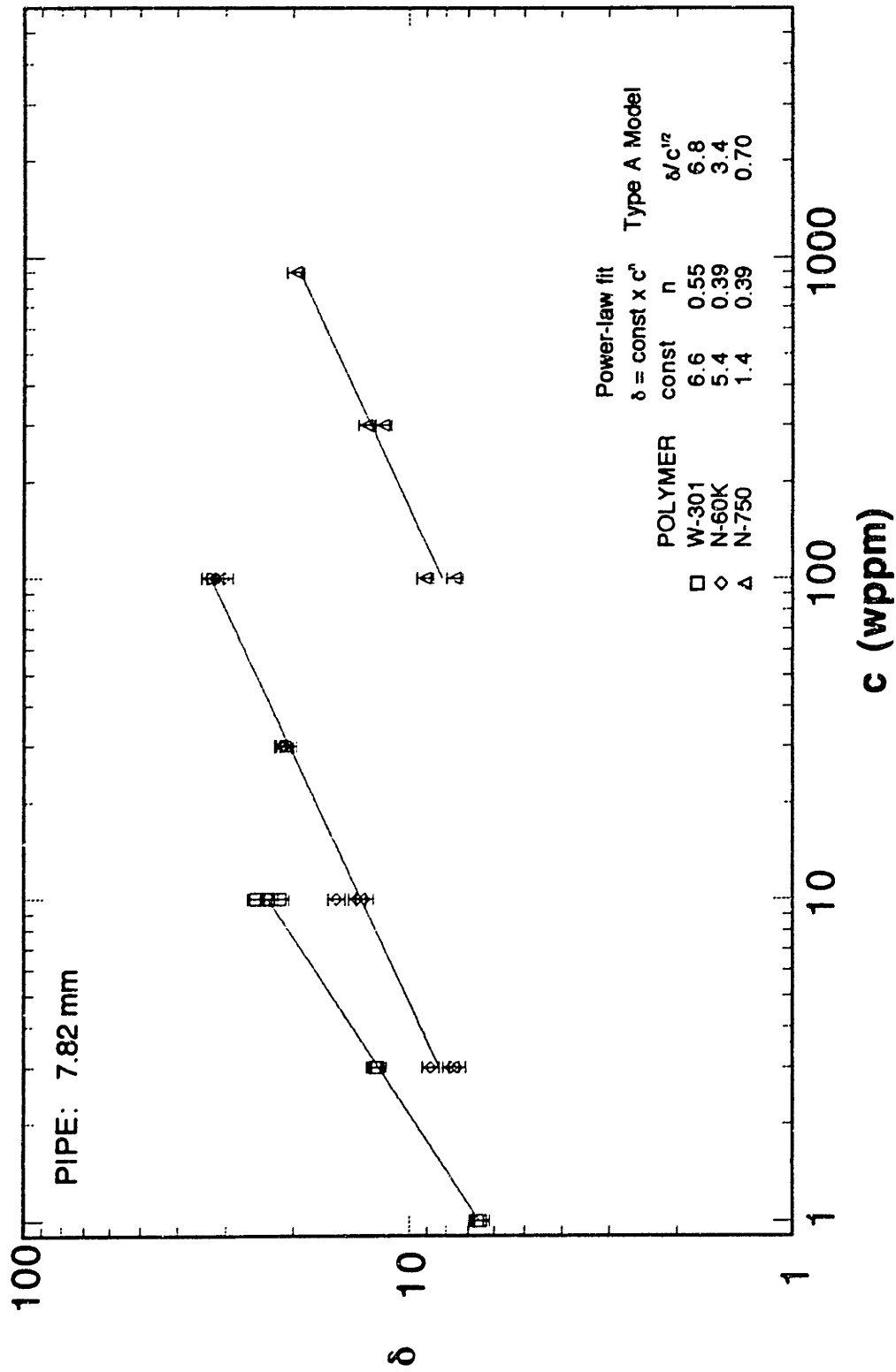


Figure 4.6.5 Slope increments in the 7.82 mm smooth pipe

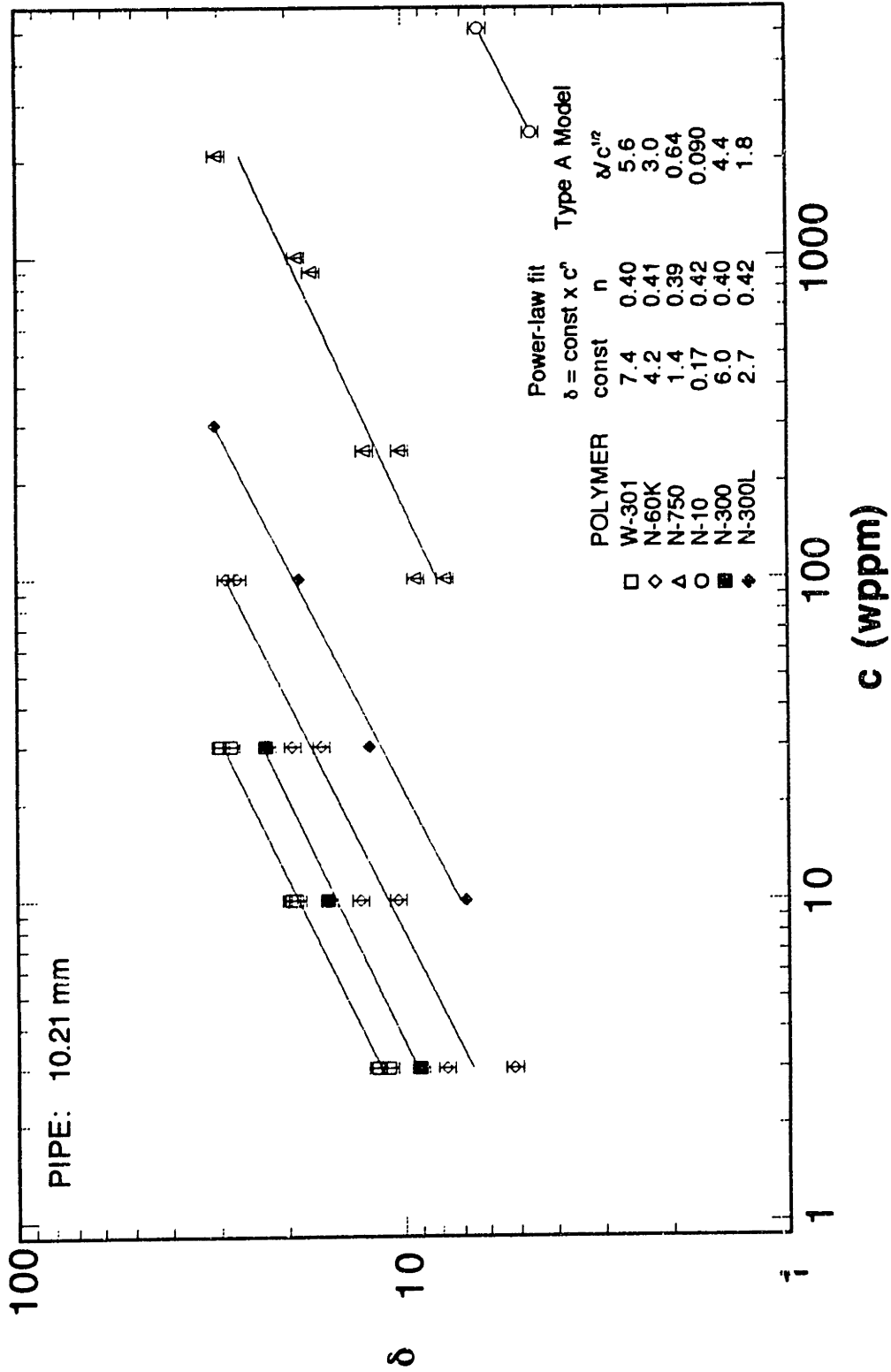


Figure 4.6.6 Slope increments in the 10.21 mm smooth pipe

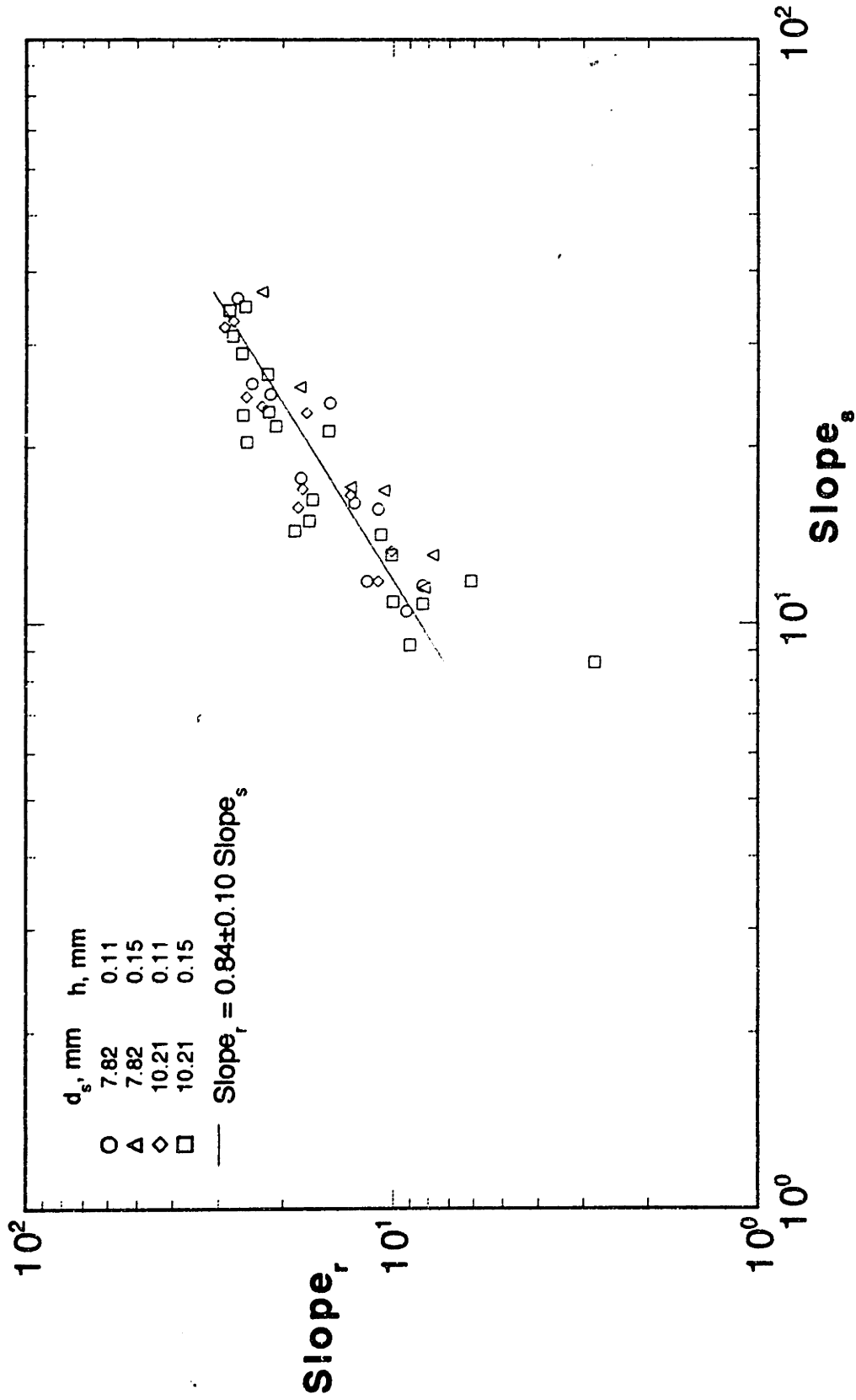


Figure 4.6.7 Variation of the slope of the first polymeric segment in a riblet pipe with the slope of the linear polymeric segment in the corresponding smooth pipe.

Chapter 5

Discussion

In this chapter the results presented in Chapter 4 are analyzed, correlated, physically interpreted wherever possible, and compared to the literature.

5.1 Smooth Pipes

5.1.1 Onset

The wall shear stress at the onset of drag reduction, τ_w^* , does not significantly depend on either the polymer concentration or the pipe diameter, but is inversely related to the polymer-coil size in solution characterized by its r.m.s. radius of gyration, R_G . The relation between τ_w^* and R_G was generalized by Virk (1975a):

$$\tau_w^* \propto R_G^{-g} \quad (5.1-1)$$

where $g = 2$ is based on a length scale hypothesis for onset. Figure 5.1.1 depicts the relation between τ_w^* and R_G in the present experiments; the data are regressed by a power-law expression to reveal:

$$\text{PEO:} \quad \tau_w^* = (6.1 \pm 0.7) \times 10^4 R_G^{-(1.96 \pm 0.05)} \quad (5.1-2a)$$

$$\text{PAM:} \quad \tau_w^* = (1.3 \pm 0.3) \times 10^4 R_G^{-(1.70 \pm 0.20)} \quad (5.1-2b)$$

The errors for the regression of the two PAM data points were inferred from the limits defined by the errors of the individual values. The values of the exponent are seen to accord with the length scale viewpoint of onset. The length-scale onset constant, Ω_L , is determined by first regressing the data against an inverse square law expression, yielding:

$$\text{PEO:} \quad \tau_w^* = (7.3 \pm 0.8) \times 10^4 R_G^{-2} \quad (5.1-3a)$$

$$\text{PAM:} \quad \tau_w^* = (3.7 \pm 0.9) \times 10^4 R_G^{-2} \quad (5.1-3b)$$

from which the length-based “onset constant” $\Omega_L = \sqrt{(\tau_w^* R_G^2 / \rho v_s^2)} = [9.6 \pm 0.5, 6.9 \pm 0.8] \times 10^{-3}$ for [PEO, PAM], respectively with physical properties determined at 25°C. This is in approximate agreement with $\Omega_L = [7.1 \pm 1.3, 8.2 \pm 0.4] \times 10^{-3}$ obtained by Virk (1975a), and $\Omega_L = [4.7 \pm 0.5, 8.3 \pm 1.5] \times 10^{-3}$ from subsequent literature [Berman (1977), Wagger (1992)]. It must be pointed out that the disagreement is due, in part, to the refinements made to the correlations that relate polymeric properties to measured intrinsic viscosities, particularly for PAM solutions. For example, the polymeric property correlations used by Virk in his original analysis would yield with $\Omega_L = [10.7 \pm 0.5, 8.6 \pm 1.2] \times 10^{-3}$ for the present data.

5.1.2 Polymeric Regime

After onset, the experimental data exhibited an approximately linear segment in the polymeric regime, the slope of which exceeded the slope of the Newtonian line, $n = 4$, by an amount, δ . For a given additive, δ does not significantly depend on the pipe diameter but is roughly proportional to the square-root of the concentration, yielding a specific slope increment, $\delta/c^{1/2}$, that is an increasing function of the polymer molecular weight. Figure 5.1.2 depicts the variation of the specific slope increment with molecular weight for the present experiments. The data are regressed with a power-law expression yielding:

$$\text{PEO:} \quad \delta/c^{1/2} = (1.14 \pm 0.10) \times 10^{-6} M_w^{(1.11 \pm 0.08)} \quad (5.1-4a)$$

$$\text{PAM:} \quad \delta/c^{1/2} = (0.65 \pm 0.15) \times 10^{-6} M_w^{(0.96 \pm 0.15)} \quad (5.1-4b)$$

Based on the approximate linear relation between $\delta/c^{1/2}$ and M_w , Virk (1975a) defined a slope increment per macromolecule or intrinsic slope increment, $\Pi = \delta/\sqrt{c/M_w}$, that is related solely to the number of backbone chain links, via a slope modulus, where:

$$\Pi = \kappa N^{3/2} \quad (5.1-5)$$

Since $N = M/m_0$, then $\kappa = m_0^{3/2} (\delta/M_w c^{1/2}) = [68.8 \pm 5.1, 129 \pm 5] \times 10^{-6}$ for [PEO, PAM] for the present data, which is in approximate agreement with $\kappa = [70 \pm 30, 95 \pm 20] \times 10^{-6}$ obtained by Virk (1975a) and $\kappa = [102 \pm 22, 80 \pm 20] \times 10^{-6}$ from [Berman (1977), Wagger (1992)]. Again, the differences are, in part, due to the intrinsic viscosity correlations used to derive polymeric parameters, the present data would yield $\kappa = [63.0 \pm 3.0, 110 \pm 2] \times 10^{-6}$ based on Virk's original analysis.

5.1.3 Maximum Drag Reduction

The polymer-independent maximum drag reduction asymptote was attained by several polymer solutions of different concentrations, molecular weights and skeletal structures in both of the smooth pipes used in the present experiments. Though the scatter in the data, earlier illustrated in Figures 4.4.2 and 4.4.3, was greater than that for solvent flow, the coefficients of the logarithmic regressions: $1/\sqrt{f} = (19.2 \pm 0.4)\log(\text{Re}\sqrt{f}) - (33.4 \pm 0.5)$ in the 7.82 mm pipe and $1/\sqrt{f} = (18.9 \pm 0.2)\log(\text{Re}\sqrt{f}) - (33.4 \pm 0.8)$ in the 10.21 mm pipe were well within the uncertainties of Virk's (1975a) original correlation: $1/\sqrt{f} = (19 \pm 0.4)\log\text{Re}\sqrt{f} - (32.4 \pm 1.2)$ correlated by Virk (1975a). The present results also accord with later results of Berman (1977), Mizushima and Usui (1977), Schummer and Thielen (1980) and Wagger (1992) at maximum drag reduction.

5.1.4 Polymer Degradation

Polymer degradation is invariably associated with polymeric drag reduction, because the extension of the macromolecular chain required to induce drag reduction also causes scission of its bonds, commonly near the chain midpoint (Merrill and Horn, 1984). Since degradation and riblet drag enhancement produce similar effects relative to the undegraded solution in the smooth pipe, analysis of drag enhancement can be masked by degradation effects, especially for high molecular weight polymers in the polymeric regime. The object of this section is to correlate the degradation data described in section 4.3.3, so that these can be systematically applied to “correct” for degradation effects in our riblet pipe results, particularly those at the highest flowrates, that were the most affected.

Let us view degradation as a chemical reaction by which the original macromolecular substrate responsible for drag reduction is “converted” to ineffective species, of lower molecular weight, by turbulent stresses encountered during its flow through the pipe. Then, at a fixed $Re\sqrt{f}$, the ratio $(-\Delta'_{jk}/S'_k)$ of the observed degradation parameter normalized by upstream flow enhancement should reflect the fractional substrate conversion, X . Further, the earlier observation in Figure 4.3.6 that both $-\Delta'_{jk}$ and S'_k varied as \sqrt{c} , that is, their ratio was independent of c , suggests that degradation is kinetically a first order process, in which conversion should be related to severity by: $-\ln[1-X] = k_{deg} \cdot t_{res}$, where k_{deg} is a first-order degradation rate constant and t_{res} the residence (transit) time between stations j and k . The degradation rate constant, $k_{deg} = \{-\ln[1-(\Delta'_{jk}/S'_k)]\}/t_{res}$, should depend only upon the turbulent stresses causing degradation, and these latter are reasonably scaled by the wall shear stress, τ_w , which is here analogous to the temperature in conventional kinetics. In the limit of low conversion, $X \approx (-\Delta'/S') \ll 1$, we have $k_{deg} \rightarrow (-\Delta'_{jk}/S'_k)/t_{res}$ which suggests a degradation correlation of the form, $(\Delta'_{jk}/S'_k)/t_{res} \text{ s}^{-1}$ vs. τ_w , Pa, as shown in Figure 5.1.3a-d. This evidently effects a considerable superposition of the original degradation data presented in Figures 4.3.6a-b and 4.3.7a-d. For each pipe and

polymer combination, results for all polymer concentrations in the polymeric regime of drag reduction, and, in (b), both downstream distances as well, collapse onto a single band. The respective bands of data, which exhibit some curvature on the semi-log coordinates of Figure 5.1.3, have been approximated by relations of the form:

$$(-\Delta'_{jk}/S'_k)/t_{res} = 0; \quad \tau_w < \tau_w^\wedge \quad (5.1-6a)$$

$$(-\Delta'_{jk}/S'_k)/t_{res} = \Gamma \log(\tau_w/\tau_w^\wedge); \quad \tau_w \geq \tau_w^\wedge \quad (5.1-6b)$$

Values of the characteristic degradation-inducing wall shear stress τ_w^\wedge Pa and the characteristic degradation rate constant Γ s⁻¹ are given in Table 5.1.1.

5.2 Riblet Pipes: Solvent Flow

5.2.1 Laminar Flow

For laminar flow in riblet pipes, our present experimental results yielded $fRe = [16.26, 16.66, 16.34, 16.22]$ for pipes [R1A, R1B, R2A, R2B], respectively, for which $d_r/2h = [36, 26, 47, 34]$; thus, for laminar flow over riblets, $(fRe)_r > (fRe)_s$. Figure 5.2.1 depicts the variation of $(fRe)_r/(fRe)_s$ with h/H , where H is the channel half width ($=d_r/2$ for pipe flow); included are the computational results of Chu and Karniadakis (1993) in a semi-infinite rectangular channel ($h/H = 0.2$) and some present preliminary computational work using a commercial finite element fluid dynamics software package, FIDAP, in a semi-infinite rectangular channel with $h/H = [0.01, 0.02, 0.04]$. The computational results show that as h/H increases, $(fRe)_r/(fRe)_s$ also increases; the present experiments roughly follow the trends exhibited by the computations with the exception of pipe R2A which exhibited a larger than expected $(fRe)_r$.

5.2.2 Comparison to Previous Work

Figure 5.2.2 is a comparison between present data for solvent flow in riblet pipes and the results of previous workers.

- (i) In the hydraulically smooth regime, $h^+ < 5$, there is considerable scatter amongst the literature data, including some apparent riblet drag reduction, which is probably due to the various authors' definitions of pipe diameter.
- (ii) The extent of the riblet drag reduction regime, $5 < h^+ < 22$, as well as the magnitude and location of the greatest effect, $R' = 0.6$ at $h^+ = 14$, obtained in the present experiments were similar to those reported by earlier workers using V-groove riblets with $h/s \approx 1$.
- (iii) In the riblet drag enhancement regime, the present data accord with previous work for $22 < h^+ < 70$, but extend to somewhat higher $h^+ = 160$ and suggest an asymptotic $R' \rightarrow -2.1$, constant, for $h^+ > 80$. This differs from rough-walled pipes, depicted by a solid line, wherein drag enhancement increases monotonically with increasing $h^+ > 5$, according to Nikuradse's roughness function (Nikuradse, 1933), with $R' = 1.71 - 4 \log h^+$ for $h^+ > 70$. Thus the view of riblets as roughness elements (Tani, 1988), derived from early riblet data at $h^+ < 50$, $R' > -1$, is not borne out by our solvent results at high $h^+ > 80$. However, one can see from the figure that for $20 < h^+ < 60$, the riblet data lie approximately parallel to, but displaced rightwards by a factor of 4 from, the sand roughness line, which might have led to the earlier inference of riblet-roughness similarity.

5.2.3 Serrated Sublayer Model

5.2.3.1 Model Development

Riblet pipe friction observations presented in Chapter 4 are the net result of two opposing effects namely, (i) a drag reduction induced by the riblets, that possibly stems from their interactions with spanwise vortices near the pipe wall and (ii) a drag enhancement due to the increased wetted surface area offered by the riblets. To understand the interaction between the riblets and turbulent flow, it is desirable to decouple these two effects. This is the objective of the present “serrated sublayer model”, wherein the wetted surface area is presumed to be directly related to the ratio of viscous sublayer (VSL) thickness to riblet height.

Our model begins with the observation that a riblet pipe is non-circular and may therefore be described by the conventional “geometric” hydraulic diameter:

$$d_H = \frac{4A_c}{P_w} \quad (5.2-1)$$

where A_c is cross sectional area and P_w the “wetted” perimeter, that is the length of physical boundary exposed to fluid. For weakly concave cross-sectional shapes, such as rectangles of small aspect ratios and triangles, Nikuradse (1930) showed that the use of d_H led to friction factor relations that were essentially identical to those for circular pipes. This is not the case for convex surfaces, such as eccentric annuli and conduits formed from arrays of parallel rods (Malak et al., 1975). Neeves et al. (1994) showed in direct numerical simulations of axial flows over curved cylinders that the VSL and logarithmic velocity profiles are functions of (i) the ratio of the boundary layer thickness to radius of curvature, $\gamma = \delta/r$ and (ii) non-dimensional radius of curvature, $r^+ = ru_\tau/\nu$. If γ is small, the curved boundary layer is similar to the planar case. If γ is large, curvature affects the outer layer if r^+ is also large, and both the outer and inner layers if r^+ is small.

Malak et al. (1975) proposed that there is some characteristic diameter, which we call an “equivalent” hydraulic diameter, $d_h = \omega_T d_H$, for which non-circular conduits obey circular friction factor relations; ω_T is a “shape factor” that relates the effective surface area exposed to the fluid to the geometric area with difference between these areas possibly arising from the effects of secondary flows which “shield” part of the physical surface from the flow. They correlated ω_T in terms of laminar flow relations, $Re_H f_H = \text{constant}$, where:

$$\omega_T = \frac{4}{1 + 3\sqrt{Re_H f_H / 16}} \quad (5.2-2)$$

[It is not readily apparent why a turbulent flow parameter, such as ω_T , should be related to laminar flow, so Eq. (5.2-2) should be viewed primarily as a correlation of the authors’ observations.] For laminar flow in the present V-groove riblet pipes, $Re_H f_H = Re_f / (1 + 4h^2/s^2) \approx 3.4$, therefore $\omega_T \approx 1.68$ from Eq. (5.2-2).

For turbulent, Newtonian flow, the pressure gradient depends on both the cross-sectional and equivalent hydraulic diameters. Using the Blasius friction factor relation:

$$|\nabla P| \propto Q^{1.75} d_c^{3.5} d_h^{1.25} \quad \text{for } Re < 10^5 \quad (5.2-3)$$

For a circular pipe, $d_c = d_h = d_H = d_s$, so that Eq. (5.2-3) reduces to Eq. (4.2-4), as expected. From the definition of the pressure gradient ratio of riblet to smooth pipes, we have:

$$P_T = \frac{d_c^{3.5} d_h^{1.25}}{d_s^{4.75}} \quad (5.2-4)$$

where d_c and d_h are, respectively, the cross-sectional and equivalent hydraulic diameters of the riblet pipe. In the hydraulically smooth regime, we postulate that the riblets are wholly within the viscous sublayer, $h^+ < y_v^+$, as depicted schematically in Figure 5.2.3a. In this regime, $P_T = P_{T0}$, therefore:

$$d_h = d_{h0} = \left(\frac{P_{T0} d_s^{4.75}}{d_c^{3.5}} \right)^{1/1.25} \quad (5.2-5)$$

Values of d_{h0} are summarized for all riblet pipes in the middle of Table 5.2.1, which also notes all other relevant riblet pipe diameters (see also section 3.1.5 where they were defined).

As $h^+ \gg y_v^+$, we assume that the drag reduction associated with riblets vanishes, because the scales of turbulence which interacted with the riblets to produce drag reduction in the vicinity of $h^+ = 14$ become much smaller than the riblets. The viscous sublayer now closely follows the contours of the riblet surface, as depicted in Figure 5.2.3c, such that $P_T = P_{T\infty}$, therefore:

$$d_h = d_{h\infty} = \left(\frac{P_{T\infty} d_s^{4.75}}{d_c^{3.5}} \right)^{1/1.25} \quad (5.2-6)$$

Values of $d_{h\infty}$ are summarized in Table 5.2.1, along with the geometric hydraulic diameter, d_H . The experimentally observed $d_H/d_{h\infty} = 0.63 \pm 0.03$ in three riblet pipes suggests that 37% of the physical riblet surface area is shielded from the outer flow at high $h^+ \gg y_v^+$. It is also interesting that the observed $d_H/d_{h\infty} \approx 0.63$ agrees with the value $1/\omega_T = 0.61$ estimated for our riblet pipes from Malak's relation (Eq. 5.2-2)

Between the two asymptotic limits, d_{h0} for $h^+ < y_v^+$ and $d_{h\infty}$ for $h^+ \gg y_v^+$, the hydraulic diameter is a function of viscous sublayer thickness. We consider a viscous sublayer of triangular shape, depicted in Figure 5.2.3b. This is the simplest model that reflects the physical shape of the viscous sublayer over riblets which is thinnest at the peak where the local wall shear stress, τ_w , is a maximum, and increases to a maximum in the valley, where τ_w is a minimum (Choi et al., 1989a, Vukoslavcevic et al., 1992). The hydraulic diameter thus varies with h^+ as follows:

$$\xi = \frac{d_h}{d_{h0}} = 1 \quad h^+ < y_v^+ \quad (5.2-7a)$$

$$\xi = \frac{d_h}{d_{h0}} = \left[1 + (\xi_\infty^2 - 1) \left(\frac{h^+ - y_v^+}{h^+} \right)^2 \right]^{1/2} \quad h^+ > y_v^+ \quad (5.2-7b)$$

where $\xi_\infty = d_{h\infty}/d_{h0}$. Figure 5.2.4 depicts the variation of ξ with h^+ for solvent flow, with $\xi_\infty = 0.80$, which is the average experimentally observed value. The effect of experimental error, ± 0.02 units in ξ_∞ , is illustrated in the figure by the dashed lines, and has only a small effect on the ξ - h^+ profile.

The original Prandtl-Karman coordinates previously used may now be converted to a coordinate system based on the equivalent hydraulic diameter, by the transformation:

$$\begin{bmatrix} \text{Re}_h \sqrt{f_h} \\ 1/\sqrt{f_h} \end{bmatrix} = \begin{bmatrix} \xi^{3/2} & 0 \\ 0 & \xi^{-1/2} \end{bmatrix} \begin{bmatrix} \text{Re} \sqrt{f} \\ 1/\sqrt{f} \end{bmatrix} \quad (5.2-8)$$

Newtonian flows in non-circular pipes are then presumed to follow the smooth pipe relationship based upon the transformed P-K coordinates:

$$\frac{1}{\sqrt{f_h}} = 4 \log \text{Re}_h \sqrt{f_h} - 0.4 \quad (5.2-9)$$

By analogy to the riblet-induced physical and fractional flow enhancement parameters, R' and R_F , we now define the corresponding "inherent" riblet-induced flow enhancement parameters, R_h' and $R_{h,F}$:

$$R_h' = \left[\left(\frac{1}{\sqrt{f_h}} \right)_r - \left(\frac{1}{\sqrt{f_h}} \right)_s \right]_{\text{Re}_h \sqrt{f_h}} \quad (5.2-10a)$$

$$R_{h,F} = \left[\left(\frac{1}{\sqrt{f_h}} \right)_r / \left(\frac{1}{\sqrt{f_h}} \right)_s - 1 \right]_{\text{Re}_h \sqrt{f_h}} = R_h' / \left(\frac{1}{\sqrt{f_h}} \right)_s \quad (5.2-10b)$$

R' reflects the flow enhancement that would be observed in a riblet pipe relative to an imaginary smooth pipe of equal wetted surface area.

5.2.3.2 Riblet Drag Reduction

The variation of the “inherent” riblet-induced flow enhancement R_h' versus h^+ in solvent is depicted in Figure 5.2.5 being derived from the data in the earlier Figure 5.2.2 showing R' vs. h^+ and application of Eq. (5.2-8). The inherent riblet-induced flow enhancement exhibits three regimes, namely:

- (i) Hydraulically smooth. For $h^+ < 5$, $R_h' \approx 0$. The riblets are within the viscous sublayer, being too small to interact with the turbulence structures in the buffer layer above them.
- (ii) Riblet-induced drag reduction. For $5 < h^+ < 65 \pm 15$, $R_h' > 0$, exhibiting a maximum $R_h' = 1.40 \pm 0.10$ at $h^+ = 17 \pm 3$. The riblets are now large enough to interfere with the vortex structures in the buffer layer and it is significant that their maximum effectiveness occurs when their tips are in the vicinity of the plane of peak turbulence production.
- (iii) Equivalently smooth. For $65 \pm 15 < h^+ < 160$, $R_h' \approx 0$. The riblets are now large enough relative to the turbulent flow scales that they contain, and cannot impede, the near-wall structures.

Figure 5.2.6 compares the physical and inherent riblet-induced flow enhancements, R' and R_h' , respectively depicted by the solid and dashed lines derived from the present data. The inherent and physical hydraulically smooth regimes are the same, $h^+ < 5$, with $R' = R_h' = 0$. The inherent riblet drag reduction regime extends over a larger range of h^+ , $5 < h^+ < 65$ in R_h' than that physically observed, $5 < h^+ < 22$, with the inherent maximum

$R_h' \approx 1.5$ at $h^+ \approx 17$ being nearly thrice the physical $R' \approx 0.5$ at $h^+ \approx 14$. The observed region of asymptotic riblet drag enhancement is transformed to the equivalently smooth regime in the inherent case $R_h' \approx 0$.

The foregoing features described for the inherent R_h' are also apparent in the variation of R_F with h^+ , depicted in Figure 5.2.7.

5.2.3.3 Comparison to Rough Pipes

The foregoing inferences for Newtonian flows in riblet pipes may now be compared those in rough pipes, the latter being described by Nikuradse's (1933) roughness function:

$$\beta = \sqrt{\frac{2}{f}} + \frac{3}{2\chi} - \frac{1}{\chi} \ln\left(\frac{d}{2k}\right) \quad (5.2-11)$$

Figure 5.2.8 depicts the variation of the inherent riblet-induced flow enhancement, R_h' versus h^+ , the nondimensional riblet height, in registry with a semi-logarithmic plot of the roughness function β versus k^+ , the nondimensional roughness height; both abscissae and ordinates have the same scale. For Newtonian flows in rough pipes, the data of Nikuradse (1933) exhibited (i) a hydraulically smooth regime for $k^+ < 5$, wherein $\beta = 2.5 \ln(k^+) + 5.5$, (ii) a transitional region $5 < k^+ < 70$, within which β exhibited a maximum at $(k^+, \beta) = (11, 9.5)$ and (iii) a fully rough regime, $k^+ > 70$, wherein $\beta = 8.5$. It is striking that the range of k^+ that defines the transitional region for Newtonian flow in rough pipes coincides with the range of h^+ that comprises the inherent riblet drag reduction regime. This suggests that drag reduction by riblets is confined to the buffer layer, approximately $5 < y^+ < 70$.

5.2.3.4 Comparison with other Models of Riblet Drag Reduction

Prompted by the analysis of longitudinal viscous flow over riblet surfaces by Bechert et al. (1989), Luchini et al. (1991) proposed that within the viscous sublayer (modeled as a quasi-steady solution of Stokes flow), the virtual plane wall seen by a fluid in cross-flow over a riblet surface is closer to the riblet peak than the one seen in parallel flow. The difference between the protrusion heights, Δh_p , was taken to be the quantitative characterization of how much the riblet wall impedes cross-flow more than longitudinal flow; the greater the difference, the greater the expected drag reduction, though no attempt was made to predict drag reduction using Δh_p . If we assume that Δh_p is of the order of the shift in the viscous flow velocity profile, then $\Delta u^+ \sim \Delta h_p^+$ and $R' \sim \Delta h_p^+/\sqrt{2}$. From the viscous flow calculations of Luchini et al. (1991), $\Delta h_p/h \approx 0.09$ for V-groove riblets with $h = s$, therefore $R' \approx 0.06 h^+$; the drag reduction would increase linearly (and indefinitely) with non-dimensional riblet height (and spacing). Figure 5.2.9 illustrates how this viscous sublayer origin shift model compares with our inherent riblet-induced flow enhancement, R_h' . Our model presumes $R_h' \approx 0$ for $h^+ < 5$ whereas Luchini's viscous sublayer model assumes a linear variation of R_h' with $h^+ (= s^+)$. Further experimental work is required for $h^+ < 5$ to resolve this difference.

Baron et al. (1993) extended the idea of Luchini et al. (1991) and showed that the experimentally observed maximum riblet-induced drag reduction in the prevailing literature is roughly proportional to $\Delta h_p/s$. Further, they modeled the drag over a riblet surface relative to that of a smooth one as the product of a riblet drag reducing effect, $F(s^+)$, and the effect of the wetted surface, $G(h_{p1}^+)$, where h_{p1} is the longitudinal protrusion height ($\approx 0.18 h^+$ for V-groove riblets with $h = s$). Their drag reduction function, which is analogous to our inherent flow enhancement parameter, is illustrated in Figure 5.2.9; it empirically embraced the viscous sublayer model of Luchini et al (1991) but extended the model to higher s^+ with $R' \rightarrow 0$ for $s^+ \gg 5$. However, their maximum drag reducing

effect of riblets is ≈ 0.5 units, because they assumed that riblet area only affected the flow if the protrusion height exceeded the viscous sublayer thickness, $h_{pl}^+ > y_v^+$ which implies $h^+ > 5.6y_v^+ \approx 28$. This differs from our model in which the area effect commences at $h^+ = y_v^+$. Further, their model accords with the observation that for $h^+ \gg y_v^+$, the drag enhancement should approach an asymptotic value, though they had no experimental data to assess the riblet wetted surface area at asymptotic conditions (Quadrio, 1995).

5.3 Riblet Pipes: Polymer Solution Flow

5.3.1 Riblet-Polymer Matrix

Since turbulent drag reduction by riblets and by polymer solutions each exhibit distinct flow regimes, their mutual interaction is considered in terms of a “Riblet-Polymer Matrix”, shown in Tables 5.3.1 - 5.3.4 for riblet pipes R1A, R1B, R2A, R2B, respectively. Each table is constructed with columns representing riblet regimes, (i) hydraulically smooth, (ii) riblet drag reduction, (iii) riblet drag enhancement, and rows representing polymer regimes, (i) Newtonian, (ii) polymeric, (iii) asymptotic maximum drag reduction. The matrix in Tables 5.3.1- 5.3.4 has been filled, using data from Tables in Chapter 4, to show the [8, 7, 8, 8] of 9 possible, elements traversed in the present experiments for [R1A, R1B, R2A, R2B], respectively. Only element (1,3) is absent in all riblet pipes which results from the observation that no polymer solution exhibited the onset of polymer-induced drag reduction in the riblet drag enhancement regime. The implications of this are examined in section 5.3.2.

5.3.2 Onset

For all experimental data, the onset of polymeric drag reduction in the riblet pipe occurred at the same onset wall shear stress as observed in the smooth pipe. Nondimensional riblet heights at onset, h^{+*} , are summarized in Table 5.3.5; some values are expressed as range of h^{+*} at a given τ_w^* because of differences in solution viscosities. It can be seen that solutions of the highest molecular weight polymers, PEO W-301 and PAM N-300, onset in the hydraulically smooth regime; in all other cases, onset occurred in the regime of riblet drag reduction.

Anderson et al. (1993), using 2, 4, and 8 wppm solutions of PEO W301, have previously reported equal onset wall shear stresses of $\tau_w^* \approx 3.5 \text{ N/m}^2$ for flows of W-301 in smooth and riblet pipes, their onset $h^{+*} \approx 10$ lying in the riblet drag reduction regime. Virk (1971a) proposed that onset is associated with incipient polymer-turbulence interaction in the vicinity of the plane of peak production, $y_{pp}^+ \approx 12$. It is therefore expected that for $y_{pp}^+ > h^{+*}$, the elastic sublayer characteristic of polymer-turbulence interaction will form beyond the riblet tips, in which case equality between smooth and riblet onsets is expected. For $y_{pp}^+ < h^{+*}$, however, the elastic sublayer is expected to form within the riblet valleys, so that the onset shear stress in the riblet pipe should be governed by the average wall shear stress on the riblet surface, which is $\approx \sqrt{5}$ times lower than that in the smooth pipe. Access to Riblet-Polymer matrix element (1,3) is therefore required to resolve the physics of the onset of polymeric drag reduction over a riblet surface. Criteria for access to the omitted matrix element can be derived from the observation that randomly-coiling polymers onset at wavenumbers (u_τ^*/ν) inversely proportional to their r.m.s radii of gyration, R_G :

$$(u_\tau^*/\nu) = \Omega_L/R_G \quad (5.3-1)$$

with onset constant $\Omega_L = [8.5, 6.7] \times 10^{-3}$ for the [PEO, PAM] skeletons. The nondimensional riblet height at onset:

$$h^{+*} = h\Omega_L/R_G \quad (5.3-2)$$

is thus essentially proportional to the ratio of riblet height to polymer radius of gyration. Since access to element (1,3) requires onset in the regime of riblet drag enhancement, at a characteristic $h^{+*} \approx 50$, say, this could be gained by increasing (h/R_G) beyond the range $410 < h/R_G < 3500$ traversed in the present experiments.

5.3.3 Polymeric Regime

5.3.3.1 Effectively Smooth

Virk (1971a) demonstrated that for drag reduction by polymer solutions in rough pipes, there exists a flow regime in which the fractional slip relative to solvent, S_F , is the same in smooth and rough pipes of the same id operating at a fixed friction velocity. This “effectively smooth” regime is distinct from the hydraulically smooth regime which exhibits equality of friction factors. For a given polymer, at all concentrations, the effectively smooth regime persisted up to a nondimensional roughness height, $k_{es}^+ \approx 50$ at which the fractional slip in the rough pipe diverged downward from that in the smooth pipe. An extension of this “effectively smooth” notion to riblet pipes is attempted in Figure 5.3.1, parts (a-d) of which respectively depict four plots of S_F versus $Re\sqrt{f}$ in both horizontal and vertical registry for [3, 10, 30, 100] wppm N-60K in pipes R1A, R1B, R2A, and R2B. Consider first the data for pipe R1A. For 3 wppm solutions, the fractional slip in the riblet pipe is essentially the same as that in the smooth pipe S1 for all $Re\sqrt{f}$, up to the highest $Re\sqrt{f} = 9500$. For 10 wppm solutions, the slips are the same up to $Re\sqrt{f} = 1700$, then the riblet data diverge slightly from the smooth pipe in the direction of lower fractional slip, but subsequently returns to the smooth pipe trajectory for $Re\sqrt{f} > 5000$. For 30 and 100 wppm solutions, the slip diverges at $Re\sqrt{f} = 1200$ and 1000, respectively, and remains below the

smooth pipe data up to the highest $Re\sqrt{f}$, the more so for 100 wppm solutions. Similar trends are observed in pipes R1B and R2A. For pipe R2B, depicted in Figure 5.3.1d, the riblet fractional slip actually exceeds that in the smooth pipe over the ranges $1500 < Re\sqrt{f} < 7500$, $Re\sqrt{f} > 1000$ and $Re\sqrt{f} > 1000$ for 3, 10 and 30 wppm solutions respectively. For 100 wppm solutions, the riblet fractional slip is approximately the same for $Re\sqrt{f} < 2200$, then diverges to lower fractional slips. The observation that the riblet pipe fractional slip may be either greater or smaller than that in the smooth pipe is further borne out by the data for N-750 and W-301 solutions, depicted in Figure 5.3.2 and 5.3.3, respectively. For example, for 100, 300 and 1000 wppm N-750 solutions in riblet pipe R1A, $S_{F,r} > S_{F,s}$ for $Re\sqrt{f} > 4000$; $S_{F,r} \approx S_{F,s}$ for $Re\sqrt{f} < Re\sqrt{f}_{max} = 6000$, and $S_{F,r} < S_{F,s}$ for $Re\sqrt{f} > 1800$, respectively. There is, therefore, some critical trajectory along which the riblet pipes are effectively smooth over all $Re\sqrt{f}$. Below this trajectory the fractional slips in the riblet pipes are slightly greater than that in the tandem smooth pipe over a certain range of $Re\sqrt{f}$, and above the critical trajectory, the fractional slips in the riblet pipes are lower, with both the range and magnitude of this region of lower slip increasing as MDR is approached. The effectively smooth regime in riblet pipes is therefore a function of slip and pipe geometry; there is apparently no single, concentration-independent k_{es}^+ (≈ 50 in rough pipes) that may be used to describe riblet pipes.

Figure 5.3.4 plots fractional slips versus $Re\sqrt{f}$ from the previous works of Anderson et al. (1993) and Christodoulou et al (1991). All of the data of Anderson et al. (1993) lie in the polymeric regime and exhibit effectively smooth behavior, $S_{F,r} \approx S_{F,s}$ at all $Re\sqrt{f} > Re\sqrt{f}^*$, as does the one 10 wppm PEO solution for which friction factors were reported by Christodoulou et al (1991); neither of these authors' data reach an effectively smooth limit. It should also be noted that all of these authors' data are at relatively low polymer-induced flow enhancements, $S_F < 0.3$, in riblet pipes of considerably smaller $d/2h$ than the present.

5.3.4 Maximum Drag Reduction

5.3.4.1 Riblet-Induced Flow Enhancement

Figure 5.3.5 depicts the variation of riblet-induced flow enhancement for the four riblet pipes at the maximum polymer-induced drag reduction, including the replicated pipes; individual polymer solutions and pipe replications are not differentiated for clarity. The solid line shown on the figure is the best fit curve through the solvent data in all pipes. Despite considerable scatter, some interesting trends are observed that reflect the earlier discussion of the pressure gradient ratio:

- (i) A hydraulically smooth regime, with $R' \approx 0$, is visible for $3 < h^+ < 9$.
- (ii) A riblet drag reduction regime occurs for $9 \pm 2 < h^+ < 14 \pm 2$, within which the riblets enhanced flow beyond the maximum flow enhancement induced by polymer additives, by an amount $R'_{m,max} = 1.2 \pm 0.8$ at $h^+ = 11 \pm 1$. The extent of the riblet drag reduction regime at MDR is considerably narrower than that observed in solvent, $5 < h^+ < 23 \pm 1$, and a maximum riblet-induced flow enhancement therein is roughly greater than the solvent $R'_{n,max} = 0.5 \pm 0.1$. The role of riblet pipe geometry, $d/2h$, is not readily apparent from the data, on account of their scatter; however, pipe R2A, with the smallest relative riblet height $d/2h = 47$, exhibited by far the greatest riblet flow enhancement at MDR.
- (iii) Riblet drag enhancement occurred for $14 \pm 2 < h^+ < 70$. In this region, the slopes of the R - $\log h^+$ relations in all pipes were considerably steeper than in solvent, reaching $R'_{m,min} = -7 \pm 1$ at $h^+ \approx 60$.

The scaling by nondimensional riblet height h^+ observed in all riblet pipes in solvent flow thus persists, to some degree, at maximum polymer drag reduction as well.

5.3.4.1 Serrated Sublayer Model at MDR

Maximum drag reduction has often been described in the literature as being akin to solvent flow because the maximum drag reduction asymptote has a semi logarithmic form identical to the Prandtl-Karman law, with mixing length constant, $\chi_m \approx 0.085$. Following the arguments in section 5.2.1.2, we consider flow enhancement at MDR to be the net result of a favorable riblet-turbulence interaction offset by the adverse increase in wetted surface area. The application of the serrated sublayer model at MDR requires knowledge of y_v^+ , d_{h0} , and $d_{h\infty}$ extracted from the P-Q plots. Unfortunately, we cannot determine $d_{h\infty}$ directly, because the experiments provided no asymptotic value of P at high flowrates. However, at the highest flowrates investigated, $Q \approx 1.1$ l/s, $P \approx 0.5$ for the 7.82 mm pipes, which is lower than the asymptotic value for solvent, $P_{\infty,n} \approx 0.60$. This implies that, at MDR, a larger fraction of the geometric area is exposed to the flow than for solvent flow. If we attribute the differences between the geometric, d_H , and the asymptotic equivalent, $d_{h\infty}$, hydraulic diameters to secondary flows within the riblets, then the foregoing suggests that at maximum drag reduction these secondary flows are weaker than in Newtonian flows. Independently, Nouri et al. (1993) have reported “considerable suppression of cross-flow fluctuations” for the flow of a 0.2% cellulosic polymer solution at conditions close to MDR in an eccentric annulus of unit eccentricity, while Einstein and Li (1958) have linked secondary flows to Reynolds stress gradients. Based on the foregoing, it seemed reasonable to set $d_h = d_H$, and $\xi_\infty \approx 1/\sqrt{5}$ at MDR.

By analogy to solvent flow, the original Prandtl-Karman coordinates presented previously may now be converted to a coordinate system based on the equivalent hydraulic diameter, via Eq. (5.2-8). We further assume that flows at maximum polymer-induced drag reduction in non-circular pipes follow smooth circular pipe relationships when based upon the equivalent hydraulic diameter:

$$\frac{1}{\sqrt{f_h}} = 19 \log Re_b \sqrt{f_h} - 32.4 \quad (5.3-3)$$

from which an inherent riblet flow enhancement at maximum drag reduction, $R_h'_{m} = ((1/\sqrt{f_{h,m}})_r - (1/\sqrt{f_{h,m}})_s)Re_h/\sqrt{f_h}$. Figure 5.3.6 depicts the variation of $R_h'_{m}$ versus h^+ , obtained by using model parameters $y_v^+ = 10$, and $\xi_\infty = 1/\sqrt{5}$ based on the foregoing discussion. Qualitatively, the inherent riblet induced flow enhancement increases with increasing h^+ from $R'_h \approx 0$ for $h^+ < \approx 10$, to $R'_h \approx 7$ at $h^+ \approx 60$. Further interpretation is cautioned without experimental evidence of an asymptotic limit at MDR, which is beyond the limitation of our present experimental setup, since the model is very sensitive to y_v^+ and ξ_∞ .

5.3.4.3 Comparison to Rough Pipes

The preceding observations on maximum drag reducing flows in riblet pipes may now be compared to similar flows in rough pipes (Virk, 1971a) via the roughness function, $\beta = \sqrt{\frac{2}{f}} + \frac{3}{2\chi} - \frac{1}{\chi} \ln\left(\frac{d}{2k}\right)$. The mixing length constants will have different values according to the flow regime, with $\chi_n \approx 0.40$ for Newtonian flows and $\chi_n \approx 0.085$ for maximum drag reduction. Figure 5.3.7 depicts the variation of the inherent riblet-induced flow enhancement, R_h' , with h^+ , in registry with a semi-logarithmic plot of β versus k^+ ; both abscissae have the same scale, but the ordinates differ by a factor ≈ 2 ; Newtonian results are depicted by solid lines. At maximum drag reduction, the rough pipe data of Virk (1971a) exhibited (i) a hydraulically smooth regime, for $4 < k^+ < 12$, wherein $\beta = 11.7 \ln(k^+) - 17$, (ii) a transitional regime for $12 < k^+ < k^+_{max} = 150$ with a maximum $(k^+, \beta) \approx (30, 17)$; no fully rough regime was observed. The range of k^+ that define the transitional region in maximum drag reducing flows in rough pipes approximately coincides with the range of h^+ that define the inherent riblet drag reduction regime. Further, in the transitional

regime, $\beta_{\max,m} > \beta_{\max,n}$, implying that rough pipes have a bigger effect at MDR than in Newtonian flows; this is also observed for inherent flow enhancement in the riblet pipes, wherein $R_h'm > R_h'n$.

5.3.5 Effect of Degradation

The riblet-induced flow enhancement, R' , was defined by Eq. (4.2-8) as the difference between $1/\sqrt{f_r}$ measured in the riblet pipe and $1/\sqrt{f_s}$ measured in the upstream smooth pipe. We may equally define R' relative to the downstream smooth section; differences between R' values referenced to the two smooth pipe locations reflect polymer degradation. Figure 5.3.8 depicts the variation of R' with h^+ for 3, 10, 30 and 100 wppm W-301 in pipe R2B, with open symbols representing measurements relative to the upstream smooth pipe, $R'_{rs(1)}$ (= our original R' used in Chapter 4), and smaller closed symbols relative to the downstream smooth pipe, $R'_{rs(2)}$ ($= R'_{rs(1)} - \Delta'_{12}$). For 3 and 10 wppm solutions, the original observations are not significantly altered, with degradation primarily affecting the riblet drag enhancement regime, increasing our original $R'_{rs(1)}$ by at most ≈ 1 unit at the highest h^+ . For 30 and 100 wppm solutions, which exhibit maximum polymer drag reduction, only the data point at the highest h^+ for 30 wppm solutions is altered. (Note that though the difference between the two smooth locations is negligible for the 30 and 100 wppm solutions, this does not imply that degradation is not occurring, since a degraded solution may still exhibit MDR.)

The effect of degradation is more pronounced in the smaller pipe, illustrated by 1, 10, and 100 wppm W-301 in R1AR by Figure 5.3.9. For the 1 wppm solution, $R'_{rs(1)}$ follow the solvent data, whereas $R'_{rs(2)}$ measured relative to the downstream section now exhibits a slightly broadened riblet drag reduction regime, $5 < h^+ < 30$. For the 10 wppm solution, R' measured with respect to the downstream section exhibits a sharper minimum

in the riblet drag enhancement regime, then increases with increasing h^+ exhibiting $R_p' > R_n'$ for $h^+ > 60$. The riblet flow enhancement is therefore sensitively dependent on the reference smooth pipe. The data for the 100 wppm solution, which follow MDR, are not significantly altered. It is important to note that the broadened riblet drag reduction regime for 1 wppm W-301 in R1A is similar to that observed for 3 wppm W-301 in R2B. This implies that the two pipes, which have similar d/h , may now be consolidated once degradation has been accounted for. It is also necessary to correct for degradation at the riblet pipe location, that is, R' must be determined based on $1/\sqrt{f_s}$ that would have been observed in a smooth pipe at the riblet location, the exact value must therefore be bounded by the upstream and downstream R' values, $R_{rs(1)}$ and $R_{rs(j>1)}$.

We now show how the foregoing degradation correlations might be applied to correct R' . Assume that the pipe, either 7.82 or 10.21 mm, and polymer, either N-60K or W-301, are both given, along with sets of smooth and riblet pipe data for a range of polymer concentrations.

1. For a given polymer, the value of the wall shear stress at incipient degradation, τ_w^\wedge is obtained from Table 5.1.1.
2. For a particular $\tau_w > \tau_w^\wedge$, calculate the corresponding $u_\tau = \sqrt{(\tau_w/\rho)}$ and the ratio (τ_w / τ_w^\wedge) .
3. Now for a particular c , at the chosen τ_w , find $1/\sqrt{f_s}$ from the data, and hence $S'_s = (1/\sqrt{f_s} - 1/\sqrt{f_n})Re\sqrt{f}$ and $U_s = \sqrt{2}u_\tau \cdot (1/\sqrt{f_s})$, which lead to first estimates of $U_{s,1} = U_s$, so $t_{res} = L_{rs} / U_s$, where L_{rs} is the distance between the upstream smooth and riblet pressure drop measurement stations.
4. Find Γ for the given pipe and polymer from Table 5.1.1, and use Eq. 5.1.6b to estimate $(-\Delta'_{jk} / S'_k) / t_{res} = \Gamma \log(\tau_w / \tau_w^\wedge)$, and thence a first estimate of the expected degradation, $\Delta'_{rs,1}$.

5. This provides a first degradation-corrected estimate of the smooth pipe friction factor at the riblet pipe location: $1/\sqrt{f_s} = 1/\sqrt{f_s} + \Delta'_{rs}$.
6. Notice that t_{res} should strictly be based on the average mean velocity between the smooth and riblet stations at the chosen constant $Re\sqrt{f}$. We can therefore iterate steps 3-5 as follows:
 - 3 (iteration 2). The second estimate $U_{s,2} = \sqrt{2}u_{\tau}(1/\sqrt{f_s} + \Delta'_{rs}/2)$, so $t_{res,2} = L_{rs}/U_{s,2}$.
 - 4 (iteration 2). The second estimate of $\Delta'_{rs,2}$.
 - 5 (iteration 2). The second degradation-corrected estimate of the smooth pipe friction factor at the riblet pipe location is: $1/\sqrt{f_{s,corr,2}} = 1/\sqrt{f_s} + \Delta'_{rs,2}$.
7. Continue to convergence, that is, till $1/\sqrt{f_{s,corr,n}} = 1/\sqrt{f_{s,corr,n-1}}$, to within experimental uncertainty, say 0.05 units of $1/\sqrt{f}$.
8. Use the final $1/\sqrt{f_{s,corr,n}}$ to obtain the corrected $R'_{corr} = (1/\sqrt{f_r} - 1/\sqrt{f_{s,corr,n}})Re\sqrt{f}$.
9. Continue for other $\tau_w > \tau_w^{\wedge}$ for the same c , and for all c at all $\tau_w > \tau_w^{\wedge}$, to generate a complete set of riblet-induced drag reductions corrected for polymer degradation.

These corrections are, strictly speaking, only valid for N-60K and W-301 solution data in the polymeric regime. For the lower molecular weight polymers, namely N-750 and N-10, degradation was not perceived in the sense that their smooth friction factor plots exhibited no downward curvature; therefore results for these polymers required no corrections. At maximum drag reduction, values of τ_w^{\wedge} are determined directly from the data at which they depart from the MDR asymptote, and corrected using values of Γ for W-301 solutions; only one or two data points at the highest $Re\sqrt{f}$ are affected. In Chapter 4, we concluded that solutions of PAM N300L and N-300 exhibited essentially the same

gross flow physics as PEO N-60K and W-301 solutions, respectively, and are thus modeled here using the values of τ_w^* and Γ of the PEO analog in Table 5.1.1.

To illustrate the effect of degradation using the foregoing correlations, again consider the flows of [3, 10] wppm W-301 in R2B and [1, 10] wppm W-301 in R1AR depicted in Figures 5.3.10 and 5.3.11, respectively. The solid lines are the lower and upper bounds of $R'_{rs(1)}$ and $R'_{rs(2)}$, respectively measured relative to the upstream (Station 1) and downstream (Station 2) smooth sections, respectively. The data predicted by the model lie between these bounds, the exact trajectory depending on the position of the riblet test section and on the universality of the model for all $[c, M_w, d_s]$.

The effect of degradation on our original results is illustrated in Figures 5.3.12-5.3.15 for flows of [3, 10, 30, 100] wppm N60K in riblet pipes R1AR and R2B, [1, 3, 10, 30, 100] wppm W-301 in pipe R1AR, and [3, 10, 30, 100] wppm W301 in R2B, respectively, using the three part flow enhancement graphs presented in Chapter 4. The solid and dashed lines refer to the original and degradation corrected data, respectively, and only S_s' is plotted in part (b) for clarity. For solutions of N-60K, perusal of Figures 5.3.12 and 5.3.13 reveal only small corrections to the original data using the degradation model, those for the 7.82 mm pipe were corrected more than the corresponding solution in the 10.21 mm pipe, with the greatest correction $-\Delta' \approx 1$ at the highest $h^+ \approx 60$. The data for 3 and 10 wppm in R2B were corrected for degradation in both the riblet drag reduction and enhancement regimes, those corrections in the riblet drag reduction regime were $0 < -\Delta' < 0.3$ for $30 < h^+ < 45$, $1.8 > R' > 0$. The data for [30, 100] wppm N-60K in R2B and [3, 10, 30, 100] wppm N-60K in R1AR were corrected for degradation only in the riblet drag enhancement regime.

For W-301 solutions, the corrections made were greater than those for N-60K solutions at comparable (h^+, S_s') , and the corrections were greater in pipe R1AR than in R2B. Only the data for the 3 wppm solution in R2B was corrected for degradation in both

the riblet drag reduction and enhancement regimes, those for the drag reduction regime were small, $0 < -\Delta' < 0.3$ for $20 < h^+ < 33$, $1.6 > R' > 0$. The data for [1, 3, 10, 30, 100] wppm W-301 in R1AR and [10, 30, 100] wppm W-301 in R2B were corrected for degradation only in the riblet drag enhancement regime, with a maximum $-\Delta' \approx 1.6$ for 10 wppm W-301 in R1AR at $h^+ \approx 75$.

Though the degradation corrections are significant for some polymer solutions, the essential features and general comparisons made in Chapter 4 are not significantly altered. Now that a first order correction of polymer degradation has been made, we may focus on correlating the riblet-induced flow enhancement with the polymer-induced flow enhancement and flow scales.

5.4. Relation Between Riblet- and Polymer-induced Flow Enhancements

5.4.1 Additive Equivalence

Figure 5.4.1 depicts, in P-K coordinates, the trajectories of 3 wppm W-301 and 300 wppm N-750 in pipes S1 and R1A, the data for the smooth pipe are corrected for degradation to facilitate comparison between smooth and riblet pipe trajectories at the riblet pipe location. It is seen that the smooth pipe trajectories intersect at $(Re\sqrt{f}, 1/\sqrt{f}) = (3900, 20.6)$. This is termed an “isoslip” point because it corresponds to a point of equal flow enhancement for different polymer solutions. The iso-slip point in the riblet pipe occurs at approximately the same $Re\sqrt{f}$ as that in the smooth pipe, $(Re\sqrt{f}, 1/\sqrt{f}) = (3800, 18.6)$. The term “additive equivalence” is used to describe such a case where two different additive solutions produce the same flow enhancement at the same $Re\sqrt{f}$ in both the smooth and riblet pipes. This suggests that at a fixed $(Re\sqrt{f}, 1/\sqrt{f}_s)$, $1/\sqrt{f}_r$ is independent of the additive that produced the flow enhancement; so that $R' = f(h^+, S_s')$. This is important because it

allows immediate comparison for all polymers in a given riblet pipe. Figure 5.4.2 illustrates a second example of additive equivalence in pipes S2 and R2B for 3 wppm W-301 and 10 wppm N-60K. Here the iso-slip points occur at $Re\sqrt{f} = 4100$, at which $[1/\sqrt{f_s}, 1/\sqrt{f_r}] = [20.6, 20.6]$, or $R' = 0$.

5.4.2 3-D Representation

The mutual relationships between riblet- and polymer-induced drag reductions, R' and S' , and turbulent flow parameters, either $Re\sqrt{f}$ or h^+ , are qualitatively illustrated in 3-D contour plots. Figures 5.4.3 - 5.4.6 depict contours of R' for riblet pipes R1A, R1B, R2A and R2B, respectively, each on a semi-log basal grid of S'_s ordinate versus dual abscissae of $Re\sqrt{f}$ (lower) and h^+ (upper); positive and negative R' are distinguished by solid and dashed contour-lines, and the basal grid is bounded between solvent, N, with $S'_s = 0$, and the smooth maximum drag reduction asymptote, M, with $S'_s = 1.5 \log Re\sqrt{f} - 32$. The contours were extracted from the results for all polymer solutions in each riblet pipe, the results for the replicated pipes being merged into the results for the corresponding original pipes. The contours were generated manually in order to capture all the physics observed previously, using both computer contour plotting software and parsed data sets as aids; details of the construction of the contour plots are presented for a representative example in Appendix B. Perusal of the four figures reveal qualitative similarities between the riblet pipes; the terrain can be divided into four regions, respectively termed:

- (1) The Flats; $h^+ < 8 \pm 2$, $0 < S'_s < S'_{MDR}$, $R' \approx 0$. A flat region bounded between N and MDR, with only the low h^+ segment of the null contour $R' = 0$ seen in it. This corresponds to the region wherein the riblets are contained wholly within the viscous sublayer.

- (2) The Dome; $10 < h^+ < 30$, $0 < S_s' < 10$, $0 < R' < 1.5$. A region mostly contained within the null contour, which fairs into elliptical contours, that ascend to a broad maximum at $(h^+, S_s', R') = (11, 5, 1)$, $(10, 4, 0.7)$, $(11, 13, 1.5)$, $(14, 5, 1.5)$ for pipes [R1A, R1B, R2A, R2B], respectively. For R2A, the “dome” has a more ridge-like appearance because the maximum riblet-induced flow enhancement occurs in the vicinity of maximum polymer-induced drag reduction. The null contours of R1A, R1B, and R2A are open at MDR over the range $9 \pm 1 < h^+ < 13 \pm 1$. It is not certain whether the null contour of R2BR is open at MDR because of the differences between the original and replicated pipes; the broken line emanating from the 0.5 contour level is drawn in an attempt to illustrate the differences between the two pipes.
- (3) The Solvent Extrudate; $30 < h^+ < 100$, $0 < S_s' < 10$, $-2 < R' < 0$. In this region the contours essentially maintain the spacings with which they emanate from the solvent line, N, with R' only weakly dependent on S_s' , but decreasing with increasing h^+ , to a lower shelf of $R' \approx R_n' \approx -2$ for $h^+ > 50$.
- (4) The MDR Ravine; $40 < h^+ < 100$, $10 < S_s' < S_{\text{mdr}}'$, $-8 < R' < -2.5$. This region lies between solvent extrudate region and the MDR line. Contours, all negative, show R' varying slowly with h^+ but decreasing with increasing S_s' ; thus the terrain descends steeply towards the MDR line, to greater depths at the higher h^+ .

Details of the topology of the riblet-induced flow enhancement in all the riblet pipes are summarized in Table 5.4.1.

A comparison with previous work, in terms of the 3-D domains discerned above, is illustrated in Figure 5.4.7 relative to the contours of R2A. The early data of Rohr et al (1990) all lie in the flats, while their more recent results (Anderson et al., 1993) lie partly in the dome and mostly in the solvent extrudate regions, $5 < h^+ < 80$ at low $S_p' < 5$. These placements are consistent with the authors' earlier observations of $R' \approx 0$, identically, as

well as their recent reports of $R_p' \approx R_n'$, that is, riblet-induced drag reduction in the polymer solutions essentially the same as that in solvent. We cannot easily accommodate the data of Christodoulou et al. (1991), which, based on their reported friction factors for 10 wppm PEO WSR301, should be similar to those of Anderson et al. (1993), albeit over a narrower range, $4 < h^+ < 22$. However, this does not accord with their stated observations of $R_p' < R_n'$, the more so at higher polymer concentrations. The difficulty in reconciling all observations might partly arise from the different pipe diameter to riblet height ratios used, being $d/2h = 26-47$ (present), 57 (Rohr et al., 1990), 83 (Anderson et al., 1993) and 114 (Christodoulou et al., 1991).

5.4.3 Scaling

Though there are qualitative similarities between the contour plots, there are significant differences that possibly reflect the dependence on the riblet pipe geometry, $d/2h$. First, we examine how two riblet pipes with approximately the same $d/2h$, namely, R1A and R2B ($d/2h \approx 35$) differ by comparing Figures 5.4.3 and 5.4.6. The peak of the dome occurred at $(h^+, S_s', R') = (11, 5, 1)$, and $(14, 5, 1.5)$ for R1A and R2B, respectively. The null contour that defines the transition from riblet drag reduction to drag enhancement regimes exhibited a more pronounced curvature in R2B than in R1A, which consequently affected both the MDR ravine and the solvent extrudate; this reflected the observation that the upper bound of the riblet drag reduction regime in R2B significantly exceeded that of solvent at low slips, $S_s' < 5$. It is not known if subtle differences in pipe fabrication are responsible for these differences. Next, we compare the contours for the two riblet pipes with the smallest and largest $d/2h$, namely R1B ($d/2h = 26$) and R2A ($d/2h = 47$) in Figures 5.4.4 and 5.4.5. Though the maximum R' occurred at approximately the same $h^+ \approx 11$, the corresponding slip $S_s' \approx 13$ in R2A is significantly larger than $S_s' \approx 5$ in

R2B. Both the solvent extrudate and MDR ravine apparently extended over similar ranges of $[h^+, S_s', R']$ for both pipes R1B and R2A.

It is apparent from the comparisons in Figures 5.4.3-5.4.6 and Table 5.4.1 that an approximate h^+ scaling exists for all riblet pipes, which accords with previous conclusions for solvent and at maximum drag reduction. Whether these observations scale as S_s' is difficult to ascertain because at MDR, say, $S_s' = 15 \log(\text{Re}\sqrt{f}) - 32 = 15 \log(h^+) - 32 - 15 \log(d/\sqrt{2}h)$, is a function of $d/2h$. This means that at a given (h^+, S_s') , the flow is perturbed closer to MDR for smaller $d/2h$. Figure 5.4.8 attempts to account for this by using the ordinate $S_s'/S_s'_{\text{MDR}}$ instead of S_s' , which scales both solvent and MDR, transforming all the data to $0 < S_s'/S_s'_{\text{MDR}} < 1$, regardless of the riblet pipe. The similarities and differences alluded to previously are still apparent.

Finally, if we assume that the riblet-induced flow enhancement, R' , is a function of the nondimensional riblet height, h^+ , and the normalized polymer-induced flow enhancement in the smooth pipe, $S_s'/S_s'_{\text{MDR}}$, only, and average over the differences between the contours observed for all riblet pipes, then we may produce a single contour plot of all the data from our present experiments shown in Figure 5.4.9, which represents a striking summary of all our experimental results.

5.4.3 Other 3D representations: Prandtl-Karman and f - Re

Figure 5.4.10a-d depicts contours of R' on Prandtl-Karman coordinates for all riblet pipes investigated. These plots were generated by transforming (h^+, S_s') to $(\text{Re}\sqrt{f}=\sqrt{2}h^+.d/h, 1/\sqrt{f}=4 \log(\text{Re}\sqrt{f})-0.4+S_s')$ coordinates for each contour value, the regions of which, namely the flats, dome, solvent extrudate and MDR ravine illustrated in Figure 5.4.10a.

We may also present our results in f - Re coordinates which are commonly used in the literature. However, the additive equivalence hypothesis discussed in section 5.4.1 allowed us to treat all the results independent of the polymeric additive at a given $Re\sqrt{f}$, not at a constant Re , since the riblet-induced drag reduction at a given (Re, f) is a function of the additive that produced it. Nonetheless, contours of the percentage riblet-induced drag reduction, $\%DR = 100(1-f_r/f_s)_{Re}$, are plotted in Figure 5.4.11 on f - Re coordinates using data for solvent, and a single polymer, namely [1, 3, 10, 30, 100] wppm W-301 in pipe R1AR, which spanned the Newtonian, polymeric, and maximum drag reduction regimes.

5.5 Mechanism

The most significant observations in regard to mechanism stem from the dome region, $8 < h^+ < 31$, $0 < S_s' < 10$, $0 < R' < 1.5$. Within the dome, riblet-induced flow enhancement is of order $R' \approx 1$, even under conditions where the polymer-induced flow enhancement is many times greater, of order $S_s' \approx 5$. The elements of turbulence that riblets affect to induce drag reduction in Newtonian flows must therefore still exist in the flows associated with polymeric drag reduction up to moderate $S_s' < 10$. This implies that riblets and polymers reduce drag by separate mechanisms, since if both shared a common mechanism, then the riblets could scarcely be expected to have an additional effect on a flow that was already suffering the much larger polymer-induced perturbation.

We can tentatively envisage how riblet and polymer drag reduction mechanisms might differ in terms of an elementary three-stage turbulent burst cycle (Kline, 1967), comprising (1) lift-up, (2) growth, and (3) breakdown. As noted in Chapter 1, riblets reduce all turbulent intensities but do not much alter u - v correlation, which implies that they mainly affect stage (2), associated with bursting strength, whereas polymeric additives increase the axial intensity and reduce u - v correlation, which implies that they primarily

affect stage (3), associated with axial to transverse energy transfer. If the burst cycle is reasonably robust, and continues to resemble the basic Newtonian case up to moderate drag reductions, then simultaneous perturbations of stage (2) by the riblets and of stage (3) by the polymer additives could lead to a dome region, wherein both $R' > 0$ and $S_s' > 0$.

The riblet drag reduction regime in solvent, $5 < h^+ < 22$, with $(R_n', h_n^+)_{\max} = (0.6, 14)$, shows that the riblets become effective only when their tips protrude past the viscous sublayer, $y_v^+ \approx 5$; their greatest effectiveness occurs when the tips are at the plane of peak production, $y_{pp}^+ \approx 12$, and they lose effectiveness when the tips lie beyond $\approx 2y_{pp}^+$. During polymer drag reduction, the elastic sublayer originates at the plane of peak production, and then increases in radial extent (that is, thickness, as reflected by the slip S'), with corresponding increases in y_v^+ and y_{pp}^+ . Under these conditions, a higher h^+ should be required for the riblet tips to protrude past the viscous sublayer, prolonging the hydraulically smooth regime. This is observed in the present experiments, the somewhat diffuse boundary between the hydraulically smooth and riblet drag reduction regimes shifting from $h^+ \approx 5$ in solvent to $h^+ \approx 10$ in the most drag-reducing polymer solutions. Also, since y_{pp}^+ is increased relative to Newtonian, we should expect the greatest riblet-induced drag reduction to occur at higher h^+ , the more so as S' increases. This suggests that contours should emanate from solvent in the direction of increasing S_s' and h^+ . Though this is tentatively observed at low slips, $S_s' < 4$, in the vicinity of the dome, the effect is reversed at high slips. As suggested by the serrated sublayer model, these results possibly reflect the pronounced adverse effects of the riblet wetted surface at the higher polymeric drag reductions, and point to the need for better understanding this drag enhancing aspect of riblet behavior.

Table 5.1.1. Degradation parameters in the polymeric regime.

Pipe id, mm	Polymer	M_w	c, wppm	τ_w^\wedge , N/m ²	Γ , s ⁻¹
7.82	N-60K	1.9×10^6	3, 10	21 ± 3	5.0 ± 1.0
7.82	W-301	5.3×10^6	1, 3, 10	16 ± 3	4.2 ± 0.5
10.21	N-60K	1.9×10^6	3, 10, 30	41 ± 4	2.4 ± 0.2
10.21	W-301	5.3×10^6	3, 10	13 ± 2	2.7 ± 0.6

$$\text{Model: } \left(\frac{-\Delta'_{jk}}{S_k} \right) / t_{res} = \Gamma \log \left[\frac{\tau_w}{\tau_w^\wedge} \right]$$

τ_w^\wedge = characteristic degradation-inducing wall shear stress

Γ = characteristic degradation rate constant, s⁻¹.

Table 5.2.1. Smooth and riblet pipe data

PIPE DESIGNATION	S 1	S 2	R1A	R1B	R2A	R2B
h, mm	-	-	0.105	0.145	0.105	0.145
s, mm	-	-	0.108	0.165	0.108	0.165
d _s , mm	7.82	10.21	7.82	7.82	10.21	10.21
d _v , mm	-	-	7.66	7.66	10.05	10.05
d _c , mm	-	-	7.55	7.51	9.94	9.90
d _r , mm	-	-	7.54	7.44	9.93	9.80
d _t , mm	-	-	7.45	7.37	9.84	9.76
P_{T0}	-	-	0.843	(0.790)	0.875	0.824
$P_{\Gamma\infty}$	-	-	0.627	0.577	-	0.643
d _{h0} , mm	-	-	7.52	(7.25)	9.89	9.53
d _{h∞} , mm	-	-	5.94	5.64	-	7.82
d _H , mm	-	-	3.50	3.79	4.60	4.97
d _H /d _{h∞}			0.59	0.66	-	0.64
$\xi_{\infty} = d_{h\infty}/d_{h0}$			0.79	(0.78)	-	0.82

Notes: $d_v = d_s - 2t$;

$$d_c = d_s - 2t - h;$$

$$d_t = d_s - 2t - 2h;$$

$$d_H = 4A_c / P_w = d_v / \sqrt{1 + \frac{4h^2}{s^2}}$$

Values in parentheses are estimated from sparse data

Table 5.3.1. The Riblet-Polymer Matrix for all polymers in the 7.82 mm pipe, 0.11 mm riblets.

Riblet Regime →	(i) Hydraulically Smooth	(ii) Riblet Drag Reduction	(iii) Riblet Drag Enhancement
Polymer Regime ↓			
(i) Newtonian			
N-750	100, 300, 1000	100, 300, 1000	-
N-60K	3, 10	30, 100	-
W-301	1, 3	-	-
P-309	-	-	-
N-300	-	-	-
(ii) Polymeric			
N-750	-	100, 300, 1000	100, 300, 1000
N-60K	3	3, 10, 30, 100	3, 10, 30, 100
W-301	1, 3, 10, 30	1, 3, 10	1, 3, 10
P-309	-	-	-
N-300	-	-	-
(iii) MDR			
N-750	-	-	-
N-60K	-	-	100
W-301	30, 100	30?, 100?	30, 100
P-309	50, 100	50?, 100?	50, 100
N-300	100	100?	100

Note: (i) Entries within a particular matrix element are the concentrations, wppm, of polymer solutions that traversed it in the present experiments.
(ii) Numbers with ? indicate uncertainty due to experimental scatter.

Table 5.3.2. The Riblet-Polymer Matrix for all polymers in the 7.82 mm pipe, 0.15 mm riblets.

Riblet Regime →	(i) Hydraulically Smooth	(ii) Riblet Drag Reduction	(iii) Riblet Drag Enhancement
Polymer Regime ↓			
(i) Newtonian			
N-750	100, 300	100, 300	-
N-60K	3, 10, 30	3, 10, 30, 100	-
W-301	-	-	-
P-309	-	-	-
N-300	-	-	-
(ii) Polymeric			
N-750	-	100, 300	100, 300
N-60K	-	3, 10, 30, 100	3, 10, 30, 100
W-301	-	-	-
P-309	-	-	-
N-300	-	-	-
(iii) MDR			
N-750	-	-	-
N-60K	-	-	100
W-301	100	100	100
P-309	50, 100	50, 100	50, 100
N-300	100	100	100

Note: Entries within a particular matrix element are the concentrations, wppm, of polymer solutions that traversed it in the present experiments.

Table 5.3.3. The Riblet-Polymer Matrix for all polymers in the 10.21 mm pipe, 0.11 mm riblets.

Riblet Regime →	(i) Hydraulically Smooth	(ii) Riblet Drag Reduction	(iii) Riblet Drag Enhancement
Polymer Regime ↓			
(i) Newtonian			
N-750	100, 250, 1000	100, 250, 1000	-
N-60K	3, 10, 30, 100	-	-
W-301	3, 10	-	-
P-309	-	-	-
(ii) Polymeric			
N-750	-	100, 250, 1000	100, 250, 1000
N-60K	-	3, 10, 30, 100	3, 10, 30, 100
W-301	10, 30, 100	3, 10, 30	3, 10
P-309	-	-	-
(iii) MDR			
N-750	-	-	-
N-60K	-	-	-
W-301	-	100	30, 100
P-309	50, 100	50, 100	50, 100

Note: Entries within a particular matrix element are the concentrations, wppm, of polymer solutions that traversed it in the present experiments.

Table 5.3.4. The Riblet-Polymer Matrix for all polymers in the 10.21 mm pipe, 0.15 mm riblets.

Riblet Regime →	(i) Hydraulically Smooth	(ii) Riblet Drag Reduction	(iii) Riblet Drag Enhancement
Polymer Regime ↓			
(i) Newtonian			
N-10	2435, 5138	2435, 5138	-
N-750	100, 250, 900, 2073	100, 250, 900	-
N-60K	3, 10, 30, 100	3, 10, 30, 100	-
W-301	3, 10	-	-
P-309	-	-	-
N-300LMW	10, 30, 100	10, 30, 100	-
N-300	3	-	-
(ii) Polymeric			
N-10	-	5138	2435, 5138
N-750	2073	100, 250, 900, 2073	100, 250, 900, 2073
N-60K	-	3, 10, 30, 100	3, 10, 30, 100
W-301	3, 10, 30, 100	3, 10	3, 10
P-309	-	-	-
N-300LMW	-	10, 30, 100, 300	10, 30, 100, 300
N 300	3, 10, 30, 100	3, 10	3, 10, 30
(iii) MDR			
N-10	-	-	-
N-750	-	-	-
N-60K	-	-	-
W-301	-	-	30, 100
P-309	50, 100	-	50, 100
N-300LMW	-	-	300
N-300	-	-	30, 100

Note: Entries within a particular matrix element are the concentrations, wppm, of polymer solutions that traversed it in the present experiments.

Table 5.3.5. Onset wall shear stress and non-dimensional riblet height in riblet pipes.

Polymer→ Pipe↓	N-10	N-750	N-60K	W-301	N-300L	N-300
R1A $d_s = 7.82 \text{ mm}$ $h = 0.11 \text{ mm}$ $d_r/2h = 36$ c range, wppm τ_w^* , N/m ² h^{+*} range	-	100-1000	3-100	1-10	-	-
	-	12.4	3.6	1.8	-	-
	-	14-11	8-7	6	-	-
R1B $d_s = 7.82 \text{ mm}$ $h = 0.15 \text{ mm}$ $d_r/2h = 26$ c range, wppm τ_w^* , N/m ² h^{+*} range	-	300-1000	3-100	-	-	-
	-	12.4	3.6	-	-	-
	-	19-15	11-10	-	-	-
R2A $d_s = 10.21 \text{ mm}$ $h = 0.11 \text{ mm}$ $d_r/2h = 47$ c range, wppm τ_w^* , N/m ² h^{+*} range	-	100-1000	3-100	3-10	-	-
	-	13.7	3.6	1.3	-	-
	-	15-12	8-7	5	-	-
R2B $d_s = 10.21 \text{ mm}$ $h = 0.15 \text{ mm}$ $d_r/2h = 34$ c range, wppm τ_w^* , N/m ² h^{+*} range	2435-5138	100-2073	3-100	3-10	3-100	3-10
	38	13.7	3.6	1.3	2.3	0.87
	24-19	19-10	11-10	6	9-8	5

Note: Values of τ_w^* in the riblet pipes are ensemble averages inferred assuming riblet pipes behave as an equivalently smooth one.

Table 5.4.1. Summary of the regions that define the relation between the riblet-induced flow enhancement, R' , the polymer-induced flow enhancement, S'_s , and the non-dimensional riblet height, h^+ .

Region	Pipe d_s h $d_r/2h$	R1A 7.82 0.11 34	R1B 7.82 0.15 26	R2A 10.21 0.11 47	R2B 10.21 0.15 36
Flats	h^+ range S' range	< 5 - 8 0 - 11	< 5 - 9 0 - 10	< 5 - 7 0 - 11	< 5 - 9±1 0 - 11
Dome	R' max h^+ @ max S' @ max	1.5 10 5	1.0 11 4.5	1.5 11 13	1.5 14 5
Extrudate	h^+ range S' range R' range	30 - 80 0 - 7 (-0.5) - (-2)	37 - 112 0 - 7 (-0.5) - (-3)	26 - 67 0 - 9 (-0.5) - (-2)	50 - 90 0 - 9 (-0.5) - (-2)
MDR Ravine	h^+ range S' range R' range	24 - 80 11 - 21 (-2.5) - (-8)	29 - 100 8 - 21 (-4) - (-8)	20 - 40 11 - 21 (-2.5) - (-5)	20 - 57 12 - 21 (-0.5) - (-8)

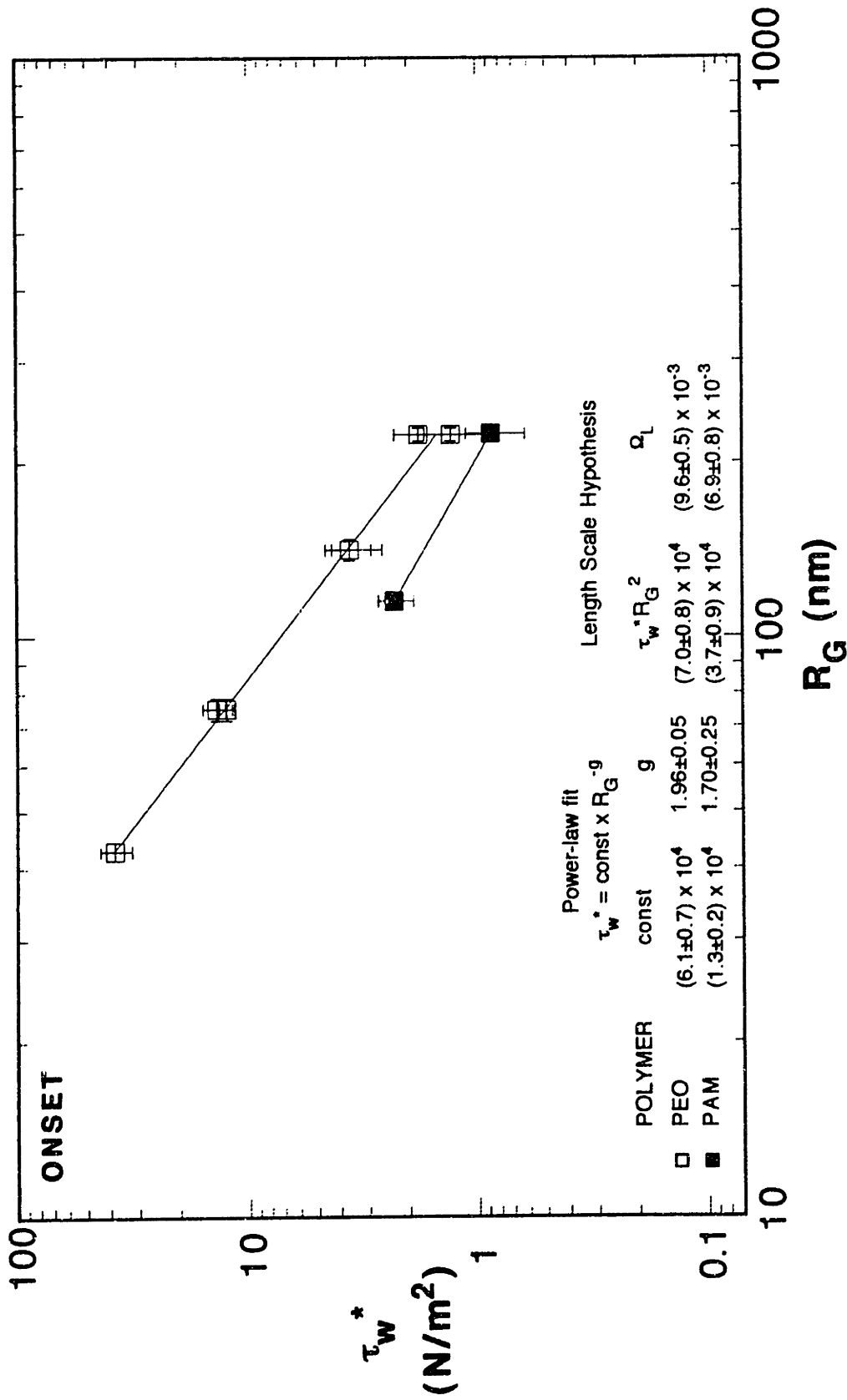


Figure 5.1.1 Onset correlations for PEO and PAM solutions in the smooth 7.82 mm and 16.21 mm pipes

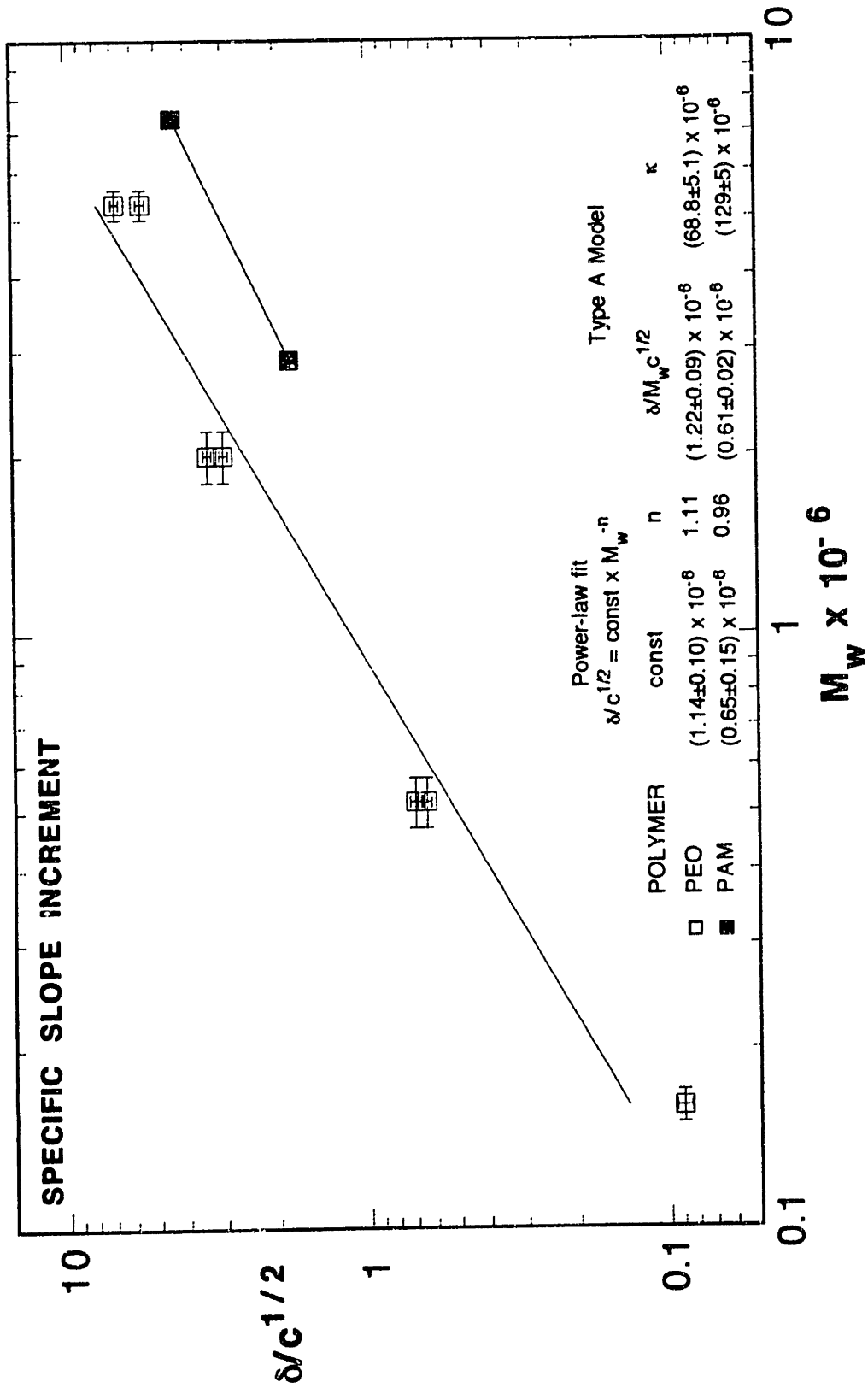


Figure 5.1.2 Specific slope increment correlations for PEO and PAM solutions in the smooth 7 and 10.21 mm pipes.

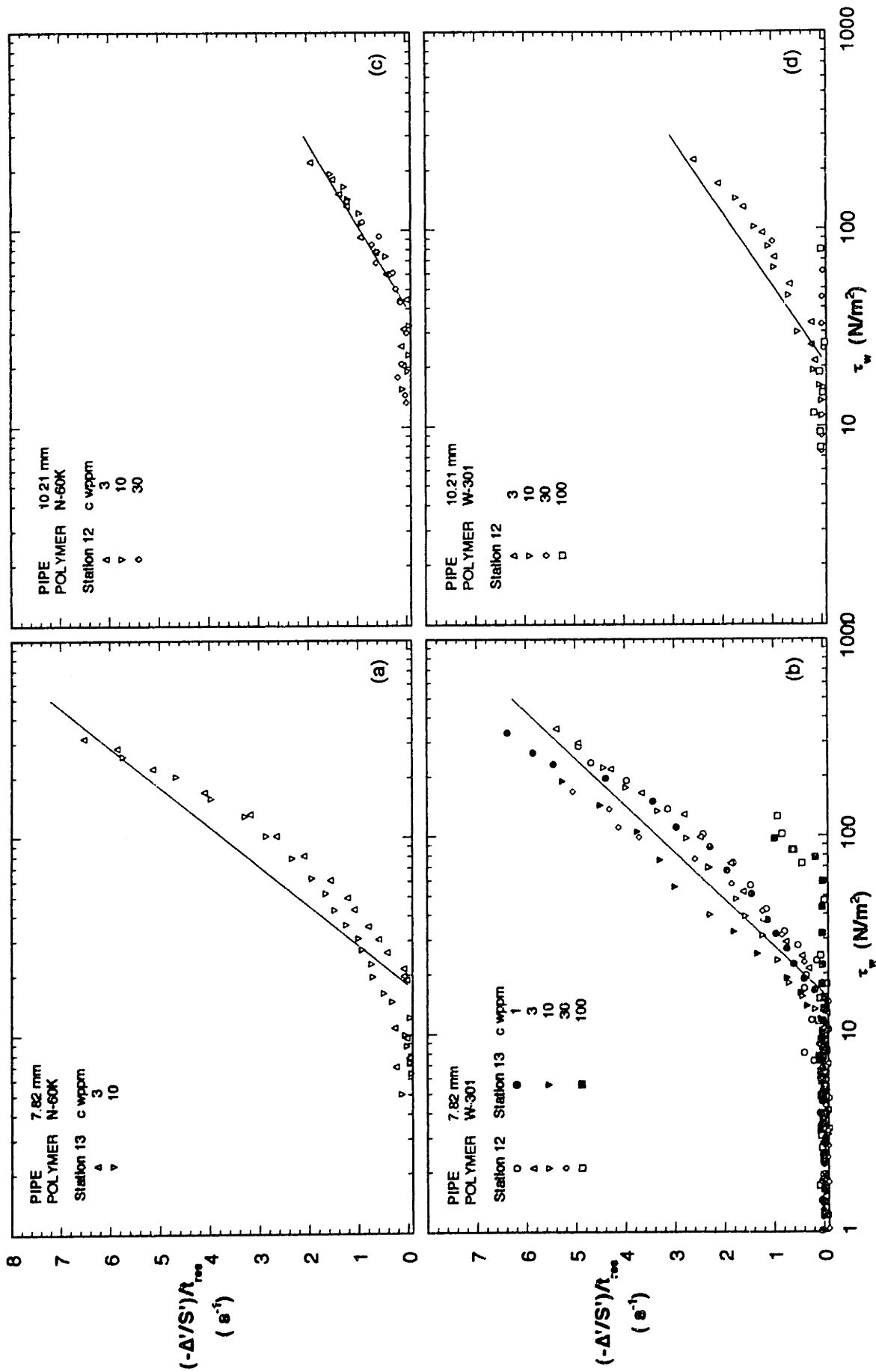


Figure 5.1.3 Variation of the apparent degradation rate constant with wall shear stress

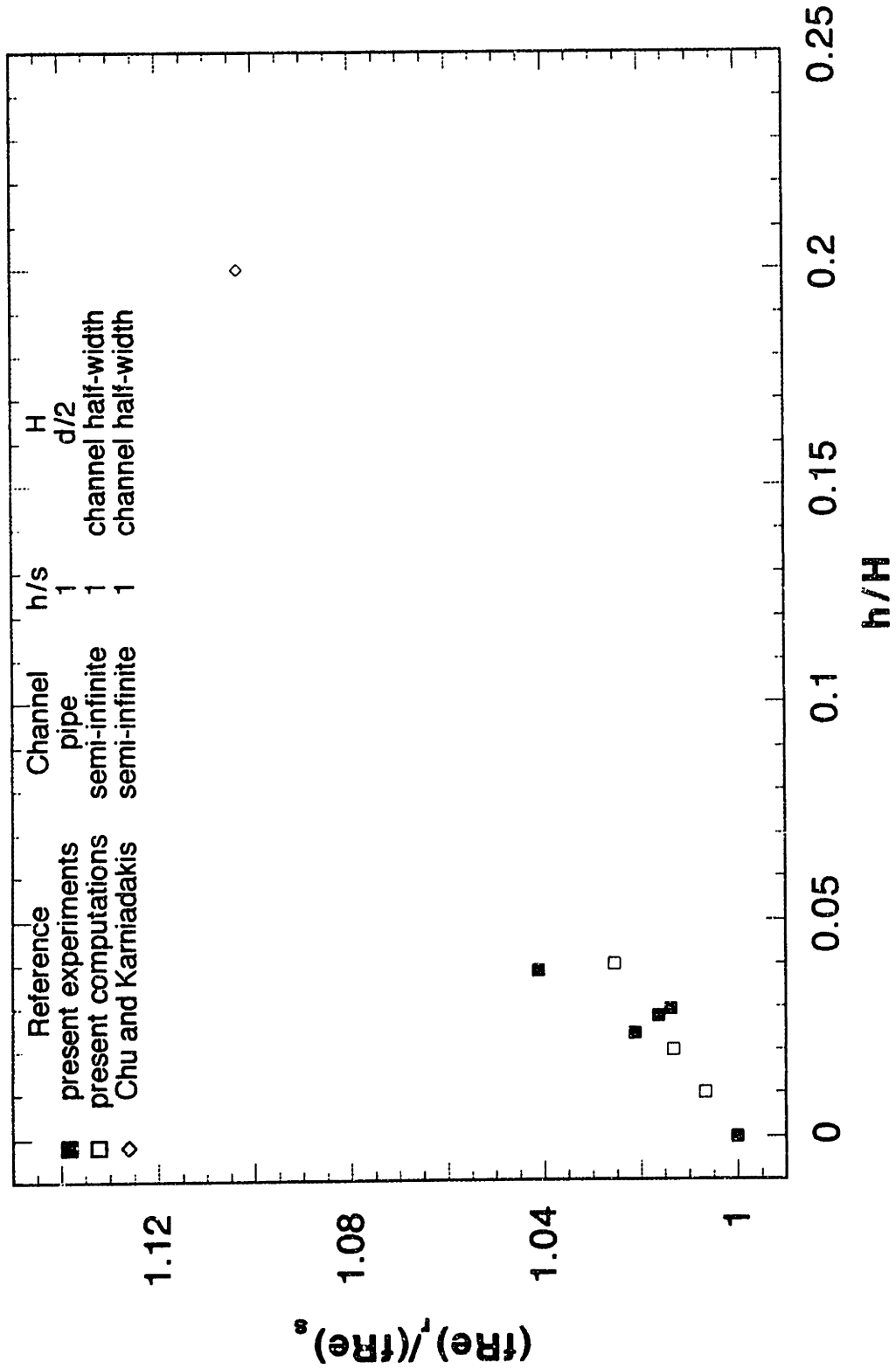


Figure 5.2.1 Experimental and computational laminar flow in riblet channels.

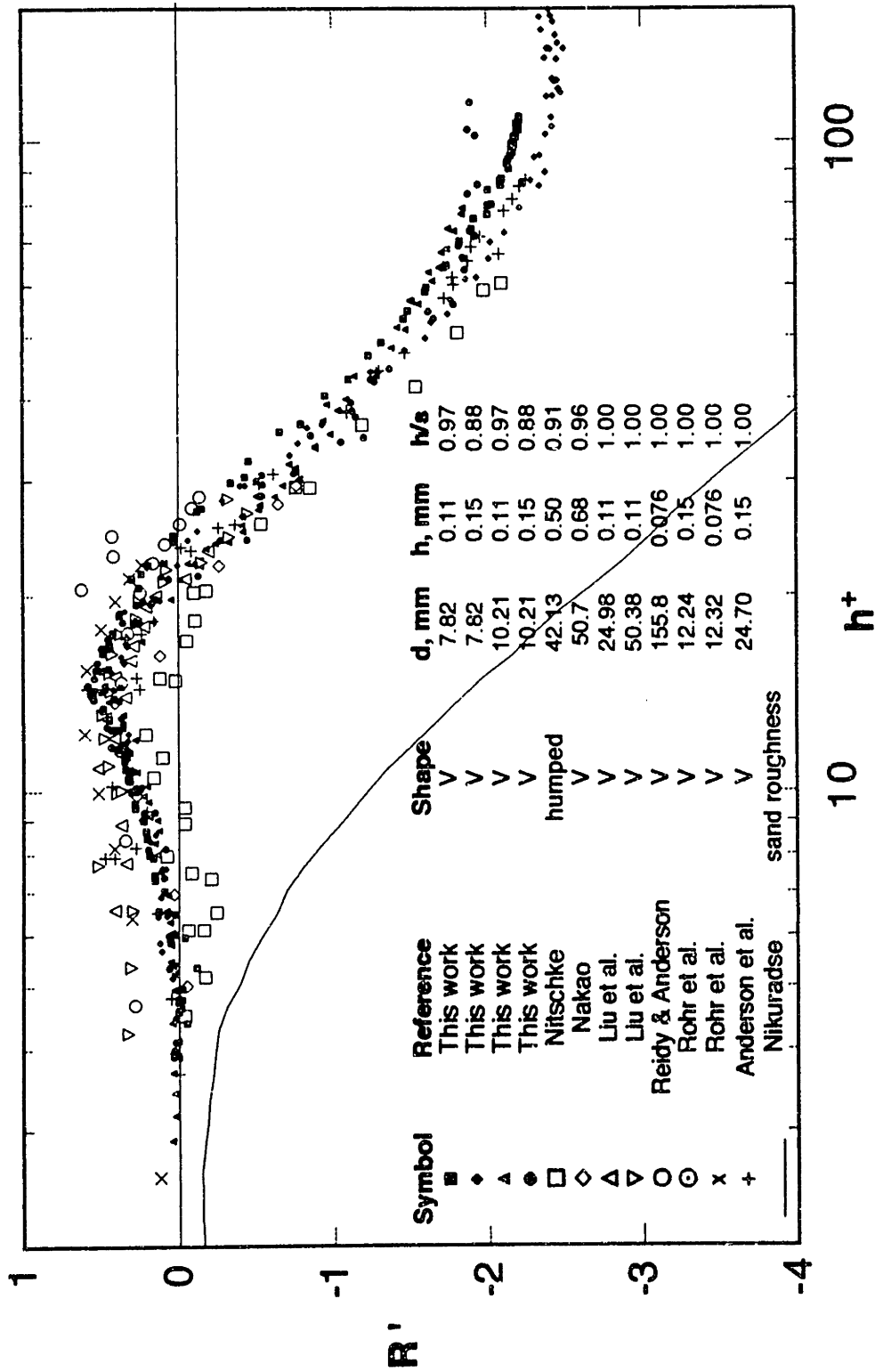


Figure 5.2.2 Comparison of riblet-induced flow enhancement between current work and previous work for riblets with $h/s \approx 1$

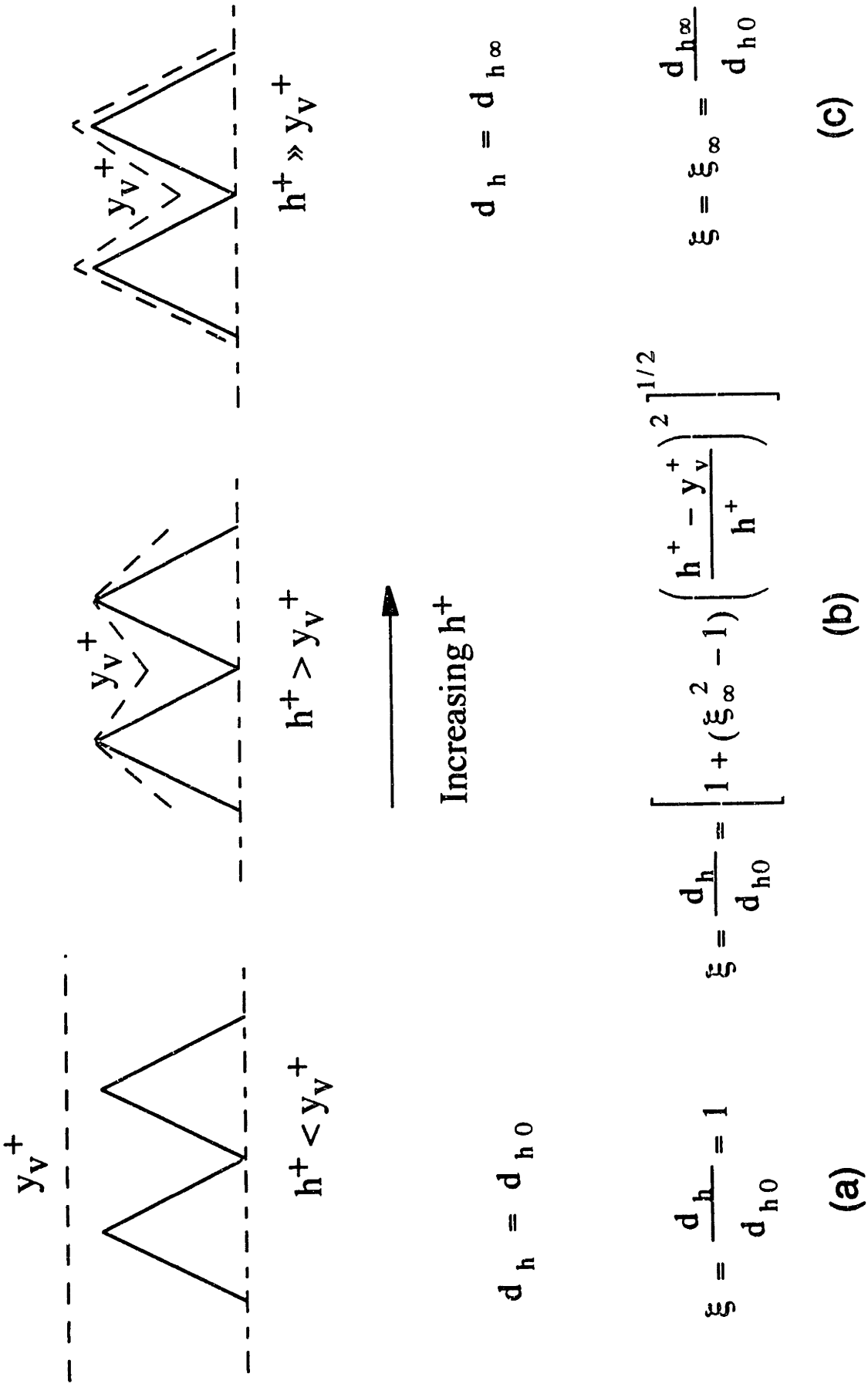


Figure 5.2.3. Serrated-sublayer model

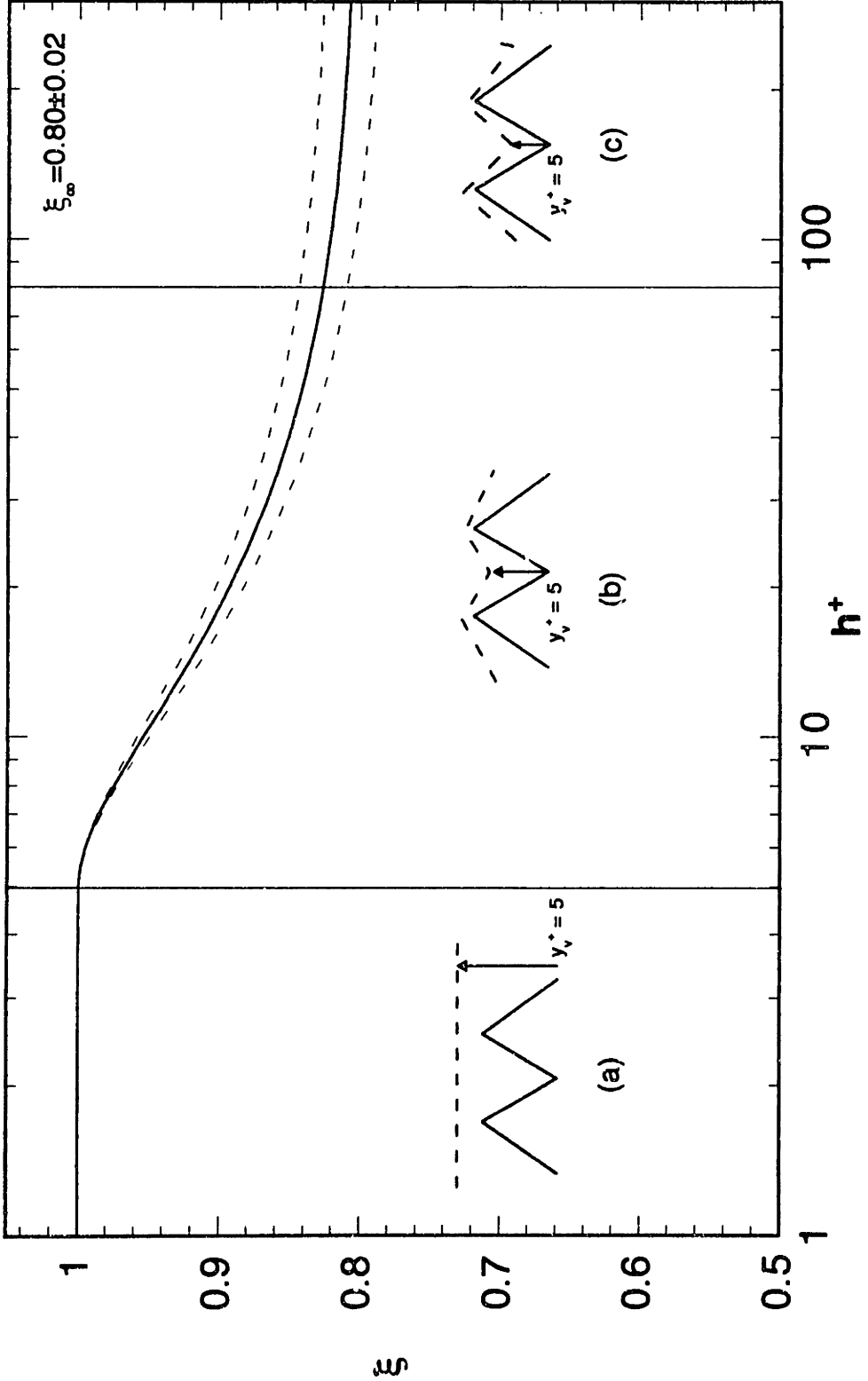


Figure 5.2.4 Variation of normalized equivalent hydraulic diameter, $\xi = d_h/d_{h0}$, with h^+

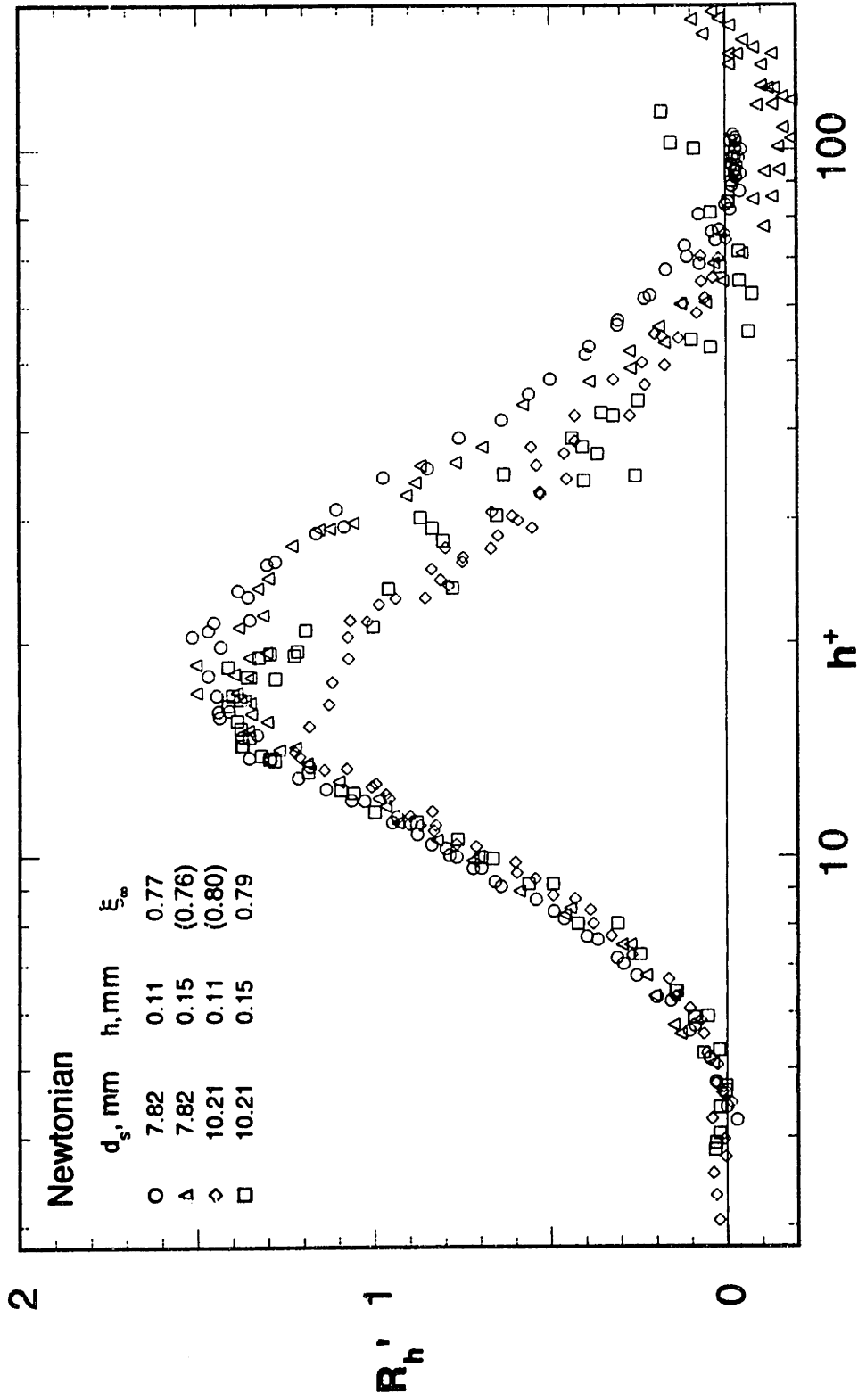


Figure 5.2.5 The inherent riblet induced flow enhancement in Newtonian pipe flows.

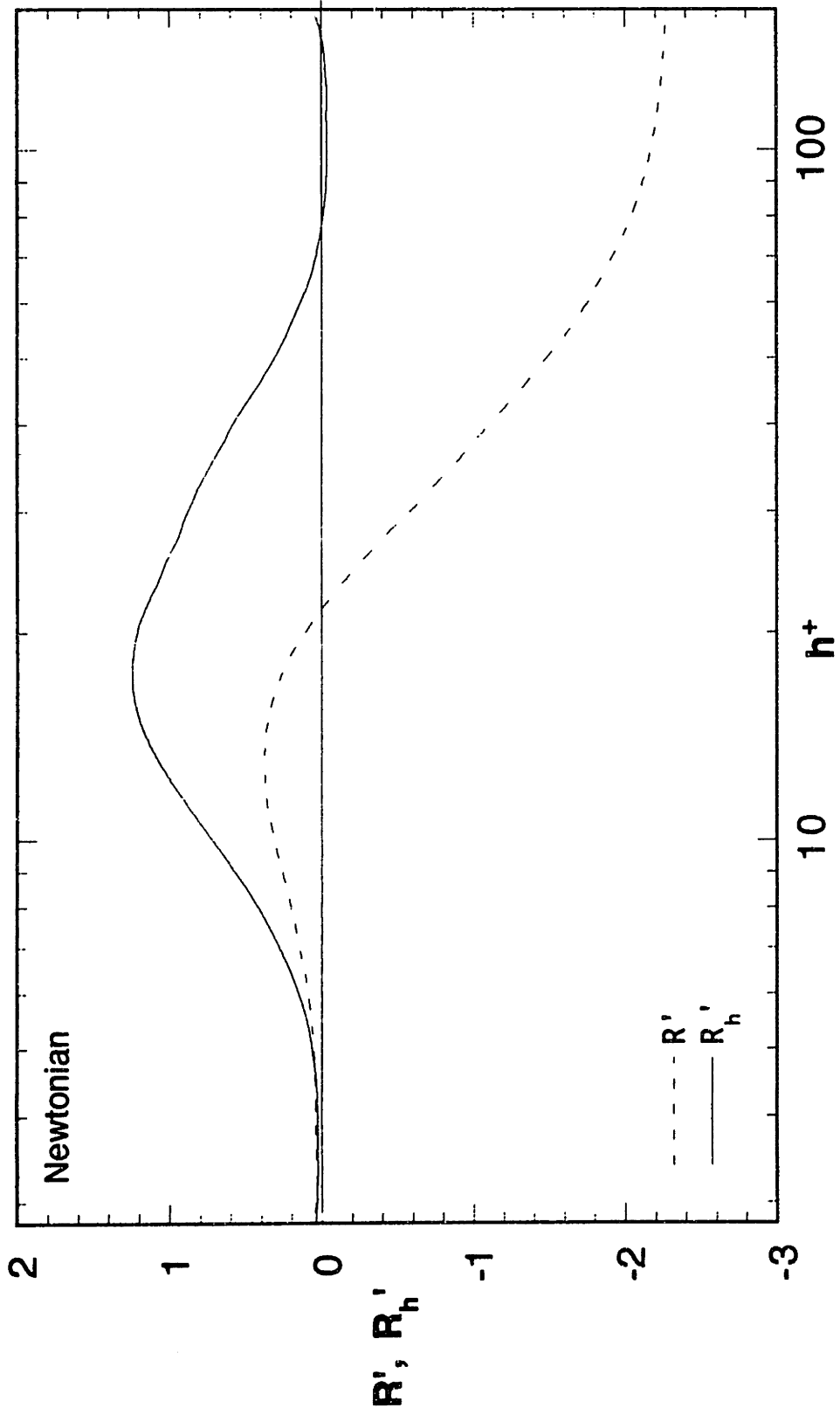


Figure 5.2.6 Comparison between physical and inherent riblet-induced flow enhancements

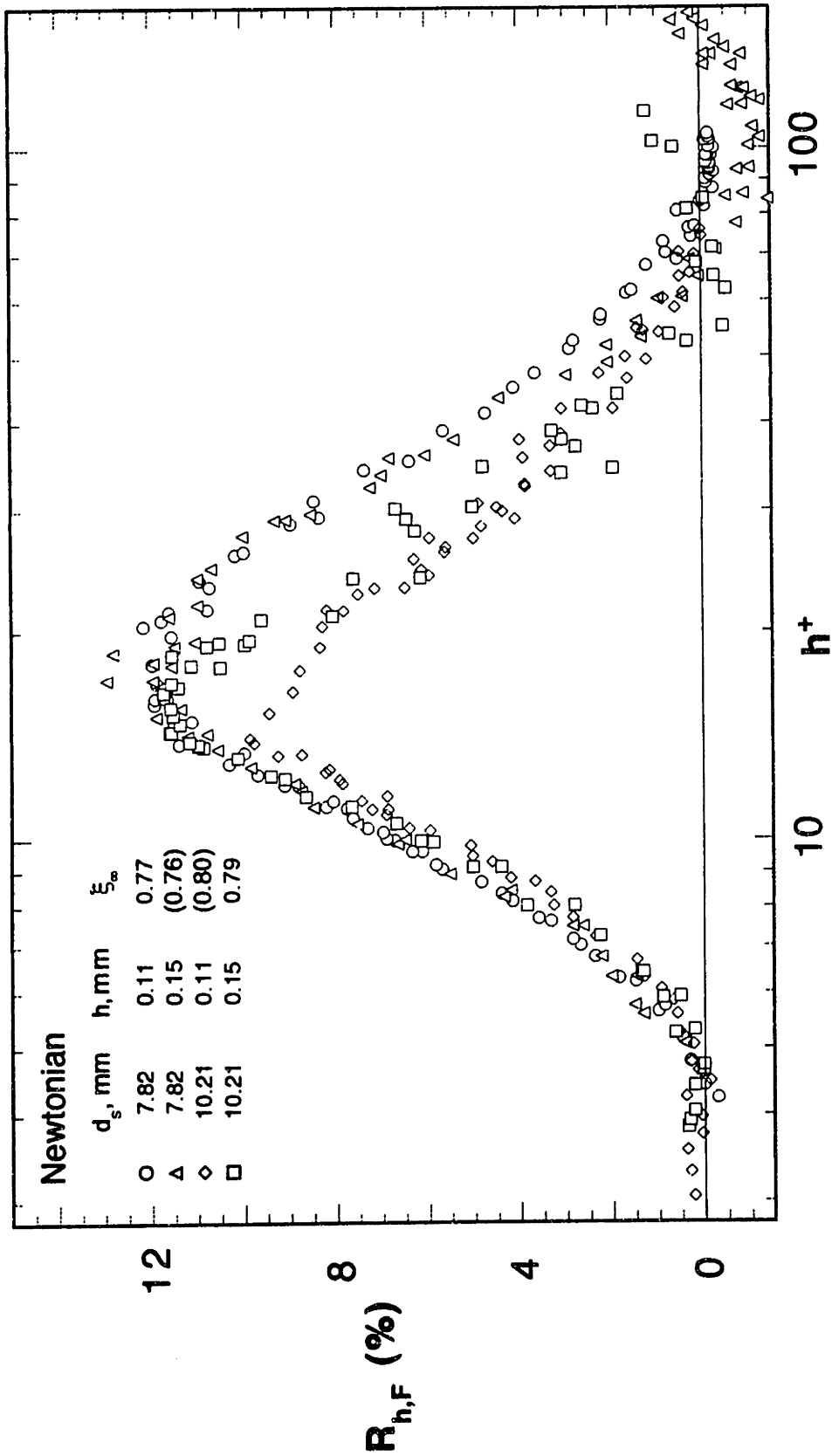


Figure 5.2.7 The inherent riblet-induced fractional flow enhancement for Newtonian pipe flows

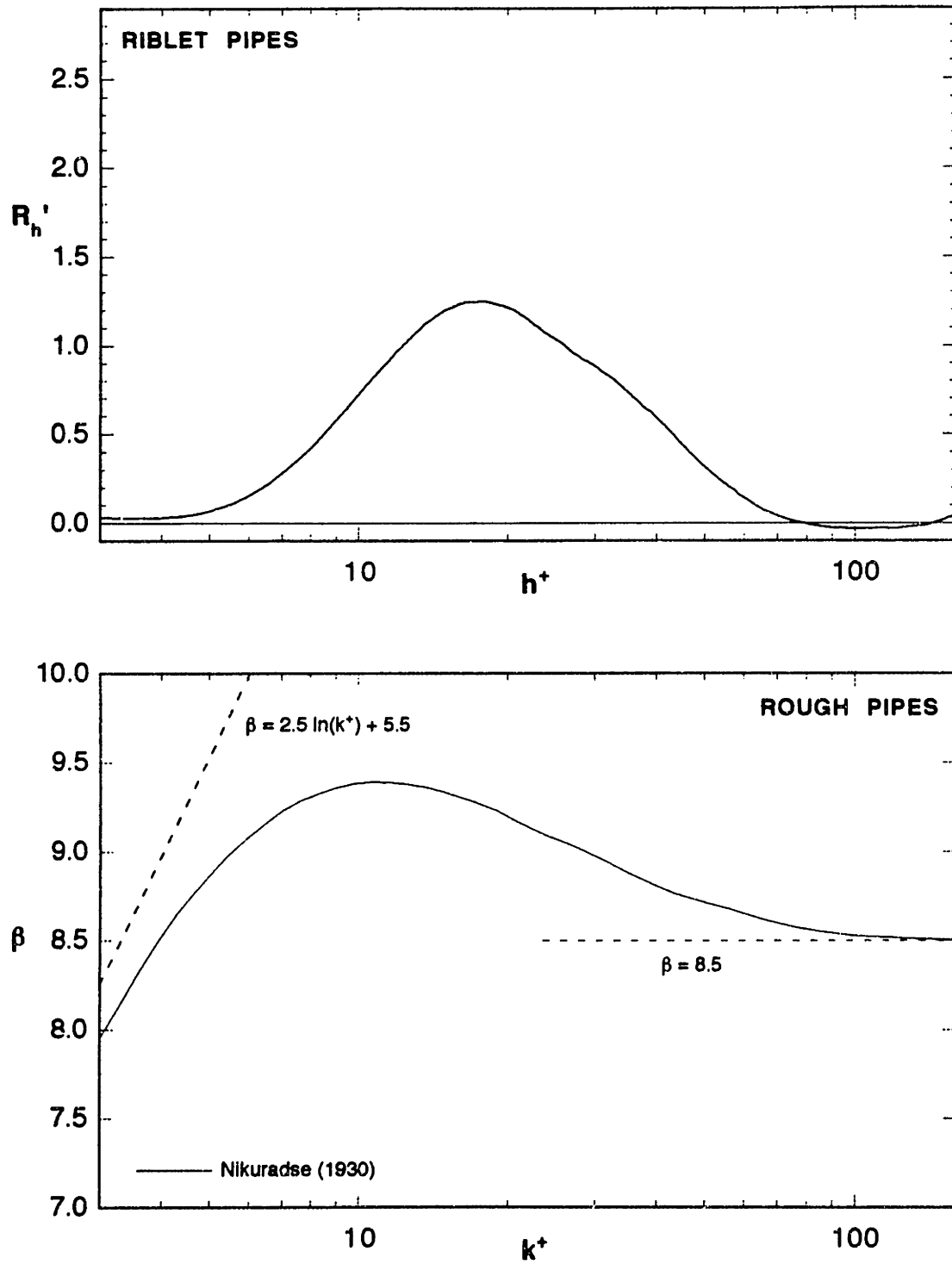


Figure 5.2.8 Comparison between riblet and rough pipes for Newtonian flows

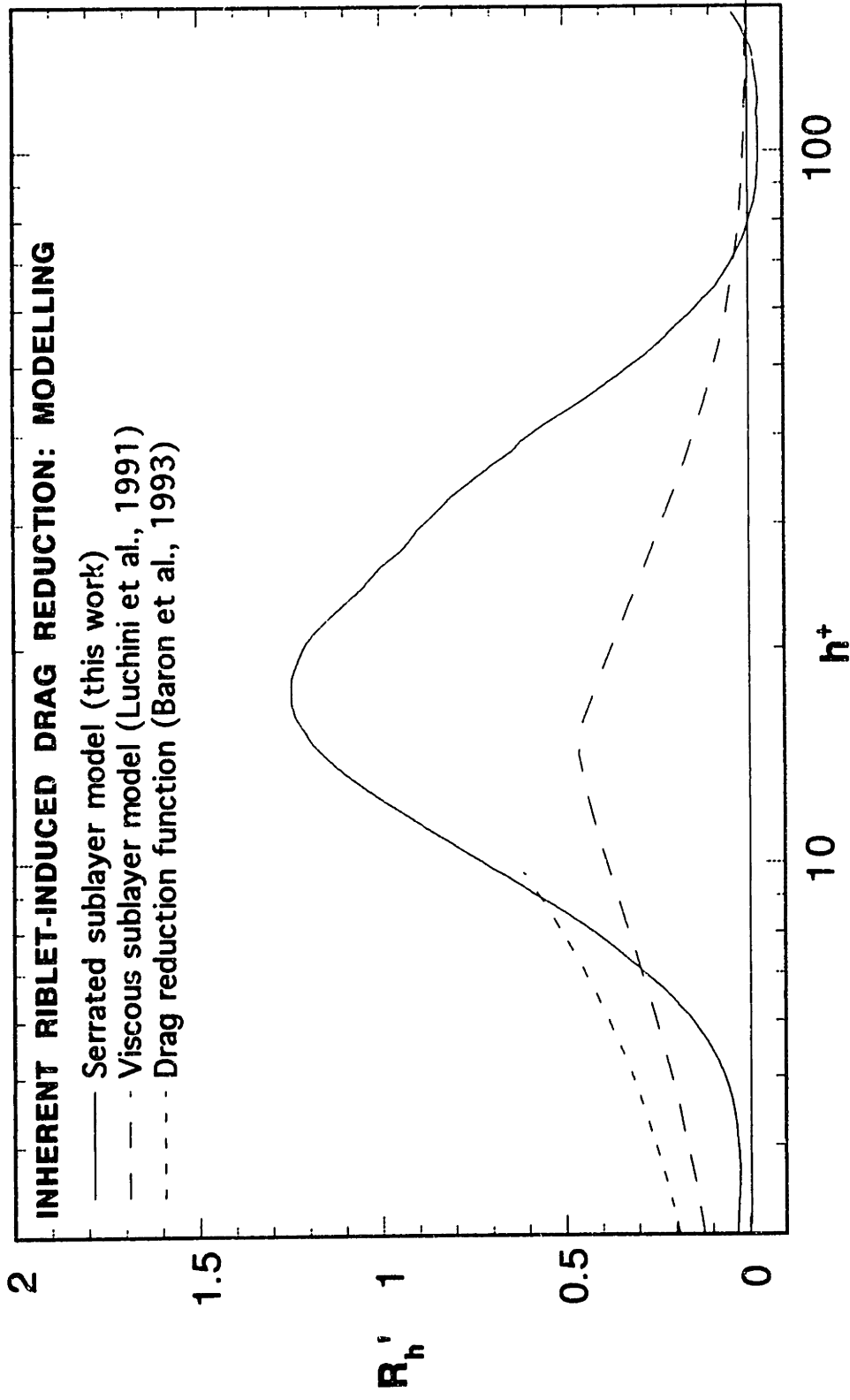


Figure 5.2.9 Comparison between predictive models for inherent riblet-induced flow enhancement

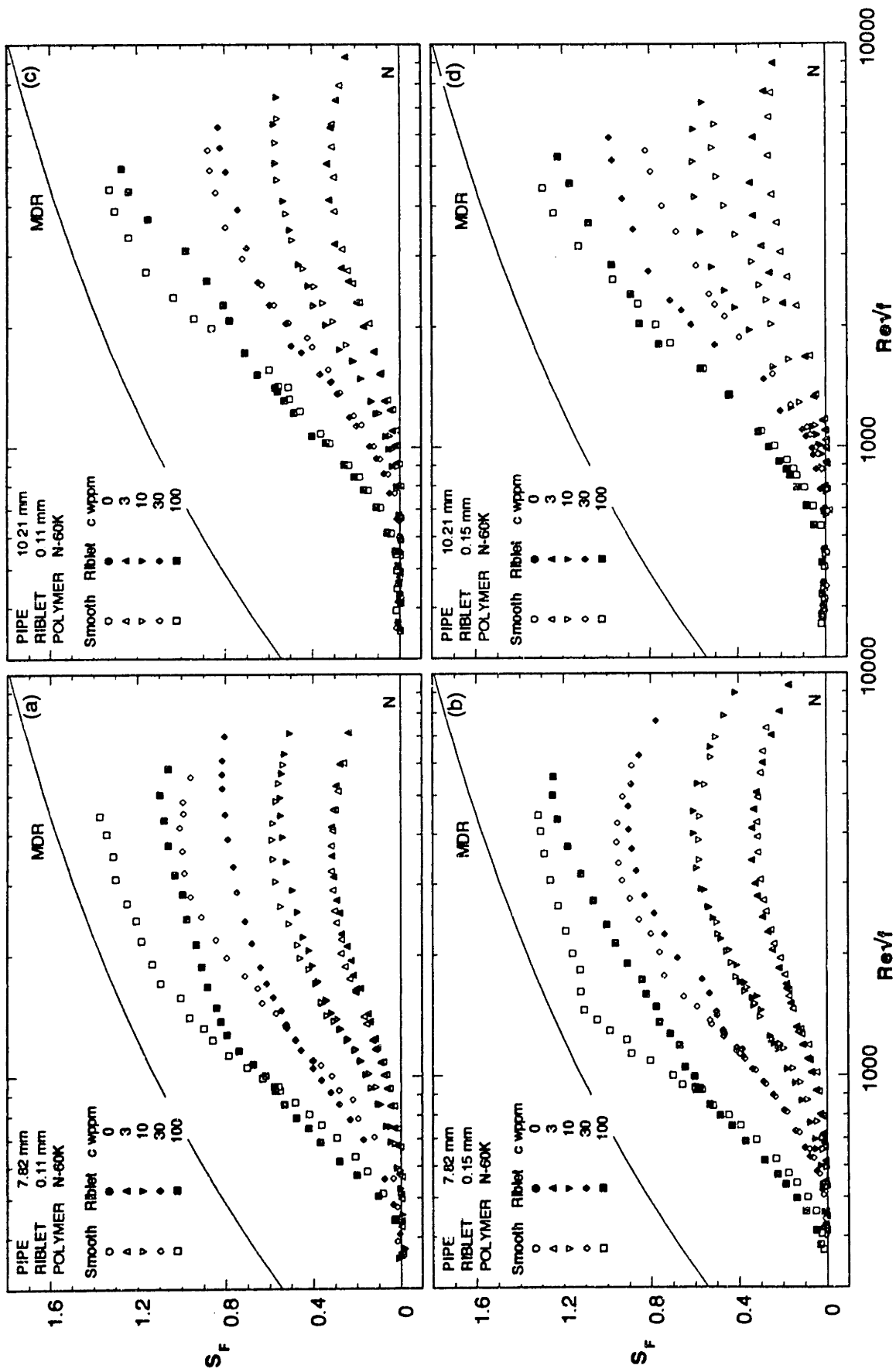


Figure 5.3.1 Comparison of polymer-induced fractional flow enhancements for PEO N-60K in all pipes

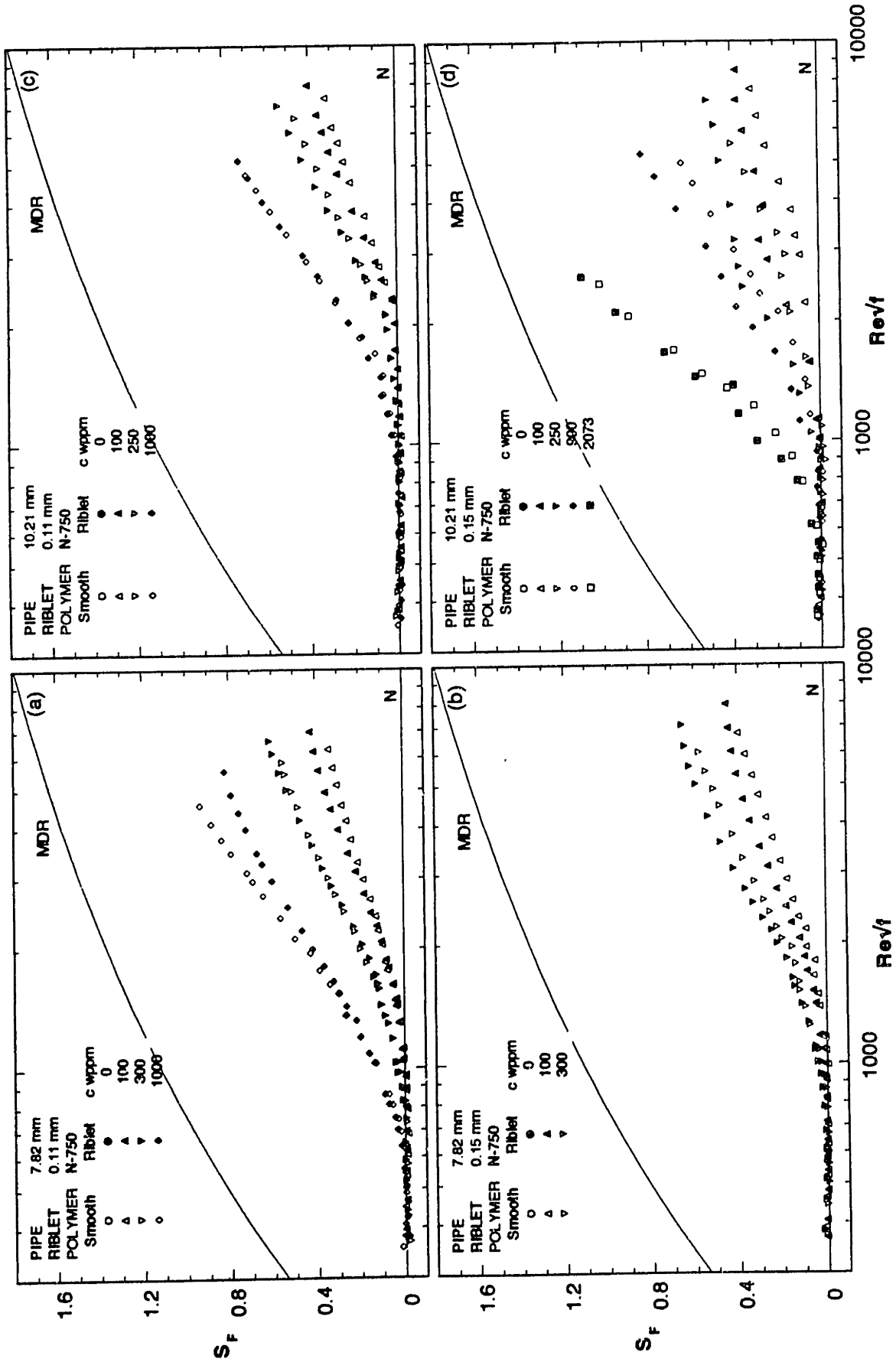


Figure 5.3.2 Comparison of polymer-induced fractional flow enhancements for PEO N-750 in all pipes

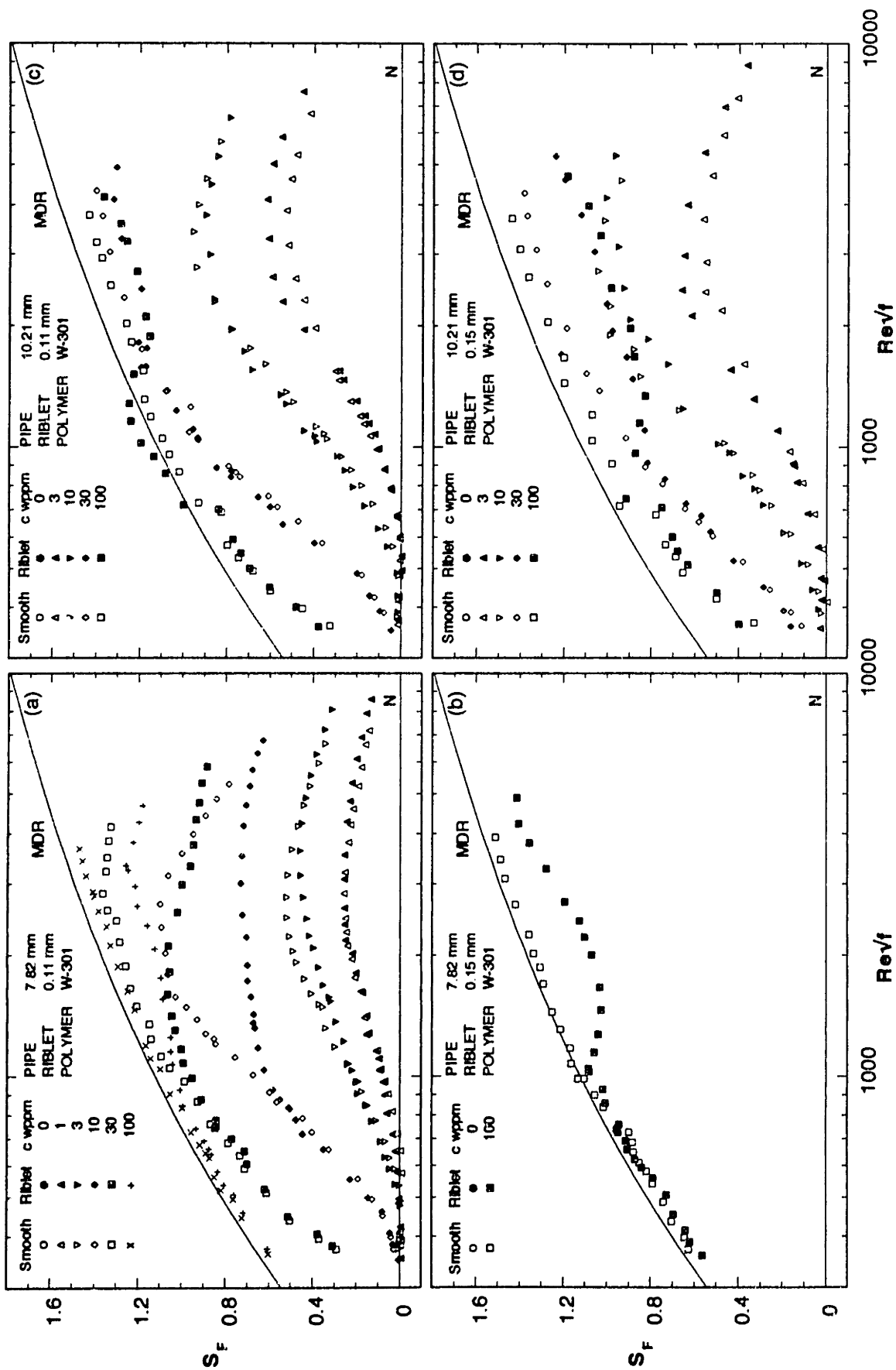


Figure 5.3.3 Comparison of polymer-induced fractional flow enhancements for PEO W-301 in all pipes

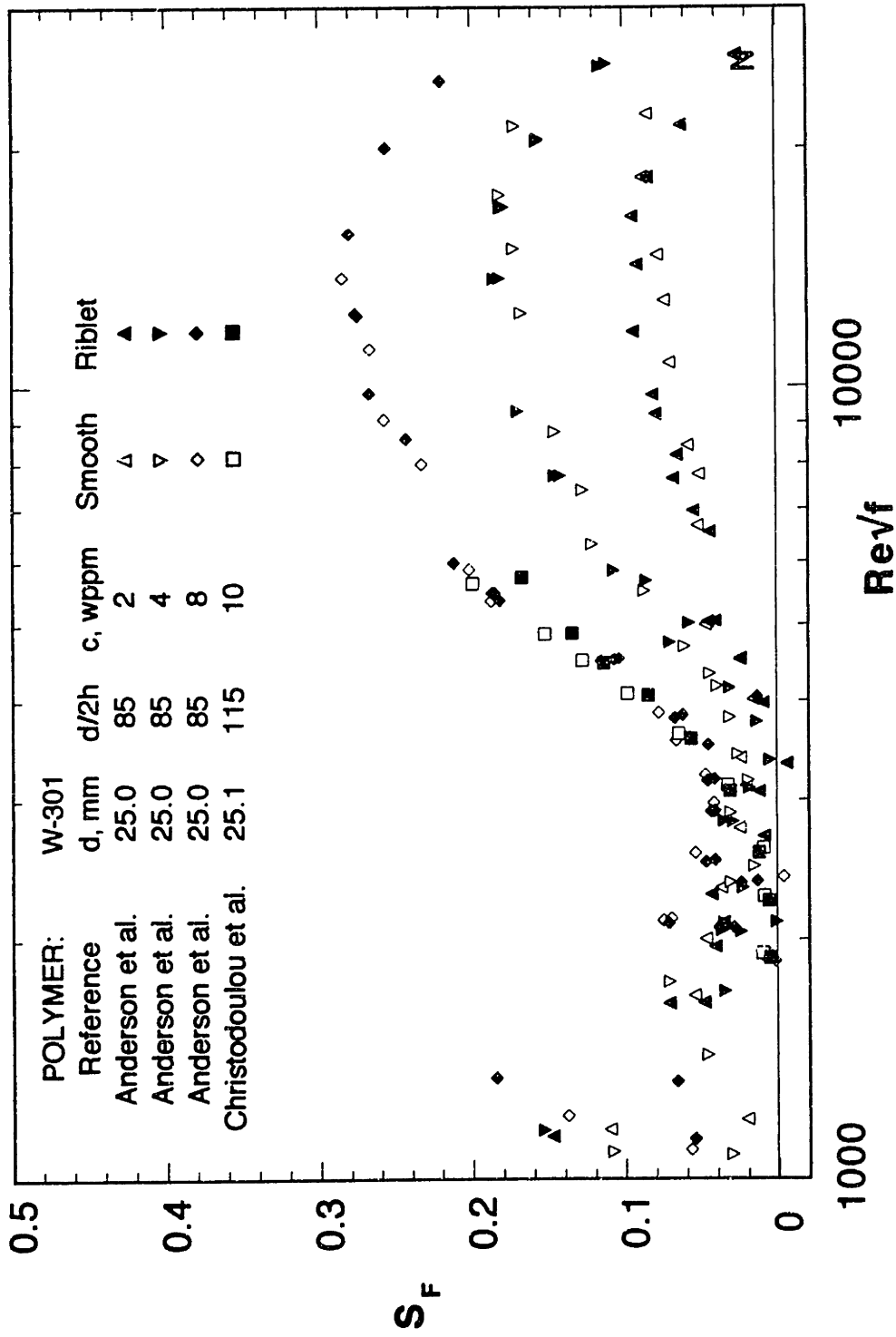


Figure 5.3.4 Analysis of polymer-induced fractional flow enhancements from Anderson et al (1993) and Christodoulou et al (1991).

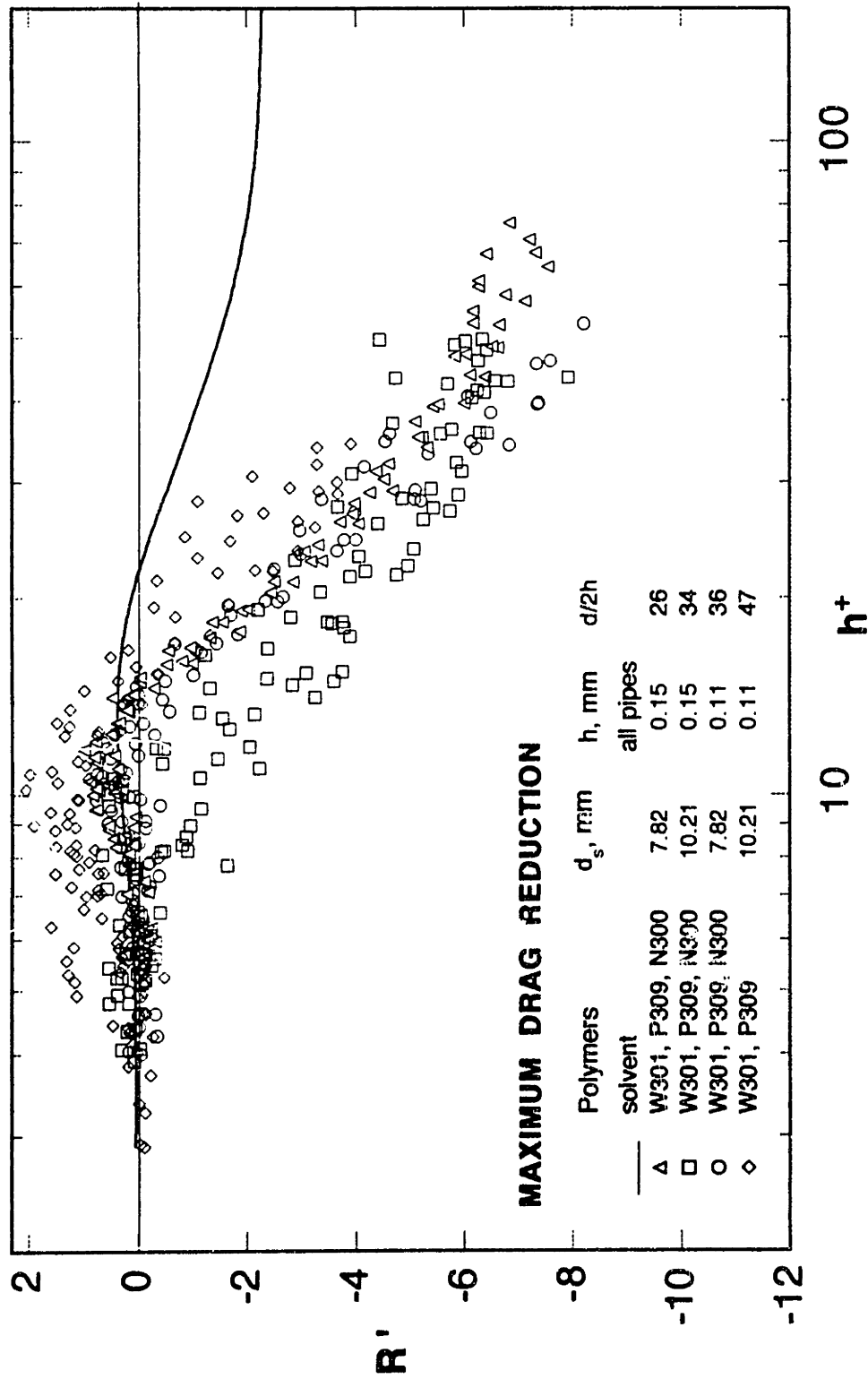


Figure 5.3.5 The riblet induced flow enhancement for flows in riblet pipes at maximum drag reduction

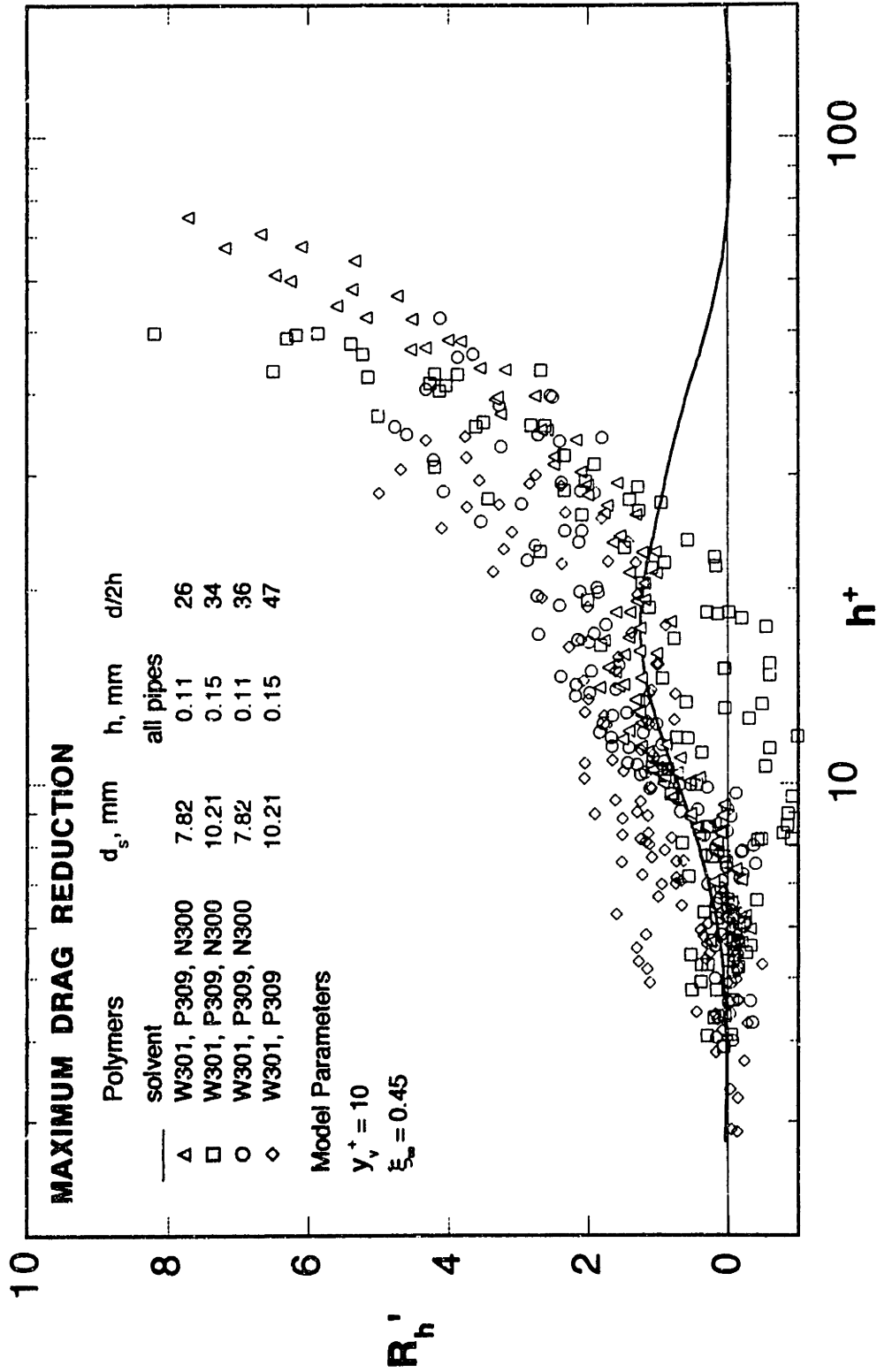


Figure 5.3.6 The inherent riblet induced flow enhancement flows in riblet pipes at maximum drag reduction

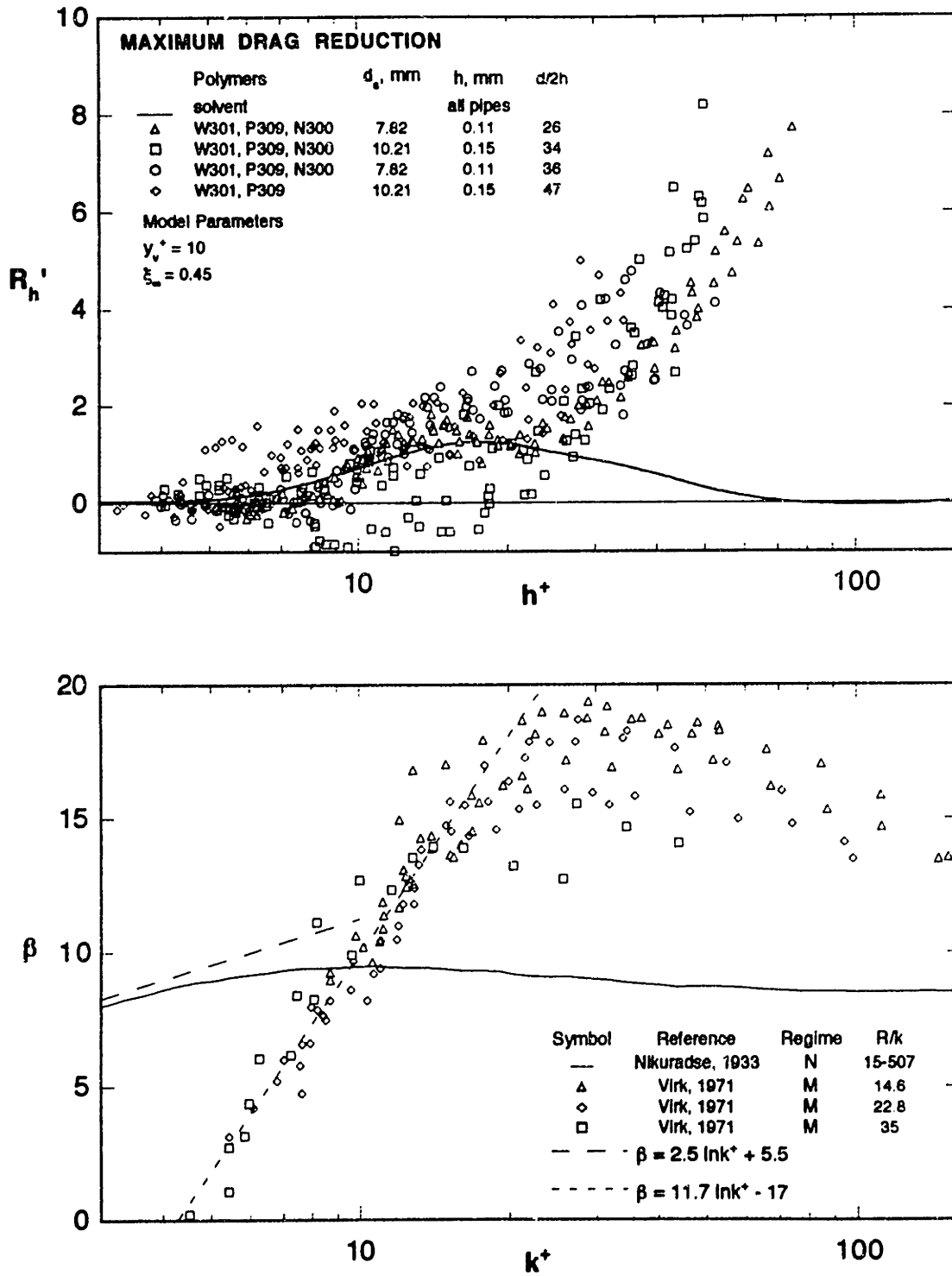


Figure 5.3.7 Comparison between riblet and rough pipes for Newtonian and maximum drag reducing flows

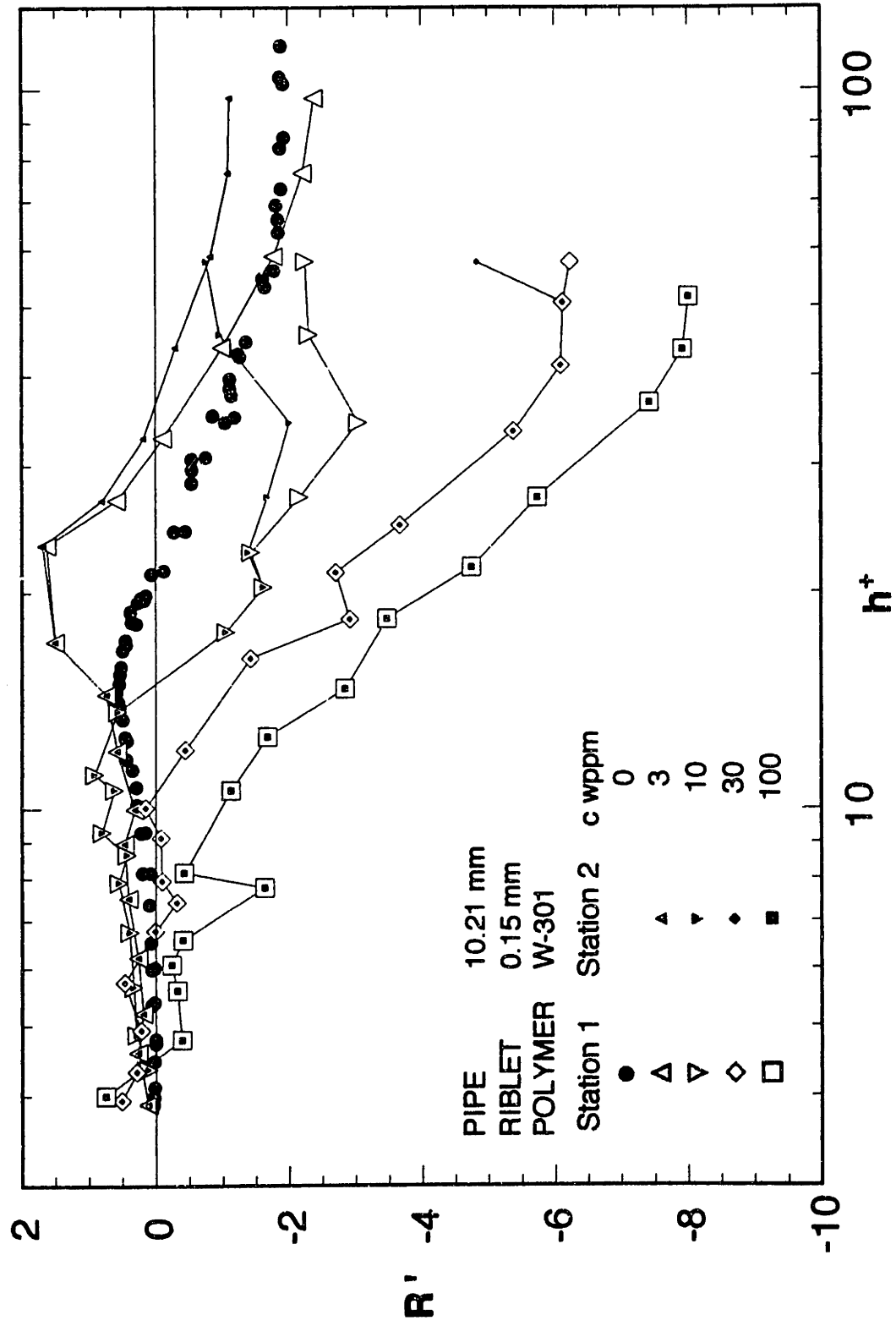


Figure 5.3.8 The riblet-induced flow enhancement for the flows of PEO W-301 in R2B based on upstream and downstream smooth pipe results

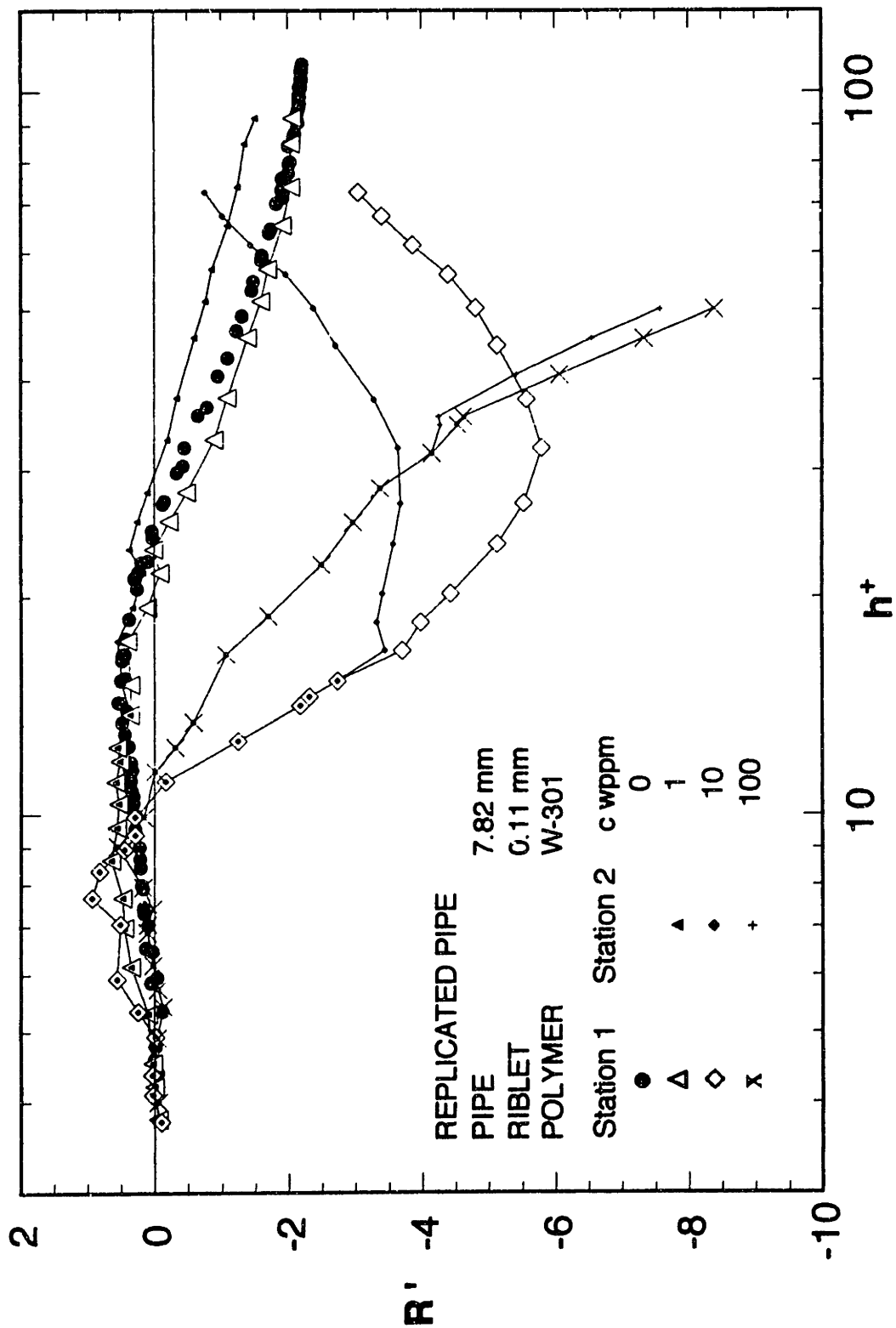


Figure 5.3.9 The riblet-induced flow enhancement for the flows of PEO W-301 in R1A based on upstream and downstream smooth pipe results

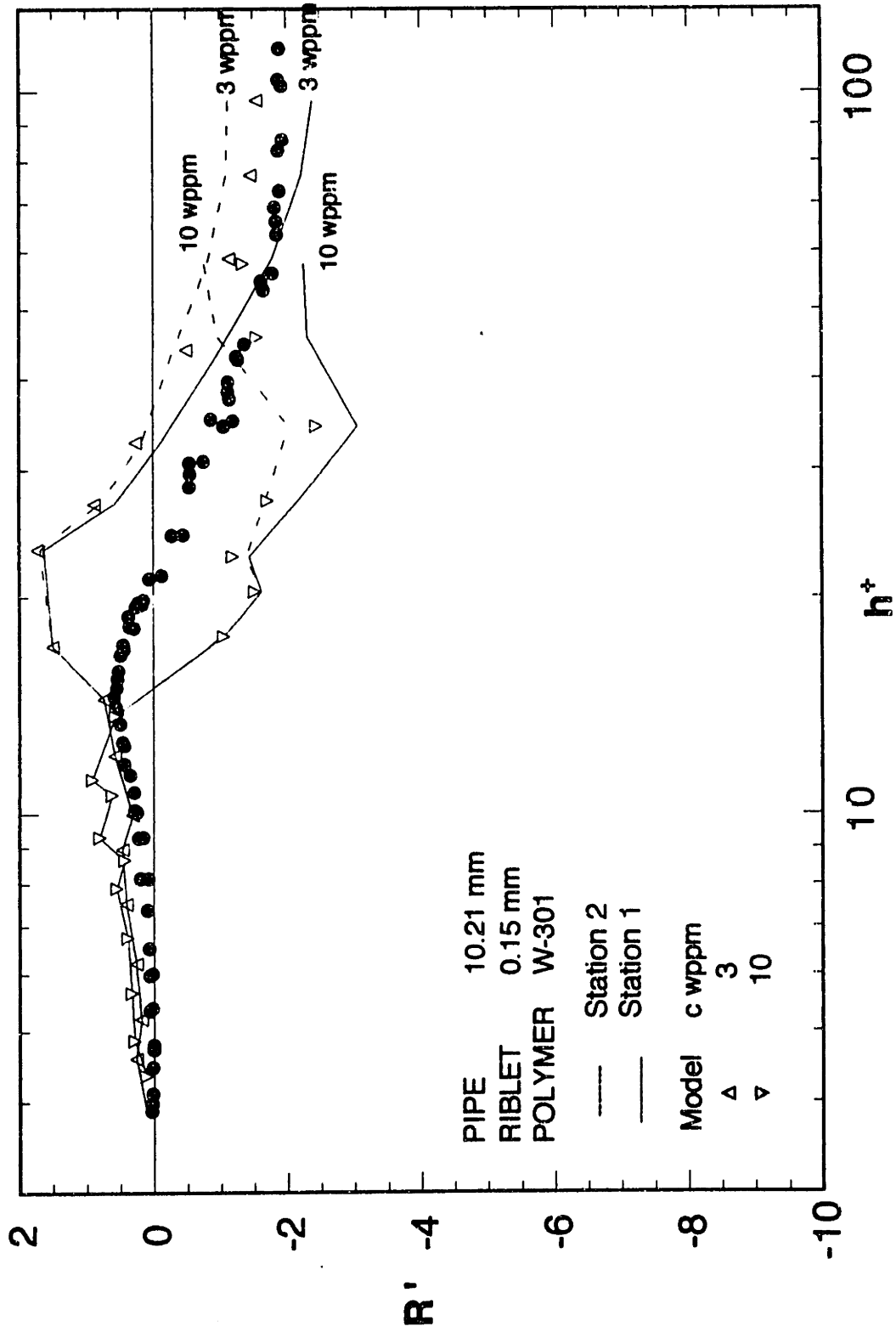


Figure 5.2.10 The degradation model riblet-induced flow enhancement for the flows of PEO W-301 in R2B; bounded by upstream and downstream smooth pipe results

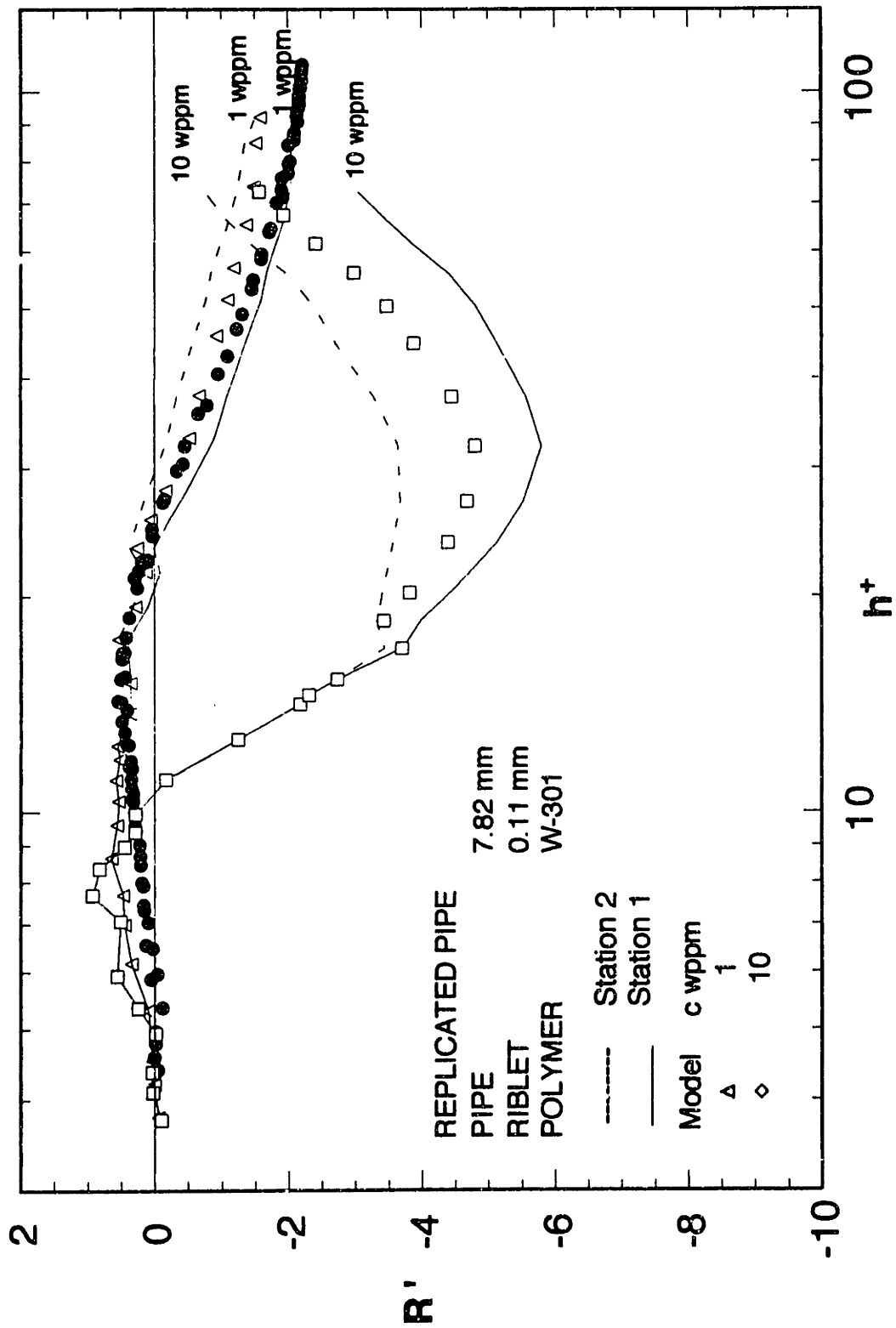


Figure 5.3.11 The degradation model riblet-induced flow enhancement for the flows of PEO W-301 in R1A; bounded by upstream and downstream smooth pipe results

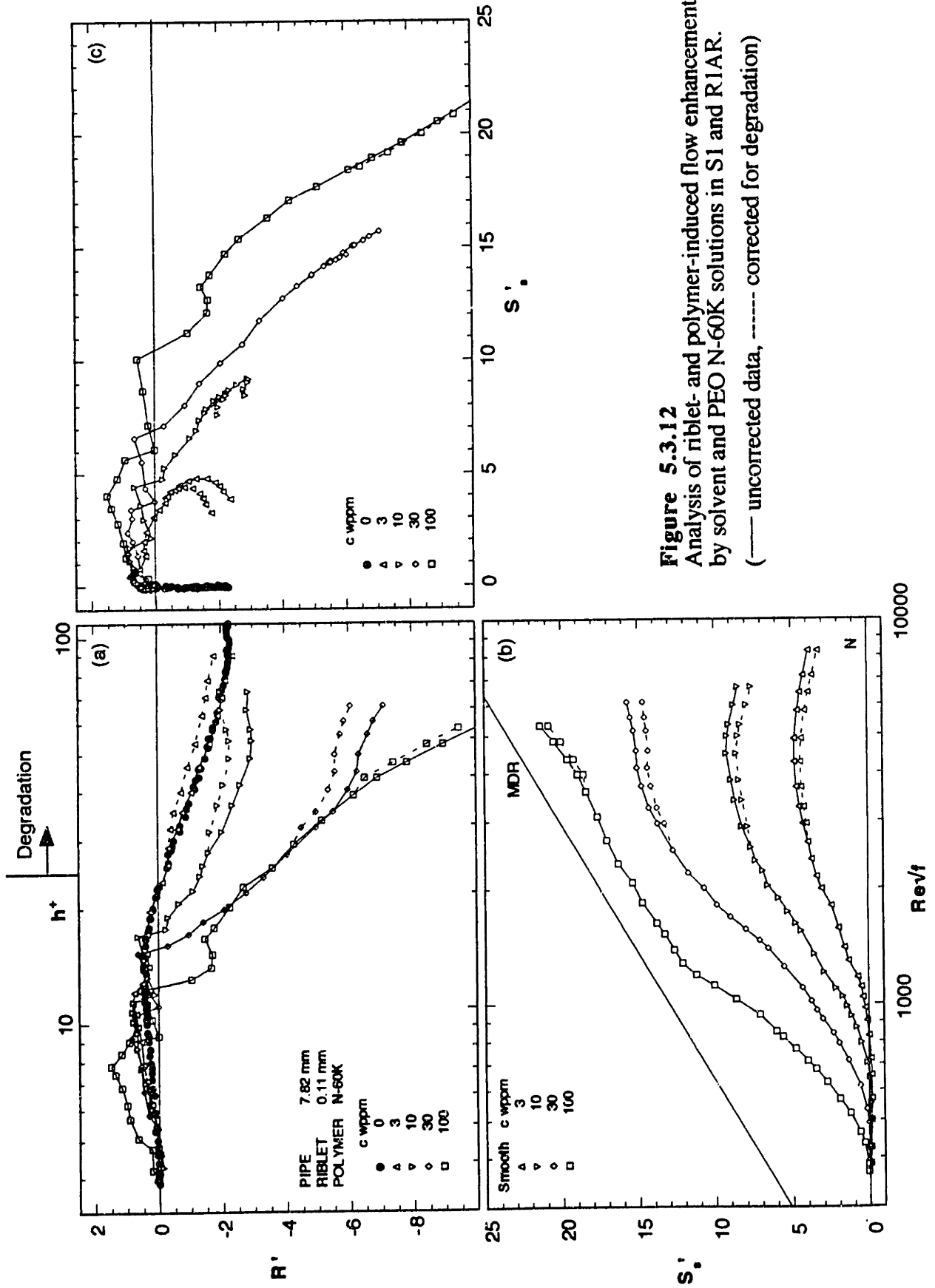


Figure 5.3.12
 Analysis of riblet- and polymer-induced flow enhancements
 by solvent and PEO N-60K solutions in S1 and R1AR.
 (— uncorrected data, ---- corrected for degradation)

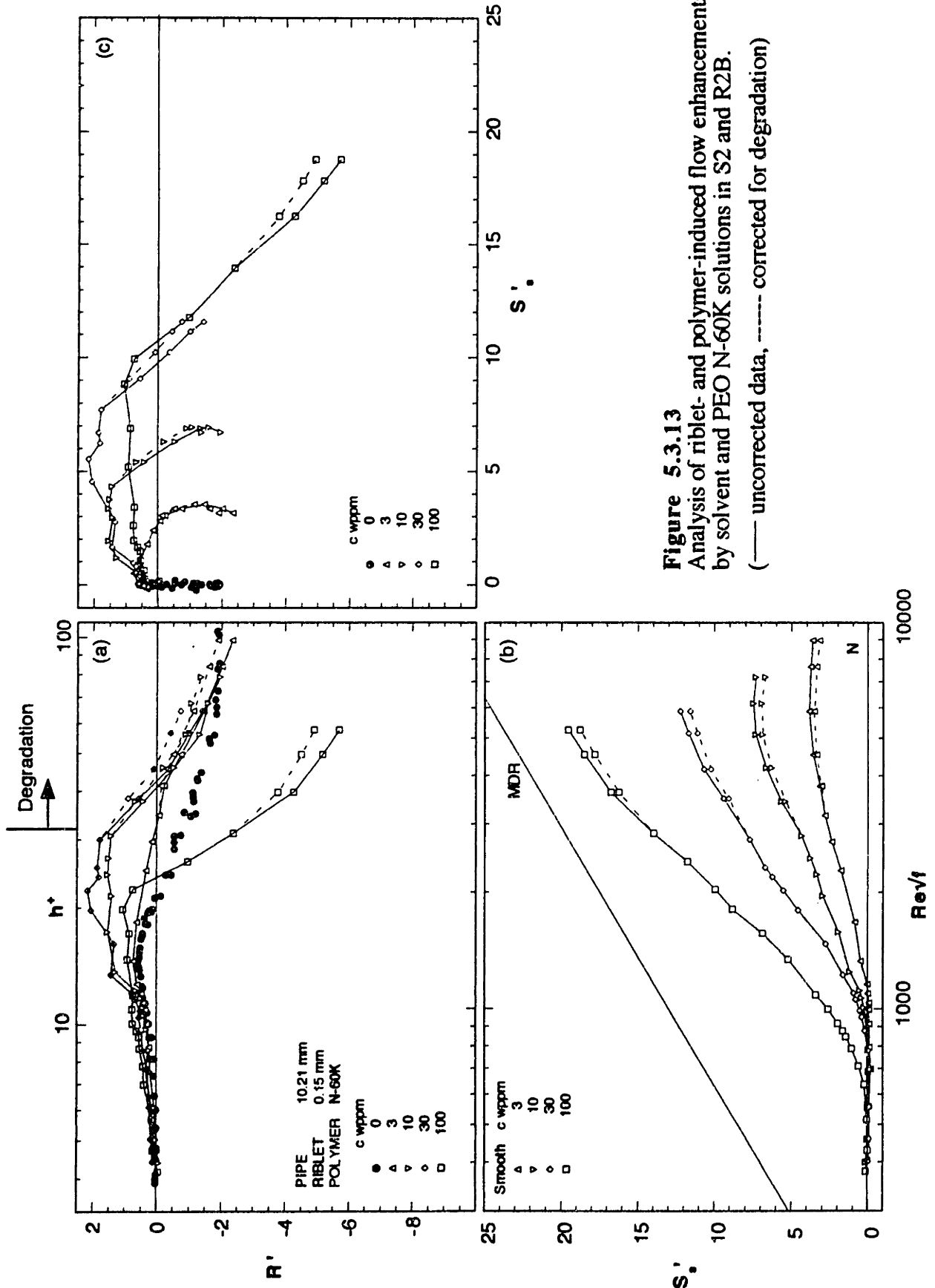


Figure 5.3.13
 Analysis of riblet- and polymer-induced flow enhancements
 by solvent and PEO N-60K solutions in S2 and R2B.
 (— uncorrected data, - - - - - corrected for degradation)

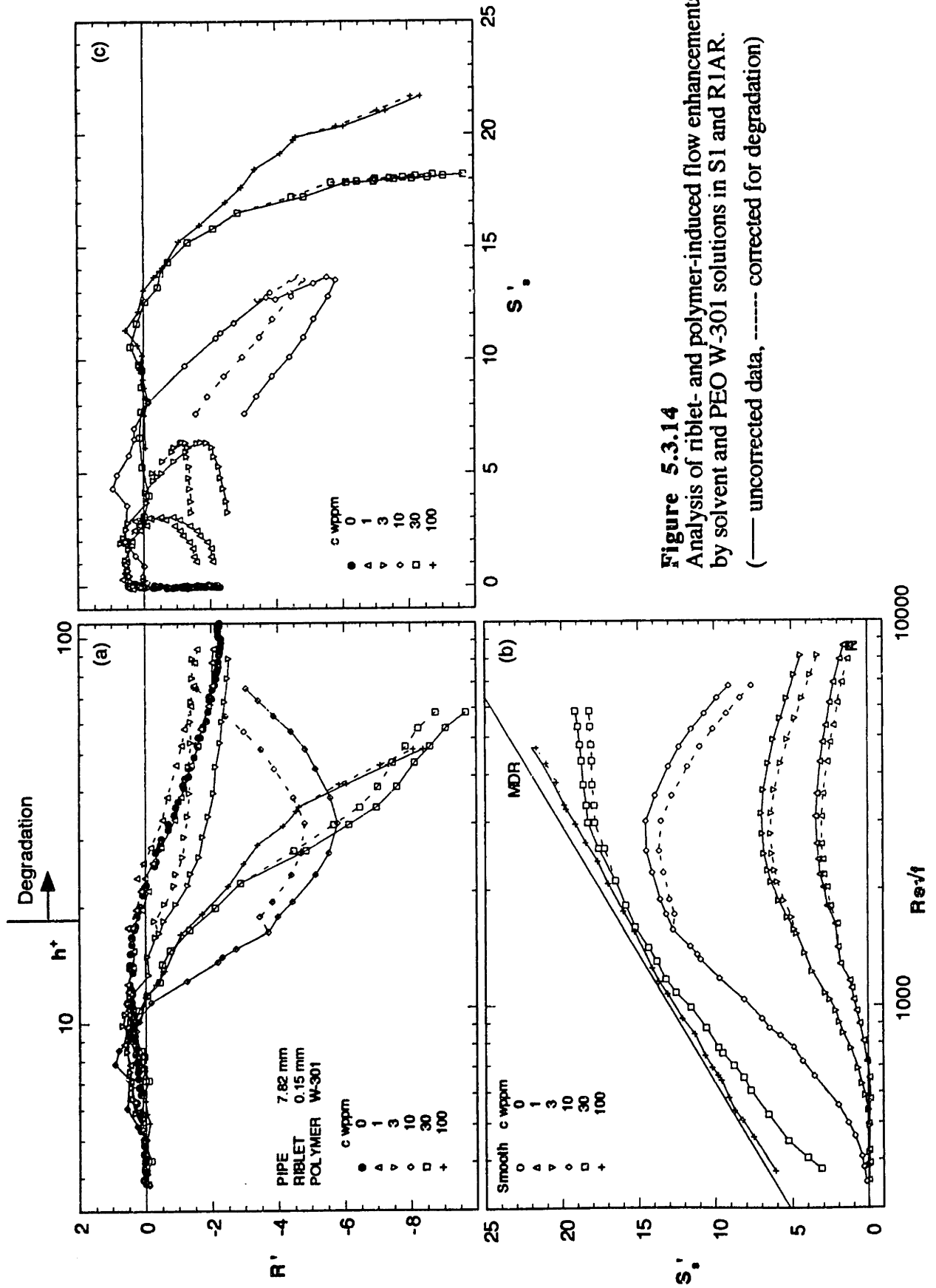


Figure 5.3.14
 Analysis of riblet- and polymer-induced flow enhancements
 by solvent and PEO W-301 solutions in S1 and R1AR.
 (— uncorrected data, ----- corrected for degradation)

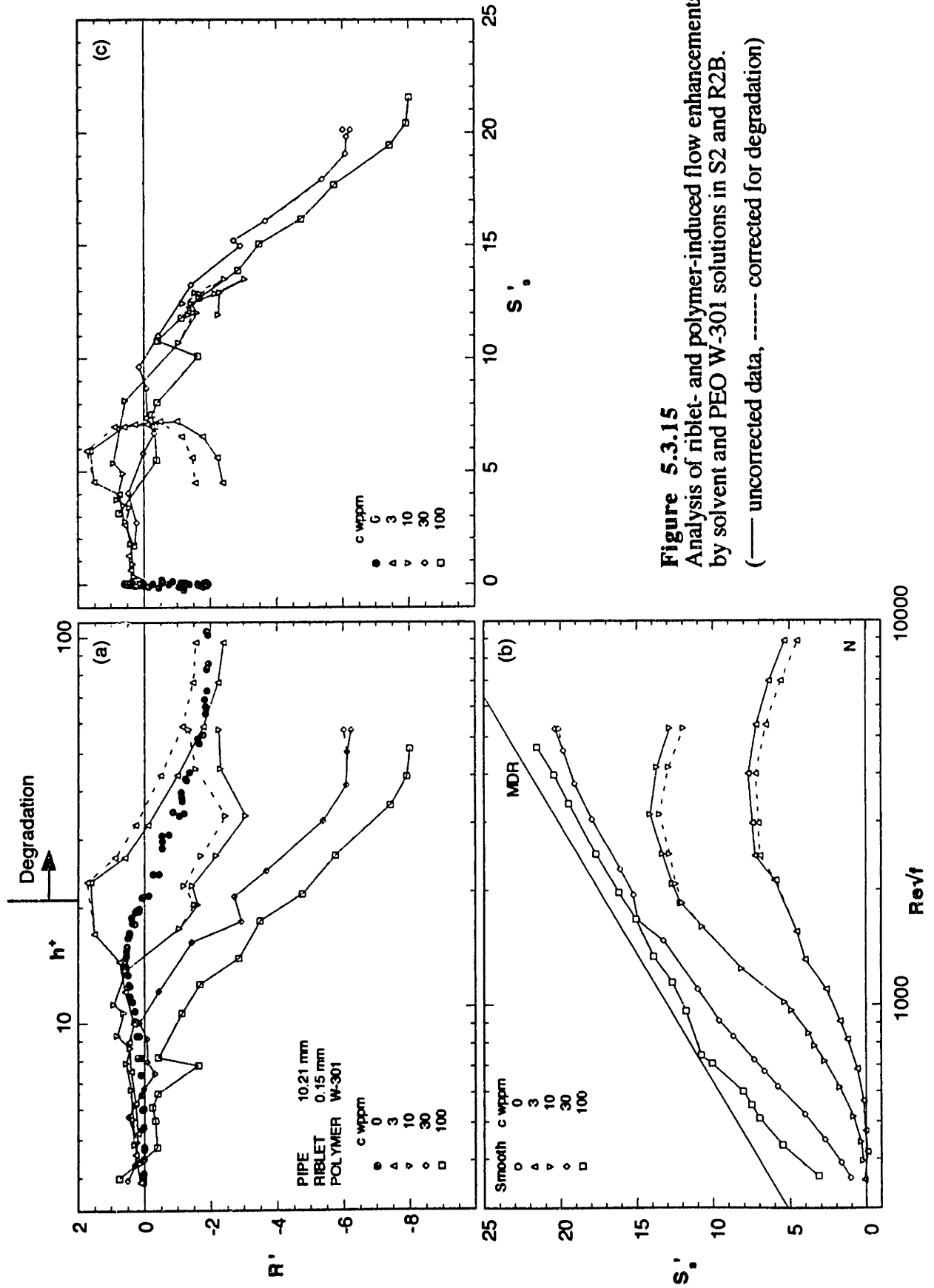


Figure 5.3.15
 Analysis of riblet- and polymer-induced flow enhancements by solvent and PEO W-301 solutions in S2 and R2B.
 (— uncorrected data, - - - - - corrected for degradation)

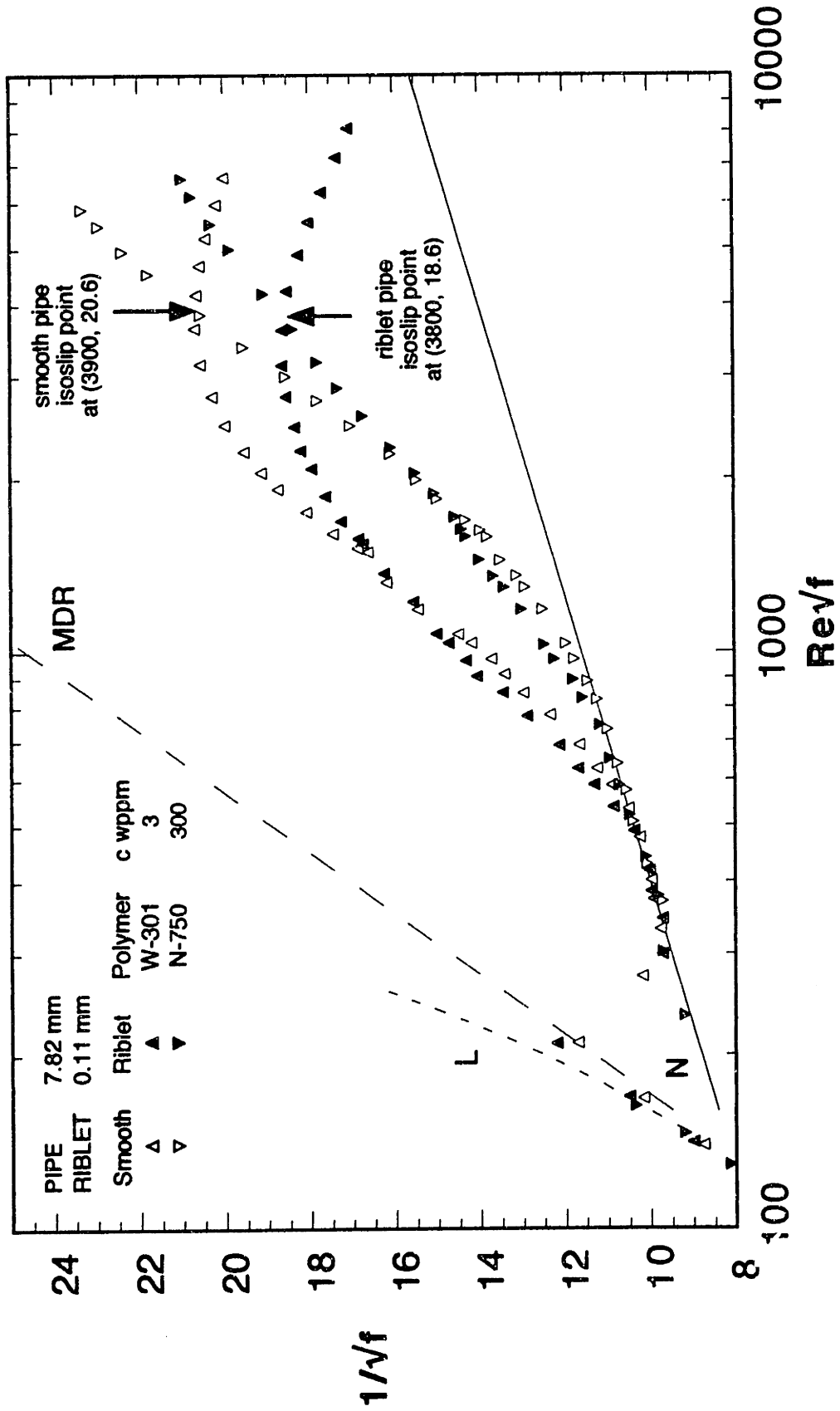


Figure 5.4.1 Example of additive equivalence at an isoslip point in the 7.82 mm pipe system.

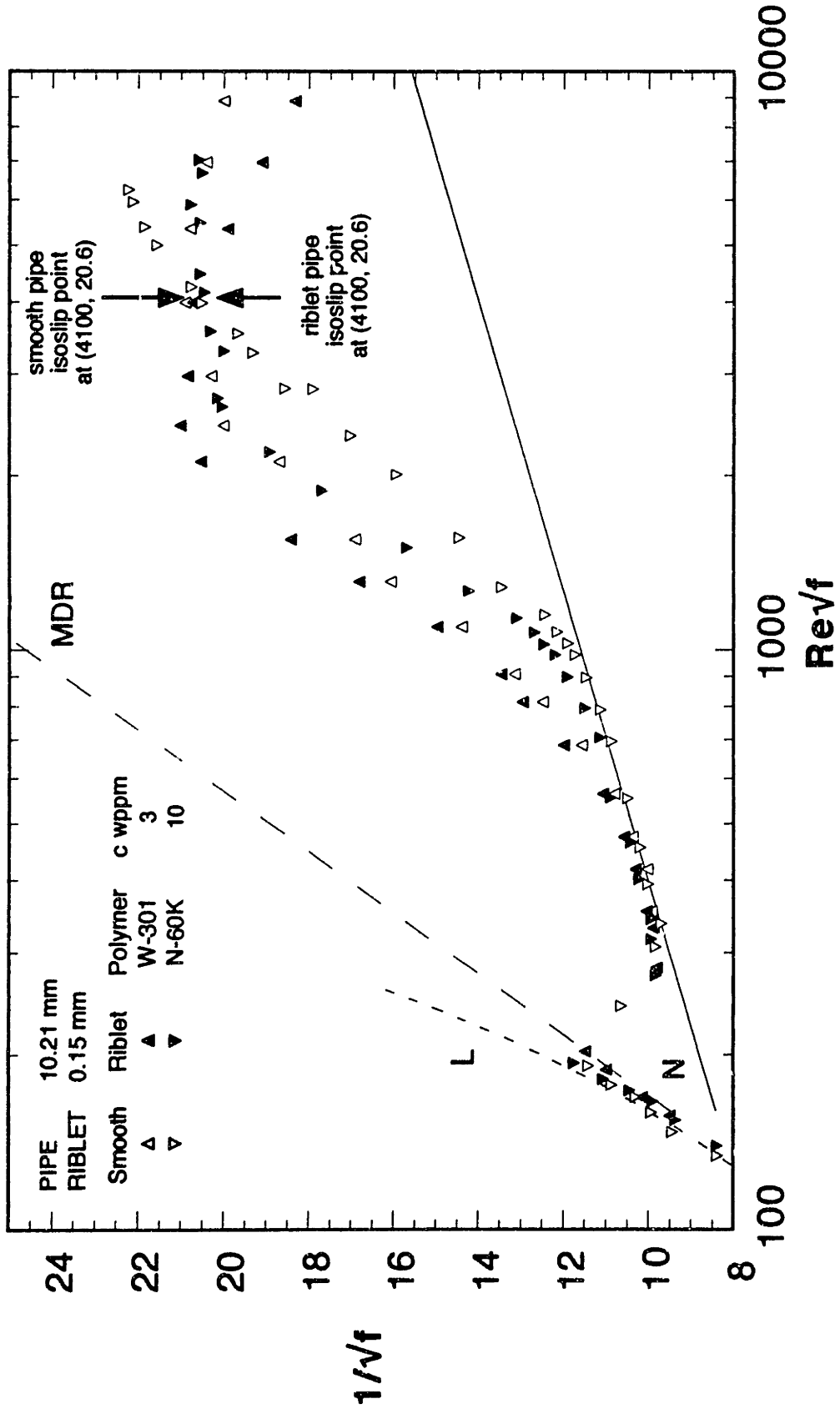


Figure 5.4.2 Example of additive equivalence at an isoslip point in the 10.21 mm pipe system.

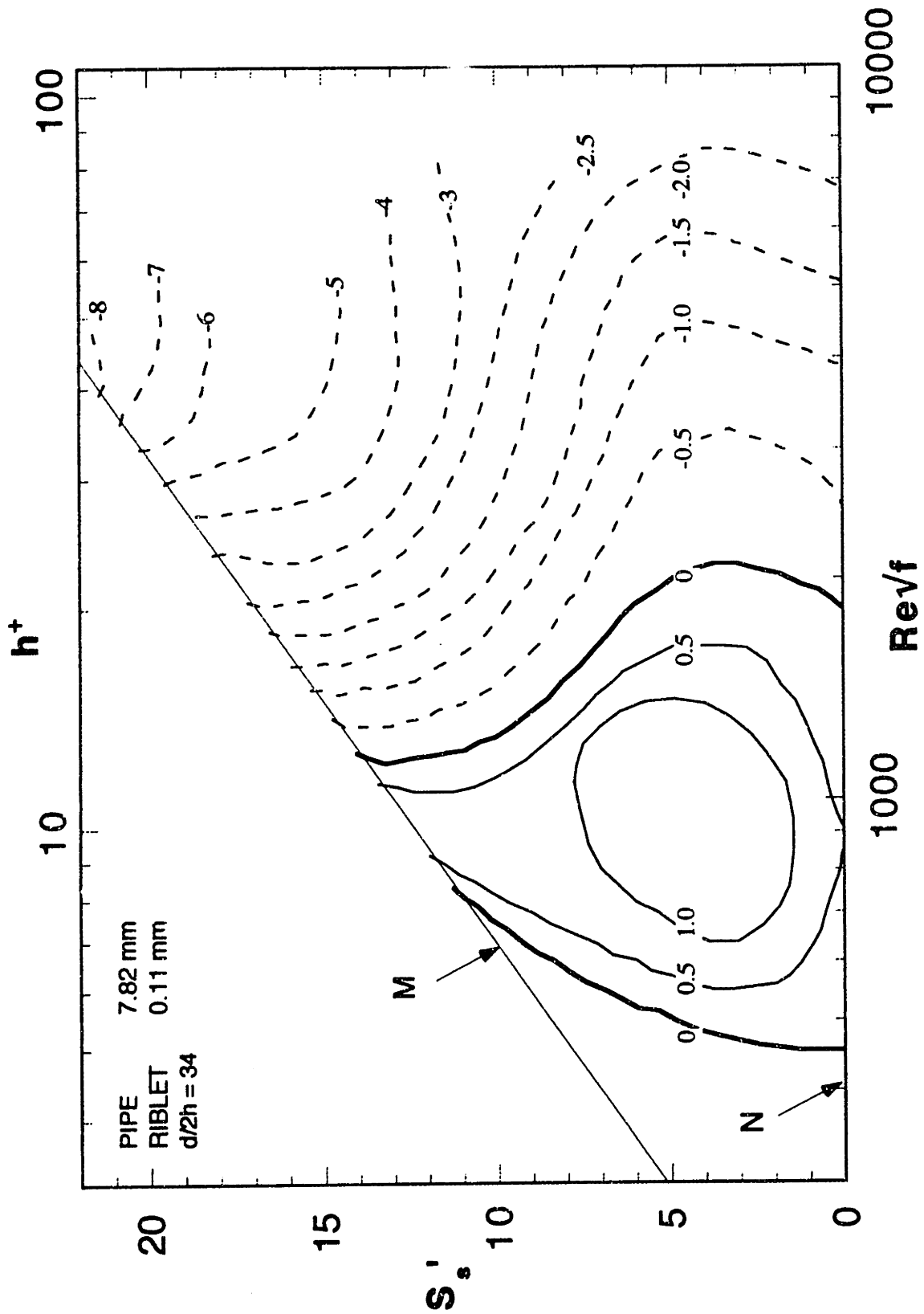


Figure 5.4.3 3-D contour representation of the relation between riblet- and polymer-induced drag reduction in turbulent flow of all polymer solutions in R1A

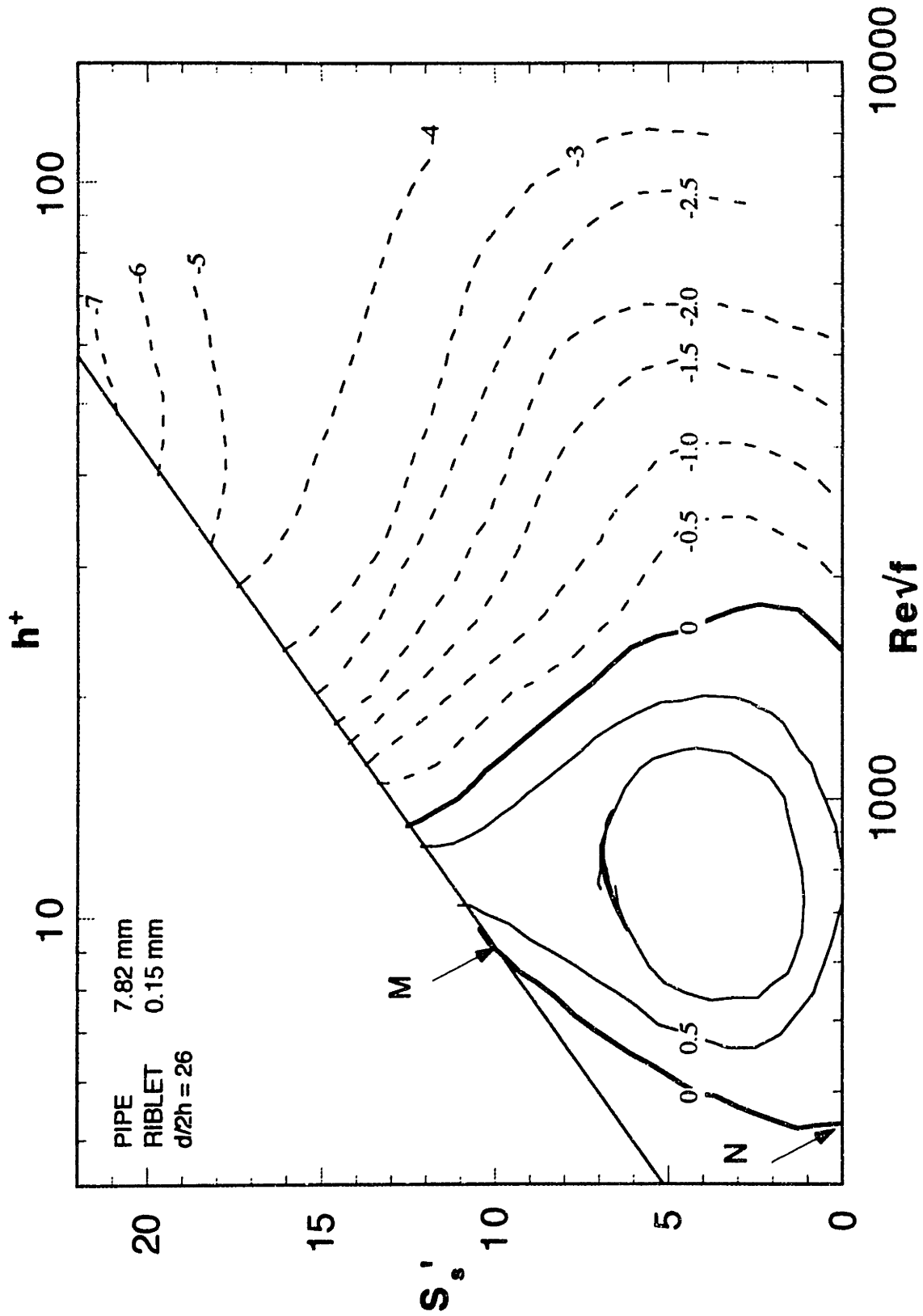


Figure 5.4.4 3-D contour representation of the relation between riblet- and polymer-induced drag reduction in turbulent flow of all polymer solutions in RIB

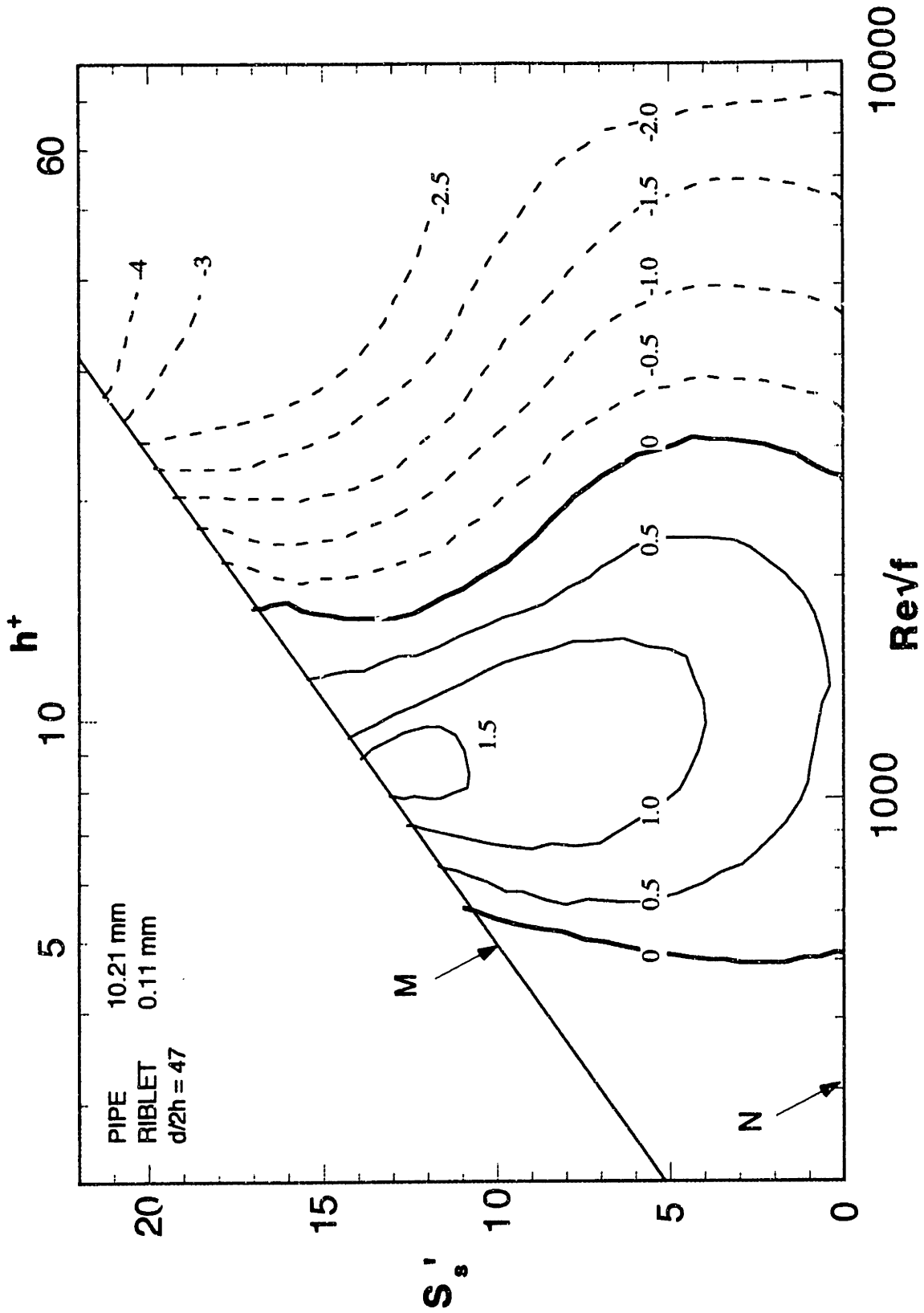


Figure 5.4.5 3-D contour representation of the relation between riblet- and polymer-induced drag reduction in turbulent flow of all polymer solutions in R2A

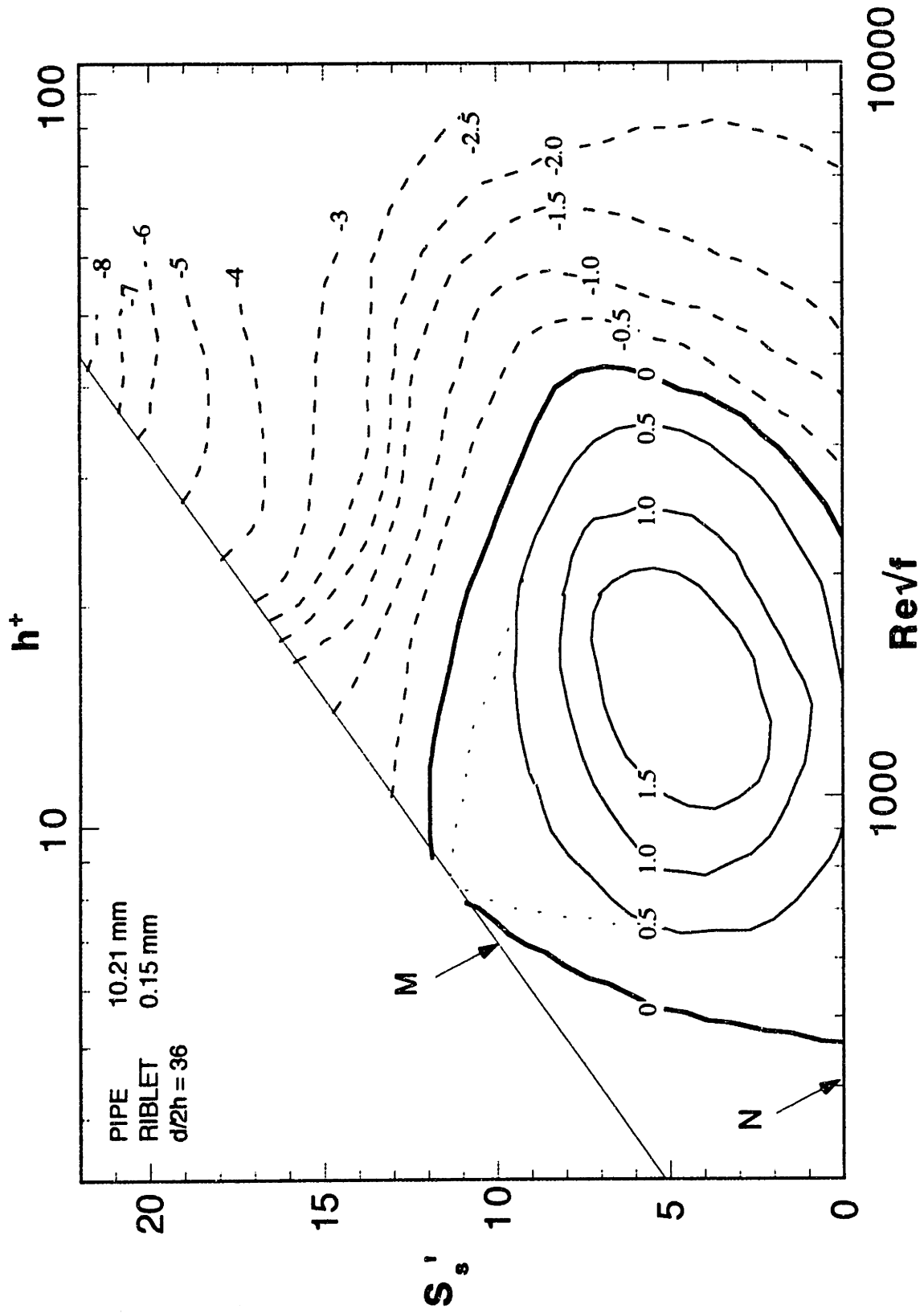


Figure 5.4.6 3-D contour representation of the relation between riblet- and polymer-induced drag reduction in turbulent flow of all polymer solutions in R2B

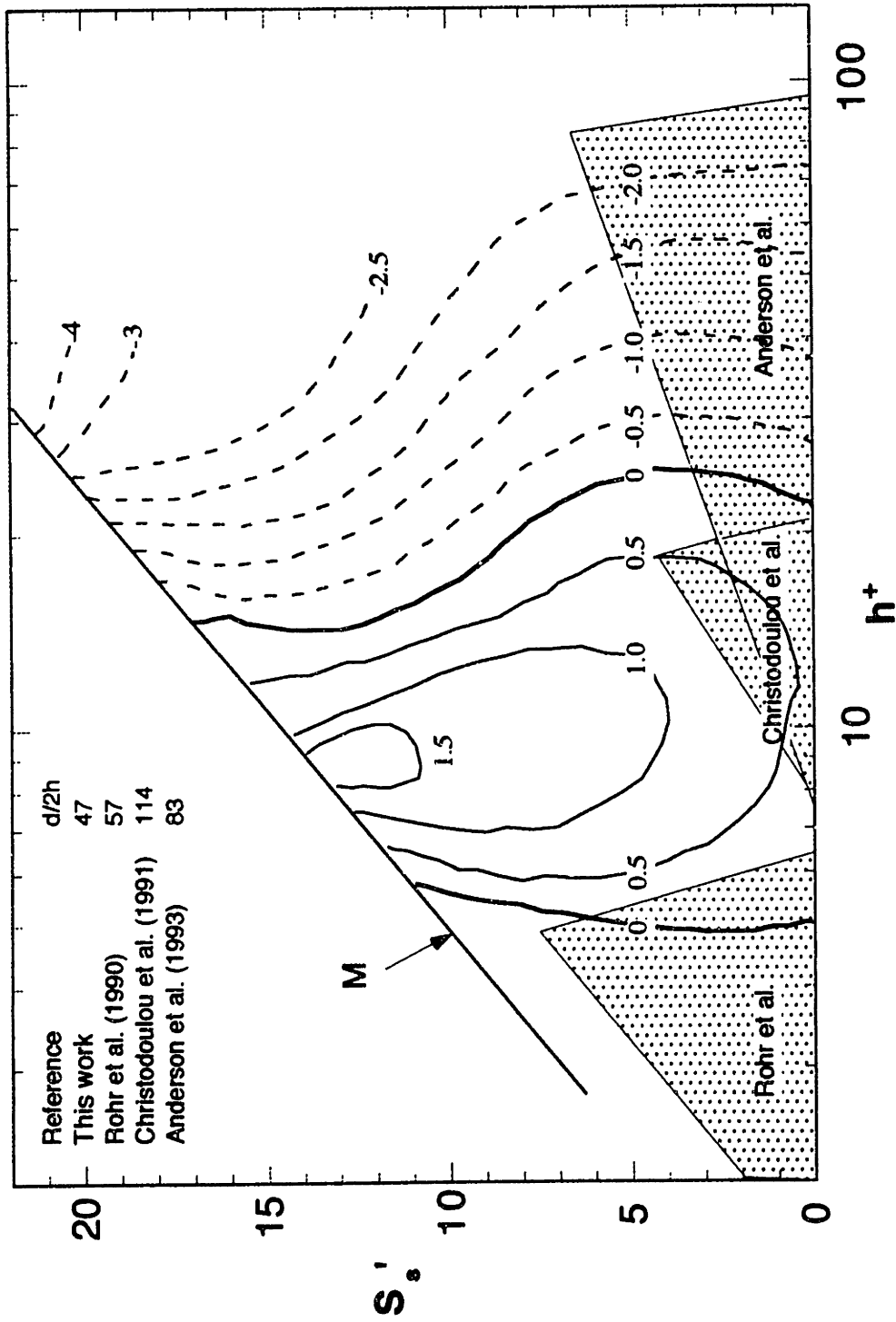


Figure 5.4.7 Analysis of literature in relation to 3-D contour representation of the polymer- and riblet-induced flow enhancement in pipe R2A

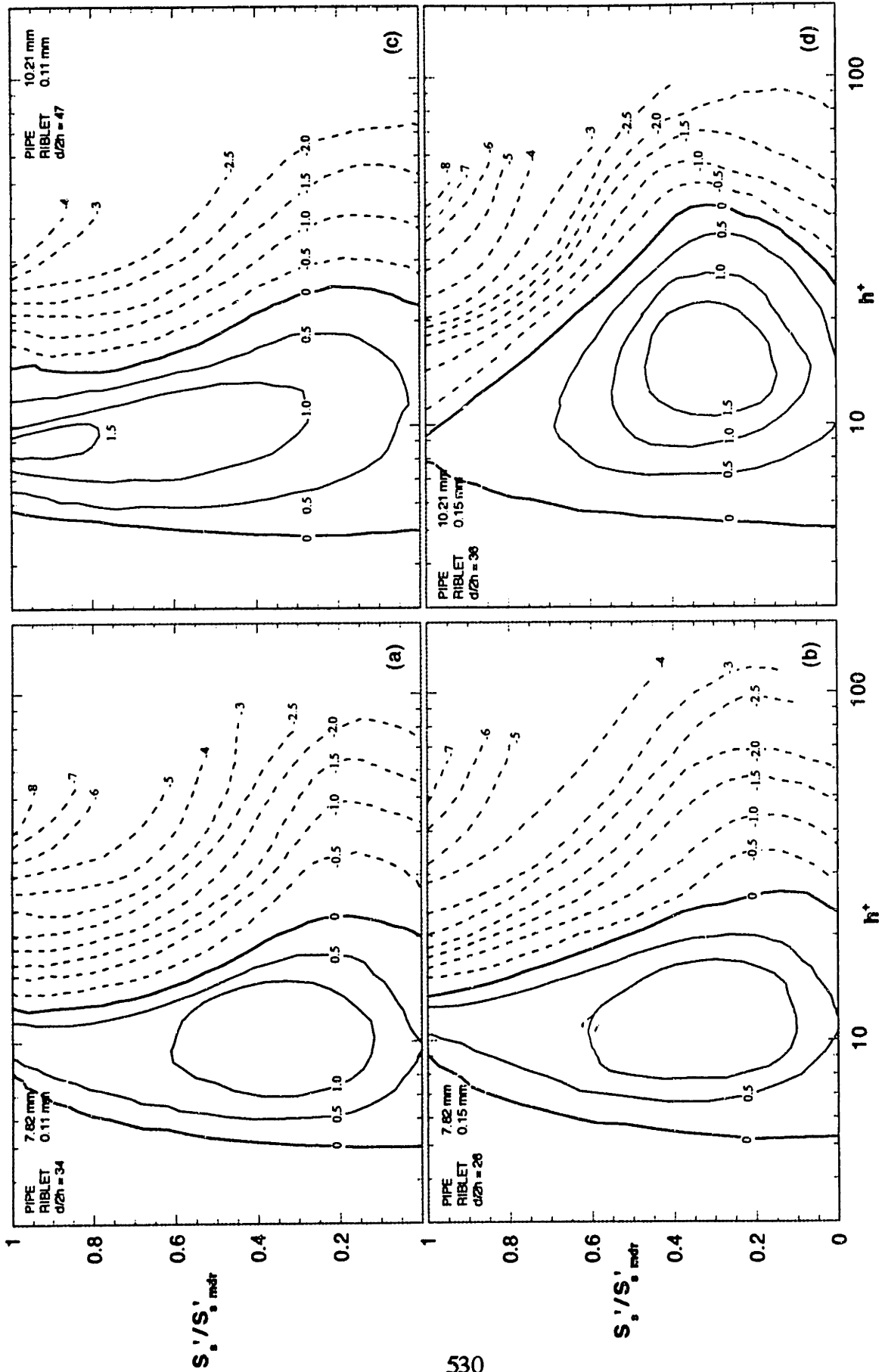


Figure 5.4.8 3-D contour representations of the riblet-induced flow enhancement, R' , using a normalized polymer-induced flow enhancement.

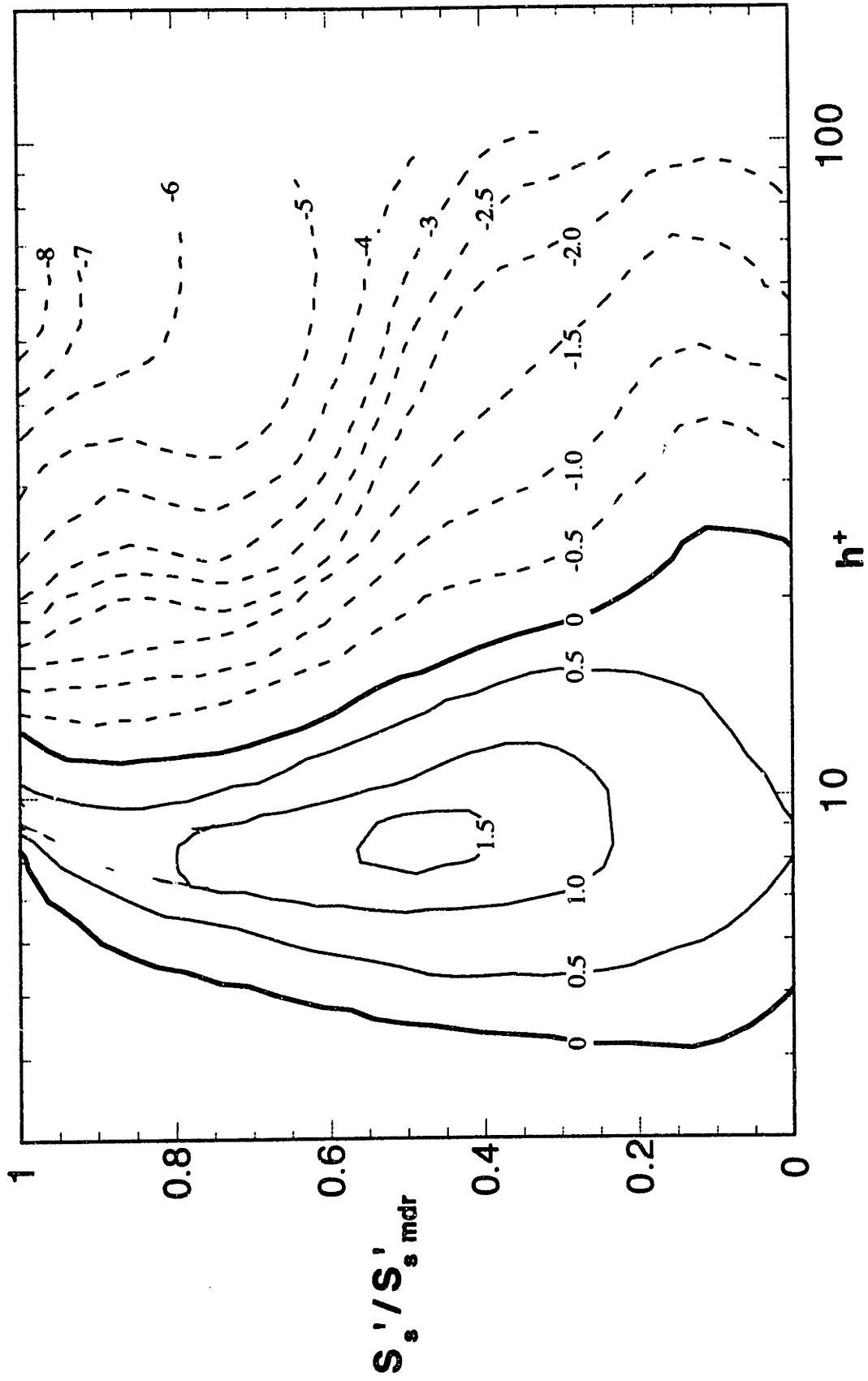


Figure 5.4.9 3-D contour representations of the average riblet-induced flow enhancement, R' , on normalized coordinates for all riblet pipes.

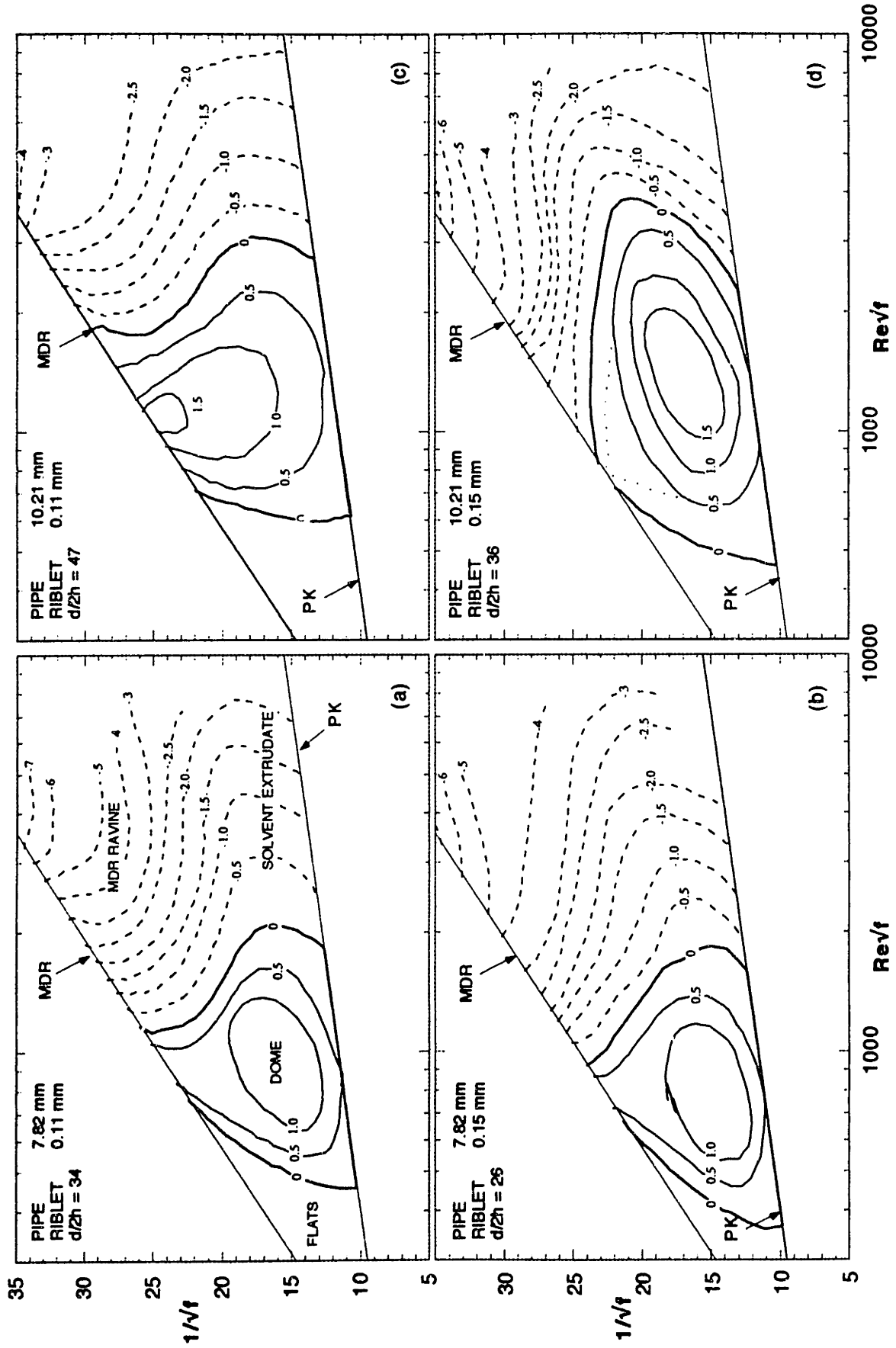


Figure 5.4.10 3-D contour representation of the riblet-induced flow enhancement, R' , on Prandtl-Karman coordinates

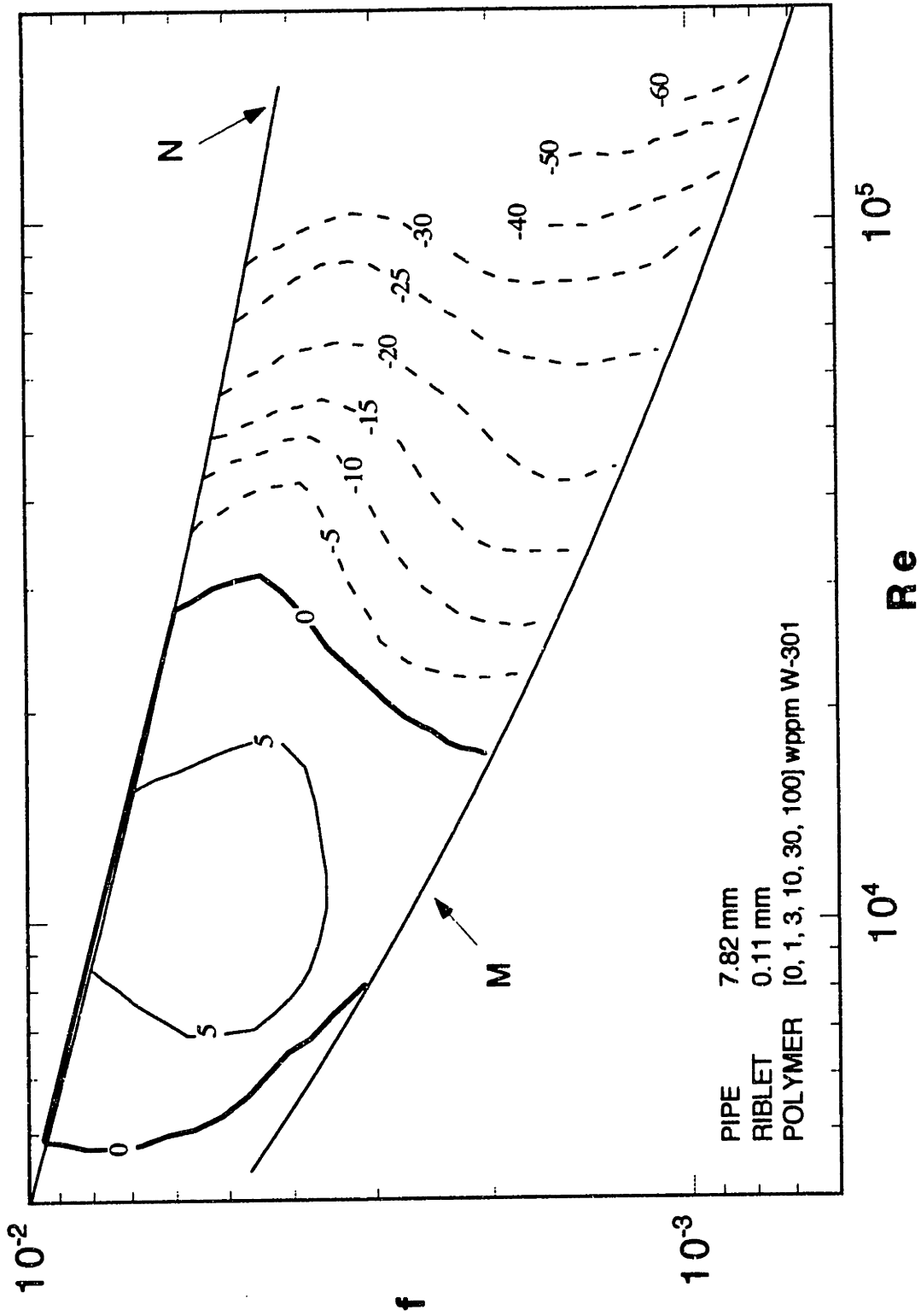


Figure 5.4.11 3-D contour representation of the riblet-induced percentage drag reduction, %DR, on f-Re coordinates

Chapter 6

Summary

6.1 Background

The primary aim of this thesis was to investigate the interaction between two established drag reducing devices, namely, dilute polymer solutions and small streamwise-aligned grooves called riblets. It was hoped that this study would yield insight into the behavior of each device separately and into the features of turbulence that are affected to produce drag reduction.

The turbulent flow of solutions of initially randomly-coiled polymers is characterized by three regimes (Virk, 1975a), in order of increasing flow rate:

- (i) **Newtonian:** In this regime, the flow of a polymer solution is identical to that of the solvent, with no drag reduction.
- (ii) **Polymeric:** The onset of drag reduction occurs at a characteristic wall shear stress, τ_w^* , that depends upon the molecular weight of the polymer but is essentially independent of polymer concentration and pipe diameter. Following onset, the extent of drag reduction increases with increasing flow rate, polymer molecular weight and polymer concentration.
- (iii) **Maximum Drag Reduction:** The maximum drag reduction is ultimately limited by an asymptote that is independent of polymeric parameters and universal in Prandtl-Karman coordinates.

The mechanism of polymeric drag reduction is still imperfectly understood, but some physical insights have emerged (Virk, 1975a, Virk and Wagger, 1989). The onset wall shear stress seems to signify the turbulent flow strength required to stretch an initially

coiled macromolecule towards its contour length. The extended conformation of the macromolecule is apparently capable of interfering with the normal Newtonian wall turbulence. This polymer-turbulence interaction commences in the vicinity of the plane of peak turbulent energy production, and one of its main consequences is a decoupling of the axial and transverse turbulent velocities, which retards radial turbulent transport and induces drag reduction. After onset, the zone of interaction, called the “elastic sublayer”, expands in radial extent, the asymptotic maximum drag reduction being reached when it pervades the entire pipe cross section. Relative to Newtonian, flows at maximum drag reduction exhibit the following structural differences: the viscous sublayer is thickened about twofold, from $y_v^+ \approx 5$ to 12, the plane of peak production is moved outward, from $y_{pp}^+ \approx 12$ to 30, and the mixing length constant in the law of the wall is reduced, from $\kappa = 0.4$ to 0.085.

Among passive drag reduction devices, turbulent boundary layer flows over small longitudinal grooves, called “riblets”, have been extensively studied by Walsh and co-workers (see Walsh, 1990 for a comprehensive review). These workers found first that triangular grooves of roughly equal height and azimuthal spacing, that is, $h/s \approx 1$, provided the optimal drag reduction performance. They further found that, relative to a smooth wall, riblets with $h/s \approx 1$ exhibited two general flow regimes:

- (i) For non-dimensional riblet height $h^+ < 25$, the riblets reduced drag, with the greatest reduction of order 10% at $h^+ \approx 15$.
- (ii) For non-dimensional riblet height $h^+ > 25$, the riblets enhanced drag, by as much as 30% at $h^+ \approx 50$.

Internal flows of air and water in riblet-lined pipes have been investigated by Nitschke (1983); Liu et al. (1989); Rohr et al. (1990); Nakao (1990), and Anderson et al. (1993), and their results show the same behavior as external flows over riblets.

In regard to the mechanism of riblet drag reduction, Walsh (1990) originally devised riblets as “fences” to isolate the low speed streaks that exist near the wall (Kline et al., 1967) and thence retard their bursting. More recently, Bechert et al. (1986) and Choi (1989) have both proposed that riblets impede spanwise motions of the streamwise vortex-pairs associated with sublayer streaks, resulting in weakened bursts and lower shear stresses. These notions are supported by measurements (Choi, 1989, Pulles et al., 1989) over riblet surfaces in their drag-reducing regime, which show all three r.m.s. turbulent intensities, as well as the turbulent shear stress, reduced relative to their respective magnitudes over smooth surfaces at the same free stream velocities. Interestingly, despite the general reduction in turbulent intensities, axial to transverse velocity correlations near the riblet surface remain much the same as those near a smooth surface. This constitutes a mechanistic difference between riblet and polymer drag reduction, because the latter is invariably accompanied by significant reductions in the axial to transverse velocity correlation relative to solvent (Virk, 1975a). Drag enhancement by riblets at high h^+ was attributed by Walsh (1990) to the adverse effects of the increased riblet wetted surface area overwhelming the riblet-induced drag reduction. However, Tani (1988) viewed riblet drag enhancement as being akin to that by sand-roughened pipes, and estimated the equivalent sand roughness of riblets to be about a quarter of their actual height. Most recently, Choi et al. (1993) have presented a direct numerical simulation of turbulent flow over riblets at $h^+ \approx 20$ and 40, respectively in the drag reducing and enhancing regimes. Interpreting their calculations in terms of coherent structures, they suggest that riblets reduce drag when the streamwise vortices above them are aligned such that only a small portion of the riblet, near the tip, is exposed to their “downwash”; at higher h^+ , the streamwise vortices become smaller relative to the riblets, and their downwash affects a greater fraction of the riblet surface, enhancing drag.

The combined effects of riblets and polymers have been investigated in external flow by Philips et al. (1987); Beauchamps and Philips (1988) and Choi et al. (1990) and in

pipe flow by two research groups: one at the Naval Ocean System Center in San Diego, California (Reidy and Anderson, 1988; Rohr et al., 1990; Anderson et al., 1993) and the other at the University of Minnesota (Christodoulou et al., 1991), summarized in Table 1.2.7.

6.2 Experimental

6.2.1 Riblets

The riblets used in this investigation were 3M Scotchcal™ Brand Drag Reduction Tape; a thin, flexible, clear, PVC tape with a precoated pressure sensitive adhesive, protected by a plastic liner. Two types of riblets were tested of nominal heights 0.11 mm and 0.15 mm. Figures 2.2.1 (a) and (b) are photographs of the riblets cross-section taken at 220x magnification using an environmental scanning electron microscope (ESEM). The triangular riblet serrations had sharp peaks, but blunt valleys, with a flat gap, g , at the bottom of adjacent serrations. For the nominal 0.11 and 0.15 mm riblets, $[h, s, g, t] = [0.145 \pm 0.001, 0.165 \pm 0.001, 0.011 \pm 0.001, 0.081 \pm 0.001]$ mm and $[h, s, g, t] = [0.105 \pm 0.001, 0.108 \pm 0.001, 0.015 \pm 0.001, 0.081 \pm 0.001]$, respectively where s is now defined as the peak-to-peak distance. The values were averaged over several snapshots. A schematic of the riblets indicating the dimensions $[h, s, g, t]$ is shown in Figure 2.2.1 (c).

6.2.2 Flow System

A schematic diagram of the experimental flow system is shown in Figure 2.1.1. Each test assembly comprised three sequential sections, namely: (i) an upstream smooth section with wall roughness < 0.0001 mm, (ii) a middle riblet-lined section, and (iii) a trailing smooth section. Six pipes were tested, two hydraulically smooth of nominal

internal diameters, $d_s = 7.82$ mm and 10.21 mm designated S1 and S2, respectively, and four riblet-lined pipes with nominal $[h, d_s] = [0.11, 7.82]$, $[0.15, 7.82]$, $[0.11, 10.21]$ and $[0.11, 10.21]$ mm designated R1A, R1B, R2A, and R2B, respectively.

Each riblet-lined test section, henceforth termed the riblet pipe, was fabricated by first cutting a strip of riblet tape with length and width equal to the length and inner circumference of the pipe respectively. Next, the self adhesive backing of the strip was sprayed with a copious amount of detergent solution and wrapped around a felt-covered dowel, with the adhesive facing outward. With the dowel as a guide, the riblets were inserted into the pipe. Once the riblets were in place, excess detergent was removed by inserting and then carefully pressurizing a length of gum rubber tubing which expanded against the riblets inside the pipe, squeezing detergent out through the tube ends and permanently sticking the riblets to the inner pipe surface. Each test section contained pressure taps ≈ 30 pipe diameters apart which were connected to a set of calibrated 0.7, 7 and 70 kPa differential transducers. At the entrance to the test system, the flow was triggered by a partially closed ball valve, and an entry length of ≈ 60 pipe diameters was provided to ensure fully developed flow by the first pressure tap. Smaller flow re-development lengths, ≈ 35 pipe diameters were provided in the riblet and trailing smooth test sections.

At the most upstream end of the flow system, two 55-gallon tanks, 1.7 m above the laboratory floor, were used to maintain the solutions under investigation. A calibrated Moyno positive displacement pump delivered flowrates from 0.13 to 1.2 l/s through the flow system. Flowrates less than 0.13 l/s were achieved by gravity-driven flow, bypassing the pump. Under gravity driven flow, the flowrate was controlled by a 10-turn needle valve in parallel with a ball valve and determined by measuring the mass of effluent diverted to a 6 l container, per unit time. Fluid temperature, measured by a thermistor placed in the

effluent stream, was held constant at $25\pm 1^\circ\text{C}$ in all experiments. Pressure transducer and thermistor outputs were measured and recorded with a data logger.

Five homologous polyethyleneoxides (PEO), namely N-10; N-750; N-60K; W-301, and P-309, and two homologous polyacrylamides (PAM), N-300L and N-300, were used to investigate drag reduction in the riblet pipes. The polymer concentrations used are summarized in Table 4.1.1, and the polymeric properties summarized in Table 4.5.2. Polymer degradation in the flow system was detected from differences between the pressure gradients in the upstream and trailing smooth sections.

6.3 Results

6.3.1 Solvent Flow

In the smooth pipes, flows of distilled water exhibited regimes of (i) laminar flow, $Re\sqrt{f} < 180$, wherein the data adhere to Poiseuille's law, $f.Re = 16$; (ii) laminar to turbulence transition, $180 < Re\sqrt{f} < 300$, and (iii) turbulent flow, $Re\sqrt{f} > 300$, wherein the data were correlated by the Prandtl-Karman law, $1/\sqrt{f} = 4.0 \log(Re\sqrt{f}) - 0.4$.

In the riblet pipes, flows of distilled water exhibited regimes of (i) laminar flow, $Re\sqrt{f} < 180$, in which the data were downwardly displaced 1.5 to 4% from Poiseuille's law; (ii) transition, $180 < Re\sqrt{f} < 300$, and (iii) turbulent flows, $Re\sqrt{f} > 300$. Within the turbulent regime, the data may be further divided into three regimes:

- (i) Hydraulically smooth, $h^+ < 5$, wherein the P-K law for smooth pipes was obeyed. This was the basis for defining the riblet pipe diameter.
- (ii) Riblet drag reduction, $5 < h^+ < 22$, wherein $1/\sqrt{f}$ exceeded the P-K law, with the greatest riblet-induced flow enhancement $R_n' = 0.5\pm 0.05$ ($1/\sqrt{f}$ units) at $h^+ = 14\pm 1$.

- (iii) Riblet drag enhancement, $h^+ > 22$, wherein $1/\sqrt{f}$ lay below the P-K law, the more so at the higher h^+ , until $R_n' \rightarrow -2.2 \pm 0.4$ for $h^+ > 70$.

6.3.2 Polymer Solution Flow

6.3.2.1 Example

Figure 4.3.1 depicts the flow of solvent and a 3 wppm W-301 polymer solution through the smooth and riblet pipes using P-K coordinates. In the smooth pipe, the polymer solution exhibits regimes of laminar, $Re\sqrt{f} < 180$, transitional, $180 < Re\sqrt{f} < 300$, and turbulent flow, $300 < Re\sqrt{f} < 9000$, the latter having two segments:

- (i) Newtonian: $300 < Re\sqrt{f} < 550$. The polymer solution data follow the solvent.
- (ii) Polymeric: $550 < Re\sqrt{f} < 9000$. A well defined onset of drag reduction occur at $Re\sqrt{f}^* = 550$, beyond which the polymer solution data diverge upwards from solvent. The segment is approximately linear from onset to $Re\sqrt{f} = 4000$, with slope $d(1/\sqrt{f})/d(\log Re\sqrt{f}) = 15$ exceeding that of the solvent line by an amount $\delta = 11$. The data exhibit a shallow maximum at $Re\sqrt{f} = 5000$ and then decline slightly to $1/\sqrt{f} = 21$ at $Re\sqrt{f} = 9000$, their decline at the highest $Re\sqrt{f}$ likely caused by polymer degradation.

In the riblet pipe, the polymer solution exhibits laminar, transitional and turbulent flow regimes similar to those seen in the smooth pipe. The turbulent flow data are viewed in two ways. First, the effect of the polymeric additive is revealed by viewing the polymer solution relative to solvent flow in the riblet pipe. The polymer solution data exhibit two segments, akin to those seen in the smooth pipe, namely:

- (i) Newtonian: $300 < Re\sqrt{f} < 550$. The polymer solution follows the solvent.

(ii) Polymeric: $550 < Re\sqrt{f} < 9000$. The onset of polymeric drag reduction in the riblet pipe occurs at $Re\sqrt{f}^* = 550$, the same as that in the smooth pipe. After onset, the polymeric segment in the riblet pipe is initially akin to that seen in the smooth pipe, increasing roughly linearly, with slope 17, from onset to $Re\sqrt{f} = 2500$, at which point it reaches a maximum and abruptly switches to a second roughly linear segment, slope -5, that persists to the highest $Re\sqrt{f} = 9000$. Detailed scrutiny of the riblet polymeric segment shows it to possess a complex sigmoidal shape that differs from that of the corresponding smooth polymeric segment in much the same manner as the riblet solvent curve differs from the smooth solvent line.

Second, the influence of the riblet wall is seen by viewing the flow of the same polymer solution in the riblet and smooth pipes. The data exhibit three turbulent regimes that mirror those earlier seen for solvent flow, namely:

- (i) Hydraulically smooth: $Re\sqrt{f} < 900$ ($h^+ < 10$). The riblet pipe data essentially follow those in the smooth pipe.
- (ii) Riblet drag reduction: $900 < Re\sqrt{f} < 2700$ ($10 < h^+ < 30$). The riblet pipe data lie above those in the smooth pipe, by as much as 1.6 units of $1/\sqrt{f}$ at $Re\sqrt{f} = 1900$ ($h^+ = 21$).
- (iii) Riblet drag enhancement: $2700 < Re\sqrt{f} < 9000$ ($30 < h^+ < 100$). The riblet pipe data lie below those in the smooth pipe, by 2.3 units of $1/\sqrt{f}$ at the highest $Re\sqrt{f} = 9000$ ($h^+ = 100$).

The extents of the three riblet regimes in the polymer solution flow differed from those in solvent, and the greatest riblet-induced drag reduction in the polymer solution considerably exceeded that seen in the solvent.

6.3.2.2 Drag Reduction Parameters

The two facets of drag reduction by polymer solutions in riblet pipes, as described above, was quantified as follows. First, the effect of the polymer solution (p) relative to the solvent (n) at a fixed $Re\sqrt{f}$ for a given pipe, either smooth (s) or riblet (r) is defined by S' , the polymer-induced flow enhancement:

$$S' = \left[\left(\frac{1}{\sqrt{f}} \right)_p - \left(\frac{1}{\sqrt{f}} \right)_n \right]_{Re\sqrt{f}, \text{ pipe}} \quad (6.3-1)$$

The evaluation of S' from experimental data is illustrated in Figure 4.3.2; the dashed vertical line abcd at $Re\sqrt{f} = 1510$ provides the smooth pipe $S_s' = \underline{ac} = 4.5$ (in units of $1/\sqrt{f}$) and the riblet pipe $S_r' = \underline{bd} = 5.6$.

Second, the effect of the riblet pipe (r) relative to the smooth pipe (s) at a fixed $Re\sqrt{f}$ for a given fluid, either solvent (n) or polymer solution (p) is defined by R' , the riblet-induced flow enhancement:

$$R' = \left[\left(\frac{1}{\sqrt{f}} \right)_r - \left(\frac{1}{\sqrt{f}} \right)_s \right]_{Re\sqrt{f}, \text{ fluid}} \quad (6.2-2)$$

Figure 4.3.2 also shows the evaluation of R' ; at $Re\sqrt{f} = 1510$, line abcd provides for the solvent $R_n' = \underline{ab} = 0.4$ and the polymer solution $R_p' = \underline{cd} = 1.5$.

6.3.2.3 Polymer-induced Flow Enhancement in the Smooth Pipes

Polymer solution flows in the smooth pipe followed previously established patterns of Type A drag reduction, exhibiting:

- (1) A well defined onset of drag reduction, which was characterized by an onset wall shear stress, τ_w^* , and examined in terms of:

- (i) molecular weight. For a fixed solution concentration, τ_w^* decreased with increasing molecular weight.
 - (ii) concentration. The onset wall shear stress, τ_w^* was, at most, a weak function of concentration, $\propto c^{-0.15 \pm 0.08}$.
 - (iii) pipe diameter. For a solution of fixed concentration and molecular weight, τ_w^* was approximately independent of pipe diameter.
- (2) A polymeric regime "fan", in which the extent of drag reduction increased with increasing $Re\sqrt{f}$. The trajectory exhibited an initially linear segment, with slope that exceeded that of the solvent line by an amount δ (slope increment) that was examined in terms of:
- (i) concentration. δ increased with increasing concentration, $\propto c^{0.40 \pm 0.01}$
 - (ii) molecular weight. For a fixed solution concentration, δ increased with increasing molecular weight.
 - (iii) pipe diameter. For a fixed polymer solution, δ was approximately independent of pipe diameter.
- (3) Polymer degradation. In certain cases, associated with the highest molecular weight polymers at high $Re\sqrt{f}$, polymer solution data deviated downwards from a linear trajectory in P-K coordinates. The extent of deviation depended on:
- (i) downstream location. Degradation was detected as a bifurcation between the friction factors measured at an upstream and a downstream smooth pipe measuring station. This occurred at a characteristic wall shear stress, τ_w^\wedge , that was roughly independent of concentration for flows in the polymeric regime. At a fixed τ_w , the severity of degradation at the downstream measuring station was more severe than at the upstream one.
 - (ii) molecular weight. For a given concentration, the wall shear stress for incipient degradation in the polymeric regime was roughly proportional to polymer

molecular weight. Furthermore, at a fixed τ_w , the extent of degradation increased with increasing molecular weight .

(iii) pipe diameter. The wall shear stress at incipient degradation was approximately independent of pipe diameter. For a given concentration and τ_w , degradation was more severe in the smaller pipe.

(4) Maximum drag reduction was attained by solutions of the highest molecular weight polymers, in which the data closely followed the universal MDR asymptote:
 $1/\sqrt{f} = 19 \log Re\sqrt{f} - 32.4$.

6.3.2.4 Polymer-induced Flow Enhancement in the Riblet Pipes

In the riblet pipes the flow of polymer solutions was first viewed relative to solvent, to discern the effect of the polymeric additive:

- (1) The onset of drag reduction in the riblet pipe occurred at the same $Re\sqrt{f}^*$ as in the smooth pipe, and the corresponding onset wall shear stress was also approximately the same as in the smooth pipe.
- (2) In the polymeric regime, following onset, the polymer solutions initially exhibited linear segments on P-K coordinates, akin to those seen in the smooth pipe, with slopes that depended on:
 - (i) concentration. The slope increased with increasing polymer concentration.
 - (ii) molecular weight. For a fixed solution concentration, the slope increased with increasing molecular weight.
 - (iii) pipe diameter. For a fixed polymer solution, the slope was approximately independent of pipe diameter.

However, beyond a characteristic $Re\sqrt{f}$, which decreased with increasing concentration, each polymer solution trajectory switched to a second roughly linear segment of lower slope, which persisted to the highest $Re\sqrt{f}$. The slope of this segment was typically 18 units less than the initial segment.

- (3) The maximum drag reduction in the riblet pipe was limited by an asymptote attained by the highest molecular weight polymer solutions. The maximum asymptotic drag reduction asymptote approximately followed the smooth pipe asymptote up to $Re\sqrt{f} \approx 1000 - 1400$, then switched to a second, polymer independent segment, the equation of which depended on the riblet pipe geometry, $d/2h$.

6.3.2.5 Riblet-induced Flow Enhancement

The flow of each polymer solution in the riblet pipe was also viewed relative to its flow in the smooth pipe, to discern the influence of the riblet wall. Three regimes of riblet-induced flow enhancement were observed, namely:

- (i) **Hydraulically smooth.** This regime, with negligible riblet-induced drag reduction was observed in all of the riblet pipes, amid varying, and considerable, polymer-induced drag reduction, $0 < S_s' < 10$. At low slips, $S_s' < 4$, the hydraulically smooth regime was observed for $3 < h^+ < 5$, as in solvent. Close to the maximum polymer-induced drag reduction, this regime appeared to extend for $3 < h^+ < 10$, somewhat beyond that in solvent, but this is uncertain, on account of both the greater scatter in the polymer solution data relative to solvent and the inherently diffuse upper boundary of this regime.
- (ii) **Riblet drag reduction.** The regime of riblet-induced drag reduction was defined in terms of an h^+ range (the upper bound being better defined than the more diffuse lower

bound), and the magnitude and position of the maximum flow enhancement, R'_{\max} . It was found that the riblet drag reduction regime depended on:

- (1) the polymer-induced flow enhancement, S_s' . For solvent flow, $S_s' = 0$, riblet drag reduction occurred over the range $5 < h^+ < 22$, with the greatest riblet-induced flow enhancement $R_n' = 0.5$ at $h^+ = 14$. For low to moderate slips, $0 < S_s' < 5$, the upper h^+ bound was typically close to or greater than the solvent upper bound, $h^+ = 22$, depending on the riblet pipe. Within this range of polymer-induced flow enhancement, the maximum R' increased with S_s' from $R_n' = 0.50$ to $R_p' \approx 1-2$ depending on the riblet pipe, occurring at $h^+ \leq 14$ for R1A, R1B, R2A and $h^+ \geq 14$ for R2B. For moderate to high slips, $S_s' > 7$, the upper bound $h^+ < 22$, typically, with a maximum $R_p' \approx 0.5-1.0$ at $h^+ < 14$ for pipes R1A and R2A; pipe R2A exhibited a maximum $R_p' \approx 1.5$ even at high $S_s' \approx 12$, and pipe R2B exhibited no discernible drag reduction regime at high slips.
- (2) riblet pipe. All riblet pipes exhibited a riblet drag reduction regime, the upper bound of which followed the same trends in pipes R1A, R1B, and R2A, but not in R2B which exhibited larger upper bounds than the solvent for $S_s' < 7$. The maximum enhancement exhibited similar trends in R1A, R1B, R2A and R2B at low to moderate slips, $S_s' < 5$, but at the highest slips, $S_s' \approx 10$, the maximum enhancement in pipe R2A exceeded those of the smaller diameter riblet pipes, and R2B exhibited no perceptible riblet drag reduction. However, the uncertainty in the results at high polymer-induced drag reductions, $\approx 0.5 1/\sqrt{f}$ units, precludes firmer conclusions concerning the effect of the riblet pipe.
- (iii) Riblet drag enhancement, $R_p' < 0$. At the highest h^+ , the riblets enhanced drag in all polymer solutions, and in all riblet pipes investigated. For low $S_s' < 5$, the riblet drag enhancement was essentially the same as in solvent, that is R_p' decreased with increasing h^+ , with $R_p' \rightarrow -2$ for $h^+ > 70$. At higher $S_s' > 5$, and at higher $h^+ > 30$,

R_p' generally decreased with increasing S_s' for flows in the polymeric regime. Close to the asymptotic maximum drag reduction, R_p' decreased monotonically, and approximately linearly, with increasing h^+ the slopes of these segments, $dR_p'/d\log(h^+) \approx -9.0 \pm 0.2$, being considerably steeper than in solvent.

6.4 Discussion

6.4.1 Smooth Pipes

In the smooth pipes, solutions of a particular polymer series exhibited an average onset wall shear stress τ_w^* which was approximately inversely proportional to the square of the r.m.s. radius of gyration, R_G , and an average specific slope increment, δ/\sqrt{c} , proportional to the polymer molecular weight, M_w . These results yielded a length-scale onset constant $\Omega_L = R_G u_{\tau^*}/\nu = [9.6, 6.9] \times 10^{-3}$ and a slope modulus $\kappa = \delta(M_w/c)^{1/2}/N^{3/2} \approx [68.8, 129] \times 10^{-6}$ for [PEO, PAM], respectively, both of which accord with previous literature (Virk, 1975a). Also, the maximum drag reduction eventually attained by the highest molecular weight polymer solutions in the smooth pipe was shown to closely approach the well known MDR asymptote: $1/\sqrt{f} = 19 \log(Re\sqrt{f}) - 32.4$.

The effect of degradation was accounted for by correlating an apparent degradation rate constant between smooth pipe measuring stations j and k , $(\Delta'_{jk}/S'_k)/t_{res} s^{-1}$ with wall shear stress, τ_w , Pa, as shown in Figure 5.1.3a-d. For each pipe and polymer combination investigated, the results for all polymer concentrations in the polymeric regime of drag reduction collapse onto a single band of the form:

$$(-\Delta'_{jk}/S'_k)/t_{res} = 0; \quad \tau_w < \tau_w^{\wedge} \quad (6.4-1a)$$

$$(-\Delta'_{jk}/S'_k)/t_{res} = \Gamma \log(\tau_w/\tau_w^{\wedge}); \quad \tau_w \geq \tau_w^{\wedge} \quad (6.4-1b)$$

Values of the characteristic degradation-inducing wall shear stress τ_w^* Pa and the inherent degradation rate constant Γ s⁻¹ are given in Table 5.1.1.

6.4.2 Riblet Pipes

6.4.2.1 Solvent Flow

For solvent flow in the riblet pipes, both the extent of the riblet drag reduction regime, $5 < h^+ < 22$, as well as the magnitude and location of the greatest effect, $R' = 0.6$ at $h^+ = 14$, were similar to those reported by earlier workers. In the riblet drag enhancement regime, the data accord with previous work for $22 < h^+ < 70$, but extend to somewhat higher $h^+ = 110$ and suggest an asymptotic $R' \rightarrow -2.2$, constant, for $h^+ > 70$. This differs from rough-walled pipes, wherein drag enhancement increases monotonically with increasing h^+ according to Nikuradse's roughness function, with $R' = 1.71 - 4 \log h^+$ for $h^+ > 70$. Thus the view of riblets as roughness elements (Tani, 1988), derived from early riblet data at $h^+ < 50$, $R' > -1$, is not borne out by our solvent results at high $h^+ > 70$.

A serrated sublayer model was proposed to decouple the drag reducing effect associated with the impedance of spanwise vortices by the riblets and the drag enhancing effect due to their increase in wetted surface area. The model related the equivalent hydraulic diameter, d_h , to the shape of the viscous sublayer over the riblet surface, illustrated schematically in Figure 5.2.3; values of d_h associated with the hydraulically smooth and asymptotic riblet drag enhancement regimes were extracted from the pressure gradient data in Figure 4.2.4. It was then assumed that a non-circular riblet pipe obeyed the smooth pipe friction factor relation when based on d_h , yielding an inherent riblet-induced flow enhancement:

$$R_h' = \left[\left(\frac{1}{\sqrt{f_{h,p}}} \right)_r - \left(\frac{1}{\sqrt{f_{h,n}}} \right)_s \right]_{Re_h \sqrt{f_h}} \quad (6.4-2)$$

Figure 5.2.5 depicts the variation of R_h' with h^+ . For $h^+ < 5$, $R_h' = 0$, the riblets are within the viscous sub-layer so that, by analogy to roughness elements, the riblets are shielded from vortical structures they affect to produce drag reduction. For $h^+ > 80$, the riblets are large enough relative to the scales of flow to contain, and not impede, the near-wall structures, therefore $R_h' = 0$. Riblet drag reduction is confined to the region, $5 < h^+ < 80$, which, coincidentally, corresponds to the region of active turbulence dynamics, that is in the buffer layer. In this region, the maximum $R_h' \approx 1.40$ occurred at $h^+ = 16$, the riblet peak is in the vicinity of the plane of peak turbulence production. This is consistent with the hypothesis that riblet drag reduction is confined to a region close to the riblet peak.

6.4.2.2 Polymer Solution Flow

The onset of polymeric drag reduction in the riblet pipes occurred at the same wall shear stress observed in the tandem smooth pipes, which accord with previous literature (Anderson et al.), 1993. Virk (1971a) proposed that onset is associated with incipient polymer-turbulence interaction in the vicinity of the plane of peak production, $y_{pp}^+ \approx 12$. It is therefore expected that for $y_{pp}^+ > h^{+*}$, the elastic sublayer is formed beyond the riblet tips, for which equality between smooth and riblet onsets is expected. It was not possible to obtain for the (more interesting) case of polymeric onset in riblet pipes with $y_{pp}^+ \ll h^{+*}$, which would force the elastic sublayer to form within the riblet valleys; this would require $h^{+*} = h\Omega_L/R_G \approx 50$.

In the polymeric regime, the riblet and smooth pipes provided approximately equal fractional flow enhancements, $S_{F,r} \approx S_{F,s}$, for $h^{+*} < h^+ < h_{es}^+$, beyond which $S_{F,r}$ may be greater than or less than $S_{F,s}$ depending on the flow enhancement. This behavior is

reminiscent of the “effectively smooth” regime that often follows onset during drag reduction in rough pipes (Virk, 1971a). Of previous work, the data of Anderson (1993) lie in the polymeric regime and exhibit effectively smooth behavior, $S_{F,r} \approx S_{F,s}$ at all $h^+ > h^{+*}$, as does the one 10 wppm PEO solution for which friction factors were reported by Christodoulou (1991).

A polymeric maximum drag reduction asymptote has not previously been reported in riblet pipes. The present experiments show existence of such an asymptote that is a function of d/h . The riblet induced flow enhancement at maximum drag reduction, depicted in Figure 5.3.5, exhibited similar regimes observed in solvent flow, namely: (i) a hydraulically smooth regime, $3 < h^+ < 9 \pm 2$; (ii) a riblet drag reduction regime for $9 \pm 2 < h^+ < 14 \pm 2$, within which the riblets reduced drag beyond that observed by polymer-induced maximum drag reduction by an amount $R'_{m,max} = 1.2 \pm 1.0$ at $h^+ = 11 \pm 1$; it is uncertain whether the variation between the maximum riblet-induced drag reduction is due to the scatter in the data or to d/h ; (iii) riblet drag enhancement $14 \pm 2 < h^+ < 100$, the riblets are drag enhancing relative to the smooth pipe, in which the slope of the $R-h^+$ relation exceeded solvent, reaching $R'_{m,min} = -7 \pm 1$ at $h^+ \approx 60$. The h^+ scaling observed for all pipes in solvent flow is therefore tentatively maintained at maximum polymer drag reduction. The application of the serrated sublayer model at MDR requires the existence of an asymptotic regime of riblet induced drag enhancement, not attained in our present experimental setup; however, the application of the model with judicious choice of model constants suggested that both the viscous sublayer and buffer layer are increased relative to solvent flow.

Since the polymer solution degraded between the smooth pipe and riblet pipe locations at the highest flowrates, it was necessary to correct for the smooth pipe data at the riblet location by invoking the degradation model developed previously. This produced first

order corrections for the polymer-induced flow enhancement in the smooth pipe, S_s' and the riblet-induced flow enhancement, R' .

For a given riblet pipe, it was shown that R' depended only on h^+ and S_s' , and was independent of the additive that produced the flow enhancement. This additive equivalence hypothesis allowed the mutual relationships between R' , h^+ , and S_s' to be illustrated by 3-D contour plots, in Figures 5.4.3 - 5.4.6, for all polymer solutions in each of the riblet pipes investigated. The terrain exhibited by the contours was divided into four regions:

- (1) The flats, $h^+ < 8 \pm 2$, $0 < S_s' < S_{\text{mdr}'}$, $R' \approx 0$, associated with the hydraulically smooth regime.
- (2) The dome, $10 < h^+ < 30$, $0 < S_s' < 10$, $0 < R' < 1.5$, which included a broad maximum at $h^+ \approx 11$.
- (3) The solvent extrudate, $30 < h^+ < 100$, $0 < S_s' < 10$, $-2 < R' < 0$, wherein contours maintained the spacings with which they emanated from the solvent line.
- (4) The MDR ravine, $40 < h^+ < 100$, $10 < S_s' < S_{\text{mdr}'}$, $-8 < R' < -2.5$, in which the terrain descended steeply towards the MDR line, to greater depths at the higher h^+ .

The foregoing regions scaled approximately as h^+ , and possibly with $S'/S'_{\text{mdr}'}$. If the scalings are correct, then our experimental results for all polymer concentrations, polymer molecular weights, polymer types, pipe diameters and riblet heights may be summarized onto a single 3-D contour plot (Figure 5.4.9) that depicts how the riblet induced flow enhancement varied with the polymer-induced drag reductions and riblet height scaled by turbulent flow parameters.

6.4.3 Mechanism

Within the dome region, riblet-induced flow enhancement was of order $R' \approx 1$, even under conditions where the polymer-induced flow enhancement was many times greater, of order $S_s' \approx 5$. The elements of turbulence that riblets affect to induce drag reduction in Newtonian flows must therefore still exist in the flows associated with polymeric drag reduction. This implies that riblets and polymers reduce drag by separate mechanisms. One possibility, in terms of a turbulent burst cycle, is that riblets inhibit the growth stage, reducing burst strength, while polymers alter the breakdown stage, reducing axial to transverse energy transfer.

During polymer drag reduction, the elastic sublayer originates at the plane of peak production, and then increases in radial extent (that is, thickness, as reflected by the slip S'), with corresponding increases in y_v^+ and y_{pp}^+ . Under these conditions, a higher h^+ should be required for the riblet tips to protrude past the viscous sublayer, prolonging the hydraulically smooth regime. This is observed in the present experiments, the somewhat diffuse boundary between the hydraulically smooth and riblet drag reduction regimes shifting from $h^+ \approx 5$ in solvent to $h^+ \approx 9$ in the drag-reducing polymer solutions. Also, since y_{pp}^+ is increased relative to Newtonian, we should expect the greatest riblet-induced drag reduction to occur at higher h^+ , the more so as S' increases. This is tentatively observed when the data for solvent flow and maximum drag reduction are examined in terms of the inherent riblet-induced flow enhancement, R_h' , and therefore requires a further experimental study on the adverse effects of the riblet wetted surface at the higher polymeric drag reductions.

Chapter 7

Recommendations

1. Further gross flow measurements are required to elucidate the asymptotic riblet drag enhancement regime, $h^+ > 70$, for Newtonian flows. Values of h^+ up to $h^+ \approx 500$ are recommended; this may be achieved by increasing flowrates or decreasing d/h . Under the present experimental setup, $h^+ \approx 500$ at $Re\sqrt{f} = 10000$, requires, $d/h = 14$, or $h = 0.55$ mm riblets in the 7.82 mm pipe.
2. The onset of polymer-induced drag reduction occurring in the regime of riblet drag enhancement requires investigation since this sheds light on the relation between the structure of the elastic layer within the riblet valleys. This requires $h^{+*} = h\Omega_L/R_G \approx 50$.
3. The existence of an asymptotic limit at maximum drag reduction needs to be confirmed. This limit may be achieved for $h^+ > 200$, about 2.5 times that of the Newtonian value.
4. The present data suggest the existence of a hydraulically smooth regime within which a riblet surface appears hydraulically smooth. This differs from some preliminary experimental results of Bechert (1995) and computational modeling by Luchini et al. (1991) who suggested the drag reduction by riblets is linear within the viscous sublayer. This requires some further investigation both experimentally and computationally with direct numerical simulation.
5. The observation that conduits with convex cross-sections exhibit different Newtonian f - Re relationships than for smooth circular pipes when based on the geometric hydraulic diameter requires further analysis. One approach would be to investigate both Newtonian and maximum drag reducing flows in non-circular conduits such a

square, triangular, and convex conduits, focusing on the gross flow, the instantaneous velocity and vorticity fields.

Appendix A

Laminar Flow Re-Development After A Sudden Contraction In Pipe Flow

Consider laminar, incompressible flow through a pipe with a sudden contraction as shown in Figure A.1. We follow the analysis of Sparrow et al. (1964) in which the velocity downstream of the contraction, $v_z(r,z)$, may be represented as a perturbation from the fully developed velocity profile downstream of the contraction:

$$v_z(r,z) = v_{z \rightarrow \infty}(r) + v_z^*(r,z) \quad (\text{A.1})$$

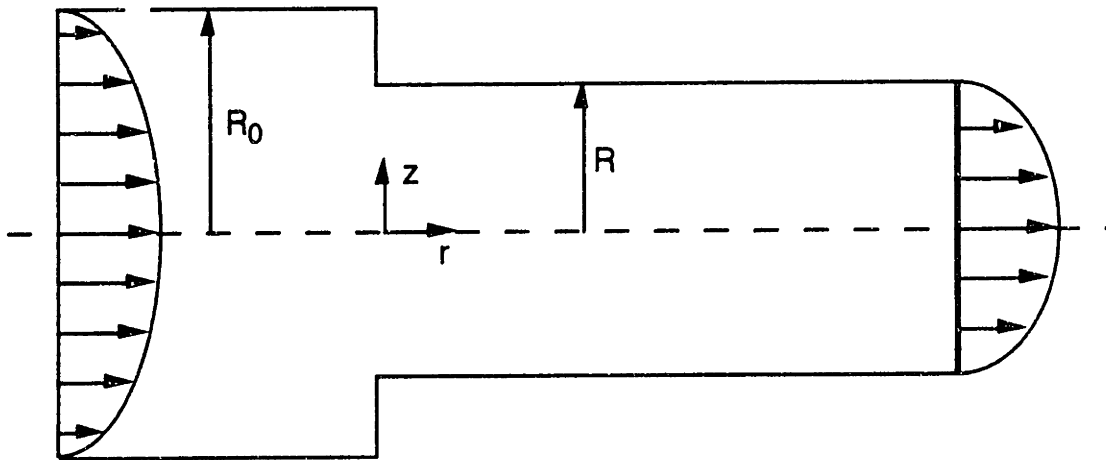


Figure A.1. Flow redevelopment in a pipe contraction.

Assuming (i) the static pressure is uniform across each z ; (ii) the component, $\eta \partial^2 v_z / \partial z^2$, of the axial shear stress is negligible relative to the components of $\eta \nabla^2 v_z$, it may be shown that:

$$w = \frac{u}{U} = 2(1-\xi^2) + \sum_{i=1}^{\infty} A_i \left\{ \frac{J_0(\alpha_i \xi)}{J_0(\alpha_i)} - 1 \right\} \exp(-\alpha_i^2 Z^*) \quad (\text{A.2})$$

where the eigenvalues, α_i , are the roots of:

$$J_1(\alpha_i)/J_0(\alpha_i) = 0.5\alpha_i \quad (\text{A.3})$$

and $w = u/U$, $\xi = \frac{r}{R}$, $Z = \frac{z/R}{UR/\nu}$, $Z^* = \frac{z^*/R}{UR/\nu}$. z^* is a "stretched" axial coordinate which would form a linearized momentum equation, defined by:

$$dz = \epsilon(z) dz^* \quad (\text{A.4})$$

where:

$$\epsilon = \frac{\int_0^1 \{2w - 1.5w^2\} \{\partial w / \partial Z^*\} \xi d\xi}{\partial w / \partial \xi + \int_0^1 (\partial w / \partial \xi)^2 \xi d\xi} \sim 1 \quad (\text{A.5})$$

Eq. (A.5) has been computed numerically by Sparrow et al. (1964). The only unknowns in Eq. (A.2) are the values of A_i for each eigenvalue, determined from the initial condition at $z = 0$. For a plug flow initial velocity profile, $u/U = 1$, $A_i = 2/\alpha_i$.

Considering the velocity along the centerline, $\xi = 0$, and truncating the expansion to first order terms only ($A_1 \gg A_2 \gg A_3 \dots$), then:

$$\frac{u_c}{U} \approx 2 + A_1 \left\{ \frac{1}{J_0(\alpha_1)} - 1 \right\} \exp(-\alpha_1^2 Z^*) \quad (\text{A.6})$$

For $Z^* = 0$, $u_c/U = 2/(R_0/R)^2$, hence:

$$A_1 = \frac{2 \left\{ \left[\frac{R}{R_0} \right]^2 - 1 \right\}}{\left\{ \frac{1}{J_0(\alpha_1)} - 1 \right\}} \quad (\text{A.7})$$

and:

$$\frac{u_c}{U} \approx 2 - 2 \left\{ 1 - \left[\frac{R}{R_0} \right]^2 \right\} \exp(-\alpha_1^2 Z^*) \quad (\text{A.8})$$

Figure A.2 depicts the variation of u_c/U with Z^* for $R/R_0 = 0.96$, which is chosen to closely approximate the contraction from smooth to riblet pipes. Also included are the results for an initial plug flow profile:

$$\frac{u_c}{U} \approx 2 - \exp(-\alpha_1^2 Z^*) \quad (\text{A.9})$$

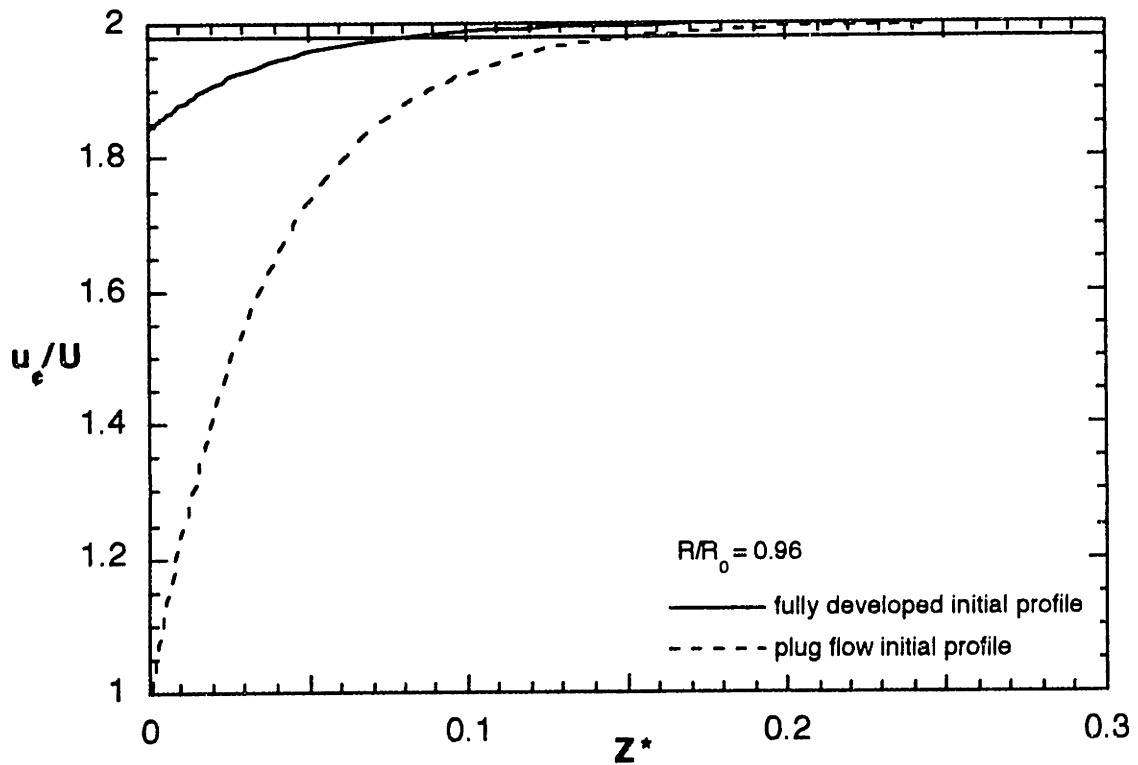


Figure A.2. Variation of the centerline velocity with scaled distance downstream of contraction.

The centerline velocity is within 98% of the fully developed downstream velocity at $Z^* \approx 0.07 \Rightarrow Z = 0.08$. In laminar flow, the flow development length, $L_e/d \approx Re/50$.

Appendix B

Contour Plot Generation

The contour plots generated in section 5.3.2 were created in the following manner:

- (1) For a given riblet pipe, including the corresponding replicated pipe, data for solvent and all polymer solutions were imputed into a single computer spreadsheet file named $abbC.WKS$, where $a = 3$ or 4 refers to the 7.82 and 10.1 mm pipes, and $bb = 45$ or 60 refers to the 0.11 mm and 0.15 mm riblets, respectively. Each column contained pipe and riblet information, polymer type and concentration, the non-dimensional riblet height, h^+ , $\log h^+$, the degradation corrected polymer-induced flow enhancement in the smooth pipe, $S_s'_{corr}$, and the degradation corrected riblet induced flow enhancement, R'_{corr} .
- (2) Solvent flow data were inserted for each polymer type, thereby weighting the solvent data, ensuring that computer software used for generating the contour plots would be forced to capture the physics exhibited by solvent flow.
- (3) The data were sorted in order of ascending R' . Contours were plotted in 1 unit intervals for $R' < -3$ and 0.5 unit intervals for $R' > -3$. A contour level, l , was assigned to each value of R' to which it closely corresponded. For example, for $-5.5 < R' < -4.5$ a contour level, $l = -5$, was assigned, and for $0.25 < R' < 0.75$, $l = 0.5$.
- (4) The data were parsed for each contour level, producing separate $(x(l), y(l), z(l), l)$ columns, where $x = \log h^+$, $y = S_s'_{corr}$, $z = R'_{corr}$.
- (5) The new file was then named $abbP.WKS$.

- (6) Both files abbC.WKS and abbP.WKS were imported into a contour plotting computer software package, AXUM™, then the contours were generated; the settings, which included grid density and coarseness of fit, were adjusted to produce contours that reasonably matched the parsed data. However, since the data were irregularly spaced and the program interpolated on a rectangular grid, contours were created in regions where there were no data. An output of such a result generated by AXUM is illustrated for pipe R1A in Figure B.1, with parsed data represented by separate symbols for each contour level.
- (7) Using the parsed data, and with the computer generated contours as a guide, a better estimate of the contours was made by manually tracing over the contours, paying particular care to capture all the physics observed in Chapter 4. The tracing generally commenced with the null contour, $l = 0$.
- (8) The contours were then digitized, producing $(\log h^+, S_s')$ data at each contour level. This allowed manipulation and coordinate transformation of the data to produce high quality graphical outputs. Figure B.2 illustrates how the final output compares to the parsed data.

Effect of Riblets on Polymeric Drag Reduction
 0.11 mm Riblets, 7.82 mm id Pipe, All Polymers

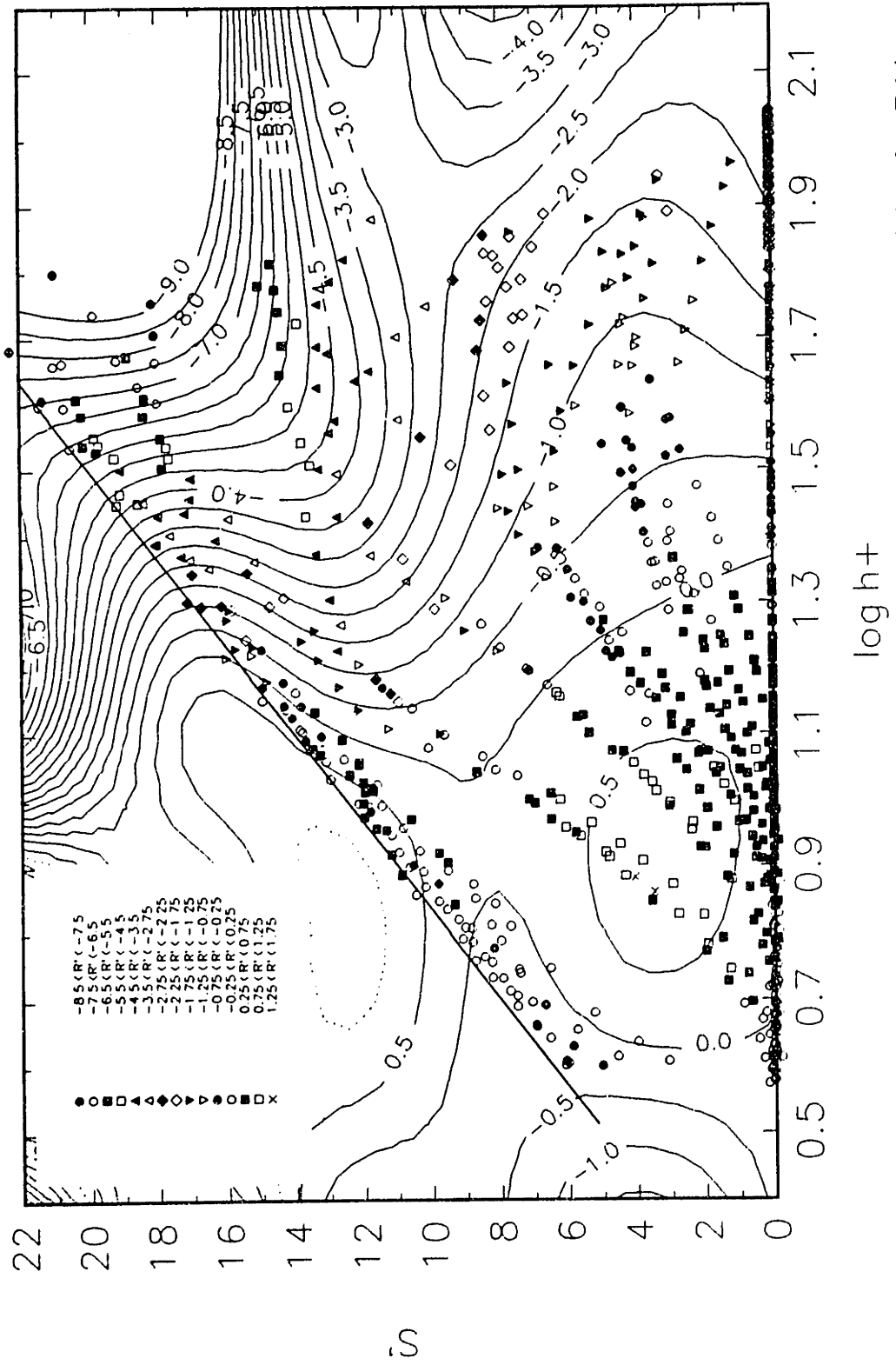


Figure B.1 Overlay of parsed data plot and computer generated contours for riblet pipe R1A

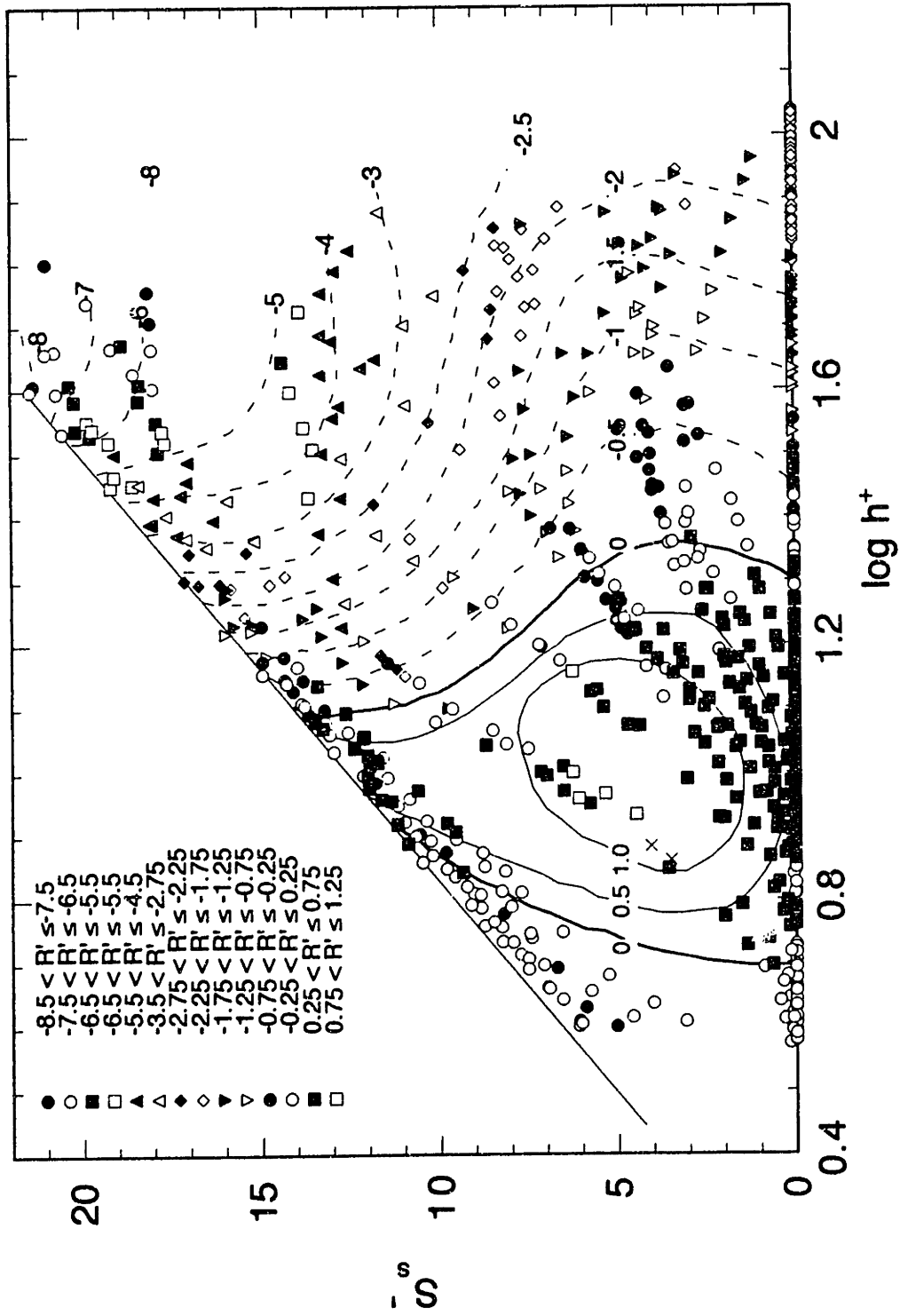


Figure B.2 Overlay of parsed data plot and traced contours for riblet pipe R1A

Appendix C

Nomenclature

English Symbols

a, K	Mark-Houwink parameters (Eq. 1.3-7)
A	area
c	polymer solution concentration, in parts per million
C	generalized constant
C_{uv}	u-v correlation coefficient
d	pipe inside diameter
%DR	percentage drag reduction
f	Fanning's friction factor
f	friction coefficient of polymer molecules in solvent
F	frequency
g	gap between triangular serrations
\mathbf{g}	gravity vector
G	stress deficit
h	riblet height
H	heterogeneity index
k	roughness height
k_1, k_2	constants in Huggins' intrinsic viscosity relation
K_{PT}	pressure transducer calibration constant
ℓ	mixing length
l_0	backbone chain link length
L	length
L_c	polymer contour length
L_e	entry length
m	mass
m_0	molecular weight per backbone chain link
M	monodisperse polymer molecular weight
M_n	number average molecular weight
M_w	weight average molecular weight
M_v	viscosity average molecular weight
M_z	z-average molecular weight
N	number of backbone chain links

N_A	Avogadro's constant
P	mean pressure
P	pressure gradient ratio
P_w	wetted perimeter
Q	volumetric flow rate
r	radius of curvature
R	pipe radius
R	molar gas constant
R'	riblet-induced flow enhancement
R_F	riblet-induced fractional flow enhancement
R_G	macromolecule root mean square radius of gyration, z-average
Re	Reynolds number
s	riblet spacing
S'	polymer-induced flow enhancement
S^+	effective slip
S_F	polymer-induced fractional flow enhancement
t	time
t_{res}	residence time
t	riblet pedestal thickness
T	temperature
T_b	turbulence burst times
u, v, w	fluctuating velocity components in x, y, z directions
U	mean velocity
w	weight fraction
w	wake function
Z	azimuthal streak spacing

Greek Symbols

α	expansion coefficient
β	roughness function
χ	mixing length constant
δ	slope increment
Δ'	degradation-induced flow enhancement parameter
ϵ	eddy viscosity
Φ	Flory's viscosity constant

Φ	profile parameter
Γ	slope of degradation segments
η	viscosity
φ_1, φ_2	correlation coefficients of Eq. (1.3-11)
κ	slope modulus
ν	kinematic viscosity
Π	intrinsic slope increment
ρ	density
τ	shear stress
ω_{Γ}	ratio of equivalent to geometric hydraulic diameters
ξ	ratio of equivalent hydraulic diameter to that in the VSL
ψ	polymer solution parameter
Ω	onset constant

Superscripts

*	at onset of polymeric drag reduction
+	normalized by inner scales, u_{τ} and ν
#	critical condition
^	at onset of observed polymer degrdation

Subscripts

av	average
c	at the riblet cross-section
d	downstream
e	elastic sub-layer
es	effectively smooth
E	energy-based
h	at the “equivalent” hydraulic plane
H	at the “geometric” hydraulic plane, $4A_{\sigma}/P_w$
inh	inherent
L	length-based
m	maximum drag reduction
max	maximum
min	minimum
MB	master batch
n	solvent

p	polymer solution
pp	at plane of peak turbulence production
r	riblet pipe
red	reduced
rel	relative
s	smooth pipe
sp	specific
t	at the riblet peak
T	time-based
u	upstream
v	at the riblet valley
v	viscous sub-layer
w	at wall
z	at the cross-over from riblet-induced drag reduction to drag enhancement regime

Other Symbols

< >	time average
	intrinsic

Appendix D

References

- Achia, B. U. & Thompson, D. W. 1977 Structure of the turbulent boundary in drag reducing pipe flow, *J. Fluid Mech.* **81**(3), 439-464.
- Alhousseini, A. A. 1989 Numerical Simulation of Turbulent Flows with Drag Reducing Polymeric Additives, *M.S. Thesis*, Arizona State University.
- American Cyanamid Co. 1955 *New Product Bulletin* No. 34.
- Anderson, G. W., Rohr, J. J. & Stanley, S. D. 1993 The combined drag effects of riblets and polymers in pipe flow, *J. Fluids Engin.* **115**, 213-221.
- Atkinson, B., Brocklebank, M. P., Card, C. C. H. & Smith, J. M. 1969 Low Reynolds number developing flows, *AIChE. J.* **15**(4), 548.
- Aydin, M. & Leutheusser, H. J. 1986 Flow visualization of coherent structures in turbulent open-channel flow. In: Turbulence Measurements and Flow Modeling, C. J. Chen, L.-D. Chen and F. M. Holly Jr. (eds.), Hemisphere.
- Bacher, E. V. & Smith, C. R. 1985 A combined visualization anemometry study of the turbulent drag reducing mechanisms of triangular micro-groove surface modifications, *AIAA Paper* 85-0548.
- Bailey, F. E. & Callard, R. W. 1959 Some properties of poly(ethylene oxide) in aqueous solution, *J. Appl. Poly. Sci.* **1**, 373.
- Bailey, F. E., Kucera, J. L. & Imhof, L. G. 1958 Molecular weight relations of poly(ethylene oxide), *J. Poly. Sci.* **32**, 517.
- Barbour, K. L. 1972 Degradation Kinetics of Dilute Polymer Solutions, *M.S. Thesis*, M.I.T.
- Baron, A., Quadrio, M. & Vigevano, L. 1993 On the boundary layer/riblets interaction mechanisms and the prediction of turbulent drag reduction, *Int. J. Heat and Fluid Flow* **14**(4), 324-332.
- Bartels, P. V., Markus, A. & Smith, J. M. 1985 The turbulent mixing of viscoelastic fluids in pipe flow. In: The Influence of Polymer Additives on Velocity and Temperature Fields, B. Gampert (ed.), Springer-Verlag.
- Beauchamps, C. H. & Philips, R. B. 1988 Riblet and polymer drag reduction on an axysymmetric body, *Proc. Symposium on Hydrodynamic Performance Enhancement for Marine Applications*, pp. 127-134, Newport, Rhode Island.
- Bechert, D. W. 1987 Experiments on three-dimensional riblets. In: Turbulent Drag Reduction by Passive Means, Royal Aeronautical Society.

- Bechert, D. W. 1995 3-D riblets, *Euromech Colloquium 332 - Drag Reduction (Proc. 9th European Drag Reduction Meeting)*, Ravello, Italy.
- Bechert, D. W. & Bartenwerfer, M. 1989 The viscous flow on surfaces with longitudinal ribs, *J. Fluid Mech.* **206**, 105-129.
- Bechert, D. W., Bartenwerfer, M., Hoppe, G. & Reif, W.-E. 1986 Drag reduction mechanism derived from shark skin, *ICAS Paper* 86-1.8.3.
- Bechert, D. W., Hoppe, G. & Reif, W.-E. 1985 On the drag reduction of a shark skin, *AIAA Paper* 85-0546.
- Berman, N. S. 1977 Flow time scales and drag reduction, *Phys. Fluids* **20**(10), S168-S174.
- Berman, N. S. 1978 Drag reduction by polymers, *Ann. Rev. Fluid Mech.* **10**, 47-64.
- Berman, N. S. 1990 Polymer contributions to the transport equations, *Proc. Drag Reduction in Fluid Flows*, R. H. J. Sellin and R. T. Moses (eds.), Ellis Horwood.
- Bewersdorff, H.-W. 1984 Heterogeneous drag reduction in turbulent pipe flows, *Rheol. Acta.* **23**(5), 522-543.
- Bewersdorff, H.-W. & Pertersmann, A. 1987 Drag reduction in artificially roughened pipes, *Chem. Eng. Comm.* **60**, 293-309.
- Brachet, M. E. 1991 Direct simulation of three-dimensional turbulence in the Taylor-Green vortex, *Fluid Dyn. Res.* **8**(1-4), 1-8.
- Brachet, M. E. 1994 Numerical Simulations (Direct), *NATO Advanced Study Institute Series B341*, 45.
- Bushnell, D. M. & Hefner, J. N. (eds.) 1990, Viscous Drag Reduction in Boundary Layers, Progress in Astronautics and Aeronautics, Volume 123, AIAA.
- Choi, H., Moin, P. & Kim, J. 1993 Direct numerical simulation of turbulent flow over riblets, *J. Fluid Mech.* **255**, 503-539.
- Choi, K.-S. 1989 Near wall structure of a turbulent boundary layer with riblets, *J. Fluid Mech* **208**, 417-458.
- Choi, K.-S. 1989 Drag reduction mechanisms and near-wall turbulence structure with riblets. In: Structure of Turbulence and Drag Reduction, A. Gyr (ed.), pp. 553-560, Springer-Verlag.
- Choi, K. S., Gadd, G. E., Pearcey, H. H., Savill, A. M. & Svensson, S. 1990 Drag reduction with a combined use of riblets and polymer coating. In: Drag Reduction in Fluid Flows, R. H. J. Sellin and R. T. Moses (ed.), pp. 263-270, Ellis Horwood.
- Choi, K. S. & Fujisawa, N. 1993 Possibility of drag reduction using d-type roughness, *Appl. Sci. Res.* **50**(3-4), 315-324.
- Christodoulou, C., Liu, K. N. & Joseph, D. D. 1991 Combined effects of riblets and polymers on drag reduction in pipes, *Phys. Fluids A* **3**(5), 995-996.

- Chu, D. C. & Garniadakis, G. E. 1993 A direct numerical simulation of laminar and turbulent flow over riblet-mounted surfaces, *J. Fluid Mech.* **250**, 1-42.
- Clark, J. A. & Markland, E. 1970 Vortex structures in turbulent boundary layers, *Aeronaut. J.* **74**, 243-244.
- Clauser, F. H. 1954 Turbulent boundary layers in adverse pressure gradients, *J. Aero. Sci.* **21**, 91-108.
- Coles, D. 1956 The law of the wake in the turbulent boundary layer, *J. Fluid Mech.* **1**, 191.
- Collinson, E., Dainton, F. S. & McNaughton, G. S. 1956 The polymerization of acrylamide in aqueous solution. Part 2. The effect of ferric perchlorate on the X- and γ -ray initiated reaction, *Trans. Far. Soc.* **53**, 489-498.
- Corino, E. R. & Brodkey, R. S. 1969 A visual study of the wall region in turbulent flow, *J. Fluid Mech.* **37**, 1.
- Crouzet, C. & Marchal, J. 1973 Characterizations des reactions primaires de degradation oxydante au cours de l'autooxydation de polyethylenes a 25°C: l'étude en solution avec amorçage par radiolyse du solvant, *Makromol. Chem.* **166**, 69.
- Deissler, R. G. 1955 Analysis of turbulent heat transfer, mass transfer and friction in smooth tubes at high Prandtl and Schmidt numbers, *NACA Tech. Report* No. 1210.
- den Toonder, J. M. J., Hulsen, M. A., Kuiken, G. D. C. & Nieuwstadt, F. T. M. 1995 Drag reduction by polymer additives: numerical and laboratory experiments, *Proc. Euromech Colloquium 332 - Drag Reduction (9th European Drag Reduction Meeting)*, Ravello, Italy.
- den Toonder, J. M. J., Nieuwstadt, F. T. M. & Kuiken, G. D. C. 1995 The role of elongational viscosity in the mechanism of drag reduction by polymer additives, to appear in *Appl. Sci. Res.*
- Djenidi, L., Liandrat, J., Anselmet, F. & Fulachier, L. 1989 Numerical and experimental investigation of the laminar boundary layer over riblets, *Appl. Sci. Res.* **46**, 263-270.
- Donohue, G. L., Tiederman, W. G. & Reischman, M. M. 1972 Flow visualisation of the near wall region in a drag reducing channel flow, *J. Fluid Mech.* **56**(3), 559-575.
- Douady, S., Couder, Y. & Brachet, M. E. 1991 Direct observation of the intermittency of intense vorticity filaments in turbulence, *Phys. Rev. Lett.* **67**, 983-986.
- Einstein, H. A. & Li, H. 1958 Secondary currents in straight channels, *Trans. Am. Geophysical Union* **39**(6), 1085-1088.
- Enyutin, G. V., Lashkov, Y. A., Samoilo, N. V., Fadeev, I. V. & Shumilkina, E. A. 1987 Experimental investigation of the effect of longitudinal riblets on the friction drag reduction of a flat plate, *Fluid Dynamics* **22**(2), 284-289.

- Fabula, A. G., Lumley, J. L. & Taylor, W. D. 1966 Some interpretations of the Toms effect. In: Modern Developments in the Mechanics of Continua, S. Eskinazi (ed.), Academic Press.
- Flory, P. J. & Fox, T. G. 1951 Treatment of intrinsic viscosities, *J. Amer. Chem. Soc.* **73**, 1904-1908.
- Gallager, J. A. & Thomas, A. S. W. 1984 Turbulent boundary layer characteristics over streamwise grooves, *AIAA Paper* 84-2185.
- Gampert, B. & Rensch, A. 1993 Schwankungsgrößen und lösungsstruktur bei der turbulenten strömung von polymerlösungen, *Z. angew. Math. Mech.* **73**(6), T529-T531.
- Gampert, B. & Rensch, A. 1995 Turbulence structure and polymer solution structure in drag reduced turbulent channel flow, *Euromech Colloquium 332 - Drag Reduction (Proc. 9th European Drag Reduction Meeting)*, Ravello, Italy.
- Gampert, B. & Yong, C. K. 1989 The influence of polymer additives on the coherent structure of turbulent channel flow. In: Structure of Turbulence and Drag Reduction, A. Gyr (ed.), pp. 223-232, Springer-Verlag.
- Giesekus, H. & Hibberd, M. F. 1989 Turbulence phenomenon in drag reducing fluids. In: Transport Phenomena in Polymeric Systems, R. A. Mashelkar, A. S. Mujumdar and R. Kamal (eds.), Ellis Horwood.
- Grass, A. J. 1971 Structural features of turbulent flow over smooth and rough boundaries, *J. Fluid Mech.* **50**, 233.
- Gyr, A. 1993 Personal Communication.
- Gyr, A., Hoyer, K. & Tsinober, A. 1995 On the mechanism of drag reduction in dilute polymer solutions, *Euromech Colloquium 332 - Drag Reduction (Proc. 9th European Drag Reduction Meeting)*, Ravello, Italy.
- Hammes, G. G. & Roberts, P. B. 1968 Cooperativity of solvent-macromolecule interactions in aqueous solutions of polyethylene glycol and polyethylene glycol-urea, *J. Amer. Chem. Soc.* **90**, 7119.
- Hinze, J. O. 1975 Turbulence, 2nd Edition, McGraw Hill.
- Hooshmand, A. 1985 An Experimental Investigation of the Influence of a Drag Reducing, Longitudinally Aligned, Triangular Riblet Surface on the Velocity and Streamwise Vorticity Fields of a Zero-Pressure Gradient Turbulent Boundary Layer, *Ph.D. Thesis*, University of Maryland.
- Hooshmand, D., Youngs, R. & Wallace, J. M. 1983 An experimental study of changes in the structure of a turbulent boundary layer due to surface geometry changes, *AIAA Paper* 83-0230.
- Huggins, M. L. 1942 The viscosity of dilute solutions of long-chain molecules. IV. Dependence on concentration, *J. Amer. Chem. Soc.* **64**, 2716-2718.

- Kane, R. S. 1990 Drag reduction by particle addition. In: Viscous Drag Reduction in Boundary Layers, Progress in Astronautics and Aeronautics, D. M. Bushnell and J. N. Hefner (eds.), pp. 433-432, AIAA.
- Kenedy, J. F., Hsu, S.-T. & Liu, J.-T. 1973 Turbulent flows past boundaries with small streamwise fins, *J. Hydraul. Div.* **99**(HY4), 605-616.
- Kezirian, M. T. 1993 The Effects of Polymer Additives on the Hydrodynamic Stability of Thin Liquid Films, *Doctoral Thesis Proposal*, Massachusetts Institute of Technology.
- Kim, H. T., Kline, S. J. & Reynolds, W. C. 1971 The production of turbulence near a smooth wall in a turbulent boundary layer, *J. Fluid Mech.* **50**, 133.
- Kirkwood, J. G. & Riseman, J. 1948 The intrinsic viscosities and diffusion constants of flexible macromolecules in solution, *J. Chem. Phys.* **16**, 565-573.
- Klein, J. & Conrad, K. 1978 Molecular weight determination of poly(acrylamide) and poly(acrylamide-co-sodium acrylate), *Makromol. Chem.* **179**, 1635-1638.
- Kline, S. J., Reynolds, W. C., Schraub, F. A. & Runstadler, P. W. 1967 The structure of turbulent boundary layers, *J. Fluid Mech.* **30**, 741.
- Kramer, M. 1937 Einrichtung zur Verminderung des Reibungsweite stands, *German Patent No 669897, March 17*.
- Kulicke, W., Kniewske, R. & Klein, J. 1982 Preparation, characterization, solution properties and rheological behavior of polyacrylamide, *Prog. Polym. Sci.* **8**, 373-468.
- Landahl, M. T. 1972 Drag reduction by polymer addition, *Proc. 13th International Congress of Theoretical and Applied Mechanics*, E. Becker and G. K. Mikhailov (eds.), Moscow, USSR.
- Laufer, J. 1954 The structure of turbulence in fully developed pipe flow, *NACA Tech. Report 1174*.
- Laufer, J. & Badri Narayanan, M. A. 1971 Mean period of the turbulent production mechanism in a boundary layer, *Phys. Fluids* **14**(182), 182-183.
- Liu, K. N., Christodoulou, C., Riccius, O. & Joseph, D. D. 1989 Drag reduction in pipes lined with riblets. In: Structure of Turbulence and Drag Reduction, A. Gyr (ed.), pp. 545-552, Springer-Verlag.
- Luchik, T. S. & Tiederman, W. G. 1988 Turbulent structure in low-concentration drag reducing channel flows, *J. Fluid Mech.* **190**, 241-264.
- Luchini, P., Manzo, F. & Pozzi, A. 1991 Resistance of a grooved surface to parallel flow and cross flow, *J. Fluid Mech.* **228**, 87-109.
- Lumley, J. L. 1969 Drag reduction by additives, *Ann. Rev. Fluid Mech.* **1**, 367-384.
- Malák, J., Hejna, J. & Schmid, J. 1975 Pressure losses and heat transfer in non-circular channels with hydraulically smooth walls, *Int. J. Heat Mass Transfer* **18**, 139-149.

- McComb, W. D. & Rabie, L.H. 1982 Local drag reduction due to injection of polymer solutions into turbulent flow in a pipe, *AIChE J.* **28**(4), 547.
- McCormick, C. L., Hester, R. D., Morgan, S. E. & Safieddine, A. M. 1990 Water soluble copolymers, *Macromolecules* **23**, 2124-2131; 2132-2139.
- Merrill, E. W. & Horn, A. F. 1984 Scission of macromolecules in dilute solutions: Extensional and turbulent flows, *Polym. Comm.* **25**(5), 144-146.
- Minoura, Y., Tanekazu, T., Kawamura, S. & Nakano, A. 1967 Dregadation of poly(ethylene oxide) by high speed stirring, *J. Polym. Sci.* **5**(A-2), 125-142.
- Mizushina, T. & Usui, H. 1977 Reduction of eddy diffusion for momentum and heat in viscoelastic fluid flow in a circular tube, *Phys. Fluids* **20**(10), S100-S108.
- Muller, G., Laine, J. P. & Fenyo, J. C. 1979 High-molecular-weight hydrolyzed polyacrylamides. I. Characterisation. Effect of salts on the conformational properties, *J Poly Sci: Poly. Chem. Ed.* **17**, 659-672.
- Munk, P., Aminabhavi, T. M., Williams, P., Hoffman, D. E. & Chemlir, M. 1980 Some solution properties of polyacrylamide, *Macromolecules* **13**, 871-875.
- Mysels, K. J. 1949 Flow of thickened fluids, *U.S. Patent* , No. 2,492,173.
- Nabi, G. 1968 Light-scattering studies of aqueous solutions of poly(ethylene oxide), *Pak. J. Sci. Res.* **20**, 136.
- Nakao, S.-I. 1990 Application of V-shape riblets to pipe flows, *J. Fluids Eng.* **113**, 587-90.
- Neves, J. C., Moin, P. & Moser, R. D. 1994 Effects of convex transverse curvature on wall-bounded turbulence. Part 1. The velocity and vorticity, *J. Fluid Mech.* **272**, 349-381.
- Nikuradse, J. 1930 Turbulente Strömung in nichtkreisförmigen rohren, *Ing. -Arch.* **1**, 306-332.
- Nikuradse, J. 1933 Laws of flow in rough pipes, *NACA TM* No. 1292.
- Nitschke, P. 1983 Experimental investigation of the turbulent flow in smooth and longitudinal grooved tubes, *NASA TM* No. 77480.
- Nouri, J. M., Umar, H. & Whitelaw, J. H. 1993 Flow of Newtonian and non-Newtonian fluids in concentric and eccentric annuli, *J. Fluid Mech.* **253**, 617-641.
- Oldaker, D. K. & Tiederman, W. G. 1977 Spatial structure of the viscous sublayer in drag reducing channel flows, *Phys. Fluids* **20**(10), S133-S144.
- Paterson, R. W. & Abernathy, F. H. 1970 Turbulent flow drag reduction and degradation with dilute polymer solutions, *J. Fluid Mech.* **43**(4), 689-710.
- Patterson, G. K. 1984 "Model for the effects of degradation on polymer drag reduction". In: The Influence of Polymer Additives on Velocity and Temperature Fields, B. Gampert (ed.), pp. 173-179, Springer-Verlag.

- Perry, R. H. & Green, D. 1984 Perry's Chemical Engineers Handbook 6th Edition, McGraw-Hill,
- Philips, R. B., Beauchamps, C. H. & Castano, J. M. 1987 Polymer-riblet interaction study, *NUSC TM* 87-2115.
- Prandtl, L. 1925 Bericht über Untersuchungen zur ausgebildeten Turbulenz, *Z. Angew. Math. Mech.* **5**, 136-137.
- Prandtl, L. 1945 Über ein neues Formelsystem für die ausgebildeten Turbulenz, *Nachr. Ges. Wiss. Göttingen, Math.-phys. Kl.*, 6-19.
- Pulles, C. J. A. 1988 Drag Reduction of Turbulent Boundary Layers by Means of Grooved Surfaces, *Ph.D. Thesis*, Eindhoven University of Technology, The Netherlands.
- Pulles, C. J. A., Krishna Prasad, K. & Nieuwstadt, F. T. M. 1989 Turbulence measurements over longitudinal micro-grooved surfaces, *Appl. Sci. Res.* **46**, 197-208.
- Quadrio, M. 1995 Personal Communication.
- Rannie, W. D. 1956 Heat transfer in turbulent shear flow, *J Aero. Sci.* **23**, 485.
- Rao, K., Narasimha, R. & Badri Narayanan, M. A. 1971 The "bursting" phenomenon in a turbulent boundary layer, *J. Fluid Mech.* **48**, 339-352.
- Reichardt, H. 1951 Vollständige Darstellung der turbulenten Geschwindigkeitsverteilung in glatten Leitungen, *Z. Angew. Math. Mech.* **31**, 208-219.
- Reidy, L. W. & Anderson, G. W. 1988 Drag reduction for external and internal boundary layers using riblets and polymers, *AIAA Paper* 88-0138.
- Reif, W.-E. 1978 Protective and hydrodynamic function of the dermal skeleton of elamolranshs, *Neues J. für Geologie und Palaontologie* **157**, 133-141.
- Rempp, J. 1957 Contribution à l'étude des solutions de molécules en chaîne à squelette oxygéné. II. Viscosités intrinsèques et coefficients de diffusion de translation des polyéthylène-glycols, *J. Chim. Phys.* **54**, 432.
- Ring, W., Cantow, H.-J. & Holtrup, W. 1966 Molekulargewichte und molekulargewichtverteilungen von polyäthylenoxiden, *Eur. Poly. J.* **2**, 151.
- Rohr, J., Anderson, G. W. & Reidy, L. W. 1990 An experimental investigation of the drag reducing effects of riblet in pipes. In: Drag Reduction in Fluid Flows, R. H. J. Sellin and R. T. Moses (eds.), pp. 263-270, Ellis Horwood.
- Rossi, C. & Cuniberti, C. 1964 Intrinsic viscosities of low poly(ethylene) oxide POEG in different solvents, *Poly. Lett.* **2**, 681.
- Rouse, P. E. 1953 A theory of linear viscoelastic properties of dilute solutions of coiling polymers, *J. Chem. Phys.* **21**, 1272.

- Sawyer, W. G. & Winter, K. J. 1987 An investigation of the effect on turbulent skin friction on surfaces with streamwise grooves. In: Turbulent Drag Reduction by Passive Means, Royal Aeronautical Society.
- Schlichting, H. 1979 Boundary-Layer Theory, 7th Edition, McGraw Hill.
- Scholtan, W. 1954 Molekulargewichtsbestimmung von polyacrylamid mittels der ultrazentrifuge, *Makromol. Chem.* **14**, 169-178.
- Schummer, P. & Thielen, W. 1980 Structure of turbulence in viscoelastic fluids, *Chem. Eng. Commun.* **4**, 593-606.
- Schwarz-van Manen, A. D., Thijsses, J. H. H., Nieuwvelt, C., Krishna Prasad, K. & Nieuwestadadt, F. T. M. 1989 The bursting process over drag reducing grooved surfaces. In: Structure of Turbulence and Drag Reduction, A. Gyr (ed.), pp. 561-568, Springer-Verlag.
- Sellin, R. H. J., Hoyt, J. W. & Scrivener, O. 1982 The effect of drag-reducing additives on fluid flows and their industrial applications, Part 1: Basic aspects, *J. Hydraulic Res.* **20**, 29-68.
- Sharma, R. S., Seshadri, V. & Mulhotra, J. P. 1978 Turbulent drag reduction by injection of fibers, *J. Rheol.* **22**(6), 643-659.
- She, Z.-S., Jackson, E. & Orszag, S. A. 1990 Intermittent vortex structures in homogeneous isotropic turbulence, *Nature* **344**, 263.
- Shin, H. 1965 Reduction of drag in turbulence by dilute polymer solutions, *Sc.D. Thesis*, Massachusetts Institute of Technology.
- Solomon, O. F. & Ciuta, I. Z. 1962 Détermination de la viscosité intrinsèque des solutions de polymères par une simple détermination de la viscosité, *J. Appl. Polym. Sci.* **6**, 683-686.
- Spalding, D. B. 1961 A single formula for the "law of the wall", *J. Appl. Mech.* **28**(9), 455-458.
- Sparrow, E. M., Lin, S. H. & Lundgren, T. S. 1964 Flow development in the hydrodynamic entrance region of tubes and ducts, *Phys. Fluids* **7**(3), 338-347.
- Squire, L. C. & Savill, A. M. 1987 Some experiences of riblets at transonic speeds. In: Turbulent Drag Reduction by Passive Means, Royal Aeronautical Society.
- Suzuki, Y. & Kasagi, N. 1994 Turbulent drag reduction mechanism above a riblet surface, *AIAA J.* **32**(9), 1781-1790.
- Tani, I. 1988 Drag reduction by riblet viewed as roughness problem, *Proc. Japan Acad.* **64 B**, 21-24.
- Tiederman, W. G., Luchik, T. S. & Bogard, D. G. 1985 Wall-layer structure and drag reduction, *J. Fluid Mech.* **156**, 419-437.

- Toms, B. A. 1948 Some observations on the flow of linear polymer solutions through straight tubes at high Reynolds numbers, *Proc. First International Congress on Rheology*, pp 135-141, Amsterdam.
- Tritton, D.J. 1988 Physical Fluid Dynamics 2nd Edition, Oxford Science.
- van Dam, P. H. J. 1993 Turbulent Dynamics in Dilute Polymer Solutions, *PhD. Thesis*, University of Amsterdam.
- van Driest, E. R. 1956 On turbulent flow near a wall, *J. Aero. Sci.* **23**, 1007.
- Vaseleski, R. C. & Metzner, A. B. 1974 Drag reduction in the turbulent flow of fiber suspensions, *AIChE J.* **20**(2), 301-306.
- Virk, P. S. 1966 The Toms Phenomenon: Turbulent Pipe Flow of Dilute Polymer Solutions, *Sc.D. Thesis*, M.I.T.
- Virk, P. S. 1971a Drag reduction in rough pipes, *J. Fluid Mech.* **45**(2), 225-246.
- Virk, P. S. 1971b An elastic sublayer model for drag reduction by dilute solutions of linear macromolecules, **45**(3), 417-440.
- Virk, P. S. 1975 Drag reduction fundamentals, *AIChE J.* **21**(4), 625-656.
- Virk, P. S. 1975 Drag reduction by collapsed and extended polyelectrolytes, *Nature* **253**, 109.
- Virk, P. S. & Merrill, E. W. 1969 The onset of dilute polymer solution phenomena. In: Viscous Drag Reduction, C. Sinclair Wells (ed.), Plenum Press.
- Virk, P. S. & Suraiya, T. 1977 Mass transfer at maximum drag reduction, *Proc. 2nd International Conference on Drag Reduction*, Cambridge, England.
- Virk, P. S. & Wagger, D. L. 1989 Aspects of type B drag reduction. In: Structure of Turbulence and Drag Reduction, A. Gyr (ed.), pp. 201-214, Springer-Verlag.
- Vukoslavcevic, P., Wallace, J. M. & Balint, J.-L. 1987 On the mechanism of viscous drag reduction using streamwise aligned riblets: A review with some new results. In: Turbulent Drag Reduction by Passive Means, Royal Aeronautical Society.
- Vukoslavcevic, P., Wallace, J. M. & Balint, J.-L. 1992 Viscous drag reduction using streamwise-aligned riblets, *AIAA J.* **30**, 1119-1122.
- Wagger, D. L. 1992 Turbulent Flow Enhancement by Polyelectrolyte Additives: Mechanistic Implications for Drag Reduction, *PhD Thesis*, M.I.T.
- Wallace, J. M. & Balint, J.-L. 1987 On the mechanism of viscous drag reduction using streamwise aligned riblets: A review with some new results. In: Turbulent Drag Reduction by Passive Means, Royal Aeronautical Society.
- Walsh, M. 1967 Theory of drag reduction in dilute high polymer flow, *Intern. Shipbuilding Progress* **14**(152), 134-139.

- Walsh, M. J. 1979 Drag characteristics of V-groove and transverse curvature riblets. In: Viscous Flow Drag Reduction, G. R. Hough (ed.), AIAA.
- Walsh, M. J. 1982 Turbulent boundary layer drag reduction using riblets, *AIAA Paper* 82-0169.
- Walsh, M. J. 1983 Riblets as a viscous drag reduction technique, *AIAA J.* **21**(4), 485-486.
- Walsh, M. J. 1990 Effect of detailed surface geometry on riblet drag reduction performance, *J. Aircraft* **27**(6), 572-573.
- Walsh, M. J. 1990 Riblets. In: Viscous Drag Reduction in Boundary Layers, Progress in Astronautics and Aeronautics, D. M. Bushnell and J. N. Hefner (eds.), pp. 351-412, AIAA.
- Walsh, M. J. & Linemann, A. M. 1984 Optimisation and applications of riblets for turbulent drag reduction, *AIAA Paper* 84-0347.
- Walsh, M. J. & Weinstein, L. M. 1979 Drag and heat transfer characteristics of small longitudinal ribbed surfaces, *AIAA J.* **17**(7), 770-771.
- Wardle, C. S. 1975 Limit of fish swimming speed, *Nature* **255**, 725-727.
- Weihs, D. 1977 Effects of size on sustained swimming speeds of aquatic organisms. In: Scale Effects in Animal Locomotion, T. J. Pedley (ed.), 333-338, Academic Press.
- White, A. & Hemmings, J. A. G. 1976 Drag Reduction by Additives: Review and Bibliography, BHRA Fluid Engineering.
- Wilkinson, S. P. & Lazos, B. S. 1987 Direct drag and hot wire measurements on thin-element riblet arrays. In: Turbulence Management and Relaminarisation, H. W. Liepmann and R. Narasimha (eds.), Springer-Verlag.
- Willmarth, W. W. & Lu, S. S. 1972 Structure of the Reynolds stress near the wall, *J. Fluid Mech* **55**, 65.
- Willmarth, W. W., Wei, T. & Lee, C. O. 1987 Laser anemometer measurements of Reynolds stress in a turbulent channel flow with drag reducing polymer additives, *Phys. Fluids* **30**(4), 933-935.
- Zimm, B. H. 1956 Dynamics of polymer molecules in dilute solution: Viscoelasticity, flow birefringence and dielectric loss, *J. Chem. Phys.* **54**(2), 269-278.

Appendix E

Data

E.1 Pipe Information:

PIPE DESIGNATION	S1	S2	R1A	R1B	R2A	R2B
h, mm	-	-	0.105	0.145	0.105	0.145
s, mm	-	-	0.108	0.165	0.108	0.165
d _s , mm	7.82	10.21	7.82	7.82	10.21	10.21
d _r , mm	-	-	7.54	7.44	9.93	9.80

Notes: Values in data outputs are in units of inches and nominal riblet heights

E.2 Polymer Information:

Polymer Type	Species	η_l (dl/g)	Polymer Parameters inferred via Eqs. 2.3-12 2.3-15			
			$M_w \times 10^{-6}$ (g/mole)	$N \times 10^{-5}$	R_G (nm)	L_c (μm)
PEO	P-309	27.5	7.9	5.25	267	168
	W-301	20.0	5.3	3.53	223	113
	N-60K	9.11	2.0	1.33	141	42
	N-750	3.10	0.52	0.35	75.1	ii
	N-10	1.18	0.16	0.10	42.8	3.4
PAM	N-300	16.6	7.4	2.09	224	104
	N-300L	8.00	2.9	0.82	115	41

E3. Data Analysis Nomenclature

RUN	=	run number
DATE	=	date
POLY	=	polymer species nomenclature
c wppm	=	c, wppm
nr	=	η_r
Station ij	=	measurements made at stations i and j during degradation studies
ΔL	=	distance, in m, between measuring strations during degradation studies
Q (L/s)	=	Q
T_w	=	τ_w
Ressqf	=	$Re_n \sqrt{f}$
1/sqf	=	$1/\sqrt{f}$
Resqf	=	$Re \sqrt{f}$
S'	=	S'
SF	=	S_F
h+	=	h ⁺
1/sqfli	=	$1/\sqrt{f_s}$ interpolated at $Re \sqrt{f}$ of riblet
S'li	=	S' interpolated at $Re \sqrt{f}$ of riblet pipe
fli	=	f_s interpolated at Re of riblet pipe
R'	=	R'
RF	=	R_F
P	=	P
Δ'/t_{res}	=	Δ'/t_{res}
corrected R'	=	R' corrected for degradation = $R' - \Delta'$
corrected S'	=	S' corrected for degradation = $S' + \Delta'$

Parentheses denote pipe name

R = Replicated pipe

PIPE: 7.82 mm

RIBBLETS: 0.11 mm

POLYMERS:

NONE (Solvent)

PEO N-750

N60K

W-301

P-309

PAM N-300

0.0045" Riblets/0.308" Pipe
Resqfit= 350

Series

DW

PPE

S1:
d= 0.308
h= smooth
R1A:
d= 0.297
h= 0.0045
R/h 33.0

RUR 233
DATE 8/25/93
POLY -
c wppm -
nr 1.000

Q (L/s)	Tw (S1)	1/sqrt(S1)	Resqf (S1)	S' (S1)	SF (S1)	Tw (R1A)	1/sqrt(R1A)	Resqf (R1A)	h*	S' (R1A)	SF (R1A)	R'	RF	P	
0.00331	0.060	6.245	97.8	-0.01	0.00	0.068	6.350	99.9	1.07	0.00	0.001	0.000	0.857	0.857	
0.00511	0.094	7.711	122.4	-0.01	0.00	0.104	7.899	124.1	1.33	0.00	-0.018	-0.002	0.851	0.851	
0.00706	0.122	9.365	139.4	-0.08	-0.01	0.144	9.273	146.3	1.57	0.00	0.056	0.005	0.848	0.848	
0.00889	0.165	10.140	162.4	-0.11	-0.01	0.182	10.401	164.5	1.76	0.00	0.130	0.012	0.855	0.855	
0.01029	0.195	10.776	177.2	-0.13	-0.01	0.403	9.237	245.2	2.63	0.00	0.154	0.014	0.868	0.868	
0.01174	0.232	11.293	193.1	-0.14	-0.01	0.524	9.636	279.9	3.00	0.00	0.000	0.000	0.554	0.554	
0.01396	0.323	11.380	228.2	-0.15	-0.01	0.784	9.873	342.8	3.67	0.00	0.211	0.019	0.594	0.594	
0.01715	0.656	9.805	325.6	-0.11	-0.01	1.219	10.125	427.7	4.58	-0.01	0.000	0.000	0.859	0.859	
0.02238	1.060	10.062	414.3	-0.06	0.00	1.429	10.246	463.5	4.97	-0.04	0.00	-0.018	0.858	0.858	
0.02464	1.260	10.161	452.1	-0.08	-0.01	1.989	10.608	547.2	5.86	0.00	0.056	0.005	0.862	0.862	
0.03004	1.775	10.438	536.9	-0.08	-0.01	2.470	10.875	610.4	6.54	0.00	0.130	0.012	0.860	0.860	
0.03421	2.229	10.608	602.3	-0.11	-0.01	3.084	11.090	682.3	7.31	0.00	0.000	0.000	0.870	0.870	
0.03899	2.800	10.797	675.3	-0.13	-0.01	3.685	11.279	745.9	7.99	0.02	0.000	0.188	0.017	0.876	0.876
0.04335	3.367	10.936	740.6	-0.14	-0.01	4.346	11.446	810.7	8.69	0.00	0.000	0.211	0.019	0.884	0.884
0.04778	3.984	11.081	806.2	-0.15	-0.01	5.113	11.660	879.5	9.42	0.02	0.000	0.304	0.026	0.888	0.888
0.05275	4.707	11.263	876.6	-0.13	-0.01	5.764	11.785	933.8	10.00	0.00	0.000	0.328	0.028	0.895	0.895
0.05665	5.341	11.347	933.7	-0.13	-0.01	6.271	11.882	973.9	10.43	0.00	0.000	0.377	0.032	0.899	0.899
0.05958	5.818	11.434	974.3	-0.12	-0.01	6.732	11.957	1008.7	10.81	-0.01	0.000	0.342	0.029	0.907	0.907
0.06212	6.262	11.491	1010.4	-0.13	-0.01	7.797	12.115	1082.7	11.60	-0.01	0.000	0.377	0.032	0.900	0.900
0.06773	7.273	11.626	1086.2	-0.12	-0.01	8.866	12.241	1160.8	12.44	-0.04	0.000	0.382	0.032	0.885	0.885
0.07298	8.135	11.845	1154.9	-0.01	0.00	9.578	12.371	1206.5	12.93	0.00	0.000	0.445	0.037	0.891	0.891
0.07666	8.854	11.926	1204.9	0.00	0.00	11.026	12.465	1296.2	13.89	-0.05	0.000	0.414	0.034	0.877	0.877
0.08287	10.032	12.112	1284.2	0.08	0.01	11.558	12.588	1329.4	14.24	0.03	0.000	0.493	0.041	0.899	0.899
0.08569	10.762	12.091	1332.5	-0.01	0.00	13.394	12.719	1431.5	15.34	0.03	0.000	0.496	0.041	0.895	0.895
0.09320	12.438	12.233	1432.9	0.01	0.00	15.816	12.838	1553.7	16.65	0.02	0.000	0.472	0.038	0.900	0.900
0.10222	14.766	12.314	1559.3	-0.06	0.00	18.169	13.085	1980.1	21.21	0.05	0.000	0.298	0.023	0.858	0.858
0.13330	23.043	12.855	1940.4	0.10	0.01	28.169	13.067	2081.0	22.50	0.01	0.000	0.194	0.015	0.861	0.861
0.13886	25.138	12.820	2042.0	-0.02	0.00	33.202	13.042	2259.5	24.21	-0.03	0.000	0.026	0.002	0.848	0.848
0.15047	29.181	12.893	2200.3	-0.08	-0.01	41.063	13.081	2512.8	26.92	0.01	0.000	-0.120	-0.009	0.831	0.831
0.16783	35.389	13.060	2423.0	-0.08	-0.01	50.294	13.039	2780.9	29.79	-0.01	0.000	-0.337	-0.025	0.814	0.814
0.18516	42.471	13.152	2654.5	-0.14	-0.01	58.804	13.059	3006.9	32.22	0.03	0.000	-0.453	-0.034	0.796	0.796
0.20051	48.519	13.325	2837.1	-0.09	-0.01	72.087	13.034	3329.6	35.67	0.04	0.000	-0.656	-0.048	0.773	0.773
0.22157	57.750	13.497	3095.5	-0.07	0.00	92.918	12.962	3781.5	40.51	0.00	0.000	-0.948	-0.068	0.740	0.740
0.25018	71.302	13.715	3440.9	-0.03	0.00	123.814	12.932	4365.9	46.78	-0.01	0.000	-1.228	-0.087	0.711	0.711
0.28812	91.275	13.960	3893.7	0.00	0.00	160.319	12.927	4967.3	53.22	-0.02	0.000	-1.458	-0.101	0.693	0.693
0.32772	115.177	14.135	4373.3	-0.03	0.00	194.245	12.953	5468.1	58.58	0.00	0.000	-1.598	-0.110	0.676	0.676
0.36146	136.171	14.339	4755.6	0.03	0.00	235.416	12.979	6020.2	64.50	0.00	0.000	-1.739	-0.118	0.665	0.665
0.39874	162.409	14.483	5194.0	0.02	0.00	302.898	13.035	6830.1	73.18	0.00	0.000	-1.903	-0.127	0.648	0.648
0.45423	203.516	14.739	5815.3	0.08	0.01	357.170	13.071	7415.0	79.44	-0.01	0.000	-2.010	-0.133	0.643	0.643
0.49460	238.251	14.833	6290.5	0.04	0.00	435.034	13.151	8174.7	87.58	-0.01	0.000	-2.099	-0.138	0.637	0.637
0.54921	287.499	14.993	6902.8	0.04	0.00	0.080	6.818	107.3	1.15	0.00	0.000	-0.048	-0.005	0.858	0.858
0.00386	0.073	6.640	106.0	-0.05	-0.01	0.119	8.302	130.7	1.40	0.00	0.000	-0.015	-0.001	0.862	0.862
0.00572	0.106	8.124	128.6	-0.05	0.00	0.158	9.525	150.8	1.62	0.00	0.000	-0.111	-0.011	0.866	0.866
0.00757	0.143	9.261	149.4	-0.05	0.00	0.201	10.624	170.5	1.83	0.00	0.000	-0.110	-0.011	0.865	0.865
0.00953	0.195	9.996	174.4	-0.05	0.00	0.256	11.542	200.1	2.80	0.00	0.000	-0.101	-0.010	0.868	0.868
0.01261	0.256	11.542	200.1	-0.05	0.00	0.323	12.115	233.1	3.00	0.00	0.000	-0.101	-0.010	0.868	0.868
0.01654	0.827	9.672	313.6	-0.05	-0.01	1.154	10.004	410.2	4.39	-0.06	0.000	-0.048	-0.005	0.788	0.788
0.02156	1.007	9.947	398.0	-0.05	0.00	1.361	10.182	445.9	4.78	-0.03	0.000	-0.015	-0.001	0.862	0.862
0.02383	1.193	10.100	433.6	-0.05	0.00	1.711	10.286	500.2	5.36	-0.01	0.000	-0.111	-0.011	0.866	0.866
0.02735	1.536	10.218	492.3	-0.05	0.00	2.114	10.547	556.4	5.96	-0.16	0.000	-0.101	-0.010	0.866	0.866
0.03099	1.903	10.400	548.3	-0.16	-0.01	2.492	10.752	604.4	6.48	-0.06	0.000	-0.01	0.026	0.874	0.874
0.03420	2.259	10.534	597.7	-0.17	-0.02	2.933	10.962	656.1	7.03	-0.15	0.000	0.000	0.009	0.878	0.878
0.03776	2.670	10.698	650.1	-0.15	-0.01										

0.04033	2.995	10.789	689.0	-0.16	-0.01	3.279	11.125	694.1	7.44	0.02	0.00	0.159	0.015	0.681
0.04337	3.406	10.879	735.0	-0.19	-0.02	3.714	11.241	736.9	7.92	0.00	0.00	0.167	0.015	0.684
0.04704	3.906	11.019	787.5	-0.17	-0.01	4.251	11.396	790.9	8.47	0.00	0.00	0.204	0.018	0.686
0.05063	4.447	11.116	840.5	-0.18	-0.02	4.813	11.528	841.8	9.02	-0.01	0.00	0.228	0.020	0.691
0.05442	5.010	11.255	892.2	-0.15	-0.01	5.407	11.689	892.4	9.56	0.01	0.00	0.286	0.025	0.693
0.05720	5.483	11.310	933.5	-0.17	-0.01	5.904	11.760	932.6	9.99	-0.02	0.00	0.281	0.024	0.696
0.05991	5.911	11.408	969.1	-0.14	-0.01	6.369	11.857	968.5	10.38	-0.01	0.00	0.313	0.027	0.695
0.06175	6.272	11.414	997.5	-0.18	-0.02	6.710	11.906	993.4	10.64	-0.02	0.00	0.318	0.027	0.901
0.06532	6.864	11.543	1043.1	-0.13	-0.01	7.371	12.018	1040.6	11.15	-0.02	0.00	0.349	0.030	0.898
0.06796	7.396	11.570	1080.1	-0.16	-0.01	7.923	12.061	1076.2	11.53	-0.05	0.00	0.333	0.028	0.900
0.07053	7.865	11.643	1103.3	-0.13	-0.01	8.459	12.114	1101.5	11.80	-0.05	0.00	0.346	0.029	0.897
0.07389	8.377	11.818	1162.4	-0.04	0.00	9.038	12.276	1162.3	12.45	-0.01	0.00	0.415	0.035	0.894
0.08076	9.767	11.963	1256.2	-0.03	0.00	10.458	12.473	1251.5	13.41	0.03	0.00	0.483	0.040	0.901
0.08726	11.204	12.068	1347.4	-0.05	0.00	11.872	12.649	1335.3	14.31	0.08	0.01	0.547	0.045	0.910
0.09446	12.810	12.218	1441.1	-0.02	0.00	13.839	12.682	1442.0	15.45	-0.02	0.00	0.447	0.036	0.893
0.10102	14.344	12.348	1524.9	0.02	0.00	15.486	12.822	1525.4	16.34	0.03	0.00	0.489	0.040	0.893
0.10300	14.882	12.360	1553.1	-0.01	0.00	16.129	12.809	1556.5	16.68	-0.01	0.00	0.441	0.036	0.890
0.10895	16.433	12.442	1632.2	-0.01	0.00	17.853	12.879	1637.9	17.55	0.00	0.00	0.422	0.034	0.888
0.11658	18.447	12.565	1728.6	0.01	0.00	20.230	12.946	1742.8	18.67	0.00	0.00	0.381	0.030	0.879
0.12829	21.833	12.710	1887.3	0.01	0.00	24.350	12.985	1916.8	20.56	-0.03	0.00	0.253	0.020	0.865
0.13673	24.428	12.807	1980.9	0.02	0.00	27.357	13.057	2018.1	21.62	0.01	0.00	0.238	0.019	0.861
0.13968	25.052	12.937	2021.9	0.11	0.01	28.990	12.975	2099.9	22.43	-0.08	-0.01	0.091	0.007	0.833
0.15530	30.458	13.027	2229.5	0.03	0.00	35.136	13.086	2305.4	24.70	0.01	0.00	0.035	0.003	0.836
0.17070	36.071	13.157	2426.4	0.02	0.00	42.571	13.067	2537.7	27.19	0.00	0.00	-0.151	-0.011	0.817
0.18992	43.588	13.317	2667.5	0.01	0.00	53.354	12.986	2841.2	30.44	-0.04	0.00	-0.793	-0.052	0.788
0.22825	59.977	13.643	3129.7	0.06	0.00	77.545	12.946	3426.0	36.71	-0.05	0.00	-0.428	-0.036	0.746
0.26643	78.117	13.954	3571.3	0.14	0.01	106.195	12.913	4008.7	42.95	-0.04	0.00	-1.099	-0.078	0.709
0.30446	99.963	14.097	4039.7	0.07	0.01	138.378	12.927	4575.8	49.02	-0.01	0.00	-1.415	-0.092	0.697
0.34046	122.216	14.256	4465.7	0.06	0.00	172.480	12.948	5107.3	54.72	0.00	0.00	-1.385	-0.103	0.683
0.37067	142.514	14.374	4821.0	0.04	0.00	203.793	12.969	5550.2	59.46	0.01	0.00	-1.609	-0.110	0.674
0.39891	162.567	14.483	5144.9	0.04	0.00	235.494	12.983	5961.5	63.87	0.01	0.00	-1.718	-0.117	0.666
0.44017	193.926	14.632	5613.9	0.04	0.00	284.314	13.039	6544.0	70.11	0.03	0.00	-1.825	-0.123	0.658
0.47753	224.349	14.759	6021.1	0.04	0.00	332.236	13.085	7084.0	75.90	0.03	0.00	-1.916	-0.128	0.651
0.53330	274.850	14.893	6543.1	0.03	0.00	408.754	13.175	7857.5	84.18	0.05	0.00	-2.006	-0.132	0.648
0.43991	194.616	14.597	5675.2	-0.02	0.00	289.567	12.974	6664.5	71.40	-0.05	0.00	-1.921	-0.129	0.648
0.47688	225.087	14.714	6103.0	-0.03	0.00	337.829	13.027	7198.1	77.12	-0.04	0.00	-2.002	-0.133	0.642
0.49529	240.426	14.786	6306.4	-0.01	0.00	362.691	13.061	7456.9	79.89	-0.03	0.00	-2.030	-0.135	0.639
0.53199	273.579	14.889	6726.3	-0.02	0.00	415.309	13.115	7978.5	85.48	-0.03	0.00	-2.068	-0.138	0.635
0.54845	289.482	14.923	6832.2	-0.02	0.00	439.526	13.147	8104.9	86.83	-0.01	0.00	-2.068	-0.137	0.635
0.56669	306.824	14.976	7122.9	-0.03	0.00	468.050	13.166	8469.5	90.74	-0.03	0.00	-2.146	-0.140	0.632
0.57762	316.659	15.025	7246.3	-0.01	0.00	483.349	13.207	8613.0	92.34	-0.01	0.00	-2.135	-0.139	0.632
0.59216	332.802	15.026	7359.7	-0.04	0.00	506.689	13.227	8742.6	93.67	0.00	0.00	-2.140	-0.139	0.633
0.59398	332.448	15.080	7428.8	0.00	0.00	509.496	13.230	8853.8	94.86	-0.01	0.00	-2.158	-0.140	0.629
0.60305	342.657	15.080	7525.3	-0.03	0.00	524.851	13.236	8966.3	96.06	-0.02	0.00	-2.174	-0.141	0.630
0.61030	350.375	15.093	7566.6	-0.02	0.00	536.181	13.254	9011.4	96.55	-0.01	0.00	-2.165	-0.140	0.630
0.61030	349.265	15.116	7619.2	-0.01	0.00	535.358	13.264	9201.4	97.30	-0.01	0.00	-2.169	-0.141	0.629
0.61935	357.850	15.155	7715.3	0.01	0.00	549.385	13.289	9203.3	98.60	0.00	0.00	-2.167	-0.140	0.628
0.62116	361.569	15.121	7729.0	-0.03	0.00	553.514	13.279	9206.5	98.64	-0.01	0.00	-2.178	-0.141	0.630
0.62658	367.353	15.133	7756.5	-0.03	0.00	561.905	13.296	9235.5	98.95	0.00	0.00	-2.166	-0.140	0.630
0.63742	376.162	15.213	7914.5	0.02	0.00	579.681	13.318	9458.7	101.34	0.00	0.00	-2.186	-0.141	0.626
0.63922	379.735	15.184	7919.3	-0.01	0.00	583.787	13.309	9453.1	101.28	-0.01	0.00	-2.193	-0.141	0.627
0.64283	384.836	15.169	7944.4	-0.03	0.00	589.099	13.324	9462.8	101.38	0.00	0.00	-2.180	-0.141	0.630
0.65724	400.461	15.203	8129.2	-0.04	0.00	615.007	13.335	9698.6	103.91	-0.02	0.00	-2.212	-0.142	0.628
0.66084	403.099	15.237	8137.9	-0.01	0.00	620.291	13.352	9718.7	104.12	0.00	0.00	-2.199	-0.141	0.627
0.67342	413.491	15.330	8301.1	0.05	0.00	640.330	13.393	9945.1	106.55	0.01	0.00	-2.198	-0.141	0.623
0.67701	421.960	15.256	8331.9	-0.03	0.00	648.619	13.379	9945.0	106.55	-0.01	0.00	-2.211	-0.142	0.627
0.68419	430.450	15.265	8425.6	-0.04	0.00	660.949	13.395	10051.4	107.69	-0.01	0.00	-2.214	-0.142	0.628

RUN 235
DATE 8/27/93
POLY
c:\pppm
1.000

0.0045" Riblets/0.308" Pipe
Result= 350

Series

DW

PIPE

SI: 256
d = 0.308
h = smooth
R1A:
d = 0.293
h = 0.0045
R/h 32.6

Q (L/s)	Tw (SI)	1/sqrt(SI)	Resqf (SI)	S' (SI)	SF (SI)	Tw (R1A)	1/sqrt(R1A)	Resqf (R1A)	h+	S' (R1A)	Sh (R1A)	R'	RF	P
0.00915	0.175	10.132	163.6	0.04	0.00	0.192	10.423	165.2	1.79	-0.07	-0.01	-0.072	-0.007	0.824
0.01218	0.249	11.296	195.5	0.00	0.00	0.465	6.919	257.3	2.79	0.00	0.00	-0.030	-0.003	0.486
0.01574	0.560	9.741	233.4	0.00	0.00	0.721	9.260	320.6	3.48	-0.03	0.00	0.013	-0.003	0.704
0.02022	0.891	9.915	370.5	0.00	0.00	1.046	9.876	386.3	4.20	-0.05	0.00	0.013	-0.003	0.784
0.02303	1.121	10.073	415.8	0.00	0.00	1.296	10.106	430.5	4.68	-0.03	0.00	0.013	-0.003	0.796
0.02767	1.546	10.304	489.1	-0.01	-0.01	1.760	10.418	502.5	5.46	0.00	0.00	0.039	0.006	0.810
0.03164	1.964	10.453	551.7	-0.11	-0.11	2.199	10.658	562.0	6.10	-0.01	0.00	0.088	0.008	0.818
0.03605	2.457	10.649	617.4	-0.11	-0.11	2.740	10.879	627.7	6.82	-0.02	0.00	0.107	0.010	0.818
0.03936	2.868	10.762	667.0	-0.13	-0.13	3.180	11.027	676.2	7.34	-0.02	0.00	0.160	0.014	0.823
0.04437	3.521	10.948	738.8	-0.13	-0.13	3.880	11.253	746.7	8.11	-0.01	0.00	0.229	0.020	0.823
0.05235	4.640	11.251	849.6	-0.07	-0.07	5.113	11.564	858.6	9.32	-0.02	0.00	0.428	0.026	0.815
0.05948	5.686	11.549	939.3	0.06	0.01	6.325	11.815	933.7	10.36	-0.02	0.00	0.336	0.029	0.828
0.06525	6.752	11.627	1022.9	-0.01	0.00	7.393	11.989	1030.5	11.19	-0.02	0.00	0.485	0.041	0.835
0.07200	7.953	11.820	1116.8	0.03	0.00	8.651	12.227	1121.4	12.18	0.02	0.00	0.428	0.036	0.834
0.07800	9.153	11.936	1199.3	0.02	0.00	9.894	12.425	1196.8	13.00	0.07	0.01	0.512	0.043	0.844
0.08456	10.605	12.022	1293.7	-0.03	0.00	11.370	12.527	1289.6	14.01	0.02	0.00	0.485	0.040	0.846
0.09192	12.091	12.238	1381.7	0.08	0.01	13.140	12.666	1386.7	15.06	0.03	0.00	0.498	0.041	0.835
0.09830	13.572	12.353	1463.6	0.09	0.01	14.604	12.848	1461.6	15.87	0.12	0.01	0.589	0.048	0.843
0.10326	14.785	12.433	1528.3	0.10	0.01	15.970	12.907	1529.1	16.61	0.11	0.01	0.569	0.046	0.840
0.13065	22.365	12.790	1872.3	0.10	0.01	25.009	13.050	1906.0	20.70	0.04	0.00	0.330	0.026	0.811
0.13101	22.859	12.742	1902.0	0.02	0.00	25.689	13.024	1949.7	21.17	0.00	0.00	0.264	0.021	0.814
0.15006	28.394	13.037	2129.4	0.12	0.01	33.823	13.007	2237.5	24.30	-0.06	-0.01	0.008	0.001	0.775
0.16905	35.049	13.219	2366.3	0.12	0.01	43.284	12.950	2531.6	27.49	-0.11	-0.01	-0.254	-0.019	0.749
0.18798	42.906	13.286	2618.2	0.01	0.00	54.476	12.853	2840.2	30.84	-0.19	-0.01	-0.361	-0.048	0.729
0.20686	50.871	13.427	2850.9	0.01	0.00	65.384	12.917	3111.6	33.79	-0.10	-0.01	-0.655	-0.048	0.721
0.22567	59.165	13.583	3074.7	0.03	0.00	78.248	12.868	3404.2	36.97	-0.10	-0.01	-0.840	-0.061	0.701
0.25380	72.514	13.798	3405.1	0.07	0.01	98.317	12.941	3817.1	41.45	-0.02	0.00	-0.986	-0.071	0.685
0.28296	93.387	14.034	3864.3	0.09	0.01	131.532	12.929	4415.1	47.95	-0.01	0.00	-1.250	-0.068	0.661
0.35002	116.477	14.156	4315.9	0.02	0.00	168.115	12.897	4991.8	54.21	-0.05	0.00	-1.496	-0.104	0.647
0.36685	141.559	14.274	4757.3	-0.04	0.00	206.422	12.952	5530.5	60.06	0.00	0.00	-1.619	-0.111	0.641
0.40346	168.562	14.386	5190.4	-0.07	-0.01	248.253	13.003	6064.1	65.86	0.02	0.00	-1.728	-0.117	0.636
0.44347	200.765	14.489	5663.0	-0.12	-0.01	298.586	13.048	6648.7	72.20	0.03	0.00	-1.843	-0.124	0.632
0.49758	247.394	14.645	6279.6	-0.15	-0.01	372.449	13.130	7417.8	80.56	0.04	0.00	-1.951	-0.129	0.626
0.54051	287.480	14.758	6746.2	-0.16	-0.01	435.904	13.202	7997.5	86.85	0.06	0.00	-2.010	-0.132	0.623
0.01102	0.214	11.028	186.0	0.02	0.00	0.349	9.320	228.6	2.48	-0.13	-0.01	-0.129	-0.013	0.556
0.01427	0.456	9.779	272.0	0.02	0.00	0.530	9.789	282.2	3.07	-0.05	-0.01	-0.026	-0.003	0.781
0.01966	0.845	9.901	370.7	-0.08	-0.01	0.999	9.826	388.0	4.21	-0.05	-0.01	-0.037	-0.003	0.795
0.02453	1.254	10.139	451.9	-0.12	-0.01	1.431	10.242	464.7	5.05	-0.04	0.00	0.037	0.003	0.808
0.02978	1.758	10.398	535.4	-0.18	-0.02	1.974	10.586	546.3	5.93	-0.04	0.00	0.062	0.006	0.818
0.03610	2.469	10.636	634.9	-0.18	-0.02	2.738	10.897	643.7	6.99	-0.03	0.00	0.124	0.011	0.824
0.04174	3.164	10.863	719.3	-0.16	-0.01	3.484	11.169	726.6	7.89	-0.03	0.00	0.184	0.016	0.829
0.04705	3.884	11.050	796.9	-0.16	-0.01	4.247	11.402	802.3	8.71	-0.02	0.00	0.242	0.021	0.833
0.05592	5.221	11.330	923.5	-0.13	-0.01	5.687	11.712	927.9	10.08	-0.05	0.00	0.267	0.023	0.838
0.06313	6.472	11.488	1026.2	-0.16	-0.01	7.003	11.911	1027.7	11.16	-0.09	-0.01	0.350	0.047	0.858
0.06912	7.437	11.733	1107.3	-0.04	0.00	7.865	12.310	1096.3	12.81	0.15	0.01	0.585	0.049	0.861
0.07538	8.654	11.861	1194.6	-0.05	0.00	9.111	12.473	1180.0	13.91	0.15	0.01	0.607	0.050	0.862
0.08278	10.168	12.017	1296.7	-0.03	0.00	10.704	12.637	1260.8	13.91	0.15	0.01	0.607	0.050	0.862
0.08609	10.860	12.093	1342.7	-0.02	0.00	11.528	12.664	1331.8	14.46	0.10	0.01	0.565	0.047	0.854

0.09426	12.723	12.232	1453.1	-0.02	0.00	13.427	12.847	1437.1	15.61	0.15	0.01	0.617	0.050	0.859
0.10256	14.677	12.392	1560.2	0.02	0.00	15.547	12.991	1546.0	16.79	0.16	0.01	0.634	0.051	0.856
0.10659	15.726	12.442	1614.0	0.01	0.00	16.672	13.038	1592.9	17.38	0.18	0.01	0.622	0.050	0.855
0.12820	21.662	12.745	1865.4	0.04	0.00	24.355	12.974	1923.8	20.89	-0.05	0.00	0.238	0.019	0.807
0.13143	22.705	12.768	1937.3	0.02	0.00	25.550	12.986	1978.5	21.49	-0.05	0.00	0.201	0.016	0.806
0.13602	23.852	12.892	1982.1	0.10	0.01	28.088	12.818	2070.7	22.49	-0.23	-0.02	-0.046	-0.004	0.770
0.14932	28.408	12.986	2162.8	0.05	0.00	33.304	12.940	2254.4	24.48	-0.13	-0.01	-0.072	-0.006	0.774
0.16878	35.507	13.111	2417.9	-0.02	0.00	43.035	12.850	2562.7	27.83	-0.21	-0.02	-0.365	-0.029	0.748
0.19376	44.894	13.386	2718.2	0.05	0.00	55.784	12.957	2917.1	31.68	-0.08	-0.01	-0.503	-0.037	0.730
0.22251	56.956	13.648	3061.0	0.16	0.01	73.237	12.986	3341.6	36.29	-0.01	0.00	-0.710	-0.052	0.705
0.26071	74.914	13.944	3509.9	0.16	0.01	100.677	12.977	3917.2	42.54	0.02	0.00	-0.995	-0.071	0.675
0.30446	99.980	14.095	4054.0	0.06	0.00	137.167	12.984	4571.4	49.65	0.04	0.00	-1.256	-0.088	0.661
0.36124	135.193	14.362	4712.2	0.09	0.01	192.160	13.015	5408.5	58.74	0.06	0.00	-1.517	-0.104	0.638
0.39891	161.519	14.530	5148.3	0.09	0.01	232.657	13.062	5948.6	64.60	0.09	0.01	-1.636	-0.111	0.630
0.43643	189.580	14.673	5574.8	0.08	0.01	276.272	13.114	6478.9	70.36	0.11	0.01	-1.732	-0.117	0.622
0.49616	238.699	14.866	6249.6	0.08	0.01	352.775	13.194	7314.4	79.43	0.12	0.01	-1.863	-0.124	0.614
0.55182	289.098	15.024	6852.4	0.08	0.01	431.233	13.271	8057.6	87.51	0.12	0.01	-1.953	-0.128	0.608
0.00649	0.121	8.639	136.8			0.135	8.821	139.2	1.51					0.812
0.00897	0.173	9.979	163.9			0.187	10.356	164.1	1.78					0.839
0.01108	0.220	10.936	185.0			0.353	9.322	225.4	2.45					0.566
0.01339	0.291	11.480	213.0			0.513	9.359	272.0	2.95					0.516
0.01918	0.807	9.884	354.7	0.08	0.01	9.792	9.792	371.9	4.04	-0.09	-0.01	-0.090	-0.009	0.765
0.02404	1.212	10.109	434.9	-0.04	0.00	1.369	10.188	448.3	4.87	-0.04	0.00	-0.018	-0.002	0.791
0.02911	1.688	10.373	513.5	-0.07	-0.01	1.905	10.534	525.3	5.70	0.00	0.00	0.052	0.005	0.803
0.03501	2.336	10.603	604.6	-0.12	-0.01	2.606	10.833	614.7	6.68	-0.01	0.00	0.078	0.007	0.813
0.04076	3.034	10.833	688.9	-0.12	-0.01	3.356	11.114	697.5	7.57	0.00	0.00	0.139	0.013	0.820
0.04620	3.778	11.005	769.0	-0.14	-0.01	4.146	11.325	775.5	8.42	-0.01	0.00	0.177	0.016	0.827
0.05447	5.038	11.236	868.5	-0.16	-0.01	5.472	11.631	891.6	9.68	-0.04	0.00	0.231	0.020	0.835
0.06214	6.279	11.481	980.2	-0.10	-0.01	6.813	11.892	992.9	10.78	-0.03	0.00	0.305	0.026	0.836
0.06786	7.242	11.675	1066.1	-0.04	0.00	7.784	12.150	1064.1	11.56	0.06	0.01	0.442	0.038	0.844
0.07531	8.650	11.855	1163.4	-0.01	0.00	9.304	12.333	1161.5	12.61	0.05	0.00	0.473	0.040	0.843
0.08076	9.752	11.973	1236.4	0.00	0.00	10.506	12.446	1235.5	13.42	0.03	0.00	0.478	0.040	0.842
0.08645	10.992	12.072	1315.0	0.00	0.00	11.772	12.586	1310.2	14.23	0.05	0.00	0.517	0.043	0.847
0.09944	13.983	12.312	1483.1	0.03	0.00	15.042	12.808	1481.0	16.08	0.06	0.00	0.525	0.043	0.843
0.10960	16.498	12.492	1612.0	0.06	0.01	17.847	12.959	1614.1	17.53	0.09	0.01	0.527	0.042	0.838
0.12504	20.834	12.683	1811.2	0.05	0.00	22.594	13.140	1815.8	19.72	0.16	0.01	0.504	0.040	0.836
0.13409	23.434	12.823	1922.7	0.09	0.01	26.000	13.135	1945.7	21.17	0.11	0.01	0.375	0.029	0.617
0.14759	28.142	12.880	2106.6	-0.01	0.00	31.758	13.082	2154.4	23.40	0.02	0.00	0.149	0.012	0.804
0.16685	34.623	13.128	2336.1	0.05	0.00	40.811	13.047	24.17	26.52	-0.02	0.00	-0.104	-0.008	0.769
0.18608	42.409	13.229	2585.0	-0.02	0.00	50.974	13.019	2728.4	29.63	-0.03	0.00	-0.325	-0.024	0.755
0.20527	50.376	13.389	2816.1	-0.01	0.00	62.654	12.954	3023.5	32.84	-0.07	-0.01	-0.568	-0.042	0.729
0.23530	64.114	13.639	3176.3	0.03	0.00	83.212	12.917	3483.7	37.83	-0.07	-0.01	-0.851	-0.062	0.699
0.27405	83.634	13.873	3627.1	0.04	0.00	112.810	12.888	4055.4	44.04	-0.06	0.00	-1.144	-0.082	0.672
0.30826	102.950	14.065	4021.9	0.05	0.00	142.877	12.882	4561.5	49.54	-0.06	0.00	-1.354	-0.095	0.653
0.35558	132.873	14.281	4566.2	0.04	0.00	189.553	12.901	5250.5	57.02	-0.05	0.00	-1.560	-0.109	0.636
0.41206	172.524	14.524	5199.5	0.06	0.00	252.760	12.947	6058.9	65.80	-0.04	0.00	-1.783	-0.121	0.619
0.46821	216.643	14.727	5822.4	0.07	0.00	323.188	13.010	6846.3	74.55	-0.03	0.00	-1.932	-0.129	0.608
0.54626	285.513	14.968	6672.5	0.07	0.00	432.571	13.120	7906.9	85.87	-0.01	0.00	-2.072	-0.136	0.599
0.00859	0.168	9.706	155.7			0.193	9.766	160.7	1.75					0.789
0.01053	0.208	10.682	173.3			0.234	10.872	176.8	1.92					0.807
0.01406	0.344	11.093	223.0			0.554	9.435	272.3	2.96					0.564
0.01857	0.761	9.861	331.5			0.909	9.732	348.9	3.79					0.759

IR	1.000	1.157	10.107	406.9	0.06	0.01	1.339	10.136	423.5	4.60	0.02	0.00	0.029	0.003	0.784
0.02347	1.633	10.289	486.0	-0.06	-0.01	1.843	10.448	497.1	5.40	0.02	0.00	0.062	0.006	0.803	
0.02839	2.192	10.553	563.3	-0.05	0.00	2.451	10.768	573.4	6.23	0.07	0.01	0.134	0.013	0.811	
0.04018	2.960	10.815	654.7	-0.05	0.00	3.289	11.071	664.3	7.21	0.06	0.01	0.182	0.017	0.816	
0.04582	3.740	10.971	736.0	-0.10	-0.01	4.121	11.276	743.8	8.08	0.02	0.00	0.190	0.017	0.823	
0.05391	4.943	11.228	846.2	-0.08	-0.01	5.396	11.595	851.2	9.24	0.03	0.00	0.275	0.024	0.831	
0.06081	6.090	11.412	939.2	-0.08	-0.01	6.617	11.812	942.5	10.24	0.01	0.00	0.314	0.027	0.835	
0.06689	7.176	11.564	1018.9	-0.07	-0.01	7.736	12.017	1018.4	11.06	0.03	0.00	0.385	0.033	0.841	
0.07385	8.426	11.731	1107.1	0.00	0.00	9.031	12.278	1103.4	11.98	0.11	0.01	0.507	0.043	0.846	
0.07786	9.217	11.876	1158.9	0.02	0.00	9.871	12.388	1154.6	12.54	0.11	0.01	0.533	0.045	0.847	
0.08264	10.179	11.995	1219.2	0.05	0.00	11.007	12.445	1220.6	13.26	0.05	0.00	0.499	0.042	0.839	
0.09354	12.655	12.176	1359.2	0.04	0.00	13.565	12.689	1354.8	14.71	0.09	0.01	0.562	0.046	0.846	
0.10007	14.153	12.317	1437.3	0.09	0.01	15.214	12.818	1434.6	15.58	0.12	0.01	0.591	0.048	0.844	
0.11436	17.918	12.511	1617.0	0.08	0.01	19.338	12.994	1617.2	17.56	0.13	0.01	0.559	0.045	0.840	
0.13357	23.513	12.756	1848.1	0.09	0.01	25.798	13.139	1863.6	20.24	0.14	0.01	0.458	0.036	0.827	
0.13409	23.570	12.789	1854.7	0.12	0.01	26.278	13.069	1895.3	20.47	0.06	0.00	0.367	0.029	0.813	
0.14566	27.613	12.836	2007.5	0.03	0.00	30.777	13.118	2040.4	22.16	0.07	0.01	0.279	0.022	0.814	
0.16878	36.152	12.998	2297.3	-0.05	0.00	41.329	13.117	2364.8	25.68	0.05	0.00	0.022	0.002	0.795	
0.18000	42.723	13.319	2497.4	0.13	0.01	50.993	13.154	2626.7	28.53	0.09	0.01	-0.124	-0.009	0.760	
0.21102	53.572	13.350	2796.8	-0.04	0.00	65.939	12.983	2987.2	32.44	-0.04	0.00	-0.518	-0.038	0.737	
0.23972	66.123	13.651	3107.3	0.08	0.01	86.304	12.892	3417.6	37.12	-0.10	-0.01	-0.843	-0.061	0.695	
0.31015	104.771	14.031	3911.1	0.06	0.00	145.040	12.867	4430.2	48.11	-0.07	-0.01	-1.319	-0.093	0.655	
0.35558	133.522	14.249	4415.3	0.07	0.00	190.362	12.876	5075.5	55.12	-0.07	-0.01	-1.546	-0.107	0.636	
0.41206	172.818	14.515	5022.9	0.11	0.01	253.389	12.993	5855.3	63.59	-0.04	0.00	-1.737	-0.118	0.619	
0.44953	201.715	14.656	5424.2	0.12	0.01	299.843	12.970	6366.7	69.14	-0.03	0.00	-1.845	-0.125	0.610	
0.54256	283.366	14.925	6419.1	0.10	0.01	429.097	13.086	7604.6	82.59	-0.02	0.00	-2.038	-0.135	0.599	
0.00783	0.151	9.339	148.6	0.06	-0.01	0.167	9.573	150.6	1.64	-0.03	0.00	-0.023	-0.032	0.780	
0.00989	0.195	10.369	169.0	-0.09	-0.01	0.211	10.756	169.2	1.84	-0.07	-0.01	-0.030	-0.003	0.791	
0.01129	0.225	11.025	181.4	-0.09	-0.01	0.384	9.102	228.2	2.48	-0.04	0.00	0.029	0.003	0.803	
0.01348	0.295	11.494	207.8	-0.12	-0.01	0.538	9.183	270.2	2.93	-0.04	0.00	0.090	0.007	0.813	
0.01842	0.755	9.816	332.5	-0.12	-0.01	0.900	9.700	349.5	3.80	-0.05	0.00	0.109	0.010	0.816	
0.02278	1.101	10.052	401.7	-0.13	-0.01	1.281	10.058	417.0	4.53	-0.07	-0.01	0.167	0.015	0.823	
0.02785	1.576	10.271	480.6	-0.18	-0.02	1.807	10.350	495.4	5.38	-0.07	-0.01	0.233	0.020	0.837	
0.03360	2.187	10.518	566.2	-0.11	-0.01	2.470	10.680	579.2	6.29	-0.04	0.00	0.258	0.022	0.831	
0.03933	2.880	10.730	649.7	-0.12	-0.01	3.214	10.960	660.7	7.18	-0.04	0.00	0.289	0.025	0.829	
0.04458	3.575	10.917	723.9	-0.13	-0.01	3.973	11.174	734.7	7.98	-0.05	0.00	0.339	0.029	0.831	
0.05257	4.758	11.160	835.1	-0.18	-0.02	5.242	11.472	843.9	9.16	-0.07	-0.01	0.401	0.033	0.836	
0.05964	5.966	11.306	935.2	-0.11	-0.01	6.463	11.885	1015.4	11.03	-0.10	-0.01	0.483	0.040	0.841	
0.06552	8.001	11.668	1082.6	-0.07	0.00	8.749	12.038	1089.9	11.84	-0.10	-0.01	0.502	0.041	0.840	
0.07127	9.154	11.820	1158.7	-0.04	0.00	9.993	12.205	1165.5	12.66	-0.09	-0.01	0.454	0.035	0.838	
0.07723	10.904	11.966	1266.2	-0.04	0.00	11.796	12.413	1267.8	13.77	-0.06	0.00	0.401	0.033	0.836	
0.08534	12.546	12.144	1352.0	0.01	0.00	13.535	12.615	1357.9	14.75	0.01	0.00	0.483	0.040	0.841	
0.09289	13.924	12.256	1429.9	0.03	0.00	15.037	12.724	1430.6	15.54	0.03	0.00	0.502	0.041	0.840	
0.09876	16.860	12.371	1574.6	-0.02	0.00	18.257	12.826	1577.5	17.13	-0.01	0.00	0.454	0.035	0.838	
0.12521	21.350	12.548	1772.3	-0.05	0.00	23.564	12.887	1792.5	19.47	-0.05	-0.01	0.273	0.022	0.822	
0.13602	23.824	12.904	1872.9	0.21	0.02	27.641	12.925	1942.2	21.09	-0.10	-0.01	0.172	0.013	0.782	
0.14952	28.676	12.929	2054.9	0.08	0.01	33.242	12.956	2129.9	23.13	-0.10	-0.01	0.043	0.003	0.782	
0.16878	35.937	13.037	2300.2	-0.01	0.00	42.120	12.993	2397.4	26.04	-0.08	-0.01	-0.126	-0.010	0.774	
0.18600	43.402	13.214	2527.9	0.00	0.00	52.240	12.995	2669.9	29.00	-0.06	0.00	-0.311	-0.023	0.754	
0.20719	51.049	13.428	2741.5	0.08	0.01	63.879	12.951	2952.4	32.06	-0.08	-0.01	-0.530	-0.039	0.725	
0.22633	59.122	13.630	2950.3	0.15	0.01	76.288	12.946	3226.5	35.04	-0.06	0.00	-0.688	-0.050	0.703	
0.25880	75.707	13.773	3338.8	0.08	0.01	100.289	12.911	3699.5	40.18	-0.06	0.00	-0.961	-0.069	0.685	

0.29687	96.014	14.029	5760.3	0.13	0.01	132.376	12.891	4250.7	46.16	-0.05	0.00	-1.223	-0.087	0.658
0.39327	158.029	14.486	4825.7	0.15	0.01	229.975	12.956	5604.5	60.86	0.00	0.00	-1.638	-0.112	0.623
0.44953	199.772	14.727	5426.4	0.19	0.01	297.133	13.029	6371.3	69.19	0.03	0.00	-1.788	-0.121	0.610
0.54256	279.997	15.014	6427.6	0.18	0.01	425.225	13.145	7625.7	82.82	0.04	0.00	-1.984	-0.131	0.597
0.00484	0.094	7.323	112.5			0.105	7.473	114.6	1.24					0.611
0.00694	0.139	8.631	136.9			0.153	8.847	138.7	1.51					0.619
0.00877	0.176	9.671	154.5			0.194	9.943	156.1	1.70					0.623
0.01084	0.226	10.558	175.1			0.266	10.503	182.8	1.99					0.771
0.01402	0.325	11.390	210.1			0.541	9.521	261.0	2.83					0.544
0.01886	0.783	9.872	326.3			0.938	9.732	343.8	3.73					0.757
0.02329	1.147	10.073	395.1	0.09	0.01	1.330	10.093	409.6	4.45	0.03	0.00	0.044	0.004	0.782
0.02821	1.625	10.250	470.4	-0.04	0.00	1.861	10.334	484.7	5.26	-0.04	0.00	-0.007	-0.001	0.792
0.03401	2.257	10.484	554.7	-0.09	-0.01	2.577	10.586	570.7	6.20	-0.11	-0.01	-0.039	-0.004	0.794
0.04013	3.004	10.725	640.0	-0.10	-0.01	3.346	10.963	650.4	7.06	0.00	0.00	0.110	0.010	0.814
0.04535	3.703	10.915	710.7	-0.09	-0.01	4.107	11.183	720.6	7.83	0.00	0.00	0.153	0.014	0.818
0.05340	4.915	11.156	818.8	-0.10	-0.01	5.401	11.483	826.3	8.97	-0.01	0.00	0.214	0.019	0.825
0.06054	6.087	11.364	910.8	-0.07	-0.01	6.565	11.717	917.6	9.96	-0.02	0.00	0.267	0.023	0.828
0.06677	7.234	11.497	992.1	-0.09	-0.01	7.868	11.895	996.1	10.82	-0.04	0.00	0.301	0.026	0.834
0.07308	8.309	11.743	1068.0	0.03	0.00	9.069	12.127	1074.2	11.67	0.02	0.00	0.403	0.034	0.831
0.07765	9.346	11.764	1133.5	-0.05	0.00	10.176	12.164	1138.6	12.37	-0.08	-0.01	0.339	0.029	0.833
0.08588	10.982	12.002	1230.7	0.04	0.00	12.063	12.355	1241.8	13.49	-0.07	-0.01	0.379	0.032	0.826
0.09594	13.505	12.091	1364.7	-0.05	0.00	14.764	12.477	1373.7	14.92	-0.14	-0.01	0.325	0.027	0.830
0.10208	14.994	12.209	1438.3	-0.02	0.00	16.401	12.595	1448.2	15.73	-0.12	-0.01	0.351	0.029	0.829
0.12118	20.210	12.484	1669.7	-0.01	0.00	22.301	12.822	1688.6	18.34	-0.09	-0.01	0.312	0.025	0.822
0.12829	22.402	12.553	1763.0	-0.03	0.00	24.889	12.850	1789.1	19.43	-0.12	-0.01	0.239	0.019	0.816
0.14141	26.518	12.718	1911.0	-0.01	0.00	29.879	12.927	1952.9	21.21	-0.10	-0.01	0.164	0.013	0.805
0.14373	27.239	12.754	1944.0	0.00	0.00	30.947	12.911	1994.9	21.66	-0.13	-0.01	0.111	0.009	0.798
0.16300	34.185	12.912	2177.8	-0.04	0.00	39.592	12.946	2256.1	24.50	-0.12	-0.01	-0.067	-0.005	0.783
0.18224	41.592	13.087	2402.2	-0.04	0.00	49.732	12.913	2528.9	27.46	-0.15	-0.01	-0.299	-0.023	0.758
0.20143	49.896	13.207	2631.2	-0.07	-0.01	61.204	12.866	2805.5	30.47	-0.18	-0.01	-0.526	-0.039	0.739
0.22059	58.701	13.334	2854.1	-0.09	-0.01	74.014	12.812	3085.3	33.51	-0.20	-0.02	-0.745	-0.055	0.719
0.25308	74.131	13.613	3207.3	-0.01	0.00	97.617	12.799	3543.3	38.48	-0.18	-0.01	-0.998	-0.072	0.689
0.29117	93.831	13.921	3608.7	0.09	0.01	129.901	12.765	4087.8	44.39	-0.18	-0.01	-1.281	-0.091	0.655
0.32911	118.035	14.029	4047.5	0.00	0.00	165.540	12.781	4614.6	50.11	-0.16	-0.01	-1.475	-0.103	0.647
0.38386	154.226	14.315	4626.6	0.05	0.00	224.047	12.814	5368.5	58.30	-0.14	-0.01	-1.705	-0.117	0.624
0.45887	211.643	14.608	5419.2	0.07	0.00	316.330	12.892	6378.3	69.27	-0.11	-0.01	-1.927	-0.130	0.607
0.55182	292.559	14.941	6364.6	0.13	0.01	447.005	13.042	7574.0	82.25	-0.06	0.00	-2.076	-0.137	0.594

RUN 254
DATE 10/13/93
POLY -
c wppm -
nr 1.000

0.0045" Ribbed 0.308" Pipe
 Radius = 350

Series

PEO

PRE

S1:
 d = 0.308
 h = smooth
 RIA:
 POLY M-750
 c = 100
 h = 1.034
 Rn = 32.6

Run
 DATE 9/16/93
 POLY M-750
 c = 100
 h = 1.034

Q(L/s)	T _{eq} (S)	T _{avg} (S)	1/ρ _{avg} (S)	Re _{avg} (S)	S(S)	S _r (S)	1 _{eq} (RIA)	1/ρ _{avg} (RIA)	Re _{avg} (RIA)	h _r	S(RIA)	S _r (RIA)	1/ρ _{avg} (S)	5 _r (S)	R	R _r	P	ΔT _{ires}	connected R	connected S
0.00482	0.093	7.342	115.3	0.05	0.00	0.00	0.104	7.489	117.4	1.27	-0.02	0.00	7.464	0.03	-0.041	-0.004	0.811	0.00	-0.041	0.03
0.00674	0.129	8.677	136.5	0.00	0.00	0.00	0.145	8.829	139.3	1.51	-0.09	-0.01	10.272	-0.01	-0.059	-0.006	0.778	0.00	-0.059	-0.01
0.00888	0.175	9.834	158.8	0.00	0.00	0.00	0.193	10.099	160.6	1.74	-0.17	-0.01	10.652	-0.12	0.123	0.012	0.801	0.00	0.123	-0.12
0.01075	0.218	10.662	177.6	0.00	0.00	0.00	0.206	9.702	202.7	2.20	-0.08	-0.01	10.796	-0.17	0.229	0.021	0.816	0.00	0.229	-0.17
0.01718	0.648	9.683	306.6	0.00	0.00	0.00	0.790	9.599	327.9	3.56	-0.08	-0.01	11.069	-0.14	0.267	0.024	0.821	0.00	0.267	-0.14
0.02146	0.994	9.965	380.0	0.00	0.00	0.00	1.155	9.472	394.4	4.28	-0.09	-0.01	11.314	-0.08	0.265	0.023	0.820	0.00	0.265	-0.08
0.02809	1.392	10.217	448.8	0.00	0.00	0.00	1.622	10.213	467.4	5.89	-0.07	-0.01	11.499	-0.03	0.257	0.022	0.820	0.00	0.257	-0.03
0.03173	1.972	10.463	535.7	0.00	0.00	0.00	2.254	10.557	551.5	8.04	-0.05	-0.01	11.790	0.10	0.321	0.027	0.824	0.00	0.321	0.10
0.03640	2.516	10.624	605.3	0.10	-0.01	0.00	2.847	10.775	619.9	6.73	-0.09	-0.01	11.926	0.13	0.315	0.026	0.824	0.00	0.315	0.13
0.04166	3.207	10.771	683.5	0.17	-0.02	0.00	3.562	11.025	693.6	7.53	-0.07	-0.01	12.361	0.30	0.378	0.031	0.830	0.00	0.378	0.30
0.04926	4.264	11.044	789.0	0.14	-0.01	0.00	4.711	11.336	798.4	8.67	-0.08	-0.01	12.703	0.47	0.363	0.029	0.827	0.00	0.363	0.47
0.05597	5.269	11.268	877.3	0.08	-0.01	0.00	5.830	11.579	888.4	9.65	-0.09	-0.01	13.133	0.53	0.359	0.028	0.827	0.00	0.359	0.53
0.06157	6.188	11.459	948.6	0.05	0.00	0.00	6.844	11.756	960.4	10.43	-0.05	0.00	13.591	0.69	0.356	0.027	0.827	0.00	0.356	0.69
0.06910	7.379	11.776	1042.0	0.10	0.01	0.00	8.122	12.111	1052.5	11.43	-0.05	0.00	14.177	0.89	0.359	0.028	0.818	0.00	0.359	0.89
0.07421	8.333	11.902	1109.2	0.12	0.01	0.00	9.169	12.241	1120.2	12.17	0.04	0.00	14.600	1.11	0.210	0.015	0.812	0.00	0.210	1.11
0.08975	11.336	12.341	1296.0	0.28	0.02	0.00	12.384	12.739	1304.1	14.16	0.21	0.02	15.359	1.57	0.093	0.006	0.799	0.00	0.093	1.57
0.10167	13.784	12.678	1428.2	0.46	0.04	0.00	15.107	13.066	1439.5	15.63	0.36	0.03	16.241	2.18	-0.109	-0.007	0.787	0.00	-0.109	2.18
0.10831	14.792	12.797	1479.9	0.52	0.04	0.00	16.206	13.183	1492.2	16.21	0.43	0.03	16.817	2.67	-0.371	-0.031	0.767	0.00	-0.371	2.67
0.11862	17.600	13.090	1612.8	0.66	0.05	0.00	19.294	13.489	1625.7	17.66	0.62	0.05	17.535	3.52	-0.680	-0.039	0.744	0.00	-0.680	3.52
0.13416	21.092	13.525	1759.3	0.94	0.07	0.00	23.392	13.856	1783.7	19.37	0.89	0.07	18.131	4.27	-1.078	-0.050	0.733	0.00	-1.078	4.27
0.14181	22.828	13.740	1840.5	1.08	0.09	0.00	25.408	14.052	1869.3	20.30	1.05	0.08	18.646	4.68	-1.285	-0.067	0.721	0.00	-1.285	4.68
0.16108	27.997	14.094	2038.5	1.26	0.10	0.00	31.277	14.387	2074.3	22.53	1.33	0.10	19.264	5.02	-1.498	-0.076	0.698	-1.87	-1.498	4.95
0.18032	33.110	14.507	2217.0	1.52	0.12	0.00	37.577	14.693	2273.7	24.69	1.62	0.12	20.407	5.43	-1.793	-0.088	0.684	-3.03	-1.793	5.32
0.19952	38.894	14.811	2403.1	1.69	0.13	0.00	43.787	15.061	2454.8	26.66	1.99	0.15	21.790	5.82						
0.22025	47.401	15.348	2653.2	2.05	0.15	0.00	54.641	15.424	2742.4	29.78	2.37	0.18	23.392	6.19						
0.26643	59.491	15.992	2972.4	2.50	0.19	0.00	70.122	15.870	3111.3	33.79	2.85	0.22	25.408	6.57						
0.30446	72.660	16.536	3285.0	2.87	0.21	0.00	87.012	16.404	3460.8	37.58	3.32	0.26	27.997	6.96						
0.36124	94.238	17.227	3740.5	3.34	0.24	0.00	114.879	16.935	3975.9	43.10	3.88	0.30	30.926	7.33						
0.41543	117.340	17.755	4171.6	3.87	0.26	0.00	145.206	17.221	4467.6	48.52	4.28	0.33	33.110	7.71						
0.46821	140.887	18.262	4571.1	4.02	0.28	0.00	172.227	17.568	4935.0	53.60	4.63	0.36	35.269	8.08						
0.54256	172.785	18.839	5131.3	4.40	0.30	0.00	227.216	17.979	5594.7	60.65	5.02	0.39	37.577	8.46						
0.61633	217.679	19.340	5670.1	4.73	0.32	0.00	282.927	18.703	6223.3	67.59	5.31	0.41	40.166	8.84						
0.70772	272.137	19.862	6299.4	5.07	0.34	0.00	360.697	18.614	6981.9	75.82	5.57	0.43	43.787	9.22						

0.0045" Ribbed 10.306" Pipe
 Resol= 350

Series
 PEO

TIME
 S1:
 d= 0.306
 h= smooth
 RTA:
 POLY M-750
 c= 300
 w= 1.101
 h= 0.0045
 Rn 32.6

Q (L/A)	Te (S1)	Vavg(S1)	ReSp(S1)	S (S1)	Sf (S1)	Te (RTA)	Vavg(RTA)	ReSp(RTA)	h _s	S (RTA)	Sf (RTA)	Vavg(S1)h	St (S1)	R	Rf	P	ΔPres	connected R	connected S
0.00411	0.085	6.525	104.0	0.04	0.01	0.085	6.666	104.8	1.15	0.04	0.01	6.638	0.03	0.011	0.003	0.00	0.00	0.103	-0.21
0.00608	0.126	7.939	126.5	0.08	0.01	0.126	8.119	128.5	1.40	0.08	0.01	8.057	0.05	0.034	0.003	0.00	0.00	0.034	-0.12
0.00780	0.163	9.057	144.1	0.13	0.01	0.163	9.189	145.9	1.58	0.13	0.01	9.072	0.07	0.065	0.008	0.00	0.00	0.065	-0.09
0.00981	0.204	10.066	161.4	0.18	0.01	0.204	10.239	163.2	1.77	0.18	0.01	10.161	0.10	0.117	0.016	0.00	0.00	0.117	-0.13
0.01247	0.272	11.076	186.6	0.25	0.01	0.272	11.251	189.3	2.04	0.25	0.01	11.136	0.14	0.161	0.021	0.00	0.00	0.161	-0.17
0.01702	0.357	12.086	220.3	0.33	0.01	0.357	12.361	223.6	2.39	0.33	0.01	12.241	0.19	0.214	0.028	0.00	0.00	0.214	-0.23
0.02146	0.459	13.096	269.1	0.43	0.01	0.459	13.336	272.4	2.81	0.43	0.01	13.216	0.25	0.281	0.037	0.00	0.00	0.281	-0.30
0.02514	0.571	14.106	328.1	0.53	0.01	0.571	14.386	331.4	3.31	0.53	0.01	14.266	0.32	0.351	0.048	0.00	0.00	0.351	-0.38
0.03159	0.699	15.116	398.1	0.64	0.01	0.699	15.436	401.4	3.91	0.64	0.01	15.316	0.41	0.431	0.061	0.00	0.00	0.431	-0.47
0.03637	0.843	16.126	478.1	0.76	0.01	0.843	16.486	481.4	4.61	0.76	0.01	16.366	0.51	0.511	0.077	0.00	0.00	0.511	-0.57
0.04117	1.003	17.136	568.1	0.89	0.01	1.003	17.536	571.4	5.41	0.89	0.01	17.446	0.62	0.611	0.097	0.00	0.00	0.611	-0.67
0.04811	1.173	18.146	668.1	1.03	0.01	1.173	18.636	671.4	6.31	1.03	0.01	18.546	0.74	0.711	0.123	0.00	0.00	0.711	-0.77
0.05557	1.353	19.156	778.1	1.18	0.01	1.353	19.736	781.4	7.31	1.18	0.01	19.646	0.87	0.811	0.157	0.00	0.00	0.811	-0.86
0.06108	1.543	20.166	898.1	1.34	0.01	1.543	20.816	901.4	8.41	1.34	0.01	20.756	1.01	0.891	0.201	0.00	0.00	0.891	-0.94
0.06850	1.743	21.176	1028.1	1.51	0.01	1.743	21.906	1031.4	9.61	1.51	0.01	21.846	1.16	0.951	0.255	0.00	0.00	0.951	-1.03
0.07390	1.953	22.186	1168.1	1.69	0.01	1.953	22.996	1171.4	10.91	1.69	0.01	22.886	1.32	1.011	0.321	0.00	0.00	1.011	-1.13
0.08848	2.173	23.196	1318.1	1.88	0.01	2.173	24.086	1321.4	12.31	1.88	0.01	23.976	1.49	1.081	0.397	0.00	0.00	1.081	-1.24
0.09961	2.403	24.206	1478.1	2.08	0.01	2.403	25.176	1481.4	13.81	2.08	0.01	24.866	1.67	1.161	0.483	0.00	0.00	1.161	-1.36
0.10603	2.643	25.216	1648.1	2.29	0.01	2.643	26.266	1641.4	15.41	2.29	0.01	25.756	1.86	1.251	0.579	0.00	0.00	1.251	-1.49
0.11618	2.893	26.226	1828.1	2.51	0.01	2.893	27.356	1801.4	17.11	2.51	0.01	26.646	2.06	1.351	0.685	0.00	0.00	1.351	-1.63
0.13022	3.153	27.236	2018.1	2.74	0.01	3.153	28.446	1961.4	18.91	2.74	0.01	27.536	2.27	1.461	0.801	0.00	0.00	1.461	-1.78
0.14373	3.423	28.246	2218.1	2.98	0.01	3.423	29.536	2121.4	20.81	2.98	0.01	28.426	2.49	1.581	0.927	0.00	0.00	1.581	-1.94
0.15904	3.703	29.256	2438.1	3.23	0.01	3.703	30.626	2291.4	22.81	3.23	0.01	29.316	2.72	1.711	1.063	0.00	0.00	1.711	-2.11
0.17224	3.993	30.266	2668.1	3.49	0.01	3.993	31.716	2481.4	24.91	3.49	0.01	30.206	2.96	1.851	1.211	0.00	0.00	1.851	-2.29
0.20910	4.593	32.276	3118.1	4.06	0.01	4.593	33.806	2931.4	29.41	4.06	0.01	32.096	3.41	2.001	1.371	0.00	0.00	2.001	-2.49
0.24736	5.203	34.286	3598.1	4.64	0.01	5.203	35.896	3401.4	34.11	4.64	0.01	33.986	3.87	2.161	1.541	0.00	0.00	2.161	-2.71
0.28546	5.833	36.296	4108.1	5.23	0.01	5.833	37.986	3891.4	39.11	5.23	0.01	35.876	4.34	2.331	1.721	0.00	0.00	2.331	-2.94
0.32532	6.483	38.306	4648.1	5.83	0.01	6.483	40.076	4401.4	44.31	5.83	0.01	37.766	4.82	2.511	1.911	0.00	0.00	2.511	-3.18
0.45887	8.143	44.316	5708.1	7.43	0.01	8.143	46.166	5451.4	54.81	7.43	0.01	43.656	5.71	2.811	2.211	0.00	0.00	2.811	-3.64
0.57029	9.903	50.516	6808.1	9.03	0.01	9.903	52.256	6501.4	65.61	9.03	0.01	49.546	6.61	3.111	2.511	0.00	0.00	3.111	-4.10
0.64384	11.763	56.716	7948.1	10.63	0.01	11.763	58.346	7651.4	76.61	10.63	0.01	55.436	7.51	3.411	2.811	0.00	0.00	3.411	-4.56
0.73496	13.723	62.916	9188.1	12.23	0.01	13.723	64.436	8891.4	88.61	12.23	0.01	61.326	8.41	3.711	3.111	0.00	0.00	3.711	-5.02
0.80719	15.783	69.116	10528.1	13.83	0.01	15.783	70.526	10231.4	103.11	13.83	0.01	67.216	9.31	4.011	3.411	0.00	0.00	4.011	-5.48

0.0045" Ribbed 0.308" Pipe
Resident - 350

Series PEO

PWE
S1:
d = 0.308
h = smooth
RIA:
d = 0.293
h = 0.0045
Nom 32.6

M-750
RUN
DATE
M-750
POLY
c temp
M-750

Q (L/A)	T _w (S1)	1/A _{sp} (S1)	Re _{sp} (S1)	S (S1)	SF (S1)	T _w (RIA)	1/A _{sp} (RIA)	Re _{sp} (RIA)	h _s	S (RIA)	SF (RIA)	1/A _{sp} (S1M)	S ₁ (S1)	R	RF	D	Δ/Inch	connected R	connected S
0.00340	0.087	5.354	85.9	0.16	0.02	0.095	5.517	86.6	0.94	-0.18	-0.02	5.396	0.09	-0.261	-0.026	0.744	0.00	-0.261	0.09
0.00546	0.138	6.802	108.7	0.02	0.00	0.156	6.910	111.1	1.21	-0.09	-0.01	6.965	0.00	-0.080	-0.008	0.774	0.00	-0.080	0.00
0.00740	0.186	7.951	126.0	0.03	0.00	0.211	8.049	129.3	1.40	-0.04	0.00	8.127	0.00	0.028	0.003	0.781	0.00	0.028	-0.03
0.00917	0.234	8.777	141.6	0.01	0.00	0.263	8.943	144.4	1.57	0.04	0.00	8.925	0.00	0.103	0.010	0.802	0.00	0.103	0.00
0.01289	0.336	10.301	170.0	0.05	0.00	0.368	10.620	171.3	1.86	0.17	0.02	10.368	0.00	0.199	0.018	0.815	0.00	0.199	0.07
0.01760	0.477	11.749	202.8	0.19	0.02	0.515	9.191	202.6	2.84	0.35	0.03	10.372	0.00	0.285	0.026	0.824	0.00	0.285	0.20
0.02176	1.018	9.983	296.8	0.81	0.05	1.300	9.535	322.7	3.51	0.81	0.07	9.943	0.09	0.465	0.035	0.836	0.00	0.465	0.36
0.02608	1.468	9.967	356.5	1.52	0.13	1.790	9.740	379.0	4.12	1.04	0.09	10.001	0.09	0.483	0.040	0.842	0.00	0.483	0.62
0.03011	1.918	10.065	407.6	2.41	0.20	2.246	10.035	424.7	4.61	1.64	0.16	10.115	0.00	0.469	0.034	0.837	0.00	0.469	1.89
0.03690	2.738	10.325	487.2	4.11	0.33	3.178	10.406	502.1	5.45	2.76	0.22	10.378	-0.03	0.519	0.036	0.837	0.00	0.519	2.40
0.04216	3.431	10.537	545.6	5.21	0.43	3.882	10.688	548.7	6.07	3.34	0.26	10.585	0.00	0.654	0.043	0.833	0.00	0.654	3.13
0.04989	4.538	10.843	627.7	6.26	0.50	5.053	11.086	637.6	6.92	4.16	0.32	10.887	0.07	0.590	0.038	0.840	0.00	0.590	3.22
0.05660	5.527	11.147	744.3	8.25	0.68	6.081	11.466	699.2	7.59	5.21	0.30	11.171	0.20	0.624	0.039	0.841	0.00	0.624	3.68
0.06244	6.407	11.421	744.3	10.81	0.81	7.019	11.773	750.0	8.14	6.46	0.37	11.457	0.36	0.316	0.028	0.828	0.00	0.316	0.20
0.06991	7.475	11.659	807.1	13.35	1.05	8.112	12.261	809.5	8.79	8.14	0.42	11.851	0.62	0.410	0.035	0.836	0.00	0.410	0.62
0.07616	8.434	12.141	858.3	18.88	1.33	9.086	12.620	857.7	9.31	1.04	0.09	12.137	0.80	0.463	0.040	0.842	0.00	0.463	0.80
0.08664	12.032	13.166	1026.5	24.11	1.88	13.029	13.651	1028.4	11.17	1.64	0.16	13.186	1.54	0.485	0.045	0.837	0.00	0.485	1.54
0.10603	13.482	13.622	1095.8	32.66	2.41	14.627	14.110	1088.8	11.82	1.97	0.16	13.641	1.89	0.469	0.034	0.836	0.00	0.469	1.89
0.12515	16.377	14.314	1195.5	41.11	3.26	17.751	14.838	1198.2	13.01	2.49	0.20	14.319	2.40	0.519	0.036	0.837	0.00	0.519	2.40
0.14153	19.775	14.735	1316.0	52.27	4.43	21.333	15.306	1315.9	14.29	2.76	0.22	14.771	2.69	0.535	0.036	0.841	0.00	0.535	2.69
0.15264	21.094	15.387	1353.3	62.27	5.21	22.956	15.914	1359.1	14.76	3.31	0.26	15.260	3.13	0.654	0.043	0.833	0.00	0.654	3.13
0.16086	23.285	15.434	1426.1	74.26	6.26	25.135	16.078	1426.5	15.51	3.34	0.26	15.438	3.22	0.590	0.038	0.840	0.00	0.590	3.22
0.19018	27.095	16.026	1540.5	93.68	8.25	29.209	16.654	1539.9	16.72	3.85	0.30	16.030	3.68	0.624	0.039	0.841	0.00	0.624	3.68
0.19756	30.031	16.691	1622.0	108.1	10.81	33.514	17.047	1649.6	17.92	4.16	0.32	16.855	4.39	0.192	0.011	0.813	0.00	0.192	4.39
0.22457	35.413	17.472	1761.4	133.5	13.35	38.984	17.738	1802.0	19.57	4.76	0.37	17.652	5.03	0.086	0.005	0.803	0.00	0.086	5.03
0.25926	43.231	18.256	1945.8	164.7	18.88	48.936	18.513	1993.1	21.64	5.47	0.42	18.550	5.75	-0.037	-0.002	0.801	0.00	-0.037	5.75
0.29968	51.301	19.371	2119.5	204.9	24.11	60.837	19.192	2222.1	24.13	6.12	0.47	19.819	6.83	-0.627	-0.032	0.765	0.00	-0.627	6.83
0.33732	64.364	20.525	2304.9	274.2	32.66	75.622	20.003	2541.8	27.60	6.94	0.53	21.205	7.98	-1.202	-0.052	0.740	0.00	-1.202	7.98
0.43599	83.910	21.955	2711.1	368.3	41.11	107.702	20.869	2957.0	32.11	7.86	0.60	22.852	9.37	-1.965	-0.086	0.707	0.00	-1.965	9.37
0.49136	99.313	22.827	2948.7	487.2	52.27	131.334	21.418	3264.6	35.45	8.42	0.65	23.912	10.26	-2.494	-0.104	0.686	0.00	-2.494	10.26
0.52954	110.393	23.334	3109.4	627.7	62.27	148.655	21.695	3473.7	37.72	8.71	0.67	24.693	10.93	-2.998	-0.121	0.674	0.00	-2.998	10.93
0.62476	137.363	24.680	3469.2	825.6	74.26	195.175	22.339	3981.2	43.24	9.38	0.72	26.170	12.17	-3.831	-0.146	0.638	0.00	-3.831	12.17
0.70070	161.049	25.563	3756.2	1081.1	93.68	236.919	22.740	4386.0	47.63	9.80	0.76	27.156	12.99	-4.416	-0.163	0.617	0.00	-4.416	12.99
0.79534	193.117	26.498	4109.4	1244.4	108.1	293.338	23.197	4875.9	52.95	10.26	0.79	28.233	13.88	-5.036	-0.178	0.597	0.00	-5.036	13.88
0.92728	242.084	27.593	4584.1	1335.5	133.5	365.186	23.602	5566.8	60.46	10.64	0.82	29.747	15.16	-6.145	-0.207	0.570	0.00	-6.145	15.16

0.0045" Ribbed 0.306" Pipe
Residence 350

Series
PEO

PIPE
SI:
d = 0.306
h = smooth
RI/A: 3
d = 0.293
h = 0.0045
RA: 32.6

RUN 243
DATE 9/11/93
POLY H-50K
c wppam 3
TR 1.003

Q(L/s)	Tw(S1)	1/nd(S1)	Resol(S1)	S(S1)	Sf(S1)	Tw(R1A)	1/nd(R1A)	Resol(R1A)	h	S(R1A)	Sf(R1A)	1/nd(S1)h	S(S1)	R	RF	P	d/Vres	corrected R	corrected S
0.00410	0.017	6.939	107.0	-0.03	0.00	0.087	6.949	109.4	1.19	-0.01	0.00	7.002	0.08	-0.178	-0.021	0.804	0.00	-0.178	0.06
0.00615	0.116	8.381	131.3	-0.03	0.00	0.130	8.539	131.8	1.45	-0.01	0.00	8.524	0.09	-0.006	-0.001	0.209	0.00	-0.006	-0.04
0.00786	0.150	9.391	149.8	-0.03	0.00	0.166	9.655	151.4	1.64	-0.01	0.00	9.477	0.08	-0.004	-0.001	0.823	0.00	-0.004	-0.04
0.00993	0.193	10.468	170.0	-0.03	0.00	0.212	10.785	171.4	1.86	-0.01	0.00	10.494	0.08	0.083	0.008	0.797	0.00	0.083	-0.07
0.01121	0.227	10.903	184.4	-0.03	0.00	0.367	8.888	234.9	2.55	-0.01	0.00	11.853	0.08	0.296	0.027	0.825	0.00	0.296	0.01
0.01352	0.276	11.910	203.7	-0.03	0.00	0.527	9.302	270.9	2.94	-0.01	0.00	10.993	0.08	0.314	0.042	0.844	0.00	0.314	0.11
0.01903	0.788	9.926	344.5	-0.03	0.00	0.952	9.747	364.4	3.96	-0.10	0.00	9.925	0.08	0.460	0.038	0.838	0.00	0.460	0.34
0.02377	1.193	10.076	424.2	-0.03	0.00	1.377	10.120	438.8	4.77	-0.07	0.00	10.126	0.08	0.514	0.042	0.844	0.00	0.514	0.75
0.02862	1.639	10.352	497.4	-0.03	0.00	1.864	10.472	510.7	5.55	-0.06	0.00	10.389	0.08	0.557	0.044	0.847	0.00	0.557	0.92
0.03304	2.099	10.528	563.4	-0.07	0.01	2.338	10.762	572.5	6.22	0.06	0.01	10.925	0.01	0.376	0.034	0.834	0.00	0.376	0.11
0.04036	2.937	10.902	666.9	0.01	0.00	3.228	11.221	673.1	7.31	0.19	0.02	11.200	0.11	0.430	0.037	0.840	0.00	0.430	0.34
0.04607	3.636	11.187	742.2	0.10	0.01	3.953	11.576	745.0	8.09	0.32	0.03	11.648	0.34	0.460	0.038	0.838	0.00	0.460	0.58
0.04452	4.700	11.643	843.8	0.34	0.03	5.085	12.078	844.9	9.18	0.53	0.05	12.057	0.58	0.460	0.038	0.840	0.00	0.460	0.58
0.06231	5.726	12.057	930.8	0.58	0.05	6.186	12.517	931.4	10.11	0.74	0.06	12.362	0.75	0.514	0.042	0.844	0.00	0.514	0.75
0.07645	6.732	12.370	1009.3	0.75	0.06	7.234	12.876	1007.2	10.94	0.92	0.08	12.660	0.92	0.557	0.044	0.847	0.00	0.557	0.92
0.08530	7.801	12.674	1085.5	0.93	0.08	8.350	13.217	1081.2	11.74	1.09	0.09	12.660	0.92	0.557	0.044	0.847	0.00	0.557	0.92
0.09137	8.896	13.242	1166.1	1.38	0.12	9.758	13.641	1175.8	12.77	1.33	0.11	13.272	1.39	0.369	0.028	0.827	0.00	0.369	1.39
0.10434	11.906	14.078	1288.6	1.52	0.13	10.849	13.858	1241.2	13.48	1.43	0.12	13.531	1.56	0.327	0.024	0.824	0.00	0.327	1.56
0.11080	12.952	14.254	1407.4	2.06	0.17	14.419	14.576	1429.6	15.53	1.89	0.15	14.346	2.13	0.230	0.016	0.815	0.00	0.230	2.13
0.13457	17.292	14.983	1619.7	2.55	0.20	19.357	15.279	1649.8	17.92	2.39	0.19	15.067	2.60	0.452	0.030	0.833	0.00	0.452	2.59
0.13602	17.619	15.003	1639.7	2.54	0.20	19.193	15.509	1647.6	17.89	2.62	0.20	15.057	2.59	0.452	0.030	0.833	0.00	0.452	2.59
0.14952	19.947	15.500	1745.0	2.93	0.23	22.426	15.773	1781.2	19.34	2.81	0.22	15.629	3.03	0.144	0.009	0.807	0.00	0.144	3.03
0.16463	23.006	15.920	1874.2	3.23	0.25	26.631	15.965	1941.3	21.08	2.94	0.23	16.115	3.36	-0.150	-0.009	0.774	0.00	-0.150	3.36
0.18224	26.729	16.320	2028.2	3.50	0.27	31.323	16.266	2105.4	22.85	3.21	0.25	16.406	3.51	-0.140	-0.009	0.774	0.00	-0.140	3.51
0.19952	31.466	16.484	2189.7	3.52	0.27	35.975	16.617	2256.2	24.63	3.55	0.27	16.630	3.62	-0.013	-0.001	0.782	0.00	-0.013	3.62
0.22633	38.020	16.995	2409.2	3.87	0.29	43.786	16.709	2545.3	27.64	3.65	0.28	17.193	3.97	-0.484	-0.028	0.753	0.00	-0.484	3.97
0.24545	43.479	17.235	2576.2	3.99	0.30	52.939	16.852	2746.7	29.72	3.60	0.29	17.437	4.09	-0.585	-0.034	0.745	-0.26	-0.585	4.06
0.28356	55.404	17.638	2907.9	4.18	0.31	69.368	17.008	3132.5	34.02	3.99	0.31	17.888	4.30	-0.880	-0.049	0.724	-1.08	-0.880	4.21
0.32153	68.495	17.968	3233.0	4.35	0.32	88.401	17.033	3536.0	38.40	4.10	0.32	18.194	4.40	-1.111	-0.061	0.703	-1.80	-1.111	4.26
0.37821	91.627	18.294	3738.2	4.40	0.32	123.035	17.033	4170.4	45.29	4.09	0.32	18.437	4.36	-1.404	-0.076	0.675	-2.78	-1.404	4.17
0.41581	109.318	18.413	4082.4	4.37	0.31	150.937	16.938	4609.9	50.06	4.00	0.31	18.521	4.27	-1.583	-0.085	0.659	-3.38	-1.583	4.06
0.47194	139.172	18.522	4603.6	4.27	0.30	197.984	16.755	5286.2	57.41	3.81	0.29	18.558	4.07	-1.803	-0.097	0.638	-4.20	-1.803	3.84
0.52774	173.412	18.555	5132.1	4.11	0.28	253.962	16.543	5979.2	64.93	3.57	0.27	18.535	3.83	-1.992	-0.107	0.619	-4.95	-1.992	3.59
0.62000	239.929	18.533	6006.1	3.82	0.26	366.983	16.168	7151.2	77.64	3.11	0.24	18.459	3.44	-2.291	-0.124	0.593	-6.05	-2.291	3.20

0.0045" Ribbed 0.308" Pipe
 Pendent: 350

Series

PEO

PIFF
 S1:
 d = 0.308
 h = 0.0045
 RIA: M-50K
 POLY
 c: mason
 r: 1.010
 Rn: 32.6

RUN 242
 DATE 9/10/93
 POLY M-50K
 c: mason
 r: 1.010

Q (L/s)	Tw (S1)	1/Agf(S1)	Respf(S1)	S (S1)	Sf (S1)	Tm (RIA)	1/Agf(RIA)	Respf(RIA)	Ns	S (RIA)	Sf (RIA)	1/Agf(S1M)	S1(S1)	R	RF	P	d/ries	corrected R	corrected P
0.00527	0.099	7.748	124.5	0.05	0.00	0.111	7.904	126.8	1.38	-0.71	-0.02	7.925	0.00	-0.206	-0.021	0.753	0.00	-0.206	0.00
0.00677	0.125	8.865	140.1	0.06	0.01	0.140	9.043	142.6	1.55	-0.11	-0.01	10.166	-0.06	-0.027	-0.003	0.784	0.00	-0.027	-0.06
0.00814	0.152	9.674	154.7	0.07	0.02	0.170	9.870	157.5	1.71	0.00	0.00	10.450	-0.03	0.081	0.008	0.799	0.00	0.081	-0.03
0.00985	0.190	10.654	173.4	0.09	0.03	0.212	10.627	176.4	1.92	0.15	0.01	10.740	0.04	0.190	0.018	0.814	0.00	0.190	0.04
0.01147	0.225	11.092	190.7	0.11	0.05	0.262	11.020	190.7	2.16	0.48	0.04	11.233	0.28	0.327	0.029	0.829	0.00	0.327	0.28
0.01445	0.338	11.860	236.6	0.15	0.09	0.385	11.720	240.8	2.62	0.74	0.07	11.628	0.52	0.391	0.034	0.835	0.00	0.391	0.52
0.01894	0.492	12.851	295.3	0.20	0.14	0.547	12.619	295.3	3.20	1.20	0.10	12.345	1.02	0.424	0.034	0.835	0.00	0.424	1.02
0.02394	0.644	13.988	355.3	0.26	0.20	0.731	13.359	344.2	3.92	1.58	0.13	12.739	1.26	0.620	0.049	0.853	0.00	0.620	1.26
0.02880	0.844	15.398	419.2	0.33	0.28	0.945	14.100	394.2	4.71	1.91	0.16	13.276	1.66	0.595	0.045	0.847	0.00	0.595	1.66
0.03376	1.095	16.995	485.1	0.41	0.36	1.184	14.900	449.1	5.56	2.25	0.19	13.852	2.10	0.538	0.039	0.841	0.00	0.538	2.10
0.04123	1.400	18.888	562.4	0.50	0.46	1.451	15.740	507.4	6.46	2.52	0.20	14.403	2.54	0.407	0.028	0.830	0.00	0.407	2.54
0.04696	1.766	20.992	650.7	0.60	0.55	1.744	16.620	590.7	7.42	2.96	0.24	14.924	2.96	0.455	0.030	0.832	0.00	0.455	2.96
0.05475	2.194	23.335	750.2	0.71	0.66	2.064	17.540	684.2	8.46	3.39	0.27	15.467	3.39	0.463	0.030	0.831	0.00	0.463	3.39
0.06475	2.688	25.922	861.2	0.83	0.78	2.414	18.500	784.2	9.54	3.85	0.29	16.017	3.85	0.269	0.017	0.824	0.00	0.269	3.85
0.07266	3.240	28.766	984.2	0.96	0.89	2.794	19.490	894.2	10.71	4.35	0.31	16.388	4.16	0.311	0.019	0.816	0.00	0.311	4.16
0.08131	3.862	31.888	1120.2	1.10	1.01	3.204	20.500	1000.2	11.84	4.89	0.34	16.811	4.46	0.345	0.021	0.820	0.00	0.345	4.46
0.08963	4.544	35.292	1270.2	1.25	1.14	3.644	21.540	1114.2	12.86	5.46	0.34	16.859	4.50	0.318	0.019	0.815	0.00	0.318	4.50
0.09602	5.288	39.000	1436.2	1.41	1.28	4.114	22.620	1236.2	13.84	6.00	0.38	17.475	4.93	0.351	0.020	0.819	0.00	0.351	4.93
0.10795	6.094	43.122	1618.2	1.58	1.42	4.614	23.740	1374.2	14.84	6.60	0.40	18.191	5.49	0.061	0.003	0.804	0.00	0.061	5.49
0.11644	6.966	47.666	1816.2	1.76	1.58	5.144	24.900	1526.2	15.84	7.14	0.42	18.831	5.98	-0.312	-0.017	0.769	0.00	-0.312	5.98
0.12443	7.904	52.644	2030.2	1.95	1.75	5.714	26.090	1684.2	16.84	7.74	0.44	19.266	6.28	-0.398	-0.021	0.771	0.00	-0.398	6.28
0.13220	8.914	58.060	2262.2	2.15	1.94	6.324	27.300	1846.2	17.84	8.34	0.47	20.326	7.09	-1.121	-0.055	0.731	0.00	-1.121	7.09
0.13795	10.000	63.920	2514.2	2.36	2.14	6.974	28.540	2014.2	18.84	8.94	0.49	21.046	7.59	-1.570	-0.075	0.699	-0.49	-1.529	7.55
0.15915	11.272	70.266	2786.2	2.58	2.34	7.654	29.800	2194.2	19.84	9.54	0.52	21.730	8.00	-1.933	-0.090	0.673	-0.49	-1.792	7.84
0.17839	12.734	77.100	3078.2	2.81	2.53	8.374	31.090	2386.2	20.84	10.14	0.54	22.139	8.21	-2.260	-0.102	0.652	-2.24	-2.025	7.97
0.19760	14.386	84.526	3390.2	3.05	2.73	9.134	32.400	2590.2	21.84	10.74	0.54	22.408	8.21	-2.379	-0.106	0.637	-5.20	-2.097	7.93
0.21675	16.228	92.560	3724.2	3.30	2.92	9.914	33.740	2814.2	22.84	11.34	0.55	22.533	8.16	-2.483	-0.110	0.627	-6.38	-2.171	7.85
0.25498	18.270	101.100	4080.2	3.56	3.10	10.734	35.100	3054.2	23.84	11.94	0.54	22.618	8.00	-2.619	-0.116	0.615	-7.95	-2.280	7.67
0.29307	20.422	110.240	4458.2	3.82	3.28	11.594	36.490	3314.2	24.84	12.54	0.54	22.541	7.73	-2.670	-0.118	0.602	-9.22	-2.317	7.38
0.34091	22.684	120.000	4848.2	4.08	3.46	12.494	37.900	3604.2	25.84	13.14	0.51	22.446	7.44	-2.787	-0.124	0.590	-10.54	-2.423	7.07

0.0045" Fiberglass® Pipe
Resin: 350

Series

PEO

PIE

SI:
d = 0.308
h = smooth
R1A:
d = 0.293
h = 0.0045
Rn 32.6

241
9/9/93
M-60K
30
1.031

Q(L/A)	T ₁ (SI)	V _{avg} (SI)	Re _{avg} (SI)	S ₁ (SI)	S ₂ (SI)	T ₂ (R1A)	V _{avg} (R1A)	Re _{avg} (R1A)	h ₂	S ₁ (R1A)	S ₂ (R1A)	V _{avg} (SI)W	S ₁ (SI)	R	RF	P	Δ/T _{res}	corrected R	corrected S
0.00354	0.066	6.388	99.1	0.16	0.02	0.074	6.489	101.3	1.10	0.074	0.00	6.537	0.17	-0.120	-0.012	0.773	0.00	-0.120	0.17
0.00547	0.102	7.932	123.6	0.15	0.01	0.114	8.076	126.1	1.37	0.114	0.03	8.078	0.16	0.222	0.021	0.818	0.00	0.222	0.16
0.00780	0.149	9.355	149.6	0.37	0.04	0.163	9.638	150.8	1.64	0.163	0.07	9.448	0.36	0.488	0.045	0.848	0.00	0.488	0.36
0.00879	0.167	9.972	158.4	0.16	0.01	0.183	10.258	159.9	1.74	0.183	0.10	10.043	0.36	0.801	0.066	0.867	0.00	0.801	1.24
0.01047	0.208	10.624	177.1	0.20	0.02	0.311	9.386	208.3	2.26	0.311	0.28	10.100	2.38	1.122	0.082	0.889	0.00	1.122	2.38
0.01195	0.306	9.499	215.0	0.45	0.09	0.455	8.846	236.5	2.74	0.455	0.36	9.611	2.74	1.019	0.070	0.865	0.00	1.019	3.02
0.01709	0.694	3.241	391.1	0.15	0.01	0.809	9.490	337.0	3.66	0.809	0.00	9.593	3.66	1.098	0.073	0.878	0.00	1.098	3.53
0.02196	1.008	10.127	591.1	0.15	0.01	1.183	10.067	407.8	4.43	1.183	0.00	10.207	4.43	1.123	0.071	0.868	0.00	1.123	4.08
0.02754	1.487	10.458	475.1	0.37	0.04	1.649	10.714	481.8	5.23	1.649	0.03	10.492	5.23	0.602	0.037	0.839	0.00	0.602	4.69
0.03393	2.055	10.957	559.1	0.37	0.04	2.198	11.430	556.7	6.05	2.198	0.07	10.942	6.05	0.769	0.042	0.843	0.00	0.769	6.24
0.04855	3.315	12.342	708.7	1.34	0.12	3.463	13.018	697.9	7.58	3.463	0.23	12.217	7.58	0.801	0.066	0.857	0.00	0.801	7.24
0.05817	4.049	13.363	787.6	2.20	0.20	4.307	14.000	782.0	8.49	4.307	0.28	13.308	8.49	0.692	0.052	0.853	0.00	0.692	2.14
0.06718	5.021	13.878	877.1	2.51	0.22	5.125	14.871	853.0	9.26	5.125	0.28	13.699	9.26	1.122	0.082	0.889	0.00	1.122	2.38
0.07509	5.596	14.695	925.3	3.23	0.26	5.871	15.480	912.3	9.91	5.871	0.32	14.461	9.91	1.019	0.070	0.865	0.00	1.019	3.02
0.08447	6.569	15.256	1002.1	3.65	0.31	6.785	16.197	980.4	10.65	6.785	0.36	15.099	10.65	1.098	0.073	0.878	0.00	1.098	3.53
0.09420	7.438	15.990	1064.9	4.28	0.37	7.769	16.881	1047.7	11.38	7.769	0.40	15.758	11.38	1.123	0.071	0.868	0.00	1.123	4.08
0.09860	7.714	16.433	1092.4	4.68	0.40	8.342	17.050	1093.6	11.88	8.342	0.40	16.448	11.88	0.602	0.037	0.839	0.00	0.602	4.69
0.11037	8.762	17.259	1163.1	5.40	0.45	9.480	17.903	1164.7	12.65	9.480	0.46	17.233	12.65	0.670	0.039	0.838	0.00	0.670	5.37
0.12016	9.886	17.692	1233.5	5.73	0.46	10.631	18.407	1231.5	13.37	10.631	0.48	17.680	13.37	0.727	0.041	0.843	0.00	0.727	5.72
0.13520	11.601	18.376	1323.9	6.29	0.52	12.511	19.092	1323.6	14.37	12.511	0.52	18.323	14.37	0.769	0.042	0.841	0.00	0.769	6.24
0.13766	11.950	18.435	1344.9	6.32	0.52	12.809	19.212	1340.4	14.56	12.809	0.54	18.428	14.56	0.784	0.043	0.846	0.00	0.784	6.32
0.15133	13.607	19.218	1435.3	6.99	0.57	15.144	19.654	1457.7	15.83	15.144	0.54	19.447	15.83	0.207	0.011	0.815	0.00	0.207	7.19
0.17052	15.346	20.151	1524.3	7.82	0.63	17.597	20.304	1571.4	17.07	17.597	0.61	20.348	17.07	0.044	-0.002	0.791	0.00	0.044	7.96
0.18984	18.098	20.658	1655.5	8.18	0.66	20.686	20.848	1704.0	18.51	20.686	0.64	21.030	18.51	-0.182	-0.009	0.793	0.00	-0.182	8.50
0.21300	20.852	21.593	1777.5	8.99	0.71	24.822	21.354	1867.1	20.28	24.822	0.68	22.236	20.28	9.55	-0.882	0.762	0.00	-0.882	9.55
0.25155	25.754	22.947	1975.5	10.16	0.80	32.720	21.966	2143.7	23.28	32.720	0.71	23.725	23.28	-1.759	-0.074	0.714	0.00	-1.759	10.80
0.29006	31.530	23.914	2186.4	10.95	0.85	41.990	22.358	2429.1	26.38	41.990	0.71	24.949	26.38	-2.591	-0.104	0.681	0.00	-2.591	11.81
0.34964	41.176	25.224	2498.6	12.03	0.91	58.689	22.796	2871.9	31.19	58.689	0.75	26.418	31.19	3.622	-0.137	0.636	0.00	3.622	12.97
0.40718	51.639	26.231	2798.5	12.84	0.96	78.458	22.961	3320.9	36.06	78.458	0.77	27.250	36.06	-4.269	-0.157	0.597	-0.23	-4.269	13.40
0.48181	67.779	27.092	3206.8	13.47	0.99	107.390	23.222	3886.0	42.20	107.390	0.79	27.969	42.20	-4.747	-0.170	0.572	-0.66	-4.747	13.72
0.55914	87.278	27.657	3639.4	13.81	1.00	142.951	23.317	4484.0	48.70	142.951	0.80	28.332	48.70	5.015	-0.177	0.554	-0.26	5.015	13.75
0.65326	114.212	28.298	4164.3	14.22	1.01	192.932	23.491	5210.6	56.59	192.932	0.81	28.703	56.59	-5.212	-0.182	0.537	-1.117	-5.212	13.81
0.71018	134.660	28.331	4521.2	14.11	0.99	226.629	23.563	5846.7	61.32	226.629	0.82	28.521	61.32	-4.938	-0.174	0.539	-1.394	-4.938	13.46
0.76698	153.979	28.614	4833.7	14.28	1.00	284.004	23.578	6093.3	66.17	284.004	0.82	28.283	66.17	-4.705	-0.166	0.529	-1.437	-4.705	13.07
0.88023	203.452	28.568	5559.2	13.99	0.96	348.475	23.552	7004.4	76.07	348.475	0.80	27.796	76.07	-4.244	-0.153	0.530	-1.736	-4.244	12.32

0.0045" Ribbed 0.306" Pipe
Resist = 350

Series
PEO

PIPE

d = 0.308
h = smooth
R/A = 9/16/93
M-60K
POLY
c = mpmm
Rn = 32.6

M-60K
RUN
DATE
POLY
c = mpmm
Rn = 32.6

Q (L/s)	T _e (S)	V _{avg} (S)	Re _{avg} (S)	S (S)	SF (S)	T _e (R/A)	V _{avg} (R/A)	Re _{avg} (R/A)	h _s	S (R/A)	SF (R/A)	V _{avg} (S/M)	S _h (S)	R	Rf	P	Δ/ires	corrected R	corrected S	
0.00402	0.083	6.446	1036	0.26	0.03	0.092	6.613	1049	1.14	0.092	0.03	6.547	0.00	-0.038	-0.004	0.820	0.00	-0.038	0.00	
0.00487	0.099	7.167	1130	0.84	0.08	0.109	7.359	1143	1.24	0.109	0.07	7.247	0.00	0.043	0.004	0.822	0.00	0.043	0.25	
0.00717	0.148	8.646	1382	1.65	0.15	0.144	8.859	1401	1.52	0.144	0.10	8.754	0.00	0.346	0.031	0.818	0.00	0.346	0.76	
0.00868	0.180	9.462	1529	2.25	0.21	0.198	9.722	1546	1.68	0.198	0.15	9.517	0.00	0.703	0.058	0.823	0.00	0.703	1.51	
0.01013	0.219	10.019	1687	3.22	0.29	0.243	10.274	1709	1.86	0.243	0.20	10.107	0.00	1.073	0.084	0.819	0.00	1.073	2.07	
0.01241	0.277	10.917	1898	4.68	0.36	0.466	10.979	2071	2.57	0.466	0.27	10.384	0.00	1.243	0.086	0.539	0.00	1.243	2.96	
0.01469	0.428	10.390	2363	5.48	0.42	0.615	9.354	2727	2.96	0.615	0.37	10.080	0.00	1.666	0.073	0.631	0.00	1.666	4.48	
0.02036	0.926	9.798	3478	6.68	0.48	1.078	9.796	3613	3.92	1.078	0.42	9.894	0.00	1.061	0.064	0.863	0.00	1.061	5.33	
0.02756	1.484	10.438	4423	8.20	0.55	1.604	10.471	4411	4.79	1.604	0.58	10.428	0.00	0.641	0.056	0.843	0.00	0.641	6.50	
0.03460	2.015	11.287	5138	9.30	0.63	2.102	11.521	5053	5.49	2.102	0.62	11.175	0.00	0.816	0.051	0.817	0.00	0.816	7.49	
0.04272	2.583	12.307	5821	10.28	0.70	2.678	12.840	5707	6.20	2.678	0.67	12.137	0.00	0.962	0.045	0.809	0.00	0.962	8.50	
0.04927	3.052	13.056	6331	11.75	0.79	3.134	13.901	6176	6.71	3.134	0.74	12.928	0.00	1.116	0.033	0.809	0.00	1.116	9.62	
0.05975	3.788	14.212	7054	12.44	0.86	4.570	15.154	6972	7.46	4.570	0.82	13.911	0.00	1.431	0.024	0.789	0.00	1.431	10.55	
0.06854	4.385	15.152	7591	13.74	0.96	5.145	16.014	7461	8.10	5.145	0.88	14.927	0.00	1.595	0.019	0.749	0.00	1.595	12.09	
0.07648	4.950	15.916	8066	14.41	1.00	5.862	17.210	8527	8.60	5.862	0.91	15.649	0.00	1.819	0.013	0.745	0.00	1.819	13.39	
0.08657	5.673	16.827	8640	15.31	1.08	6.376	18.500	9233	9.26	6.376	0.93	16.649	0.00	2.016	0.008	0.697	0.00	2.016	14.31	
0.09783	6.480	17.792	9242	15.86	1.18	7.292	18.647	9447	10.26	7.292	0.98	17.699	0.00	2.257	0.005	0.675	0.00	2.257	15.16	
0.10081	6.774	17.931	9458	16.63	1.21	8.273	19.346	10048	10.91	8.273	1.00	19.102	0.00	2.439	0.004	0.652	0.00	2.439	15.93	
0.11140	7.454	18.890	9907	17.63	1.25	9.598	20.272	10738	11.66	9.598	1.06	20.221	0.00	2.618	0.003	0.626	0.00	2.618	16.72	
0.12547	8.526	19.893	10535	18.10	1.31	11.105	21.358	11590	12.59	11.105	1.10	21.474	0.00	2.819	0.002	0.607	0.00	2.819	17.02	
0.14250	9.766	21.109	11290	18.48	1.34	13.388	22.382	12726	13.82	13.388	1.08	22.571	0.00	3.032	0.001	0.586	0.00	3.032	17.73	
0.16395	11.644	22.244	12328	18.80	1.37	15.521	22.992	13703	14.88	15.521	0.96	23.566	0.00	3.257	0.001	0.562	0.00	3.257	18.26	
0.18134	13.370	22.950	13210	18.80	1.34	18.230	23.473	14851	16.13	18.230	0.96	24.880	0.00	3.490	0.000	0.539	0.00	3.490	18.98	
0.20065	15.055	23.940	14019	11.75	1.34	20.092	24.285	16716	18.15	20.092	1.00	26.000	0.00	3.732	0.000	0.515	0.00	3.732	19.95	
0.23363	18.971	24.833	15738	12.44	1.37	29.150	24.841	18754	20.37	29.150	1.06	28.000	0.00	4.009	0.000	0.491	0.00	4.009	21.15	
0.26850	22.395	26.267	17074	13.74	1.41	37.414	25.257	21283	23.11	37.414	1.10	29.076	0.00	4.267	0.000	0.465	0.00	4.267	21.50	
0.30820	27.845	27.135	19071	14.41	1.41	50.296	25.842	24678	26.80	50.296	1.18	30.932	0.00	4.509	0.000	0.439	0.00	4.509	21.83	
0.36681	36.139	28.256	21729	15.31	1.38	66.368	26.023	28954	30.79	66.368	1.21	31.330	0.00	4.743	0.000	0.413	0.00	4.743	21.95	
0.42442	45.845	29.019	24478	15.86	1.21	82.943	26.425	31702	34.43	82.943	1.25	32.333	0.00	4.965	0.000	0.387	0.00	4.965	21.83	
0.48161	55.475	29.947	26930	16.63	1.25	116.460	26.715	31572	40.81	116.460	1.06	33.405	0.00	5.187	0.000	0.361	0.00	5.187	21.83	
0.57719	73.364	31.197	30980	17.63	1.30	155.582	26.920	43434	47.17	155.582	1.06	34.805	0.00	5.409	0.000	0.335	0.00	5.409	21.83	
0.67225	95.241	31.890	35259	18.10	1.31	208.823	27.165	50325	54.65	208.823	1.10	36.322	0.00	5.621	0.000	0.309	0.00	5.621	21.83	
0.78569	122.866	32.823	40097	19.81	1.34	281.993	26.743	58159	63.16	281.993	1.06	37.777	0.00	5.833	0.000	0.283	0.00	5.833	21.83	
0.89906	152.818	33.671	44472	19.48	1.37															

0.0048" Fiberglass 300" Pipe
 Modulus = 350

Series
 PEO

WSR-301
 RUN 252
 DATE 10/10/93
 POLY WSR-301
 c temp 100
 W 1.205

PIPE
 S1:
 d = 0.308
 h = smooth
 R/A: 10/10/93
 d = 0.293
 h = 0.0045
 Rn 32.6

Q (L/s)	Tw (S1)	1/Amp(S1)	Reag(S1)	S (S1)	SF (S1)	Tw (R1A)	1/Amp(R1A)	Reag(R1A)	h	S (R1A)	SF (R1A)	1/Amp(S1M)	S1 (S1)	R	RF	P	d/ires	corrected R	corrected S
0.00405	0.094	6.122	98.3	5.81	0.59	0.102	6.329	98.7	1.07	5.72	0.58	6.147	6.09	-0.370	-0.023	0.777	0.00	-0.370	6.09
0.00504	0.117	6.836	109.8	6.41	0.64	0.127	7.059	112.3	1.20	6.53	0.65	15.960	6.55	-0.016	-0.001	0.796	0.00	-0.016	6.55
0.00618	0.141	7.614	120.9	7.02	0.69	0.154	7.858	121.7	1.32	7.25	0.71	17.338	7.09	0.183	0.011	0.805	0.00	0.183	7.09
0.00739	0.173	8.447	134.1	7.84	0.75	0.187	8.762	134.3	1.46	7.61	0.73	17.909	7.46	0.194	0.011	0.811	0.00	0.194	7.46
0.01061	0.245	9.919	160.1	8.74	0.82	0.283	9.965	165.5	1.80	8.27	0.74	18.770	8.20	-0.268	-0.014	0.791	0.00	-0.268	8.20
0.01729	0.440	12.483	214.8	9.24	0.86	0.579	11.353	237.1	2.58	9.53	0.87	19.544	9.34	0.293	0.015	0.813	0.00	0.293	9.34
0.02161	0.643	14.660	293.9	9.86	0.90	0.763	12.359	272.7	2.96	9.92	0.89	20.175	10.25	-0.184	-0.009	0.800	0.00	-0.184	10.25
0.02605	0.817	13.347	324.1	10.60	0.96	0.983	13.176	310.0	3.37	10.84	0.96	21.285	10.97	0.064	0.003	0.815	0.00	0.064	10.97
0.03114	0.994	14.460	324.1	11.42	1.02	1.173	14.358	339.0	3.68	11.69	1.01	22.117	10.97	0.298	0.013	0.817	0.00	0.298	11.62
0.03732	1.222	15.634	359.6	11.90	1.04	1.426	15.610	374.1	4.06	12.37	1.06	22.913	11.62	0.772	0.033	0.831	0.00	0.772	11.87
0.04282	1.463	16.389	393.9	11.80	1.03	1.647	16.567	404.8	4.40	12.37	1.05	23.297	11.87	0.772	0.033	0.831	0.00	0.772	11.87
0.05133	2.223	17.232	449.5	12.23	1.06	2.141	17.521	459.2	4.99	12.38	1.05	23.467	11.96	0.738	0.031	0.846	0.00	0.738	11.96
0.05944	3.463	18.363	505.6	12.99	1.11	2.690	18.103	514.8	5.59	12.83	1.05	24.008	12.39	0.322	0.013	0.813	0.00	0.322	12.39
0.06544	4.04	17.748	537.4	12.99	1.11	3.122	18.502	554.0	6.02	12.83	1.05	24.961	13.19	0.042	0.002	0.797	0.00	0.042	13.19
0.07380	2.223	19.340	576.6	13.51	1.14	3.567	19.540	592.8	6.44	13.32	1.08	25.741	13.85	-0.095	-0.004	0.797	0.00	-0.095	13.85
0.08378	3.247	20.040	632.1	14.29	1.20	4.181	20.466	642.9	6.98	13.32	1.08	26.356	14.32	-0.444	-0.017	0.759	0.00	-0.444	14.32
0.09528	4.486	20.626	695.1	14.29	1.20	5.209	21.101	721.0	7.83	13.33	1.05	27.000	14.81	-1.018	-0.038	0.752	0.00	-1.018	14.81
0.10628	5.144	21.689	743.5	15.26	1.25	5.916	22.181	771.4	8.38	13.16	1.02	27.858	15.42	-1.825	-0.056	0.695	0.00	-1.825	15.42
0.12174	6.186	22.661	813.4	15.48	1.24	7.073	23.211	837.3	9.09	13.45	1.04	28.769	16.13	-2.334	-0.081	0.686	0.00	-2.334	16.13
0.13730	7.438	23.307	896.6	16.49	1.30	8.150	24.059	903.5	9.81	13.55	1.04	30.259	17.31	-3.648	-0.121	0.646	0.00	-3.648	17.31
0.14024	7.811	23.233	908.0	16.49	1.30	9.229	24.205	950.3	10.32	13.69	1.05	30.259	18.57	-5.062	-0.160	0.601	0.00	-5.062	18.57
0.15509	9.090	23.817	991.4	17.46	1.40	10.166	24.330	1009.4	10.96	14.10	1.08	33.333	19.76	-6.216	-0.186	0.567	0.00	-6.216	19.76
0.17442	10.675	24.716	1074.6	18.52	1.47	12.266	25.003	1104.2	11.99	14.24	1.10	34.558	20.71	-7.350	-0.213	0.536	0.00	-7.350	20.71
0.19181	12.266	25.355	1152.0	19.33	1.43	13.962	25.646	1183.3	12.85	14.48	1.12	36.009	21.99	-8.577	-0.238	0.518	0.00	-8.577	21.99
0.21111	13.867	26.246	1225.3	20.02	1.47	16.548	26.546	1286.6	13.99	14.40	1.11	37.583	23.39	-10.240	-0.272	0.500	0.00	-10.240	23.39
0.23040	16.274	26.442	1327.5	20.34	1.48	19.580	26.982	1401.9	15.22	14.40	1.11	39.423	25.04	-12.711	-0.322	0.457	0.00	-12.711	25.04
0.26701	20.112	27.565	1476.1	21.00	1.51	26.135	28.033	1619.9	17.59	13.77	1.06	27.858	15.42	-1.825	-0.056	0.695	0.00	-1.825	15.42
0.30551	25.571	27.970	1664.5	16.49	1.30	33.098	28.435	1833.1	19.80	13.45	1.04	28.769	16.13	-2.334	-0.081	0.686	0.00	-2.334	16.13
0.36698	33.813	29.218	1914.2	17.46	1.40	44.946	28.611	2171.4	23.58	13.69	1.05	30.259	17.31	-3.648	-0.121	0.646	0.00	-3.648	17.31
0.44364	45.499	30.450	2221.0	18.52	1.47	67.560	26.750	2605.4	28.30	13.69	1.05	31.832	18.57	-5.062	-0.160	0.601	0.00	-5.062	18.57
0.53917	61.712	31.776	2586.3	19.33	1.43	131.876	27.117	3113.7	33.81	14.10	1.08	33.333	19.76	-6.216	-0.186	0.567	0.00	-6.216	19.76
0.64937	80.147	32.806	2947.3	19.33	1.43	161.830	27.432	3679.7	39.53	14.24	1.10	34.558	20.71	-7.350	-0.213	0.536	0.00	-7.350	20.71
0.71030	95.481	33.654	3215.9	20.02	1.47	161.830	27.432	4090.7	43.77	14.48	1.12	36.009	21.99	-8.577	-0.238	0.518	0.00	-8.577	21.99
0.78602	113.748	34.121	3502.9	20.34	1.48	198.471	27.343	4454.5	48.38	14.40	1.11	37.583	23.39	-10.240	-0.272	0.500	0.00	-10.240	23.39
0.86153	130.722	34.888	3728.6	21.00	1.51	248.589	26.712	4950.1	53.76	13.77	1.06	39.423	25.04	-12.711	-0.322	0.457	0.00	-12.711	25.04

0.0045" Ribbed 0.300" Pipe
 Residual = 350

Series	PEO	Q (UM)	Tm (S1)	1/Aq(S1)	Resid (S1)	S (S1)	Sf (S1)	Tm (R1A)	1/Aq(R1A)	Resid (R1A)	h _s	S (R1A)	Sf (R1A)	1/Aq(S1A)	S1 (S1)	R	W	P	Δ/True	connected R	connected S
		0.00485	0.105	6.921	111.6	4.29	0.43	0.112	7.243	110.7	1.20	0.45	0.112	6.965	4.59	-0.146	-0.010	0.800	0.00	-0.146	4.59
	250	0.00688	0.147	8.304	132.1	5.45	0.54	0.159	8.319	132.4	1.44	0.55	0.159	8.319	5.77	-0.163	-0.010	0.799	0.00	-0.163	5.77
	107793	0.00842	0.181	9.168	146.7	6.37	0.63	0.195	9.176	146.8	1.59	0.61	0.195	9.176	6.71	-0.118	-0.024	0.778	0.00	-0.118	6.71
	P-309	0.01009	0.216	10.048	160.4	7.26	0.70	0.270	9.697	172.7	1.88	0.72	0.270	10.666	7.44	-0.116	-0.007	0.789	0.00	-0.116	7.44
	SO	0.01312	0.293	11.217	187.0	8.17	0.77	0.463	9.627	226.4	2.46	0.82	0.463	11.105	8.00	-0.194	-0.010	0.800	0.00	-0.194	8.00
	1.138	0.01640	0.410	14.904	270.0	10.18	0.98	0.673	11.207	275.9	2.96	1.01	0.673	12.355	9.54	-0.198	-0.009	0.785	0.00	-0.198	9.54
		0.02310	0.766	12.223	302.6	11.14	0.83	0.846	12.549	306.2	3.33	0.86	0.846	13.453	10.36	-0.007	0.000	0.796	0.00	-0.007	10.36
		0.02748	0.919	13.271	331.7	12.51	0.92	1.036	13.486	339.1	3.68	0.91	1.036	14.504	11.46	-0.045	-0.002	0.799	0.00	-0.045	11.46
		0.03277	1.146	14.169	370.6	14.16	1.01	1.299	14.358	379.9	4.13	1.04	1.299	15.848	12.03	0.640	0.028	0.813	0.00	0.640	12.03
		0.03926	1.378	15.485	406.6	15.66	1.01	1.563	15.685	417.0	4.53	1.01	1.563	17.302	12.13	0.505	0.021	0.809	0.00	0.505	12.13
		0.04505	1.591	16.534	437.4	16.53	1.03	1.854	16.525	454.5	4.94	1.03	1.854	19.610	12.11	0.714	0.030	0.834	0.00	0.714	12.11
		0.05403	2.013	17.629	492.0	17.62	1.03	2.314	17.742	507.8	5.51	1.03	2.314	23.799	12.11	0.427	0.017	0.816	0.00	0.427	12.11
		0.06272	2.496	18.383	548.0	18.38	1.06	2.892	18.425	567.9	6.17	1.06	2.892	24.449	12.63	0.251	0.010	0.800	0.00	0.251	12.63
		0.06890	2.987	18.842	597.1	18.84	1.11	3.229	19.154	598.9	6.51	1.11	3.229	25.415	13.42	0.029	0.001	0.764	0.00	0.029	13.42
		0.07644	3.338	19.369	634.4	19.36	1.14	3.676	19.441	656.5	7.13	1.14	3.676	26.098	13.96	0.029	0.001	0.764	0.00	0.029	13.96
		0.08821	4.114	20.136	704.9	20.13	1.19	4.676	20.377	723.6	7.86	1.19	4.676	27.341	14.96	-0.673	-0.025	0.794	0.00	-0.673	14.96
		0.09956	4.689	21.890	812.1	21.89	1.23	5.345	21.511	774.8	8.41	1.23	5.345	28.526	15.91	-1.654	-0.028	0.723	0.00	-1.654	15.91
		0.11036	5.449	23.375	941.3	23.37	1.28	6.275	22.007	993.1	9.11	1.28	6.275	29.986	17.06	-2.990	-0.008	0.672	0.00	-2.990	17.06
		0.12393	6.466	25.565	1084.4	25.56	1.32	7.340	23.874	1141.5	10.40	1.32	7.340	31.158	19.24	-3.336	-0.163	0.595	0.00	-3.336	19.24
		0.13643	7.301	28.170	1250.1	28.17	1.37	8.148	24.676	1348.5	11.46	1.37	8.148	32.775	20.20	-4.483	-0.191	0.523	0.00	-4.483	20.20
		0.13702	7.497	23.170	950.1	23.17	1.05	8.359	24.317	1046.0	11.36	1.05	8.359	32.775	20.91	-7.590	-0.211	0.523	0.00	-7.590	20.91
		0.15334	8.855	23.693	1048.0	23.69	1.03	9.838	24.513	1052.2	11.43	1.03	9.838	35.023	21.21	-8.209	-0.231	0.492	0.00	-8.209	21.21
		0.15392	9.046	23.693	1048.0	23.69	1.03	9.838	24.513	1052.2	11.43	1.03	9.838	35.023	21.21	-8.209	-0.231	0.492	0.00	-8.209	21.21
		0.16946	10.415	24.311	1124.5	24.31	1.06	11.579	24.876	1141.5	12.40	1.06	11.579	36.771	21.60	-9.562	-0.267	0.451	0.00	-9.562	21.60
		0.19276	12.543	25.198	1234.3	25.19	1.11	14.074	25.666	1258.6	13.67	1.11	14.074	38.541	22.03	-10.833	-0.281	0.422	0.00	-10.833	22.03
		0.21022	14.148	25.875	1310.9	25.87	1.14	16.154	26.127	1348.5	14.64	1.14	16.154	40.408	22.44	-12.111	-0.281	0.422	0.00	-12.111	22.44
		0.24898	18.329	26.924	1492.1	26.92	1.19	21.750	26.668	1564.8	16.99	1.19	21.750	42.311	22.85	-13.400	-0.281	0.422	0.00	-13.400	22.85
		0.28769	22.789	27.901	1663.7	27.90	1.23	26.589	26.872	1794.3	19.49	1.23	26.589	44.214	23.26	-14.689	-0.281	0.422	0.00	-14.689	23.26
		0.34566	30.301	29.072	1918.6	29.07	1.28	40.908	26.996	2407.7	23.31	1.28	40.908	46.117	23.67	-15.970	-0.281	0.422	0.00	-15.970	23.67
		0.40351	38.619	30.061	2163.7	30.06	1.32	54.979	27.184	2407.7	23.31	1.32	54.979	48.020	24.08	-17.260	-0.281	0.422	0.00	-17.260	24.08
		0.49987	54.243	31.410	2566.9	31.41	1.37	82.741	27.439	3052.0	24.07	1.37	82.741	50.000	24.49	-18.550	-0.281	0.422	0.00	-18.550	24.49
		0.58019	68.830	32.377	2891.3	32.37	1.41	111.012	27.507	3535.0	24.07	1.41	111.012	52.000	24.90	-19.840	-0.281	0.422	0.00	-19.840	24.90
		0.69482	92.298	33.484	3346.3	33.48	1.44	160.067	27.493	4242.6	24.07	1.44	160.067	54.000	25.31	-21.130	-0.281	0.422	0.00	-21.130	25.31
		0.78999	112.907	34.421	3697.1	34.42	1.48	208.339	27.340	4834.8	24.07	1.48	208.339	56.000	25.72	-22.420	-0.281	0.422	0.00	-22.420	25.72
		0.88483	138.120	34.859	4058.1	34.85	1.48	277.895	26.515	5541.7	24.07	1.48	277.895	58.000	26.13	-23.710	-0.281	0.422	0.00	-23.710	26.13

0.0045" Fiberglass 300" Pipe
Residual = .350

Series
PEO

PIPE
SI:
d = 0.308
h = smooth
RIA = 10.6/93
d = 0.293
h = 0.0045
Rh = 32.6

P-309 249
DATE 10/6/93
PCY P-309
c uppm 100
w 1.260

Q (L/A)	Te (SI)	1/Amp(SI)	Amp(SI)	S (SI)	Sf (SI)	Tw (RIA)	1/Amp(RIA)	Amp(RIA)	Ns	S (RIA)	Sf (RIA)	1/Amp(SI)	Sf (SI)	R	Rf	P	d/hrs	corrected R	corrected S
0.00351	0.083	5.629	89.8	5.91	0.60	0.091	5.819	90.3	0.98	6.20	0.63	15.911	6.03	0.170	0.011	0.00	0.00	0.170	6.03
0.00453	0.108	6.389	102.3	6.80	0.68	0.119	6.575	103.3	1.12	6.92	0.68	17.042	6.94	-0.005	0.000	0.00	0.00	-0.005	6.94
0.00506	0.120	6.755	106.3	7.34	0.72	0.133	6.950	109.3	1.19	7.42	0.72	17.804	7.52	-0.069	-0.004	0.00	0.00	-0.069	7.52
0.00592	0.141	7.318	117.0	7.73	0.75	0.153	7.564	117.6	1.28	7.83	0.75	18.336	7.94	-0.077	-0.004	0.00	0.00	-0.077	7.94
0.01071	0.259	9.745	159.1	8.37	0.80	0.277	10.155	158.6	1.72	8.53	0.81	19.001	8.48	0.104	0.005	0.00	0.00	0.104	8.48
0.01602	0.401	11.704	198.4	8.73	0.82	0.478	11.572	206.5	2.26	8.87	0.82	19.732	9.04	-0.083	-0.004	0.00	0.00	-0.083	9.04
0.01998	0.529	12.720	227.9	8.94	0.84	0.636	12.570	240.5	2.61	8.99	0.84	12.870	9.04	-0.083	-0.004	0.00	0.00	-0.083	9.04
0.02340	0.688	13.058	260.2	9.08	0.85	0.819	12.911	273.4	2.97	9.02	0.85	13.708	9.04	-0.083	-0.004	0.00	0.00	-0.083	9.04
0.02895	0.851	14.527	286.6	9.16	0.86	1.064	14.014	311.8	3.39	9.04	0.86	14.836	9.04	-0.083	-0.004	0.00	0.00	-0.083	9.04
0.03402	1.093	15.070	328.4	9.16	0.86	1.252	15.187	330.5	3.68	9.04	0.86	15.248	9.04	-0.083	-0.004	0.00	0.00	-0.083	9.04
0.03950	1.346	15.761	364.9	9.16	0.86	1.506	16.081	371.5	4.03	9.04	0.86	15.911	9.04	-0.083	-0.004	0.00	0.00	-0.083	9.04
0.04751	1.703	16.857	410.6	9.16	0.86	1.940	17.037	429.0	4.58	9.04	0.86	17.042	9.04	-0.083	-0.004	0.00	0.00	-0.083	9.04
0.05501	2.099	17.578	456.1	9.16	0.86	2.400	17.735	469.6	5.10	9.04	0.86	17.804	9.04	-0.083	-0.004	0.00	0.00	-0.083	9.04
0.06014	2.373	18.073	485.3	9.16	0.86	2.707	18.258	499.0	5.42	9.04	0.86	18.336	9.04	-0.083	-0.004	0.00	0.00	-0.083	9.04
0.06773	2.769	18.845	524.5	9.16	0.86	3.136	19.105	537.4	5.84	9.04	0.86	19.001	9.04	-0.083	-0.004	0.00	0.00	-0.083	9.04
0.07697	3.380	19.382	580.3	9.16	0.86	3.829	19.649	594.6	6.46	9.04	0.86	19.732	9.04	-0.083	-0.004	0.00	0.00	-0.083	9.04
0.08260	4.147	21.052	644.0	10.22	0.94	4.777	21.163	665.4	7.23	10.15	0.92	21.376	10.48	-0.213	-0.010	0.00	0.00	-0.213	10.48
0.10409	4.894	21.783	699.5	10.80	0.98	5.481	22.209	712.7	7.74	11.05	0.99	21.867	10.88	0.322	0.015	0.00	0.00	0.322	10.88
0.11392	5.645	22.198	751.1	11.09	1.00	6.314	22.646	764.7	8.30	11.33	1.00	22.318	11.18	0.328	0.015	0.00	0.00	0.328	11.18
0.13694	7.450	23.227	861.4	11.89	1.05	8.240	23.829	872.1	9.47	12.21	1.05	23.335	11.97	0.494	0.021	0.00	0.00	0.494	11.97
0.16332	9.606	24.396	973.3	12.84	1.11	10.847	24.770	995.7	10.91	12.84	1.08	24.548	12.96	0.222	0.009	0.00	0.00	0.222	12.96
0.18791	11.946	25.169	1095.7	13.41	1.14	13.136	25.894	1106.3	12.01	13.72	1.13	25.259	13.48	0.635	0.025	0.00	0.00	0.635	13.48
0.23228	16.146	26.762	1274.0	14.74	1.23	18.435	27.023	1310.6	14.23	14.49	1.16	27.026	14.96	-0.003	0.000	0.00	0.00	-0.003	14.96
0.27081	20.347	27.794	1430.4	15.57	1.27	24.822	27.151	1520.9	16.52	14.37	1.12	28.311	15.98	-1.160	-0.041	0.00	0.00	-1.160	15.98
0.32851	27.467	29.019	1662.0	16.54	1.32	36.607	27.121	1847.2	20.06	14.13	1.09	29.777	17.11	-2.656	-0.089	0.00	0.00	-2.656	17.11
0.40526	38.560	30.214	1969.5	17.44	1.36	54.907	27.318	2262.5	24.57	14.25	1.09	31.103	18.08	-3.785	-0.122	0.00	0.00	-3.785	18.08
0.48181	51.333	31.132	2272.1	18.11	1.39	77.642	27.312	2690.2	29.22	14.26	1.09	32.403	19.08	-5.091	-0.157	0.00	0.00	-5.091	19.08
0.57219	68.783	32.219	2638.5	18.94	1.43	108.370	27.644	3182.2	34.58	14.64	1.13	33.765	20.15	-6.121	-0.181	0.00	0.00	-6.121	20.15
0.67225	87.866	33.202	2964.9	19.71	1.46	144.510	27.933	3660.5	39.75	14.96	1.15	35.299	21.44	-7.366	-0.209	0.00	0.00	-7.366	21.44
0.76698	108.497	34.089	3304.0	20.41	1.49	186.719	28.036	4172.8	45.32	15.09	1.17	37.018	23.04	-9.082	-0.245	0.00	0.00	-9.082	23.04
0.86159	129.242	35.078	3598.3	21.25	1.54	237.292	27.931	4693.9	50.98	14.99	1.16	38.970	24.68	-11.039	-0.283	0.00	0.00	-11.039	24.68

0.0045" Ribbed 40.308" Pipe
 Rev/Ver = 3/0

Series

PAM

PIPE
 S1:
 d = 0.308
 h = smooth
 RIA: M-300
 POLY: 100
 c: mpans
 w: 1.176

M-300
 RUN: 253
 DATE: 10/12/2013
 M-300
 POLY: 100
 c: mpans
 w: 1.176

Q (L/A)	Te (S)	V _{1/2} (S)	Re _v (S)	S (S)	Sf (S)	Te (RIA)	V _{1/2} (RIA)	Re _v (RIA)	N	S (RIA)	Sf (RIA)	V _{1/2} (S)	Sv (S)	R	RF	P	Δ/rev	connected R	connected S
0.00363	0.082	5.860	94.5	4.64	0.47	0.090	6.048	95.1	1.03	4.43	0.45	5.903	5.03	-0.601	-0.040	0.765	0.00	-0.601	5.03
0.00485	0.108	6.824	108.6	5.42	0.55	0.119	7.033	109.5	1.18	5.54	0.55	6.826	5.89	-0.348	-0.022	0.796	0.00	-0.348	5.89
0.00526	0.140	7.744	123.8	6.63	0.66	0.152	8.009	124.3	1.35	6.64	0.66	7.777	6.97	-0.314	-0.018	0.786	0.00	-0.314	6.97
0.00799	0.179	8.743	140.2	7.58	0.74	0.198	9.104	139.9	1.52	7.58	0.73	8.742	7.23	-0.124	-0.007	0.787	0.00	-0.124	7.23
0.00826	0.221	9.788	156.5	8.07	0.77	0.265	10.086	142.3	1.55	8.23	0.78	8.917	8.27	0.009	0.000	0.800	0.00	0.009	8.27
0.00955	0.281	10.987	176.7	9.16	0.86	0.353	10.986	157.8	1.71	8.67	0.81	9.865	8.83	-0.140	-0.007	0.790	0.00	-0.140	8.83
0.01259	0.526	11.338	242.0	10.19	0.93	0.367	10.375	194.3	2.11	9.29	0.86	11.213	9.82	-0.117	0.006	0.798	0.00	-0.117	9.24
0.02173	0.708	12.172	281.3	11.29	1.00	0.766	12.628	251.5	2.73	10.02	0.84	11.492	10.54	-0.359	-0.017	0.783	0.00	-0.359	10.54
0.02664	0.853	13.350	309.0	11.99	1.05	0.999	13.314	321.8	3.06	11.12	0.95	12.194	11.79	-0.401	-0.017	0.790	0.00	-0.401	11.79
0.03260	1.095	14.423	350.5	11.99	1.04	1.298	14.291	367.4	3.99	12.03	1.04	13.695	12.00	0.654	0.028	0.825	0.00	0.654	12.00
0.03782	1.301	15.353	382.7	11.99	1.04	1.482	15.221	392.2	4.27	12.03	1.08	14.892	12.00	1.258	0.053	0.861	0.00	1.258	12.01
0.04400	1.491	16.685	410.1	11.99	1.05	1.719	16.764	424.0	4.60	13.44	1.11	15.869	13.26	0.576	0.023	0.821	0.00	0.576	13.26
0.05282	1.898	17.833	461.8	11.99	1.04	2.126	17.921	472.3	5.18	13.81	1.11	16.550	13.26	0.154	0.006	0.800	0.00	0.154	13.27
0.06121	2.244	18.513	514.9	11.99	1.04	2.655	18.765	527.6	5.73	13.86	1.11	18.756	13.26	0.001	0.000	0.794	0.00	0.001	14.27
0.06751	2.661	19.161	548.6	11.99	1.04	3.053	19.301	563.7	6.14	13.86	1.11	19.441	13.26	0.000	0.000	0.776	0.00	0.000	14.94
0.07380	3.124	19.855	595.1	11.99	1.04	3.459	20.097	610.7	6.63	13.81	1.11	19.980	13.26	-0.505	-0.019	0.720	0.00	-0.505	15.72
0.08695	3.929	20.308	667.8	11.99	1.04	4.579	20.387	691.0	7.50	13.81	1.11	20.773	13.26	-2.559	-0.087	0.695	0.00	-2.559	16.72
0.09687	4.477	21.197	711.9	11.99	1.04	5.184	21.254	737.5	8.01	13.81	1.11	21.613	13.26	-4.001	-0.129	0.627	0.00	-4.001	18.03
0.11269	5.489	22.268	789.7	11.99	1.00	6.371	22.301	819.1	8.90	13.81	1.11	22.434	13.26	-5.200	-0.160	0.609	0.00	-5.200	19.19
0.12521	6.562	22.630	861.5	11.99	1.00	7.535	22.785	888.7	9.65	13.81	1.11	23.186	13.26	-6.824	-0.200	0.555	0.00	-6.824	20.54
0.13382	7.014	23.392	894.8	11.99	1.05	7.915	23.759	915.1	9.94	13.81	1.11	23.441	13.26	-8.154	-0.231	0.513	0.00	-8.154	21.42
0.14838	8.517	23.541	973.7	11.99	1.04	9.363	24.225	982.8	10.67	13.81	1.11	23.571	13.26	-9.749	-0.265	0.475	0.00	-9.749	22.82
0.15123	8.776	23.633	1001.1	12.03	1.04	9.243	24.847	989.1	10.74	13.81	1.11	24.988	13.26	-10.996	-0.291	0.454	0.00	-10.996	24.15
0.17056	10.051	24.907	1071.5	13.19	1.13	11.097	25.574	1084.0	11.77	13.81	1.11	25.650	13.26	-13.908	-0.351	0.401	0.00	-13.908	30.84
0.18601	11.432	25.469	1142.9	13.64	1.15	12.966	26.804	1171.7	12.72	13.81	1.11	26.282	13.26	-14.400	-0.351	0.401	0.00	-14.400	30.84
0.20532	13.331	26.035	1234.2	14.07	1.18	15.227	26.283	1269.9	13.79	13.81	1.11	27.089	13.26	-15.720	-0.400	0.351	0.00	-15.720	30.84
0.22461	15.234	26.642	1319.5	14.56	1.21	17.812	26.584	1373.6	14.92	13.81	1.11	28.104	13.26	-17.440	-0.451	0.300	0.00	-17.440	30.84
0.25378	18.452	27.740	1452.0	15.49	1.26	21.249	28.664	1589.0	17.04	13.81	1.06	29.355	13.26	-20.000	-0.500	0.250	0.00	-20.000	30.84
0.29974	23.912	28.378	1652.9	15.90	1.28	31.219	28.786	1818.2	19.75	13.81	1.06	31.050	13.26	-22.559	-0.559	0.200	0.00	-22.559	30.84
0.37659	33.447	30.146	1955.0	17.38	1.36	48.362	27.049	2589.6	28.12	13.81	1.09	32.440	13.26	-25.200	-0.600	0.150	0.00	-25.200	30.84
0.43407	42.523	30.818	2203.7	17.84	1.38	63.359	27.240	3423.0	34.23	13.81	1.10	34.135	13.26	-28.154	-0.654	0.100	0.00	-28.154	30.84
0.52963	57.462	32.347	2562.0	19.11	1.44	93.834	27.311	4515.9	40.61	13.81	1.09	35.314	13.26	-31.440	-0.700	0.050	0.00	-31.440	30.84
0.62487	74.682	33.476	2920.7	20.01	1.49	132.067	27.160	3738.2	48.23	13.81	1.09	36.764	13.26	-34.940	-0.750	0.000	0.00	-34.940	30.84
0.73872	97.685	34.603	3337.8	20.91	1.53	186.569	27.015	4440.9	48.23	13.81	1.09	37.788	13.26	-38.940	-0.800	0.000	0.00	-38.940	30.84
0.81436	115.405	35.096	3623.9	21.26	1.54	230.529	26.792	4930.9	53.55	13.81	1.07	39.638	13.26	-42.940	-0.850	0.000	0.00	-42.940	30.84
0.92743	143.235	35.877	4016.2	21.86	1.56	324.152	25.730	5816.9	63.17	12.76	0.98	39.638	13.26	-46.940	-0.900	0.000	0.00	-46.940	30.84

PIPE: 7.82 mm

RIBBLETS: 0.11 mm Replicated Pipe

POLYMERS:

NONE (Solvent)

PEO N-60K

W-301

0.0045b" Riblets/0.308" Pipe
 Reference = 350

Series

DW

PIPE

S1:
 d = 0.308
 h = smooth
 RIAR:
 d = 0.297
 h = 0.0045
 R/h 33.0

RUN 276
 DATE 7/28/93
 POLY -
 c system
 nr 1.000

Q (L/s)	Tw (S1)	1/sqrt(S1)	Reyn(S1)	S'(S1)	SF(S1)	Tw(R1A)	1/sqrt(R1A)	Reyn(R1A)	h+	S'(R1A)	SF(R1A)	R'	RF	P
0.61673	356.871	15.113	7631.4	-0.02	0.00	548.909	13.148	9111.7	97.62	-0.05	0.00	-2.291	-0.148	0.627
0.59866	337.913	15.076	7436.6	-0.01	0.00	520.995	13.100	8889.7	95.24	-0.06	0.00	-2.296	-0.148	0.625
0.58054	319.747	15.029	7237.6	0.01	0.00	492.116	13.071	8644.2	92.81	-0.05	0.00	-2.276	-0.148	0.627
0.56420	303.363	14.995	7051.3	0.00	0.00	466.848	13.042	8421.2	90.22	-0.04	0.00	-2.260	-0.148	0.627
0.52775	269.211	14.889	6643.7	0.00	0.00	413.116	12.968	7923.3	84.89	-0.04	0.00	-2.227	-0.147	0.628
0.51128	254.777	14.828	6464.2	-0.01	0.00	390.077	12.929	7700.4	82.50	-0.05	0.00	-2.217	-0.146	0.630
0.49295	238.188	14.786	6250.1	0.00	0.00	363.404	12.915	7432.3	79.63	-0.03	0.00	-2.169	-0.144	0.632
0.47456	222.129	14.740	6035.2	0.02	0.00	338.867	12.876	7176.4	76.89	-0.03	0.00	-2.148	-0.143	0.632
0.45613	208.608	14.619	5846.6	-0.05	0.00	313.926	12.858	6907.2	74.00	-0.02	0.00	-2.099	-0.140	0.641
0.41914	177.904	14.547	5401.1	0.02	0.00	267.154	12.808	6371.9	68.27	-0.02	0.00	-2.009	-0.136	0.642
0.36330	137.450	14.344	4753.3	0.02	0.00	203.237	12.728	5564.5	59.62	-0.05	0.00	-1.854	-0.127	0.652
0.34646	126.511	14.259	4560.6	0.04	0.00	184.253	12.748	5298.7	56.77	-0.02	0.00	-1.749	-0.121	0.662
0.32959	115.530	14.195	4358.6	0.04	0.00	166.941	12.741	5044.0	54.04	-0.03	0.00	-1.671	-0.116	0.667
0.31080	104.271	14.090	4142.2	0.02	0.00	149.116	12.712	4768.8	51.09	-0.05	0.00	-1.602	-0.112	0.674
0.27498	83.676	13.915	3713.8	0.04	0.00	131.490	12.717	4479.8	47.98	-0.05	0.00	-1.486	-0.105	0.683
0.25984	75.862	13.810	3537.6	0.02	0.00	116.417	12.729	4217.2	45.18	-0.05	0.00	-1.372	-0.097	0.693
0.24278	67.244	13.705	3332.0	0.01	0.00	104.484	12.696	3996.8	42.82	-0.09	-0.01	-1.311	-0.094	0.700
0.22378	58.158	13.583	3100.2	0.02	0.00	90.977	12.713	3731.2	39.98	-0.08	-0.01	-1.176	-0.085	0.713
0.20664	50.296	13.468	2893.8	0.05	0.00	76.820	12.752	3430.3	36.75	-0.06	0.00	-0.989	-0.072	0.730
0.18946	43.247	13.336	2674.1	0.03	0.00	65.745	12.728	3174.1	34.01	-0.10	-0.01	-0.878	-0.065	0.738
0.17416	37.544	13.157	2492.6	-0.03	0.00	55.045	12.754	2905.2	31.13	-0.09	-0.01	-0.699	-0.052	0.758
0.15691	31.084	13.028	2286.6	0.01	0.00	45.882	12.842	2652.8	28.42	-0.02	0.00	-0.453	-0.034	0.789
						37.526	12.793	2399.7	25.71	-0.08	-0.01	-0.327	-0.025	0.799
0.62033	358.670	15.162	7691.8	0.02	0.00	550.101	13.210	9170.7	98.25	0.00	0.00	-2.240	-0.145	0.629
0.54782	287.211	14.962	6940.3	0.00	0.00	440.259	13.038	8272.4	88.63	-0.02	0.00	-2.231	-0.146	0.629
0.49295	236.984	14.822	6317.7	0.02	0.00	361.669	12.945	7513.8	80.50	-0.01	0.00	-2.158	-0.143	0.632
0.43786	191.303	14.647	5679.6	0.03	0.00	288.158	12.876	6710.8	71.90	0.02	0.00	-2.031	-0.136	0.640
0.38196	149.459	14.461	5021.6	0.06	0.00	222.458	12.789	5898.0	63.19	-0.01	0.00	-1.894	-0.129	0.648
0.34834	126.699	14.324	4624.8	0.05	0.00	185.401	12.776	5386.0	57.70	0.00	0.00	-1.749	-0.120	0.659
0.31080	103.340	14.152	4177.2	0.07	0.00	148.039	12.757	4813.3	51.57	-0.01	0.00	-1.573	-0.110	0.673
0.27309	82.237	13.939	3726.9	0.05	0.00	114.283	12.758	4229.5	46.32	-0.02	0.00	-1.348	-0.096	0.694
0.24488	67.465	13.789	3375.8	0.08	0.01	91.471	12.777	3784.3	40.54	-0.01	0.00	-1.135	-0.082	0.711
0.21428	53.401	13.572	3003.6	0.06	0.00	70.250	12.767	3316.6	35.53	-0.05	0.00	-0.916	-0.067	0.733
0.19519	45.159	13.445	2787.4	0.08	0.01	57.862	12.815	3010.3	32.2E	-0.02	0.00	-0.699	-0.052	0.753
0.16842	34.652	13.243	2419.8	0.11	0.01	42.947	12.835	2593.5	27.79	-0.03	0.00	-0.421	-0.032	0.778
0.15116	28.913	13.012	2210.4	0.03	0.00	34.846	12.788	2336.2	25.03	-0.08	-0.01	-0.286	-0.022	0.800
0.13578	23.656	12.668	2007.9	0.06	0.00	27.833	12.853	2088.0	22.37	-0.01	0.00	-0.026	-0.002	0.826
0.08199	10.004	12.000	1278.8	-0.03	0.00	10.734	12.499	1275.2	13.66	0.03	0.00	0.477	0.040	0.889
0.08290	10.058	12.100	1296.4	0.05	0.00	10.914	12.533	1300.1	13.93	0.03	0.00	0.477	0.040	0.889
0.08934	11.527	12.181	1390.4	0.01	0.00	12.467	12.637	1392.1	14.91	0.04	0.00	0.463	0.038	0.892
0.09910	13.862	12.321	1524.9	-0.01	0.00	15.090	12.741	1531.7	16.41	0.04	0.00	0.400	0.032	0.886
0.10396	15.011	12.420	1587.1	0.02	0.00	16.571	12.754	1605.5	17.20	0.01	0.00	0.331	0.027	0.873
0.11277	17.171	12.596	1698.0	0.08	0.01	17.317	12.829	1731.7	18.55	0.03	0.00	0.276	0.022	0.859
0.11879	18.756	12.696	1774.8	0.10	0.01	21.413	12.820	1825.7	19.58	-0.01	0.00	0.176	0.014	0.845
0.12832	21.586	12.785	1903.5	0.07	0.01	24.872	12.850	1967.1	21.07	0.00	0.00	0.075	0.006	0.837
0.07346	8.149	11.913	1150.2	0.07	0.01	8.860	12.327	1154.6	12.37	0.02	0.00	0.468	0.040	0.890
0.07007	7.530	11.821	1109.3	0.04	0.00	8.160	12.252	1111.7	11.91	0.02	0.00	0.458	0.040	0.890
0.06510	6.624	11.708	1043.4	0.03	0.00	7.192	12.123	1046.6	11.21	0.01	0.00	0.444	0.038	0.886
0.06177	6.079	11.598	1000.7	0.00	0.00	6.600	12.009	1003.8	10.75	-0.02	0.00	0.403	0.035	0.868

0.06726	5.338	11.472	938.1	-0.02	0.00	5.803	11.871	941.6	10.09	-0.02	0.00	0.376	0.033	0.887
0.05094	4.360	11.294	847.8	-0.02	0.00	4.771	11.649	853.8	9.15	-0.02	0.00	0.324	0.029	0.881
0.04843	3.713	11.153	782.1	-0.02	0.00	4.086	11.472	789.8	8.46	-0.02	0.00	0.282	0.025	0.876
0.04081	2.975	10.952	690.5	-0.03	0.00	3.295	11.229	708.7	7.59	-0.01	0.00	0.227	0.021	0.871
0.03349	2.124	10.637	590.7	-0.05	0.00	2.369	10.866	600.5	6.43	-0.01	0.00	0.154	0.014	0.865
0.02930	1.681	10.462	525.0	-0.02	0.00	1.893	10.638	536.3	5.75	0.00	0.00	0.120	0.011	0.858
0.02438	1.212	10.253	445.4	0.06	0.01	1.395	10.310	460.1	4.93	-0.02	0.00	0.059	0.008	0.838
0.02216	1.034	10.088	410.4	0.04	0.00	1.194	10.126	424.6	4.55	-0.05	0.00	0.014	0.001	0.835
0.02076	0.910	10.075	384.9	0.13	0.01	1.067	10.041	401.1	4.39	-0.02	0.00	0.028	0.003	0.823
0.01926	0.796	9.993	359.7	0.17	0.02	0.944	9.902	377.1	4.04	-0.04	0.00	-0.004	0.000	0.813
0.01798	0.703	9.913	337.7			0.837	9.804	354.7	3.80	-0.03	0.00	0.005	0.001	0.810

0.07681	9.047	11.827	1114.7	0.04	0.00	9.659	12.224	1120.3	12.00	-0.02	0.00	0.427	0.036	0.885
0.07076	7.749	11.769	1086.7	0.03	0.00	8.448	12.162	1092.4	11.70	-0.04	0.00	0.408	0.035	0.884
0.06794	7.189	11.731	1061.9	0.03	0.00	7.780	12.166	1063.6	11.39	0.02	0.00	0.459	0.039	0.891
0.06557	6.756	11.679	1036.5	0.02	0.00	7.345	12.085	1040.4	11.15	-0.02	0.00	0.416	0.036	0.887
0.06305	6.320	11.610	1004.8	0.00	0.00	6.874	12.012	1008.9	10.81	-0.02	0.00	0.396	0.034	0.887
0.05995	5.768	11.556	963.9	0.02	0.00	6.315	11.917	970.9	10.40	-0.04	0.00	0.368	0.032	0.881
0.05811	5.491	11.481	940.3	-0.01	0.00	5.952	11.897	942.5	10.10	0.01	0.00	0.400	0.035	0.890
0.05589	5.169	11.380	914.6	-0.06	-0.01	5.572	11.826	914.2	9.79	0.01	0.00	0.382	0.033	0.895
0.05292	4.896	11.305	889.5	-0.05	0.00	5.078	11.729	870.5	9.33	0.02	0.00	0.370	0.033	0.892
0.04960	4.180	11.230	822.3	-0.03	0.00	4.563	11.598	827.0	8.86	0.00	0.00	0.328	0.029	0.883
0.04506	3.539	11.089	756.4	-0.03	0.00	3.875	11.434	762.0	8.16	0.03	0.00	0.306	0.027	0.881
0.04248	3.210	10.976	719.5	-0.05	0.00	3.525	11.301	725.8	7.76	0.01	0.00	0.257	0.023	0.878
0.03977	2.859	10.888	679.3	-0.04	0.00	3.155	11.183	687.0	7.36	0.01	0.00	0.236	0.022	0.874
0.03794	2.642	10.807	653.1	-0.05	0.00	2.912	11.106	660.1	7.07	0.02	0.00	0.227	0.021	0.875
0.03565	2.362	10.739	616.9	-0.02	0.00	2.624	10.995	625.9	6.71	0.03	0.00	0.209	0.019	0.868
0.03238	1.999	10.601	566.5	-0.01	0.00	2.203	10.897	572.1	6.13	0.12	0.01	0.265	0.025	0.875
0.03020	1.776	10.489	532.9	-0.02	0.00	1.992	10.687	543.2	5.82	0.02	0.00	0.148	0.014	0.860
0.02653	1.413	10.331	475.6	0.02	0.00	1.595	10.494	486.5	5.21	0.06	0.01	0.147	0.014	0.855
0.02351	1.162	10.100	431.1	-0.04	0.00	1.321	10.218	442.6	4.74	-0.03	0.00	0.034	0.003	0.848
0.02236	1.048	10.111	409.1	0.06	0.01	1.207	10.168	422.5	4.53	0.01	0.00	0.065	0.006	0.838
0.02076	0.917	10.035	382.3	0.11	0.01	1.073	10.011	398.1	4.26	-0.04	0.00	0.012	0.001	0.824
0.01871	0.763	9.984	346.1			0.889	9.911	362.2	3.88	0.04	0.00	0.075	0.008	0.816
0.01715	0.643	9.901	319.3			0.777	9.719	337.9	3.62					0.798
0.01536	0.522	9.837	287.5			0.636	9.623	305.2	3.27					0.793
0.01353	0.319	11.098	224.3			0.374	11.054	233.9	2.51					0.622
0.01078	0.206	11.000	180.1			0.229	11.253	182.8	1.96					0.667
0.00937	0.175	10.388	165.6			0.195	10.603	168.5	1.81					0.863
0.00726	0.135	9.158	145.3			0.151	9.347	147.8	1.58					0.863
0.00463	0.089	7.200	117.8			0.100	7.321	120.3	1.29					0.855

0.08107	9.916	11.920	1239.8	-0.05	0.00	10.737	12.360	1242.0	13.31	-0.07	-0.01	0.384	0.032	0.691
0.08304	10.176	12.050	1284.1	0.02	0.00	11.130	12.432	1292.9	13.85	-0.06	-0.01	0.385	0.032	0.882
0.08981	11.707	12.150	1369.2	-0.02	0.00	12.729	12.572	1394.6	14.94	0.03	0.00	0.395	0.032	0.887
0.09550	12.952	12.283	1462.8	0.02	0.00	14.123	12.691	1470.6	15.76	0.03	0.00	0.421	0.034	0.884
0.10034	14.190	12.330	1532.7	-0.01	0.00	15.400	12.770	1537.2	16.47	0.06	0.00	0.423	0.034	0.889
0.10655	15.514	12.522	1603.7	0.10	0.01	17.417	12.851	1636.8	17.53	-0.01	0.00	0.296	0.024	0.859
0.11307	17.236	12.607	1690.5	0.09	0.01	19.461	12.801	1729.4	18.53	0.00	0.00	0.249	0.020	0.854
0.12011	19.094	12.724	1779.9	0.12	0.01	21.894	12.821	1834.9	19.66	-0.01	0.00	0.166	0.013	0.841
0.13544	23.917	12.820	1991.2	0.02	0.00	27.581	12.880	2056.6	22.06	-0.03	0.00	0.226	0.002	0.836
0.07103	446.531	15.356	8624.1	0.01	0.00	663.522	13.392	10272.3	110.05	0.02	0.00	-0.255	-0.144	0.630
0.88676	430.371	15.323	8498.8	0.01	0.00	652.387	13.428	10073.7	107.93	0.05	0.00	-2.185	-0.140	0.636
0.67066	413.925	15.256	8340.1	-0.03	0.00	626.053	13.386	9874.6	105.79	0.04	0.00	-2.192	-0.141	0.638

0.65632	398.023	15.227	8176.8	-0.02	0.00	602.562	13.353	9688.3	103.80	0.06	0.00	-2.192	-0.141	0.637
0.64015	380.191	15.197	7984.6	-0.01	0.00	577.562	13.303	9474.4	101.51	0.04	0.00	-2.203	-0.142	0.635
0.62755	366.414	15.175	7835.0	0.00	0.00	557.682	13.271	9305.7	99.70	0.04	0.00	-2.204	-0.142	0.634
0.64554	384.977	15.229	8029.1	0.01	0.00	586.884	13.308	9544.0	102.26	0.03	0.00	-2.211	-0.142	0.633
0.66349	405.587	15.250	8242.1	-0.01	0.00	619.526	13.313	9806.7	105.07	-0.02	0.00	-2.253	-0.145	0.631
0.67782	420.235	15.305	8392.5	0.01	0.00	643.459	13.346	9997.9	107.11	-0.02	0.00	-2.255	-0.145	0.630
0.56965	309.944	14.977	7203.6	-0.05	0.00	469.997	13.123	8539.8	91.49	0.02	0.00	-2.203	-0.144	0.636
0.49662	241.743	14.785	6359.5	-0.03	0.00	368.632	12.918	7560.4	81.00	-0.04	0.00	-2.196	-0.145	0.632
0.42284	180.581	14.566	5491.5	0.01	0.00	268.259	12.894	6444.0	69.04	0.06	0.00	-1.943	-0.131	0.649
0.32959	115.801	14.177	4395.0	0.01	0.00	165.168	12.808	5053.2	54.14	0.04	0.00	-1.606	-0.111	0.676
0.27309	83.169	13.861	3723.7	-0.02	0.00	113.691	12.791	4191.4	44.91	0.02	0.00	-1.298	-0.092	0.705
0.25606	73.957	13.782	3510.8	0.00	0.00	100.172	12.777	3933.6	42.14	-0.01	0.00	-1.202	-0.086	0.712
0.17990	39.380	13.270	2561.2	0.04	0.00	48.800	12.862	2744.8	29.41	0.01	0.00	-0.492	-0.037	0.778
0.16650	34.672	13.089	2402.9	-0.03	0.00	41.501	12.908	2530.9	27.12	0.04	0.00	-0.305	-0.023	0.806

0.00-450" Ribbed 0.308" Pipe

Residue = 350

Series

PEO

PIE
 SI:
 d = 0.308
 h = smooth
 R1AR: 3
 d = 0.297
 h = 0.0045
 RA 33.0

NUM 290
 DATE 8/16/94
 POLY M-60K
 c wppm 3
 W 1.00

Q (L/h)	T _w (S1)	1/μg(S1)	Resq(S1)	S (S1)	SF (S1)	T _w (RIA)	1/μg(RIA)	Resq(RIA)	h _s	S (RIA)	SF (RIA)	1/μg	S _h (S1)	R	RF	P	Δ/hrs	corrected R	corrected S
0.01157	0.228	11.218	190.4			0.259	11.351	195.5	2.09							0.848			
0.01462	0.483	9.742	277.2			0.544	9.902	283.3	3.03							0.856			
0.01731	0.672	9.174	327.3			0.797	9.686	343.1	3.68							0.813			
0.01989	0.875	9.843	373.9			1.005	9.911	395.7	4.13							0.840			
0.02218	1.053	10.005	410.3			1.215	10.051	424.3	4.55							0.836			
0.02707	1.487	10.278	487.6			1.687	10.411	500.1	5.36							0.850			
0.03169	1.963	10.470	561.3			2.177	10.727	569.1	6.10							0.869			
0.03775	2.651	10.733	653.3			2.872	11.127	654.6	7.01							0.890			
0.04284	3.258	10.936	724.5			3.481	11.414	721.1	7.73							0.902			
0.05068	4.301	11.314	832.8			4.562	11.853	825.7	8.85							0.909			
0.05705	5.187	11.596	915.2			5.441	12.215	902.5	9.67							0.919			
0.06292	6.048	11.844	988.9			6.320	12.500	973.2	10.43							0.923			
0.06951	6.962	12.195	1060.3			7.226	12.915	1040.0	11.14							0.928			
0.07494	7.906	12.338	1127.9			8.215	13.059	1106.9	11.86							0.928			
0.08063	8.724	12.638	1174.5			9.395	13.140	1173.4	12.57							0.895			
0.09187	10.151	13.348	1281.3			11.205	13.709	1295.9	13.88							0.900			
0.10225	11.852	13.749	1391.1			13.009	14.159	1403.2	15.03							0.878			
0.11960	14.925	14.331	1562.5			16.436	14.735	1578.5	16.91							0.878			
0.14237	19.432	14.950	1782.9			21.501	15.335	1892.6	19.34							0.872			
0.16300	23.084	15.702	1945.1			26.151	15.920	1995.6	21.35							0.852			
0.17839	26.115	16.160	2068.5			30.213	16.210	2142.0	22.95							0.852			
0.20143	31.444	16.629	2270.0			37.101	16.317	2373.9	25.43							0.817			
0.22825	38.241	17.086	2503.9			45.453	16.909	2628.0	28.16							0.811			
0.25880	47.261	17.427	2783.6			56.969	17.126	2942.2	31.52							0.800			
0.29117	56.389	17.949	3099.9			69.952	17.388	3259.6	34.92							0.777			
0.32911	69.601	18.261	3377.5			88.264	17.496	3661.7	39.23							0.760			
0.38386	90.094	18.721	3842.4			118.550	17.608	4243.3	45.46							0.733			
0.44017	115.422	18.961	4350.5			157.176	17.536	4886.1	52.35							0.709			
0.51475	153.805	19.214	5019.3			216.967	17.374	5765.7	61.77							0.677			
0.57029	188.304	19.238	5551.4			272.529	17.254	6429.5	68.88							0.666			
0.62551	224.521	19.325	6053.6			334.353	17.086	7111.9	76.20							0.648			
0.71681	297.140	19.251	6902.9			456.187	16.763	8234.4	88.22							0.628			

0.00456" Ribbed 0.308" Pipe
 L = 350

PEE
 S1:
 d = 0.308
 h = smooth
 R1/R2:
 c = 1.0
 d = 0.297
 h = 0.0045
 Ph = 33.0

PEO
 RUN: 289
 DATE: 8/14/94
 POLY: M-60K
 c = 1.0
 w = 1.01

Q (L/s)	T _{in} (S)	1/√gH(S)	Re _{eff} (S)	S ₁ (S)	S ₂ (S)	T _{in} (R1A)	1/√gH(R1A)	Re _{eff} (R1A)	h _r	S ₁ (R1A)	S ₂ (R1A)	1/√gH	SV(S1)	R	RF	P	Δ/ft _{res}	corrected R
0.00493	0.090	7.590	118.0	0.01	0.00	0.101	7.728	120.4	1.29	-0.18	-0.018	9.944	-0.02	-0.116	-0.012	0.859	0.00	-0.116
0.01023	0.198	10.652	174.9	0.21	-0.06	0.211	11.132	173.8	1.86	-0.16	-0.016	10.053	-0.07	-0.028	-0.003	0.905	0.00	-0.028
0.01281	0.264	11.540	202.1	0.27	-0.10	0.271	12.295	197.1	2.11	-0.13	-0.013	10.281	-0.10	0.059	0.006	0.946	0.00	0.059
0.01549	0.342	9.746	269.9	0.633	-0.09	0.633	9.724	301.8	3.23	0.01	0.001	10.477	-0.09	0.235	0.022	0.870	0.00	0.235
0.01776	0.711	9.747	332.7	0.823	-0.03	0.823	9.760	344.4	3.69	0.00	0.000	10.810	-0.03	0.435	0.040	0.896	0.00	0.435
0.02022	0.895	9.898	373.4	0.01	0.00	1.056	9.026	390.6	4.18	0.45	0.040	11.127	0.14	0.553	0.050	0.908	0.00	0.553
0.02259	1.092	10.004	413.1	0.06	0.05	1.266	10.025	428.2	4.59	0.88	0.076	11.699	0.50	0.672	0.057	0.916	0.00	0.672
0.02702	1.494	10.233	483.4	-0.10	-0.01	1.703	10.340	486.9	5.32	1.17	0.100	12.196	0.84	0.676	0.055	0.913	0.00	0.676
0.03109	1.896	10.451	544.8	-0.09	0.01	2.102	10.712	552.1	5.92	1.56	0.132	12.621	1.15	0.801	0.063	0.922	0.00	0.801
0.03807	2.656	10.813	645.5	0.00	0.00	2.860	11.245	644.8	6.91	1.87	0.156	13.018	1.45	0.834	0.064	0.924	0.00	0.834
0.04316	3.208	11.157	710.1	0.15	0.01	3.407	11.680	704.5	7.55	2.17	0.174	13.403	1.73	0.807	0.060	0.919	0.00	0.807
0.05141	4.093	11.764	802.0	0.55	0.05	4.309	12.371	792.2	8.49	1.87	0.156	13.930	2.17	0.125	0.009	0.887	0.00	0.125
0.05856	4.892	12.258	877.7	0.88	0.08	5.164	12.872	868.2	9.30	1.56	0.132	14.889	2.95	0.361	0.024	0.878	0.00	0.361
0.06538	5.659	12.722	944.0	1.22	0.11	5.919	13.422	920.5	9.96	1.87	0.156	15.732	3.61	0.452	0.029	0.859	0.00	0.452
0.07157	6.367	13.131	999.9	1.53	0.13	6.660	13.852	984.5	10.55	2.17	0.174	16.795	4.43	0.652	0.039	0.859	0.00	0.652
0.07804	7.169	13.482	1053.9	1.79	0.15	7.524	14.210	1044.3	11.18	2.17	0.174	17.220	4.78	-0.234	-0.014	0.833	0.00	-0.234
0.08367	7.771	13.896	1092.9	2.14	0.18	8.447	14.580	1096.9	11.75	2.17	0.174	17.854	5.29	-0.299	-0.017	0.833	0.00	-0.299
0.09660	9.117	14.811	1199.9	2.89	0.24	10.019	15.244	1210.9	12.97	2.86	0.231	18.581	5.87	-0.644	-0.035	0.807	0.00	-0.644
0.11194	11.007	15.620	1323.2	3.53	0.29	12.362	15.902	1350.0	14.46	3.35	0.266	19.416	6.58	-1.094	-0.056	0.755	0.00	-1.094
0.13515	14.483	16.499	1518.7	4.11	0.33	16.376	16.680	1554.7	16.66	3.96	0.311	20.464	7.37	-1.407	-0.069	0.711	0.00	-1.407
0.14373	15.429	16.939	1569.3	4.56	0.37	17.863	16.986	1625.6	17.42	4.23	0.332	20.905	7.68	-1.568	-0.075	0.744	0.00	-1.568
0.15915	17.718	17.503	1682.1	5.00	0.40	20.503	17.555	1742.1	18.66	4.75	0.371	21.700	8.25	-2.009	-0.093	0.726	0.00	-2.009
0.17647	20.208	18.173	1796.5	5.55	0.44	24.147	17.937	1890.6	20.25	5.10	0.397	22.414	8.69	-2.342	-0.104	0.685	0.00	-2.342
0.19376	23.014	18.697	1917.3	5.97	0.47	27.898	18.322	2032.3	21.77	5.46	0.425	22.863	8.94	-2.596	-0.114	0.681	0.00	-2.596
0.21485	26.086	19.473	2041.5	6.63	0.52	33.338	18.585	2221.9	23.80	5.71	0.444	23.424	9.22	-2.907	-0.124	0.665	0.00	-2.907
0.23908	30.053	19.759	2191.2	6.80	0.52	37.606	19.057	2359.7	25.28	6.15	0.481	23.566	9.05	-2.922	-0.124	0.641	0.00	-2.922
0.25690	33.992	20.398	2330.5	7.33	0.56	44.030	19.337	2553.5	27.36	6.47	0.503	23.459	8.75	-2.801	-0.119	0.636	0.00	-2.801
0.29687	42.678	21.936	2611.3	7.77	0.59	56.704	19.691	2897.8	31.05	6.95	0.533	23.459	8.48	-2.862	-0.122	0.630	0.00	-2.862
0.33589	55.851	21.908	2987.5	8.41	0.62	71.456	20.072	3387.0	36.29	7.26	0.567	23.459	8.13	-2.862	-0.122	0.630	0.00	-2.862
0.40267	69.515	22.957	3322.5	8.67	0.63	98.473	20.267	3818.4	40.91	7.48	0.585	23.459	7.85	-2.862	-0.122	0.630	0.00	-2.862
0.47759	93.162	22.903	3856.8	8.96	0.64	135.140	20.517	4472.0	47.91	7.75	0.607	23.459	7.58	-2.862	-0.122	0.630	0.00	-2.862
0.53330	112.734	23.252	4242.4	9.14	0.65	167.091	20.606	4972.4	53.27	7.84	0.614	23.459	7.32	-2.862	-0.122	0.630	0.00	-2.862
0.57029	126.832	23.442	4496.6	9.23	0.65	190.721	20.626	5308.4	56.87	7.85	0.615	23.459	7.06	-2.862	-0.122	0.630	0.00	-2.862
0.64384	159.710	23.584	5041.3	9.17	0.64	242.319	20.658	5973.2	64.05	7.86	0.614	23.459	6.81	-2.862	-0.122	0.630	0.00	-2.862
0.71681	199.222	23.511	5589.8	8.92	0.61	304.816	20.507	6656.5	71.32	7.65	0.595	23.459	6.55	-2.862	-0.122	0.630	0.00	-2.862

0.00-456" Ribbed 0.500" Pipe
 Paragraph 350

Series

PEO

PIPE
 S1:
 d = 0.306
 h = smooth
 R1AR:
 d = 0.297
 h = 0.0045
 RA: 33.0

RUM 288
 DATE 8/12/94
 POLY H-50K
 c 30
 w 1.03

Q (L/h)	Tw (S1)	1/Avg(S1)	Reyn(S1)	S (S1)	Sf (S1)	Te (RIA)	1/Sqf(RIA)	Reyn(RIA)	h	S (RIA)	Sf (RIA)	1/Sqf(RIA)	Reyn(RIA)	h	S (RIA)	Sf (RIA)	1/Sqf(RIA)	V/Avg	St(S1)	R	Rf	P	Δ/hrs	corrected R	corrected S
0.00483	0.092	7.350	118.5	0.13	0.01	0.106	7.405	122.2	1.31	-0.01	-0.001	-0.001	10.055	0.09	-0.055	-0.005	0.824	0.00	0.00	-0.055	0.824	0.00	0.00	-0.055	0.09
0.00690	0.128	8.804	138.4	0.05	0.00	0.147	8.866	143.8	1.54	0.00	0.008	0.008	10.127	0.03	-0.048	-0.005	0.828	0.00	0.00	-0.048	0.828	0.00	0.00	-0.048	0.03
0.00966	0.184	10.411	167.8	0.16	0.02	0.202	10.738	169.0	1.81	0.01	0.001	0.001	10.130	0.07	0.040	0.004	0.846	0.00	0.00	0.040	0.846	0.00	0.00	0.040	0.07
0.01341	0.259	11.079	219.0	0.61	0.02	0.401	10.570	238.5	2.56	0.06	0.036	0.036	11.357	0.18	0.327	0.031	0.884	0.00	0.00	0.327	0.884	0.00	0.00	0.327	0.18
0.01576	0.339	9.942	287.2	1.38	0.13	2.825	9.821	302.0	3.24	0.39	0.096	0.096	11.357	0.61	0.473	0.042	0.897	0.00	0.00	0.473	0.897	0.00	0.00	0.473	0.61
0.01826	0.477	9.913	333.8	2.05	0.18	3.368	9.850	347.6	3.72	0.67	0.148	0.148	12.382	1.37	0.598	0.044	0.900	0.00	0.00	0.598	0.900	0.00	0.00	0.598	1.37
0.02076	0.619	10.027	375.5	2.49	0.27	4.349	10.000	391.0	4.19	1.00	0.209	0.209	13.094	1.99	0.706	0.054	0.909	0.00	0.00	0.706	0.909	0.00	0.00	0.706	1.99
0.02253	0.771	10.081	405.6	3.09	0.30	5.876	10.079	421.4	4.51	1.38	0.266	0.266	13.694	2.39	0.870	0.064	0.920	0.00	0.00	0.870	0.920	0.00	0.00	0.870	2.39
0.02424	0.941	10.362	477.4	3.48	0.33	6.995	10.200	463.0	4.79	1.66	0.317	0.317	14.479	3.04	0.723	0.050	0.905	0.00	0.00	0.723	0.905	0.00	0.00	0.723	3.04
0.03110	1.323	10.661	530.5	4.38	0.37	7.338	10.178	507.8	5.26	1.85	0.344	0.344	14.598	3.42	0.762	0.051	0.906	0.00	0.00	0.762	0.906	0.00	0.00	0.762	3.42
0.03838	1.843	11.366	614.3	4.38	0.37	8.493	10.178	552.6	5.26	1.85	0.344	0.344	14.598	3.42	0.762	0.051	0.906	0.00	0.00	0.762	0.906	0.00	0.00	0.762	3.42
0.04890	2.445	12.406	717.2	5.42	0.45	10.911	10.178	607.4	5.26	1.85	0.344	0.344	14.598	3.42	0.762	0.051	0.906	0.00	0.00	0.762	0.906	0.00	0.00	0.762	3.42
0.05800	3.329	13.257	797.3	5.42	0.45	12.866	10.178	662.2	5.26	1.85	0.344	0.344	14.598	3.42	0.762	0.051	0.906	0.00	0.00	0.762	0.906	0.00	0.00	0.762	3.42
0.06477	4.708	13.818	854.1	6.34	0.52	13.481	10.178	717.0	5.26	1.85	0.344	0.344	14.598	3.42	0.762	0.051	0.906	0.00	0.00	0.762	0.906	0.00	0.00	0.762	3.42
0.07347	5.470	14.542	920.0	6.34	0.52	14.865	10.178	771.8	5.26	1.85	0.344	0.344	14.598	3.42	0.762	0.051	0.906	0.00	0.00	0.762	0.906	0.00	0.00	0.762	3.42
0.08021	6.104	15.070	968.8	6.34	0.52	16.160	10.178	826.6	5.26	1.85	0.344	0.344	14.598	3.42	0.762	0.051	0.906	0.00	0.00	0.762	0.906	0.00	0.00	0.762	3.42
0.08786	6.908	15.476	1025.7	6.34	0.52	17.390	10.178	881.4	5.26	1.85	0.344	0.344	14.598	3.42	0.762	0.051	0.906	0.00	0.00	0.762	0.906	0.00	0.00	0.762	3.42
0.09822	7.916	16.160	1108.8	6.34	0.52	18.481	10.178	936.2	5.26	1.85	0.344	0.344	14.598	3.42	0.762	0.051	0.906	0.00	0.00	0.762	0.906	0.00	0.00	0.762	3.42
0.11776	9.825	17.390	1238.8	6.34	0.52	19.119	10.178	991.0	5.26	1.85	0.344	0.344	14.598	3.42	0.762	0.051	0.906	0.00	0.00	0.762	0.906	0.00	0.00	0.762	3.42
0.13994	12.090	18.498	1374.8	6.34	0.52	20.107	10.178	1045.8	5.26	1.85	0.344	0.344	14.598	3.42	0.762	0.051	0.906	0.00	0.00	0.762	0.906	0.00	0.00	0.762	3.42
0.14759	12.866	19.047	1420.7	6.34	0.52	20.107	10.178	1045.8	5.26	1.85	0.344	0.344	14.598	3.42	0.762	0.051	0.906	0.00	0.00	0.762	0.906	0.00	0.00	0.762	3.42
0.16108	14.401	19.649	1503.1	7.34	0.60	20.107	10.178	1045.8	5.26	1.85	0.344	0.344	14.598	3.42	0.762	0.051	0.906	0.00	0.00	0.762	0.906	0.00	0.00	0.762	3.42
0.17839	16.085	20.590	1588.7	8.19	0.66	20.107	10.178	1045.8	5.26	1.85	0.344	0.344	14.598	3.42	0.762	0.051	0.906	0.00	0.00	0.762	0.906	0.00	0.00	0.762	3.42
0.19568	17.922	21.396	1677.0	8.90	0.71	22.809	20.463	1821.4	19.51	7.84	0.573	0.573	22.525	9.88	-2.062	-0.092	0.758	0.00	0.00	-2.062	0.758	0.00	0.00	-2.062	9.88
0.21823	20.457	22.381	1791.8	9.77	0.77	27.685	20.757	2068.7	21.50	7.90	0.614	0.614	23.520	10.71	-2.763	-0.117	0.713	0.00	0.00	-2.763	0.713	0.00	0.00	-2.763	10.71
0.24736	24.375	23.192	1955.9	10.43	0.82	33.270	21.418	2200.0	23.57	8.55	0.664	0.664	24.719	11.75	-3.301	-0.134	0.706	0.00	0.00	-3.301	0.706	0.00	0.00	-3.301	11.75
0.26927	28.716	24.564	2160.0	11.63	0.90	43.500	21.904	2516.0	26.96	9.04	0.702	0.702	25.947	12.74	-4.043	-0.156	0.659	0.00	0.00	-4.043	0.659	0.00	0.00	-4.043	12.74
0.34613	36.735	25.744	2466.3	12.58	0.96	60.243	22.272	2961.1	31.72	9.43	0.734	0.734	27.228	13.74	-4.956	-0.182	0.620	0.00	0.00	-4.956	0.620	0.00	0.00	-4.956	13.74
0.36786	44.899	26.518	2655.0	13.22	0.98	72.842	22.463	3255.6	34.88	9.64	0.752	0.752	27.949	14.30	-5.486	-0.196	0.594	-1.16	-5.411	-5.411	0.594	-1.16	-5.411	14.22	
0.44017	55.990	27.233	2964.0	13.75	1.02	93.963	22.679	3696.9	39.61	9.88	0.772	0.772	28.629	14.76	-5.950	-0.208	0.574	-3.52	-5.749	-5.749	0.574	-3.52	-5.749	14.56	
0.49616	67.453	27.964	3253.6	14.31	1.05	117.284	22.882	4130.4	44.25	10.10	0.791	0.791	29.125	15.06	-6.243	-0.214	0.555	-5.52	-5.965	-5.965	0.555	-5.52	-5.965	14.78	
0.55182	80.995	28.383	3565.2	14.57	1.06	143.606	22.998	4570.3	48.96	10.23	0.801	0.801	29.308	15.07	-6.310	-0.215	0.544	-7.48	-6.970	-6.970	0.544	-7.48	-6.970	14.73	
0.62551	99.021	29.098	3940.3	15.12	1.08	182.106	23.150	5144.4	55.12	10.38	0.813	0.813	29.730	15.28	-6.580	-0.221	0.524	-9.64	-6.194	-6.194	0.524	-9.64	-6.194	14.90	
0.68040	116.774	29.146	4274.3	15.02	1.06	213.478	23.258	5563.8	59.61	10.48	0.820	0.820	30.038	15.46	-6.780	-0.226	0.527	-11.41	-6.360	-6.360	0.527	-11.41	-6.360	15.04	
0.75307	140.772	29.382	4670.9	15.10	1.06	259.254	23.360	6102.5	65.38	10.55	0.824	0.824	30.434	15.69	-7.074	-0.232	0.524	-13.41	-6.628	-6.628	0.524	-13.41	-6.628	15.25	

0.00450" Fiberglass 0.300" Pipe
 Height: 350

Series: PEO

PIPE
 S1: 287
 d = 0.308
 h = smooth
 R1/R2: 100
 d = 0.297
 h = 0.0045
 RA: 33.0

Q (L/s)	Te (S1)	1/μm(S1)	Repl(S1)	S (S1)	Sf (S1)	Te (R1A)	1/μm(R1A)	Repl(R1A)	N	S (R1A)	Sf (R1A)	1/μm	S1(S1)	R	RF	P	Δ/Inch	connected R	connected S
0.00443	0.093	6.746	109.3			0.104	6.854	111.8	1.20							0.855			
0.00547	0.110	7.623	119.3			0.127	7.662	123.2	1.48							0.841			
0.00682	0.141	8.400	135.4			0.159	8.530	138.4	1.32							0.854			
0.00973	0.207	9.906	163.9			0.239	9.941	169.6	1.82							0.834			
0.01380	0.320	11.292	204.0			0.355	11.566	206.9	2.22							0.869			
0.01608	0.482	10.720	250.6			0.708	9.546	292.3	3.13							0.657			
0.01812	0.728	9.837	307.9			0.859	9.770	322.0	3.45							0.817			
0.02110	0.966	9.938	355.1	0.14		1.113	9.990	367.0	3.93	0.10	0.010	9.964	0.11	0.027	0.003	0.837	0.00	0.027	0.11
0.02255	1.092	9.988	377.9	0.08		1.210	10.238	383.0	4.10	0.26	0.026	10.019	0.04	0.029	0.022	0.870	0.00	0.029	0.09
0.02697	1.424	10.463	431.6	0.32		1.570	10.751	436.3	4.67	0.53	0.051	10.523	0.36	0.228	0.022	0.875	0.00	0.228	0.36
0.03094	1.693	11.009	470.8	0.72		1.780	11.582	464.8	4.98	1.23	0.119	10.923	0.65	0.659	0.060	0.917	0.00	0.659	0.65
0.03791	2.162	11.937	532.2	1.43		2.230	12.679	520.5	5.58	2.10	0.199	11.749	1.28	0.930	0.079	0.935	0.00	0.930	1.28
0.04415	2.558	12.779	573.1	2.13		2.643	13.585	566.7	6.07	2.81	0.262	12.557	1.94	1.008	0.080	0.933	0.00	1.008	1.94
0.05320	3.165	13.844	644.1	3.01	0.28	3.246	14.750	628.0	6.73	3.78	0.344	13.960	2.79	1.170	0.086	0.940	0.00	1.170	2.79
0.06145	3.720	14.750	699.2	3.77	0.34	3.784	15.780	678.9	7.27	4.64	0.416	14.415	3.49	1.365	0.095	0.948	0.00	1.365	3.49
0.06793	4.118	15.499	735.8	4.43	0.40	4.189	16.579	714.4	7.65	5.32	0.473	15.065	4.05	1.514	0.101	0.948	0.00	1.514	4.05
0.07539	4.656	16.175	782.6	5.00	0.45	4.827	17.140	767.1	8.22	5.72	0.501	15.952	4.81	1.188	0.074	0.930	0.00	1.188	4.81
0.08438	5.263	17.029	832.0	5.75	0.51	5.582	17.840	824.9	8.84	6.25	0.540	16.907	5.64	0.933	0.055	0.909	0.00	0.933	5.64
0.09002	5.652	17.531	855.9	6.20	0.55	6.026	18.319	850.8	9.11	6.66	0.571	17.393	6.07	0.921	0.001	0.905	0.00	0.921	6.07
0.10311	6.638	18.528	933.4	7.05	0.61	7.249	19.130	939.1	10.06	7.25	0.610	18.629	7.14	0.215	0.012	0.883	0.00	0.215	7.14
0.12258	7.908	20.181	1022.1	8.54	0.73	8.687	20.774	1031.4	11.05	8.69	0.719	20.328	8.67	0.365	0.018	0.878	0.00	0.365	8.67
0.13925	9.100	21.370	1096.1	9.61	0.82	10.302	21.671	1122.7	12.03	9.42	0.769	21.891	10.09	0.548	0.025	0.852	0.00	0.548	10.09
0.15145	9.869	22.318	1144.4	10.48	0.89	11.702	22.113	1199.8	12.85	9.74	0.787	23.154	11.24	-1.041	-0.045	0.813	0.00	-1.041	11.24
0.16493	10.899	23.170	1200.7	11.25	0.94	13.395	22.509	1293.8	13.75	10.03	0.803	24.161	12.13	-1.652	-0.068	0.782	0.00	-1.652	12.13
0.18416	12.420	24.192	1284.2	12.16	1.01	15.741	23.183	1391.8	14.91	10.59	0.840	24.858	12.66	-1.673	-0.067	0.761	0.00	-1.673	12.66
0.21102	15.232	25.030	1422.2	12.82	1.05	19.017	24.170	1529.9	16.39	11.47	0.909	25.617	13.28	-1.447	-0.056	0.772	0.00	-1.447	13.28
0.22825	17.170	25.500	1510.2	13.18	1.07	21.664	24.494	1633.1	17.50	11.73	0.920	26.237	13.78	-1.743	-0.066	0.764	0.00	-1.743	13.78
0.26452	17.306	26.530	1682.6	14.03	1.12	27.613	25.144	1844.1	19.76	12.31	0.960	27.390	14.73	-2.246	-0.082	0.744	0.00	-2.246	14.73
0.30256	26.007	27.466	1838.9	14.79	1.17	34.934	25.569	2074.2	22.22	12.70	0.988	28.239	15.37	-2.670	-0.095	0.718	0.00	-2.670	15.37
0.34235	31.707	28.146	2052.4	15.30	1.19	43.955	25.792	2326.4	24.92	12.92	1.004	29.377	16.31	-3.585	-0.122	0.696	0.00	-3.585	16.31
0.39891	39.793	29.275	2299.3	16.23	1.24	58.265	26.103	2678.6	28.70	13.24	1.030	30.366	17.05	-4.283	-0.140	0.659	0.00	-4.283	17.05
0.45887	49.684	30.138	2569.2	16.90	1.28	77.261	26.075	3084.5	31.05	13.24	1.032	31.210	17.65	-5.135	-0.165	0.620	0.00	-5.135	17.65
0.53330	64.038	30.852	2917.6	17.59	1.29	104.410	26.069	3586.6	38.43	13.27	1.036	32.204	18.39	-6.135	-0.191	0.591	-1.28	-6.075	18.39
0.58874	75.406	31.866	3165.3	17.78	1.31	127.608	26.032	3964.2	42.47	13.27	1.036	32.917	18.92	-6.885	-0.209	0.570	-4.47	-6.695	18.73
0.64384	87.195	31.920	3402.7	18.19	1.33	153.631	25.946	4348.2	46.59	13.17	1.032	33.762	19.61	-7.816	-0.232	0.547	-7.32	-7.532	19.32
0.71681	104.747	32.424	3724.8	18.54	1.34	181.197	25.883	4844.8	51.91	13.13	1.028	34.854	20.51	-8.961	-0.257	0.528	-10.91	-8.579	20.13
0.78919	122.506	33.010	4006.4	19.00	1.36	232.228	25.868	5310.5	56.90	13.10	1.025	35.878	21.38	-10.010	-0.279	0.509	-13.98	-9.567	20.93

0.00405" Ribbed 3.008" Pipe
Residuals = 350

PEO

DATE 8/6/94
POLY W-301
c-mpgm 1
w 1.00

NUM	DATE	POLY	c-mpgm	w	O (L/A)	T _w (S2)	1/μg(S2)	Reps(S2)	S (S2)	SF (S2)	T _w (R4)	1/μg(R4)	Reps(R4)	h	S (R4)	SF (R4)	1/μg	S1(S1)	R	Rf	P	Δ/hrs	corrected R	corrected S
0.00660					0.121	8.722	138.4		-0.06	-0.01	0.137	8.908	141.6	1.52	-0.08	-0.08	9.799	0.01	-0.058	-0.006	0.854	0.00	-0.058	0.01
0.01041					0.202	10.735	178.9		0.04	0.00	0.217	11.170	178.6	1.91	-0.10	0.10	9.921	-0.05	0.001	0.000	0.839	0.00	0.001	-0.05
0.01326					0.271	11.784	207.8		0.04	0.00	0.271	12.217	200.0	2.14	-0.06	-0.06	10.072	-0.03	0.027	0.003	0.843	0.00	0.027	-0.03
0.01509					0.383	11.288	247.2		0.04	0.00	0.617	9.582	302.1	3.24	0.01	0.00	10.392	0.01	0.098	0.009	0.840	0.00	0.098	0.01
0.01789					0.719	9.767	338.3		-0.11	-0.01	0.842	9.741	353.3	3.79	0.09	0.009	10.534	-0.11	0.344	0.033	0.885	0.00	0.344	-0.11
0.02022					0.902	9.860	380.1		-0.06	-0.01	1.036	9.922	392.4	4.20	0.19	0.018	10.764	-0.06	0.453	0.042	0.898	0.00	0.453	-0.06
0.02214					1.048	10.011	410.5		0.10	0.01	1.199	10.099	422.7	4.53	0.32	0.029	11.116	0.10	0.471	0.042	0.899	0.00	0.471	0.10
0.02690					1.442	10.370	482.3		0.04	0.00	1.640	10.490	495.3	5.31	0.86	0.057	11.551	0.32	0.846	0.056	0.916	0.00	0.846	0.32
0.03237					2.028	10.524	573.1		-0.06	-0.01	2.209	10.878	575.9	6.17	0.78	0.066	11.998	0.59	0.562	0.047	0.904	0.00	0.562	0.32
0.03783					2.629	11.126	718.2		0.35	0.03	3.406	11.587	716.3	7.87	0.89	0.074	12.301	0.76	0.531	0.043	0.900	0.00	0.531	0.76
0.05085					3.174	11.598	817.8		0.60	0.05	4.335	12.197	807.8	8.65	1.12	0.092	12.635	0.97	0.572	0.045	0.902	0.00	0.572	0.97
0.05800					4.987	12.024	901.8		0.77	0.07	5.320	12.560	896.7	9.61	1.86	0.117	12.901	1.10	0.518	0.040	0.896	0.00	0.518	1.10
0.06405					5.798	12.314	971.0		0.99	0.09	7.133	13.207	1035.6	11.09	2.25	0.152	13.072	1.22	0.553	0.042	0.898	0.00	0.553	1.22
0.07062					6.670	12.658	1040.2		1.23	0.10	8.221	13.390	1107.2	11.86	3.28	0.177	13.072	1.22	0.553	0.042	0.898	0.00	0.553	1.22
0.07687					7.637	12.876	1108.5		1.81	0.15	9.084	13.625	1156.1	12.39	4.26	0.200	13.072	1.22	0.553	0.042	0.898	0.00	0.553	1.22
0.08222					8.463	13.084	1159.1		1.97	0.16	10.842	14.226	1281.9	13.73	5.48	0.255	13.072	1.22	0.553	0.042	0.898	0.00	0.553	1.22
0.09379					9.860	13.827	1269.8		2.13	0.21	13.058	14.536	1413.5	15.14	6.38	0.293	13.072	1.22	0.553	0.042	0.898	0.00	0.553	1.22
0.10517					11.837	14.150	1397.9		2.62	0.21	17.202	15.008	1624.4	17.40	7.29	0.322	14.510	2.17	0.398	0.027	0.880	-0.29	0.456	2.11
0.12463					15.707	14.557	1612.3		2.78	0.24	21.187	15.386	1805.0	19.34	8.29	0.350	15.281	2.66	0.105	0.007	0.849	-0.29	0.324	2.44
0.14181					18.657	15.197	1759.4		2.78	0.24	26.430	15.386	2016.6	21.61	9.29	0.350	15.734	2.92	-0.083	-0.005	0.839	-2.39	0.289	2.54
0.16108					22.979	15.554	1953.6		3.09	0.24	30.658	16.091	2172.6	23.28	10.29	0.350	16.077	3.13	0.014	0.001	0.839	-3.22	0.466	2.68
0.17839					26.680	15.987	2105.2		3.19	0.24	36.703	16.131	2377.9	25.48	11.29	0.350	16.341	3.24	-0.216	-0.013	0.820	-4.08	0.306	2.72
0.19568					31.199	16.216	2277.3		3.29	0.25	44.198	16.140	2610.3	27.97	12.29	0.350	16.612	3.35	-0.472	-0.028	0.796	-4.95	0.105	2.77
0.21485					36.507	16.460	2464.2		3.44	0.26	61.638	16.100	3082.4	33.02	13.29	0.350	16.987	3.43	-0.887	-0.052	0.757	-6.50	-0.244	2.79
0.23308					48.359	16.846	2836.0		3.44	0.26	61.638	16.100	3082.4	33.02	13.29	0.350	17.143	3.35	-1.082	-0.063	0.735	-7.84	-0.403	2.67
0.28927					61.636	17.055	3201.7		3.30	0.24	80.906	16.061	3531.4	37.83	14.29	0.350	17.270	3.15	-1.394	-0.081	0.705	-9.72	-0.691	2.44
0.34613					86.636	17.214	3794.6		3.17	0.23	118.570	15.876	4273.7	45.79	15.29	0.350	17.206	2.96	-1.593	-0.092	0.685	-10.83	-0.886	2.26
0.38386					105.943	17.263	4197.6		3.05	0.21	149.233	15.693	4796.3	51.39	16.29	0.350	17.253	2.75	-1.692	-0.098	0.670	-11.84	-0.989	2.05
0.42144					127.127	17.302	4597.1		2.78	0.19	182.962	15.561	5309.4	56.88	17.29	0.350	17.254	2.51	-1.915	-0.111	0.655	-13.25	-1.220	1.82
0.47753					164.192	17.251	5222.3		2.61	0.18	241.742	15.339	6100.5	65.36	18.29	0.350	17.189	2.24	-2.036	-0.119	0.638	-14.46	-1.378	1.56
0.53330					204.402	17.267	5822.6		2.34	0.16	308.957	15.153	6891.7	73.84	19.29	0.350	17.189	2.24	-2.036	-0.119	0.628	-15.92	-1.378	1.18
0.60714					266.074	17.230	6625.2		2.12	0.14	408.827	14.997	7506.2	84.71	19.99	0.350	17.032	1.84	-2.035	-0.119	0.628	-15.92	-1.378	1.18
0.66214					319.623	17.146	7169.1		2.12	0.14	495.511	14.857	8593.6	92.07	1.75	0.133	16.926	1.59	-2.069	-0.122	0.622	-16.93	-1.428	0.95

0.0045h² Ribbet®.308" Pipe
Respirator 350

Series

PEO

PIPE
SI:
d = 0.308
h = smooth
RIAR:
d = 0.297
h = 0.0045
RH: 33.0

REIN
DATE
POLY
W-301
c-mpam
1.00

Z84
B/G/94

Q (L/s)	T _{eq} (S)	1/ρ _{eq} (S)	Re _{eq} (S)	S (S)	Sf (S)	T _{eq} (RIA)	1/ρ _{eq} (RIA)	Re _{eq} (RIA)	h _{eq}	S (RIA)	Sf (RIA)	1/ρ _{eq} (S)	R	ρ	d/h _{eq}	corrected ρ
0.00424	0.079	6.379	110.4	0.01	0.00	0.090	7.053	113.5	1.22	-0.01	-0.001	9.944	0.00	0.003	0.00	0.026
0.00670	0.125	8.765	136.3	0.01	0.00	0.138	8.997	140.9	1.51	-0.02	-0.012	10.033	-0.00	-0.002	0.00	-0.020
0.00939	0.182	10.188	168.2	0.01	0.00	0.199	10.503	169.5	1.82	-0.02	-0.008	10.308	-0.04	0.006	0.00	0.062
0.01345	0.263	11.714	210.0	0.01	0.00	0.303	12.207	209.3	2.24	-0.08	-0.008	10.536	-0.01	0.013	0.00	0.313
0.01527	0.481	10.197	274.3	0.01	0.00	0.617	9.716	299.1	3.20	0.20	0.019	10.904	0.23	0.037	0.00	0.403
0.01762	0.698	9.765	330.7	0.01	0.00	0.822	9.707	345.5	3.70	0.48	0.044	10.904	0.23	0.037	0.00	0.403
0.02014	0.884	9.917	372.4	0.01	0.00	1.018	9.970	384.7	4.12	0.71	0.065	11.250	0.46	0.030	0.00	0.430
0.02187	1.029	9.982	401.9	0.01	0.00	1.190	10.013	416.2	4.46	0.96	0.085	11.250	0.46	0.030	0.00	0.430
0.02663	1.446	10.251	476.7	0.01	0.00	1.645	10.370	489.5	5.24	1.45	0.127	12.320	1.17	0.067	0.00	0.466
0.03070	1.828	10.510	535.1	0.02	0.02	2.377	11.307	587.4	6.29	2.26	0.191	12.320	1.17	0.067	0.00	0.466
0.03490	2.198	10.898	586.7	0.04	0.04	2.660	11.680	627.0	6.72	2.37	0.199	13.700	2.16	0.088	0.00	0.466
0.03814	2.464	11.249	626.8	0.07	0.07	3.197	12.128	687.5	7.37	2.84	0.233	14.534	2.81	0.100	0.00	0.470
0.04341	2.968	11.665	688.2	0.11	0.11	4.038	12.887	722.6	8.28	3.15	0.254	15.643	3.70	0.090	0.00	0.470
0.05185	3.779	12.348	776.2	0.15	0.15	4.864	13.444	848.5	9.09	3.67	0.292	16.304	4.16	0.064	0.00	0.464
0.05936	4.492	13.415	914.2	0.17	0.17	5.560	14.059	906.1	9.71	4.02	0.316	17.020	4.68	0.029	0.00	0.468
0.07237	5.961	13.723	970.9	0.21	0.21	6.376	14.316	966.7	10.36	4.47	0.349	17.240	4.86	0.024	0.00	0.411
0.08071	6.938	14.187	1035.8	0.25	0.22	7.494	14.728	1036.3	11.10	4.77	0.372	17.240	4.86	0.024	0.00	0.411
0.08545	7.445	14.500	1071.3	0.28	0.24	8.094	15.004	1075.4	11.52	5.07	0.394	18.208	5.29	0.024	0.00	0.411
0.09849	8.723	15.438	1184.3	0.34	0.30	10.006	15.553	1221.1	13.08	5.47	0.425	19.208	6.34	0.024	0.00	0.411
0.09849	8.723	15.438	1184.3	0.34	0.30	10.006	15.553	1221.1	13.08	5.47	0.425	19.208	6.34	0.024	0.00	0.411
0.11442	10.711	16.184	1318.5	0.41	0.34	12.384	16.240	1364.9	14.62	5.81	0.455	20.276	6.90	0.024	0.00	0.411
0.13235	13.988	16.621	1487.7	0.53	0.37	15.616	16.728	1570.6	16.83	6.29	0.485	20.276	6.90	0.024	0.00	0.411
0.13602	13.951	16.858	1509.5	0.53	0.40	16.295	16.829	1608.0	18.05	6.59	0.507	20.276	6.90	0.024	0.00	0.411
0.14952	15.737	17.448	1603.8	0.50	0.44	18.742	17.250	1695.0	19.87	6.81	0.529	20.276	6.90	0.024	0.00	0.411
0.16878	18.693	18.071	1748.4	0.61	0.47	22.916	17.609	1863.7	19.87	7.27	0.574	20.276	6.90	0.024	0.00	0.411
0.19184	22.446	18.744	1916.4	0.69	0.49	28.527	17.939	2073.9	22.28	7.59	0.607	20.276	6.90	0.024	0.00	0.411
0.20910	25.996	19.132	2046.8	0.75	0.50	32.946	18.194	2235.6	23.95	7.91	0.641	20.276	6.90	0.024	0.00	0.411
0.23207	30.232	19.538	2224.7	0.81	0.52	39.952	18.338	2462.1	26.36	8.24	0.674	20.276	6.90	0.024	0.00	0.411
0.26452	37.528	19.989	2478.7	0.90	0.52	50.760	18.544	2775.3	29.73	8.58	0.707	20.276	6.90	0.024	0.00	0.411
0.30067	47.110	20.278	2777.1	0.96	0.51	64.877	18.644	3137.5	33.61	8.81	0.739	20.276	6.90	0.024	0.00	0.411
0.34613	60.732	20.560	3154.5	0.96	0.51	86.163	18.624	3617.2	38.75	9.05	0.771	20.276	6.90	0.024	0.00	0.411
0.40267	81.183	20.688	3646.9	0.96	0.49	117.907	18.521	4231.2	45.33	9.29	0.804	20.276	6.90	0.024	0.00	0.411
0.45887	105.870	20.645	4162.3	0.96	0.44	157.705	18.250	4890.7	52.60	9.53	0.837	20.276	6.90	0.024	0.00	0.411
0.51475	134.072	20.579	4683.3	0.96	0.44	204.121	17.995	5563.2	59.60	9.77	0.870	20.276	6.90	0.024	0.00	0.411
0.57029	167.054	20.426	5223.4	0.96	0.41	258.847	17.704	6259.7	67.06	9.99	0.903	20.276	6.90	0.024	0.00	0.411
0.64384	218.156	20.179	5962.3	0.96	0.37	343.499	17.351	7202.7	77.17	10.22	0.936	20.276	6.90	0.024	0.00	0.411
0.71681	275.504	19.992	6658.8	0.96	0.34	440.004	17.068	8101.5	86.80	10.45	0.969	20.276	6.90	0.024	0.00	0.411

0.00-453" Ribbed 3.008" Pipe
 Neoprene 350

Series

PEO

SI: 203
 d: 0.308
 P: 0.5794
 W: 3.01
 POLY: 10
 c: 1.02
 W:

SI: 203
 d: 0.308
 P: 0.5794
 W: 3.01
 POLY: 10
 c: 1.02
 W:

Q (L/s)	Ts (SI)	V (m/s)	Reyn (SI)	S (SI)	Sf (SI)	Te (RIA)	V (m/s)	Reyn (RIA)	h	S (RIA)	Sf (RIA)	V (m/s)	Reyn (RIA)	R	Rf	P	d/rms	connected	P connected
0.00531	0.100	7.780	1226	0.27	0.03	0.113	7.685	125.6	1.35	0.04	0.004	9.949	0.17	-0.100	-0.010	0.851	0.00	-0.100	0.17
0.00572	0.148	9.292	1496	0.38	0.04	0.164	9.511	151.9	1.63	0.30	0.030	10.238	0.31	0.027	0.003	0.831	0.00	0.027	0.31
0.00974	0.109	10.393	1893	0.77	0.06	0.204	10.773	169.5	1.82	0.44	0.043	10.493	0.45	0.037	0.004	0.852	0.00	0.037	0.45
0.01340	0.302	11.291	2143	1.30	0.13	0.448	10.000	231.4	2.69	1.51	0.144	11.153	0.90	-0.012	-0.001	0.852	0.00	-0.012	0.90
0.01582	0.567	9.730	294.0	2.02	0.19	0.659	9.664	307.5	3.29	2.43	0.227	12.567	1.99	0.252	0.021	0.876	0.00	0.252	1.99
0.01833	0.745	9.832	377.6	3.54	0.33	0.864	9.849	350.1	3.75	3.86	0.349	14.432	1.99	0.563	0.045	0.900	0.00	0.563	1.99
0.02079	0.899	10.150	391.1	4.45	0.40	1.023	10.265	381.7	4.09	5.02	0.446	15.355	4.33	0.936	0.061	0.916	0.00	0.936	4.33
0.02275	1.029	10.381	396.1	4.96	0.44	1.164	10.530	407.7	4.37	5.44	0.475	16.078	4.91	0.822	0.051	0.908	0.00	0.822	4.91
0.02714	1.309	10.984	449.6	5.67	0.50	1.481	11.141	460.5	4.93	5.89	0.507	17.068	5.77	0.452	0.027	0.884	0.00	0.452	5.77
0.03166	1.577	11.672	493.9	6.83	0.56	1.736	12.000	499.0	5.35	6.49	0.548	17.863	6.49	0.287	0.016	0.868	0.00	0.287	6.49
0.03839	1.991	12.596	555.5	8.22	0.60	2.133	13.170	553.6	5.93	6.87	0.580	18.431	6.96	0.289	0.016	0.869	0.00	0.289	6.96
0.05196	2.786	14.412	657.4	10.08	0.76	3.010	14.940	658.7	7.06	7.52	0.622	19.784	8.12	-1.250	-0.008	0.844	0.00	-1.250	8.12
0.06189	3.420	15.493	726.4	12.05	0.84	3.601	16.291	719.4	8.35	8.02	0.650	21.610	9.72	-1.250	-0.008	0.844	0.00	-1.250	9.72
0.06950	3.971	16.145	785.4	14.08	0.88	4.218	16.901	778.4	8.35	8.33	0.665	23.033	10.95	-2.307	-0.099	0.743	0.00	-2.307	10.95
0.07710	4.435	16.948	830.8	16.20	0.85	4.837	17.510	835.3	8.95	8.47	0.671	23.307	11.17	-2.307	-0.099	0.743	0.00	-2.307	11.17
0.08393	4.803	17.729	862.7	18.32	0.89	5.335	18.150	873.3	9.36	8.7C	0.683	23.833	11.61	-2.733	-0.115	0.714	0.00	-2.733	11.61
0.09264	5.508	18.274	914.1	20.71	0.93	6.110	18.720	926.9	9.93	8.96	0.700	25.743	13.20	-3.983	-0.155	0.664	0.00	-3.983	13.20
0.10730	6.530	19.438	1008.7	24.134	1.03	7.461	19.620	1039.0	11.12	9.00	0.701	26.271	13.57	-4.428	-0.169	0.626	0.00	-4.428	13.57
0.12572	7.903	20.702	1115.8	28.106	1.06	8.512	20.360	1178.5	12.63	9.07	0.705	27.074	14.10	-5.130	-0.189	0.588	-0.35	-4.601	13.57
0.14373	9.146	22.000	1205.4	32.165	1.08	9.512	20.860	1320.5	14.15	9.30	0.723	27.680	14.49	-5.525	-0.200	0.575	-0.35	-4.710	13.67
0.14953	9.748	22.170	1240.2	36.004	1.09	10.648	21.000	1360.0	15.37	9.39	0.723	28.024	14.51	-5.800	-0.200	0.545	-0.35	-4.742	13.66
0.15723	10.256	22.727	1276.3	39.906	1.06	11.829	21.100	1427.9	16.91	9.30	0.727	27.678	13.90	-5.567	-0.201	0.518	-0.35	-4.975	12.70
0.17647	12.094	23.490	1386.4	44.859	1.06	13.615	21.430	1578.5	18.47	9.02	0.707	27.098	13.02	-5.128	-0.189	0.508	-0.35	-4.975	12.70
0.19568	13.883	24.310	1487.3	50.300	1.00	15.915	21.760	1724.0	20.21	8.68	0.691	26.600	12.31	-4.813	-0.181	0.515	-0.35	-4.813	10.94
0.21485	15.662	25.130	1578.3	55.988	0.95	18.134	21.843	1886.1	23.70	8.68	0.679	25.996	11.51	-4.391	-0.169	0.519	-0.35	-4.391	10.10
0.23408	17.442	26.039	1794.4	62.079	0.89	20.171	21.760	2039.0	26.99	8.40	0.655	24.630	10.69	-3.861	-0.152	0.530	-0.35	-3.861	9.26
0.25308	20.242	26.610	2020.0	68.948	0.84	22.117	21.972	2211.7	30.04	8.10	0.629	24.002	9.08	-3.040	-0.127	0.542	-0.35	-3.040	8.39
0.29117	25.654	28.610	2345.9	76.849	0.79	24.134	21.843	2411.7	32.18	8.10	0.629	24.002	9.08	-3.040	-0.127	0.542	-0.35	-3.040	7.63
0.34802	34.574	27.398	2739.9	84.851	0.79	26.169	22.224	2604.0	34.18	8.10	0.629	24.002	9.08	-3.040	-0.127	0.542	-0.35	-3.040	7.63
0.40454	44.892	28.055	3143.6	92.851	0.79	28.189	21.972	2809.6	36.18	8.10	0.629	24.002	9.08	-3.040	-0.127	0.542	-0.35	-3.040	7.63
0.47753	62.079	28.610	3565.1	100.851	0.79	30.171	21.760	3009.6	38.18	8.10	0.629	24.002	9.08	-3.040	-0.127	0.542	-0.35	-3.040	7.63
0.53330	79.882	27.621	3960.8	108.851	0.79	32.117	21.843	3204.0	40.18	8.10	0.629	24.002	9.08	-3.040	-0.127	0.542	-0.35	-3.040	7.63
0.58874	99.747	27.287	4418.9	116.851	0.79	34.063	21.972	3409.6	42.18	8.10	0.629	24.002	9.08	-3.040	-0.127	0.542	-0.35	-3.040	7.63
0.64384	123.225	26.849	4859.1	124.851	0.79	36.010	21.760	3609.6	44.18	8.10	0.629	24.002	9.08	-3.040	-0.127	0.542	-0.35	-3.040	7.63
0.69862	148.474	26.452	5293.2	132.851	0.79	37.957	21.225	3804.0	46.18	8.10	0.629	24.002	9.08	-3.040	-0.127	0.542	-0.35	-3.040	7.63
0.75307	181.022	25.912	5732.2	140.851	0.79	39.904	20.962	4004.0	48.18	8.10	0.629	24.002	9.08	-3.040	-0.127	0.542	-0.35	-3.040	7.63

0.00453" Ribbed 2.000" Pipe
Residual = 350

Series

PEO

PIPE
SI:
d = 0.308
h = smooth
RIAB:
d = 0.297
h = 0.0045
RA 33.0

RUN 291
DATE 8/2/94
POLY W-301
c wppm 30
IR 1.07

Q (L/A)	Tm (S)	1/√g(S)	Reyd (S)	S (S)	Sf (S)	Tm (RIA)	1/√g(RIA)	Reyd (RIA)	h	S (RIA)	Sf (RIA)	1/√g	Sv (S)	R	IR	P	Δ/hrs	corrected R	corrected S
0.00518	0.105	7.410	118.7	2.86	0.29	0.119	7.540	121.2	1.30	3.05	0.306	13.010	3.10	-0.010	-0.001	0.863	0.00	-0.010	3.10
0.00592	0.120	7.928	127.1	3.69	0.37	0.133	8.110	128.1	1.38	3.79	0.376	14.029	4.00	-0.159	-0.011	0.852	0.00	-0.159	4.00
0.00623	0.165	9.372	149.8	5.10	0.50	0.176	9.792	148.9	1.60	5.24	0.510	15.470	5.26	0.051	0.003	0.856	0.00	0.051	5.26
0.01009	0.200	10.389	165.9	6.39	0.61	0.231	10.490	170.6	1.63	6.55	0.619	17.027	6.55	0.114	0.007	0.859	0.00	0.114	6.55
0.01413	0.300	11.946	202.4	7.92	0.73	0.283	10.129	248.0	2.66	7.62	0.700	18.440	7.71	0.070	0.004	0.848	0.00	0.070	7.71
0.01642	0.478	10.993	256.0	9.36	0.84	0.593	10.658	274.3	2.94	7.88	0.713	19.029	8.17	-0.089	-0.005	0.847	0.00	-0.089	8.17
0.01890	0.686	10.561	306.9	10.50	0.93	0.872	11.175	301.3	3.73	8.63	0.770	19.776	8.80	0.064	0.003	0.854	0.00	0.064	8.80
0.02106	0.773	11.090	326.0	11.39	0.99	0.950	11.263	333.4	3.57	9.40	0.842	20.643	9.53	0.040	0.002	0.850	0.00	0.040	9.53
0.02306	0.835	11.687	339.1	12.31	1.05	1.274	11.820	348.3	3.73	10.65	0.908	21.972	10.60	0.409	0.019	0.869	0.00	0.409	10.60
0.02755	1.002	12.739	371.9	13.66	1.14	1.274	13.000	378.6	4.06	11.39	0.950	23.179	11.60	0.212	0.009	0.861	0.00	0.212	11.60
0.03135	1.126	13.676	395.1	14.83	1.15	1.598	13.870	404.7	4.34	12.07	0.991	24.296	12.56	-0.045	-0.002	0.846	0.00	-0.045	12.56
0.03879	1.383	15.270	438.5	15.96	1.26	2.125	15.521	448.1	4.80	12.82	1.029	25.085	13.21	0.495	-0.019	0.811	0.00	0.495	13.21
0.05002	1.893	16.831	513.4	16.62	1.28	2.832	17.141	523.6	5.61	13.52	1.064	25.869	13.81	-0.499	-0.028	0.813	0.00	-0.499	13.81
0.06891	2.491	18.291	589.3	17.06	1.34	3.302	18.510	604.9	6.48	14.15	1.084	26.541	14.34	-1.328	-0.048	0.779	0.00	-1.328	14.34
0.08831	3.355	19.540	683.6	18.35	1.35	3.789	19.840	693.3	7.49	15.21	1.054	27.628	15.21	-2.109	-0.074	0.739	0.00	-2.109	15.21
0.07731	3.996	20.451	744.1	18.86	1.36	4.428	20.961	754.2	8.08	15.96	1.062	28.457	15.82	-2.862	-0.097	0.710	0.00	-2.862	15.82
0.09175	4.181	20.772	761.0	19.35	1.36	4.723	21.088	778.6	8.34	16.62	1.062	29.394	16.50	-3.472	-0.131	0.598	0.00	-3.472	16.50
0.10885	5.319	21.848	864.8	20.27	1.36	5.901	22.381	890.2	10.61	17.75	1.019	30.812	17.59	-4.840	-0.193	0.598	0.00	-4.840	17.59
0.12837	6.712	22.937	972.1	21.31	1.36	7.514	23.391	990.2	11.58	18.20	0.999	31.792	18.30	-6.131	-0.217	0.544	0.00	-6.131	18.30
0.14543	7.869	24.001	1051.7	22.31	1.36	8.972	24.251	1081.2	12.54	19.35	0.999	32.076	18.39	-6.960	-0.233	0.511	0.00	-6.960	18.39
0.18224	10.830	25.634	1241.1	23.82	1.36	12.872	25.370	1302.6	13.96	20.27	1.029	32.470	18.57	-7.577	-0.247	0.495	0.00	-7.577	18.57
0.20143	12.813	26.050	1350.0	24.11	1.36	15.202	25.804	1415.7	15.17	21.31	1.045	32.839	18.70	-8.114	-0.247	0.495	0.00	-8.114	18.70
0.23207	15.094	27.127	1494.0	24.83	1.34	19.424	26.300	1600.6	17.15	22.59	1.062	33.110	18.80	-8.589	-0.259	0.479	0.00	-8.589	18.80
0.26452	19.276	27.891	1656.7	25.41	1.24	25.144	26.348	1821.6	19.52	23.82	1.062	33.454	18.95	-9.061	-0.271	0.465	0.00	-9.061	18.95
0.30626	24.799	28.655	1879.2	25.96	1.26	33.673	26.532	2108.1	22.59	25.96	1.062	33.781	19.11	-9.670	-0.286	0.449	0.00	-9.670	19.11
0.36501	32.689	29.553	2157.5	26.62	1.28	49.271	25.972	2550.0	27.32	28.62	1.019	34.029	19.26	-10.286	-0.299	0.425	0.00	-10.286	19.26
0.42144	41.709	30.208	2437.1	27.06	1.30	67.283	25.661	2980.0	31.93	31.11	0.999	34.296	19.40	-10.840	-0.311	0.400	0.00	-10.840	19.40
0.45987	46.957	30.999	2585.0	27.75	1.34	83.268	25.116	3314.0	35.51	32.30	0.959	34.541	19.53	-11.414	-0.323	0.379	0.00	-11.414	19.53
0.51475	56.571	31.681	2837.4	28.27	1.36	106.648	24.893	3751.0	40.19	33.52	0.946	34.781	19.66	-12.028	-0.333	0.354	0.00	-12.028	19.66
0.58874	72.643	31.976	3215.6	28.35	1.35	141.442	24.725	4319.7	46.28	34.54	0.936	34.981	19.77	-12.689	-0.341	0.339	0.00	-12.689	19.77
0.64384	85.427	32.247	3483.6	28.48	1.34	171.991	24.521	4758.4	50.98	35.54	0.921	35.110	19.80	-13.301	-0.349	0.324	0.00	-13.301	19.80
0.71681	103.986	32.541	3836.0	28.61	1.34	215.422	24.393	5315.4	56.95	36.54	0.910	35.291	19.91	-13.961	-0.354	0.310	0.00	-13.961	19.91
0.78919	124.597	32.732	4145.6	28.66	1.33	267.300	24.111	5845.7	62.63	37.54	0.895	35.454	20.00	-14.670	-0.358	0.295	0.00	-14.670	20.00

0.00480" Ribbed 0.308" Pipe
 Modulus: 350

PEE
 S1:
 d = 0.308
 h = smooth
 RIAC
 d = 0.297
 h = 0.0045
 N/A 33.0

Series
 PEO

NUM 280
 DATE 8/27/94
 POLY W.301
 c.ripps 100
 IV 1.20

Q(L/A)	Tot(S1)	1/Exp(S1)	S(S1)	SF(S1)	Tv(RIA)	1/Exp(RIA)	Repd(RIA)	Nv	S(RIA)	SF(RIA)	1/Exp	St(S1)	R	RF	P	Δ/mes	connected R	connected S
0.00399	0.090	6.167	99.2	0.60	0.099	6.327	100.4	1.08	6.00	0.605	15.989	6.10	-0.059	-0.004	0.00	0.00	-0.059	6.10
0.00590	0.130	7.556	119.7	0.72	0.146	7.713	121.8	1.31	7.41	0.718	17.767	7.52	-0.036	-0.002	0.00	0.00	-0.036	7.52
0.00771	0.171	8.620	137.4	0.76	0.166	8.929	137.8	1.48	8.02	0.762	18.655	8.24	-0.122	-0.007	0.00	0.00	-0.122	8.24
0.01140	0.256	10.426	168.2	0.82	0.236	9.829	185.3	1.99	8.38	0.808	19.266	8.75	-0.051	-0.003	0.00	0.00	-0.051	8.75
0.01431	0.341	11.354	194.1	0.85	0.382	11.570	197.9	2.12	8.39	0.833	19.771	9.12	0.020	0.001	0.00	0.00	0.020	9.12
0.01610	0.383	12.045	206.2	0.87	0.432	12.233	210.9	2.26	8.49	0.861	20.404	9.58	0.106	0.005	0.00	0.00	0.106	9.58
0.01834	0.470	12.386	228.8	0.89	0.538	12.497	235.5	2.52	8.69	0.875	20.679	9.80	0.091	0.004	0.00	0.00	0.091	9.80
0.01994	0.526	12.729	242.2	0.90	0.597	12.800	248.4	2.66	8.94	0.894	21.159	10.20	0.031	0.001	0.00	0.00	0.031	10.20
0.02163	0.590	13.037	256.9	0.92	0.660	13.300	261.6	2.80	9.05	0.912	21.744	10.66	0.176	0.008	0.00	0.00	0.176	10.66
0.02397	0.731	14.056	286.5	0.96	0.825	14.300	293.0	3.14	11.55	0.992	22.638	11.33	0.549	0.024	0.00	0.00	0.549	11.33
0.02680	0.885	14.667	315.5	0.96	0.993	14.940	321.8	3.45	11.91	1.005	23.605	12.14	-0.006	-0.000	0.00	0.00	-0.006	12.14
0.02982	1.169	15.766	363.2	1.00	1.333	15.930	373.4	4.01	12.64	1.039	24.806	13.09	0.000	0.000	0.00	0.00	0.000	13.09
0.03390	1.737	17.370	445.6	1.05	2.008	17.331	459.7	4.91	12.81	1.049	25.517	14.08	-0.307	-0.012	0.00	0.00	-0.307	14.08
0.03916	2.162	18.310	494.7	1.05	2.455	18.543	507.4	5.44	13.05	1.087	26.072	14.08	-0.576	-0.022	0.00	0.00	-0.576	14.08
0.04376	2.401	19.050	521.2	1.14	2.747	19.215	538.8	5.75	13.82	1.087	27.611	15.24	-1.068	-0.039	0.00	0.00	-1.068	15.24
0.07085	2.795	19.620	562.4	1.16	3.197	19.791	579.2	6.20	14.48	1.096	28.550	15.97	-1.701	-0.060	0.00	0.00	-1.701	15.97
0.08121	3.464	20.200	626.9	1.25	3.912	20.310	641.4	6.87	14.84	1.126	29.842	16.96	-2.494	-0.084	0.00	0.00	-2.494	16.96
0.08578	3.771	20.450	644.7	1.25	4.256	20.700	693.3	7.06	14.84	1.126	29.842	16.96	-2.965	-0.096	0.00	0.00	-2.965	16.96
0.09101	4.053	20.928	675.2	1.33	4.602	21.190	742.9	7.96	15.59	1.214	31.707	18.42	-3.372	-0.106	0.00	0.00	-3.372	18.42
0.10028	4.619	21.600	725.8	1.38	5.221	21.920	742.9	7.96	15.59	1.214	31.707	18.42	-4.151	-0.127	0.00	0.00	-4.151	18.42
0.12046	6.123	23.437	904.7	1.44	6.732	23.187	844.3	9.05	16.67	1.340	33.531	19.70	-4.540	-0.136	0.00	0.00	-4.540	19.70
0.16300	8.484	24.501	1044.3	1.44	10.776	24.800	1071.7	11.48	17.59	1.448	34.488	20.57	-6.064	-0.176	0.00	0.00	-6.064	20.57
0.19558	10.709	25.234	1110.2	1.44	12.491	25.210	1154.3	12.37	18.01	1.480	35.341	21.29	-7.337	-0.207	0.00	0.00	-7.337	21.29
0.19568	12.359	25.766	1193.0	1.16	14.694	25.496	1252.3	13.42	18.01	1.480	35.341	21.29	-8.383	-0.231	0.00	0.00	-8.383	21.29
0.25308	18.601	27.163	1464.0	1.40	22.678	26.543	1556.2	16.67	19.84	1.526	36.233	21.95	-10.668	-0.276	0.00	0.00	-10.668	21.95
0.28927	22.948	27.952	1626.5	1.51	26.955	26.849	1758.9	18.84	20.67	1.547	37.107	22.79	-12.494	-0.296	0.00	0.00	-12.494	22.79
0.34613	30.394	29.062	1872.3	1.29	31.959	27.348	2066.7	22.14	21.48	1.579	38.000	23.62	-14.840	-0.337	0.00	0.00	-14.840	23.62
0.40257	38.569	30.013	2109.3	1.33	35.456	27.767	2368.2	25.37	22.14	1.599	38.944	24.48	-17.000	-0.372	0.00	0.00	-17.000	24.48
0.45887	47.944	30.670	2352.0	1.38	41.784	28.428	2956.4	28.33	23.35	1.622	39.844	25.37	-19.700	-0.415	0.00	0.00	-19.700	25.37
0.51475	57.222	31.499	2568.7	1.40	47.805	28.800	3233.5	34.64	24.48	1.646	40.744	26.29	-22.494	-0.454	0.00	0.00	-22.494	26.29
0.57029	67.578	32.113	2791.8	1.41	54.000	29.100	3533.8	35.61	25.37	1.667	41.644	27.29	-25.494	-0.494	0.00	0.00	-25.494	27.29
0.58874	71.210	32.295	2864.6	1.41	60.364	28.424	3798.2	40.69	26.29	1.688	42.544	28.29	-28.494	-0.534	0.00	0.00	-28.494	28.29
0.66214	85.560	33.137	3136.6	1.44	67.000	28.800	4069.6	45.64	27.29	1.709	43.444	29.29	-31.494	-0.574	0.00	0.00	-31.494	29.29
0.73496	101.795	33.721	3414.0	1.46	74.000	28.072	4259.7	45.64	28.29	1.729	44.344	30.29	-34.494	-0.614	0.00	0.00	-34.494	30.29
0.86719	119.280	34.215	3661.5	1.47	81.000	27.850	4672.6	50.06	29.29	1.749	45.244	31.29	-37.494	-0.654	0.00	0.00	-37.494	31.29

PIPE: 7.82 mm

RIBLETS: 0.15 mm

POLYMERS:

NONE (Solvent)

PEO N-750

N60K

W-301

P-309

PAM N-300

0.0060" Riblets/0.308" Pipe
ReaderIt= 350

Series	Q (L/s)	Tw(S1)	1/Spd(S1)	ReSpd(S1)	S'(S1)	SF(S1)	Tw(R1B)	1/Spd(K1B)	ReSpd(R1B)	h*	S'(R1B)	SF(R1)	K'	RF	P
RUN 216	0.07533	6.66	11.850	1184.4	-0.04	0.00	9.80	12.351	1198.5	17.32	0.10	0.01	0.44	0.037	0.841
DATE 7/2/93	0.08264	10.15	12.009	1266.7	-0.03	0.00	11.67	12.415	1310.4	18.97	0.08	0.01	0.35	0.029	0.837
POLY -	0.09302	12.47	12.195	1427.1	-0.02	0.00	14.84	12.390	1479.1	21.42	-0.02	0.00	0.11	0.009	0.799
smooth	0.09625	13.27	12.229	1476.8	-0.05	0.00	15.98	12.357	1538.9	22.26	-0.06	-0.01	0.01	0.001	0.790
IR 1.000	0.10587	15.56	12.425	1599.0	0.01	0.00	19.08	12.439	1681.7	24.36	0.01	0.00	-0.06	-0.006	0.776
	0.10935	16.46	12.476	1644.7	0.01	0.00	20.36	12.437	1737.2	25.16	0.01	0.00	-0.12	-0.010	0.769
	0.12198	19.70	12.721	1799.3	0.10	0.01	25.23	12.463	1933.8	28.00	0.06	0.00	-0.28	-0.022	0.743
	0.12829	21.78	12.726	1889.5	0.02	0.00	28.15	12.409	2040.1	29.54	0.02	0.00	-0.43	-0.033	0.736
	0.12829	21.77	12.727	1891.1	0.02	0.00	28.02	12.437	2037.9	29.51	0.05	0.00	-0.40	-0.031	0.739
	0.13019	22.38	12.738	1916.7	0.01	0.00	29.19	12.367	2078.7	30.10	-0.01	0.00	-0.50	-0.039	0.730
	0.14181	26.01	12.872	2064.9	0.01	0.00	34.95	12.309	2273.5	32.92	-0.03	0.00	-0.72	-0.055	0.708
	0.14759	28.05	12.900	2146.3	-0.03	0.00	37.78	12.322	2366.0	34.26	0.00	0.00	-0.77	-0.059	0.706
	0.15653	30.66	13.086	2243.6	0.08	0.01	42.23	12.360	2501.2	36.22	0.06	0.01	-0.83	-0.063	0.691
	0.15723	30.84	13.105	2248.9	0.10	0.01	43.17	12.280	2528.9	36.59	-0.01	0.00	-0.93	-0.070	0.680
	0.16493	33.71	13.150	2352.9	0.06	0.00	47.66	12.260	2657.4	38.48	0.07	0.01	-1.04	-0.078	0.673
	0.18992	43.57	13.319	2672.9	0.01	0.00	62.87	12.292	3049.4	44.16	0.01	0.00	-1.24	-0.092	0.659
	0.20335	49.61	13.365	2854.3	-0.06	0.00	73.14	12.203	3291.5	47.66	0.00	0.00	-1.47	-0.107	0.645
	0.21102	52.72	13.453	2940.7	-0.02	0.00	79.56	12.140	3493.1	49.68	-0.06	0.00	-1.64	-0.116	0.630
	0.22442	58.98	13.530	3111.4	-0.04	0.00	89.05	12.204	3631.8	52.59	0.01	0.00	-1.74	-0.126	0.612
	0.23016	60.79	13.665	3157.8	0.07	0.00	94.55	12.147	3740.1	54.16	-0.05	0.00	-1.86	-0.132	0.614
	0.24354	67.25	13.747	3322.5	0.06	0.00	104.64	12.217	3936.4	57.00	0.01	0.00	-1.76	-0.126	0.611
	0.25262	76.73	13.878	3548.3	0.08	0.01	122.31	12.186	4254.8	61.61	0.03	0.00	-1.93	-0.137	0.597
	0.26262	78.16	13.751	3581.6	-0.07	0.00	121.14	12.245	4235.0	61.32	0.03	0.00	-1.86	-0.132	0.614
	0.28166	88.13	13.889	3802.8	-0.03	0.00	139.91	12.220	4550.8	65.90	0.02	0.00	-2.01	-0.141	0.590
	0.30067	98.13	14.050	4013.4	0.04	0.00	157.08	12.311	4822.7	69.83	0.04	0.00	-2.02	-0.141	0.594
	0.31015	102.78	14.162	4106.8	0.11	0.01	168.04	12.279	4987.3	72.22	-0.01	0.00	-2.11	-0.147	0.582
	0.34046	123.32	14.192	4498.6	-0.02	0.00	200.76	12.331	5451.6	78.94	-0.01	0.00	-2.22	-0.152	0.562
	0.37821	146.91	14.372	4911.4	0.01	0.00	239.99	12.466	5961.9	86.33	0.05	0.00	-2.24	-0.152	0.582
	0.41393	173.72	14.533	5341.1	0.03	0.00	243.90	12.428	6099.0	87.01	0.00	0.00	-2.29	-0.155	0.579
	0.41581	175.54	14.528	5368.8	0.01	0.00	286.72	12.548	6517.0	94.37	0.04	0.00	-2.31	-0.165	0.576
	0.45140	203.76	14.638	5783.5	-0.01	0.00	290.58	12.518	6560.4	94.99	0.00	0.00	-2.35	-0.158	0.575
	0.52588	266.81	14.909	6816.4	0.03	0.00	337.28	12.613	7067.1	102.33	0.01	0.00	-2.38	-0.159	0.575
	0.52588	266.43	14.914	6816.9	0.03	0.00	444.24	12.804	8111.5	117.46	0.01	0.00	-2.43	-0.160	0.571
	0.56291	302.57	14.980	7045.7	-0.01	0.00	441.74	12.840	8092.0	117.17	0.05	0.00	-2.39	-0.157	0.574
	0.63652	375.81	15.203	7843.4	0.03	0.00	500.71	12.910	8608.3	124.77	0.01	0.00	-2.43	-0.158	0.575
	0.63652	374.90	15.218	7851.2	0.04	0.00	620.97	13.108	9578.1	138.9	0.02	0.00	-2.42	-0.156	0.575
	0.01041	0.20	10.906	178.2	0.00	0.00	618.95	13.129	9581.3	138.74	0.04	0.00	-2.40	-0.154	0.576
RUN 216	0.01041	0.20	10.906	178.2	0.00	0.00	0.24	10.938	187.0	2.71	0.00	0.00	0.779	0.037	0.841
DATE 7/4/93	0.01265	0.26	11.559	204.0	0.35	0.00	0.24	11.025	225.8	3.27	0.00	0.00	0.701	0.029	0.837
POLY -	0.01618	0.59	9.749	310.0	0.68	0.00	0.68	10.043	316.9	4.59	0.00	0.00	0.821	0.009	0.799
smooth	0.02079	0.93	9.973	390.5	0.01	0.00	1.11	10.149	404.0	5.85	0.04	0.00	0.612	0.012	0.802
IR 1.000	0.02009	1.11	10.136	427.1	0.01	0.00	1.33	10.267	443.9	6.43	-0.03	0.00	0.08	0.008	0.794
	0.02815	1.57	10.382	508.7	-0.04	0.00	1.86	10.591	525.1	7.80	-0.05	0.00	0.11	0.011	0.805
	0.03247	2.02	10.575	576.6	-0.07	-0.01	2.38	10.841	592.2	8.58	-0.06	-0.01	0.15	0.014	0.813
	0.03963	2.91	10.818	691.7	-0.14	-0.01	3.32	11.226	701.8	10.16	-0.05	0.00	0.24	0.022	0.833
	0.04977	4.24	11.185	835.9	-0.10	-0.01	4.32	11.631	846.4	12.26	-0.05	0.00	0.32	0.028	0.837
	0.06054	5.89	11.543	985.9	-0.03	0.00	6.74	11.968	1001.2	14.50	-0.03	0.00	0.35	0.030	0.832
	0.06858	6.95	11.692	1070.1	-0.03	0.00	7.98	12.099	1088.9	15.77	-0.03	0.00	0.37	0.032	0.829
	0.07229	8.00	11.829	1145.5	-0.01	0.00	9.24	12.207	1168.8	16.92	-0.01	0.00	0.34	0.028	0.824
	0.07968	9.42	12.018	1234.8	0.05	0.00	11.07	12.293	1271.0	18.40	-0.02	0.00	0.28	0.023	0.810

0.36501	141.57	14.200	4867.6	-0.15	-0.01	230.46	12.338	5998.4	85.41	-0.07	-0.01	-2.34	-0.160	0.594
0.38386	154.02	14.317	5077.8	-0.11	-0.01	253.09	12.392	6182.0	89.52	-0.07	-0.01	-2.38	-0.161	0.579
0.45887	211.15	14.617	5947.7	-0.08	-0.01	348.41	12.815	7256.3	105.07	-0.02	0.00	-2.43	-0.161	0.677
0.47753	225.70	14.713	6148.5	-0.04	0.00	373.56	12.878	7512.7	108.78	-0.01	0.00	-2.42	-0.161	0.575
0.52588	267.77	14.876	6700.2	-0.03	0.00	446.40	12.772	8216.5	118.97	-0.05	0.00	-2.49	-0.163	0.571
0.53330	274.39	14.902	6782.0	-0.02	0.00	456.46	12.809	8307.9	120.30	-0.03	0.00	-2.47	-0.162	0.572
0.55182	292.86	14.926	7008.4	-0.06	0.00	484.16	12.869	8536.4	123.93	-0.02	0.00	-2.46	-0.161	0.575
0.55182	291.79	14.953	6992.8	-0.03	0.00	483.14	12.883	8546.0	123.75	0.00	0.00	-2.44	-0.159	0.575
0.60714	346.36	15.101	7547.0	-0.01	0.00	574.35	13.001	9230.2	133.65	-0.02	0.00	-2.46	-0.159	0.574
0.62551	364.95	15.156	7826.4	-0.02	0.00	566.97	13.084	9260.5	134.09	0.06	0.00	-2.38	-0.154	0.580
0.64384	383.39	15.221	7989.4	0.01	0.00	607.42	13.024	9599.7	138.86	-0.07	-0.01	-2.50	-0.161	0.572
0.66305	405.93	15.233	8240.8	-0.03	0.00	658.72	13.157	10045.7	145.46	-0.03	0.00	-2.45	-0.157	0.577
0.68040	421.44	15.341	8410.8	0.04	0.00	691.09	13.281	10229.4	148.12	0.06	0.00	-2.36	-0.151	0.580
0.69862	444.66	15.335	8636.0	-0.01	0.00	731.80	13.252	10522.2	152.36	-0.03	0.00	-2.44	-0.155	0.578
0.71681	464.76	15.391	8833.2	0.01	0.00	764.00	13.308	10756.4	155.75	-0.02	0.00	-2.42	-0.154	0.579
0.71681	459.34	15.481	8784.6	0.11	0.01	756.87	13.370	10709.7	155.08	0.05	0.00	-2.35	-0.149	0.577
0.73496	485.21	15.444	9029.8	0.02	0.00	797.52	13.355	10995.0	159.21	-0.02	0.00	-2.41	-0.153	0.579
0.00365	0.07	6.486	104.4			0.08	6.506	109.0	1.59					0.779
0.00498	0.09	7.547	122.4			0.11	7.597	128.0	1.85					0.784
0.00657	0.12	8.600	133.9			0.15	8.787	146.5	2.12					0.772
0.00788	0.14	9.610	152.7			0.18	9.632	160.4	2.32					0.776
0.00918	0.17	10.391	184.7			0.21	10.234	176.1	2.55					0.751
0.01049	0.20	10.920	179.4			0.24	10.974	188.0	2.72					0.782
0.01169	0.23	11.408	191.6			0.27	11.506	200.0	2.90					0.787
0.01277	0.27	11.422	209.2			0.37	10.785	233.3	3.38					0.690
0.01394	0.37	10.540	247.8			0.51	10.036	274.0	3.97					0.702
0.01584	0.54	9.949	298.5			0.67	9.965	313.8	4.54					0.776
0.01773	0.70	9.842	336.4			0.85	9.848	356.0	5.16					0.775
0.01989	0.85	10.015	375.2			1.03	10.088	392.2	5.68					0.785
0.02309	1.11	10.145	428.2	0.12	0.01	1.32	10.320	443.2	6.42	0.03	0.00	0.13	0.013	0.801
0.02491	1.27	10.239	456.5	-0.01	0.00	1.51	10.420	474.3	6.87	-0.01	0.00	0.12	0.011	0.802
0.02798	1.56	10.385	507.8	-0.04	0.00	1.85	10.568	525.4	7.61	-0.07	-0.01	0.09	0.008	0.802
0.03163	1.92	10.575	584.2	-0.03	0.00	2.24	10.838	579.7	8.39	-0.01	0.00	0.19	0.017	0.813
0.03477	2.27	10.691	613.7	-0.06	-0.01	2.62	11.028	626.4	9.07	0.01	0.00	0.24	0.022	0.824
0.03915	2.78	10.373	678.9	-0.06	-0.01	3.20	11.233	692.9	10.03	-0.01	0.00	0.27	0.025	0.826
0.04225	3.18	10.973	727.3	-0.07	-0.01	3.63	11.377	738.6	10.69	-0.01	0.00	0.30	0.027	0.832
0.04627	3.56	11.100	770.7	-0.05	0.00	4.07	11.523	781.7	11.32	0.01	0.00	0.35	0.031	0.834
0.05285	4.67	11.322	882.7	-0.06	-0.01	4.53	11.595	825.5	11.95	-0.03	0.00	0.33	0.029	0.836
0.05862	5.29	11.434	939.9	-0.06	-0.01	5.30	11.775	893.6	12.94	-0.01	0.00	0.37	0.032	0.837
0.05983	5.79	11.512	982.9	-0.06	-0.01	6.00	11.902	950.7	13.77	0.00	0.00	0.39	0.034	0.839
0.05451	6.59	11.629	1047.1	-0.05	0.00	7.45	12.130	1057.0	15.30	0.05	0.00	0.43	0.037	0.842
0.06810	7.23	11.725	1098.8	-0.04	0.00	8.26	12.156	1115.8	16.16	0.00	0.00	0.37	0.031	0.832
0.07086	7.74	11.791	1136.5	-0.03	0.00	8.90	12.186	1157.8	16.77	-0.02	0.00	0.33	0.028	0.827
0.07368	8.27	11.859	1172.0	-0.02	0.00	9.54	12.243	1195.3	17.31	0.00	0.00	0.33	0.028	0.825
0.07731	9.00	11.929	1223.8	-0.02	0.00	10.51	12.239	1255.9	18.19	-0.06	0.00	0.24	0.020	0.815
0.08326	10.21	12.064	1296.2	0.01	0.00	12.09	12.289	1339.8	19.40	-0.06	-0.01	0.18	0.015	0.803
0.08495	10.62	12.070	1312.3	0.00	0.00	12.66	12.255	1360.9	19.71	-0.11	-0.01	0.12	0.010	0.798

RUN 217
DATE 7/8/93
POLY -
e wppm
in 1.000

0.0000' RH(B)@0.300' Pipes
Resident = 350

Series

DW

PIPE
S1:
d = 0.300
h = smooth
R1E:
d = 0.293
h = 0.0060
RA 24.4

RUN 221
DATE 7/14/93
POLY -
c 1.000
w

Q (US)	T (S)	1/√g(S)	Resd(S)	S (S)	Sf (S)	T (R)	1/√g(R)	Resd(R)	M	S (R)	Sf (R)	F	W	P
0.00980	0.18	10.553	171.9			0.23	10.393	183.1	2.65					0.756
0.01166	0.23	11.314	191.0			0.28	11.207	202.4	2.93					0.764
0.01285	0.30	10.857	219.6			0.37	10.745	237.8	3.37					0.763
0.01518	0.51	9.834	286.7			0.58	10.125	292.2	4.23					0.826
0.01833	0.74	9.892	344.7			0.86	10.058	355.7	5.15					0.805
0.02298	1.11	10.095	423.9	-0.01	0.00	1.29	10.297	436.0	6.31	0.19	0.02	0.25	0.028	0.811
0.02567	1.34	10.260	466.3	-0.01	0.00	1.59	10.444	480.7	6.96	-0.01	0.00	0.12	0.011	0.807
0.03117	1.88	10.536	552.1	-0.03	0.00	2.16	10.806	564.8	8.18	0.01	0.00	0.20	0.019	0.820
0.03589	2.42	10.706	628.1	-0.09	-0.01	2.76	11.045	638.9	9.25	-0.02	0.00	0.22	0.021	0.829
0.04366	3.37	11.007	741.5	-0.07	-0.01	3.79	11.439	746.7	10.84	0.00	0.00	0.34	0.031	0.841
0.04973	4.98	11.359	901.3	-0.06	-0.01	5.53	11.861	905.7	13.11	0.05	0.00	0.43	0.038	0.850
0.06669	6.98	11.683	1088.4	-0.03	0.00	7.78	12.186	1074.7	15.56	0.08	0.01	0.46	0.039	0.848
0.07297	8.18	11.809	1156.3	-0.04	0.00	9.18	12.275	1167.2	16.90	0.06	0.00	0.41	0.034	0.842
0.07925	9.41	11.959	1237.6	-0.01	0.00	10.68	12.360	1256.5	18.19	0.06	0.00	0.36	0.030	0.832
0.07953	9.49	11.947	1245.5	-0.03	0.00	10.79	12.337	1265.6	18.33	0.03	0.00	0.33	0.027	0.831
0.08888	11.48	12.146	1366.4	0.00	0.00	13.30	12.424	1401.7	20.30	0.04	0.00	0.24	0.019	0.815
0.09447	12.82	12.214	1449.8	-0.03	0.00	14.92	12.466	1490.6	21.58	0.06	0.00	0.17	0.014	0.811
0.10138	14.53	12.309	1549.5	-0.05	0.00	17.20	12.458	1606.4	23.26	0.03	0.00	0.03	0.003	0.798
0.10393	15.07	12.392	1579.2	0.00	0.00	18.33	12.468	1659.8	24.03	0.04	0.00	-0.01	-0.001	0.789
0.10942	16.45	12.488	1649.8	0.02	0.00	20.20	12.511	1742.0	25.22	0.08	0.01	-0.05	-0.004	0.782
0.12029	21.88	12.695	1900.2	-0.02	0.00	27.89	12.381	2044.5	29.60	-0.01	0.00	-0.46	-0.036	0.741
0.13155	22.65	12.794	1936.5	0.05	0.00	30.16	12.356	2129.4	30.89	-0.01	0.00	-0.56	-0.043	0.727
0.14181	25.91	12.897	2087.7	0.03	0.00	34.85	12.243	2283.5	33.09	-0.10	-0.01	-0.79	-0.061	0.702
0.15635	30.52	13.100	2288.1	0.09	0.01	42.73	12.191	2534.9	36.71	-0.10	-0.01	-1.03	-0.078	0.675
0.15915	31.73	13.080	2288.5	0.04	0.00	43.82	12.254	2563.2	37.12	-0.03	0.00	-0.96	-0.074	0.684
0.17647	37.85	13.278	2499.8	0.09	0.01	54.49	12.185	2858.3	41.39	-0.06	0.00	-1.24	-0.092	0.656
0.19376	45.04	13.364	2727.4	0.02	0.00	66.25	12.133	3152.1	45.64	-0.08	-0.01	-1.46	-0.107	0.642
0.23207	61.71	13.675	3192.6	0.06	0.00	94.31	12.180	3761.3	54.46	-0.02	0.00	-1.72	-0.129	0.618
0.25117	71.13	13.786	3427.7	0.05	0.00	109.74	12.221	4057.4	58.75	0.01	0.00	-1.81	-0.129	0.612
0.28927	90.99	14.037	3873.4	0.08	0.01	144.18	12.279	4651.3	67.35	0.03	0.00	-1.99	-0.146	0.596
0.32721	113.09	14.243	4323.4	0.10	0.01	182.05	12.361	5227.5	75.69	0.05	0.00	-2.11	-0.146	0.587
0.36501	137.49	14.410	4767.7	0.12	0.01	224.15	12.426	5801.5	84.01	0.03	0.00	-2.23	-0.152	0.579
0.42144	177.32	14.650	5415.1	0.12	0.01	292.08	12.569	6623.3	95.91	0.04	0.00	-2.32	-0.156	0.573
0.48616	237.02	14.918	6262.6	0.13	0.01	393.47	12.749	7698.6	111.35	0.03	0.00	-2.39	-0.138	0.569
0.57029	304.06	15.139	7094.8	0.14	0.01	503.63	12.950	8703.3	126.02	0.04	0.00	-2.41	-0.137	0.570
0.62551	358.86	15.295	7703.6	0.14	0.01	593.42	13.088	9440.8	136.70	0.03	0.00	-2.41	-0.156	0.571
0.00606	0.11	8.499	133.0			0.14	8.453	140.8	2.04					0.771
0.00785	0.14	9.598	152.6			0.18	9.494	162.5	2.35					0.762
0.01017	0.19	10.781	176.5			0.26	10.337	193.8	2.81					0.716
0.01261	0.25	11.641	202.8			0.43	9.838	252.7	3.66					0.556
0.01532	0.52	9.848	291.8			0.62	10.007	302.4	4.38					0.804
0.01971	0.83	10.001	370.3			1.00	10.111	385.6	5.58	0.09	0.01	0.17	0.017	0.796
0.02440	1.23	10.192	450.4	-0.02	0.00	1.43	10.468	461.7	6.69	0.09	0.01	0.21	0.021	0.822
0.02715	1.48	10.345	494.1	-0.03	0.00	1.71	10.652	505.2	7.31	0.09	0.01	0.24	0.023	0.826
0.03261	2.03	10.602	580.2	-0.05	0.00	2.34	10.952	591.4	8.56	0.06	0.01	0.26	0.025	0.831
0.03737	2.57	10.786	653.1	-0.07	-0.01	2.92	11.215	661.4	9.58	0.03	0.01	0.33	0.031	0.842
0.04591	3.70	11.056	782.8	-0.12	-0.01	4.16	11.558	788.4	11.42	0.03	0.00	0.37	0.033	0.851
0.05744	3.70	11.068	782.8	-0.11	-0.01	4.16	11.567	789.3	11.43	0.04	0.00	0.38	0.034	0.851
0.05744	5.42	11.425	949.8	-0.09	-0.01	5.94	12.092	944.9	13.68	0.20	0.02	0.59	0.051	0.873
0.06986	7.58	11.748	1122.9	-0.05	0.00	6.54	12.269	1130.0	16.39	0.09	0.01	0.45	0.038	0.850
0.07681	8.96	11.878	1219.4	-0.07	-0.01	10.20	12.343	1235.6	17.89	0.06	0.00	0.38	0.031	0.841
0.08333	10.27	12.034	1300.9	-0.03	0.00	11.84	12.430	1328.1	19.23	0.08	0.01	0.34	0.028	0.831
0.08595	10.49	12.283	1322.7	0.20	0.02	12.52	12.465	1372.4	19.87	0.10	0.01	0.31	0.026	0.802
0.09108	11.77	12.288	1405.9	0.10	0.01	14.07	12.460	1459.8	21.14	0.06	0.00	0.20	0.017	0.801
0.09628	12.90	12.410	1455.0	0.16	0.01	15.76	12.448	1527.3	22.12	0.03	0.00	0.11	0.009	0.784
0.10563	15.32	12.493	1593.5	0.08	0.01	18.86	12.480	1679.6	24.32	0.05	0.00	-0.02	-0.002	0.777
0.11358	17.25	12.659	1694.3	0.14	0.01	21.89	12.456	1813.0	26.25	0.01	0.00	-0.18	-0.014	0.754
0.13048	21.93	12.897	1913.1	0.17	0.01	28.88	12.459	2085.3	30.19	0.08	0.01	-0.42	-0.032	0.727
0.13602	24.24	12.788	1995.1	-0.01	0.00	31.43	12.450	2157.7	31.24	0.09	0.01	-0.49	-0.038	0.738
0.15530	30.54	13.010	2299.1	0.01	0.00	42.02	12.294	2494.7	36.12	0.00	0.00	-0.89	-0.068	0.696
0.17455	37.66	13.167	2488.4	-0.02	0.00	54.21	12.166	2833.3	41.03	-0.08	-0.01	-1.24	-0.093	0.665
0.19184	44.38	13.330	2698.7	0.01	0.00	64.73	12.236	3095.5	44.82	0.02	0.00	-1.44	-0.098	0.656
0.20910	51.51	13.495	2907.0	0.03	0.00	76.54	12.266	3365.3	48.73	0.06	0.01	-1.44	-0.105	0.644

RUN 223
DATE 7/17/93
POLY -
c 1.000
w

0.24736	69.30	13.755	3371.1	0.04	0.00	106.14	12.207	3999.6	57.91	0.00	0.00	-1.80	-0.129	0.614
0.20166	86.72	14.001	3770.2	0.10	0.01	137.45	12.329	4509.1	65.28	0.05	0.01	-1.89	-0.133	0.604
0.33857	120.69	14.266	4447.3	0.17	0.01	194.55	12.452	5362.7	77.65	0.13	0.01	-2.06	-0.142	0.594
0.31744	144.39	14.425	4863.8	0.08	0.00	295.32	12.526	5997.3	85.39	0.12	0.01	-2.16	-0.147	0.588
0.43081	185.96	14.624	5519.5	0.06	0.00	394.33	12.673	6706.2	97.11	0.13	0.01	-2.23	-0.150	0.585
0.48685	223.17	14.886	6105.7	0.14	0.01	391.01	12.800	7477.1	108.27	0.12	0.01	-2.29	-0.152	0.576
0.54256	278.75	15.043	6747.8	0.13	0.01	460.60	12.974	8239.1	119.74	0.15	0.01	-2.29	-0.150	0.579
0.63468	369.47	15.285	7781.3	0.12	0.01	608.50	13.204	9484.3	137.33	0.13	0.01	-2.30	-0.149	0.581
0.00947	0.18	10.432	168.1	0.04	0.00	0.21	10.539	174.9	2.53	0.00	0.00	0.95	0.026	0.828
0.01136	0.22	11.184	188.6	0.07	0.00	0.28	11.046	200.8	2.91	0.00	0.00	0.31	0.026	0.828
0.01482	0.40	10.790	255.1	0.06	0.00	0.56	10.123	265.9	4.14	0.00	0.00	0.30	0.025	0.828
0.01793	0.71	9.851	338.5	0.03	0.00	0.83	10.050	348.9	5.05	0.00	0.00	0.30	0.025	0.828
0.02298	1.10	10.176	422.6	0.02	0.00	1.30	10.314	435.4	6.30	0.08	0.01	0.18	0.018	0.811
0.02584	1.34	10.318	466.5	0.05	0.00	1.59	10.498	482.2	6.98	0.04	0.00	0.16	0.016	0.805
0.03054	1.82	10.492	542.5	0.04	0.00	2.10	10.795	554.9	8.04	0.03	0.00	0.21	0.020	0.823
0.03493	2.28	10.709	608.4	-0.03	0.00	2.62	11.041	620.4	8.98	0.04	0.00	0.27	0.025	0.828
0.03997	2.88	10.909	683.9	-0.03	0.00	3.29	11.277	695.6	10.07	0.02	0.00	0.31	0.028	0.833
0.04373	3.36	11.048	738.5	-0.02	0.00	3.83	11.441	749.9	10.86	0.00	0.00	0.34	0.031	0.835
0.04996	4.21	11.247	828.6	-0.03	0.00	4.78	11.673	839.5	12.16	0.01	0.00	0.38	0.033	0.839
0.05916	5.70	11.473	962.2	-0.06	-0.01	6.42	11.950	971.4	14.07	0.01	0.00	0.40	0.035	0.845
0.06738	7.10	11.706	1075.9	-0.02	0.00	8.16	12.070	1097.1	15.89	-0.07	-0.01	0.31	0.026	0.828
0.07395	8.36	11.838	1166.4	-0.03	0.00	9.62	12.201	1189.9	17.23	0.00	0.00	0.30	0.025	0.828
0.07833	9.32	11.879	1217.8	-0.06	-0.01	10.76	12.273	1244.4	18.02	-0.07	-0.01	0.24	0.020	0.825
0.08054	9.54	12.070	1246.8	0.09	0.01	11.37	12.249	1291.7	18.70	-0.07	-0.01	0.20	0.017	0.802
0.08830	11.21	12.208	1345.5	0.09	0.01	13.41	12.343	1399.2	20.26	-0.04	0.00	0.16	0.013	0.796
0.09636	13.18	12.288	1470.9	0.02	0.00	15.82	12.397	1533.0	22.20	-0.02	0.00	0.06	0.004	0.793
0.10365	15.03	12.378	1562.5	-0.02	0.00	18.21	12.432	1635.9	23.69	0.00	0.00	-0.02	-0.002	0.786
0.11359	17.65	12.509	1707.2	-0.02	0.00	21.84	12.431	1806.3	26.16	0.01	0.00	-0.20	-0.016	0.769
0.12430	20.81	12.613	1839.4	-0.05	0.00	26.15	12.440	1961.0	28.40	0.04	0.00	-0.33	-0.028	0.758
0.14165	26.38	12.767	2070.7	-0.10	-0.01	34.92	12.268	2265.8	32.81	-0.07	0.01	-0.75	-0.058	0.719
0.16663	34.75	13.086	2376.4	-0.02	0.00	48.44	12.253	2688.4	38.64	-0.02	0.00	-1.05	-0.079	0.683
0.18389	41.78	13.169	2605.7	-0.03	0.00	59.74	12.177	2963.2	42.91	-0.06	0.00	-1.31	-0.097	0.666
0.20111	48.53	13.364	2807.9	-0.09	-0.01	71.47	12.175	3240.9	46.93	-0.03	0.00	-1.47	-0.108	0.647
0.22783	60.40	13.571	3132.2	-0.01	0.00	91.44	12.184	3665.2	53.07	0.00	0.00	-1.66	-0.120	0.629
0.24686	69.91	13.668	3388.6	-0.04	0.00	107.13	12.207	3965.8	57.43	0.00	0.00	-1.79	-0.128	0.621
0.29048	92.28	13.998	3869.3	0.05	0.00	147.19	12.254	4647.5	67.30	0.01	0.00	-2.01	-0.141	0.598
0.33576	119.95	14.192	4410.0	0.01	0.00	194.32	12.327	5338.3	77.30	0.00	0.00	-2.18	-0.150	0.588
0.37330	145.04	14.349	4847.9	0.01	0.00	237.31	12.402	5987.7	85.40	0.00	0.00	-2.28	-0.155	0.582
0.44787	200.09	14.657	5692.7	0.04	0.00	332.15	12.577	6975.5	101.01	-0.01	0.00	-2.40	-0.160	0.574
0.54013	280.41	14.932	6733.6	0.02	0.00	466.04	12.805	8256.0	119.55	-0.02	0.00	-2.46	-0.161	0.573
0.63132	370.12	15.191	7718.5	0.04	0.00	617.30	13.005	9480.1	137.27	-0.06	0.00	-2.50	-0.161	0.571
0.00867	0.16	10.025	159.3	0.11	0.01	0.20	10.078	165.9	2.42	0.02	0.02	0.30	0.030	0.816
0.01083	0.20	11.089	180.1	0.02	0.00	0.25	11.119	189.2	2.74	0.01	0.01	0.26	0.025	0.822
0.01340	0.29	11.559	214.1	0.01	0.00	0.53	9.457	275.5	3.99	0.01	0.01	0.31	0.029	0.830
0.01659	0.61	9.860	313.0	0.72	0.10	0.72	10.106	321.6	4.66	0.21	0.02	0.30	0.030	0.816
0.02091	0.93	10.050	385.1	0.11	0.01	1.09	10.287	396.1	5.74	0.21	0.02	0.26	0.025	0.822
0.02380	1.17	10.169	433.6	0.02	0.00	1.37	10.447	444.3	6.43	0.15	0.01	0.26	0.025	0.822
0.02890	1.64	10.448	512.7	0.01	0.00	1.89	10.783	523.1	7.57	0.15	0.01	0.31	0.029	0.830
0.03287	2.06	10.608	574.7	-0.03	0.00	2.35	11.013	582.8	8.44	0.15	0.01	0.35	0.033	0.840
0.03764	2.61	10.794	646.9	-0.05	0.00	2.96	11.232	654.5	9.48	0.11	0.01	0.37	0.034	0.844
0.04061	2.97	10.913	690.4	-0.04	0.00	3.34	11.396	696.2	10.08	0.14	0.01	0.42	0.039	0.850
0.04632	3.72	11.123	773.3	-0.03	0.00	4.18	11.626	778.9	11.28	0.12	0.01	0.46	0.041	0.851
0.05488	4.98	11.380	896.0	-0.03	0.00	5.59	11.917	901.0	13.05	0.11	0.01	0.50	0.044	0.854
0.06196	6.17	11.546	996.8	-0.05	0.00	6.50	12.107	1000.9	14.48	0.11	0.01	0.50	0.044	0.857
0.06785	7.17	11.731	1169.0	0.00	0.00	8.10	12.238	1096.0	15.73	0.12	0.01	0.49	0.042	0.848
0.07400	8.46	11.971	1339.5	-0.08	-0.01	9.48	12.335	1175.1	17.02	0.11	0.01	0.45	0.038	0.855
0.07479	8.50	11.874	1177.0	-0.01	0.00	9.66	12.346	1192.0	17.26	0.10	0.01	0.44	0.037	0.842
0.08171	9.94	12.000	1267.0	-0.01	0.00	11.41	12.417	1289.2	18.67	0.09	0.01	0.38	0.031	0.834
0.09363	12.53	12.245	1431.1	0.02	0.00	14.80	12.491	1477.1	21.39	0.09	0.01	0.21	0.017	0.811
0.10352	14.91	12.411	1560.6	0.04	0.00	18.14	12.474	1634.9	23.67	0.05	0.00	0.02	0.002	0.787
0.12902	21.98	12.741	1890.9	-0.03	0.00	28.35	12.436	2039.7	29.54	0.05	0.00	-0.40	-0.031	0.742
0.13988	25.60	12.757	2052.0	-0.05	0.00	34.34	12.500	2257.2	30.69	-0.09	0.01	-0.76	-0.059	0.714
0.15915	32.30	12.963	2305.0	-0.09	-0.01	44.61	12.229	2572.6	31.75	0.06	0.00	-1.01	-0.076	0.693
0.17939	39.38	13.160	2544.8	-0.06	0.00	56.17	12.215	2896.7	41.80	0.03	0.00	-1.23	-0.091	0.671
0.19588	45.95	13.362	2748.9	0.01	0.00	67.90	12.187	3286.7	45.95	0.02	0.00	-1.42	-0.104	0.648
0.21485	54.27	13.501	2986.7	0.00	0.00	81.89	12.184	3484.6	50.46	-0.02	0.00	-1.56	-0.115	0.635
0.23998	62.98	13.652	3208.9	0.07	0.00	96.71	12.210	3786.3	54.93	0.01	0.00	-1.70	-0.122	0.620

NUM 228
DATE 7/24/93
POLY -
c wpm -
W 1.000

NUM 232
DATE 7/30/93
POLY -
c wpm -
W 1.000

0.27214	81.82	13.927	3665.9	0.07	0.01	126.75	12.261	4384.4	63.49	0.03	0.00	-1.91	-0.135	0.604
0.31015	102.89	14.155	4109.6	0.10	0.01	166.65	12.330	4967.4	71.81	0.05	0.00	-2.05	-0.143	0.591
0.34802	126.01	14.351	4547.0	0.12	0.01	207.48	12.399	5541.3	80.24	0.04	0.00	-2.18	-0.149	0.582
0.40454	164.54	14.599	5193.2	0.14	0.01	274.46	12.532	6370.1	92.24	0.05	0.00	-2.29	-0.154	0.574
0.46821	213.50	14.833	5911.9	0.15	0.01	357.77	12.703	7268.5	105.73	0.06	0.01	-2.34	-0.156	0.571
0.56106	294.57	15.133	6934.2	0.17	0.01	485.19	12.939	8538.9	123.64	0.06	0.00	-2.39	-0.156	0.570
0.63468	366.23	15.312	7691.8	0.17	0.01	617.05	13.113	9458.8	138.93	0.05	0.00	-2.39	-0.154	0.571

0.0000" Ribbed 9.500" Pipe
 Resid/ctm = 350

Series
 PEO

MM
 S1:
 d = 0.308
 h = smooth
 R1B:
 d = 0.293
 h = 0.0060
 R/A 24.4

Q (L/A)	Wt(S1)	1/ncp(S1)	Resid(S1)	S(S1)	SF(S1)	Wt(R1B)	1/ncp(R1B)	Resid(R1B)	N	S(R1B)	SF(R1B)	1/ncp(S1A)	S1(S1)	R	MF	P	Δ/View	corrected R	corrected S
0.00462	0.09	7.298	111.8	0.11	0.01	0.11	7.187	110.5	1.73	0.11	0.01	7.8	0.14	-0.014	-0.001	0.286	0.00	-0.014	0.14
0.00646	0.12	8.608	132.6	0.17	0.01	0.17	8.143	147.6	2.14	0.17	0.01	10.14	0.11	0.034	0.003	0.793	0.00	0.034	0.11
0.00779	0.15	9.401	146.5	0.21	0.01	0.21	8.807	164.7	2.39	0.21	0.01	10.41	0.04	0.093	0.009	0.801	0.00	0.093	0.04
0.00909	0.17	10.113	159.2	0.24	0.01	0.24	9.456	179.2	2.59	0.24	0.01	11.03	0.01	0.170	0.016	0.812	0.00	0.170	0.01
0.01033	0.20	10.732	170.6	0.32	0.01	0.32	9.340	206.5	2.99	0.32	0.01	11.34	0.00	0.244	0.023	0.819	0.00	0.244	0.00
0.01250	0.26	11.371	195.0	0.45	0.01	0.45	9.521	245.3	3.55	0.45	0.01	10.44	0.00	0.276	0.025	0.825	0.00	0.276	0.00
0.01549	0.32	9.934	272.0	0.60	0.01	0.60	10.223	283.4	4.10	0.60	0.01	9.99	0.00	0.334	0.030	0.831	0.00	0.334	0.00
0.01856	0.37	9.942	350.0	0.81	0.01	0.81	9.986	366.9	5.31	0.81	0.01	10	0.00	0.385	0.034	0.839	0.00	0.385	0.00
0.02202	1.02	10.093	388.5	0.11	0.01	1.23	10.174	405.4	5.87	0.06	0.01	10.14	0.00	0.417	0.036	0.839	0.00	0.417	0.00
0.02683	1.45	10.320	462.7	0.06	0.01	1.73	10.463	480.5	6.46	0.01	0.00	10.37	0.00	0.452	0.038	0.839	0.00	0.452	0.00
0.03070	1.84	10.478	521.9	0.01	0.00	2.17	10.700	538.1	7.79	0.01	0.00	10.53	0.00	0.485	0.041	0.839	0.00	0.485	0.00
0.03494	2.29	10.691	582.1	0.03	0.00	2.67	10.964	597.7	8.65	0.01	0.00	10.72	0.00	0.516	0.045	0.839	0.00	0.516	0.00
0.03788	2.64	10.784	626.0	0.00	0.00	3.07	11.096	640.6	9.78	0.02	0.00	10.82	0.00	0.547	0.049	0.839	0.00	0.547	0.00
0.04314	3.31	10.981	700.6	0.00	0.00	3.81	11.344	714.1	11.34	0.03	0.00	11.01	0.00	0.578	0.054	0.839	0.00	0.578	0.00
0.05108	4.43	11.240	810.1	0.01	0.00	5.06	11.655	822.6	11.91	0.04	0.00	11.27	0.00	0.609	0.059	0.839	0.00	0.609	0.00
0.05819	5.51	11.473	903.9	0.05	0.00	6.29	11.907	917.0	13.20	0.07	0.01	11.49	0.00	0.640	0.064	0.839	0.00	0.640	0.00
0.06402	6.58	11.554	987.6	0.02	0.00	7.34	12.086	984.1	14.30	0.10	0.01	11.57	0.00	0.671	0.069	0.839	0.00	0.671	0.00
0.07042	7.77	11.759	1073.5	0.04	0.00	8.74	12.294	1081.1	15.65	0.18	0.01	11.77	0.00	0.702	0.074	0.839	0.00	0.702	0.00
0.07742	9.02	11.932	1156.0	0.08	0.01	10.13	12.480	1163.1	16.84	0.27	0.02	12.01	0.00	0.733	0.079	0.839	0.00	0.733	0.00
0.07819	9.05	12.032	1163.0	0.17	0.01	10.14	12.602	1163.9	16.94	0.38	0.03	12.04	0.00	0.764	0.084	0.839	0.00	0.764	0.00
0.09465	12.72	12.544	1381.7	0.38	0.01	14.59	12.985	1405.4	20.35	0.60	0.05	12.84	0.00	0.815	0.091	0.839	0.00	0.815	0.00
0.10559	14.66	12.784	1482.0	0.48	0.04	16.94	13.164	1513.0	21.91	0.75	0.06	12.84	0.00	0.846	0.096	0.839	0.00	0.846	0.00
0.12179	18.30	13.178	1650.8	0.71	0.06	21.39	13.515	1644.8	24.34	1.09	0.09	13.45	0.00	0.877	0.101	0.839	0.00	0.877	0.00
0.13300	21.51	13.276	1798.0	0.66	0.05	24.87	13.661	1819.9	26.64	1.24	0.10	13.45	0.00	0.908	0.106	0.839	0.00	0.908	0.00
0.15060	25.18	13.895	1945.5	1.14	0.09	31.08	13.865	2025.9	28.73	1.48	0.12	14.02	0.00	0.939	0.111	0.839	0.00	0.939	0.00
0.17016	31.06	14.135	2161.1	1.20	0.09	37.28	14.302	2248.8	32.56	1.96	0.16	14.45	0.00	0.970	0.116	0.839	0.00	0.970	0.00
0.18972	35.70	14.700	2317.2	1.64	0.13	44.86	14.537	2467.1	35.72	2.23	0.18	15.05	0.00	1.001	0.121	0.839	0.00	1.001	0.00
0.21710	43.50	15.240	2557.9	2.01	0.15	55.07	15.014	2733.7	39.58	2.75	0.22	15.55	0.00	1.032	0.126	0.839	0.00	1.032	0.00
0.25427	55.35	15.822	2885.5	2.38	0.18	71.70	15.454	3110.5	45.04	3.24	0.26	16.26	0.00	1.063	0.131	0.839	0.00	1.063	0.00
0.29339	68.24	16.441	3204.0	2.92	0.21	90.00	15.871	3494.6	50.60	3.67	0.30	16.93	0.00	1.094	0.136	0.839	0.00	1.094	0.00
0.35206	89.67	17.211	3672.5	3.35	0.24	121.07	16.421	4025.8	58.68	4.21	0.35	17.78	0.00	1.125	0.141	0.839	0.00	1.125	0.00
0.41074	113.11	17.879	4123.9	3.82	0.27	154.23	16.865	4603.3	66.66	4.62	0.41	18.54	0.00	1.156	0.146	0.839	0.00	1.156	0.00
0.48098	146.99	18.671	4702.5	4.38	0.31	209.10	17.354	5237.0	77.13	5.03	0.41	19.39	0.00	1.187	0.151	0.839	0.00	1.187	0.00
0.58721	184.62	19.325	5289.3	4.84	0.33	268.99	17.752	6039.7	87.45	5.32	0.43	20.18	0.00	1.218	0.156	0.839	0.00	1.218	0.00
0.66501	235.09	20.078	5943.2	5.38	0.37	354.16	18.135	6928.1	100.32	5.46	0.44	21.02	0.00	1.249	0.161	0.839	0.00	1.249	0.00
0.78236	302.20	20.835	6728.4	5.92	0.40	469.57	18.530	7968.5	115.46	5.74	0.45	21.96	0.00	1.280	0.166	0.839	0.00	1.280	0.00

0.0060" Ribbed 0.500" Pipe
 Height = 350

Series
 PEO

WFE
 S1:
 d = 0.308
 h = smooth
 RIB
 d = 0.293
 h = 0.0060
 Rh = 24.4

M-750
 RUN 230
 DATE 7/27/93
 POLY M-750
 c 300
 w 1.102

Q (L/s)	Ted(S1)	1/Avg(S1)	Req(S1)	S (S1)	Sf (S1)	1/W(RIB)	1/Avg(RIB)	Req(RIB)	N	S (RIB)	Sf (RIB)	1/Avg(S1h)	Sb (S1)	R	W	P	D/Req	Corrected R	Corrected S
0.00362	0.08	6.118	98.0	0.06	0.01	0.09	6.296	100.3	1.45	0.18	0.02	9.91	0.05	0.209	0.021	0.818	0.00	0.209	0.05
0.00476	0.10	7.038	112.0	0.00	0.00	1.25	10.189	302.4	5.54	0.08	0.01	9.96	-0.01	0.200	0.000	0.816	0.00	0.200	-0.01
0.00606	0.13	7.927	126.8	-0.05	0.00	2.75	10.830	455.9	6.60	0.07	0.01	10.23	-0.05	0.227	0.027	0.826	0.00	0.227	-0.05
0.00785	0.16	9.037	144.3	0.00	0.01	2.78	10.870	513.7	7.44	0.05	0.00	10.39	-0.06	0.300	0.028	0.830	0.00	0.300	-0.06
0.00905	0.19	9.658	155.7	0.00	0.00	3.17	11.039	609.7	8.83	0.08	0.01	10.69	-0.07	0.349	0.033	0.835	0.00	0.349	-0.05
0.01262	0.27	11.192	187.5	-0.08	0.01	3.90	11.250	676.7	9.80	0.06	0.01	10.85	-0.07	0.400	0.037	0.842	0.00	0.400	-0.07
0.01568	0.40	11.416	208.5	0.00	0.00	6.38	11.949	865.4	12.53	0.15	0.01	11.15	0.05	0.500	0.045	0.853	0.00	0.500	-0.02
0.02000	0.87	9.913	336.0	0.14	0.01	7.48	12.207	937.2	13.57	0.33	0.03	11.64	0.15	0.567	0.049	0.859	0.00	0.567	0.05
0.02222	1.07	9.945	372.1	0.26	0.02	8.60	12.493	1004.4	14.54	0.49	0.04	11.89	0.28	0.603	0.051	0.861	0.00	0.603	0.28
0.02709	1.51	10.191	443.2	0.39	0.03	9.98	12.760	1080.7	15.65	0.64	0.05	12.22	0.48	0.590	0.044	0.863	0.00	0.590	0.49
0.03120	1.95	10.359	502.4	0.50	0.04	10.26	12.764	1100.5	15.94	0.62	0.05	12.32	0.55	0.444	0.036	0.846	0.00	0.444	0.55
0.03533	2.41	10.510	559.8	0.80	0.08	13.56	13.305	1268.8	18.34	1.00	0.09	12.35	0.94	0.356	0.027	0.832	0.00	0.356	0.94
0.03831	2.77	10.663	599.5	1.16	0.10	16.81	13.755	1408.4	20.39	1.37	0.11	13.41	1.22	0.345	0.026	0.831	0.00	0.345	1.22
0.04331	3.43	10.823	668.1	1.49	0.12	20.65	14.216	1554.5	22.51	1.79	0.14	13.87	1.50	0.346	0.025	0.825	0.00	0.346	1.50
0.05163	4.61	11.135	774.2	1.52	0.12	22.56	14.306	1634.4	23.67	1.88	0.15	14.02	1.57	0.286	0.020	0.822	0.00	0.286	1.57
0.05882	5.72	11.390	862.3	1.75	0.14	28.32	14.618	1831.1	26.51	2.22	0.18	14.47	1.82	0.168	0.012	0.811	0.00	0.168	1.82
0.06506	6.71	11.626	934.5	1.96	0.15	33.63	15.145	1995.4	28.88	2.75	0.22	15.05	2.25	0.095	0.006	0.825	0.00	0.095	2.25
0.07137	7.73	11.881	1003.1	2.59	0.20	39.36	15.421	2158.5	31.25	3.06	0.25	15.76	2.82	-0.339	-0.021	0.778	0.00	-0.339	2.82
0.07855	8.99	12.126	1080.0	2.91	0.22	45.21	15.862	2314.0	33.51	3.53	0.29	16.23	3.17	-0.368	-0.023	0.778	0.00	-0.368	3.17
0.08548	9.06	12.249	1093.1	3.35	0.26	54.23	16.363	2534.6	36.70	4.07	0.33	16.88	3.66	-0.517	-0.031	0.769	0.00	-0.517	3.66
0.10988	14.59	13.319	1381.4	3.73	0.26	63.21	16.770	2736.6	39.63	4.51	0.37	17.45	4.10	-0.680	-0.039	0.761	0.00	-0.680	4.10
0.12885	17.79	13.813	1519.4	4.37	0.31	80.42	17.372	3090.5	44.75	5.15	0.42	18.36	4.80	-0.988	-0.054	0.742	0.00	-0.988	4.80
0.13241	19.37	13.926	1594.6	5.12	0.38	108.82	18.055	3590.9	52.00	5.86	0.48	19.45	5.63	-1.395	-0.072	0.720	0.00	-1.395	5.63
0.15178	23.99	14.345	1774.6	5.89	0.42	146.73	18.772	4170.4	60.38	6.56	0.54	20.56	6.48	-1.788	-0.087	0.701	0.00	-1.788	6.48
0.17113	28.97	14.720	1949.9	6.84	0.48	213.04	19.545	5025.7	72.37	7.28	0.59	21.9	7.50	-2.335	-0.107	0.674	0.00	-2.335	7.50
0.18852	31.98	15.432	2048.6	6.84	0.51	261.59	20.038	5567.9	80.62	7.88	0.62	22.66	8.08	-2.822	-0.116	0.665	-1.61	-2.822	8.01
0.20781	36.74	15.873	2196.3	7.34	0.51	330.26	20.467	6251.3	90.52	8.00	0.64	23.48	8.70	-3.013	-0.128	0.647	-3.46	-3.013	8.56
0.23479	43.57	16.467	2392.1	7.92	0.58	424.13	20.828	7058.8	102.31	8.23	0.65	24.44	9.44	-3.612	-0.148	0.627	-5.43	-3.612	9.26

0.0090" Ribbed 0.500" Pipe
 Resol: 350

Saves
 PEO

RUN 227
 DATE 7/22/93
 POLY M-50K
 c. wpsn 3
 # 1.003

P/E
 S1:
 d = 0.308
 n = smooth
 RIB:
 d = 0.293
 h = 0.0060
 Rn = 24.4

Q (L/A)	Twr(S1)	1/Avg(S1)	Resp(S1)	S(S1)	Sf(S1)	Twr(R1R)	1/Avg(R1R)	Resp(R1R)	N	S(R1R)	Sf(R1R)	1/Avg(S1R)	S(S1R)	R	#	P	Δ/Pms	connected	IF	connected
0.01739	0.68	9.772	378.8	0.01	0.00	0.79	10.046	336.7	4.88	0.06	0.01	9.8	0.00	0.157	0.016	0.823	0.00	0.157	0.00	
0.02265	1.08	10.060	415.4	0.01	0.00	1.28	10.287	428.6	6.21	0.07	0.01	10.13	0.00	0.183	0.018	0.814	0.00	0.183	0.00	
0.02473	1.26	10.214	447.4	0.01	0.00	1.48	10.443	461.2	6.68	0.07	0.01	10.26	0.00	0.219	0.021	0.820	0.00	0.219	0.00	
0.03034	1.78	10.525	533.2	0.02	0.00	2.08	10.799	547.1	7.92	0.07	0.01	10.58	0.03	0.215	0.020	0.818	0.00	0.215	0.00	
0.03475	2.23	10.777	596.7	0.07	0.01	2.61	11.045	613.0	8.88	0.07	0.01	10.83	0.08	0.299	0.027	0.829	0.00	0.299	0.00	
0.03845	2.76	10.988	665.8	0.09	0.01	3.19	11.318	679.4	9.84	0.14	0.01	11.04	0.11	0.307	0.027	0.830	0.00	0.307	0.00	
0.04217	3.08	11.132	702.9	0.14	0.01	3.55	11.487	717.2	10.39	0.16	0.01	11.18	0.16	0.450	0.029	0.846	0.00	0.450	0.00	
0.04874	3.91	11.419	792.0	0.22	0.02	4.42	11.900	800.1	11.59	0.34	0.03	11.45	0.24	0.529	0.045	0.853	0.00	0.529	0.00	
0.05907	5.15	11.850	909.8	0.41	0.04	5.78	12.399	915.5	13.26	0.37	0.05	11.87	0.34	0.681	0.056	0.868	0.00	0.681	0.00	
0.06853	6.41	12.166	1015.7	0.54	0.05	7.07	12.841	1013.2	14.67	0.83	0.07	12.16	0.34	0.825	0.041	0.846	0.00	0.825	0.00	
0.07410	7.36	12.647	1088.4	0.90	0.08	8.31	13.195	1098.4	15.91	1.06	0.09	12.67	0.31	1.000	0.051	0.863	0.00	1.000	0.00	
0.08242	8.76	12.890	1186.7	0.99	0.08	9.72	13.543	1187.5	17.19	1.32	0.11	12.9	1.00	0.663	0.051	0.863	0.00	0.663	0.00	
0.09108	9.93	13.390	1262.1	1.38	0.11	11.31	13.901	1279.1	18.52	1.59	0.13	13.43	1.40	0.471	0.075	0.841	0.00	0.471	0.00	
0.09491	10.60	13.493	1301.0	1.44	0.12	12.03	14.044	1316.1	19.06	1.70	0.14	13.55	1.47	0.494	0.076	0.844	0.00	0.494	0.00	
0.11094	13.17	14.150	1458.5	1.89	0.15	15.55	14.436	1505.2	21.80	2.02	0.16	14.32	2.01	0.116	0.009	0.811	0.00	0.116	0.00	
0.12226	15.16	14.534	1569.7	2.15	0.17	18.27	14.677	1636.6	23.70	2.25	0.18	14.63	2.17	0.047	0.009	0.795	0.00	0.047	0.00	
0.12701	16.23	14.593	1621.5	2.15	0.17	19.39	14.728	1682.9	24.37	2.30	0.18	14.76	2.26	-0.032	-0.002	0.794	0.00	-0.032	0.00	
0.14263	19.38	14.999	1721.8	2.41	0.19	23.23	15.099	1842.4	26.68	2.68	0.27	15.18	2.52	-0.081	-0.005	0.790	0.00	-0.081	0.00	
0.16216	23.55	15.470	1953.4	2.71	0.21	26.59	15.461	2044.2	29.60	3.07	0.25	15.77	2.93	-0.309	-0.020	0.778	0.00	-0.309	0.00	
0.18168	27.61	16.006	2115.5	3.10	0.24	30.51	15.640	2262.5	32.76	3.30	0.27	16.31	3.28	-0.670	-0.041	0.744	0.00	-0.670	0.00	
0.20119	32.39	16.366	2291.4	3.33	0.26	41.49	15.895	2463.3	35.67	3.59	0.28	16.72	3.55	-0.825	-0.049	0.735	0.00	-0.825	0.00	
0.23046	39.93	16.882	2544.7	3.66	0.28	52.70	16.138	2768.4	40.20	3.88	0.32	17.25	3.88	-1.114	-0.065	0.712	0.00	-1.114	0.00	
0.24997	45.47	17.160	2715.6	3.82	0.29	61.79	16.215	2994.3	43.86	3.95	0.33	17.54	4.03	-1.325	-0.076	0.696	0.00	-1.325	0.00	
0.28897	57.66	17.616	3058.4	4.07	0.30	80.03	16.376	3425.0	49.55	4.17	0.34	18.01	4.27	-1.634	-0.091	0.673	0.00	-1.634	0.00	
0.34745	78.55	18.148	3569.7	4.34	0.31	115.32	16.360	4107.9	59.48	4.15	0.34	18.52	4.47	-2.160	-0.117	0.633	0.00	-2.160	0.00	
0.38642	94.55	18.396	3916.9	4.42	0.32	143.14	16.304	4577.2	66.28	4.06	0.33	18.74	4.50	-2.436	-0.130	0.612	0.00	-2.436	0.00	
0.42537	112.00	18.606	4264.1	4.49	0.31	174.89	16.209	5060.7	73.28	3.92	0.32	18.89	4.47	-2.681	-0.142	0.591	0.00	-2.681	0.00	
0.49740	149.14	18.854	4920.8	4.49	0.31	243.62	16.207	5973.3	86.48	3.59	0.29	19.06	4.36	-3.053	-0.160	0.562	0.00	-3.053	0.00	
0.57521	196.07	19.016	5641.7	4.41	0.30	334.61	15.741	6996.7	101.36	3.15	0.25	19.15	4.17	-3.409	-0.178	0.534	0.00	-3.409	0.00	
0.65296	250.38	19.103	6375.7	4.28	0.29	441.03	15.510	8036.7	116.37	2.73	0.21	19.22	4.00	-3.710	-0.193	0.514	0.00	-3.710	0.00	
0.75007	327.97	19.173	7282.3	4.12	0.27	595.63	15.264	9333.6	135.15	2.22	0.17	19.3	3.82	-4.036	-0.209	0.494	0.00	-4.036	0.00	

0.0000" Ribbed 300" Pipe
 Reference: 350

Series
 PEO

PRE
 S1:
 d = 0.308
 h = smooth
 RIB:
 d = 0.293
 h = 0.0060
 N = 24.4

MIN 226
 DATE 7/21/93
 POLY M-60K
 c wipam
 W 1.009

Q(L/N)	Tem(S1)	1/Amp(S1)	Reof(S1)	S'(S1)	Sf(S1)	1/Amp(RIB)	Reof(RIB)	Ns	S'(RIB)	Sf(RIB)	1/Amp(S1)	S'(S1)	R	W	P	Δ/hrs	connected/R	connected/S
0.00547	0.10	7.98	125.1	-0.02	0.00	0.12	8.069	1.88	0.13	0.01	8.22	-0.02	0.243	0.024	0.00	0.00	0.243	-0.02
0.00799	0.15	5.32	152.2	0.00	0.00	0.18	9.690	2.26	0.10	0.01	9.82	0.01	0.213	0.021	0.01	0.00	0.213	0.01
0.00993	0.19	10.503	171.9	0.04	0.00	0.25	10.245	2.69	0.16	0.01	10.41	-0.04	0.362	0.035	0.00	0.00	0.362	-0.04
0.01194	0.24	10.280	192.7	0.53	0.00	0.43	9.353	3.54	0.20	0.03	10.41	0.03	0.453	0.042	0.00	0.00	0.453	0.03
0.01440	0.42	10.257	256.0	0.65	0.00	0.76	10.148	272.4	0.51	0.05	10.1	0.22	0.620	0.052	0.00	0.00	0.620	0.22
0.01718	0.65	9.849	318.2	0.65	0.00	1.24	10.116	326.2	0.76	0.06	9.84	0.48	0.703	0.061	0.00	0.00	0.703	0.48
0.02236	1.07	10.017	407.6	0.49	0.04	1.49	10.303	417.3	0.85	0.07	10.06	0.22	0.820	0.055	0.00	0.00	0.820	0.22
0.02492	1.28	10.222	446.5	0.04	0.00	1.49	10.463	450.4	0.85	0.07	10.06	0.22	0.820	0.055	0.00	0.00	0.820	0.22
0.03015	1.78	10.454	527.7	0.00	0.00	2.04	10.842	535.8	1.16	0.10	10.25	0.01	0.913	0.021	0.01	0.00	0.913	0.01
0.03470	2.25	10.713	592.8	0.02	0.00	2.53	11.193	597.4	0.76	0.16	10.48	-0.04	0.962	0.042	0.00	0.00	0.962	-0.04
0.03957	2.74	11.063	654.8	0.20	0.00	3.05	11.636	655.4	0.49	0.20	10.71	0.03	1.071	0.033	0.00	0.00	1.071	0.03
0.04256	3.10	11.185	697.0	0.21	0.02	3.42	11.810	695.0	0.51	0.05	11.06	0.18	1.176	0.052	0.00	0.00	1.176	0.18
0.04874	3.76	11.634	767.6	0.49	0.04	4.13	12.313	763.7	0.76	0.16	11.19	0.22	1.262	0.055	0.00	0.00	1.262	0.22
0.05860	4.84	12.327	870.4	0.97	0.04	5.32	13.041	866.3	1.32	0.11	11.61	0.48	1.408	0.061	0.00	0.00	1.408	0.48
0.07399	5.85	12.883	958.8	1.36	0.12	6.44	13.611	955.5	1.34	0.11	12.3	0.95	1.541	0.060	0.00	0.00	1.541	0.95
0.08968	6.86	13.429	1038.1	1.76	0.15	7.55	14.190	1034.4	1.70	0.14	12.86	1.34	1.674	0.059	0.00	0.00	1.674	1.34
0.09395	8.61	14.147	1161.6	2.29	0.19	9.54	14.902	1161.1	2.14	0.18	13.4	1.74	1.790	0.058	0.00	0.00	1.790	1.74
0.09985	9.07	14.443	1193.6	2.54	0.21	10.10	15.174	1196.2	2.93	0.22	14.14	2.28	1.876	0.054	0.00	0.00	1.876	2.28
0.10995	9.58	14.932	1225.9	2.98	0.25	11.04	15.422	1249.7	3.13	0.25	14.54	2.63	1.932	0.044	0.00	0.00	1.932	2.63
0.12038	12.37	15.846	1396.6	3.67	0.30	14.76	16.092	1449.0	3.30	0.32	15.03	3.01	2.026	0.031	0.00	0.00	2.026	3.01
0.13215	14.00	16.349	1485.4	4.06	0.33	17.20	16.354	1547.7	3.68	0.30	16.13	3.89	2.104	0.026	0.00	0.00	2.104	3.89
0.13290	14.24	16.303	1502.4	4.00	0.32	16.89	16.597	1553.8	4.18	0.34	16.59	4.22	2.182	0.021	0.00	0.00	2.182	4.22
0.14952	16.49	17.043	1616.8	4.61	0.37	20.16	17.088	1697.9	4.66	0.39	17.34	4.82	2.252	0.015	0.00	0.00	2.252	4.82
0.15170	17.07	16.997	1646.0	4.53	0.36	20.21	17.318	1701.0	4.89	0.41	17.34	4.82	2.252	0.015	0.00	0.00	2.252	4.82
0.16878	19.38	17.747	1753.0	5.17	0.41	24.61	17.462	1875.8	5.05	0.44	18.13	5.44	2.322	0.003	0.00	0.00	2.322	5.44
0.18800	22.83	18.216	1902.6	5.50	0.43	29.20	17.858	2043.6	5.47	0.44	18.69	5.85	2.392	0.003	0.00	0.00	2.392	5.85
0.20527	25.99	18.641	2030.3	5.81	0.45	33.23	18.276	2180.4	5.92	0.48	19.2	6.25	2.462	0.003	0.00	0.00	2.462	6.25
0.23590	31.65	19.111	2240.6	6.41	0.49	42.15	18.648	2455.7	6.34	0.52	19.86	6.70	2.532	0.003	0.00	0.00	2.532	6.70
0.25499	36.05	19.659	2392.1	6.54	0.50	48.02	18.884	2621.9	6.61	0.54	20.36	7.11	2.602	0.003	0.00	0.00	2.602	7.11
0.32721	42.76	20.343	2605.4	7.08	0.53	59.04	19.193	2907.6	6.96	0.57	20.92	7.47	2.672	0.003	0.00	0.00	2.672	7.47
0.40267	52.58	20.890	2889.5	7.45	0.55	74.89	19.405	3275.3	7.20	0.59	21.48	7.82	2.742	0.003	0.00	0.00	2.742	7.82
0.45887	73.99	21.671	3428.3	7.93	0.58	111.37	19.582	3994.8	7.38	0.60	22.12	8.11	2.812	0.003	0.00	0.00	2.812	8.11
0.53330	93.04	22.023	3945.0	8.08	0.58	144.09	19.619	4544.6	7.38	0.60	22.38	8.15	2.882	0.003	0.00	0.00	2.882	8.15
0.64384	122.15	22.338	4406.4	8.16	0.58	196.61	19.519	5309.5	7.20	0.58	22.51	8.01	2.952	0.003	0.00	0.00	2.952	8.01
0.75307	175.28	22.513	5279.1	8.02	0.55	298.85	19.114	6546.9	6.60	0.53	22.51	7.64	3.022	0.003	0.00	0.00	3.022	7.64
0.84309	239.99	22.504	6177.6	7.74	0.52	428.75	18.665	7842.3	5.92	0.46	22.46	7.28	3.092	0.003	0.00	0.00	3.092	7.28
	301.23	22.487	6906.8	7.53	0.50	559.22	18.297	8937.7	5.34	0.41	22.43	7.03	3.162	0.003	0.00	0.00	3.162	7.03

0.0050" Fiberglass Pipe
Residue: 350

Series PEO

PIPE
S1:
d = 0.308
h = smooth
RIB:
d = 0.293
h = 0.0050
RH 24.4

RUN 225
DATE 7/20/83
POLY M-60K
Cmpsn 30
W 1.032

Q (L/A)	Tef(S1)	Vadef(S1)	Repad(S1)	S(S1)	Sf(S1)	Tef(R1R)	Vadef(R1R)	Repad(R1R)	h _w	S(R1R)	Sf(R1R)	Vadef(S1)*	Sf(S1)	R	W	P	Δ/area	connected R	connected S	
0.00477	0.09	7.346	116.2	0.07	0.01	0.11	7.426	121.1	1.75	0.01	0.00	10.14	0.05	0.035	0.003	0.796	0.00	0.015	0.05	
0.00611	0.12	8.278	132.4	0.05	0.01	0.14	8.369	137.9	2.00	0.05	0.00	10.31	0.07	0.088	0.009	0.796	0.00	0.088	0.07	
0.00799	0.15	9.479	151.4	0.16	0.02	0.19	9.470	159.5	2.31	0.21	0.02	10.67	0.20	0.159	0.015	0.778	0.00	0.159	0.20	
0.00947	0.18	10.246	166.1	0.25	0.03	0.22	10.430	171.8	2.49	0.51	0.08	11.05	0.40	0.311	0.028	0.807	0.00	0.311	0.40	
0.01101	0.22	10.956	180.7	0.28	0.04	0.25	10.956	180.7	3.17	0.85	0.08	11.49	0.69	0.396	0.034	0.589	0.00	0.396	0.40	
0.01279	0.26	11.723	196.2	0.26	0.06	0.30	11.723	196.2	3.77	1.10	0.10	11.88	0.92	0.451	0.038	0.481	0.00	0.451	0.32	
0.01518	0.30	9.948	214.5	0.29	0.08	0.36	9.948	214.5	4.20	1.62	0.14	12.48	1.43	0.498	0.040	0.772	0.00	0.498	1.43	
0.01829	0.73	9.908	332.3	0.28	0.18	4.30	13.864	820.8	11.89	2.25	0.19	13.37	2.11	0.494	0.037	0.848	0.00	0.494	2.11	
0.02250	1.07	10.064	401.8	0.28	0.28	5.81	14.657	893.7	12.94	2.87	0.24	14.14	2.74	0.517	0.037	0.847	0.00	0.517	2.74	
0.02506	1.29	10.229	441.1	0.32	0.32	6.72	15.345	962.0	13.93	3.42	0.29	14.8	3.27	0.545	0.037	0.847	0.00	0.545	3.27	
0.02976	1.69	10.581	506.1	0.40	0.40	7.80	16.112	1035.5	14.99	4.06	0.34	15.47	3.81	0.642	0.042	0.852	0.00	0.642	3.81	
0.03476	2.15	10.973	569.9	0.46	0.46	9.01	16.763	1113.2	16.12	4.60	0.38	16.29	4.50	0.473	0.029	0.841	0.00	0.473	4.50	
0.03947	2.56	11.421	623.5	0.41	0.41	9.82	16.899	1160.2	16.80	4.69	0.38	16.82	4.96	0.079	0.005	0.819	0.00	0.079	4.96	
0.04272	2.84	11.740	656.7	0.47	0.47	11.80	17.229	1178.1	16.97	5.01	0.41	16.94	5.06	0.269	0.017	0.830	0.00	0.269	5.06	
0.05981	4.34	13.291	813.2	0.46	0.46	12.05	18.006	1278.1	18.51	5.77	0.47	17.81	5.78	0.276	0.016	0.822	0.00	0.276	5.78	
0.06882	5.13	14.058	885.0	0.52	0.52	14.26	18.540	1405.2	18.72	5.79	0.47	17.94	5.89	0.171	0.010	0.829	0.00	0.171	5.89	
0.07754	5.95	14.718	952.6	0.52	0.52	14.87	18.612	1436.7	20.35	6.16	0.50	18.87	6.68	-0.330	-0.017	0.796	0.00	-0.330	6.68	
0.08766	6.94	15.403	1026.8	0.53	0.53	14.87	18.612	1436.7	20.80	6.22	0.50	19.13	6.90	-0.518	-0.027	0.780	0.00	-0.518	6.90	
0.10321	8.41	16.480	1130.0	0.47	0.47	18.37	19.054	1592.1	23.13	6.63	0.53	20.69	8.29	-1.636	-0.079	0.743	0.00	-1.636	8.29	
0.10591	8.63	16.692	1148.6	0.41	0.41	21.63	19.472	1732.9	23.09	7.04	0.57	21.71	9.15	-2.238	-0.103	0.708	0.00	-2.238	9.15	
0.12107	10.14	17.603	1247.2	0.46	0.46	27.54	20.824	1955.4	28.31	8.42	0.68	22.4	9.64	-1.576	-0.070	0.704	0.00	-1.576	9.64	
0.12250	10.42	17.570	1265.7	0.56	0.56	36.13	21.445	2240.1	32.44	9.10	0.74	23.4	10.40	-1.955	-0.084	0.703	0.00	-1.955	10.40	
0.13641	11.70	18.462	1340.3	0.63	0.63	45.75	21.947	2521.2	36.54	9.65	0.79	24.68	11.47	-2.733	-0.111	0.685	0.00	-2.733	11.47	
0.13988	12.13	18.595	1365.8	0.45	0.45	56.17	22.406	2793.6	40.45	10.15	0.83	25.47	12.09	-3.064	-0.120	0.657	0.00	-3.064	12.09	
0.15915	14.25	19.517	1480.8	0.45	0.45	74.64	22.801	3220.8	46.64	10.59	0.89	26.47	12.84	-3.669	-0.139	0.630	0.00	-3.669	12.84	
0.17647	15.99	20.430	1588.7	0.45	0.45	96.22	23.028	3650.5	52.93	10.83	0.89	27.1	13.25	-4.072	-0.150	0.604	0.00	-4.072	13.25	
0.21235	20.24	21.910	1765.1	0.74	0.74	120.33	23.212	4090.5	59.23	11.00	0.90	27.47	13.42	-4.258	-0.155	0.589	0.00	-4.258	13.42	
0.25117	26.51	22.583	2020.4	0.86	0.86	157.38	23.329	4678.3	67.74	11.08	0.90	27.7	13.42	-4.371	-0.158	0.571	0.00	-4.371	13.42	
0.28927	32.72	23.410	2244.8	0.90	0.90	201.37	23.284	5293.1	76.64	10.96	0.90	27.76	13.27	-4.476	-0.161	0.556	0.00	-4.476	13.27	
0.38386	48.12	25.354	2437.0	1.25	1.25	280.27	23.084	6245.6	90.44	10.62	0.85	27.62	12.84	-4.536	-0.164	0.540	0.00	-4.536	12.84	
0.44017	60.67	26.161	3057.4	1.30	1.30	416.55	22.545	7614.4	110.26	9.84	0.77	27.37	12.24	-4.825	-0.176	0.516	0.00	-4.825	12.24	
0.49616	73.86	26.724	3374.4	1.33	1.33															
0.57029	93.86	27.250	3803.0	1.33	1.33															
0.64384	116.90	27.565	4246.3	1.345	1.345															
0.75307	157.92	27.740	4936.2	1.337	1.337															
0.89665	224.67	27.691	5987.9	1.301	1.301															

0.0000" Ribbed 3.000" Pipe
 Product = 350

Series

PEO

MPE
 SI: 224
 d = 0.308
 h = smooth
 RIR: 7/15/93
 POLY: H-60K
 c: 100
 w: 1.092
 R/h: 24.4

Q(L/H)	Te(S1)	1/mag(S1)	Reag(S1)	S(S1)	Sf(S1)	Te(R1B)	1/mag(R1B)	Reag(R1B)	Ns	S(R1B)	Sf(R1B)	1/mag(S1)	S(S1)	R	W	P	Δ/Yes	connected R	connected S
0.00416	0.09	6.604	104.6	0.14	0.01	0.10	6.600	108.7	1.57	0.10	0.03	6.84	0.16	0.210	0.021	0.822	0.00	0.210	0.16
0.00473	0.10	7.022	111.9	0.24	0.02	0.11	7.239	114.3	1.65	0.11	0.05	7.16	0.27	0.300	0.029	0.835	0.00	0.300	0.27
0.00532	0.12	7.829	125.7	0.52	0.05	0.14	8.050	129.7	1.88	0.14	0.09	8.07	0.564	0.562	0.064	0.864	0.00	0.564	0.53
0.00736	0.15	8.728	140.4	1.44	0.14	0.18	8.950	145.8	2.11	0.18	0.14	9.06	1.278	0.702	0.062	0.873	0.00	0.702	0.89
0.00863	0.18	9.458	152.1	2.48	0.21	0.22	9.404	159.6	2.31	0.22	0.19	9.87	1.809	0.788	0.066	0.875	0.00	0.788	1.39
0.00998	0.21	10.127	161.6	3.51	0.27	0.26	10.127	171.3	2.51	0.26	0.20	10.5	2.41	0.809	0.065	0.875	0.00	0.809	1.80
0.01210	0.26	10.920	185.0	4.35	0.34	0.34	10.920	185.0	2.78	0.34	0.26	11.32	3.11	0.924	0.070	0.880	0.00	0.924	2.41
0.01428	0.34	11.414	209.1	5.01	0.45	0.44	9.663	206.1	3.27	0.44	0.37	10.51	3.43	0.987	0.069	0.878	0.00	0.987	3.43
0.01716	0.40	9.798	309.5	5.84	0.52	0.53	10.017	312.6	4.53	0.53	0.48	9.78	4.32	0.915	0.059	0.870	0.00	0.915	4.32
0.02221	1.05	10.019	371.6	6.52	0.58	1.23	10.290	380.9	5.52	0.79	0.53	10.08	5.00	0.948	0.059	0.871	0.00	0.948	5.00
0.02493	1.26	10.279	406.6	6.52	0.65	1.45	10.640	413.6	5.99	0.48	0.48	10.34	5.91	0.677	0.039	0.849	0.00	0.677	5.91
0.02957	1.61	10.773	460.6	6.52	0.65	1.79	11.344	460.6	6.67	0.98	0.58	10.78	6.64	0.247	0.013	0.846	0.00	0.247	7.01
0.03372	1.90	11.321	500.1	6.52	0.65	2.09	11.982	497.5	7.20	1.45	0.14	11.28	7.20	0.351	0.019	0.841	0.00	0.351	7.16
0.03864	2.23	11.973	542.2	1.44	0.14	2.44	12.698	538.3	7.78	2.01	0.19	11.91	7.78	0.446	-0.023	0.789	0.00	0.446	8.05
0.04252	2.49	12.462	573.0	1.85	0.17	2.72	13.229	569.2	8.24	2.42	0.27	12.42	8.24	0.600	-0.030	0.788	0.00	0.600	8.05
0.04908	2.94	13.260	622.9	2.48	0.27	3.18	14.094	617.0	8.93	3.11	0.26	13.17	8.93	0.775	-0.024	0.788	0.00	0.775	8.05
0.05939	3.63	14.476	693.2	3.51	0.32	3.96	15.367	687.5	9.96	4.14	0.37	14.38	9.96	0.875	-0.024	0.788	0.00	0.875	8.05
0.06900	4.27	15.459	752.1	4.35	0.34	4.70	16.335	748.4	10.85	4.92	0.48	15.42	10.85	0.915	-0.024	0.788	0.00	0.915	8.05
0.07690	4.82	16.222	796.9	5.01	0.45	5.30	17.148	795.7	11.52	5.60	0.48	16.2	11.52	0.948	-0.024	0.788	0.00	0.948	8.05
0.08545	5.33	17.139	840.4	5.84	0.52	6.01	17.897	847.4	12.27	6.22	0.53	17.22	12.27	0.977	-0.024	0.788	0.00	0.977	8.05
0.09804	6.38	17.975	926.4	6.52	0.58	6.70	18.991	931.5	13.47	6.96	0.58	18.64	13.47	0.987	-0.024	0.788	0.00	0.987	8.05
0.09996	6.41	18.274	922.3	6.81	0.58	8.29	19.194	993.1	14.38	7.21	0.60	19.84	14.38	0.987	-0.024	0.788	0.00	0.987	8.05
0.10751	6.81	19.071	949.2	7.56	0.66	9.10	19.826	1046.5	15.15	7.76	0.64	20.43	15.15	0.987	-0.024	0.788	0.00	0.987	8.05
0.11653	7.49	19.715	995.5	8.12	0.70	11.67	20.436	1188.9	17.21	8.20	0.67	22.65	17.21	0.987	-0.024	0.788	0.00	0.987	8.05
0.13602	8.82	21.197	1088.6	9.45	0.80	13.25	21.079	1287.2	18.35	8.77	0.71	23.56	18.35	0.987	-0.024	0.788	0.00	0.987	8.05
0.14952	9.60	22.345	1135.3	10.52	0.89	15.13	21.759	1354.2	19.61	9.40	0.76	24.66	19.61	0.987	-0.024	0.788	0.00	0.987	8.05
0.16493	11.17	22.849	1224.8	10.90	0.91	18.04	22.020	1478.7	21.41	9.61	0.77	25.92	21.41	0.987	-0.024	0.788	0.00	0.987	8.05
0.18224	12.42	23.943	1291.6	11.90	0.99	20.85	22.640	1589.9	23.02	10.21	0.82	26.31	23.02	0.987	-0.024	0.788	0.00	0.987	8.05
0.20143	14.04	24.886	1373.7	12.73	1.05	24.51	22.869	1723.9	24.96	10.44	0.84	26.63	24.96	0.987	-0.024	0.788	0.00	0.987	8.05
0.22059	15.68	25.786	1452.1	13.54	1.11	29.60	23.632	1894.9	27.44	11.29	0.91	27.16	27.44	0.987	-0.024	0.788	0.00	0.987	8.05
0.25117	19.42	26.387	1615.9	13.95	1.12	37.41	24.271	2130.6	30.85	11.90	0.96	28.07	30.85	0.987	-0.024	0.788	0.00	0.987	8.05
0.28927	24.83	26.872	1827.7	14.22	1.12	46.29	24.683	2370.4	34.32	12.36	1.00	28.07	34.32	0.987	-0.024	0.788	0.00	0.987	8.05
0.32721	30.00	27.657	2009.2	14.84	1.16	60.61	25.305	2712.6	39.28	13.04	1.06	29.75	39.28	0.987	-0.024	0.788	0.00	0.987	8.05
0.38386	38.75	28.547	2283.7	15.51	1.19	82.70	25.887	3168.8	45.88	13.68	1.12	30.85	45.88	0.987	-0.024	0.788	0.00	0.987	8.05
0.45887	51.69	29.547	2637.8	16.26	1.22	113.26	26.609	3709.7	53.72	14.41	1.18	31.63	53.72	0.987	-0.024	0.788	0.00	0.987	8.05
0.55182	89.60	30.620	3061.7	17.08	1.26	158.83	27.222	4351.6	62.01	15.00	1.23	32.75	62.01	0.987	-0.024	0.788	0.00	0.987	8.05
0.66214	94.15	31.592	3561.3	17.79	1.28	205.07	27.637	4991.9	72.28	15.35	1.25	33.62	72.28	0.987	-0.024	0.788	0.00	0.987	8.05
0.77115	121.94	32.328	4053.1	18.30	1.30	253.38	27.759	5544.2	80.28	15.40	1.25	34.38	80.28	0.987	-0.024	0.788	0.00	0.987	8.05
0.86098	146.98	32.876	4446.1	18.68	1.32														

0.00900" Ribbed 0.508" Pipe
Residence 350

PEE
S1: 0.300
h = smooth
RIB: 301
d = 0.293
h = 0.0060
RA: 24.4

Series
PEO

WR3-301
RUN
DATE 7/15/93
POLY 301
c temp
1.209

Q (L/s)	Tet(S1)	1/Avg(S1)	Reyn(S1)	S(S1)	SF(S1)	Tet(RIB)	1/Avg(RIB)	Reyn(RIB)	h _s	S(RIB)	SF(RIB)	1/Avg(S1)h	S1(S1)	R	#	Δ/h _s	connected R	connected S
0.00399	0.09	6.061	99.2	6.18	0.63	0.11	6.242	100.5	1.46	5.55	0.54	6.24	6.01	-0.390	-0.025	0.00	-0.390	6.01
0.00482	0.11	6.717	107.1	6.43	0.64	0.13	6.862	110.6	1.60	6.70	0.62	6.277	6.33	-0.046	-0.033	0.00	-0.046	6.33
0.00639	0.15	7.754	123.4	7.13	0.70	0.17	7.901	127.7	1.85	6.48	0.64	6.794	6.73	-0.156	-0.009	0.00	-0.156	6.73
0.00739	0.17	8.315	133.2	7.66	0.74	0.20	8.446	138.3	2.00	7.16	0.69	17.547	7.32	-0.049	-0.003	0.00	-0.049	7.32
0.00899	0.20	9.190	146.8	8.30	0.79	0.25	9.222	154.3	2.23	7.66	0.73	18.321	7.90	-0.098	-0.005	0.00	-0.098	7.90
0.01079	0.25	10.079	160.9	9.00	0.85	0.30	10.067	169.9	2.46	8.46	0.79	19.066	8.48	0.165	0.009	0.00	0.165	8.48
0.01368	0.32	11.273	182.6	9.71	0.92	0.41	10.938	198.4	2.87	9.56	0.87	20.021	9.25	0.538	0.027	0.00	0.538	9.25
0.01810	0.45	12.426	219.5	10.49	0.98	0.58	12.203	235.7	3.41	10.05	0.90	20.395	9.53	0.781	0.038	0.00	0.781	9.53
0.02294	0.61	13.649	253.6	11.17	1.05	0.78	13.357	273.3	3.96	10.74	0.95	20.631	9.67	0.879	0.041	0.00	0.879	9.67
0.02557	0.71	14.064	274.5	11.45	1.01	0.90	13.873	293.5	4.25	11.75	1.00	21.839	10.15	0.887	0.042	0.00	0.887	10.15
0.03011	0.89	14.785	307.4	12.01	1.05	1.10	14.782	324.5	4.70	12.06	1.02	22.957	11.63	0.492	0.021	0.00	0.492	12.06
0.03466	1.08	15.435	338.8	12.78	1.10	1.34	15.433	357.3	5.18	13.07	1.08	25.18	13.50	-0.047	-0.002	0.00	-0.047	13.50
0.03940	1.29	16.054	370.9	13.11	1.13	1.56	16.231	388.9	5.60	13.70	1.06	25.073	13.78	-0.550	-0.021	0.00	-0.550	13.78
0.04317	1.48	16.424	397.0	13.65	1.16	1.79	16.638	413.3	5.98	14.85	1.08	25.619	14.41	-1.357	-0.051	0.00	-1.357	14.41
0.04959	1.76	17.285	434.7	14.62	1.21	2.13	17.498	452.9	6.56	16.62	1.06	26.43	15.38	-2.498	-0.090	0.00	-2.498	15.38
0.05773	2.20	18.007	485.9	15.31	1.25	2.66	18.223	506.4	7.33	18.274	1.03	28.555	16.07	-3.306	-0.116	0.00	-3.306	16.07
0.06695	2.71	18.927	538.9	16.16	1.29	3.22	19.225	556.6	8.06	19.996	1.07	29.888	17.08	-4.249	-0.142	0.00	-4.249	17.08
0.07401	3.13	19.363	579.6	16.54	1.34	3.62	20.020	591.2	8.56	21.176	1.10	30.547	17.57	-4.604	-0.151	0.00	-4.604	17.57
0.07965	3.44	19.869	607.7	16.82	1.36	3.98	20.559	619.5	8.97	22.274	1.13	31.316	18.17	-5.153	-0.165	0.00	-5.153	18.17
0.08694	3.92	20.333	647.2	17.12	1.36	4.47	21.176	655.4	9.49	24.282	1.19	32.32	18.99	-5.421	-0.168	0.00	-5.421	18.99
0.09379	4.46	20.574	683.0	17.45	1.42	5.06	21.470	690.3	10.00	26.899	1.28	33.837	20.18	-6.031	-0.178	0.00	-6.031	20.18
0.10052	4.94	20.938	723.9	17.65	1.44	5.50	22.080	724.0	10.48	28.729	1.35	34.884	20.97	-6.155	-0.176	0.00	-6.155	20.97
0.10600	5.15	21.633	737.0	17.82	1.49	6.04	22.214	752.1	10.86	30.824	1.40	35.642	21.54	-6.285	-0.176	0.00	-6.285	21.54
0.12559	6.53	22.741	836.2	18.89	1.49	7.80	23.449	855.3	12.39	34.875	1.41	36.816	22.46	-7.204	-0.196	0.00	-7.204	22.46
0.13845	7.49	23.425	896.6	19.89	1.49	8.89	23.918	926.1	13.41	37.929	1.40	38.000	23.79	-8.285	-0.176	0.00	-8.285	23.79
0.15796	9.02	24.354	984.5	20.46	1.49	11.29	25.133	1044.3	15.12	40.000	1.40	39.837	25.18	-9.285	-0.176	0.00	-9.285	25.18
0.16006	9.10	24.686	986.3	20.46	1.49	10.95	25.035	1025.7	14.85	40.000	1.40	39.837	25.18	-9.285	-0.176	0.00	-9.285	25.18
0.18018	10.82	25.360	1075.6	21.12	1.51	13.70	25.069	1147.6	16.62	42.87	1.06	42.87	26.43	-10.41	-0.176	0.00	-10.41	26.43
0.19949	12.89	25.728	1173.8	21.85	1.17	16.79	25.073	1270.4	18.39	42.87	1.04	42.87	26.43	-10.41	-0.176	0.00	-10.41	26.43
0.23035	15.97	26.687	1306.6	22.27	1.21	22.27	25.147	1462.8	21.18	42.87	1.03	42.87	26.43	-10.41	-0.176	0.00	-10.41	26.43
0.26311	19.55	27.551	1445.9	22.80	1.25	28.80	25.249	1664.1	24.10	42.87	1.07	42.87	26.43	-10.41	-0.176	0.00	-10.41	26.43
0.32083	26.84	28.672	1694.8	24.62	1.29	41.56	25.631	1999.6	28.95	42.87	1.04	42.87	26.43	-10.41	-0.176	0.00	-10.41	26.43
0.35924	32.40	29.218	1862.6	25.31	1.30	50.86	25.943	2212.4	32.04	42.87	1.10	42.87	26.43	-10.41	-0.176	0.00	-10.41	26.43
0.39760	37.81	29.935	2012.1	26.16	1.34	61.26	26.163	2428.2	35.16	42.87	1.13	42.87	26.43	-10.41	-0.176	0.00	-10.41	26.43
0.45504	47.21	30.660	2248.5	27.03	1.36	75.90	26.899	2703.1	39.14	42.87	1.19	42.87	26.43	-10.41	-0.176	0.00	-10.41	26.43
0.56767	65.57	32.211	2689.8	28.91	1.42	110.55	27.806	3252.0	47.23	42.87	1.28	42.87	26.43	-10.41	-0.176	0.00	-10.41	26.43
0.68174	85.06	33.446	3089.0	29.89	1.47	149.36	28.729	3782.9	54.92	42.87	1.35	42.87	26.43	-10.41	-0.176	0.00	-10.41	26.43
0.77644	110.45	34.205	3498.3	30.46	1.49	185.29	29.377	4222.4	61.14	42.87	1.40	42.87	26.43	-10.41	-0.176	0.00	-10.41	26.43
0.90847	143.67	35.091	3910.4	31.12	1.51	249.66	29.612	4877.5	70.77	42.87	1.41	42.87	26.43	-10.41	-0.176	0.00	-10.41	26.43

0.0060" Ribbed 306" Pipe
 Report No. 350

Series

PEO

PER

S1:
 d = 0.308
 h = smooth
 RIR:
 d = 0.293
 h = 0.0060
 Rn 24.4

RUN 220
 DATE 7/12/93
 POLY R-309
 campaign 50
 nr 1,135

6/1res corrected R Corrected S

Q(L/A)	Ted(S1)	Ved(S1)	Reed(S1)	S(S1)	Sf(S1)	Ted(R1B)	Ved(R1B)	Reed(R1B)	Nr	S(R1B)	Sf(R1B)	Ved(S1B)	Sv(S1)	R	NR	P	6/1res corrected R Corrected S
0.00369	0.08	5.978	96.6			0.10	6.046	100.6	1.46			6.235				0.717	5.75
0.00486	0.11	6.893	110.6			0.13	7.056	113.7	1.65			7.107				0.816	-0.240
0.00604	0.16	7.725	122.9			0.16	7.828	127.7	1.85			8.021				0.900	6.13
0.00729	0.16	8.478	135.3			0.19	8.576	140.8	2.04			8.84				0.797	-0.315
0.00866	0.19	9.258	147.3			0.24	9.085	158.0	2.28			9.85				0.750	6.54
0.00983	0.21	9.832	157.6			0.27	9.640	169.2	2.45			10.374				0.749	7.02
0.01279	0.29	10.979	183.9			0.38	10.594	200.6	2.90			11.592				0.726	-0.046
0.01680	0.41	12.186	217.7			0.53	11.827	236.2	3.42			12.826				0.734	7.93
0.02121	0.54	13.323	251.4			0.71	12.901	273.4	3.96			13.784				0.731	8.56
0.02375	0.64	13.763	272.7			0.83	13.362	295.7	4.28			14.345				0.734	8.95
0.02809	0.79	14.594	305.7			1.00	14.394	326.3	4.72			15.09				0.758	9.72
0.03250	0.96	15.329	336.9			1.19	15.310	355.2	5.14	5.45	0.55	15.55	5.75	-0.240	-0.015	0.00	10.24
0.03610	1.14	15.683	366.0		5.83	1.37	15.812	382.2	5.53	5.81	0.58	16.06	6.13	-0.248	-0.015	0.00	10.54
0.03994	1.29	16.263	390.7		6.30	1.59	16.281	410.9	5.95	6.14	0.61	16.596	6.54	-0.315	-0.019	0.00	10.78
0.04592	1.59	16.932	431.6		6.79	1.88	17.180	447.8	6.48	6.87	0.67	17.226	7.02	-0.046	-0.003	0.00	11.32
0.05544	2.03	18.004	490.2		7.64	2.43	18.249	509.2	7.37	7.67	0.73	18.355	7.93	-0.106	-0.006	0.00	11.94
0.06461	2.49	18.966	542.3		8.43	2.95	19.316	560.6	8.12	8.54	0.78	19.153	8.56	0.163	0.009	0.00	12.47
0.07117	2.89	19.377	584.0		8.71	3.38	19.852	600.2	8.65	8.92	0.82	19.662	8.95	0.190	0.010	0.00	13.49
0.07752	3.24	19.939	616.1		9.18	3.86	20.240	639.1	9.25	9.17	0.83	20.188	9.37	0.052	0.003	0.00	14.07
0.08880	4.01	20.939	690.6		9.58	4.58	21.309	700.8	10.15	10.04	0.89	20.584	9.60	0.725	0.035	0.00	14.74
0.09227	4.30	20.600	703.9		9.61	4.94	21.301	723.9	10.38	9.98	0.88	20.737	9.72	0.564	0.027	0.00	15.09
0.10208	4.93	21.284	765.1		10.15	5.59	22.154	773.9	11.21	10.67	0.93	21.396	10.24	0.758	0.035	0.00	15.74
0.11005	5.47	21.780	805.0		10.56	6.14	22.795	809.8	11.73	11.21	0.97	21.817	10.58	0.978	0.045	0.00	16.25
0.12274	6.45	22.375	870.9		11.02	7.44	23.102	888.1	12.86	11.33	0.96	22.711	11.32	0.991	0.017	0.00	16.81
0.13290	7.12	23.065	905.9		11.64	8.31	23.664	929.7	13.46	11.80	0.99	23.467	11.99	0.197	0.008	0.00	17.32
0.14153	7.60	23.775	948.5		12.27	8.84	24.438	971.6	14.07	12.50	1.05	23.969	12.42	0.469	0.020	0.00	17.94
0.16086	9.27	24.462	1048.0		12.78	10.9	24.717	1092.1	15.81	12.59	1.04	25.24	13.49	-0.523	-0.021	0.00	18.49
0.17632	10.24	25.517	1101.3		13.75	11.16	24.656	1199.6	17.37	12.41	1.01	25.984	14.07	-1.318	-0.051	0.00	19.07
0.19370	11.95	25.939	1190.3		14.04	16.26	24.657	1318.5	19.09	12.32	1.00	26.549	14.47	-1.892	-0.071	0.00	19.74
0.23228	16.05	26.846	1379.5		14.69	23.17	24.769	1574.2	22.79	12.35	0.99	28.13	15.74	-3.361	-0.119	0.00	20.47
0.27081	19.95	28.073	1538.5		15.72	30.49	25.176	1806.3	26.16	12.75	1.03	28.877	16.25	-3.701	-0.128	0.00	21.25
0.30006	22.59	28.255	1637.5		15.80	34.58	25.320	1923.9	27.86	12.91	1.04	29.263	16.55	-3.963	-0.135	0.00	22.08
0.32851	27.89	28.504	1813.3		16.27	43.14	25.672	2149.7	31.13	13.31	1.08	30.046	17.12	-4.376	-0.146	0.00	22.94
0.40527	38.98	30.055	2151.9		17.12	61.76	26.469	2522.8	37.25	14.18	1.15	31.567	18.33	-5.099	-0.162	0.00	23.82
0.53908	60.53	31.977	2691.1		18.66	98.14	27.931	3244.0	46.94	15.72	1.29	33.747	20.10	-5.816	-0.172	0.00	24.77
0.61526	75.33	32.821	2992.5		19.32	123.24	28.447	3635.3	52.64	16.25	1.33	34.615	20.77	-6.168	-0.178	0.00	25.74
0.71019	93.24	34.053	3330.4		20.36	159.12	28.898	4132.1	59.83	16.69	1.38	35.172	21.11	-6.274	-0.177	0.00	26.77
0.80479	115.21	34.715	3701.8		20.84	201.01	29.136	4643.9	67.24	16.89	1.38	35.522	21.28	-6.416	-0.180	0.00	27.82
0.89907	140.41	35.130	4084.3		21.09	257.66	29.090	5193.1	75.20	16.78	1.36	35.925	21.46	-6.835	-0.190	0.00	28.97
1.01178	174.33	35.480	4537.6		21.25	320.57	29.006	5844.0	84.62	16.61	1.34	36.368	21.70	-7.362	-0.202	0.00	30.16

0.0000" Ribbed 0.300" Pipe
Resistivity = 350

Series PEO

PWE
S1:
d = 0.300
h = smooth
RIR:
d = 0.293
h = 0.0060
RA, 24.4

P-309
RUN
DATE 7/11/93
POLY P-309
c-wagon
W 1.251

Q(LA)	Tim(S1)	1/Amp(S1)	Resp(S1)	S(S1)	SF(S1)	Tim(RIB)	1/Amp(RIB)	Resp(RIB)	No	S(RIB)	SF(RIB)	1/Amp(S1M)	S(S1)	R	W	P	d/Pres	corrected R	corrected S
0.00348	0.08	5.604	89.5	5.72	0.58	0.10	5.611	91.9	1.36	5.86	0.59	5.86	5.98	-0.057	-0.004	0.806	0.00	-0.057	5.98
0.00440	0.10	6.291	101.0	6.19	0.62	0.13	6.333	105.5	1.53	6.48	0.62	6.48	6.48	-0.192	-0.012	0.795	0.00	-0.192	6.48
0.00531	0.13	6.942	110.9	6.86	0.68	0.15	6.933	115.9	1.68	7.09	0.68	7.09	7.09	-0.069	-0.004	0.801	0.00	-0.069	7.09
0.00663	0.16	7.755	124.0	7.70	0.75	0.19	7.837	129.0	1.87	7.94	0.76	7.94	7.94	0.213	0.012	0.816	0.00	0.213	7.94
0.00806	0.19	8.564	136.8	8.86	0.84	0.23	8.644	141.5	2.06	8.85	0.85	8.85	8.85	0.151	0.008	0.815	0.00	0.151	8.85
0.00961	0.23	9.351	149.9	9.35	0.88	0.27	9.396	156.8	2.27	9.22	0.85	9.22	9.22	0.416	0.021	0.825	0.00	0.416	9.22
0.01220	0.29	10.419	171.2	10.41	0.96	0.36	10.427	179.8	2.60	9.61	0.88	9.61	9.61	0.536	0.027	0.830	0.00	0.536	9.61
0.01694	0.43	11.941	207.7	11.94	0.98	0.54	11.749	221.9	3.21	10.15	0.91	10.15	10.15	0.758	0.037	0.845	0.00	0.758	9.65
0.02106	0.59	12.658	244.0	12.65	0.98	0.72	12.670	256.3	3.71	10.18	0.90	10.18	10.18	0.439	0.039	0.842	0.00	0.439	10.03
0.02392	0.67	13.485	260.5	13.48	0.92	0.81	13.430	274.9	3.98	10.60	0.94	10.60	10.60	0.768	0.036	0.838	0.00	0.768	10.13
0.02698	0.90	14.156	301.0	14.15	1.00	1.05	14.449	310.0	4.49	11.65	1.01	11.65	11.65	0.900	0.034	0.839	0.00	0.900	11.48
0.03285	1.03	15.000	322.3	15.00	1.00	1.22	15.214	334.0	4.84	11.88	1.02	11.88	11.88	0.335	0.014	0.817	0.00	0.335	11.92
0.03750	1.25	15.524	355.9	15.52	1.03	1.48	15.786	367.9	5.33	12.41	1.04	12.41	12.41	0.178	0.007	0.809	0.00	0.178	12.62
0.04117	1.40	16.094	377.2	16.09	1.08	1.68	16.261	392.4	5.68	12.08	1.01	12.08	12.08	0.291	0.012	0.782	0.00	0.291	12.76
0.04752	1.69	16.927	414.3	16.92	1.08	2.01	17.158	429.6	6.22	12.08	1.01	12.08	12.08	0.999	0.039	0.767	0.00	0.999	13.65
0.05766	2.20	17.997	473.0	17.99	1.11	2.56	18.416	485.9	7.04	12.28	1.01	12.28	12.28	1.865	0.071	0.703	0.00	1.865	14.21
0.06706	2.72	18.830	526.0	18.83	1.17	3.17	19.254	540.7	7.83	12.02	0.98	12.02	12.02	-2.030	-0.076	0.707	0.00	-2.030	14.69
0.07405	3.10	19.416	561.1	19.41	1.18	3.57	20.045	573.0	8.30	12.40	1.00	12.40	12.40	-2.846	-0.104	0.663	0.00	-2.846	15.11
0.08085	3.53	19.926	599.4	19.92	1.21	4.04	20.572	610.2	8.84	12.30	0.99	12.30	12.30	-4.049	-0.140	0.633	0.00	-4.049	16.41
0.09021	4.18	20.434	651.0	20.43	1.24	4.70	21.278	657.1	9.51	12.55	1.01	12.55	12.55	-5.305	-0.171	0.593	0.00	-5.305	18.82
0.09688	4.62	20.828	681.4	20.82	1.28	5.32	21.436	686.0	10.08	12.82	1.03	12.82	12.82	-5.996	-0.186	0.575	0.00	-5.996	19.68
0.10120	4.95	21.055	702.3	21.05	1.32	5.54	21.893	706.5	10.23	13.00	1.06	13.00	13.00	-6.516	-0.191	0.569	0.00	-6.516	20.96
0.11868	6.74	22.352	782.3	22.35	1.38	6.78	23.179	788.4	11.42	13.30	1.14	13.30	13.30	-6.766	-0.189	0.568	0.00	-6.766	21.70
0.12657	6.67	22.685	823.8	22.68	1.42	7.52	23.539	832.1	12.05	13.74	1.19	13.74	13.74	-7.317	-0.197	0.562	0.00	-7.317	22.90
0.13572	7.40	23.100	868.3	23.10	1.45	8.61	23.659	891.2	12.90	14.12	1.26	14.12	14.12						
0.15313	8.80	23.898	945.9	23.89	1.48	10.34	24.359	975.5	14.56	14.56	1.31	14.56	14.56						
0.15573	8.99	24.039	958.1	24.03	1.49	10.94	24.081	1005.3	15.87	15.87	1.35	15.87	15.87						
0.17246	10.53	24.602	1035.1	24.60	1.53	13.05	24.418	1096.3	15.87	15.87	1.35	15.87	15.87						
0.19177	12.04	25.585	1107.4	25.58	1.57	16.30	24.295	1225.8	17.75	17.75	1.40	17.75	17.75						
0.21107	14.15	26.974	1200.8	26.97	1.58	19.03	24.747	1324.9	19.18	19.18	1.44	19.18	19.18						
0.23036	16.09	26.586	1280.4	26.58	1.59	23.10	24.517	1459.5	21.13	21.13	1.44	21.13	21.13						
0.24963	18.37	26.963	1368.3	26.96	1.62	26.69	24.718	1568.9	22.72	22.72	1.44	22.72	22.72						
0.26814	23.16	27.717	1536.7	27.71	1.62	34.83	24.974	1782.7	25.96	25.96	1.44	25.96	25.96						
0.32659	28.07	28.535	1691.8	28.53	1.62	43.91	25.211	2012.8	29.15	29.15	1.44	29.15	29.15						
0.38610	36.43	29.614	1927.7	29.61	1.62	59.38	25.628	2341.4	33.90	33.90	1.44	33.90	33.90						
0.46269	49.08	30.574	2237.8	30.57	1.35	81.16	26.271	2737.6	39.64	39.64	1.44	39.64	39.64						
0.52000	59.05	31.327	2454.8	31.32	1.38	98.38	26.816	3014.4	43.65	43.65	1.44	43.65	43.65						
0.59623	73.25	32.251	2733.5	32.25	1.42	121.75	27.640	3352.7	48.55	48.55	1.26	48.55	48.55						
0.65327	84.31	32.937	2932.6	32.93	1.45	141.00	28.141	3607.9	52.24	52.24	1.31	52.24	52.24						
0.74807	104.32	33.908	3260.5	33.90	1.48	174.75	28.946	4014.7	58.13	58.13	1.37	58.13	58.13						
0.89907	140.14	35.161	3770.3	35.16	1.53	237.17	29.863	4666.2	67.57	67.57	1.44	67.57	67.57						

0.0060" Ribbed 0.306" Pipe
 Req./ft. = 350

Series
PAM

N-300
 RUN 231
 DATE 7/27/93
 POLY M-300
 c 100
 w 1.178
 Nn 24.4

Q (L/A)	Td(S2)	1/A(S2)	Re-1/2(S2)	S'(S2)	S'(S2)	1/A(R3)	Re-1/2(R3)	h	S(R3)	Sf(R3)	1/A(S2)h	S1(S2)	R	RF	P	Δ/ftes	connected R	connected S
0.00410	0.09	6.311	100.8	4.99	0.51	0.10	6.567	102.0	5.58	0.56	6.39	5.18	0.477	0.032	0.852	0.00	0.477	5.18
0.00539	0.12	7.223	116.0	5.78	0.58	0.13	7.583	116.3	6.21	0.62	7.25	6.04	0.256	0.016	0.834	0.00	0.256	6.04
0.00627	0.14	7.800	125.0	6.75	0.67	0.16	8.071	127.2	6.82	0.67	7.94	7.16	-0.243	-0.014	0.801	0.00	-0.243	7.16
0.00831	0.18	9.020	143.6	7.83	0.76	0.21	9.228	147.8	7.70	0.73	9.27	8.02	-0.188	-0.010	0.786	0.00	-0.188	8.02
0.00989	0.22	9.811	157.2	8.29	0.79	0.26	9.669	168.0	8.47	0.79	10.39	18.38	0.174	0.009	0.813	0.00	0.174	8.47
0.01271	0.28	10.989	180.5	8.76	0.83	0.34	11.215	186.4	8.96	0.83	11.07	18.59	0.106	0.005	0.816	0.00	0.106	8.96
0.01569	0.42	11.153	220.0	9.37	0.88	0.58	10.571	244.4	9.40	0.86	11.37	9.54	0.086	0.004	0.804	0.00	0.086	9.54
0.01952	0.60	11.658	262.0	9.88	0.90	0.69	12.099	265.8	10.09	0.89	11.83	10.10	0.284	0.013	0.821	0.00	0.284	10.10
0.02284	0.70	12.563	282.1	11.08	0.99	0.98	13.927	318.7	11.32	0.98	12.7	11.24	0.424	0.019	0.824	0.00	0.424	11.24
0.02652	0.87	13.329	316.2	12.00	1.05	1.17	14.788	347.6	11.99	1.01	14.59	12.65	0.375	0.003	0.807	0.00	0.375	12.65
0.03115	1.00	14.423	338.5	12.36	1.07	1.34	15.537	372.2	12.23	1.03	15.06	13.46	-0.807	-0.038	0.739	0.00	-0.807	13.46
0.03502	1.19	14.861	369.6	12.96	1.12	1.48	16.266	392.2	12.28	1.01	16.42	14.40	-0.954	-0.059	0.742	0.00	-0.954	14.40
0.03859	1.29	15.720	385.4	13.12	1.12	1.79	17.057	431.3	12.33	1.03	16.01	15.01	-1.549	-0.059	0.742	0.00	-1.549	15.01
0.04450	1.50	16.826	415.2	13.38	1.14	2.30	18.192	489.0	12.39	1.00	18.38	16.95	-3.046	-0.107	0.669	0.00	-3.046	16.95
0.05386	1.89	18.108	466.6	14.33	1.19	2.79	19.164	538.0	12.56	1.02	18.59	17.76	-4.518	-0.147	0.622	0.00	-4.518	17.76
0.06233	2.37	18.759	522.0	14.33	1.24	3.21	19.805	577.3	12.92	1.04	20.34	18.72	-5.221	-0.164	0.599	0.00	-5.221	18.72
0.06914	2.73	19.354	561.1	14.33	1.24	3.64	20.386	615.8	13.27	1.07	21.09	19.37	-5.513	-0.169	0.591	0.00	-5.513	19.37
0.07577	3.06	20.066	594.1	14.33	1.24	4.74	21.374	703.9	13.75	1.11	22.44	20.91	-6.111	-0.181	0.580	0.00	-6.111	20.91
0.08072	4.07	20.822	686.2	14.33	1.24	6.03	22.864	794.3	14.33	1.16	23.67	22.65	-6.615	-0.191	0.572	0.00	-6.615	20.91
0.09460	5.19	22.239	775.6	14.33	1.24	8.22	23.842	926.5	14.33	1.16	24.22	23.67	-7.126	-0.200	0.547	0.00	-7.126	21.74
0.13323	6.94	23.406	896.4	14.33	1.24	9.18	24.295	982.3	14.33	1.16	25.24	24.22	-7.551	-0.208	0.531	0.00	-7.551	21.74
0.14346	7.74	23.874	949.4	14.33	1.24	11.83	24.433	1066.4	14.33	1.16	26.42	25.24	-7.551	-0.208	0.531	0.00	-7.551	21.74
0.16373	9.89	25.101	1073.5	14.33	1.24	12.82	24.446	1160.6	14.33	1.16	26.42	25.24	-7.551	-0.208	0.531	0.00	-7.551	21.74
0.17052	9.89	25.491	1176.9	14.33	1.24	15.34	24.871	1270.0	14.33	1.16	26.42	25.24	-7.551	-0.208	0.531	0.00	-7.551	21.74
0.18984	11.89	25.491	1255.5	14.33	1.24	18.77	24.775	1404.7	14.33	1.16	26.42	25.24	-7.551	-0.208	0.531	0.00	-7.551	21.74
0.20914	13.53	26.325	1431.7	14.33	1.24	25.16	25.344	1627.0	14.33	1.16	26.42	25.24	-7.551	-0.208	0.531	0.00	-7.551	21.74
0.24770	17.57	27.353	1777.6	14.33	1.24	32.71	25.683	1855.5	14.33	1.16	26.42	25.24	-7.551	-0.208	0.531	0.00	-7.551	21.74
0.28621	21.99	28.254	1602.0	14.33	1.24	41.66	26.122	2094.4	14.33	1.16	26.42	25.24	-7.551	-0.208	0.531	0.00	-7.551	21.74
0.32651	27.07	29.230	1777.6	14.33	1.24	55.88	26.799	2425.9	14.33	1.16	26.42	25.24	-7.551	-0.208	0.531	0.00	-7.551	21.74
0.38601	34.99	30.368	2021.1	14.33	1.24	70.66	27.197	3027.9	14.33	1.16	26.42	25.24	-7.551	-0.208	0.531	0.00	-7.551	21.74
0.44547	43.58	31.238	2255.8	14.33	1.24	87.04	27.659	3728.0	14.33	1.16	26.42	25.24	-7.551	-0.208	0.531	0.00	-7.551	21.74
0.49282	52.72	32.057	2481.2	14.33	1.24	105.48	27.985	3332.5	14.33	1.16	26.42	25.24	-7.551	-0.208	0.531	0.00	-7.551	21.74
0.55005	63.04	32.655	2712.5	14.33	1.24	146.60	28.574	3928.6	14.33	1.16	26.42	25.24	-7.551	-0.208	0.531	0.00	-7.551	21.74
0.67415	83.79	34.094	3127.2	14.33	1.24	187.35	28.829	4437.9	14.33	1.16	26.42	25.24	-7.551	-0.208	0.531	0.00	-7.551	21.74
0.76888	103.90	34.920	3479.7	14.33	1.24	255.10	28.601	5556.1	14.33	1.16	26.42	25.24	-7.551	-0.208	0.531	0.00	-7.551	21.74
0.95735	151.13	36.052	4186.4	14.33	1.24	295.10	28.601	5556.1	14.33	1.16	26.42	25.24	-7.551	-0.208	0.531	0.00	-7.551	21.74

PIPE: 10.21 mm

RIBLETS: 0.11 mm

POLYMERS:

NONE (Solvent)

PEO N-750

N60K

W-301

P-309

0.0045" Ribbed 0.402" Pipe
Reed/crit= 350

Series DW

PIPE
S2:
d = 0.402
h = smooth
R2A:
g = 0.391
h = 0.0045
R/h: 43.5

RUN 036-038
DATE 10/1/91
POLY -
c wppm -
nr 1.000

Q (l/s)	Tw(S2)	1/sgt(S2)	Reagf(S2)	S(S2)	SF(S2)	Tw(R2A)	1/sgt(R2A)	Reagf(R2A)	h*	S(R2A)	SF(R2A)	R	RF	P
0.00102	0.01	2.913	46.4											
0.00136	0.01	3.323	53.2											
0.00147	0.01	3.477	55.5											
0.00155	0.01	3.593	57.2											
0.00201	0.02	4.065	65.0											
0.00216	0.02	4.221	67.5											
0.00225	0.02	4.322	69.0											
0.00249	0.02	4.505	71.9											
0.00256	0.02	4.591	73.2											
0.00277	0.03	4.789	76.1											
0.00304	0.03	4.972	79.5											
0.00342	0.03	5.324	84.9											
0.00346	0.03	5.337	85.2											
0.00367	0.03	5.500	87.7											
0.00377	0.03	5.571	87.8											
0.00379	0.03	5.580	88.1											
0.00411	0.04	5.815	93.2											
0.00424	0.04	5.906	94.3											
0.00479	0.04	6.240	99.6											
0.00494	0.04	6.372	101.8											
0.00502	0.05	6.384	102.1											
0.00542	0.05	6.675	106.6											
0.00543	0.05	6.712	107.0											
0.00560	0.05	6.803	108.4											
0.00585	0.05	6.891	109.8											
0.00597	0.05	7.009	111.8											
0.00646	0.06	7.239	115.6											
0.00697	0.06	7.562	120.7											
0.00715	0.06	7.693	122.6											
0.00723	0.07	7.652	122.3											
0.00733	0.07	7.779	123.7											
0.00772	0.07	7.921	127.7											
0.00774	0.07	7.977	127.5											
0.00778	0.07	7.911	127.3											
0.00832	0.08	8.282	132.5											
0.00867	0.08	8.340	134.6											
0.00885	0.08	8.529	136.5											
0.00888	0.08	8.481	137.4											
0.00932	0.09	8.649	139.4											
0.00944	0.09	8.786	141.4											
0.01014	0.09	9.042	145.2											
0.01074	0.10	9.321	151.6											
0.01079	0.10	9.350	152.1											
0.01088	0.10	9.294	151.6											
0.01150	0.11	9.593	155.8											
0.01191	0.11	9.813	160.0											
0.01209	0.11	9.827	161.8											
0.01377	0.12	10.478	172.9											
0.00231	0.02	4.381	69.6											
0.00259	0.02	4.618	74.0											
0.00353	0.03	5.414	86.0											
0.00559	0.05	6.809	108.2											
0.00720	0.07	7.701	123.0											
0.01031	0.09	9.198	147.5											
0.01282	0.12	10.190	165.4											
0.01662	0.17	11.054	197.5											

RUN 40
DATE 10/27/92
POLY -
c wppm -
nr 1.000

RUN	DATE	POLY	c	temp	hr
0.02184	0.38	9.642	297.4	-0.09	-0.01
0.02819	0.61	9.820	377.0	-0.02	0.00
0.03383	0.83	10.143	437.9	-0.01	0.00
0.03938	1.07	10.377	498.2	-0.08	-0.01
0.04864	1.56	10.628	600.9	-0.10	-0.01
0.04876	1.57	10.620	602.7	-0.05	0.00
0.04985	1.56	10.665	601.3	-0.03	0.00
0.05287	2.41	11.063	746.1	-0.07	-0.01
0.05339	2.46	11.035	754.1	-0.02	0.00
0.06016	3.66	11.435	926.4	0.04	0.00
0.09140	4.56	11.689	1026.6	0.06	0.00
0.09956	5.28	11.831	1104.8	-0.02	0.00
0.11042	6.39	11.923	1215.9	0.03	0.00
0.11617	6.93	12.048	1271.9	0.00	0.00
0.01617	0.16	11.046	192.1	-0.02	0.00
0.01775	0.22	10.265	227.0	-0.12	-0.01
0.01880	0.28	9.776	252.5	-0.08	-0.01
0.02023	0.34	9.505	278.4	-0.04	0.00
0.02149	0.38	9.524	295.9	0.06	0.01
0.02377	0.45	9.633	323.3	-0.11	-0.01
0.02652	0.55	9.783	355.0	-0.10	-0.01
0.03157	0.74	10.038	411.9	-0.02	0.00
0.03633	0.95	10.162	468.3	-0.08	-0.01
0.04093	1.16	10.375	518.0	-0.04	0.00
0.04403	1.30	10.526	550.4	-0.05	-0.01
0.04476	1.35	10.533	559.0	0.06	0.01
0.04945	1.57	10.780	603.6	-0.11	-0.01
0.05625	2.01	10.826	682.1	-0.10	-0.01
0.07267	3.13	11.216	850.7	-0.10	-0.01
0.08540	4.14	11.463	978.1	-0.10	-0.01
0.09742	5.20	11.661	1096.9	-0.10	-0.01
0.10900	6.26	11.696	1205.7	-0.03	0.00
0.11452	6.81	11.978	1271.5	-0.04	0.00
0.29066	35.79	13.266	2869.8	-0.17	-0.01
0.96885	298.25	15.317	8255.6	0.05	0.00
0.77508	201.31	14.916	6782.4	-0.01	0.00
0.58131	121.03	14.427	5259.0	-0.06	0.00
0.48443	87.55	14.136	4472.8	-0.07	0.00
0.58131	121.35	14.405	5504.5	-0.16	-0.01
0.48443	87.48	14.138	4678.9	-0.14	-0.01
0.39754	58.15	13.872	3829.8	-0.06	0.00
0.29066	35.09	13.393	2983.8	-0.11	-0.01
0.87197	244.62	15.218	7905.1	0.03	0.00
0.77508	198.01	15.035	7120.4	0.02	0.00
0.67820	156.36	14.804	6327.4	0.00	0.00
0.29569	36.65	13.336	2843.0	-0.08	-0.01
0.31003	38.73	13.599	3098.9	0.03	0.00
0.32941	44.85	13.431	3144.9	-0.16	-0.01
0.34879	48.32	13.701	3264.2	0.05	0.00
0.34879	48.63	13.653	3464.5	-0.11	-0.01
0.42629	69.60	13.949	4184.7	-0.12	-0.01
0.46567	74.93	14.058	4664.9	0.02	0.00
0.46567	75.02	14.047	4268.2	-0.07	-0.01
0.54256	106.79	14.332	5133.9	-0.11	-0.01
0.55612	112.29	14.330	4976.2	-0.06	0.00
0.56213	112.68	14.467	5212.9	-0.01	0.00
0.58131	121.60	14.395	5178.2	-0.06	0.00
0.61813	133.64	14.596	5743.3	-0.04	0.00

RUN 41
DATE 10/28/91
POLY -
c 1.000

RUN 42
DATE 10/29/91
POLY -
c 1.000

0.62006	135.26	14.555	5704.7	-0.07	0.00
0.67620	157.69	14.744	6152.6	-0.01	0.00
0.77508	200.07	14.960	6922.0	0.00	0.00
0.77508	200.71	14.935	7054.6	-0.06	0.00
0.87197	246.76	15.153	7822.2	-0.02	0.00
0.96885	297.58	15.332	8589.9	0.00	0.00
0.07009	2.99	11.077	805.6	-0.15	-0.01
0.07463	3.77	11.269	843.4	-0.03	0.00
0.07643	3.57	11.331	881.2	-0.05	0.00
0.08615	4.20	11.472	956.0	-0.05	0.00
0.09226	4.72	11.598	1012.8	-0.02	0.00
0.09546	5.05	11.663	1047.4	-0.08	-0.01
0.11074	6.43	11.978	1176.3	0.05	0.00
0.11846	7.79	11.977	1256.2	-0.02	0.00
0.12820	8.55	11.974	1363.1	-0.16	-0.01
0.12834	8.47	12.044	1353.3	-0.08	-0.01
0.14458	10.50	12.185	1510.7	-0.13	-0.01
0.14468	10.31	12.318	1493.8	0.02	0.00
0.15658	12.36	12.160	1639.3	-0.30	-0.02
0.15675	12.03	12.341	1617.0	-0.09	-0.01
0.15735	12.07	12.401	1619.5	-0.04	0.00
0.18925	16.68	12.654	1908.6	-0.07	-0.01
0.25403	29.26	12.864	2521.9	-0.34	-0.03
0.29441	36.28	13.347	2608.2	-0.05	0.00
0.18984	17.06	12.550	1925.8	-0.19	-0.02
0.20775	20.07	12.664	2088.6	-0.22	-0.02
0.16393	12.57	12.622	1761.4	0.04	0.00
0.17633	14.32	12.722	1873.3	0.03	0.00
0.20650	19.42	12.915	2189.4	-0.05	0.00
0.23466	23.84	13.120	2411.7	-0.01	0.00
0.26798	30.06	13.344	2701.7	0.02	0.00
0.27783	31.74	13.221	2721.9	-0.12	-0.01
0.31991	42.28	13.432	3141.5	-0.16	-0.01
0.36506	53.04	13.684	3584.8	-0.13	-0.01
0.40866	64.70	13.871	3886.1	-0.09	-0.01
0.43637	73.28	13.917	4133.7	-0.15	-0.01
0.49469	88.87	14.327	4554.3	0.09	0.01
0.50574	95.44	14.134	4719.8	-0.16	-0.01
0.53364	105.06	14.215	4951.9	-0.16	-0.01
0.57666	120.73	14.328	5408.4	-0.20	-0.01
0.65010	148.67	14.557	5904.5	-0.13	-0.01
0.68905	164.01	14.689	6216.3	-0.09	-0.01
0.73187	182.90	14.773	6657.0	-0.12	-0.01
0.82895	226.10	15.050	7401.5	-0.03	0.00
0.94540	286.88	15.238	8337.1	-0.05	0.00
1.02311	327.17	15.442	8903.3	0.04	0.00
0.00635	0.06	7.253	116.2		
0.01095	0.10	9.453	154.2		
0.01560	0.15	11.033	188.2		
0.01660	0.16	11.182	197.7		
0.01764	0.19	11.141	210.8		
0.01851	0.23	10.488	235.0		
0.01909	0.25	10.374	245.0		
0.02255	0.40	9.753	307.9		
0.02477	0.48	9.773	337.5		
0.02980	0.66	10.016	396.2	0.02	0.00
0.03482	0.86	10.236	453.4	0.01	0.00
0.03902	1.06	10.367	502.3	-0.04	0.00

RUN 43
DATE 10/30/91
POLY -
c. wppm -
IN 1.000

RUN 44
DATE 10/30/91
POLY -
c. wppm -
IN 1.000

RUN 45
DATE 10/30/91
POLY -
c. wppm -
IN 1.000

0.04285	1.24	10.525	543.3	-0.02	0.00	0.09	6.875	143.8	1.17	0.07	0.01	0.044	0.004	0.955
0.05898	2.12	11.070	710.9	0.06	0.01	0.12	10.136	165.9	1.35	0.04	0.00	0.023	0.002	0.878
0.06804	2.78	11.144	814.8	0.10	-0.01	0.14	10.976	180.3	1.47	0.03	0.00	0.031	0.003	0.875
0.07703	3.41	11.369	902.6	-0.03	0.00	0.16	11.504	192.9	1.57	0.03	0.00	0.040	0.004	0.876
0.08346	3.91	11.521	987.0	-0.02	0.00	0.20	11.301	213.3	1.73	0.03	0.00	0.006	0.001	0.871
0.09034						0.31	10.068	267.1	2.17	0.03	0.00	0.000	0.000	0.875
0.01228						0.41	9.748	305.8	2.49	0.02	0.00	0.016	0.001	0.896
0.01444						0.48	9.757	330.5	2.69	0.02	0.00	0.016	0.001	0.898
0.01617						0.55	9.852	356.5	2.90	0.02	0.00	0.033	0.003	0.876
0.01755						0.66	9.982	398.8	3.16	0.04	0.00	0.028	0.003	0.875
0.01957						0.77	10.132	421.8	3.43	0.03	0.00	0.055	0.005	0.879
0.02167						0.89	10.266	453.3	3.69	0.03	0.00	0.050	0.005	0.878
0.02342						0.99	10.324	478.1	3.89	0.01	0.00	0.045	0.004	0.878
0.02549						1.11	10.427	506.7	4.12	-0.01	0.00	-0.012	-0.001	0.869
0.02813						1.27	10.578	541.6	4.40	0.02	0.00	0.016	0.001	0.873
0.03097						1.41	10.612	570.3	4.64	0.02	0.00	0.033	0.003	0.876
0.03371						1.51	10.701	590.6	4.80	0.02	0.00	0.028	0.003	0.875
0.03576						1.80	10.769	608.1	4.94	0.00	0.00	0.055	0.005	0.879
0.04145						1.95	10.964	671.8	5.46	0.01	0.00	0.050	0.005	0.878
0.04380						2.20	11.064	713.5	5.80	0.00	0.00	0.045	0.004	0.878
0.04572						2.40	11.134	745.4	6.06	-0.01	0.00	0.059	0.005	0.880
0.04733						2.59	11.216	774.6	6.30	0.00	0.00	0.083	0.007	0.883
0.05065						3.16	11.307	805.4	6.55	0.02	0.00	0.070	0.006	0.881
0.05324						3.21	11.395	853.8	6.94	0.00	0.00	0.123	0.011	0.889
0.05703						4.21	11.586	924.5	7.52	0.03	0.00	0.136	0.012	0.891
0.05996						4.57	11.709	984.7	8.01	0.02	0.00	0.155	0.013	0.894
0.06277						5.01	11.848	1024.5	8.33	0.03	0.00	0.178	0.011	0.890
0.06585						5.42	11.924	1112.0	9.04	-0.03	0.00	0.140	0.012	0.891
0.07032						5.62	11.996	1125.2	9.15	0.02	0.00	0.191	0.016	0.899
0.07350						6.53	12.092	1185.8	9.64	-0.01	0.00	0.196	0.016	0.899
0.08351						7.31	12.160	1210.5	9.84	0.01	0.00	0.228	0.019	0.904
0.08759						7.34	12.195	1251.1	10.17	-0.04	0.00	0.205	0.017	0.901
0.09211						7.78	12.345	1316.7	10.71	-0.01	0.00	0.267	0.022	0.909
0.09646						8.64	12.504	1387.7	11.28	0.02	0.00	0.313	0.026	0.916
0.09882						8.94	12.513	1411.2	11.48	0.03	0.00	0.334	0.027	0.919
0.10735						8.93	12.555	1411.5	11.48	0.04	0.00	0.315	0.026	0.916
0.11417						9.44	12.606	1451.7	11.80	0.02	0.00	0.356	0.029	0.922
0.11474						9.98	12.559	1476.9	12.01	-0.01	0.00	0.359	0.029	0.911
0.11961						10.64	12.709	1540.4	12.53	-0.01	0.00	0.359	0.029	0.927
0.12114						10.98	12.730	1561.8	12.70	-0.02	0.00	0.356	0.029	0.921
0.12768						12.90	12.903	1696.6	13.80	-0.01	0.00	0.384	0.031	0.925
0.12999						12.84	12.962	1692.0	13.76	0.06	0.00	0.448	0.036	0.934
0.13031						13.99	13.061	1766.3	14.36	0.09	0.01	0.473	0.038	0.937
0.13457						10.82	12.788	1599.9	13.01	-0.01	0.00	0.372	0.030	0.923
0.13779						13.59	13.086	1781.9	14.57	0.09	0.01	0.473	0.038	0.937
0.14398						16.16	13.117	1952.7	15.88	0.01	0.00	0.354	0.028	0.919
0.14655						18.65	13.121	2095.6	17.04	-0.05	0.00	0.236	0.018	0.903
0.15181														
0.16100														
0.16131														
0.16371														
0.16761														
0.18321														
0.19685														

0.21244	1.000	0.2155	13.172	2251.6	18.31	-0.04	0.00	0.162	0.012	0.892
0.22998		25.18	13.193	2431.5	19.77	-0.03	0.00	0.049	0.004	0.877
0.24752		29.90	13.253	2602.2	21.16	0.03	0.00	-0.008	-0.001	0.869
0.26117		32.19	13.249	2743.8	22.31	0.03	0.00	-0.104	-0.008	0.857
0.27676		36.05	13.298	2901.7	23.60	0.06	0.00	-0.163	-0.014	0.847
0.29235		41.01	13.139	3085.6	25.09	-0.06	0.00	-0.418	-0.031	0.818
0.31099		45.48	13.235	3254.1	26.46	0.04	0.00	-0.415	-0.030	0.818
0.33133		52.64	13.145	3486.8	28.35	-0.05	0.00	-0.624	-0.045	0.793
0.35082		58.84	13.166	3626.7	29.49	-0.03	0.00	-0.672	-0.049	0.788
0.25922	134	32.39	13.298	2753.1	22.39	0.08	0.01	-0.061	-0.005	0.862
0.27676	11/27/92	37.68	13.165	2966.6	24.12	-0.04	0.00	-0.374	-0.024	0.829
0.27676		37.24	13.243	2959.3	24.06	0.03	0.00	-0.742	-0.016	0.839
0.29430		42.50	13.180	3147.4	25.59	-0.02	0.00	-0.411	-0.030	0.819
0.31184	1.000	47.75	13.177	3333.1	27.10	-0.02	0.00	-0.515	-0.039	0.806
0.31574		48.84	13.191	3387.1	27.54	0.00	0.00	-0.528	-0.038	0.805
0.32938		52.55	13.267	3493.3	28.41	0.07	0.01	-0.506	-0.037	0.808
0.34692		59.79	13.101	3722.1	30.27	-0.10	-0.01	-0.782	-0.056	0.775
0.35472		61.92	13.162	3811.6	31.00	-0.04	0.00	-0.767	-0.055	0.778
0.36057		63.69	13.192	3865.3	31.43	-0.01	0.00	-0.757	-0.054	0.779
0.37031		64.50	13.260	3921.7	31.89	0.05	0.00	-0.714	-0.051	0.784
0.38980		74.47	13.189	4146.9	33.72	-0.03	0.00	-0.882	-0.063	0.765
0.39980		74.37	13.198	4176.0	33.96	-0.07	0.00	-0.885	-0.063	0.764
0.40929		82.32	13.172	4354.1	35.41	0.06	0.00	-0.983	-0.069	0.754
0.42878		88.60	13.300	4555.2	37.04	0.06	0.00	-0.934	-0.066	0.760
0.44827		97.33	13.268	4732.0	38.48	0.01	0.00	-1.032	-0.072	0.749
0.45802		99.94	13.377	4831.9	39.29	0.11	0.01	-0.959	-0.067	0.758
0.46776		105.72	13.284	4927.7	40.07	0.01	0.00	-1.087	-0.076	0.744
0.50674		125.03	13.233	5354.6	43.54	-0.07	-0.01	-1.282	-0.088	0.723
0.50674		122.36	13.376	5349.8	43.50	0.07	0.01	-1.138	-0.078	0.739
0.54376		152.76	13.307	5914.1	48.09	-0.04	0.00	-1.380	-0.094	0.715
0.57496		156.71	13.411	6023.5	48.98	0.05	0.00	-1.309	-0.089	0.723
0.60224		174.04	13.330	6307.9	51.29	-0.05	0.00	-1.469	-0.099	0.706
0.60419		173.31	13.400	6366.3	51.77	0.01	0.00	-1.415	-0.096	0.712
0.66266		208.47	13.402	6899.5	56.11	-0.03	0.00	-1.554	-0.104	0.699
0.66266		208.81	13.454	6951.3	56.53	0.02	0.00	-1.514	-0.101	0.703
0.67241		212.12	13.481	6995.4	56.89	0.04	0.00	-1.499	-0.100	0.705
0.72113		245.07	13.451	7477.0	60.80	-0.03	0.00	-1.644	-0.109	0.691
0.74062		255.59	13.527	7723.4	62.81	0.02	0.00	-1.625	-0.107	0.694
0.76011		270.71	13.490	7854.5	63.87	-0.03	0.00	-1.690	-0.111	0.687
0.79909		295.72	13.568	8298.2	67.48	0.01	0.00	-1.708	-0.112	0.687
0.81663		309.62	13.552	8392.6	68.25	-0.02	0.00	-1.744	-0.114	0.683
0.87510		352.11	13.618	8941.6	72.71	-0.01	0.00	-1.788	-0.116	0.680
0.87705		350.83	13.672	9007.8	73.25	0.04	0.00	-1.746	-0.113	0.684
0.93552		399.15	13.674	9498.9	77.24	-0.01	0.00	-1.837	-0.118	0.676
0.97450		431.20	13.705	9705.6	78.97	0.00	0.00	-1.843	-0.119	0.676
0.00255	126-127	0.02	4.729	74.0						0.892
0.00350		0.03	5.518	87.0						0.886
0.00400		0.04	5.851	92.2						0.886
0.00431		0.04	6.114	96.5						0.884
0.00466		0.05	6.364	100.6						0.883
0.00571	1.000	0.06	6.996	110.2						0.886
0.00589		0.06	7.131	113.2						0.879
0.00645		0.06	7.513	117.4						0.893
0.00694		0.07	7.547	122.6						0.871
0.00725		0.07	7.896	126.1						0.873
0.00753		0.07	8.050	127.8						0.879
0.00767		0.08	8.086	130.2						0.867
0.00800		0.08	8.166	132.3						0.862

0.890
0.871
0.859
0.862
0.878
0.850
0.860
0.901

131.0
135.9
141.9
147.5
146.3
155.5
161.8
159.1

R.354
B.489
R.726
9.106
9.201
9.471
9.964
10.270

0.08
0.08
0.09
0.10
0.10
0.11
0.12
0.12

0.00800
0.00845
0.00902
0.00984
0.00984
0.01079
0.01183
0.01193

0.0045" Ribbed/0.402" Pipe
 Riserfit= 350

Series

DW

PIPE

SZ:

d = 0.402

h = smooth

RZL

d = C.391

h = 0.0045

R/h 43.5

Q (L/h)	Tw(SZ)	1/avg(SZ)	Rmpf(SZ)	S'(SZ)	SF(SZ)	Tw(RZA)	1/avg(RZA)	Rmpf(RZA)	h*	S'(RZA)	SF(RZA)	R'	RF	P
0.01390	0.13	10.674	172.9	0.14	0.01	0.14	10.661	177.8	1.45	-0.06	-0.01	-0.003	-0.004	0.872
0.01681	0.16	11.545	193.2	0.16	0.00	0.18	11.557	198.3	1.61	-0.05	0.00	-0.015	-0.001	0.876
0.02022	0.31	9.975	268.6	0.36	0.00	0.36	9.694	284.2	2.31	-0.05	0.00	0.021	0.001	0.884
0.02295	0.40	9.843	309.2	0.45	0.00	0.45	9.868	316.9	2.68	-0.06	0.00	0.002	0.000	0.887
0.02544	0.48	9.996	337.4	0.54	0.00	0.54	9.927	349.0	2.84	-0.01	0.00	0.057	0.004	0.893
0.03097	0.69	10.163	404.1	0.79	0.01	0.79	10.032	420.6	3.42	-0.08	-0.01	0.103	0.007	0.899
0.03625	0.92	10.320	465.7	1.02	0.00	1.02	10.314	478.7	3.89	-0.02	0.00	-0.006	0.000	0.873
0.04538	1.38	10.619	566.6	1.51	0.00	1.51	10.641	580.9	4.72	-0.06	0.00	-0.015	-0.001	0.878
0.04547	1.37	10.613	567.9	1.50	0.00	1.50	10.678	580.0	4.72	-0.01	0.00	0.021	0.001	0.884
0.05889	2.15	10.964	712.1	-0.05	0.00	2.38	11.046	726.1	5.90	-0.06	0.00	0.002	0.000	0.887
0.06859	2.79	11.199	812.0	-0.04	0.00	3.04	11.323	825.1	6.71	-0.01	0.00	0.057	0.004	0.893
0.07676	3.31	11.353	864.8	-0.03	0.00	3.59	11.513	896.4	7.29	0.02	0.00	0.103	0.007	0.899
0.08510	4.12	11.572	965.6	0.00	0.00	4.48	11.710	1001.2	8.14	-0.01	0.00	0.113	0.007	0.898
0.09513	5.01	11.713	1068.5	-0.03	0.00	5.39	11.920	1098.9	8.94	-0.01	0.00	0.157	0.010	0.905
0.10320	5.68	11.818	1159.8	-0.04	0.00	6.04	12.099	1163.9	9.48	0.04	0.00	0.235	0.015	0.916
0.10501	5.94	11.866	1185.8	-0.03	0.00	6.36	12.097	1194.9	9.72	-0.02	0.00	0.187	0.012	0.908
0.11247	6.55	11.988	1247.8	0.00	0.00	7.02	12.215	1258.1	10.23	-0.03	0.00	0.216	0.013	0.907
0.11888	7.27	12.023	1314.9	-0.05	0.00	7.72	12.320	1318.3	10.72	-0.04	0.00	0.240	0.015	0.917
0.12612	8.09	12.219	1487.5	-0.07	-0.01	9.70	12.651	1476.0	12.00	0.03	0.00	0.375	0.022	0.937
0.14812	10.86	12.261	1803.5	-0.16	-0.01	11.34	12.661	1596.2	12.97	-0.13	-0.01	0.250	0.015	0.932
0.17172	13.82	12.597	1809.4	-0.03	0.00	14.27	13.084	1789.7	14.66	0.09	0.01	0.473	0.028	0.943
0.17541	14.94	12.377	1880.9	-0.32	-0.03	15.07	13.008	1838.5	14.95	-0.03	0.00	0.351	0.020	0.965
0.20659	19.50	12.759	2148.7	-0.17	-0.01	21.10	12.946	2175.6	17.69	-0.25	-0.02	-0.004	0.000	0.900
0.25337	28.04	13.050	2576.1	-0.19	-0.01	30.91	13.119	2632.5	21.41	-0.10	-0.01	-0.162	-0.009	0.883
0.31184	40.88	13.302	3110.6	-0.27	-0.02	46.29	13.194	3221.7	26.20	0.00	0.00	-0.438	-0.024	0.860
0.37031	55.19	13.595	3614.6	-0.24	-0.02	65.10	13.212	3821.1	31.07	0.01	0.00	-0.717	-0.039	0.325
0.42878	71.27	13.852	4108.0	-0.20	-0.01	87.86	13.168	4439.6	36.10	-0.07	-0.01	-1.021	-0.055	0.790
0.52623	102.51	14.176	4928.0	-0.19	-0.01	132.57	13.156	5455.1	44.36	-0.16	-0.01	-1.391	-0.073	0.753
0.60419	130.92	14.402	5570.6	-0.18	-0.01	173.29	13.212	6238.2	50.73	-0.17	-0.01	-1.568	-0.081	0.735
0.72113	178.76	14.710	6513.7	-0.14	-0.01	244.04	13.288	7408.1	60.24	-0.19	-0.01	-1.791	-0.091	0.713
0.87705	252.72	15.047	7752.8	-0.11	-0.01	352.92	13.439	8917.5	72.52	-0.18	-0.01	-1.932	-0.099	0.697
0.92578	274.87	15.235	8103.0	0.00	0.00	391.56	13.467	9417.1	76.58	-0.20	-0.01	-2.028	-0.101	0.683
0.01451	0.13	10.784	177.2	0.13	0.00	0.14	10.980	178.6	1.45					0.906
0.01736	0.17	11.408	200.3	0.20	0.00	0.20	11.171	210.1	1.71					0.838
0.02170	0.36	9.853	289.7	0.41	0.00	0.41	9.793	299.5	2.44					0.863
0.02600	0.51	9.953	343.6	0.56	0.00	0.56	9.974	352.3	2.86					0.877
0.03132	0.70	10.174	404.8	0.70	0.01	0.70	10.199	414.8	3.37	0.13	0.01	0.128	0.009	0.878
0.03639	0.92	10.361	462.2	0.09	0.01	1.03	10.311	476.7	3.88	-0.01	0.00	-0.002	0.000	0.867
0.04587	1.39	10.606	568.4	-0.01	0.00	1.52	10.717	577.8	4.70	0.04	0.00	0.070	0.005	0.892
0.05944	2.18	10.984	711.2	-0.02	0.00	2.38	11.083	724.1	5.99	-0.01	0.00	0.044	0.003	0.890
0.06901	2.83	11.183	811.1	-0.05	0.00	3.10	11.289	825.4	6.71	-0.04	0.00	0.023	0.001	0.891
0.07622	3.35	11.362	881.6	-0.02	0.00	3.62	11.532	892.4	7.26	0.05	0.00	0.129	0.008	0.900
0.08654	4.16	11.672	982.8	0.00	0.00	4.46	11.798	990.3	8.05	0.10	0.01	0.215	0.014	0.908
0.09671	5.04	11.747	1081.4	0.01	0.00	5.39	11.992	1088.3	8.85	0.09	0.01	0.245	0.015	0.911
0.10730	6.02	11.935	1184.5	0.04	0.00	6.40	12.213	1189.1	9.67	0.10	0.01	0.312	0.019	0.915
0.10863	6.17	11.929	1200.0	0.01	0.00	6.52	12.242	1201.3	9.77	0.11	0.01	0.324	0.020	0.920
0.11368	6.65	12.023	1252.5	0.03	0.00	7.07	12.307	1257.1	10.22	0.08	0.01	0.310	0.019	0.916
0.11784	7.14	12.029	1291.1	-0.01	0.00	7.49	12.395	1287.3	10.47	0.10	0.01	0.357	0.022	0.928
0.13825	9.46	12.261	1488.3	-0.03	0.00	9.86	12.577	1478.8	12.03	0.06	0.00	0.397	0.024	0.934

0.16792	13.19	12.809	1754.4	0.03	0.09	13.84	13.089	1736.3	14.12	0.14	0.01	0.530	0.031	0.942
0.19002	17.78	12.860	2025.6	-0.16	-0.01	18.80	13.015	2027.4	16.49	-0.13	-0.01	0.187	0.011	0.921
0.21780	21.36	12.854	2219.7	-0.13	-0.01	27.83	12.973	2224.0	18.09	-0.23	-0.02	-0.016	-0.001	0.890
0.26136	29.17	13.200	2593.4	-0.06	0.00	31.77	13.139	2634.7	21.42	-0.08	0.00	-0.144	-0.008	0.868
0.29700	36.42	13.424	2897.6	-0.02	0.00	40.45	13.233	2972.4	24.17	0.03	0.00	-0.259	-0.014	0.849
0.33660	45.22	13.653	3229.0	0.02	0.00	52.02	13.325	3371.1	27.41	0.03	0.00	-0.488	-0.027	0.829
0.40929	65.32	13.813	3881.6	-0.14	-0.01	79.43	13.221	4186.5	33.86	0.00	0.00	-0.858	-0.046	0.800
0.46776	82.49	14.048	4362.5	-0.11	-0.01	103.74	13.221	4762.1	38.72	-0.04	0.00	-1.090	-0.058	0.774
0.51649	98.38	14.203	4766.3	-0.11	-0.01	127.34	13.176	5278.5	42.92	-0.12	0.00	-1.314	-0.069	0.752
0.63343	141.11	14.544	5721.6	-0.09	-0.01	190.05	13.227	6463.4	52.56	-0.17	-0.01	-1.615	-0.084	0.723
0.75037	190.39	14.833	6646.2	-0.06	0.00	283.63	13.204	7612.5	61.90	-0.19	-0.01	-1.822	-0.093	0.703
0.80629	265.67	15.165	7946.1	-0.04	0.00	375.77	13.458	9201.1	74.82	-0.19	-0.01	-1.997	-0.100	0.688

0.01400	0.13	10.698	173.5			0.14	10.758	177.2	1.44					0.684
0.01742	0.17	11.531	200.3			0.16	11.914	199.2	1.62					0.933
0.02082	0.33	9.868	279.7			0.37	9.829	288.5	2.35					0.667
0.02394	0.44	9.892	320.8			0.48	9.897	328.4	2.68					0.875
0.02918	0.62	10.073	384.0	0.14	0.01	0.69	10.112	393.0	3.20	0.14	0.01	0.135	0.010	0.881
0.03502	0.86	10.296	450.7	0.06	0.01	0.95	10.343	460.9	3.75	0.06	0.01	0.088	0.006	0.882
0.04000	1.08	10.488	505.3	0.07	0.01	1.20	10.531	517.0	4.20	0.06	0.01	0.077	0.005	0.881
0.04688	1.43	10.690	581.1	0.03	0.00	1.56	10.791	591.4	4.81	0.07	0.01	0.104	0.007	0.890
0.05419	1.85	10.872	660.5	-0.01	0.00	2.01	11.008	670.1	5.45	0.06	0.01	0.103	0.007	0.896
0.06631	2.61	11.165	785.7	0.00	0.00	2.82	11.368	794.2	6.46	0.11	0.01	0.168	0.011	0.903
0.07767	3.44	11.418	901.5	0.00	0.00	3.71	11.605	911.2	7.41	0.08	0.01	0.166	0.011	0.903
0.08824	4.29	11.619	1006.7	0.01	0.00	4.64	11.791	1012.1	8.29	0.03	0.00	0.159	0.010	0.900
0.10149	5.46	11.848	1135.9	0.03	0.00	5.87	12.055	1146.8	9.33	0.03	0.00	0.218	0.013	0.905
0.10997	6.33	11.921	1223.2	-0.03	0.00	6.66	12.265	1221.4	9.93	0.09	0.01	0.317	0.019	0.925
0.11498	6.77	12.056	1265.6	0.05	0.00	7.21	12.326	1271.9	10.34	0.06	0.00	0.308	0.019	0.913
0.12289	7.67	12.106	1346.9	-0.01	0.00	8.05	12.466	1343.8	10.93	0.06	0.01	0.353	0.021	0.927
0.13901	9.56	12.261	1506.3	-0.05	0.00	9.93	12.695	1494.6	12.15	0.04	0.00	0.397	0.024	0.937
0.16992	13.41	12.654	1782.5	0.05	0.00	13.85	13.144	1762.9	14.34	0.17	0.01	0.559	0.033	0.943
0.20854	19.59	12.851	2154.5	-0.08	-0.01	20.98	13.106	2170.3	17.65	-0.09	-0.01	0.160	0.009	0.909
0.22414	22.42	12.910	2304.8	-0.14	-0.01	24.06	13.155	2323.7	18.90	-0.06	0.00	0.090	0.005	0.907
0.26312	29.80	13.146	2657.0	-0.15	-0.01	32.88	13.209	2716.6	22.09	-0.01	0.00	-0.127	-0.007	0.882
0.32159	42.83	13.403	3185.2	-0.21	-0.02	48.27	13.324	3291.7	26.77	0.13	0.01	-0.346	-0.019	0.864
0.38006	57.36	13.686	3696.8	-0.18	-0.01	66.22	13.246	3913.4	31.82	0.04	0.00	-0.724	-0.039	0.819
0.47751	85.64	14.073	4505.5	-0.14	-0.01	107.76	13.241	4919.6	40.01	-0.03	0.00	-1.126	-0.060	0.774
0.57496	119.48	14.346	5323.3	-0.16	-0.01	156.80	13.217	5935.9	48.27	-0.14	-0.01	-1.477	-0.077	0.742
0.67241	157.38	14.619	6112.6	-0.13	-0.01	212.76	13.270	6918.1	56.26	-0.17	-0.01	-1.680	-0.087	0.720
0.78935	209.39	14.878	7055.1	-0.12	-0.01	289.34	13.358	8072.5	65.64	-0.18	-0.01	-1.870	-0.095	0.704
0.90629	267.21	15.121	7982.3	-0.09	-0.01	374.79	13.476	9201.8	74.83	-0.17	-0.01	-1.980	-0.099	0.694

0.00923	0.08	8.696	140.3			0.09	8.780	142.9	1.16					0.691
0.01114	0.10	9.528	154.6			0.11	9.809	157.6	1.28					0.889
0.01386	0.13	10.589	173.4			0.14	10.729	176.9	1.43					0.897
0.01766	0.19	11.198	208.5			0.20	11.500	208.7	1.70					0.922
0.02278	0.41	9.759	308.5			0.45	9.764	316.4	2.57					0.878
0.02598	0.51	9.886	347.4	0.09	0.01	0.57	9.890	357.0	2.90	0.10	0.01	0.079	0.006	0.875
0.03127	0.71	10.136	407.7	0.04	0.00	0.80	10.093	421.0	3.42	0.00	0.00	-0.004	0.000	0.866
0.03660	0.94	10.322	468.6	0.04	0.00	1.05	10.289	483.3	3.93	-0.06	-0.01	-0.047	-0.003	0.866
0.04214	1.20	10.487	530.9	-0.01	0.00	1.33	10.519	544.3	4.43	-0.05	0.00	-0.025	-0.002	0.879
0.04623	1.41	10.602	576.1	-0.04	0.00	1.56	10.666	586.8	4.79	-0.05	0.00	-0.014	-0.001	0.884
0.05949	2.19	10.973	716.2	-0.05	0.00	2.40	11.082	729.1	5.93	-0.02	0.00	0.031	0.002	0.891
0.06909	2.85	11.169	817.3	-0.08	-0.01	3.10	11.306	830.1	6.75	-0.04	0.00	0.030	0.002	0.895
0.07591	3.35	11.311	886.9	-0.08	-0.01	3.64	11.469	899.3	7.31	-0.03	0.00	0.054	0.003	0.898
0.08558	4.17	11.562	989.9	-0.02	0.00	4.53	11.728	1003.3	8.16	0.00	0.00	0.122	0.008	0.899

0.09452	4.87	11.677	1070.3	-0.04	0.00	5.26	11.684	1081.3	8.79	-0.01	0.00	0.148	0.009	0.905
0.09955	5.32	11.773	1119.8	-0.02	0.00	6.74	11.981	1131.3	9.20	-0.01	0.00	0.187	0.010	0.905
0.10453	5.77	11.865	1165.9	0.00	0.00	6.23	12.078	1177.4	9.67	-0.01	0.00	0.195	0.012	0.908
0.11291	6.52	12.063	1243.6	0.08	0.01	7.01	12.293	1254.9	10.20	0.02	0.00	0.299	0.018	0.907
0.11911	7.25	12.064	1306.9	0.00	0.00	7.71	12.387	1312.7	10.67	0.02	0.00	0.294	0.018	0.918
0.13564	9.12	12.247	1485.5	-0.02	0.00	9.68	12.566	1488.6	11.94	-0.05	0.00	0.298	0.018	0.920
0.14622	10.40	12.377	1564.5	0.00	0.00	10.91	12.762	1558.7	12.68	0.02	0.00	0.391	0.023	0.929
0.01396	0.13	10.654	169.8			0.14	10.781	172.3	1.40					0.895
0.01699	0.16	11.542	190.7			0.16	11.562	195.6	1.59					0.877
0.02232	0.38	9.838	293.9			0.43	9.815	302.6	2.46					0.870
0.02602	0.51	9.980	337.6			0.56	9.980	346.9	2.82					0.874
0.03113	0.70	10.141	397.3	0.14	0.01	0.78	10.135	408.4	3.32	0.10	0.01	0.091	0.006	0.873
0.03630	0.92	10.344	454.2	0.12	0.01	1.02	10.329	467.3	3.80	0.04	0.00	0.050	0.004	0.871
0.04558	1.37	10.637	554.4	0.06	0.01	1.50	10.702	568.1	4.60	0.06	0.01	0.091	0.008	0.865
0.05869	2.12	10.984	691.2	0.03	0.00	2.31	11.125	701.2	5.70	0.10	0.01	0.141	0.009	0.898
0.06810	2.76	11.176	788.8	-0.01	0.00	2.98	11.349	798.0	6.49	0.08	0.01	0.141	0.009	0.901
0.07500	3.27	11.321	857.6	0.00	0.00	3.52	11.511	865.6	7.05	0.08	0.01	0.159	0.010	0.903
0.08502	4.05	11.519	955.6	0.00	0.00	4.35	11.729	964.1	7.84	0.09	0.01	0.193	0.012	0.906
0.09381	4.90	11.555	1051.7	-0.13	-0.01	5.24	11.793	1058.8	8.61	-0.05	0.00	0.094	0.006	0.910
0.11010	6.34	11.927	1197.0	0.01	0.00	6.77	12.184	1203.8	9.79	0.04	0.00	0.262	0.016	0.912
0.11324	6.72	11.916	1234.8	-0.05	0.00	7.02	12.302	1228.7	9.99	0.11	0.01	0.345	0.021	0.931
0.12952	8.48	12.133	1384.1	-0.03	0.00	8.85	12.533	1376.7	11.19	0.07	0.01	0.377	0.023	0.932
0.13573	9.21	12.197	1442.5	-0.04	0.00	9.57	12.630	1431.2	11.64	0.08	0.01	0.407	0.024	0.937
0.15386	11.47	12.392	1609.7	-0.03	-0.01	11.86	12.868	1592.5	12.96	0.06	0.01	0.460	0.027	0.942
0.19900	16.27	12.700	2029.0	-0.13	-0.01	16.56	13.297	1990.8	16.19	0.17	0.01	0.501	0.029	0.958
0.25870	26.32	13.260	2526.1	0.05	0.00	30.09	13.578	2534.4	20.81	0.35	0.03	0.363	0.020	0.916
0.29650	36.60	13.459	2871.7	0.03	0.00	39.84	13.615	2916.5	23.72	0.40	0.03	0.156	0.009	0.894
0.33830	45.53	13.677	3202.8	0.05	0.00	51.31	13.597	3309.6	26.91	0.40	0.03	0.082	-0.004	0.864
0.45770	77.51	14.181	4180.3	0.10	0.01	95.19	13.508	4509.4	36.87	0.27	0.02	-0.711	-0.038	0.793
0.55720	110.95	14.429	5003.4	0.03	0.00	141.77	13.473	5505.2	44.77	0.16	0.01	-1.091	-0.057	0.762
0.67241	158.36	14.575	5980.1	-0.13	-0.01	214.85	13.207	6780.0	55.13	-0.22	-0.02	-1.718	-0.089	0.717
0.78935	209.89	14.862	6889.9	-0.09	-0.01	292.46	13.286	7916.5	64.38	-0.24	-0.02	-1.906	-0.097	0.699
0.90629	266.92	15.131	7783.5	-0.03	0.00	378.61	13.409	9023.3	73.38	-0.22	-0.02	-2.012	-0.101	0.666
0.01396	0.13	10.854	169.8			0.14	10.781	172.3	1.40					0.895
0.01699	0.16	11.542	190.7			0.16	11.562	195.6	1.59					0.877
0.02232	0.38	9.838	293.9			0.43	9.815	302.6	2.46					0.870
0.02602	0.51	9.980	337.6			0.56	9.980	346.9	2.82					0.874
0.03113	0.70	10.141	397.3	0.14	0.01	0.78	10.135	408.4	3.32	0.10	0.01	0.091	0.006	0.873
0.03630	0.92	10.344	454.2	0.12	0.01	1.02	10.329	467.3	3.80	0.04	0.00	0.050	0.004	0.871
0.04558	1.37	10.637	554.4	0.06	0.01	1.50	10.702	568.1	4.60	0.06	0.01	0.091	0.008	0.865
0.05869	2.12	10.984	691.2	0.03	0.00	2.31	11.125	701.2	5.70	0.10	0.01	0.141	0.009	0.898
0.06810	2.76	11.176	788.8	-0.01	0.00	2.98	11.349	798.0	6.49	0.08	0.01	0.141	0.009	0.901
0.07500	3.27	11.321	857.6	0.00	0.00	3.52	11.511	865.6	7.05	0.08	0.01	0.159	0.010	0.903
0.08502	4.05	11.519	955.6	0.00	0.00	4.35	11.729	964.1	7.84	0.09	0.01	0.193	0.012	0.906
0.09381	4.90	11.555	1051.7	-0.13	-0.01	5.24	11.793	1058.8	8.61	-0.05	0.00	0.094	0.006	0.910
0.11010	6.34	11.927	1197.0	0.01	0.00	6.77	12.184	1203.8	9.79	0.04	0.00	0.262	0.016	0.912
0.11324	6.72	11.916	1234.8	-0.05	0.00	7.02	12.302	1228.7	9.99	0.11	0.01	0.345	0.021	0.931
0.12952	8.48	12.133	1384.1	-0.03	0.00	8.85	12.533	1376.7	11.19	0.07	0.01	0.377	0.023	0.932
0.13573	9.21	12.197	1442.5	-0.04	0.00	9.57	12.630	1431.2	11.64	0.08	0.01	0.407	0.024	0.937
0.15386	11.47	12.392	1609.7	-0.03	-0.01	11.86	12.868	1592.5	12.96	0.06	0.01	0.460	0.027	0.942
0.19900	16.27	12.700	2029.0	-0.13	-0.01	16.56	13.297	1990.8	16.19	0.17	0.01	0.501	0.029	0.958
0.25870	26.32	13.260	2526.1	0.05	0.00	30.09	13.578	2534.4	20.81	0.35	0.03	0.363	0.020	0.916
0.29650	36.60	13.459	2871.7	0.03	0.00	39.84	13.615	2916.5	23.72	0.40	0.03	0.156	0.009	0.894
0.33830	45.53	13.677	3202.8	0.05	0.00	51.31	13.597	3309.6	26.91	0.40	0.03	0.082	-0.004	0.864
0.45770	77.51	14.181	4180.3	0.10	0.01	95.19	13.508	4509.4	36.87	0.27	0.02	-0.711	-0.038	0.793
0.55720	110.95	14.429	5003.4	0.03	0.00	141.77	13.473	5505.2	44.77	0.16	0.01	-1.091	-0.057	0.762
0.67241	158.36	14.575	5980.1	-0.13	-0.01	214.85	13.207	6780.0	55.13	-0.22	-0.02	-1.718	-0.089	0.717
0.78935	209.89	14.862	6889.9	-0.09	-0.01	292.46	13.286	7916.5	64.38	-0.24	-0.02	-1.906	-0.097	0.699
0.90629	266.92	15.131	7783.5	-0.03	0.00	378.61	13.409	9023.3	73.38	-0.22	-0.02	-2.012	-0.101	0.666
0.01396	0.13	10.854	169.8			0.14	10.781	172.3	1.40					0.895
0.01699	0.16	11.542	190.7			0.16	11.562	195.6	1.59					0.877
0.02232	0.38	9.838	293.9			0.43	9.815	302.6	2.46					0.870
0.02602	0.51	9.980	337.6			0.56	9.980	346.9	2.82					0.874
0.03113	0.70	10.141	397.3	0.14	0.01	0.78	10.135	408.4	3.32	0.10	0.01	0.091	0.006	0.873
0.03630	0.92	10.344	454.2	0.12	0.01	1.02	10.329	467.3	3.80	0.04	0.00	0.050	0.004	0.871
0.04558	1.37	10.637	554.4	0.06	0.01	1.50	10.702	568.1	4.60	0.06	0.01	0.091	0.008	0.865
0.05869	2.12	10.984	691.2	0.03	0.00	2.31	11.125	701.2	5.70	0.10	0.01	0.141	0.009	0.898
0.06810	2.76	11.176	788.8	-0.01	0.00	2.98	11.349	798.0	6.49	0.08	0.01	0.141	0.009	0.901
0.07500	3.27	11.321	857.6	0.00	0.00	3.52	11.511	865.6	7.05	0.08	0.01	0.159	0.010	0.903
0.08502	4.05	11.519	955.6	0.00	0.00	4.35	11.729	964.1	7.84	0.09	0.01	0.193	0.012	0.906
0.09381	4.90	11.555	1051.7	-0.13	-0.01	5.24	11.793	1058.8	8.61	-0.05	0.00	0.094	0.006	0.910
0.11010	6.34	11.927	1197.0	0.01	0.00	6.77	12.184	1203.8	9.79	0.04	0.00	0.262	0.016	0.912
0.11324	6.72	11.916	1234.8	-0.05	0.00	7.02	12.302	1228.7	9.99	0.11	0.01	0.345	0.021	0.931
0.12952	8.48	12.133	1384.1	-0.03	0.00	8.85	12.533	1376.7	11.19	0.07	0.01	0.377	0.023	0.932
0.13573	9.21	12.197	1442.5	-0.04	0.00	9.57	12.630	1431.2	11.64	0.08	0.01	0.407	0.024	0.937
0.15386	11.47	12.392	1609.7	-0.03	-0.01	11.86	12.868	1592.5	12.96	0.06	0.01	0.460	0.027	0.942
0.19900	16.27	12.700	2029.0	-0.13	-0.01	16.56	13.297	1990.8	16.19	0.17	0.01	0.501	0.029	0.958
0.25870	26.32	13.260	2526.1	0.05	0.00	30.09	13.578	2534.4	20.81	0.35	0.03	0.363	0.020	0.916
0.29650	36.60	13.459	2871.7	0.03	0.00	39.84	13.615	2916.5	23.72	0.40	0.03	0.156	0.009	0.894
0.33830	45.53	13.677	3202.8	0.05	0.00	51.31	13.597	3309.6	26.91	0.40	0.03	0.082	-0.004	0.864
0.45770	77.51	14.181	4180.3	0.10	0.01	95.19	13.508	4509.4	36.87	0.27	0.02	-0.711	-0.038	0.793
0.55720	110.95	14.429	5003.4	0.03	0.00	141.77	13.473	5505.2	44.77	0.16	0.01	-1.091	-0.057	0.762
0.67241	158.36	14.575</												

RUM	163	0.45770	14.181	4180.3	0.10	0.01	96.19	13.506	4509.4	36.67	0.27	0.02	-0.711	-0.038	0.793
DATE	2/20/83	110.95	14.429	5003.4	0.03	0.00	141.77	13.473	5505.2	44.77	0.16	0.01	-1.091	-0.057	0.762
POLY	-	156.36	14.575	5980.1	-0.13	-0.01	214.85	13.207	6780.0	55.13	-0.22	-0.02	-1.718	-0.089	0.717
e wppm	-	209.89	14.862	6889.9	-0.09	-0.01	292.46	13.288	7916.5	64.38	-0.24	-0.02	-1.906	-0.097	0.699
IV	1.000	266.92	15.131	7783.5	-0.03	0.00	378.61	13.409	9023.3	73.38	-0.22	-0.02	-2.012	-0.101	0.686
RUM	163	0.01045	9.070	146.6	0.10	0.00	0.11	9.116	149.9	1.22	0.00	0.00	0.014	0.001	0.862
DATE	2/20/83	0.01472	10.634	176.0	0.15	0.00	0.15	10.818	177.8	1.45	0.00	0.00	-0.019	-0.001	0.870
POLY	-	0.01783	11.584	195.6	0.20	0.00	0.20	11.491	202.6	1.65	-0.03	0.00	-0.003	0.000	0.884
e wppm	-	0.02270	9.740	296.1	0.46	0.00	0.46	9.874	306.3	2.49	0.04	0.00	0.044	0.003	0.891
IV	1.000	0.02667	9.880	342.9	0.61	0.00	0.61	9.814	354.7	2.88	0.00	0.00	0.014	0.001	0.862
RUM	163	0.03566	10.227	442.7	0.07	0.01	0.83	10.055	411.6	3.35	0.00	0.00	0.014	0.001	0.870
DATE	2/20/83	0.04086	11.16	500.2	-0.03	0.00	1.27	10.431	455.4	3.70	-0.03	0.00	-0.019	-0.001	0.872
POLY	-	0.04634	10.557	557.1	-0.03	0.00	1.57	10.658	565.9	4.61	0.02	0.00	-0.003	0.000	0.884
e wppm	-	0.05345	10.733	631.9	-0.07	-0.01	2.01	10.853	642.1	5.22	-0.02	0.00	0.044	0.003	0.891
IV	1.000	0.06556	11.019	755.0	-0.09	-0.01	2.83	11.218	761.8	6.20	0.04	0.00	0.090	0.006	0.906
RUM	163	0.07685	11.255	866.4	-0.10	-0.01	3.71	11.493	871.8	7.09	0.05	0.00	0.131	0.008	0.911
DATE	2/20/83	0.08768	11.477	959.4	-0.07	-0.01	4.65	11.707	976.3	7.94	0.04	0.00	0.149	0.009	0.909
POLY	-	0.09801	11.639	1067.7	-0.08	-0.01	5.60	11.921	1071.0	8.71	0.05	0.00	0.202	0.013	0.917
e wppm	-	0.11405	11.865	1218.5	-0.08	-0.01	7.24	12.202	1217.2	9.90	0.04	0.00	0.260	0.016	0.924
IV	1.000	0.11838	11.912	1265.8	-0.10	-0.01	7.72	12.263	1263.3	10.27	0.01	0.00	0.257	0.016	0.926
RUM	163	0.13875	12.145	1450.8	-0.10	-0.01	11.99	12.550	1442.3	11.73	-0.02	0.00	0.314	0.019	0.933
DATE	2/20/83	0.15345	12.317	1581.3	-0.08	-0.01	11.99	12.759	1568.3	12.75	0.00	0.00	0.377	0.022	0.938
POLY	-	0.16775	12.699	1874.5	0.01	0.00	16.99	13.114	1864.9	15.16	0.06	0.00	0.431	0.025	0.932
e wppm	-	0.22170	12.960	2169.0	0.02	0.00	21.78	13.330	2166.5	17.62	0.14	0.01	0.387	0.022	0.924
IV	1.000	0.25965	13.222	2490.1	0.04	0.00	30.63	13.509	2503.9	20.36	0.28	0.02	0.314	0.018	0.912
RUM	163	0.29960	13.501	2813.9	0.10	0.01	40.74	13.514	2888.2	23.49	0.30	0.02	0.072	0.004	0.875
DATE	2/20/83	0.33964	13.690	3145.6	0.10	0.01	53.86	13.319	3321.8	27.01	0.12	0.01	-0.367	-0.020	0.827
POLY	-	0.39147	13.936	3563.4	0.13	0.01	71.63	13.317	3830.9	31.15	0.12	0.01	-0.616	-0.033	0.798
e wppm	-	0.45139	14.162	4044.1	0.14	0.01	95.84	13.276	4432.1	36.04	0.04	0.00	-0.911	-0.049	0.768
IV	1.000	0.53115	14.491	4828.5	0.16	0.01	143.69	13.241	5428.8	44.15	-0.07	-0.01	-1.298	-0.068	0.730
RUM	163	0.61125	14.750	5433.1	0.21	0.01	187.95	13.255	6211.1	50.51	-0.12	-0.01	-1.617	-0.079	0.706
DATE	2/20/83	0.71104	14.946	6043.5	0.22	0.01	236.32	13.317	6968.2	56.66	-0.12	-0.01	-1.855	-0.085	0.694
POLY	-	0.81090	15.169	6796.5	0.24	0.02	304.64	13.377	7917.7	64.39	-0.15	-0.01	-1.818	-0.092	0.680
e wppm	-	0.82874	15.418	7687.2	0.27	0.02	393.49	13.480	9032.6	73.45	-0.15	-0.01	-1.943	-0.097	0.665
IV	1.000	0.01037	8.970	146.3	0.10	0.00	0.11	9.129	147.7	1.20	0.00	0.00	-0.087	-0.006	0.860
RUM	167	0.01427	10.438	173.1	0.15	0.00	0.15	10.686	173.6	1.41	0.00	0.00	-0.058	-0.004	0.875
DATE	2/20/83	0.01725	11.357	192.3	0.19	0.00	0.19	11.472	195.6	1.59	-0.07	-0.01	-0.214	-0.015	0.881
POLY	-	0.02244	9.713	292.3	0.46	0.00	0.46	9.536	305.8	2.49	0.04	0.00	0.003	0.000	0.898
e wppm	-	0.02602	9.801	335.8	0.52	0.00	0.50	9.689	349.0	2.84	0.00	0.00	0.086	0.006	0.907
IV	1.000	0.03150	10.044	396.7	0.05	0.00	0.83	9.956	410.7	3.34	-0.08	-0.01	-0.081	-0.005	0.884
RUM	163	0.03680	10.216	453.7	-0.02	0.00	1.07	10.222	467.8	3.80	-0.07	-0.01	-0.214	-0.015	0.884
DATE	2/20/83	0.04144	10.223	512.7	-0.22	-0.02	1.35	10.265	524.6	4.27	-0.24	-0.02	-0.214	-0.015	0.881
POLY	-	0.04607	10.478	556.0	-0.10	-0.01	1.58	10.537	568.0	4.62	-0.11	-0.01	-0.081	-0.005	0.884
e wppm	-	0.05312	10.677	629.2	-0.12	-0.01	2.00	10.822	637.8	5.19	-0.04	0.00	0.003	0.000	0.898
IV	1.000	0.06519	10.991	750.1	-0.11	-0.01	2.81	11.201	756.2	6.15	0.03	0.00	0.086	0.006	0.907
RUM	163	0.07670	11.203	866.2	-0.15	-0.01	3.73	11.434	871.9	7.09	-0.01	0.00	0.072	0.005	0.910
DATE	2/20/83	0.08728	11.400	969.1	-0.15	-0.01	4.68	11.620	976.7	7.94	-0.05	0.00	0.061	0.004	0.908
POLY	-	0.09809	11.577	1073.3	-0.15	-0.01	5.71	11.819	1080.0	8.78	-0.07	-0.01	0.085	0.005	0.911
e wppm	-	0.11329	11.822	1214.8	-0.12	-0.01	7.26	12.104	1218.9	9.91	-0.06	-0.01	0.160	0.010	0.916
IV	1.000	0.11995	11.946	1276.0	-0.08	-0.01	9.98	12.232	1250.2	10.41	-0.05	0.00	0.203	0.012	0.916
RUM	163	0.13648	12.145	1424.1	-0.07	-0.01	12.45	12.488	1422.9	11.67	-0.05	0.00	0.275	0.017	0.924
DATE	2/20/83	0.15683	11.97	12368	-0.06	0.00	12.52	12.763	1599.1	13.00	-0.03	0.00	0.348	0.021	0.931
POLY	-	0.16979	17.90	12819	0.05	0.00	19.22	13.056	1982.7	16.12	-0.07	-0.01	0.267	0.015	0.906

0.21855	22.02	12.707	2179.9	-0.25	-0.02	22.96	13.133	2186.9	17.62	-0.06	0.00	0.189	0.011	0.933
0.24814	26.85	13.065	2407.1	-0.06	0.00	29.37	13.184	2450.6	19.93	-0.04	0.00	0.027	0.002	0.890
0.27789	32.62	13.263	2853.5	-0.03	0.00	36.44	13.245	2729.8	22.20	0.03	0.00	-0.100	-0.006	0.871
0.31111	40.39	13.355	2952.4	-0.13	-0.01	46.37	13.155	3079.3	25.04	-0.05	0.00	-0.399	-0.032	0.848
0.36994	54.35	13.690	3425.1	-0.05	0.00	66.51	13.081	3688.1	29.99	-0.14	-0.01	-0.806	-0.044	0.795
0.44417	74.48	14.040	4010.9	0.03	0.00	95.08	13.054	4432.0	36.04	-0.18	-0.01	-1.133	-0.081	0.755
0.52196	102.08	14.093	4898.3	-0.19	-0.01	133.18	13.023	5223.5	42.48	-0.27	-0.02	-1.449	-0.077	0.746
0.63798	143.35	14.536	5570.0	-0.05	0.00	199.84	12.984	6401.5	52.08	-0.40	-0.03	-1.831	-0.095	0.698
0.77233	202.60	14.802	6631.5	-0.08	-0.01	290.98	13.036	7735.8	62.91	-0.47	-0.03	-2.118	-0.108	0.678
0.90559	268.98	15.062	7714.1	-0.09	-0.01	395.68	13.107	9107.2	74.06	-0.53	-0.04	-2.330	-0.117	0.662

0.0045" Finished 4.022" Pipe
 h=0.0045 350

Series

PEO

WFE 168
 d= 0.402
 h= smooth
 R2/A 100
 d= 0.391
 h= 0.0045
 R/A 43.5

Q(U/A)	Tot(SZ)	Vpnt(SZ)	Repd(SZ)	S(SZ)	SF(SZ)	Tot(R2A)	Vpnt(R2A)	Repd(R2A)	h=	S(R2A)	SF(R2A)	Vpnt(S2)	R	RF	P	d/vres	connected	R	connected
0.00591	0.06	7.615	121.4	0.01	0.00	0.07	7.572	125.4	1.02	0.07	0.00	7.83	0.003	0.000	0.081	0.00	0.003	0.000	0.000
0.00926	0.07	8.273	133.6	0.01	0.00	0.08	8.423	134.8	1.10	0.08	-0.01	10.23	-0.004	-0.004	0.071	0.00	-0.044	-0.001	-0.044
0.01005	0.09	9.059	148.6	-0.07	-0.01	0.10	9.200	150.3	1.22	0.10	-0.10	10.35	-0.005	-0.005	0.079	0.00	-0.005	-0.000	-0.005
0.01349	0.12	10.428	173.5	-0.10	-0.01	0.13	10.580	175.7	1.43	0.13	-0.11	10.47	0.023	0.002	0.084	0.00	0.023	0.002	0.002
0.01546	0.14	11.145	186.2	-0.12	-0.01	0.16	11.276	189.1	1.54	0.16	-0.11	10.66	0.056	0.005	0.087	0.00	0.056	0.005	0.005
0.02054	0.29	10.386	263.7	-0.16	-0.01	0.37	9.675	293.1	2.38	0.37	-0.08	10.94	0.124	0.011	0.098	0.00	0.124	0.011	0.124
0.02361	0.43	9.800	323.8	-0.16	-0.01	0.49	9.733	315.0	2.72	0.49	-0.06	11.18	0.158	0.014	0.092	0.00	0.158	0.014	0.158
0.02855	0.61	9.954	385.9	-0.16	-0.01	0.68	9.993	394.3	3.21	0.68	-0.09	11.36	0.175	0.015	0.094	0.00	0.175	0.015	0.175
0.03366	0.81	10.203	444.0	-0.07	-0.01	1.12	10.345	456.9	3.72	1.12	-0.10	11.52	0.246	0.021	0.913	0.00	0.246	0.021	0.246
0.03811	1.01	10.314	497.7	-0.10	-0.01	1.33	10.493	553.9	4.50	1.33	-0.11	11.77	0.270	0.023	0.916	0.00	0.270	0.023	0.270
0.04197	1.20	10.435	542.1	-0.12	-0.01	1.70	10.716	627.1	5.10	1.70	-0.11	12.92	0.362	0.028	0.925	0.00	0.362	0.028	0.362
0.04851	1.55	10.634	615.2	-0.16	-0.01	2.41	11.064	746.8	6.07	2.41	-0.08	14.04	0.478	0.031	0.899	0.00	0.478	0.031	0.478
0.05363	2.22	10.913	737.0	-0.16	-0.01	3.15	11.338	855.1	6.95	3.15	-0.09	15.32	0.617	0.037	0.877	0.00	0.617	0.037	0.617
0.05996	2.92	11.160	845.7	-0.16	-0.01	3.94	11.535	954.9	7.76	3.94	-0.07	16.12	0.748	0.040	0.867	0.00	0.748	0.040	0.748
0.07851	3.85	11.342	945.3	-0.12	-0.01	4.80	11.766	1053.4	8.57	4.80	-0.05	17.54	0.875	0.044	0.824	0.00	0.875	0.044	0.875
0.08962	4.50	11.514	1047.9	-0.12	-0.01	6.06	12.040	1178.7	9.59	6.06	-0.05	18.23	0.955	0.044	0.824	0.00	0.955	0.044	0.955
0.10296	5.70	11.760	1174.6	-0.07	-0.01	8.46	12.451	1360.7	11.31	8.46	-0.03	19.54	1.044	0.055	0.817	0.00	1.044	0.055	1.044
0.11187	6.53	11.934	1284.0	-0.01	0.00	10.27	12.704	1544.1	12.56	10.27	-0.02	20.27	1.261	0.062	0.792	0.00	1.261	0.062	1.261
0.12582	7.97	12.154	1386.7	-0.01	0.00	8.46	12.451	1360.7	11.31	8.46	-0.03	19.54	1.044	0.055	0.817	0.00	1.044	0.055	1.044
0.14148	9.76	12.350	1546.1	-0.01	0.00	10.27	12.704	1544.1	12.56	10.27	-0.02	20.27	1.261	0.062	0.792	0.00	1.261	0.062	1.261
0.16218	12.15	12.686	1725.5	0.14	0.01	12.78	13.054	1722.7	14.01	12.78	0.12	22.35	1.404	0.078	0.899	0.00	1.404	0.078	1.404
0.19174	16.37	12.923	2013.0	0.11	0.01	17.26	13.282	2012.1	16.36	17.26	0.14	23.38	1.532	0.089	0.899	0.00	1.532	0.089	1.532
0.22569	21.37	13.313	2300.4	0.27	0.02	23.14	13.502	2300.3	18.95	23.14	0.28	25.97	1.717	0.100	0.877	0.00	1.717	0.100	1.717
0.26364	26.52	13.960	2562.8	0.72	0.05	28.74	14.152	2597.1	21.12	28.74	0.93	30.07	2.041	0.112	0.808	0.00	2.041	0.112	2.041
0.29960	31.82	14.480	2807.3	1.09	0.08	35.32	14.507	2878.7	23.41	35.32	1.30	33.07	2.341	0.122	0.808	0.00	2.341	0.122	2.341
0.35951	41.68	15.184	3213.1	1.56	0.11	46.62	15.153	3307.7	26.90	46.62	1.96	36.90	2.670	0.130	0.808	0.00	2.670	0.130	2.670
0.43941	56.53	15.936	3741.8	2.04	0.15	63.47	15.872	3859.6	31.99	63.47	2.67	40.27	3.020	0.141	0.808	0.00	3.020	0.141	3.020
0.53922	83.86	17.246	4558.0	3.01	0.21	97.69	16.865	4788.5	38.94	97.69	3.60	44.17	3.369	0.155	0.808	0.00	3.369	0.155	3.369
0.67908	106.50	17.942	5135.9	3.50	0.24	125.74	17.428	5431.9	44.17	125.74	4.12	47.84	3.699	0.164	0.808	0.00	3.699	0.164	3.699
0.77895	131.75	18.504	5709.7	3.86	0.27	156.90	17.896	6064.9	49.32	156.90	4.53	50.34	3.944	0.164	0.808	0.00	3.944	0.164	3.944
0.87881	156.87	19.132	6221.9	4.36	0.29	191.33	18.284	6688.5	54.39	191.33	4.87	54.39	4.211	0.164	0.808	0.00	4.211	0.164	4.211
1.09852	225.03	19.968	7403.0	4.89	0.32	276.59	19.009	7988.9	64.36	276.59	5.48	64.36	4.644	0.164	0.808	0.00	4.644	0.164	4.644

0.0045" Ribbed 0.402" Pipe
Resistor - 350

Series

PEO

PPE
SZ-
d- 0.402
h- smooth
R2K
d- 0.381
h- 0.0045
RA 43.5

NUM 169
DATE 3/2/93
POLY IN-750
c program 250
w 1.080

Q (L/A)	Tet(SZ)	1/vol(SZ)	Revol(SZ)	S (SZ)	SF (SZ)	Tet(R2A)	1/vol(R2A)	Revol(R2A)	h _s	S (R2A)	SF (R2A)	1/vol(S2A)	St (S2)	R	RF	P	Δ/Trns	connected/R	connected/S	
0.00283	0.03	4.773	76.1			0.09	9.317	137.6	1.12			6.58	0.12	-0.077	-0.008	0.975				
0.00419	0.04	5.796	93.0			0.14	10.284	169.9	1.38			10.33	0.05	-0.080	-0.008	0.892				
0.00600	0.06	6.965	111.0			0.16	11.247	185.7	1.51			11.03	-0.01	-0.093	0.000	0.879				
0.00776	0.07	7.900	126.7			0.38	9.608	283.6	2.31			10.09	-0.05	0.015	0.001	0.862				
0.00966	0.09	8.822	141.4			0.49	9.694	323.4	2.63			9.81	-0.08	0.063	0.008	0.891				
0.01315	0.12	10.179	167.1			0.68	9.973	382.2	3.11	0.06	0.01	10.05	0.12	-0.077	-0.008	0.867			0.12	
0.02046	0.15	11.077	183.5			0.90	10.140	440.2	3.58	-0.04	0.00	10.22	0.05	-0.080	-0.008	0.867			0.05	
0.02353	0.29	10.359	255.0			1.13	10.357	493.8	4.02	-0.03	0.00	10.36	-0.01	-0.093	0.000	0.879			-0.01	
0.02860	0.43	9.778	312.0	0.13	0.01	1.32	10.475	532.9	4.33	-0.05	-0.01	10.46	-0.05	0.015	0.001	0.862			-0.05	
0.03347	0.61	10.010	370.6	-0.09	-0.01	1.67	10.713	600.1	4.88	-0.02	0.00	10.63	-0.09	0.063	0.008	0.891			-0.09	
0.03832	0.80	10.180	426.8	-0.09	-0.01	2.36	11.044	712.9	5.80	-0.02	0.00	10.92	-0.10	0.124	0.011	0.896			-0.10	
0.04182	1.02	10.324	482.2	-0.09	-0.01	3.09	11.270	816.4	6.64	-0.04	0.00	11.15	-0.10	0.120	0.011	0.896			-0.10	
0.04817	1.53	10.607	590.0	-0.09	-0.01	3.82	11.515	908.2	7.39	-0.01	0.00	11.34	-0.09	0.175	0.015	0.904			-0.09	
0.05899	2.18	10.898	703.2	-0.09	-0.01	4.66	11.683	1001.8	8.15	-0.04	0.00	11.5	-0.10	0.183	0.016	0.905			-0.10	
0.06883	2.84	11.129	804.7	-0.09	-0.01	5.91	12.003	1250.3	10.51	0.02	0.00	11.75	-0.05	0.253	0.022	0.913			-0.05	
0.07823	3.55	11.321	899.1	-0.11	0.01	7.86	12.373	1459.2	12.1	0.06	0.01	12.1	-0.05	0.273	0.023	0.915			-0.05	
0.08766	4.33	11.740	1119.6	-0.06	0.00	9.91	12.789	1459.4	11.87	0.19	0.02	12.45	0.19	0.339	0.027	0.922			0.05	
0.10142	5.55	12.073	1287.1	0.05	0.00	12.50	13.198	1642.0	13.35	0.35	0.03	12.79	0.33	0.408	0.032	0.929			0.19	
0.12053	7.39	12.450	1459.2	0.19	0.02	17.31	13.675	1943.4	15.80	0.57	0.04	13.3	0.55	0.375	0.028	0.923			0.33	
0.13989	9.39	12.797	1648.3	0.33	0.03	20.85	13.847	2132.3	17.34	0.66	0.05	13.59	0.67	0.257	0.019	0.912			0.55	
0.16216	11.94	13.304	1944.4	0.55	0.04	26.24	14.586	2392.7	19.46	1.36	0.10	14.54	1.42	0.046	0.003	0.891			0.67	
0.19773	16.42	13.554	2120.3	0.65	0.05	32.08	15.119	2655.4	21.51	1.90	0.14	15.15	1.86	-0.031	-0.002	0.885			1.42	
0.21970	19.59	14.447	2351.4	1.36	0.10	36.87	15.671	2912.3	23.88	2.46	0.19	15.75	2.29	-0.079	-0.005	0.881			1.86	
0.25985	24.01	15.026	2590.9	1.77	0.13	53.45	16.509	3415.1	27.77	3.31	0.25	16.85	3.12	-0.341	-0.020	0.864			2.29	
0.30760	28.16	15.608	2846.1	2.19	0.16	68.77	17.327	3874.3	31.51	4.12	0.31	17.82	3.87	-0.493	-0.028	0.853			3.12	
0.33954	33.18	16.607	3304.8	2.93	0.21	90.65	18.110	4447.4	36.17	4.87	0.37	18.8	4.61	-0.690	-0.037	0.840			3.87	
0.41943	47.42	17.537	3726.0	3.65	0.26	124.80	19.036	5216.9	42.42	5.74	0.43	19.97	5.50	-0.934	-0.047	0.828			4.61	
0.49933	60.27	18.467	4245.3	4.36	0.31	169.43	19.870	6071.7	49.37	6.51	0.49	21.13	6.40	-1.260	-0.060	0.810			5.50	
0.59919	78.26	18.467	4942.6	5.18	0.36	233.06	20.707	7081.6	57.59	7.26	0.54	22.29	7.29	-1.583	-0.071	0.795			6.40	
0.73900	106.13	19.558	4942.6	6.02	0.41															7.29
0.89879	140.97	20.639	5689.8	6.84	0.46															-1.61
1.09852	190.30	21.712	6574.3	6.84	0.46															-1.523

0.0045" \pm 1lb/inch² Pipe
 Resilient 350

Series
 PEO

PIPE
 SC:
 d = 0.402
 h = smooth
 R2A:
 d = 0.391
 h = 0.0045
 RA: 43.5

Q(L/s)	Vel(SC)	1/vel(SC)	1/vel(SC) ²	Reof(SC)	S(SC)	SF(SC)	1/vel(R2A)	Reof(R2A)	h _s	S(R2A)	SF(R2A)	1/vel(SC) ²	St(SC)	R	W	P	Δ /ves	connected R	connected S
0.00279	0.03	4.297	67.7	0.09	0.09	0.01	0.03	67.8	0.55	-0.09	0.01	4.3	0.06	-0.174	-0.018	0.851	0.00	-0.174	0.06
0.00387	0.04	5.021	80.4	0.05	0.01	0.00	0.05	83.0	0.68	-0.11	-0.01	5.18	0.00	-0.108	-0.011	0.862	0.00	-0.108	0.00
0.00577	0.07	6.116	98.6	0.07	-0.02	0.00	0.07	102.0	0.83	-0.14	-0.01	6.33	0.00	-0.105	-0.010	0.864	0.00	-0.105	-0.04
0.00754	0.09	6.998	112.7	0.10	-0.06	-0.01	0.10	115.9	0.94	-0.14	-0.01	7.16	0.00	-0.021	-0.002	0.876	0.00	-0.021	-0.07
0.00981	0.12	7.868	130.6	0.13	-0.08	-0.01	0.13	133.3	1.04	-0.14	-0.01	8.03	0.00	0.016	0.002	0.882	0.00	0.016	-0.12
0.01311	0.15	9.092	151.2	0.16	-0.12	-0.01	0.16	150.9	1.23	-0.06	-0.01	9.07	0.00	0.097	0.009	0.885	0.00	0.097	-0.12
0.01577	0.19	9.912	167.0	0.21	-0.12	-0.01	0.21	170.2	1.38	-0.02	0.00	10.08	0.00	0.147	0.013	0.888	0.00	0.147	-0.11
0.01990	0.24	11.060	189.0	0.26	-0.10	-0.01	0.26	192.3	1.56	-0.02	0.00	11.1	0.00	0.184	0.016	0.899	0.00	0.184	-0.10
0.02340	0.33	11.100	221.6	0.35	-0.01	0.00	0.35	222.4	1.81	-0.02	0.00	11.09	0.00	0.201	0.012	0.892	0.00	0.201	-0.07
0.02841	0.63	9.791	305.2	0.74	0.09	0.01	0.74	323.1	2.63	0.32	0.11	9.81	0.00	0.317	0.027	0.923	0.00	0.317	0.44
0.03303	0.83	9.877	352.0	1.18	0.01	0.00	0.95	374.6	2.98	0.33	-0.11	9.92	0.00	0.359	0.029	0.931	0.00	0.359	0.44
0.03745	1.04	9.998	394.7	1.40	-0.02	0.00	1.18	406.2	3.32	-0.14	-0.01	10.04	0.00	0.402	0.026	0.920	0.00	0.402	2.86
0.04135	1.24	10.115	431.0	1.79	-0.06	-0.01	1.40	445.4	3.62	-0.14	-0.01	10.34	0.00	0.432	0.026	0.891	0.00	0.432	3.82
0.04794	1.61	10.303	490.8	2.53	-0.12	-0.01	1.79	503.5	4.09	-0.14	-0.01	10.59	0.00	0.462	0.026	0.860	0.00	0.462	4.92
0.05860	2.29	10.554	585.8	3.26	-0.12	-0.01	2.53	598.9	4.87	-0.14	-0.01	10.81	0.00	0.492	0.026	0.860	0.00	0.492	5.89
0.06841	0.7780	10.780	669.2	4.03	-0.12	-0.01	3.26	679.5	5.53	-0.06	-0.01	10.81	0.00	0.522	0.026	0.860	0.00	0.522	6.82
0.07780	3.74	10.976	746.7	4.93	-0.10	-0.01	4.03	753.3	6.14	-0.02	0.00	11	0.00	0.552	0.026	0.860	0.00	0.552	7.75
0.08738	4.55	11.165	825.1	5.91	-0.01	0.00	4.93	835.8	6.80	0.09	0.01	11.19	0.00	0.582	0.026	0.860	0.00	0.582	8.68
0.10065	5.74	11.453	924.9	6.17	0.00	0.00	5.91	932.9	7.59	0.09	0.01	11.48	0.00	0.612	0.026	0.860	0.00	0.612	9.61
0.11970	7.56	11.867	1055.2	7.99	0.04	0.01	7.99	1055.6	8.58	0.35	0.05	11.87	0.18	0.642	0.026	0.860	0.00	0.642	10.54
0.14049	9.62	12.353	1196.9	10.12	0.17	0.01	10.12	1195.2	9.72	0.59	0.05	12.35	0.44	0.672	0.026	0.860	0.00	0.672	11.47
0.16308	11.91	12.886	1334.2	12.46	0.06	0.00	12.46	1329.3	10.80	0.92	0.07	12.85	0.76	0.702	0.026	0.860	0.00	0.702	12.40
0.18375	14.59	13.117	1486.0	15.18	0.07	0.00	15.18	1475.3	12.00	0.95	0.08	13.1	0.82	0.732	0.026	0.860	0.00	0.732	13.33
0.21870	18.89	13.783	1690.9	18.87	0.17	0.01	18.87	1645.0	13.38	1.70	0.13	13.59	1.13	0.762	0.026	0.860	0.00	0.762	14.26
0.25965	22.66	14.871	1852.7	24.33	0.20	0.10	24.33	1868.5	15.19	2.09	0.16	14.95	2.26	0.792	0.026	0.860	0.00	0.792	15.19
0.29960	27.13	15.683	2027.0	28.70	0.22	0.08	28.70	2029.5	16.50	2.95	0.22	15.69	2.86	0.822	0.026	0.860	0.00	0.822	16.12
0.43941	34.35	16.725	2281.5	37.51	0.28	0.08	37.51	2320.6	18.87	3.68	0.28	16.88	3.82	0.852	0.026	0.860	0.00	0.852	17.05
0.51930	44.40	17.980	2594.2	49.24	0.36	0.10	49.24	2639.4	21.63	4.80	0.36	18.22	4.92	0.882	0.026	0.860	0.00	0.882	18.00
0.65911	55.23	19.052	2893.2	62.47	0.42	0.10	62.47	2995.3	24.36	5.70	0.43	19.4	5.89	0.912	0.026	0.860	0.00	0.912	19.00
0.79892	75.61	20.668	3385.2	87.47	0.51	0.10	87.47	3544.0	28.82	7.08	0.54	21.15	7.35	0.942	0.026	0.860	0.00	0.942	20.00
0.95870	97.84	22.021	3849.3	115.96	0.58	0.10	115.96	4079.1	33.17	8.14	0.62	22.57	8.53	0.972	0.026	0.860	0.00	0.972	21.00
1.09852	126.20	23.268	4368.3	153.25	0.64	0.10	153.25	4685.6	38.10	9.03	0.68	24.03	9.75	1.002	0.026	0.860	0.00	1.002	22.00
	152.68	24.240	4772.5	189.52	0.69	0.10	189.52	5175.7	42.09	9.67	0.73	25.21	10.75	1.032	0.026	0.860	0.00	1.032	23.00

0.0045" Riblets 0.402" Pipe
 Rev 04-08-350

Sizes
 PEO

SIZE: .62
 d = 0.402
 h = smooth
 RZ/A: 3
 d = 0.391
 h = 0.0045
 R/h: 43.5

Q (L/h)	Vel (ft/s)	1/vel (s)	Reof (S)	S (S)	Sf (S)	1+vel (ft/s)	Reof (ft/s)	h	S (ft/s)	Sf (ft/s)	1/vel (ft/s)	S (ft/s)	Sf (ft/s)	R	RF	P	Δ/ves	connected P	connected P
0.00395	0.03	5.939	92.1			0.11	10.116	164.2	1.33							0.889			
0.00604	0.05	7.254	115.5			0.15	11.105	1900	1.54		10.18					0.874			
0.00845	0.07	8.593	136.6			0.18	11.420	213.5	1.74		11.26					0.848			
0.01007	0.09	9.381	149.3			0.41	8.912	317.5	2.58		9.86					0.869			
0.01160	0.10	10.029	161.2			0.54	9.919	367.7	2.99		10.18					0.865			
0.01473	0.16	11.582	204.7			0.73	10.105	426.4	3.47		10.36					0.867			
0.02170	0.36	9.841	306.2			0.95	10.355	488.1	3.97		10.53					0.878			
0.02539	0.48	9.969	356.1	0.16	0.02	1.19	10.609	546.6	4.44		10.68					0.891			
0.03513	0.86	10.330	476.3	0.02	0.00	1.43	10.764	586.6	4.87		10.86					0.892			
0.04028	1.09	10.505	537.3	0.02	0.00	1.83	11.013	676.8	5.50		10.96					0.901			
0.04474	1.31	10.653	588.8	-0.03	0.00	2.57	11.377	802.9	6.33		11.16					0.910			
0.05171	1.69	10.845	669.0	-0.06	-0.01	3.29	11.714	906.5	7.40		11.44					0.917			
0.06335	2.40	11.146	797.8	-0.06	-0.00	4.06	12.016	1010.1	8.21		11.73					0.918			
0.07307	3.10	11.435	906.9	0.00	0.00	4.81	12.319	1098.1	8.93		11.96					0.927			
0.08417	3.83	11.725	1007.6	0.11	0.01	6.13	12.746	1237.0	10.06		12.36					0.930			
0.09391	4.58	11.963	1100.6	0.20	0.02	6.84	13.177	1302.3	10.59		12.67					0.936			
0.10965	5.85	12.357	1242.0	0.38	0.03	9.23	13.632	1524.3	12.40		13.38					0.931			
0.11979	6.58	12.728	1312.3	0.66	0.05	11.85	14.465	1729.4	14.06		14					0.929			
0.14602	8.83	13.399	1531.7	1.06	0.09	15.83	15.311	2002.0	16.28		14.56					0.920			
0.17300	11.31	14.028	1735.8	1.47	0.12	20.98	15.847	2299.5	18.70		15.44					0.900			
0.21171	15.55	14.637	2036.5	1.80	0.14	26.50	16.302	2590.2	21.06		16.14					0.883			
0.25166	19.73	15.447	2296.3	2.40	0.18	30.97	16.732	2800.3	22.77		16.63					0.870			
0.29161	24.50	16.064	2558.6	2.83	0.21	40.71	17.115	3210.5	26.11		17.28					0.813			
0.32956	28.42	16.947	2756.1	3.19	0.26	67.57	17.480	4136.4	31.64		18.27					0.790			
0.37949	36.40	17.150	3118.6	3.57	0.30	101.60	17.676	5072.4	41.25		18.81					0.741			
0.49933	56.45	18.121	3883.9	4.16	0.30	153.80	17.611	6238.8	50.73		19.37					0.675			
0.61916	82.50	18.585	4695.9	4.30	0.30	211.08	17.407	7305.0	59.40		19.49					0.675			
0.75897	117.02	19.129	5590.9	4.54	0.31	343.85	17.045	9283.8	75.49		19.13					0.675			
0.87881	152.46	19.406	6376.1	4.59	0.31											0.675			
1.09852	230.58	19.351	7943.5	4.19	0.28											0.675			

0.0045" Ribbed 0.402" Pipe

Rev'd 11-1-35

Series

PEO

P/E
 S/E
 d = 0.402
 h = smooth
 R2A
 c = 10
 d = 0.391
 h = C.D.045
 R/A 43.5

Q (L/A)	Ted(S2)	1/sof(S2)	Refod(S2)	S (S2)	Sf (S2)	Ted(R2A)	1/sof(R2A)	Refod(R2A)	h _s	S (R2A)	Sf (R2A)	1/sof(S2)	R	W	P	d/nms	corrected R	corrected S	
0.00458	0.04	6.229	101.0	0.05	0.00	0.11	10.126	165.2	1.34	0.03	0.00	10.07	-0.017	-0.002	0.901	0.00	-0.017	0.03	
0.00707	0.06	7.793	124.6	0.01	0.00	0.14	11.325	182.4	1.48	0.00	0.00	10.92	-0.026	-0.003	0.933	0.00	-0.026	-0.01	
0.00879	0.08	8.667	139.7	0.00	0.00	0.20	11.232	222.7	1.81	-0.04	-0.04	10.89	-0.002	0.000	0.930	0.00	-0.002	-0.04	
0.01028	0.09	9.350	151.7	0.00	0.00	0.40	9.776	313.6	2.55	0.03	0.03	9.8	0.03	0.00	0.966	0.00	0.03	-0.08	
0.01178	0.10	9.969	163.3	0.00	0.00	0.55	9.883	368.7	3.00	-0.01	-0.01	9.9	-0.01	0.005	0.988	0.00	0.051	-0.10	
0.01454	0.13	10.959	183.4	0.00	0.00	0.78	10.124	437.5	3.56	0.00	0.00	10.15	-0.01	0.013	0.976	0.00	0.145	-0.10	
0.01759	0.19	10.888	223.6	0.00	0.00	1.01	10.348	498.3	4.05	-0.06	-0.06	10.35	-0.04	0.005	0.989	0.00	0.211	-0.10	
0.02154	0.36	9.819	303.9	0.00	0.00	1.46	10.681	600.0	4.88	0.07	0.07	10.63	-0.10	0.019	0.910	0.00	0.330	0.11	
0.02557	0.50	9.869	359.4	0.00	0.00	1.87	10.975	676.3	5.52	0.14	0.14	11.19	0.11	0.028	0.925	0.00	0.308	0.37	
0.03106	0.70	10.111	426.4	0.00	0.00	2.57	11.401	746.0	6.47	0.35	0.35	11.51	0.30	0.026	0.919	0.00	0.356	0.52	
0.03614	0.91	10.312	486.7	0.00	0.00	3.24	11.840	893.7	7.27	0.56	0.56	11.95	0.37	0.029	0.925	0.00	0.348	1.54	
0.04488	1.33	10.506	588.7	0.00	0.00	3.97	12.298	998.3	8.04	0.73	0.73	12.23	0.52	0.033	0.928	0.00	0.372	2.17	
0.05213	2.40	11.169	790.9	0.00	0.00	4.59	12.586	1063.5	8.65	1.29	1.29	13.02	0.58	0.026	0.919	0.00	0.490	1.06	
0.07402	3.08	11.950	987.8	0.00	0.00	5.97	13.450	1213.1	9.86	1.62	1.62	13.6	0.54	0.033	0.928	0.00	0.348	1.54	
0.08485	3.75	12.231	1065.2	0.00	0.00	6.97	13.948	1303.6	10.60	1.62	1.62	14.46	0.54	0.026	0.920	0.00	0.372	2.17	
0.09374	4.37	13.048	1217.2	0.00	0.00	8.90	14.832	1483.8	12.07	2.20	2.20	15.13	0.52	0.026	0.923	0.00	0.423	2.67	
0.11429	5.70	13.602	1301.2	0.00	0.00	10.85	15.553	1641.3	13.35	3.54	3.54	15.53	0.52	0.026	0.968	0.00	0.979	2.95	
0.12799	6.58	14.452	1482.3	0.00	0.00	12.41	16.509	1757.3	14.29	4.44	4.44	16.6	0.52	0.026	0.961	0.00	0.887	4.48	
0.15374	8.41	14.452	1482.3	0.00	0.00	16.43	17.583	2022.0	16.44	5.18	5.18	17.5	0.52	0.026	0.951	0.00	0.887	4.48	
0.17799	10.29	15.131	1642.1	0.00	0.00	20.54	18.367	2261.0	18.39	5.18	5.18	18.36	0.52	0.026	0.914	0.00	0.374	5.15	
0.20213	12.35	15.683	1800.6	0.00	0.00	25.63	19.234	2525.3	20.53	6.07	6.07	19.44	0.52	0.026	0.878	0.00	-0.152	6.02	
0.24767	16.22	16.769	2063.7	0.00	0.00	32.73	19.288	2854.1	23.21	6.07	6.07	20.67	0.52	0.026	0.823	0.00	-0.877	6.90	
0.28961	20.07	17.627	2295.9	0.00	0.00	46.61	19.785	3478.1	26.28	6.58	6.58	21.56	0.52	0.026	0.800	0.00	-1.200	7.39	
0.32955	24.06	18.319	2513.8	0.00	0.00	67.80	20.242	4107.3	33.40	7.03	7.03	22.61	0.52	0.026	0.766	0.00	-1.570	7.96	
0.38348	29.52	19.244	2784.4	0.00	0.00	104.14	20.839	5090.4	41.39	7.56	7.56	23.15	0.52	0.026	0.740	0.00	-1.793	8.08	
0.47935	41.11	20.395	3285.9	0.00	0.00	163.83	21.105	6380.8	51.89	7.71	7.71	23.39	0.52	0.026	0.720	0.00	-2.070	8.03	
0.57932	55.70	21.161	3824.7	0.00	0.00	225.55	21.050	7448.5	60.57	7.57	7.57	23.39	0.52	0.026	0.720	0.00	-2.070	8.03	
0.73960	81.93	22.260	4638.5	0.00	0.00														
0.93873	124.62	22.928	5717.2	0.00	0.00														
1.09852	166.80	23.192	6580.6	0.00	0.00														

0.0045" Ribbed 0.402" Pipe
Residues: 350

Series
PEO

WFE
SZ: 160
d = 0.402
h = smooth
R24:
d = 0.391
h = 0.0045
RN = 43.5

Q (t/h)	Temp(SZ)	1/nd(SZ)	Reprod(SZ)	S (SZ)	SF (SZ)	Temp(R2A)	1/nd(R2A)	Reprod(R2A)	h	S (R2A)	SF (R2A)	1/nd(SZ)	S (SZ)	R	R	P	ΔT/hrs	connected R	connected S
0.00525	0.05	6.652	106.4	0.15	0.02	0.13	10.262	171.0	1.39	0.07	0.01	10.33	0.12	-0.061	0.00	0.887	0.00	-0.061	0.12
0.00789	0.07	8.143	130.8	-0.08	-0.01	0.17	11.179	196.9	1.60	0.07	0.00	11.15	-0.08	0.054	0.00	0.884	0.00	0.054	-0.08
0.00966	0.09	9.966	145.6	-0.06	-0.01	0.22	11.018	228.0	1.85	0.06	0.00	11.13	-0.06	0.026	0.00	0.868	0.00	0.026	-0.06
0.01146	0.10	9.750	159.0	0.01	0.00	0.43	9.767	319.6	2.60	0.05	0.01	9.83	0.02	0.015	0.00	0.885	0.00	0.015	0.02
0.01262	0.11	10.184	167.7	0.25	0.02	0.57	9.919	368.0	2.89	0.05	0.01	9.98	0.25	0.309	0.00	0.868	0.00	0.309	0.25
0.01580	0.15	11.115	192.8	0.61	0.05	0.79	10.114	432.3	3.52	0.04	0.00	10.06	0.61	0.054	0.00	0.885	0.00	0.054	0.61
0.01800	0.19	11.185	218.6	0.75	0.02	1.27	10.526	548.5	4.46	0.06	0.01	10.5	0.75	0.026	0.00	0.885	0.00	0.026	0.75
0.02337	0.39	9.902	310.0	0.25	0.02	1.85	11.061	661.6	5.38	0.14	0.01	10.9	0.25	0.309	0.00	0.904	0.00	0.309	0.25
0.02613	0.51	9.959	356.8	0.61	0.05	2.47	11.699	765.3	6.22	0.07	0.05	11.39	0.61	0.286	0.00	0.868	0.00	0.286	0.61
0.03125	0.72	10.034	424.1	1.03	0.09	3.10	12.236	857.4	6.97	0.83	0.07	11.95	1.03	0.027	0.00	0.918	0.00	0.027	1.03
0.04124	1.16	10.460	537.3	1.37	0.12	3.71	12.834	937.5	7.62	1.25	0.11	12.53	1.37	0.304	0.00	0.918	0.00	0.304	1.16
0.05225	1.72	10.876	654.9	2.06	0.18	4.28	13.337	1006.8	8.19	1.60	0.14	12.99	2.06	0.347	0.00	0.922	0.00	0.347	1.72
0.06390	2.34	11.385	765.6	2.50	0.21	5.40	14.360	1129.6	9.19	2.37	0.20	13.86	2.50	0.500	0.00	0.932	0.00	0.500	2.34
0.07483	2.92	11.937	855.5	3.33	0.27	6.04	14.892	1188.1	9.67	2.78	0.23	14.34	3.33	0.552	0.00	0.933	0.00	0.552	2.92
0.08584	3.50	12.516	935.7	3.81	0.31	7.77	15.890	1359.2	11.04	3.55	0.29	14.94	3.81	0.562	0.00	0.930	0.00	0.562	3.50
0.11600	5.18	13.900	1335.9	4.05	0.33	8.86	16.572	1452.3	11.81	3.99	0.32	16.01	4.05	0.683	0.00	0.930	0.00	0.683	5.18
0.15477	7.44	15.471	1965.6	5.08	0.40	9.72	17.333	1524.6	12.40	4.64	0.37	16.28	5.08	0.757	0.00	0.930	0.00	0.757	7.44
0.18775	8.46	16.427	1565.9	5.38	0.42	12.42	18.754	1724.0	14.02	5.82	0.45	17.33	5.38	0.862	0.00	0.987	0.00	0.862	8.46
0.22269	12.59	17.648	1783.2	5.04	0.42	13.43	19.447	1792.7	14.58	6.45	0.50	17.69	5.04	0.987	0.00	1.011	0.00	0.987	12.59
0.24767	13.96	18.076	1877.4	5.38	0.51	17.38	19.993	2039.1	16.58	6.84	0.52	19.31	5.38	1.757	0.00	1.011	0.00	1.757	13.96
0.28961	16.60	19.380	2047.6	6.54	0.58	21.47	21.086	2266.8	18.43	7.88	0.60	20.52	6.54	6.47	0.00	0.930	0.00	6.47	16.60
0.33954	20.34	20.525	2266.8	7.50	0.58	27.82	21.796	2560.2	20.98	8.57	0.65	20.52	7.50	7.50	0.00	0.930	0.00	7.50	20.34
0.39946	25.52	21.560	2539.0	8.34	0.63	40.91	22.464	3129.2	25.45	9.26	0.70	21.72	8.34	8.47	0.00	0.893	0.00	8.47	25.52
0.48933	34.41	23.208	2948.2	9.73	0.72	63.83	23.021	3908.5	31.78	9.82	0.74	23.78	9.73	-1.316	0.00	0.819	0.00	-1.316	34.41
0.63914	49.39	24.797	3531.9	11.01	0.80	97.92	23.815	4839.9	39.36	10.55	0.80	25.45	11.01	-2.429	0.00	0.753	0.00	-2.429	49.39
0.81889	73.44	26.054	4306.2	11.92	0.84	129.14	24.278	5551.7	45.15	10.86	0.82	26.79	11.92	-3.975	0.00	0.715	0.00	-3.975	73.44
0.98070	94.80	26.847	4866.7	12.49	0.87	166.34	24.511	6264.4	50.94	11.13	0.83	27.14	12.49	-1.114	0.00	0.715	0.00	-1.114	94.80
1.09852	120.03	27.339	5467.0	12.79	0.88							27.91	13.12	-3.399	0.00	0.702	0.00	-3.399	120.03

0.00-38" Ribbed 0.402" Pipe
 Resonant: 350

Series

PEO

ME
 SZ:
 d = 0.402
 h = smooth
 RZA:
 d = 0.391
 h = 0.0045
 Ra = 43.5

RMN 164
 DATE 2/22/93
 POLY M-YOK
 c-sigma 100
 W 1.089

Q (Ln)	1w(SZ)	1/w(SZ)	Resp(SZ)	S (SZ)	Q (SZ)	1w(RZA)	1/w(RZA)	Resp(RZA)	N	S (RZA)	Sf (RZA)	1/w(SZ)	Sf (SZ)	R	R	P	d/hrs	connected R	connected S
0.00380	0.04	5.504	RR-1	0.15	0.01	0.12	0.01	161.1	1.31	-0.02	0.00	9.86	0.24	-0.261	-0.028	0.823	0.00	-0.281	0.24
0.00491	0.05	6.277	100.1	0.12	0.01	0.17	0.00	192.0	1.56	0.00	0.00	11.14	0.13	-0.203	-0.020	0.829	0.00	-0.203	0.13
0.00579	0.06	7.366	117.9	0.13	0.01	0.20	0.00	204.8	1.87	0.00	0.00	9.89	0.12	-0.065	-0.008	0.838	0.00	-0.065	0.12
0.00662	0.08	8.299	133.2	0.13	0.01	0.46	0.00	311.8	2.54	0.00	0.00	10.19	0.14	-0.027	-0.003	0.834	0.00	-0.027	0.14
0.01175	0.11	9.635	156.7	0.18	0.02	0.58	0.00	351.7	2.86	0.00	0.00	10.37	0.21	0.026	0.002	0.834	0.00	0.026	0.21
0.01534	0.15	10.842	182.0	0.43	0.04	0.70	0.00	411.4	3.35	0.00	0.00	10.56	0.45	0.196	0.018	0.834	0.00	0.196	0.45
0.01832	0.19	11.433	206.5	0.43	0.04	0.85	0.00	458.6	3.74	0.00	0.00	10.78	1.2	0.230	0.019	0.834	0.00	0.230	1.00
0.02262	0.29	9.800	296.6	0.209	0.18	1.21	0.00	507.5	4.13	0.00	0.00	12.0	1.63	0.286	0.022	0.834	0.00	0.286	1.63
0.03095	0.69	10.314	394.8	2.09	0.23	3.32	0.00	552.3	4.99	0.00	0.00	13.41	2.11	0.337	0.025	0.834	0.00	0.337	2.11
0.03559	0.89	10.510	446.1	2.67	0.23	3.83	0.00	608.0	6.06	0.00	0.00	14.12	2.69	0.325	0.023	0.834	0.00	0.325	2.69
0.04024	1.09	10.714	495.1	3.73	0.32	4.92	0.00	662.5	8.34	0.00	0.00	15.36	3.74	0.390	0.025	0.834	0.00	0.390	3.74
0.04493	1.31	10.714	542.3	4.26	0.36	5.41	0.00	708.3	8.68	0.00	0.00	15.84	4.13	0.294	0.050	0.834	0.00	0.294	4.13
0.05257	1.65	11.170	609.9	5.46	0.46	6.94	0.00	782.4	9.92	0.00	0.00	17.31	5.36	0.751	0.043	0.834	0.00	0.751	5.36
0.06489	2.19	11.964	704.8	6.11	0.51	7.95	0.00	843.6	10.64	0.00	0.00	18.07	6.00	0.790	0.044	0.834	0.00	0.790	6.00
0.07678	2.68	12.777	780.0	6.24	0.51	8.75	0.00	902.6	11.19	0.00	0.00	18.28	6.13	1.153	0.063	0.834	0.00	1.153	6.13
0.08699	3.14	13.394	842.8	6.77	0.55	9.19	0.00	968.0	11.45	0.00	0.00	18.48	6.29	1.178	0.064	0.834	0.00	1.178	6.29
0.09827	3.61	14.098	902.6	7.43	0.60	10.64	0.00	1025.3	12.35	0.00	0.00	19.52	7.19	1.448	0.074	0.834	0.00	1.448	7.19
0.13445	5.26	15.990	1062.5	8.89	0.71	13.65	0.00	1067.1	13.99	0.00	0.00	21.38	8.84	0.711	0.033	0.834	0.00	0.711	8.84
0.16531	6.70	17.418	1231.1	11.04	0.86	19.91	0.00	1219.7	16.89	0.00	0.00	24.76	11.89	-1.220	-0.053	0.834	0.00	-1.220	11.89
0.18478	7.67	18.196	1319.9	12.13	0.94	23.61	0.00	1376.3	18.39	0.00	0.00	26.02	13.00	-2.125	-0.082	0.834	0.00	-2.125	13.00
0.19973	8.72	18.436	1412.2	13.55	1.04	31.22	0.00	1489.3	20.11	0.00	0.00	26.07	14.81	-3.177	-0.113	0.834	0.00	-3.177	14.81
0.20710	8.85	18.881	1419.6	13.55	1.04	44.11	0.00	1601.4	21.15	0.00	0.00	26.97	16.41	-3.836	-0.128	0.834	0.00	-3.836	16.41
0.20710	8.85	18.881	1419.6	13.55	1.04	44.11	0.00	1601.4	21.15	0.00	0.00	26.97	16.41	-3.836	-0.128	0.834	0.00	-3.836	16.41
0.23768	10.70	19.809	1564.3	15.46	1.24	63.07	0.00	1719.9	25.05	0.00	0.00	31.69	17.62	-3.321	-0.105	0.834	0.00	-3.321	17.62
0.29362	13.01	21.439	1725.0	16.97	1.30	86.94	0.00	1895.9	30.05	0.00	0.00	32.88	18.73	-3.323	-0.104	0.834	0.00	-3.323	18.73
0.36351	17.29	23.831	1989.0	18.78	1.33	114.02	0.00	2061.1	40.08	0.00	0.00	33.65	19.28	-3.507	-0.100	0.834	0.00	-3.507	19.28
0.40345	19.32	25.024	2102.3	18.78	1.33	114.02	0.00	2261.8	40.08	0.00	0.00	33.65	19.28	-3.507	-0.100	0.834	0.00	-3.507	19.28
0.48335	24.45	26.650	2365.0	18.78	1.33	114.02	0.00	2489.3	40.08	0.00	0.00	33.65	19.28	-3.507	-0.100	0.834	0.00	-3.507	19.28
0.60318	32.59	28.808	2729.9	18.78	1.33	114.02	0.00	2691.4	40.08	0.00	0.00	33.65	19.28	-3.507	-0.100	0.834	0.00	-3.507	19.28
0.78294	48.47	30.662	3328.5	18.78	1.33	114.02	0.00	2836.9	40.08	0.00	0.00	33.65	19.28	-3.507	-0.100	0.834	0.00	-3.507	19.28
0.95870	66.11	32.147	3882.9	18.78	1.33	114.02	0.00	3014.3	40.08	0.00	0.00	33.65	19.28	-3.507	-0.100	0.834	0.00	-3.507	19.28
1.11849	85.67	32.948	4389.0	18.78	1.33	114.02	0.00	4928.5	40.08	0.00	0.00	33.65	19.28	-3.507	-0.100	0.834	0.00	-3.507	19.28

0.00-08" Fiberglass 402" Pipe
 Residual = 350

Series

PEO

PFE
 SC: 166
 d = 0.402
 h = smooth
 RZA: IN-60K
 POLY IN-60K
 c = 300
 w = 1.317
 R/h = 43.5

Q (L/h)	Tw(SZ)	1/Avg(SZ)	Resid(SZ)	S(SZ)	Sf(SZ)	Tw(RZA)	1/Avg(RZA)	Resid(RZA)	N	S(RZA)	Sf(RZA)	1/Avg(SZ)h	Sf(SZ)	R	RF	P	d/True	corrected R	corrected S
0.00324	0.04	4.636	73.4	0.20	0.02	0.94	9.876	305.6	2.48	0.04	0.00	10.02	0.16	-0.144	-0.014	0.854	0.00	-0.144	0.16
0.00457	0.05	5.478	87.8	0.12	0.01	1.19	10.121	411.9	3.35	0.07	0.01	10.17	0.11	-0.049	-0.005	0.872	0.00	-0.049	0.11
0.00575	0.07	6.153	98.6	0.10	0.01	1.38	10.262	445.0	3.62	0.06	0.01	10.31	0.12	-0.048	-0.005	0.875	0.00	-0.048	0.12
0.00686	0.08	6.707	108.1	0.20	0.02	1.74	10.717	499.7	4.06	0.31	0.03	10.62	0.23	0.097	0.009	0.897	0.00	0.097	0.23
0.01174	0.14	8.687	143.0	0.58	0.05	2.35	11.542	580.4	4.72	0.86	0.08	11.23	0.57	0.312	0.028	0.923	0.00	0.312	0.57
0.01647	0.19	10.214	170.8	1.13	0.10	2.90	12.396	645.0	5.24	1.52	0.14	11.92	1.08	0.476	0.040	0.936	0.00	0.476	1.08
0.02050	0.25	11.209	193.5	1.64	0.15	3.40	13.000	697.5	5.67	1.98	0.18	12.6	1.63	0.400	0.032	0.927	0.00	0.400	1.63
0.02383	0.30	11.727	214.0	2.26	0.20	3.96	13.837	751.9	6.11	2.68	0.24	13.31	2.21	0.527	0.040	0.935	0.00	0.527	2.21
0.02877	0.34	10.708	264.1	3.07	0.27	4.65	14.870	830.0	6.75	3.49	0.31	14.24	2.96	0.590	0.041	0.937	0.00	0.590	2.96
0.03330	0.83	9.888	352.9	4.18	0.36	5.96	16.233	925.2	7.52	4.68	0.40	15.54	4.08	0.693	0.045	0.939	0.00	0.693	4.08
0.03831	1.06	10.131	400.5	5.32	0.45	7.41	17.499	1044.2	8.57	6.67	0.48	17	5.31	0.499	0.029	0.925	0.00	0.499	5.31
0.04194	1.24	10.253	433.5	6.26	0.53	8.73	18.615	1154.8	9.39	6.57	0.55	18.06	6.21	0.555	0.031	0.923	0.00	0.555	6.21
0.04916	1.61	10.575	492.9	6.61	0.55	10.00	19.445	1201.9	9.77	7.31	0.60	18.42	6.50	1.025	0.056	0.956	0.00	1.025	6.50
0.05148	2.23	11.233	580.5	6.61	0.55	11.98	21.093	1315.3	10.70	7.31	0.60	18.42	6.50	1.025	0.056	0.956	0.00	1.025	6.50
0.07338	2.79	11.977	649.8	8.11	0.67	14.67	23.510	1455.4	11.84	9.92	0.79	19.9	7.82	1.193	0.080	0.952	0.00	1.193	7.82
0.08327	3.24	12.621	699.3	9.55	0.78	16.67	24.818	1622.2	13.60	11.94	0.93	24.75	9.48	0.780	0.096	0.931	0.00	0.780	9.48
0.09565	3.80	13.378	756.9	12.03	0.96	19.36	26.111	1824.7	15.65	13.02	0.99	26.93	12.26	0.068	0.003	0.897	0.00	0.068	12.26
0.11349	4.67	14.323	836.5	13.75	1.09	25.63	26.111	1924.7	18.73	14.30	1.08	29.1	16.05	-1.589	-0.055	0.820	0.00	-1.589	16.05
0.13766	5.75	15.657	933.7	15.45	1.19	36.71	27.511	2303.4	22.59	15.88	1.20	31.1	17.72	-2.504	-0.064	0.799	0.00	-2.504	17.72
0.16550	7.03	17.012	1055.5	17.17	1.30	53.42	29.096	2778.5	26.75	16.64	1.26	32.34	18.67	-2.507	-0.078	0.771	0.00	-2.507	18.67
0.19111	8.28	18.108	1155.5	18.24	1.35	75.17	29.833	3298.5	26.75	16.64	1.26	32.34	18.67	-2.507	-0.078	0.771	0.00	-2.507	18.67
0.21371	9.86	18.559	1225.7	18.90	1.37	105.01	30.852	3847.4	31.29	17.65	1.34	33.11	19.17	-2.258	-0.068	0.778	-5.09	-2.069	18.98
0.23966	11.71	20.210	1386.1	6.61	0.55	10.00	19.445	1201.9	9.77	7.31	0.60	18.42	6.50	1.025	0.056	0.956	0.00	1.025	6.50
0.29960	14.03	21.811	1462.0	8.11	0.67	14.67	23.510	1455.4	11.84	9.92	0.79	19.9	7.82	1.193	0.080	0.952	0.00	1.193	7.82
0.37949	17.84	24.495	1649.1	9.55	0.78	16.67	24.818	1622.2	13.60	11.94	0.93	24.75	9.48	0.780	0.096	0.931	0.00	0.780	9.48
0.45938	22.47	26.421	1851.5	12.03	0.96	19.36	26.111	1824.7	15.65	13.02	0.99	26.93	12.26	0.068	0.003	0.897	0.00	0.068	12.26
0.57922	30.94	28.393	2172.5	13.75	1.09	25.63	26.111	1924.7	18.73	14.30	1.08	29.1	16.05	-1.589	-0.055	0.820	0.00	-1.589	16.05
0.73900	43.88	30.419	2586.8	15.45	1.19	36.71	27.511	2303.4	22.59	15.88	1.20	31.1	17.72	-2.504	-0.064	0.799	0.00	-2.504	17.72
0.89479	59.55	31.757	3008.0	17.17	1.30	53.42	29.096	2778.5	26.75	16.64	1.26	32.34	18.67	-2.507	-0.078	0.771	0.00	-2.507	18.67
1.09852	83.96	32.691	3514.3	18.90	1.37	105.01	30.852	3847.4	31.29	17.65	1.34	33.11	19.17	-2.258	-0.068	0.778	-5.09	-2.069	18.98

0.0045" Ribbed 7.602" Pipe
Res/cft = 3.50

Series: PEO

REP# 152
DATE 1/29/93
POLY 301
c. temp 3
IR 1.000

PEE
SZ: d = 0.402
h = smooth
R2A: d = 0.391
h = 0.0045
RN = 43.5

Q (L/A)	Td(SZ)	1/Ap(SZ)	Rep(SZ)	S (SZ)	SF (SZ)	Td(R2A)	1/Ap(R2A)	Rep(R2A)	h _a	S (R2A)	SF (R2A)	1/Ap(SZ) _h	S ₁ (SZ)	R	RF	P	Δ/hrs	corrected R	corrected S
0.00464	0.04	6.439	100.4			0.14	11.313	187.6	1.53			11.16				0.901			
0.00698	0.06	7.841	124.2			0.18	11.312	211.6	1.72			9.84				0.875			
0.00929	0.08	9.008	144.0			0.35	9.694	297.5	2.42			9.88				0.842			
0.01107	0.10	9.781	158.2			0.45	9.966	370.2	3.01	0.11	0.01	9.99	0.12	-0.024	-0.002	0.876	0.00	-0.024	0.12
0.01248	0.11	10.359	168.6			0.71	10.199	424.7	3.45	0.08	0.01	10.42	0.09	-0.001	0.000	0.879	0.00	-0.001	0.09
0.01472	0.13	11.138	185.5			0.97	10.362	494.4	4.02	-0.03	-0.01	10.55	0.03	-0.058	-0.006	0.872	0.00	-0.058	0.04
0.01659	0.16	11.306	206.1			1.14	10.505	536.5	4.36	-0.04	-0.01	10.55	0.03	-0.045	-0.004	0.874	0.00	-0.045	0.03
0.01998	0.20	9.875	284.3			1.53	10.830	602.0	4.90	0.08	0.00	10.76	0.04	0.070	0.006	0.891	0.00	0.070	0.04
0.02354	0.24	9.951	360.9			1.81	11.208	678.1	5.51	0.24	0.02	11.1	0.17	0.108	0.010	0.898	0.00	0.108	0.17
0.02996	0.28	10.170	414.5			2.45	11.858	788.3	6.41	0.61	0.05	11.69	0.50	0.168	0.014	0.905	0.00	0.168	0.50
0.03541	0.31	10.505	522.2			3.06	12.454	881.2	7.17	0.89	0.07	12.23	0.85	0.224	0.018	0.911	0.00	0.224	0.85
0.04503	0.36	11.652	780.9			3.87	13.131	991.2	8.06	1.43	0.10	12.91	1.33	0.221	0.017	0.910	0.00	0.221	1.33
0.05246	0.41	12.200	875.6			4.57	13.619	1075.5	8.75	1.74	0.12	13.41	1.68	0.209	0.016	0.908	0.00	0.209	1.68
0.06451	0.48	12.866	984.7			5.26	14.143	1144.5	9.31	2.12	0.15	13.87	2.04	0.273	0.020	0.913	0.00	0.273	2.04
0.08981	0.57	13.359	1067.3			6.73	14.491	1193.6	9.71	2.37	0.17	14.19	2.28	0.301	0.021	0.915	0.00	0.301	2.28
0.10121	0.63	13.835	1138.9			8.45	15.207	1289.9	10.57	2.88	0.21	14.89	2.83	0.317	0.021	0.915	0.00	0.317	2.83
0.11954	0.72	14.158	1189.2			9.39	16.156	1464.9	11.91	3.55	0.26	15.77	3.51	0.386	0.024	0.918	0.00	0.386	3.51
0.13709	0.82	14.865	1294.6			10.45	16.445	1566.4	12.58	3.72	0.28	16.09	3.73	0.355	0.022	0.915	0.00	0.355	3.73
0.16318	0.93	15.761	1461.7			14.90	18.463	1952.0	15.87	5.35	0.45	17.76	5.00	0.703	0.040	0.938	0.00	0.703	5.00
0.17513	0.97	16.070	1540.4			20.41	19.589	2285.0	18.58	6.38	0.55	18.82	5.78	0.769	0.041	0.940	0.00	0.769	5.78
0.24767	1.36	17.819	1968.7			27.00	20.130	2627.9	21.37	6.91	0.59	19.79	6.51	0.940	0.017	0.969	-3.86	0.940	-3.86
0.30758	1.72	18.884	2307.2			42.00	20.398	3277.7	26.65	7.20	0.61	20.8	7.14	-0.402	-0.019	0.953	-6.67	-0.402	-6.67
0.36351	25.21	19.740	2608.6			65.98	20.519	4108.4	33.41	7.30	0.62	21.4	7.35	-0.881	-0.041	0.810	-9.61	-0.881	-9.61
0.45938	36.81	20.643	3152.6			98.49	20.269	5018.9	40.81	6.99	0.59	21.46	7.06	-1.191	-0.055	0.779	-12.29	-1.191	-12.29
0.57922	54.89	21.315	3849.7			133.26	19.915	5835.5	47.45	6.57	0.55	21.36	6.70	-1.445	-0.068	0.754	-14.27	-1.445	-14.27
0.69906	78.84	21.465	4613.2			226.46	19.096	7591.7	61.73	5.60	0.45	20.85	5.73	-1.754	-0.084	0.713	-17.77	-1.754	-17.77
0.79832	103.18	21.444	5275.2																
0.99865	165.90	21.139	6675.5																

0.0045" Ribbed 60.402" Pipe
Resident: 350

Series

PEO

PKR 153
SZ 1/20/93
d = 0.402
h = smooth
POLY 301
c 10
r 1.019
R2A:
d = 0.391
h = 0.0045
N = 43.5

Q(L/A)	Tot(SZ)	1/ndf(SZ)	Reof(SZ)	S(SZ)	Sf(SZ)	Tot(R2A)	1/ndf(R2A)	Reof(R2A)	h	S(R2A)	Sf(R2A)	1/ndf(S2)	Sf(S2)	R	Rf	P	d/hrs	connected R	connected S	
0.00303	0.03	5.065	81.9	0.13	0.01	0.14	10.972	181.2	1.47	0.11	0.01	10.88		-0.027	-0.003	0.900				
0.00412	0.04	5.891	95.6	0.08	0.01	0.16	11.578	197.2	1.60	0.31	0.01	11.33				0.908				
0.00536	0.06	7.341	118.9	0.06	0.01	0.31	10.014	275.0	2.24	0.50	0.01	10.07				0.855				
0.00913	0.08	8.803	142.4	0.08	0.01	0.50	9.911	346.1	2.81	0.62	0.01	9.92				0.878				
0.01130	0.10	9.750	159.3	0.10	0.01	0.62	10.053	388.9	3.16	0.75	0.01	10.08				0.875				
0.01409	0.13	10.809	179.0	0.13	0.01	0.75	10.226	426.7	3.47	0.88	0.01	10.15				0.885				
0.01617	0.15	11.355	195.8	0.15	0.01	0.88	10.536	486.6	3.96	1.01	0.01	10.45				0.895				
0.01948	0.20	10.120	264.8	0.20	0.01	1.01	11.281	566.6	4.61	1.11	0.01	10.98				0.901				
0.02425	0.45	9.890	337.6	0.45	0.01	1.11	11.938	627.3	5.10	1.11	0.01	11.49				0.936				
0.02760	0.56	10.046	378.9	0.56	0.01	1.32	12.912	715.3	5.82	1.85	0.17	12.37				0.941				
0.03086	0.69	10.161	418.0	0.69	0.01	1.62	11.938	627.3	5.10	1.11	0.10	12.37				0.941				
0.03629	0.90	10.408	479.5	0.90	0.01	2.11	12.912	715.3	5.82	1.85	0.17	12.37				0.941				
0.04508	1.25	10.978	565.7	1.25	0.01	2.60	13.729	793.4	6.45	2.47	0.22	13.16				0.940				
0.05290	1.56	11.533	632.0	1.56	0.01	3.13	14.382	873.0	7.10	2.94	0.26	13.92				0.929				
0.06510	2.04	12.441	722.7	2.04	0.18	3.70	14.998	948.8	7.72	3.39	0.29	14.67				0.917				
0.07638	2.51	13.226	801.1	2.51	0.23	4.44	16.334	1031.7	8.39	4.55	0.39	15.48				0.952				
0.08846	2.99	13.951	876.0	2.99	0.27	4.68	16.530	1069.2	8.66	4.67	0.39	15.76				0.948				
0.10031	3.49	14.643	945.9	3.49	0.34	5.02	17.225	1149.2	8.94	5.30	0.44	16.13				0.963				
0.11953	4.34	15.651	1048.0	4.34	0.35	5.02	17.225	1149.2	8.94	5.30	0.44	16.13				0.963				
0.12425	4.56	15.868	1079.5	4.56	0.39	5.02	17.225	1149.2	8.94	5.30	0.44	16.13				0.963				
0.13409	4.97	16.405	1123.4	4.97	0.49	6.75	18.737	1277.2	10.39	6.46	0.53	17.87				0.946				
0.16915	6.56	18.007	1293.5	6.56	0.49	7.51	19.282	1348.2	10.96	6.87	0.55	18.4				0.947				
0.18366	7.31	18.525	1366.0	7.31	0.62	9.84	21.438	1552.9	12.63	8.70	0.68	19.8				0.882				
0.23368	9.98	20.169	1606.6	9.98	0.62	12.16	22.250	1726.5	14.04	9.31	0.72	21.06				0.987				
0.26864	11.93	21.284	1756.8	11.93	0.69	15.59	23.291	1954.9	15.90	10.18	0.78	22.72				0.955				
0.31957	14.72	22.710	1951.5	14.72	0.78	21.91	24.557	2317.9	18.85	11.34	0.86	24.34				0.919				
0.39946	20.23	24.216	2287.9	20.23	0.86	36.41	24.765	2988.2	24.30	11.56	0.88	26.37				0.899				
0.51930	29.77	25.948	2776.0	29.77	0.94	57.52	25.008	3755.9	30.54	11.81	0.89	26.59				0.798				
0.65911	44.85	26.834	3407.1	44.85	0.95	81.80	24.783	4478.4	38.42	11.55	0.87	27				0.759				
0.77895	61.89	27.040	3995.4	61.89	0.93	111.59	24.484	5227.2	42.51	11.19	0.84	26.87				0.734				
0.89873	82.48	26.983	4616.8	82.48	0.89	174.75	23.914	6529.6	53.10	10.51	0.78	26.51				0.719				
1.09852	125.38	26.749	5682.2	125.38	0.89												0.698			

0.0048" Ribbed 8.002" Pipe
 Resistor - 350

Series

PEO

PK# 154
 d= 0.402
 h= smooth
 R2K 30
 d= 0.391
 h= 0.0045
 RN 43.5

RUN 154
 DATE 2/17/93
 POLY 301
 c equip 30
 W 1.056

Q (U/I)	Tim(SZ)	1/mpt(SZ)	Rept(SZ)	S (SZ)	SF (SZ)	Tim(R2A)	1/mpt(R2A)	Rept(R2A)	h=	S (R2A)	SF (R2A)	1/mpt(S2)	SN(SZ)	R	W	P	D/mms	connected	R corrected	S
0.00405	0.04	5.745	82.1			0.16	11.185	186.9	1.52							0.879				
0.00574	0.05	6.852	109.7			0.27	10.393	246.8	2.01							0.777				
0.00787	0.07	8.028	128.6			0.45	9.948	315.9	2.57							0.872				
0.00993	0.09	9.024	144.6			0.55	10.187	350.3	2.85							0.873				
0.01201	0.11	9.953	158.6			0.69	10.898	391.5	3.18							0.905				
0.01543	0.14	11.154	182.4			0.81	11.556	426.6	3.47							0.911				
0.01890	0.22	11.023	226.5			1.05	12.433	485.2	3.95							0.910				
0.02314	0.40	9.957	307.2			1.49	14.911	578.2	4.70							0.924				
0.02823	0.49	10.191	340.8			1.93	16.759	642.1	5.22							0.960				
0.03134	0.64	10.707	387.8	0.75		2.24	17.712	711.4	5.78							0.919				
0.03621	0.76	11.319	423.9	1.21		2.51	18.502	751.9	6.11							0.923				
0.04426	0.98	12.186	481.8	1.85		3.21	20.255	840.3	6.83							0.924				
0.05314	1.41	14.502	578.7	3.85		3.28	20.346	871.1	7.08							0.940				
0.07878	1.80	15.996	655.1	5.13		3.53	21.208	885.8	7.20							0.944				
0.09221	2.12	17.272	710.1	6.27		4.98	22.884	1053.7	8.57							0.999				
0.10192	2.41	17.905	756.3	6.79		5.51	23.356	1108.3	9.01							0.987				
0.12616	3.05	19.696	841.2	8.40		6.63	24.784	1229.1	9.99							0.963				
0.12992	3.14	19.975	863.7	8.63		8.30	25.940	1375.4	11.18							0.925				
0.13855	3.41	20.448	894.2	9.04		10.97	27.761	1581.5	12.86							0.912				
0.17746	4.60	22.555	1040.6	10.89		13.76	28.128	1756.3	14.28							0.911				
0.19047	5.02	23.187	1086.6	11.44		14.79	28.717	1815.2	14.76							0.908				
0.22170	6.55	23.610	1255.8	11.61		19.47	28.658	2106.8	17.13							0.854				
0.25965	7.88	25.211	1377.5	13.76		26.48	29.041	2457.3	19.98							0.833				
0.31957	10.26	27.177	1572.5	14.79		47.02	30.175	3274.5	26.63							0.798				
0.35951	12.66	27.546	1745.7	14.98		74.29	30.674	4114.0	33.45							0.758				
0.37949	13.89	28.172	1801.0	15.55		106.59	30.619	4921.6	40.02							0.710				
0.43941	17.07	28.995	2026.9	16.17																
0.51930	22.66	29.745	2353.3	16.67																
0.71903	38.31	31.675	3036.4	18.15																
0.91876	57.85	32.936	3729.5	19.05																
1.09952	77.72	33.975	4317.4	19.83																

0.0045" Rbblat0.402" Pipe
 Residues = 350

Series
 PEO

PKZ
 SZ: 0.402
 h = smooth
 RZAL
 d = 0.391
 h = 0.0045
 R/h 43.5

W201-301
 RUN 159
 DATE 2/10/93
 POLY 301
 c mpags
 nr 1,201

Q (h)	Tot(SZ)	1/Inf(SZ)	Band(SZ)	S(SZ)	SF(SZ)	Tot(RZAL)	1/Inf(RZAL)	Band(RZAL)	Ns	S(RZAL)	SF(RZAL)	1/Inf(SZ)	St(SZ)	R	IR	P	A/7ms	connected R	connected S	
0.00355	0.04	5.063	81.1	3.20	0.33	0.12	9.261	145.5	1.18	3.67	0.38	12.92	3.11	0.538	0.042	0.334	0.00	0.538	3.11	
0.00435	0.04	5.616	89.6	4.52	0.45	0.19	10.974	180.9	1.47	4.79	0.48	14.65	4.64	-1.159	0.010	0.307	0.00	0.139	4.64	
0.00585	0.06	6.509	104.1	6.10	0.60	0.25	12.121	208.8	1.70	6.15	0.60	16.49	6.28	-0.123	-0.007	0.884	0.00	-0.123	6.28	
0.00710	0.07	7.196	114.5	7.06	0.68	0.31	12.560	230.0	1.87	7.24	0.70	17.6	7.20	0.057	0.003	0.896	0.00	0.057	7.20	
0.00879	0.09	8.009	127.5	7.84	0.75	0.34	11.342	306.4	2.49	7.77	0.73	18.64	8.09	-0.299	-0.016	0.874	0.00	-0.299	8.09	
0.01129	0.12	8.997	145.8	8.49	0.80	0.49	11.358	297.8	2.71	8.24	0.84	19.35	8.66	-0.361	-0.019	0.862	0.00	-0.361	8.66	
0.01661	0.17	10.860	177.0	9.06	0.83	0.54	12.075	313.5	2.91	8.24	0.84	20.42	9.44	-0.156	-0.008	0.896	0.00	-0.156	9.44	
0.02415	0.24	11.700	210.5	10.27	0.93	0.64	13.458	354.8	2.90	8.24	0.84	22.82	11.49	0.950	0.042	0.941	0.00	0.950	11.49	
0.02903	0.34	11.235	250.3	11.56	1.02	0.71	14.789	400.7	3.26	8.24	0.84	24.32	12.19	1.089	0.046	0.946	0.00	1.089	12.19	
0.03364	0.49	11.358	297.8	12.29	1.07	0.72	14.789	400.7	3.26	8.24	0.84	25.38	13.53	1.609	0.063	0.970	0.00	1.609	13.53	
0.04008	0.70	13.018	359.1	13.72	1.15	0.76	14.789	400.7	3.26	8.24	0.84	26.18	14.15	1.478	0.056	0.965	0.00	1.478	14.15	
0.04943	0.86	14.513	397.4	14.65	1.19	0.93	14.789	400.7	3.26	8.24	0.84	28.91	14.59	1.347	0.050	0.937	0.00	1.347	14.59	
0.08120	1.05	16.272	439.2	15.68	1.24	1.16	16.367	448.6	3.65	8.24	0.84	28.91	15.83	-0.383	-0.013	0.863	0.00	-0.383	15.83	
0.07364	1.33	17.436	493.2	16.18	1.26	1.44	17.657	500.4	4.07	8.24	0.84	29.29	16.40	-0.669	-0.023	0.851	0.00	-0.669	16.40	
0.08350	1.54	18.343	531.7	17.84	1.38	1.72	18.341	546.3	4.44	8.24	0.84	31.4	18.07	-2.143	-0.068	0.788	0.00	-2.143	18.07	
0.09359	1.78	19.114	571.7	18.51	1.40	2.01	18.989	591.2	4.81	8.24	0.84	32.76	19.13	-2.927	-0.089	0.744	0.00	-2.927	19.13	
0.11843	2.60	20.015	690.5	19.93	1.43	3.00	20.264	700.7	5.70	8.24	0.84	33.51	19.70	-3.310	-0.099	0.744	0.00	-3.310	19.70	
0.13325	2.91	21.315	726.0	20.17	1.43	4.25	22.137	718.1	5.84	8.24	0.84	33.51	20.48	-3.288	-0.095	0.744	0.00	-3.288	20.48	
0.17022	4.10	22.911	866.3	22.84	1.10	5.15	23.770	857.8	6.98	8.24	0.84	33.51	23.69	1.089	0.046	0.946	0.00	1.089	23.69	
0.19534	5.00	23.812	957.5	22.84	1.10	5.99	24.779	945.3	7.69	8.24	0.84	33.51	24.32	1.609	0.063	0.970	0.00	1.609	24.32	
0.21970	5.97	24.521	1049.2	23.72	1.15	7.66	25.832	1023.2	8.32	8.24	0.84	33.51	25.38	1.478	0.056	0.965	0.00	1.478	25.38	
0.25965	7.64	25.613	1195.8	24.25	1.18	9.46	26.989	1156.1	9.40	8.24	0.84	33.51	26.18	1.347	0.050	0.937	0.00	1.347	26.18	
0.29560	9.38	26.321	1312.1	24.65	1.19	13.11	28.257	1282.8	10.43	8.24	0.84	33.51	28.91	-0.383	-0.013	0.863	0.00	-0.383	28.91	
0.35552	12.89	26.999	1543.0	25.68	1.19	20.18	28.147	1314.6	12.32	8.24	0.84	33.51	29.29	-0.669	-0.023	0.851	0.00	-0.669	29.29	
0.43941	17.80	28.318	1818.5	26.18	1.24	25.21	28.621	1479.6	15.28	8.24	0.84	33.51	31.4	-2.143	-0.068	0.788	0.00	-2.143	31.4	
0.49333	22.04	28.996	2017.9	26.96	1.26	42.03	29.257	1700.3	17.08	8.24	0.84	33.51	32.76	-3.310	-0.099	0.744	0.00	-3.310	32.76	
0.65911	34.01	30.816	2506.3	27.62	1.34	59.39	29.833	3222.2	26.20	8.24	0.84	33.51	33.51	-3.288	-0.095	0.744	0.00	-3.288	33.51	
0.79852	46.40	31.980	2925.9	28.51	1.38	73.35	30.200	3574.5	29.07	8.24	0.84	33.51	34.56	-3.288	-0.095	0.744	0.00	-3.288	34.56	
0.89879	56.05	32.733	3210.2	19.11	1.40	102.20	31.272	4171.5	33.92	8.24	0.84	33.51	35.92	-3.288	-0.095	0.744	0.00	-3.288	35.92	
1.09852	78.40	33.829	3753.5	19.93	1.43															

0.0045" Ribbed 0.402" Pipe

Rev/rev = 350

Scores

PEO

RIB
 SE: 148
 d = 0.402
 h = smooth
 R2A: P-309
 c: 50
 TR: 1.151
 d = 0.391
 h = 0.0045
 RA: 43.5

Q (L/A)	T (S)	1/amp(S)	1/amp(S) ²	Revol (S)	S (S)	SF (S)	1/amp(R2A)	1/amp(R2A) ²	Revol (R2A)	h	S (R2A)	SF (R2A)	1/amp(S) ²	St (S)	R	RE	P	d/mex	connected IF	connected S
0.00295	0.03	4.713	25.4	75.4	4.24	0.43	0.15	10.619	170.1	1.38	4.82	0.49	10.52	4.11	0.690	0.049	0.942	0.00	0.690	4.11
0.00426	0.04	5.672	90.8	90.8	6.60	0.64	0.20	11.681	192.9	1.57	6.73	0.65	17.08	6.80	-0.053	-0.003	0.892	0.00	-0.053	6.80
0.00555	0.05	6.483	103.6	103.6	7.79	0.75	0.32	11.592	244.2	1.99	7.72	0.74	18.49	8.01	-0.272	-0.015	0.874	0.00	-0.272	8.01
0.00706	0.07	7.312	116.9	116.9	8.41	0.80	0.43	11.104	285.4	2.32	8.39	0.79	19.16	8.54	-0.196	-0.007	0.877	0.00	-0.196	8.54
0.00878	0.09	8.155	130.6	130.6	8.82	0.86	0.52	12.085	315.3	2.56	8.80	0.82	19.70	8.95	-0.116	-0.006	0.879	0.00	-0.116	8.95
0.01062	0.11	9.101	144.2	144.2	9.38	0.94	0.59	13.097	344.2	2.72	9.38	0.86	20.47	9.56	-0.138	-0.007	0.881	0.00	-0.138	9.56
0.01447	0.14	10.339	168.4	168.4	10.33	0.94	0.73	14.687	372.5	3.03	10.33	0.94	21.79	10.73	-0.043	-0.002	0.904	0.00	-0.043	10.73
0.01802	0.18	11.460	191.3	191.3	10.96	0.99	1.15	17.022	463.6	3.80	11.25	1.01	22.11	11.02	0.287	0.013	0.903	0.00	0.287	11.02
0.02532	0.26	11.104	275.8	275.8	10.33	0.94	1.69	19.504	611.9	4.98	12.34	1.11	23.06	11.69	0.733	0.032	0.929	0.00	0.733	11.69
0.03042	0.31	11.649	318.4	318.4	10.96	0.99	2.37	20.328	671.1	5.46	12.34	1.11	23.82	12.35	0.637	0.027	0.920	0.00	0.637	12.35
0.03493	0.37	12.654	386.7	386.7	12.36	1.08	4.11	23.796	878.8	7.15	12.34	1.11	24.460	12.81	0.804	0.033	0.930	0.00	0.804	12.81
0.04364	0.51	14.143	476.5	476.5	13.18	1.11	5.45	25.232	1013.2	8.24	13.48	1.24	24.81	13.04	1.908	0.079	0.987	0.00	1.908	13.04
0.06346	1.05	16.950	693.3	693.3	14.68	1.21	6.34	26.716	1101.9	8.96	14.78	1.24	26.07	14.08	2.058	0.079	0.987	0.00	2.058	14.08
0.07599	1.29	18.215	809.5	809.5	15.60	1.24	8.18	28.130	1252.4	10.18	15.86	1.30	26.67	14.56	1.583	0.059	0.969	0.00	1.583	14.56
0.08600	1.53	18.966	853.4	853.4	16.19	1.28	9.31	28.248	1336.1	10.87	15.86	1.29	27.68	15.30	1.261	0.046	0.948	0.00	1.261	15.30
0.09548	1.78	19.523	897.5	897.5	16.33	1.27	12.78	28.943	1564.5	12.72	16.19	1.27	28.42	15.77	0.359	0.013	0.908	0.00	0.359	15.77
0.10875	2.14	20.248	955.8	955.8	16.33	1.27	17.58	28.782	1836.4	14.93	16.78	1.29	28.28	16.18	0.384	0.014	0.933	0.00	0.384	16.18
0.12725	2.63	21.375	1096	1096	16.33	1.27	16.44	29.765	1775.0	14.43	16.78	1.29	29.28	16.43	0.181	0.006	0.892	0.00	0.181	16.43
0.13470	2.78	22.032	1236.6	1236.6	17.64	1.33	21.52	29.461	2050.4	16.67	16.31	1.24	29.28	16.43	-0.341	-0.011	0.868	0.00	-0.341	16.43
0.16764	3.92	23.078	1820.0	1820.0	18.45	1.37	35.78	30.748	2619.3	21.30	17.52	1.33	31.09	17.82	-0.856	-0.027	0.844	0.00	-0.856	17.82
0.18261	4.36	23.833	931.0	931.0	19.08	1.40	48.49	31.365	3049.0	24.79	18.16	1.38	32.22	18.68	-1.087	-0.033	0.834	0.00	-1.087	18.68
0.20474	5.21	24.455	1017.5	1017.5	19.95	1.43	77.87	31.956	3458.8	28.13	18.80	1.42	33.08	19.33	-1.087	-0.033	0.834	0.00	-1.087	19.33
0.23368	6.49	25.016	1145.5	1145.5	19.95	1.43	93.90	32.624	4229.4	34.39	19.40	1.47	34.38	20.27	-1.752	-0.051	0.807	0.00	-1.752	20.27
0.27982	8.30	26.465	1295.7	1295.7	14.68	1.21														
0.29960	9.27	26.827	1368.4	1368.4	14.68	1.21														
0.33951	12.45	27.782	1586.5	1586.5	15.60	1.24														
0.41943	16.40	28.238	1821.9	1821.9	16.19	1.28														
0.47935	20.10	29.152	2016.9	2016.9	16.33	1.27														
0.63914	31.89	30.857	2540.6	2540.6	17.64	1.33														
0.75987	42.06	31.909	2917.2	2917.2	18.45	1.37														
0.87881	53.54	32.746	3289.6	3289.6	19.08	1.40														
1.09652	77.87	33.942	3956.8	3956.8	19.95	1.43														

0.0045" Ribbed 40.02" Pipe
Residuals: 350

Serve
PEO

PWF
SZ:
d = 0.402
h = smooth
RZA:
d = 0.391
h = 0.0045
RA: 43.5

P-309
RUN
DATE 1/13/93
POLY P-309
c espans
nr 1.300

Q(L/W)	T _{mid} (SZ)	1/A _{mid} (SZ)	Resid(SZ)	S(SZ)	SF(SZ)	1/A _{mid} (RZA)	Resid(RZA)	H _r	S _r (RZA)	S _f (RZA)	1/A _{mid} (SZ)H	SV(SZ)	R	WF	P	d/Trans	connected R	corrected S	
0.00186	0.02	3.486	57.1			0.20	10.256	171.6	1.40		10.4								
0.00329	0.04	4.680	75.3			0.24	11.149	188.6	1.53		11.23				0.895	0.00		-0.122	5.16
0.00414	0.05	5.287	83.9			0.26	11.619	203.9	1.66		11.52				0.874	0.00		-0.126	6.93
0.00508	0.06	5.870	92.9			0.32	12.141	217.7	1.77		11.82				0.909	0.00		-0.228	7.74
0.00715	0.08	6.955	110.4			0.47	12.026	264.6	2.15		12.24				0.888	0.00		-0.088	8.88
0.01000	0.11	8.201	131.1			0.55	12.947	285.5	2.32		12.49				0.854	0.00		-0.148	8.36
0.01591	0.16	10.189	168.1			0.72	14.070	326.2	2.65		14.25				0.936	0.00		-0.130	9.17
0.01900	0.22	11.150	183.6			0.85	15.168	355.5	2.89		15.29				0.888	0.00		-0.476	9.57
0.02140	0.26	11.391	202.5			1.08	16.811	401.3	3.26		16.94				0.882	0.00		-0.272	10.10
0.02386	0.29	12.045	213.5			1.40	17.752	452.1	3.72		17.98				0.873	0.00		-0.025	11.00
0.02871	0.41	12.168	254.5			1.65	18.547	495.8	4.03		18.53				0.885	0.00		0.676	11.85
0.03334	0.53	12.511	287.6			1.89	19.029	531.1	4.32		18.88				0.899	0.00		0.742	11.89
0.04138	0.65	14.000	319.1			2.17	19.192	568.0	4.62		19.34				0.885	0.00		0.948	12.53
0.04859	0.78	15.045	340.9			2.70	19.830	628.9	5.11		19.96				0.873	0.00		1.126	13.04
0.07308	1.26	17.764	444.6		6.75	2.82	19.934	645.5	5.25		20.41				0.888	0.00		1.486	13.31
0.08282	1.50	18.428	485.8		7.57	3.26	21.272	670.0	5.45		21				0.895	0.00		1.240	15.68
0.09102	1.75	19.198	524.3		8.28	3.81	22.085	756.3	6.15		20.96				0.884	0.00		1.810	16.03
0.09824	1.95	19.198	552.7		8.63	4.03	23.093	795.8	6.47		22.11				0.884	0.00		1.093	19.17
0.11527	2.45	19.722	615.5		8.97	4.58	23.972	860.0	6.99		23.23				0.933	0.00		-1.812	20.01
0.11628	2.54	19.889	628.7		9.09	4.98	25.236	988.6	8.04		24.11				0.924	0.00		-2.096	20.73
0.12783	2.75	21.014	660.2		10.14	5.51	26.123	1108.5	9.01		24.82				0.948	0.00		0.000	20.73
0.13347	3.04	20.868	688.9		9.92	6.11	26.271	1193.7	10.76		26.28				0.959	0.00		0.000	20.73
0.14980	3.46	21.860	740.4		10.88	6.51	25.236	988.6	8.04		24.11				0.948	0.00		0.000	20.73
0.18578	3.56	22.427	797.6		11.22	7.05	23.876	867.5	7.05		23.23				0.924	0.00		0.000	20.73
0.18575	4.80	23.106	872.6		11.74	8.04	23.972	860.0	6.99		23.23				0.924	0.00		0.000	20.73
0.18590	4.73	23.318	860.6		11.98	8.04	25.236	988.6	8.04		24.11				0.948	0.00		0.000	20.73
0.22370	6.34	24.227	1002.3		12.62	8.18	26.123	1108.5	9.01		24.82				0.959	0.00		0.000	20.73
0.25965	8.06	24.939	1130.2		13.13	8.18	26.271	1193.7	10.76		26.28				0.968	0.00		0.000	20.73
0.33555	11.84	26.584	1370.2		14.44	11.11	26.123	1108.5	9.01		24.11				0.948	0.00		0.000	20.73
0.41544	16.50	27.886	1616.8		15.45	12.24	26.271	1193.7	10.76		26.28				0.959	0.00		0.000	20.73
0.43741	17.77	28.293	1679.7		15.79	16.33	29.400	1867.7	13.90		27.71				0.986	0.00		0.000	20.73
0.53927	24.73	29.566	1982.1		16.78	18.33	30.138	2380.0	17.01		29.63				0.968	0.00		0.000	20.73
0.65911	33.66	30.972	2312.9		17.92	26.51	31.487	2893.1	23.04		31.21				0.968	0.00		0.000	20.73
0.79992	45.78	32.193	2697.2		18.87	31.62	31.487	2893.1	23.04		31.21				0.968	0.00		0.000	20.73
0.93873	59.46	33.193	3073.8		19.64	31.62	31.487	2893.1	23.04		31.21				0.968	0.00		0.000	20.73
1.09852	77.15	34.098	3498.3		20.32	31.62	31.487	2893.1	23.04		31.21				0.968	0.00		0.000	20.73
0.00248	0.03	4.054	65.4			0.13	8.796	139.6	1.14		8.95				0.890	0.00		-0.356	6.37
0.00357	0.04	4.892	78.1			0.19	10.450	169.3	1.38		10.99				0.866	0.00		-0.048	7.18
0.00483	0.05	5.689	90.9			0.22	11.554	195.6	1.46		11.03				0.950	0.00		-0.095	7.57
0.00556	0.07	6.648	105.8			0.26	12.123	195.2	1.59		11.63				0.939	0.00		-0.068	7.54
0.00844	0.09	7.516	120.6			0.34	11.657	225.2	1.83		11.9				0.841	0.00		-0.327	8.70
0.01113	0.12	8.717	137.1			0.46	12.105	260.5	2.12		11.85				0.913	0.00		-0.010	8.87
0.01602	0.16	10.683	158.2			0.68	14.526	318.3	2.59		11.98				0.968	0.00		0.000	8.87
0.01876	0.21	11.074	182.3			1.00	15.954	384.9	3.13		13.6				0.951	0.00		0.000	8.87
0.02199	0.25	11.693	197.0			1.21	17.242	424.0	3.45		16.31				0.869	0.00		0.000	8.87
0.02372	0.30	11.886	215.0			1.41	17.905	457.2	3.72		17.81				0.889	0.00		0.000	8.87
0.02849	0.43	11.842	259.2			1.44	17.905	457.2	3.72		17.81				0.889	0.00		0.000	8.87
0.03316	0.56	12.096	295.6			1.75	18.398	510.3	4.15		18.39				0.876	0.00		-0.356	6.37
0.04171	0.67	13.923	323.3			2.07	18.398	510.3	4.15		18.39				0.876	0.00		-0.048	7.18
0.05590	0.89	16.002	373.5		6.11	2.07	18.398	510.3	4.15		18.39				0.876	0.00		-0.068	7.54
0.07387	1.27	17.847	447.0		7.02	2.48	19.793	607.3	4.94		19.28				0.866	0.00		-0.327	8.70
0.08459	1.58	18.375	497.4		7.55	2.60	19.814	617.0	5.02		19.72				0.889	0.00		-0.253	8.96
0.09481	1.84	19.036	538.1		8.51	2.83	20.197	647.3	5.26		20.45				0.889	0.00		-0.094	8.96
0.10840	2.25	19.724	593.2		9.03	2.83	20.197	647.3	5.26		20.45				0.889	0.00		-0.253	8.96
0.11105	2.39	19.585	607.9		8.85	2.83	20.197	647.3	5.26		20.45				0.889	0.00		-0.253	8.96
0.11806	2.58	20.029	635.0		9.22	3.05	21.397	671.7	5.46		21.14				0.903	0.00		-0.025	10.23
0.12993	2.83	21.045	664.7		10.15	3.89	23.431	769.2	6.25		22.47				0.942	0.00		-0.061	11.33
0.16258	3.86	22.562	777.5		11.40	1.02	23.431	769.2	6.25		22.47				0.942	0.00		-0.061	11.33

P-309
RUN
DATE 1/17/93
POLY P-309
c espans
nr 1.305

Q(L/W)	T _{mid} (SZ)	1/A _{mid} (SZ)	Resid(SZ)	S(SZ)	SF(SZ)	1/A _{mid} (RZA)	Resid(RZA)	H _r	S _r (RZA)	S _f (RZA)	1/A _{mid} (SZ)H	SV(SZ)	R	WF	P	d/Trans	connected R	corrected S	
0.00248	0.03	4.054	65.4			0.13	8.796	139.6	1.14		8.95				0.890	0.00		-0.356	6.37
0.00357	0.04	4.892	78.1			0.19	10.450	169.3	1.38		10.99				0.866	0.00		-0.048	7.18
0.00483	0.05	5.689	90.9			0.22	11.554	195.6	1.46		11.03				0.950	0.00		-0.095	7.57
0.00556	0.07	6.648	105.8			0.26	12.123	195.2	1.59		11.63				0.939	0.00		-0.068	7.54
0.00844	0.09	7.516	120.6			0.34	11.657	225.2	1.83		11.9				0.841	0.00		-0.327	8.70
0.01113	0.12	8.717	137.1			0.46	12.105	260.5	2.12		11.85				0.913	0.00		-0.010	8.87
0.01602	0.16	10.683	158.2			0.68	14.526	318.3	2.59		11.98				0.968	0.00		0.000	8.87
0.01876	0.21	11.074	182.3			1.00	15.954	384.9	3.13		13.6				0.951	0.00		0.000	8.87
0.02199	0.25	11.693	197.0			1.21	17.242	424.0	3.45		16.31				0.869	0.00		0.000	8.87
0.02372	0.30	11.886	215.0			1.41	17.905	457.2	3.72		17.81				0.889	0.00		0.000	8.87
0.02849	0.43	11.842	259.2			1.44	17.905	457.2	3.72		17.81				0.889	0.00		0.000	8.87
0.03316	0.56	12.096	295.6			1.75	18.398	510.3	4.15		18.39				0.876	0.00		-0.	

0.20013	527	23,763	908.8	1233	1.08	5.47	24,614	901.4	733	13.11	1.14	23.7	12.28	0.914	0.039	0.938	0.00	0.914	12.28
0.21970	607	24,319	970.4	1276	1.10	6.24	25,308	968.8	786	13.66	1.17	24.22	12.68	1.088	0.045	0.946	0.00	1.088	12.68
0.25965	772	25,479	1104.7	1371	1.16	7.93	26,574	1099.8	886	14.63	1.23	25.35	13.60	1.184	0.047	0.948	0.00	1.184	13.60
0.33954	1156	27,273	1351.2	1511	1.25	11.39	28,945	1306.1	1062	16.61	1.35	26.96	14.90	1.985	0.074	0.987	0.00	1.985	14.90
0.39946	1505	28,070	1541.2	1572	1.27	15.11	29,567	1503.2	1222	16.90	1.33	27.87	15.56	1.697	0.061	0.969	0.00	1.697	15.56
0.43941	1732	28,791	1634.4	1634	1.31	18.02	29,786	1623.0	1320	16.96	1.32	28.71	16.27	1.076	0.037	0.935	0.00	1.076	16.27
0.51930	2247	29,868	1862.1	1719	1.36	23.99	30,511	1872.7	1523	17.45	1.34	29.92	17.23	0.591	0.020	0.912	0.00	0.591	17.23
0.63914	3113	31,234	2191.9	1827	1.41	35.06	31,065	2264.1	1841	17.86	1.35	31.47	18.45	-0.405	-0.013	0.864	0.00	-0.405	18.45
0.71903	3773	31,916	2413.5	1879	1.43	43.24	31,467	2514.9	2045	18.24	1.38	32.2	19.00	-0.733	-0.023	0.849	0.00	-0.733	19.00
0.83887	4865	32,793	2740.5	1944	1.46	52.39	31,865	2897.4	2356	18.65	1.41	33.18	19.73	-1.315	-0.040	0.825	0.00	-1.315	19.73
0.99865	6498	33,780	3162.0	2018	1.48	78.63	32,410	3385.7	2753	19.22	1.46	34.27	20.55	-1.860	-0.054	0.804	0.00	-1.860	20.55

PIPE: 10.21 mm

RIBLETS: 0.11 mm Replicated Pipe

POLYMERS:

NONE (Solvent)

PEO W-301

 P-309

0.0045b Riblets/0.402" Pipe
Refract- 350

Series Q (L/s) Tw(S1) 1/sqrt(S1) Reqf(S1) S'(S1) SF(S1) Tw(R2) 1/sqrt(R2) Reqf(R2) h. S'(R2) SF(R2) R RF P

DW

PIPE

SZ:
d = 0.402
h = smooth
REAR:
d = 0.391
h = 0.0045
R/n 43.5

ITEM	303	304	305										
ITEM	303	304	305										
DATE	3/13/95	3/14/95	3/15/95										
POLY	-	-	-										
crippen	1.000	1.000	1.000										
W													
17.17	12.879	2046.2	0.04	0.00	18.12	13.230	2046.3	16.64	0.00	0.01	0.286	0.022	0.824
19.74	13.080	2194.5	0.11	0.01	21.28	13.297	2217.7	18.03	-0.01	0.01	0.313	0.018	0.913
21.36	13.146	2292.2	0.11	0.01	23.27	13.292	2318.8	18.86	-0.05	0.01	0.291	0.013	0.902
23.22	13.158	2380.1	0.05	0.00	25.20	13.331	2418.4	19.63	-0.04	0.01	0.200	0.011	0.897
24.53	13.223	2446.4	0.07	0.01	26.47	13.439	2472.9	20.11	0.06	0.02	0.266	0.015	0.906
26.67	13.299	2551.1	0.07	0.01	29.26	13.402	2500.8	21.15	0.01	0.01	0.141	0.008	0.889
28.85	13.250	2559.1	0.02	0.00	29.15	13.428	2594.6	21.10	0.02	0.02	0.170	0.010	0.893
32.35	13.470	2809.2	0.06	0.00	36.15	13.448	2890.7	23.51	0.03	0.02	0.004	0.000	0.871
38.88	13.558	3078.1	0.00	0.00	43.79	13.483	3179.7	25.86	0.09	0.02	-0.126	-0.007	0.854
45.12	13.765	3317.7	0.06	0.01	53.28	13.370	3509.2	28.54	0.01	0.01	-0.411	-0.032	0.819
47.84	13.750	3414.0	0.02	0.00	55.97	13.417	3594.5	29.23	0.06	0.02	-0.406	-0.032	0.820
53.4071	14.006	3910.2	0.04	0.00	76.97	13.347	4215.2	34.28	0.06	0.01	-0.752	-0.044	0.780
62.76	14.006	3910.2	0.04	0.00	81.05	13.317	4328.4	35.20	0.04	0.01	-0.828	-0.044	0.772
65.15	14.073	3986.8	0.07	0.01	101.49	13.284	4840.1	39.36	0.05	0.00	-1.053	-0.056	0.747
79.38	14.232	4397.7	0.06	0.00	101.49	13.294	4840.1	39.36	0.05	0.00	-1.053	-0.056	0.747
88.47	14.328	4646.7	0.05	0.00	115.21	13.248	5161.5	41.97	0.03	0.00	-1.204	-0.064	0.732
97.66	14.435	4877.6	0.06	0.01	130.34	13.168	5484.9	44.60	0.01	-0.01	-1.369	-0.072	0.714
108.22	14.475	5140.2	0.03	0.00	144.60	13.216	5783.6	47.03	0.02	-0.01	-1.482	-0.075	0.709
140.69	14.699	5952.8	0.03	0.00	144.60	13.216	5783.6	47.03	0.02	-0.01	-1.482	-0.077	0.704
168.09	14.877	6407.7	0.05	0.00	150.14	13.198	5886.1	47.86	0.00	-0.01	-1.612	-0.083	0.692
172.93	14.866	6488.5	0.02	0.00	181.82	13.234	6476.7	52.67	0.04	-0.02	-1.812	-0.093	0.674
186.48	14.888	6774.1	0.05	0.00	187.57	13.233	6588.8	53.58	0.03	-0.01	-1.642	-0.085	0.689
140.69	14.699	5952.8	0.03	0.00	194.06	13.210	6690.9	54.41	0.01	-0.02	-1.812	-0.093	0.674
168.09	14.877	6407.7	0.05	0.00	235.55	13.262	7384.7	60.05	0.04	-0.02	-2.040	-0.103	0.654
172.93	14.866	6488.5	0.02	0.00	242.92	13.238	7485.7	60.87	0.01	-0.02	-1.859	-0.099	0.661
190.61	14.925	6812.4	-0.01	0.00	269.82	13.240	7889.4	64.16	0.00	-0.02	-1.949	-0.099	0.661
211.76	15.068	7194.9	0.04	0.00	302.54	13.205	8371.1	68.07	0.04	-0.02	-1.987	-0.100	0.659
226.43	15.093	7425.4	0.02	0.00	324.80	13.309	8654.0	70.37	0.03	-0.02	-2.040	-0.103	0.654
239.08	15.263	7958.2	0.06	0.00	374.94	13.391	9318.9	75.78	0.08	-0.02	-2.066	-0.104	0.652
269.01	15.462	8104.8	0.23	0.01	400.40	13.376	9624.7	78.27	0.05	-0.02	-2.157	-0.108	0.645
0.10	9.376	150.9			0.11	9.406	154.4	1.26					0.880
0.15	11.480	187.9			0.17	11.429	192.9	1.58					0.866
0.33	9.857	280.5			0.26	9.803	269.8	2.26					0.864
0.46	9.843	328.5			0.30	9.918	335.0	2.72					0.887
0.65	9.985	392.1			0.72	10.004	402.0	3.27	0.04	0.00	-0.018	-0.001	0.868
0.86	10.175	451.1			0.95	10.242	460.4	3.74	0.03	0.00	-0.011	-0.001	0.869
1.09	10.348	506.7			1.18	10.482	518.9	4.18	0.06	0.00	0.099	0.003	0.877
1.30	10.509	553.5			1.41	10.638	561.7	4.57	0.04	0.00	0.040	0.003	0.877
1.49	10.539	592.2			1.60	10.734	597.3	4.86	0.01	0.00	0.080	0.002	0.875
1.69	10.711	630.9			1.81	10.914	636.1	5.17	0.06	0.01	0.100	0.007	0.887
2.05	10.902	695.6			2.21	11.099	701.9	5.71	0.08	0.01	0.114	0.008	0.889
2.40	11.045	733.0			2.57	11.277	757.7	6.16	0.05	0.01	0.159	0.010	0.896
2.70	11.182	788.5			2.89	11.409	804.0	6.54	0.03	0.01	0.188	0.012	0.900
3.24	11.326	873.6			3.44	11.596	876.5	7.13	0.04	0.01	0.225	0.014	0.905
4.18	11.530	992.8			4.39	11.871	990.7	8.06	0.03	0.01	0.287	0.018	0.914
5.05	11.801	1091.7			5.36	12.091	1094.6	8.90	0.03	0.01	0.394	0.021	0.921
5.91	11.948	1180.2			6.28	12.234	1194.2	9.63	-0.01	0.01	0.340	0.021	0.921
6.72	11.991	1258.8			6.95	12.430	1245.5	10.13	0.07	0.02	0.449	0.027	0.937
5.86	11.890	1188.7			6.10	12.807	1177.9	9.58	0.08	0.02	0.422	0.026	0.938
6.20	11.940	1221.1			6.53	12.277	1221.0	9.93	-0.04	0.01	0.390	0.020	0.919
6.65	11.892	1264.6			6.85	12.369	1249.3	10.16	0.01	0.01	0.382	0.023	0.927
6.99	11.998	1289.2			7.22	12.410	1280.4	10.41	-0.01	0.01	0.381	0.023	0.926
8.04	12.175	1393.0			8.21	12.714	1370.4	11.14	0.15	0.02	0.485	0.029	0.954
10.08	12.499	1559.7			10.59	12.876	1555.5	12.65	0.06	0.01	0.508	0.030	0.944
11.32	12.561	1652.7			11.85	12.957	1646.0	13.38	0.04	0.01	0.492	0.029	0.940
12.51	12.480	1667.0			11.79	13.016	1642.0	13.35	0.10	0.01	0.553	0.033	0.950
13.51	12.541	1721.6			12.64	13.048	1700.2	13.83	0.07	0.01	0.524	0.031	0.945
13.84	12.676	1828.0			14.27	13.175	1806.8	14.69	0.10	0.01	0.547	0.032	0.948
14.27	12.553	1855.7			14.48	13.150	1819.9	14.80	0.07	0.01	0.510	0.030	0.942

0.19373	17.18	12.746	2038.5	-0.09	-0.01	17.69	13.357	2013.5	16.97	0.04	0.01	0.441	0.025	0.931
0.20923	19.81	12.820	2188.9	-0.14	-0.01	20.50	13.301	2167.4	17.62	0.01	0.01	0.357	0.020	0.919
0.22666	22.57	13.013	2336.1	-0.06	0.00	23.88	13.352	2339.1	19.02	0.00	0.01	0.276	0.018	0.908
0.26541	30.10	13.193	2698.1	-0.13	-0.01	31.83	13.541	2700.3	21.96	0.14	0.02	0.216	0.012	0.899
0.28283	33.52	13.324	2846.9	-0.09	-0.01	36.51	13.474	2892.1	23.52	0.07	0.02	0.029	0.002	0.874
0.30222	37.65	13.433	3017.2	-0.09	-0.01	42.14	13.402	3108.9	25.26	0.00	0.02	-0.168	-0.009	0.868
0.31965	41.34	13.539	3161.4	-0.04	0.00	46.46	13.499	3262.3	26.33	0.11	0.02	-0.155	-0.009	0.851
0.37777	55.58	13.820	3665.5	-0.04	0.00	65.97	13.388	3887.0	31.61	0.07	0.01	-0.370	-0.031	0.801
0.51338	95.73	14.310	4811.1	-0.02	0.00	123.78	13.283	5324.9	43.20	0.08	0.00	-1.223	-0.064	0.780
0.72649	178.11	14.846	6583.7	-0.02	0.00	248.02	13.278	7539.3	61.31	0.05	-0.02	-1.831	-0.093	0.672
0.90084	260.78	15.214	7938.3	0.01	0.00	373.76	13.413	9250.5	75.22	0.10	-0.02	-2.052	-0.103	0.655

0.0045" Repeated Riblets0.402" P1

Respect = 350

PEO

WFE SC: 310
d = 0.402
h = smooth
R2A: 301
c: wppm 3
w 1.006
h = 0.391
R/h = 43.5

Q(L/A)	Tw(S2)	1/Spf(S2)	Respf(S2)	S(S2)	Sf(S2)	Tw(R2A)	1/Spf(R2A)	Respf(R2A)	h	S(R2A)	Sf(R2A)	1/Spf(S2)h	St(S2)	R	W	P	d'	Fract	Score
0.00750	0.07	7.884	127.9	0.03	0.00	0.07	7.971	132.0	1.06	0.14	0.01	9.835	0.01	0.662	0.006	0.888	0.00	0.662	0.01
0.01299	0.12	10.296	169.7	0.03	0.00	0.13	10.336	173.6	1.41	0.14	0.01	10.444	-0.10	0.665	0.008	0.694	0.00	0.665	-0.10
0.01748	0.18	11.132	211.4	0.03	0.00	0.21	11.043	218.9	1.78	0.14	0.01	10.595	-0.06	0.730	0.017	0.907	0.00	0.730	-0.06
0.02269	0.41	9.816	314.5	0.03	0.00	0.44	9.879	319.9	2.60	0.14	0.01	10.295	-0.01	0.730	0.022	0.915	0.00	0.730	-0.01
0.03569	0.51	9.816	352.6	0.03	0.00	0.56	9.897	359.3	2.92	0.14	0.01	10.595	0.16	0.695	0.003	0.690	0.00	0.695	0.16
0.03161	0.74	10.015	425.3	-0.10	-0.01	0.81	10.129	432.1	3.51	0.03	0.02	10.295	0.28	0.133	0.012	0.902	0.00	0.133	0.28
0.03696	0.96	10.278	484.8	-0.06	-0.01	1.03	10.469	489.0	3.98	0.14	0.02	10.595	0.39	0.217	0.019	0.912	0.00	0.217	0.39
0.04228	1.20	10.519	541.9	-0.02	0.00	1.28	10.765	543.9	4.42	0.23	0.02	10.895	0.71	0.116	0.010	0.901	0.00	0.116	0.71
0.04666	1.39	10.788	583.2	0.12	0.01	1.52	10.890	591.5	4.83	0.18	0.02	10.895	1.08	0.148	0.012	0.903	0.00	0.148	1.08
0.05076	1.57	11.030	620.5	0.26	0.02	1.70	11.205	621.1	5.10	0.38	0.03	11.072	1.58	0.305	0.024	0.937	0.00	0.305	1.58
0.05468	1.76	11.241	656.0	0.37	0.03	1.88	11.484	659.7	5.36	0.55	0.05	11.267	2.25	0.578	0.042	0.940	0.00	0.578	2.25
0.06228	2.11	11.690	718.6	0.66	0.06	2.28	11.870	727.1	5.91	0.73	0.07	11.754	3.07	0.694	0.044	0.940	0.00	0.694	3.07
0.07142	2.54	12.225	788.2	1.04	0.09	2.74	12.430	796.4	6.48	1.09	0.10	12.282	4.59	0.746	0.044	0.940	0.00	0.746	4.59
0.08190	3.06	12.759	866.1	1.41	0.12	3.18	13.216	859.0	6.99	1.70	0.15	12.911	6.21	0.888	0.042	0.937	0.00	0.888	6.21
0.09613	3.81	13.439	965.1	1.90	0.16	3.96	13.898	958.7	7.80	2.14	0.18	13.394	8.53	0.940	0.042	0.940	0.00	0.940	8.53
0.10977	4.58	13.990	1058.5	2.29	0.20	4.74	14.510	1048.5	8.53	2.54	0.21	13.932	10.46	0.940	0.044	0.940	0.00	0.940	10.46
0.12156	5.28	14.434	1135.2	2.61	0.22	5.31	14.510	1129.0	9.18	2.77	0.23	14.396	12.69	0.940	0.044	0.940	0.00	0.940	12.69
0.13801	6.21	15.105	1230.1	3.14	0.26	6.43	15.671	1218.1	9.91	3.36	0.27	15.012	15.96	0.940	0.044	0.940	0.00	0.940	15.96
0.15104	6.88	15.705	1298.9	3.65	0.30	7.12	16.290	1286.4	10.46	3.86	0.31	15.596	18.04	0.940	0.044	0.940	0.00	0.940	18.04
0.17972	8.39	16.920	1435.4	4.69	0.38	8.69	17.550	1421.7	11.56	4.91	0.39	16.804	21.53	0.940	0.044	0.940	0.00	0.940	21.53
0.20372	9.95	17.616	1563.8	5.24	0.42	10.30	18.268	1549.3	12.60	5.46	0.43	17.531	25.88	0.940	0.042	0.940	0.00	0.940	25.88
0.21970	10.85	18.193	1633.1	5.74	0.46	11.39	18.740	1628.8	13.25	5.84	0.45	18.33	30.99	0.940	0.022	0.940	0.00	0.940	30.99
0.23668	12.20	18.712	1732.0	6.16	0.49	13.25	18.950	1757.1	14.29	5.92	0.45	18.785	35.69	0.940	0.009	0.940	0.00	0.940	35.69
0.25664	14.35	19.123	1878.6	6.43	0.51	15.59	19.370	1905.4	15.49	6.22	0.47	19.269	40.12	0.940	0.005	0.940	0.00	0.940	40.12
0.28962	15.65	19.554	1961.3	6.78	0.53	17.44	19.549	2015.5	16.39	6.33	0.48	19.717	44.63	0.940	0.009	0.940	0.00	0.940	44.63
0.31957	18.00	20.101	2149.8	7.17	0.55	21.24	19.957	2224.5	18.09	6.64	0.50	20.349	49.12	0.940	0.019	0.940	0.00	0.940	49.12
0.37354	20.36	20.402	2237.2	7.40	0.57	23.44	20.066	2336.9	19.00	6.72	0.50	20.618	54.12	0.940	0.027	0.940	0.00	0.940	54.12
0.37949	24.64	20.849	2461.3	7.69	0.58	28.98	20.290	2590.3	21.13	6.89	0.51	21.082	60.12	0.940	0.038	0.940	0.00	0.940	60.12
0.45938	34.05	21.469	2893.7	8.02	0.60	41.55	20.513	3111.4	25.30	7.11	0.53	21.594	66.12	0.940	0.050	0.940	0.00	0.940	66.12
0.49933	39.73	21.602	3125.8	8.02	0.59	49.21	20.487	3386.0	27.53	7.11	0.53	21.755	72.12	0.940	0.059	0.940	0.00	0.940	72.12
0.55924	48.92	21.804	3468.3	8.04	0.58	62.33	20.399	3810.6	30.99	7.06	0.53	21.914	78.12	0.940	0.077	0.940	0.00	0.940	78.12
0.63914	63.22	21.921	3942.4	7.94	0.57	82.64	20.236	4387.4	35.69	6.97	0.53	21.914	84.12	0.940	0.102	0.940	0.00	0.940	84.12
0.77895	94.46	21.857	4818.0	7.53	0.53	129.37	19.711	5488.5	44.63	6.51	0.49	21.699	90.12	0.940	0.168	0.940	0.00	0.940	90.12
0.85884	113.97	21.749	5336.3	7.24	0.50	163.75	19.318	6172.2	50.19	6.12	0.46	21.401	96.12	0.940	0.269	0.940	0.00	0.940	96.12
0.95870	148.24	21.473	6002.2	6.76	0.46	215.24	18.808	7061.2	57.42	5.60	0.42	20.977	102.12	0.940	0.403	0.940	0.00	0.940	102.12

0.0045" Repeated Fillets @ .040"
Revol (crits) 350

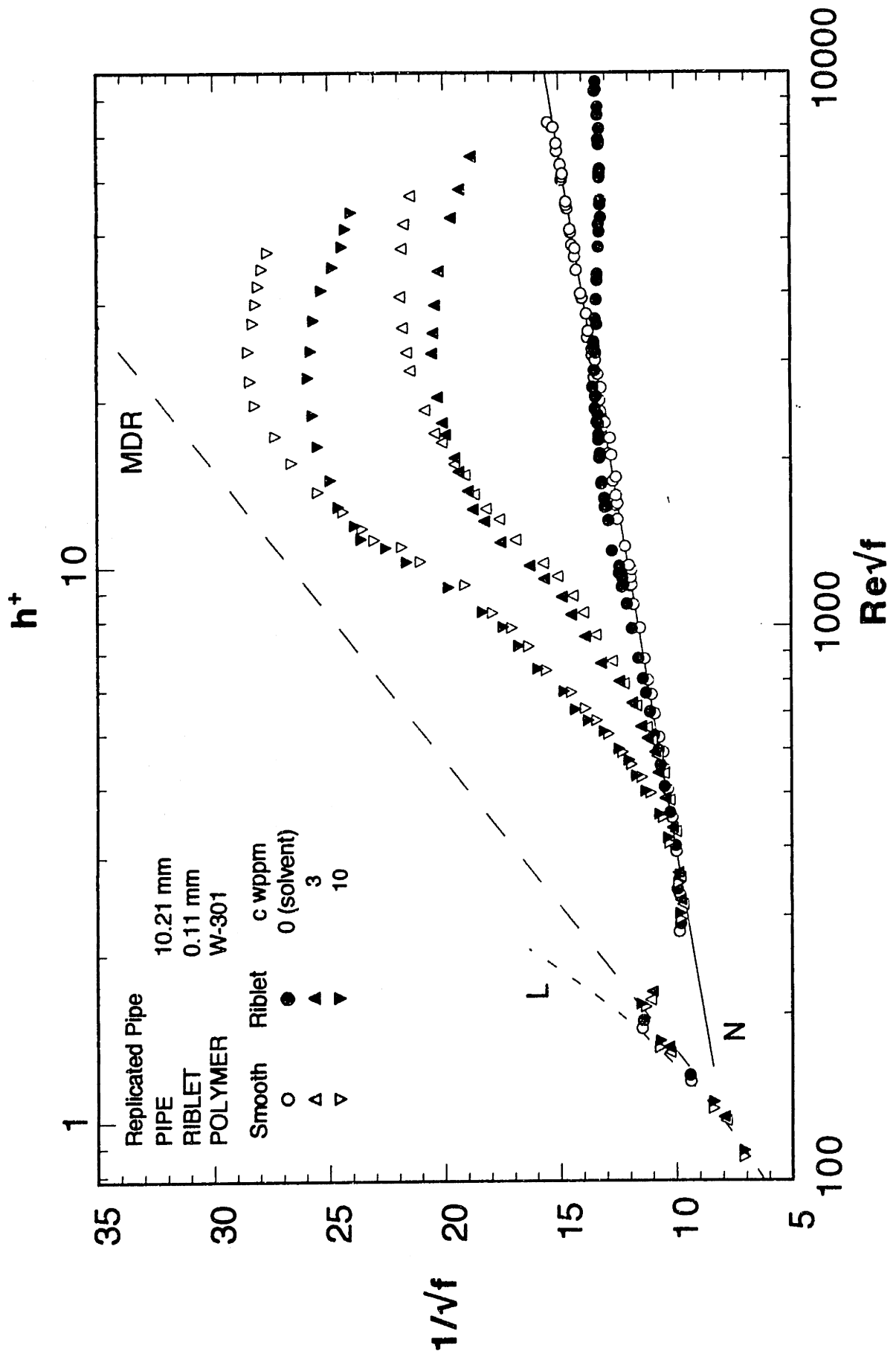
Series

PEO

PIPE
S2:
d = 0.402
h = smooth
RZA:
d = 0.391
h = 0.0045
R/h = 43.5

RUN 309
DATE 5/9/95
POLY 301
c 10
w 1.019

O (L/S)	Twr(S2)	1/sgf(S2)	Revol(S2)	S (S2)	SF (S2)	Twr(R2A)	1/sgf(R2A)	Revol(R2A)	h	S (R2A)	SF (R2A)	1/sgf(S2)	S (S2)	R	RF	P	Rcorr	Storr
0.00593	0.05	7.073	117.1	0.23	0.02	0.06	7.072	113.1	0.92	0.06	0.01	9.942	0.14	-0.140	-0.014	0.874	-0.140	0.14
0.00559	0.06	8.364	134.7	0.31	0.03	0.09	8.360	130.7	1.13	0.28	0.03	10.316	0.24	-0.015	-0.001	0.881	-0.015	0.24
0.01407	0.13	10.691	173.0	0.46	0.06	0.14	10.661	170.2	1.45	0.47	0.05	10.598	0.35	0.076	0.007	0.906	0.076	0.35
0.01765	0.18	11.799	205.5	0.66	0.06	0.20	11.485	207.7	1.69	0.89	0.09	11.096	0.69	0.175	0.016	0.909	0.175	0.69
0.02194	0.37	9.778	295.3	0.94	0.09	0.41	9.806	302.6	2.46	1.17	0.11	11.508	0.99	0.170	0.015	0.910	0.170	0.99
0.03572	0.50	9.872	342.9	1.26	0.12	0.49	12.000	573.6	4.66	1.36	0.13	12.025	1.39	-0.025	-0.002	0.890	-0.025	1.39
0.03158	0.70	10.760	405.4	1.57	0.15	0.63	12.420	600.9	4.89	1.66	0.16	12.376	1.66	0.044	0.004	0.896	0.044	1.66
0.03613	0.88	10.532	452.0	2.05	0.19	0.89	13.060	646.8	5.26	2.17	0.20	12.980	2.14	0.080	0.006	0.900	0.080	2.14
0.04195	1.07	11.454	500.2	2.47	0.23	2.07	13.756	676.8	5.50	2.77	0.25	13.389	2.47	0.367	0.027	0.922	0.367	2.47
0.04634	1.22	11.446	533.6	2.85	0.26	2.27	14.307	708.6	5.76	3.22	0.29	13.871	2.82	0.486	0.035	0.931	0.486	2.82
0.05083	1.36	11.893	563.4	3.34	0.30	2.63	14.809	763.5	6.21	3.56	0.32	14.499	3.37	0.310	0.021	0.916	0.310	3.37
0.05509	1.50	12.265	592.3	4.28	0.38	3.18	15.919	838.7	6.82	4.46	0.39	15.579	4.28	0.340	0.022	0.914	0.340	4.28
0.06236	1.75	12.870	639.9	4.89	0.43	3.86	16.785	924.0	7.51	5.09	0.44	16.366	4.90	0.399	0.024	0.919	0.399	4.90
0.06673	1.96	13.990	676.9	5.47	0.47	4.55	17.437	999.7	8.13	5.58	0.47	17.123	5.52	0.425	0.025	0.915	0.425	5.52
0.07485	2.17	13.864	711.8	6.20	0.53	5.19	18.370	1062.4	8.64	6.32	0.53	17.927	6.22	0.525	0.029	0.915	0.525	6.22
0.08343	2.48	14.463	761.0	7.19	0.60	6.25	19.803	1177.9	9.58	7.57	0.62	18.988	7.10	0.615	0.043	0.940	0.615	7.10
0.09855	2.98	15.565	834.9	8.93	0.74	7.80	21.610	1309.6	10.65	9.14	0.73	20.955	8.89	0.655	0.031	0.925	0.655	8.89
0.11444	3.64	16.349	922.3	10.80	0.88	8.77	23.520	1388.4	11.29	9.93	0.79	21.864	9.71	0.636	0.029	0.931	0.636	9.71
0.12917	4.27	17.058	994.5	11.22	0.91	9.45	23.570	1400.9	11.72	10.90	0.86	22.824	10.59	0.435	0.019	0.915	0.435	10.59
0.14493	4.88	17.900	1058.4	11.94	0.96	10.58	23.860	1575.1	12.40	11.08	0.87	23.664	11.35	0.176	0.007	0.898	0.176	11.35
0.17206	6.04	19.090	1189.3	12.89	1.03	12.33	24.560	1646.4	13.39	11.64	0.90	24.671	12.15	-0.061	-0.002	0.887	-0.061	12.15
0.20972	7.42	21.000	1311.8	13.81	1.08	15.39	24.910	1839.8	14.96	11.81	0.90	25.982	13.37	-1.072	-0.041	0.836	-1.072	13.37
0.23169	8.39	21.820	1394.8	14.31	1.10	16.79	25.470	2116.8	17.21	12.20	0.92	27.014	14.11	-1.544	-0.057	0.802	-1.544	14.39
0.25166	8.88	23.029	1435.5	14.98	1.13	26.52	25.679	2414.6	19.63	12.31	0.92	27.891	14.76	-2.212	-0.079	0.774	-2.212	14.55
0.25964	9.76	23.371	1505.1	15.47	1.05	36.00	25.870	2813.4	22.88	12.46	0.93	28.372	14.98	-2.502	-0.088	0.737	-2.502	14.30
0.33954	13.22	25.467	1751.6	16.86	1.09	44.87	25.748	3140.7	25.54	12.35	0.92	28.435	14.85	-2.687	-0.095	0.720	-2.687	14.30
0.39946	16.79	26.587	1974.0	17.47	1.05	58.13	25.637	3575.0	29.07	12.28	0.92	28.743	14.43	-2.606	-0.092	0.710	-2.606	13.91
0.45938	21.07	27.293	2211.4	18.11	1.02	74.63	25.289	4050.5	32.94	11.99	0.90	28.057	14.03	-2.768	-0.099	0.700	-2.768	13.45
0.53927	27.25	28.176	2514.4	18.98	1.02	90.36	24.797	4456.9	36.24	11.54	0.87	27.824	13.63	-3.027	-0.109	0.679	-3.027	13.00
0.59919	33.21	28.356	2775.9	19.86	0.99	107.59	24.387	4962.7	39.54	11.16	0.84	27.527	13.18	-3.140	-0.114	0.661	-3.140	12.51
0.67908	42.41	28.441	3136.8	20.86	0.96	124.38	24.229	5276.7	42.50	11.02	0.83	27.255	12.78	-3.026	-0.111	0.662	-3.026	12.08
0.75897	53.64	28.264	3527.6	21.97	0.96	143.43	24.002	5607.8	45.60	10.80	0.82	26.469	12.37	-2.967	-0.110	0.660	-2.967	11.64
0.81889	63.01	28.137	3823.4	23.11	0.96	163.43												
0.87881	73.11	28.031	4118.0	24.31	0.96	183.48												
0.93873	84.54	27.845	4426.9	25.54	0.96	203.53												
0.99865	97.27	27.616	4744.2	26.81	0.93	223.58												



0.00450" R/PhenolD_402" Pipe
Respect = 350

Series

PEO

P/E
S2:
d = 0.402
h = smooth
RZAC:
d = 0.391
h = 0.0045
R/h 43.5

P-309 307
DATE 3/29/95
POLY P-309
c/wppm 50
IR 1.106

Q (L/V)	1w(SZ)	1/w(SZ)	Resq(SZ)	S (SZ)	SF (SZ)	1w(R2A)	1/w(R2A)	Resq(R2A)	h*	S (R2A)	SF (R2A)	1/w(SZ)H	ST(SZ)	R	R*	P	d	Rcor	Score
0.00228	0.02	4.144	65.0	3.95	0.40	0.03	3.933	70.5	0.57	4.11	0.42	14.007	4.16	-0.107	-0.008	0.891	0.00	-0.107	4.16
0.00533	0.05	6.321	96.9	4.63	0.47	0.06	6.315	102.7	0.84	5.21	0.53	14.439	4.54	0.608	0.042	0.935	0.00	0.608	4.54
0.00866	0.09	8.091	126.9	5.22	0.52	0.09	8.073	130.7	1.06	5.56	0.56	15.322	5.32	0.207	0.014	0.912	0.00	0.207	5.32
0.01227	0.12	9.705	150.2	5.89	0.59	0.14	9.458	158.3	1.29	6.20	0.62	16.071	6.00	0.138	0.009	0.904	0.00	0.138	6.00
0.01541	0.15	10.918	167.9	6.56	0.65	0.18	10.570	178.2	1.45	6.66	0.66	17.119	6.91	-0.215	-0.013	0.881	0.00	-0.215	6.91
0.01986	0.21	11.773	200.8	7.31	0.71	0.24	11.699	207.6	1.68	7.37	0.72	17.825	7.51	-0.176	-0.010	0.890	0.00	-0.176	7.51
0.02377	0.30	11.890	238.1	8.27	0.79	0.33	11.836	245.7	2.00	8.51	0.81	18.844	8.31	0.184	0.010	0.898	0.00	0.184	8.31
0.02619	0.39	11.485	272.0	8.69	0.81	0.43	11.565	277.5	2.26	8.77	0.82	19.502	8.78	0.008	0.000	0.886	0.00	0.008	8.78
0.03105	0.51	11.912	311.2	9.51	0.87	0.53	12.275	310.3	2.52	9.51	0.87	20.110	9.24	0.326	0.016	0.908	0.00	0.326	9.24
0.03634	0.59	12.896	356.7	10.14	0.89	0.61	13.405	332.7	2.71	9.80	0.89	20.885	9.87	0.350	0.017	0.914	0.00	0.350	9.87
0.04124	0.67	13.765	398.4	10.68	0.91	0.75	13.900	364.6	2.96	10.14	0.91	21.207	10.16	0.390	0.018	0.914	0.00	0.390	10.16
0.04598	0.74	14.543	378.4	10.80	0.91	0.77	15.047	375.7	3.06	10.45	0.94	22.190	11.03	-0.183	-0.008	0.895	0.00	-0.183	11.03
0.05018	0.81	15.203	395.2	10.98	0.95	0.87	15.529	397.5	3.23	10.73	0.95	22.186	11.03	0.119	0.005	0.893	0.00	0.119	11.03
0.05451	0.87	15.940	409.5	11.54	0.98	0.94	16.209	413.7	3.36	11.03	0.98	22.979	11.70	0.075	0.003	0.891	0.00	0.075	11.70
0.06180	1.00	16.831	440.1	11.58	1.00	1.11	16.904	450.2	3.66	11.61	1.01	23.826	12.35	0.734	0.031	0.927	0.00	0.734	12.35
0.06942	1.13	17.582	466.7	12.37	1.08	1.25	17.649	477.7	3.88	12.87	1.10	24.216	12.67	0.904	0.037	0.935	0.00	0.904	12.67
0.08343	1.47	18.775	533.1	12.77	1.10	1.59	19.028	540.4	4.39	13.33	1.13	24.960	12.74	1.250	0.051	0.961	0.00	1.250	12.74
0.09538	1.80	19.374	590.8	12.99	1.10	1.98	19.510	602.7	4.90	13.73	1.16	24.960	12.88	1.514	0.061	0.972	0.00	1.514	12.88
0.10898	2.20	20.049	652.5	13.99	1.10	2.36	20.486	657.6	5.35	14.32	1.18	25.255	13.41	1.252	0.050	0.947	0.00	1.252	13.41
0.12288	2.61	20.761	710.2	14.53	1.22	2.77	21.235	713.3	5.80	15.00	1.22	26.181	14.25	1.110	0.042	0.929	0.00	1.110	14.25
0.12907	2.78	21.120	725.5	14.28	1.18	2.96	21.597	728.9	5.93	15.00	1.22	26.362	14.30	0.906	0.034	0.936	0.00	0.906	14.30
0.13819	3.00	21.750	762.4	14.80	1.22	3.27	22.007	774.1	6.29	15.29	1.22	26.873	14.73	0.969	0.036	0.932	0.00	0.969	14.73
0.14068	3.02	22.064	761.3	15.88	1.29	3.30	22.305	833.3	6.78	15.06	1.24	26.873	14.73	0.327	0.012	0.902	0.00	0.327	15.98
0.15611	3.48	22.830	819.1	15.97	1.28	3.80	23.054	833.3	6.78	15.06	1.24	26.873	14.73	0.281	0.010	0.902	0.00	0.281	16.47
0.18552	4.50	23.847	932.8	15.56	1.32	4.73	24.560	930.5	7.57	16.30	1.26	28.990	16.47	0.199	0.007	0.895	0.00	0.199	16.69
0.19574	4.83	24.280	976.0	16.56	1.35	5.03	25.120	969.2	7.88	16.43	1.26	29.226	16.69	0.033	0.001	0.885	0.00	0.033	17.27
0.20772	5.38	24.420	1030.0	17.15	1.35	5.45	25.610	1009.0	8.20	17.22	1.28	30.008	17.27	0.033	0.001	0.885	0.00	0.033	17.27
0.22769	6.29	24.770	1133.2	18.70	1.42	6.29	26.131	1084.0	8.82	18.00	1.30	31.249	18.20	-0.688	-0.022	0.851	0.00	-0.688	18.20
0.24567	6.93	25.457	1168.6	19.24	1.44	7.12	26.507	1153.0	9.38	18.00	1.30	32.314	19.00	-1.454	-0.045	0.817	0.00	-1.454	19.00
0.26564	7.49	26.465	1215.6	19.67	1.45	7.85	27.291	1211.1	9.85	18.00	1.34	33.089	19.57	-1.683	-0.051	0.809	0.00	-1.683	19.57
0.28561	8.74	26.351	1312.3	20.11	1.47	9.09	27.268	1302.9	11.10	18.20	1.36	33.815	20.13	-2.298	-0.061	0.787	0.00	-2.298	20.13
0.30559	9.56	26.953	1372.6	20.37	1.48	9.98	27.847	1365.1	11.10	18.20	1.36	34.380	20.49	-3.277	-0.094	0.749	0.00	-3.277	20.49
0.35552	11.81	28.213	1523.7	20.70	1.49	12.75	28.659	1541.0	12.53	18.34	1.38	34.921	20.95	-3.899	-0.110	0.730	0.00	-3.899	21.42
0.39946	14.63	28.483	1695.1	20.70	1.49	15.43	29.271	1694.5	13.78	18.34	1.38	35.520	21.42						
0.40545	14.66	29.077	1690.8	20.70	1.49	15.73	29.425	1716.3	13.96	18.34	1.38								
0.46537	17.07	29.855	1890.4	20.70	1.49	19.68	30.041	1930.1	15.69	18.34	1.38								
0.56524	24.79	30.963	2214.0	20.70	1.49	28.34	30.561	2304.5	18.74	17.22	1.28								
0.66510	32.31	31.909	2528.1	18.70	1.42	38.49	30.860	2685.6	21.84	17.46	1.30								
0.75997	40.21	32.642	2819.5	19.24	1.44	48.39	31.406	3010.5	24.48	18.00	1.34								
0.83887	47.46	33.210	3061.9	19.67	1.45	58.70	31.517	3314.6	26.95	18.13	1.35								
0.91876	55.01	33.784	3294.9	20.11	1.47	70.26	31.551	3624.5	29.47	18.20	1.36								
0.99865	63.54	34.168	3536.8	20.37	1.48	82.53	31.644	3923.4	31.90	18.33	1.38								
1.07854	72.29	34.598	3759.9	20.70	1.49	96.40	31.621	4226.4	34.37	18.34	1.38								

0.00-055" Ribbed, 4.02" Pipe

Resol: 350

Series

PEO

MPE

SC:

d = 0.402

h = smooth

RZARC

d = 0.391

h = 0.0045

Rn = 43.5

P-309

IRUN

DATE

P-309

POLY

C

W

Q (L/s)

Tim(S)

1/sqrt(S)

Reof(S)

S (S)

Sf (S)

Tim(R2A)

1/sqrt(R2A)

Reof(R2A)

h

S (R2A)

Sf (R2A)

1/sqrt(S)

St(S)

R

RF

P

A

FCov

Score

Q (L/s)	Tim(S)	1/sqrt(S)	Reof(S)	S (S)	Sf (S)	Tim(R2A)	1/sqrt(R2A)	Reof(R2A)	h	S (R2A)	Sf (R2A)	1/sqrt(S)	St(S)	R	RF	P	A	FCov	Score
0.00311	0.03	4.568	72.6	7.00	0.70	0.04	4.658	73.2	0.60	5.79	0.59	15.584	5.77	-0.41	-0.003	0.909		-0.041	5.77
0.00494	0.06	5.736	92.1	7.55	0.73	0.06	5.717	94.9	0.77	7.05	0.70	17.081	7.02	-0.21	-0.001	0.877		-0.021	7.02
0.00617	0.07	6.408	104.4	8.67	0.83	0.08	6.438	104.7	0.85	7.98	0.78	18.05	7.76	0.181	0.010	0.913		0.181	7.76
0.00930	0.10	7.874	126.5	10.02	0.92	0.11	7.926	129.1	1.05	8.85	0.85	19.178	8.75	0.084	0.004	0.892		0.084	8.75
0.01532	0.18	9.823	167.5	12.65	1.08	0.19	10.097	167.4	1.36	9.48	0.90	19.567	9.02	0.454	0.023	0.915		0.454	9.02
0.01773	0.20	10.750	177.3	13.36	1.14	0.22	10.795	181.4	1.48	10.26	0.95	19.983	9.16	1.120	0.056	0.966		1.120	9.16
0.02111	0.26	11.336	201.8	14.42	1.24	0.27	11.706	200.8	1.63	10.41	0.96	20.1	9.29	1.160	0.058	0.967		1.160	9.29
0.02415	0.30	12.074	215.8	15.05	1.28	0.31	12.389	215.9	1.76	10.66	0.98	20.288	9.43	1.280	0.063	0.960		1.280	9.43
0.02901	0.36	13.186	237.9	15.85	1.38	0.39	13.381	240.8	1.96	11.09	1.01	21.797	9.65	1.312	0.063	0.969		1.312	9.65
0.03450	0.46	13.907	270.3	16.80	1.49	0.51	13.954	274.8	2.23	11.64	1.08	22.902	11.64	1.594	0.073	0.980		1.594	11.64
0.04219	0.58	15.079	303.1	18.05	1.63	0.66	15.000	313.0	2.55	12.49	1.09	23.275	11.88	1.999	0.044	0.936		1.999	11.64
0.05202	0.75	15.705	345.0	19.53	1.78	0.86	15.543	358.1	2.91	12.92	1.11	23.514	12.04	2.274	0.053	0.961		2.274	11.88
0.06329	1.03	17.025	403.1	21.44	1.96	1.14	17.060	413.3	3.36	13.35	1.14	23.514	12.70	1.175	0.048	0.947		1.175	12.70
0.07699	1.39	19.069	468.6	23.80	2.16	1.48	18.231	470.9	3.83	13.62	1.16	24.295	12.96	1.138	0.046	0.945		1.138	12.96
0.08828	1.59	19.669	502.2	24.77	2.24	1.74	19.262	510.8	4.15	13.82	1.16	24.612	13.47	1.149	0.046	0.945		1.149	13.47
0.09791	1.86	19.974	542.7	26.18	2.41	1.98	20.021	544.8	4.43	14.68	1.19	25.231	13.95	1.087	0.042	0.940		1.087	13.95
0.11449	2.44	19.974	618.0	27.5	2.66	2.46	21.003	633.8	4.91	15.67	1.25	25.879	14.98	1.106	0.041	0.940		1.106	14.98
0.12257	2.73	20.214	648.5	28.9	2.84	2.75	21.568	652.4	5.31	16.67	1.25	27.146	15.49	1.061	0.041	0.940		1.061	15.49
0.12843	2.90	20.578	665.6	29.9	2.97	3.11	22.100	683.8	5.56	17.78	1.24	27.811	15.48	0.718	0.026	0.934		0.718	15.48
0.13533	3.09	20.965	700.9	31.1	3.07	3.97	23.391	822.4	6.69	18.24	1.24	28.566	16.05	-0.073	-0.003	0.882		-0.073	16.05
0.16188	3.99	22.089	794.6	33.91	3.33	4.56	23.901	897.2	7.21	19.53	1.22	29.477	16.78	-0.351	-0.012	0.868		-0.351	16.78
0.17740	4.39	23.088	828.7	35.4	3.53	5.33	24.499	997.0	7.55	20.00	1.22	30.761	17.83	-1.317	-0.043	0.830		-1.317	17.83
0.19650	5.26	23.360	906.7	37.19	3.84	5.84	25.036	998.5	8.12	21.28	1.24	31.697	18.57	-1.667	-0.053	0.808		-1.667	18.57
0.21026	5.85	23.710	954.8	38.5	4.06	6.75	25.470	998.5	8.37	22.49	1.24	32.528	19.20	-2.472	-0.076	0.776		-2.472	19.20
0.22991	6.57	24.466	1011.8	40.18	4.31	7.18	26.390	1095.6	8.91	23.86	1.25	33.107	19.66	-2.929	-0.088	0.760		-2.929	19.66
0.23973	6.98	24.737	1043.4	41.06	4.42	8.13	26.966	1208.5	9.83	24.49	1.25	33.754	20.16	-3.243	-0.096	0.749		-3.243	20.16
0.26135	7.89	25.370	1108.9	43.59	4.71	9.90	28.252	1383.1	11.25	25.67	1.24	34.46	20.66	-3.666	-0.106	0.728		-3.666	20.66
0.29475	9.59	25.956	1222.1	46.01	5.06	12.98	28.550	1535.2	12.48	26.94	1.24	34.714	20.85	-3.648	-0.105	0.730		-3.648	20.85
0.35370	12.54	27.241	1396.2	49.17	5.42	15.70	28.546	1682.0	13.76	28.44	1.22	34.46	20.66	-3.666	-0.106	0.728		-3.666	20.66
0.39200	14.75	27.907	1509.0	51.59	5.78	19.31	28.493	1880.8	15.29	30.00	1.22	34.46	20.66	-3.666	-0.106	0.728		-3.666	20.66
0.39546	15.25	27.615	1544.7	52.26	5.84	19.31	28.493	1880.8	15.29	30.00	1.22	34.46	20.66	-3.666	-0.106	0.728		-3.666	20.66
0.43501	17.49	28.365	1654.3	55.89	6.31	23.86	29.126	2047.0	17.55	31.42	1.25	34.46	20.66	-3.666	-0.106	0.728		-3.666	20.66
0.49433	21.28	29.223	1824.6	60.31	6.86	29.11	30.030	2407.0	19.57	33.10	1.24	34.46	20.66	-3.666	-0.106	0.728		-3.666	20.66
0.57342	26.79	30.214	2046.7	66.18	7.42	39.11	30.030	2696.5	21.93	36.65	1.24	34.46	20.66	-3.666	-0.106	0.728		-3.666	20.66
0.63251	31.230	31.230	2252.9	72.29	7.97	49.08	30.056	2902.5	23.60	39.11	1.25	34.46	20.66	-3.666	-0.106	0.728		-3.666	20.66
0.73160	39.14	31.892	2473.7	81.72	8.42	56.90	30.178	2902.5	23.60	39.11	1.28	34.46	20.66	-3.666	-0.106	0.728		-3.666	20.66
0.79092	44.44	32.353	2635.2	89.07	8.96	67.36	30.511	3156.7	25.67	41.46	1.28	34.46	20.66	-3.666	-0.106	0.728		-3.666	20.66
0.87001	51.84	32.951	2845.2	95.53	9.46	85.39	30.794	3549.1	28.86	44.46	1.31	34.46	20.66	-3.666	-0.106	0.728		-3.666	20.66
0.98865	63.83	33.746	3152.4	101.5	1.48	94.28	30.794	3549.1	28.86	44.46	1.33	34.46	20.66	-3.666	-0.106	0.728		-3.666	20.66
1.04797	70.73	33.983	3283.5	104.2	1.49	94.28	31.066	3690.1	30.01	44.46	1.33	34.46	20.66	-3.666	-0.106	0.728		-3.666	20.66

PIPE: 10.21 mm

RIBBLETS: 0.15 mm

POLYMERS:

NONE (Solvent)

PEO N-10

N-750

N60K

W-301

P-309

PAM N-300L

N-300

0.006" Ribbed 0.402" Pipe
 Report = 350

Sizes

DW

PIPE
 SZ: 036-038
 d = 0.402
 h = smooth

RZR: 1.000
 d = 0.386
 h = 0.006
 R/h 32.2

Q (L/s)	T ₁ (S2)	1/r ₀₁ (S2)	Re ₀₁ (S2)	S (S2)	Sf (S2)	T ₁ (s2B)	1/r ₀₁ (s2B)	Re ₀₁ (s2B)	h _s	S (s2B)	Sf (s2B)	R	RF	P
0.00102	0.01	2.913	46.4											
0.00136	0.01	3.323	53.2											
0.00147	0.01	3.477	55.5											
0.00155	0.01	3.593	57.2											
0.00201	0.02	4.065	65.0											
0.00216	0.02	4.221	67.5											
0.00225	0.02	4.322	69.0											
0.00249	0.02	4.505	71.9											
0.00256	0.02	4.591	73.2											
0.00277	0.03	4.789	76.1											
0.00304	0.03	4.972	79.5											
0.00342	0.03	5.324	84.9											
0.00346	0.03	5.337	85.2											
0.00367	0.03	5.500	87.2											
0.00377	0.03	5.571	87.8											
0.00379	0.03	5.590	88.1											
0.00411	0.04	5.815	93.2											
0.00424	0.04	5.906	94.3											
0.00479	0.04	6.240	99.6											
0.00494	0.04	6.372	101.8											
0.00502	0.05	6.384	102.1											
0.00542	0.05	6.675	106.6											
0.00543	0.05	6.712	107.0											
0.00560	0.05	6.803	108.4											
0.00595	0.05	6.891	109.8											
0.00597	0.05	7.009	111.8											
0.00646	0.06	7.239	115.6											
0.00697	0.06	7.562	120.7											
0.00715	0.06	7.693	122.6											
0.00723	0.07	7.652	122.3											
0.00733	0.07	7.779	123.7											
0.00772	0.07	7.921	127.7											
0.00774	0.07	7.977	127.5											
0.00778	0.07	7.911	127.3											
0.00832	0.08	8.282	132.5											
0.00867	0.08	8.340	134.6											
0.00885	0.08	8.529	136.5											
0.00888	0.08	8.461	137.4											
0.00932	0.09	8.649	139.4											
0.00944	0.09	8.786	141.4											
0.01014	0.09	9.042	145.2											
0.01074	0.10	9.321	151.6											
0.01079	0.10	9.350	152.1											
0.01088	0.10	9.294	151.6											
0.01150	0.11	9.593	155.8											
0.01191	0.11	9.813	160.0											
0.01209	0.11	9.827	161.8											
0.01377	0.13	10.478	172.9											
0.00231	0.02	4.381	69.6											
0.00259	0.02	4.618	74.0											
0.00353	0.03	5.414	86.0											
0.00559	0.05	6.809	108.2											
0.00720	0.07	7.701	123.0											
0.01031	0.09	9.198	147.5											
0.01282	0.12	10.190	165.4											
0.01662	0.17	11.054	197.5											
0.02194	0.38	9.642	297.4											
0.02819	0.61	9.820	377.0	-0.09	-0.01									
0.03383	0.83	10.143	437.9	-0.02	0.00									
0.03938	1.07	10.377	498.2	-0.01	0.00									

PIPE
 SZ: 40
 d = 0.402
 h = smooth

RZR: 1.000
 d = 0.386
 h = 0.006
 R/h 32.2

0.04864	1.56	10.628	600.9	0.09	0.01
0.04876	1.57	10.620	602.7	-0.10	0.01
0.04885	1.56	10.665	601.3	-0.05	0.00
0.06287	2.41	11.063	746.1	-0.01	0.00
0.06339	2.46	11.035	754.1	-0.07	-0.01
0.08016	3.66	11.435	820.4	-0.02	0.00
0.09140	4.56	11.689	1026.6	0.04	0.00
0.09456	5.28	11.831	1104.8	0.06	0.00
0.11042	6.39	11.923	1215.9	-0.02	0.00
0.11617	6.93	12.046	1271.9	0.03	0.00
0.01617	0.16	11.046	192.1		
0.01775	0.22	10.265	277.0		
0.01880	0.28	9.726	252.5		
0.02073	0.34	9.505	279.4		
0.02149	0.38	9.524	295.9		
0.02377	0.45	9.633	323.3		
0.02652	0.55	9.783	355.0	-0.02	0.00
0.03157	0.74	10.038	411.9	0.02	0.00
0.03633	0.95	10.162	468.3	-0.12	-0.01
0.04093	1.16	10.375	518.0	-0.09	-0.01
0.04403	1.30	10.526	550.4	0.04	0.00
0.04476	1.35	10.533	558.0	-0.05	0.01
0.04945	1.57	10.780	601.6	0.06	0.01
0.05655	2.01	10.826	602.1	-0.11	-0.01
0.07267	3.13	11.216	850.7	-0.10	-0.01
0.08540	4.14	11.463	978.1	-0.10	-0.01
0.09742	5.20	11.661	1096.9	-0.10	-0.01
0.10900	6.26	11.896	1205.7	-0.03	0.00
0.11452	6.81	11.978	1271.5	-0.04	0.00
0.29066	35.79	13.266	2069.8	-0.17	-0.01
0.96885	298.25	15.317	8235.6	0.05	0.00
0.72508	201.31	14.916	6782.4	-0.01	0.00
0.58131	121.03	14.427	5239.0	-0.06	0.00
0.48443	87.55	14.136	4472.8	-0.07	0.00
0.38131	121.35	14.405	5504.5	-0.16	-0.01
0.48443	87.48	14.138	4678.9	-0.14	-0.01
0.38754	58.15	13.872	3829.8	-0.06	0.00
0.29066	35.09	13.393	2983.8	-0.11	-0.01
0.87197	244.62	15.218	7905.1	0.03	0.00
0.72508	198.01	15.035	7120.4	0.02	0.00
0.67820	156.36	14.804	6327.4	0.00	0.00

0.29569	36.65	13.336	2843.0	-0.08	0.01
0.31003	38.73	13.599	3098.9	0.03	0.00
0.32041	44.85	13.431	3144.9	-0.16	-0.01
0.34879	48.32	13.701	3264.2	0.05	0.02
0.34879	48.63	13.653	3464.5	-0.11	0.01
0.42629	69.60	13.949	4144.7	-0.12	-0.01
0.44567	74.93	14.058	4064.9	0.02	0.00
0.44567	75.02	14.047	4268.2	-0.07	-0.01
0.54256	106.79	14.332	5133.9	-0.11	-0.01
0.55812	112.29	14.330	4976.2	-0.06	0.00
0.56213	112.68	14.457	5212.9	0.01	0.00
0.58131	121.60	14.395	5178.2	-0.06	0.00
0.61013	133.64	14.596	5743.3	-0.04	0.00
0.62006	135.26	14.555	5704.7	0.07	0.00
0.67820	157.69	14.744	6152.6	-0.01	0.00
0.77508	200.07	14.860	6922.0	0.00	0.00
0.77508	200.71	14.935	7054.6	-0.06	0.00
0.87197	246.76	15.153	7822.2	-0.02	0.00
0.96885	297.58	15.332	8589.9	0.00	0.00
0.07009	2.99	11.077	805.6	-0.15	-0.01
0.07465	3.27	11.269	843.4	0.03	0.00

RUN 41
DATE 10/28/91
POLY -
C temp 1.000
tr

RUN 42
DATE 10/29/91
POLY -
C temp 1.000
tr

RUN 43
DATE 10/30/91

0.46505	116.17	12.765	4867.2	54.60	0.02	0.00	-1.620	-0.113	0.670
0.60069	187.61	12.974	6282.7	69.05	0.06	0.00	-1.816	-0.123	0.654
0.73633	271.22	13.228	7536.1	82.83	0.08	0.01	-1.881	-0.124	0.652
0.93010	412.97	13.541	9277.3	101.97	0.01	0.00	-1.929	-0.125	0.643
1.06574	543.38	13.782	10444.0	114.79	0.07	0.00	-1.893	-0.121	0.641
0.15502	12.34	12.795	1540.1	16.93	-0.01	0.00	0.444	0.036	0.902
0.16485	14.04	12.754	1647.0	18.10	-0.07	-0.01	0.288	0.023	0.840
0.17439	15.33	12.913	1712.5	18.82	0.10	0.01	0.379	0.030	0.845
0.18000	16.52	12.836	1786.8	19.64	0.04	0.00	0.228	0.018	0.834
0.19377	19.76	12.636	1951.6	21.45	-0.12	-0.01	-0.125	-0.010	0.825
0.19391	19.27	12.806	1929.5	21.21	0.04	0.00	0.064	0.005	0.848
0.27128	37.89	12.776	2692.5	29.59	0.13	0.01	-0.545	-0.041	0.760
0.31063	52.42	12.413	3182.6	34.98	-0.24	-0.02	-1.198	-0.088	0.696
0.34879	63.87	12.651	3495.9	38.42	-0.01	0.00	-1.123	-0.082	0.706
0.38754	78.46	12.683	3874.7	42.59	0.01	0.00	-1.270	-0.091	0.693
0.48443	122.55	12.685	4842.5	53.22	-0.05	0.00	-1.655	-0.115	0.659
0.58131	173.65	12.788	5764.4	63.36	-0.05	0.00	-1.855	-0.127	0.659
0.67820	228.97	12.992	6619.2	72.75	0.02	0.00	-1.891	-0.127	0.630
0.01302	0.13	10.616	171.6						0.841
0.01018	0.10	9.403	151.5						0.844
0.00887	0.09	8.759	141.6						0.841
0.00758	0.08	8.096	130.9						0.841
0.00565	0.06	6.993	113.0						0.842
0.00323	0.03	5.284	85.2						0.845
0.01380	0.15	10.691	175.2						0.830
0.01244	0.13	10.203	165.0						0.741
0.01101	0.12	9.569	155.6						0.837
0.00939	0.10	8.813	144.1						0.832
0.00827	0.09	8.316	134.3						0.842
0.00619	0.06	7.225	116.0						0.847
0.00316	0.03	5.105	84.0						0.827

0.29647	13.531	3079.9	41673	5.46e+03	-0.02	0.00	44.76	13.105	3311.7	36.40	0.45	0.04	-0.575	-0.042	0.766
0.31003	13.690	3204.7	43873	5.34e+03	0.02	0.00	48.06	13.116	3483.8	38.79	0.46	0.04	-0.653	-0.047	0.749
0.38754	56.91	14.007	3880.4	54352	5.10e+03	0.05	0.00	74.63	13.267	4266.6	0.58	0.05	-0.653	-0.060	0.732
0.50386	88.95	14.565	4840.3	70499	4.71e+03	0.23	0.02	126.99	13.271	5553.3	61.04	0.03	-1.357	-0.093	0.673
0.60069	118.39	15.053	5558.9	83679	4.41e+03	0.47	0.03	174.33	13.455	6477.1	71.19	0.04	-1.391	-0.094	0.652
0.65882	140.33	15.165	6038.3	91570	4.35e+03	0.44	0.03	206.18	13.570	7027.9	77.25	0.04	-1.418	-0.095	0.654
0.02094	0.34	9.773	297.2	2904	1.05e+02		0.40	9.786	309.1	3.40					0.818
0.02483	0.46	9.937	347.3	3451	1.01e+02		0.54	9.973	360.4	3.96	0.15	0.01	0.146	0.015	0.822
0.03006	0.66	10.107	413.4	4179	9.79e+03	0.04	0.00	10.208	426.3	4.69	0.07	0.01	0.089	0.009	0.833
0.03513	0.87	10.288	475.7	4894	9.65e+03	0.02	0.00	10.403	489.9	5.38	0.00	0.00	0.043	0.004	0.835
0.04405	1.29	10.583	579.8	6136	8.93e+03	-0.07	-0.01	10.759	593.9	6.53	0.00	0.00	0.065	0.006	0.844
0.05685	2.00	10.965	723.8	7937	8.32e+03	-0.07	-0.01	11.203	737.9	8.11	0.01	0.00	0.131	0.012	0.852
0.06596	2.59	11.174	824.7	9209	8.01e+03	-0.09	-0.01	11.447	838.3	9.21	-0.03	0.00	0.148	0.013	0.856
0.06618	2.58	11.240	822.1	9240	7.92e+03	-0.07	0.00	11.482	838.1	9.21	0.01	0.00	0.189	0.017	0.852
0.07254	3.05	11.333	893.6	10177	7.79e+03	-0.07	-0.01	11.669	903.9	9.93	0.01	0.00	0.244	0.021	0.865
0.08213	3.81	11.471	1001.9	11483	7.60e+03	-0.13	-0.01	11.893	1006.4	11.06	-0.06	-0.01	0.282	0.024	0.877
0.09058	4.49	11.655	1086.3	12661	7.36e+03	-0.09	-0.01	12.117	1088.2	11.96	-0.06	0.00	0.370	0.032	0.882
0.10544	5.76	11.975	1229.3	14722	7.07e+03	0.02	0.00	12.385	1237.9	13.61	-0.12	-0.01	0.414	0.035	0.873
0.12188	7.50	12.133	1408.9	17084	6.79e+03	-0.06	-0.01	12.576	1415.6	15.56	-0.17	-0.01	0.372	0.031	0.877
0.23252	24.02	12.936	2532.3	32758	5.98e+03	-0.28	-0.02	12.874	13.033	26.17	0.39	0.03	-0.239	-0.018	0.829
0.29066	35.05	13.385	3052.3	40856	5.58e+03	-0.15	-0.01	14.422	12.926	32.91	0.27	0.02	-0.743	-0.054	0.761
0.31003	38.41	13.640	3187.8	43882	5.37e+03	0.03	0.00	50.40	12.915	35.06	0.26	0.02	-0.864	-0.063	0.732
0.34879	48.57	13.645	3584.9	48917	5.37e+03	-0.17	-0.01	63.21	12.974	39.26	0.30	0.02	-1.002	-0.072	0.738
0.40692	64.28	13.839	4114.6	56942	5.22e+03	-0.22	-0.02	88.73	12.775	46.41	0.06	0.00	-1.491	-0.105	0.696
0.48443	86.52	14.201	4762.9	67635	4.96e+03	-0.11	-0.01	126.63	12.731	55.32	60.81	-0.07	-1.841	-0.126	0.656
0.58131	117.48	14.624	5537.5	80979	4.68e+03	0.05	0.00	178.16	12.880	65.47	71.97	-0.08	-1.984	-0.133	0.633
0.01798	0.12	10.415	173.3	1805	9.22e+03		0.13	10.530	178.4	1.96					0.834
0.01667	0.15	11.703	198.6	2324	7.30e+03		0.18	11.670	207.3	2.28	0.12	0.00	0.054	0.005	0.810
0.01943	0.28	10.041	269.1	2702	9.92e+03		0.36	9.583	293.5	3.23	0.05	0.01	0.070	0.002	0.833
0.02294	0.40	9.837	324.2	3189	1.03e+02		0.48	9.774	339.7	3.73	0.06	0.01	-0.006	-0.001	0.823
0.02490	0.47	9.854	351.8	3502	1.01e+02	0.17	0.02	9.915	367.6	4.04	0.05	0.01	-0.038	-0.004	0.834
0.03000	0.66	10.058	419.5	4219	9.89e+03	-0.03	0.00	9.76	432.2	4.75	-0.01	0.00	0.029	0.003	0.847
0.03487	0.85	10.318	474.5	4896	9.39e+03	0.01	0.00	10.361	491.9	5.41	-0.05	0.00	0.074	0.006	0.853
0.04382	1.28	10.568	584.4	6176	8.95e+03	-0.10	-0.01	10.680	601.9	6.62	-0.11	-0.01	0.074	0.006	0.853
0.05682	2.01	10.927	734.6	8027	8.30e+03	-0.14	-0.01	11.131	750.7	8.25	-0.09	-0.01	0.074	0.006	0.853
0.07248	3.07	11.284	907.4	10239	7.85e+03	-0.15	-0.01	11.537	923.9	10.15	-0.18	-0.02	0.074	0.006	0.853
0.08229	3.76	11.589	1003.1	11625	7.45e+03	-0.02	0.00	11.793	1076.1	11.28	-0.22	-0.02	0.074	0.006	0.853
0.09111	4.56	11.647	1107.6	12900	7.37e+03	-0.13	-0.01	12.023	1116.9	12.28	-0.22	-0.02	0.074	0.006	0.853
0.10436	5.74	11.887	1234.6	14676	7.08e+03	-0.08	-0.01	12.240	1248.1	13.72	-0.29	-0.02	0.074	0.006	0.853
0.12983	8.29	12.306	1493.7	16381	6.60e+03	0.01	0.00	12.772	1498.1	16.47	-0.02	0.00	0.074	0.006	0.853
0.15502	11.45	12.503	1759.3	21996	6.40e+03	-0.08	-0.01	13.12	1726.8	19.88	-0.14	-0.01	0.074	0.006	0.853
0.25190	26.94	13.246	2686.4	35585	5.70e+03	-0.07	-0.01	15.13	2947.3	37.39	-0.08	-0.01	0.074	0.006	0.853
0.30422	37.89	13.489	3185.9	42976	5.50e+03	-0.12	-0.01	15.22	3558.7	39.11	-0.09	-0.01	0.074	0.006	0.853
0.36235	52.60	13.635	3754.1	51188	5.30e+03	-0.26	-0.02	16.32	4169.8	45.83	0.09	0.01	0.074	0.006	0.853
0.42629	69.49	13.957	4314.9	60221	5.13e+03	-0.18	-0.01	17.36	4906.4	53.93	0.04	0.00	0.074	0.006	0.853
0.50380	93.31	14.234	4999.8	71170	4.94e+03	-0.16	-0.01	18.10	5779.8	63.53	-0.02	0.00	0.074	0.006	0.853
0.58131	120.51	14.452	5662.1	82119	4.79e+03	-0.17	-0.01	17.50	6587.4	72.40	0.01	0.00	0.074	0.006	0.853
0.01174	0.10	10.016	162.9	1632	9.92e+03		0.12	10.091	168.4	1.85					0.829
0.01534	0.14	11.211	190.6	2136	7.94e+03		0.16	11.351	196.0	2.15					0.837
0.01821	0.17	11.950	212.7	2542	7.00e+03		0.32	9.496	278.8	3.06					0.515
0.02195	0.37	9.798	313.5	3572	1.04e+02		0.42	9.965	321.1	3.53					0.844
0.02648	0.52	9.992	371.7	3714	1.00e+02	0.11	0.01	0.61	9.997	386.9	4.25	0.04	0.047	0.005	0.817
0.03249	0.75	10.250	445.6	4567	9.52e+03	0.05	0.01	0.87	10.297	461.9	5.08	0.00	0.039	0.004	0.824
0.04039	1.10	10.510	540.2	5677	9.05e+03	-0.02	0.00	1.25	10.691	553.0	6.08	0.01	0.039	0.004	0.824
0.05245	1.74	10.837	681.8	7389	8.51e+03	-0.10	-0.01	1.97	11.048	696.5	7.66	-0.02	0.076	0.007	0.848
0.06703	2.66	11.205	842.8	9444	7.96e+03	-0.10	-0.01	2.97	11.512	854.3	9.39	-0.01	0.186	0.016	0.862
0.07577	3.32	11.344	941.0	10675	7.77e+03	-0.15	-0.01	3.64	11.751	946.1	10.40	-0.03	0.247	0.021	0.876
0.08254	3.90	11.398	1017.9	11602	7.70e+03	-0.23	-0.02	4.23	11.871	1017.9	11.19	-0.12	0.240	0.021	0.885

0.00786	5.17	11.738	1169.2	13724	7.26e-03	-0.13	-0.01	5.67	12.158	1175.6	12.92	-0.22	-0.02	0.277	0.023	0.876
0.12576	7.94	12.170	1468.8	17676	6.75e-03	-0.10	-0.01	8.65	12.643	1472.5	16.18	-0.14	-0.01	0.371	0.030	0.881
0.14688	10.41	12.412	1685.8	20924	6.49e-03	-0.10	-0.01	11.70	12.698	1716.1	18.86	-0.12	-0.01	0.160	0.013	0.854
0.17439	14.29	12.576	1875.5	24844	6.32e-03	-0.21	-0.02	16.89	12.548	2062.0	22.66	-0.18	-0.01	-0.309	-0.024	0.813
0.25190	27.44	13.111	2737.0	35886	5.87e-03	-0.24	-0.02	34.72	12.651	2956.3	35.49	0.01	0.00	-0.832	-0.062	0.760
0.33810	46.06	13.622	3538.3	48201	5.39e-03	-0.17	-0.01	62.00	12.735	3941.9	43.33	0.06	0.00	-1.248	-0.089	0.713
0.45923	77.98	14.178	4614.3	63423	4.97e-03	-0.08	-0.01	111.94	12.835	5308.5	58.35	0.06	0.00	-1.665	-0.115	0.669
0.61425	129.68	14.763	5927.5	82507	4.59e-03	0.07	0.00	187.07	13.280	6862.5	75.43	0.27	0.02	-1.666	-0.111	0.660
0.87197	231.20	15.635	7945.2	124221	4.09e-03	0.43	0.03	348.46	13.413	9366.0	102.94	-0.16	-0.01	-2.074	-0.134	0.601
0.01294	0.11	10.534	170.4	1795	9.01e-03			0.13	10.495	178.1	1.96					0.810
0.01677	0.16	11.386	204.8	2331	7.71e-03			0.22	10.630	228.2	2.51					0.712
0.02313	0.41	9.861	376.7	3222	1.03e-02			0.48	9.842	340.9	3.75					0.813
0.02865	0.60	10.097	396.2	4000	9.81e-03	0.11	0.01	0.70	10.125	411.4	4.52	0.05		0.067	0.007	0.821
0.03546	0.87	10.379	477.0	4951	9.28e-03	0.06	0.01	1.00	10.485	492.7	5.42	0.05	0.00	0.095	0.009	0.830
0.04421	1.28	10.659	590.4	6187	8.89e-03	0.00	0.00	1.47	10.785	597.4	6.57	0.01	0.00	0.080	0.008	0.836
0.05716	2.00	11.017	727.7	8017	8.24e-03	-0.03	0.00	2.76	11.234	743.2	8.17	0.03	0.00	0.150	0.014	0.849
0.06647	2.59	11.269	827.3	9323	7.89e-03	0.00	0.00	3.93	11.494	844.7	9.28	0.00	0.00	0.187	0.017	0.849
0.07298	3.04	11.408	897.2	10235	7.68e-03	0.00	0.00	3.45	11.616	917.7	10.09	-0.09	-0.01	0.165	0.014	0.846
0.08265	3.79	11.575	1001.4	11592	7.46e-03	-0.03	0.00	4.29	11.802	1022.9	11.24	-0.20	-0.02	0.163	0.014	0.849
0.09261	4.61	11.760	1104.5	12986	7.23e-03	-0.01	0.00	5.08	12.148	1113.5	12.24	-0.09	-0.01	0.361	0.031	0.871
0.10562	5.77	11.987	1235.8	14813	6.96e-03	0.02	0.00	6.42	12.324	1251.8	13.76	-0.21	-0.02	0.334	0.028	0.863
0.12944	8.51	12.097	1507.4	18235	6.83e-03	-0.22	-0.02	9.26	12.578	1509.8	16.59	-0.22	-0.02	0.263	0.021	0.882
0.16645	13.32	12.435	1881.5	23397	6.47e-03	-0.26	-0.02	14.72	12.829	1899.3	20.88	0.06	0.00	0.115	0.009	0.869
0.21722	21.20	12.862	2373.8	30533	6.04e-03	-0.24	-0.02	25.32	12.766	2490.8	27.38	0.11	0.01	-0.419	-0.032	0.804
0.29414	36.24	13.323	3103.3	41346	5.63e-03	-0.24	-0.02	46.30	12.516	3440.3	37.81	-0.14	-0.01	-1.230	-0.089	0.720
0.32941	44.41	13.478	3435.5	46303	5.50e-03	-0.27	-0.02	59.59	12.620	3821.1	42.00	-0.05	0.00	-1.309	-0.094	0.716
0.40692	64.30	13.836	4133.9	57198	5.22e-03	-0.23	-0.02	91.53	12.578	4736.0	52.05	-0.14	-0.01	-1.724	-0.121	0.675
0.48443	87.35	14.132	4818.4	68093	5.01e-03	-0.20	-0.01	128.71	12.627	5616.0	61.73	-0.19	-0.01	-1.970	-0.135	0.652
0.54256	106.44	14.338	5318.9	78264	4.86e-03	-0.16	-0.01	159.72	12.646	6258.0	68.76	-0.21	-0.02	-2.089	-0.141	0.640
0.65882	149.70	14.681	6307.7	92606	4.64e-03	-0.12	-0.01	227.14	12.927	7460.5	85.00	-0.21	-0.02	-2.164	-0.143	0.633
0.73633	182.63	14.856	6966.9	103501	4.53e-03	-0.12	-0.01	277.47	13.072	8245.7	90.63	-0.23	-0.02	-2.193	-0.144	0.632
0.01087	0.09	10.146	150.5	1527	9.71e-03			0.11	9.617	165.4	1.82					0.823
0.01571	0.14	11.373	194.1	2288	7.73e-03			0.17	11.306	203.4	2.24					0.807
0.01896	0.24	10.603	251.4	2665	6.90e-03			0.34	9.618	280.6	3.17					0.672
0.02362	0.43	9.819	338.9	3328	1.04e-02			0.50	9.880	350.8	3.86	0.10	0.01	0.100	0.010	0.876
0.02860	0.61	10.008	402.2	4025	9.98e-03	-0.01	0.00	0.70	10.133	413.7	4.55	0.05	0.00	0.066	0.007	0.837
0.03330	0.79	10.214	460.4	4702	9.98e-03	-0.04	0.00	0.90	10.360	472.7	5.20	0.02	0.00	0.062	0.006	0.840
0.04224	1.20	10.499	569.4	5978	9.07e-03	-0.12	-0.01	1.35	10.740	579.7	6.37	0.02	0.00	0.087	0.008	0.854
0.05499	1.90	10.882	713.4	7764	8.44e-03	-0.13	-0.01	2.12	11.173	723.7	7.95	0.03	0.00	0.135	0.012	0.860
0.07004	2.88	11.244	881.6	9912	7.91e-03	-0.14	-0.01	3.14	11.610	895.2	9.77	-0.01	0.00	0.214	0.019	0.870
0.07937	3.59	11.422	981.2	11207	7.64e-03	-0.14	-0.01	3.96	11.794	989.5	10.88	-0.16	-0.01	0.212	0.018	0.870
0.08791	4.30	11.563	1075.9	12440	7.46e-03	-0.16	-0.01	4.70	11.991	1080.4	11.89	-0.16	-0.01	0.257	0.022	0.878
0.10115	5.46	11.804	1212.7	14314	7.18e-03	-0.13	-0.01	5.91	12.304	1211.7	13.32	-0.15	-0.01	0.370	0.031	0.887
0.13176	8.65	12.217	1526.2	18646	6.70e-03	-0.12	-0.01	9.41	12.702	1528.8	16.80	-0.10	-0.01	0.364	0.030	0.882
0.16625	13.03	12.559	1873.3	23577	6.34e-03	-0.13	-0.01	14.41	12.951	1891.9	20.79	0.18	0.01	0.243	0.019	0.868
0.22458	22.06	13.035	2438.0	31781	5.89e-03	-0.11	-0.01	27.98	12.554	2636.4	28.98	-0.09	-0.01	-0.730	-0.055	0.757
0.29066	35.22	13.353	3073.4	41039	5.61e-03	-0.20	-0.01	48.91	12.290	3477.6	38.72	-0.37	-0.03	-1.475	-0.107	0.691
0.34646	47.36	13.727	3563.8	48010	5.31e-03	-0.08	-0.01	68.14	12.412	4104.7	45.12	-0.27	-0.02	-1.641	-0.117	0.667
0.35847	50.50	13.753	3688.5	50728	5.29e-03	-0.11	-0.01	70.95	12.585	4107.8	46.14	-0.10	-0.01	-1.507	-0.102	0.684
0.45536	77.27	14.123	4562.5	64439	5.01e-03	-0.11	-0.01	114.40	12.590	5330.4	58.59	-0.19	-0.01	-1.917	-0.132	0.649
0.51349	95.53	14.324	5073.1	72665	4.87e-03	-0.10	-0.01	143.16	12.691	5963.1	65.54	-0.17	-0.01	-2.011	-0.137	0.641
0.59100	122.57	14.555	5746.1	83633	4.72e-03	-0.08	-0.01	185.39	12.836	6785.7	74.58	-0.16	-0.01	-2.091	-0.140	0.635
0.67820	156.36	14.787	6490.1	95972	4.57e-03	-0.06	0.00	237.51	13.013	7680.6	84.42	-0.17	-0.01	-2.128	-0.141	0.632
0.01158	0.10	10.016	163.0	1633	9.97e-03			0.11	10.117	168.1	1.85					0.833
0.01411	0.12	10.986	181.3	1982	8.79e-03			0.14	11.062	187.5	2.06					0.828
0.01650	0.15	11.444	203.6	2330	7.64e-03			0.19	11.087	218.0	2.41					0.766
0.01945	0.29	9.850	278.8	2746	1.03e-02			0.35	9.726	294.0	3.23					0.796
0.02457	0.46	9.937	349.3	3467	1.01e-02			0.52	10.042	359.6	3.95	0.22	0.02	0.219	0.022	0.835

0.02951	10.105	411.4	4158	9.79e-03	0.05	0.00	0.73	10.185	425.1	4.67	0.05	0.00	0.071	0.007	0.029	
0.03496	10.321	482.0	4974	9.39e-03	-0.01	0.00	0.34	10.514	492.7	5.42	0.10	0.01	0.144	0.014	0.047	
0.04293	1.23	576.5	6116	8.95e-03	-0.08	-0.01	1.37	10.627	508.3	6.47	0.08	0.01	0.149	0.014	0.056	
0.05546	1.91	10.945	7796	8.35e-03	-0.09	-0.01	2.12	11.255	731.6	8.04	0.06	0.01	0.198	0.018	0.063	
0.07043	2.89	11.294	889.2	7.84e-03	-0.10	-0.01	3.23	11.581	903.1	9.93	-0.08	-0.01	0.158	0.014	0.058	
0.07969	3.57	11.487	987.9	7.57e-03	-0.08	-0.01	4.01	11.773	1004.7	11.04	-0.18	-0.01	0.165	0.014	0.056	
0.08753	4.24	11.595	1074.0	7.46e-03	-0.13	-0.01	4.72	11.911	1088.0	11.97	-0.26	-0.02	0.164	0.014	0.061	
0.10190	5.51	11.832	1219.2	7.14e-03	-0.11	-0.01	6.10	12.200	1231.5	13.54	-0.29	-0.02	0.238	0.020	0.066	
0.14533	10.22	12.390	1680.6	2.082e-02	6.51e-03	-0.11	0.01	11.05	1677.2	18.43	0.11	0.01	0.432	0.035	0.089	
0.16277	12.50	12.569	1865.3	2.332e-02	6.39e-03	-0.17	-0.01	13.70	13.002	1868.9	20.54	0.22	0.202	0.075	0.082	
0.23252	23.42	13.100	2504.4	3.332e-02	5.83e-03	-0.12	-0.01	20.60	12.840	2703.6	29.72	0.20	0.02	-0.488	-0.032	0.784
0.27128	30.65	13.360	3087.9	5.69e-03	-0.10	-0.01	40.03	12.879	3193.6	35.10	0.03	0.00	-0.939	-0.069	0.735	
0.37941	43.01	13.694	3436.9	4.706e-03	-0.05	0.00	56.91	12.911	3786.2	41.73	0.24	0.02	-1.006	-0.072	0.726	
0.38754	58.11	13.860	4007.2	5.554e-03	5.21e-03	-0.15	-0.01	82.68	12.603	4589.7	50.45	-0.11	-0.01	-1.644	-0.115	0.675
0.50380	92.80	14.258	5064.1	7.270e-03	4.92e-03	-0.16	-0.01	139.49	12.611	5961.7	65.53	-0.25	-0.02	-2.068	-0.142	0.639
0.60089	126.44	14.564	5909.8	8.607e-03	4.71e-03	-0.12	-0.01	191.34	12.774	7017.4	77.13	-0.27	-0.02	-2.211	-0.148	0.620
0.71695	172.85	14.867	5905.3	10.266e-03	4.52e-03	-0.09	-0.01	266.46	12.987	8237.4	90.48	-0.32	-0.02	-2.275	-0.149	0.623
0.81383	216.58	15.077	7705.4	1.1617e-02	4.40e-03	-0.07	0.00	334.45	13.159	9184.2	101.06	-0.37	-0.03	-2.295	-0.149	0.622
0.01695	0.17	11.337	208.2	2.361e-03	7.70e-03	0.03	0.20	11.218	219.2	2.41	0.20	0.00	0.799	0.079	0.799	
0.01921	0.28	9.954	268.9	2.676e-03	1.01e-02	0.03	0.34	9.795	284.6	3.13	0.34	0.00	0.790	0.790	0.790	
0.02190	0.37	9.830	310.5	3.052e-03	1.03e-02	0.03	0.43	9.864	322.3	3.54	0.43	0.00	0.804	0.804	0.804	
0.02725	0.54	12.086	376.8	3.800e-03	9.83e-03	0.18	0.63	10.192	388.3	4.27	0.23	0.02	0.235	0.024	0.834	
0.03305	0.76	10.310	447.3	4.611e-03	9.41e-03	0.11	0.87	10.490	458.2	5.04	0.20	0.02	0.236	0.023	0.843	
0.03863	1.01	10.496	513.5	5.391e-03	9.08e-03	0.05	1.14	10.703	524.6	5.77	0.17	0.02	0.224	0.021	0.849	
0.04726	1.42	10.814	610.2	6.599e-03	8.55e-03	0.07	1.60	11.061	621.3	6.83	0.21	0.02	0.298	0.027	0.854	
0.06027	2.15	11.200	751.3	8.414e-03	7.97e-03	0.10	2.40	11.497	762.2	8.38	0.24	0.02	0.369	0.033	0.860	
0.07441	3.13	11.461	906.2	10.385e-03	7.61e-03	0.03	3.50	11.768	919.1	10.10	0.06	0.01	0.314	0.027	0.861	
0.08296	3.75	11.678	988.9	1.1549e-02	7.33e-03	0.10	4.23	11.975	1028.6	11.09	-0.04	0.00	0.310	0.027	0.861	
0.09040	4.40	11.753	1067.9	1.2551e-02	7.24e-03	0.04	4.91	12.068	1083.2	11.91	-0.09	-0.01	0.379	0.028	0.860	
0.10005	5.32	11.826	1169.8	1.3834e-02	7.15e-03	-0.05	5.91	12.176	1183.2	13.01	-0.22	-0.02	0.264	0.024	0.865	
0.14727	10.34	12.486	1646.4	2.0556e-02	6.41e-03	0.02	11.42	12.885	1661.4	18.26	0.07	0.01	0.404	0.032	0.869	
0.15889	12.05	12.483	1767.9	2.2766e-02	6.42e-03	-0.11	-0.01	13.43	12.874	1792.3	19.70	0.02	0.00	0.710	0.017	0.863
0.23252	23.39	13.111	2462.8	3.2290e-02	5.82e-03	-0.05	28.66	12.845	2617.9	28.77	0.20	0.02	-0.476	-0.032	0.783	
0.31003	39.04	13.529	3180.7	4.5033e-02	5.46e-03	-0.08	-0.01	52.35	12.673	3536.4	38.07	0.01	0.00	-1.121	-0.081	0.716
0.33910	44.96	13.790	3421.6	4.7185e-02	5.26e-03	0.05	61.96	12.739	3857.6	42.40	0.07	0.01	-1.207	-0.087	0.697	
0.40692	63.42	13.933	4052.0	5.6456e-02	5.15e-03	-0.10	-0.01	91.36	12.659	51.33	-0.13	-0.01	-1.686	-0.116	0.667	
0.48443	86.32	14.217	4724.1	6.7163e-02	4.95e-03	-0.08	-0.01	176.99	12.714	5501.7	60.47	-0.09	-0.01	-1.848	-0.127	0.653
0.67820	156.16	14.799	6346.7	9.3922e-02	4.57e-03	-0.01	0.00	239.04	13.001	7523.9	82.70	-0.15	-0.01	-2.105	-0.139	0.630
0.77508	196.37	15.082	7104.0	1.0714e-01	4.40e-03	0.08	0.01	301.61	13.199	8463.9	92.92	-0.15	-0.01	-2.109	-0.138	0.625
0.01063	0.09	9.564	154.3	1.475e-03	1.09e-02	0.03	0.10	9.952	154.4	1.70	0.10	0.00	0.854	0.854	0.854	
0.01159	0.10	9.978	167.1	1.610e-03	1.01e-02	0.03	0.11	10.168	164.9	1.81	0.11	0.00	0.856	0.856	0.856	
0.01314	0.12	10.531	173.5	1.827e-03	9.02e-03	0.03	0.14	10.549	180.3	1.98	0.14	0.00	0.819	0.819	0.819	
0.01514	0.14	11.176	188.3	2.105e-03	8.01e-03	0.03	0.16	11.313	193.8	2.13	0.13	0.00	0.836	0.836	0.836	
0.01719	0.16	11.670	204.9	2.391e-03	7.34e-03	0.03	0.19	11.684	213.1	2.34	0.19	0.00	0.818	0.818	0.818	
0.02212	0.38	9.840	317.9	3.079e-03	1.03e-02	0.03	0.44	9.850	325.5	3.58	0.44	0.00	0.818	0.818	0.818	
0.02595	0.50	9.966	362.6	3.614e-03	1.01e-02	0.03	0.60	9.935	378.8	4.16	0.60	0.01	0.021	0.002	0.872	
0.03102	0.69	10.173	424.9	4.323e-03	9.66e-03	0.06	0.81	10.212	440.9	4.85	0.81	0.00	0.034	0.003	0.872	
0.03655	0.93	10.344	492.8	5.097e-03	9.35e-03	-0.03	1.07	10.458	507.6	5.58	-0.01	0.00	0.036	0.003	0.834	
0.04519	1.34	10.628	593.5	6.308e-03	8.85e-03	-0.07	1.53	10.790	608.8	6.69	-0.02	0.00	0.052	0.005	0.841	
0.05010	2.08	10.994	738.1	8.116e-03	8.27e-03	-0.08	2.32	11.280	749.3	8.24	0.06	0.01	0.181	0.016	0.859	
0.07365	3.14	11.325	908.1	1.0284e-02	7.80e-03	-0.11	3.49	11.656	918.9	10.10	-0.05	0.00	0.203	0.018	0.865	
0.08272	3.84	11.504	1002.7	1.1535e-02	7.56e-03	-0.10	4.27	11.839	1014.7	11.15	-0.14	-0.01	0.214	0.018	0.865	
0.09057	4.49	11.655	1080.0	1.2586e-02	7.36e-03	-0.08	4.97	12.019	1090.6	11.99	-0.16	-0.01	0.269	0.023	0.868	
0.10196	5.52	11.819	1186.3	1.4056e-02	7.16e-03	-0.08	6.10	12.201	1199.8	13.19	-0.23	-0.02	0.285	0.024	0.870	
0.12176	7.39	12.212	1386.2	1.6929e-02	6.70e-03	0.05	8.37	12.445	1418.7	15.57	-0.30	-0.02	0.240	0.020	0.848	
0.18003	15.19	12.595	1987.1	2.5027e-02	6.30e-03	-0.20	12.42	12.757	2043.2	22.46	0.03	0.00	-0.084	-0.007	0.837	
0.22282	21.69	13.032	2376.1	3.0967e-02	5.89e-03	-0.20	17.07	12.653	2548.8	28.01	0.00	0.00	-0.572	-0.043	0.769	
0.25746	29.10	13.013	2740.9	3.5786e-02	5.80e-03	-0.34	37.13	12.466	2993.5	32.78	-0.15	-0.01	-1.002	-0.074	0.753	
0.33489	45.17	13.587	3425.8	4.6544e-02	5.42e-03	-0.15	63.10	12.449	3887.8	42.73	-0.20	-0.02	-1.491	-0.107	0.687	

RUN 106
DATE 9/29/92
POLY -
c.w.r.p.p.m. -
W 1.000

RUN 113
DATE 10/9/92
POLY -
c.w.r.p.p.m. -
W 1.000

0.008" Ribbed 0.402" Pipe

Resol = 350

Series

PRE
S2: 0.402
h = smooth
RZB:
d = 0.386
h = 0.006
R/h 32.2

N=10

RAM 95
DATE 8/4/92
POLY N=10
c wppm 2435.1
w 1.303

Q (L/A)	Tw(S2)	1/w(S2)	Resol(S2)	S(S2)	Sf(S2)	Tw(R2B)	1/w(R2B)	Resol(R2B)	h _s	S(R2B)	Sf(R2B)	1/w(S2)h	Sf(S2)h	R	Rf	P	Δ/ries	corrected R	corrected R
0.00189	0.02	3.584	57.5	0.00	0.00	0.12	7.734	126.4	1.42	0.08	0.01	9.93	-0.02	0.116	0.012	0.841	0.00	0.116	-0.02
0.00267	0.03	4.176	66.4	0.00	0.00	0.13	8.269	136.4	1.50	0.08	0.01	10.3	-0.01	0.164	0.016	0.848	0.00	0.164	-0.01
0.00336	0.04	4.678	74.7	0.06	-0.01	0.15	9.088	144.6	1.59	0.11	0.01	10.54	-0.07	0.235	0.022	0.856	0.00	0.235	-0.07
0.00433	0.05	5.177	85.0	-0.10	-0.01	0.23	10.391	178.0	1.96	0.10	0.01	10.74	-0.10	0.289	0.027	0.864	0.00	0.289	-0.10
0.00545	0.06	5.667	95.4	-0.12	-0.01	0.41	10.191	240.5	2.64	0.17	0.02	10.9	-0.12	0.398	0.036	0.878	0.00	0.398	-0.12
0.00660	0.07	6.572	105.1	-0.12	-0.01	0.41	10.191	240.5	2.64	0.17	0.02	10.9	-0.12	0.398	0.036	0.878	0.00	0.398	-0.12
0.00731	0.08	6.923	110.8	-0.13	-0.01	0.43	11.298	287.6	4.26	0.12	0.01	11.05	-0.13	0.381	0.035	0.875	0.00	0.381	-0.13
0.00913	0.10	7.704	124.8	-0.13	-0.01	0.567	11.641	392.0	8.59	0.12	0.01	11.27	-0.13	0.371	0.033	0.872	0.00	0.371	-0.13
0.01026	0.12	8.155	132.7	-0.13	-0.01	0.77	12.272	482.3	13.00	-0.13	-0.01	11.88	-0.01	0.392	0.033	0.873	0.00	0.392	-0.01
0.01193	0.14	8.809	143.2	0.00	0.00	1.399	13.999	618.0	15.59	0.04	0.00	12.2	-0.01	0.590	0.048	0.893	0.00	0.590	-0.01
0.01680	0.20	10.371	171.2	0.00	0.00	2.266	13.019	804.3	19.83	0.22	0.02	12.61	-0.02	0.409	0.032	0.872	0.00	0.409	-0.02
0.02216	0.24	11.433	205.8	0.11	0.01	4.201	13.477	1056.8	27.00	0.82	0.06	13.28	0.12	0.197	0.015	0.847	0.00	0.197	0.12
0.03517	0.34	13.994	317.8	0.19	0.01	53.47	13.722	2765.5	30.40	1.08	0.09	13.59	0.22	0.132	0.010	0.841	0.00	0.132	0.22
0.04485	0.42	15.267	464.9	0.38	0.03	76.19	13.524	3306.6	36.37	0.87	0.07	14.08	0.58	-0.556	-0.040	0.768	0.00	-0.556	0.58
0.05471	0.51	16.519	554.7	0.44	0.03	108.48	13.600	3948.0	43.39	0.93	0.07	14.57	0.58	-0.970	-0.047	0.742	0.00	-0.970	0.58
0.06432	0.60	17.718	636.7	1.20	0.08	223.94	14.199	5672.3	62.35	1.38	0.11	16.15	1.53	-1.951	-0.121	0.678	0.00	-1.951	1.53
0.07279	0.69	18.896	712.6	1.63	0.11	327.39	14.679	6658.5	75.38	1.67	0.13	16.99	2.05	-2.311	-0.136	0.650	0.00	-2.311	2.05

0.006" Ribbed 402" Pipe
 Resolcut = 350

Sewer

RPE
 SZ: d = 0.402
 h = smooth
 R2B: d = 0.386
 h = 0.006
 RA: 32.2

IN-10

RUN 115
 DATE 10/14/92
 POLY H-10
 c wppm 5136.4
 W 1.777

Q (L/s)	Tw(SZ)	1/Spd(SZ)	Revd(SZ)	S (SZ)	SF (SZ)	Tw(R2B)	1/Spd(R2B)	Revd(R2B)	Ns	S (R2B)	SF (R2B)	1/Spd(S2N)	S _N (S2N)	R	Rf	P	Δ/ires	connected R	connected S
0.00249	0.04	3.498	56.1			0.09	5.273	84.6	0.83			5.28				0.848			
0.00338	0.05	4.080	65.2			0.11	5.994	94.1	1.03			5.89				0.864			
0.00381	0.06	4.339	69.2			0.13	6.425	102.1	1.12			6.38				0.857			
0.00468	0.07	4.797	77.0			0.15	6.957	106.5	1.19			6.77				0.860			
0.00542	0.08	5.172	82.8			0.17	7.300	115.9	1.27			7.21				0.860			
0.00685	0.10	5.876	93.0			0.23	8.535	135.3	1.49			8.39				0.864			
0.00796	0.12	6.272	100.4			0.30	9.526	154.2	1.69			9.43				0.858			
0.00902	0.14	6.680	106.9			0.36	10.379	168.7	1.85			10.19				0.863			
0.01398	0.21	8.284	133.7			0.83	9.581	254.2	2.75			10.53				0.887			
0.01777	0.27	9.293	151.8			1.26	9.753	314.3	3.45			9.76				0.821			
0.02117	0.33	10.094	166.6			1.96	10.143	392.2	4.31	0.16	0.02	10.02	0.05	0.123	0.012	0.842	0.00	0.123	0.05
0.02943	0.50	11.295	207.1			2.95	10.499	481.5	5.29	0.13	0.01	10.31	-0.02	0.189	0.018	0.851	0.00	0.189	-0.02
0.03703	1.08	9.722	302.8	0.06	0.01	3.60	10.732	531.2	5.84	0.18	0.02	10.46	-0.04	0.272	0.026	0.863	0.00	0.272	-0.04
0.04802	1.72	9.987	382.5	-0.01	0.00	4.28	10.979	578.5	6.36	0.27	0.02	10.64	-0.01	0.339	0.032	0.872	0.00	0.339	-0.01
0.06102	2.62	10.284	472.0	-0.04	0.00	5.42	11.240	648.4	7.13	0.31	0.03	10.91	0.06	0.330	0.030	0.869	0.00	0.330	0.06
0.06882	3.23	10.440	524.3	-0.01	0.00	10.89	11.908	928.7	10.21	0.16	0.01	11.63	0.16	0.278	0.024	0.867	0.00	0.278	0.16
0.07678	3.88	10.622	574.2	0.06	0.01	19.03	12.556	1227.6	13.49	0.07	0.01	12.08	0.12	0.476	0.039	0.882	0.00	0.476	0.12
0.08950	4.91	10.892	642.5	0.16	0.01	31.39	13.168	1576.8	17.33	0.35	0.03	12.88	0.49	0.288	0.022	0.861	0.00	0.288	0.49
0.12892	9.25	11.556	891.3	0.12	0.01	41.50	13.944	1813.2	19.93	1.15	0.09	13.51	0.88	0.434	0.032	0.873	0.00	0.434	0.88
0.24948	28.16	12.818	1555.3	0.45	0.04	59.80	14.656	2198.1	23.95	1.96	0.15	13.28	1.43	0.276	0.019	0.859	0.00	0.276	1.43
0.30376	37.74	13.481	1800.8	0.86	0.07	80.80	15.245	2500.7	27.82	2.59	0.21	15.29	2.08	-0.045	-0.003	0.830	0.00	-0.045	2.08
0.38359	53.56	14.250	2145.5	1.36	0.11	116.66	15.966	3041.4	33.43	3.32	0.26	16.07	2.54	-0.104	-0.006	0.820	0.00	-0.104	2.54
0.46342	69.83	15.120	2450.2	1.96	0.15	171.15	16.542	3685.8	40.51	3.88	0.31	16.83	2.96	-0.288	-0.017	0.813	0.00	-0.288	2.96
0.56317	99.58	15.933	2926.3	2.47	0.18	190.02	16.749	3881.4	42.66	4.08	0.32	17.09	3.13	-0.341	-0.020	0.805	0.00	-0.341	3.13
0.73186	144.91	16.575	3532.0	2.78	0.20	246.40	17.174	4426.4	48.65	4.47	0.35	17.8	3.62	-0.626	-0.035	0.790	0.00	-0.626	3.62
0.78076	159.35	16.863	3701.7	2.99	0.22	295.70	17.458	4749.0	52.20	4.73	0.37	18.26	3.95	-0.802	-0.044	0.781	0.00	-0.802	3.95
0.91168	202.68	17.459	4180.9	3.37	0.24														
0.99790	232.31	17.851	4459.8	3.65	0.26														

0.008" Ribbed 0.402" Pipe

Revised - 350

Series M-750

PER
 SZ d = 0.402
 h = smooth
 R2B: d = 0.386
 h = 0.006
 h = 32.2
 W 1.038

M-750
 RUN 90
 DATE 7/27/92
 POLY M-750
 c 100
 W 1.038

Q1(L/S)	Twd(SZ)	1/4wd(SZ)	Revd(SZ)	S(SZ)	Sf(SZ)	Twd(R2B)	1/4wd(R2B)	Revd(R2B)	h _s	S(R2B)	Sf(R2B)	1/4wd(S2h)	S1(SZ)	R	W	P	ΔT/hrs	connected R	connected S
0.00850	0.07	8.520	133.1	0.15	0.01	0.09	8.709	134.6	1.48	0.03	0.00	8.62	0.12	-0.075	-0.007	0.00	0.00	-0.075	0.12
0.01061	0.09	9.517	149.3	0.06	0.01	0.11	9.693	152.8	1.68	0.10	0.01	9.7	0.08	0.053	0.005	0.00	0.00	0.053	0.08
0.01189	0.10	10.021	159.3	0.01	0.00	0.12	10.116	164.1	1.81	0.00	0.00	10.28	0.05	0.010	0.001	0.00	0.00	0.010	0.05
0.01364	0.12	10.643	172.0	0.03	0.00	0.14	10.887	175.1	1.97	-0.05	0.00	10.76	0.01	0.039	0.004	0.00	0.00	0.039	0.01
0.01523	0.14	11.097	184.7	0.03	0.00	0.25	9.055	235.6	2.58	0.04	0.00	10.87	0.03	0.202	0.018	0.00	0.00	0.202	0.03
0.01845	0.20	11.143	223.2	0.01	0.00	0.31	9.841	263.2	2.88	0.02	0.00	10.33	0.02	0.272	0.024	0.00	0.00	0.272	0.02
0.02094	0.32	10.029	281.4	0.00	0.00	0.39	9.938	295.8	3.25	0.03	0.00	9.97	0.04	0.335	0.029	0.00	0.00	0.335	0.04
0.02366	0.42	5.949	321.3	0.00	0.00	0.51	9.822	318.9	3.73	0.02	0.00	10.33	0.04	0.352	0.053	0.00	0.00	0.352	0.04
0.02855	0.60	10.061	383.5	0.01	0.00	0.70	10.055	400.4	4.40	0.03	0.00	9.97	0.04	0.352	0.053	0.00	0.00	0.352	0.04
0.03343	0.79	10.261	441.1	0.01	0.00	1.34	10.363	454.9	5.00	0.00	0.00	10.31	0.08	0.053	0.005	0.00	0.00	0.053	0.08
0.04167	1.15	10.572	533.7	0.06	0.01	0.91	11.009	552.8	6.08	0.00	0.00	10.62	0.05	0.010	0.001	0.00	0.00	0.010	0.05
0.05397	1.82	10.914	671.1	0.01	0.00	2.10	11.009	692.9	7.62	-0.05	0.00	10.97	0.01	0.039	0.004	0.00	0.00	0.039	0.01
0.06868	2.75	11.298	826.9	0.03	0.00	3.10	11.532	843.7	9.27	0.04	0.00	11.33	0.03	0.202	0.018	0.00	0.00	0.202	0.03
0.07776	3.42	11.466	922.5	0.01	0.00	3.82	11.772	935.8	10.29	0.02	0.00	11.5	0.02	0.272	0.024	0.00	0.00	0.272	0.02
0.08583	4.04	11.642	1000.6	0.04	0.00	4.48	11.995	1071.4	10.29	0.03	0.00	11.86	0.04	0.335	0.029	0.00	0.00	0.335	0.04
0.09845	5.21	11.876	1134.0	0.06	0.00	5.54	12.492	1122.8	12.34	0.23	0.02	11.86	0.06	0.352	0.053	0.00	0.00	0.352	0.06
0.14769	9.72	12.914	1562.6	0.54	0.04	10.58	13.423	1565.7	17.21	0.61	0.05	12.82	0.54	0.503	0.059	0.00	0.00	0.503	0.54
0.22273	19.32	13.817	2207.6	0.84	0.06	20.37	14.592	2176.9	23.93	1.89	0.15	13.78	0.83	0.812	0.059	0.00	0.00	0.812	0.83
0.31055	33.50	14.628	2907.1	1.17	0.09	34.56	15.622	2835.1	31.16	2.98	0.24	14.54	1.13	1.082	0.074	0.00	0.00	1.082	1.13
0.35824	42.06	15.103	3250.1	1.46	0.11	43.49	16.109	3173.3	34.88	3.46	0.27	15	1.39	1.109	0.074	0.00	0.00	1.109	1.39
0.43029	56.12	15.661	3762.6	1.76	0.13	64.21	15.880	3864.5	47.48	3.21	0.25	15.81	1.86	0.070	0.004	0.00	0.00	0.070	1.86
0.54226	78.05	16.734	4437.4	2.55	0.18	95.36	16.421	4709.6	51.76	3.70	0.29	17.12	2.83	-0.699	-0.041	0.00	0.00	-0.699	2.83
0.72008	118.13	18.063	5459.2	3.51	0.24	151.35	17.308	5933.3	65.21	4.45	0.38	18.54	3.85	-1.232	-0.066	0.00	0.00	-1.232	3.85
0.89811	166.01	19.004	6471.6	4.16	0.28	218.06	17.985	7121.9	78.28	4.92	0.38	19.48	4.47	-1.495	-0.077	0.00	0.00	-1.495	4.47
1.09769	228.89	19.781	7599.0	4.66	0.31	310.81	18.412	8502.7	93.46	5.05	0.38	20.33	5.01	-1.918	-0.094	0.00	0.00	-1.918	5.01

0.006" Ribbed 0.402" Pipe

Residm = .350

PPE
 SZ: d = 0.402
 h = smooth
 R2R: d = 0.386
 h = 0.006
 RA: 32.2
 Series: M-750
 RUN DATE 7/28/92
 POLY M-750
 c temp 250
 W 1.094

Q (L/A)	Tef(S)	Vref(S)	Repd(S)	S(S)	SF(S)	Tef(R2B)	Vref(R2B)	Repd(R2B)	N	S (R2B)	Sf (R2B)	Vref(S2)	S(S2)	P	Δ/Inch	connected R	connected S
0.00231	0.02	4.281	67.3	0.04	0.00	0.09	9.788	136.0	1.49	0.12	0.01	8.47	0.02	0.097	0.010	0.097	0.02
0.00297	0.03	4.850	76.7	-0.04	0.00	0.11	9.532	149.9	1.65	0.14	0.00	9.2	-0.05	0.115	0.011	0.115	-0.05
0.00348	0.03	5.288	82.4	-0.07	-0.01	0.14	10.318	164.8	1.81	0.16	0.00	10.05	-0.07	0.115	0.011	0.115	-0.07
0.00481	0.04	6.203	97.5	-0.15	-0.01	0.21	9.850	204.0	2.24	0.24	0.00	11.61	-0.15	0.213	0.020	0.213	-0.15
0.00559	0.05	6.700	105.2	-0.15	-0.01	0.29	9.963	241.3	2.65	0.26	0.00	10.64	-0.15	0.213	0.020	0.213	-0.15
0.00738	0.07	7.667	121.8	-0.14	-0.01	0.49	10.056	282.1	3.10	0.38	0.00	9.84	-0.14	0.246	0.023	0.246	-0.14
0.00905	0.09	8.459	135.8	-0.15	-0.01	0.68	9.776	314.8	3.46	0.49	0.00	9.75	-0.15	0.308	0.028	0.308	-0.15
0.01080	0.10	9.179	149.5	-0.15	-0.01	0.80	10.007	372.8	4.10	0.62	0.00	9.91	-0.15	0.308	0.028	0.308	-0.15
0.01282	0.12	9.884	163.5	-0.17	-0.01	0.90	10.195	430.0	4.73	0.64	0.00	10.08	-0.17	0.308	0.028	0.308	-0.17
0.01515	0.15	10.751	179.4	-0.17	-0.01	1.35	10.466	525.3	5.77	0.07	0.01	10.41	-0.17	0.308	0.028	0.308	-0.17
0.01809	0.18	11.588	199.2	-0.15	-0.01	2.07	10.923	652.0	7.17	-0.02	0.00	10.71	-0.15	0.308	0.028	0.308	-0.15
0.02129	0.24	10.003	272.3	-0.15	-0.01	2.65	11.176	738.7	8.12	-0.01	0.00	10.93	-0.15	0.308	0.028	0.308	-0.15
0.02304	0.42	9.722	303.9	-0.15	-0.01	3.10	11.348	798.6	8.78	-0.01	0.00	11.04	-0.15	0.308	0.028	0.308	-0.15
0.02794	0.59	9.882	362.5	-0.17	-0.01	3.82	11.574	886.1	9.74	-0.04	0.00	11.11	-0.17	0.308	0.028	0.308	-0.17
0.03276	0.79	10.046	419.0	-0.17	-0.01	4.44	11.859	954.1	10.49	0.05	0.00	11.34	-0.17	0.308	0.028	0.308	-0.17
0.04109	1.17	10.363	509.5	-0.17	-0.01	5.31	12.534	1043.1	11.47	0.48	0.04	11.53	-0.14	0.308	0.028	0.308	-0.14
0.05310	1.84	10.676	640.5	-0.15	-0.01	8.21	13.757	1308.4	14.38	1.14	0.09	12.55	0.48	1.207	0.096	1.207	0.48
0.06757	2.79	11.033	788.7	-0.15	-0.01	11.39	14.325	1540.6	16.93	1.52	0.12	13.05	0.70	1.275	0.096	1.275	0.70
0.07647	3.53	11.099	887.3	-0.29	-0.03	19.59	15.721	2020.8	22.21	2.99	0.23	14.36	1.54	1.361	0.095	1.361	1.54
0.08446	4.11	11.355	956.7	-0.17	-0.01	26.30	17.064	2478.7	26.69	4.40	0.35	15.25	2.11	1.814	0.119	1.814	2.11
0.09771	5.27	11.607	1081.6	-0.13	-0.01	35.79	17.264	2731.5	30.02	4.62	0.37	15.49	2.14	1.774	0.115	1.774	2.14
0.13332	8.15	12.730	1357.7	0.60	0.05	48.76	17.487	3188.2	35.04	4.84	0.38	15.96	2.35	1.527	0.096	1.527	2.35
0.16346	11.44	13.177	1608.2	0.75	0.06	72.47	17.748	3886.8	42.72	5.08	0.40	17.73	3.77	1.018	0.001	1.018	3.77
0.23530	19.44	14.552	2096.2	1.67	0.13	121.69	18.511	5086.6	53.36	5.76	0.45	19.54	5.13	-1.029	-0.053	-1.029	5.13
0.30695	29.30	15.461	2573.8	2.22	0.17	182.36	19.012	6165.5	67.77	6.12	0.47	21.31	6.55	-2.298	-0.108	-2.298	6.55
0.34927	37.73	15.503	2920.7	2.04	0.15	243.04	19.686	7117.9	78.23	6.62	0.51	22.8	7.79	-3.114	-0.137	-3.114	7.79
0.41203	48.24	16.210	3302.5	2.53	0.19												
0.51092	63.01	17.549	3774.4	3.64	0.26												
0.69055	98.00	19.018	4707.2	4.73	0.33												
0.86817	135.66	20.323	5538.2	5.75	0.39												
1.03782																	

0.006" Ribbed 0.402" Pipe
 Resol: 350

Series

RUN 93
 DATE 7/20/92
 POLY M-750
 c. wppm 900
 W 1.278

M-750

PIPE
 S2: d = 0.402
 h = smooth
 R2B: d = 0.386
 h = 0.006
 RA 32.2
 W 1.278

Q (L/s)	Tm(S2)	1/mph(S2)	Penp(S2)	S (S2)	SF (S2)	1/mph(R2B)	Penp(R2B)	h	S (R2B)	SF (R2B)	1/mph(S2)	S (S2)	W	P	d/Tree	connected R	corrected S
0.00131	0.01	2.952	47.2			0.11	7.666	125.7	1.38								
0.00206	0.02	3.706	59.2			0.13	8.295	139.9	1.54					0.837			
0.00261	0.03	4.168	66.7			0.15	8.864	148.8	1.64					0.816			
0.00312	0.03	4.548	73.0			0.17	9.380	157.5	1.73					0.831			
0.00414	0.05	5.269	84.1			0.20	10.160	172.7	1.90					0.833			
0.00496	0.06	5.761	92.3			0.24	10.765	186.8	2.08					0.829			
0.00777	0.06	6.227	99.6			0.33	10.610	221.9	2.44					0.697			
0.00704	0.08	6.874	110.3			0.52	9.411	276.8	3.04					0.535			
0.00857	0.10	7.572	122.2			0.71	9.754	324.7	3.57					0.817			
0.01028	0.11	8.285	134.3			0.91	10.003	367.9	4.04	0.14	0.01	0.01	0.001	0.825	0.00	0.013	0.13
0.01167	0.13	8.787	144.1			1.35	10.279	448.2	4.93	0.04	0.00	0.10	0.109	0.840	0.00	0.109	-0.04
0.01307	0.15	9.286	152.8			2.11	10.651	562.0	6.18	0.01	0.00	0.10	0.121	0.842	0.00	0.121	-0.07
0.01500	0.18	10.070	167.3			2.71	10.930	636.3	6.94	0.04	0.00	0.10	0.170	0.848	0.00	0.170	-0.05
0.01791	0.21	10.683	182.7			3.13	11.112	683.2	7.51	0.08	0.01	0.08	0.232	0.858	0.00	0.232	-0.06
0.02074	0.24	11.482	196.9			3.85	11.406	758.6	8.34	0.16	0.01	0.16	0.246	0.854	0.00	0.246	0.04
0.02295	0.29	11.626	215.1			4.63	11.561	831.5	9.14	0.11	0.01	0.11	0.401	0.877	0.00	0.401	0.12
0.02783	0.61	9.748	311.9			5.79	11.915	931.9	10.24	0.17	0.01	0.17	0.415	0.878	0.00	0.415	0.02
0.03227	0.78	9.952	355.0		0.15	8.22	11.377	1118.3	12.29	0.09	0.04	0.12	0.472	0.948	0.00	0.472	0.47
0.04040	1.18	10.130	436.7		0.03	11.70	14.302	1337.0	14.70	0.13	0.04	0.13	1.472	0.985	0.00	1.472	0.73
0.05237	1.85	10.489	548.0		-0.07	18.06	15.429	1661.0	18.26	0.20	0.20	0.20	1.629	0.980	0.00	1.629	1.32
0.06086	2.39	10.725	622.7		0.00	25.60	16.651	1916.4	21.06	0.38	0.38	0.38	1.911	0.968	0.00	1.911	1.91
0.06643	2.78	10.838	672.6		-0.05	33.63	17.523	2162.8	23.77	4.82	4.82	4.82	2.69	0.910	0.00	2.69	1.893
0.07370	3.43	11.149	745.1		-0.07	43.40	18.286	2574.7	28.30	5.64	5.64	5.64	4.05	0.902	0.00	4.05	0.996
0.08411	4.23	11.156	827.4		0.06	61.68	19.162	3089.6	33.74	6.52	6.52	6.52	5.41	0.850	0.00	5.41	0.202
0.08694	5.30	11.485	928.3		-0.11	94.81	20.912	3805.6	41.83	8.24	8.24	8.24	7.02	0.835	0.00	7.02	-0.028
0.12973	8.12	12.410	1197.5		0.00	139.35	22.249	4613.6	50.71	9.54	9.54	9.54	8.44	0.812	0.00	8.44	8.44
0.16545	12.01	13.217	1410.6		0.05	179.30	23.140	5233.4	57.52	10.37	10.37	10.37	9.45	0.798	0.00	9.45	-0.790
0.22173	18.43	14.081	1747.5		0.82												
0.28939	26.63	15.290	2100.4		0.19												
0.34927	32.94	16.592	2330.9		0.27												
0.40914	41.10	17.399	2609.6		0.31												
0.50893	54.62	18.774	3008.3		0.39												
0.68955	82.43	20.677	3695.5		0.81												
0.88813	117.88	22.302	4419.4		0.57												
1.04780	148.97	23.406	4968.0		0.63												

0.006" Fiberglass 402" Pipe
 Rndscr = 350

PIPE
 SZ: d = 0.402
 h = w/scrh
 RZR: M-750
 d = 0.386
 h = 0.006
 R/h 32.2

Series
 M-750
 NUM 97
 DATE 8/22/82
 POLY M-750
 C temp 2072.7
 W 1.894

Q (L/s)	Tref(SZ)	Vref(SZ)	Reof(SZ)	Sf(SZ)	Sf(SZ)	Tref(SZ)	Vref(SZ)	Reof(SZ)	h	Sf(RZR)	Sf(RZR)	Vref(SZR)	Sf(SZR)	R	W	P	Δ/hrs	connected R	connected S
0.00374	0.06	4.101	65.2			0.16	6.278	102.5	1.13			6.23				0.858			
0.00417	0.07	4.315	69.2			0.20	6.939	112.6	1.24			6.96				0.847			
0.00489	0.08	4.670	74.8			0.27	8.165	131.4	1.44			7.99				0.868			
0.00626	0.10	5.297	84.8			0.37	9.413	156.4	1.72			9.42				0.847			
0.00695	0.12	5.568	89.8			0.46	10.138	173.8	1.91			10.3				0.834			
0.00790	0.13	5.974	95.0			0.63	11.332	202.8	2.23			11.39				0.811			
0.00856	0.15	6.123	101.0			1.32	9.638	294.3	3.23			10.13				0.747			
0.01037	0.17	6.813	110.2			2.11	10.083	372.9	4.10	0.19	0.02	10.04	0.15	0.043	0.004	0.826	0.00	0.043	0.15
0.01949	0.33	9.243	153.0			2.73	10.255	424.1	4.66	0.12	0.01	10.17	0.06	0.065	0.008	0.835	0.00	0.065	0.06
0.02331	0.40	10.032	168.6			3.20	10.406	458.8	5.04	0.13	0.01	10.3	0.05	0.106	0.010	0.841	0.00	0.106	0.05
0.03034	0.53	11.369	194.1			3.91	10.662	508.2	5.59	0.19	0.02	10.46	0.04	0.202	0.019	0.849	0.00	0.202	0.04
0.03823	1.03	10.285	270.3			4.61	10.739	551.3	6.06	0.12	0.01	10.5	-0.07	0.239	0.023	0.861	0.00	0.239	-0.07
0.04953	1.82	10.022	360.2			5.12	11.304	613.8	6.75	0.48	0.04	11	0.25	0.304	0.028	0.869	0.00	0.304	0.25
0.05278	2.38	10.137	411.9			9.33	12.598	789.5	8.68	1.21	0.11	12.15	0.96	0.389	0.032	0.875	0.00	0.389	0.96
0.06290	2.80	10.254	447.1			11.87	13.704	890.4	9.76	2.08	0.18	12.82	1.42	0.484	0.029	0.875	0.00	0.484	1.42
0.07190	3.46	10.453	497.7			14.74	15.372	992.3	10.91	3.46	0.29	13.66	2.07	0.712	0.122	0.918	0.00	0.712	1.42
0.09141	5.17	10.998	608.0			20.43	16.976	1168.1	12.84	4.61	0.37	15.13	3.26	1.046	0.122	0.968	0.00	1.046	3.26
0.12953	8.50	12.114	784.7			26.25	17.767	1373.6	15.10	5.07	0.40	17.53	5.38	1.523	0.062	0.918	0.00	1.523	5.38
0.19958	11.35	12.925	906.5			31.28	20.053	1445.2	15.88	7.29	0.57	18.53	6.29	1.523	0.062	0.918	0.00	1.523	6.29
0.25945	20.60	15.587	1221.6			41.70	21.936	1668.8	18.34	9.12	0.71	20.73	8.24	1.206	0.058	0.902	0.00	1.206	8.24
0.31933	25.38	17.283	1355.9			66.63	24.585	2109.4	23.19	11.87	0.93	24.45	11.55	0.135	0.006	0.847	0.00	0.135	11.55
0.37920	29.91	18.905	1472.0			100.81	26.454	2584.6	26.52	13.81	1.09	26.98	13.72	-0.526	-0.019	0.814	0.00	-0.526	13.72
0.47899	39.18	20.867	1684.5																
0.67857	58.77	24.135	2063.2																
0.89811	85.44	26.494	2487.6																

0.008" Ribbed 0.402" Pipe
Residual = 350

PIPE	Q (L/A)	Tm(S2)	1/Amp(S2)	Resid(S2)	S (S2)	SF (S2)	Tm(R2B)	1/Amp(R2B)	Resid(R2B)	Ns	S (R2B)	SF (R2B)	1/Amp(S2)M	S1 (S2)	R	RF	P	Δ/Inch	connected R	connected S
M-60K 74 7/2/92 DATE POLY c temp Rn 32.2	0.00165	0.02	3.581	57.3	0.11	0.01	0.08	7.202	126.9	1.39	0.23	0.02	7.77	0.10	0.138	0.014	0.761	0.00	0.138	0.10
	0.00211	0.02	4.054	64.8	0.12	0.02	0.10	8.242	137.5	1.51	0.12	0.01	8.2%	0.08	0.068	0.007	0.855	0.00	0.068	0.08
	0.00269	0.03	4.599	73.3	0.14	0.03	0.11	8.818	148.0	1.64	0.12	0.01	9.05	0.08	0.182	0.017	0.822	0.00	0.182	0.08
	0.00398	0.04	5.570	89.4	0.19	0.05	0.14	10.338	167.0	1.84	0.14	0.02	9.45	0.06	0.356	0.031	0.834	0.00	0.356	0.06
	0.00524	0.05	6.402	102.6	0.22	0.06	0.19	11.243	193.4	2.13	0.15	0.03	10.17	0.06	0.69	0.031	0.846	0.00	0.69	0.06
	0.00656	0.06	7.459	117.6	0.26	0.08	0.22	11.492	211.9	2.33	0.15	0.03	11.65	0.06	1.14	0.031	0.785	0.00	1.14	0.06
	0.00864	0.09	8.055	135.1	0.31	0.11	0.28	12.932	293.0	3.22	0.18	0.05	10.05	0.06	2.21	0.038	0.597	0.00	2.21	0.06
	0.00999	0.10	8.785	143.6	0.33	0.12	0.28	13.118	315.3	3.47	0.18	0.05	9.88	0.06	3.45	0.038	0.623	0.00	3.45	0.06
	0.01089	0.11	9.144	150.7	0.33	0.12	0.28	13.118	315.3	3.47	0.18	0.05	9.88	0.06	3.45	0.038	0.623	0.00	3.45	0.06
	0.01307	0.13	10.074	164.3	0.36	0.14	0.31	13.922	427.4	4.70	0.20	0.12	10.27	0.08	4.02	0.040	0.643	0.00	4.02	0.08
	0.01642	0.16	11.045	188.0	0.41	0.19	0.41	14.820	498.9	5.48	0.25	0.16	10.75	0.09	5.27	0.040	0.669	0.00	5.27	0.09
	0.01839	0.19	11.846	200.5	0.44	0.22	0.44	15.800	548.8	6.28	0.28	0.19	11.45	0.11	6.96	0.040	0.693	0.00	6.96	0.11
	0.02127	0.26	11.265	240.5	0.52	0.28	0.52	16.800	666.9	7.55	0.32	0.22	12.09	0.12	8.75	0.040	0.726	0.00	8.75	0.12
	0.02355	0.33	8.850	304.6	0.60	0.35	0.60	17.800	753.2	8.96	0.37	0.25	13.46	0.13	10.52	0.040	0.759	0.00	10.52	0.13
	0.02498	0.39	10.125	341.2	0.66	0.41	0.66	18.800	848.1	9.37	0.40	0.27	14.05	0.14	12.21	0.040	0.785	0.00	12.21	0.14
	0.02628	0.43	11.411	416.2	0.72	0.46	0.72	19.800	946.2	10.42	0.44	0.29	14.97	0.14	14.05	0.040	0.811	0.00	14.05	0.14
	0.02805	0.51	12.861	558.6	0.84	0.56	0.84	20.800	1042.4	11.70	0.47	0.31	15.80	0.15	15.80	0.040	0.839	0.00	15.80	0.15
	0.03138	0.60	13.784	814.9	1.00	0.67	1.00	21.800	1170.0	13.62	0.50	0.34	16.98	0.16	16.98	0.040	0.866	0.00	16.98	0.16
	0.03541	0.70	14.820	867.6	1.12	0.77	1.12	22.800	1289.4	15.43	0.53	0.37	18.13	0.16	18.13	0.040	0.891	0.00	18.13	0.16
	0.03913	0.82	14.994	956.3	1.27	0.87	1.27	23.800	1403.4	16.99	0.56	0.39	19.13	0.17	19.13	0.040	0.916	0.00	19.13	0.17
	0.04352	0.96	16.576	1040.2	1.44	0.97	1.44	24.800	1529.4	18.62	0.59	0.42	20.33	0.17	20.33	0.040	0.941	0.00	20.33	0.17
	0.04724	1.06	18.733	1187.4	1.62	1.06	1.62	25.800	1653.4	20.81	0.62	0.44	21.52	0.18	21.52	0.040	0.966	0.00	21.52	0.18
	0.05123	1.20	20.085	1366.8	1.82	1.14	1.82	26.800	1777.4	23.09	0.65	0.46	22.72	0.18	22.72	0.040	0.991	0.00	22.72	0.18
	0.05528	1.36	22.348	1689.6	2.04	1.24	2.04	27.800	1901.4	25.43	0.68	0.48	23.92	0.19	23.92	0.040	1.016	0.00	23.92	0.19
	0.06010	1.46	23.865	1795.0	2.26	1.29	2.26	28.800	2025.4	27.53	0.71	0.50	25.12	0.19	25.12	0.040	1.041	0.00	25.12	0.19
	0.06502	1.56	25.165	2145.4	2.50	1.33	2.50	29.800	2149.4	29.81	0.74	0.52	26.32	0.20	26.32	0.040	1.066	0.00	26.32	0.20
	0.07000	1.66	27.411	2629.0	2.74	1.36	2.74	30.800	2273.4	31.32	0.77	0.54	27.52	0.20	27.52	0.040	1.091	0.00	27.52	0.20
	0.07500	1.76	30.547	3055.0	3.00	1.41	3.00	31.800	2397.4	33.67	0.79	0.56	28.72	0.20	28.72	0.040	1.116	0.00	28.72	0.20
	0.08000	1.86	32.084	3780.8	3.26	1.44	3.26	32.800	2521.4	35.96	0.81	0.58	29.92	0.21	29.92	0.040	1.141	0.00	29.92	0.21
	1.09769	-83.10	32.891	4317.8	3.50	1.47	1.28	28.800	5149.7	56.60	1.32	1.25	33.08	0.21	33.08	0.040	1.166	0.00	33.08	0.21
	0.00175	0.02	3.740	59.9	0.02	0.01	0.09	8.032	137.3	1.51	0.09	0.01	10.057	0.14	-0.044	-0.004	0.815	0.00	-0.044	0.14
	0.00252	0.03	4.447	71.1	0.04	0.00	0.11	9.176	154.2	1.69	0.13	0.01	10.166	0.03	0.120	0.012	0.842	0.00	0.120	0.03
	0.00302	0.04	4.785	74.8	0.04	0.00	0.14	9.867	167.0	1.84	0.13	0.01	10.503	0.06	0.151	0.014	0.847	0.00	0.151	0.06
	0.00416	0.04	5.746	91.8	0.04	0.00	0.20	10.533	202.8	2.23	0.16	0.02	11.635	0.03	0.406	0.037	0.881	0.00	0.406	0.03
	0.00578	0.05	6.761	107.9	0.05	0.02	0.32	9.909	254.3	2.80	0.16	0.05	11.049	0.24	0.406	0.037	0.881	0.00	0.406	0.24
	0.00700	0.07	7.435	119.0	0.07	0.02	0.41	10.085	287.9	3.16	0.18	0.09	10.098	0.62	0.438	0.038	0.881	0.00	0.438	0.62
	0.00835	0.08	8.050	131.5	0.08	0.02	0.50	9.871	318.2	3.50	0.18	0.09	9.7953	1.07	0.540	0.044	0.889	0.00	0.540	1.07
	0.01048	0.10	9.058	150.0	0.10	0.00	0.70	10.013	378.6	4.16	0.18	0.16	10.057	1.46	0.563	0.044	0.889	0.00	0.563	1.46
	0.01242	0.12	9.789	161.6	0.12	0.00	0.90	10.286	429.4	4.72	0.18	0.16	10.166	1.84	0.626	0.046	0.893	0.00	0.626	1.84
	0.01607	0.16	10.963	187.0	0.16	0.00	1.29	10.654	514.8	5.66	0.16	0.16	10.503	2.62	0.762	0.057	0.901	0.00	0.762	2.62
	0.01892	0.19	11.769	205.6	0.22	0.02	1.96	11.455	635.3	6.98	0.16	0.16	11.049	3.26	0.826	0.054	0.895	0.00	0.826	3.26
	0.02176	0.22	12.952	263.8	0.26	0.06	2.44	12.042	709.7	7.80	0.16	0.16	11.624	4.54	0.926	0.059	0.897	0.00	0.926	4.54
	0.02359	0.24	13.770	308.7	0.31	0.10	3.01	12.990	846.0	8.66	0.16	0.16	12.255	5.19	0.926	0.059	0.897	0.00	0.926	5.19
	0.02833	0.33	15.323	363.1	0.36	0.15	3.47	13.930	986.0	9.30	0.16	0.16	12.767	6.88	0.985	0.045	0.889	0.00	0.985	6.88
	0.03301	0.39	16.130	418.7	0.41	0.18	3.73	14.832	1160.0	10.07	0.18	0.18	13.007	8.68	1.045	0.045	0.889	0.00	1.045	8.68
	0.04090	0.46	17.457	503.6	0.46	0.20	4.69	15.783	1395.1	10.94	0.18	0.18	13.339	10.57	1.099	0.045	0.889	0.00	1.099	10.57
	0.05426	0.54	19.027	633.7	0.54	0.22	5.38	16.800	1629.5	11.76	0.18	0.18	13.671	12.52	1.166	0.045	0.889	0.00	1.166	12.52
	0.06370	0.60	21.161	708.0	0.60	0.26	6.16	17.800	1888.5	12.71	0.18	0.18	14.003	14.47	1.236	0.045	0.889	0.00	1.236	14.47
	0.07502	0.72	22.963	789.5	0.72	0.28	7.04	18.800	2147.6	13.66	0.18	0.18	14.335	16.42	1.306	0.045	0.889	0.00	1.306	16.42
	0.08991	0.84	24.779	847.4	0.84	0.31	8.01	19.800	2406.7	14.61	0.18	0.18	14.667	18.37	1.376	0.045	0.889	0.00	1.376	18.37
	0.08890	0.84	25.033	879.5	0.84	0.31	8.01	19.800	2406.7	14.61	0.18	0.18	14.667	18.37	1.376	0.045	0.889	0.00	1.376	18.37
	0.08689	0.85	25.287	924.1	0.85	0.31	8.01	19.800	2406.7	14.61	0.18	0.18	14.667	18.37	1.376	0.045	0.889	0.00	1.376	18.37
	0.10969	0.98	28.850	1002.1	0.98	0.33	9.01	20.800	2666.7	15.56	0.18	0.18	14.999	20.32	1.446	0.045	0.889	0.00	1	

0.006" Ribbed 0.402" Pipe
 Resilient = 350

PIPE S2: d = 0.402 h = smooth R2B: d = 0.386 h = 0.006 R/h 3.22
 Series WSR-301
 RUN 102 DATE 9/21/92 POLY 301 c wppm 3 nr 1

Q (L/A)	Tw(S2)	1/Aq(S2)	Resf(S2)	S (S2)	Sf (S2)	Tw(R2B)	1/Aq(R2B)	Resf(R2B)	h _s	S (R2B)	Sf (R2B)	1/Aq(S2N)	S% (S2)	R	RF	P	Δ/ires	connected R	corrected S
0.00306	0.03	5.145	R21			0.10	9.484	156.7	1.72	0.25	0.03	9.92	0.12	0.118	0.012	0.858	0.00	0.118	0.12
0.00455	0.04	6.268	1003			0.12	10.136	168.4	1.85	0.19	0.02	10.03	-0.05	0.267	0.027	0.866	0.00	0.267	-0.05
0.00606	0.05	7.238	116.0			0.15	10.988	188.5	2.07	0.22	0.02	10.37	0.07	0.195	0.019	0.855	0.00	0.195	0.07
0.00762	0.07	8.105	130.4			0.17	11.473	202.5	2.23	0.22	0.04	10.8	0.19	0.266	0.025	0.865	0.00	0.266	0.19
0.00908	0.08	8.849	142.5			0.33	9.806	283.0	3.11	0.94	0.09	11.57	0.63	0.406	0.035	0.878	0.00	0.406	0.63
0.01026	0.09	9.392	152.1			0.45	9.888	331.1	3.64	1.55	0.14	12.49	1.25	0.463	0.037	0.880	0.00	0.463	1.25
0.01175	0.10	10.000	163.9			0.51	10.038	353.9	3.89	1.79	0.15	13.15	1.72	0.310	0.024	0.864	0.00	0.310	1.72
0.01424	0.13	10.929	181.9			1.31	11.066	565.0	6.21	6.40	0.04	11.57	0.63	0.406	0.035	0.878	0.00	0.406	0.63
0.01596	0.14	11.445	194.9			2.69	12.953	813.9	8.95	1.55	0.14	12.49	1.25	0.463	0.037	0.880	0.00	0.463	1.25
0.01904	0.24	10.552	252.5			3.35	13.460	907.9	9.98	1.79	0.15	13.15	1.72	0.310	0.024	0.864	0.00	0.310	1.72
0.02245	0.39	9.860	318.8			4.95	14.969	1098.0	12.07	2.77	0.23	14.39	2.63	0.579	0.040	0.884	0.00	0.579	2.63
0.02434	0.45	9.906	344.3			6.90	16.806	1311.7	14.42	4.18	0.33	16.07	4.00	0.736	0.046	0.890	0.00	0.736	4.00
0.02942	0.64	9.995	412.8	-0.07		9.67	18.415	1553.3	17.07	5.60	0.44	16.91	4.55	1.505	0.089	0.947	0.00	1.505	4.55
0.03426	0.82	10.325	465.5	0.05		17.85	20.534	2114.2	23.24	7.82	0.62	18.9	6.00	1.634	0.086	0.938	-1.16	1.837	5.80
0.04275	1.17	10.739	586.0	0.17		24.17	21.007	2445.9	26.88	8.35	0.66	20.42	7.27	0.587	0.029	0.863	-2.78	0.998	6.86
0.05590	1.74	11.347	681.5	0.06		35.38	20.838	2977.5	32.73	8.19	0.65	20.94	7.44	-0.102	-0.005	0.817	-5.18	0.536	6.81
0.07186	2.47	12.475	811.5	0.11		63.56	20.727	3992.1	43.88	8.05	0.64	21.72	7.72	-0.983	-0.046	0.748	-8.85	-0.176	6.90
0.08333	3.01	13.086	896.7	0.15		113.84	19.913	5343.8	58.74	7.13	0.56	21.69	7.18	-1.777	-0.082	0.685	-12.50	-0.880	6.28
0.11262	4.56	14.381	1097.3	0.22		193.10	19.112	6959.7	76.50	6.08	0.47	21.33	6.38	-2.218	-0.104	0.639	-15.89	-1.305	5.45
0.14929	6.39	16.096	1315.1	0.38		313.66	18.328	8954.2	97.32	4.88	0.36	20.71	5.32	-2.382	-0.115	0.609	-19.12	-1.669	4.61
0.19339	9.52	17.093	1606.8	0.67															
0.29338	17.44	19.156	2176.0	6.21															
0.34927	21.73	20.430	2414.9	7.30															
0.41912	30.11	20.826	2860.7	7.40															
0.55982	48.52	21.652	3669.5	7.79															
0.71849	81.21	21.737	4700.4	7.45															
0.89811	128.60	21.592	5915.0	6.90															
1.09169	199.10	21.210	7346.6	6.15															

0.006" Riblets/0.402" Pipe
 Series WSR301
 Res=350

PFE
 SZ: d = 0.402
 h = smooth
 RZB: POLY 301
 d = 0.386
 h = 0.006
 R/h 32.2

Q (L/A)	T _{in} (SZ)	1/ρ _{in} (SZ)	ρ _{in} (SZ)	S (SZ)	S' (SZ)	T _{out} (RZR)	1/ρ _{out} (RZR)	ρ _{out} (RZR)	h _o	S (RZR)	S' (RZR)	1/ρ _{out} (SZ)	S _{in} (SZ)	R	R'	P	ΔT/ires	connected P	corrected S
0.0166	0.01	3.738	59.6	0.01	0.02	0.10	9.172	148.5	1.63	0.31	0.03	0.03	0.21	0.118	0.012	0.844	0.00	0.118	0.21
0.0314	0.03	5.133	81.9	0.03	0.03	0.08	10.118	365.8	4.35	0.61	0.06	0.06	0.35	0.295	0.028	0.869	0.00	0.295	0.35
0.0628	0.06	6.608	105.1	0.06	0.08	0.15	11.667	515.2	5.66	1.17	0.11	0.11	0.88	0.337	0.030	0.873	0.00	0.337	0.88
0.0942	0.09	8.002	145.3	0.09	0.15	0.24	12.911	614.0	6.75	2.09	0.19	0.19	1.25	0.391	0.031	0.875	0.00	0.391	1.25
0.1256	0.12	9.536	156.0	0.12	0.25	0.26	14.338	718.2	7.89	3.21	0.29	0.29	1.37	0.548	0.040	0.883	0.00	0.548	2.76
0.1570	0.15	10.146	166.0	0.15	0.30	0.29	15.034	787.4	8.65	3.71	0.33	0.33	1.46	0.623	0.040	0.883	0.00	0.623	3.42
0.1884	0.18	10.822	178.3	0.18	0.34	0.31	15.888	845.8	9.30	4.39	0.38	0.38	1.50	0.808	0.054	0.899	0.00	0.808	3.77
0.2198	0.21	11.381	193.9	0.21	0.42	0.41	17.073	967.6	10.63	5.23	0.44	0.44	1.65	0.823	0.038	0.882	0.00	0.823	4.91
0.2512	0.25	10.832	239.4	0.25	0.47	0.41	17.901	1016.3	11.17	5.92	0.49	0.49	1.69	0.911	0.054	0.898	0.00	0.911	5.36
0.2826	0.28	9.836	305.7	0.28	0.67	0.60	20.680	1243.8	13.67	8.16	0.65	0.65	20.11	0.570	0.028	0.872	0.00	0.570	8.13
0.3140	0.31	10.149	386.4	0.31	0.85	0.85	22.065	1602.8	17.62	9.24	0.72	0.72	23.12	-1.055	-0.065	0.770	0.00	-1.055	10.70
0.3454	0.34	11.284	436.4	0.34	0.85	1.15	14.60	23.174	18.907	10.39	0.81	0.81	24.79	-1.616	-0.065	0.787	0.00	-1.616	12.12
0.3768	0.37	12.474	610.3	0.37	1.04	1.15	24.117	2071.0	22.76	11.39	0.90	0.90	25.55	-1.433	-0.065	0.743	0.00	-1.433	12.69
0.4082	0.40	13.784	717.4	0.40	1.28	1.34	24.328	2462.7	27.15	11.67	0.92	0.92	26.49	-2.162	-0.062	0.726	-3.60	-2.162	12.97
0.4396	0.43	14.561	786.6	0.43	1.49	1.49	24.646	3135.1	34.46	12.00	0.95	0.95	27.69	-3.044	-0.110	0.668	-3.75	-3.044	13.44
0.4710	0.47	15.338	852.4	0.47	1.73	1.73	25.440	4161.0	45.73	12.75	1.01	1.01	27.74	-3.666	-0.083	0.681	-16.42	-3.666	12.75
0.5024	0.50	16.426	965.6	0.50	1.80	1.80	25.071	5250.8	57.71	12.30	0.96	0.96	27.32	-2.249	-0.062	0.674	-22.38	-2.249	11.84

0.006" Ribbed 0.402" Pipe
Resistor = 350

Series

WSP-301

PIPE
SZ: d = 0.402
h = smooth
RZR: DATE 9/15/92
POLY 301
h = 0.006
c vppm 30
R/h 32.2
w

Q (L/h)	Tef(SZ)	1/wf(SZ)	Reof(SZ)	Sf(SZ)	Sf(SZ)	1/wf(R2B)	Reof(R2B)	h	Sf(R2B)	Sf(R2B)	1/wf(S2B)	Sf(S2)	R	Rf	P	Δ/Pves	connected R	connected S
0.00259	0.02	4.581	72.0			0.11	9.441	150.6	1.65		9.39	1.07	0.509	0.047	0.891	0.00	0.509	1.07
0.00313	0.03	5.023	79.0			0.14	10.076	167.1	1.84		10.37	1.66	0.289	0.025	0.869	0.00	0.289	1.66
0.00380	0.05	5.551	87.0			0.16	10.844	183.0	2.01		11.14	2.72	0.221	0.017	0.862	0.00	0.221	2.72
0.00600	0.05	7.002	109.7			0.28	9.741	241.5	2.65		10.9	4.05	0.470	0.032	0.877	0.00	0.470	4.05
0.00780	0.07	7.976	125.5			0.36	9.362	271.6	2.99		10.36	6.68	-0.305	-0.017	0.826	0.00	-0.305	6.68
0.00931	0.09	8.704	137.4			0.44	10.159	301.9	3.32		10.03	7.36	-0.091	-0.004	0.837	0.00	-0.091	7.36
0.01060	0.10	9.232	147.8			0.50	10.513	322.3	3.54		10.29	8.44	0.010	0.001	0.844	0.00	0.010	8.44
0.01254	0.12	10.035	161.1			0.61	11.399	358.5	3.94	1.58	10.89	11.64	0.509	0.047	0.891	0.00	0.509	11.64
0.01476	0.14	10.827	176.0			0.74	11.929	392.8	4.32	1.94	11.64	14.52	0.289	0.025	0.869	0.00	0.289	14.52
0.01748	0.17	11.579	195.1			0.96	13.151	448.6	4.93	2.91	12.93	17.6	0.221	0.017	0.862	0.00	0.221	17.6
0.02007	0.25	10.980	236.6			1.30	14.990	522.3	5.74	4.47	14.52	22.78	0.470	0.032	0.877	0.00	0.470	22.78
0.02273	0.39	9.956	295.8			1.81	16.560	616.8	6.78	5.73	16.55	27.45	0.010	0.001	0.844	0.00	0.010	27.45
0.02509	0.45	10.228	318.1			2.17	17.295	675.5	7.42	6.29	17.6	34.06	-0.305	-0.017	0.826	0.00	-0.305	34.06
0.03022	0.57	10.913	359.6		1.09	2.50	18.309	723.9	7.96	7.16	18.4	40.82	0.010	0.001	0.844	0.00	0.010	40.82
0.03465	0.67	11.559	389.2		1.60	3.32	19.895	830.4	9.13	8.44	19.97	48.24	-0.091	-0.004	0.837	0.00	-0.091	48.24
0.04363	0.86	12.800	442.6		2.62	3.89	21.237	913.0	10.04	9.55	21.08	55.55	0.157	0.007	0.846	0.00	0.157	55.55
0.05786	1.19	14.464	519.8		4.00	5.65	23.346	1100.1	12.09	10.14	22.78	66.4	-0.075	-0.004	0.811	0.00	-0.075	66.4
0.07538	1.59	16.284	602.3		5.56	10.14	24.099	1475.6	16.22	13.32	25.52	77.0	0.157	0.007	0.846	0.00	0.157	77.0
0.09669	1.86	17.195	652.4		6.34	13.03	24.529	1670.4	18.36	11.71	27.45	86.4	-0.434	-0.019	0.811	0.00	-0.434	86.4
0.12260	2.17	18.089	703.5		7.10	17.71	25.245	1939.3	21.32	12.49	29.09	98.6	-0.075	-0.004	0.837	0.00	-0.075	98.6
0.14170	3.43	20.857	892.6		8.41	23.77	25.420	2261.1	24.85	12.74	31.46	106	0.157	0.007	0.846	0.00	0.157	106
0.17962	4.77	22.417	1053.0		9.92	33.32	26.082	2643.6	31.45	13.44	34.06	112	-0.434	-0.019	0.811	0.00	-0.434	112
0.25945	8.13	24.803	1376.6		12.65	43.07	26.889	3167.0	41.40	14.22	36.06	120	0.157	0.007	0.846	0.00	0.157	120
0.29937	9.86	25.859	1521.5		13.53	55.96	26.889	3767.5	50.60	15.22	38.22	126	-0.075	-0.004	0.837	0.00	-0.075	126
0.35924	12.48	27.724	1695.6		15.21	65.96	26.889	4403.2	58.60	16.90	40.71	133	0.157	0.007	0.846	0.00	0.157	133
0.41912	16.66	27.998	1971.2		15.22	98.60	27.937	4603.2	60.25	18.00	42.75	137	-0.434	-0.019	0.811	0.00	-0.434	137
0.57878	27.47	30.110	2531.5		16.90	126.98	28.584	5245.6	57.66	19.55	44.82	143	0.157	0.007	0.846	0.00	0.157	143
0.73845	40.71	31.555	3082.2		18.00	176.98	29.584	5766	57.66	19.55	46.07	148	-0.075	-0.004	0.837	0.00	-0.075	148
0.93864	60.25	32.950	3747.5		19.05	205.84	30.584	6032	60.32	19.05	48.24	150	0.157	0.007	0.846	0.00	0.157	150
1.09769	79.00	33.674	4275.6		19.55	226.98	30.584	6032	60.32	19.55	50.60	151	-0.434	-0.019	0.811	0.00	-0.434	151

0.000" Ribbed 402" Pipe
 Nondrill = 350

Series

PIPE
 SZ: d = 0.402
 h = smooth
 AZR: DATE 9/11/92
 POLY 301
 c-wagon 100
 R 1.219

Q (L/s)	T _{in} (S2)	1/A _{in} (S2)	Re _{in} (S2)	S (S2)	Sf (S2)	T _{in} (R2B)	1/A _{in} (R2B)	Re _{in} (R2B)	h _v	S (R2B)	Sf (R2B)	1/A _{in} (S2)h	St (S2)	Tr	Rf	P	ΔV _{res}	connected R	connected S
0.00217	0.02	3.872	62.2			0.11	8.491	131.4	1.44										
0.00299	0.03	4.552	73.1			0.15	9.719	154.3	1.70			8.23				0.875	0.899		
0.00404	0.04	5.303	84.8			0.19	11.037	175.2	1.93			9.2				0.875	0.899		
0.00501	0.05	5.912	94.6			0.25	11.258	198.1	2.18			10.7				0.875	0.899		
0.00544	0.06	6.167	98.6			0.41	10.392	255.2	2.80			11.31				0.875	0.899		
0.00757	0.08	7.312	115.9			0.44	10.692	265.8	2.92			10.63				0.875	0.899		
0.00955	0.10	8.198	130.7			0.56	11.391	299.2	3.29			10.59				0.875	0.899		
0.01281	0.14	9.262	155.5			0.66	12.366	323.9	3.56			11.07				0.875	0.899		
0.01646	0.18	10.658	174.2			0.83	13.740	363.2	3.99			11.59				0.875	0.899		
0.01896	0.21	11.179	191.6			1.18	15.251	434.7	4.78			12.99				0.875	0.899		
0.02252	0.29	11.456	222.2			1.62	17.110	510.0	5.61			15.64				0.875	0.899		
0.02411	0.39	10.576	258.0			1.91	17.850	553.1	6.08			17.43				0.875	0.899		
0.02888	0.51	11.023	296.9			2.26	18.258	595.7	6.59			18.08				0.875	0.899		
0.03392	0.62	11.709	328.4			3.40	21.459	743.0	7.78			21.09				0.875	0.899		
0.04224	0.77	13.093	366.0	3.24	0.33	3.05	22.194	865.0	8.17			21.88				0.875	0.899		
0.05606	1.02	15.149	420.2	5.06	0.50	5.73	22.935	965.0	10.62			23.32				0.875	0.899		
0.07370	1.37	17.156	488.4	6.80	0.66	8.08	23.151	1049.0	12.60			24.51				0.875	0.899		
0.08347	1.65	17.739	534.4	7.23	0.69	10.98	23.151	1049.0	14.71			25.59				0.875	0.899		
0.09324	1.90	18.442	573.2	7.81	0.73	14.66	24.065	1674.5	18.41			27.54				0.875	0.899		
0.11677	2.68	19.442	680.0	8.51	0.78	17.39	24.190	1971.9	21.67			28.94				0.875	0.899		
0.13372	2.89	21.437	714.1	10.42	0.95	23.33	25.118	2469.2	27.14			30.86				0.875	0.899		
0.17962	4.68	22.651	908.9	11.22	0.98	32.33	25.118	2469.2	36.70			33.15				0.875	0.899		
0.21954	6.13	24.186	1039.2	12.52	1.07	48.74	25.722	3339.4	43.56			34.4				0.875	0.899		
0.25945	8.19	24.724	1203.6	12.80	1.07	68.24	25.722	3339.4	43.56			34.4				0.875	0.899		
0.33929	11.83	26.893	1438.8	14.66	1.20	96.19	26.480	3962.4	51.49			35.82				0.875	0.899		
0.39916	15.66	27.503	1665.3	15.02	1.28	136.33	27.804	4684.9	51.49			35.82				0.875	0.899		
0.51891	23.43	29.228	2037.6	16.39	1.28	200.00										0.875	0.899		
0.71849	36.99	31.376	2628.7	18.10	1.36											0.875	0.899		
0.87815	54.00	32.584	3092.4	19.02	1.40											0.875	0.899		
1.09769	78.10	33.870	3692.8	20.00	1.44											0.875	0.899		

0.000" PIPES @ 402" PIPE
Resistor - 350

PIPE
SZ:
d = 0.402
h = smooth
R2R:
d = 0.386
h = 0.006
RA: 32.2

P-309
RUN
DATE
POLY
c
temp
re

62
4/15/92
P-309
50
1.221

Q (L/h)	T _{ref} (SZ)	1/(ref)(SZ)	Sf (SZ)	Sf (SZ)	Resid (SZ)	1/(ref)(SZ)	Resid (SZ)	h	S (R2R)	Sf (R2R)	1/(ref)(SZ)	Sx (SZ)	Rf	P	Δ/ires	connected R	connected S
0.00088	0.01	2.493	39.9	0.03	4.660	64.3	0.71	0.71	0.39	0.39	3.99	0.335	0.00	0.00	0.335	3.51	
0.00256	0.03	4.2-J	68.0	0.05	5.352	88.8	0.94	0.94	5.35	5.35	5.36	0.085	0.00	0.00	0.085	5.29	
0.00391	0.04	5.284	83.5	0.06	5.448	88.5	0.97	0.97	6.50	6.50	6.24	-0.265	0.00	0.00	-0.265	6.50	
0.0040P	0.04	5.366	86.2	0.06	6.254	100.0	1.10	1.10	6.25	6.25	6.24	0.152	0.00	0.00	0.152	7.06	
0.00530	0.06	6.123	98.1	0.09	7.622	117.7	1.29	1.29	8.17	8.17	8.83	-0.184	0.00	0.00	-0.184	8.20	
0.00758	0.08	7.330	117.5	0.12	8.917	137.8	1.51	1.51	10.786	10.786	10.14	0.025	0.00	0.00	0.025	9.14	
0.01039	0.10	8.749	134.9	0.16	10.252	167.4	1.83	1.83	11.293	11.293	10.9	-0.006	0.00	0.00	-0.006	8.41	
0.01514	0.16	10.252	167.4	0.19	11.919	191.0	2.10	2.10	12.23	12.23	11.23	0.025	0.00	0.00	0.025	9.14	
0.01669	0.17	10.950	173.6	0.23	11.919	191.0	2.10	2.10	10.684	10.684	10.86	-0.006	0.00	0.00	-0.006	8.41	
0.01916	0.21	11.279	193.9	0.26	11.772	214.9	2.42	2.42	11.452	11.452	11.09	0.025	0.00	0.00	0.025	9.14	
0.02218	0.26	11.772	214.9	0.39	10.544	262.2	3.00	3.00	12.217	12.217	11.89	0.025	0.00	0.00	0.025	9.14	
0.02864	0.50	11.053	296.2	0.65	12.217	324.4	3.57	3.57	3.85	3.85	3.85	0.025	0.00	0.00	0.025	9.14	
0.03336	0.50	11.810	322.2	0.81	13.695	364.2	4.00	4.00	5.35	5.35	5.36	0.085	0.00	0.00	0.085	5.29	
0.04179	0.74	13.259	361.3	1.10	15.485	423.8	4.66	4.66	6.50	6.50	6.24	-0.265	0.00	0.00	-0.265	6.50	
0.05498	0.98	15.120	416.7	1.33	16.505	464.6	5.11	5.11	6.20	6.20	6.24	0.152	0.00	0.00	0.152	7.06	
0.06424	1.14	16.380	449.5	1.50	17.582	493.6	5.43	5.43	7.17	7.17	7.17	0.009	0.00	0.00	0.009	8.29	
0.07271	1.32	17.224	483.8	1.69	18.196	539.9	5.93	5.93	7.61	7.61	7.85	-0.110	0.00	0.00	-0.110	8.20	
0.08251	1.55	18.026	523.3	1.79	18.730	574.4	6.31	6.31	8.03	8.03	8.41	0.025	0.00	0.00	0.025	9.14	
0.09013	1.73	18.666	553.3	2.03	19.152	612.9	6.74	6.74	8.33	8.33	8.41	-0.006	0.00	0.00	-0.006	8.41	
0.09656	2.00	19.991	593.5	2.32	20.115	668.0	7.54	7.54	9.07	9.07	9.29	0.025	0.00	0.00	0.025	9.14	
0.11613	2.57	19.747	671.0	2.82	22.112	793.7	8.61	8.61	9.79	9.79	9.2	0.088	0.00	0.00	0.088	10.82	
0.13831	3.10	21.427	741.4	3.75	22.818	834.0	9.14	9.14	10.82	10.82	10.11	-0.006	0.00	0.00	-0.006	8.41	
0.25826	7.85	25.139	1180.0	10.35	28.112	1354.0	14.88	14.88	14.88	14.88	14.88	0.025	0.00	0.00	0.025	9.14	
0.33809	11.70	26.954	1437.5	14.72	24.147	1671.1	18.37	18.37	11.33	11.33	11.33	-0.136	0.00	0.00	-0.136	15.60	
0.41513	16.34	28.004	1698.9	15.48	25.264	1961.2	21.56	21.56	12.51	12.51	12.51	0.068	0.00	0.00	0.068	16.38	
0.59794	28.74	30.412	2248.2	17.40	23.61	25.264	26.681	26.681	29.33	29.33	32.07	-0.389	0.00	0.00	-0.389	18.76	
0.75780	41.29	32.158	2694.6	18.84	64.68	27.867	3238.4	35.59	35.59	35.59	34.41	0.165	0.00	0.00	0.165	19.79	
0.93603	58.52	33.362	3201.0	19.74	92.90	28.724	42.56	42.56	16.05	16.05	20.46	-0.589	0.00	0.00	-0.589	20.46	
1.09769	76.94	34.123	3670.1	20.26	122.00	29.392	44.37.6	48.77	16.69	16.69	35.21	-0.618	0.00	0.00	-0.618	21.02	

66
5/7/92
P-309
50
1.139

P-309
RUN
DATE
POLY
c
temp
re

0.00198	0.02	3.888	62.4	0.05	5.867	101.2	1.11	1.11	6.25	6.25	6.25	0.213	0.00	0.00	0.213	0.10	
0.00284	0.03	4.665	74.7	0.07	6.463	115.1	1.27	1.27	7.35	7.35	7.35	0.213	0.00	0.00	0.213	0.10	
0.00358	0.04	5.268	84.0	0.08	6.932	124.1	1.36	1.36	8.16	8.16	8.16	0.213	0.00	0.00	0.213	0.10	
0.00462	0.06	6.564	106.9	0.10	7.071	135.6	1.49	1.49	8.49	8.49	8.49	0.213	0.00	0.00	0.213	0.10	
0.00668	0.06	7.332	112.7	0.11	7.851	147.4	1.62	1.62	8.85	8.85	8.85	0.213	0.00	0.00	0.213	0.10	
0.00743	0.07	7.555	121.9	0.13	9.021	159.2	1.75	1.75	9.55	9.55	9.55	0.213	0.00	0.00	0.213	0.10	
0.00896	0.09	8.181	135.8	0.16	11.337	176.0	1.93	1.93	10.11	10.11	10.11	0.213	0.00	0.00	0.213	0.10	
0.01112	0.12	8.765	157.3	0.19	11.730	189.6	2.08	2.08	10.38	10.38	10.38	0.213	0.00	0.00	0.213	0.10	
0.01546	0.20	10.603	201.4	0.20	12.363	196.0	2.15	2.15	9.58	9.58	9.58	0.213	0.00	0.00	0.213	0.10	
0.01881	0.22	10.683	211.9	0.49	9.705	305.8	3.36	3.36	9.59	9.59	9.59	0.213	0.00	0.00	0.213	0.10	
0.02320	0.40	9.643	266.1	0.55	9.700	321.8	3.54	3.54	0.31	0.31	0.31	0.021	0.00	0.00	0.021	0.10	
0.02423	0.48	9.675	313.0	0.73	10.203	373.2	4.10	4.10	0.31	0.31	0.31	0.021	0.00	0.00	0.021	0.10	
0.02590	0.66	9.929	366.3	0.83	10.960	396.7	4.36	4.36	0.95	0.95	0.95	0.021	0.00	0.00	0.021	0.10	
0.03367	0.78	10.380	402.2	1.08	12.028	452.9	4.98	4.98	1.77	1.77	1.77	0.046	0.00	0.00	0.046	0.10	
0.04219	1.00	11.525	453.8	1.30	13.504	534.9	5.89	5.89	2.94	2.94	2.94	0.046	0.00	0.00	0.046	0.10	
0.05589	1.39	12.936	526.1	2.42	15.362	613.7	6.77	6.77	4.52	4.52	4.52	0.060	0.00	0.00	0.060	0.10	
0.07320	1.86	14.629	621.7	3.85	22.1	16.572	649.3	7.14	5.64	5.64	4.59	0.132	0.00	0.00	0.132	4.59	
0.08335	2.09	15.706	657.9	4.83	22.1	16.572	649.3	7.20	6.22	6.22	4.59	0.132	0.00	0.00	0.132	4.59	
0.09369	2.36	16.619	700.4	5.64	22.1	16.572	649.3	7.20	6.22	6.22	4.59	0.132	0.00	0.00	0.132	4.59	
0.11667	2.96	18.421	785.2	7.24	32.6	19.095	788.8	8.67	7.76	7.76	6.85	0.068	0.00	0.00	0.068	6.85	
0.17862	4.63	22.634	982.7	11.06	32.6	19.095	788.8	8.67	7.76	7.76	6.85	0.068	0.00	0.00	0.068	6.85	
0.19100	5.36	22.497	1052.5	10.81	6.02	22.350	1071.2	11.77	10.22	10.22	8.84	0.044	0.00	0.00	0.044	8.84	
0.25866	7.68	25.446	1265.7	13.44	9.73	23.006	1368.0	15.04	11.11	11.11	8.84	-0.364	0.00	0.00	-0.364	14.03	
0.29657	9.50	26.413	1401.3	14.23	13.23	23.568	1587.9	17.45	10.75	10.75	8.84	-0.364	0.00	0.00	-0.364	14.03	
0.318173	10.35	27.012	1469.2	14.74	14.38	24.134	1662.8	18.26	11.31	11.31	8.84	-0.364	0.00	0.00	-0.364	14.03	
0.47859	20.30	28.962	2057.7	16.11	29.02	25.507	2362.4	25.97	12.84	12.84	10.1	-0.403	0.00	0.00	-0.403	16.82	
0.59854	29.15	30.227	2465.6	17.06	44.62	25.727	2929.2	32.20	13.08	13.08	10.1	-0.403	0.00	0.00	-0.403	16.82	
0.79832	46.27	31.999	3092.7	18.44	73.83	26.675	3751.3	41.23	14.01	14.01	11.1	-0.635	0.00	0.00	-0.635	19.14	
0.99790	67.85	33.030	3745.2	19.14	107.46	27.638	4525.7	49.74	14.93	14.93	11.8	-0.632	0.00	0.00	-0.632	19.75	

0.006" Ribbed/A02" Pipe
Resol/ct = 350

PIPE
 EC: 0.402
 d = 0.402
 h = smooth
 RZB:
 d = 0.386
 h = 0.006
 R/h 32.2

M-300LWP
 REM 112
 DATE 10/09/92
 POLY M-300LWP
 c wppm 10
 w 1.008

Q(L/A)	Tef(S2)	1/wd(S2)	Reof(S2)	S'(S2)	Sf(S2)	1/wd(R2B)	Reof(R2B)	h _s	S'(R2B)	Sf(R2B)	1/wd(S2)h	Sf(S2)	h _s	connected R'	connected P'
0.00242	0.02	4.591	72.6			0.09	9.109	150.3	1.65		9.37				
0.00400	0.03	5.929	93.1			0.10	9.649	157.9	1.74		9.78			0.825	0.22
0.00555	0.05	6.964	110.2			0.11	10.028	167.8	1.84		10.3			0.834	0.17
0.00710	0.06	7.889	124.5			0.12	10.431	174.1	1.91		10.63			0.824	0.07
0.00814	0.07	8.437	133.5			0.13	10.840	184.9	2.03		11.17			0.840	0.04
0.00949	0.08	9.059	145.2			0.16	11.517	205.0	2.25		11.51			0.802	0.02
0.01056	0.09	9.548	153.3			0.29	9.755	288.0	3.17		10.13			0.689	0.00
0.01165	0.10	9.900	161.9			0.41	9.806	328.9	3.62		9.91			0.809	0.00
0.01257	0.11	10.244	168.6			0.48	9.746	358.9	3.94	-0.07	10.04			0.784	0.00
0.01386	0.12	10.823	177.8			0.70	10.198	429.0	4.72	0.04	10.3			0.806	0.00
0.01631	0.15	11.620	195.1			0.90	10.386	483.5	5.31	0.01	10.41			0.819	0.00
0.01940	0.25	10.616	254.1			1.28	10.757	576.2	6.33	0.05	10.68			0.835	0.00
0.02228	0.38	9.853	314.3			1.99	11.296	715.8	7.87	0.17	11.14			0.847	0.00
0.02412	0.44	9.545	337.7	0.21	0.02	2.89	11.969	858.3	9.43	0.44	11.69			0.862	0.00
0.03015	0.64	10.262	409.4	0.10	0.01	4.13	12.385	948.1	10.42	0.60	12.04			0.868	0.00
0.03459	0.83	10.366	465.2	0.10	0.01	5.27	12.662	1021.5	11.23	0.67	12.28			0.873	0.00
0.04267	1.20	10.634	559.7	0.04	0.00	7.81	13.314	1145.0	12.56	1.00	12.9			0.874	0.00
0.05265	1.87	11.088	700.2	0.11	0.01	12.39	14.617	1405.2	15.46	1.88	13.96			0.892	0.00
0.07067	2.74	11.647	846.9	0.34	0.03	18.70	15.845	1763.0	19.38	3.04	14.95			0.910	0.00
0.08082	3.37	12.012	938.7	0.52	0.05	24.01	17.031	2483.5	27.30	4.17	15.82			0.917	0.00
0.08916	5.09	12.246	1014.2	0.62	0.05	34.47	17.376	3022.4	33.22	4.73	16.57			0.917	0.00
0.10583	7.53	13.980	1137.6	1.04	0.09	47.86	17.895	3589.9	39.46	5.22	17.61			0.868	0.00
0.14070	12.06	15.009	1787.2	1.78	0.15	73.27	18.192	4492.8	49.38	5.49	18.38			0.814	0.00
0.19120	18.28	15.911	2200.4	2.40	0.19	105.69	18.127	5476.0	60.19	5.33	19.62			0.714	0.00
0.24948	22.83	16.514	2459.3	2.94	0.23	174.66	17.937	7164.2	78.74	4.87	19.95			0.667	0.00
0.28939	28.83	17.399	2898.2	3.35	0.25	276.74	17.575	9134.1	100.40	4.06	20.03			0.632	0.00
0.35924	31.69	17.399	3395.1	3.95	0.29										
0.47908	43.46	18.156	3995.1	4.43	0.32										
0.55982	65.05	18.890	4154.5	4.82	0.34										
0.67857	91.16	19.378	4918.8	5.01	0.35										
0.87815	145.55	19.845	6217.6	5.07	0.34										
1.09769	224.50	19.974	7717.2	4.82	0.32										

0.006" Ribbed 402" Pipe
 Receptor = 350

Series

MFE

SC: 0.402
 d: 0.402
 h: wmonth
 RZR: 0.396
 d: 0.396
 h: 0.006
 R/h: 32.2

M-3000.MW

111
 10/7/92
 POLY M-3000.MW
 c. wspan 30
 m 1.025

Q (1/A)	Tet(S2)	1/Aop(S2)	Resid(S2)	S'(S2)	Sf(S2)	Tet(R2R)	1/Aop(R2R)	Resid(R2R)	h _o	S'(R2R)	Sf(R2R)	1/Aop(S2)h	S'(S2)	R'	RF	P	Δ/Tres	connected R'	corrected S
0.00471	0.04	6.373	100.2	0.11	0.01	0.11	9.578	157.9	1.74	0.18	0.02	9.84	0.09	0.104	0.010	0.831	0.00	0.104	0.09
0.00605	0.05	7.226	113.6	0.12	0.00	0.72	9.818	167.3	1.84	0.12	0.01	10.26	0.05	0.114	0.011	0.842	0.00	0.114	0.05
0.00772	0.07	8.118	129.2	0.13	0.01	0.94	10.321	172.5	1.90	0.12	0.01	10.33	0.05	0.168	0.016	0.851	0.00	0.168	0.14
0.00883	0.08	8.684	138.3	0.15	0.01	1.35	10.807	184.5	2.01	0.25	0.02	10.73	0.14	0.295	0.026	0.866	0.00	0.295	0.40
0.00979	0.09	9.082	146.6	0.17	0.04	2.02	11.591	200.8	2.21	0.60	0.05	11.35	0.40	0.443	0.037	0.880	0.00	0.443	0.80
0.01067	0.09	9.495	153.0	0.14	0.07	2.83	9.931	281.1	3.09	1.08	0.09	12.04	0.80	0.533	0.042	0.887	0.00	0.533	1.17
0.01158	0.10	9.915	159.1	0.46	0.10	3.42	9.945	327.2	3.60	1.47	0.13	12.57	1.17	0.568	0.044	0.889	0.00	0.568	1.47
0.01253	0.11	10.243	166.3	0.52	0.11	4.00	9.949	348.0	3.82	1.74	0.15	13.01	1.47	0.589	0.043	0.896	0.00	0.589	2.07
0.01426	0.13	10.894	178.6	0.72	0.04	6.06	10.244	409.5	4.50	2.26	0.19	13.8	2.07	0.599	0.043	0.910	0.00	0.599	2.45
0.01637	0.15	11.531	193.8	0.94	0.01	8.88	10.444	468.6	5.15	2.52	0.23	14.36	2.45	1.144	0.073	0.922	0.00	1.144	3.45
0.01982	0.24	10.860	246.8	1.35	0.04	14.57	10.898	560.0	6.15	4.07	0.32	15.69	3.45	1.444	0.073	0.922	0.00	1.444	4.96
0.02263	0.39	9.890	312.7	2.02	0.07	20.39	11.645	686.0	7.54	5.77	0.45	17.63	4.96	1.755	0.053	0.936	0.00	1.755	5.89
0.02431	0.45	9.918	335.2	3.42	0.10	31.42	12.483	812.7	8.93	7.93	0.54	18.85	5.89	1.965	0.047	0.933	0.00	1.965	6.45
0.02943	0.63	10.109	398.5	4.00	0.13	40.00	13.103	893.6	9.82	1.74	0.15	19.65	6.45	2.093	0.031	0.930	0.00	2.093	7.47
0.03431	0.83	10.282	457.1	5.00	0.18	50.2	13.578	1075.8	11.82	2.26	0.19	20.39	7.93	2.152	0.028	0.923	0.00	2.152	8.30
0.04274	1.19	10.676	548.9	6.47	0.21	60.6	14.399	1195.2	13.14	2.52	0.23	21.52	8.43	2.227	-0.005	0.923	-1.88	2.227	8.94
0.05592	1.82	11.308	678.3	8.88	0.29	88.8	15.339	1446.5	15.90	4.07	0.32	22.27	9.04	2.282	-0.028	0.923	-5.98	22.27	8.94
0.07099	2.59	12.024	810.1	11.47	0.36	114.7	16.834	1853.0	20.37	5.77	0.45	23.23	9.42	2.305	-0.054	0.923	-10.32	23.23	8.94
0.08138	3.16	12.572	894.3	14.7	0.49	147.0	18.556	2192.7	24.10	6.91	0.54	24.35	9.42	2.305	-0.054	0.923	-10.32	24.35	8.94
0.09177	3.70	13.013	966.2	19.62	0.58	196.2	20.580	2506.9	27.55	7.93	0.63	25.65	9.42	2.305	-0.054	0.923	-10.32	25.65	8.94
0.10911	4.64	13.818	1076.3	2.09	0.74	251.6	21.572	2924.0	32.14	8.93	0.75	26.65	9.42	2.305	-0.054	0.923	-10.32	26.65	8.94
0.12773	5.90	14.464	1217.0	3.56	0.89	349.3	22.158	3623.9	39.83	9.50	0.78	27.27	9.42	2.305	-0.054	0.923	-10.32	27.27	8.94
0.16864	8.53	15.840	1476.1	5.00	1.18	476.1	22.569	4448.5	48.89	9.87	0.78	28.23	9.42	2.305	-0.054	0.923	-10.32	28.23	8.94
0.23950	13.63	17.688	1866.6	6.47	1.47	647.0	23.174	5561.9	61.13	9.89	0.77	29.42	9.42	2.305	-0.054	0.923	-10.32	29.42	8.94
0.35924	18.76	18.846	2190.2	8.88	1.82	888.0	23.777	7015.6	77.11	9.43	0.72	30.83	9.42	2.305	-0.054	0.923	-10.32	30.83	8.94
0.43638	24.78	19.677	2517.6	11.47	2.09	1147.0	24.109	8931.6	98.2	9.40	0.64	32.14	9.42	2.305	-0.054	0.923	-10.32	32.14	8.94
0.55882	32.89	20.874	2901.4	14.7	2.52	1470.0	24.695	11195.2	118.2	9.43	0.72	33.54	9.42	2.305	-0.054	0.923	-10.32	33.54	8.94
0.69653	47.67	22.067	3493.9	19.62	3.56	1962.0	25.067	14464.5	147.6	9.43	0.72	35.00	9.42	2.305	-0.054	0.923	-10.32	35.00	8.94
0.87815	68.76	22.968	4197.3	25.65	4.96	2565.0	25.650	18530.0	185.3	9.43	0.72	36.45	9.42	2.305	-0.054	0.923	-10.32	36.45	8.94
1.09769	101.40	23.777	5097.7	34.93	6.63	3493.0	26.650	24106.5	241.0	9.43	0.72	38.00	9.42	2.305	-0.054	0.923	-10.32	38.00	8.94
	153.09	24.188	6258.5	46.4	9.40	4640.0	27.473	30815.6	308.1	9.43	0.72	39.42	9.42	2.305	-0.054	0.923	-10.32	39.42	8.94

0.006" Fiberglass 402" Pipe
Receiver = 350

Series M-300LHW

M-300LHW

PIPE
SZ: G = 0.402
h = smooth
RZR: G = 0.386
h = 0.006
RA: 32.2

RUN 110
DATE 10/6/92
POLY M-300LHW
c wppcm 100
nr 1.084

Q (L/s)	Im(SZ)	1/Im(SZ)	Reof(SZ)	S (SZ)	Sf (SZ)	Im(RZR)	1/Im(RZR)	Reof(RZR)	Nz	S (RZR)	Sf (RZR)	1/Im(SZ)	R	RF	P	ΔP/m	corrected P	corrected S
0.00367	0.03	5.414	86.6	0.16	0.02	0.11	9.015	148.0	1.83	0.31	0.03	10.12	0.162	0.016	0.848	0.00	0.152	0.16
0.00468	0.04	6.119	97.9	0.20	0.02	0.12	9.629	155.3	1.71	0.47	0.05	10.37	0.206	0.029	0.867	0.00	0.206	0.20
0.00557	0.05	6.683	106.8	0.45	0.04	0.13	10.090	165.1	1.81	0.81	0.08	10.9	0.408	0.037	0.880	0.00	0.408	0.45
0.00753	0.06	7.251	116.2	1.07	0.10	0.15	10.595	177.8	1.95	1.46	0.13	11.84	1.07	0.458	0.982	0.00	1.07	1.07
0.00871	0.07	7.768	124.4	1.93	0.18	0.18	11.298	192.1	2.17	2.19	0.20	13.06	2.00	0.501	0.865	0.00	2.00	2.00
0.00996	0.08	8.362	133.8	2.89	0.26	0.22	11.798	212.7	2.87	3.05	0.24	13.71	2.50	0.526	0.866	0.00	2.50	2.50
0.01116	0.09	8.873	144.4	3.68	0.33	0.26	12.298	233.3	3.05	4.03	0.26	14.33	2.99	0.529	0.866	0.00	2.99	2.99
0.01241	0.10	9.405	152.7	4.26	0.36	0.31	12.798	253.9	3.14	5.32	0.34	15.2	3.67	0.556	0.866	0.00	3.67	3.67
0.01402	0.12	9.885	161.8	4.26	0.36	0.31	13.298	274.5	3.14	7.81	0.44	15.71	4.04	0.561	0.866	0.00	4.04	4.04
0.01681	0.16	11.298	192.1	6.23	0.51	0.36	14.086	300.1	3.14	8.92	0.51	16.68	5.64	0.616	0.866	0.00	5.64	5.64
0.01983	0.26	10.556	242.7	6.23	0.51	0.36	14.595	320.7	3.14	9.85	0.70	17.68	7.41	0.659	0.866	0.00	7.41	7.41
0.02282	0.40	9.829	300.1	6.23	0.51	0.36	15.095	341.3	3.14	10.78	0.92	18.68	9.18	0.699	0.866	0.00	9.18	9.18
0.02446	0.46	9.847	321.3	6.23	0.51	0.36	15.595	361.9	3.14	11.71	1.15	19.68	10.95	0.735	0.866	0.00	10.95	10.95
0.02968	0.64	10.086	380.9	6.23	0.51	0.36	16.095	401.5	3.14	12.64	1.45	20.68	12.72	0.765	0.866	0.00	12.72	12.72
0.03462	0.83	10.346	431.6	6.23	0.51	0.36	16.595	441.1	3.14	13.57	1.81	21.68	14.49	0.791	0.866	0.00	14.49	14.49
0.04308	1.16	11.829	617.3	6.23	0.51	0.36	17.595	521.7	3.14	15.44	2.44	23.68	18.26	0.851	0.866	0.00	18.26	18.26
0.05627	1.68	12.976	725.0	6.23	0.51	0.36	18.595	601.3	3.14	17.31	3.22	25.68	22.03	0.899	0.866	0.00	22.03	22.03
0.07249	2.32	13.626	798.8	6.23	0.51	0.36	19.595	680.9	3.14	19.18	4.15	27.68	25.80	0.935	0.866	0.00	25.80	25.80
0.08303	2.76	13.626	798.8	6.23	0.51	0.36	20.595	760.5	3.14	21.05	5.08	29.68	29.57	0.961	0.866	0.00	29.57	29.57
0.09334	3.21	14.211	850.8	6.23	0.51	0.36	21.595	840.1	3.14	22.92	6.01	31.68	33.34	0.979	0.866	0.00	33.34	33.34
0.11394	4.17	15.218	962.0	6.23	0.51	0.36	22.595	920.7	3.14	24.79	7.04	33.68	37.11	0.989	0.866	0.00	37.11	37.11
0.13292	5.13	15.998	1084.8	6.23	0.51	0.36	23.595	1000.3	3.14	26.66	8.07	35.68	40.88	0.991	0.866	0.00	40.88	40.88
0.19319	8.21	18.378	1373.0	6.23	0.51	0.36	24.595	1100.9	3.14	28.53	9.10	37.68	44.65	0.993	0.866	0.00	44.65	44.65
0.24748	11.20	20.166	1602.9	6.23	0.51	0.36	25.595	1201.5	3.14	30.40	10.13	39.68	48.42	0.994	0.866	0.00	48.42	48.42
0.29937	14.53	21.415	1826.6	6.23	0.51	0.36	26.595	1302.1	3.14	32.27	11.16	41.68	52.19	0.995	0.866	0.00	52.19	52.19
0.37920	20.20	23.003	2154.7	6.23	0.51	0.36	27.595	1402.7	3.14	34.14	12.19	43.68	55.96	0.996	0.866	0.00	55.96	55.96
0.45903	26.01	24.538	2445.2	6.23	0.51	0.36	28.595	1503.3	3.14	36.01	13.22	45.68	59.73	0.997	0.866	0.00	59.73	59.73
0.57878	35.70	26.409	2865.5	6.23	0.51	0.36	29.595	1603.9	3.14	37.88	14.25	47.68	63.50	0.998	0.866	0.00	63.50	63.50
0.71849	49.29	27.903	3367.3	6.23	0.51	0.36	30.595	1704.5	3.14	39.75	15.28	49.68	67.27	0.999	0.866	0.00	67.27	67.27
0.89811	69.92	29.284	4010.0	6.23	0.51	0.36	31.595	1805.1	3.14	41.62	16.31	51.68	71.04	0.999	0.866	0.00	71.04	71.04
1.09769	99.05	30.072	4766.6	6.23	0.51	0.36	32.595	1905.7	3.14	43.49	17.34	53.68	74.81	0.999	0.866	0.00	74.81	74.81

0.006" Ribbed 0.402" Pipe
 Pipe Length = 350

Pipe
 S2: 0.402
 d: 0.402
 h: smooth
 R2R: POLY N-300LHW
 d: 0.386
 h: 0.006
 R/h: 32.2

Series
 N-300LHW
 RUN 114
 DATE 10/13/92
 POLY N-300LHW
 c: wppm 300
 m: 1.254

Q (L/s)	Tot(S2)	1/√g(S2)	Press(S2)	S'(S2)	Sf(S2)	Twr(R2R)	1/√g(R2R)	Re-v(R2R)	h _s	S'(R2R)	Sf(R2R)	1/√g(S2N)	Sh(S2)	R	Rf	P	ΔV/m	competed R	connected S
0.00158	0.02	3.694	59.4			0.10	7.763	121.5	1.34			7.64				0.865			
0.00305	0.03	4.609	73.7			0.11	8.373	131.1	1.44			8.24				0.862			
0.00394	0.04	5.208	84.3			0.13	8.913	143.8	1.58			8.97				0.843			
0.00479	0.05	5.768	92.7			0.16	9.854	157.7	1.73			9.77				0.856			
0.00579	0.06	6.364	101.6			0.20	10.647	175.8	1.93			10.73				0.841			
0.00725	0.08	7.132	113.6			0.24	11.397	195.8	2.15			11.47				0.817			
0.00810	0.09	7.541	120.1			0.36	10.932	236.2	2.60			10.9				0.770			
0.00941	0.10	8.146	129.4			0.53	9.739	298.0	3.17			10.03				0.730			
0.01098	0.12	8.770	140.3			0.71	10.036	333.9	3.67			10.01				0.628			
0.01331	0.14	9.625	155.0			0.90	10.399	376.4	4.14	0.49	0.05	10.29	0.99	0.109	0.011	0.844	0.00	0.109	0.39
0.01601	0.17	10.491	171.3			1.23	11.111	439.2	4.83	0.91	0.09	10.88	0.71	0.231	0.021	0.861	0.00	0.231	0.71
0.01907	0.21	11.392	188.1			1.75	12.370	524.6	5.77	1.84	0.17	11.99	1.51	0.380	0.032	0.876	0.00	0.380	1.51
0.02206	0.29	11.254	220.3			2.35	13.854	608.0	6.68	3.05	0.28	13.29	2.55	0.564	0.042	0.886	0.00	0.564	2.55
0.02396	0.40	10.301	261.5	0.36	0.04	2.67	14.818	647.1	7.11	3.89	0.36	13.89	3.05	0.928	0.067	0.910	0.00	0.928	3.05
0.02860	0.61	9.963	322.9	0.67	0.07	3.13	15.353	700.2	7.70	4.27	0.39	14.62	3.64	0.733	0.050	0.895	0.00	0.733	3.64
0.03338	0.79	10.226	367.6	0.99	0.14	4.01	16.954	788.4	8.67	5.62	0.50	16.12	4.93	0.834	0.052	0.896	0.00	0.834	4.93
0.04160	1.10	10.818	433.2	1.47	0.24	4.64	18.326	856.5	9.44	6.80	0.59	17.94	6.61	0.786	0.022	0.869	0.00	0.786	6.61
0.05529	1.59	11.941	521.8	2.56	0.45	6.13	20.735	987.0	10.85	8.84	0.74	20.37	8.79	0.365	0.018	0.861	0.00	0.365	8.79
0.07180	2.17	13.295	606.3	3.16	0.75	8.81	21.878	1183.0	13.00	9.48	0.76	22.31	10.32	-0.332	-0.015	0.830	0.00	-0.332	10.32
0.09190	2.92	14.030	656.2	3.67	1.00	13.08	22.846	1441.9	15.85	10.08	0.75	25.59	13.35	-2.744	-0.107	0.732	0.00	-2.744	13.35
0.09189	3.74	16.184	793.0	4.99	1.17	20.71	24.642	1815.1	19.95	11.85	0.99	27.93	15.29	-3.288	-0.118	0.684	0.00	-3.288	15.29
0.13352	4.20	17.761	850.6	6.44	1.30	31.07	25.413	2222.8	24.43	12.73	1.00	29.81	16.82	-4.397	-0.147	0.655	0.00	-4.397	16.82
0.17363	5.50	20.192	973.2	8.64	1.45	46.16	26.060	2710.1	29.79	13.42	1.06	31.65	18.32	-5.590	-0.177	0.617	0.00	-5.590	18.32
0.21854	7.61	21.693	1145.6	9.86	1.45	72.27	27.528	3503.1	38.50	14.87	1.17	34.07	20.29	-6.542	-0.192	0.597	0.00	-6.542	19.98
0.27941	9.98	24.120	1311.4	12.05	1.45	105.73	28.699	4077.5	44.82	16.02	1.26	35.71	21.07	-7.011	-0.196	0.585	-17.19	-6.293	19.98
0.37920	14.76	26.912	1595.9	14.50	1.45													-6.306	20.96
0.47899	21.18	28.375	1911.6	15.65	1.23														
0.59874	29.64	29.982	2261.8	16.96	1.30														
0.81828	48.00	32.200	2875.6	18.76	1.40														
0.99790	65.52	33.613	3342.8	19.92	1.45														

Series	Q (L/A)	Tm(SZ)	1/Amp(SZ)	Peak(SZ)	S (SZ)	Sf (SZ)	Tm(RZR)	1/Amp(RZR)	Peak(RZR)	N	S (RZR)	Sf (RZR)	1/Amp(SZ)	Sf (SZ)	R	Rf	P	Δ/hrs	corrected R	corrected Sf
0.008" Ribbed 0.402" Pipe Residue = 350																				
PKT																				
SZ:																				
d = 0.402																				
h = smooth																				
RZ:																				
d = 0.386																				
h = 0.026																				
h ₀ = 32.2																				
N = 300																				
MLN																				
DATE																				
POLY																				
c																				
w																				
	0.00294	0.02	5.084	79.0	0.18	0.02	0.09	9.405	147.0	1.62	0.17	0.02	9.18	0.18	0.005	0.000	0.870	0.00	0.005	0.18
	0.00433	0.04	6.131	96.7	0.18	0.02	0.10	9.799	154.5	1.70	0.25	0.02	9.59	0.19	0.100	0.010	0.840	0.00	0.100	0.19
	0.00601	0.05	7.134	115.5	0.33	0.03	0.12	10.307	165.8	1.82	0.45	0.04	10.23	0.37	0.129	0.012	0.848	0.00	0.129	0.37
	0.00760	0.06	8.129	128.2	0.82	0.08	0.13	10.905	174.5	1.92	1.06	0.10	11.74	0.85	0.291	0.025	0.865	0.00	0.291	0.85
	0.00946	0.07	9.980	135.4	1.40	0.12	0.16	11.836	191.5	2.10	1.57	0.14	12.62	1.43	0.290	0.023	0.863	0.00	0.290	1.43
	0.00966	0.08	9.111	145.7	1.40	0.13	0.30	10.278	265.1	2.91	2.00	0.17	10.33	1.37	0.685	0.055	0.901	0.00	0.685	1.37
	0.01056	0.09	9.498	153.0	1.82	0.19	0.41	10.030	313.2	3.44	2.00	0.17	9.86	1.87	0.327	0.025	0.866	0.00	0.327	1.87
	0.01191	0.10	10.078	162.8	2.66	0.23	0.50	10.043	343.6	3.78	2.66	0.23	10							
	0.01326	0.12	10.575	172.8	3.24	0.27	0.69	10.215	405.1	4.45	3.24	0.27	10.21	3.08	1.302	0.092	0.945	0.00	1.302	3.08
	0.01577	0.15	11.093	196.1	3.94	0.32	1.26	11.059	548.0	6.02	3.94	0.32	10.45	3.73	1.528	0.096	0.949	0.00	1.528	3.73
	0.01895	0.24	10.519	248.7	5.22	0.41	1.85	12.031	663.8	7.30	5.22	0.41	11.74	4.57	1.467	0.086				
	0.02183	0.37	9.821	307.1	5.55	0.42	2.62	12.810	791.0	8.69	5.55	0.42	12.53	5.13	1.391	0.078	0.934	0.00	1.391	5.13
	0.02387	0.43	9.956	332.8	5.55	0.42	2.53	13.215	777.7	8.55	5.55	0.42	18.56	5.51	1.619	0.087	0.954	-2.79	2.089	5.06
	0.02933	0.79	10.397	451.7	3.94	0.32	7.39	16.362	1190.5	13.08	3.94	0.32	14.98	3.08	1.302	0.092	0.945	0.00	1.302	3.08
	0.04200	1.11	10.846	536.5	3.94	0.32	7.39	17.368	1340.9	14.74	4.70	0.37	15.84	3.73	1.528	0.096	0.949	0.00	1.528	3.73
	0.05536	1.67	11.885	656.2	5.22	0.41	13.66	19.161	1823.5	20.04	6.37	0.50	17.77	4.57	1.467	0.086				
	0.07072	2.36	12.556	780.9	5.55	0.42	21.90	20.179	2309.2	23.38	7.51	0.59	18.56	5.51	1.619	0.087	0.954	0.00	1.619	5.51
	0.07113	2.38	12.577	784.7	5.55	0.42	21.90	19.999	2609.5	26.68	7.35	0.58	18.84	5.67	1.659	0.056				
	0.08118	2.83	13.152	855.9	2.18	0.19	47.27	18.886	3393.3	37.30	6.23	0.49	19.54	5.82	-0.654	-0.033	3.768	-6.86	0.152	5.01
	0.09352	3.48	13.675	940.9	2.18	0.19	70.27	18.307	4138.1	45.48	5.62	0.44	19.45	5.38	-1.143	-0.059	0.715	-9.26	-0.223	4.46
	0.11319	4.60	14.392	1081.8	3.43	0.23	118.02	17.385	5365.4	58.97	4.60	0.36	19.13	4.61	-1.745	-0.091	0.661	-12.50	-0.735	3.60
	0.15966	7.30	16.108	1388.2	3.43	0.23	202.88	16.575	7034.8	77.32	3.53	0.27	18.68	3.69	-2.105	-0.113	0.622	-16.05	-1.068	2.65
	0.19658	13.29	17.909	1873.3	3.43	0.23	344.47	15.900	9158.3	100.66	2.38	0.18	18.08	2.63	-2.180	-0.121	0.600	-19.70	-1.162	1.61
	0.23850	21.75	18.670	2396.6	3.43	0.23														
	0.31833	37.80	19.473	3160.1	3.43	0.23														
	0.35824	52.32	19.560	3718.8	3.43	0.23														
	0.43908	81.20	19.324	4635.0	3.43	0.23														
	0.51891	131.32	18.994	5894.2	3.43	0.23														
	0.63866	215.40	18.538	7542.3	3.43	0.23														
	0.79832																			
	0.99790																			

0.008" Ribbed 60.402" Pipe
Product = 350

Series

MPR
SZ:
 d = 0.402
 h = smooth
RZ: 107
 DATE 9/29/92
POLY M-300
 c 10
 h = 0.006
 RN 32.2
 W

Q (L/A)	Tm(SZ)	1/mpr(SZ)	Repr(SZ)	S (SZ)	SF (SZ)	1/m(RZ)	1/mpr(RZ)	Repr(RZ)	N	S (RZ)	SF (RZ)	1/mpr(SZ)	5m(SZ)	R	W	P	ΔVres	connected R	connected S
0.00421	0.04	5.918	96.4	0.46	0.05	0.12	10.084	163.6	1.80	0.79	0.08	0.08	0.47	0.335	0.032	0.874	0.00	0.335	0.47
0.00525	0.05	6.641	107.2	0.77	0.08	0.12	10.266	167.7	1.84	1.18	0.12	0.12	0.78	0.423	0.039	0.883	0.00	0.423	0.78
0.00608	0.05	7.129	115.7	1.48	0.14	0.14	10.483	176.7	1.94	1.99	0.19	0.19	1.46	0.583	0.049	0.893	0.00	0.583	1.46
0.00798	0.07	8.160	132.8	2.60	0.24	1.48	11.130	184.4	2.03	3.12	0.29	0.29	2.58	0.614	0.046	0.890	0.00	0.614	2.58
0.00950	0.09	8.876	145.5	3.70	0.34	1.99	11.484	202.0	2.22	4.52	0.41	0.41	3.58	1.035	0.071	0.917	0.00	1.035	3.58
0.01080	0.10	9.460	155.2	4.35	0.39	2.43	9.727	281.7	3.10	5.08	0.45	0.45	4.26	0.946	0.062	0.907	0.00	0.946	4.26
0.01163	0.10	9.806	161.5	5.00	0.44	2.91	9.926	315.2	3.46	5.50	0.48	0.48	4.99	0.674	0.041	0.885	0.00	0.674	4.99
0.01214	0.11	9.978	165.7	5.78	0.50	4.06	10.133	344.9	3.78	6.02	0.51	0.51	5.90	0.429	0.025	0.870	0.00	0.429	5.90
0.01304	0.12	10.283	173.0	6.80	0.58	4.60	10.775	391.4	4.30	7.21	0.60	0.60	6.77	0.815	0.044	0.887	0.00	0.815	6.77
0.01443	0.13	10.808	182.3	8.44	0.71	6.58	11.343	432.2	4.75	8.18	0.65	0.65	7.86	0.674	0.044	0.887	0.00	0.674	7.86
0.01629	0.15	11.362	196.0	9.64	0.79	8.51	12.423	496.6	5.46	9.50	0.75	0.75	9.81	0.232	0.011	0.849	0.00	0.232	9.81
0.01823	0.24	10.767	244.3	12.38	0.98	11.73	13.874	588.6	6.48	10.85	0.88	0.88	10.89	0.750	0.032	0.873	0.00	0.750	10.89
0.02195	0.37	9.816	306.0	13.05	0.98	22.53	15.555	684.1	7.52	12.20	0.96	0.96	12.65	-0.842	-0.033	0.786	-3.72	-0.460	12.20
0.02449	0.45	9.978	336.4	14.98	0.98	34.84	16.316	755.1	8.30	12.35	0.98	0.98	12.87	-1.312	-0.050	0.736	-10.18	-0.477	12.35
0.02851	0.60	10.415	386.8	16.44	0.98	54.03	17.879	825.2	9.07	12.23	0.97	0.97	12.87	-1.098	-0.042	0.740	-17.94	-0.090	12.23
0.03428	0.73	10.806	431.6	18.45	0.98	87.30	18.934	973.3	10.70	10.61	0.83	0.83	10.63	-1.625	-0.065	0.680	-26.76	-0.218	10.61
0.04312	0.98	11.875	498.9	22.60	0.98	160.14	20.266	1044.2	11.48	9.03	0.70	0.70	9.40	-2.240	-0.093	0.654	-34.78	-0.722	9.03
0.05712	1.37	13.285	591.2	26.80	0.98	248.01	24.801	1250.2	13.74	7.43	0.56	0.56	8.70	-3.227	-0.135	0.595	-40.77	-1.707	7.43
0.07423	1.90	14.671	696.4	32.38	0.98			1422.6	15.64										
0.08595	2.29	15.481	764.2	36.25	0.98			1670.4	18.36										
0.09762	2.68	16.264	825.0	40.53	0.98			2316.5	25.46										
0.12208	3.69	17.318	964.8	57.8	0.98			2498.6	31.66										
0.13971	4.25	18.480	1045.3	68.0	0.98			3587.1	39.43										
0.17962	5.77	20.385	1219.7	84.4	0.98			4816.1	52.94										
0.21954	7.53	21.820	1393.0	96.4	0.98			6172.2	67.60										
0.27941	10.67	23.326	1659.2	108.5	0.98			7673.4	84.34										
0.36916	18.45	25.339	2183.0	123.8	0.98														
0.49895	26.69	26.332	2625.8	13.05	0.98														
0.61810	41.63	26.144	2278.4	12.48	0.91														
0.77836	68.96	25.557	4222.4	11.45	0.81														
0.93803	109.15	24.480	5911.1	9.98	0.69														
1.06769	153.77	24.136	6292.5	9.34	0.63														

0.008" Ribbed 0.402" Pipe
Reynolds = 350

PWE

S1:

d = 0.402

h = smooth

R1:

d = 0.366

h = 0.006

Re = 322

M-300

RUB

DATE

POLY

c

IR

104

9/24/92

M-300

100

1.1774

Series	Q (L/s)	Vel(S1)	1/4(S1)	Re(V(S1))	Sf(S1)	Vel(R1)	1/4(R1)	Re(V(R1))	N _s	S(R1)	Sf(R1)	1/4(S1) ^{1/4}	Sf(S1)	R	Ri	P	d/Re ^{0.14}	connected	P _r connected
0.00358	0.04	5.096	81.8			0.10	8.418	133.4	1.47	3.29	0.33	8.32	0.859	-0.009	-0.001	0.852	0.00	0.009	3.31
0.00426	0.04	5.574	89.0			0.12	9.014	142.5	1.57	5.01	0.49	8.85	0.866	-0.347	-0.027	0.833	0.00	-0.347	5.38
0.00514	0.05	6.102	98.0			0.14	9.593	151.9	1.67	6.94	0.67	9.42	0.865	-0.357	-0.020	0.823	0.00	-0.357	7.34
0.00517	0.05	6.144	98.1			0.17	10.809	171.2	1.88	7.71	0.73	10.41	0.883	-0.039	-0.002	0.831	0.00	-0.039	7.80
0.00587	0.06	6.587	105.3			0.21	11.519	190.4	2.09	8.97	0.82	11.39	0.856	-0.228	-0.011	0.844	0.00	-0.228	9.29
0.00613	0.06	6.690	106.9			0.37	10.128	250.5	2.75	10.39	0.93	11.38	0.587	-0.471	-0.021	0.810	0.00	-0.471	10.98
0.00692	0.07	7.066	113.4			0.39	10.668	260.1	2.78	10.68	0.93	11.35	0.604	-0.000	0.000	0.842	0.00	0.000	11.51
0.00707	0.07	7.169	115.2			0.51	11.240	295.0	3.24	11.78	1.07	11.24	0.682	-0.000	0.000	0.879	0.00	-0.000	11.51
0.00802	0.08	7.674	122.1			0.61	11.778	323.1	3.55	11.78	1.07	11.68	0.855	-0.009	-0.001	0.852	0.00	-0.009	11.51
0.00921	0.09	8.206	131.4			0.78	13.161	368.0	4.04	3.29	0.33	13.17	0.852	-0.347	-0.027	0.833	0.00	-0.347	5.38
0.01052	0.11	8.752	140.9			1.03	15.143	423.5	4.65	5.01	0.49	15.49	0.865	-0.357	-0.020	0.823	0.00	-0.357	7.34
0.01193	0.12	9.320	150.1			1.17	17.333	487.7	5.36	6.94	0.67	17.69	0.883	-0.039	-0.002	0.831	0.00	-0.039	7.80
0.01513	0.16	10.392	170.9			1.58	18.241	523.9	5.76	7.71	0.73	18.28	0.856	-0.228	-0.011	0.844	0.00	-0.228	9.29
0.21791	0.19	11.246	187.2			2.63	19.972	671.7	7.38	8.97	0.82	20.2	0.604	-0.471	-0.021	0.810	0.00	-0.471	10.98
0.02071	0.22	11.943	204.0			3.15	21.599	745.1	8.19	10.39	0.93	22.07	0.856	-0.000	0.000	0.842	0.00	0.000	11.51
0.02074	0.22	11.701	208.6			4.64	23.013	904.9	9.95	11.35	0.97	22.94	0.856	-0.000	0.000	0.842	0.00	0.000	11.51
0.02249	0.28	11.609	228.2			6.6	23.915	1308	13.08	11.50	0.93	25.46	0.715	-1.545	-0.061	0.715	0.00	-1.545	13.56
0.02702	0.46	10.829	294.1			1.21	23.621	1407.4	15.47	10.89	0.85	27.65	0.699	-4.029	-0.146	0.699	0.00	-4.029	15.46
0.03099	0.54	11.510	317.4			16.52	25.417	1697.8	18.66	12.60	0.98	28.22	0.659	-2.803	-0.099	0.659	0.00	-2.803	15.70
0.03940	0.70	12.884	360.9			22.53	25.369	1995.9	21.94	12.63	0.99	29.55	0.659	-4.181	-0.141	0.659	0.00	-4.181	16.75
0.05206	0.90	14.907	410.9			28.27	26.237	2498.0	27.46	13.58	1.07	31.67	0.624	-5.433	-0.172	0.624	0.00	-5.433	18.48
0.06863	1.17	17.263	470.1			35.27	27.452	3257.0	35.80	14.80	1.17	35.73	0.592	-6.278	-0.186	0.592	0.00	-6.278	20.08
0.07763	1.37	18.080	507.5			86.59	28.543	3913.9	43.02	15.87	1.26	35.11	0.590	-6.567	-0.187	0.590	0.00	-6.567	21.14
0.10949	2.31	19.642	655.8			115.07	30.263	4490.6	49.36	17.56	1.38	36.28	0.618	-6.017	-0.166	0.618	0.00	-6.017	22.07
0.12973	2.66	21.680	712.8																
0.16765	4.07	22.661	882.4																
0.22952	6.00	25.543	1070.1																
0.26244	8.16	25.523	1250.7																
0.30627	11.39	28.297	1464.3																
0.40714	15.47	28.228	1722.5																
0.50809	22.91	30.015	2096.7																
0.71849	36.90	32.247	2662.3																
0.89811	53.16	33.584	3194.0																
1.09769	74.04	34.784	3751.4																

PIPE: 10.21 mm

RIBLETS: 0.15 mm Replicated Pipe

POLYMERS:

NONE (Solvent)

PEO W-301

P-309

0.0060R Fibreted 0.402" Pipe

Series	Q (L/s)	Tw(S2)	1/sef(S2)	Reof(S2)	S(S2)	Sf(S2)	Tw(R2BR)	1/sef(R2BR)	Reof(R2BR)	h+	S'(R2BR)	Sf(R2BR)	R'	RF	P
RUN 183	0.01119	0.10	9.817	158.0	0.15	0.02	0.11	9.678	164.6	1.81	0.01	0.14	0.158	0.016	0.793
DATE 4/22/93	0.01248	0.11	10.352	187.2	0.08	0.01	0.15	10.174	174.8	1.92	0.00	0.04	0.092	0.009	0.824
POLY -	0.01470	0.13	11.130	183.3	0.03	0.00	0.12	11.006	190.4	2.09	-0.04	0.05	0.034	0.003	0.823
e wppm -	0.01786	0.20	11.011	225.1	0.00	0.00	0.22	11.046	230.5	2.53	-0.04	0.00	0.053	0.005	0.830
nr 1.000	0.02284	0.40	9.891	320.5	-0.03	0.00	0.43	9.975	326.5	3.59	-0.03	0.00	0.064	0.006	0.834
	0.02597	0.50	9.980	361.3	0.00	0.00	0.56	10.028	369.4	4.06	0.00	0.00	0.094	0.009	0.842
	0.03161	0.71	10.215	429.8	-0.05	0.00	0.79	10.263	439.5	4.83	-0.05	0.00	0.154	0.014	0.851
	0.03665	0.93	10.389	490.2	-0.07	0.00	1.02	10.434	501.5	5.51	-0.07	0.00	0.177	0.015	0.854
	0.04183	1.17	10.560	550.6	-0.08	0.00	1.28	10.649	560.9	6.16	-0.08	0.00	0.212	0.018	0.859
	0.04584	1.37	10.677	596.9	-0.09	0.00	1.49	10.796	606.5	6.87	-0.09	0.00	0.273	0.023	0.862
	0.05287	1.76	10.867	676.4	-0.10	0.00	1.90	11.036	684.6	7.52	-0.10	0.00	0.385	0.032	0.873
	0.06487	2.51	11.158	807.9	-0.11	0.00	2.68	11.394	812.8	8.93	-0.11	0.00	0.532	0.047	0.884
	0.07816	3.32	11.396	928.0	-0.12	0.00	3.54	11.655	932.2	10.25	-0.12	0.00	0.719	0.064	0.894
	0.08667	4.16	11.581	1036.7	-0.13	0.00	4.41	11.878	1038.4	11.41	-0.13	0.00	0.944	0.094	0.904
	0.09964	5.28	11.827	1157.8	-0.14	0.00	5.58	12.135	1159.3	12.74	-0.14	0.00	1.219	0.124	0.914
	0.11240	6.57	11.962	1273.4	-0.15	0.00	6.93	12.293	1273.0	13.99	-0.15	0.00	1.581	0.158	0.924
	0.12174	7.49	12.130	1388.5	-0.16	0.00	8.00	12.544	1379.5	15.16	-0.16	0.00	2.029	0.202	0.934
	0.13817	9.32	12.340	1557.4	-0.17	0.00	9.80	12.699	1554.8	17.09	-0.17	0.00	2.625	0.262	0.944
	0.15858	11.61	12.529	1740.3	-0.18	0.00	12.42	12.788	1751.7	19.25	-0.18	0.00	3.419	0.341	0.954
	0.18322	15.27	12.787	1996.0	-0.19	0.00	17.12	12.743	2057.6	22.62	-0.19	0.00	4.531	0.453	0.964
	0.19880	17.77	12.861	2150.6	-0.20	0.00	20.26	12.709	2235.8	24.57	-0.20	0.00	6.011	0.601	0.974
	0.23040	22.98	13.105	2446.7	-0.21	0.00	27.73	12.592	2815.1	28.74	-0.21	0.00	8.011	0.801	0.984
	0.25013	28.46	13.259	2624.4	-0.22	0.00	32.65	12.597	2837.8	31.19	-0.22	0.00	10.511	1.051	0.994
	0.26983	30.35	13.354	2810.9	-0.23	0.00	38.37	12.538	3076.2	33.81	-0.23	0.00	13.811	1.381	1.004
	0.28951	34.18	13.503	2982.7	-0.24	0.00	43.82	12.587	3287.3	36.13	-0.24	0.00	18.111	1.811	1.014
	0.32860	42.71	13.719	3334.3	-0.25	0.00	57.19	12.512	3755.9	41.28	-0.25	0.00	24.411	2.441	1.024
	0.36605	51.67	13.886	3667.9	-0.26	0.00	70.47	12.549	4169.7	45.83	-0.26	0.00	32.711	3.271	1.034
	0.42470	67.21	14.126	4183.9	-0.27	0.00	94.67	12.561	4833.7	53.13	-0.27	0.00	44.111	4.411	1.044
	0.48315	84.71	14.314	4698.1	-0.28	0.00	122.33	12.572	5495.3	60.40	-0.28	0.00	59.111	5.911	1.054
	0.54141	103.64	14.501	5197.4	-0.29	0.00	151.40	12.663	6114.6	67.21	-0.29	0.00	78.111	7.811	1.064
	0.63806	139.11	14.751	6023.2	-0.30	0.00	206.98	12.763	7151.5	78.60	-0.30	0.00	104.111	10.411	1.074
	0.69578	162.75	14.872	6515.7	-0.31	0.00	243.75	12.825	7762.3	85.32	-0.31	0.00	138.111	13.811	1.084
	0.81064	214.53	15.091	7483.9	-0.32	0.00	323.19	12.977	8941.3	98.28	-0.32	0.00	185.111	18.511	1.094
	0.90575	262.51	15.243	8284.6	-0.33	0.00	394.56	13.123	9886.5	108.57	-0.33	0.00	248.111	24.811	1.104
RUN 187	0.01136	0.10	9.787	160.1	0.12	0.01	0.11	9.844	163.6	1.80	0.02	0.18	0.193	0.020	0.833
DATE 4/26/93	0.01515	0.14	11.047	189.4	0.03	0.00	0.15	11.231	191.4	2.10	0.05	0.00	0.098	0.010	0.832
POLY -	0.01711	0.17	11.299	209.2	0.00	0.00	0.19	11.284	216.3	2.37	-0.02	0.00	0.060	0.006	0.832
e wppm -	0.02207	0.38	9.797	311.6	0.12	0.01	0.41	9.882	317.3	3.49	0.18	0.02	0.193	0.020	0.833
nr 1.000	0.02586	0.50	9.943	359.8	0.03	0.00	0.55	10.046	365.8	4.02	0.05	0.00	0.098	0.010	0.832
	0.03150	0.71	10.160	429.3	-0.03	0.00	0.78	10.532	436.7	4.80	-0.02	0.00	0.060	0.006	0.832
	0.03866	1.02	10.433	513.1	-0.01	0.00	1.12	10.532	522.2	5.74	-0.01	0.00	0.068	0.006	0.837
	0.04556	1.36	10.650	592.6	-0.04	0.00	1.48	10.784	601.2	6.61	-0.03	0.00	0.068	0.006	0.837
	0.05288	1.77	10.849	675.5	-0.07	0.00	1.90	11.030	682.6	7.50	-0.01	0.00	0.094	0.009	0.844
	0.06450	2.49	11.149	802.0	-0.07	0.00	2.67	11.369	807.9	8.88	0.02	0.00	0.140	0.012	0.849
	0.07572	3.29	11.384	922.2	-0.08	0.00	3.48	11.680	923.4	10.15	0.06	0.01	0.219	0.019	0.859
	0.08649	4.15	11.583	1036.2	-0.08	0.00	4.36	11.922	1033.2	11.36	0.05	0.00	0.265	0.023	0.865
	0.09782	5.13	11.774	1150.0	-0.07	0.00	5.41	12.108	1148.8	12.63	-0.01	0.00	0.267	0.023	0.863
	0.10507	5.78	11.917	1219.2	-0.03	0.00	6.09	12.256	1217.9	13.39	0.00	0.00	0.314	0.026	0.863
	0.12017	7.33	12.104	1370.0	-0.04	0.00	7.51	12.622	1349.8	14.84	0.14	0.01	0.501	0.041	0.868
	0.13277	9.45	12.396	1561.6	0.02	0.00	10.00	12.722	1563.3	17.16	0.01	0.00	0.346	0.028	0.860

PIPE:
S2:
d = 0.402
h = smooth
R2BR:
d = 0.386
h = 0.006
R/h 32.2

0.17010	13.33	12.704	1856.1	0.03	0.00	14.59	12.618	1890.0	20.77	0.04	0.00	0.112	0.009	0.831
0.19650	17.65	12.753	2136.7	-0.17	-0.01	30.40	12.520	2236.0	24.58	-0.16	-0.01	-0.475	-0.037	0.787
0.22211	21.84	12.960	2376.8	-0.14	-0.01	26.62	12.389	2554.3	28.07	-0.20	-0.02	-0.840	-0.063	0.746
0.23787	24.44	13.120	2514.4	-0.05	-0.01	30.53	12.359	2735.6	30.67	-0.16	-0.01	-0.959	-0.072	0.728
0.28121	33.15	13.318	2928.6	-0.15	-0.01	42.91	12.354	3243.4	35.65	-0.15	-0.01	-1.290	-0.095	0.702
0.34631	46.37	13.626	3464.0	-0.13	-0.01	62.42	12.396	3911.8	43.00	-0.11	-0.01	-1.573	-0.113	0.678
0.37971	56.01	13.834	3807.2	-0.09	-0.01	77.15	12.441	4349.3	47.80	-0.09	-0.01	-1.712	-0.121	0.660
0.44078	72.75	14.091	4339.2	-0.06	0.00	102.76	12.514	5019.9	55.18	-0.06	0.00	-1.869	-0.131	0.644
0.55898	112.91	14.344	5406.2	-0.19	-0.01	181.35	12.665	6290.7	69.14	-0.02	0.00	-2.130	-0.144	0.636
0.65748	147.04	14.785	6169.0	0.02	0.00	217.57	12.828	7304.4	80.28	0.02	0.00	-2.226	-0.148	0.614
0.79538	205.59	15.126	7290.9	0.07	0.00	306.33	13.079	8652.9	95.22	0.07	0.01	-2.272	-0.148	0.610
0.91358	263.10	15.358	8212.5	0.10	0.01	390.98	13.297	9744.7	107.11	0.11	0.01	-2.258	-0.145	0.612
0.00942	0.08	6.945	142.9	0.03	0.00	0.09	8.925	147.3	1.62	0.03	0.00	0.101	0.010	0.820
0.01163	0.10	9.872	159.9	0.12	0.01	0.12	9.883	164.2	1.81	0.12	0.01	0.075	0.007	0.826
0.01496	0.13	11.125	182.7	0.15	0.01	0.15	11.162	187.2	2.06	0.15	0.01	0.070	0.007	0.835
0.01715	0.16	11.611	200.9	0.18	0.01	0.18	11.724	204.5	2.25	0.18	0.01	0.079	0.007	0.840
0.02261	0.40	9.799	313.8	0.44	0.01	0.44	9.841	321.2	3.53	0.44	0.01	0.167	0.014	0.852
0.02816	0.52	9.936	358.2	0.12	0.01	0.57	9.962	387.3	4.04	0.09	0.01	0.101	0.010	0.820
0.03148	0.71	10.155	421.9	0.05	0.01	0.79	10.213	431.2	4.74	0.02	0.00	0.075	0.007	0.826
0.03965	1.07	10.436	517.5	-0.02	0.00	1.17	10.554	526.1	5.78	-0.01	0.00	0.070	0.007	0.835
0.04690	1.39	10.631	589.5	-0.05	0.00	1.51	10.784	597.5	6.57	-0.02	0.00	0.079	0.007	0.840
0.05316	1.79	10.821	689.6	-0.08	-0.01	1.94	11.001	677.1	7.44	-0.03	0.00	0.079	0.007	0.844
0.05520	2.55	11.132	798.5	-0.08	-0.01	2.73	11.376	803.3	8.83	0.04	0.00	0.157	0.014	0.852
0.07648	3.37	11.360	917.8	-0.09	-0.01	3.58	11.645	920.5	10.12	0.03	0.00	0.189	0.016	0.858
0.08705	4.25	11.516	1030.4	-0.14	-0.01	4.48	11.860	1026.8	11.31	0.00	0.00	0.210	0.018	0.865
0.10002	5.36	11.776	1156.6	-0.08	-0.01	5.68	12.102	1157.1	12.72	-0.04	0.00	0.249	0.021	0.862
0.11220	6.54	11.968	1274.5	-0.05	0.00	6.91	12.302	1274.9	14.01	-0.06	-0.01	0.280	0.023	0.862
0.12085	7.34	12.164	1351.2	0.04	0.00	7.85	12.434	1359.0	14.94	-0.06	-0.01	0.301	0.025	0.853
0.13871	9.37	12.357	1534.2	0.01	0.00	10.02	12.632	1543.0	16.96	-0.07	-0.01	0.278	0.023	0.853
0.16908	13.20	12.893	1821.8	0.05	0.00	14.52	12.791	1856.7	20.43	0.01	0.00	0.114	0.009	0.829
0.18498	16.51	12.807	1966.0	0.03	0.00	17.21	12.854	2014.0	22.14	0.10	0.01	0.036	0.003	0.822
0.20078	17.89	12.947	2110.7	0.05	0.00	20.38	12.820	2191.5	24.09	0.12	0.01	-0.143	-0.011	0.800
0.22448	22.12	13.017	2347.0	-0.06	0.00	26.35	12.606	2491.9	27.39	0.00	0.00	-0.581	-0.044	0.765
0.24224	24.94	13.227	2492.3	0.04	0.00	30.28	12.694	2670.0	29.35	0.13	0.01	-0.612	-0.046	0.752
0.26983	30.66	13.290	2762.8	-0.08	-0.01	38.75	12.498	3021.0	33.20	-0.02	0.00	-1.025	-0.076	0.722
0.30327	36.50	13.689	3013.6	0.17	0.01	47.99	12.620	3360.7	36.94	0.12	0.01	-1.086	-0.079	0.694
0.36213	50.53	13.893	3544.6	0.09	0.01	68.39	12.623	4010.9	44.08	0.11	0.01	-1.390	-0.099	0.674
0.40126	60.19	14.104	3868.4	0.15	0.01	84.13	12.611	4448.1	48.69	0.08	0.01	-1.581	-0.111	0.653
0.45985	75.94	14.389	4344.7	0.24	0.02	108.78	12.650	5080.8	55.84	0.07	0.01	-1.773	-0.123	0.631
0.56678	111.01	14.515	5252.3	0.03	0.00	181.63	12.715	6164.4	67.75	0.04	0.00	-2.044	-0.139	0.626
0.67556	155.90	14.777	6222.5	0.00	0.00	229.46	12.875	7342.6	80.70	0.06	0.00	-2.188	-0.145	0.620
0.79155	208.20	14.960	7183.3	-0.06	0.00	309.67	12.967	8520.9	93.66	-0.02	0.00	-2.356	-0.154	0.613
0.90575	262.52	15.246	7979.3	0.04	0.00	393.47	13.164	9501.4	104.43	0.02	0.00	-2.348	-0.151	0.608

0.00800" Ribbets/O.402" Pipe Series

PEO

WSR-301

185

4/23/93

WSR-301

3

1.006

R/A: 3:2.2

PEE:
 SZ:
 d = 0.402
 h = smooth
 RZR:
 d = 0.386
 h = 0.006

Q (L/s)	T _{wf} (S)	1/W _f (S ²)	Re _{wf} (S ²)	S (S ²)	Sf (S ²)	1/W _f (F ₃)	1/W _f (F _{2R})	Re _{wf} (F _{2R})	N _s	S (F _{2R})	Sf (F _{2R})	1/W _f (S ₂)*	S ₂ (S ₂)	R	W _f	P	Δ/Tree	connected R	connected S
0.00812	0.07	8.315	135.3	0.08	0.01	0.09	8.383	138.0	1.52	-0.05	-0.01	8.4932	0.07	-0.081	-0.008	0.809	0.00	-0.081	0.07
0.01073	0.09	9.574	155.4	0.10	0.00	0.10	9.607	159.2	1.75	-0.04	0.00	9.7942	0.00	0.021	0.002	0.825	0.00	0.021	0.00
0.01343	0.12	10.629	175.4	0.13	0.00	0.13	10.655	179.9	1.98	-0.06	0.01	10.806	-0.03	0.046	0.004	0.828	0.00	0.046	-0.03
0.01593	0.15	11.304	195.6	0.16	0.00	0.16	11.350	200.5	2.20	-0.06	0.01	11.375	-0.06	0.069	0.008	0.834	0.00	0.069	-0.06
0.02026	0.32	9.707	290.2	0.32	0.00	0.37	9.641	300.4	3.30	-0.07	-0.01	10.688	-0.10	0.128	0.012	0.840	0.00	0.128	-0.10
0.02300	0.41	9.834	325.3	0.46	0.00	0.46	9.818	335.0	3.68	-0.07	0.01	9.8678	-0.04	0.207	0.019	0.850	0.00	0.207	-0.04
0.02818	0.58	10.048	390.2	0.66	0.01	0.66	10.005	402.9	4.43	-0.05	0.01	10.096	0.00	0.313	0.028	0.862	0.00	0.313	0.08
0.03112	0.78	10.225	451.0	0.96	0.00	0.96	10.277	461.3	5.07	-0.04	0.00	10.256	0.00	0.389	0.033	0.869	0.00	0.389	0.30
0.03732	0.96	10.377	501.0	1.04	0.00	1.04	10.450	511.5	5.62	-0.06	0.01	10.511	-0.06	0.440	0.036	0.872	0.00	0.440	0.50
0.04100	1.14	10.488	544.8	1.24	0.00	1.24	10.600	554.2	6.09	-0.06	0.01	10.688	-0.10	0.489	0.034	0.872	0.00	0.489	0.79
0.04734	1.46	10.665	618.1	-0.10	-0.01	1.59	10.816	627.6	6.90	-0.07	-0.01	11.038	-0.04	0.529	0.038	0.871	0.00	0.529	1.00
0.05806	2.06	11.020	735.0	-0.04	0.00	2.21	11.245	740.6	8.14	0.06	0.01	11.366	0.00	0.606	0.044	0.881	0.00	0.606	1.60
0.06809	2.67	11.363	836.1	0.07	0.01	2.82	11.675	836.3	9.19	0.26	0.02	11.767	0.30	0.641	0.041	0.877	0.00	0.641	2.24
0.07867	3.31	11.782	932.0	0.30	0.03	3.48	12.156	928.8	10.21	0.52	0.05	12.559	0.79	0.591	0.034	0.871	0.00	0.591	2.79
0.08916	3.97	12.195	1020.4	0.56	0.05	4.15	12.608	1014.8	11.15	0.78	0.07	13.668	1.00	0.512	0.034	0.871	0.00	0.512	3.20
0.10003	4.72	12.555	1110.6	0.77	0.07	4.93	12.980	1104.5	12.14	0.95	0.08	14.529	2.24	0.382	0.024	0.871	0.00	0.382	3.61
0.10627	5.05	12.899	1149.9	1.06	0.09	5.29	13.371	1144.8	12.58	1.21	0.10	15.272	2.79	0.300	0.024	0.871	0.00	0.300	3.61
0.13036	6.70	13.736	1322.1	1.65	0.14	6.93	14.274	1308.1	14.38	1.85	0.15	16.344	3.20	0.248	0.024	0.871	0.00	0.248	3.61
0.15621	8.52	14.587	1498.6	2.28	0.19	8.87	15.120	1486.5	16.34	2.47	0.20	17.399	4.25	0.187	0.024	0.871	0.00	0.187	3.61
0.18195	10.54	15.283	1667.1	2.80	0.22	11.04	15.784	1559.6	18.24	3.02	0.24	18.029	4.93	0.142	0.011	0.842	-2.43	0.142	4.10
0.19973	11.69	15.926	1758.9	3.34	0.27	12.02	16.686	1734.4	19.06	3.82	0.30	19.272	5.83	0.105	-0.018	0.804	-5.02	0.105	4.60
0.22869	14.50	16.445	1959.0	3.68	0.29	14.77	17.223	1923.1	21.14	4.45	0.35	20.246	6.42	0.085	-0.058	0.735	-7.75	0.085	5.28
0.25965	16.94	17.200	2117.3	4.30	0.33	17.71	17.780	2105.9	23.15	5.05	0.40	20.557	6.48	0.073	-0.073	0.713	-11.55	0.073	5.74
0.29960	20.72	17.944	2341.7	4.87	0.37	22.46	18.221	2370.9	26.06	5.58	0.44	20.97	6.18	0.052	-0.105	0.652	-14.93	0.052	5.43
0.37949	29.45	19.066	2791.6	5.68	0.42	33.42	18.918	2892.6	31.79	6.39	0.51	20.97	6.18	0.041	-0.112	0.619	-17.97	0.041	5.54
0.47935	42.62	20.021	3356.2	6.32	0.46	51.55	19.241	3592.6	39.49	6.74	0.54	20.97	6.18	0.036	-0.058	0.735	-8.73	0.036	5.77
0.55924	55.75	20.421	3841.3	6.48	0.47	69.21	19.375	4162.6	45.75	6.85	0.55	20.97	6.18	0.034	-0.058	0.735	-8.73	0.034	5.77
0.63914	71.35	20.629	4344.8	6.48	0.46	91.31	19.277	4780.5	52.54	6.72	0.54	20.97	6.18	0.034	-0.058	0.735	-8.73	0.034	5.77
0.81889	112.90	21.013	5462.6	6.46	0.44	157.96	18.779	6284.6	69.08	6.09	0.48	20.97	6.18	0.034	-0.058	0.735	-8.73	0.034	5.77
0.99865	170.48	20.854	6684.9	5.95	0.40	251.10	18.164	7891.1	86.73	5.27	0.41	20.462	5.27	0.034	-0.112	0.619	-17.97	0.034	5.54

0.0060R Riblets/0.402" Pipe Series

PEO

WSP-301

185
4/24/93

MIN
DATE
POLY
WSP-301
c temp
10
1.021

PEO

PEO

d = 0.402
h = smooth
RZRC
d = 0.386
h = 0.006
R/h 32.2

Q (L/s)	Tau(SZ)	1/psi(SZ)	Reof(SZ)	S (SZ)	Sf (SZ)	Tau(R2B)	1/psi(R2B)	Reof(R2B)	h _s	S (R2B)	Sf (R2B)	1/psi(S2B)	St(SZ)	R	Rf	P	Δ/rms	corrected R	corrected P
0.00766	0.07	8.027	129.6	0.10	0.01	0.07	8.144	131.5	1.45	0.07	0.01	8.1483	0.09	0.011	0.001	0.001	0.00	0.011	0.09
0.00933	0.08	8.075	143.1	0.08	0.01	0.09	8.377	145.6	1.60	0.09	0.01	9.0212	0.07	0.078	0.008	0.008	0.00	0.078	0.07
0.01123	0.10	9.201	157.7	0.10	0.01	0.14	9.808	166.6	1.76	0.14	0.01	9.8611	0.07	0.167	0.016	0.016	0.00	0.167	0.04
0.01404	0.13	10.799	177.3	0.13	0.01	0.16	11.472	196.4	2.16	0.16	0.01	10.923	0.08	0.245	0.023	0.023	0.00	0.245	0.08
0.01604	0.15	11.324	193.3	0.15	0.01	0.36	9.103	289.8	3.19	0.36	0.01	9.8437	0.27	0.364	0.033	0.033	0.00	0.364	0.27
0.02022	0.31	9.872	279.6	0.31	0.01	0.48	9.921	336.2	3.70	0.48	0.01	9.6892	0.68	0.528	0.045	0.045	0.00	0.528	0.68
0.02373	0.43	9.872	328.3	0.43	0.01	0.67	10.099	397.3	4.37	0.67	0.01	10.068	1.183	0.575	0.047	0.047	0.00	0.575	1.21
0.02652	0.60	10.053	387.7	0.60	0.01	0.85	10.359	449.7	4.94	0.85	0.01	10.281	1.74	0.680	0.052	0.052	0.00	0.680	1.74
0.03008	0.77	10.254	441.3	0.04	0.00	1.05	10.605	499.6	5.49	1.05	0.13	10.438	2.36	0.664	0.044	0.044	0.00	0.664	2.36
0.03759	0.97	10.593	535.2	0.08	0.01	1.21	10.852	537.9	5.91	1.21	0.24	10.607	3.01	0.729	0.050	0.050	0.00	0.729	3.01
0.04139	1.14	10.998	602.8	0.26	0.03	1.52	11.352	601.1	6.61	1.52	0.54	10.988	4.00	0.833	0.052	0.052	0.00	0.833	4.00
0.04837	1.44	11.687	695.4	0.72	0.07	1.99	12.156	688.2	7.56	1.99	1.10	11.63	5.25	0.689	0.040	0.040	0.00	0.689	5.25
0.05920	1.91	11.687	762.2	1.27	0.11	2.47	12.731	768.2	8.44	2.47	1.67	12.356	6.78	0.769	0.043	0.043	0.00	0.769	6.78
0.07031	2.38	12.451	851.4	1.82	0.16	2.95	13.713	839.9	9.23	2.95	2.29	13.033	8.06	0.861	0.054	0.054	0.00	0.861	8.06
0.08149	2.86	13.141	951.4	2.42	0.21	3.58	14.428	925.5	10.17	3.58	2.80	14.677	9.90	0.922	0.010	0.010	0.00	0.922	9.90
0.09452	3.44	13.900	933.2	3.09	0.26	4.53	15.406	1040.3	11.43	4.53	3.52	15.842	11.26	0.886	0.000	0.000	0.00	0.886	11.26
0.10813	4.39	14.776	1053.6	4.12	0.35	5.72	16.695	1165.9	12.81	5.72	4.54	17.352	11.83	0.886	0.000	0.000	0.00	0.886	11.83
0.13813	5.54	16.008	1181.1	5.30	0.44	7.44	18.041	1336.8	14.69	7.44	5.58	18.068	12.26	0.886	0.000	0.000	0.00	0.886	12.26
0.17032	7.11	17.415	1345.2	5.90	0.48	8.73	18.857	1449.1	15.93	8.73	6.24	18.068	12.26	0.886	0.000	0.000	0.00	0.886	12.26
0.19284	8.38	18.342	1502.9	6.03	0.49	8.78	19.479	1456.8	16.01	8.78	6.24	18.068	12.26	0.886	0.000	0.000	0.00	0.886	12.26
0.19973	8.81	18.342	1502.9	6.03	0.49	8.78	19.479	1456.8	16.01	8.78	6.24	18.068	12.26	0.886	0.000	0.000	0.00	0.886	12.26
0.23968	11.01	19.698	1679.4	7.20	0.58	10.80	21.076	1615.8	17.76	10.80	8.33	20.698	12.26	0.886	0.000	0.000	0.00	0.886	12.26
0.27962	13.33	20.878	1848.6	8.21	0.65	13.72	21.816	1821.2	20.02	13.72	9.03	21.816	12.26	0.886	0.000	0.000	0.00	0.886	12.26
0.35951	18.71	22.663	2189.7	9.70	0.75	20.39	23.004	2220.9	24.41	20.39	10.32	23.004	12.26	0.886	0.000	0.000	0.00	0.886	12.26
0.43941	25.16	23.865	2539.7	10.67	0.81	29.24	23.481	2659.4	29.23	29.24	10.32	23.481	12.26	0.886	0.000	0.000	0.00	0.886	12.26
0.53927	34.00	25.218	2952.5	11.74	0.87	41.73	24.121	3177.6	34.93	41.73	11.61	24.121	12.26	0.886	0.000	0.000	0.00	0.886	12.26
0.63914	45.42	25.856	3412.8	12.12	0.88	57.47	24.360	4039.9	40.99	57.47	11.66	24.360	12.26	0.886	0.000	0.000	0.00	0.886	12.26
0.79892	68.20	26.377	4180.5	12.29	0.87	90.95	24.206	4689.7	51.55	90.95	11.66	24.206	12.26	0.886	0.000	0.000	0.00	0.886	12.26
0.89879	85.87	26.445	4686.6	12.16	0.85	117.28	23.981	5320.4	58.48	117.28	11.38	23.981	12.26	0.886	0.000	0.000	0.00	0.886	12.26
1.09852	129.20	26.351	5720.7	11.72	0.80	185.35	23.315	6656.0	73.16	185.35	10.58	23.315	12.26	0.886	0.000	0.000	0.00	0.886	12.26

0.0064" Riblets/0.402" Pipe
Repeated Runs

PPE:
 SZ: d = 0.402
 h = smooth
 RZRC: POLY P-309
 c: 50
 w: 1.142
 R/A: 32.2

Series: P-309
 PEO

Q(L/A)	T _{in} (SZ)	1/√h(SZ)	Re _{in} (SZ)	S _{in} (SZ)	Sf(SZ)	T _{in} (R2B)	1/√h(R2B)	Re _{in} (R2B)	N _{in}	S _{in} (R2B)	Sf(R2B)	1/√h(S2M)	S _{in} (S2)	R	RF	P	σ/T _{res}	connected R	connected S
0.00551	0.05	6.494	102.9	102.9	0.40	0.06	6.497	105.7	1.16	4.58	0.47	6.6478	3.73	0.844	0.062	0.088	0.00	0.844	3.73
0.00671	0.07	7.134	114.1	114.1	0.52	0.07	7.199	116.3	1.28	5.30	0.53	7.2798	5.32	0.003	0.000	0.838	0.00	0.003	5.32
0.00838	0.08	8.017	127.0	127.0	0.64	0.09	8.032	130.4	1.43	6.43	0.63	8.1757	6.74	-0.247	0.015	0.821	0.00	-0.247	6.74
0.00971	0.10	8.542	138.3	138.3	0.73	0.11	8.603	141.2	1.55	7.41	0.71	8.7122	7.74	-0.253	-0.014	0.816	0.00	-0.253	7.74
0.01313	0.13	9.953	160.6	160.6	0.81	0.14	10.018	164.0	1.80	8.05	0.76	10.115	8.25	-0.110	-0.006	0.822	0.00	-0.110	8.25
0.01647	0.17	10.941	183.5	183.5	0.87	0.18	11.077	186.4	2.05	8.62	0.80	11.091	8.76	-0.048	-0.002	0.826	0.00	-0.048	8.76
0.02032	0.21	12.132	204.4	204.4	0.85	0.23	12.272	207.8	2.28	9.44	0.85	12.209	9.49	0.054	0.003	0.825	0.00	0.054	9.49
0.02330	0.26	12.370	230.1	230.1	0.87	0.31	12.082	242.2	2.66	10.27	1.01	12.318	10.27	0.264	0.013	0.843	0.00	0.264	9.50
0.02788	0.42	11.670	292.2	292.2	1.00	0.45	12.033	291.3	3.20	11.76	1.02	11.678	11.51	0.473	0.020	0.854	0.00	0.473	11.51
0.03456	0.55	12.666	334.0	334.0	1.16	0.55	13.385	324.9	3.57	11.72	0.98	12.346	11.67	0.473	0.020	0.854	0.00	0.473	11.51
0.04006	0.63	13.770	356.3	356.3	1.22	0.65	14.361	351.2	3.86	11.72	0.98	13.517	12.43	-0.482	-0.020	0.802	0.00	-0.482	12.43
0.04719	0.73	15.075	383.6	383.6	1.28	0.78	15.295	389.0	4.28	11.94	0.97	15.382	13.38	-1.121	-0.044	0.782	0.00	-1.121	13.38
0.05862	0.92	16.626	432.2	432.2	1.41	1.03	16.676	443.1	4.87	12.21	1.02	16.823	13.89	-1.319	-0.051	0.758	0.00	-1.319	13.89
0.07055	1.16	17.878	484.0	484.0	1.54	1.29	17.871	497.8	5.47	12.89	1.02	18.124	14.49	-1.231	-0.046	0.768	0.00	-1.231	14.49
0.08002	1.38	18.596	527.7	527.7	1.66	1.53	18.667	540.3	5.94	13.32	1.04	18.777	15.72	-2.196	-0.078	0.736	0.00	-2.196	15.72
0.09131	1.66	19.294	580.7	580.7	1.84	1.84	19.407	593.7	6.53	14.08	1.11	19.455	16.82	-2.879	-0.097	0.696	0.00	-2.879	16.82
0.11382	2.31	20.414	684.8	684.8	2.06	2.36	20.527	700.2	7.70	15.40	1.23	20.655	17.80	-3.659	-0.118	0.667	0.00	-3.659	17.80
0.12957	2.94	20.939	769.3	769.3	2.22	3.18	20.929	778.2	8.55	15.10	1.29	22.988	19.58	-4.683	-0.141	0.646	0.00	-4.683	19.58
0.17301	4.52	23.157	939.1	939.1	2.42	4.54	23.401	933.9	10.27	17.95	1.43	23.211	20.22	-4.726	-0.138	0.638	0.00	-4.726	20.22
0.18055	4.83	23.878	1031.6	1031.6	2.59	4.83	23.684	964.2	10.60	17.95	1.43	24.149	20.71	-4.441	-0.127	0.650	0.00	-4.441	20.55
0.19973	5.20	24.712	1156.3	1156.3	2.86	5.92	23.667	1070.0	11.76	17.95	1.43	25.314	21.16	-0.044	0.000	0.802	0.00	-0.044	12.43
0.23169	6.53	24.712	1241.8	1241.8	3.62	7.62	24.193	1214.4	13.35	11.94	0.97	25.314	21.16	-0.044	0.000	0.802	0.00	-0.044	12.43
0.25765	7.53	25.594	1403.0	1403.0	4.14	9.07	24.662	1325.0	14.56	12.21	1.02	25.981	22.89	-1.231	-0.051	0.758	0.00	-1.231	13.89
0.29960	9.62	26.342	1614.3	1614.3	5.04	11.42	25.546	1487.4	16.35	12.89	1.02	26.777	24.49	-2.196	-0.078	0.736	0.00	-2.196	15.72
0.33951	12.73	27.476	1867.5	1867.5	6.34	15.76	26.098	1747.3	19.21	13.32	1.04	28.294	28.29	-2.879	-0.097	0.696	0.00	-2.879	16.82
0.39941	17.03	29.029	2210.4	2210.4	8.29	22.31	26.811	2078.9	22.85	14.72	1.17	30.994	30.99	-3.659	-0.118	0.667	0.00	-3.659	17.80
0.53927	23.87	30.087	2471.7	2471.7	13.32	32.35	27.325	2503.2	27.51	17.95	1.43	31.869	31.86	-4.683	-0.141	0.646	0.00	-4.683	19.58
0.61916	29.85	30.901	2911.7	2911.7	17.73	40.79	27.939	2810.6	30.89	15.10	1.29	33.286	33.28	-4.726	-0.138	0.638	0.00	-4.726	20.22
0.75897	41.45	32.143	3392.6	3392.6	19.63	58.48	28.603	3364.0	36.37	16.97	1.36	34.205	34.20	-4.441	-0.127	0.650	0.00	-4.441	20.55
0.91876	56.42	33.351	3926.4	3926.4	20.20	80.69	29.479	3946.3	43.37	17.95	1.43	34.931	34.93	-4.441	-0.127	0.650	0.00	-4.441	20.55
1.09852	76.80	34.180	4525.4	4525.4	20.20	107.83	30.490	4525.4	49.74	17.95	1.43	34.931	34.93	-4.441	-0.127	0.650	0.00	-4.441	20.55

0.008" Ribs/ft/0.402" Pipe
Repeated Runs

Series	PEO	Q (L/s)	T _w (S)	1/√g(S _w)	Re _{avg} (S _w)	S (S _w)	Sf (S _w)	T _w (R _{2B})	1/√g(R _{2B})	Re _{avg} (R _{2B})	h _s	S (R _{2B})	Sf (R _{2B})	1/√g(S _{2B})	S ₁ (S ₂)	R	Rf	P	Δt (ms)	corrected F _{corrected S}	
R-309	188	0.00336	0.03	4.890	78.3	4.81	0.49	0.04	4.841	81.3	0.89	5.14	0.52	5.0949	4.85	0.301	0.020	0.800	0.000	0.301	4.85
ALJ	428/493	0.00436	0.05	5.599	89.0	6.31	0.63	0.05	5.565	92.1	1.01	6.39	0.63	5.7922	6.49	-0.058	0.032	0.806	0.006	-0.058	6.49
POLY	100	0.00549	0.06	6.283	100.2	7.33	0.71	0.06	6.262	103.4	1.14	7.31	0.70	6.4704	7.51	-0.139	-0.008	0.811	0.011	-0.139	7.51
c. mason	1258	0.00689	0.07	7.022	112.8	7.87	0.77	0.07	7.005	116.3	1.28	7.89	0.75	7.2335	8.10	-0.133	-0.007	0.812	0.012	-0.133	8.10
lv		0.00838	0.09	7.753	124.5	8.43	0.80	0.09	7.729	128.4	1.41	8.56	0.80	8.0007	8.49	0.158	0.008	0.811	0.011	0.158	8.49
		0.01184	0.12	9.245	147.8	9.18	0.85	0.12	9.171	153.2	1.68	9.65	0.84	9.5841	9.99	0.567	0.028	0.803	0.003	0.567	9.99
		0.01535	0.16	10.529	168.6	10.00	0.90	0.16	10.383	175.2	1.93	10.53	0.84	10.804	11.40	0.658	0.031	0.795	0.003	0.658	11.40
		0.01963	0.22	11.506	197.6	11.35	1.06	0.22	11.454	197.2	2.17	11.80	1.03	11.502	12.62	0.824	0.024	0.776	0.003	0.824	12.62
		0.02233	0.24	12.311	210.4	11.35	1.06	0.24	12.176	213.3	2.34	11.80	1.03	12.294	12.62	0.824	0.024	0.776	0.003	0.824	12.62
		0.02687	0.34	12.490	249.9	12.25	1.06	0.34	12.251	253.5	2.90	12.25	1.06	12.543	12.62	0.824	0.024	0.776	0.003	0.824	12.62
		0.03368	0.53	12.712	310.3	13.69	1.32	0.53	12.669	306.1	3.64	13.69	1.32	12.706	12.62	0.824	0.024	0.776	0.003	0.824	12.62
		0.03900	0.60	13.669	332.8	13.69	1.32	0.60	13.669	331.1	3.64	13.69	1.32	13.59	12.62	0.824	0.024	0.776	0.003	0.824	12.62
		0.04631	0.74	14.671	368.4	14.67	1.44	0.74	14.671	369.9	4.07	14.67	1.44	14.722	12.62	0.824	0.024	0.776	0.003	0.824	12.62
		0.05783	0.93	16.370	412.7	16.37	1.64	0.93	16.370	420.2	4.62	16.37	1.64	16.586	12.62	0.824	0.024	0.776	0.003	0.824	12.62
		0.06940	1.16	17.585	461.6	17.58	1.82	1.16	17.585	472.3	5.19	17.58	1.82	17.809	12.62	0.824	0.024	0.776	0.003	0.824	12.62
		0.07901	1.37	18.381	502.9	18.38	2.00	1.37	18.381	516.0	5.67	18.38	2.00	18.551	12.62	0.824	0.024	0.776	0.003	0.824	12.62
		0.08997	1.67	19.003	553.9	19.00	2.18	1.67	19.003	562.1	6.18	19.00	2.18	19.094	12.62	0.824	0.028	0.863	0.000	0.158	8.49
		0.11195	2.32	20.045	653.3	20.04	2.85	2.32	20.045	653.1	7.18	20.04	2.85	20.048	12.62	0.824	0.028	0.863	0.000	0.158	8.49
		0.13400	3.00	21.072	736.9	21.07	3.53	3.00	21.072	735.3	8.08	21.07	3.53	21.053	12.62	0.824	0.031	0.866	0.000	0.158	8.49
		0.16950	4.14	22.712	873.8	22.71	4.51	4.14	22.712	873.8	9.62	22.71	4.51	22.773	12.62	0.824	0.031	0.866	0.000	0.158	8.49
		0.19373	4.93	23.770	953.3	23.77	5.29	4.93	23.770	953.3	10.51	23.77	5.29	24.142	12.62	0.824	0.031	0.866	0.000	0.158	8.49
		0.23968	6.42	25.774	1094.8	25.77	6.94	6.42	25.774	1094.8	11.36	25.77	6.94	26.113	12.62	0.824	0.031	0.866	0.000	0.158	8.49
		0.31957	8.34	26.397	1248.9	26.39	9.03	8.34	26.397	1248.9	12.26	26.39	9.03	26.885	12.62	0.824	0.031	0.866	0.000	0.158	8.49
		0.49336	10.25	27.210	1504.6	27.21	10.67	10.25	27.210	1504.6	13.16	27.21	10.67	27.815	12.62	0.824	0.031	0.866	0.000	0.158	8.49
		0.49336	14.69	28.405	1657.7	28.40	12.61	14.69	28.405	1657.7	14.05	28.40	12.61	28.944	12.62	0.824	0.031	0.866	0.000	0.158	8.49
		0.57922	18.18	29.381	1843.0	29.38	15.65	18.18	29.381	1843.0	15.05	29.38	15.65	30.079	12.62	0.824	0.031	0.866	0.000	0.158	8.49
		0.73897	26.08	30.975	2207.2	30.97	19.59	26.08	30.975	2207.2	16.05	30.97	19.59	31.744	12.62	0.824	0.031	0.866	0.000	0.158	8.49
		0.89879	40.45	32.506	2747.4	32.50	26.08	40.45	32.506	2747.4	17.17	32.50	26.08	33.744	12.62	0.824	0.031	0.866	0.000	0.158	8.49
		1.09852	53.65	33.446	3156.5	33.44	33.44	53.65	33.446	3156.5	17.41	33.44	33.44	36.353	12.62	0.824	0.031	0.866	0.000	0.158	8.49
			74.69	34.650	3659.5	34.65	40.45	74.69	34.650	3659.5	17.41	34.65	40.45	36.353	12.62	0.824	0.031	0.866	0.000	0.158	8.49

PIPE: 7.82 mm (Upstream and Downstream)

RIBLETS: 0.11 mm Degradation Experiments

POLYMERS:

NONE (Solvent)

PEO W-301

0.308" Pipe/Degradation
Resq/crit= 350

Series	Q (L/s)	Tw (S1)	1/sqrt(S1)	Resqf (S1)	S (S1)	SF (S1)	Tw (SID)	1/sqrt(SID)	Resqf (SID)	S' (SID)	SF (SID)	R'	P
DW													
PIPE													
S1:													
d = 0.308													
h = smooth													
SID:													
d = 0.308													
h = smooth													
Series													
DW													
263													
7/8/94													
POLY													
c wppm													
nr													
1.000													
264													
7/10/94													
POLY													
c wppm													
nr													
1.000													

0.06537	6.738	11.657	1059.2	-0.04	0.00	6.657	11.728	1052.8	0.04	0.00	0.039	1.012
0.06304	6.332	11.596	1025.1	-0.05	0.00	6.264	11.658	1019.6	0.02	0.00	0.024	1.011
0.06006	5.832	11.512	984.1	-0.06	-0.01	5.754	11.591	977.5	0.03	0.00	0.030	1.014
0.05816	5.520	11.459	958.6	-0.07	-0.01	5.438	11.545	951.4	0.03	0.00	0.032	1.015
0.05596	5.152	11.411	926.1	-0.06	0.00	5.075	11.498	919.1	0.04	0.00	0.044	1.015
0.05326	4.736	11.329	887.7	-0.06	-0.01	4.744	11.320	888.4	-0.07	-0.01	-0.075	0.988
0.04971	4.221	11.199	837.4	-0.09	-0.01	4.201	11.227	835.3	-0.06	-0.01	-0.061	1.005
0.04776	3.930	11.152	808.4	-0.08	-0.01	3.911	11.179	806.5	-0.05	0.00	-0.048	1.005
0.04528	3.592	11.060	772.1	-0.09	-0.01	3.573	11.089	770.0	-0.06	-0.01	-0.057	1.005
0.04279	3.256	10.979	735.0	-0.09	-0.01	3.237	11.010	732.9	-0.05	0.00	-0.051	1.006
0.03997	2.902	10.861	692.8	-0.10	-0.01	2.866	10.928	688.6	-0.02	0.00	-0.023	1.012
0.03717	2.558	10.758	650.6	-0.10	-0.01	2.531	10.815	647.2	-0.03	0.00	-0.030	1.011
0.03508	2.311	10.681	618.0	-0.08	-0.01	2.283	10.746	614.2	-0.01	0.00	-0.008	1.012
0.03252	2.036	10.550	579.2	-0.10	-0.01	2.004	10.636	574.5	0.00	0.00	-0.001	1.016
0.03086	1.856	10.486	552.4	-0.08	-0.01	1.825	10.572	547.9	0.02	0.00	0.018	1.016
0.02879	1.649	10.378	520.0	-0.09	-0.01	1.605	10.517	513.1	0.08	0.01	0.077	1.027
0.02623	1.394	10.282	477.9	-0.03	0.00	1.363	10.399	472.5	0.06	0.01	0.101	1.023
0.02370	1.168	10.154	436.2	0.00	0.00	1.147	10.245	432.3	0.05	0.01	0.102	1.018
0.02270	1.082	10.103	419.6	0.01	0.00	1.061	10.203	415.5	0.01	0.01	0.129	1.020
0.02173	1.002	10.053	403.0	0.03	0.00	0.965	10.136	399.7	0.08	0.01	0.129	1.017
0.02050	0.906	9.973	382.9	0.04	0.00	0.886	10.084	378.6	0.04	0.02	0.171	1.022
0.01858	0.753	9.913	348.7			0.732	10.053	343.9				1.029
0.01659	0.621	9.751	316.1			0.574	10.139	304.0				1.081
0.01584	0.565	9.754	301.3			0.527	10.101	290.9				1.072
0.01561	0.547	9.771	296.0			0.488	10.344	279.6				1.121
0.01431	0.382	10.712	247.1			0.388	10.639	248.8				0.986
0.01194	0.234	11.435	193.0			0.251	11.026	200.1				0.930
0.00979	0.186	10.516	171.8			0.181	10.655	169.5				1.027
0.00726	0.135	9.166	145.9			0.134	9.175	145.8				1.002
0.00522	0.096	7.806	123.1			0.097	7.748	124.1				0.985
0.01154	0.240	10.915	180.0			0.237	10.987	178.9				1.013
0.01108	0.229	10.713	176.2			0.222	10.891	173.3				1.034
0.01012	0.206	10.334	167.1			0.203	10.398	166.1				1.012
0.00862	0.173	9.611	153.2			0.173	9.611	153.2				1.000
0.00698	0.137	8.725	136.8			0.140	8.634	136.3				0.979
0.00648	0.127	8.432	131.8			0.129	8.344	133.2				0.979
0.00599	0.117	8.109	127.0			0.120	8.011	128.5				0.976
0.00488	0.092	7.458	113.0			0.095	7.277	115.8				0.972
0.00418	0.080	6.859	105.4			0.081	6.725	107.5				0.985
0.00346	0.065	6.274	95.8			0.065	6.139	98.0				1.001
0.00502	0.097	7.476	116.9			0.099	7.384	118.3				0.975
0.00696	0.135	8.769	138.7			0.137	8.715	139.6				0.988
0.00835	0.161	9.635	152.1			0.163	9.579	153.0				0.988
0.00977	0.193	10.308	166.9			0.189	10.406	165.3				1.019
0.01046	0.207	10.647	173.8			0.202	10.769	171.8				1.023
0.00840	0.162	9.671	154.0			0.162	9.679	153.9				1.002
0.00599	0.114	8.228	129.3			0.116	8.135	130.8				0.977

RUN 258
 DATE 7/4/94
 POLY -
 c wppm
 nr 1.000

0.308" Pipe/Degradation/
RampRate= 350

PIPE S1:	Series	Q (L/s)	Tw (S1)	1/amp(S1)	Resp(S1)	S' (S1)	SF (S1)	Tw (S1D)	1/amp(S1D)	Resp(S1D)	S' (S1D)	SF (S1D)	1/amp(I)	A'	Δ/Tres
297	RUN	0.01209	0.238	11.472	194.3			0.226	11.759	189.6					
0.308	DATE	0.01465	0.471	9.811	273.5			0.476	9.764	274.8					
smooth	POLY	0.01693	0.638	9.817	318.1			0.632	9.861	316.7					
3	e vpppp	0.01989	0.857	9.944	368.9	0.08	0.01	0.837	10.064	364.5	0.22	0.02	9.934	0.130	0.053
1.00	nr	0.02180	1.017	10.007	402.7	-0.01	0.00	0.991	10.137	397.6	0.14	0.01	9.997	0.140	0.063
13	Stations	0.02560	1.373	10.196	467.8	-0.08	-0.01	1.348	10.288	463.6	0.02	0.00	10.184	0.104	0.055
		0.03122	1.913	10.447	552.4	-0.12	-0.01	1.874	10.555	546.7	0.00	0.00	10.430	0.125	0.080
		0.03582	2.417	10.666	622.1	-0.11	-0.01	2.372	10.765	616.4	0.01	0.00	10.648	0.117	0.087
		0.04030	2.950	10.863	687.4	-0.09	-0.01	2.910	10.937	682.7	0.00	0.00	10.847	0.090	0.075
		0.04396	3.440	10.971	742.3	-0.11	-0.01	3.377	11.074	735.4	0.01	0.00	10.961	0.113	0.102
		0.04844	4.030	11.170	803.4	-0.05	0.00	3.971	11.253	797.5	0.05	0.00	11.151	0.102	0.101
		0.05260	4.608	11.345	857.0	0.01	0.00	4.550	11.416	851.7	0.09	0.01	11.329	0.087	0.094
		0.05726	5.265	11.552	916.2	0.10	0.01	5.231	11.590	913.2	0.15	0.01	11.536	0.054	0.064
		0.06220	6.058	11.701	980.5	0.14	0.01	6.020	11.736	977.5	0.18	0.02	11.697	0.039	0.050
		0.06756	6.872	11.931	1049.1	0.25	0.02	6.906	11.901	1051.7	0.21	0.02	11.945	-0.044	-0.061
		0.07291	7.687	12.175	1107.1	0.40	0.03	7.679	12.181	1106.5	0.40	0.03	12.172	0.009	0.013
		0.08498	9.602	12.695	1245.7	0.71	0.06	9.613	12.688	1246.3	0.71	0.06	12.698	-0.010	-0.018
		0.09209	10.756	12.999	1321.3	0.92	0.08	10.923	12.899	1331.6	0.80	0.07	13.029	-0.130	-0.247
		0.11348	14.828	13.642	1554.9	1.28	0.10	14.703	13.700	1548.3	1.34	0.11	13.624	0.076	0.179
		0.13307	18.857	14.186	1753.4	1.61	0.13	18.926	14.160	1756.6	1.58	0.13	14.170	-0.010	-0.028
		0.13642	19.884	14.162	1800.6	1.54	0.12	19.836	14.180	1798.3	1.56	0.12	14.223	-0.043	-0.122
		0.14432	21.463	14.420	1870.7	1.73	0.14	21.590	14.378	1876.2	1.68	0.13	14.426	-0.047	-0.140
		0.16114	25.408	14.799	2035.3	1.96	0.15	26.096	14.602	2052.7	1.74	0.14	14.852	-0.250	-0.829
		0.17753	29.569	15.113	2195.7	2.15	0.17	30.597	14.857	2233.5	1.86	0.14	15.203	-0.346	-1.265
		0.19461	33.876	15.478	2350.2	2.39	0.18	35.543	15.111	2407.3	1.98	0.15	15.581	-0.470	-1.864
		0.21865	40.677	15.870	2575.3	2.63	0.20	43.278	15.385	2656.3	2.09	0.16	16.006	-0.621	-2.795
		0.23705	46.176	16.149	2743.8	2.80	0.21	49.506	15.596	2841.1	2.18	0.16	16.281	-0.685	-3.344
		0.26636	55.859	16.498	3017.8	2.98	0.22	60.809	15.812	3148.7	2.22	0.16	16.640	-0.828	-4.544
		0.31178	72.757	16.921	3444.2	3.17	0.23	80.724	16.064	3627.9	2.23	0.16	17.070	-1.006	-6.461
		0.35319	90.167	17.218	3834.2	3.28	0.24	101.823	16.203	4074.5	2.16	0.15	17.359	-1.156	-8.412
		0.40310	114.072	17.471	4312.6	3.33	0.24	130.838	16.313	4618.7	2.06	0.14	17.546	-1.232	-10.226
		0.45946	145.984	17.603	4878.7	3.25	0.23	169.580	16.333	5258.2	1.85	0.13	17.688	-1.355	-12.825
		0.52890	190.234	17.751	5589.2	3.17	0.22	223.350	16.383	6034.5	1.66	0.11	17.817	-1.434	-15.627
		0.59722	240.317	17.834	6259.6	3.05	0.21	283.343	16.424	6796.8	1.49	0.10	17.818	-1.394	-17.149
		0.63096	268.483	17.826	6572.1	2.96	0.20	317.991	16.380	7152.4	1.36	0.09	17.805	-1.425	-18.522

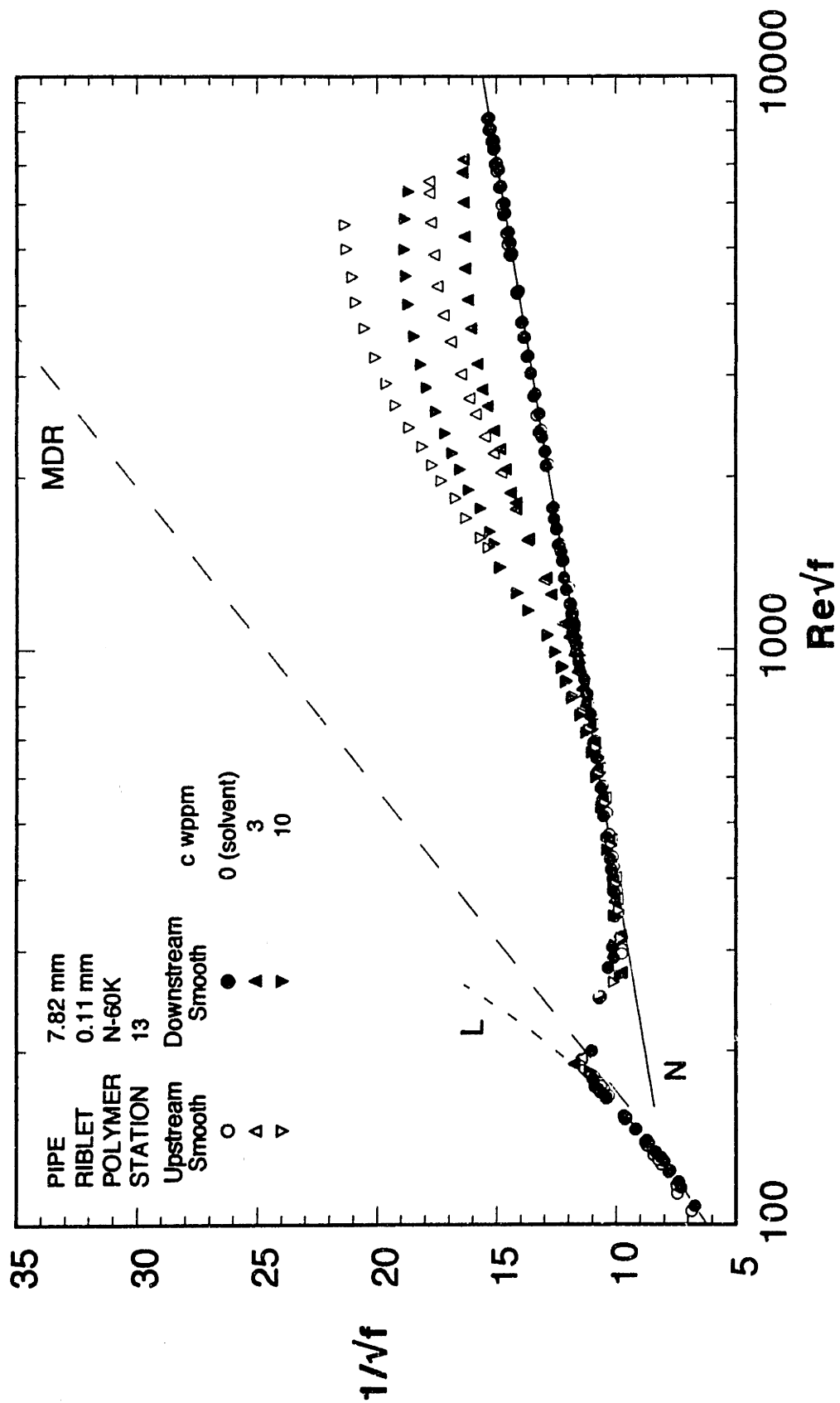
PEO

PIPE

S1:
d = 0.308
h = smooth
SID:
d = 0.308
h = smooth
ΔL = 1.01

0.308" Pipe/Degradation
Receptor1= 360

Series	Q (L/s)	Tw (S1)	1/sgf(S1)	Reopf(S1)	S'(S1)	SF(S1)	Tw(Std)	1/sgf(Std)	Reopf(Std)	S'(Std)	SF(Std)	1/sgf1	A'	Δ/Trec
PIPE														
SI:														
d = 0.308														
h = smooth														
STD:														
d = 0.308														
h = smooth														
AL = 1.01														
RUN	0.01127	0.223	11.064	184.4	0.223	0.01	0.222	11.079	184.2	0.222	0.02	9.973	0.148	0.064
DATE	0.01471	0.450	10.087	264.0	0.450	0.00	0.480	9.832	270.8	0.480	0.02	10.186	0.188	0.099
POLY	0.01702	0.649	9.782	314.9	0.649	0.00	0.615	10.048	306.5	0.615	0.01	10.417	0.186	0.119
s wppm	0.01916	0.807	9.877	351.9	0.807	0.01	0.775	10.078	344.9	0.775	0.01	10.657	0.141	0.104
nr	0.02148	0.992	9.988	390.1	0.992	0.02	0.966	10.119	385.0	0.966	0.01	10.788	0.213	0.176
Stations	0.02564	1.352	10.209	458.4	1.352	0.00	1.309	10.374	449.2	1.309	0.01	10.865	0.160	0.145
	0.03103	1.893	10.442	540.1	1.893	-0.01	1.836	10.603	532.0	1.836	0.02	11.065	0.149	0.148
	0.03568	2.386	10.692	606.5	2.386	0.00	2.335	10.808	599.9	2.335	0.01	11.331	0.137	0.137
	0.04007	2.945	10.811	673.8	2.945	-0.01	2.845	10.999	662.2	2.845	0.02	11.697	0.124	0.124
	0.04414	3.383	11.110	723.7	3.383	0.01	3.314	11.225	716.3	3.314	0.03	11.931	0.104	0.104
	0.04844	3.893	11.366	776.4	3.893	0.02	3.817	11.480	768.7	3.817	0.03	12.182	0.076	0.076
	0.05342	4.439	11.739	829.0	4.439	0.04	4.378	11.821	823.3	4.378	0.05	12.498	0.052	0.052
	0.05819	4.957	12.160	876.0	4.957	0.06	5.024	12.018	882.0	5.024	0.07	12.802	0.038	0.038
	0.06253	5.640	12.190	934.4	5.640	0.07	5.577	12.258	929.2	5.577	0.08	13.157	0.011	-0.020
	0.06841	6.408	12.514	991.4	6.408	0.08	6.369	12.550	986.6	6.369	0.09	14.157	-0.057	-0.114
	0.07459	7.268	12.809	1058.4	7.268	0.09	7.233	12.840	1055.9	7.233	0.10	14.786	0.054	0.126
	0.08716	8.739	13.650	1168.4	8.739	0.15	8.751	13.641	1169.2	8.751	0.15	15.447	-0.367	-0.946
	0.09632	9.939	14.144	1248.9	9.939	0.18	10.002	14.100	1252.8	10.002	0.18	16.447	-0.566	-1.561
	0.11223	12.320	14.803	1390.5	12.320	0.22	12.258	14.840	1386.5	12.258	0.22	16.833	-0.844	-2.898
	0.12525	14.324	16.320	1502.6	14.324	0.24	14.783	15.080	1528.5	14.783	0.25	17.574	-1.056	-4.031
	0.13307	16.516	16.840	1563.9	16.516	0.26	16.282	15.267	1602.0	16.282	0.26	18.479	-1.329	-6.088
	0.14993	18.200	16.271	1693.8	18.200	0.30	19.665	16.141	1998.6	19.665	0.30	19.050	-1.523	-7.780
	0.16573	21.334	16.711	1833.8	21.334	0.32	22.868	16.141	2062.3	22.868	0.32	19.534	-1.664	-8.313
	0.18534	24.630	17.288	1970.4	24.630	0.35	26.980	16.518	2203.9	26.980	0.35	19.944	-1.777	-11.343
	0.20202	27.971	17.683	2099.8	27.971	0.37	30.813	16.848	2382.8	30.813	0.37	20.413	-1.964	-14.285
	0.22233	32.339	18.099	2257.8	32.339	0.39	36.020	17.150	2503.9	36.020	0.39	20.843	-2.160	-18.088
	0.24806	37.874	18.660	2443.4	37.874	0.42	42.928	17.527	2801.3	42.928	0.42	21.039	-2.241	-21.213
	0.27912	45.283	19.202	2671.7	45.283	0.44	52.028	17.914	2863.8	52.028	0.44	21.276	-2.418	-25.479
	0.30998	53.590	19.602	2906.5	53.590	0.46	62.391	18.167	3136.0	62.391	0.46	21.352	-2.522	-30.136
	0.35319	66.327	20.076	3233.5	66.327	0.47	78.542	18.449	3518.6	78.542	0.47	21.393	-2.718	-36.263
	0.40664	84.019	20.637	3839.2	84.019	0.48	101.520	18.683	4000.4	101.520	0.48			
	0.45946	103.819	20.875	4045.4	103.819	0.48	128.038	18.798	4492.5	128.038	0.48			
	0.51165	125.853	21.030	4471.7	125.853	0.48	157.753	18.858	4986.7	157.753	0.48			
	0.58024	159.323	21.281	5000.2	159.323	0.48	203.497	18.830	5651.0	203.497	0.48			
	0.64772	197.399	21.344	5515.9	197.399	0.47	257.847	18.675	6304.1	257.847	0.47			



0.308" Pipe/Degradation
Resqfit= 350

PPE
SI:
d = 0.308
h = smooth
SID:
d = 0.308
h = smooth
AL = 0.73

Series	Q (L/s)	Tw (SI)	1/sqrt(SI)	Resqf (SI)	S' (SI)	SF (SI)	Tw (SID)	1/sqrt(SID)	Resqf (SID)	S' (SID)	SF (SID)	1/wqfH	Δ	Δ/ires
PEO														
RLM 274	0.01039	0.194	10.929	176.2			0.197	10.831	177.8			10.020	0.170	0.0982
DATE 7/24/94	0.01254	0.256	11.487	202.7			0.265	11.284	208.3			10.146	0.181	0.1173
POLY W-301	0.01447	0.459	9.885	272.0			0.437	10.129	265.5			10.386	0.168	0.1291
c wppm 1	0.01677	0.620	9.854	316.6	0.14	0.01	0.631	9.771	319.3	0.32	0.03	11.020	0.177	0.1597
nr 1.00	0.02026	0.873	10.028	375.9	0.09	0.01	1.037	10.327	409.8	0.28	0.03	10.146	0.168	0.1291
Station 12	0.02272	1.071	10.165	416.2	0.09	0.01	1.406	10.534	478.1	0.24	0.02	10.386	0.177	0.1597
	0.02703	1.445	10.409	484.7	0.07	0.01	1.837	10.798	548.0	0.24	0.02	11.020	0.177	0.1597
	0.03161	1.889	10.648	555.7	0.07	0.02	2.515	11.182	641.8	0.35	0.03	11.053	0.129	0.1404
	0.03851	2.561	11.061	647.6	0.24	0.02	3.731	11.906	782.3	0.73	0.07	11.798	0.108	0.1527
	0.04968	3.782	11.826	787.5	0.64	0.06	4.734	12.401	882.0	1.02	0.09	12.341	0.060	0.0998
	0.05829	4.765	12.360	884.9	0.97	0.09	5.507	12.667	950.7	1.15	0.10	12.662	0.005	0.0092
	0.06421	5.517	12.656	951.6	1.14	0.10	6.266	13.055	1013.5	1.43	0.12	13.043	0.012	0.0234
	0.07059	6.258	13.062	1012.9	1.44	0.12	7.280	13.225	1067.7	1.48	0.13	13.368	-0.143	-0.3137
	0.07708	7.220	13.280	1083.2	1.54	0.13	8.000	13.453	1119.1	1.66	0.14	13.758	-0.305	-0.7146
	0.08219	7.794	12.630	1104.5	1.86	0.16	9.631	13.958	1259.4	1.96	0.16	13.930	0.028	0.0756
	0.09358	9.672	13.929	1262.1	1.92	0.16	11.708	14.577	1393.2	2.40	0.20	14.780	-0.203	-0.6241
	0.10775	11.454	14.737	1378.0	2.58	0.21	14.432	15.110	1549.5	2.75	0.22	15.041	0.069	0.2439
	0.12401	14.559	15.044	1556.3	2.68	0.22	16.904	15.313	1681.4	2.81	0.22	15.615	-0.302	-1.1700
	0.13602	16.425	15.535	1657.4	3.06	0.25	19.550	15.653	1808.8	3.02	0.24	15.924	-0.271	-1.1548
	0.14952	18.973	15.889	1781.9	3.29	0.26	23.271	16.010	1973.5	3.23	0.25	16.110	-0.100	-0.4741
	0.16685	23.045	16.089	1963.9	3.32	0.26	27.776	16.174	2156.4	3.24	0.25	16.522	-0.348	-1.8252
	0.18416	26.890	16.457	2119.3	3.55	0.28	32.695	16.307	2339.9	3.23	0.25	16.809	-0.502	-2.8843
	0.20143	31.079	16.725	2281.3	3.69	0.28	42.324	16.512	2662.3	3.21	0.24	17.173	-0.661	-4.3718
	0.23207	39.498	17.093	2571.9	3.85	0.29	56.337	16.666	3071.1	3.12	0.23	17.388	-0.722	-5.5641
	0.27024	66.815	17.347	2950.4	3.87	0.29	72.797	16.724	3491.0	2.95	0.21	17.485	-0.761	-6.6893
	0.30826	66.815	17.456	3344.5	3.76	0.27	101.717	16.753	4126.5	2.69	0.19	17.565	-0.812	-8.4514
	0.36501	92.720	17.547	3939.7	3.56	0.25	136.380	16.704	4777.5	2.39	0.17	17.560	-0.856	-10.2770
	0.42144	123.094	17.583	4538.8	3.35	0.24	190.088	16.658	5640.0	2.05	0.14	17.472	-0.814	-11.5138
	0.49616	172.361	17.493	5370.6	2.97	0.20	236.090	16.624	6282.2	1.83	0.12	17.420	-0.796	-12.5226
	0.55182	214.373	17.445	5986.3	2.74	0.19	285.190	16.642	6893.4	1.69	0.11	17.344	-0.702	-12.1497
	0.60714	261.157	17.391	6596.6	2.51	0.17	361.678	16.562	7668.4	1.42	0.09	17.175		
	0.68040	333.633	17.244	7365.0	2.18	0.14								

0.308" Pipe/Degradation
 Refcrite= 350

Series	Q (L/s)	Tw (S1)	1/sq(S1)	Resq(S1)	S' (S1)	SF (S1)	Tw (S1D)	1/sq(S1D)	Resq(S1D)	S' (S1D)	SF (S1D)	1/sqH	A'	Δt/hrs
PEE														
S1:														
d = 0.308														
h = smooth														
S1D:														
d = 0.308														
h = smooth														
ΔL = 0.73														
PEO														
RUN	0.00726	0.133	9.216	145.7	0.15	0.02	0.135	9.143	146.9	0.36	0.04	10.040	0.195	0.1155
DATE	0.00924	0.172	10.309	165.9	0.06	0.01	0.163	10.590	161.5	0.36	0.04	10.125	0.274	0.1780
POLY	0.01221	0.253	11.230	201.5	0.12	0.01	0.266	10.952	206.6	0.30	0.03	10.403	0.200	0.1531
c wppm	0.01414	0.421	10.087	260.2	0.37	0.03	0.413	10.187	257.7	0.51	0.05	10.845	0.171	0.1525
nr	0.01549	0.531	9.843	292.3	0.76	0.07	0.531	9.838	292.4	0.92	0.09	11.472	0.198	0.2166
Station	0.01749	0.670	9.693	328.8	1.65	0.15	0.655	10.000	325.3	1.73	0.16	12.687	0.110	0.1580
	0.02058	0.880	10.060	377.5	2.24	0.20	0.850	10.235	371.0	2.31	0.21	13.464	0.105	0.1768
	0.02275	1.077	10.148	418.0	3.04	0.26	1.077	10.399	407.9	3.27	0.28	14.891	0.058	0.1110
	0.02687	1.418	10.445	479.7	4.82	0.40	1.376	10.603	472.6	5.46	0.45	17.504	0.100	0.3876
	0.03138	1.779	10.891	538.2	6.60	0.52	1.799	11.016	532.2	7.72	0.58	19.420	0.057	0.2429
	0.03852	2.367	11.530	621.1	8.60	0.60	2.310	11.670	613.7	10.43	0.65	20.964	0.208	1.0114
	0.05042	3.364	12.727	741.4	11.67	0.79	3.327	12.797	737.3	14.86	0.81	23.968	0.052	-0.0582
	0.05952	4.165	13.502	824.7	15.85	0.99	4.123	13.569	820.6	19.42	1.00	26.998	-0.849	-5.5235
	0.06673	4.839	14.042	888.8	21.29	1.32	4.813	14.080	886.4	24.96	1.23	29.964	-1.238	-9.2016
	0.07345	5.473	14.535	943.9	27.64	1.72	5.472	14.536	943.8	31.26	1.46	31.26	-3.1422	-12.1142
	0.08105	6.341	14.900	1011.7	32.59	2.08	6.348	14.891	1012.3	35.31	1.62	33.53	-1.379	-12.1142
	0.11633	10.192	16.868	1297.4	42.89	3.31	10.580	16.555	1321.9	47.47	0.50	35.31	-1.462	-17.5532
	0.13602	12.523	17.792	1444.2	55.55	4.45	12.640	17.709	1450.9	62.72	0.52	37.53	-1.376	-18.7287
	0.13606	12.947	17.504	1463.4	52.4	4.43	12.968	17.490	1464.6	52.3	0.43	35.31	-1.379	-12.1142
	0.14952	14.478	18.190	1553.2	60.52	5.55	14.739	18.028	1567.2	65.65	0.46	37.53	-1.238	-9.2016
	0.17070	17.815	18.721	1723.4	68.18	6.49	17.516	18.880	1708.8	72.79	0.51	37.53	-1.376	-18.7287
	0.18992	20.782	19.284	1861.7	73.3	7.52	21.292	19.052	1884.5	79.47	0.52	37.53	-1.379	-12.1142
	0.20910	23.500	19.967	1979.7	77.38	8.57	24.538	19.540	2022.9	81.3	0.50	37.53	-1.462	-17.5532
	0.22825	27.123	20.287	2127.3	81.3	9.57	26.998	19.620	2199.6	85.31	0.51	37.53	-1.376	-18.7287
	0.26071	33.387	20.885	2360.2	85.31	10.49	31.353	19.746	2496.5	89.47	0.50	37.53	-1.379	-12.1142
	0.30826	45.787	21.087	2764.2	89.47	11.65	37.533	19.747	2951.8	94.37	0.46	37.53	-1.462	-17.5532
	0.36501	63.680	21.173	3259.3	94.37	13.26	52.213	19.891	3469.4	100.00	0.45	37.53	-1.376	-18.7287
	0.42144	84.418	21.232	3753.1	99.43	15.00	72.156	19.664	4032.2	106.64	0.40	37.53	-1.462	-17.5532
	0.47753	110.339	21.043	4289.5	106.64	16.91	127.660	19.564	4613.9	114.37	0.37	37.53	-1.376	-18.7287
	0.53330	139.884	20.872	4827.4	114.37	19.00	165.050	19.215	5243.7	123.47	0.33	37.53	-1.379	-12.1142
	0.60714	185.671	20.625	5560.6	123.47	21.46	218.816	18.999	6036.5	133.47	0.29	37.53	-1.462	-17.5532
	0.69862	254.834	20.258	6505.3	133.47	24.46	297.400	18.752	7027.6	144.37	0.25	37.53	-1.443	-24.9688
	0.75307	302.377	20.048	7033.2	144.37	28.06	351.224	18.601	7580.0	156.64	0.23	37.53	-1.298	-25.8381
													-1.229	-26.3682

0.308" Pipe/Degradation
 Receptor1= 350

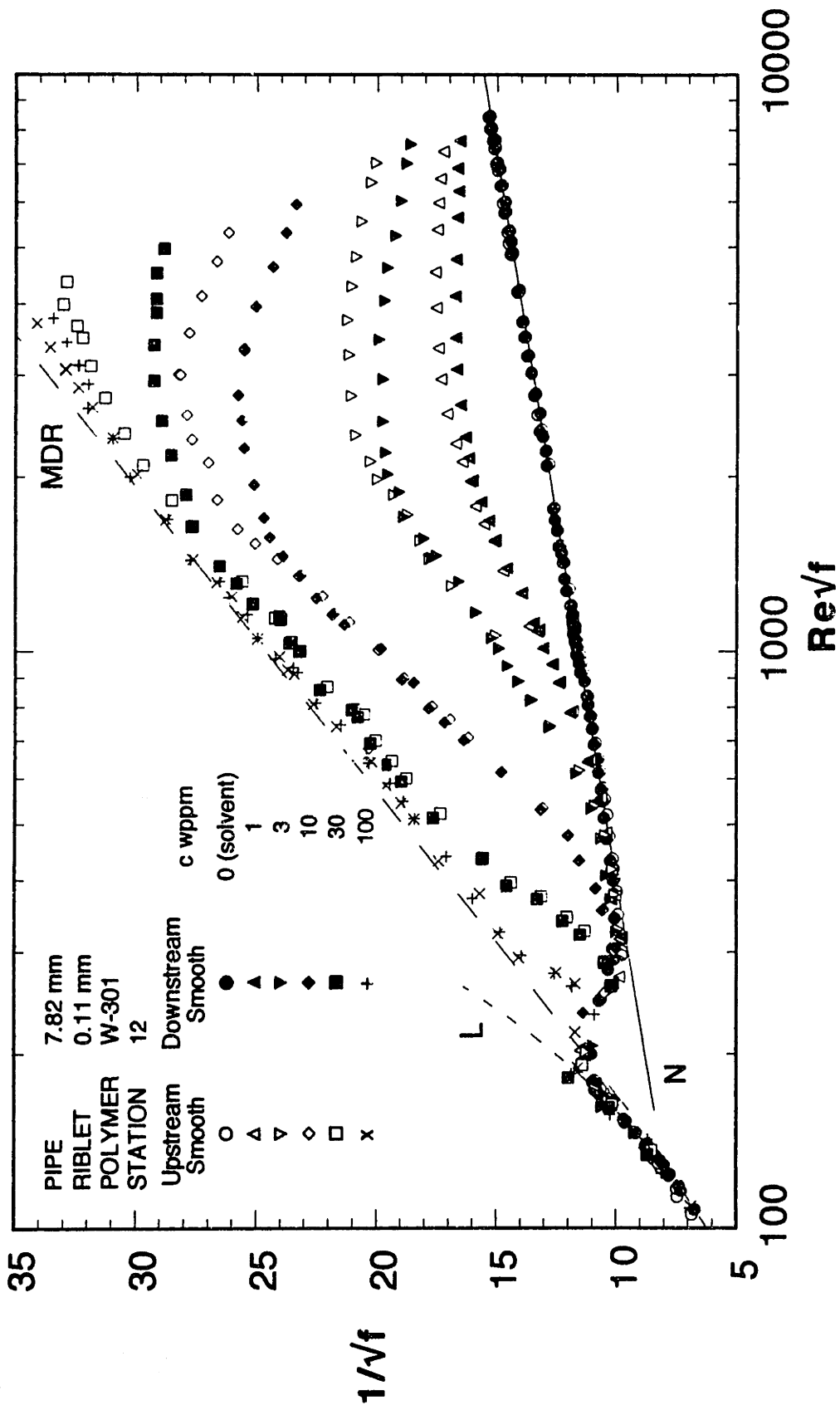
PIPE	Series	Q (L/s)	Tw (S1)	1/sgf(S1)	Reamp(S1)	S'(S1)	SF(S1)	Tw(S1D)	1/sgf(S1D)	Reamp(S1D)	S'(S1D)	SF(S1D)	1/sgf(I)	A'	d'/vres
S1:	RUN 272	0.00920	0.172	10.273	163.2			0.178	10.090	166.2					
d = 0.308	DATE 7/22/94	0.01194	0.230	11.517	189.2			0.230	11.538	188.8					
h = smooth	POLY W-301	0.01466	0.417	10.503	254.8			0.357	11.363	235.0					
S1D:	c vpppm 10	0.01663	0.582	10.090	301.6	0.79	0.08	0.593	10.000	304.3	0.72	0.07		-0.082	-0.0480
d = 0.308	nr 1.02	0.02048	0.02	10.590	354.2	0.87	0.09	0.812	10.524	356.4	0.90	0.09		0.033	0.0219
h = smooth	Staktien 12	0.02274	0.960	10.830	388.1	1.04	0.14	0.956	10.856	387.1	1.42	0.14		0.050	0.0390
		0.02724	1.196	11.528	433.6	1.38	0.16	1.454	12.000	478.7	1.68	0.16		0.180	0.0161
		0.03126	1.457	11.987	479.2	1.66	0.16	1.454	12.000	478.7	1.68	0.16		0.180	0.1943
		0.03797	1.811	13.061	534.7	2.55	0.24	1.783	13.182	530.6	2.66	0.25		0.180	0.1943
		0.04953	2.404	14.788	616.7	4.03	0.37	2.409	14.774	617.3	4.01	0.37		-0.023	-0.0327
		0.06227	3.177	16.172	709.5	5.17	0.47	3.106	16.356	701.5	5.37	0.49		0.303	0.5371
		0.07000	3.663	16.930	762.0	5.60	0.52	3.564	17.163	751.6	6.06	0.55		0.383	0.7845
		0.07700	4.064	17.682	802.2	6.47	0.58	4.001	17.820	796.0	6.62	0.59		0.254	0.5565
		0.08861	4.931	18.472	882.4	7.09	0.62	4.950	18.437	894.0	7.05	0.62		-0.068	-0.1727
		0.09317	5.240	18.841	900.3	7.42	0.65	5.184	18.943	895.5	7.53	0.66		0.201	0.5333
		0.10879	6.389	19.924	1005.2	8.32	0.72	6.461	19.812	1010.8	8.19	0.71		-0.170	-0.5255
		0.12828	7.899	21.126	1122.3	9.33	0.79	7.736	21.349	1110.7	9.57	0.81		0.340	1.2444
		0.13802	8.355	21.781	1159.2	9.92	0.84	8.310	21.840	1156.0	9.99	0.84		0.116	0.4606
		0.14952	9.665	22.262	1246.7	10.28	0.86	9.456	22.507	1233.1	10.54	0.88		0.320	1.3850
		0.16878	11.379	23.180	1352.8	11.04	0.91	11.301	23.240	1348.1	11.12	0.92		0.120	0.5769
		0.18800	12.995	24.140	1445.7	11.90	0.97	13.239	23.917	1459.2	11.66	0.95		0.320	1.3850
		0.20719	14.641	25.064	1535.1	12.72	1.03	15.360	24.470	1572.3	12.08	0.98		-0.363	-1.9450
		0.22633	16.486	25.803	1629.1	13.36	1.07	17.962	24.720	1700.5	12.20	0.97		-0.886	-5.2313
		0.26262	20.790	26.600	1829.4	14.01	1.11	23.399	25.130	1940.8	12.38	0.97		-1.388	-8.9528
		0.30828	27.809	27.019	2118.5	14.12	1.09	31.212	25.540	2241.2	12.64	0.98		-1.668	-12.4844
		0.34613	33.429	27.711	2318.9	14.65	1.12	37.108	25.620	2508.2	12.42	0.94		-1.903	-16.7175
		0.38518	40.822	27.905	2559.8	14.67	1.11	47.794	25.790	2769.8	12.42	0.93		-2.246	-24.6582
		0.45887	56.432	28.275	3015.2	14.76	1.09	69.165	25.540	3338.1	11.85	0.87		-2.465	-32.2378
		0.45887	56.795	28.185	3009.4	14.67	1.09	69.169	25.540	3321.1	11.85	0.87		-2.480	-32.4320
		0.53330	78.738	27.820	3560.2	14.01	1.02	97.111	25.050	3953.8	11.06	0.79		-2.428	-36.9017
		0.60714	105.759	27.328	4126.0	13.27	0.94	133.285	24.343	4631.9	10.08	0.71		-2.436	-42.1517
		0.68040	139.468	26.669	4733.1	12.37	0.86	175.228	23.792	5305.3	9.29	0.64		-2.415	-46.8221
		0.75307	176.933	26.207	5305.9	11.71	0.81	222.124	23.390	5945.0	8.69	0.59		-2.302	-49.4106

0.308" Pipe/Degradation
 ReamerIt= 350

PIPE		Series		Q (L/s)	Tw (S1)	1/amp(S1)	Reamp (S1)	S' (S1)	SF (S1)	Tw (S1D)	1/amp(S1D)	Reamp (S1D)	S' (S1D)	SF (S1D)	1/amp(I)	Δ'	Δ'/ave
d = 0.308	h = smooth	RUN	DATE														
S1D:	d = 0.308	271	7/21/94														
h = smooth	nr	W-301															
	ScaleIn	30															
	ScaleIn	12															
ΔL = 0.73																	
0.00661	0.126	8.535	136.3	0.124	0.124	8.692	133.0	3.42	0.35	0.124	8.692	133.0	3.42	0.35	12.976	0.318	0.2512
0.00943	0.184	10.170	163.3	0.180	0.180	10.279	161.6	4.61	0.46	0.180	10.279	161.6	4.61	0.46	14.084	0.496	0.4524
0.01237	0.252	11.412	191.1	0.228	0.228	11.998	181.8	5.40	0.53	0.228	11.998	181.8	5.40	0.53	15.638	-0.077	-0.0837
0.01512	0.472	10.193	262.3	0.469	0.469	10.219	261.7	7.20	0.69	0.469	10.219	261.7	7.20	0.69	17.153	0.490	0.7090
0.01707	0.568	10.485	288.3	0.565	0.565	10.509	287.6	8.82	0.82	0.565	10.509	287.6	8.82	0.82	18.632	0.338	0.6084
0.02087	0.728	11.327	326.7	0.705	0.705	11.503	321.7	9.39	0.85	0.705	11.503	321.7	9.39	0.85	19.213	0.421	0.8391
0.02344	0.810	12.059	344.8	0.786	0.786	12.237	339.8	9.63	0.86	0.786	12.237	339.8	9.63	0.86	19.945	0.317	0.7117
0.02772	0.954	13.136	375.1	0.932	0.932	13.294	370.6	11.01	0.97	0.932	13.294	370.6	11.01	0.97	21.893	0.446	1.3743
0.03203	1.062	14.390	396.0	1.034	1.034	14.580	390.9	11.58	1.00	1.034	14.580	390.9	11.58	1.00	23.263	-0.082	-0.3037
0.03821	1.284	15.610	436.0	1.292	1.292	15.561	437.4	12.16	1.03	1.292	15.561	437.4	12.16	1.03	24.035	-0.057	-0.2452
0.05079	1.839	17.335	522.2	1.776	1.776	17.643	513.1	13.21	1.11	1.776	17.643	513.1	13.21	1.11	26.174	-0.034	-0.1634
0.06322	2.435	18.755	600.9	2.380	2.380	18.970	594.1	13.77	1.14	2.380	18.970	594.1	13.77	1.14	26.544	0.293	1.5723
0.06996	2.803	19.342	644.6	2.721	2.721	19.634	635.0	14.35	1.18	2.721	19.634	635.0	14.35	1.18	27.723	-0.011	-0.0649
0.07870	3.304	20.042	699.7	3.232	3.232	20.262	692.1	15.19	1.22	3.232	20.262	692.1	15.19	1.22	28.698	-0.757	-6.2408
0.08948	4.069	20.532	777.1	3.977	3.977	20.769	768.2	15.61	1.26	3.977	20.769	768.2	15.61	1.26	29.963	-1.404	-13.8510
0.10810	5.147	22.056	868.4	4.337	4.337	21.013	790.4	15.75	1.29	4.337	21.013	790.4	15.75	1.29	30.765	-1.820	-20.8803
0.12982	6.688	23.236	988.9	6.719	6.719	23.181	1001.2	16.54	1.34	6.719	23.181	1001.2	16.54	1.34	31.608	-2.347	-31.9350
0.13602	7.092	23.640	1033.6	7.147	7.147	23.549	1037.6	16.78	1.35	7.147	23.549	1037.6	16.78	1.35	32.153	-2.888	-45.4238
0.15145	8.531	24.000	1134.0	8.546	8.546	23.978	1135.0	17.39	1.39	8.546	23.978	1135.0	17.39	1.39	32.798	-3.628	-64.6793
0.16424	8.894	24.214	1140.2	8.807	8.807	24.058	1147.6	18.47	1.44	8.807	24.058	1147.6	18.47	1.44	33.008	-3.832	-72.3150
0.16878	9.634	25.169	1205.6	9.656	9.656	25.140	1206.9	19.03	1.36	9.656	25.140	1206.9	19.03	1.36	32.860	-3.692	-77.3315
0.18800	11.583	25.590	1321.1	11.342	11.342	25.837	1308.5	19.78	1.32	11.342	25.837	1308.5	19.78	1.32	32.706	-3.063	-88.8625
0.20719	13.047	26.549	1403.5	13.056	13.056	26.540	1404.0	20.262	1.26	13.056	26.540	1404.0	20.262	1.26			
0.25308	17.071	27.710	1642.8	17.935	17.935	27.660	1645.7	22.982	1.31	17.935	27.660	1645.7	22.982	1.31			
0.28927	22.028	28.527	1824.0	22.982	22.982	27.941	1822.3	27.941	1.34	22.982	27.941	1822.3	27.941	1.34			
0.34613	29.037	29.731	2094.0	31.469	31.469	28.559	2179.9	31.469	1.35	31.469	28.559	2179.9	31.469	1.35			
0.40267	37.362	30.491	2375.1	41.459	41.459	28.945	2501.9	41.459	1.36	41.459	28.945	2501.9	41.459	1.36			
0.47753	49.901	31.289	2744.3	47.065	47.065	29.259	2934.6	47.065	1.34	47.065	29.259	2934.6	47.065	1.34			
0.55182	64.106	31.900	3110.7	57.172	57.172	29.265	3390.8	57.172	1.35	57.172	29.265	3390.8	57.172	1.35			
0.62551	80.639	32.241	3488.0	68.515	68.515	29.170	3855.2	68.515	1.34	68.515	29.170	3855.2	68.515	1.34			
0.66214	89.103	32.468	3664.6	76.174	76.174	29.174	4078.4	76.174	1.34	76.174	29.174	4078.4	76.174	1.34			
0.73496	106.041	33.035	3992.0	110.360	110.360	29.168	4521.2	110.360	1.36	110.360	29.168	4521.2	110.360	1.36			
0.80719	128.882	32.912	4363.5	167.787	167.787	28.845	4978.7	167.787	1.32	167.787	28.845	4978.7	167.787	1.32			

0.306" Pipe/Degradation
Resort/rt= 350

Series	Q (L/s)	Tw (SI)	1/sqrt(SI)	Resqt (SI)	S' (SI)	SF (SI)	Tw (STD)	1/sqrt(STD)	Resqt (STD)	S' (STD)	SF (STD)	1/sqrt	d'	Δ/Trms
PEE														
PEO														
RUN	0.00404	0.091	6.217	99.7			0.086	6.372	97.2					
DATE	0.00487	0.108	6.870	108.9			0.106	6.922	108.1					
POLY	0.00654	0.145	7.952	126.7			0.140	8.099	124.4					
c wppim	0.00802	0.178	8.808	140.5			0.183	8.691	142.4					
nr	0.01043	0.230	10.061	160.2			0.222	10.256	157.1					
Station	0.01418	0.321	11.594	189.3			0.306	11.875	184.9					
	0.01648	0.424	11.711	218.1			0.489	10.912	234.1					
	0.02000	0.625	11.715	265.1			0.610	11.858	261.9					
	0.02223	0.677	12.520	276.3			0.672	12.571	275.2					
	0.02649	0.761	14.060	293.4			0.774	13.944	295.8					
	0.03101	0.922	14.950	323.2			0.935	14.846	325.5					
	0.03813	1.266	15.690	379.1	5.78	0.58	1.219	15.987	372.1	6.10	0.62	15.597	0.390	0.4237
	0.04823	1.645	17.407	432.5	7.26	0.72	1.706	17.094	440.4	6.92	0.68	17.510	-0.416	-0.5717
	0.06030	2.298	18.433	510.9	8.00	0.77	2.299	18.409	511.5	7.97	0.76	18.443	-0.034	-0.0578
	0.06624	2.612	18.973	545.0	8.43	0.80	2.640	18.873	547.9	8.32	0.79	19.020	-0.147	-0.2779
	0.07335	2.998	19.610	584.0	8.94	0.84	3.049	19.446	588.9	8.77	0.82	19.660	-0.214	-0.4464
	0.08334	3.648	20.202	642.6	9.37	0.87	3.609	20.310	639.1	9.49	0.88	20.167	0.143	0.3401
	0.08749	3.976	20.312	664.0	9.42	0.87	3.942	20.400	661.1	9.52	0.87	20.297	0.103	0.2575
	0.10258	4.806	21.660	739.3	10.59	0.96	4.878	21.500	744.8	10.41	0.94	21.734	-0.234	-0.6841
	0.11682	5.713	22.624	810.5	11.39	1.01	5.769	22.513	814.5	11.27	1.00	22.655	-0.142	-0.4721
	0.13602	7.229	23.418	914.5	11.97	1.05	7.309	23.289	919.6	11.83	1.03	23.508	-0.219	-0.8479
	0.14034	7.520	23.689	929.8	12.22	1.06	7.655	23.479	938.1	11.99	1.04	23.748	-0.269	-1.0764
	0.14952	8.289	24.040	979.5	12.48	1.08	8.173	24.209	972.7	12.66	1.10	23.992	0.217	0.9250
	0.16685	9.565	24.973	1052.4	13.28	1.14	9.583	24.950	1053.3	13.26	1.13	24.979	-0.029	-0.1376
	0.18608	11.336	25.583	1145.9	13.75	1.16	11.526	25.371	1155.5	13.52	1.14	25.628	-0.257	-1.3634
	0.20527	13.320	26.035	1242.4	14.06	1.17	13.208	26.145	1237.2	14.18	1.18	26.011	0.134	0.7824
	0.22251	14.932	26.655	1315.7	14.58	1.21	15.073	26.530	1321.9	14.44	1.20	26.705	-0.175	-1.1121
	0.25308	17.930	27.666	1441.8	15.43	1.26	17.809	27.760	1437.0	15.53	1.27	27.628	0.132	0.9521
	0.30826	24.363	28.791	1688.0	16.28	1.30	24.738	28.689	1694.0	16.17	1.29	28.812	-0.123	-1.0797
	0.38366	35.144	29.973	2019.5	17.15	1.34	34.435	30.280	1999.0	17.48	1.37	29.900	0.360	4.1553
	0.45887	47.000	30.983	2335.1	17.91	1.37	46.949	31.000	2333.9	17.93	1.37	30.979	0.021	0.2733
	0.53330	60.152	31.829	2641.1	18.54	1.40	59.505	32.002	2626.8	18.72	1.41	31.789	0.213	3.2395
	0.58874	70.765	32.397	2859.5	18.97	1.41	72.532	31.989	2894.9	18.55	1.38	32.487	-0.468	-8.1800
	0.64364	81.848	32.943	3078.4	19.39	1.43	84.453	32.431	3127.0	18.85	1.39	33.055	-0.624	-11.4522
	0.64364	81.955	32.922	3065.6	19.38	1.43	84.747	32.375	3117.4	18.80	1.38	33.033	-0.658	-12.0647
	0.71681	97.611	33.585	3358.1	19.88	1.45	101.744	32.896	3428.4	19.16	1.39	33.697	-0.801	-16.3721
	0.80719	119.864	34.130	3700.6	20.26	1.46	124.820	33.445	3776.3	19.54	1.40	34.250	-0.805	-18.5099



0.308" Pipe/Degradation
Resprc(1= 350

Series
PEO

PIPE
S1:
d = 0.308
h = smatch
SID:
d = 0.308
h = smatch
AL = 1.01

RUN 294
DATE 9/77/94
POLY W-301
e supplm
vr 1.00
Stuckim
13

Q (L/s)	Tw (S1)	1/sgf(S1)	Resprc (S1)	S (S1)	SF (S1)	Tw (SID)	1/sgf(SID)	Resprc (SID)	S (SID)	SF (SID)	1/sgfI	Δ	Δ/vres
0.01150	0.235	11.070	188.2			0.225	1.311	184.2					
0.01521	0.525	9.720	281.7			0.532	9.662	283.4					
0.01922	0.833	9.750	355.5	-0.05	-0.01	0.800	9.945	348.5					
0.02174	1.038	9.880	396.9	-0.11	-0.01	1.009	10.020	391.3	0.05	0.00	9.861	0.010	0.0045
0.02654	1.460	10.170	470.6	-0.12	-0.01	1.434	10.261	466.4	-0.01	0.00	10.153	0.010	0.0055
0.03037	1.829	10.400	527.9	-0.09	-0.01	1.799	10.485	523.6	0.01	0.00	10.383	0.005	0.0031
0.03655	2.490	10.840	616.1	0.08	0.01	2.471	10.882	613.7	0.13	0.01	10.827	0.055	0.0421
0.04172	2.975	11.200	674.5	0.28	0.03	2.972	11.206	674.6	0.29	0.03	11.196	0.010	0.0084
0.04582	3.421	11.470	723.7	0.43	0.04	3.432	11.451	724.9	0.41	0.04	11.478	-0.027	-0.0257
0.05087	3.960	11.790	778.7	0.62	0.06	3.978	11.763	780.4	0.59	0.05	11.804	-0.041	-0.0429
0.05545	4.487	12.120	828.9	0.85	0.08	4.554	12.032	835.0	0.74	0.07	12.155	-0.025	-0.0286
0.06108	5.151	12.460	888.0	1.07	0.09	5.159	12.451	888.7	1.06	0.09	12.463	-0.012	-0.0156
0.06710	5.910	12.780	951.2	1.27	0.11	5.947	12.740	954.2	1.22	0.11	12.795	-0.055	-0.0756
0.07249	6.615	13.050	1006.4	1.44	0.12	6.625	13.040	1007.2	1.43	0.12	13.086	-0.026	-0.0388
0.07835	7.374	13.360	1055.3	1.67	0.14	7.472	13.272	1062.3	1.67	0.13	13.400	-0.100	-0.1614
0.08861	8.736	13.880	1181.8	2.02	0.17	8.702	13.907	1189.5	2.05	0.17	13.864	0.043	0.0787
0.09968	10.607	14.170	1283.0	2.14	0.18	10.482	14.254	1275.5	2.23	0.19	14.152	0.102	0.2094
0.10941	11.939	14.660	1364.3	2.52	0.21	11.794	14.750	1355.9	2.62	0.22	14.610	0.140	0.3155
0.13575	16.127	15.650	1585.5	3.25	0.26	16.462	15.490	1602.0	3.07	0.25	15.702	-0.212	-0.5928
0.14569	17.950	16.920	1672.9	3.43	0.27	18.769	15.569	1710.6	3.04	0.24	16.007	-0.438	-1.3141
0.16087	21.058	16.230	1811.9	3.60	0.28	22.417	15.731	1859.4	3.04	0.24	16.370	-2.1190	-2.7767
0.17787	24.639	16.590	1959.9	3.82	0.30	26.746	15.923	2042.0	3.08	0.24	16.681	-0.758	-2.7767
0.19490	28.950	16.770	2124.5	3.86	0.30	31.804	16.000	2226.7	3.01	0.23	16.901	-0.901	-3.6174
0.21187	33.410	16.970	2282.2	3.94	0.30	37.258	16.070	2410.1	2.94	0.22	17.065	-0.995	-4.3426
0.24945	45.032	17.210	2649.5	3.92	0.29	50.534	16.230	2809.6	2.84	0.21	17.301	-1.071	-5.5029
0.28670	58.192	17.400	3012.0	3.88	0.29	66.884	16.230	3229.1	2.69	0.19	17.462	-1.232	-7.2753
0.32948	75.982	17.500	3441.7	3.75	0.27	87.475	16.310	3692.9	2.44	0.18	17.525	-1.215	-8.2464
0.38636	93.620	17.530	3820.4	3.60	0.26	110.303	16.150	4146.8	2.08	0.15	17.507	-1.357	-10.2402
0.42684	128.101	17.460	4466.9	3.26	0.23	149.730	16.150	4831.4	1.81	0.13	17.378	-1.228	-10.7982
0.48652	169.324	17.310	5137.8	2.87	0.20	196.463	16.070	5534.3	1.50	0.10	17.279	-1.209	-12.1156
0.52229	195.816	17.280	5525.1	2.71	0.19	231.418	15.895	6006.5	1.18	0.08	17.213	-1.318	-14.1758
0.55794	224.768	17.230	5906.2	2.54	0.17	264.379	15.887	6405.5	1.06	0.07	17.136	-1.249	-14.3551
0.62943	291.140	17.080	6646.1	2.19	0.15	334.937	15.924	7128.5	0.91	0.06	16.967	-1.043	-13.5197

0.308" Pipe/Degradation
Reoffer11= 360

Series	Q (L/s)	Tw (S1)	1/wpf(S1)	Rmpf(S1)	S'(S1)	SF(S1)	Tw(S1D)	1/wpf(S1D)	Rmpf(S1D)	S'(S1D)	SF(S1D)	1/wpf1	d'	d'/d
PIPE														
SZ:														
d = 0.308														
h = smooth														
SZD:														
d = 0.308														
h = smooth														
AL = 1.01														
PEO														
RUN 296	0.01138	0.233	10.910	185.2	0.27	0.03	0.237	10.820	186.8	0.33	0.03	10.071	0.074	0.0309
DATE 9/8/94	0.01539	0.551	9.603	285.3			0.543	9.673	283.2					0.0559
POLY W-301	0.01788	0.714	9.801	324.8			0.698	9.926	320.7					0.0389
e upper 10	0.02039	0.875	10.090	359.6	0.27	0.03	0.866	10.145	357.7	0.33	0.03	10.071	0.074	0.0309
nr 1.02	0.02281	1.016	10.480	387.4	0.53	0.05	1.000	10.559	384.5	0.62	0.06	10.438	0.121	0.0559
Station 13	0.02751	1.271	11.300	434.4	1.15	0.11	1.262	11.341	432.8	1.20	0.12	11.272	0.069	0.0389
	0.03325	1.598	12.180	487.1	1.83	0.18	1.579	12.253	484.2	1.91	0.16	12.136	0.117	0.0800
	0.03869	1.887	13.040	529.3	2.55	0.24	1.854	13.168	524.7	2.68	0.26	12.947	0.209	0.1602
	0.04472	2.213	13.920	573.2	3.29	0.31	2.185	14.009	569.5	3.39	0.32	13.846	0.163	0.1502
	0.04969	2.483	14.800	608.5	3.86	0.36	2.457	14.876	605.3	3.95	0.37	14.539	0.137	0.1406
	0.05542	2.805	15.320	646.8	4.48	0.41	2.761	15.442	641.7	4.61	0.43	15.223	0.219	0.2606
	0.06166	3.176	16.020	685.2	5.07	0.46	3.228	16.890	693.8	4.93	0.45	16.121	-0.231	-0.2931
	0.06823	3.557	16.750	726.4	5.70	0.52	3.519	16.841	724.4	5.80	0.53	16.860	0.180	0.2537
	0.07438	4.009	17.200	773.3	6.05	0.54	3.994	17.254	770.9	6.11	0.55	17.188	0.066	0.1006
	0.08470	4.633	18.220	833.1	6.94	0.61	4.639	18.207	833.7	6.92	0.61	18.226	-0.019	-0.0330
	0.09111	5.062	18.750	865.9	7.40	0.65	5.008	18.850	862.3	7.51	0.66	18.876	0.174	0.3264
	0.10380	5.994	19.630	947.6	8.12	0.71	6.067	19.511	953.4	7.99	0.69	19.891	-0.180	-0.3844
	0.12088	7.331	20.670	1050.4	8.98	0.77	7.384	20.595	1054.2	8.90	0.76	20.705	-0.110	-0.2736
	0.14179	9.110	21.750	1170.9	9.88	0.83	9.119	21.739	1171.5	9.86	0.83	21.933	-0.194	-0.5654
	0.14863	9.249	22.170	1182.5	10.28	0.86	9.316	22.090	1186.8	10.19	0.86	22.259	-0.169	-0.5075
	0.15891	10.232	23.000	1243.8	11.02	0.92	10.298	22.926	1247.8	10.94	0.91	23.022	-0.098	-0.3139
	0.17598	11.748	23.770	1332.7	11.67	0.96	11.822	23.690	1336.9	11.59	0.96	23.840	-0.144	-0.6227
	0.19297	13.082	24.700	1406.4	12.61	1.03	13.770	24.075	1442.8	11.84	0.97	25.083	-1.008	-4.0049
	0.21180	14.752	25.530	1493.4	13.23	1.08	15.999	24.515	1555.3	12.15	0.98	25.844	-1.329	-5.7971
	0.23060	16.822	26.030	1594.7	13.62	1.10	19.042	24.465	1696.7	11.95	0.95	26.478	-2.013	-9.5604
	0.26236	20.002	26.760	1764.9	14.17	1.13	25.223	24.185	1952.8	11.02	0.89	27.452	-3.267	-17.6652
	0.29590	24.924	27.440	1941.2	14.69	1.15	32.639	23.979	2221.4	10.99	0.85	27.989	-4.010	-24.4427
	0.32545	29.482	27.750	2111.2	14.85	1.15	39.872	23.862	2455.2	10.70	0.81	28.484	-4.622	-30.9853
	0.37889	38.177	28.390	2402.4	15.27	1.16	55.392	23.569	2893.8	10.12	0.75	28.843	-5.274	-41.1577
	0.43717	49.217	28.850	2727.8	15.51	1.16	75.431	23.304	3377.0	9.59	0.70	28.424	-6.120	-46.1053
	0.50432	66.322	28.670	3166.5	15.07	1.11	104.425	22.848	3973.3	8.85	0.63	27.755	-4.907	-50.9698
	0.57543	90.266	28.040	3694.2	14.17	1.02	142.876	22.288	4647.6	8.02	0.56	27.141	-4.854	-57.5259
	0.64635	118.069	27.540	4205.9	13.44	0.95	189.480	21.741	5327.8	7.23	0.50	26.526	-4.785	-63.7086

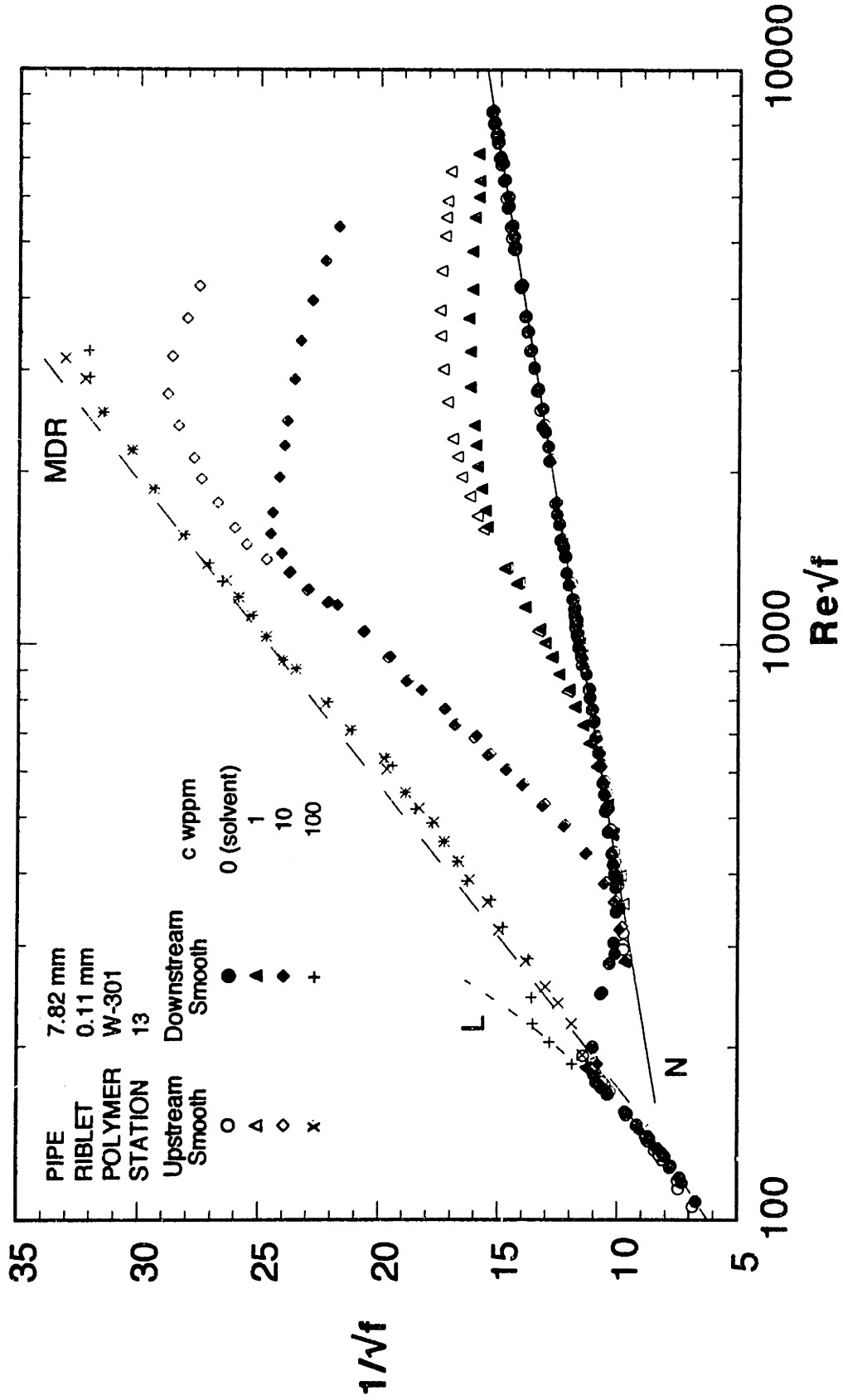
0.308" Pipe/Degradation
 Reference: 350

Series
 PEO

PIPE
 SZ:
 d = 0.308
 h = smooth
 SZD:
 d = 0.308
 h = smooth
 AL = 1.01

RUN 296
 DATE 9/9/94
 PLY W-301
 c vpppm 100
 nr 1.20
 Stellen 13

Q (L/s)	Tw (S1)	1/sgf(S1)	Reapf (S1)	S' (S1)	SF (S1)	Tw (S1D)	1/sgf(S1D)	Reapf (S1D)	S' (S1D)	SF (S1D)	1/sgf(l)	Δ	Δ/1rsm
0.00849	0.194	8.916	143.5	5.63	0.57	0.190	9.025	141.8	5.47	0.56	15.516	-0.021	-0.0157
0.01470	0.352	11.470	193.6	6.23	0.63	0.328	11.893	186.8	6.33	0.64	16.155	0.050	0.0430
0.01733	0.453	11.920	219.6	6.57	0.65	0.391	12.828	204.0	6.80	0.65	16.650	0.040	0.0375
0.01968	0.536	12.450	238.8	7.03	0.69	0.452	13.545	219.5	7.02	0.69	17.263	-0.010	-0.0109
0.02190	0.608	13.000	255.0	7.32	0.71	0.557	13.583	244.1	7.40	0.71	17.685	0.075	0.0887
0.02584	0.749	13.830	283.0	7.84	0.75	0.760	13.731	285.0	7.97	0.76	18.238	0.100	0.1291
0.03166	0.961	14.950	320.6	8.30	0.78	0.980	14.805	323.8	8.31	0.79	18.865	0.015	0.0211
0.03635	1.188	15.440	357.2	8.92	0.83	1.406	15.295	360.6	8.89	0.82	19.810	-0.108	-0.2431
0.04171	1.421	16.200	390.8	9.35	0.83	1.638	16.290	388.5	9.35	0.83	20.244	-0.035	-0.0715
0.04614	1.644	16.660	420.3	10.17	0.92	1.924	16.690	419.5	10.14	0.92	21.185	-0.114	-0.2709
0.05168	1.922	17.260	454.4	11.02	0.98	2.238	17.253	454.6	12.02	1.05	23.488	-0.038	-0.1106
0.05739	2.256	17.690	492.3	12.04	1.05	2.479	17.760	490.4	12.51	1.09	23.962	0.000	0.0003
0.06267	2.511	18.310	520.6	13.05	1.12	2.836	18.310	520.6	13.49	1.14	25.290	-0.038	-0.1452
0.06867	2.839	18.870	553.5	13.52	1.15	3.154	18.880	553.2	14.50	1.21	25.842	0.038	0.1600
0.07867	3.433	19.660	608.6	14.33	1.19	3.761	19.702	635.7	15.73	1.27	27.224	-0.050	-0.2935
0.08253	3.739	19.760	633.8	15.81	1.28	4.066	20.068	650.2	16.68	1.32	28.189	-0.058	-0.4296
0.09857	4.652	21.180	710.2	16.74	1.32	5.816	21.150	711.2	17.34	1.34	30.329	-0.038	-0.3413
0.11527	5.774	22.210	791.2	17.37	1.34	7.586	22.130	794.1	18.30	1.38	31.542	-0.025	-0.2730
0.13950	7.573	23.470	906.1	18.32	1.39	8.111	23.450	906.9	18.64	1.39	32.346	-0.244	-3.0670
0.14763	8.111	24.000	939.8	19.53	1.44	9.754	24.000	939.8	19.53	1.44	33.476	-1.340	-18.8308
0.16662	9.754	24.700	1030.5	19.53	1.44	11.537	25.290	1030.6	19.53	1.44	25.328	0.000	0.0003
0.18554	11.510	25.320	1119.6	19.53	1.44	13.373	25.880	1206.8	19.53	1.44	26.342	0.038	0.1600
0.20442	13.404	25.850	1206.2	19.53	1.44	15.167	26.540	1285.2	19.53	1.44	27.224	0.050	0.2299
0.22325	15.351	26.380	1293.0	19.53	1.44	17.555	27.080	1366.6	19.53	1.44	28.189	-0.100	-0.5062
0.24577	17.513	27.190	1381.0	19.53	1.44	20.068	28.069	1550.2	19.53	1.44	29.428	-0.058	-0.4296
0.26501	21.941	28.170	1545.8	19.53	1.44	22.068	28.069	1668.3	19.53	1.44	30.329	-0.038	-0.3413
0.35834	31.800	29.420	1865.1	19.53	1.44	24.000	29.370	1868.3	19.53	1.44	31.542	-0.025	-0.2730
0.43154	43.422	30.320	2179.5	19.53	1.44	26.342	30.291	2181.6	19.53	1.44	32.346	-0.244	-3.0670
0.52187	58.683	31.540	2533.7	19.53	1.44	28.189	31.517	2535.5	19.53	1.44	33.476	-1.340	-18.8308
0.61075	76.684	32.290	2898.3	19.53	1.44	29.428	32.102	2913.3	19.53	1.44	33.476	-1.340	-18.8308
0.68251	91.027	33.120	3141.4	19.53	1.44	31.542	32.137	3237.5	19.53	1.44	33.476	-1.340	-18.8308



PIPE: 10.21 mm (Upstream and Downstream)

RIBBLETS: 0.11 mm Degradation Experiments

POLYMERS:

NONE (Solvent)

PEO N-60K

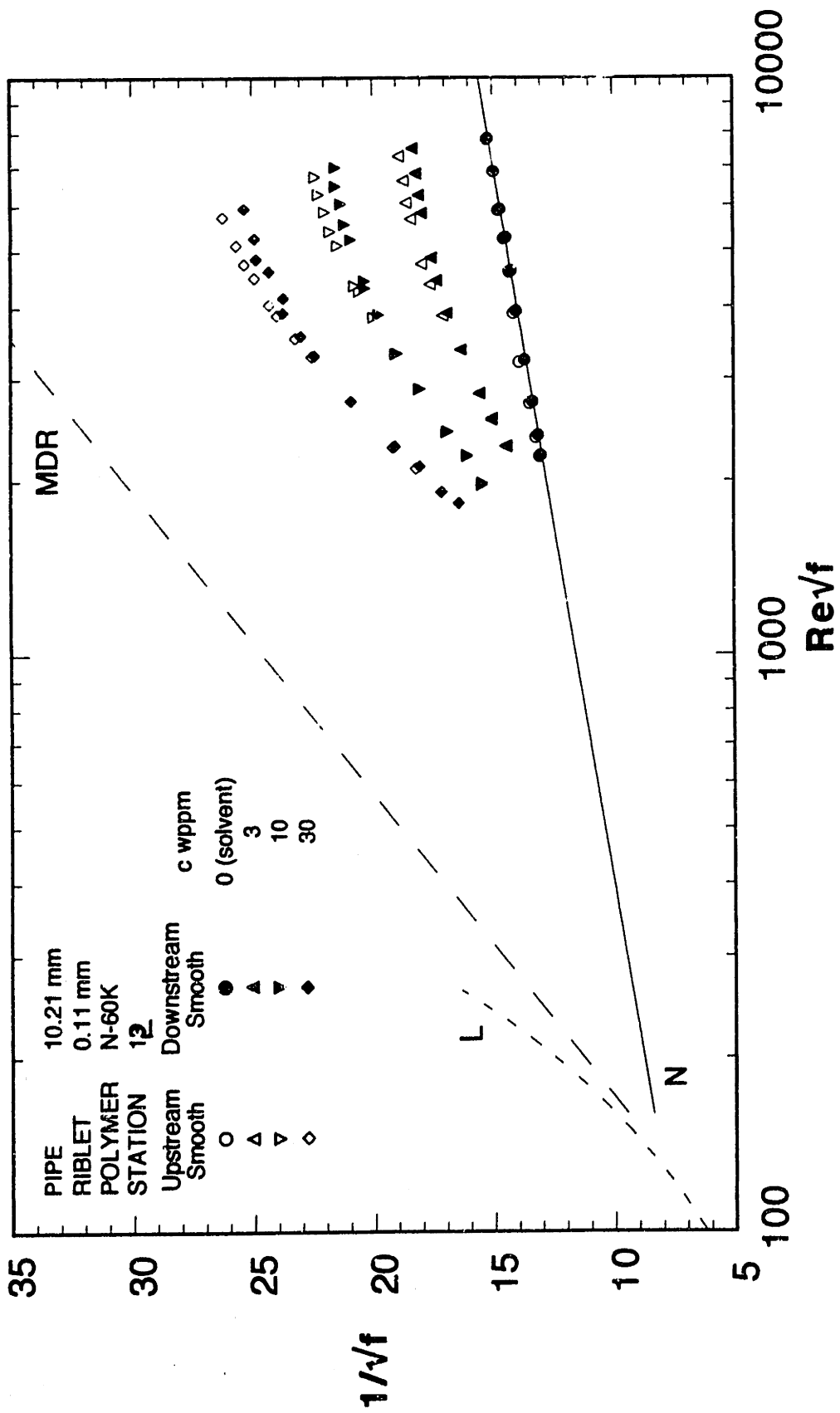
W-301

0.402" Pipe/Degradation
Resqfit = 350

PIPE

SZ:
d = 0.402
h = smooth
SZD:
d = 0.402
h = smooth

Series	Q (L/s)	TW(SZ)	1/sqrt(SZ)	Resqf (SZ)	S' (SZ)	TW(SZD)	1/sqrt(SZD)	Resqf (SZD)	S' (SZD)	1/sqrt(SZD)H	Δ'	Δ/tres
DW												
N-60K	0.87053	244.45	15.184	7824.2	0.01	243.33	15.218	7806.3	0.05	15.170	0.049	
RUN	0.75413	189.44	14.941	6887.2	-0.01	189.11	14.955	6881.2	0.00	14.951	0.004	
DATE	0.63773	139.07	14.747	5987.7	0.06	140.42	14.676	5927.4	-0.02	14.691	-0.015	
POLY	0.56013	110.31	14.543	5252.8	0.06	111.64	14.456	5284.3	-0.04	14.492	-0.036	
c wppm	0.48253	84.65	14.302	4600.8	0.05	85.53	14.228	4624.6	-0.03	14.260	-0.032	
nr	0.40493	60.90	14.150	3901.5	0.18	62.06	14.017	3938.6	0.04	13.981	0.035	
Station	0.32733	41.17	13.911	3207.4	0.19	41.89	13.684	3227.5	0.05	13.635	0.049	
	0.26913	29.66	13.476	2721.9	0.08	29.93	13.368	2734.1	0.02	13.347	0.019	
	0.23033	22.52	13.235	2371.9	0.01	22.90	13.124	2391.9	0.01	13.115	0.009	
	0.21093	19.42	13.053	2202.2	0.08	19.55	13.008	2209.9	0.03	12.977	0.030	
N-60K	0.23968	20.51	14.483	2290.4	1.44	20.47	14.445	2288.4	1.41	14.478	-0.033	-0.0877
RUN	0.27962	25.35	15.086	2546.7	1.86	25.64	15.057	2581.6	1.82	15.115	-0.058	-0.1803
DATE	0.31957	31.30	15.575	2830.3	2.17	31.41	15.548	2835.2	2.14	15.583	-0.035	-0.1239
POLY	0.39946	44.45	16.339	3373.0	2.63	44.44	16.341	3372.6	2.63	16.338	0.003	0.0119
c wppm	0.47935	58.51	17.088	3870.5	3.14	59.75	16.910	3911.3	2.94	17.138	-0.226	-1.2135
nr	0.55924	75.00	17.609	4382.9	3.44	77.32	17.342	4450.4	3.15	17.675	-0.333	-2.0856
Station	0.61916	88.32	17.965	4756.9	3.66	92.47	17.558	4867.4	3.21	18.037	-0.479	-3.3261
	0.75897	126.21	18.422	5688.6	3.80	132.81	17.959	5835.3	3.29	18.487	-0.528	-4.4916
	0.81889	144.27	18.591	6082.6	3.85	152.70	18.070	6257.8	3.28	18.631	-0.561	-5.1424
	0.89879	171.62	18.708	6634.8	3.82	181.41	18.197	6821.2	3.28	18.755	-0.558	-5.6231
	0.99865	207.72	18.894	7300.3	3.84	221.06	18.316	7531.0	3.21	18.967	-0.651	-7.2888
N-60K	0.22170	15.29	15.464	1965.5	2.69	15.56	15.427	1983.0	2.64	15.50	-0.072	-0.1796
RUN	0.25965	19.38	16.082	2212.4	3.10	19.15	16.079	2199.1	3.11	16.04	0.039	0.1143
DATE	0.29960	23.39	16.893	2430.3	3.75	23.20	16.921	2420.7	3.78	16.86	0.061	0.2036
POLY	0.37949	32.98	18.021	2885.9	4.58	32.78	18.075	2877.3	4.64	18.00	0.075	0.3186
c wppm	0.45938	43.26	19.046	3305.8	5.37	43.62	18.967	3319.5	5.28	19.07	-0.107	-0.5502
nr	0.55924	58.39	19.957	3841.0	6.02	59.65	19.745	3882.2	5.79	20.02	-0.274	-1.7150
Station	0.63914	71.87	20.559	4263.2	6.44	73.67	20.306	4316.3	6.17	20.66	-0.357	-2.5529
	0.65911	75.09	20.741	4356.5	6.58	78.09	20.340	4442.6	6.15	20.85	-0.508	-3.7548
	0.79692	103.08	21.458	5104.9	7.03	108.55	20.911	5238.5	6.43	21.60	-0.691	-6.1874
	0.85884	115.56	21.786	5408.1	7.25	122.48	21.162	5587.7	6.50	21.86	-0.698	-6.7195
	0.93873	135.64	21.980	5857.3	7.31	144.57	21.290	6047.0	6.56	22.09	-0.802	-8.4303
	1.01862	156.05	22.236	6284.6	7.44	166.63	21.518	6494.2	6.67	22.31	-0.795	-9.0704
	1.09852	179.28	22.373	6734.8	7.46	193.61	21.529	6998.8	6.55	22.43	-0.901	-11.0896
N-60K	0.21970	13.30	16.429	1827.4	3.78	13.29	16.432	1827.1	3.78	16.43	0.005	0.0113
RUN	0.23968	14.52	17.154	1909.6	4.43	14.56	17.129	1912.3	4.40	17.17	-0.044	-0.1183
DATE	0.27962	17.51	18.223	2097.3	5.34	17.85	18.046	2117.9	5.14	18.34	-0.290	-0.9088
POLY	0.31957	20.64	19.183	2277.1	6.15	20.86	19.081	2289.3	6.04	19.24	-0.158	-0.5665
c wppm	0.41943	29.95	20.900	2743.3	7.55	29.93	20.906	2742.5	7.55	20.90	0.009	0.0440
nr	0.53927	42.60	22.532	3271.9	8.87	43.03	22.417	3288.7	8.75	22.58	-0.162	-0.9774
Station	0.59919	49.52	23.220	3527.2	9.43	50.47	23.000	3561.0	9.19	23.30	-0.303	-2.0352
	0.67908	59.61	23.985	3870.1	10.03	60.94	23.723	3912.8	9.75	24.07	-0.345	-2.6246



0.71903	65.08	24.305	4045.2	10.28	68.45	23.700	4148.5	9.63	24.48	-0.757	-6.0978
0.81889	80.27	24.925	4493.0	10.71	84.40	24.308	4607.1	10.05	25.10	-0.791	-7.2612
0.87881	89.63	25.314	4746.9	11.01	93.28	24.814	4842.5	10.47	25.82	-0.601	-5.9194
0.95870	103.71	25.671	5108.3	11.24	110.10	24.916	5283.1	10.43	25.42	-0.902	-9.6860
1.09852	130.40	26.233	5728.1	11.60	140.02	25.316	5935.7	10.62	26.41	-1.096	-13.4947

WSR-301												
RUN	198d	15.26	16.594	1961.9	3.82	15.19	16.630	1957.7	3.86	16.571	0.059	0.1571
DATE	5/15/93	18.67	17.522	2170.7	4.58	18.85	17.435	2181.5	4.48	17.552	-0.117	-0.3634
POLY	301	20.96	17.846	2300.0	4.80	21.32	17.694	2319.8	4.63	17.9	-0.206	-0.6914
c vppm	3	32.56	19.090	2867.2	5.66	25.77	18.241	2550.4	5.01	18.537	-0.296	-1.1277
nr	1	49.09	20.212	3521.2	6.43	33.30	18.876	2899.7	5.43	19.147	-0.271	-1.2126
Station	13	66.21	20.750	4090.4	6.70	52.03	19.632	3625.3	5.79	20.338	-0.706	-4.1075
		87.04	21.016	4690.5	6.73	71.64	19.948	4254.7	5.83	20.847	-0.899	-6.2345
		117.25	21.125	5445.4	6.58	95.29	20.086	4907.7	5.72	21.056	-0.970	-7.8112
		152.04	21.202	6201.8	6.43	129.77	20.081	5728.5	5.45	21.158	-1.077	-10.1203
		199.28	21.220	7097.2	6.22	170.84	20.002	6574.0	5.13	21.214	-1.212	-13.0195
						225.15	19.964	7543.8	4.85	21.223	-1.259	-15.4970
WSR-301												
RUN	198c	10.90	19.799	1622.2	7.36	11.20	19.531	1644.4	7.07	19.94	0.005	0.0134
DATE	5/15/93	13.35	20.868	1795.8	8.25	13.36	20.862	1796.3	8.24	20.871	-0.009	-0.0289
POLY	301	15.95	21.819	1963.0	9.05	16.05	21.752	1969.1	8.97	21.853	-0.101	-0.3627
c vppm	10	18.65	22.700	2122.7	9.79	19.10	22.434	2147.8	9.51	22.83	-0.396	-1.5954
nr	1.02	27.86	24.766	2594.5	11.51	29.75	23.965	2681.1	10.65	24.989	-1.024	-5.4973
Station	13	42.41	25.928	3201.5	12.30	45.70	24.976	3323.2	11.29	26.131	-1.155	-8.0141
		56.98	26.698	3710.9	12.82	63.51	25.288	3917.9	11.32	26.721	-1.433	-11.8659
		73.15	26.746	4205.2	12.65	81.17	25.392	4429.6	11.21	26.799	-1.407	-13.2270
		90.82	26.861	4685.4	12.58	102.29	25.311	4972.3	10.92	26.872	-1.561	-18.4158
		125.09	26.784	5494.1	12.22	143.22	25.032	5878.8	10.35	26.673	-1.641	-20.2006
WSR-301												
RUN	198b	7.43	23.986	1276.3	11.96	7.45	23.945	1278.4	11.92	24.009	0.002	0.0054
DATE	5/15/93	9.12	25.252	1414.5	13.05	8.93	25.518	1399.7	13.33	25.144	0.002	0.0063
POLY	301	11.26	25.966	1572.1	13.58	11.26	25.976	1571.5	13.59	25.964	0.012	0.0417
c vppm	30	15.61	27.573	1850.8	14.90	15.52	27.650	1845.6	14.99	27.545	0.080	0.3580
nr	1.066	24.77	29.550	2331.8	16.48	24.64	29.626	2325.7	16.56	29.529	0.097	0.5884
Station	13	32.54	30.555	2672.7	17.25	32.77	30.446	2682.3	17.13	30.582	-0.005	-0.0258
		46.44	31.969	3193.4	18.35	44.95	32.496	3141.6	18.91	31.85	0.025	0.2238
		61.36	32.679	3670.7	18.82	60.75	32.844	3652.3	18.99	32.651	0.050	0.5259
		79.94	33.505	4187.9	19.42	86.29	32.249	4351.0	18.09	33.774	-1.525	-18.7681
WSR-301												
RUN	198a	7.74	23.490	1131.2	11.68	7.78	23.430	1134.1	11.61	23.539	-0.109	-0.2916
DATE	5/15/93	9.28	25.030	1238.8	13.06	9.35	24.940	1243.2	12.96	25.078	-0.138	-0.4321
POLY	301	11.22	26.016	1362.2	13.88	11.64	25.546	1387.3	13.38	26.153	-0.607	-2.1728
c vppm	100	14.74	26.954	1561.6	14.58	14.70	26.996	1559.2	14.62	26.943	0.053	0.2273
nr	1.219	18.59	27.789	1754.1	15.21	18.75	27.676	1761.3	15.09	27.823	-0.147	-0.7214
Station	13	26.48	29.637	2093.6	16.75	26.27	29.755	2085.3	16.88	29.597	0.158	0.9687
		35.87	30.921	2436.5	17.77	35.34	31.151	2418.5	18.02	30.862	0.289	2.2009
		44.82	31.731	2722.7	18.39	44.16	31.966	2702.7	18.64	31.674	0.292	2.5463

0.89879	56.32	32.662	3050.0	19.13	55.72	32.837	3033.8	19.31	32.617	0.220	2.2111
1.09852	78.31	33.853	3586.6	20.03	78.40	33.836	3588.5	20.02	33.857	-0.021	-0.2639

